

# Complexity Arising in Financial Modelling and its Applications

Lead Guest Editor: Sameh S. Askar

Guest Editors: Delfim F. M. Torres, Junhai Ma, Mohamed El-Dessoky Ahmed, and Yingqian Zhang





---

# **Complexity Arising in Financial Modelling and its Applications**

Complexity

---

## **Complexity Arising in Financial Modelling and its Applications**

Lead Guest Editor: Sameh S. Askar

Guest Editors: Delfim F. M. Torres, Junhai Ma,  
Mohamed El-Dessoky Ahmed, and Yingqian  
Zhang




---

Copyright © 2023 Hindawi Limited. All rights reserved.

This is a special issue published in "Complexity." All articles are open access articles distributed under the Creative Commons Attribution License, which permits unrestricted use, distribution, and reproduction in any medium, provided the original work is properly cited.

# Chief Editor

Hiroki Sayama , USA

## Associate Editors

Albert Diaz-Guilera , Spain  
Carlos Gershenson , Mexico  
Sergio Gómez , Spain  
Sing Kiong Nguang , New Zealand  
Yongping Pan , Singapore  
Dimitrios Stamovlasis , Greece  
Christos Volos , Greece  
Yong Xu , China  
Xinggang Yan , United Kingdom


## Academic Editors

Andrew Adamatzky, United Kingdom  
Marcus Aguiar , Brazil  
Tarek Ahmed-Ali, France  
Maia Angelova , Australia  
David Arroyo, Spain  
Tomaso Aste , United Kingdom  
Shonak Bansal , India  
George Bassel, United Kingdom  
Mohamed Boutayeb, France  
Dirk Brockmann, Germany  
Seth Bullock, United Kingdom  
Diyi Chen , China  
Alan Dorin , Australia  
Guilherme Ferraz de Arruda , Italy  
Harish Garg , India  
Sarangapani Jagannathan , USA  
Mahdi Jalili, Australia  
Jeffrey H. Johnson, United Kingdom  
Jurgen Kurths, Germany  
C. H. Lai , Singapore  
Fredrik Liljeros, Sweden  
Naoki Masuda, USA  
Jose F. Mendes , Portugal  
Christopher P. Monterola, Philippines  
Marcin Mrugalski , Poland  
Vincenzo Nicosia, United Kingdom  
Nicola Perra , United Kingdom  
Andrea Rapisarda, Italy  
Céline Rozenblat, Switzerland  
M. San Miguel, Spain  
Enzo Pasquale Scilingo , Italy  
Ana Teixeira de Melo, Portugal

Shahadat Uddin , Australia  
Jose C. Valverde , Spain  
Massimiliano Zanin , Spain




## Contents

### **Decision-Making Techniques Based on $q$ -Rung Orthopair Probabilistic Hesitant Fuzzy Information: Application in Supply Chain Financing**

Shahzaib Ashraf , Noor Rehman , Muhammad Naeem , Sumayya Gul , Bushra Batool , and Shamsullah Zaland 

Research Article (19 pages), Article ID 3587316, Volume 2023 (2023)

### **The Effect of Utilizing Business Model Canvas on the Satisfaction of Operating Electronic Business**

Bahjat Fakieh , Abdullah S. AL-Malaise AL-Ghamdi , and Mahmoud Ragab 



Research Article (10 pages), Article ID 1649160, Volume 2022 (2022)

### **Corrigendum to “Asymmetric Risk Spillover Networks and Risk Contagion Driver in Chinese Financial Markets: The Perspective of Economic Policy Uncertainty”**

Zongxin Zhang, Ying Chen, and Weijie Hou


Corrigendum (1 page), Article ID 9853049, Volume 2022 (2022)

### **Fama–French Three-Factor Versus Daniel–Titman Characteristics Model: A Comparative Study of Asset Pricing Models from India**

Samreen Akhtar , Valeed Ahmad Ansari, Saghir Ahmad Ansari, and Alam Ahmad 



Research Article (12 pages), Article ID 6768434, Volume 2022 (2022)

### **More Efficient Prediction for Ordinary Kriging to Solve a Problem in the Structure of Some Random Fields**

Mohammad Mehdi Saber  and Ramy Abdelhamid Aldallal




Research Article (6 pages), Article ID 9712576, Volume 2022 (2022)

### **Evaluation of Hot Money Drivers in China: A Structural VAR Approach**

Weigang Hu , Yan Zhou , and Jun Liu






Research Article (12 pages), Article ID 1066096, Volume 2022 (2022)

### **Estimation for Akshaya Failure Model with Competing Risks under Progressive Censoring Scheme with Analyzing of Thymic Lymphoma of Mice Application**

Tahani A. Abushal , Jitendra Kumar, Abdisalam Hassan Muse , and Ahlam H. Tolba 

Research Article (27 pages), Article ID 5151274, Volume 2022 (2022)

### **On Extended Neoteric Ranked Set Sampling Plan: Likelihood Function Derivation and Parameter Estimation**

Fathy H. Riad, Mohamed A. Sabry , Ehab M. Almetwally , Ramy Aldallal , Randa Alharbi , and Md. Moyazzem Hossain 





Research Article (13 pages), Article ID 1697481, Volume 2022 (2022)

### **Constructing Multiple-Objective Portfolio Selection for Green Innovation and Dominating Green Innovation Indexes**

Meng Li , Kezhi Liao , Yue Qi , and Tongyang Liu 


Research Article (19 pages), Article ID 8263720, Volume 2022 (2022)

**The Impact of Internet Use on Corporate Tax Avoidance: Evidence from Chinese Enterprises**

Gaoyi Lin , Yanyan Zhao , Wanmin Liu , and Jianjun Zhou 


Research Article (17 pages), Article ID 5638593, Volume 2022 (2022)

**On Statistical Properties of a New Bivariate Modified Lindley Distribution with an Application to Financial Data**

Ahmed Elhassanein 


Research Article (19 pages), Article ID 2328831, Volume 2022 (2022)

**Economic Policy Uncertainty and Sectoral Trading Volume in the U.S. Stock Market: Evidence from the COVID-19 Crisis**

Dohyun Pak and Sun-Yong Choi 



Research Article (15 pages), Article ID 2248731, Volume 2022 (2022)

**On the Dynamics of Cournot Duopoly Game with Governmental Taxes**

S. S. Askar 





Research Article (11 pages), Article ID 5195337, Volume 2022 (2022)

**Mathematical and Statistical Models with Applications of Spread of Private Tutoring in Saudi Arabia**

Alanazi Talal Abdulrahman  and Adel A. Attiya 


Research Article (9 pages), Article ID 7842971, Volume 2022 (2022)

**The Catastrophe Analysis of Shanghai Crude Oil Futures Price from the Perspective of Volatility Factors**

Weifeng Gong , Yahui Li , Chuanhui Wang , Haixia Zhang , and Zhengjie Zhai


Research Article (12 pages), Article ID 5367693, Volume 2022 (2022)

**A Novel Modeling Technique for the Forecasting of Multiple-Asset Trading Volumes: Innovative Initial-Value-Problem Differential Equation Algorithms for Reinforcement Machine Learning**

Mazin A. M. Al Janabi 


Research Article (16 pages), Article ID 4965556, Volume 2022 (2022)

**A Combined Prediction Model for Hog Futures Prices Based on WOA-LightGBM-CEEMDAN**

Xiang Wang , Shen Gao, Yibin Guo, Shiyu Zhou, Yonghui Duan, and Daqing Wu




Research Article (15 pages), Article ID 3216036, Volume 2022 (2022)

**Prediction and Classification of Financial Criteria of Management Control System in Manufactories Using Deep Interaction Neural Network (DINN) and Machine Learning**

Amir Yousefpour  and Hamid Mazidabadi Farahani

Research Article (12 pages), Article ID 2295105, Volume 2022 (2022)




**Multifactor Stock Selection Strategy Based on Machine Learning: Evidence from China**

Jieying Gao , Huan Guo , and Xin Xu 

Research Article (17 pages), Article ID 7447229, Volume 2022 (2022)






# Contents

## **A Composite Index for Measuring Stock Market Inefficiency**

Raffaele Mattera , Fabrizio Di Sciorio , and Juan E. Trinidad-Segovia 

Research Article (13 pages), Article ID 9838850, Volume 2022 (2022)

## **Jumping Risk Communities in the Energy Industry: An Empirical Analysis Based on Time-Varying Complex Networks**

Hui Wang , Lili Jiang , Hongjun Duan , Yifeng Wang , Yichen Jiang , and Xiaolei Zhang 




Research Article (12 pages), Article ID 8642443, Volume 2022 (2022)

## **Workforce Participation, Ageing, and Economic Welfare: New Empirical Evidence on Complex Patterns across the European Union**

Mirela S. Cristea , Marilen G. Pirtea , Marta C. Suciuc , and Gratiela G. Noja 


Research Article (13 pages), Article ID 7313452, Volume 2022 (2022)

## **A Novel Approach to Improving E-Government Performance from Budget Challenges in Complex Financial Systems**

Enkeleda Lulaj , Ismat Zarin , and Shawkat Rahman 


Research Article (16 pages), Article ID 2507490, Volume 2022 (2022)

## **Local Asymptotic Normality Complexity Arising in a Parametric Statistical Lévy Model**

Wissem Jedidi 



Research Article (18 pages), Article ID 3143324, Volume 2021 (2021)

## **The New Novel Discrete Distribution with Application on COVID-19 Mortality Numbers in Kingdom of Saudi Arabia and Latvia**

M. Nagy, Ehab M. Almetwally, Ahmed M. Gemeay, Heba S. Mohammed, Taghreed M. Jawa, Neveen Sayed-Ahmed, and Abdisalam Hassan Muse 



Research Article (20 pages), Article ID 7192833, Volume 2021 (2021)

## **Nonlinear Cointegration and Asymmetric Adjustment in Purchasing Power Parity of the USA, Germany, and Pakistan**

Kashif Ali, Hafsa Hina, Muhammad Ijaz , and Mahmoud El-Morshedy 


Research Article (7 pages), Article ID 1555091, Volume 2021 (2021)

## **The Arctan-X Family of Distributions: Properties, Simulation, and Applications to Actuarial Sciences**

Ibrahim Alkhairy, M. Nagy, Abdisalam Hassan Muse , and Eslam Hussam 


Research Article (14 pages), Article ID 4689010, Volume 2021 (2021)

## **The Traditional Influence on Increasing Acceptance of Commercial Smartphone Applications in Specific Regions of the Arabic World**

Adel A. Bahaddad 

Research Article (16 pages), Article ID 4336772, Volume 2021 (2021)



## **Inferences for Generalized Pareto Distribution Based on Progressive First-Failure Censoring Scheme**

Rashad M. El-Sagheer, Taghreed M. Jawa, and Neveen Sayed-Ahmed 

Research Article (11 pages), Article ID 9325928, Volume 2021 (2021)




**Maximize Expected Profits by Dynamic After-Sales Service Investment Strategy Based on Word-of-Mouth Marketing in Social Network Shopping**

Ying Yu , Jiaomin Liu, Jiadong Ren , Qian Wang, and Cuiyi Xiao  
Research Article (15 pages), Article ID 4237712, Volume 2021 (2021)

**Credit Rating Model of Small Enterprises Based on Optimal Discriminant Ability and Its Empirical Study**

Zhanjiang Li  and Lin Guo   
Research Article (12 pages), Article ID 5605499, Volume 2021 (2021)

**Netizens' Perspective towards Electronic Money and Its Essence in the Virtual Economy: An Empirical Analysis with Special Reference to Delhi-NCR, India**

Mohammed Arshad Khan   
Research Article (18 pages), Article ID 7772929, Volume 2021 (2021)

**The Influence of Industrial Policy on Innovation in Startup Enterprises: An Empirical Study Based on China's GEM Listed Companies**

Fang Wang and Deyong Zhu   
Research Article (15 pages), Article ID 9650741, Volume 2021 (2021)


**Truncated Cauchy Power Odd Fréchet-G Family of Distributions: Theory and Applications**

M. Shrahili  and I. Elbatal  
Research Article (9 pages), Article ID 4256945, Volume 2021 (2021)


**Regional Bank Consolidation and SMEs' Credit Availability: Evidence from China**

Xiaohui Hou , Wei He, and Kong-Lin Ke  
Research Article (4 pages), Article ID 8509991, Volume 2021 (2021)

**Economic Policy Uncertainty and Chinese Stock Market Volatility: A CARR-MIDAS Approach**

Xinyu Wu , Tianyu Liu, and Haibin Xie  
Research Article (10 pages), Article ID 4527314, Volume 2021 (2021)

**Asymmetric Risk Spillover Networks and Risk Contagion Driver in Chinese Financial Markets: The Perspective of Economic Policy Uncertainty**

Zongxin Zhang, Ying Chen , and Weijie Hou  
Research Article (10 pages), Article ID 3169534, Volume 2021 (2021)

## Research Article

# Decision-Making Techniques Based on $q$ -Rung Orthopair Probabilistic Hesitant Fuzzy Information: Application in Supply Chain Financing

Shahzaib Ashraf <sup>1</sup>, Noor Rehman <sup>2</sup>, Muhammad Naeem <sup>3</sup>, Sumayya Gul <sup>2</sup>,  
Bushra Batool <sup>4</sup>, and Shamsullah Zaland <sup>5</sup>

<sup>1</sup>Institute of Mathematics, Khwaja Fareed University of Engineering and Information Technology, Rahim Yar Khan 64200, Pakistan

<sup>2</sup>Department of Mathematics and Statistics, Bacha Khan University, Charsadda 24420, Pakistan

<sup>3</sup>Department of Mathematics, Deanship of Applied Sciences, Umm Al-Qura University, Makkah, Saudi Arabia

<sup>4</sup>Department of Mathematics, University of Sargodha, Sargodha 40100, Pakistan

<sup>5</sup>Faculty of Mathematics, Kabul Polytechnic University, Kabul, Afghanistan

Correspondence should be addressed to Shamsullah Zaland; [shamszaland@kpu.edu.af](mailto:shamszaland@kpu.edu.af)

Received 19 November 2021; Revised 6 January 2022; Accepted 19 May 2023; Published 29 June 2023

Academic Editor: M. M. El-Dessoky

Copyright © 2023 Shahzaib Ashraf et al. This is an open access article distributed under the Creative Commons Attribution License, which permits unrestricted use, distribution, and reproduction in any medium, provided the original work is properly cited.

The influence of COVID-19 on individuals, businesses, and corporations is indisputable. Many markets, particularly financial markets, have been severely shaken and have suffered significant losses. Significant issues have arisen in supply chain networks, particularly in terms of financing. The COVID-19 consequences had a significant effect on supply chain financing (SCF), which is responsible for finance supply chain components and improved supply chain performance. The primary source of supply chain financing is financial providers. Among financial providers, the banking sector is referred to as the primary source of financing. Any hiccup in the banking operational systems can have a massive influence on the financing process. In this study, we attempted to comprehend the key consequences of the COVID-19 epidemic and how to mitigate COVID-19's impact on Pakistan's banking industry. For this, three extended hybrid approaches which consists of TOPSIS, VIKOR, and Grey are established to address the uncertainty in supply chain finance under  $q$ -rung orthopair probabilistic hesitant fuzzy environment with unknown weight information of decision-making experts as well as the criteria. The study is split into three parts. First, the novel  $q$ -rung orthopair probabilistic hesitant fuzzy (qROPHF) entropy measure is established using generalized distance measure under qROPHF information to determine the unknown weights information of the attributes. The second part consists of three decision-making techniques (TOPSIS, VIKOR, and GRA) in the form of algorithm to tackle the uncertain information under qROPHF settings. Last part consists of a real-life case study of supply chain finance in Pakistan to analyze the effects of emergency situation of COVID-19 on Pakistani banks. Therefore, to help the government, we chose the best alternative form list of consider five alternatives (investment, government support, propositions and brands, channels, and digital and markets segments) by using proposed algorithm that minimize the effect of COVID-19 on supply chain finance of Pakistani banks. The results indicate that the proposed techniques are applicable and effective to cope with ambiguous data in decision-making challenges.

## 1. Introduction

The origins of supply chain finance (SCF) may be traced back to the 1970s, when the influence of trade-credit adjustments and inventory regulations on net cash flow was explored by

Budin and Eapen [1]. At the turn of the twenty-first century, the first formal definition of SCF appeared. Stemmler [2] identified financial flows into the physical supply chain as a key SCF feature. According to the findings of this study, SCF is an essential component of supply chain management.

In recent years, SCF has played a crucial role in operational and financial transactions and has attracted the interest of academics and business [3–5]. In literature, there are various definitions of SCF. The SCF is defined as the intercompany optimization of financing to maximize the value of all participating firms by consolidating financing activities with consumers, suppliers, and service providers [6]. Many authors contribute many techniques to tackle the supply chain financing problems [7–10].

Buyers and suppliers are looking for ways to improve working capital efficiency and liberate cash stuck in the financial supply chain in the face of an economic slump caused by a global pandemic and the increasing complexity of global supply chains. Integration of financial and physical supply chains is required in a global economy where supply networks are becoming increasingly complex [11]. In integrating financial and physical supply chains, financial service providers serve a significant role in meeting capital requirements throughout the supply chain [12]. Due to the strategic relationship between suppliers, purchasers, and financial service providers, it would be difficult for either side to fail to deliver on mutual contractual promises [13]. Among all financial service providers, banks are the conventional and primary source of financial resources for supply chain finance. According to [14], about 30% of finance supply in the supply chain finance belongs to global/regional banks. Also, 50% of this finance supply belongs to domestic banks. Anything that affects financial networks has unavoidable and irreversible consequences for supply chain financing activity. Due to the emergence of the coronavirus (COVID-19) in the early 2020s, numerous markets were hit by the pandemic's ramifications. Financial markets and banks were no exception. As a consequence, banks' financial supply had significant challenges. A vast number of banks have been exposed to a variety of risks and uncertainties. Banks should develop and coordinate emergency/crisis management implementation plans so that they can be carried out in an emergency with the least amount of disruption to the bank. The unpredictability of loss in the process through which financial institutions such as banks deliver supply chain financial services is known as supply chain finance risk [15]. As a result, in order to minimize risk, a risk assessment is required to investigate the hazards of supply chain financing. Risk recognition, evaluation, measurement, and control are the fundamental aspects of risk management in SCF [16].

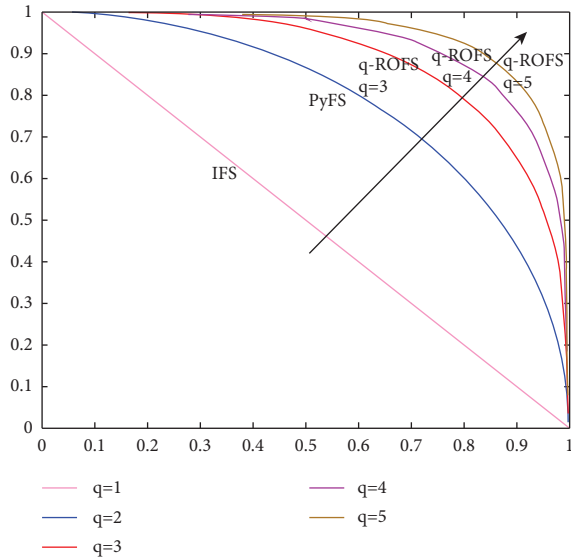
As previously stated, SCF and particularly financial suppliers like banks have faced numerous uncertainties, particularly in emergency situations such as pandemics. Fuzzy set [17] is a handy and reliable strategy to cope with such ambiguities in decision-making problems [7–9, 18, 19]. By proposing the notion of positive and negative grades, Atanassov [20] established the fortuitous of intuitionistic fuzzy sets (IFSs) as a refinement of FSs. IFS theory has been applied by a number of academics in a variety of fields [21–23]. Furthermore, Yager [24] developed the Pythagorean fuzzy set (PFS) theory that is more effective and superior to IFS theory in resolving with challenges that IFS theory cannot answer. The PFS has been applied by

a number of academics in a variety of fields [25–27]. However, if a decision-maker faces such obstacles that the sum of the squares of both degrees cannot be surpassed from a unit interval, there are several concerns. Furthermore, Yager discovered the theory of  $q$ -rung orthopair fuzzy set (QROFS), which employs the rule that the sum of the  $q$ -power of both degrees cannot beyond from the unit interval and is more effective and superior to PFS theory in answering issues that PFS theory cannot respond.

The limitation of QROFS would be that the total of the membership degree (MD) power and the nonmembership degree (NMD) power of  $q$  may be less than or identical to one. Clearly, the greater the rung  $q$ , the more the bounding condition is fulfilled by orthopair and thus the greater the space of fuzzy data that can be expressed by QROFSs [28]. In ability to cope with both the complete absence of clarity and flouted information, QROFSs are better and more efficient than IFS and PFS. Figure 1 depicts the distinction between them.

Many researchers contribute to the QROFS to tackle the uncertain and ambiguity in decision-making problems (DMPs) such as Wei et al. [29] established the novel list of aggregation operators (AGOp) based on QROF information and discussed their application in DMPs. Liu and Wang [30] proposed algebraic norm-based lists of QROF AGoP under QROF environment. Liu and Wang [31] proposed Archimedean Bonferroni mean-based lists of QROF AGoP under QROF environment and discussed their application to tackle uncertainty in DMPs. Peng et al. [32] established the list of exponential operations-based AGoP under QROF environment. Shu et al. [33] presented the integrations rules using QROFs and also discussed applicability in DMPs. Peng and Liu [34] discussed the information measures under  $q$ -ROF settings. Ali [35] discussed the novel operational rules and algebraic relations under QROF information. Xing et al. stated that [36], based on the QROF interaction, a new multicriteria group decision-making methodology has been developed. Gao et al. [37] stated the continuities, derivatives, and differentials of QROF functions and discussed in their applicability in real word problems. Wei et al. [38] established the novel list of aggregation operators based on Maclaurin symmetric mean under QROF information and also discussed their application related to emerging technology. Habib et al. [39] proposed the fuzzy competition graphs under QROF settings and also presented the real-life application related to soil ecosystem. Liu et al. [40] established the novel list of AGoP based on power Maclaurin symmetric mean under QROF information. Yang and Pang [41] proposed partitioned Bonferroni mean-based lists of QROF AGoP under QROF environment. Liao et al. [42] established the QROF GLDS approach for BE angel capital investment assessment in China.

Hesitancy is a common occurrence in our universe. In real life, choosing one of the finest options (alternative) under list of attributes is difficult. Experts are having difficulty making decisions due to the data's ambiguity and hesitation. Torra [43] proposed the concept of hesitant fuzzy set to overcome the hesitancy (HFS). Khan et al. [44] proposed an improved version of hesitating fuzzy sets called

FIGURE 1:  $q$ -ROFSs space.

the Pythagorean hesitant fuzzy set. Overhead ideas can be utilized to efficiently determine randomness. However, the frameworks described above are incapable of dealing with circumstances in which a specialist's rejection is a critical factor in the decision-making process. For example, in the staffing procedure, a board of five professionals is regarded to determine the best applicant, and three of them are rejected from making any judgement. While using existing strategies to examine the information, the number of decision-makers is kept to three rather than five, i.e., the rejected professionals are completely ignored, and the choice is made solely on the basis of the three professionals' preferences. It results in significant data loss and may result in inadequate grades. To deal with such situations, Xu and Zhou [45] proposed a new concept known as probabilistic hesitant fuzzy sets (PHFSs).

As a result of the foregoing motivation, this study provides three novel expanded decision-making techniques, which are "technique for order of preference by similarity to ideal solution" (TOPSIS), "Vlsekriterijumska Optimizacija I Kompromisno Resenje" (VIKOR) and "Grey" (GRA) approaches to tackle the uncertain information in real-life decision-making problems under  $q$ -rung orthopair probabilistic hesitant fuzzy environment with unknown weight information. To determine the unknown weight information of the decision-making experts as well as the weight information of the consider attributes/criteria, entropy measure based on generalized distance measures is provided under  $q$ -rung orthopair probabilistic hesitant fuzzy environment. Meanwhile, this study provides a weight calculation technique that can effectively deal with the bias expert's extreme value and solve the problem of huge differences of opinion among experts. Furthermore, the proposed method will produce a more accurate evaluation result by employing the improved relative closeness formula. As a result, the following are the primary characteristics of this paper's innovations: First, it introduces the  $q$ -rung orthopair

probabilistic hesitant fuzzy set, which is a novel idea ( $q$ -ROPHFS). The motivation for the new concept is that while only positive membership degrees are considered with probabilistic information in probabilistic hesitant fuzzy sets. However, the innovative concept of  $q$ -ROPHFS is defined by the presence of both positive and negative hesitant grades, with the restriction that the square sum of both hesitant grades be not more than one.

The decision-makers in  $q$ -ROPHFS are limited to a single domain and ignore the negative membership degree and its likelihood of occurrence. In comparison to others, every negative reluctant membership degree has some preferences. For example, in DM-problems, decision-makers may express their view in the form of multiple alternative values; for example, if one DM delivers values 0.3, 0.4, and 0.6 for positive membership degree with matching preference values 0.1 and 0.9, the other may reject. The proposed concept considers the possibility of a higher rejection level with reluctance. Despite HFSs and  $q$ -ROHFSs, the information about chances will decrease. The probability of occurrence with positive and negative membership degrees provides extra information about the DMs' level of disagreement. The innovative notion of Pythagorean probabilistic hesitant fuzzy set is proposed to deal with uncertainty in decision-making situations. The following is a list of the paper's originality:

- (1)  $q$ -ROPHFS is a generalization of the PHFS
- (2)  $q$ -ROPHF extended TOPSIS and VIKOR methods-based algorithms using unidentified weight data of attributes as well as the decision-making experts
- (3) The  $q$ -ROPHF multicriteria group decision-making problems are tackled by the proposed three generalized decision-making techniques
- (4) We apply the distance measures and entropy measure to determine the unknown information of weights
- (5) To demonstrate the efficacy and application of the suggested technique, a case study related to supply chain finance is considered to analyze the effect of emergency situation of COVID-19 on Pakistani banks
- (6) A comparative study is proposed based on the GRY method to validate the proposed methodologies

The rest of this manuscript is organized as follows. Section 2 briefly retrospect's some basic concepts of  $q$ -ROFSs, HFSs, and probabilistic fuzzy set theory. A novel notion of  $q$ -rung orthopair probabilistic hesitant fuzzy sets is presented in Section 3. Section 4 highlights a novel entropy measures based on the generalized distance measures under QROPHFSs to determine the unknown weight information of the attributes. Section 5 is devoted the three decision-making methodologies based on TOPSIS, VIKOR, and GRA to address the uncertainty in decision-making problems and also presents the numerical illustration related to finance supply chain is consider analyzing the effects of emergency situation of COVID-19 on Pakistani banks in Section 6. The

comparative study of the proposed technique using extended GRY method is presented in Section 7. Section 8 concludes this study.

## 2. Preliminaries

In this segment, we briefly recall the rudiments of fuzzy sets and their generalized structures like intuitionistic FSs (IFSs),  $q$ -rung orthopair FSs (QROFSs), hesitant FSs (HFSs), and  $q$ -rung orthopair hesitant FSs ( $q$ -ROHFSs). The following are some related definitions.

*Definition 1* (see [28]). Let  $S$  be a fixed set. A  $q$ -ROFSs in  $S$  is defined as follows:

$$s = \{(m, P_s(m), N_s(m)) \mid m \in S\}, \quad (1)$$

for each  $m \in S$ ,  $P_s(m)$  and  $N_s(m) \in [0, 1]$  are known to be positive and negative MGs, respectively. In addition,  $0 \leq (P_s(m))^q + (N_s(m))^q \leq 1$  for all  $m \in S$ .

We shall symbolize the  $q$ -rung orthopair fuzzy number ( $q$ -ROFN) by a pair  $s = (P_s, N_s)$ . Conventionally,  $\mathbb{E}_m = \sqrt[q]{1 - P_s^q - N_s^q}$  is the degree of hesitancy of  $m \in S$  to  $s$ .

*Definition 2* (see [28]). Let  $s_1, s_2, s \in q$ -ROFNs, the operational rules are defined as follows:

- (1)  $s_1 \leq s_2$  iff  $P_{s_1}(m) \leq P_{s_2}(m)$  and  $N_{s_1}(m) \geq N_{s_2}(m) \forall m \in S$
- (2)  $s_1 = s_2$  iff  $s_1 \leq s_2$  and  $s_2 \leq s_1$
- (3)  $s_1 \cup s_2 = \{\max(P_{s_1}(m), P_{s_2}(m)), \min(N_{s_1}(m), N_{s_2}(m)) \mid m \in S\}$
- (4)  $s_1 \cap s_2 = \{\min(P_{s_1}(m), P_{s_2}(m)), \max(N_{s_1}(m), N_{s_2}(m)) \mid m \in S\}$
- (5)  $s^c = \{N_s(m), P_s(m) \mid m \in S\}$

*Definition 3* (see [28]). Let  $s_1, s_2, s \in q$ -ROFNs with  $h > 0$ , the basic operational rules are defined as follows:

- (1)  $s_1 \otimes s_2 = (P_{s_1} P_{s_2}, \sqrt[q]{(N_{s_1})^q + (N_{s_2})^q - (N_{s_1})^q (N_{s_2})^q})$ ;
- (2)  $s_1 \oplus s_2 = (\sqrt[q]{(P_{s_1})^q + (P_{s_2})^q - (P_{s_1})^q (P_{s_2})^q}, N_{s_1} N_{s_2})$ ;
- (3)  $h \cdot s = (\sqrt[q]{1 - (1 - (P_s)^q)^h}, (N_s)^h)$ ;
- (4)  $(s)^h = ((P_s)^h, \sqrt[q]{1 - (1 - (N_s)^q)^h})$ .

*Definition 4* (see [43]). Let  $S$  be a fixed set. A HFSs in  $S$  is defined as follows:

$$s = \{(m, P_s(m)) \mid m \in S\}, \quad (2)$$

for each  $m \in S$ ,  $P_s(m)$  be a set of some values in  $[0, 1]$  known to be hesitant membership grade (MG).

*Definition 5* (see [43]). Let  $s_1, s_2 \in$  HFS, the operational rules are defined as follows:

- (1)  $s_1^c = \cup_{h \in P_{s_1}(m)} \{1 - h\}$
- (2)  $s_1 \cup s_2 = P_{s_1}(m) \vee P_{s_2}(m) = \cup_{h_1 \in P_{s_1}, h_2 \in P_{s_2}} \max\{h_1, h_2\}$
- (3)  $s_1 \cap s_2 = P_{s_1}(m) \wedge P_{s_2}(m) = \cup_{h_1 \in P_{s_1}, h_2 \in P_{s_2}} \min\{h_1, h_2\}$

*Definition 6.* Let  $S$  be a fixed set. A PHFS in  $S$  is defined as follows:

$$s = \{(m, P_s(m), N_s(m)) \mid m \in S\}, \quad (3)$$

for each  $m \in S$ ,  $P_s(m)$  and  $N_s(m) \in [0, 1]$  are the set of some values in  $[0, 1]$  known to be positive and negative hesitant MGs. In addition  $(\max(P_s(m)))^2 + (\min(N_s(m)))^2 \leq 1$  and  $(\min(P_s(m)))^2 + (\max(N_s(m)))^2 \leq 1$ .

We will use pair  $s = (P_s, N_s)$  to represent the Pythagorean hesitant fuzzy number (PHFN).

*Definition 7.* Let  $s_1, s_2 \in$  PHFS, the operational rules are defined as follows:

- (1)  $s^c = \{N_s(m), P_s(m) \mid m \in S\}$
- (2)  $s_1 \cup s_2 = \left\{ \begin{array}{l} P_{s_1}(m) \vee P_{s_2}(m), \\ N_{s_1}(m) \wedge N_{s_2}(m) \end{array} \right\} = \left\{ \begin{array}{l} \cup_{h_1 \in P_{s_1}, h_2 \in P_{s_2}} \max(h_1, h_2) \\ \cup_{r_1 \in N_{s_1}, r_2 \in N_{s_2}} \min(r_1, r_2) \end{array} \right\}$
- (3)  $s_1 \cap s_2 = \left\{ \begin{array}{l} P_{s_1}(m) \wedge P_{s_2}(m), \\ N_{s_1}(m) \vee N_{s_2}(m) \end{array} \right\} = \left\{ \begin{array}{l} \cup_{h_1 \in P_{s_1}, h_2 \in P_{s_2}} \min(h_1, h_2), \\ \cup_{r_1 \in N_{s_1}, r_2 \in N_{s_2}} \max(r_1, r_2) \end{array} \right\}$

*Definition 8.* Let  $S$  be a fixed set. A PPHFS in  $S$  is defined as follows:

$$s = \left\{ \left( m, \frac{P_s(m)}{p_s}, \frac{N_s(m)}{n_s} \right) \mid m \in S \right\}, \quad (4)$$

for each  $m \in S$ ,  $P_s(m)$  and  $N_s(m) \in [0, 1]$  are the set of some values in  $[0, 1]$  and  $p_o, n_o$  are probabilistics terms. Here,  $P_o(m)/p_o$  and  $N_o(m)/n_o$  are known to be positive and negative probabilistic hesitant MGs. In addition  $0 < \alpha_i, \beta_i < 1$  and  $0 < p_i, n_i \leq 1$  with  $\sum_{i=1}^k p_i \leq 1, \sum_{i=1}^k n_i \leq 1$  ( $k$  is a positive integer to describe the number of elements contained in PPHFS, where  $\alpha_i \in P_s(m), \beta_i \in N_s(m), p_i \in p_s, n_i \in n_s$ )  $(\max(P_s(m)))^2 + (\min(N_s(m)))^2 \leq 1$  and  $(\min(P_s(m)))^2 + (\max(N_s(m)))^2 \leq 1$ .

We will use pair  $s = (P_s/p_s, N_s/n_s)$  to represent the Pythagorean probabilistics hesitant fuzzy number (PPHFN).

*Definition 9.* Let  $s_1 = (P_{s_1}/p_{s_1}, N_{s_1}/n_{s_1})$  and  $s_2 = (P_{s_2}/p_{s_2}, N_{s_2}/n_{s_2})$  are two PyPHFNs with  $\alpha > 0$ , the operational rules are defined as follows:

- (1)  $s_1 \oplus s_2 = \left\{ \begin{array}{l} \cup_{h_1 \in P_{s_1}(m), h_2 \in P_{s_2}(m), p_1 \in p_{s_1}, p_2 \in p_{s_2}} (\sqrt{h_1^2 + h_2^2 - h_1^2 h_2^2 / p_1 p_2}) \\ \cup_{r_1 \in N_{s_1}(m), r_2 \in N_{s_2}(m), n_1 \in n_{s_1}, n_2 \in n_{s_2}} (r_1 r_2 / n_1 n_2) \end{array} \right\}$
- (2)  $s_1 \otimes s_2 = \left\{ \begin{array}{l} \cup_{h_1 \in P_{s_1}(m), h_2 \in P_{s_2}(m), p_1 \in p_{s_1}, p_2 \in p_{s_2}} (h_1 h_2 / p_1 p_2) \\ \cup_{r_1 \in N_{s_1}(m), r_2 \in N_{s_2}(m), n_1 \in n_{s_1}, n_2 \in n_{s_2}} (\sqrt{r_1^2 + r_2^2 - r_1^2 r_2^2 / n_1 n_2}) \end{array} \right\}$
- (3)  $\alpha s_1 = \left\{ \begin{array}{l} \cup_{h_1 \in P_{s_1}(m), p_1 \in p_{s_1}} (\sqrt{1 - (1 - h_1^2)^\alpha} / p_1), \cup_{r_1 \in N_{s_1}(m), n_1 \in n_{s_2}} (r_1^\alpha / n_1) \end{array} \right\}$
- (4)  $s_1^\alpha = \left\{ \begin{array}{l} \cup_{h_1 \in P_{s_1}(m), p_1 \in p_{s_1}} (h_1^\alpha / p_1), \cup_{r_1 \in N_{s_1}(m), n_1 \in n_{s_2}} (\sqrt{1 - (1 - r_1^2)^\alpha} / n_1) \end{array} \right\}$

### 3. $q$ -Rung Orthopair Probabilistic Hesitant Fuzzy Sets

*Definition 10.* Let  $S$  be a fixed set. APPHFS in  $S$  is defined as follows:

$$s = \left\{ \left( m, \frac{P_s(m)}{p_s}, \frac{N_s(m)}{n_s} \right) \mid m \in S \right\}, \quad (5)$$

for each  $m \in S$ ,  $P_s(m)$  and  $N_s(m) \in [0, 1]$  are the set of some values in  $[0, 1]$  and  $p_s, n_s$  are probabilistics terms, where  $P_s(m)/p_s$  and  $N_s(m)/n_s$  are known to be positive and negative probabilistic hesitant MGs. In addition  $0 \leq \alpha_i, \beta_i \leq 1$  and  $0 \leq p_i, n_i \leq 1$  with  $\sum_{i=1}^k p_i \leq 1, \sum_{i=1}^k n_i \leq 1$  ( $k$  is a positive integer to describe the number of elements contained in PPHFS, where  $\alpha_i \in P_s(m), \beta_i \in N_s(m), p_i \in p_s, n_i \in n_s$ )  $(\max(P_s(m)))^q + (\min(N_s(m)))^q \leq 1$  and  $(\min(P_s(m)))^q + (\max(N_s(m)))^q \leq 1$ .

We shall symbolize the  $q$ -rung orthopair probabilistics hesitant fuzzy number ( $q$ -ROPHFN) by a pair  $s = (P_s/p_s, N_s/n_s)$ .

*Definition 11.* Let  $s_1 = (P_{s_1}/p_{s_1}, N_{s_1}/n_{s_1})$  and  $s_2 = (P_{s_2}/p_{s_2}, N_{s_2}/n_{s_2})$  are two  $q$ -ROPHFNs. Then, the basic operational laws are defined as follows:

$$\begin{aligned} (1) \quad s_1 \cup s_2 &= \left\{ \begin{array}{l} \cup_{h_1 \in P_{s_1}(m), p_1 \in p_{s_1}} (\max(h_1/p_1, h_2/p_2)) \\ \cup_{r_1 \in N_{s_1}(m), n_1 \in n_{s_2}} (\min(r_1/n_1, r_2/n_2)) \end{array} \right\} \\ (2) \quad s_1 \cap s_2 &= \left\{ \begin{array}{l} \cup_{h_1 \in P_{s_1}(m), p_1 \in p_{s_1}} (\min(h_1/p_1, h_2/p_2)) \\ \cup_{r_1 \in N_{s_1}(m), n_1 \in n_{s_2}} (\max(r_1/n_1, r_2/n_2)) \end{array} \right\} \\ (3) \quad s^c &= \{N_s/n_s, P_s/p_s\} \end{aligned}$$

*Definition 12.* Let  $s_1 = (P_{s_1}/p_{s_1}, N_{s_1}/n_{s_1})$  and  $s_2 = (P_{s_2}/p_{s_2}, N_{s_2}/n_{s_2})$  are two  $q$ -ROPHFNs with  $\alpha > 0$ , then the operation are defined as follows:

$$\begin{aligned} (1) \quad s_1 \oplus s_2 &= \left\{ \begin{array}{l} \cup_{h_1 \in P_{s_1}(m), h_2 \in P_{s_2}(m), p_1 \in p_{s_1}, p_2 \in p_{s_2}} (\sqrt[q]{h_1^q + h_2^q - h_1^q h_2^q / p_1 p_2}) \\ \cup_{r_1 \in N_{s_1}(m), r_2 \in N_{s_2}(m), n_1 \in n_{s_1}, n_2 \in n_{s_2}} (r_1 r_2 / n_1 n_2) \end{array} \right\} \\ (2) \quad s_1 \otimes s_2 &= \left\{ \begin{array}{l} \cup_{h_1 \in P_{s_1}(m), h_2 \in P_{s_2}(m), p_1 \in p_{s_1}, p_2 \in p_{s_2}} (h_1 h_2 / p_1 p_2) \\ \cup_{r_1 \in N_{s_1}(m), r_2 \in N_{s_2}(m), n_1 \in n_{s_1}, n_2 \in n_{s_2}} (\sqrt[q]{r_1^q + r_2^q - r_1^q r_2^q / n_1 n_2}) \end{array} \right\}; \\ (3) \quad \alpha s_1 &= \left\{ \begin{array}{l} \cup_{h_1 \in P_{s_1}(m), p_1 \in p_{s_1}} (\sqrt[q]{1 - (1 - h_1^q)^\alpha / p_1}) \\ \cup_{r_1 \in N_{s_1}(m), n_1 \in n_{s_2}} (r_1^\alpha / n_1) \end{array} \right\} \\ (4) \quad s_1^\alpha &= \left\{ \begin{array}{l} \cup_{h_1 \in P_{s_1}(m), p_1 \in p_{s_1}} (h_1^\alpha / p_1), \cup_{r_1 \in N_{s_1}(m), n_1 \in n_{s_2}} \\ (\sqrt[q]{1 - (1 - r_1^q)^\alpha / n_1}) \end{array} \right\} \end{aligned}$$

*Definition 13.* For any  $q$ -ROPHFNs  $= (P_s(m)/p_s, N_s(m)/n_s)$ . The score value of  $q$ -ROPHFNs is defined as follows:

$$\alpha(s) = \left( \frac{1}{A_s} \sum_{h_i \in P_s, p_i \in p_s} h_i \cdot p_i \right)^q - \left( \frac{1}{B_s} \sum_{r_i \in N_s, n_i \in n_s} r_i \cdot n_i \right)^q, \quad (6)$$

where  $A_s$  stands for the number of entries in  $P_s(m)$  and  $B_s$  stands for the number of entries in  $N_s(m)$ .

*Definition 14.* For any  $q$ -ROPHFN  $s = (P_s(m)/p_s, N_s(m)/n_s)$ . The accuracy value of  $q$ -ROPHFNs is defined as follows:

$$\beta(s) = \left( \frac{1}{A_s} \sum_{h_i \in P_s, p_i \in p_s} h_i \cdot p_i \right)^q + \left( \frac{1}{B_s} \sum_{r_i \in N_s, n_i \in n_s} r_i \cdot n_i \right)^q, \quad (7)$$

where  $A_s$  stands for the number of entries in  $P_s(m)$  and  $B_s$  stands for the number of entries in  $N_s(m)$ .

*Definition 15.* Let  $s_1 = (P_{s_1}/p_{s_1}, N_{s_1}/n_{s_1})$  and  $s_2 = (P_{s_2}/p_{s_2}, N_{s_2}/n_{s_2})$  are two  $q$ -ROPHFNs. Then, using the Definitions 16 E 17, comparison of  $q$ -ROPHFNs are defined as follows:

- (1) If  $\alpha(s_1) > \alpha(s_2)$ , then  $s_1 > s_2$
- (2) If  $\alpha(s_1) = \alpha(s_2)$  and  $\beta(s_1) > \beta(s_2)$ , then  $s_1 > s_2$

### 4. Development of an Approach under the $q$ -ROPHFS

The proposed extended distance measures and the weighted extended distance measurements for the  $q$ -ROPHFSs are defined in this section. Furthermore, entropy measures for  $q$ -ROPHFS are presented for quantitative evaluation of randomness of a  $q$ -ROPHFSs.

#### 4.1. Distance Measure for $q$ -ROPHFSs

*Definition 16.* For any two  $q$ -ROPHFSs  $= \{s_1, s_2, \dots, s_n\}$  and  $r = \{r_1, r_2, \dots, r_n\}$ , where  $s_j = (P_s/p_s(x_j), N_s/n_s(x_j))$  and  $r_j = (P_r/p_r(x_j), N_r/n_r(x_j))$ ,  $j = 1, 2, \dots, n$ . For any number  $\alpha > 0$ , the generalized distance measure between  $s$  and  $r$  as follows:

$$d(s, r) = \left( \frac{1}{2n} \sum_{j=1}^n \left( \left| \left( \frac{1}{A_s} \sum_{h_j \in P_s, p_j \in p_s} (h_j p_j) \right)^2 - \left( \frac{1}{A_r} \sum_{h_j \in P_r, p_j \in p_r} (h_j p_j) \right)^2 \right|^\alpha \right)^{1/\alpha} \right)^{1/\alpha}, \quad (8)$$

where  $A_s, B_s, A_r,$  and  $B_r$  are the possible numbers of elements in  $P_s/p_s, N_s/n_s, P_r/p_r,$  and  $N_r/n_r.$

*Definition 17.* For any two  $q$ -ROPHFSs  $s = \{s_1, s_2, \dots, s_n\}$  and  $r = \{r_1, r_2, \dots, r_n\},$  where  $s_j = (P_s/p_s(x_j), N_s/n_s(x_j))$  and  $r_j = (P_r/p_r(x_j), N_r/n_r(x_j)), j = 1, 2, \dots, n.$  For any number  $\alpha > 0,$  the generalized distance measure between  $s$  and  $r$  as follows:

$$d(s, r) = \left( \frac{1}{2n} \sum_{j=1}^n w_j \left( \left| \left( \frac{1}{A_s} \sum_{h_{s_j} \in P_s, p_{s_j} \in P_s}^{A_s} (h_{s_j} p_{s_j}) \right)^2 - \left( \frac{1}{A_r} \sum_{h_{r_j} \in P_r, p_{r_j} \in P_r}^{A_r} (h_{r_j} p_{r_j}) \right)^2 \right|^{\alpha} \right)^{1/\alpha} \right)^{1/\alpha}, \quad (9)$$

where  $w_j (j = 1, 2, \dots, n)$  be the weights vector assigned for each  $(x_j)$  and  $A_s, B_s, A_r, B_r$  are the possible numbers of elements in  $P_s/p_s, N_s/n_s, P_r/p_r, N_r/n_r.$

**Theorem 18.** Let  $s$  and  $r$  are two  $q$ -ROPHFSs, the distance measure has the following constraints:

- (A1)  $0 \leq d(s, r) \leq 1$
- (A2)  $d(s, r) = 1 \iff s = r$
- (A3)  $d(s, r) = d(r, s)$

*Proof.* Straightforward.  $\square$

**4.2. Entropy Measure for  $q$ -ROPHFSs.** In decision-making, the weights information of attributes/criteria is crucial. Many researchers study decision-making challenges in fuzzy settings with incomplete or undetermined weight data of attributes. Entropy measure is a conventional concept to determine attribute weight effectively.

*Definition 19.* The Shannon entropy information  $E(E_1, E_2, \dots, E_n)$  for  $q$ -ROPHFS is defined as follows:

$$E = \frac{-1}{(2 \log (n))} \sum_{i=1}^n (P_s (\log P_s) \times p_s + N_s (\log N_s) \times n_s). \quad (10)$$

List of some properties of entropy measure as follows:

- (1)  $E(s) = 0 \iff s$  is a crisp set
- (2)  $E(s) = 1 \iff h_{s_i}(m) = v_{s_i}(m) \forall m \in E$

(3)  $E(s) \leq E(r)$  if  $s \leq r$

(4)  $E(s) = E(s^c)$

## 5. Multiattribute Decision-Making Techniques for $q$ -ROPHFSs

Let  $\mathcal{F} = \{\mathcal{F}_1, \mathcal{F}_2, \dots, \mathcal{F}_m\}$  be a set of alternatives,  $C = \{C_1, C_2, \dots, C_n\}$  be a set of criteria and  $r$  be the number of DMs,  $DM_f (f = 1, 2, 3, \dots, r)$  to demonstrate their perception about “ $m$ ” alternatives with respect to the “ $n$ ” criteria by taking  $q$ -ROPHFSs  $S_{ij}^{(f)} = (P_{ij}^{(f)}, N_{ij}^{(f)})$ . The decision matrix of experts information is presented in Table 1.

$$S^{(f)} = [S_{ij}^{(f)}]_{m \times n} = \left[ \left( \frac{P_{ij}^{(f)}}{P_{S_{ij}}} \frac{N_{ij}^{(f)}}{n_{S_{ij}}} \right) \right]_{m \times n}. \quad (11)$$

**5.1.  $q$ -ROPHF Extended TOPSIS Method.** There are two primary parts to this method. First, a method for calculating the weights of criteria/attributes is presented using the proposed entropy measure for  $q$ -ROPHFNs. A ranking procedure based on the degree of similarity to the ideal solution is considered in the last part. Steps are presented as follows for the  $q$ -ROPHF extended TOPSIS method:

Step 1: first, we collect the data provided by the decision-makers in the form of  $q$ -ROPHFNs.

Step 2: we normalized the information defined by DMs in this step, as the decision matrix may have some benefit and cost parameters altogether, as follows:

$$e_{ij}^{(f)} = \begin{cases} S_{ij}^{(f)}, & \text{for benefit criteria,} \\ (S_{ij}^{(f)})^c, & \text{for cost criteria,} \end{cases}$$

$f = 1, 2, 3, \dots, r, i = 1, 2, 3, \dots, m, j = 1, 2, 3, \dots, n$  where  $(S_{ij}^{(f)})^c$  is complement of  $S_{ij}^{(f)}$ , that is  $(S_{ij}^{(f)})^c = (N_{S_{ij}}^{(f)}, P_{S_{ij}}^{(f)})$ .

(12)

TABLE 1: Expert information  $S^{(f)}$ .

	$C_1$	$C_2$	...	$C_n$
$J_1$	$(P_{S_{11}}^{(f)}/p_{S_{11}}, N_{S_{11}}^{(f)}/n_{S_{11}})$	$(P_{S_{12}}^{(f)}/p_{S_{12}}, N_{S_{12}}^{(f)}/n_{S_{12}})$	...	$(P_{S_{1n}}^{(f)}/p_{S_{1n}}, N_{S_{1n}}^{(f)}/n_{S_{1n}})$
$J_2$	$(P_{S_{21}}^{(f)}/p_{S_{21}}, N_{S_{21}}^{(f)}/n_{S_{21}})$	$(P_{S_{22}}^{(f)}/p_{S_{22}}, N_{S_{22}}^{(f)}/n_{S_{22}})$	...	$(P_{S_{2n}}^{(f)}/p_{S_{2n}}, N_{S_{2n}}^{(f)}/n_{S_{2n}})$
$J_3$	$(P_{S_{31}}^{(f)}/p_{S_{31}}, N_{S_{31}}^{(f)}/n_{S_{31}})$	$(P_{S_{32}}^{(f)}/p_{S_{32}}, N_{S_{32}}^{(f)}/n_{S_{32}})$	...	$(P_{S_{3n}}^{(f)}/p_{S_{3n}}, N_{S_{3n}}^{(f)}/n_{S_{3n}})$
$\vdots$	$\vdots$	$\vdots$	$\ddots$	$\vdots$
$J_m$	$(P_{S_{m1}}^{(f)}/p_{S_{m1}}, N_{S_{m1}}^{(f)}/n_{S_{m1}})$	$(P_{S_{m2}}^{(f)}/p_{S_{m2}}, N_{S_{m2}}^{(f)}/n_{S_{m2}})$	...	$(P_{S_{mn}}^{(f)}/p_{S_{mn}}, N_{S_{mn}}^{(f)}/n_{S_{mn}})$

Step 3: the weights of the parameters are determined in the following manner by the proposed entropy measure. The calculation of entropy corresponding to each criterion is as follows:

$$\begin{aligned}
 E(S_j) &= E(S_{1j}, S_{2j}, S_{3j}, \dots, S_{mj}), j = 1, 2, 3, \dots, n \\
 &= \frac{-1}{(2 \log(n))} \sum_{i=1}^n (P_s(\log P_s) \times p_s + N_s(\log N_s) \times n_s). \quad (13)
 \end{aligned}$$

then

$$w(S_j) = \frac{(1 - E(S_j))}{\sum_{j=1}^n (1 - E(S_j))}. \quad (14)$$

Thus, weights of criteria are found as follows:

$$w(S_j) = (w(S_1), w(S_2), w(S_3), \dots, w(S_n))^T. \quad (15)$$

Step 4: in this step, the best alternative according to given list of criteria/attribute are determined.

Step 4(a): determine the weighted NDM<sup>(f)</sup> using the weights of the assessed parameters in the following manner:

$$\text{NDM}_{i_j}^{(f)} = w(S_j) \cdot S_{i_j}^{(f)} = \begin{pmatrix} \bigcup_{h_i \in P_{S_{ij}}, p_i \in p_{S_{ij}}} \frac{\sqrt[q]{1 - \prod_{i=1}^m (1 - (h_{S_{ij}}^{(f)})^q)^{w(S_j)}}}{\prod_{i=1}^m p_{S_{ij}}^{(f)}} \\ \bigcup_{v_i \in N_{S_{ij}}, n_i \in n_{S_{ij}}} \frac{\prod_{i=1}^m \prod_{i=1}^m (v_{S_{ij}}^{(f)})^{w(S_j)}}{\prod_{i=1}^m n_{S_{ij}}^{(f)}} \end{pmatrix}. \quad (16)$$

for all  $f = 1.2.3 \dots \checkmark$ .

Step 4(b): derive PIS<sup>(f)</sup> and NIS<sup>(f)</sup> for all weighted NDM<sup>(f)</sup>, as follows for all DM<sup>(f)</sup>:



$$\begin{aligned}
\text{PIS}^{(f)} &= \{\text{PIS}_j^{(f)}\}_{r \times n} \\
&= \{(\text{NDM}_{ij}^{(f)}): m[s(\text{NDM}_{ij}^{(f)})]\}, \\
\text{NIS}^{(f)} &= \{\text{NIS}_j^{(f)}\}_{r \times n} \\
&= \{(\text{NDM}_{ij}^{(f)}): m[s(\text{NDM}_{ij}^{(f)})]\}.
\end{aligned} \tag{17}$$

for  $j = 1, 2, 3, \dots, n$ .

Step 4(c): consider the weight of the measured requirements.  $\text{EIS}_i^+$  and  $\text{EIS}_i^-$  are denoted using the weighted distance calculation of weighted  $\text{NDM}^{(f)}$  from  $\text{PIS}^{(f)}$  and  $\text{NIS}^{(f)}$  and are measured according to each  $DM_f$  in the following manner:

$$\begin{aligned}
\text{EIS}_i^{+(f)} &= \frac{1}{2n} \sum_{j=1}^n w_j \left( \left| \left( \frac{1}{A_s} \sum_{h_{s_j} \in P_s, p_{s_j} \in P_s}^{A_s} h_{\text{NDM}_{ij}^{(f)}} p_{\text{NDM}_{ij}^{(f)}} \right)^{2^\alpha} \right. \right. \\
&\quad \left. \left. + \left( \frac{1}{A_r} \sum_{h_{r_j} \in P_r, p_{r_j} \in P_r}^{A_r} h_{\text{PIS}_j^{(f)}} p_{\text{PIS}_j^{(f)}} \right)^2 \right| \right. \\
&\quad \left. \left| \left( \frac{1}{B_s} \sum_{v_{s_j} \in N_s, n_{s_j} \in n_s}^{B_s} v_{\text{NDM}_{ij}^{(f)}} n_{\text{NDM}_{ij}^{(f)}} \right)^{2^\alpha} \right. \right. \\
&\quad \left. \left. - \left( \frac{1}{B_r} \sum_{v_{r_j} \in N_r, n_{r_j} \in n_r}^{B_r} v_{\text{PIS}_j^{(f)}} n_{\text{PIS}_j^{(f)}} \right)^2 \right| \right)^{1/\alpha}, \\
\text{EIS}_i^{-(f)} &= \frac{1}{2n} \sum_{j=1}^n w_j \left( \left| \left( \frac{1}{A_s} \sum_{h_{s_j} \in P_s, p_{s_j} \in P_s}^{A_s} h_{\text{NDM}_{ij}^{(f)}} p_{\text{NDM}_{ij}^{(f)}} \right)^{2^\alpha} \right. \right. \\
&\quad \left. \left. + \left( \frac{1}{A_r} \sum_{h_{r_j} \in P_r, p_{r_j} \in P_r}^{A_r} h_{\text{NIS}_j^{(f)}} p_{\text{NIS}_j^{(f)}} \right)^2 \right| \right. \\
&\quad \left. \left| \left( \frac{1}{B_s} \sum_{v_{s_j} \in N_s, n_{s_j} \in n_s}^{B_s} v_{\text{NDM}_{ij}^{(f)}} n_{\text{NDM}_{ij}^{(f)}} \right)^{2^\alpha} \right. \right. \\
&\quad \left. \left. - \left( \frac{1}{B_r} \sum_{v_{r_j} \in N_r, n_{r_j} \in n_r}^{B_r} v_{\text{NIS}_j^{(f)}} n_{\text{NIS}_j^{(f)}} \right)^2 \right| \right)^{1/\alpha}.
\end{aligned} \tag{18}$$

Step 4(d): the revised indices of closeness are calculated in the following manner for all DM alternatives:

$$\text{RCI}_i^{(f)} = \frac{(\text{EIS}_i^-(f))}{(\text{EIS}_i^-(f) + \text{EIS}_i^+(f))}, \tag{19}$$

Step 5: alternative selection and pick the most suitable alternative with a minimum distance.

**5.2.  $q$ -ROPHF Extended VIKOR Method.** There are two primary parts to this method. Firstly, a method for calculating the weights of criteria/attributes is presented using the proposed entropy measure for  $q$ -ROPHFNs. A ranking procedure based on the degree of similarity to the ideal solution is considered in the last part. Steps are presented as follows for the  $q$ -ROPHF extended VIKOR method.

Step 1: first, we collect the data provided by the decision-makers in the form of a-ROPHFNs.

Step 2: we normalized the information defined by DMs in this step, as the decision matrix may have some benefit and cost parameters altogether, as follows:

$$e_{ij}^{(f)} = \begin{cases} S_{ij}^{(f)} & \text{for benefit criteria,} \\ (S_{ij}^{(f)})^c & \text{for cost criteria,} \end{cases} \quad (20)$$

$f = 1, 2, 3, \dots, r$ ,  $i = 1, 2, 3, \dots, m$ ,  $j = 1, 2, 3, \dots, n$  where  $(S_{ij}^{(f)})^c$  is complement of  $S_{ij}^{(f)}$ , that is  $(S_{ij}^{(f)})^c = (N_{S_{ij}^{(f)}}, P_{S_{ij}^{(f)}})$ .

Step 3: the weights of the parameters are determined in the following manner by the proposed entropy measure. The calculation of entropy corresponding to each criterion is as follows:

$$\begin{aligned} E(S_j) &= E(S_{1j}, S_{2j}, S_{3j}, \dots, S_{mj}), j = 1, 2, 3, \dots, n \\ &= \frac{(-1)}{(2 \log(n))} \sum_{i=1}^n (P_s(\log P_s) \times p_s) \\ &\quad + N_s(\log N_s) \times n_s. \end{aligned} \quad (21)$$

then

$$w(S_j) = \frac{1 - E(S_j)}{\sum_{j=1}^n (1 - E(S_j))}. \quad (22)$$

Thus, weights of criteria are found as follows:

$$w(S_j) = (w(S_1), w(S_2), w(S_3), \dots, w(S_n))^T. \quad (23)$$

Step 4: in this step, the best alternative according to given list of criteria/attribute are determined.

Step 4(a): determine the weighted NDM( $f$ ) using the weights of the assessed parameters in the following manner:

$$\text{NDM}_{ij}^{(f)} = w(S_j) \cdot S_{ij}^{(f)} = \begin{pmatrix} \bigcup_{h_i \in P_{S_{ij}}, p_i \in P_{S_{ij}}} \frac{\sqrt[q]{1 - \prod_{i=1}^m (1 - (h_{S_{ij}}^{(f)})^q)^{w(S_j)}}}{\prod_{i=1}^m P_{S_{ij}}^{(f)}} \\ \bigcup_{v_i \in N_{S_{ij}}, n_i \in n_{S_{ij}}} \frac{\prod_{i=1}^m (v_{S_{ij}}^{(f)})^{w(S_j)}}{\prod_{i=1}^m n_{S_{ij}}^{(f)}} \end{pmatrix} \text{ for all } f = 1, 2, 3, \dots, r. \quad (24)$$

Step 4(b): derive  $\text{PIS}^{(f)}$  and  $\text{NIS}^{(f)}$  for all weighted  $\text{NDM}^{(f)}$ , as follows for all  $\text{DM}^{(f)}$ :

$$\begin{aligned} \text{PIS}^{(f)} &= \{\text{PIS}_j^{(f)}\}_{r \times n} \\ &= \{(\text{NDM}_{ij}^{(f)}): m[s(\text{NDM}_{ij}^{(f)})]\}, \\ \text{NIS}^{(f)} &= \{\text{NIS}_j^{(f)}\}_{r \times n} \\ &= \{(\text{NDM}_{ij}^{(f)}): m[s(\text{NDM}_{ij}^{(f)})]\}. \end{aligned} \quad (25)$$

for  $j = 1, 2, 3, \dots, n$

Step 4(c): the useful calculation of the  $q$ -ROPHF category over the attributes of profit types is obtained from the following formula:

$$M_i = \frac{\sum_{j=1}^n (w_j d(\text{PIS}_j^+, e_{ij}))}{d(\text{PIS}_j^+, \text{NIS}_j)}, \quad (26)$$

$$i = 1, 2, 3, \dots, m.$$

From the following formula, the measure of  $q$ -ROPHF regret over the benefit type attribute is obtained.

$$R_i = \max_j \frac{w_j d(\text{PIS}_j^+, e_{ij})}{d(\text{PIS}_j^+, \text{NIS}_j^-)}, \quad (27)$$

$$i = 1, 2, 3, \dots, m,$$

where the distance of any two  $q$ -ROPHFNs is as follows:

$$d(s, r) = \left( \frac{1}{2n} \sum_{j=1}^n \left( \left| \left( \frac{1}{A_s} \sum_{h_{s_j} \in P_s, P_{s_j} \in P_s}^{A_s} (h_{s_j} p_{s_j}) \right)^2 - \left( \frac{1}{A_r} \sum_{h_{r_j} \in P_r, P_{r_j} \in P_r}^{A_r} (h_{r_j} p_{r_j}) \right)^2 \right|^{2\alpha} \right)^{1/\alpha} \right. \\ \left. \left( \left| \left( \frac{1}{B_s} \sum_{v_{s_j} \in N_s, n_{s_j} \in n_s}^{B_s} (v_{s_j} n_{s_j}) \right)^2 - \left( \frac{1}{B_r} \sum_{v_{r_j} \in N_r, n_{r_j} \in n_r}^{B_r} (v_{r_j} n_{r_j}) \right)^2 \right|^{2\alpha} \right)^{1/\alpha} \right), \quad (28)$$

where  $A_s, B_s, A_r,$  and  $B_r$  are the possible numbers of elements in  $P_s/p_s, N_s/n_s, P_r/p_r$  and  $N_r/n_r$ .

Step 5: from the following formula, the  $q$ -ROPHF compromise measure value of  $G_i (i = 1, 2, 3, \dots, m)$  is obtained:

$$G_i = V \left( \frac{(M_i - M^+)}{(M^- - M^+)} \right) + (1 - V) \left( \frac{(R_i - R^+)}{(R^- - R^+)} \right), \quad (29)$$

where

$M^+ = \min_i M_i, M^- = \max_i M_i, R^+ = \min_i R_i, R^- = \max_i R_i$  and  $V$  is the weight of the majority attribute strategy or the overall total utility. The greater the value of  $V$ , the greater average of the decision-preferences maker's over various attributes. The value 0.55 also arrives without loss of overview.

We can understand from equation (29) that the  $q$ -ROPHF compromise measure combines two components: the distance in terms of group utility is the preceding one. In terms of individual remorse, the finale is the gap. The smaller the value of the compromise measure of  $q$ -ROPHF, the superior the alternative would be. So between  $G_i (i = 1, 2, 3, \dots, m)$ , we need to choose the smallest one.

Step 6(a): rank the  $X_i (i = 1, 2, 3, \dots, m)$  alternatives according to  $M_i, R_i$  and  $G_i (i = 1, 2, 3, \dots, m)$  values. The solution needed must fulfill the two requirements set out as follows:

Condition 1.  $G(X_2) - G(X_1) \geq 1/m - 1$  where  $X_1$  and  $X_2$  are the first and second place alternatives in the ranking list, respectively.

Condition 2. The highest graded by  $M$  and  $R$  should be  $X_1$ . It is said that the Condition 1 is an acceptable gain, while the Condition 2 is said to be an acceptable stability.

If both circumstances are not met, go to the next stage.

Step 6(b): gain the alternative to compromise: explore the maximum value of  $M$  according to the following equation:

$$G(X^N) - G(X_1) \leq DG. \quad (30)$$

If Condition 1 does not hold, the compromise options are all the alternative  $X_1, X_2, X_3, \dots, X^N$ . If the Condition 2 does not hold, then the compromise solutions are the alternatives  $X_1$  and  $X_2$ .

## 6. Numerical Applications of Proposed Methodology

### 6.1. Case Study: COVID-19 and Pakistan

*The Economic Fallout.* Pakistan's financial industry is still in its early stages of growth, although it controls the bulk of the market. Following the onset of the coronavirus epidemic, numerous industries have been impacted by the virus's devastation. The halting of the economy's growth came as a huge shock to a wide range of industries and businesses. The longer the COVID-19 pandemic continues, the more severe the outbreak's impact on the world economy will ultimately to recession. Many small and medium enterprises, especially service businesses are experiencing cash flow issues. The need for banks to continue to assist the economy is unavoidable. The principal repercussions of the COVID-19 outbreak on the Pakistani financial sector are anticipated to cause liquidity issues for businesses and families. The impact of a pandemic like COVID-19 on Pakistan's financial industry can be divided into four categories:

6.2. *Exchange Rate ( $C_1$ ).* The exchange rate fluctuated due to the uncertainty over when the COVID-19 epidemic would cease. Since the first case was reported in Pakistan on February 26, 2020, the nominal exchange rate versus the US dollar has been steadily increasing. Reduced employment, decreased country exports, increased bankruptcies, increased credit volume, high risk of loan nonrepayment, and a fall in tourism earnings may be cited as factors for the exchange rate fluctuation.

6.3. *Interest Rate ( $C_2$ ).* Prior to the outbreak of the pandemic, banks took the initiative to lower lending interest rates. Banks conveyed their thanks by granting their clients a lower interest rate. Following the outbreak of the epidemic, Pakistan's central bank was obliged to hike interest rates due to economic and banking sector pressures. Certain enterprises, such as hotel cooperatives, have asked banks to cut lending rates. The effort was effective, and practically all banks amended their interest rate policies with the goal of assisting the most vulnerable businesses.

6.4. *Customer Behavior Changes ( $C_3$ ).* COVID-19 reduced consumption and influenced consumer behavior as their demands changed. Banks should classify their clients

according to a variety of criteria and dimensions. In response to changing consumer behavior, banks must change their service sectors and present unique Opportunities to their clients. Clients' consumption habits altered throughout the epidemic. Customers who were keen to invest in gold and foreign currencies before to the outbreak replaced those who were prepared to take out loans because to low interest rates. They are averse to taking out bank loans.

*6.5. Credit Risk, Loss of Income, and Liquidity ( $\mathcal{C}_4$ ).* As the crisis worsens expect a drop in income due to difficulties recovering loans and lower transaction volumes. These have a detrimental influence on liquidity, the amount of risky assets, profitability, and capital adequacy. Banks should undertake scenario analysis based on numerous assumptions in these conditions in order to manage any potential financial effects. During the COVID-19 pandemic, this study believes these four criteria to be substantial hazards for the banking industry as the concrete nucleus of supply chain financing. We may approach it as an MCDM problem and solve it using a decision-making technique if we consider the needs and characteristics of decision-making problems. The goal of this study was to look at the banking sector's top risk factors as a result of the COVID-19 pandemic, calculate the banking sector's performance index, and recommend some risk management techniques to preserve financial management efficiency.

In this scenario, the government must prepare an action plans that prioritizes the social and economic well-being of Pakistanis; a plan that lays out the multifaceted aspects of the COVID-19 response, as well as a clear policy for effectively and successfully minimizing, mitigating, and managing the pandemic's negative consequences. This also entails mobilizing technical and financial resources through government-owned sources, donor assistance, and collaboration with development partners to define and develop new economic priorities; making precise plans to keep economic activities and jobs; achieve food security; and protecting the health and social needs of the most vulnerable in a coordinated and effective manner. Following are the five alternatives on the base of which Pakistani bank sectors select the best socioeconomic response plan to protect the needs and rights of people living under the duress of the pandemic.

*6.6. Investment ( $\mathcal{I}_1$ ).* The economy was expected to expand up moderately before the outbreak of COVID-19, due to structural improvements. In the medium to long term, Pakistan will need to double its private investment rate and human capital investment, increase more revenue, simplify the business regulatory regime, integrate with global value chains, and sustainably manage its natural endowments in order to recover from the effects of COVID-19 and continue on its path to becoming an upper middle-income country.

To reduce the negative economic effects of the outbreak, focus on economic recovery strategies that promote small and medium companies owned by women. During this epidemic, strong market connections should be developed

for homebased female workers who can sell their products while working from home.

*6.7. Government Support ( $\mathcal{F}_2$ ).* Cities and counties took the brunt of increased public health costs while losing "own-source" money from parking penalties, user fees, restaurant taxes, conferences, airports, and other sources. While dealing with the loss of small companies, school closures, and other issues, local governments must provide assistance to vulnerable populations.

*6.8. Propositions and Brands ( $\mathcal{F}_3$ ).* Customers would be expecting availability in the form of discounts, free services, payment deferrals, and other benefit packages to adjust for their loss of income during this time. Brands must also express empathy and support for their users. To take advantage of the scenario, banks must be aware of the potential and develop mechanisms to gather, monitor, and identify all the potential for improvement that arise as a result of greater digital banking usage.

*6.9. Channels and Digital ( $\mathcal{F}_4$ ).* Customers' participation with digital platforms will grow throughout this period since they are the primary way of performing transactions. Cheque clearance, for example, has been delayed. As a result, digital channels will become increasingly important.

*6.10. Markets Segments ( $\mathcal{F}_5$ ).* Corporates and individuals, who are banking customers, are under a lot of pressure. As economic activity slows, household income will suffer, and SMEs' operations would likely slow as well. Banks may be able to help companies in the health and pharmaceuticals sectors remodel and renovate hospitals and expand their manufacturing capacity.

We have looked at the present scenario and identified several particular subjects as options that the banking sector should think about and address while taking the required steps to deal with this "new normal."

#### *6.11. Using Extended TOPSIS Methodology*

Step 1: information of decision-makers in the form of q-ROPHFNs is given in Table 2

Step 2: expert normalized information is provided in Table 3 as follows

Step 3: using the proposed entropy measure of q-ROPHFNs, compute the weight information for attributes/criteria as follows:

$$w = (w_1 = 0.221877, w_2 = 0.231623, w_3 = 0.193205, w_4 = 0.353295). \quad (31)$$

Step 4(a): in Tables 4 and 5, the weighted normalized matrix is computed as follows:

Step 4(b): in Tables 6 and 7, positive and negative ideal solutions are determined as follows:

TABLE 2: Expert information.

$S^{(f)}$	$C_1$	$C_2$	$C_3$	$C_4$
$J_1$	(0.2/0.6, 0.3/0.4) (0.2/0.6, 0.5/0.4)	(0.2/1) (0.4/0.6, 0.4/0.4)	(0.3/0.9, 0.4/0.1) (0.8/0.7, 0.2/0.3)	(0.2/0.4, 0.5/0.6) (0.2/1)
$J_2$	(0.4/0.3, 0.8/0.7) (0.6/1)	(0.4/0.4, 0.5/0.6) (0.8/0.7, 0.4/0.3)	(0.8/1) (0.5/0.6, 0.3/0.4)	(0.3/0.2, 0.4/0.8) (0.2/0.5, 0.2/0.5)
$J_3$	(0.8/0.5, 0.6/0.5) (0.2/0.5, 0.2/0.5)	(0.3/1) (0.4/0.4, 0.8/0.6)	(0.4/0.5, 0.6/0.5) (0.7/0.9, 0.2/0.1)	(0.2/0.1, 0.3/0.9) (0.8/1)
$J_4$	(0.2/0.4, 0.8/0.6) (0.5/1)	(0.5/0.5, 0.6/0.5) (0.5/0.5, 0.2/0.5)	(0.8/1) (0.4/0.2, 0.4/0.8)	(0.3/0.5, 0.4/0.5) (0.2/0.9, 0.5/0.1)
$J_5$	(0.7/0.3, 0.4/0.7) (0.3/0.6, 0.8/0.4)	(0.4/1) (0.2/0.8, 0.4/0.2)	(0.7/0.4, 0.2/0.6) (0.2/0.4, 0.4/0.6)	(0.6/0.3, 0.2/0.7) (0.3/1)

TABLE 3: Expert normalized information.

$S^{(f)}$	$C_1$	$C_2$	$C_3$	$C_4$
$J_1$	(0.2/0.6, 0.3/0.4) (0.2/0.6, 0.5/0.4)	(0.2/1) (0.4/0.6, 0.4/0.4)	(0.3/0.9, 0.4/0.1) (0.8/0.7, 0.2/0.3)	(0.2/0.4, 0.5/0.6) (0.2/1)
$J_2$	(0.4/0.3, 0.8/0.7) (0.6/1)	(0.4/0.4, 0.5/0.6) (0.8/0.7, 0.4/0.3)	(0.8/1) (0.5/0.6, 0.3/0.4)	(0.3/0.2, 0.4/0.8) (0.2/0.5, 0.2/0.5)
$J_3$	(0.8/0.5, 0.6/0.5) (0.2/0.5, 0.2/0.5)	(0.3/1) (0.4/0.4, 0.8/0.6)	(0.4/0.5, 0.6/0.5) (0.7/0.9, 0.2/0.1)	(0.2/0.1, 0.3/0.9) (0.8/1)
$J_4$	(0.2/0.4, 0.8/0.6) (0.5/1)	(0.5/0.5, 0.6/0.5) (0.5/0.5, 0.2/0.5)	(0.8/1) (0.4/0.2, 0.4/0.8)	(0.3/0.5, 0.4/0.5) (0.2/0.9, 0.5/0.1)
$J_5$	(0.7/0.3, 0.4/0.7) (0.3/0.6, 0.8/0.4)	(0.4/1) (0.2/0.8, 0.4/0.2)	(0.7/0.4, 0.2/0.6) (0.2/0.4, 0.4/0.6)	(0.6/0.3, 0.2/0.7) (0.3/1)

TABLE 4: Weighted normalized information (a).

$S^{(f)}$	$C_1$	$C_2$
$J_1$	(0.042197/0.6, 0.077811/0.4) (0.699705/0.6, 0.857449/0.4)	(0.043113/1) (0.808775/0.6, 0.808775/0.4)
$J_2$	(0.120697/0.3, 0.383614/0.7) (0.892347/1)	(0.1233/0.4, 0.174515/0.6) (0.949628/0.7, 0.808775/0.3)
$J_3$	(0.383614/0.5, 0.229262/0.5) (0.699705/0.5, 0.699705/0.5)	(0.079497/1) (0.808775/0.4, 0.949628/0.6)
$J_4$	(0.042197/0.4, 0.383614/0.6) (0.857449/1)	(0.174515/0.5, 0.234106/0.5) (0.851676/0.5, 0.688815/0.5)
$J_5$	(0.298316/0.3, 0.120697/0.7) (0.765571/0.6, 0.951695/0.4)	(0.1233/1) (0.688815/0.8, 0.808775/0.2)

TABLE 5: Weighted normalized information (b).

$S^{(f)}$	$C_3$	$C_4$
$J_1$	(0.072624/0.9, 0.112682/0.1) (0.957804/0.7, 0.73275/0.3)	(0.053233/0.4, 0.214664/0.6) (0.0566314/1)
$J_2$	(0.359771/1) (0.874661/0.6, 0.79246/0.4)	(0.0981/0.2, 0.151974/0.8) (0.566314/0.5, 0.566314/0.5)
$J_3$	(0.112682/0.5, 0.214307/0.5) (0.9334/0.9, 0.73275/0.1)	(0.053233/0.1, 0.0981/0.9) (0.924192/1)
$J_4$	(0.359771/1) (0.837753/0.2, 0.837753/0.8)	(0.0981/0.5, 0.151974/0.5) (0.566314/0.9, 0.782794/0.1)
$J_5$	(0.279202/0.4, 0.039378/0.6) (0.73275/0.4, 0.837753/0.6)	(0.287021/0.3, 0.053233/0.7) (0.653536/1)

TABLE 6: Positive ideal solution (PIS).

$C_1$	$C_2$	$C_3$	$C_3$
(0.383614/0.5, 0.229262/0.5)	(0.123/1)	(0.35977/1)	(0.0981/0.2, 0.151974/0.8)
(0.699705/0.5, 0.699705/0.5)	(0.688815/0.8, 0.808775/0.2)	(0.837753/0.2, 0.837753/0.8)	(0.566314/0.5, 0.566314/0.5)

TABLE 7: Negative ideal solution (NIS).

$C_1$	$C_2$	$C_3$	$C_3$
(0.120697/0.3, 0.383614/0.7)	(0.079497/1)	(0.112682/0.5, 0.214307/0.5)	(0.053233/0.1, 0.0981/0.9)
(0.892847/1)	(0.808775/0.4, 0.949628/0.6)	(0.93341/0.9, 0.73275/0.1)	(0.924192/1)

Step 4(c): the calculation of the weighted distance of PIS and NIS to the weighted normalized matrix is calculated as follows:

$$\begin{aligned} &0.018493 \quad 0.054316 \quad 0.065317 \quad 0.04416 \quad 0.024829, \\ &0.084221 \quad 0.071465 \quad 0.030669 \quad 0.080368 \quad 0.07835. \end{aligned} \quad (32)$$

Step 5: the ranking of the alternative is as follows:

$$0.819957 \quad 0.568172 \quad 0.319515 \quad 0.645384 \quad 0.759357. \quad (33)$$

Therefore,  $\mathcal{F}_3$  alternative has the least distance, so it is the best alternative in the given list of alternatives.

### 6.12. Using Extended VIKOR Methodology

Step 1: information of decision-makers in the form of  $q$ -ROPFNs is given in Table 2.

Step 2: expert normalized information is provided in Table 3.

Step 3: using the proposed entropy measure of  $q$ -ROPFNs, compute the weight information for attributes/criteria as follows:

$$\begin{aligned} w &= (w_1 = 0.221877, w_2 = 0.231623, w_3 \\ &= 0.193205, w_4 = 0.353295). \end{aligned} \quad (34)$$

Step 4(a): in Tables 8 and 9, the weighted normalized matrix is computed as follows.

Step 4(b): in Tables 6 and 7, positive and negative ideal solutions are determined as follows.

Step 4(c): calculations of  $M_i$  and  $R_i$  is presented in the Table 10.

Step 5: the values of  $G_i$  is calculated in the Table 11.

Step 6(a): we can sort the alternatives according to  $M$ ,  $R$ , and  $G$  values. Which alternative has lower  $M$ ,  $R$ , and  $G$  values, will be the best alternative according to given list of attributes. The values are calculated in Tables 12 and 13.

Step 6(b): according to the value of  $G$ , the best alternative is  $\mathcal{F}_3$  with  $G(\mathcal{F}_3) = 0.024978$  and alternative  $\mathcal{F}_1$

is second with  $G(\mathcal{F}_1) = 0.035898$  Since  $DG = 1/M - 1 = 1/5 - 1 = 0.25$ ,  $G(\mathcal{F}_1) - G(\mathcal{F}_3) = 0.01092 < 0.25$ , which does not fulfill  $G(X_1) - G(X_3) \geq DG$ . Alternatively,  $\mathcal{F}_3$  fulfills condition 2 that it is the best option sorted by  $M$  and  $R$ . Then, we get  $G(\mathcal{F}_1) - G(\mathcal{F}_3) = 0.01092 < 0.25$ ,  $G(\mathcal{F}_2) - G(\mathcal{F}_3) = 0.796495 > 0.25$ ,  $\mathcal{F}_1$  and  $\mathcal{F}_3$  were therefore a compromise solution. These results indicate that  $\mathcal{F}_3$  is the best choice among the five alternatives, while  $\mathcal{F}_1$  could be compromise solutions.

## 7. Comparison Study

In this section, we presented the comparison study of the proposed technique to show the applicability and effectiveness of the proposed methods. In this regards we presented the extended GRY method to validate the proposed techniques.

**7.1.  $q$ -ROPHF Extended GRA Method.** There are two primary parts to this method. First, a method for calculating the weights of criteria/attributes is presented using the proposed entropy measure for  $q$ -ROPFNs. A ranking procedure based on the degree of similarity to the ideal solution is considered in the last part. Steps are presented as follows for the  $q$ -ROPHF extended GRA method.

Step 1: first, we collect the data provided by the decision-makers in the form of  $q$ -ROPFNs.

Step 2: we normalized the information defined by DMs in this step, as the decision matrix may have some benefit and cost parameters altogether, as follows:

$$e_{ij}^{(f)} = \begin{cases} S_{ij}^{(f)} & \text{for benefit criteria,} \\ (S_{ij}^{(f)})^c & \text{for cost criteria.} \end{cases} \quad (35)$$

$f = 1, 2, 3, \dots, r, i = 1, 2, 3, \dots, m, j = 1, 2, 3, \dots, n$  where  $(S_{ij}^{(f)})^c$  is complement of  $S_{ij}^{(f)}$ , that is  $(S_{ij}^{(f)})^c = (N_{S_{ij}^{(f)}}^{(f)}, P_{S_{ij}^{(f)}}^{(f)})$

Step 3: the weights of the parameters are determined in the following manner by the proposed entropy

TABLE 8: Weighted normalized information (a).

$S^{(f)}$	$C_1$	$C_2$
$J_1$	(0.042197/0.6, 0.077811/0.4) (0.699705/0.6, 0.857449/0.4)	(0.043113/1) (0.808775/0.6, 0.808775/0.4)
$J_2$	(0.120697/0.3, 0.383614/0.7) 0.892347/1	(0.1233/0.4, 0.174515/0.6) (0.949628/0.7, 0.808775/0.3)
$J_3$	(0.383614/0.5, 0.229262/0.5) (0.699705/0.5, 0.699705/0.5)	(0.079497/1) (0.808775/0.4, 0.949628/0.6)
$J_4$	(0.042197/0.4, 0.383614/0.6) (0.857449/1)	(0.174515/0.5, 0.234106/0.5) (0.851676/0.5, 0.688815/0.5)
$J_5$	(0.298316/0.3, 0.120697/0.7) (0.765571/0.6, 0.951695/0.4)	(0.1233/1) (0.688815/0.8, 0.808775/0.2)

TABLE 9: Weighted normalized information (b).

$S^{(f)}$	$C_3$	$C_4$
$J_1$	(0.072624/0.9, 0.112682/0.1) (0.957804/0.7, 0.73275/0.3)	(0.053233/0.4, 0.214664/0.6) (0.0566314/1)
$J_2$	(0.359771/1) (0.874661/0.6, 0.79246/0.4)	(0.0981/0.2, 0.151974/0.8) (0.566314/0.5, 0.566314/0.5)
$J_3$	(0.112682/0.5, 0.214307/0.5) (0.9334/0.9, 0.73275/0.1)	(0.053233/0.1, 0.0981/0.9) (0.924192/1)
$J_4$	(0.359771/1) (0.837753/0.2, 0.837753/0.8)	(0.0981/0.5, 0.151974/0.5) (0.566314/0.9, 0.782794/0.1)
$J_5$	(0.279202/0.4, 0.039378/0.6) (0.73275/0.4, 0.837753/0.6)	(0.287021/0.3, 0.053233/0.7) (0.653536/1)

TABLE 10: The values of M & R.

	$J_1$	$J_2$	$J_3$	$J_4$	$J_5$
$M$	0.731165	1.213087	0.767741	1.463348	1.061134
$R$	0.299427	0.819749	0.258508	0.828442	0.557226

TABLE 11: G when  $V = 0.5$ .

	$J_1$	$J_2$	$J_3$	$J_4$	$J_5$
$G$	0.035898	0.821473	0.024978	1	0.487296

TABLE 12: Values of M, R and G.

	$\mathcal{F}_1$	$\mathcal{F}_2$	$\mathcal{F}_3$	$\mathcal{F}_4$	$\mathcal{F}_5$
$M$	0.731165	1.213087	0.767741	1.463348	1.061134
$R$	0.299427	0.819749	0.258508	0.828442	0.557226
$G$	0.035898	0.821473	0.024978	1	0.487296

TABLE 13: Ranking.

Ranking	Best alternative
$M$	$\mathcal{F}_1 > \mathcal{F}_3 > \mathcal{F}_5 > \mathcal{F}_2 > \mathcal{F}_4$
$R$	$\mathcal{F}_3 > \mathcal{F}_1 > \mathcal{F}_5 > \mathcal{F}_2 > \mathcal{F}_4$
$G$	$\mathcal{F}_3 > \mathcal{F}_1 > \mathcal{F}_5 > \mathcal{F}_2 > \mathcal{F}_4$

TABLE 14:  $K^{(+)}$ .

	$C_1$	$C_2$	$C_3$	...	$C_n$
$J_1$	$(K_{11}^{(+)})$	$(K_{12}^{(+)})$	$(K_{13}^{(+)})$		$(K_{1n}^{(+)})$
$J_2$	$(K_{21}^{(+)})$	$(K_{22}^{(+)})$	$(K_{23}^{(+)})$		$(K_{2n}^{(+)})$
$J_3$	$(K_{31}^{(+)})$	$(K_{32}^{(+)})$	$(K_{33}^{(+)})$		$(K_{3n}^{(+)})$
$J_m$	$(K_{m1}^{(+)})$	$(K_{m2}^{(+)})$	$(K_{m3}^{(+)})$		$(K_{mn}^{(+)})$

TABLE 15:  $K^{(-)}$ .

	$C_1$	$C_2$	$C_3$	$\dots$	$C_n$
$J_1$	$(K_{11}^{(-)})$	$(K_{12}^{(-)})$	$(K_{13}^{(-)})$		$(K_{1n}^{(-)})$
$J_2$	$(K_{21}^{(-)})$	$(K_{22}^{(-)})$	$(K_{23}^{(-)})$		$(K_{2n}^{(-)})$
$J_3$	$(K_{31}^{(-)})$	$(K_{32}^{(-)})$	$(K_{33}^{(-)})$		$(K_{3n}^{(-)})$
$J_m$	$(K_{m1}^{(-)})$	$(K_{m2}^{(-)})$	$(K_{m3}^{(-)})$		$(K_{mn}^{(-)})$

measure. The calculation of entropy corresponding to each criterion is as follows:

$$\begin{aligned}
E(S_j) &= E(S_{1j}, S_{2j}, S_{3j}, \dots, S_{mj}), j = 1, 2, 3, \dots, n \\
&= (-1)/(2 \log(n)) \sum_{i=1}^n (P_s(\log P_s) \times p_s \\
&\quad + N_s(\log N_s) \times n_s).
\end{aligned} \tag{36}$$

then,

$$w(S_j) = \frac{(1 - E(S_j))}{(\sum_{j=1}^n (1 - E(S_j)))}. \tag{37}$$

Thus, weights of criteria are found as follows:

$$w(S_j) = (w(S_1), w(S_2), w(S_3), \dots, w(S_n))^T. \tag{38}$$

Step 4: in this step, the best alternative according to given list of criteria/attribute are determined.

Step 4(a): determine the weighted NDM( $f$ ) using the weights of the assessed parameters in the following manner:

$$\begin{aligned}
\text{NDM}_{ij}^{(f)} &= w(S_j) \cdot S_{ij}^{(f)} \\
&= \left( \begin{array}{c} \bigcup_{h_i \in P_{S_{ij}}, p_i \in P_{S_{ij}}} \frac{\sqrt[q]{1 - \prod_{i=1}^m (1 - (h_{S_{ij}}^{(f)})^q)^{w(S_j)}}}{\prod_{i=1}^m P_{S_{ij}}^{(f)}} \\ \bigcup_{v_i \in N_{S_{ij}}, n_i \in N_{S_{ij}}} \frac{\prod_{i=1}^m (v_{S_{ij}}^{(f)})^{w(S_j)}}{\prod_{i=1}^m N_{S_{ij}}^{(f)}} \end{array} \right).
\end{aligned} \tag{39}$$

for all  $f = 1, 2, 3, \dots, r$ .

Step 4(b): derive PIS $^{(f)}$  and NIS $^{(f)}$  for all weighted NDM $^{(f)}$ , as follows for all DM $^{(f)}$ :

$$\begin{aligned}
\text{PIS}^{(f)} &= \{\text{PIS}_j^{(f)}\}_{r \times n} \\
&= \{(\text{NDM}_{ij}^{(f)}): m[s(\text{NDM}_{ij}^{(f)})]\}, \\
\text{NIS}^{(f)} &= \{\text{NIS}_j^{(f)}\}_{r \times n} \\
&= \{(\text{NDM}_{ij}^{(f)}): m[s(\text{NDM}_{ij}^{(f)})]\}.
\end{aligned} \tag{40}$$

for  $j = 1, 2, 3, \dots, n$ .

Step 4(c): measure distance of PIS and NIS with each element of the alternative to determine the positive ideal separation matrix  $K^+$  and negative ideal separation matrix  $K^-$  as follow (see Tables 14 and 15):

where

$$d(s, r) = \left( \frac{1}{2n} \sum_{j=1}^n \sum_{h_s} \left| \left( \sum_{v_{s_j} \in N_{s_j}, n_{s_j} \in n_s}^{B_s} \left( \frac{1}{A_s} h_{s_j} \in p_s \right) (h_{s_j} p_{s_j}) \right)^2 - \left( \frac{1}{A_r} \left( \sum_{h_{r_j} \in P_{r_j}, p_{r_j} \in p_r}^{A_r} (h_{r_j} p_{r_j}) \right) \right)^{2/a} \right| \right)^{1/\alpha}. \tag{41}$$

where  $A_s, B_s, A_r$ , and  $B_r$  are the possible numbers of elements in  $P_s/p_s, N_s/n_s, P_r/p_r$  and  $N_r/n_r$ .

Step 5: determine matrices with Grey coefficients using the following formulas:



TABLE 16: Grey relational coefficient ( $\varphi_{ij}^+$ ).

0.833758	0.852003	0.796283	0.876161
0.727805	0.996317	0.431545	0.846628
0.617427	0.975802	0.93921	0.556616
0.993145	0.69808	0.428526	0.872206
0.860693	0.660276	0.678921	1

TABLE 17: Grey relational coefficient ( $\varphi_{ij}^-$ ).

0.591037	0.880002	0.989586	0.539976
0.666481	0.979524	0.512448	0.532206
0.505373	0.965965	0.918441	1
0.645767	0.762128	0.509554	0.538953
0.599572	0.731093	0.803636	0.569494

TABLE 18:  $\Phi_i^+$ .

$J_1$	0.845724
$J_2$	0.774739
$J_3$	0.741121
$J_4$	0.772987
$J_5$	0.828369

TABLE 19:  $\Phi_i^-$ .

$J_1$	0.716930
$J_2$	0.661790
$J_3$	0.866613
$J_4$	0.608665
$J_5$	0.658835

$$\varphi_{ij}^+ = \frac{\min_{1 < i < m} \min_{1 < i < m} k_{ij}^+ + \rho \left( \min_{1 < i < m} \max_{1 < i < m} k_{ij}^+ \right)}{k_{ij}^+ + \rho \left( \min_{1 < i < m} \max_{1 < i < m} k_{ij}^+ \right)}, \quad (42)$$

$$\varphi_{ij}^- = \frac{\min_{1 < i < m} \min_{1 < i < m} k_{ij}^- + \rho \left( \min_{1 < i < m} \max_{1 < i < m} k_{ij}^- \right)}{k_{ij}^- + \rho \left( \min_{1 < i < m} \max_{1 < i < m} k_{ij}^- \right)},$$

where  $i \in m, j \in n$  and  $\rho = 0.5$  be fixed coefficient.

Step 6: attributes weight information which is calculated using proposed entropy measure for  $q$ -ROPHFSs. Consider that attributes weights  $W = \{\rho_1, \rho_2, \rho_3, \dots, \rho_n\}$  subject to  $\rho_j \in [0, 1]$  such that  $\sum_{j=1}^n \rho_j = 1$ . Then, Grey coefficients are obtained as follows:

$$\begin{aligned} \Phi_i^+ &= \sum_{j=1}^n \rho_j \varphi_{ij}^+, i \in m, \\ \Phi_i^- &= \sum_{j=1}^n \rho_j \varphi_{ij}^-, i \in m. \end{aligned} \quad (43)$$

Step 7: measure the closeness coefficients are obtained as follows:

$$\phi_i = \frac{\Phi_i^-}{\Phi_i^+ + \Phi_i^-}, i \in m. \quad (44)$$

Rank the  $\phi_i$  according to descending order. Choose the larger  $\phi_i$  for best alternative.

## 7.2. Numerical Illustration

Step 1: information of decision-makers in the form of  $q$ -ROPHFNs is given in Table 2

Step 2: expert normalized information is provided in Table 3

Step 3: using the proposed entropy measure of  $q$ -ROPHFNs, compute the weight information for attributes/criteria as follows:

$$\begin{aligned} w &= (w_1 = 0.221877, w_2 = 0.231623, w_3 \\ &= 0.193205, w_4 = 0.353295). \end{aligned} \quad (45)$$

Step 4(a): in Tables 4 and 5, the weighted normalized matrix is computed

TABLE 20:  $\phi_i$ .

$\mathcal{F}_1$	0.45879
$\mathcal{F}_2$	0.460687
$\mathcal{F}_3$	0.539028
$\mathcal{F}_4$	0.440534
$\mathcal{F}_5$	0.443002

Step 4(b): in Tables 6 and 7, positive and negative ideal solutions are determined

Step 4(c): in order to calculate the positive ideal separation matrix  $K^+$  and negative ideal separation  $K^-$ , evaluate the distance of PIS and NIS for each part of the alternative as follows:

$$K^+ = \begin{bmatrix} 0.052936 & 0.049711 & 0.060025 & 0.045647 \\ 0.074864 & 0.028361 & 0.19332 & 0.050647 \\ 0.10571 & 0.031011 & 0.036025 & 0.127931 \\ 0.028764 & 0.082211 & 0.19537 & 0.046297 \\ 0.048223 & 0.092511 & 0.087288 & 0.027897 \end{bmatrix},$$

$$K^- = \begin{bmatrix} 0.190902 & 0.088165 & 0.064896 & 0.220487 \\ 0.155486 & 0.066815 & 0.238883 & 0.225487 \\ 0.243936 & 0.069465 & 0.079371 & 0.06295 \\ 0.164386 & 0.120665 & 0.240933 & 0.221137 \\ 0.186448 & 0.130965 & 0.108133 & 0.202737 \end{bmatrix}.$$

(46)

Step 5: calculate the grey relational coefficient of each alternative from  $K^+$  and  $K^-$  in the Tables 16 and 17

Step 6: Grey closeness coefficient of each alternative from  $K^+$  and  $K^-$  is calculated in Tables 18 and 19 as follows

Step 7: calculated relative closeness coefficient  $\phi_i$  for each alternative is presented in Table 20

Hence,  $\mathcal{F}_3$  alternative has the maximum relative closeness coefficient, so it is the best alternative in the given list of alternatives.

## 8. Conclusion

The impact of the COVID-19 pandemic on the Pakistani financial sector under supply chain finance was investigated using a hybrid decision-making framework. Based on both the literature and banker's judgements, four primary characteristics that have a substantial impact on Pakistan's banking system were identified. By consulting three experts, we were able to identify which of these four factors was the most essential and which was the least important. The advanced TOPSIS, VIKOR, and GRA methods was extended to the  $q$ -rung orthopair probabilistic hesitant Fuzzy TOPSIS, VIKOR, and GRA methods with unknown weight information about the decision-making experts as well as the criteria. Three decision-making algorithms are designed to address the uncertain information in supply chain finance for Pakistan's Banks under  $q$ -rung orthopair probabilistic

hesitant fuzzy environment. To determine the rationality and reliability of the elaborated techniques, a numerical example about supply chain finance in Pakistan to analyze the effects of emergency situation of COVID-19 on Pakistani banks is illustrated. The results indicate that the proposed technique is applicable and effected to tackle the uncertainty and ambiguity in real-life decision-making problems.

In future research, the other techniques like VIKOR, TODAM, and Electric-I, II, and III with real-life problems are investigated under the novel concept of  $q$ -rung orthopair probabilistic hesitant fuzzy information.

## Data Availability

The data used in this study are hypothetical and can be used by anyone by just citing this article.

## Ethical Approval

This article does not contain any studies with human participants or animals performed by any of the authors.

## Conflicts of Interest

The authors declare that they have no conflicts of interest to report regarding the present study.

## Authors' Contributions

All authors have contributed equally to this article.

## Acknowledgments

The authors extend their appreciation to the Deputyship for Research & Innovation, Ministry of Education in Saudi Arabia for funding this research work through the project number : IFP22UQU4310396DSR35.

## References

- [1] M. Budin and A. T. Eapen, "Cash generation in business operations: some simulation models," *The Journal of Finance*, vol. 25, no. 5, pp. 1091–1107, 1970.
- [2] L. Stemmler, "The role of finance in supply chain management," in *Cost Management in Supply Chains*, pp. 165–176, Physica, 2002.
- [3] B. Milder, "Closing the gap: reaching the missing middle and rural poor through value chain finance," *Enterprise Development & Microfinance*, vol. 19, no. 4, p. 301, 2008.
- [4] X. Xu, X. Chen, F. Jia, S. Brown et al., "Supply chain finance: a systematic literature review and bibliometric analysis," *International Journal of Production Economics*, vol. 204, pp. 160–173, 2018.
- [5] N. Yan, B. Sun, H. Zhang, and C. Liu, "A partial credit guarantee contract in a capital-constrained supply chain: financing equilibrium and coordinating strategy," *International Journal of Production Economics*, vol. 173, pp. 122–133, 2016.
- [6] H. C. Pfohl and M. Gomm, "Supply chain finance: optimizing financial flows in supply chains," *Logistics research*, vol. 1, no. 3-4, pp. 149–161, 2009.

- [7] W. H. Jiang, L. Xu, Z. S. Chen, K. Govindan, and K. S. Chin, "Financing equilibrium in a capital constrained supply Chain: the impact of credit rating," *Transportation Research Part E: Logistics and Transportation Review*, vol. 157, Article ID 102559, 2022.
- [8] J. Wang, S. Yao, X. Wang, P. Hou, and Q. Zhang, "Analysis of sales and financing modes in a green platform supply chain with a capital-constrained manufacturer," *Kybernetes*, vol. 52, 2021.
- [9] D. Tang and X. Zhuang, "Financing a capital-constrained supply chain: factoring accounts receivable vs a bct-scf receivable chain," *Kybernetes*, vol. 50, 2020.
- [10] S. A. Seyfi-Shishavan, F. K. Gündoğdu, and E. Farrokhizadeh, "An assessment of the banking industry performance based on Intuitionistic fuzzy Best-Worst Method and fuzzy inference system," *Applied Soft Computing*, vol. 113, Article ID 107990, 2021.
- [11] R. Silvestro and P. Lustrato, "Integrating financial and physical supply chains: the role of banks in enabling supply chain integration," *International Journal of Operations & Production Management*, vol. 34, 2014.
- [12] D. More and P. Basu, "Challenges of supply chain finance: a detailed study and a hierarchical model based on the experiences of an Indian firm," *Business Process Management Journal*, vol. 19, pp. 624–647.
- [13] A. Group, E. Cavenaghi, B. Santander, E. Camerinelli, A. Group, and I. C. C. B. Committee, *Technology-Enabled Supply Chain Finance for Small and Medium Enterprises Is a Major Growth Opportunity for Banks*, International Finance Corporation, Washington, DC, USA, 2017.
- [14] M. Sommer and R. O'Kelly, "Corporate Banking Insights-Supply Chain Finance: Riding the Waves," 2017, <https://www.oliverwyman.com/index.html>.
- [15] C. L. Zhang, "Risk assessment of supply chain finance with intuitionistic fuzzy information," *Journal of Intelligent and Fuzzy Systems*, vol. 31, pp. 1967–1975, 2016.
- [16] M. Zhang, J. Zhang, R. Ma, and X. Chen, "Quantifying credit risk of supply chain finance: a Chinese automobile supply chain perspective," *IEEE Access*, vol. 7, pp. 144264–144279, 2019.
- [17] L. A. Zadeh, "Fuzzy sets," *Information and Control*, vol. 8, pp. 338–353, 1965.
- [18] B. Batool, S. Abdullah, S. Ashraf, and M. Ahmad, "Pythagorean probabilistic hesitant fuzzy aggregation operators and their application in decision-making," *Kybernetes*, vol. 51, 2021.
- [19] B. Batool, S. S. Abosuliman, S. Abdullah, and S. Ashraf, "EDAS method for decision support modeling under the Pythagorean probabilistic hesitant fuzzy aggregation information," *Journal of Ambient Intelligence and Humanized Computing*, vol. 13, no. 12, pp. 5491–5504, 2022.
- [20] K. T. Atanassov, "Intuitionistic fuzzy sets," *Fuzzy Sets and Systems*, vol. 20, p. 87, 1986.
- [21] S. K. De, R. Biswas, and A. R. Roy, "Some operations on intuitionistic fuzzy sets," *Fuzzy sets and Systems*, vol. 114, no. 3, pp. 477–484, 2000.
- [22] E. Szmidt and J. Kacprzyk, "Distances between intuitionistic fuzzy sets," *Fuzzy Sets and Systems*, vol. 114, no. 3, pp. 505–518, 2000.
- [23] Z. Xu, "Intuitionistic fuzzy aggregation operators," *IEEE Transactions on Fuzzy Systems*, vol. 15, no. 6, pp. 1179–1187, 2007.
- [24] R. R. Yager, "Pythagorean fuzzy subsets," in *Proceedings of the 2013 Joint IFSA World congress and NAFIPS Annual Meeting (IFSA/NAFIPS)*, pp. 57–61, IEEE, Edmonton, Alberta, Canada, June 2013.
- [25] S. Ashraf, S. Abdullah, and S. Khan, "Fuzzy decision support modeling for internet finance soft power evaluation based on sine trigonometric Pythagorean fuzzy information," *Journal of Ambient Intelligence and Humanized Computing*, vol. 12, no. 2, pp. 3101–3119, 2021.
- [26] B. Batool, M. Ahmad, S. Abdullah, S. Ashraf, and R. Chinram, "Entropy based Pythagorean probabilistic hesitant fuzzy decision making technique and its application for fog-haze factor assessment problem," *Entropy*, vol. 22, no. 3, p. 318, 2020.
- [27] A. A. Khan, S. Ashraf, S. Abdullah, and M. Qiyas, "Pythagorean fuzzy Dombi aggregation operators and their application in decision support system," *Symmetry*, vol. 11, no. 3, p. 383, 2019.
- [28] R. R. Yager, "Generalized orthopair fuzzy sets," *IEEE Transactions on Fuzzy Systems*, vol. 25, no. 5, pp. 1222–1230, 2016.
- [29] G. Wei, H. Gao, and Y. Wei, "Some q-rung orthopair fuzzy Heronian mean operators in multiple attribute decision making," *International Journal of Intelligent Systems*, vol. 33, no. 7, pp. 1426–1458, 2018.
- [30] P. Liu and P. Wang, "Some q-rung orthopair fuzzy aggregation operators and their applications to multiple-attribute decision making," *International Journal of Intelligent Systems*, vol. 33, no. 2, pp. 259–280, 2018.
- [31] P. Liu and P. Wang, "Multiple-attribute decision-making based on Archimedean Bonferroni operators of q-rung orthopair fuzzy numbers," *IEEE Transactions on Fuzzy Systems*, vol. 27, no. 5, pp. 834–848, 2018.
- [32] X. Peng, J. Dai, and H. Garg, "Exponential operation and aggregation operator for q-rung orthopair fuzzy set and their decision-making method with a new score function," *International Journal of Intelligent Systems*, vol. 33, no. 11, pp. 2255–2282, 2018.
- [33] X. Shu, Z. Ai, Z. Xu, and J. Ye, "Integrations of q-rung orthopair fuzzy continuous information," *IEEE Transactions on Fuzzy Systems*, vol. 27, no. 10, pp. 1974–1985, 2019.
- [34] X. Peng and L. Liu, "Information measures for q-rung orthopair fuzzy sets," *International Journal of Intelligent Systems*, vol. 34, no. 8, pp. 1795–1834, 2019.
- [35] M. I. Ali, "Another view on q-rung orthopair fuzzy sets," *International Journal of Intelligent Systems*, vol. 33, no. 11, pp. 2139–2153, 2018.
- [36] Y. Xing, R. Zhang, J. Wang, K. Bai, and J. Xue, "A new multi-criteria group decision-making approach based on q-rung orthopair fuzzy interaction Hammy mean operators," *Neural Computing & Applications*, vol. 1, 2019.
- [37] J. Gao, Z. Liang, J. Shang, and Z. Xu, "Continuities, Derivatives, and Differentials of q-Rung Orthopair Fuzzy Functions," *IEEE Transactions on Fuzzy Systems*, vol. 27, no. 8, pp. 1687–1699, 2018.
- [38] G. Wei, C. Wei, J. Wang, H. Gao, and Y. Wei, "Some q-rung orthopair fuzzy McLaurin symmetric mean operators and their applications to potential evaluation of emerging technology commercialization," *International Journal of Intelligent Systems*, vol. 34, no. 1, pp. 50–81, 2019.
- [39] A. Habib, M. Akram, and A. Farooq, "q-Rung orthopair fuzzy competition graphs with application in the soil ecosystem," *Mathematics*, vol. 7, no. 1, p. 91, 2019.
- [40] P. Liu, S. M. Chen, and P. Wang, "Multiple-attribute group decision-making based on q-rung orthopair fuzzy power

- McLaurin symmetric mean operators,” *IEEE Transactions on Systems, Man, and Cybernetics*, vol. 50, no. 10, pp. 3741–3756, 2018.
- [41] W. Yang and Y. Pang, “New q-rung orthopair fuzzy partitioned Bonferroni mean operators and their application in multiple attribute decision making,” *International Journal of Intelligent Systems*, vol. 34, no. 3, pp. 439–476, 2019.
- [42] H. Liao, H. Zhang, C. Zhang, X. Wu, and A. Mardani, “A q-rung orthopair fuzzy GLDS method for investment evaluation of BE angel capital in China,” *Technological and Economic Development of Economy*, vol. 26, no. 1, pp. 103–134, 2020.
- [43] V. Torra, “Hesitant fuzzy sets,” *International Journal of Intelligent Systems*, vol. 25, pp. 529–539, 2010.
- [44] M. S. A. Khan, S. Abdullah, A. Ali, N. Siddiqui, and F. Amin, “Pythagorean hesitant fuzzy sets and their application to group decision making with incomplete weight information,” *Journal of Intelligent and Fuzzy Systems*, vol. 33, pp. 3971–3985, 2017.
- [45] Z. Xu and W. Zhou, “Consensus building with a group of decision makers under the hesitant probabilistic fuzzy environment,” *Fuzzy Optimization and Decision Making*, vol. 16, pp. 481–503, 2017.

## Research Article

# The Effect of Utilizing Business Model Canvas on the Satisfaction of Operating Electronic Business

**Bahjat Fakieh** <sup>1</sup>, **Abdullah S. AL-Malaise AL-Ghamdi** <sup>1,2,3</sup> and **Mahmoud Ragab** <sup>2,4,5</sup>

<sup>1</sup>Information Systems Department, Faculty of Computing and Information Technology, King Abdulaziz University, Jeddah 21589, Saudi Arabia

<sup>2</sup>Center of Excellence in Smart Environment Research, King Abdulaziz University, Jeddah 21589, Saudi Arabia

<sup>3</sup>Information Systems Department, HECI School, Dar Alhekma University, Jeddah, Saudi Arabia

<sup>4</sup>Information Technology Department, Faculty of Computing and Information Technology, King Abdulaziz University, Jeddah 21589, Saudi Arabia

<sup>5</sup>Department of Mathematics, Faculty of Science, Al-Azhar University, Naser 11884, Cairo, Egypt

Correspondence should be addressed to Mahmoud Ragab; [mragab@kau.edu.sa](mailto:mragab@kau.edu.sa)

Received 11 October 2021; Accepted 15 July 2022; Published 1 September 2022

Academic Editor: Abdellatif Ben Makhlouf

Copyright © 2022 Bahjat Fakieh et al. This is an open access article distributed under the Creative Commons Attribution License, which permits unrestricted use, distribution, and reproduction in any medium, provided the original work is properly cited.

The Business Model Canvas (BMC) is a strategic model for developing business organizations' roadmap toward achieving their goals. While several organizations utilize the Business Model Canvas (BMC) to establish and operate their businesses well, the utilization of BMC seems to be limited in the local market of Saudi Arabia, especially when businesses utilize electronic business channels. This paper aims to explore the status of the utilization of BMC among Saudi SMEs, as a critical sector. The paper highlights the awareness and practice of BMC's nine factors before and during the operation of e-commerce stores by Saudi SMEs. Then, it aims to explore the significance of practicing those factors in increasing the satisfaction level of running businesses. In this paper, a quantitative survey was distributed conveniently to 200 SMEs in the two largest Saudi cities, which are Riyadh (the capital) and Jeddah (the country's main seaport), resulting in 63 valid participations from different industries. After operating e-commerce stores, most SMEs gained more knowledge of five BMC factors: key partners, value propositions, customer relationships, customer segments, and cost structures. Meanwhile, they found some issues in the other four factors: key activities, key resources, channels, and revenue streams. The proposed method exposes the variety of results and indicates a lack of understanding of BMC by the examined e-commerce SME samples, as they depend on traditional methods of identifying the elements of each of the BMC factors.

## 1. Introduction

The Business Model Canvas (BMC) is a tool for strategic management that firms can use to define their business key factors and ideas [1]. The BMC offers a one-page concentrated template that allows the firm to document fundamental elements of the business, its products, and services or to structure a business idea in a coherent way [2, 3]. Figure 1 shows a common BMC that covers all nine fundamental elements. In the presented figure, the right side of the canvas focuses on the customer and the external needs of the business, while the left side of the BMC focuses on the business itself and the internal needs of the business [4].

As such, it is notable that both the external and internal needs of the business meet at the value proposition corner, which entails exchanging the values between the business and the clients [5]. Companies use the BMC for various reasons, including the need to quickly draw a picture of what the idea entails, to understand the business by connecting with the idea, to understand the different kinds of customer decisions that influence the use of the business systems, to provide a clear idea of what the business is likely to be, and to reach a sustainable transition to utilizing information systems [6, 7].

The focus of the study was on Saudi Arabian Small and Medium-sized Enterprises (SMEs) with an e-commerce presence. The study was drawn from the fact that a majority

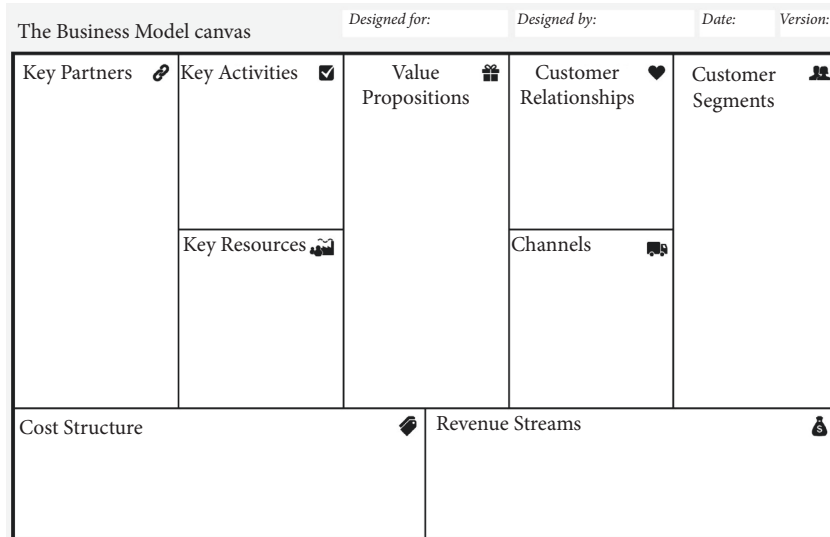


FIGURE 1: The Business Model Canvas [4].

of the businesses in the country are family owned, and, as such, very few of them apply conventional models of business management and administration, such as corporate governance, corporate social responsibility (CSR), sustainable business management, and the application of various business models, such as the Business Model Canvas [1, 8]. Nonetheless, due to globalization and the exposure of the Saudi Arabian markets to the global economy, many firms are taking up these universal corporate standards and applying them in their operations. SMEs in the country, irrespective of their ownership, are also taking up these universal corporate standards and applying them in their operations [9].

## 2. Literature Review

**2.1. Components of the Business Model Canvas.** Figure 1 shows one of the most common BMC templates, which incorporates nine elements of strategic management, including key partners, key activities, and key resources as the internal factors, customer relationships, customer segments, and customer channels as the external factors, which meet up under value propositions of the firm, factored with cost structures and revenue streams to ensure the maximization of returns on investment. The following section evaluates the nine elements of BMC, with a specific focus on how each element works, and the expected outcome for the firms, particularly SMEs [3], when they practice these concepts.

**2.1.1. Key Partners.** According to Aji, Yusop, Dahari, and Mohd, a company requires a network of partners to help it progress and expand its operations within its primary markets [3, 10]. In this regard, the key partners refer to the external companies, suppliers, contractors, or parties that the company requires to achieve or implement its key activities, and, in the process, deliver desired value to the customers. Baraibar-Diez, Odriozola, Llorente, and Sánchez support the above claims, citing that the partner networks

are instrumental in optimizing the operations of the firm, reducing all business risks that the firm might face in the course of its operations, as well as cultivating strong and long-lasting strategic business alliances, such as buyer-supplier relationships [11]. For instance, the global pandemic issue of COVID 19 is one of the severe risks that wiped several businesses—including well-known brands—from the market [12]. Thus, the existence of a robust business model would help to mitigate the harsh impact of such a crisis. These not only boost the sustainability of the firm but also allow it to focus more on core business activities, thereby boosting productivity margins.

**2.1.2. Key Activities.** Bocken, Schuit, and Kraaijenhagen asserted that key activities of the firm should focus on the execution of the firm's value proposition [13]. This means that a company should not promise its esteemed customers what it cannot deliver, as delivering on its value proposition is what differentiates it from its competitors in the market, giving it an edge over other industry players. Bocken, Boons, and Baldassarre support the above claims, citing that the key activities of the business are the actions, processes, programs, or projects undertaken by the firm to deliver on its outlined value propositions to the customers [14]. As such, a firm's management must question various aspects of its operations and activities to ensure that each one of them delivers on the promises set for the firm.

**2.1.3. Key Resources.** Bryant, Straker, and Wrigley stated that key resources refer to resources that the firm requires to create value for its customers, given its respective line of products and services [15]. As such, resources are a company's assets that are instrumental in facilitating production activities, thereby supporting and sustaining the operations of the business [1]. The resources can come in various forms, including human resources or human capital, financial resources or financial capital, and intellectual resources such as

patents, trademarks, and copyrights. Carayannis, Grigoriadis, Stamati, and Valvi agreed with the above claims, stating that identifying the resources that the business needs to achieve its objectives under key activities is the most effective way to improve the firm's competitiveness, as well as boost its marginal earnings [16].

*2.1.4. Value Propositions.* Chua, Chiu, and Bool stated that customers come to purchase and consume a company's products and services because of the perceived values that they derive from their consumption, as opposed to what their competitors offer [3, 5]. As such, the value proposition of the firm entails the collection of products and services that a business offers to meet the needs of its customers [17]. Crick and Crick agreed with the above claims, stating that the company's value proposition is what distinguishes the firm from its competitors, enabling it to stand out from the competition, as well as attracting and retaining the potential and target customers as loyal consumers of the brand [18]. Davies and Chambers noted that value proposition provides value to the products and services that the firm offers to its customers through different elements, including performance, customization, newness, uniqueness, getting the job done, cost efficiencies, brand or status, pricing, risk reduction, accessibility, and convenience and usability [9].

*2.1.5. Customer Relationships.* Heyes, Sharmina, Mendoza, Gallego-Schmid, and Azapagic stated that customer relationships are essential for the growth and expansion of any business, as well as its sustainability in the long run [3, 19]. Therefore, companies must identify the types of relationships they want to create with their respective customer segments to ensure the survival and success of the business [20]. Horváth and Szabó supported the above claims, arguing that businesses must engage in various forms of business relationships, including personal assistance, dedicated personal assistance, self-service, automated services, communities, and cocreation [21]. Similarly, Hruska and Maresova added that close customer relationships are strategic in improving sales volumes and expanding the company's market thresholds, given that the firm is capable of maintaining strong and long-lasting business relationships with its loyal customers on a long-term basis [22].

*2.1.6. Customer Segments.* Klimas stated that customer segments are defined by where the business, as well as its products and services, fit into the value chain [23]. To survive in the market competition, businesses are supposed to identify the consumer markets that they serve and build an effective business model around them [24, 25]. Customers of the company are what shape the growth and development of the firm by patronizing the firm's products and services in the market, as opposed to purchasing products from its competitors [26]. Ladd supports the above claims, citing that market segmentation is an effective strategy for businesses to create a competitive edge over other industry players by understanding the customers' tastes and preferences, and

then delivering products and services tailor-made to match these needs [27]. Lüdeke-Freund, Bohnsack, Breuer, and Massa added that the segmentation of customers follows various frameworks, including their needs and attributes, to facilitate the implementation of an appropriate corporate strategy that aligns with the characteristics of the market segment [28].

*2.1.7. Channels.* According to Davies and Chambers, a business channel refers to the avenues that the business uses to reach its customers, with a particular focus on delivering their respective products and services [3, 29]. In essence, the channels that the business uses must be not only efficient but also convenient for the customers, to ensure ease in the accessibility of their products and services. This enhances the company's brand image through improved place utility. Ojasalo and Ojasalo support the above claims, arguing that a company can deliver its value proposition to its target and potential customers using different channels; however, the most effective channels are those that deliver the company's value proposition through means that are not only fast and efficient but also cost-effective [30]. Similarly, Pedersen, Gwozdz, and Hvass added that the different channels that the company can use to reach its potential and target clients include its channels or storefronts, partner channels or major distributors, or a combination of both [31].

*2.1.8. Cost Structures.* Santonen and Julin stated that the element of the cost structure in the Business Model Canvas describes the most important monetary consequences of the firm when operating under different business models [32, 33]. In this regard, the cost structure is usually shaped in line with the business structure, with a particular focus on the firm's specific goals and objectives [26]. Schoormann, Behrens, and Knackstedt were in favor of the above claims, stating that the business structure falls into two distinct classes: the cost-driven class and the value-driven class [34]. A cost-driven class is a business model that focuses on the minimization of all costs and having no frills, such as low-cost airlines. On the other hand, a value-driven class is less concerned with the costs incurred in the operations of the firm, and, rather, more focused on the creation of value for products and services for the firm. In most cases, the latter class maintains a premium brand of products and services, such as Louis Vuitton and Mercedes Benz. Setiawan, Surjokusumo, Ma'some, Johan, Hasyim, Kurniasi, and Nasihien also added that the best strategy for ensuring efficient management of cost structures is to understand the firm's business class structure and the role that cost plays in maintaining the firm's value propositioning [33, 35].

*2.1.9. Revenue Streams.* Urban, Klemm, Ploetner, and Hornung defined revenue streams as the way a company makes income from each customer segment [36]. The primary purpose of a company engaging in business activities is to maximize its shareholders' wealth. As such, most companies are for-profit, meaning that they aim to maximize

their profits through successful delivery of their value propositions, and, hence, maintain steady revenue streams for the business. Uusitalo and Antikainen supported the above claims, citing that a business should identify and pursue one or more of the different models of revenue streams, including asset sales, usage fees, subscription fees, licensing, brokerage fees, advertising, lending, leasing, or renting, among many others [37]. Asset sale or service sale is the most common type of revenue stream pursued by most businesses; it entails the sale of ownership rights to a physical good or the rendering of specific professional services to the target clients (the sale of goods and services). Santonen and Julin added that “usage fees” refer to the revenues generated from the use of a particular service, such as UPS, and “subscription fees” refer to revenues generated by selling access to a continuous service, such as Netflix. Brokerage fees are revenues generated from an immediate service between two or more parties, such as a broker selling a house for a commission [38].

## 2.2. Analysis of the Existing Gap in the Practice of BMC in Saudi Arabia and Globally

**2.2.1. Global View.** Franco-Santos stated that, from the global perspective, companies, both small and large, are adopting and implementing the BMC framework to improve their performance standards and efficiency [39]. Companies based in western countries, including Europe and America, are particularly leading in the adoption and implementation of the BMC framework, given the successes attributed to its integration into business operations. However, Osterwalder and Euchner noted that the degree of inception and integration of the BMC framework in the rest of the world cannot be compared to that of Saudi Arabia, as the integration of the framework in the Arab country seems lower and less prevalent as compared to its counterparts, such as the United States and the United Kingdom [40]. Indrawan, Nasution, Adil, and Rossanty added that while in the UK 9 out of every 10 SMEs implemented the BMC framework, the statistics in Saudi Arabia were a little lower, at 3 to 5 out of 10 [41]. In this regard, it is advisable for more SMEs in the Saudi Arabian market to consider adopting and implementing the BMC framework to improve their operational excellence.

**2.2.2. In Saudi Arabia.** According to Toro-Jarrín, Ponce-Jaramillo, and Güemes-Castorena, the Saudi Arabian market has begun adopting and implementing the BMC concept, as evidenced by the adoption of conventional business frameworks by both large multinational corporations and SMEs [42], though the adoption of BMC for e-commerce is still undeclared. The adoption of these conventional business frameworks by Saudi Arabian firms has enabled them to compete on a global scale. Joyce and Paquin agree with the above claims, citing that many different SMEs in the country have also adopted and implemented the BMC framework to facilitate improved success margins in strategic planning and management [43]. Jbara and Darnton noted that Souq, one of the leading brands in Saudi Arabia, had adopted and

implemented the business framework to improve its productivity and efficiency in operations [44]. The scholars added that the entry of western firms into the market, taking advantage of the conducive foreign direct investment (FDI) policies in the country as the Saudi government focuses on diversifying its streams of income, has been a major contributor to the integration of BMC in the Saudi Arabian context.

## 3. Current Research Gap

Saudi Arabia is one of the leading global economic countries, given the fact that it has the second-largest deposits of crude oil and natural gas in the world. As such, the circular flow of money in the economy derived from the proceeds of oil and gas exports creates a business environment conducive for firms to operate and prosper [45]. Most of the companies operating in Saudi Arabia are either state-owned or family owned. The state-owned companies make up the majority of the large-cap companies in the country, with a few family owned companies. However, most of the start-ups or SMEs in the country are family owned. Given the stiff competition in the market, and the need to grow and expand both nationally and regionally, these SMEs are expected to integrate various strategies to give them an edge over their competitors, as well as to ensure efficient management of their operations. Therefore, the integration of the Business Model Canvas in their activities provides the right framework for achieving their strategic management goals and lean start-ups [46]. The problem examined in the research paper involves how these SMEs apply the Business Model Canvas to improve the success rates of their business operations, especially in their e-businesses.

The research study aimed to address the gap regarding the absence of adequate background information on the integration of the BMC framework in the Saudi Arabian market. As noted in the literature review analysis, the BMC framework is one of the many conventional business frameworks that are slowly penetrating the Saudi Arabian business context, triggered by the move by the country’s leadership to diversify its revenues by making the country open for business and to reduce overreliance on oil and gas revenues. As such, there is little information regarding the adoption and implementation of the BMC framework by businesses in Saudi Arabia, particularly among SMEs. The research study focuses on addressing this research gap and providing information regarding the awareness and practice of the BMC by Saudi Arabian SMEs. In addition, this research paper aims to evaluate the awareness of SMEs’ practice of the BMC components in the Saudi Arabian market. In other words, this study aims to answer the following questions:

- (i) What is the level of awareness among Saudi Arabian SMEs regarding the practice of BMC before starting online businesses?
- (ii) What is the level of awareness among Saudi Arabian SMEs regarding the practice of BMC when running online businesses?



To answer the developed research questions, the level of satisfaction would be explored by looking at the utilization of the nine BMC factors, as shown in Figure 2.

This study considered every SME that includes any sort of online process in running its business. This means that a particular SME might use a specific online solution but not run a business-to-consumer (B2C) direct e-commerce store.

## 4. Research Methodology

*4.1. Research Design and Method.* The study used an explorative research design to address the gap, which is discussed early in the literature concerning the awareness and practice of the BMC components by Saudi Arabian SMEs. The literature gap arises from the fact that Saudi Arabia is a wealthy Arab country whose main source of revenue is oil and gas that aimed recently to diversify its sources of income. As such, the explorative research design is instrumental in facilitating a critical analysis of the awareness and practice of the BMC framework by these SMEs, because most of the private businesses in the country are family owned, and, as such, likely to disregard most of the conventional business practices.

The study used the quantitative research method, focusing on the collection and analysis of figurative data from the study population. In this particular case, the study population for the research was Saudi Arabian SMEs. The choice of the qualitative research method was informed by the fact that the study aimed to establish the prevalence of the BMC concept in the target market, based on the background that its prevalence in the country was slightly lower compared to that of its global counterparts—a fact attributable to the country's economic setup. Therefore, the quantitative research method was instrumental in the collection and analysis of data required to address the research aim and questions raised in the study.

*4.2. Data Collection.* Survey questionnaires were passed to 200 firms at the initial stage. All SMEs without an online presence were excluded from this study. As a result, data were collected from 63 Saudi SMEs. Those participating SMEs were selected conveniently from the two largest cities in Saudi Arabia, which are Riyadh (the capital of Saudi Arabia) and Jeddah (the main Saudi seaport on the west coast). In this regard, the sample framework comprised  $n = 63$ , and the response rate was 31.5% of 200 SMEs. The Saudi Arabian market operates in different lines of business, including phones, computers, footwear, clothes, convenience stores, pharmacy, fuel stations, and restaurants, among many others. The diversity of business fields was instrumental in facilitating the inclusivity of the research data, such that it would not appear that the research focused only on a particular industry or business alone. In the same regard, this boosted the quality and validity of the data collected and used for the study analysis.

## 5. Results and Discussion

The explored SMEs in the sample were asked to identify their consideration of the BMC factors before and while running the online business to answer the research questions. The following sections reveal the results of the analyzed data.

*5.1. Exploring the Utilization of BMC Factors before and While Running the Business.* The level of considering the utilization of BMC practices before and while running an online business by Saudi SMEs are the main two questions that this study aims to address. Table 1 shows the average of considering the BMC's nine practices.

Table 1 shows some kind of uncertainty in terms of considering and understanding BMC practices by Saudi SMEs. To visualize the result, the graph in Figure 3 presents the percentage of considering the practices before the online business started and the percentage after the online business had been in operation.

At the initial stage of analyzing the presented data, it is good to understand the three possible situations:

- (1) If the percentage of understanding a specific BMC practice is similar before and while running the online business, this would indicate that the business had accurate plans before establishing its online activities. Surprisingly, Figure 3 does not show any stable percentage before and while running online businesses. This result would negatively affect the ratio of achieving complete satisfaction among business stakeholders.
- (2) If the percentage of understanding a specific BMC practice has increased after launching the online activities, this would indicate that the business might start with some thoughts and learned to correct its direction upon understanding the reality of the online business environment. Five practices fit into this situation: key partners, value propositions, customer relationships, customer segments, and cost structures. The practices in this group would improve the satisfaction level of running the online business.
- (3) If the percentage of understanding of a specific BMC practice has decreased after the online business had been in operation, the indication is that the business would have had some understanding, adaptation, and adoption while the firm is planning the adoption of e-business, but that the reality of the business situation mixed up those plans and led to this reduction. Stakeholders in this group could be more likely to be less satisfied with their business outcomes. The graph shows four practices in this category: key activities, key resources, channels, and revenue streams.

The next stage of this research explored the average satisfaction level among the studied sample.

*5.2. Satisfaction with Business Success from 1 to 10.* The graph in Figure 4 shows the extent to which the Saudi Arabian SMEs were satisfied with the success of their businesses, on a scale of 1–10, taking into consideration their respective application of the BMC framework for strategic planning and management. The results indicate that most of the businesses were satisfied with the success of their business, as they reported a score between 4 and 10, with levels 7 and 8 being the highest. This could be evidence that the SMEs that

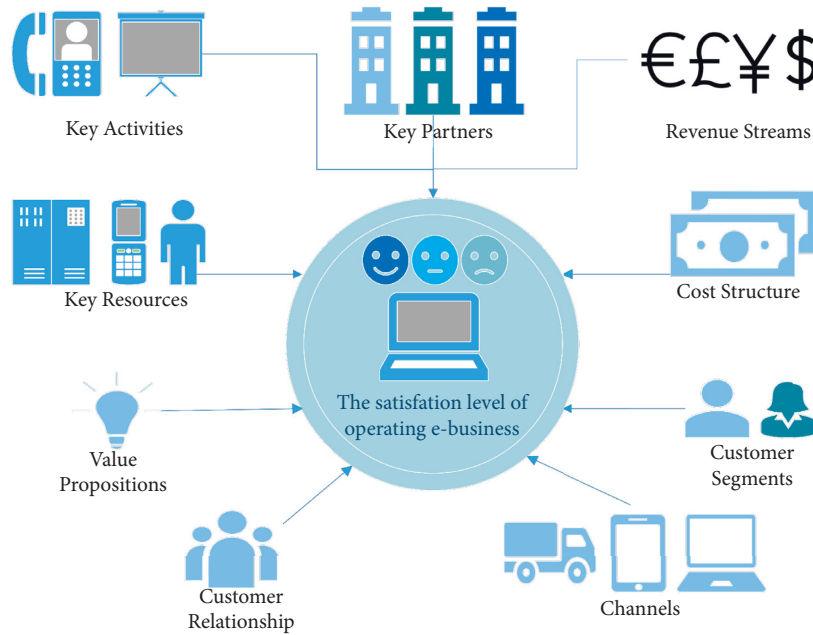


FIGURE 2: Exploring the statistically significant relationship between nine BMC factors and the satisfaction of the business owners.

TABLE 1: Considering BMC practices before and during the running of the online business.

BMC practice	N = 63	Before operating the business			While operating the business		
		Yes	Not sure	No	Yes	Not sure	No
Key partners	<i>n</i> 32 (%) 50.8	18 28.6	9 14.3	39 61.9	0 0.0	2 3.2	
Key activities	<i>n</i> 46 (%) 73.0	10 15.9	1 1.6	39 61.9	1 1.6	0 0.0	
Key resources	<i>n</i> 45 (%) 71.4	11 17.5	2 3.2	38 60.3	3 4.8	0 0.0	
Value proposition	<i>n</i> 21 (%) 33.3	31 49.2	1 1.6	41 65.1	6 9.5	0 0.0	
Customer relationship	<i>n</i> 23 (%) 36.5	16 25.4	10 15.9	36 57.1	7 11.1	3 4.8	
Channels	<i>n</i> 49 (%) 77.8	7 11.1	1 1.6	40 63.5	2 3.2	0 0.0	
Customer segments	<i>n</i> 17 (%) 27.0	17 27.0	18 28.6	28 44.4	7 11.1	8 12.7	
Cost structure	<i>n</i> 31 (%) 49.2	18 28.6	5 7.9	41 65.1	4 6.3	2 3.2	
Revenue streams	<i>n</i> 40 (%) 63.5	14 22.2	1 1.6	37 58.7	5 7.9	1 1.6	

were aware of the BMC components and that practiced the framework reported a higher level of success as compared to those that did not.

5.3. Regression Analysis. This study employed the stepwise regression forward selection procedure to build the model and examine the importance of survey variables

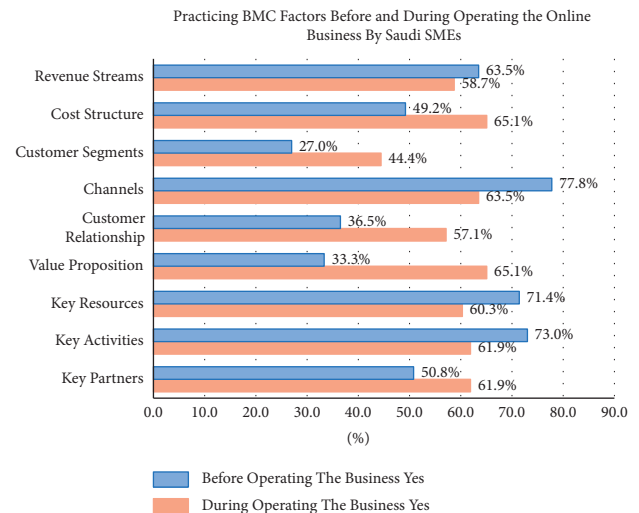


FIGURE 3: Practicing BMC factors before and while operating an online business by Saudi SMEs.

entered into the model for testing the relationship between the independent variables and the satisfaction of the business owners or the number of employees. Stepwise regression is a statistical method that is considered in multiple regression to enter variables into the model based on a statistical criterion [47]. Also, stepwise regression is used to mitigate over-fitting and multicollinearity in a model containing numerous predictors with traces of linear combinations [48]. The forward selection procedure is particularly relevant when the predictor variables are observed to correlate with one another, as it will add the predictors to the model in the

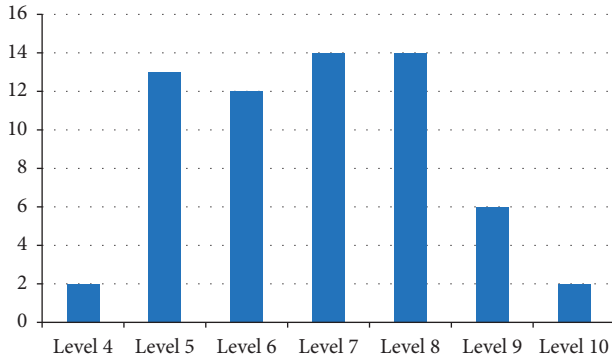


FIGURE 4: The satisfaction levels to business success.

order of relevance and will discard variables that can be dropped without seriously impairing the overall goodness of fit.

This study used F-statistic to compute all potential variables related to the satisfaction of the business owners or the number of employees and added the variable whose  $p$  value is highest as the first variable; any variable entering the model will not be removed. The study iterated the process until all the significant variables were completely added to the model. This was done to mitigate multicollinearity within the estimated model and excluded all the potential collinear variables in the model. Multicollinearity occurs when two or more independent variables are closely and linearly related [47]. The forward selection procedure includes only variables that are capable of uniquely establishing a significant relationship.

To form research hypotheses to establish a relationship between the survey variables and the satisfaction of the business owners or the number of employees by using the quantitative correlational nonexperimental study design, the study estimated a linear regression model to establish a relationship between the survey variables and the satisfaction of the business owners or the number of employees, using the computed mean score from the construct listed in the methodology section of this report and setting the satisfaction of the business owners or the number of employees, which was computed on a 10-point scale with 10 indicating best satisfaction experience as the dependent variable. The determined statistical significance of the research model was 0.05. The study presented the estimated result of the linear regression model by using Table 2, computing the R-Square statistics. Because the study considered the forward selection procedure, the first variable added to the model is key partners, where the model computed an R-Square of 0.665 and  $F_{(1,61)} = (23.471, p < .001)$ . The procedure added the remaining variables, which increased the R-Squared statistics to 0.974 and  $F_{(8,54)} = (10.416, p < .001)$ . The indication is that the  $r$  final model improved on the first model when estimated with fewer variables.

Regarding the overall significance of the research model, the study observed that the linear regression model was statistically significant,  $F_{(8,54)} = 10.416, p < 0.0001$ , overall  $R^2 = 0.974$ . This is an indication that a significant relationship exists between the survey variables and the satisfaction

TABLE 2: Linear regression model.

Satisfaction	B	SE ( $\beta$ )	$t$ value	$p$
Key partners	3.330	0.105	3.153	0.002
Key activities	2.285	0.093	3.079	0.003
Key resources	5.228	0.228	2.882	0.005
Value proposition	1.415	0.477	2.966	0.071
Customer relationship	4.036	0.837	4.822	0.003
Channels	2.022	0.748	2.703	0.045
Customer segments	2.275	0.512	3.942	0.024
Cost structure	-2.002	0.545	-4.002	0.048
Revenue streams	-0.344	0.148	-0.085	0.323

$N=63$ . The test of the hypotheses of  $\beta=0$  is based on  $t$ -values,  $df=62$ ,  $R^2=0.974$ , Adj.  $R^2=.0971$ , and  $*p < 0.05$ .

of the business owners or the number of employees. Moreover, 97.4% of the satisfaction of the business owners or the number of employees is explainable by the survey variables.

To estimate the relationship between the survey variables and the satisfaction of the business owners or the number of employees, a regression model was estimated. The significant raw or unstandardized regression coefficients correspond to the hypothesis and model path. The result provides information that can help to evaluate how much controlling for key partners, key activities, key resources, value proposition, customer relationships, channels, customer segments, cost structure, and revenue streams increases the strength of the association between the satisfaction of the business owners or the number of employees.

#### 5.4. Discussion and Analysis of the Results and Findings.

The results presented above were used to examine the significance of the model coefficients and to test the research hypotheses, providing informed responses sufficient to answer the research questions. Table 2 indicates whether there is a statistically significant relationship between each of the BMC factors and the satisfaction of businesses. The result shows that practicing most of the BMC factors would affect the satisfaction level of operating business activities online. The findings are described as follows.

$H_0$ : There is no statistically significant relationship between the following factors and the satisfaction of the business owners. The factors are as follows:

- (i) Value proposition
- (ii) Revenue streams

Although those two factors play a significant role in leading the business to success, Saudi SMEs seemed to not consider them as they should. Not considering the value proposition and the complete understanding of the revenue stream might mean that they use the online platforms to run their internal processes but not to sell or contact the customer. Also, they might use them to provide the same products or services as their competitors in the market, and not for the sake of being distinct.

$H_1$ : There is a statistically significant relationship between the following factors and the satisfaction of the business owners. The factors are as follows:

- (i) Key partners
- (ii) Key activities
- (iii) Key resources
- (iv) Customer relationship
- (v) Channels
- (vi) Customer segment
- (vii) Cost structure

*5.5. Recommendation of an Appropriate Framework to Incorporate IT Solutions into the Business Model.* The theory of organizational creativity is an appropriate framework that SMEs in Saudi Arabia can apply in incorporating IT solutions into the Business Model Canvas, thereby further improving the degree of effectiveness and efficiency derived from integrating the concept into their operations [49]. As discussed earlier, the theory of organizational creativity focuses on promoting the differentiation of a company's brand by facilitating the development of unique products and services through continuous Research and Development (R&D) programs that inspire creativity and innovation within these firms [13]. The BMC framework encourages firms to be the best in their respective markets by providing them with an effective strategic management and planning framework for use in pursuing their respective goal and objectives. Therefore, by using the theory of organizational creativity, Saudi SMEs can easily incorporate IT solutions into their respective business models, including the BMC framework, to improve the level of business success [40].

## 6. Conclusions

The Business Model Canvas (BMC) is one of the common strategic models to help businesses plan and foresee their progress and status from the early stages. The BMC can benefit all businesses of all sizes, from micro to small, medium, or even large enterprises. Thus, it is one of the models recommended by the industry to increase the likelihood of business success.

The market offers several versions of business models. The common BMC consists of nine main factors or practices to be identified. Large enterprises would have wide experience in adapting the BMC to their firms, while the practice of BMC by SMEs was uncovered. Therefore, this study focused on exploring the practice of BMC among SMEs in Saudi Arabia.

The study included 63 SMEs from different industry sectors to answer two main questions. Those questions explored the practicing and understanding level of SMEs to practice the BMC factors. The organizations were asked whether they practiced and identified each factor before and while running the business.

The results of this study revealed the instability of SMEs in Saudi Arabia when practicing BMC factors. Their understanding and awareness of some factors increased after they started their online businesses. This would indicate that those SMEs might not plan their start-ups well before running the online business, and they learned to correct

their direction after running the online channel. On the other hand, the realization level of some factors decreased after the launch of the online business. This would be the result of an optimistic plan for some SMEs that found themselves lost when they went online.

It is recommended that companies, especially SMEs, adopt and integrate the BMC framework into their operations, as this framework facilitates the achievement of their value propositions. The value that companies offer their customers is integral to ensure customer loyalty to the company's brand, as well as the continuous consumption of the firm's products and services. As such, with an elaborate BMC framework, these firms know how to work with each component of the framework to successfully achieve and deliver on their respective value propositions.

*6.1. Study Limitations.* The main limitation experienced during the research study involved reaching out to all the SMEs in the country, to ensure a comprehensive analysis of the entire nation, such that the results and findings obtained would reflect the real situation on the ground regarding the awareness and practice of BMC by Saudi Arabian SMEs. To overcome this challenge and ensure that sampling and data collection represented the entire study population, the study used online platforms to select the participants and administer the survey questionnaires. This not only introduced efficiencies in the administration and monitoring of the survey process but also reduced the research costs.

## Abbreviations

B2B:	Business to Business
BMC:	Business Model Canvas
FDI:	Foreign Direct Investment
R&D:	Research and Development
ROI:	Return on Investment
SEM:	Search Engine Marketing
SMEs:	Small and Medium-Sized Enterprises.

## Data Availability

The data are not publicly available due to privacy reasons and are available from the corresponding author upon request.

## Consent

Informed consent was obtained from all subjects involved in the study.

## Conflicts of Interest

The authors declare that they have no conflicts of interest.

## Acknowledgments

The authors gratefully thank the valuable technical support provided by the Faculty of Computing and Information Technology, King Abdulaziz University, Jeddah, Saudi

Arabia. The authors also acknowledge the support provided by the Center of Excellence in Smart Environment Research, King Abdulaziz University, Jeddah, Saudi Arabia.

## References

- [1] J. Shakeel, A. Mardani, A. G. Chofreh, F. A. Goni, and J. J. Klemeš, "Anatomy of sustainable business model innovation," *Journal of Cleaner Production*, vol. 261, Article ID 121201, 2020.
- [2] J. Rose, J. Holgersson, and E. Soderstrom, "Designing innovative digital services for government: a business model canvas adaptation," in *Proceedings of the In 27th European Conference on Information Systems (ECIS), Stockholm & Uppsala*, Association for Information Systems, Sweden, June 2019.
- [3] F. Cosenz and E. Bivona, "Fostering growth patterns of SMEs through business model innovation. A tailored dynamic business modelling approach," *Journal of Business Research*, vol. 130, pp. 658–669, 2021.
- [4] A. Baskara, E. Kaburuan, L. Ardiansyah, S. Sfenrianto, and T. Hwa, "Business model canvase of motorcycle after-sales service mobile application," *International Journal of Civil Engineering & Technology*, vol. 10, no. 4, p. 344, 2019.
- [5] E. Chua, J. Chiu, and N. Bool, "Sharing economy: an analysis of airbnb business model and the factors that influence consumer adoption," *Review of Integrative Business and Economics Research*, vol. 8, p. 19, 2019.
- [6] S. Sparviero, "The case for a socially oriented business model canvas: the social enterprise model canvas," *Journal of Social Entrepreneurship*, vol. 10, no. 2, pp. 232–251, 2019.
- [7] R. Amoussouhoui, A. Arouna, M. Bavorova, H. Tsangari, and J. Banout, "An extended Canvas business model: a tool for sustainable technology transfer and adoption," *Technology in Society*, vol. 68, Article ID 101901, 2022/02/01/2022.
- [8] J. Roselund and C. Legrand, "The Circular Economy Business Model of Algoland," *Short Communication*, vol. 10, 2019.
- [9] I. A. Davies and B. Doherty, "Balancing a hybrid business model: the search for equilibrium at Cafédirect," *Journal of Business Ethics*, vol. 157, no. 4, pp. 1043–1066, 2019.
- [10] Z. Ali, "Business model canvas for smart tailor platform," in *Proceedings of the Knowledge Management International Conference (KMICe)*, Miri Sarawak, Malaysia, 2018.
- [11] E. Baraibar-Diez, M. Odriozola, I. Llorente, and J. Sanchez, *Evaluating the business model of a work integration social enterprise in cantabria*, pp. 51–67, Springer, Cham, 2019.
- [12] P. Seetharaman, "Business models shifts: impact of covid-19," *International Journal of Information Management*, vol. 54, Article ID 102173, 2020.
- [13] N. Bocken, C. Schuit, and C. Kraaijenhagen, "Experimenting with a circular business model: lessons from eight cases," *Environmental Innovation and Societal Transitions*, vol. 28, pp. 79–95, 2018.
- [14] N. Bocken, F. Boons, and B. Baldassarre, "Sustainable business model experimentation by understanding ecologies of business models," *Journal of Cleaner Production*, vol. 208, pp. 1498–1512, 2019.
- [15] S. T. Bryant, K. Straker, and C. Wrigley, "The typologies of power: energy utility business models in an increasingly renewable sector," *Journal of Cleaner Production*, vol. 195, pp. 1032–1046, 2018.
- [16] E. Carayannis, E. Grigoroudis, D. Stamati, and T. Valvi, "Social Business Model Innovation: A Quadruple/Quintuple Helix-Based Social Innovation Ecosystem," *IEEE Transactions on Engineering Management*, vol. 68, 2019.
- [17] T. Burström, V. Parida, T. Lahti, and J. Wincent, "AI-enabled business-model innovation and transformation in industrial ecosystems: a framework, model and outline for further research," *Journal of Business Research*, vol. 127, pp. 85–95, 2021/04/01/2021.
- [18] J. M. Crick and D. Crick, "Angel investors' predictive and control funding criteria: the importance of evolving business models," *Journal of Research in Marketing and Entrepreneurship*, vol. 20, no. 1, pp. 34–56, 2018.
- [19] G. Heyes, M. Sharmina, J. M. F. Mendoza, A. Gallego-Schmid, and A. Azapagic, "Developing and implementing circular economy business models in service-oriented technology companies," *Journal of Cleaner Production*, vol. 177, pp. 621–632, 2018.
- [20] M.-A. Latifi, S. Nikou, and H. Bouwman, "Business model innovation and firm performance: exploring causal mechanisms in SMEs," *Technovation*, vol. 107, Article ID 102274, 2021/09.
- [21] D. Hovarth and R. Szabo, "Evolution of photovoltaic business models: overcoming the main barriers of distributed energy deployment," *Renewable and Sustainable Energy Reviews*, vol. 90, pp. 623–635, 2019.
- [22] J. Hruska and P. Maresova, "Design of business model canvas for social media," in *Emerging Technologies In Data Mining And Information Security Singapore*, vol. 813, p. 63, Springer, 2019.
- [23] P. Klimas, "Game developers' business models - the key activities exploration," *International Journal of Contemporary Management*, vol. 17, no. 1, pp. 99–17, 2018.
- [24] S. Wu, W. C. Yau, T. S. Ong, and S. C. Chong, "Integrated churn prediction and customer segmentation framework for telco business," *IEEE Access*, vol. 9, pp. 62118–62136, 2021.
- [25] O. Jewinly, M. Z. Zakaria, and S. Abdul-Rahman, "Customer segmentation analysis on retail transaction data," in *Proceedings of the 8th International Conference on Computational Science and Technology*, pp. 235–248, Springer Singapore, Singapore, September 2022.
- [26] N. Iheanachor, Y. David-West, and I. O. Umukoro, "Business model innovation at the bottom of the pyramid – a case of mobile money agents," *Journal of Business Research*, vol. 127, pp. 96–107, 2021/04/01/2021.
- [27] T. Ladd, "Does the business model canvas drive venture success?" *Journal of Research in Marketing and Entrepreneurship*, vol. 20, no. 1, pp. 57–69, 2018.
- [28] F. Lüdeke-Freund, R. Bohnsack, H. Breuer, and L. Massa, *Research on sustainable business model patterns: status quo, methodological issues, and a research agenda*, pp. 25–60, Springer, Palgrave Macmillan, Cham, 2019.
- [29] I. A. Davies and L. Chambers, "Integrating hybridity and business model theory in sustainable entrepreneurship," *Journal of Cleaner Production*, vol. 177, pp. 378–386, 2018.
- [30] J. Ojasalo and K. Ojasalo, "Service logic business model canvas," *Journal of Research in Marketing and Entrepreneurship*, vol. 20, no. 1, pp. 70–98, 2018.
- [31] E. R. G. Pedersen, W. Gwozdz, and K. K. Hvass, "Exploring the relationship between business model innovation, corporate sustainability, and organisational Values within the fashion industry," *Journal of Business Ethics*, vol. 149, no. 2, pp. 267–284, 2018.
- [32] T. Santonen and M. Julin, "Comparison of health and well-being living lab business models: preliminary results based on business model canvas evaluation," in *Proceedings of the*

- Research and Innovation Conference*, European Network of Living Labs, Geneva, Switzerland, 2018.
- [33] R. G. Chammassian and V. Sabatier, "The role of costs in business model design for early-stage technology startups," *Technological Forecasting and Social Change*, vol. 157, Article ID 120090, 2020.
- [34] T. Schoormann, D. Behrens, and R. Knackstedt, "Design Principles of Leveraging Sustainability in Business Modelling Tools," in *Proceedings of the Business Model Development Tools for Sustainability SmartHybridECIS*, vol. 71, Portsmouth, UK, June 2018.
- [35] M. Setiawan, S. Surjokusumo, D. Ma'soem et al., "Business centre development model of airport area in supporting airport sustainability in Indonesia," *Journal of Physics: Conference Series*, vol. 954, no. 1, Article ID 012024, 2018.
- [36] M. Urban, M. Klemm, K. O. Ploetner, and M. Hornung, "Airline categorisation by applying the business model canvas and clustering algorithms," *Journal of Air Transport Management*, vol. 71, pp. 175–192, 2018.
- [37] T. Uusitalo and M. Antikainen, "The concept of value in circular economy business models," in *Proceeding of the ISPIM Innovation Forum*, pp. 25–28, Boston, MA, USA, March 2018.
- [38] T. Santonen and M. Julin, "Identifying health and well-being living lab business model attributes," in *Proceedings of the ISPIM Conference Proceedigs. The International Society for professional Innovation Management (ISPIM)*, pp. 1–13, Finland, June 2018.
- [39] M. Franco-Santos, "Designing Better Performance Measurement Systems in Universities Using the Business Model Canvas," 2016.
- [40] A. Osterwalder and J. Euchner, "Business model innovation: an interview with alex osterwalder," *Research-Technology Management*, vol. 62, no. 4, pp. 12–18, 2019.
- [41] M. I. Indrawan, M. D. T. P. Nasution, E. Adil, and Y. Rossanty, "A business model canvas: traditional restaurant 'melayu' in north sumatra, Indonesia," *Business Management and Strategy*, vol. 7, no. 2, pp. 102–120, 2016.
- [42] M. Toro-Jarrin, I. Ponce-Jaramillo, and D. Guemes-Castorena, "Methodology for the building process integration of business model canvas and technological roadmap," *Technological Forecasting and Social Change*, vol. 110, pp. 213–225, 2016.
- [43] A. Joyce and R. L. Paquin, "The triple layered business model canvas: a tool to design more sustainable business models," *Journal of Cleaner Production*, vol. 135, pp. 1474–1486, 2016.
- [44] N. Jbara and G. Darnton, "The innovation of a hybrid business model for social enterprises," in *Proceedings of the International Conference on Innovation and Entrepreneurship*, Academic Conferences International Limited, Houston, March 2019.
- [45] M. P. Pieroni, T. C. McAloone, and D. C. Pigosso, "Business model innovation for circular economy and sustainability: a review of approaches," *Journal of Cleaner Production*, vol. 215, pp. 198–216, 2019.
- [46] M. Geissdoerfer and R. Weerdmeester, "Managing Business Model Innovation for Relocalization in the Process and Manufacturing Industry," *The Journal of Business*, vol. 16, 2019.
- [47] A. Field, "Why Is My Evil Lecturer Forcing Me to Learn Statistics? (Discovering Statistics Using SPSS Statistics)," Sage, 2018.
- [48] R. F. Gunst and R. L. Mason, "Biased estimation in regression: an evaluation using mean squared error," *Journal of the American Statistical Association*, vol. 72, no. 359, pp. 616–628, 1977.
- [49] S. Widhoyoko, E. Peranginangin, J. Gultom, and S. Handayani, "An epistemology of fraudulent financial reporting: a business model canvas adoption," *International Journal of Engineering and Technology*, vol. 7, pp. 305–308, 2018.

## Corrigendum

# Corrigendum to “Asymmetric Risk Spillover Networks and Risk Contagion Driver in Chinese Financial Markets: The Perspective of Economic Policy Uncertainty”

Zongxin Zhang,<sup>1</sup> Ying Chen,<sup>2</sup> and Weijie Hou<sup>3</sup>

<sup>1</sup>*Institute of Finance, Fudan University, Shanghai 200433, China*

<sup>2</sup>*School of Economics, Fudan University, Shanghai 200433, China*

<sup>3</sup>*Antai College of Economics & Management, Shanghai Jiao Tong University, Shanghai 200030, China*

Correspondence should be addressed to Ying Chen; [chenying18@fudan.edu.cn](mailto:chenying18@fudan.edu.cn)

Received 21 July 2022; Accepted 21 July 2022; Published 13 August 2022

Copyright © 2022 Zongxin Zhang et al. This is an open access article distributed under the Creative Commons Attribution License, which permits unrestricted use, distribution, and reproduction in any medium, provided the original work is properly cited.

In the article titled “Asymmetric Risk Spillover Networks and Risk Contagion Driver in Chinese Financial Markets: The Perspective of Economic Policy Uncertainty” [1], there was an error in the grant number in the Acknowledgements section. It should read as follows:

### Acknowledgments



This work was supported by the National Natural Science Foundation of China (72073035).

### References

- [1] Z. Zhang, Y. Chen, and W. Hou, “Asymmetric Risk Spillover Networks and Risk Contagion Driver in Chinese Financial Markets: The Perspective of Economic Policy Uncertainty,” *Complexity*, vol. 2021, Article ID 3169534, 10 pages, 2021.

## Research Article

# Fama–French Three-Factor Versus Daniel-Titman Characteristics Model: A Comparative Study of Asset Pricing Models from India

Samreen Akhtar <sup>1</sup>, Valeed Ahmad Ansari,<sup>2</sup> Saghir Ahmad Ansari,<sup>3</sup> and Alam Ahmad <sup>1</sup>

<sup>1</sup>College of Administrative and Financial Sciences, Saudi Electronic University, Jeddah Campus, Saudi Arabia

<sup>2</sup>Department of Business Administration, Aligarh Muslim University, Aligarh, India

<sup>3</sup>Department of Agricultural Economics and Business Management, Aligarh Muslim University, Aligarh, India

Correspondence should be addressed to Samreen Akhtar; [s.akhtar@seu.edu.sa](mailto:s.akhtar@seu.edu.sa)

Received 12 November 2021; Revised 10 June 2022; Accepted 16 June 2022; Published 20 July 2022

Academic Editor: Sheng Du

Copyright © 2022 Samreen Akhtar et al. This is an open access article distributed under the Creative Commons Attribution License, which permits unrestricted use, distribution, and reproduction in any medium, provided the original work is properly cited.

This study compares the three-factor model (F&F model) proposed by Eugene Fama and Kenneth French with Daniel and Titman's Characteristics Model (D&T model) using the data of Indian stock returns for the period of 25 years from 1993 to 2018. Three-way sorting ( $3 \times 2 \times 2$ ) of stocks based on the B/M ratio and size of the firms, and then by SMB, HML, or ex-ante  $\beta$  loadings, is formulated to design thirty-six portfolios. Regression and rolling regression are applied to the data under study. Results obtained by the F&F model, despite its shortcomings, are found more conclusive than the D&T model for distinguishing between characteristics and covariances for returns on Indian stock. This study favors the F&F model over the D&T model.

## 1. Introduction

This study explores and compares Fama- French three factor model (F&F Model) with Daniel and Titman's characteristics model (D&T Model) using the data of Indian stock returns. F&F Model is a kind of Capital Asset Pricing Model (CAPM). The CAPM was initially developed by Sharpe [1] and Lintner [2]. It has been used as one of the most recognized models of asset pricing in the history of finance (Ross, Westerfield, and Jordan, 1996) since its development. However, in the late 1970s, it came under attack as many anomalous pricing patterns emerged from empirical research works which could not be explained by CAPM [3, 4]. Book to Market (B/M) equity ratio and Firm size (size) are two such anomalies that are relevant to this research work. Fama and French analyzed in 1992 that B/M equity ratio and size can record the cross-sectional differences in the rate of return better than beta. Fama and French were motivated by the findings of other researchers similar to these findings. They extended their research in the same field and proposed F&F Model in 1993 [5]. They added two additional portfolios of risk factors in already existing CAPM to record the B/M ratio and

size premiums. However, this F&F model was questioned by Daniel and Titman [6] with their competing hypothesis, which put forth the following argument: It is not the price loadings on risk factors but the usual firm's characteristics with comparable B/M ratio and size that explicate variations (cross-sectional) in the stock returns. It is clear that the firms with the same characteristics, like size and B/M ratio, provide similar results due to their same level of risk exposure. According to Daniel and Titman [6], the problem is whether the B/M ratio or size are proxies for the risk-related factors which cannot be diversified and, consequently, can prompt the variations in the stock's returns [7].

The study was needed and had great importance in the field of CAPMs in the Indian context. It contributes and adds value to literature mainly in two ways. First, the F&F model is tested by using a long period (quarter of a century) data set of the Indian stock market and provides fresh evidence on whether B/M premium (value effect) and size premium (size effect) prevail in Indian Market [8]. Therefore, the results of this study provide an out-of-sample analysis of the F&F Model. Second, this work happens to be



the first study using the data of the Indian market, which provides a comparison between the F&F and D&T models.

## 2. Review of Literature (Theoretical Framework)

*2.1. Fama–French 3-Factor (F&F) Model.* According to Fama and French [5], B/M ratio and size are the two factors of risk that should be rewarded. It was also suggested by them that the high B/M ratio and a high average return on small shares are a type of recompense for bearing distress risk. The duo created mimicking portfolios that record (expected) return premiums related to B/M ratio and size. Their model is mathematically demonstrated through the following equation:

$$R_{pt} - R_{ft} = \alpha_p + \beta_p(R_{mt} - R_{ft}) + S_p(SMB)_t + h_p(HML)_t + \varepsilon_{pt}, \quad (1)$$

where  $R_p$  stands for the rate of return on portfolio  $p$ ,  $R_f$  is the rate of return on the risk-free asset,  $R_m$  is market portfolio's rate of return,  $HML$  is the return on the portfolio mimicking for the value factor (B/M equity), and  $SMB$  is the return on the portfolio mimicking for the market capitalization (size).

The return on stocks is shown by two factors. The first factor is  $SMB$  which depicts Small minus Big (i.e., returns on small size market cap firms minus big size market cap firms). Another one is  $HML$  which means High minus Low (i.e., returns on high B/M equity firms minus low B/M equity firms). Fama and French [5] tested the F&F model by taking the following steps. They sorted (a) stocks based on size and (b) B/M equity into quintiles. Based on the same, they formed 25 more portfolios by using the intersection of sorted data. It is worth noting that Fama and French tested their model against the dependent variables. The time-series regressions are computed for every portfolio. They found in their research that all factor loadings on each of these three factors were significant in the case of all 25 portfolios. The implication of such loadings on  $SMB$  and  $HML$  factors was that they captured time-series variation in the expected returns, and it was clarified that the slopes which are obtained from time-series regressions on  $SMB$  and  $HML$  are the loadings on priced factors.

In a stream of related articles, Fama and French [9, 10] argue, following Merton's [11] Intertemporal CAPM (ICAPM) framework, that the discernible superior returns of size and value portfolios are the compensation for some extramarket risk. There is substantial evidence to suggest that the premiums earned by these fundamental risk characteristics are indeed pervasive across emerging and developed markets [10, 12–19]; Sehgal and Jain, 2011, [20, 21], and [22]. Momani [23], in his study on Amman stock Exchange, favors using Carhart Model over the F&F model in practical applications. Fathi et al. [24] study the influence of trading characteristics in the Tehran Stock Exchange and report these to be the main determinants of liquidity.

The evidence of the effects of size and B/M ratio led researchers to study the F&F model in the Indian context

[25]. The F&F model was studied specifically for the Indian stock market for the first time by Connor and Sehgal [26], followed by Taneja [27], Sehgal and Balakrishnan [28], and Rossi [29]. All of them provided evidence in favor of the F&F model.

However, the literature is silent on whether it is the characteristics of the exposure to the risk factors which define cross-sectional variation in the mean of stock returns for the Indian stock market. In the recent studies over factor models, a new factor “human capital” has also been explored by Maiti and Balakrishnan [30]. Maiti [31] has conducted a review study on the evolution of risk factors in CAPMs and stressed that risk factors' evolution is a continuous process. Amihud [32], Amihud and Levi [33], and Adrian, Fleming, Shachar, and Vogt [34] have shown the effect of illiquidity on stock returns.

*2.2. Daniel and Titman's Study Characteristic Model (D&T Model).* Daniel and Titman's study (1997) is the first study that raised the questions on the inclusion of risk factors in the F&F model and argues that returns are better described by firm characteristics like firm size and B/M equity ratio than the factor loadings. According to them, the F&F model does not describe the average rate of returns directly. It describes average returns due to the correlation between factor loadings and firm Characteristics. Daniel and Titman formed portfolios by categorizing stocks according to B/M equity ratios and a second sort of factor loadings to unclasp the explanatory power of these two models. They reported results consistent with the mispricing story, as a powerful relation is observed between B/M equity ratio and expected rate of returns than between expected rate of return and factor loadings. They provided an argument that distressed stocks, which were exposed to a unique ‘distress’ factor, were not the reason behind the comovement of high B/M equity ratio stocks. It (comovement) was due to stocks with similar factor sensitivities, which tended to become distressed at the same time. It means that the results favored the characteristics of the firm model as opposed to the assumption of the factor of risk. Low B/M equity ratio, which is one of the characteristics of large firms, produces a low return, which cannot be, essentially, linked to a risk factor. Thus, Daniel and Titman's work supported the Characteristics of Firm Model (D&T model) as against the F&F model. D&T model also rejected the risk-based interpretations provided by Fama and French initially.

A response was provided to Daniel and Titman for their characteristics model by Davis, Fama, and French [35]. They perform the same investigation spanning 68 years (1929–1997). They executed a  $3 \times 3 \times 3$  sort where they took size, B/M equity, and factor loading instead of  $3 \times 3 \times 5$  sorts, which were used by Daniel and Titman because of this long time period, availability of data of very less number of firms was available. To confirm that this study is not prejudiced to reject the Characteristics Model, they show that the  $HML$  premiums come out to be comparable over different periods. For the period from 1929 to 1997,  $HML$  is 0.46 percent per month, and for the period from 1973 to 1993, it is 0.50 percent per month. Both the premiums are significant statistically.

They report varying results for the period (1973–1993) taken by Daniel and Titman for their analysis and for the extended period, that is, 1929–1997. Hence, similar to the results provided by Daniel and Titman in 1997, Davis et al. [35] also supported Characteristics Model but only over 20 years. But when the period of study is extended, they observe that the F&F model cannot be rejected or disapproved. Thus, they provided an argument that the interpretation of Daniel and Titman is subsample-specific and demonstrate their results to be consistent with the F&F model.

Similarly, Lewellen [36], in his study, also found that Fama–French Model is superior to the Titman Model. On the other hand, Ferson and Harvey [37] presented in their study that the F&F model is unable to explain the conditional expected returns.

Daniel, Titman, and Wei [38] provided the very first evidence from outside of the USA by studying the Japanese stock market, and the French Stock market was studied by Lajili-Jarjir [7].

Daniel et al. [38] provided the evidence which supports the story of the D&T model, while Lajili and Jarjir [7] found evidence that favors of F&F model.

To respond to the findings provided by Davis et al. [35], in favor of the F&F model, Daniel et al. [38] replicated the same testing on Japan's data for the period spanning 1975–1997. Their results suggest that the value premium in average stock returns of Japan's Stocks was more vigorous than in the USA. Consistent with Daniel and Titman's findings, they reveal that characteristics and not the factor loadings explain the stock returns in Japan and they find out some key differences between evidence from Japan and USA. They discarded the F&F model in all those experiments that construct characteristic-balanced portfolios with HML factor loading. The results of Daniel and Titman's study are more realistic because they did not accept those characteristic-balanced portfolios which have the loadings on the market, SMB, and HML factors [39].

Gharghori et al. [40] conduct an investigation of the F&F model versus the D&T Model on Australian data. They approved the F&F model as against D&T Model. Lajili-Jarjir [7] also tested both models using data from the stock market of France. They formed portfolios based on the triple sort on B/M ratio, size, and then by ex-ante beta, SMB, or HML loadings, and the results of this study rejected the F&F model. However, regression tests of this study favored the F&F model. Fieberg et al. [41] tried to explain that the characteristics (covariance) make-up of returns explicates the cross-sectional variation in German stock returns. Their results report that widely accepted factors like HML, WML, or SMB were not priced. This observation became inconsistent with the literature available currently, which claimed that these factors should be priced. They found that B/M equity and characteristics momentum explained the differences at a cross-sectional level, and returns on the stocks confirm the findings/results [42, 43]; (Schierack et al., 1999).

Further, their results report the lack of size effect. That is, firm size does not define the returns at cross-sectional. This finding supports the recent literature on Germany [42, 44]. It was also pointed out in this study that cross-sectional dispersion

in average stock returns for the stock market of Germany can be explained by characteristics instead of exposure to the risk factors. So, they reported their results consistent with Daniel and Titman's findings and the findings of [38].

### 3. Data and Methodology

**3.1. Data.** This section focuses on the data utilized for conducting this research. The relevant data of the S&P BSE-500 index for the period July 1993 to June 2018 is obtained from Prowess, the Reserve Bank of India's weekly auction database (<http://www.rbi.org.in>), and BSE Sensex. The Prowess, which is a database maintained by the Centre for Monitoring Indian Economy (CMIE), provided the data of monthly closing prices on common stocks, market capitalization, and price-to-book ratio for each month of the sample period.

The monthly closing prices of common stocks were used to calculate monthly return data. While S&P BSE-500 index covers about 90 percent of the total market capitalization and trading activities in the Indian stock market, and hence, it fairly represents market performance. Market capitalization is used as a measure of company size, and the price-to-book value ratio is inverted to obtain the B/M equity ratio (BE/ME). BE/ME is used to construct a value factor to be used as one of the variables in the study [45, 46].

Firms having negative BE are excluded while reckoning the breakpoints for the B/M equity ratio. Reserve Bank of India's weekly auction data is used to compute the rate of the 91-day treasury bill. A risk-free rate is obtained by converting the implicit yields into the monthly rate of return. The rate of return of BSE stocks served as the market return proxy. Finally, to calculate the market risk premium, the risk-free rate was reduced from the monthly rate of return on the market portfolios.

The average number of business firms considered in the study across years is given in Table 1. The number of firms taken for the analysis significantly rises from the year 1993 to the year 2016. The minimum number of firms analyzed during any one year is 157 for the year 1993, and the maximum number of firms is 496 for the year 2018. Stocks of the rest of the firms were excluded due to incomplete or missing data on some variables.

The sample for the study of the D&T model spans from July 1993 to June 2018. However, the main analysis is from July 1996 to June 2018, as prior data for three years is used to measure the preformation factor loadings. The main idea behind taking the data up to 2018 was to make a round figure of 25 years when we originally started working on this manuscript in 2020.

The number of firms ranges between 157 and 496 between 1993–1994 and 2017–2018. The average number of firms/stocks is 311.

#### 3.2. Methodology

**3.2.1. Portfolios Sorting Based on Size and Book-to-Market.** In June of each year, stocks are sorted on their market capitalization in increasing order and grouped into two types of

TABLE 1: Number of stocks in the sample across years.

Year	Number of business firms	Year	Number of business firms
1993–1994	157	2006–2007	307
1994–1995	180	2007–2008	327
1995–1996	198	2008–2009	350
1996–1997	216	2009–2010	354
1997–1998	222	2010–2011	365
1998–1999	231	2011–2012	380
1999–2000	234	2012–2013	383
2000–2001	243	2013–2014	385
2001–2002	246	2014–2015	477
2002–2003	253	2015–2016	481
2003–2004	262	2016–2017	490
2004–2005	269	2017–2018	496
2005–2006	282		

portfolios “small and big” by the median (Therefore, the breakpoint for constructing “size portfolios” is 50% based on median). Then these small and big portfolios are sorted into three groups by their ranked book equity to market equity ratio (value portfolios) at the end of the previous financial year (i.e., March). These value portfolios are broken down into three groups at the breakpoints of top 30% (High), middle 40% (Medium), and bottom 30% (low). Six test portfolios named small-high (SH), small-medium (SM), small-low (SL), big-high (BH), big-medium (BM), and big-low (BL) are made (mimicking to F&F model 1993) with the intersection of size (big/small) and B/M Ratio (High/Medium/Low). Two portfolios, named as “high minus low” (HML) and “Small minus Big” (SMB), are formed further from these six portfolios.

$$SMB = \frac{(SL - BL) + (SM - BM) + (SH - BH)}{3}, \quad (2)$$

$$HML = \frac{(SH - SL) + (BH - BL)}{2}.$$

**3.2.2. Construction of Triple-Sorted Portfolios Based on Factor Loadings by Using Rolling Regression.** To test Titman Model, all six portfolios formed on independent B/M ratio and size are further sorted into two portfolios based on preformation HML slopes. This  $3 \times 2 \times 2$  sort on B/M ratio, size, and HML loadings (low and high) produces a total of 12 portfolios that are known as the dependent variables, the same as Fama–French regression. This portfolio formation process is repeated for the remaining two factors in the Fama–French model, that is, SMB and market factor. Hence, a total of three sets of 12 portfolios each are formed on HML, SMB, and market factor loadings (Figure 1).

Following Daniel and Titman [6], the preformation factor slopes are prepared by doing *rolling regression* on returns of every stock of the three-factor portfolios (HML, SMB, and Market) of Fama–French for the period starting from  $-35$  to  $0$  relative to the date of portfolio formation.

After constructing these three sets of portfolios, we begin our tests of the F&F model by using the methodology of Daniel and Titman. First, we analyze the returns on the 12 B/M equity, size, and market factor loading portfolios. According to Daniel and Titman’s Characteristics Model, the returns which are expected from low and high factor loading portfolios are the

same because their factor risk does not carry any reward. Alternatively, the F&F model envisions that average returns of the high factor loading portfolios are more than the portfolios with low loadings because the prior are rewarded for higher risk. If the difference in portfolio returns between high and low factor loadings (i.e.,  $h-l$ ) is positive and significant, the D&T model will get the rejection against the F&F model.

### 3.2.3. Construction of Characteristics-Balanced Portfolios.

We perform a formal inspection of the F&F model against the D&T model, the same as it was conducted by Daniel and Titman (1997) in their study. This inspection is based on the significance level and the time-series regression of the returns of D&T model portfolios on the returns of the F&F model portfolios.

Returns of D&T model portfolios are also computed. It is computed by reducing the low factor loading from high factor loading ( $h-l$ ) portfolios of each B/M ratio group size. Accordingly, a set of six CB portfolios were composed against every set of factor-loading portfolios. There were a total of three sets of factor loading portfolios. Therefore researcher got a total of three sets of characteristic-balanced portfolios, where each set consisted of 6 stocks.

It was predicted by the F&F model that the regressions’ intercepts of the returns of CB portfolios on the F&F model portfolios cannot be distinguished from zero. On the contrary, the D&T model reveals that the value of  $h-l$  (intercepts) in the time-series regression should be negative.

According to the anticipation of the D&T model, the mean rate of return of CB portfolios must be distinguishable from zero because these CB portfolios also present the short as well as the long asset having the same characteristics. On the other hand, the F&F model says that the returns of these portfolios should be positive.

## 4. Results and Discussion

It is examined whether expected returns generated by the F&F model are better described by factor loadings or by firm characteristics. Furthermore, a comparative analysis of the F&F model and D&T model is conducted.

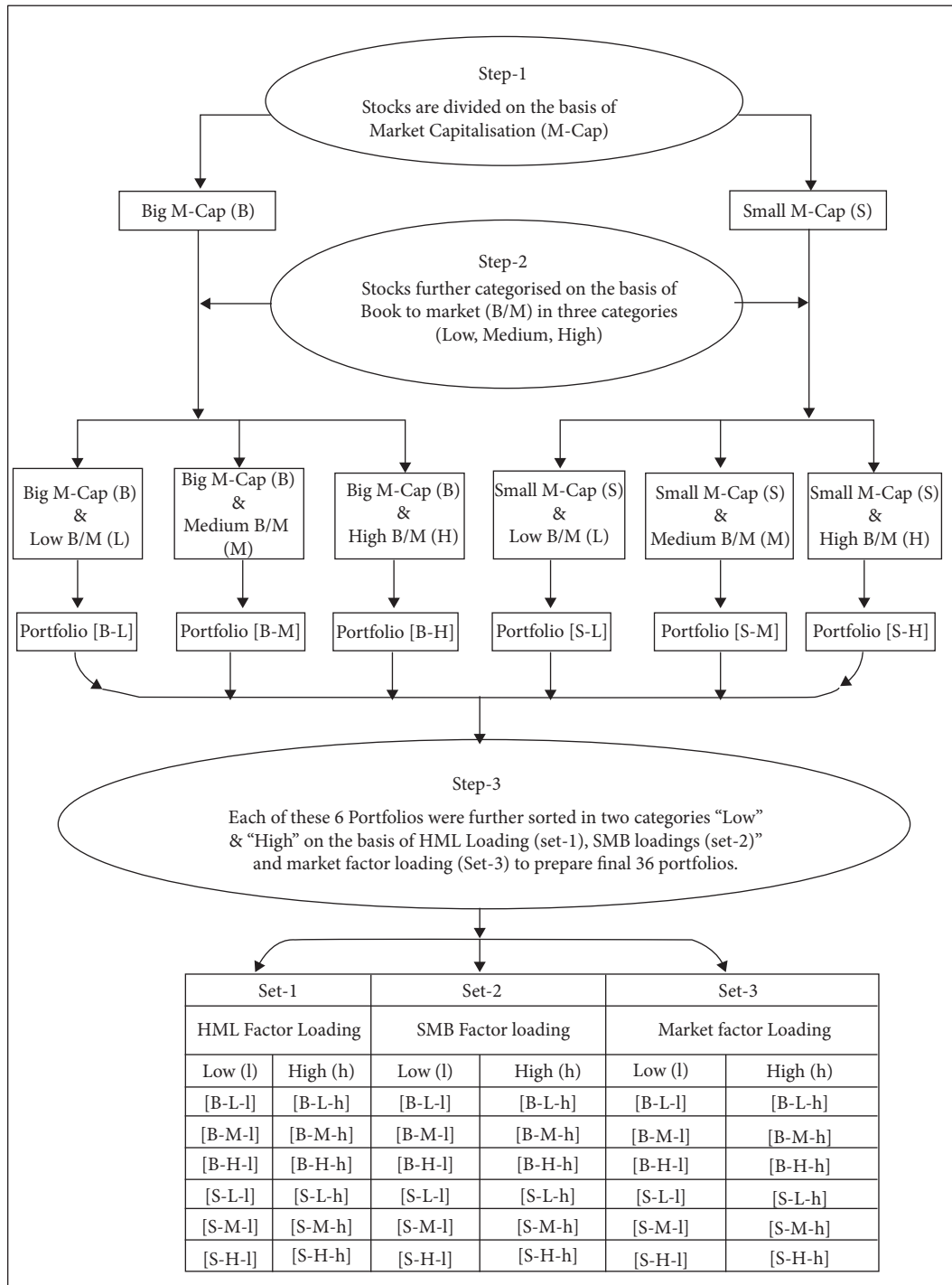


FIGURE 1: Conceptual Framework (Portfolios construction) for the study (prepared by Authors).

It is evident from the descriptive statistics (Table 2) that the mean monthly return of the HML factor portfolio is 0.859 percent with 2.685 *t*-statistics, while the Size factor SMB yields a mean monthly premium equalling 1.373 percent and *t*-statistics of 6.162. The mean excess monthly return of the market portfolio is 0.518 percent with *t*-statistics of 1.198 (Table 2). Fama and French, via the F&F model (1993), reported a mean

return for the market portfolio of about 0.89 percent per month. Inconsistent with Fama and French [5], portfolio returns on HML are positively correlated with both excess market returns and SMB portfolio returns. A negative correlation is reported between SMB and market portfolio returns (Table 2, Panel-B).

Numbers in bold denote significance at the five percent level or better.

4.1. *Analysis of Portfolios Sorted on Size, B/M Equity Ratio, and HML Factor Loadings.* Daniel and Titman's [6] study is followed for this sorting. Expected future loadings of stocks on the HML factor are estimated. Factor loadings of F&F Model factors are estimated for each stock at the end of June each year, while using 3 years' time-series regressions based on the return per month.

Based on an independent sort on market capitalization (size) and B/M equity, six test portfolios are obtained. Every portfolio is divided into two subportfolios on the basis of their preformation factor (HML/SMB/Market) loadings to get a total of 12 s.

Table 3 reports mean monthly excess returns for the 12 portfolios constructed using size, B/M ratio, and preformation HML factor loadings. The results depict a negative relationship between ex-ante HML factor loadings and average monthly excess returns for portfolios having low B/M equity. Nevertheless, this negative relationship inverts portfolios having medium and high B/M equity. So, evidence of higher mean returns for portfolios with greater factor loading than for portfolios with lower factor loading in four out of six cases is supportive of the F&F model or, as their model of risk hypothesizes that portfolios with greater factor loading yield average return higher than portfolios with lower factor loading.

Table 4 reports the average B/M ratio and size against the median for the test portfolios. Applying value weight, the mean market capitalization, and B/M equity ratio for every portfolio may be computed every year at the construction date:

$$\overline{SZ}_t = \frac{1}{\sum_i ME_{i,t}} \sum_i ME_{i,t}^2, \quad (3)$$

$$\overline{BM}_t = \frac{1}{\sum_i ME_{i,t}} \sum_i ME_{i,t} BM_{i,t}.$$

After that, these can be divided by the median of market capitalization and the B/M ratio of the Indian Market at all the points. Then, these, at all points, are divided by the median values of market capitalization and B/M equity of the Indian market. The numbers displayed in the table below are obtained by averaging both the time series independently.

For every market capitalization and book equity to market equity group, the B/M ratio concerning the median is found to be greater in the case of portfolios with high loadings on the high HML factor compared to low HML loading portfolios. Big portfolios have a negative relation with HML factor loadings.

For each market capitalization and B/M equity class, the highest average excess monthly returns are reported for the portfolio having the highest mean market value concerning median, as is evident from panel A and panel B of Table 3.

Panel 5 shows the regression results based on the F&F model for the 12 portfolios constructed on Size, B/M equity, and preformation HML factor loadings. Numbers given in bold font present a significance level at the five percent or better.

TABLE 2: Descriptive statistics of factor portfolio (Mimicking Portfolios) returns.

Panel A: Excess return (on monthly basis in percent)					
	Mean	t-value (mean)	Std. Dev.	Skewness	Kurtosis
SMB	1.373	6.162	3.722	0.290	4.102
HML	0.859	2.685	5.348	1.209	6.647
MKT	0.518	1.198	7.227	0.046	3.671
S/L	1.531	2.877	0.0889	0.505	6.317
S/M	1.782	3.215	0.0926	0.363	4.975
S/H	2.602	4.008	0.1084	0.469	4.072
B/L	0.390	0.877	0.0742	0.038	6.366
B/M	0.462	0.925	0.0835	0.194	5.199
B/H	0.944	1.517	0.1039	0.637	4.821
Panel B: Correlations					
	SMB	HML	MKT		
SMB	1.000	0.181	-0.019		
HML	0.181	1.000	0.210		
MKT	-0.019	0.210	1.000		

TABLE 3: Mean excess monthly returns for the 12 portfolios constructed on size, BM, and HML loadings.

Size	BM	HML factor loading group	
		Low (l)	High (h)
Mean monthly excess returns			
S	L	0.012	0.006
B	L	0.004	0.001
S	M	0.017	0.019
B	M	0.006	0.008
S	H	0.026	0.030
B	H	0.009	0.018

TABLE 4: Average BM and size of the 12 portfolios constructed on size, B/M equity, and HML loadings.

Size	BM	HML factor loading portfolios	
		Low (l)	High (h)
BM with respect to median			
S	L	0.389	0.423
B	L	0.306	0.368
S	M	0.986	1.057
B	M	0.947	1.056
S	H	2.754	3.583
B	H	2.154	2.509
Size with respect to median			
S	L	1.425	1.339
B	L	53.391	35.172
S	M	0.580	0.580
B	M	34.620	29.847
S	H	0.302	0.309
B	H	13.056	5.941

Table 5 further displays that the ordering pattern of preformation HML slopes is reproduced by the postformation slopes in four out of six cases.

Indeed, for portfolios with high and medium ratios of B/M equity (HS, HB, MS, and MB), postformation slopes can be judged on the basis of preformation slopes. Moreover,

TABLE 5: Fama–French regression results for the portfolios constructed on size, B/M equity, and HML loadings.

	$A$	$\beta$	$s$	$H$	Adj. $R^2$
S-L-l	-0.002 (-0.711)	<b>0.994</b> (19.746)	<b>0.797</b> (7.042)	<b>-0.168</b> (-2.360)	0.728
S-L-h	<b>-0.010</b> (-3.581)	<b>1.005</b> (14.081)	<b>0.784</b> (7.075)	0.033 (0.487)	0.758
B-L-l	-0.001 (-0.692)	<b>0.921</b> (22.341)	<b>0.194</b> (2.309)	<b>-0.169</b> (-3.366)	0.789
B-L-h	-0.005 (-1.875)	<b>0.967</b> (11.425)	0.078 (0.864)	0.057 (1.042)	0.726
S-M-l	-0.002 (-0.488)	<b>0.914</b> (17.157)	<b>0.977</b> (9.957)	0.086 (1.068)	0.716
S-M-h	-0.005 (-1.391)	<b>1.019</b> (15.447)	<b>1.211</b> (10.012)	<b>0.243</b> (2.532)	0.777
B-M-l	-0.004 (-1.421)	<b>0.982</b> (26.659)	<b>0.198</b> (2.639)	<b>0.282</b> (6.654)	0.809
B-M-h	<b>-0.007</b> (-2.320)	<b>1.117</b> (14.299)	<b>0.289</b> (2.736)	<b>0.533</b> (6.767)	0.812
S-H-l	-0.003 (-1.052)	<b>0.909</b> (17.246)	<b>1.422</b> (11.950)	<b>0.601</b> (6.379)	0.824
S-H-h	-0.002 (-0.746)	<b>1.018</b> (18.793)	<b>1.470</b> (10.820)	<b>0.768</b> (12.241)	0.842
B-H-l	<b>-0.008</b> (-3.315)	<b>0.971</b> (15.607)	<b>0.488</b> (4.083)	<b>0.661</b> (8.510)	0.810
B-H-h	<b>0.001</b> (0.117)	0.944 (8.970)	-0.007 (-0.025)	1.375 (5.650)	0.771

regression intercepts, as anticipated by the F&F model, must be zero. Table 3 reports an absolute value of  $t$ -statistics of less than two for nine intercepts. This evidence supports the F&F model.

As predicted by the Titman Model, the alpha values of the portfolios having lower loading on risk factors should be greater than zero, and those of the portfolios having high loading on risk factors should be less than zero, or it suggests a declining pattern in intercepts from low to high factor loadings. However, this study documents that all the intercepts except one are negative. These findings also support the F&F model against the D&T Model.

**4.2. Characteristic-Balanced Portfolios Regressions.** The returns on the characteristic-balanced portfolio ( $h-l$ ) of each class of size and B/M equity are calculated by subtracting the returns on low HML factor loading portfolios from that on portfolios having high HML factor loading. Thus, a total of six such characteristic-balanced portfolios are obtained.

Intercepts that are generated by doing a regression of the returns of these portfolios on the returns of the portfolios of the F&F model cannot be distinguished from zero. In contrast, the D&T Model hypothesizes that the time-series regressions of ( $h-l$ ) should yield negative intercepts. To confirm the validity of the regression model, a GRS test was conducted and GRS Statistics for the model is 0.3160, which is statistically insignificant and confirms the validity of the model.

The mean return of characteristic-balanced portfolios, as conjectured by D&T, must not be distinguishable from zero because small size and big size portfolios have same characteristics. But as per F&F Model, returns generated by these portfolios cannot be negative. The D&T model portfolios carry higher HML factor loading.

Panel A of Table 6 shows the descriptive statistics of the CB portfolios. The first column of Panel A presents the mean returns of the CB portfolios. It reveals that out of six portfolios, only two portfolios have a negative difference in mean monthly return, and both cases are insignificant. This condition supports the F&F model.

Table 6 (panel-B) reveals that the results which are consistent with the Fama–French Model. The table also shows that the regressions of portfolio returns of CB

portfolios against the returns of all three factors generated intercepts that have  $t$ -statistics less than two in five out of six instances.

It can be summarized that the evidence coming from Table 3 and panel A of Table 6 points out that the D&T model cannot be accepted, and the evidence from Table 5 and Panel B of Table 6 does not discard the F&F model. As a whole, the present analysis shows the F&F model is superior and accepts it over the D&T.

**4.3. Analysis of Portfolios Sorted on Size, B/M Ratio, and SMB Factor Loadings.** The procedure, same as the HML factor loadings, was used to analyze the performance of SMB factor loadings. The results display a positive relationship between average excess monthly returns and ex-ante SMB loadings for all the portfolios. Thus, the F&F model is supported as it predicts that higher average returns are observed in the case of portfolios with greater factor loading than in portfolios with lower factor loading.

The analysis further shows that the average B/M ratio and size with respect to the median for the test portfolios, Applying value weighting, the mean market capitalization, and B/M equity are computed for each portfolio every year at the construction date: Then, these at all points are divided by the median values of market capitalization and B/M equity of Indian stock market.

For the low B/M equity class, the average B/M equity against the median is observed to be higher for low SMB loading portfolios in comparison to the high SMB factor loading portfolios. This pattern is reversed for the group with medium B/M equity.

For every group of size and B/M equity, the average market capitalization concerning the median is recorded to be higher for portfolios having lower SMB factor loadings than the higher SMB factor loading portfolios.

It is also found that the results produced by regressions of each of the 12 test portfolios on the three risk factors. The market betas for all the portfolios are either one or close to one. HML slopes are positively related to B/M equity as with the increase in B/M equity, HML slopes also increase, and values that were negative for a group having lower B/M equity become positive for a group having higher B/M equity.

TABLE 6: Mean monthly excess returns and regression results for the characteristic-balanced portfolios sorted on size, B/M, and HML factor loadings.

Panel A: Mean excess monthly returns					
	Mean		Std. Dev.		t-statistic
SL ( $h_h-l_h$ )	-0.006		0.049		-1.795
BL ( $h_h-l_h$ )	-0.003		0.047		-1.016
SM ( $h_h-l_h$ )	0.002		0.054		0.631
BM ( $h_h-l_h$ )	0.002		0.048		0.680
SH ( $h_h-l_h$ )	0.004		0.066		0.942
BH ( $h_h-l_h$ )	0.009		0.073		1.864
Avg. ( $h_h-l_h$ )	0.001		0.030		0.707
Panel B: Fama-French regression results					
	$\alpha$	$\beta$	$s$	$h$	Adj. $R^2$
SL ( $h-l$ )	<b>-0.0075</b> (-2.3784)	0.0112 (0.1742)	-0.0137 (-0.0971)	<b>0.2011</b> (3.0129)	0.0402
BL ( $h-l$ )	-0.0039 (-1.1884)	0.0458 (0.5805)	-0.1160 (-0.9779)	<b>0.2265</b> (3.6028)	0.0729
SM ( $h-l$ )	-0.0030 (-0.7632)	0.1055 (1.6393)	<b>0.2339</b> (2.1521)	<b>0.1575</b> (2.4250)	0.0754
BM ( $h-l$ )	-0.0021 (-0.7256)	0.1346 (1.6738)	0.0902 (1.0499)	<b>0.2507</b> (3.5982)	0.1488
SH ( $h-l$ )	0.0013 (0.3434)	<b>0.1091</b> (2.8170)	0.0478 (0.2360)	0.1675 (1.5278)	0.0309
BH ( $h-l$ )	0.0089 (1.6530)	-0.0261 (-0.2688)	-0.4949 (-1.5028)	<b>0.7140</b> (2.4471)	0.2947
Avg ( $h-l$ )	-0.0010 (-0.6910)	0.0633 (1.4559)	-0.0421 (-0.6354)	<b>0.2862</b> (6.7566)	0.3173

Numbers in bold denote significance at the 5 percent level or better.

In the same way, SMB slopes are also related to size, but they are negatively related. Every B/M-HML loading class witnesses a reduction in SMB slopes on moving from smaller to bigger capitalization portfolios. And the ordering of the preformation SMB slopes is reproduced by the post-formation slopes in all six cases. Indeed, preformation slopes seem educative about their postformation slopes: portfolios that carry High factor loading comparatively observe higher SMB loading than the portfolios that carry low factor loading in comparison to the low factor loading portfolios observe higher SMB loading.

Moreover, regression intercepts, as anticipated by the factor model, should be zero. The table reports that  $t$ -statistics has an absolute value of less than two in ten instances of intercepts. This evidence supports the F&F model.

**4.4. Characteristic-Balanced Portfolios Regressions.** As in the previous section, a new set of six characteristics-balanced portfolios is formed using preformation HML factor loadings. The characteristic-balanced portfolio returns ( $h-l$ ) of every size and B/M ratio group are calculated by subtracting the returns on high SMB factor loading portfolios from that on portfolios having low SMB factor loading. Thus, a total of six such characteristic-balanced portfolios are obtained.

All means except one are indistinguishable from zero. Evidence of positive mean returns in five out of six instances does not let us reject the factor model. Thus, no conclusive result is obtained based on mean returns.

Panel B of Table 7 shows the results which seem supportive of the Fama-French model. The table reports that the

time-series regressions of portfolio returns of characteristic-balanced portfolios on the three-factor returns generate intercepts that have  $t$ -statistics below two in all six instances. Also, there is no significant negative intercept in any of the characteristic-balanced portfolios.

To conclude, the evidence in Panel A of Tables 6 and 7 favors the Fama-French model, and the evidence in Panels C of Table 5 and panel B of 6 also supports the Fama-French model.

**4.5. Analysis of Portfolios Sorted on Size, B/M Equity, and Market Factor Loadings.** Panel A of Table 8 shows the mean excess monthly returns for the 12 portfolios constructed by sorting the stocks based on size, B/M equity ratio, and market factor slopes. A positive relationship is found between average excess monthly returns and ex-ante market factor loadings for four portfolios out of six. Thus, the F&F model is supported as it predicts that high factor loading portfolios observe higher average returns than that of low factor loading portfolios.

Panel B reports the average B/M ratio to market equity and size against the median for the test portfolios. Applying value weighting, the mean market capitalization and B/M equity for each portfolio are calculated every year at the construction date.

Then, all of these points are divided by the median values of market capitalization and B/M equity of the Indian market. The numbers displayed in the table below are obtained by averaging both the time series independently.

TABLE 7: Mean excess monthly returns and Fama–French regression results for the characteristic-balanced portfolios sorted on size, B/Mand SMB factor loadings.

Panel A: Mean excess monthly returns					
	Mean		Std. Dev.	t-statistic	
SL ( $h-l$ )	0.005		0.048	1.720	
BL ( $h-l$ )	0.002		0.043	0.543	
SM ( $h-l$ )	0.006		0.049	1.788	
BM ( $h-l$ )	0.002		0.042	0.815	
SH ( $h-l$ )	0.011		0.068	2.437	
BH ( $h-l$ )	-0.001		0.073	-0.174	
Avg ( $h-l$ )	0.004		0.029	2.156	
Panel B: FF regression results					
	$A$	$\beta$	$s$	$h$	Adj. $R^2$
SL ( $h-l$ )	0.002 (0.649)	0.214 (4.030)	0.268 (2.600)	-0.147 (-1.797)	0.118
BL ( $h-l$ )	0.000 (0.004)	0.055 (0.952)	0.187 (2.136)	<b>-0.142</b> (-2.120)	0.036
SM ( $h-l$ )	0.002 (0.541)	0.054 (0.990)	0.284 (2.864)	-0.032 (-0.665)	0.035
BM ( $h-l$ )	-0.001 (-0.279)	0.105 (2.253)	0.271 (2.716)	-0.118 (-1.766)	0.072
SH ( $h-l$ )	0.003 (0.887)	0.117 (1.929)	0.573 (2.796)	-0.085 (-0.943)	0.089
BH ( $h-l$ )	-0.007 (-1.325)	0.127 (1.435)	0.859 (2.648)	<b>-0.629</b> (-2.046)	0.314
Avg ( $hs-ls$ )	0.000 -0.142	0.112 3.951	0.407 6.610	-0.192 -4.936	0.332

Numbers in bold denote significance at the 5 percent level or better.

TABLE 8: Mean excess monthly returns and F&amp;F regression for the CB portfolios sorted on size, B/M, and market factor loadings.

Panel A: Mean excess monthly returns					
	Mean		Std. Dev.	t-statistic	
SL ( $h-l$ )	0.003		0.052	0.976	
BL ( $h-l$ )	0.001		0.054	0.169	
SM ( $h-l$ )	0.003		0.050	0.950	
BM ( $h-l$ )	-0.001		0.044	-0.357	
SH ( $h-l$ )	0.006		0.066	1.400	
BH ( $h-l$ )	-0.001		0.073	-0.173	
Avg. ( $h-l$ )	0.002		0.031	0.930	
Panel B: FF regression results					
	$\alpha$	$\beta$	$s$	$h$	Adj. $R^2$
SL ( $h-l$ )	0.002 (0.620)	0.287 (4.835)	0.084 (0.765)	-0.131 (-2.067)	0.140
BL ( $h-l$ )	-0.001 (-0.402)	0.356 (3.924)	0.102 (0.958)	-0.144 (-2.332)	0.201
SM ( $h-l$ )	-0.002 (-0.757)	0.181 (3.248)	0.307 (2.405)	0.020 (0.354)	0.105
BM ( $h-l$ )	0.000 (0.135)	0.219 (4.541)	-0.106 (-1.092)	-0.105 (-1.495)	0.127
SH ( $h-l$ )	-0.001 (-0.403)	0.224 (4.422)	0.378 (1.914)	0.113 (1.360)	0.113
BH ( $h-l$ )	0.002 (0.231)	0.019 (0.173)	-0.458 (-1.204)	0.402 (1.134)	0.114
Avg ( $h-l$ )	0.000 (-0.063)	0.214 (4.982)	0.051 (0.578)	0.026 (0.400)	0.254

For the low B/M equity class, the average B/M equity against the median is observed to be higher for low Market factor loading portfolios in comparison to the high Market

factor loading portfolios. This pattern is reversed for the group with medium B/M equity while no such pattern is observed in the case of the high B/M class.



For each group of size and B/M equity, the average market capitalization concerning the median is recorded to be higher for portfolios having low market factor loadings than the high market factor loading portfolios. This pattern is reversed for the group with medium B/M equity, while no such pattern is observed in the case of the high B/M equity class.

Panel C reports the results produced by regressions of each of the 12 test portfolios on the three risk factors. HML slopes are positively related to B/M equity as with the increase in B/M equity, HML slopes also increase and values that were negative for the group having lower B/M equity become positive for the group having higher B/M equity. Similarly, SMB slopes are related to size, but these are negatively related.

Panel C also displays that the ordering of the preformation SMB slopes is reproduced by the postformation slopes in all six cases. Indeed, preformation slopes are educative about postformation slopes: Higher Market loading ( $\beta$ ) is observed for higher factor loading portfolios than that for lower factor loading portfolios.

Moreover, regression intercepts, as anticipated by the Fama–French model, must be zero. The table reports that  $t$ -statistics has a value of less than two in eleven instances of intercepts. This evidence also supports the Fama–French model.

**4.6. Characteristic-Balanced Portfolios Regressions.** As in the previous section, a new set of six characteristics-balanced portfolios is formed using preformation market factor loadings. The characteristic-balanced portfolio returns ( $h-l$ ) of each size and B/M equity ratio group are calculated by reducing the portfolio returns on.

Low market factor loading portfolios from the portfolio are having high market factor loading. Thus, a total of six such characteristic-balanced portfolios are obtained.

Mean monthly returns for all ( $h-l$ ) portfolios are indistinguishable from zero. The evidence of four out of six means monthly returns being positive supports the factor model. Thus, on the basis of mean returns of the characteristics-balanced portfolios, no satisfactory conclusion can be derived about the two models.

Panel B of Table 8 shows the results generated from the Fama–French regressions of CB portfolio returns. The table reports all the intercept values statistically indistinguishable from zero. Thus, the factor model is accepted. However, three intercepts are negative. These findings favor the F&F over the Characteristics Model and hence refute the findings of the Characteristics Model (1997).

## 5. Conclusion

This study examines the returns on the Indian stocks on the basis of the period from July 1993 to June 2018. The value effect in average stock returns, measured by *HML* Portfolios, is 0.859% with  $t$  statistics of 2.685 and the market effect, measured by *MKT* Portfolios, is only 0.518% with a  $t$  statistics of 1.198, while the size effect, measured by *SMB* Portfolios, is robust. It is 1.73% with  $t$  statistics of 6.162 [7, 8, 20, 30].

Fama and French [5] contend that stock returns can be described by three factors, namely, market, size, and book-to-market equity. However, the model lacks any well-built academic justification as to why size and book-to-market describe the cross-sectional differences in predicted returns of stocks. Fama and French [5] argue that higher return earned by firms with small size and a high book-to-market ratio is a reward for distress risk. This risk-based explanation, on account of a paucity of theoretical justification, has faced criticism from many scholars. The characteristics model propounded by Daniel and Titman [6] is the most severe of all the attacks that maintain that cross-sectional differences in predicted returns are described not by priced loadings on risk factors but by the characteristics of firms similar in size and book-to-market equity. The study examined whether expected returns generated by the Fama–French model (1993) are determined by loadings on risk factors or by characteristics of firms.

For testing these models, the authors used the methodology of Daniel and Titman to form characteristic-balanced portfolios. These portfolios are long and short assets with equal characteristics. D&T model predicted zero average rates of return on these portfolios.

However, the F&F model suggested the positive returns on these portfolios because the characteristic-balanced portfolios' loading on the HML factor (or SMB or  $\beta$  loadings) was very high.

The F&F risk model predicted that the intercepts of time-series regressions of the returns of these characteristic-balanced portfolios on the Fama and French factor portfolios are indistinguishable from zero.

In contrast, the hypothesis of the characteristic model says that these intercepts should be negative. But the results of this study revealed that, except in a few cases, all the intercepts have  $t$ -statistics below two. And the results of this study favor the F&F model over the D&T model. These results are consistent for the F&F model and not consistent for the D&T model.

It is found that most of the test portfolios displayed high returns for high loadings. Moreover, most of the intercepts from Fama–French regressions are not significant. And for the characteristic-based portfolios (D&T model), all the intercept terms are nonsignificant.

To conclude, the methodology proposed by Daniel and Titman distinguishes the factor model and does not allow one to make clear conclusions about the Indian context. Results obtained by the F&F model, despite its shortcomings, are more conclusive than the results obtained by D&T Model. These shortcomings are not those predicted by the characteristic model.

To show that covariances and characteristics are not the same and can be differentiated for the Indian stock market, this evidence favors the F&F model over the D&T Model. In a pragmatic way, we can say that the F&F model is a good tool for describing returns. It can be useful for many fields in finance, such as portfolio analysis, performance evaluation, or corporate finance. However, the debate regarding its theoretical legitimacy remains open [47, 48].

## 6. Implication and the Future Scope of the Study

The present work is useful for academicians as well as professionals in the different fields of finance like portfolio analysis, corporate finance, shares trading, etc. It provides good insights/trends and performance analysis of Indian Stocks. The study opens up the ways for the other researchers to use these models (1) to analyze the performance of the different portfolios, (2) corporate financing, (3) performance evaluation and comparison, (4) addition of other factors in the F&F model, and (5) review and comparative study of other models.

Researchers are especially expected to conduct a comparative study of 5-factor model of Fama–French with Daniel and Titman’s characteristics model. Researchers may also add illiquidity as a risk factor and analyze the results.

### Data Availability

The quantitative data used to support the findings of this study can be obtained from the corresponding author upon request.

### Conflicts of Interest

There are no conflicts of interest among the authors of this manuscript.

### References

- [1] W. F. Sharpe, “Capital asset prices: a theory of market equilibrium under conditions of risk,” *The Journal of Finance*, vol. 19, no. 3, 1964.
- [2] J. Lintner, “The valuation of risk assets and the selection of risky investments in stock portfolios and capital budgets,” *The Review of Economics and Statistics*, vol. 47, no. 1, 1965.
- [3] M. Rossi and G. Fattoruso, “The EMH and the market anomalies: an empirical analysis on Italian stock market,” *International Journal of Managerial and Financial Accounting*, vol. 9, no. 3, 2017.
- [4] V. A. Ansari, “Capital asset pricing model: should we stop using it?” *Vikalpa: The Journal for Decision Makers*, vol. 25, no. 1, pp. 55–64, 2000.
- [5] E. F. Fama and K. R. French, “Common risk factors in the returns on stocks and bonds,” *Journal of Financial Economics*, vol. 33, no. 1, pp. 3–56, 1993.
- [6] K. D. Daniel and S. Titman, “Evidence on the characteristics of cross-sectional variation in stock returns,” *The Journal of Finance*, vol. 52, no. 1, pp. 1–33, 1997.
- [7] S. Lajili-Jarjir, “Explaining the cross-section of stock returns in France: characteristics or risk factors?” *The European Journal of Finance*, vol. 13, no. 2, pp. 145–158, 2007.
- [8] S. Sehgal and V. Tripathi, “Size effect in Indian stock market: some empirical evidence,” *Vision*, vol. 9, no. 4, pp. 27–42, 2005.
- [9] E. F. Fama and K. R. French, “Multifactor explanations of asset pricing anomalies,” *The Journal of Finance*, vol. 51, no. 1, pp. 55–84, 1996.
- [10] E. F. Fama and K. R. French, “Value versus growth: the international evidence,” *The Journal of Finance*, vol. 53, no. 6, pp. 1975–1999, 1998.
- [11] R. C. Merton, “An intertemporal capital asset pricing model,” *Econometrica*, vol. 41, no. 5, 1973.
- [12] E. F. Fama and K. R. French, “The cross-section of expected stock returns,” *The Journal of Finance*, vol. 47, no. 2, pp. 427–465, 1992.
- [13] K. G. Rouwenhorst, “International momentum strategies,” *The Journal of Finance*, vol. 53, no. 1, pp. 267–284, 1998.
- [14] K. G. Rouwenhorst, “Local return factors and turnover in emerging stock markets,” *The Journal of Finance*, vol. 54, no. 4, pp. 1439–1464, 1999.
- [15] Y. W. Ho, R. Strange, and J. Piesse, “CAPM anomalies and the pricing of equity: evidence from the Hong Kong market,” *Applied Economics*, vol. 32, no. 12, pp. 1629–1636, 2000.
- [16] C. G. de Groot and W. F. C. Verschoor, “Further evidence on asian stock return behavior,” *Emerging Markets Review*, vol. 3, no. 2, pp. 179–193, 2002.
- [17] K. S. K. Lam, “The relationship between size, book-to-market equity ratio, earnings–price ratio, and return for the Hong Kong stock market,” *Global Finance Journal*, vol. 13, no. 2, pp. 163–179, 2002.
- [18] S. T. Lau, C. T. Lee, and T. H. McInish, “Stock returns and beta, firms size, E/P, CF/P, book-to-market, and sales growth: evidence from Singapore and Malaysia,” *Journal of Multi-national Financial Management*, vol. 12, no. 3, pp. 207–222, 2002.
- [19] H. W. Chan and R. W. Faff, “An investigation into the role of liquidity in asset-pricing: Australian evidence,” *Pacific-Basin Finance Journal*, vol. 11, no. 5, pp. 555–572, 2003.
- [20] A. Pandey and S. Sehgal, “Explaining size effect for Indian stock market,” *Asia-Pacific Financial Markets*, vol. 23, no. 1, pp. 45–68, 2016.
- [21] M. Rossi and A. Gunardi, “Efficient market hypothesis and stock market anomalies: empirical evidence in four European countries,” *Journal of Applied Business Research*, vol. 34, no. 1, pp. 183–192, 2018.
- [22] I. A. Ekaputra and B. Sutrisno, “Empirical tests of the Fama–French five-factor model in Indonesia and Singapore,” *Afro-Asian Journal of Finance and Accounting*, vol. 10, no. 1, 2020.
- [23] M. Q. M. Momani, “On the robustness of the Fama–French three-factor and the Carhart four-factor models on the amman stock Exchange,” *Afro-Asian Journal of Finance and Accounting*, vol. 11, no. 1, 2021.
- [24] S. Fathi, S. Jalali, A. Ajam, and O. M. Sadeghi, “Analysing the effect of trading characteristics on liquidity measures – a combined approach to liquidity: evidences from Tehran Stock Exchange,” *Afro-Asian Journal of Finance and Accounting*, vol. 10, no. 2, 2020.
- [25] A. Balakrishnan and M. Maiti, “Dynamics of size and value factors in stock returns: evidence from India,” *Indian Journal of Finance*, vol. 11, no. 6, p. 21, 2017.
- [26] G. Connor and S. Sehgal, “Tests of the Fama and French model in India,” *Decision*, vol. 30, no. 2, pp. 1–20, 2003.
- [27] Y. P. Taneja, “Revisiting Fama–French three-factor model in Indian stock market,” *Vision: The Journal of Business Perspective*, vol. 14, no. 4, pp. 267–274, 2010.
- [28] S. Sehgal and A. Balakrishnan, “Robustness of Fama–French three-factor model: further evidence for Indian stock market,” *Vision: The Journal of Business Perspective*, vol. 17, no. 2, pp. 119–127, 2013.
- [29] M. Rossi, “The efficient market hypothesis and calendar anomalies: a literature review,” *International Journal of Managerial and Financial Accounting*, vol. 7, no. 3/4, 2015.

- [30] M. Maiti and A. Balakrishnan, "Is human capital the sixth factor?" *Journal of Economics Studies*, vol. 45, no. 4, pp. 710–737, 2018.
- [31] M. Maiti, "A critical review on evolution of risk factors and factor models," *Journal of Economic Surveys*, vol. 34, no. 1, pp. 175–184, 2020.
- [32] Y. Amihud, "Illiquidity and stock returns: cross-section and time-series effects," *Journal of Financial Markets*, vol. 5, no. 1, pp. 31–56, 2002.
- [33] Y. Amihud and S. Levi, *The Effect of Stock Liquidity on the Firm's Investment and Production*, *Review of Financial Studies*, 2019, doi. 10.2139/ssrn.3183091.
- [34] T. Adrian, M. Fleming, O. Shachar, and E. Vogt, "Market liquidity after the financial crisis," *Annual Review of Financial Economics*, vol. 9, no. 1, pp. 43–83, 2017.
- [35] J. L. Davis, F. Fama, and R. French, "Characteristics, covariances, and average returns: 1929 to 1997," *The Journal of Finance*, vol. 55, no. 1, pp. 389–406, 2000.
- [36] J. Lewellen, "The time series relations among expected return, risk, and book to market," *Journal of Financial Economics*, vol. 54, no. 1, pp. 5–43, 1999.
- [37] W. E. Ferson and C. R. Harvey, "Conditioning variables and the cross section of stock returns," *The Journal of Finance*, vol. 54, no. 4, pp. 1325–1360, 1999.
- [38] K. D. Daniel, S. Titman, and K. J. Wei, "Explaining the cross-section of stock returns in Japan: factors or characteristics," *The Journal of Finance*, vol. 56, no. 2, pp. 743–766, 2001.
- [39] M. Ben Ltaifa, "Do book to market and size explain stock returns of banks? An empirical investigation from MENA economies," *International Journal of Managerial and Financial Accounting*, vol. 10, no. 3, Article ID 223, 2018.
- [40] P. Gharghori, H. Chan, and R. Faff, "Factors or characteristics? That is the question," *Pacific Accounting Review*, vol. 18, no. 1, pp. 21–46, 2006.
- [41] C. Fieberg, A. Varmaz, and T. Poddig, "Covariances vs. Characteristics: what does explain the cross section of the German stock market returns?" *Business Research*, vol. 9, no. 1, pp. 27–50, 2016.
- [42] A. Schrimpf, M. Schroder, and R. Stehle, "Cross-sectional tests of conditional asset pricing models: evidence from the German stock market," *European Financial Management*, vol. 13, no. 5, pp. 880–907, 2007.
- [43] M. Glaser and M. Weber, "Momentum and turnover: evidence from the German stock market," *Schmalenbach Business Review*, vol. 55, no. 2, pp. 108–135, 2003.
- [44] S. Artmann, P. Finter, and A. Kempf, "Determinants of expected stock returns: large sample evidence from the German market," *Journal of Business Finance & Accounting*, vol. 39, no. 5–6, 2012.
- [45] F. É. Racicot, "Engineering robust instruments for GMM estimation of panel data regression models with errors in variables: a note," *Applied Economics*, vol. 47, no. 10, pp. 981–989, 2015.
- [46] F. E. Racicot, W. F. Rentz, A. Kahl, and O. Mesly, "Examining the dynamics of illiquidity risks within the phases of the business cycle," *Borsa Istanbul Review*, vol. 19, no. 2, pp. 117–131, 2019.
- [47] S. Ross, R. Westerfield, and J. Jaffe, *Corporate Finance*, McGraw–Hill Primis, Pennsylvania, PA, USA, 2008.
- [48] S. Sehgal and I. Balakrishnan, "Contrarian and momentum strategies in the Indian capital market," *Vikalpa*, vol. 27, no. 1, pp. 13–20, 2002.

## Research Article

# More Efficient Prediction for Ordinary Kriging to Solve a Problem in the Structure of Some Random Fields

Mohammad Mehdi Saber <sup>1</sup> and Ramy Abdelhamid Aldallal<sup>2</sup>

<sup>1</sup>Department of Statistics, Higher Education Center of Eghlid, Eghlid, Iran

<sup>2</sup>College of Business Administration in Hotat Bani Tamim, Prince Sattam Bin Abdulaziz University, Al-Kharj, Saudi Arabia

Correspondence should be addressed to Mohammad Mehdi Saber; [mmsaber@eghlid.ac.ir](mailto:mmsaber@eghlid.ac.ir)

Received 5 November 2021; Revised 28 May 2022; Accepted 24 June 2022; Published 6 July 2022

Academic Editor: Atila Bueno

Copyright © 2022 Mohammad Mehdi Saber and Ramy Abdelhamid Aldallal. This is an open access article distributed under the Creative Commons Attribution License, which permits unrestricted use, distribution, and reproduction in any medium, provided the original work is properly cited.

Recently, some specific random fields have been defined based on multivariate distributions. This paper will show that almost all these random fields have a deficiency in spatial autocorrelation structure. The paper recommends a method for coping with this problem. Another application of these random fields is spatial data prediction, and the Kriging estimator is the most widely used method that does not require defining the mentioned random fields. Although it is an unbiased estimator with a minimum mean-squared error, it does not necessarily have a minimum mean-squared error in the class of all linear estimators. In this work, a biased estimator is introduced with less mean-squared error than the Kriging estimator under some conditions. Asymptotic behavior of its basic component will be investigated too.

## 1. Introduction

Random fields (RFs) as a statistical model can be applied in many real-life events, such as biological sequences, management of soil resources in agriculture and forestry, text and image processing, designing environmental monitoring networks, artificial intelligence, and road and tunnel planning.

An RF is usually constructed based on a multivariate distribution's finite-dimensional distributions. For example, the skew-normal (SN) RF based on multivariate SN distribution [1] has been defined by Kim and Mallick [2]. The closed skew-normal (CSN) RF based on multivariate CSN distribution [GF\_2004] has been established by Allard and Naveau [3]. Similar work has been performed by Karimi et al [4], Hosseini et al. [5], and Karimi and Mohammadzadeh [6]. Zareifard and Jafari Khaledi [7] defined a second-order stationary RF named unified skew-normal (SUN) RF by using multivariate SUN distribution [8]. The generalized Skew-Normal (GSN) RF introduced by Mahmoudian [9] has also been constructed from multivariate GSN distribution as shown by Sahu et al. [10], while the generalized asymmetric

Laplace (GAL) RF is defined by multivariate GAL distribution as shown by Kozubowski et al. [11] and was introduced by Saber et al. [12]. Some other RFs may be defined by multivariate skew-t distribution and its general form or multivariate extended skew-t (EST) distribution as shown by Arellano-Valle and Genton [13].

For the spatial structure of the model, Wall [14] studied the spatial structure implied by the CAR and SAR models. According to Saber et al. [12] and Mahmoudian [15], almost all mentioned RFs in the previous paragraph are not well defined by the Kolmogorov existence theorem. Saber et al. [12] showed that these RFs do not consider proper spatial autocorrelation structure (PSAS). In the present article, we will show that almost all aforementioned skew RFs have this deficiency. In fact, they do not consider PSAS.

A final application of any random field is spatial data prediction, which has been applied in some works of authors such as Basu and Reinsel [16], Saber and Nematollahi [17], and Saber [18]. Many researchers have studied the prediction of spatial data using mentioned unsuitable RFs. To solve the previously discussed problem, some authors such as

Mojiri et al. [19] have considered a univariate distribution for detection of errors of the process, which results in a new problem in modeling spatial correlation. Some others such as Hosseini and Karimi [21] have used an approximate skew-normal RF. Although this work has some benefits for reaching a high percentage of PSAS, it has some fundamental problems, and it cannot solve the two mentioned problems.

Kriging is a spatial prediction methodology and is the most widely used method of spatial data prediction that has increased during recent years. Because this method does not require defining the previously mentioned random fields that have problem in PSAS, Cressie [22] presented an unbiased linear estimator for Kriging and has a minimum mean-squared error (MSE), although it is not the best estimator in the larger class of all linear estimators. On the other hand, according to Moyeed and Papritz [23] linear Kriging is as good as any nonlinear method, especially for symmetric data. However, for skewed data, some of the nonlinear methods perform better in estimating prediction uncertainty. The focus of this article is on linear Kriging as we suggested a biased estimator for Kriging where the only interest is to minimize the MSE. Our recommended estimator has less MSE than the Cressie estimator under some conditions. Therefore, it is appropriate to use it for skewed data when we have a problem in defining a valid RF and for ordinary Kriging that does not have precision for nonlinear methods.

The paper is organized as follows: In Section 2, some requirements of the previously mentioned multivariate distributions are reviewed to show defined RFs that do not consider the PSAS property. After that, an estimator for the mean of the process and then a predictor with a minimum MSE in all the linear predictors for ordinary Kriging are presented in Section 3. Finally, Section 4 is devoted to investigating some asymptotic behavior for the recommended estimator.

## 2. A Problem in Some RFs

The first part of this section reviews the variance matrix of multivariate SN, CSN, EST, GSN, SUN, and GAL distributions.

Consider a  $p$ -dimensional continuous random vector  $\mathbf{X} = (X_1, \dots, X_p)'$  that has an SN distribution, denoted by  $\mathbf{X} \sim SN_p(\mu, \Sigma, \lambda)$ . Then, we have

$$\text{Var}(\mathbf{X}) = \Sigma - \frac{2}{\pi(1 + \lambda^T \lambda)} \Sigma^{1/2} \lambda \lambda^T \Sigma^{1/2}, \quad (1)$$

and consider another  $p$ -dimensional continuous random vector  $\mathbf{X} = (X_1, \dots, X_p)'$  but with a CSN distribution, denoted by  $\mathbf{X} \sim CSN_{p,q}(\mu, \Sigma, \Gamma, \xi, \Delta)$ . Then, we have

$$\text{Var}(\mathbf{X}) = \Sigma + \Sigma \Gamma^T \Lambda \Gamma \Sigma - \Sigma \Gamma^T \Psi \Psi^T \Gamma \Sigma, \quad (2)$$

where  $\Lambda$  and  $\Psi$  are complicated matrices based on  $\Phi_q(\mathbf{0}; \xi, \Delta + \Gamma \Sigma \Gamma^T)$ . The detail about these matrices is not essential for us, although they are present in the study conducted by González-Farías *et al.* [24].

The variance matrix of a multivariate EST distribution is denoted by  $\mathbf{X} \sim EST_p(\mu, \Sigma, \lambda, \nu, \tau)$ , which is given as follows:

$$\text{Var}(\mathbf{X}) = \alpha_*^2 (\omega^{-1} \Sigma \omega^{-1} - \delta \delta^T) + \sigma_*^2 \delta \delta^T. \quad (3)$$

However, the variance matrix of a multivariate GSN distribution is denoted by  $\mathbf{X} \sim GSN_p(\mu, \Sigma, \lambda)$ , which is given as follows:

$$\text{Var}(\mathbf{X}) = \Sigma + \left(1 - \frac{2}{\pi}\right) \text{diag}(\lambda^2). \quad (4)$$

Arellano-Valle and Azzalini [25] recently provided a very complicated and cumbersome computation of the variance matrix of multivariate SUN. Let  $\mathbf{X} \sim SUN_{d,m}(\xi, \Sigma, \Delta, \tau, \Gamma)$ . Then we have,

$$\text{Var}(\mathbf{X}) = \Sigma + \omega \Delta \mathbf{H} \Delta^T \omega. \quad (5)$$

Finally, the variance matrix of the GAL distribution continuous  $p$ -dimensional random vector  $\mathbf{X}$  denoted by  $\mathbf{X} \sim GAL_p(\mu, \Sigma, q)$  is given as follows:

$$\text{Var}(\mathbf{X}) = q(\Sigma + \mu \mu^T). \quad (6)$$

After that, we state the following remark.

*Remark 1.* Let  $Z(\mathbf{s}_1), \dots, Z(\mathbf{s}_n)$  be the observations from an RF  $\{Z(\mathbf{s}): \mathbf{s} \in \mathbf{D} \subseteq \mathbf{R}^d\}$  at  $n$  locations  $(\mathbf{s}_1, \dots, \mathbf{s}_n)$  in the area  $\mathbf{D}$ . It is assumed that  $\text{Cov}(Z(\mathbf{s}_i), Z(\mathbf{s}_j)) = q(|\mathbf{s}_i - \mathbf{s}_j|)$  where  $|\mathbf{h}|$  is the norm of the vector  $\mathbf{h}$  and  $q$  is a real value function. In a matrix form,  $\text{Var}(\mathbf{Z}) = \mathbf{C}$  where  $\mathbf{Z} = (Z(\mathbf{s}_1), \dots, Z(\mathbf{s}_n))$  and  $\mathbf{C} = [C_{i,j}]_{i,j=1}^n$  with a notation  $C_{i,j} = q(|\mathbf{s}_i - \mathbf{s}_j|)$ . Some RFs have been defined so that they satisfy the condition  $\text{Var}(\mathbf{Z}) = \mathbf{C}$ , while in some other cases, the covariance matrix  $\mathbf{C}$  has been used somehow in which  $\text{Var}(\mathbf{Z}) \neq \mathbf{C}$ .

In continuation of this section, we investigate the condition where  $\text{Var}(\mathbf{Z}) = \mathbf{C}$  is named as PSAS in some well-known RFs.

Gaussian RF:  $\mathbf{Z} \sim N_n(\mu, \Sigma)$  and  $\text{Var}(\mathbf{Z}) = \Sigma$ . Therefore, we choose  $\Sigma = \mathbf{C}$  to have a spatial correlation between variables.

$t$  RF:  $\mathbf{Z} \sim t_n(\mu, \Sigma, d)$  ( $d \geq 3$ ) and  $\text{Var}(\mathbf{Z}) = d/d - 2\Sigma$ . It seems to be an appropriate choice to reach the PSAS when  $\Sigma = d - 2/d\mathbf{C}$ .

SN RF:  $\mathbf{Z} \sim SN_n(\mu, \Sigma, \lambda)$  and  $\text{ar}(\mathbf{Z}) = \Sigma - 2/\pi(1 + \lambda^T \lambda) \Sigma^{1/2} \lambda \lambda^T \Sigma^{1/2}$  where it is convenient to substitute  $\Sigma - 2/\pi(1 + \lambda^T \lambda) \Sigma^{1/2} \lambda \lambda^T \Sigma^{1/2} = \mathbf{C}$  to get to the PSAS.

CSN RF:  $\mathbf{Z} \sim CSN_{n,q}(\mu, \Sigma, \Gamma, \xi, \Delta)$  and  $\text{ar}(\mathbf{Z}) = \Sigma + \Sigma \Gamma^T \Lambda \Gamma \Sigma - \Sigma \Gamma^T \Psi \Psi^T \Gamma \Sigma$ . Choosing  $\Sigma + \Sigma \Gamma^T \Lambda \Gamma \Sigma - \Sigma \Gamma^T \Psi \Psi^T \Gamma \Sigma = \mathbf{C}$  provides an adequate choice to reach the PSAS.

EST RF:  $\mathbf{Z} \sim EST_n(\mu, \Sigma, \lambda, \nu, \tau)$  and  $\text{ar}(\mathbf{Z}) = \alpha_*^2 (\omega^{-1} \Sigma \omega^{-1} - \delta \delta^T) + \sigma_*^2 \delta \delta^T$ . By substituting  $\alpha_*^2 (\omega^{-1} \Sigma \omega^{-1} - \delta \delta^T) + \sigma_*^2 \delta \delta^T = \mathbf{C}$ , we will obtain the PSAS.

SUN RF:  $\mathbf{Z} \sim SUN_{n,m}(\xi, \Sigma, \Delta, \tau, \Gamma)$  and  $\text{ar}(\mathbf{Z}) = \Sigma + \omega \Delta \mathbf{H} \Delta^T \omega$ . Making  $\Sigma + \omega \Delta \mathbf{H} \Delta^T \omega = \mathbf{C}$  will fulfill the PSAS.

GSN RF:  $\mathbf{Z} \sim GSN_n(\mu, \Sigma, \lambda)$  and  $\text{ar}(\mathbf{Z}) = \Sigma + \lambda(1 - 2/\pi)I$ . It provides a suitable choice to choose  $\Sigma + \lambda(1 - 2/\pi)I = \mathbf{C}$  and then consider  $\lambda$  as a nugget and  $\Sigma + \lambda(1 - 2/\pi)I = \mathbf{C}$  to accomplish the PSAS.

GAL RF:  $\mathbf{Z} \sim \text{GAL}_n(\mu, \Sigma, q)$  and  $ar(\mathbf{Z}) = q(\Sigma + \mu\mu^T)$ . After finding the PSAS, we will choose  $q(\Sigma + \mu^2 \mathbf{1}\mathbf{1}^T) = \mathbf{C}$ , which results as  $\mu = \mathbf{X}\beta$  and  $\Sigma = 1/q\mathbf{C} - \mathbf{X}\beta\beta^T\mathbf{X}^T$  where  $\mathbf{X}$  is the matrix of covariates and  $\beta$  is the regression coefficient.

As previously shown, some of the RFs satisfy the PSAS, while others do not. In the following remark, we denote this matter concisely.

*Remark 2.* The Gaussian RF,  $t$  RF, GSN RF, and GAL RF satisfy the PSAS. Other RFs containing the SN RF, CSN RF, EST RF, and SUN RF do not satisfy the PSAS. In some of the previous works that applied a second group of RFs, it was supposed that  $\Sigma = \mathbf{C}$ , although it does not lead to  $\text{Var}(\mathbf{Z}) = \mathbf{C}$  for achieving the PSAS.

Imposing the equality  $\text{Var}(\mathbf{Z}) = \mathbf{C}$ , without any other constraints, may result in a nonpositive definite for the matrix  $\Sigma$ . There is a method from which we can add a small value to the diagonal of  $\Sigma$ , but it does not work in every case. So, there is still a problem in getting the PSAS and positive definiteness for the matrix.  $\Sigma$

### 3. Linear Kriging as an Alternative for the Nonlinear Predictors Conducted by RFs

Let RF  $\{Z(\mathbf{s}): \mathbf{s} \in \mathbf{D} \subseteq \mathbb{R}^d\}$  satisfies the following model:

$$Z(\mathbf{s}) = \mu + Y(\mathbf{s}) + \varepsilon(\mathbf{s}), \quad (7)$$

where  $\mu$  is the mean value,  $Y(\cdot)$  is the zero-mean intermediate-scale variation, and a white noise error denoted by  $\varepsilon(\cdot)$  with a variance  $\sigma_\varepsilon^2$ .

Kriging belongs to the family of linear least square estimation algorithms. Given the observations  $Z = (Z(\mathbf{s}_1), \dots, Z(\mathbf{s}_n))$ , a common task is to predict  $Z(\mathbf{s}_0)$  at an unobserved location  $\mathbf{s}_0$  and to calculate the prediction error variance at each such location. The Kriging estimator is a linear predictor for  $\widehat{Z}(\mathbf{s}_0)$ , which is as follows:

$$\widehat{Z}(\mathbf{s}_0) = \sum_{i=1}^n l_i Z(\mathbf{s}_i), \quad (8)$$

where  $l_i$ s (the Kriging weights) are some scalars that may be found under two conditions:

- (a)  $E(\widehat{Z}(\mathbf{s}_0) - Z(\mathbf{s}_0)) = 0$  (unbiased condition)
- (b)  $\text{Argmin}\{\text{MSE}(\widehat{Z}(\mathbf{s}_0)) = E(\widehat{Z}(\mathbf{s}_0) - Z(\mathbf{s}_0))^2\}$

Simple Kriging (known mean) and ordinary Kriging (unknown but constant mean) are two well-known divisions of Kriging based on the mean value specification. In fact, in simple Kriging  $\mu$  is assumed to be known, but it is unknown in the case of ordinary Kriging, which occurs more in the application. As in the previous section, let  $\mathbf{C} = (\text{cov}(Z(\mathbf{s}_i), Z(\mathbf{s}_j)))_{i,j}$  denotes the covariance matrix of the observations and let  $\boldsymbol{\gamma} = (\text{cov}(Z(\mathbf{s}_0), Z(\mathbf{s}_1)), \dots, \text{cov}(Z(\mathbf{s}_0), Z(\mathbf{s}_n)))$  denotes the vector containing the covariances between observed and unobserved location  $\mathbf{s}_0$ .

According to Cressie [22], the simple Kriging estimator and its error variance are given, respectively, by

$$\widehat{Z}_{\text{simple}}(\mathbf{s}_0) = \boldsymbol{\gamma}' \mathbf{C}^{-1} \mathbf{Z}, \quad (9)$$

and

$$\text{Var}(\widehat{Z}_{\text{simple}}(\mathbf{s}_0) - Z(\mathbf{s}_0)) = \sigma_z^2(\mathbf{s}_0) - \boldsymbol{\gamma}' \mathbf{C}^{-1} \boldsymbol{\gamma}. \quad (10)$$

Also, the ordinary Kriging and its error variance are given, respectively, by

$$\widehat{Z}(\mathbf{s}_0) = \left( \boldsymbol{\gamma}' \mathbf{1} + \frac{(\mathbf{1}' \mathbf{C}^{-1} \boldsymbol{\gamma})}{\mathbf{1}' \mathbf{C}^{-1} \mathbf{1}} \right) \mathbf{C}^{-1} \mathbf{Z}, \quad (11)$$

and

$$\begin{aligned} \sigma_r^2(\mathbf{s}_0) &= V(\widehat{Z}(\mathbf{s}_0) - Z(\mathbf{s}_0)) \\ &= \sigma_z^2(\mathbf{s}_0) - \boldsymbol{\gamma}' \mathbf{C}^{-1} \boldsymbol{\gamma} + \frac{(\mathbf{1}' \mathbf{C}^{-1} \boldsymbol{\gamma})^2}{\mathbf{1}' \mathbf{C}^{-1} \mathbf{1}}, \end{aligned} \quad (12)$$

where  $\mathbf{1}' = (1, \dots, 1)$  is the row vector of size  $n$  in which its components are 1 s.

*3.1. New Estimator.* The Kriging estimator for ordinary Kriging is the best estimator regarding unbiasedness and the minimum MSE. However, a biased estimator with a less MSE is preferable in some circumstances. An estimator with this condition exists, and we denote our motivation for recommending this estimator in the following theorem.

**Theorem 1.** *An unbiased linear estimator for the mean of the process given in (7) exists and has a minimum MSE among all unbiased linear estimators for the mean. This estimator is in the form of*

$$\widehat{\mu} = \frac{\mathbf{1}' \mathbf{C}^{-1} \mathbf{Z}}{\mathbf{1}' \mathbf{C}^{-1} \mathbf{1}}, \quad (13)$$

and its variance is given by

$$\text{Var}(\widehat{\mu}) = \frac{1}{\mathbf{1}' \mathbf{C}^{-1} \mathbf{1}}. \quad (14)$$

*Proof.* A linear estimator for  $\mu$  is in the form of  $\sum_{i=1}^n a_i Z(\mathbf{s}_i) = \mathbf{a}' \mathbf{Z}$ . Unbiasedness implies that  $\mathbf{a}' \mathbf{1} = \sum_{i=1}^n a_i = 1$ . Hence, under this condition,  $\text{Var}(\mathbf{a}' \mathbf{Z}) = \mathbf{a}' \mathbf{C} \mathbf{a}$  must be minimized. By using the Lagrange equation  $\Gamma = \mathbf{a}' \mathbf{C} \mathbf{a} + \lambda(\mathbf{a}' \mathbf{1} - 1)$  and by vector differentiating, one can solve this problem to reach  $\widehat{\mathbf{a}} = \mathbf{C}^{-1} \mathbf{1} / (\mathbf{1}' \mathbf{C}^{-1} \mathbf{1})$ , and its results are shown in (13). Now, we have  $\text{Var}(\mathbf{1}' \mathbf{C}^{-1} / \mathbf{1}' \mathbf{C}^{-1} \mathbf{1} \mathbf{Z}) = \mathbf{1}' \mathbf{C}^{-1} \mathbf{C} \mathbf{C}^{-1} \mathbf{1} / (\mathbf{1}' \mathbf{C}^{-1} \mathbf{1})^2 = \mathbf{1}' \mathbf{C}^{-1} \mathbf{1} / (\mathbf{1}' \mathbf{C}^{-1} \mathbf{1})^2 = 1 / \mathbf{1}' \mathbf{C}^{-1} \mathbf{1}$ , which completes the proof.

Now, a simple Kriging method can be applied instead of an ordinary Kriging method. By substituting (13) in (7), we can reach  $Z(\mathbf{s}) - \widehat{\mu} = Y(\mathbf{s}) + \varepsilon(\mathbf{s})$  and  $Z(\mathbf{s}) - \mathbf{1}' \mathbf{C}^{-1} \mathbf{Z} / \mathbf{1}' \mathbf{C}^{-1} \mathbf{1} = Y(\mathbf{s}) + \varepsilon(\mathbf{s})$ . From (9), we can conclude that

$$\begin{aligned}\widehat{Z}_{\text{new}}(\mathbf{s}_0) &= \boldsymbol{\gamma}' \mathbf{C}^{-1} \left( \mathbf{Z} - \frac{1}{1' \mathbf{C}^{-1} \mathbf{1}} \mathbf{C}^{-1} \mathbf{Z} \right) \\ &= \left( \boldsymbol{\gamma} - \frac{1}{1' \mathbf{C}^{-1} \mathbf{1}} \right)' \mathbf{C}^{-1} \mathbf{Z},\end{aligned}\quad (15)$$

which is the new estimator for interpolation.  $\widehat{Z}_{\text{new}}(\mathbf{s}_0)$  is a special case of  $\widehat{Z}(\mathbf{s}_0)$  when  $\boldsymbol{\gamma}' \mathbf{C}^{-1} \mathbf{1} = 2$ .  $\square$

**Corollary 1.** *The biasedness and prediction error variance of the estimator  $\widehat{Z}_{\text{new}}$  is given by*

$$\begin{aligned}E(\widehat{Z}_{\text{new}}(\mathbf{s}_0) - Z(\mathbf{s}_0)) &= \mu(\boldsymbol{\gamma}' \mathbf{C}^{-1} \mathbf{1} - 2), \\ \text{Var}(\widehat{Z}_{\text{new}}(\mathbf{s}_0) - Z(\mathbf{s}_0)) &= \sigma_z^2(\mathbf{s}_0) - \boldsymbol{\gamma}' \mathbf{C}^{-1} \boldsymbol{\gamma} + \frac{1}{1' \mathbf{C}^{-1} \mathbf{1}}.\end{aligned}\quad (16)$$

*Proof.* The proof comes from Theorem 1, and a direct computation is presented in the following equations:

$$\begin{aligned}E(\widehat{Z}_{\text{new}}(\mathbf{s}_0) - Z(\mathbf{s}_0)) &= \left( \boldsymbol{\gamma} - \frac{1}{1' \mathbf{C}^{-1} \mathbf{1}} \right)' \mathbf{C}^{-1} \boldsymbol{\mu} \mathbf{1} - \mu \\ &= \mu(\boldsymbol{\gamma}' \mathbf{C}^{-1} \mathbf{1} - 2), \\ \text{Var}(\widehat{Z}_{\text{new}}(\mathbf{s}_0) - Z(\mathbf{s}_0)) &= \text{Var}(\widehat{Z}_{\text{new}}(\mathbf{s}_0)) + \text{Var}(Z(\mathbf{s}_0)) - 2\text{cov}(\widehat{Z}_{\text{new}}(\mathbf{s}_0), Z(\mathbf{s}_0)) \\ &= \left( \boldsymbol{\gamma} - \frac{1}{1' \mathbf{C}^{-1} \mathbf{1}} \right)' \mathbf{C}^{-1} \left( \boldsymbol{\gamma} - \frac{1}{1' \mathbf{C}^{-1} \mathbf{1}} \right) + \sigma_z^2(\mathbf{s}_0) - 2 \left( \boldsymbol{\gamma} - \frac{1}{1' \mathbf{C}^{-1} \mathbf{1}} \right)' \mathbf{C}^{-1} \boldsymbol{\gamma} \\ &= \sigma_z^2(\mathbf{s}_0) - \boldsymbol{\gamma}' \mathbf{C}^{-1} \boldsymbol{\gamma} + \frac{1}{1' \mathbf{C}^{-1} \mathbf{1}}.\end{aligned}\quad (17)$$

Because of this fact, we deduce that  $\widehat{Z}_{\text{new}}(\mathbf{s}_0)$  is a biased estimator. Now, to compare with the ordinary Kriging estimator given by (11), variance is not a useful criterion. The MSE is better when solving this problem and not only in this case but also while comparing between estimators even though at least one of them is biased. Finally, Theorem 2 shows that  $\widehat{Z}_{\text{new}}(\mathbf{s}_0)$  is better than the ordinary Kriging estimator (11) regarding the MSE under some conditions.  $\square$

**Theorem 2.** *Under one of the following two conditions (i) and (ii),  $\widehat{\text{MSE}} \widehat{Z}_{\text{new}}(\mathbf{s}_0)$  will be less than  $\widehat{\text{MSE}}(\widehat{Z}(\mathbf{s}_0))$ .*

- (i)  $(1' \mathbf{C}^{-1} \mathbf{Z})^2 > 1' \mathbf{C}^{-1} \mathbf{1}$  and  $\boldsymbol{\gamma}' \mathbf{C}^{-1} \mathbf{1}$  are between 2 and  $2(1' \mathbf{C}^{-1} \mathbf{Z})^2 / (1' \mathbf{C}^{-1} \mathbf{Z})^2 - 1' \mathbf{C}^{-1} \mathbf{1}$
- (ii)  $(1' \mathbf{C}^{-1} \mathbf{Z})^2 < 1' \mathbf{C}^{-1} \mathbf{1}$  and  $\boldsymbol{\gamma}' \mathbf{C}^{-1} \mathbf{1} > 2$  or  $\boldsymbol{\gamma}' \mathbf{C}^{-1} \mathbf{1} < 2(1' \mathbf{C}^{-1} \mathbf{Z})^2 / (1' \mathbf{C}^{-1} \mathbf{Z})^2 - 1' \mathbf{C}^{-1} \mathbf{1}$

*Proof.* From Corollary 1, we have  $\text{MSE}(\widehat{Z}_{\text{new}}(\mathbf{s}_0)) = (\mu(\boldsymbol{\gamma}' \mathbf{C}^{-1} \mathbf{1} - 2))^2 + \sigma_z^2(\mathbf{s}_0) - \boldsymbol{\gamma}' \mathbf{C}^{-1} \boldsymbol{\gamma} + 1/1' \mathbf{C}^{-1} \mathbf{1}$ . On the other hand, Equation (12) results in  $\text{MSE}(\widehat{Z}(\mathbf{s}_0)) = \sigma_z^2(\mathbf{s}_0) - \boldsymbol{\gamma}' \mathbf{C}^{-1} \boldsymbol{\gamma} + (1 - \boldsymbol{\gamma}' \mathbf{C}^{-1} \mathbf{1})^2 / 1' \mathbf{C}^{-1} \mathbf{1}$ . Then, by defining  $c = \boldsymbol{\gamma}' \mathbf{C}^{-1} \mathbf{1}$  and  $a = 1' \mathbf{C}^{-1} \mathbf{1}$ , one can show that  $d = \text{MSE}(\widehat{Z}_{\text{new}}(\mathbf{s}_0)) - \text{MSE}(\widehat{Z}(\mathbf{s}_0)) = 2c - c^2/a + \mu^2(2 - c)^2$

From the positive definiteness of  $\mathbf{C}$ , it is found that  $a > 0$ . By multiplying the above equality by  $a$ , we get  $ad = 2c - c^2 + a\mu^2(2 - c)^2$ . Replacing  $\mu$  by  $\widehat{\mu}$  leads to

$$\widehat{ad} = c^2(e - a) + c(2a - 4e) + 4e, \quad (18)$$

where  $e = (1' \mathbf{C}^{-1} \mathbf{Z})^2$ . The quadratic form (18) has two roots  $c_1 = 2$  and  $c_2 = 2e/e - a$  with respect to  $c$ . Under condition (i) or (ii), Equation (18) will be negative; hence,  $\widehat{d} \leq 0$  under condition (i) or (ii) as well. This completes the proof.  $\square$

#### 4. Asymptotic Behavior of the Mean Estimator

Since the estimator of  $\mu$  (13) in Theorem 1 has an essential role, its asymptotic behavior should be interesting for this study. First, we denote the following lemma, which is required for the continuation of this section.

**Lemma 1.** *For two sequences of unbiased estimators  $\widehat{\theta}_n^{(1)}$  and  $\widehat{\theta}_n^{(2)}$  we can say that  $\widehat{\theta}_n^{(2)} \xrightarrow{L} 2\theta$ ,  $\widehat{\theta}_n^{(1)} \xrightarrow{L} 2\theta$ , if  $\text{Var}(\widehat{\theta}_n^{(2)}) \geq \text{Var}(\widehat{\theta}_n^{(1)})$ . Here,  $\xrightarrow{L} 2$  states the mean square convergence.*

**Theorem 3.** *Let a random process  $Z(\mathbf{s})$  exists on a lattice  $\Lambda$  in  $R^k$  with coordinates,  $\mathbf{s}_1, \dots, \mathbf{s}_n$ ,  $\text{Var}(Z(\mathbf{s}_i)) \leq c < \infty$  for all  $i = 1, \dots, n$  and  $\text{cov}(Z(\mathbf{s}_i), Z(\mathbf{s}_j)) \rightarrow 0$  as  $|\mathbf{s}_i - \mathbf{s}_j|$  tends to infinity, then  $\overline{Z}_n \xrightarrow{L} 2\mu$  and  $\widehat{\mu} \xrightarrow{L} 2\mu$ .*

*Proof.* Without losing generality, assume  $Z_i$  denotes  $Z(\mathbf{s}_i)$ . First, we know that  $E(\overline{Z}_n) = 1/n(\sum_{i=1}^n E(Z_i)) = \mu$ . Now, we can compute the variance of  $\overline{Z}_n$

$$\begin{aligned}
\text{Var}(\bar{Z}_n) &= \frac{1}{n^2} \sum_{i=1}^n \sum_{j=1}^n \text{Var}(Z_i) \text{Var}(Z_j) \rho(Z_i, Z_j) \\
&\leq \frac{c}{n^2} \sum_{i=1}^n \sum_{j=1}^n |\rho(Z_i, Z_j)| \\
&= \frac{c}{n^2} \sum_{i=1}^n \sum_{j=1}^n |\rho(Z_i, Z_j)| I_{\{|s_i - s_j| \geq N_\varepsilon\}} \\
&\quad + \frac{c}{n^2} \sum_{i=1}^n \sum_{j=1}^n |\rho(Z_i, Z_j)| I_{\{|s_i - s_j| < N_\varepsilon\}}.
\end{aligned} \tag{19}$$

The last term has  $n^2$  components. The assumption which  $\rho(Z(\mathbf{s}_i), Z(\mathbf{s}_j)) \rightarrow 0$ , as  $|\mathbf{s}_i - \mathbf{s}_j|$  tends to infinity gives that for all  $\varepsilon > 0$ , there exists an integer  $N_\varepsilon$  enough large such that  $|\rho(Z(\mathbf{s}_i), Z(\mathbf{s}_j))| \leq \varepsilon$  for all  $Z(\mathbf{s}_i)$  and  $Z(\mathbf{s}_j)$  and that  $|\mathbf{s}_i - \mathbf{s}_j| \geq N_\varepsilon$ . For a fixed  $\mathbf{s}_i$ , the number of  $\mathbf{s}_j$  so that  $|\mathbf{s}_i - \mathbf{s}_j| \leq N_\varepsilon$  is less than  $(2N_\varepsilon)^k$ . Therefore, the total number of points with condition  $|\mathbf{s}_i - \mathbf{s}_j| \leq N_\varepsilon$  is at last  $n(2N_\varepsilon)^k$  which leads to  $\text{Var}(\bar{Z}_n) \leq c/n^2 (n(2N_\varepsilon)^k + (n^2 - n(2N_\varepsilon)^k)\varepsilon) = c(1/n(2N_\varepsilon)^k + (1 - 1/n(2N_\varepsilon)^k)\varepsilon)$

which clearly proves  $\bar{Z}_n \xrightarrow{L} 2\mu$ . By Theorem 1,  $\hat{\mu}$  is unbiased for  $\mu$  and  $\text{Var}(\hat{\mu}) < \text{Var}(\bar{Z}_n)$ . Finally, by Lemma 1 we get that  $\hat{\mu} \xrightarrow{L} 2\mu$ .  $\square$

**Corollary 2.** *It is an immediate consequence of Theorem 4 that under its conditions  $1/C^{-1}1$  tends to infinity as  $n$  tends to infinity.*

**Theorem 4.** *Under conditions of Theorem 4 and at least one of the followings (i) or (ii) and  $\hat{Z}_n(\mathbf{s}_0) \xrightarrow{L} 2\mu$ .*

- (i)  $\gamma' C^{-1} \gamma \rightarrow 0$  as  $n$  tends to infinity.
- (ii)  $1' C^{-1} 1 \gamma' C^{-1} \gamma - (\gamma' C^{-1} 1)^2$  is bounded.

*Proof.* Regarding Lemma 1 and the unbiasedness of  $\hat{Z}_n(\mathbf{s}_0)$ , we see that  $\text{var}(\hat{Z}_n(\mathbf{s}_0)) \rightarrow 0$  if it satisfies condition (i) or (ii). Since  $\hat{\mu}_n$  is the linear unbiased estimator for  $\mu$  with the minimum variance and  $\hat{Z}_n(\mathbf{s}_0)$  is the linear unbiased estimator for  $\mu$ , we obtain that

$$0 \leq \text{var}(\hat{\mu}_n) - \text{var}(\hat{Z}_n(\mathbf{s}_0)) = k_n. \tag{20}$$

Corollary 1 and equation (20) result in  $\text{var}(\hat{Z}_n(\mathbf{s}_0)) \rightarrow 0$  if and only if  $k_n \rightarrow 0$ . On the other hand, a direct computation shows that  $k_n = 1' C^{-1} 1 \gamma' C^{-1} \gamma - (\gamma' C^{-1} 1)^2 / 1' C^{-1} 1$  and under condition (ii), it obviously tends to 0. Another form of  $k_n$  is  $k_n = \gamma' C^{-1} \gamma - (\gamma' C^{-1} 1)^2 / 1' C^{-1} 1$ , with the fact that  $(\gamma' C^{-1} 1)^2 / 1' C^{-1} 1 > 0$  and if (i) satisfies, it will tend to 0.  $\square$

## 5. Conclusion

In this paper, we showed some previously defined RFs that have been extensively applied to modeling time series, spatial, and spatiotemporal data. However, they have a few limitations that they cannot consider the PSAS, which has a

crucial and basic role in modeling the previously mentioned data. For that, we presented some alternative RFs without the mentioned problem, and having a more general solution is still needed. The paper recommended a method for coping with this problem by finding a new predictor in ordinary Kriging. The customary predictor for ordinary Kriging has a minimum MSE in the class of all linear unbiased predictors. However, it does not necessarily have a minimum MSE in the class of all linear predictors. Therefore, we obtained a biased predictor with a less MSE than the Kriging predictor. Asymptotic behavior of this predictor alongside the past Kriging predictor was provided.

We studied six well-known multivariate distributions in this article. Some other multivariate distributions studied by Kotz et al. [26] such as the truncated multivariate normal distribution, truncated multivariate  $t$  distribution, Linnik's distribution, gamma distribution, and logistic distribution can be surveyed under this paper's point of view.

Despite providing some solutions for the problem of lacking PSAS, it seems that the best method for modeling skew spatial data is defining a consistent skew RF. This matter may be performed in the future.

## Data Availability

There are no data related to this paper.

## Conflicts of Interest

The authors declare that they have no conflicts of interest.

## Authors' Contributions

The idea of the paper was conceived and planned by Mohammad Mehdi Saber. Ramy Abdelhamid Aldallal was involved in writing the manuscript. All authors provided critical feedback and helped shape the manuscript's research, analysis, and construction.

## References

- [1] A. Azzalini, "A class of distributions which includes the normal ones," *Scandinavian Journal of Statistics*, vol. 12, pp. 171–178, 1985.
- [2] H.-M. Kim and B. Mallick, "A Bayesian prediction using the skew Gaussian distribution," *Journal of Statistical Planning and Inference*, vol. 120, no. 1-2, pp. 85–101, 2004.
- [3] D. Allard and P. Naveau, "A new spatial skew-normal random field model," *Communications in Statistics - Theory and Methods*, vol. 36, no. 9, pp. 1821–1834, 2007.
- [4] O. Karimi, H. Omre, and M. Mohammadzadeh, "Bayesian closed-skew Gaussian inversion of seismic AVO data for elastic material properties," *Geophysics*, vol. 75, pp. 1–11, 2010.
- [5] F. Hosseini, J. Eidsvik, and M. Mohammadzadeh, "Approximate Bayesian inference in spatial GLMM with skew normal latent variables," *Computational Statistics & Data Analysis*, vol. 55, no. 4, pp. 1791–1806, 2011.
- [6] O. Karimi and M. Mohammadzadeh, "Bayesian spatial prediction for discrete closed skew Gaussian random field," *Mathematical Geosciences*, vol. 43, no. 5, pp. 565–582, 2011.



- [7] H. Zareifard and M. J. Jafari Khaledi, "Non-Gaussian modeling of spatial data using scale mixing of a unified skew Gaussian process," *Journal of Multivariate Analysis*, vol. 114, pp. 16–28, 2013.
- [8] R. B. Arellano-Valle and A. Azzalini, "On the unification of families of skew-normal distributions," *Scandinavian Journal of Statistics*, vol. 33, no. 3, pp. 159–188, 2006.
- [9] B. Mahmoudian, "A skewed and heavy-tailed latent random field model for spatial extremes," *Journal of Computational & Graphical Statistics*, vol. 26, no. 3, pp. 658–670, 2017.
- [10] S. K. Sahu, D. K. Dey, and M. D. Branco, "A new class of multivariate skew distributions with applications to Bayesian regression models," *Canadian Journal of Statistics*, vol. 31, no. 2, pp. 129–150, 2003.
- [11] T. J. Kozubowski, K. Podgórski, and I. Rychlik, "Multivariate generalized Laplace distribution and related random fields," *Journal of Multivariate Analysis*, vol. 113, pp. 59–72, 2013.
- [12] M. M. Saber, A. R. Nematollahi, and M. Mohammadzadeh, "Generalized asymmetric Laplace random fields: existence and application," *Journal of Data Science*, vol. 18, pp. 51–68, 2018.
- [13] R. B. Arellano-Valle and M. G. Genton, "Multivariate extended skew-t distributions and related families," *Metron*, vol. 68, no. 3, pp. 201–234, 2010.
- [14] M. Wall, "A close look at the spatial structure implied by the CAR and SAR models," *Journal of Statistical Planning and Inference*, vol. 121, no. 2, pp. 311–324, 2004.
- [15] B. Mahmoudian, "On the existence of some skew-Gaussian random field models," *Statistics & Probability Letters*, vol. 137, pp. 331–335, 2018.
- [16] S. Basu and G. C. Reinsel, "Properties of the spatial unilateral first-order ARMA model," *Advances in Applied Probability*, vol. 25, no. 3, 1993.
- [17] M. M. Saber and A. R. Nematollahi, "Comparison of spatial interpolation methods in the first order stationary multiplicative spatial autoregressive models," *Communications in Statistics - Theory and Methods*, vol. 46, no. 18, pp. 9230–9246, 2017.
- [18] M. M. Saber, "Performance of extrapolation based on Pitman's measure of closeness in spatial regression models with extended skew t innovations," *Communications in Statistics - Theory and Methods*, vol. 48, no. 2, pp. 282–299, 2019.
- [19] A. Mojiri, Y. Waghei, H. R. Sani, and G. ., R. Borzadaran, "Comparison of predictions by kriging and spatial autoregressive models," *Communications in Statistics - Simulation and Computation*, vol. 47, no. 6, pp. 1785–1795, 2018.
- [20] A. Mojiri, Y. Waghei, H. R. Nili Sani, and G. R. Mohtashami Borzadaran, "Non-stationary spatial autoregressive modeling for the prediction of lattice data," *Communications in Statistics - Simulation and Computation*, forthcoming, 2021.
- [21] F. Hosseini and O. Karimi, "Approximate pairwise likelihood inference in SGLM models with skew normal latent variables," *Journal of Computational and Applied Mathematics*, vol. 398, 2021.
- [22] N. A. C. Cressie, *Statistics for Spatial Data*, Wiley, New York, NY, USA, 1993.
- [23] R. A. Moyeed and A. Papritz, "An empirical comparison of kriging methods for nonlinear spatial point prediction," *Mathematical Geology*, vol. 34, no. 4, pp. 365–386, 2002.
- [24] G. Gonzales-Farias, G. Dominguez-Molin, and A. K. Gupta, M. G. Genton, "The closed skew normal distribution," in *Skew-Elliptical Distribution and Their Applications: A Journey beyond Normality*, pp. 25–42, Chapman & Hall, Boca Rayton, FL, USA, 2004.
- [25] R. B. Arellano-Valle and A. Azzalini, "Some properties of the unified skew-normal distribution," *Mathematics arXiv: Statistics Theory*, vol. 63, pp. 461–487, 2020.
- [26] S. Kotz, N. Balakrishnan, and N. L. Johnson, *Continuous Multivariate Distributions. Models and Applications*, Wiley, vol. 1, New York, NY, USA, , 2000.

## Research Article

# Evaluation of Hot Money Drivers in China: A Structural VAR Approach

Weigang Hu <sup>1,2</sup>, Yan Zhou <sup>3,4</sup> and Jun Liu<sup>2</sup>

<sup>1</sup>*Institute of World Economy, Shanghai Academy of Social Sciences, Shanghai 200235, China*

<sup>2</sup>*School of Finance, Tongling University, Tongling 244061, China*

<sup>3</sup>*Endicott College of International Studies, Woosong University, Daejeon 34606, Republic of Korea*

<sup>4</sup>*School of Accounting, Tongling University, Tongling 244061, China*

Correspondence should be addressed to Weigang Hu; [huweigang08@163.com](mailto:huweigang08@163.com) and Yan Zhou; [yanzhou@tlu.edu.cn](mailto:yanzhou@tlu.edu.cn)

Received 8 June 2021; Revised 6 April 2022; Accepted 17 May 2022; Published 4 July 2022

Academic Editor: Atila Bueno

Copyright © 2022 Weigang Hu et al. This is an open access article distributed under the Creative Commons Attribution License, which permits unrestricted use, distribution, and reproduction in any medium, provided the original work is properly cited.

This paper investigates the drivers of hot money in China. It develops a model based on expectation-variance utility theory in the theoretical analysis section. The model considers a foreign investor who faces the question of how to distribute his wealth between foreign and domestic assets. The model's analysis suggests that economic variations, such as expected domestic currency appreciation, rise in domestic asset return, drop in foreign asset return, domestic economic growth, decrease in domestic inflation, and rise in foreign asset risk will cause foreign investors to distribute more wealth in domestic assets. Therefore, hot money flows in, and vice versa. In the empirical analysis section, the paper estimates structural VAR models using data from 2000 to 2019 in China. The impulse response functions are consistent with the theoretical predictions: when there is a positive domestic inflation shock, hot money outflows increase (inflows decline) in the current period, but the response is not significant. When there is a positive domestic growth rate shock or positive domestic asset return rate shock, hot money inflows increase (outflows decline) in the current period, and the response reaches its peak in the next period. Furthermore, when there is a positive expected exchange rate shock, hot money outflows increase (inflows decline) in the current period. Of these drivers, the expected exchange rate has the largest impact on hot money, and the domestic growth rate has the most enduring effect.

## 1. Introduction

Since the 1980s, global financial integration has progressed rapidly and has been an important phenomenon in the world economy, facilitating large quantities of cross-border capital flows [1–4]. Latin America's debt crisis, the Mexican financial crisis, the Asian financial crisis, and the 2008 financial crisis have one thing in common: they were all accompanied by huge amounts of international capital flows. A large share of these flows constitutes hot money, defined as cross-border speculative capital flow [5].

Hot money attracts scholarly attention because of its multiple influences on recipient countries. Firstly, hot money can influence recipient countries' economic output [6]. Secondly, hot money affects stock markets [7–10].

Thirdly, it can inflate property prices and accelerate market volatilities [11]. Lastly, hot money is closely connected with crises. Hot money not only exacerbates economic volatilities and damages economic growth prospects during the crisis period [12] but also makes recipient countries more vulnerable to future adverse shocks [13]. These speculative capital flows can also cause systemic risk through banking system channels [14, 15]. Based on these findings, hot money is widely considered detrimental to the recipient country's financial stability.

Several previous studies have analyzed the drivers of hot money. The interest rate differential and expectation of an appreciation of the China Yuan (CNY), which is the official currency of China, are suggested to be the main drivers of hot money in China [16, 17]. Cheung and Qian (2010) show

that China's hot money outflow (capital flight) is well explained by its history and covered interest differentials. The other possible determinants offer relatively small additional explanatory power [18]. Zhang and Shen (2008) show that the appreciation of the CNY and higher capital market returns are the determinants of hot money in China [19]. Zhao et al. (2013) find that hot money flows to China are related to the expected appreciation of the CNY, the change in house prices, and the change in the stock market index [20]. Zhang and Fung (2006) and Guo and Huang (2010) stress the importance of the stock market and real estate market factors [21, 22]. Davis et al. (2021) find that the energy price factor accounts for a significant share of the variance of capital flows [23]. Some researchers find that global risk is also an important factor in explaining hot money dynamics [24, 25]. Steinkamp and Westermann (2021) find that capital flight is positively correlated with development aid in Nepal [26]. Fratzscher et al. (2018) find that the Federal Reserve's quantitative easing increased the procyclicality of international portfolio flows [27]. Investors' experiences may also impact capital flows, and Malmendier et al. (2020) argue that investment experience effects can explain the tendency of investors to invest in domestic stock markets in periods of domestic crises and withdraw capital from foreign stock markets in periods of foreign crises [28]. Previous studies do not come to a consistent conclusion. The first possible reason is that they use different approaches to measure hot money, and some papers only consider hot money outflow (capital flight). The second possible reason is that the studies mainly use autoregressive distributed lag (ARDL) models or VAR models. These approaches have the problem that the reduced form residuals are typically not the shocks of interest in the viewpoint of economics.

This study evaluates the influence of different drivers of hot money in China.

As the first step in our analysis, we develop a foreign investor's asset allocation decision model based on expectation-variance utility theory. In this model, the foreign investor adjusts his portfolio when macroeconomic variables change and, therefore, short-term speculative capital flows across the border. We derive two findings from analyzing the model: firstly, the expected appreciation of the domestic currency, increase in the return of domestic assets, and decline in the return of foreign assets lead to hot money inflows. Secondly, domestic inflation, the domestic growth rate, and the risk of foreign assets' impact on hot money depend on whether the current position is long or short. If domestic and foreign positions are all long, which is typically the case, the expected appreciation of the domestic currency, increase in the domestic growth rate, the decline in the domestic inflation rate, and the increase of foreign asset risk cause hot money inflows.

The second step in our analysis involves studying the drivers of hot money in China, using the monthly data from 2000 to 2019. We estimate the structural VAR (SVAR) models and use impulse response functions to investigate drivers of hot money. Essentially, empirical results are consistent with our model's predictions: firstly, an increase in domestic inflation leads to a decline in hot money net

inflows. However, the results are insignificant, both economically and statistically. Secondly, the expected appreciation of the domestic currency, an increase in the domestic growth rate, and a rise in domestic asset return rate lead to hot money inflows. We find currency appreciation to be the most significant of the three drivers. Moreover, the impact of the growth rate is persistent. We perform the robust test in two ways: alternative measurement of hot money and different sample periods. The test results indicate that our conclusions are not sensitive to the choice of sample data.

This study makes two contributions to the literature. Firstly, it analyzes the impact of the main economic variables on hot money through a simple short-term investment decision model. The model considers the possibility of a short sale, which extant studies have ignored. Secondly, we use the SVAR model to measure macroeconomic variables' impact on hot money. The SVAR method is superior to the VAR method in measuring economic shocks.

The paper is organized as follows: we develop a foreign investors' portfolio decision model in Section 2. Then, Section 3 discusses and estimates the SVAR model. Furthermore, robust tests are performed in Section 4, and finally, conclusions are drawn in Section 5.

## 2. Theoretical Analysis

We develop a foreign investors' portfolio decision model based on mean-variance utility theory [29]. In this model, foreign investors distribute their wealth between domestic and foreign assets, and hot money flows when investors increase the share of domestic asset and vice versa. Hot money flows are endogenously decided in this way.

We assume that a foreign investor is ready to distribute one unit of foreign currency between domestic and foreign financial assets. The shares invested in the domestic and foreign assets are  $f_h$  and  $f_m$ , respectively. Since the total wealth of the investor is one unit of foreign currency,  $f_h$  and  $f_m$  are also the market values of his assets, can be any real number, and must satisfy the following equation:

$$f_h + f_m = 1. \quad (1)$$

When the share is a negative number, the investor has short sold the relevant asset. For instance, when  $f_h = 2$  and  $f_m = -1$ , the investor borrows one unit of foreign currency, converts the two units of foreign currency into domestic currency, and invests them in the domestic asset.

The return rates of the domestic and foreign assets are  $I$  and  $I_f$ , respectively. The domestic growth and inflation rates are  $y$  and  $p$ , respectively. The current exchange rate is  $e$  units of domestic currency per unit of foreign currency. The procedure surrounding the foreign investor's short-term speculative investment in the domestic asset is such that, firstly, they convert foreign currency into domestic currency at the current exchange rate  $e$ . Secondly, he buys and holds domestic assets. At last, they sell the domestic asset and convert domestic currency back into foreign currency. When the investor decides to invest in domestic asset, the expected exchange rate is  $e_f$ . It is easy to see that an increase

in  $e$  indicates a depreciation of the domestic currency. The foreign investor's expected rate of return from the investment in domestic asset is  $(1+I)e/e_f - 1$ . The expected return rate from his portfolio is as follows:

$$E[R] = f_h \left( \frac{e}{e_f} (1+I) - 1 \right) + f_m I_f. \quad (2)$$

It is assumed that the variance of the return rate of his domestic investment is  $\sigma_h^2$  and the variance of the return rate of his foreign asset is  $\sigma_m^2$ . Furthermore, it is assumed that the return rate of the domestic investment and that of the foreign asset are uncorrelated, which is plausible when strict restrictions are imposed on domestic financial account transactions, and the domestic economy is sufficiently large, as in the case of China. It is also assumed that  $\sigma_h^2$  is a function of domestic growth rate  $y$  and inflation rate  $p$ . For the sake of simplicity, it is assumed further that the function is linear as follows:

$$\sigma_h^2 = a_0 - a_1 y + a_2 p^2. \quad (3)$$

In this regard, the parameters  $a_0$ ,  $a_1$ , and  $a_2$  are all positive. The  $-a_1$  before  $y$  indicates that domestic investment risk is negatively correlated with domestic growth rate. The positive  $a_2$  indicates that the more stable the domestic prices, the less risky the domestic investment. Having summarized the above assumptions, the investor's portfolio return variance can be expressed as follows:

$$\sigma_R^2 = f_h^2 (a_0 - a_1 y + a_2 p^2) + f_m^2 \sigma_m^2. \quad (4)$$

Based on classic mean-variance utility theory, we assume the foreign investor's utility function as  $U(R, \sigma_R^2) = E[R] - 0.5\gamma\sigma_R^2$ , where  $R$  denotes portfolio return rate and  $\gamma$  measures his risk aversion. Therefore, we derive the investor's utility maximization problem as follows:

$$\max_{f_h, f_m} f_h \left( \frac{e}{e_f} (1+I) - 1 \right) + f_m I_f - 0.5\gamma (f_h^2 (a_0 - a_1 y + a_2 p^2) + f_m^2 \sigma_m^2), \text{ s.t. } f_h + f_m = 1. \quad (5)$$

We express the Lagrange function for the above problem and develop first-order conditions as

$$\frac{\partial L}{\partial f_h} = \frac{e(1+I)}{e_f} - 1 - \gamma f_h (a_0 - a_1 y + a_2 p^2) - \lambda = 0,$$

$$\frac{\partial L}{\partial f_m} = I_f - \gamma f_m \sigma_m^2 - \lambda = 0, \quad (6)$$

$$\frac{\partial L}{\partial \lambda} = f_h + f_m - 1 = 0.$$

Solving the simultaneous equations, we have derived the following:

$$f_h = \frac{e(1+I)/e_f - 1 - I_f + \gamma\sigma_m^2}{\gamma[\sigma_m^2 + (a_0 - a_1 y + a_2 p^2)]}. \quad (7)$$

It is evident that  $\partial f_h / \partial e_f < 0$ ,  $\partial f_h / \partial I > 0$ , and  $\partial f_h / \partial I_f < 0$ . The signs of those inequalities mean that expected domestic currency appreciation, an increase in the domestic asset return rate, and a decline in the foreign asset return rate cause the foreign investor to distribute more wealth in domestic asset, therefore, causing an inward flow of hot money.

$$\frac{\partial f_h}{\partial y} = \frac{a_1 (e(1+I)/e_f - 1 - I_f + \gamma\sigma_m^2)}{\gamma[\sigma_m^2 + (a_0 - a_1 y + a_2 p^2)]^2}. \quad (8)$$

The sign of the above derivative is the same as the sign of the part  $e(1+I)/e_f - 1 - I_f + \gamma\sigma_m^2$  in the numerator. Hence, it is the same as that of  $f_h$ . Therefore, when  $f_h > 0$ ,  $\partial f_h / \partial y > 0$ ; when  $f_h < 0$ ,  $\partial f_h / \partial y < 0$ . The economic meaning of this outcome is that when the foreign investor

holds a long position on the domestic asset, the high domestic growth rate will entice him to hold more of this long position, and there will be an inward flow of hot money. When the foreign investor holds a short position on the domestic asset, the high domestic growth rate will cause him to hold more of a short position on the domestic asset, causing an outward flow of hot money. The mechanism of the second result (the case of  $f_h < 0$ ) is that when  $f_h < 0$ , the high domestic growth rate reduces the risk of the short position, low risk causes the investor to take more of both the short and long positions, causing an outward flow of hot money.

$$\frac{\partial f_h}{\partial p^2} = -\frac{a_2 (e(1+I)/e_f - 1 - I_f + \gamma\sigma_m^2)}{\gamma[\sigma_m^2 + (a_0 - a_1 y + a_2 p^2)]^2}. \quad (9)$$

The analysis of equation (9) is similar to that of equation (8). The sign of  $\partial f_h / \partial p^2$  is contrary to that of  $e(1+I)/e_f - 1 - I_f + \gamma\sigma_m^2$  in the numerator, so it is contrary to that of  $f_h$ . Therefore, when  $f_h > 0$ ,  $\partial f_h / \partial p^2 < 0$ ; when  $f_h < 0$ ,  $\partial f_h / \partial p^2 > 0$ . The economic meaning in this regard is that when the foreign investor holds a long position on the domestic asset, the domestic price volatility will cause him to hold less domestic asset in the long position, causing an outward flow of hot money. Furthermore, when the foreign investor holds a short position on the domestic asset, the domestic price volatility will cause him to hold less domestic asset in the short position, causing a decline in the outflow of hot money. The mechanism underpinning the second result (the case of  $f_h < 0$ ) is that when  $f_h < 0$ , domestic price volatility increases the risk of the short position, high risk leads the investor to take less of both positions, causing a decline in the outflow of hot money.

$$\frac{\partial f_h}{\partial \sigma_m^2} = \frac{\gamma[\sigma_m^2 + (a_0 - a_1\gamma + a_2p^2)] - (e(1+I)/e_f - 1 - I_f + \gamma\sigma_m^2)}{\gamma[\sigma_m^2 + (a_0 - a_1\gamma + a_2p^2)]^2} \quad (10)$$

Regarding equation (10), the sign of derivative  $\partial f_h/\partial \sigma_m^2$  is determined by the numerator's sign, which is determined by the two terms in the numerator. Those two terms happen to be the denominator and numerator of  $f_h$ , so we analyze the sign of derivative  $\partial f_h/\partial \sigma_m^2$  in different subregions of  $f_h$ .

- (i)  $f_h > 1$ : in this case,  $e(1+I)/e_f - 1 - I_f + \gamma\sigma_m^2 > \gamma[\sigma_m^2 + (a_0 - a_1\gamma + a_2p^2)] > 0$ , so  $\partial f_h/\partial \sigma_m^2 < 0$ . This outcome means that when the foreign investor holds foreign asset in the short position and domestic asset in the long position, an increase in foreign asset risk causes the investor to reduce both positions, and therefore, there is an outflow of hot money.
- (ii)  $1 > f_h > 0$ : in this case,  $\gamma[\sigma_m^2 + (a_0 - a_1\gamma + a_2p^2)] > e(1+I)/e_f - 1 - I_f + \gamma\sigma_m^2 > 0$ , so  $\partial f_h/\partial \sigma_m^2 > 0$ , meaning that when the foreign investor holds both assets in long positions, an increase in foreign asset risk causes the investor to reduce the foreign asset long position and increase the domestic asset long position, and therefore, there is an inward flow of hot money.
- (iii)  $f_h < 0$ : in this case,  $e(1+I)/e_f - 1 - I_f + \gamma\sigma_m^2 < 0$ ; therefore,  $\partial f_h/\partial \sigma_m^2 > 0$ , showing that when the foreign investor holds domestic asset in a short position and foreign asset in a long position, an increase in foreign asset risk causes the investor to reduce both positions, and therefore, there is a decline in the outflow of hot money.

In summary, foreign investors typically hold both assets in long positions ( $1 > f_h > 0$ ). In this case, expected domestic currency appreciation, a rise in the return on domestic asset, a decrease in the return on foreign asset, domestic economic growth, decreased domestic inflation, and increased foreign asset risk may all lead foreign investors to distribute more wealth in domestic asset, therefore causing inflows of hot money.

### 3. Empirical Analysis

**3.1. Sample and Data.** In this study, we use an SVAR model comprising seven variables. A large sample is preferred for producing robust results. Therefore, we choose the longest sample range available for the period 2000.9–2019.11. Variable definitions and explanations are as follows:

- (1) Hot money (HM): for the time being, there are two main approaches to measuring hot money. The first one is the direct approach, the main idea of which is that hot money is hidden in the section titled “Net Errors and Omissions” of the Balance of Payments

(BOPS). Thus, scholars may measure net flows of hot money based on net errors and omissions with some adjustments. The second method is the indirect approach. The main idea of the indirect approach is to attribute the inexplicable part of the variation in foreign exchange reserves (FER) to hot money. The World Bank report (1985) suggests measuring hot money using the following equation: hot money net inflow = variation in FER – current account surplus – foreign direct investment (FDI) – the variation in short-term foreign debts [30]. This paper uses the indirect approach. Data on FER, the current account, and short-term foreign debt are taken from China's State Administration of Foreign Exchange (SAFE) website. FDI data are taken from the Wind Economic Database. Hot money net flows in China for the period 2000.9–2019.11 are shown in Figure 1. Hot money net flows were relatively small before the 2008 financial crisis and increased gradually over 2008–2015. Before 2013, hot money inflows were more frequent than outflows, and the peak inflow occurred in September 2013. Since 2014, there has been an outward flow of hot money, with a peak in outflows occurring in December 2015. After 2015, hot money outflows are on a smaller scale.

- (2) Economic growth rate Y: although this study uses monthly data, China's National Bureau of Statistics offers only quarterly GDP data. We substitute industrial value-added growth rate, which is monthly data, for GDP growth rate. Industrial value-added data are taken from the Chinese Economic Information Statistics Database.
- (3) Inflation rate p: this study uses the consumer price index to measure the inflation rate, and the data come from the China Stock Market and Accounting Research Database.
- (4) Domestic asset return rate (DAR): this study uses the Chinese three-month interbank offered rate to measure the domestic asset return rate, and the data in this regard are also taken from the Chinese Economic Information Statistics Database. We use the log difference of the original data.
- (5) Foreign asset return rate (FAR): this study uses the three-month US dollar LIBOR to measure the foreign asset return rate, and the data are from CEIC Data's Global Database. We use the log difference of the original data.
- (6) Expected exchange rate (EER): this study uses a three-month nondeliverable forward in Hong Kong's offshore CNY market to measure the

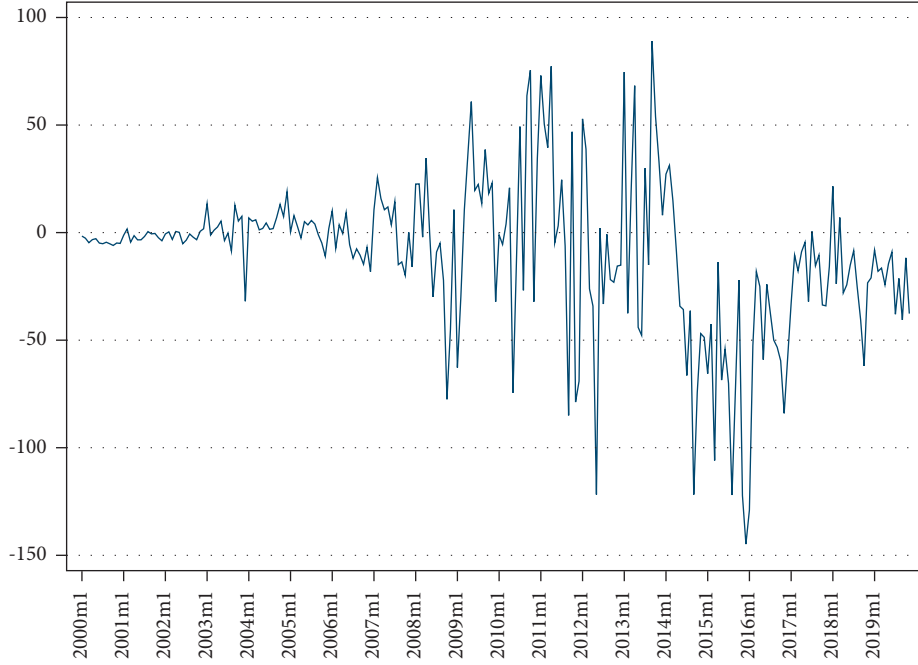


FIGURE 1: The hot money flows in China (billion USD). Source: Authors' calculations.

expected exchange rate of CNY against USD. In the offshore CNY market, CNY/USD exchange rates are in a direct quote. Therefore, the increase in the exchange rate indicates that the market expects CNY depreciation. The data are taken from CEIC Data's Global Database, and we use the log difference of the original data.

- (7) Foreign asset risk: this study uses the market volatility index (VIX) offered by the Chicago Board Options Exchange (CBOE) to measure foreign asset risk. The VIX measures the expected price fluctuations in the S&P 500 index option and is often referred to as the "fear index." The higher the VIX, the higher investors' expected stock market fluctuation risk. The data are taken from the Wind Economic Database.

Table 1 shows the summary statistics of previous variables.

**3.2. SVAR Model Specification.** We have suggested that the SVAR model is more appropriate for this study, and now we discuss the model's specifications. Firstly, we introduce the general method of SVAR model identification. Then, we expound on the model's specification in this study.

We consider a general SVAR model. It consists of  $M$  endogenous variables and  $K$  exogenous variables, and the maximum lag length is  $p$ . The SVAR model is written as follows:

$$Ay_t = A_1^S y_{t-1} + A_2^S y_{t-2} + \dots + A_p^S y_{t-p} + C^S x_t + Bu_t, \quad (11)$$

where  $y_t$  is  $M \times 1$  endogenous variables vector;  $x_t$  is  $K \times 1$  exogenous variables vector; and  $C^S$  is  $M \times K$  coefficients

TABLE 1: Descriptive statistics.

	Mean	Max	Min	SD	p50
P	2.369	8.700	-1.800	1.974	2.100
Y	11.263	23.200	-1.100	4.822	10.300
DAR	0.002	0.600	-0.703	0.170	0.004
EER	-0.001	0.053	-0.033	0.009	-0.001
HM	10.591	89.018	144.799	36.760	-4.481
VIX	19.309	59.890	9.510	8.005	16.860
FAR	-0.014	0.434	-0.951	0.128	0.000

matrix;  $A$ ,  $A_1^S$ ,  $A_2^S$ ,  $\dots$ ,  $A_p^S$ , and  $B$  are  $M \times M$  coefficients matrix. Furthermore,  $u_t$  is a column vector that comprises  $M$  random errors, reflecting the structural innovations. The components of  $u_t$  are independently distributed with zero means, and the correlation matrix of  $u_t$  is a unit matrix. Assuming that matrix  $A$  is nonsingular, left-multiply equation (11) by the inverse of  $A$ , to generate the following:

$$y_t = A^{-1}A_1^S y_{t-1} + A^{-1}A_2^S y_{t-2} + \dots + A^{-1}A_p^S y_{t-p} + A^{-1}C^S x_t + A^{-1}Bu_t. \quad (12)$$

Let  $A_1 = A^{-1}A_1^S$ ,  $A_2 = A^{-1}A_2^S$ ,  $\dots$ ,  $A_p = A^{-1}A_p^S$ ,  $C = A^{-1}C^S$ ,  $\varepsilon_t = A^{-1}Bu_t$ , we have reduced VAR

$$y_t = A_1 y_{t-1} + A_2 y_{t-2} + \dots + A_p y_{t-p} + Cx_t + \varepsilon_t. \quad (13)$$

The specification of exogenous variables: the FAR and foreign asset risk VIX are data from the United States. The United States is the largest economy in the world. According to OECD statistics, the total value of US financial assets is 213,105.459 billion dollars, while the estimated hot money net flow in China in 2018 is -243.3 billion dollars (the negative sign indicates net inflow). Even if we consider the

difference between net value and gross value, hot money flows in China are small compared to the size of the US financial market. Considering that hot money flows in China do not have to be between China and the United States, the impacts of hot money flows from China (to China) on the United States are negligible. Therefore, it is plausible to assume that hot money in China does not affect the US financial market. Therefore, we specify the FAR and the foreign asset risk VIX as exogenous variables.

We can consistently estimate the reduced VAR by the ordinary least square method. We need additional restrictions to identify structural VAR parameters from the reduced VAR. Specifically, we need  $M(M-1)/2$  restrictions for the model with  $M$  endogenous variables.

We add identification conditions based on economic reality. For the convenience of further explanation, it is noted that the variables are ranked in the same order as in Table 1. Because price stickiness, growth rate shocks, and financial market shocks (including DAR, EER, and HM) do not contemporaneously affect inflation rate  $p$ , we assume  $a_{12} = 0$ ,  $a_{13} = 0$ ,  $a_{14} = 0$ , and  $a_{15} = 0$ . Since output adjustment is slow, and this study uses monthly data, we assume that the growth rate will be contemporaneously unaffected by financial market shocks. Then, we have  $a_{23} = 0$ ,  $a_{24} = 0$ , and  $a_{25} = 0$ . One thing that should be pointed out is that we use the nominal growth rate rather than the real growth rate. Then, price shocks will contemporaneously affect the growth rate, and we do not assume  $a_{21} = 0$ . The monetary policy (represented by the official central bank benchmark rate) is a significant and powerful factor determining and affecting China's interbank rate [31]. Other factors are negligible, so we assume  $a_{34} = 0$  and  $a_{35} = 0$ . It takes time for the monetary authority to perceive price and output shocks. It also takes time for the monetary authority to formulate and implement monetary policy to affect domestic asset return rates (the interbank rate in this study). Therefore, we assume that price and output shocks will not contemporaneously impact the domestic interest rate, and we assume that  $a_{31} = 0$  and  $a_{32} = 0$ . Finally, we assume that hot money is not strong enough to affect the expected exchange rate, which means  $a_{45} = 0$ . There are five endogenous variables in the model; therefore, we need at least  $5 \times (5-1)/2 = 10$  restrictions to identify the structural model. Previous analysis suggests 12 short-term restrictions, so the model is identifiable. All the restrictions are summarized as follows:

$$A = \begin{bmatrix} 1 & 0 & 0 & 0 & 0 \\ a_{21} & 1 & 0 & 0 & 0 \\ 0 & 0 & 1 & 0 & 0 \\ a_{41} & a_{42} & a_{43} & 1 & 0 \\ a_{51} & a_{52} & a_{53} & a_{54} & 1 \end{bmatrix} B = \begin{bmatrix} b_{11} & 0 & 0 & 0 & 0 \\ 0 & b_{22} & 0 & 0 & 0 \\ 0 & 0 & b_{33} & 0 & 0 \\ 0 & 0 & 0 & b_{44} & 0 \\ 0 & 0 & 0 & 0 & b_{55} \end{bmatrix}. \quad (14)$$

**3.3. Model Specification Test.** Unit root test: the unit root test results are shown in Table 2, and all variables are stationary.

TABLE 2: Unit root test.

Series	$z$	Constant, trend, and lags	Stationary
P	-3.49	(C, 0, 3)	Yes
Y	-4.78	(C, t, 1)	Yes
DAR	-11.02	(C, 0, 2)	Yes
EER	-13.80	(C, 0, 0)	Yes
HM	-4.30	(C, 0, 2)	Yes
VIX	-4.62	(C, 0, 0)	Yes
FAR	-9.60	(C, 0, 0)	Yes

TABLE 3: Choice of VAR lags.

Lags	FPE	AIC	HQIC	SBIC
1	0.341	13.11	13.39*	13.80*
2	0.318	13.04	13.47	14.10
3	0.321	13.05	13.63	14.49
4	0.301*	12.99*	13.72	14.80

TABLE 4: Granger causality test.

Null hypothesis	F statistics	P value
HM does not Granger cause p	6.210	0.013
p does not Granger cause HM	3.451	0.063
HM does not Granger cause Y	9.594	0.002
Y does not Granger cause HM	7.421	0.006
HM does not Granger cause DAR	0.160	0.689
DAR does not Granger cause HM	0.988	0.320
HM does not Granger cause EER	0.577	0.448
EER does not Granger cause HM	0.824	0.364

Choice of lag length: as shown in Table 3, the Hannan–Quinn information criterion (HQIC) and Schwarz's Bayesian information criterion (SBIC) recommend a model of one lag, whereas the Akaike information criterion (AIC) and final prediction error criterion (FPE) select a model of four lags. In this VAR model that includes five variables, the coefficient number will dramatically increase if we choose four lags. Therefore, to keep the model simple and stable, we choose a model of one lag.

VAR stationary test: we verify that the VAR system is stationary by checking that the reciprocal of the autoregression roots are all in the unit circle. We find that they are in the unit circle; however, the results are not displayed to keep the paper concise.

Granger causality test: this study investigates the Granger causality between hot money and macroeconomic variables, such as the domestic inflation rate, domestic economic growth rate, domestic asset return rate, and the expected exchange rate. The results are summarized in Table 4. The result reveals the existence of bidirectional causality between hot money and the domestic inflation rate and between hot money and the domestic growth rate. No statistically significant evidence supported Granger causality between hot money and the domestic asset return rate and between hot money and expected exchange rate. The main reason for the above results is that hot money, the domestic asset return rate, and the expected exchange rate are financial market variables, and the interactions among them

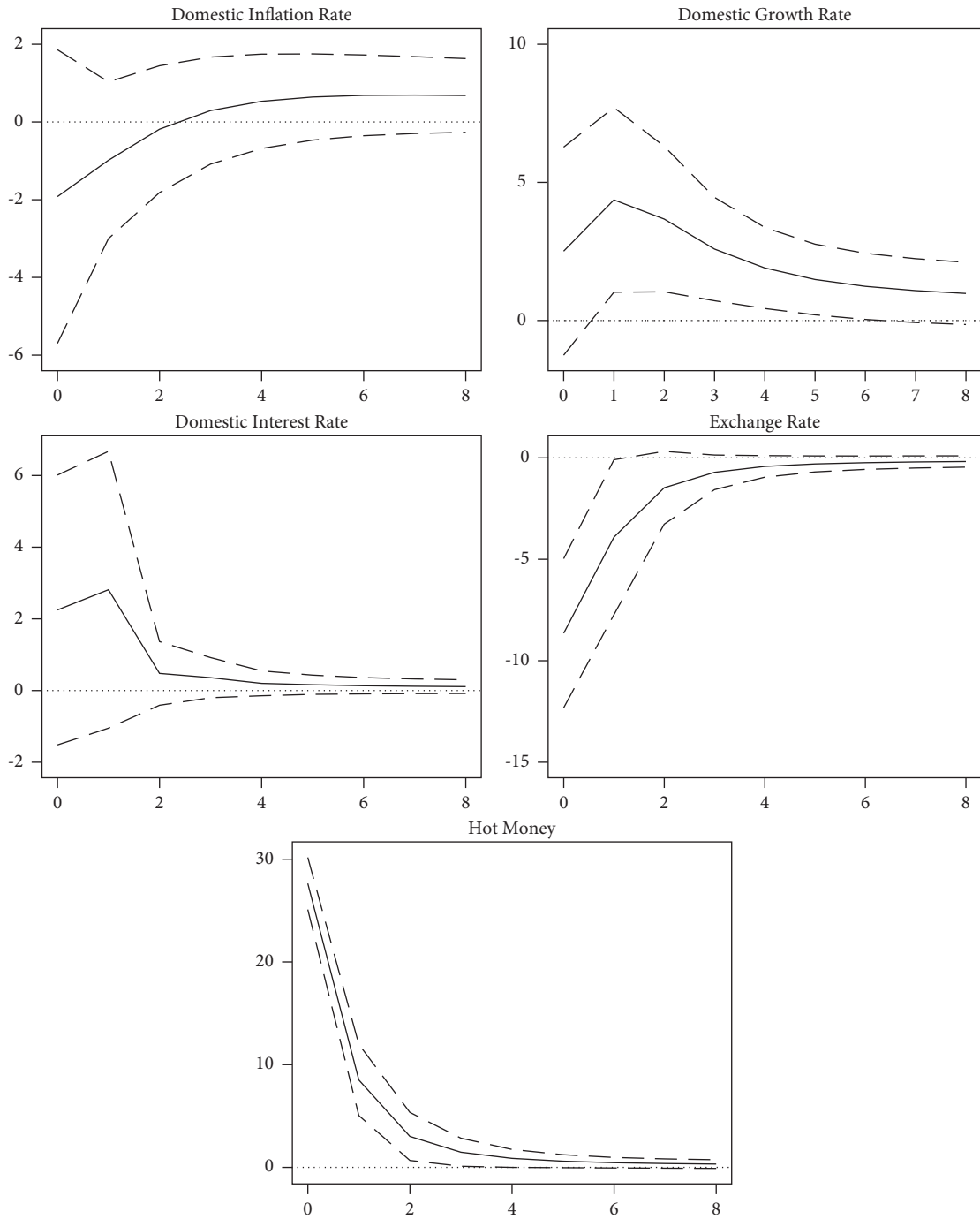


FIGURE 2: Impulse response functions of SVAR (full sample).

are so fast that we can only find a contemporaneous relationship in our monthly data. The discovery corroborates our view that it is necessary to consider contemporaneous relations and use the SVAR model.

*3.4. Impulse Response Analysis.* Because the coefficients in the SVAR model have no clear economic meaning when considered individually, this study uses the impulse response function (IRF) to analyze the economic meaning of the SVAR model. Figure 2 shows the responses of hot

money to a positive standard deviation shock of five variables.

- (i) When there is a positive domestic inflation shock of one standard deviation, hot money outflows increase (inflows decline) in the current period, and the response has diminished ever since. The response diminishes to zero two months later. The response is not statistically significant.
- (ii) When there is a positive domestic growth rate shock of one standard deviation, hot money inflows



increase (outflows decline) in the current period. The response peaks in the next period (month) and has diminished ever since. The response's attenuation is very slow, and the response is still statistically significant after eight periods (months). One standard deviation of  $u_{2t}$  is 2.48, and the response peak is 4.37. Therefore, if the economic growth rate increases by 1%, hot money inflow will increase by 1.76 (4.37/2.48) billion dollars in the next month. Six months later, the response is 1.24. Therefore, if the economic growth rate increases by 1%, the hot money inflow will increase by 0.5 (1.24/2.48) billion dollars even after six months. Therefore, economic growth has a long-term effect on hot money.

- (iii) One positive standard deviation shock in the domestic asset return rate attracts hot money inflow in the current period. The response peaks in the next period (month) and rapidly declines to zero after two months. One standard deviation of  $u_{3t}$  is 0.16, and the hot money response in the current period is 2.25; then, if the domestic return rate increases by 0.1%, hot money inflow will increase by 1.41 ( $2.25 * 0.1/0.16$ ) billion dollars in the current period. The response in the next period is 2.81, which is the peak value. If the domestic return rate increases by 0.1%, hot money inflow will increase by 1.76 ( $2.81 * 0.1/0.16$ ) billion dollars in the next period. The above results are not statistically significant but economically significant.
- (iv) When there is a positive expected exchange rate shock of one standard deviation, hot money responds by peaking in the current period. The response peak is  $-8.64$  billion dollars. The response rapidly declines to  $-3.91$  and  $-1.47$  billion dollars in the next two months, respectively, and it is not statistically significant three months later. One standard deviation of  $u_{4t}$  is 0.0086. When the expected exchange rate increases by 1%, hot money outflow increases by 10.05 ( $86.4 * 1\%/0.0086$ ) billion dollars in the current month and 4.55 ( $3.91 * 1\%/0.0086$ ) billion dollars in the next month. The results are statistically and economically significant.
- (v) For a positive standard deviation shock in hot money, the response of hot money itself over the next three months is 8.51, 3.02, and 1.48 billion dollars, respectively. As the standard deviation of  $u_{5t}$  is 27.6 billion dollars, 10 billion dollars of hot money inflows in the current month will bring in 3.08, 1.09, and 0.54 billion dollars of hot money in the next three months, respectively. It appears that the hot money flow is quite persistent.

Table 5 presents forecast error variance decomposition for hot money in the model over 24 months. The results show that errors in the forecast of the hot money are greatly attributed to other variables than are ascribed to the variables in the model. In the first month, the error in the forecast of the hot money dominated itself. The EER

TABLE 5: Forecast error variance decomposition.

Step	P	Y	DAR	EER	HM
1	0.0043	0.0074	0.0059	0.0875	0.8949
6	0.0054	0.0508	0.0132	0.0918	0.8388
12	0.0079	0.0560	0.0132	0.0912	0.8317
18	0.0095	0.0585	0.0132	0.0908	0.8281
24	0.0104	0.0598	0.0131	0.0906	0.8260

accounts for 9% in the 24th month, while economic growth accounts for about 6%. The inflation and interest rates are insignificant in the forecast of hot money throughout all months.

## 4. Robustness Test

*4.1. Postcrisis Subsample.* In this section, we analyze the subsample after the subprime mortgage crisis to see whether the results in the previous section are robust. We choose the postcrisis subsample for three reasons. Firstly, as shown in Figure 1, the hot money flows in China are greater in volume and variation after the financial crisis. Secondly, financial supervision and regulation policies varied considerably after the financial crisis in China. The internationalization of the CNY and financial opening-up in China progressed steadily during this period, marked by the pilot CNY settlement of cross-border trade, which began in 2009. At last, hot money flows were relatively small before the financial crisis, so the measurement error is a more serious problem for the precrisis subsample.

The postcrisis subsample started in January 2008. The HQIC and SBIC recommend a model of one lag. Furthermore, the model specification and identification conditions are the same as those of the full sample model. Impulse response functions are shown in Figure 3. The qualitative characteristics of the postcrisis subsample IRF are identical to those of the full sample IRF. Next, we quantitatively analyze the subsample IRFs.

- (1) The standard deviation of  $u_{2t}$  is 1.38, and IRF reaches the maximum value of 5.79 one month later. Therefore, when there is a positive shock of 1% of the economic growth rate, hot money inflow will increase by 4.2 (5.79/1.38) billion dollars in the next month.
- (2) The standard deviation of  $u_{3t}$  is 0.12, and IRF reaches the maximum value of 4.22. When the domestic interest rate rises by 0.1%, hot money inflow will increase by 3.52 ( $4.22 * 0.1/0.12$ ) billion dollars in the next month.
- (3) The standard deviation of  $u_{4t}$  is 0.01, and IRF reaches the maximum value of  $-10.44$  in the current period (month). Therefore, when the EER rises by 1%, hot money outflow will increase by 10.44 billion dollars in the current month.

Comparing the postcrisis result with the full sample result, we can see that the impact of all drivers has intensified since the financial crisis. The impact of

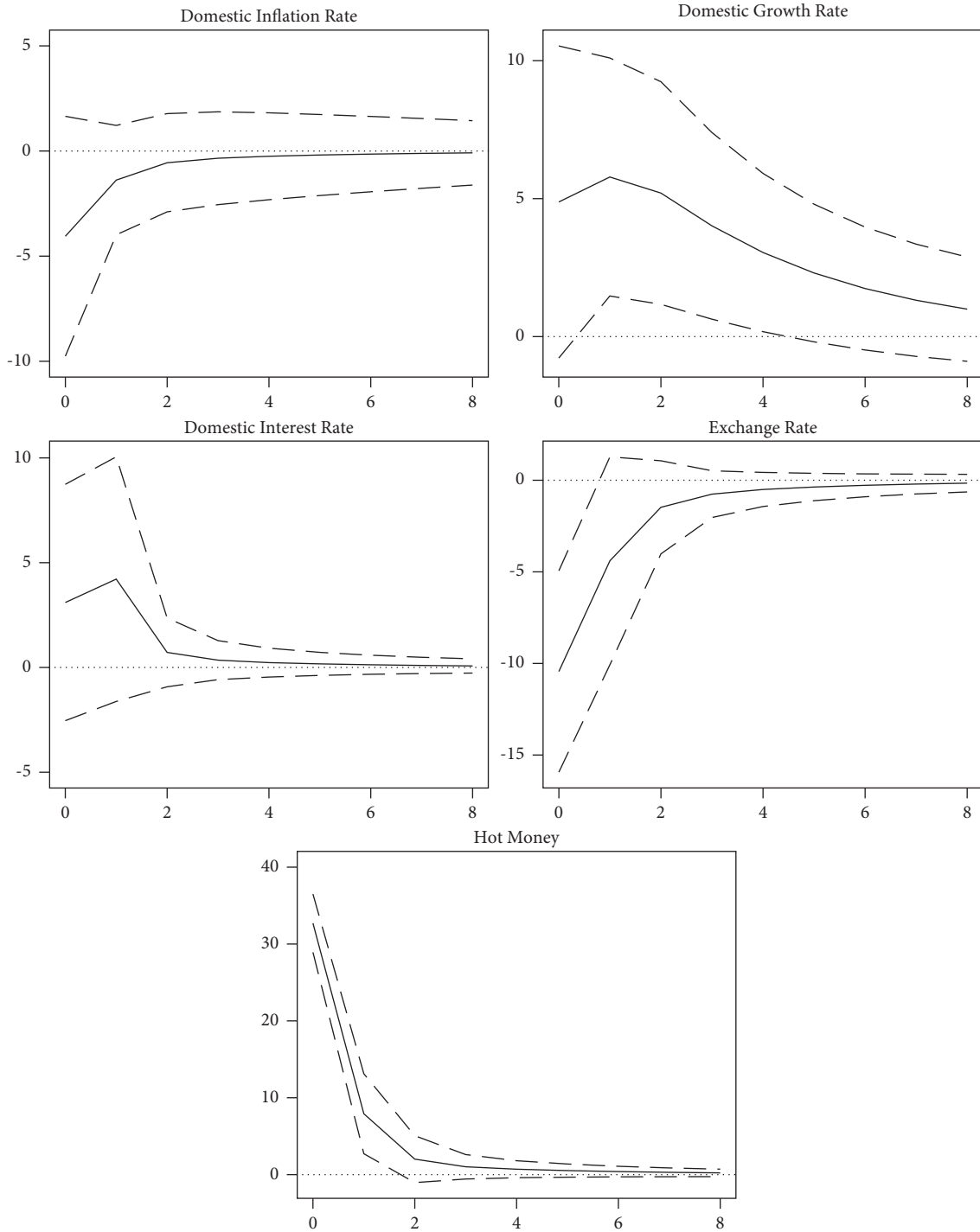


FIGURE 3: Impulse response functions of SVAR (postcrisis subsample).

the economic growth and domestic interest rates increased considerably, while that of the EER increased slightly.

*4.2. Alternative Measurement of Hot Money.* We measure hot money flow in China by an alternative approach to see whether the SVAR model is sensitive to the measurement approach. This section calculates hot money inflow using the following equation: hot money net inflow = variation in

FER-net export-FDI. The sample period is 2000.9–2019.11, as we previously referred to as the full sample. The HQIC and SBIC recommend a model of one lag, and the model specification and identification conditions are the same as those of the full sample model.

Figure 4 shows the IRFs. The estimated matrix B is similar to that of the baseline model, which means that the sizes of standard deviation shocks are similar. We can compare IRFs directly. The two results are qualitatively the

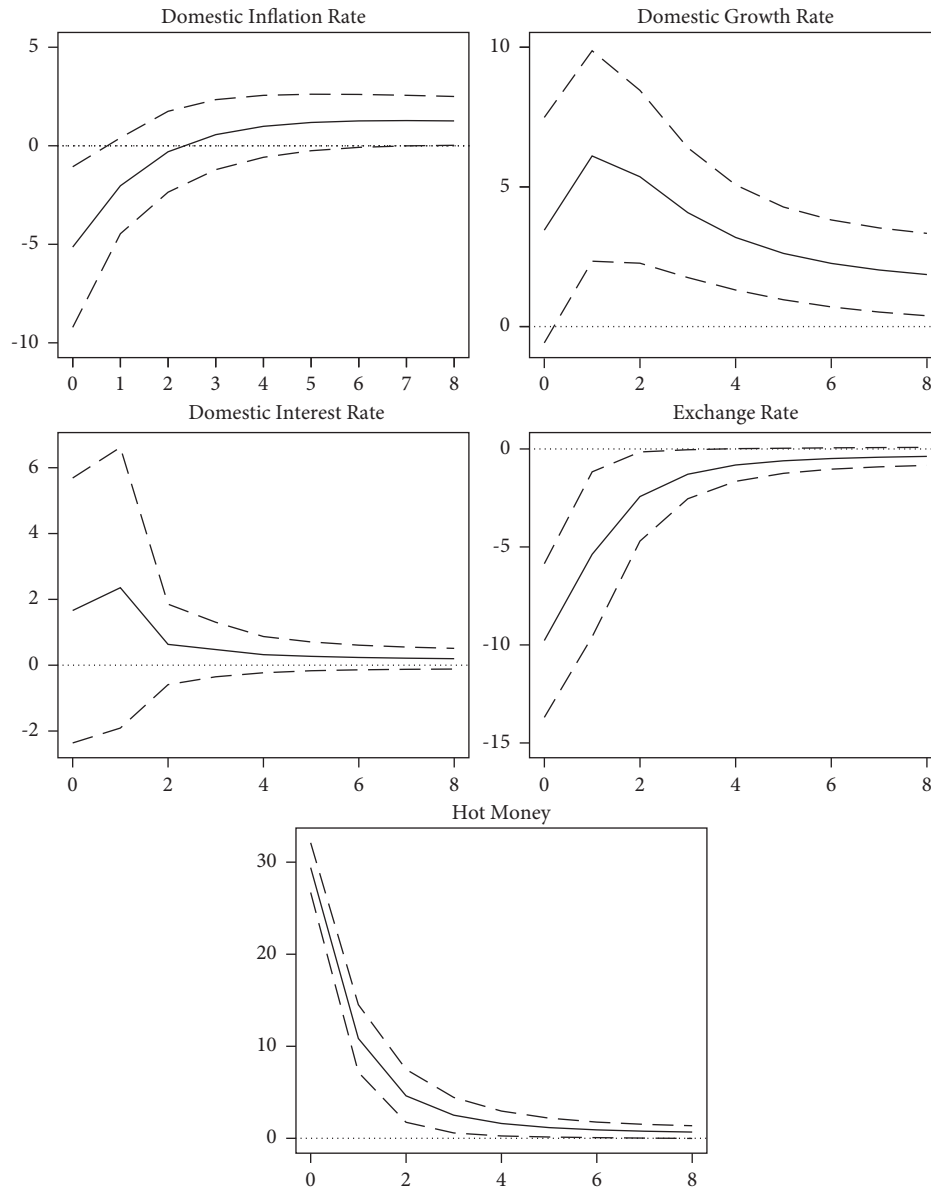


FIGURE 4: Impulse response functions of SVAR (alternative measurement of hot money).

same: hot money negatively responds to price shock. It positively responds to growth rate shock, and the IRF peaks in the next period. Additionally, it positively responds to domestic return rate shock and negatively responds to EER shock. It positively responds to its own shock. IRFs are quantitatively very close, except that hot money's response to price shock is slightly larger.

## 5. Conclusions and Policy Implications

This paper explores the main drivers of hot money and quantifies their influence in China. Firstly, we develop a portfolio decision model from the viewpoint of a foreign investor (speculator) according to expectation-variance utility theory. We show that in the case of the foreign investor holding both long positions of the two countries' assets, the factors that cause the foreign investor to allocate

more wealth to domestic asset and cause hot money net inflows to increase include the following: expected domestic currency appreciation, rise in domestic asset return, drop in the foreign asset return, domestic economic growth, decrease in domestic inflation, and increase in foreign asset risk. Secondly, we estimate the SVAR models and find the empirical results accord with theoretical model predictions. We also find that the expected exchange rate is the most influential of all the hot money drivers, and the domestic growth rate is the most enduring.

The theoretical implications of the study are twofold. The first implication is that the expected exchange rate is the most important driver of hot money in China. The other drivers are not as important as existing theories predicted. The second implication is that the majority of variations in hot money are left unexplained. Therefore, it is necessary to advance a better theory to describe hot money flows, such as

a theory including expectations of political change. Furthermore, the regime shift caused by the adoption of electronic money may also explain part of the variations in hot money flows [32].

The policy implications of this study are as follows: firstly, when hot money flows out, raising the domestic interest rate helps mitigate hot money outflows. Our findings show that the policy effect is not significant, so monetary policy is not an effective policy tool to control capital flight. Secondly, the expected exchange rate is the most influential driver of hot money in the short run. Therefore, it is important to enhance investors' confidence in the domestic economy to reverse the trend of capital flight. Credible policy declaration is an efficient and low-cost way to ameliorate investors' expectations if the monetary authority is trusted, so policy declaration is an ideal way to control hot money. Thirdly, stable economic growth can attract hot money in both the short and long run. Thus, the steady growth of the economy is the ultimate way to keep hot money under control.

### Data Availability

The Foreign Exchange Reserve data, Current Account data, and foreign debts data used to support the findings of this study are deposited on the website of the State Administration of Foreign Exchange of China (<http://www.safe.gov.cn/safe/tjsj1/>). The Foreign Direct Investment and Market Volatility Index data used to support the findings of this study were supplied by Wind Information Technology Company Limited under license and so cannot be made freely available. Requests for access to these data should be made to Wind Information Technology Company Limited ([www.wind.com.cn](http://www.wind.com.cn)). The economic growth rate and Chinese interbank offered rate data used to support the findings of this study were supplied by the Chinese Economic Information Statistics Database under license and so cannot be made freely available. Requests for access to these data should be made to China Economic Information Network ([www.cei.cn](http://www.cei.cn)). The inflation rate data used to support the findings of this study were supplied by China Stock Market and Accounting Research Database under license and so cannot be made freely available. Requests for access to these data should be made to Shenzhen CSMAR Data Technology Company ([www.gtarsc.com/](http://www.gtarsc.com/)). The US dollar LIBOR and 3-month NDF data used to support the findings of this study were supplied by CEIC Data's Global database under license and so cannot be made freely available. Requests for access to these data should be made to CEIC Data (<https://www.ceicdata.com/en>).

### Conflicts of Interest

The authors declared that they have no conflicts of interest.

### Acknowledgments

Hu gratefully acknowledges the financial support of the Anhui Province Federation of Social Sciences (2020CX056) and the Education Department of Anhui Province (SK2021A0654, SK2019A0586).

### References

- [1] J. De Gregorio, S. Edwards, and R. O. Valdés, "Controls on capital inflows: do they work?" *Journal of Development Economics*, vol. 63, no. 1, pp. 59–83, 2000.
- [2] A. Korinek, "Regulating capital flows to emerging markets: an externality view," *Journal of International Economics*, vol. 111, pp. 61–80, 2018.
- [3] A. Chari, K. Dilts Stedman, and C. Lundblad, "Taper tantrums: quantitative easing, its aftermath, and emerging market capital flows," *Review of Financial Studies*, vol. 34, no. 3, pp. 1445–1508, 2021.
- [4] M. B. Devereux and C. Yu, "International financial integration and crisis contagion," *The Review of Economic Studies*, vol. 87, no. 3, pp. 1174–1212, 2019.
- [5] S. Claessens, M. P. Dooley, and A. Warner, "Portfolio capital flows: hot or cold?" *The World Bank Economic Review*, vol. 9, no. 1, pp. 153–174, 1995.
- [6] Y. Zhang, F. Chen, J. Huang, and C. Shenoy, "Hot money flows and production uncertainty: evidence from China," *Pacific-Basin Finance Journal*, vol. 57, Article ID 101070, 2019.
- [7] I.-C. Tsai, M.-C. Chiang, H.-C. Tsai, and C.-H. Liou, "Hot money effect or foreign exchange exposure? Investigation of the exchange rate exposures of Taiwanese industries," *Journal of International Financial Markets, Institutions and Money*, vol. 31, pp. 75–96, 2014.
- [8] D. Kim and S. Iwasawa, "Hot money and cross-section of stock returns during the global financial crisis," *International Review of Economics & Finance*, vol. 50, pp. 8–22, 2017.
- [9] Y.-H. Lee, Y.-L. Huang, and T.-H. Chen, "Does hot money impact stock and exchange rate markets on China?" *Asian Academy of Management Journal of Accounting and Finance*, vol. 13, no. 2, pp. 95–108, 2018.
- [10] C. Yan, "Hot money in disaggregated capital flows," *The European Journal of Finance*, vol. 24, no. 14, pp. 1190–1223, 2018.
- [11] F. Guo and Y. Huang, "Hot money and business cycle volatility: evidence from China," *China and World Economy*, vol. 18, no. 6, pp. 73–89, 2010.
- [12] L. Yang and S. Hamori, "Hot money and business cycle volatility: evidence from selected ASEAN countries," *Emerging Markets Finance and Trade*, vol. 52, no. 2, pp. 351–363, 2016.
- [13] A. Korinek, "Hot money and serial financial crises," *IMF Economic Review*, vol. 59, no. 2, pp. 306–339, 2011.
- [14] M. A. Ali, A. Pervez, R. Bansal, and M. A. Khan, "Analyzing performance of banks in India: a robust regression analysis approach," *Discrete Dynamics in Nature and Society*, vol. 2022, Article ID 8103510, 9 pages, 2022.
- [15] M. A. Khan, P. Roy, S. Siddiqui, and A. A. Alakkas, "Systemic risk assessment: aggregated and disaggregated analysis on selected Indian banks," *Complexity*, vol. 2021, Article ID 8360778, 14 pages, 2021.
- [16] M. Martin and W. Morrison, "China's "hot money" problems," Congressional Research Service Report, Washington DC, 2008.
- [17] X. Fang, P. Pei, and Y. Zhang, "International speculative capital inflow: motivations and shocks - an empirical test based on the 1999–2011 sample data of mainland China," *Journal of Financial Research*, vol. 33, pp. 67–77, 2012, in Chinese.
- [18] Y.-W. Cheung and X. Qian, "Capital flight: China's experience," *SSRN Electronic Journal*, vol. 14, 2010.

- [19] Y. Zhang and X. Shen, "An empirical Research on the appreciation of RMB, rising of stock price and hot money inflow," *Journal of Financial Research*, vol. 30, pp. 87–98, 2008, in Chinese.
- [20] Y. Zhao, J. de Haan, B. Scholtens, and H. Yang, "The dynamics of hot money in China," in *Proceedings of the BOFIT and CityU HK Conference on Renminbi and the Global Economy*, vol. 30, Hong Kong, China, May 2013.
- [21] G. Zhang and H. G. Fung, "On the imbalance between the real estate market and the stock markets in China," *The Chinese Economy*, vol. 39, no. 2, pp. 26–39, 2006.
- [22] F. Guo and Y. S. Huang, "Does "hot money" drive China's real estate and stock markets?" *International Review of Economics & Finance*, vol. 19, no. 3, pp. 452–466, 2010.
- [23] J. S. Davis, G. Valente, and E. van Wincoop, "Global drivers of gross and net capital flows," *Journal of International Economics*, vol. 128, Article ID 103397, 2021.
- [24] H. Yang and F. Shi, "The dynamics and driving factors of China's hot money flows since the financial crisis of 2007," *Management Review*, vol. 28, pp. 12–19, 2016, in Chinese.
- [25] T. Cai, V. Q. T. Dang, and J. T. Lai, "China's capital and "hot" money flows: an empirical investigation," *Pacific Economic Review*, vol. 21, no. 3, pp. 276–294, 2016.
- [26] S. Steinkamp and F. Westermann, "Development aid and illicit capital flight: evidence from Nepal," *The World Economy*, 2021.
- [27] M. Fratzscher, M. Lo Duca, and R. Straub, "On the international spillovers of US quantitative easing," *The Economic Journal*, vol. 128, no. 608, pp. 330–377, 2017.
- [28] U. Malmendier, D. Pouzo, and V. Vanasco, "Investor experiences and international capital flows," *Journal of International Economics*, vol. 124, Article ID 103302, 2020.
- [29] Y. Kroll, H. Levy, and H. M. Markowitz, "Mean-variance versus direct utility maximization," *The Journal of Finance*, vol. 39, no. 1, pp. 47–61, 1984.
- [30] J. Hanson, S. V. Wijnbergen, K. T. Yurukogl et al., *World Development Report 1985*, Oxford University Press, New York, NY, USA, 1985.
- [31] N. Porter and T. Xu, "Money-market rates and retail interest regulation in China: the disconnect between interbank and retail credit conditions," *International Journal of Central Banking*, vol. 12, pp. 143–198, 2016.
- [32] M. A. Khan, "Netizens' perspective towards electronic money and its essence in the virtual economy: an empirical analysis with special reference to Delhi-ncr, India," *Complexity*, vol. 2021, Article ID 7772929, 18 pages, 2021.

## Research Article

# Estimation for Akshaya Failure Model with Competing Risks under Progressive Censoring Scheme with Analyzing of Thymic Lymphoma of Mice Application

Tahani A. Abushal <sup>1</sup>, Jitendra Kumar,<sup>2</sup> Abdisalam Hassan Muse <sup>3</sup>,  
and Ahlam H. Tolba <sup>4</sup>

<sup>1</sup>Department of Mathematical Science, Faculty of Applied Science, Umm Al-Qura University, Mecca, Saudi Arabia

<sup>2</sup>Directorate of Economics and Statistics, Planning Department, New Delhi, India

<sup>3</sup>Department of Mathematics (Statistics Option) Programme, Pan African University, Institute for Basic Science, Technology and Innovation (PAUSTI), Nairobi, 6200-00200, Kenya

<sup>4</sup>Department of Mathematics, Faculty of Science, Mansoura University, Mansoura 35516, Egypt

Correspondence should be addressed to Tahani A. Abushal; [taabushal@uqu.edu.sa](mailto:taabushal@uqu.edu.sa) and Abdisalam Hassan Muse; [abdisalam.hassan@amoud.edu.so](mailto:abdisalam.hassan@amoud.edu.so)

Received 19 November 2021; Accepted 5 May 2022; Published 30 June 2022

Academic Editor: Junhai Ma

Copyright © 2022 Tahani A. Abushal et al. This is an open access article distributed under the Creative Commons Attribution License, which permits unrestricted use, distribution, and reproduction in any medium, provided the original work is properly cited.

In several experiments of survival analysis, the cause of death or failure of any subject may be characterized by more than one cause. Since the cause of failure may be dependent or independent, in this work, we discuss the competing risk lifetime model under progressive type-II censored where the removal follows a binomial distribution. We consider the Akshaya lifetime failure model under independent causes and the number of subjects removed at every failure time when the removal follows the binomial distribution with known parameters. The classical and Bayesian approaches are used to account for the point and interval estimation procedures for parameters and parametric functions. The Bayes estimate is obtained by using the Markov Chain Monte Carlo (MCMC) method under symmetric and asymmetric loss functions. We apply the Metropolis–Hasting algorithm to generate MCMC samples from the posterior density function. A simulated data set is applied to diagnose the performance of the two techniques applied here. The data represented the survival times of mice kept in a conventional germ-free environment, all of which were exposed to a fixed dose of radiation at the age of 5 to 6 weeks, which was used as a practice for the model discussed. There are 3 causes of death. In group 1, we considered thymic lymphoma to be the first cause and other causes to be the second. On the base of mice data, the survival mean time (cumulative incidence function) of mice of the second cause is higher than the first cause.

## 1. Introduction

In several lifetime experiments of survival and reliability analysis, the cause of death or failure of subjects may be characterized by more than one cause. Consider an example involving more than one cause of failure, Hoel [1] supported a laboratory survival experiment where the mice were given a dose of radiation at 6 weeks of age. In this experiment, there is more than one cause of death. The researcher records the causes of death as reticulum cell sarcoma, thymic lymphoma, or others. We discussed one more example in

which the cause of the death of the subject was recorded as breast cancer or other cancer presented by Boag [2]. In reliability experiments, there are promiscuous examples where subjects may fail due to one among all causes. In traditional analysis of survival samples, first, the experimenter is interested in the lifetime distribution under single cause of failure, such as heart attack or cancer, and any other causes are combined and/or considered as censored data. In the last decade, the scientist considered the different types of failure distribution for specific risk and developed the model for two or more causes of failure. In competing risk models,

there are two observable variables considered, one is the failure time and second is the indicator variable, denoting the failure and specific cause of failure of the item or individual, respectively.

In literature, many authors considered the independent and dependent cause of failure rates. For instance, Sarhan et al. [3] discussed the competing risks model with the presence of covariates using Weibull subdistributions. In this regard and in most situations, the statistical analysis of competing risk sample data assumes independent and/or dependent causes of failure. Abushal [4] studied the parametric inference of Akash distribution with type-II censoring with analyzing of relief times of patients. Abushal [5] studied the Bayesian estimation of the reliability characteristic of Shanker distribution. Furthermore, Tan [6] developed a probabilistic conditional model to evaluate the efficient estimate of component failure probabilities in the binomial system testing-masked data using EM algorithm. He also discussed the accuracy and capability of the probabilistic model in this case when the system configurations are in series and parallel. Sarhan et al. [7] considered the geometric distribution for components lifetimes and obtained ML and Bayes estimators for the component reliability measures in a multicomponent system in the presence of partial dependent masked system life test data. Sarhan and Kundu [8] discussed the masked system lifetime data from geometric distribution and obtained Bayes estimators of the parameters and component reliability function when the prior information of success probabilities assumed to be beta population. They also discussed the Bayesian procedure for obtaining minimum posterior risk associated with parametric function under square error loss function. Jiang [9] considered the Poisson shock model using masked system life data and obtained ML and Bayes estimator of parameter and survival function of each component with influence of the making level. Almarashi et al. [10] considered the two causes of failure, where the lifetime units come from the exponential failure distribution. The units is censored under a hybrid progressive type-I censoring scheme. They have discussed maximum likelihood and Bayesian estimation procedure with their asymptotic confidence as well as the Bayesian credible intervals, respectively. Almalki et al. [11] discussed the statistical analysis of type-II censored competing risks data under reduced new modified Weibull baseline. Abushal et al. [12] considered the two independent cause of failure under type-I censoring scheme and obtained the ML and Bayes estimate of given parameter of the lifetime model. They also presented the confidence intervals of unknown parameters under both paradigm. For more reading, see [12]. The numerical procedures used to characterise the quality of theoretical conclusions are examined via the analysis of actual data and Monte Carlo simulations.

Although the assumption of cause dependence may be more realistic, there is some anxiety about the identifiability of the underlying lifetime model. The authors [13, 14] and several more authors such as in [15–17] have argued that without information on covariance, it is not possible to use the sample data of experiment, such as the assumption of independent failure times. Competing risks models are

studied by several authors based on both dependent and/or independent causes of failures with parametric and non-parametric setup [14, 18, 19]. It is assumed, in the parametric setup, that the risks follow a variety of lifetime distributions.

All researchers have the same goal in mind: to examine the competing risk data. This information is from their experiments, which could be in areas such as demography, engineering, life science, health management, and so on. The main focus of an analytic technique is on statistics that can be used to plan future events. Modeling data can be obtained in a variety of ways, both basic and complicated. A well-established methodology is to fit the data using a distribution-based procedure and then acquire the relevant statistics. The advantage of this strategy is that once a good model for the gathered observations in an experiment is found, all of the model's properties can be used immediately. However, nowadays, the biggest challenge is searching for an appropriate model for the study.

Shankar and Ramadan et al. [20, 21] proposed a new one-parameter continuous distribution named Akshaya distribution and its generalized power Akshaya distribution for lifetime modeling in medical and engineering science. The behavior of hazard function of Akshaya distribution is increasing or decreasing (based on its parameter), so this distribution is flexible to throughout used to analysis of real area. Various properties of Akshaya distribution are discussed by Shankar [20]. They obtained the maximum likelihood estimator of parameter when cause of failures are either unknown or known. Shankar [20] discussed the statistical properties of Akshaya distribution and calculate the maximum likelihood function for complete and censored sample situation. They show the fitting the real data set and analysis for it.

In life-testing experiments, researchers conduct tests on human beings, electrical appliances, natural, and in many more aspects. In such studies, the primary objective is to understand the basic nature of observed lifetimes. Generally, conducting life-testing experiments is time taking and expensive which demands a large amount of money, labor, and time. For reducing the cost and time of the experiments, various types of censoring schemes are developed in the literature. The censoring is inevitable in reliability and life-testing experiment, and the researcher is unable to achieve overall information for all individuals. Censoring in a life-testing experiment occur when the experiment is terminated before the failure of all the units put to test. The decision of termination the experiment is taken according to any available censoring scheme. In the clinical trial, example, the patients may depart from the trial and the experiment may have to be restricted at a prefixed time point. The experiment subjects may fail accidentally in industrial experiments.

In many research, the removal of units at given failure is preplanned in order to provide resources such cost associated with testing and savings in terms of time. The type-II and type-I censoring schemes are two most usual and regular censoring schemes in life experiment. However, in some life experiments, some number of patients leave the experiments cannot be prefixed and which are random. Here, we consider the independent competing risk or multiple failure data

under progressive type-II censored with binomial removal. Cohen [22] considered the sample specimens that remain after each step of censoring are observed until they fail or until a future stage of censoring is performed. They explained that the maximum likelihood estimators for the normal and exponential distributions are generated when the data are gradually suppressed. A novel technique based on regression to estimate unknown parameters of the Pareto distribution using the progressive type-II censoring scheme is proposed by Seo et al. [23]. Kishan and Kumar [24] discussed the Bayesian estimation for the Lindley distribution under progressive type-II censoring with binomial removals. Salah et al. [25] obtained the estimate of the parameter of the two-parameter-power exponential distribution under progressive type-II censored data with fixed shape parameter. Li and Gui [26] obtained the ML estimates with their confidence intervals for the parameter of generalized Pareto distribution. They present Bayes estimators by using the Adaptive Rejection Metropolis Sampling algorithm to derive the point estimate and credible intervals. In this continuation, the authors also find the estimates of survival function and hazard function of the distribution. The Monte Carlo simulation study is carried out to compare the performances of the three proposed methods based on different data schemes. The broad list of related references and further details on progressive censored sample may refer to [27, 27–29].

The process of the progressive scheme is as follows: first, the experimenter put  $n$  subject on test at the introductory period. At initially stage, we assume the total number of failure  $m$  and binomial probability  $p$  in advance. On the basis of  $n, m$ , and  $p$ , generate the censored values  $R_1, R_2, \dots, R_m$  for further analysis. At the first failure of unit, the time  $T_{1:m:n}$  is observed and  $R_1$  of surviving units is selected using simple random sampling without replacement (SRSWOR) and removed from  $n - 1$  surviving unit. At the second failure from  $n - m - R_1$  unit, we get the failure time  $T_{2:m:n}$  and  $R_2$  of surviving units is randomly selected and removed from the experiment. At the  $i^{\text{th}}$  failure, the time  $T_{i:m:n}$  is observed and  $R_i$  of surviving units is randomly selected with SRSWOR from  $n - m - \sum_{j=1}^{i-1} R_j$  units and removed. Similarly, when the  $(m - 1)^{\text{th}}$  subject fails,  $T_{m-1:m:n}$  is observed and  $R_{m-1}$  of surviving units is removed from the  $n - m - \sum_{j=1}^{m-2} R_j$  unit. At the termination of the experiment, i.e.,  $m^{\text{th}}$  failure,  $T_{m:m:n}$  failure time is observed and all remaining units, i.e.,  $R_m = n - m - \sum_{i=1}^{m-1} R_i$ , are completely removed from the experiment and stopped the experiment, when the censoring scheme  $R_i, i = 1, 2, \dots, m$  is all prefixed [22].

In competing risk scenario, the data from the progressive type-II censoring with binomial removal is as follows. Here,  $(T_{1:m:n}, R_1, \delta_1), (T_{2:m:n}, R_2, \delta_2), \dots, (T_{m:m:n}, R_m, \delta_m)$  denoted the total observed failure times,  $\delta_1 < \delta_2 < \dots < \delta_m$  indicate the cause of failure,  $R_1, R_2, \dots, R_m$  denote the number of subjects removed from the experiment at the respected failure times  $t_{1:m:n} < t_{2:m:n} < \dots < t_{m:m:n}$ . Since, we observed that the type-II censoring and complete sample are the special case of the progressive type-II censoring

scheme by putting  $R_1 = R_2 = \dots = R_{m-1} = 0, R_m = n - m$  and  $R_1 = R_2 = \dots = R_m = 0$ , respectively.

The state of research on competing risk models is steadily growing. As a baseline hazard rate, many probability distributions for the number of competing causes of the event of interest have been offered. An interesting survey for the classical distributions and their survey can be referred to [30–35]. Table 1 shows the chronological review on the competing risk models under progressive censoring scheme with different baseline distributions.

The main goal of this paper is to explicate the competing risks model under progressive type-II censored with binomial removals. We considered that the cause of failure are mutually independent and follows to Akshaya distribution. We have drive the point and interval estimation of the parameter and its function under the classical and Bayesian paradigm. In the Bayesian estimation procedure, the experimenter considered the three loss function (one is symmetric and two are asymmetric) under gamma prior.

The paper is organized in the following frame. Section 2 describes the competing risk model based on progressive censored sample for Akshaya distribution. In Section 3, we drive the maximum likelihood function and obtain the maximum likelihood estimator of given parameter. The estimator of the component reliability and cumulative incidence function is also discussed here. The two-sided asymptotic confidence intervals of the unknown parameters included in the model. Furthermore, in Section 4, we discuss the Bayes estimators of parameter with two-sided Bayesian intervals. The Bayesian procedure is driven by the Markov chain Monte Carlo (MCMC) technique by using the prior information. The Bayesian confidence intervals are also discussed here. Finally, in Section 5, the reviewed methodologies are illustrated with simulation data. Analysis of a real data set is provided in Section 6 to illustrate the use of the method applied in this paper.

## 2. Model Assumptions

In life-testing experiment, we consider that there are  $n$  identical and independent (iid) subjects put in test. Every subject of the test works under some risk factors such as cause of failure. So, each subject assign  $k, k > 2$ , and cause of failure. Since any one subject fails by only one cause among all causes, we noted the cause of failure and study about the environment of the all cause because some causes have low and some have high risk. In a life test, some countable subjects may fail or be removed or be censored during the test. So, the test will be terminated when it fails or reach to a censoring time. There are two noticeable quantities for the failed subject. These quantities are the subject life time ( $T_i$ ) and the cause of failure ( $\delta$ ), say  $\delta = \{1, 2, \dots, k\}$ . In the censoring scheme, there is only one quantity which is the censoring time and we set it as  $\delta = 0$ . Also, we need the following assumptions throughout this paper:

- (1) We put  $n$  iid subjects on the life time test and the given test is terminated at the  $m^{\text{th}}$  failure,  $m \leq n, m$ .



TABLE 1: Chronological review on competing risk models under progressive censoring scheme and their baseline distributions.

S. no.	Developers (year)	Competing risk model based on progressive censoring scheme
1	Debasis et al. (2003)	Discussed the analysis of progressively censored competing risks data [36].
2	Pareek et al. (2009)	Explored the application of Weibull distribution to competing risk model under progressive censoring scheme [37].
3	Debasis and Biswabrata (2011)	Discussed the Bayesian analysis of progressive censored competing risks data [38].
4	Bundel et al. (2016)	Applied the inverse Lindley distribution for modeling competing risks for progressive censored data [39].
5	Kumar et al. (2016)	Studied the Bayesian analysis of modified Weibull distribution under progressive censored competing risk model [40].
6	Liang (2018)	Used the Kumaraswamy distribution to model competing risk data under progressive censored data [41].
7	Hongyi and Wenhao (2019)	Used the Rayleigh distribution to model competing risk data under progressive type-II censored data [42].
8	Manoj and Rakhi (2019)	Presented the Bayesian analysis of Weibull distribution based on progressive type-II censored competing risks data with binomial removals [43].
9	Ahmed et al. (2020)	Introduced the inference of progressive type-II censored competing risks data from Chen distribution [44].
10	Fariba et al. (2020)	Presented the inference for competing risks model under progressive interval censored using Weibull data [45].
11	Shuhan and Wenhao (2020)	Discussed the estimation of the parameters of the two-parameter Rayleigh distribution based on adaptive type-II progressive hybrid censored data with competing risks [46].
12	Chandrakant et al. (2021)	Presented the analysis of a progressively censored competing risks data using Gompertz distribution [47].
13	El-Rahem et al. (2021)	Used the extension of the exponential distribution to model competing risk under progressive censoring scheme [48].
14	Almarashi et al. (2021)	Used exponential lifetimes for modeling competing risk model with the presence of joint hybrid censoring scheme [10].
15	Elshahhat (2021)	Introduced using Xgamma under type-II adaptive progressive hybrid censoring
16	Kumar et al. (2021)	Presented the inference for partially observed competing risks model for Kumaraswamy distribution under generalized progressive hybrid censoring [49].
17	Yuge and Wenhao. (2022)	Presented Burr-XII distribution under adaptive type-II progressive censored schemes with the presence of competing risks data [50].
18	Qi et al. (2022)	Presented the statistical inference for the Gompertz distribution under general progressive type-II censored competing risks sample [51].

There are  $k, k \geq 2$  mutually independent causes of failure engaged to each object.

- (2) Assume that  $T_i$  is the lifetime of  $i (i = 1, 2, \dots, N)$  subject with cumulative distribution function (*cdf*)  $F(\cdot)$ ,  $\bar{F}(\cdot)$  is the survival function of  $T_i$ , and  $f(\cdot)$  is the probability density function (*pdf*) of  $T_i$ .
- (3) Assume that  $T_{ji}$  is the lifetime of  $j (j = 1, 2, \dots, k)$  cause with *cdf*  $F_j(\cdot)$ ,  $\bar{F}_j(\cdot)$  is the survival function of  $T_{ji}$ ,  $f_j(\cdot)$  is the *pdf*, and  $h_j(\cdot)$  is the hazard rate function of  $T_{ji}$ .
- (4) Assume that  $\delta_i, (i = 1, 2, \dots, n)$  is integer observable variables signifying the cause of failure of  $i^{\text{th}}$  system or censored data.
- (5) At the first failure,
  - (a) We observed two observable quantities  $T_{1:m:n}$  and  $\delta_1 \in \{1, 2, \dots, k\}$ , and
  - (b) The surviving subject, say  $R_1$ , is removed randomly where the removed  $R_1$  follows binomial distribution with parameters  $n - m$  and  $p$ . Here, we assume that

the binomial parameter  $p$  is predefined as based on the required environment scenario.

- (6) In the continuation, when the  $i^{\text{th}}$  subject fails  $i = 1, 2, \dots, (m - 1)$ : (a) we observed the two quantities  $T_i$  and  $\delta_i$ . (b) The surviving subject, say  $R_i$ , is randomly removed provided that  $R_i$  follows binomial distribution with parameters  $n - m - \sum_{j=1}^{i-1} R_j$  and  $p$ .
- (7) At the last failure or termination of the experiment, i.e.,  $m^{\text{th}}$  failure, we observed the following quantities  $T_{m:m:n}$  and  $\delta_m$ . Secondly, the rest of the survival subject  $R_m (= n - \sum_{j=1}^{m-1} R_j - m)$  is completely removed from the experiment.
- (8) Here,  $\delta_i = j, j = 1, 2, \dots, k$  denotes the unit  $i$  has failed due to cause  $j$  at time  $X_{i:m:n}$ .
- (9) For the given study, the parameter  $p$  of the binomial distribution is to be considered same in the whole experiment.
- (10) We assume that the random variable  $T_{ji}$  follows Akshaya distributions with unknown parameter  $\theta_j$ ,

say Akshaya  $(\theta_j)$ , for  $i = 1, 2, \dots, n$  and  $j = 1, 2, \dots, k$ , i.e.,  $T_{ji}$  has the *cdf*

$$F_j(t) = 1 - \left[ 1 + \frac{\theta_j^3 t^3 + 3\theta_j^2(\theta_j + 1)t^2 + 3\theta_j(\theta_j^2 + 2\theta_j + 2)t}{\theta_j^3 + 3\theta_j^2 + 6\theta_j + 6} \right] e^{-\theta_j t}. \quad (1)$$

and the survival function of Akshaya distribution is given by

$$h_j(t) = \frac{\theta_j^4 (1+t)^3}{\theta_j^3 t^3 + 3\theta_j^2(\theta_j + 1)t^2 + 3\theta_j(\theta_j^2 + 2\theta_j + 2)t + (\theta_j^3 + 3\theta_j^2 + 6\theta_j + 6)}, \quad (3)$$

where  $\theta_j$  is the shape parameter. Based on the above discussed assumptions, the observed data  $(T_{j1: m: n}, \delta_1, R_1), (T_{j2: m: n}, \delta_2, R_2), \dots, (T_{jm: m: n}, \delta_m, R_m)$  is the type-II progressive censored sample, where  $T_{j1: m: n} < T_{j2: m: n} < \dots < T_{jm: m: n}$  indicate the failure time of  $m$  observation. Now,  $\delta_i, i = 1, 2, \dots, m$  denote the respected causes of  $i^{\text{th}}$  failures, and  $R_i, i = 1, 2, \dots, m$  indicate the number of units which are randomly selected and removed from the experiment at the respected failure times  $T_{j1: m: n} < T_{j2: m: n} < \dots < T_{jm: m: n}$ . We will use henceforth  $T_{ji}$  instead of  $T_{ji: m: n}, j = 1, 2, \dots, k$  to simplify the given notation.

**2.1. Cumulative Incidence Function (CIF).** A very interested quantity in the competing risk is cumulative incidence function. It is defined as the risk when other causes are present in the experiment. The CIF provides the estimate quantity of the cumulative probability of locoregional recurrences in the presence of other causes. In presence of competing risks, the probability for occurrence of each event of type  $j$  out of the possible event types  $i = 1, 2, \dots, k$ , up to a

$$\overline{F}_j(t) = \left[ 1 + \frac{\theta_j^3 t^3 + 3\theta_j^2(\theta_j + 1)t^2 + 3\theta_j(\theta_j^2 + 2\theta_j + 2)t}{\theta_j^3 + 3\theta_j^2 + 6\theta_j + 6} \right] e^{-\theta_j t}. \quad (2)$$

and the hazard function is

mission time  $t^*$ , can be described in term of  $\mathcal{C}$  for event type  $j$ . The  $\mathcal{C}$  of  $j^{\text{th}}$  cause is

$$\begin{aligned} \mathcal{C}_j &= P(T_{ij} \leq t^*, \delta = j) \\ &= \int_0^{t^*} h_j(u|x)S(u)du, \end{aligned} \quad (4)$$

where  $h_j$  is the cause-specific hazard rate which is the hazard function allied with a specific cause when there are multiple events under consideration and  $S(u)$  is overall survival function.

### 3. Maximum Likelihood Estimates

Now, we discuss parameter estimation for this model. We define the likelihood function of observed sample of  $T_{1: m: n}, T_{2: m: n}, \dots, T_{m: m: n}$  from InvMWD under progressively type-II censored binomial removals. On the basis of the available data obtained in the previous section, the likelihood function of given data can be written as

$$L(\theta; t, \delta; R) = L_1(\theta; t, \delta | R = r)P(R, p), \quad (5)$$

where

$$L_1(\theta; t, \delta | R = r) = \prod_{i=1}^n \left[ \prod_{j=1}^k \left[ f_j(t_i) \prod_{\substack{l=1 \\ l \neq j}}^k \overline{F}_j(t_i) \right]^{I(\delta_i = j)} [\overline{F}(t_i)]^{I(\delta_i = 0)} [\overline{F}(t_i)]^{r_i} \right]. \quad (6)$$

and  $\theta = (\alpha_1, \alpha_2, \dots, \alpha_k, \beta_1, \beta_2, \dots, \beta_k)$ .

From the relation between the survival function, the hazard rate, and *pdf*, the likelihood function becomes

$$L_1(\theta; t, \delta | R = r) = \left[ \prod_{i=1}^n \prod_{j=1}^k [h_j(t_i)]^{I(\delta_i = j)} \right] \left[ \prod_{i=1}^n \prod_{j=1}^k [\overline{F}_j(t_i)]^{r_i + 1} \right]. \quad (7)$$

Now, the number of items randomly selected and removed at the failure time of subject where removal follows to the binomial distribution with parameter  $p$ , such that

$$P(R_1 = r_1) = \binom{n-m}{r_1} p^{r_1} (1-p)^{n-m-r_1},$$

$$P(R_i = r_i | R_{i-1} = r_{i-1}, \dots, R_1 = r_1) = \binom{n-m - \sum_{l=1}^{i-1} r_l}{r_i} p^{r_i} (1-p)^{n-m - \sum_{l=1}^i r_l}, \quad (8)$$

where  $0 \leq r_i \leq n-m - \sum_{l=1}^i r_l$ ,  $i = 1, 2, \dots, m-1$ . At the last failure in the experiment, the remaining items, if exist, are removed from the experiment with probability one. In

this regard, it is assumed that  $R_i$  and  $T_i$  are mutually independent for all  $i$ . Then,

$$P(R, p) = P(R_1 = r_1)P(R_2 = r_2 | R_1 = r_1) \dots P(R_m = r_m | R_{m-1} = r_{m-1}, \dots, R_1 = r_1). \quad (9)$$

Therefore,

$$P(R, p) = \frac{(n-m)!}{(n-m - \sum_{i=1}^{m-1} r_i)! \prod_{i=1}^{m-1} r_i!} p^{\sum_{i=1}^{m-1} r_i} (1-p)^{(n-m)(m-1) \sum_{i=1}^{m-1} r_i (m-i)}. \quad (10)$$

Substituting the expression of equations (7) and (10) into (5), the observed likelihood function takes the following form:

$$L(\theta; t, \delta; R) \propto \left[ \prod_{i=1}^n \prod_{j=1}^k [h_j(t_i)]^{I(\delta_i=j)} \right] \left[ \prod_{i=1}^n \prod_{j=1}^k [\bar{F}_j(t_i)]^{r_i+1} \right] \quad (11)$$

$$\times p^{\sum_{i=1}^{m-1} r_i} (1-p)^{(n-m)(m-1) \sum_{i=1}^{m-1} r_i (m-i)}.$$

$$\alpha \left[ \prod_{i=1}^n \prod_{j=1}^k \left[ \frac{\theta_j^4 (1+t_i)^3}{\theta_j^3 t_i^3 + 3\theta_j^2 (\theta_j+1) t_i^2 + 3\theta_j (\theta_j^2 + 2\theta_j + 2) t_i + (\theta_j^3 + 3\theta_j^2 + 6\theta_j + 6)} \right]^{I(\delta_i=j)} \right]$$

$$\left[ \prod_{i=1}^N \prod_{j=1}^K \left[ 1 + \frac{\theta_j^3 t_i^3 + 3\theta_j^2 (\theta_j+1) t_i^2 + 3\theta_j (\theta_j^2 + 2\theta_j + 2) t_i}{\theta_j^3 + 3\theta_j^2 + 6\theta_j + 6} \right] e^{-\theta_j t} \right]^{(r_i+1)} \quad (12)$$

$$\times p^{\sum_{i=1}^{m-1} r_i} (1-p)^{(n-m)(m-1) \sum_{i=1}^{m-1} r_i (m-i)}.$$

Thus, the log-likelihood function takes the natural logarithm of equation (12) and defined in the following form:

$$\begin{aligned}
\mathcal{L} &= \sum_{j=1}^k \sum_{i=1}^n I(\delta_i = j) (4 \ln \theta_j + 3 \ln(1 + t_i) - \log(\theta_j^3 t_i^3 + 3\theta_j^2(\theta_j + 1)t_i^2)) \\
&\quad + I(\delta_i = j) (+3\theta_j(\theta_j^2 + 2\theta_j + 2)t_i + (\theta_j^3 + 3\theta_j^2 + 6\theta_j + 6)) \\
&\quad + (r_i + 1) \left[ -\theta_j t_i + \log \left\{ \left( 1 + \frac{\theta_j^3 t_i^3 + 3\theta_j^2(\theta_j + 1)t_i^2 + 3\theta_j(\theta_j^2 + 2\theta_j + 2)t_i}{\theta_j^3 + 3\theta_j^2 + 6\theta_j + 6} \right) \right\} \right] \\
&\quad + \sum_{i=1}^{m-1} r_i \log p + \left( (n - m)(m - 1) - \sum_{i=1}^{m-1} r_i(m - i) \right) \log(1 - p).
\end{aligned} \tag{13}$$

The first partial derivatives of  $\mathcal{L}$  with respect to  $\theta_l$ ,  $l = 1, 2, \dots, k$ , and  $p$  are

$$\begin{aligned}
\frac{\partial \mathcal{L}}{\partial \theta_l} &= \sum_{i=1}^N \sum_{j=1}^k \delta_{jl} \left[ \begin{aligned} &I(\delta_i = j) \left( \frac{4}{\theta_j} \right) - \frac{3\theta_j^2 t_i^3 + 6\theta_j(\theta_j + 1)t_i^2 + 3\theta_j^2 t_i^2 + 3(\theta_j^2 + 2\theta_j + 2)t_i + 3\theta_j(2\theta_j + 2)t}{\theta_j^3 t_i^3 + 3\theta_j^2(\theta_j + 1)t_i^2 + 3\theta_j(\theta_j^2 + 2\theta_j + 2)t_i} \\ &\quad + I(\delta_i = j) (3\theta_j^2 + 6\theta_j + 6) - (r_i + 1)t_i \\ &\quad + (r_i + 1) \frac{(3\theta_j^2 t_i^3 + 6\theta_j(\theta_j + 1)t_i^2 + 3\theta_j^2 t_i^2 + 3(\theta_j^2 + 2\theta_j + 2)t_i + 3\theta_j(2\theta_j + 2)t_i)(\theta_j^3 + 3\theta_j^2 + 6\theta_j + 6)}{1 + \theta_j^3 t_i^3 + 3\theta_j^2(\theta_j + 1)t_i^2 + 3\theta_j(\theta_j^2 + 2\theta_j + 2)t_i / \theta_j^3 + 3\theta_j^2 + 6\theta_j + 6} \\ &\quad + (r_i + 1) \frac{-(3\theta_j^2 + 6\theta_j + 6)(\theta_j^3 t_i^3 + 3\theta_j^2(\theta_j + 1)t_i^2 + 3\theta_j(\theta_j^2 + 2\theta_j + 2)t_i)}{1 + \theta_j^3 t_i^3 + 3\theta_j^2(\theta_j + 1)t_i^2 + 3\theta_j(\theta_j^2 + 2\theta_j + 2)t_i / \theta_j^3 + 3\theta_j^2 + 6\theta_j + 6} \end{aligned} \right] \\
\frac{\partial \mathcal{L}}{\partial p} &= \frac{1}{p} \sum_{i=1}^{m-1} r_i - \frac{(m - 1)(n - m) - \sum_{i=1}^{m-1} (m - i)r_i}{(1 - p)},
\end{aligned} \tag{14}$$

where  $\delta_{lj}$ ,  $j = 1, 2, \dots, k$ ,  $l = 1, 2, \dots, m$  is the Kronecker delta. Using the observed data set, one can calculate the MLEs of the distribution parameters  $\theta_j$  and  $p$  by solving the following equations with respect to  $\theta_l$  and  $p$ ,

$$\frac{\partial \mathcal{L}}{\partial \theta_l} = 0, \tag{15}$$

$$\frac{\partial \mathcal{L}}{\partial p} = 0. \tag{16}$$

Suppose that  $\hat{\theta}_l$  and  $\hat{p}$  be the MLE of  $\theta_l$ ,  $l = 1, 2, \dots, k$ , and  $p$ , respectively. Using invariance property of the MLEs, MLEs of the component reliability and component cumulative incidence function, at a given time  $t$  are obtained accordingly.

**3.1. Confidence Intervals.** Along with the point estimator, another statistic of interest is the interval estimator. A confidence interval defines the range of numbers, which contains the true population value. The probability that

interval includes the parameter value is what we call the confidence level. Since the ML estimators of the parameters cannot be defined in analytic forms. Therefore, the actual distributions of ML estimators cannot be derived.

**3.1.1. Asymptotic Confidence Intervals.** Here, the confidence interval (CI) is obtained using the asymptotic normal property of the ML estimator. As the estimator in equations (13) and (14) is not in the closed-form, it is not possible to derive their exact distribution of given parameters. However, we use the asymptotic distribution of ML estimator to derive CIs for  $(\theta_k, p)$ . We know that

$$\hat{\theta} \longrightarrow N_{2k+1}(\theta, I^{-1}(\hat{\theta})), \tag{17}$$

where  $I^{-1}(\hat{\theta})$  is the variance-covariance matrix and  $N_{2k+1}$  indicates the  $(2k + 1)^{\text{th}}$  multidimension normal distribution. It can be calculated by the inverse of the matrix of  $\hat{\theta}$ . In Fisher information matrix, the element  $\mathcal{L}$  is with respect to  $\theta_l$  and  $p$ , that is,  $I(\theta) = (I_{ij}(\theta))$ ,  $j, i = 1, 2, \dots, k$ , and is defined as

$$I_{ij}(\theta) = -E \left[ \frac{\partial^2 \mathcal{L}(\theta)}{\partial \theta_i \partial \theta_j} \right], \quad i, j = 1, 2, \dots, k. \quad (18)$$

and  $(\theta_k, p)$ . Now, we use the delta method to obtain the asymptotic confidence interval of  $w(\theta)$ , say, parametric function. The delta method (Qehlert (1992)) allows a normal approximation for a continuous and differentiable function of a sequence of random variables that already has a normal limit in distribution. According to the delta method, the variance of  $w(\theta)$  is estimated by

$$\sqrt{n}[w(x) - w(\theta)] \longrightarrow N(0, V(\theta)[w'(\theta)]^2). \quad (19)$$

So, the ACI of  $w(\theta)$  is obtained as follows:

$$\hat{w}(\theta) \pm z_{\gamma/2} \text{S.E.}(\hat{w}(\theta)), \quad (20)$$

where  $z_{\gamma/2}$  is the upper  $100(\gamma/2)^{\text{th}}$ % of standard normal variate.

**3.1.2. Boot-p Confidence Interval.** In this subsection, Efron and Tibshirani [52] proposed the parametric bootstrap confidence intervals for the parameters. The bootstrap method is utilized when a normality assumption is invalid. Consider  $\theta = \{\text{set of all parameter}\}$ . Let  $\Phi(z) = P(\hat{\theta}^* \leq z)$  be *cdf* of  $\hat{\theta}^*$ . Define  $\hat{\theta}_{\text{Boot}}^* = \Phi^{-1}(z)$  for given  $z$ . For boot-p CIs, the necessarily computational algorithm is defined as the following manner:

- (1) To calculate the ML, estimate  $\theta$  as  $\hat{\theta}$  under the progressive type-II censored with binomial removal.
- (2) Generate failure censored sample  $\{t_1^*, t_2^*, \dots, t_m^*\}$  with given  $R_i, i = 1, 2, \dots, m$  of size  $m$  form  $f(t; \hat{\theta})$  by using  $\hat{\theta}$ .
- (3) Using the sample from step-2 to obtained the boot-p estimate for the parameter  $\theta$ , say  $\hat{\theta}^*$ .
- (4) Repeat the above mention steps 2-3 for the  $B$  times, we get the sequence of boot-p estimators  $(\hat{\theta}_j^*; j = 1, 2, \dots, B)$ .
- (5) Set the obtained sequence  $(\hat{\theta}_j^*; j = 1, 2, \dots, B)$  in ascending order and receive  $(\hat{\theta}_{[1]}^*, \hat{\theta}_{[2]}^*, \dots, \hat{\theta}_{[B]}^*)$ .
- (6) A two-sided  $100(1 - \gamma)\%$  boot-p parameter confidence interval is given by

$$(\hat{\theta}_L^*, \hat{\theta}_U^*) = (\hat{\theta}_{[B(\alpha/2)]}^*, \hat{\theta}_{[B(1-\alpha/2)]}^*), \quad (21)$$

where  $[\varphi]$  denote the integer part of  $\varphi$ .

## 4. Bayesian Procedure

We obtain Bayesian estimates of the parameters  $\theta_j, j = 1, 2, \dots, k$ , and  $p$ . To do so, we need the following assumptions:

*Assumption 1.* Assume that  $\theta_j, j = 1, 2, \dots, k$ , and  $p$  are independent.

*Assumption 2.* Also  $\theta_j, j = 1, 2, \dots, k$ , have gamma prior distributions  $g_{\theta_j}(\theta_j)$  and  $g_p(p)$  with different known and nonnegative hyperparameters  $\alpha_j$  and  $\beta_j, j = 1, 2, \dots, k$ , respectively, and  $p$  has the beta distribution with  $g_p(p)$  with known and nonnegative hyperparameters  $c_1$  and  $c_2$ , respectively. The gamma prior density function has the following form:

$$g(u; a, b) = \frac{b^a}{\Gamma(a)} u^{a-1} e^{-ub}, \quad u > 0 \text{ and } a, b > 0, \quad (22)$$

and the beta density function has the following form:

$$g(x; c, d) = \frac{x^{c-1} (1-x)^{d-1}}{B(x; c, d)}, \quad (23)$$

where

$$B(x; c, d) = \int_0^1 x^{c-1} (1-x)^{d-1} dx = \frac{\Gamma(c)\Gamma(d)}{\Gamma(c+d)}, \quad (24)$$

$$x \in (0, 1) \text{ and } c, d > 0.$$

The joint prior density function is

$$g(\theta) = \prod_{j=1}^k g_{\theta_j}(\theta_j) g_p(p) \propto \prod_{j=1}^k \theta_j^{\alpha_j-1} p^{c_1-1} e^{-(\theta_j \beta_j + p c_2)}. \quad (25)$$

*Assumption 3.* A quadratic loss function is used, that is, the loss function is

$$l(\underline{\theta}, p; \hat{\underline{\theta}}, \hat{p}) = \sum_{v=1}^k k_{1v} (\hat{\theta}_v - \theta_v)^2 + k_2 (\hat{p} - p)^2, \quad (26)$$

where  $\underline{\theta} = (\theta_1, \theta_2, \dots, \theta_k)$ .

Therefore, the posterior density function of  $\theta = (\theta_1, \theta_2, \dots, \theta_k, p)$ , up to a normalized constant, is

$$g(\theta | \cdot) \propto \prod_{j=1}^k \prod_{i=1}^k \theta_j^{\alpha_j-1} p^{c_1-1} e^{-(\theta_j \beta_j + p c_2)} \left[ \prod_{i=1}^n \prod_{j=1}^k [h_j(t_i)]^{I(\delta_i=j)} \right] \\ \times \left[ \prod_{i=1}^n \prod_{j=1}^k [\bar{F}_j(t_i)]^{(r_i+1)} \right] p^{\sum_{i=1}^{m-1} r_i} (1-p)^{(n-m)(m-1) - \sum_{i=1}^{m-1} r_i (m-i)}. \quad (27)$$

According to the Assumption 3, the Bayes estimates of given function of the parameters  $\theta = \{(\theta_1, \theta_2, \dots, \theta_k), p\}$ , say  $v(\theta)$  is

$$\hat{v} = E_{\theta_l} (v(\theta)) = \int_0^\infty v(\theta)g(\theta)d\theta. \quad (28)$$

The integral in equation (28) and the normalized constant present in equation (28) have no analytical solutions. Therefore, we will use the MCMC simulation method for obtaining the Bayes estimate of the parameters.

To generate random samples from the joint posterior density function in equation (28) and to compute the Bayes estimate of  $\theta$  and also construct associated credible intervals.

**4.1. Markov Chain Monte Carlo (MCMC) Method.** The Markov Chain Monte Carlo (MCMC) method is one of the most important technique in Bayesian paradigm. The MCMC method is the main computational tools which have been broadly used in Bayesian inference [53–57]. In MCMC algorithm, we have summarized the posterior distribution without requiring the given normalized constant. One of the common technique of the MCMC method is the Metropolis–Hasting to generate the random sample observation from the unknown density. The main aim of the MCMC method is to discover the suitable distribution function and its called the “proposal density.” The proposal density satisfies the two conditions (i) it mimics the actual posterior distribution function and (ii) easy to simulate. We obtain the random sample from the proposal density by using the acceptance-rejection rule. The following steps represents to the Metropolis–Hastings algorithm to generate the random sample drawn from the posterior density  $g(\theta)$ .

- (1) To set the initial point of the sequence, say  $\theta^{(0)}$ .
- (2) To set a size of sequence for getting the random sample, say  $M$ .
- (3) For repeat  $i = 1, \dots, M$ , we take the following steps:
  - (a) Set  $\theta = \theta^{(i-1)}$ .
  - (b) Generate a new candidate point  $\theta^*$  from a candidate distribution  $p(\theta^*|\theta)$ .
  - (c) The acceptance probability  $\wp$  calculate as by  $\wp = \min\{r, 1\}$ , where  $r = g(\theta^*|.)p(\theta|\theta^*)/g(\theta|.)p(\theta^*|\theta)$ .
  - (d) Accept  $\theta^{(i)} = \theta^*$  with probability  $\wp$  or otherwise set  $\theta^{(i)} = \theta$ .

The proposal density  $p(\theta^*|\theta)$ , under some regularity condition, the sequence of the simulated sample  $\{\theta^{(i)}\}_{i=1}^M$  will be random draws and follow the posterior density  $g(\theta|.)$ . The Gibbs sampler algorithms will help to generate random samples from the proposal distributions under the MH algorithm which is used as a cover for the conditional posterior distributions. The necessary steps for the MH algorithm is presented in the following Algorithm 1.

We discard first some values from generated chain to avoid initial value effects. Also, by using some diagnostic

tools such as Cumsum and ACF plots, we get some help in making the chain stationary. At end, we get a chain of size  $N$ , based on which we draw the required inferences. We will calculate the Bayesian credible intervals (BCIs) and highest posterior density (HPD) intervals.

**4.2. Bayes Estimate using Balanced Loss Functions.** In the estimation theory, some difference is always observed between the true and estimate value of the parameter. In symmetric loss function, the amount of risk define by the particular loss function to a negative error is equal to positive of the magnitude. Since the assumption of the equal loss is not appropriate in practical situations scenarios and may be guide with misleading results. In this regards, asymmetric loss function are appropriate for that situation. In those cases, given negative error may be more serious than a given positive error of their magnitude or vice-versa. Now, we will discuss the asymmetric loss function. Here, we considered three loss functions: (i) balanced squared error loss function (BSEL), (ii) balanced LINEX loss function (BLINEX), and (iii) balanced entropy loss unction (BEL), which are introduced by (Jozani et al. [? ]). Let us consider that  $\delta$  be an estimator of the unknown parameter  $\psi$ . The Bayes estimates of  $\psi$  are given in Table 2 under given loss functions.

$w$  and  $q$  are both nonzero real numbers. The Gibbs sampling is one of the easiest algorithms in MCMC techniques and is introduced by [58]. Azzalini [59] helped to vindicate the magnitude of Gibbs algorithms for the problems in Bayesian paradigm. Using the Gibbs sampling technique, the translation kernel is build up by the full conditional distributions.

**4.3. Bayesian Intervals.** First, we generated the sample from the given posterior densities of  $\theta_l, l = 1, 2, \dots, k$ , and  $p$ , and find out the credible intervals for the unknown parameters and its functions. Here, we discussed the process based on the algorithm of [60] to evaluate Bayesian credible and highest posterior density (HPD) intervals. The necessary steps in the this algorithm are as follows:

- (a) Credible intervals
  - (i) We generate a random sample through the M-H algorithm and set in ordered values such as

$$\theta_{l(1)} \leq \theta_{l(2)} \leq \dots \leq \theta_{l(h)}. \quad (29)$$

- (ii) The  $100(1 - \gamma)\%$  Bayesian credible interval for  $\theta_l$  is given by

$$(\theta_{l[(\gamma/2)h]}, \theta_{l[(1-\gamma/2)h]}). \quad (30)$$

- (b) Highest posterior density (HPD) intervals
  - (i) For calculation, all possible  $100(1 - \gamma)\%$  Bayesian credible intervals with corresponding lengths as given by

- (1) Consider an arbitrary initial point  $\theta^{(0)} = \{\theta_1^{(0)}, \theta_2^{(0)}, \dots, \theta_d^{(0)}\}$ , for which  $g(\theta^{(0)}) > 0$ .
- (2) Put  $t = 1$ .
- (3) Get  $\theta_1^{(t)}$  from full conditional distribution  $g(\theta_1 | \theta_2^{(t-1)}, \theta_3^{(t-1)}, \dots, \theta_d^{(t-1)})$ .
- (4) Obtain  $\theta_2^{(t)}$  from full conditional distribution  $g(\theta_2 | \theta_1^{(t)}, \theta_3^{(t-1)}, \dots, \theta_d^{(t-1)})$ .
- ⋮
- (5) Obtain  $\theta_d^{(t)}$  from full conditional distribution  $g(\theta_d | \theta_1^{(t)}, \theta_2^{(t)}, \dots, \theta_{d-1}^{(t)})$ .
- (6) Put  $t = 2$ .
- (7) Repeat steps 2–6.

ALGORITHM 1: The steps for the MH algorithm.

TABLE 2: Loss functions and their corresponding form of the Bayes estimates.

Loss function name	Loss function expression	Bayes estimates
BSEL	$\delta_w(\underline{x}) = w\delta_0(\underline{x}) + (1-w)E(\psi   \underline{x})$	$w\hat{\psi} + 1 - w/N - M \sum_{i=M}^N \psi^{(i)}$
BLINEX	$\delta_w(\underline{x}) = -1/q * \text{Log}[we^{-q\delta_0(\underline{x})} + (1-w)E(e^{-q\psi}   \underline{x})]$	$-1/q \text{Log}[we^{-q\hat{\psi}} + 1 - w/N - M \sum_{i=M}^N e^{-q\psi^{(i)}}]$
BGELF	$\delta_w(\underline{x}) = (\delta_0/\delta_m)^q - q * \text{Log}(\delta_0/\delta_m) - 1$	$[E(\delta_m^q)]^{-1/q}$

$$(\theta_{l(j)}, \theta_{l(j+(1-\gamma)h)}), \quad l_j = \theta_{l(j+(1-\gamma)h)} - \theta_{l(j)}; \quad (31)$$

$$j = 1, 2, \dots, \gamma h, \quad l = 1, 2, \dots, k.$$

- (ii) Search for the credible intervals which have smallest length for  $l_j^\theta$ . The credible intervals with smallest length is HPD interval of  $\theta$ .

## 5. Simulation Study

Shankar [20] proposed the Akshaya distribution by considered the mixture of the Gamma distribution  $\gamma(1, \theta)$ ,  $\gamma(2, \theta)$ ,  $\gamma(3, \theta)$ , and  $\gamma(4, \theta)$  with their respective mixing proportions,

$$\frac{\theta^3}{\theta^3 + 3\theta^2 + 6\theta + 6}, \frac{3\theta_2}{\theta^3 + 3\theta^2 + 6\theta + 6}, \frac{6\theta}{\theta^3 + 3\theta^2 + 6\theta + 6} \& \frac{6}{\theta^3 + 3\theta^2 + 6\theta + 6}. \quad (32)$$

In this case, we consider the statistical analysis of a simulated data set in real-life problem. Here, in our study, we considered that a system have two components. We have assume that both the components follow Akshaya distribution with parameters  $\theta_1$  and  $\theta_2$ , respectively. Furthermore, we treated the values of  $\theta_1 = 1.6$  and  $\theta_2 = 1.8$  and we generate the lifetimes of  $X_1$  and  $X_2$ , which are considered to be the lifetimes of component 1 and component 2 of a system, respectively. Since we are considering series systems of the components, the lifetime of the failed systems becomes  $X_i = x_i$  and is the failure time of  $i^{\text{th}}$  system. We generate  $n$  observations in this way and also note down their cause of failures, say  $c_i$ . We assume that  $m$  observations are failed and remaining  $(n - m)$  observations are removed from the experiment by progressive type-II binomial removals with parameters  $n$  and  $p$ . Now, we have discussed to generate the progressive type-II binomial removal sample.

Table 3 shows the patterns of progressive binomial removals at every failure. The removals pattern is based on the probability value of binomial distribution. In our study, we assume different values of  $p = \{0.05, 0.10, 0.15 \& 0.20\}$  for particulars  $n$  and  $m$  for the generated type-II progressive binomial censored lifetime data. We provide these estimates under various type of schemes by choosing several patterns

of removals by using the different parameters of binomial distribution. In simulation study, we obtained the ML estimate of parameter and also obtained the MSE's. In interval estimation, the asymptotic confidence and boot-p intervals also obtained based on different methods. The ML estimate of component cumulative incidence function, say,  $\mathfrak{C}_1$  and  $\mathfrak{C}_2$ , is calculated based on given time. The component reliability and cumulative incidence functions are also obtained at given time  $t = 1.2$  and  $t = 1.4$ , respectively. The confidence interval of also find by using the delta method. The coverage probability (CP) of a confidence interval of parameter is defined by the proportion of the number of times that the interval comprise the true value of interest. In simulation, the CP is the ratio of number of times the true parameter value lies outside the confidence interval and total number of simulation.

For Bayesian estimation, the system components follow gamma distribution with hyperparameters to be  $\alpha_i$  and  $\beta_i$  for  $i = 1, 2$ . For this, we assume that  $\alpha_1 = \alpha_2 = 2$  and  $\beta_1 = \beta_2 = 3$ . For these values, we obtain distribution parameters  $\theta_1$  and  $\theta_2$ , component reliability, and component cumulative incidence function using the MCMC method. We run this process for 7000 times and obtain the averages estimates of parameters and parametric function along with

TABLE 3: Sampling procedure of removals for failure time under progressive type-II censoring scheme when removals follows to the Binomial removals.

Stage	Failed unit	Removed units	Survived units
1	$x_1$	$r_1 \sim \text{Binorm}(n-1, p)$	$n-1-r_1$
2	$x_2$	$r_2 \sim \text{Binorm}(n-2-r_1, p)$	$n-2-r_1-r_2$
$\vdots$	$\vdots$	$\vdots$	$\vdots$
$i$	$x_i$	$r_i \sim \text{Binorm}(n-i-\sum_{j=1}^{i-1} r_j, p)$	$n-i-\sum_{j=1}^{i-1} r_j$
$\vdots$	$\vdots$	$\vdots$	$\vdots$
$m-1$	$x_{m-1}$	$r_{m-1} \sim \text{Binorm}(n-m-\sum_{j=1}^{m-1} r_j, p)$	$n-m-\sum_{j=1}^{m-1} r_j$
$m$	$x_m$	0	—

TABLE 4: ML and Bayes estimates of  $\theta_1$  with respected MSE's for different values of  $p$  and  $m$  for  $n$ .

$(n, m)$	$p$	$\hat{\theta}_1^M$	$\hat{\theta}_1^{BS}$	$\hat{\theta}_1^{BLL}$	$\hat{\theta}_1^{BLU}$	$\hat{\theta}_1^{BEL}$	$\hat{\theta}_1^{BEU}$	
(40, 20)	0.05	1.45213	1.49555	1.43192	1.44442	1.52096	1.54817	
		0.20451	0.14285	0.11482	0.16545	0.11745	0.17025	
	0.10	1.56978	1.53927	1.54867	1.45693	1.44132	1.59582	
		0.21452	0.16854	0.11845	0.17024	0.10554	0.16845	
	0.15	1.41991	1.46363	1.45253	1.44012	1.49525	1.57109	
		0.21584	0.16945	0.12541	0.17584	0.12453	0.17985	
	0.20	1.56608	1.51716	1.52196	1.46533	1.48354	1.41291	
		0.22455	0.17245	0.14845	0.18124	0.14241	0.19241	
	(40, 30)	0.05	1.46203	1.43992	1.57269	1.56958	1.53947	1.48194
			0.17524	0.11545	0.10458	0.14584	0.10547	0.15784
0.1		1.46173	1.52326	1.48114	1.55098	1.53247	1.47824	
		0.19455	0.14845	0.11548	0.15742	0.11145	0.16854	
0.15		1.58009	1.50285	1.5924	1.58989	1.50145	1.58399	
		0.20469	0.15421	0.13475	0.16845	0.12548	0.17201	
0.2		1.59941	1.57199	1.45703	1.57739	1.49225	1.54667	
		0.20981	0.16045	0.13845	0.17012	0.13545	0.18254	
(40, 40)		0.05	1.47224	1.43692	1.53657	1.46373	1.57129	1.48184
			0.16854	0.10548	0.10421	0.13542	0.09458	0.14527
	0.1	1.49785	1.51896	1.43902	1.5918	1.45683	1.48454	
		0.18155	0.14021	0.11984	0.14526	0.11254	0.15784	
	0.15	1.55428	1.41621	1.45803	1.48274	1.42511	1.49245	
		0.19045	0.14842	0.12254	0.15245	0.13087	0.15482	
	0.2	1.44952	1.55208	1.43182	1.56158	1.42191	1.41601	
		0.20454	1.64581	0.13489	0.15845	0.1254	0.17521	
	(60, 30)	0.05	1.41411	1.49375	1.48254	1.48264	1.48174	1.40175
			0.17558	0.10451	0.11455	0.14354	0.11245	0.15482
0.1		1.54427	1.51126	1.46933	1.51536	1.59576	1.42211	
		0.19452	0.12548	0.12485	0.15141	0.12487	0.15025	
0.15		1.50995	1.51566	1.55008	1.52906	1.55588	1.57449	
		0.19841	0.14515	0.13015	0.15472	0.12845	0.18421	
0.2		1.49395	1.42281	1.54317	1.45643	1.61842	1.42011	
		0.21055	0.17548	0.14254	0.18756	0.14855	0.19824	
(60, 45)		0.05	1.41571	1.48144	1.48384	1.45883	1.54487	1.48764
			0.15248	0.10245	0.09487	0.12055	0.09215	0.13458
	0.1	1.53667	1.49235	1.47794	1.49735	1.47714	1.53937	
		0.17256	0.13584	0.10241	0.12458	0.10215	0.14985	
	0.15	1.55988	1.47844	1.49355	1.52066	1.44052	1.48004	
		0.18425	0.14021	0.11487	0.13845	0.12547	0.16815	
	0.2	1.50425	1.53257	1.40754	1.42331	1.47274	1.55548	
		0.20418	0.15748	0.13541	0.14515	0.12845	0.17654	
	(60, 60)	0.05	1.51586	1.51476	1.55878	1.46993	1.49795	1.55668
			0.12485	0.10125	0.08125	0.12454	0.08152	0.12424
0.1		1.44452	1.53137	1.54907	1.52506	1.52236	1.42201	
		0.16541	0.11545	0.08154	0.12014	0.10242	0.1348	
0.15		1.43782	1.42611	1.49805	1.50575	1.52996	1.40593	
		0.17556	0.12458	0.10245	0.13054	0.12411	0.15844	
0.2		1.44672	1.46793	1.58679	1.47294	1.40744	1.45203	
		0.19456	0.13254	0.12514	0.14025	0.11548	0.17022	



TABLE 5: ML and Bayes estimates of  $\theta_2$  with respected MSE's for different values of  $p$  and  $m$  for  $n$ .

$(n, m)$	$p$	$\hat{\theta}_2^M$	$\hat{\theta}_2^{BS}$	$\hat{\theta}_2^{BLL}$	$\hat{\theta}_2^s$	$\hat{\theta}_2^{BEL}$	$\hat{\theta}_2^{BEU}$
(40, 20)	0.05	1.7265	1.79555	1.63192	1.74442	1.72096	1.64817
		0.15784	0.12285	0.10452	0.15146	0.10584	0.14545
	0.1	1.77613	1.84164	1.77809	1.78649	1.75358	1.79224
		0.17458	0.13484	0.12473	0.16842	0.11895	0.15455
	0.15	1.80306	1.70756	1.64359	1.69642	1.69893	1.62127
		0.18454	0.14258	0.14257	0.17584	0.13584	0.16585
	0.2	1.73494	1.72217	1.82158	1.69962	1.67891	1.64244
		0.20175	0.16154	0.16514	0.18459	0.15462	0.17615
(40, 30)	0.05	1.71745	1.70422	1.83251	1.66476	1.72643	1.67396
		0.13458	0.11845	0.09455	0.15478	0.09157	0.14021
	0.1	1.77602	1.63001	1.80513	1.70353	1.62104	1.78131
		0.15784	0.12454	0.12485	0.16542	0.09845	0.16484
	0.15	1.69387	1.68386	1.78568	1.78637	1.62495	1.77556
		0.16821	0.13584	0.12984	0.17021	0.12548	0.15485
	0.2	1.73322	1.68742	1.75784	1.64669	1.75266	1.68535
		0.17855	0.14815	0.15842	0.17985	0.14589	0.16945
(40, 40)	0.05	1.77751	1.77119	1.70767	1.80938	1.65486	1.83619
		0.12458	0.10256	0.09012	0.12684	0.10215	0.13254
	0.1	1.74047	1.65187	1.72171	1.68892	1.64819	1.69916
		0.12985	0.13254	0.11285	0.13256	0.10985	0.14585
	0.15	1.6345	1.84954	1.81594	1.81364	1.83458	1.77797
		0.15248	0.14251	0.11985	0.14568	0.11845	0.14525
	0.2	1.68765	1.78971	1.78476	1.63611	1.76773	1.72194
		0.16954	0.15928	0.14586	0.15854	0.12455	0.16844
(60, 30)	0.05	1.64071	1.76244	1.82445	1.83407	1.84068	1.77498
		0.14365	0.12548	0.11025	0.15478	0.10215	0.14895
	0.1	1.75324	1.66637	1.68087	1.69168	1.79742	1.74093
		0.16548	0.13588	0.12484	0.16984	0.11548	0.17528
	0.15	1.76532	1.84436	1.74288	1.80708	1.7377	1.84183
		0.17545	0.14415	0.13485	0.18485	0.14515	0.17844
	0.2	1.82538	1.77406	1.78127	1.76969	1.64991	1.76957
		0.19452	0.16848	0.16845	0.18994	0.15482	0.18452
(60, 45)	0.05	1.71101	1.7621	1.80881	1.68259	1.67672	1.83245
		0.11458	0.11564	0.10102	0.12015	0.11285	0.13876
	0.1	1.62138	1.77027	1.79512	1.6865	1.74599	1.70595
		0.12485	0.12545	0.12515	0.14285	0.12482	0.15486
	0.15	1.67569	1.84103	1.70963	1.65049	1.79063	1.71688
		0.15846	0.14559	0.12984	0.15032	0.13542	0.15982
	0.2	1.65613	1.67983	1.62978	1.81295	1.84126	1.78718
		0.17562	0.16521	0.15496	0.15487	0.13982	0.17559
(60, 60)	0.05	1.67902	1.62587	1.74843	1.71642	1.84298	1.67086
		0.09225	0.09154	0.09152	0.11561	0.09485	0.11456
	0.1	1.77211	1.72597	1.81721	1.79064	1.68501	1.78419
		0.10254	0.10255	0.11548	0.13589	0.10459	0.14525
	0.15	1.83343	1.83286	1.67258	1.83297	1.67178	1.76294
		0.13452	0.13845	0.12185	0.15128	0.11541	0.15218
	0.2	1.70848	1.76523	1.64439	1.73927	1.80248	1.79811
		0.14268	0.14625	0.13548	0.15515	0.12895	0.1587

their mean square errors (MSE). In this study, we considered the square error loss function as a symmetric loss function and LINEX and entropy function as asymmetric loss function. For LINEX loss function, we considered the value of shape parameter for under and over estimation is  $-1.5$  and  $2$ , respectively. The same value assume for the entropy loss function. We have obtained component reliability and cumulative incidence function based on the given time. We assume two sample sizes and are defined as

$$n = 40, m = \{20, 30, 40\} \text{ and } n = 60, m = \{30, 45, 60\}. \quad (33)$$

The Tables 4 and 5 represent the ML and Bayes estimate of  $\theta_1$  and  $\theta_2$ , respectively, with respected MSE's of parameter. The Bayes estimate is obtained under symmetric and asymmetric loss function. Similarly, Tables 6–8 show the ML and Bayes estimates of component cumulative incidence function and  $p$  with their MSE. The length and CP of asymptotic confidence and HPD interval of  $\theta_1$  and  $\theta_1$  are

TABLE 6: ML and Bayes estimate of  $\mathfrak{C}_1$  with respected MSE's for different values of  $p$  and  $m$  for  $n$ .

$(n, m)$	$p$	$\hat{\mathfrak{C}}_1^M$	$\hat{\mathfrak{C}}_1^{BS}$	$\hat{\mathfrak{C}}_1^{BLL}$	$\hat{\mathfrak{C}}_1^{BLU}$	$\hat{\mathfrak{C}}_1^{BEL}$	$\hat{\mathfrak{C}}_1^{BEU}$
(40, 20)	0.05	0.41359	0.42958	0.42528	0.43552	0.41827	0.41458
		0.00984	0.00654	0.00515	0.00854	0.00545	0.00942
	0.1	0.42241	0.42013	0.43778	0.41825	0.41414	0.43608
		0.01254	0.00825	0.00759	0.01025	0.00841	0.01025
	0.15	0.42924	0.42457	0.42954	0.42538	0.41009	0.43211
		0.01325	0.00915	0.00984	0.01154	0.00948	0.01258
	0.2	0.41623	0.41395	0.41624	0.43443	0.43308	0.43743
		0.01548	0.01175	0.01048	0.01315	0.01157	0.0137
(40, 30)	0.05	0.41797	0.41368	0.43284	0.41125	0.42553	0.43205
		0.00865	0.00548	0.00484	0.00874	0.00516	0.00874
	0.1	0.43892	0.43527	0.43863	0.43098	0.41027	0.42234
		0.01054	0.00745	0.00684	0.01151	0.00754	0.01058
	0.15	0.41876	0.43077	0.42049	0.43427	0.41842	0.41795
		0.01154	0.00845	0.00648	0.01027	0.01035	0.01152
	0.2	0.41035	0.42934	0.41285	0.41842	0.43766	0.43304
		0.01325	0.01056	0.00948	0.01254	0.01058	0.01254
(40, 40)	0.05	0.41746	0.43857	0.41527	0.42118	0.41985	0.43424
		0.00825	0.00512	0.0041	0.00842	0.00468	0.00784
	0.1	0.43515	0.42219	0.43032	0.42504	0.42273	0.41667
		0.01085	0.00774	0.00741	0.00952	0.00684	0.00982
	0.15	0.41543	0.41654	0.42349	0.43834	0.42871	0.41245
		0.01059	0.00748	0.00637	0.00985	0.00847	0.00975
	0.2	0.42738	0.41662	0.43971	0.43412	0.43886	0.42436
		0.01354	0.00986	0.00872	0.01325	0.01145	0.01052
(60, 30)	0.05	0.41717	0.42741	0.41006	0.41525	0.41914	0.42178
		0.00941	0.00485	0.00412	0.00908	0.00402	0.00725
	0.1	0.41836	0.43295	0.41944	0.42399	0.41198	0.42365
		0.01125	0.00542	0.00579	0.01021	0.00674	0.00941
	0.15	0.41909	0.42654	0.41236	0.42832	0.42984	0.43272
		0.01207	0.00945	0.00745	0.01154	0.00947	0.0114
	0.2	0.42717	0.43173	0.41915	0.41065	0.42975	0.43629
		0.01285	0.01041	0.01012	0.01289	0.01204	0.01287
(60, 45)	0.05	0.42894	0.43776	0.43193	0.41021	0.42772	0.41816
		0.00845	0.00384	0.00385	0.00854	0.00382	0.00741
	0.1	0.43979	0.42045	0.42378	0.42071	0.42057	0.41368
		0.00948	0.00485	0.00464	0.00907	0.00485	0.00872
	0.15	0.41407	0.42276	0.41968	0.43349	0.41498	0.43223
		0.01025	0.00874	0.00687	0.00982	0.00621	0.00943
	0.2	0.41852	0.43079	0.43865	0.41932	0.41495	0.42249
		0.01154	0.01014	0.00985	0.00987	0.00754	0.00991
(60, 60)	0.05	0.43674	0.41354	0.41186	0.42727	0.42336	0.41977
		0.00684	0.00352	0.00325	0.00646	0.00287	0.00589
	0.1	0.42216	0.41659	0.43988	0.43421	0.43155	0.42462
		0.00882	0.00312	0.00412	0.00712	0.00385	0.00712
	0.15	0.42035	0.43163	0.41216	0.43407	0.41965	0.41687
		0.0092	0.00745	0.00574	0.00864	0.00598	0.00789
	0.2	0.43611	0.43854	0.43025	0.43833	0.41522	0.42405
		0.01104	0.00984	0.00852	0.00985	0.00754	0.01058

discussed in Tables 9 and 10, respectively. Similarly, the length of asymptotic confidence interval and HPD interval of  $\mathfrak{C}_1$  and  $\mathfrak{C}_2$ ,  $p$ , with respected coverage probabilities is discussed in Tables 11–13.

From all the tables, we observe that MSEs of all function decreases when  $n$  increases. For fixed  $n$ , the MSEs of all the estimates decrease when  $m$  increases. In the Bayesian analysis, we find out the MSE's under symmetric and

asymmetric loss function. Based on the simulation study, we found the following result:

- (i) In general, as  $m$  for any  $n$  increases, MSE's of corresponding ML and Bayes estimator decrease and reverse nature exists for  $p$  at any  $n$  and  $m$ .
- (ii) The Bayes estimation, as we use some additional information in form of prior, work more efficiently

TABLE 7: ML and Bayes estimate of  $\mathfrak{C}_2$  with respected MSE's for different values of  $p$  and  $m$  for  $n$ .

$(n, m)$	$p$	$\hat{\mathfrak{C}}_2^M$	$\hat{\mathfrak{C}}_2^{BS}$	$\hat{\mathfrak{C}}_2^{BLL}$	$\hat{\mathfrak{C}}_2^{BLU}$	$\hat{\mathfrak{C}}_2^{BEL}$	$\hat{\mathfrak{C}}_2^{BEU}$
(40, 20)	0.05	0.46713	0.48552	0.47009	0.45666	0.47515	0.46259
		0.01114	0.00845	0.00751	0.00972	0.00748	0.01025
	0.1	0.46125	0.47197	0.45616	0.47593	0.48054	0.45602
		0.01352	0.00947	0.00863	0.01045	0.00954	0.01104
	0.15	0.45438	0.46845	0.45878	0.46807	0.45768	0.45428
		0.01458	0.01155	0.00987	0.01257	0.0983	0.01296
	0.2	0.45044	0.46461	0.48774	0.48654	0.47065	0.45916
		0.01587	0.01259	0.01147	0.01298	0.01054	0.01325
(40, 30)	0.05	0.47587	0.46409	0.47205	0.46755	0.4892	0.45338
		0.01048	0.00821	0.00706	0.00825	0.00684	0.00985
	0.1	0.47101	0.45494	0.48784	0.46571	0.48485	0.46927
		0.01285	0.01084	0.00821	0.00925	0.00845	0.00982
	0.15	0.47261	0.47337	0.46603	0.48796	0.46735	0.48672
		0.01394	0.01124	0.00978	0.01137	0.00946	0.01047
	0.2	0.47013	0.48592	0.47325	0.46295	0.47119	0.47339
		0.01406	0.01284	0.01054	0.01174	0.0102	0.01245
(40, 40)	0.05	0.45118	0.46113	0.48044	0.47835	0.47741	0.46629
		0.01024	0.00795	0.00684	0.00865	0.00584	0.00925
	0.1	0.46107	0.48656	0.45806	0.47433	0.45342	0.45489
		0.01154	0.00937	0.00745	0.00885	0.00754	0.01054
	0.15	0.45984	0.48174	0.48548	0.46489	0.45764	0.45546
		0.01289	0.01124	0.00937	0.01021	0.00845	0.00985
	0.2	0.48224	0.48226	0.47255	0.48845	0.47549	0.46443
		0.01296	0.01325	0.0111	0.0119	0.00925	0.01151
(60, 30)	0.05	0.48856	0.47493	0.48144	0.46209	0.46881	0.48382
		0.01125	0.00954	0.00845	0.00875	0.00701	0.00946
	0.1	0.48956	0.46181	0.48602	0.45376	0.45865	0.47669
		0.01196	0.00983	0.00715	0.00913	0.0086	0.01025
	0.15	0.46915	0.47281	0.45268	0.46115	0.48102	0.45792
		0.01287	0.01025	0.00847	0.0111	0.00879	0.00945
	0.2	0.46017	0.45604	0.47769	0.48688	0.45933	0.48065
		0.01358	0.01187	0.00984	0.01278	0.00928	0.01185
(60, 45)	0.05	0.45184	0.45822	0.48051	0.47867	0.45912	0.47607
		0.01084	0.00873	0.00796	0.00823	0.00684	0.00865
	0.1	0.48298	0.46795	0.45636	0.47861	0.45584	0.47979
		0.01098	0.00824	0.00824	0.00905	0.00824	0.00945
	0.15	0.45906	0.47417	0.48786	0.46525	0.47539	0.46911
		0.01112	0.00936	0.00868	0.00983	0.00918	0.00991
	0.2	0.45722	0.48416	0.47605	0.45858	0.48814	0.46787
		0.01298	0.01102	0.00927	0.01111	0.00912	0.01025
(60, 60)	0.05	0.46681	0.46951	0.48478	0.48726	0.48082	0.47215
		0.00945	0.00739	0.00712	0.00817	0.00587	0.00758
	0.1	0.45542	0.48965	0.45947	0.46155	0.47513	0.45572
		0.01029	0.0081	0.0079	0.00873	0.00715	0.00815
	0.15	0.46331	0.47793	0.47067	0.48824	0.48894	0.47217
		0.01098	0.00873	0.00845	0.00942	0.00845	0.00917
	0.2	0.46721	0.45056	0.45349	0.46801	0.45884	0.46493
		0.01143	0.01021	0.00893	0.01044	0.00924	0.01087

than the maximum likelihood approach. For each set of  $n, m, p$ , MSE's of the Bayes estimation is more appropriate than ML approach.

- (iii) The average lengths of the given intervals decrease as  $m$  increases for any  $n$ . This nature also exists for coverage probability. The HPD beats BCI in case of average length which is obvious and expected.
- (iv) As  $m$  increases for large value of  $p$ , the probability of getting  $m$  failures decreases.

## 6. Data Study

In this section, we considered simulated and real data to show the application of Akshaya distribution. All the data set to present that the Akshaya life times can use the results to a real-life problem.

6.1. Simulated Data. We also consider the simulated data analysis to show how the results applied in real-life

TABLE 8: ML and Bayes estimate of  $p$  with respected MSE's for different values of  $p$  and  $m$  for  $n$ .

$(n, m)$	$p$	$\hat{p}^M$	$\hat{p}^{BS}$	$\hat{p}^{BLL}$	$\hat{p}^{BLU}$	$\hat{p}^{BEL}$	$\hat{p}^{BEU}$
(40, 20)	0.05	0.05255	0.05042	0.05775	0.03889	0.03853	0.03896
		0.00642	0.00314	0.00204	0.00298	0.00198	0.00312
	0.1	0.11548	0.10838	0.11176	0.11674	0.09401	0.11714
		0.00784	0.00579	0.00309	0.00315	0.00298	0.00325
	0.15	0.14248	0.14055	0.14567	0.15017	0.15041	0.13881
0.00821		0.00584	0.00345	0.00324	0.00312	0.00382	
(40, 30)	0.05	0.05187	0.04155	0.04816	0.03969	0.06296	0.05087
		0.00547	0.00285	0.00178	0.00237	0.00164	0.00275
	0.1	0.11413	0.12155	0.11048	0.10409	0.11109	0.12431
		0.0063	0.00513	0.00278	0.00327	0.00275	0.00308
	0.15	0.14574	0.15146	0.15876	0.14656	0.14258	0.13583
0.00701		0.00468	0.00365	0.00412	0.00381	0.00425	
(40, 40)	0.05	0.05187	0.04335	0.05629	0.05846	0.04509	0.04695
		0.00523	0.00243	0.00147	0.00184	0.00134	0.00214
	0.1	0.09287	0.09661	0.10649	0.09762	0.12355	0.09248
		0.00612	0.0048	0.00243	0.00291	0.0025	0.00281
	0.15	0.14968	0.15496	0.15082	0.14836	0.16002	0.14923
0.00659		0.00438	0.00384	0.00461	0.00402	0.00431	
(60, 30)	0.05	0.05894	0.04884	0.04111	0.06477	0.04904	0.04528
		0.0056	0.00265	0.00185	0.00263	0.00174	0.00344
	0.1	0.09145	0.08508	0.12359	0.11094	0.11777	0.11861
		0.00594	0.00489	0.00315	0.00362	0.00285	0.00421
	0.15	0.15387	0.14648	0.15083	0.15142	0.16182	0.16326
0.00628		0.00498	0.00245	0.00357	0.00249	0.00382	
(60, 45)	0.05	0.04846	0.04411	0.06185	0.05455	0.04893	0.05349
		0.00534	0.00239	0.00128	0.00168	0.00141	0.00192
	0.1	0.1064	0.11916	0.10334	0.08437	0.08962	0.08533
		0.00639	0.00439	0.00272	0.00319	0.00274	0.0038
	0.15	0.15189	0.15223	0.14451	0.14145	0.15292	0.16026
0.00562		0.00462	0.00239	0.00325	0.00213	0.00372	
(60, 60)	0.05	0.05967	0.03967	0.04689	0.04321	0.06049	0.04799
		0.00482	0.00182	0.00081	0.00124	0.00108	0.00138
	0.1	0.10415	0.09411	0.11702	0.11523	0.08899	0.10588
		0.00508	0.00408	0.00241	0.00278	0.00237	0.00268
	0.15	0.1509	0.14385	0.14136	0.16149	0.15658	0.14671
0.00559		0.00379	0.00198	0.00309	0.00198	0.00348	
(60, 20)	0.05	0.21154	0.21465	0.19651	0.20576	0.20164	0.20406
		0.00597	0.00571	0.00345	0.00415	0.00298	0.00438

problems. The data are simulated from the considered Akshaya population by taking  $\theta_1 = 1.6$  and of  $\theta_2 = 1.8$ , we generated competing risk data of size  $n = 50$ . In this study, we considered total  $m = 35$  system failed out of  $n = 50$  and  $p$  takes value 0.05, 0.10, and 0.15. The pair value shows the failure time and cause of failure of system. The observe data with cause of failure is given as Table 14. The asymptotic confidence and boot-p confidence are calculated. For this continue, we assume that  $\alpha_1 = \alpha_2 = 2$  and  $\beta_1 = \beta_2 = 3$ . For these values, we obtain distribution parameters  $\theta_1$  and  $\theta_2$ ,

component reliability, and component cumulative incidence function using the MCMC method. The Bayesian estimation performed under the symmetric and asymmetric loss function. We also discussed the Bayesian credible and HPD interval for the  $\theta_1, \theta_2, \mathfrak{C}_1, \mathfrak{C}_2$ , and  $p$ . Tables 15–17 present the ML and Bayes estimate of parameter with their length of 95% confidence intervals. The component reliability and cumulative incidence function obtain at the given time  $t_0 = 1.3$ . The Bayes estimates of  $\mathfrak{C}_1$  and  $\mathfrak{C}_2$  with their length of CI for different  $m$  for  $n$  and  $p$  are discussed in Table 18.

TABLE 9: Length of confidence interval of  $\theta_1$  with their coverage probability of different  $p$  and  $m$  for  $n$ .

$(n, m)$	$p$	$\hat{\theta}_1^M$	$\hat{\theta}_1^{BS}$	$\hat{\theta}_1^{BLL}$	$\hat{\theta}_1^{BLU}$	$\hat{\theta}_1^{BEL}$	$\hat{\theta}_1^{BEU}$
(40, 20)	0.05	0.24153	0.18542	0.14207	0.15247	0.13844	0.16248
		0.92458	0.9436	0.95248	0.94825	0.95521	0.94581
	0.1	0.25218	0.18958	0.15084	0.16258	0.14025	0.16847
		0.91745	0.93954	0.94751	0.94455	0.95395	0.94358
	0.15	0.25847	0.19485	0.15358	0.16785	0.14584	0.17168
		0.91287	0.92742	0.94522	0.94912	0.95712	0.94851
	0.2	0.26025	0.20548	0.16258	0.17058	0.15125	0.17894
		0.90745	0.92455	0.94186	0.95314	0.94778	0.93752
(40, 30)	0.05	0.23451	0.16285	0.13584	0.14857	0.13012	0.15482
		0.92846	0.94842	0.95542	0.95144	0.95714	0.94862
	0.1	0.24587	0.17824	0.14785	0.15214	0.13598	0.15981
		0.92382	0.94243	0.94925	0.94708	0.95855	0.95214
	0.15	0.24924	0.17989	0.14935	0.15895	0.13915	0.16485
		0.91564	0.94825	0.94385	0.94984	0.94365	0.95084
	0.2	0.25128	0.19358	0.15824	0.16548	0.14278	0.17048
		0.91146	0.95247	0.9471	0.94751	0.9468	0.94582
(40, 40)	0.05	0.23014	0.15358	0.13025	0.14018	0.12945	0.15048
		0.93456	0.95189	0.95624	0.95428	0.95933	0.95422
	0.1	0.23759	0.16847	0.13148	0.15012	0.13129	0.14358
		0.93058	0.94732	0.95387	0.95275	0.95775	0.95384
	0.15	0.24152	0.17158	0.14078	0.15725	0.13648	0.15198
		0.92458	0.94574	0.94654	0.94751	0.94852	0.94881
	0.2	0.24852	0.18584	0.14897	0.16015	0.1398	0.16457
		0.92726	0.94188	0.94025	0.95128	0.95245	0.95284
(60, 30)	0.05	0.24584	0.17254	0.14258	0.14915	0.13284	0.1558
		0.92158	0.95214	0.95942	0.94751	0.95724	0.94822
	0.1	0.25128	0.18128	0.14948	0.15481	0.13914	0.15842
		0.92684	0.95425	0.95462	0.95314	0.95258	0.94628
	0.15	0.25485	0.18783	0.15068	0.16287	0.14357	0.16784
		0.92458	0.94852	0.95621	0.94258	0.948	0.93845
	0.2	0.26358	0.19842	0.15719	0.17349	0.15465	0.17354
		0.93584	0.94586	0.94985	0.94632	0.94951	0.94125
(60, 45)	0.05	0.23458	0.16584	0.13584	0.14645	0.13426	0.15287
		0.92694	0.95841	0.95981	0.95471	0.95833	0.95246
	0.1	0.24278	0.16901	0.13945	0.14781	0.13582	0.15924
		0.92684	0.9483	0.95812	0.95245	0.95384	0.94935
	0.15	0.24851	0.17268	0.14751	0.15845	0.14369	0.16547
		0.92457	0.94442	0.94825	0.95348	0.95645	0.94072
	0.2	0.25235	0.17981	0.15134	0.16458	0.14915	0.16845
		0.93248	0.9531	0.95142	0.94582	0.9485	0.94352
(60, 60)	0.05	0.22254	0.15248	0.12587	0.13545	0.12314	0.14218
		0.92925	0.96254	0.96342	0.95932	0.96254	0.95832
	0.1	0.22845	0.15874	0.12941	0.14359	0.13015	0.14813
		0.92548	0.95845	0.95934	0.95654	0.95842	0.95624
	0.15	0.23254	0.16248	0.13587	0.14921	0.13945	0.15284
		0.93548	0.95377	0.95388	0.94855	0.95268	0.95554
	0.2	0.23758	0.17128	0.14284	0.15460	0.14542	0.1618
		0.92458	0.9684	0.95425	0.94652	0.95562	0.9496

The cumulative incidence function for both causes are obtained for the value  $p = 0.05, 0.1, \text{ and } 0.15$

6.2. *Real Data.* The data represented the survival times of mice, kept in a conventional germ-free environment, all of which were exposed to a fixed dose of radiation at an age of 5 to 6 weeks [1]. There are 3 causes of death. Here, we considered the thymic lymphoma for first cause and other cause

for second cause in group 1. The cause-wise data are shown in Table 19 after using type-II progressive censored binomial removal with probability  $p = (0.05 \text{ and } 0.10)$ .

The ML and Bayes estimates with their respected length of confidence intervals are presented in Tables 20–22. In Bayesian paradigm, all estimation is performed under various loss functions. The graphical representation of generated sample from the MCMC method of both component is presented in Figure 1. The component reliability and

TABLE 10: Length of confidence interval of  $\theta_1$  with their coverage probability of different  $m$  for  $n$  and  $p$ .

$(n, m)$	$p$	$\hat{\theta}_2^M$	$\hat{\theta}_2^{BS}$	$\hat{\theta}_2^{BLL}$	$\hat{\theta}_2^{BLU}$	$\hat{\theta}_2^{BEL}$	$\hat{\theta}_2^{BEU}$
(40, 20)	0.05	0.28325	0.18451	0.16547	0.18254	0.16815	0.18452
		0.93254	0.95422	0.96345	0.95725	0.96524	0.95864
	0.1	0.29248	0.19848	0.1743	0.19458	0.17125	0.18924
		0.93574	0.952	0.96122	0.95425	0.96287	0.9548
	0.15	0.29745	0.20316	0.17942	0.19845	0.17841	0.19421
		0.92842	0.94875	0.95746	0.95211	0.9574	0.952
	0.2	0.30241	0.20857	0.18384	0.20489	0.18341	0.20364
		0.92644	0.94398	0.95688	0.93254	0.95804	0.94863
(40, 30)	0.05	0.27584	0.18248	0.16048	0.17924	0.16259	0.1784
		0.94255	0.95832	0.96547	0.95935	0.96808	0.96348
	0.1	0.27987	0.19384	0.16682	0.18241	0.17281	0.18416
		0.94325	0.9542	0.964	0.95475	0.96502	0.96028
	0.15	0.28547	0.19848	0.17527	0.18756	0.17924	0.18805
		0.9374	0.94793	0.95924	0.9521	0.95921	0.95712
	0.2	0.29025	0.20179	0.18038	0.19351	0.18347	0.19418
		0.93845	0.93768	0.95428	0.94511	0.95722	0.95044
(40, 40)	0.05	0.26845	0.17451	0.15743	0.17254	0.15782	0.17152
		0.951	0.96045	0.96624	0.96215	0.96952	0.96854
	0.1	0.27254	0.18252	0.16221	0.17213	0.16721	0.17846
		0.94856	0.95745	0.9647	0.95982	0.96685	0.96358
	0.15	0.27902	0.19278	0.17632	0.18179	0.16287	0.18374
		0.94251	0.95422	0.96115	0.95424	0.95904	0.95842
	0.2	0.28243	0.19484	0.17924	0.18721	0.17294	0.19108
		0.94512	0.94267	0.95632	0.94485	0.95824	0.94782
(60, 30)	0.05	0.28245	0.20474	0.1721	0.17647	0.1682	0.17684
		0.93945	0.95925	0.96454	0.96254	0.96654	0.96347
	0.1	0.28728	0.20547	0.17212	0.17849	0.1734	0.18016
		0.93475	0.96245	0.96154	0.95864	0.96425	0.96048
	0.15	0.29357	0.21258	0.18052	0.18784	0.18213	0.18805
		0.93584	0.95641	0.95874	0.95462	0.9618	0.95584
	0.2	0.29752	0.21827	0.18338	0.18894	0.18514	0.19418
		0.92845	0.9524	0.95474	0.95025	0.95485	0.95133
(60, 45)	0.05	0.27248	0.19584	0.16475	0.17255	0.16247	0.17087
		0.94582	0.96245	0.96712	0.9654	0.96845	0.96529
	0.1	0.27685	0.20187	0.17218	0.17841	0.1654	0.17424
		0.94385	0.95985	0.96384	0.96348	0.96577	0.9627
	0.15	0.28315	0.20738	0.17813	0.18115	0.17147	0.17947
		0.93954	0.95428	0.96502	0.95841	0.96472	0.95942
	0.2	0.28721	0.21421	0.1802	0.18408	0.1791	0.18225
		0.93604	0.95305	0.95882	0.95645	0.96201	0.95206
(60, 60)	0.05	0.26014	0.19021	0.15882	0.1642	0.15231	0.17158
		0.95485	0.9651	0.96845	0.96845	0.97106	0.96924
	0.1	0.2642	0.19982	0.16542	0.16974	0.16418	0.17258
		0.95388	0.96284	0.96504	0.9648	0.96754	0.96729
	0.15	0.27004	0.20608	0.1712	0.17404	0.17189	0.17518
		0.95007	0.95742	0.96488	0.96158	0.96486	0.96355
	0.2	0.27928	0.21185	0.17684	0.17915	0.17621	0.17802
		0.94856	0.95258	0.96046	0.95702	0.96122	0.95792

TABLE 11: Confidence interval of cumulative incidence function for first component  $\mathfrak{C}_1$  with their coverage probability for different  $p$  and  $m$  for  $n$ .

$(n, m)$	$p$	$\widehat{\mathfrak{C}}_1^M$	$\widehat{\mathfrak{C}}_1^{BS}$	$\widehat{\mathfrak{C}}_1^{BLL}$	$\widehat{\mathfrak{C}}_1^{BLU}$	$\widehat{\mathfrak{C}}_1^{BEL}$	$\widehat{\mathfrak{C}}_1^{BEU}$	
(40, 20)	0.05	0.02524	0.01924	0.01464	0.01584	0.01425	0.01578	
		0.92954	0.94456	0.95684	0.94925	0.95842	0.95247	
	0.1	0.02572	0.01971	0.01531	0.01668	0.01484	0.01634	
		0.92482	0.94302	0.953	0.94584	0.9569	0.95188	
	0.15	0.02608	0.01991	0.01581	0.01758	0.01524	0.01708	
		0.92563	0.93752	0.94821	0.94685	0.95712	0.94866	
	0.2	0.02642	0.02024	0.0164	0.01794	0.01574	0.01759	
		0.91632	0.93699	0.94335	0.93954	0.95	0.94754	
	(40, 30)	0.05	0.02485	0.01754	0.01425	0.01512	0.01364	0.01538
			0.9342	0.94925	0.95942	0.94635	0.96254	0.95784
0.1		0.02502	0.01794	0.01498	0.01569	0.0139	0.01571	
		0.93185	0.9521	0.95498	0.94852	0.95899	0.94277	
0.15		0.02548	0.01852	0.01535	0.01615	0.01485	0.0162	
		0.92746	0.94215	0.95077	0.94213	0.95664	0.95348	
0.2		0.02625	0.01912	0.01594	0.01683	0.01534	0.01684	
		0.92455	0.94344	0.9487	0.94355	0.95278	0.95745	
(40, 40)		0.05	0.02342	0.01634	0.01348	0.01454	0.01312	0.01528
			0.9364	0.95325	0.96244	0.95354	0.96524	0.96001
	0.1	0.02394	0.01712	0.01381	0.01538	0.01372	0.01597	
		0.93584	0.9544	0.96429	0.95046	0.96294	0.95475	
	0.15	0.02435	0.01745	0.01431	0.01619	0.01424	0.01625	
		0.93502	0.94527	0.95478	0.94557	0.95644	0.95278	
	0.2	0.02524	0.01863	0.01476	0.01673	0.01482	0.01671	
		0.99315	0.94289	0.95009	0.94472	0.955	0.95082	
	(60, 30)	0.05	0.02482	0.01784	0.01404	0.01526	0.01388	0.01569
			0.92415	0.95143	0.96148	0.95638	0.96342	0.95742
0.1		0.02537	0.01835	0.01468	0.01581	0.01425	0.01593	
		0.92358	0.94223	0.95689	0.95341	0.9618	0.9541	
0.15		0.02584	0.0189	0.01495	0.01652	0.01472	0.01652	
		0.91765	0.93865	0.95284	0.94857	0.95874	0.95144	
0.2		0.02651	0.01954	0.01583	0.01770	0.01552	0.01735	
		0.91532	0.9375	0.94884	0.94521	0.95558	0.94258	
(60, 45)		0.05	0.02419	0.01735	0.01384	0.01491	0.01362	0.01518
			0.9221	0.95621	0.96278	0.95844	0.96412	0.95714
	0.1	0.02468	0.01765	0.01425	0.01534	0.01382	0.01541	
		0.92318	0.95284	0.95985	0.95724	0.96244	0.95484	
	0.15	0.02548	0.01834	0.0149	0.01571	0.01402	0.01586	
		0.91945	0.95347	0.95824	0.94952	0.96411	0.95004	
	0.2	0.02583	0.01888	0.01548	0.01668	0.01475	0.01658	
		0.91358	0.94822	0.954	0.95004	0.95864	0.94854	
	(60, 60)	0.05	0.02354	0.01632	0.0128	0.01392	0.01322	0.01415
			0.93412	0.96004	0.96714	0.95932	0.9667	0.96
0.1		0.02384	0.01681	0.01324	0.01453	0.01258	0.01458	
		0.93155	0.95726	0.96153	0.95832	0.95924	0.95765	
0.15		0.02432	0.0171	0.01392	0.01528	0.01359	0.01541	
		0.92843	0.9426	0.95844	0.9542	0.96244	0.95384	
0.2		0.02492	0.01738	0.01453	0.01578	0.01401	0.01585	
		0.925	0.94295	0.95624	0.95247	0.96452	0.9498	

TABLE 12: Confidence interval of cumulative incidence function for first component  $\mathfrak{C}_2$  with their coverage probability for different  $m$  for  $n$  and  $p$ .

$(n, m)$	$p$	$\widehat{\mathfrak{C}}_2^M$	$\widetilde{\mathfrak{C}}_2^{BS}$	$\widetilde{\mathfrak{C}}_2^{BLL}$	$\widetilde{\mathfrak{C}}_2^{BLU}$	$\widetilde{\mathfrak{C}}_2^{BEL}$	$\widetilde{\mathfrak{C}}_2^{BEU}$	
(40, 20)	0.05	0.02912	0.01847	0.01625	0.01825	0.01681	0.01845	
		0.93845	0.95326	0.9627	0.95846	0.96355	0.96045	
	0.1	0.03041	0.01984	0.01743	0.01945	0.01712	0.01892	
		0.934128	0.95187	0.96184	0.95647	0.96174	0.95842	
	0.15	0.03091	0.02025	0.01794	0.01984	0.01784	0.01942	
		0.93254	0.94803	0.95712	0.95314	0.95784	0.9548	
	0.2	0.03254	0.0209	0.01838	0.02048	0.01834	0.02036	
		0.92748	0.94542	0.95627	0.95047	0.95429	0.95187	
	(40, 30)	0.05	0.02885	0.01854	0.01604	0.01792	0.01625	0.01784
			0.94259	0.95824	0.96482	0.9614	0.9657	0.96212
0.1		0.02925	0.01994	0.01668	0.01824	0.01728	0.01841	
		0.93845	0.95617	0.96147	0.96023	0.96254	0.95943	
0.15		0.03028	0.02004	0.01752	0.01875	0.01792	0.0188	
		0.93248	0.95208	0.9569	0.95332	0.95709	0.95384	
0.2		0.03024	0.0208	0.01803	0.01935	0.01834	0.01941	
		0.92985	0.9472	0.95355	0.95071	0.95485	0.95185	
(40, 40)		0.05	0.02756	0.01738	0.01574	0.01725	0.01578	0.01715
			0.9545	0.9624	0.96964	0.9654	0.96843	0.96487
	0.1	0.02824	0.01845	0.01622	0.01721	0.01672	0.01784	
		0.95248	0.96085	0.9672	0.96204	0.9657	0.96218	
	0.15	0.02878	0.01975	0.01763	0.01817	0.01628	0.01837	
		0.94924	0.95421	0.96318	0.96	0.96246	0.95874	
	0.2	0.02952	0.02014	0.01792	0.01872	0.01729	0.0191	
		0.9472	0.9541	0.95902	0.95842	0.96014	0.95564	
	(60, 30)	0.05	0.02824	0.02061	0.01784	0.01781	0.01725	0.01782
			0.94187	0.95723	0.96485	0.96185	0.96628	0.96084
0.1		0.02872	0.02086	0.01792	0.01824	0.01775	0.01841	
		0.9357	0.95268	0.9624	0.95682	0.96345	0.95729	
0.15		0.02935	0.02158	0.01841	0.01885	0.01864	0.01868	
		0.93284	0.94792	0.95893	0.95386	0.96015	0.9543	
0.2		0.02975	0.02222	0.01863	0.01935	0.01924	0.01957	
		0.9246	0.94384	0.95427	0.95048	0.95641	0.951	
(60, 45)		0.05	0.02724	0.01974	0.01735	0.01752	0.01684	0.01735
			0.09486	0.96172	0.96764	0.96485	0.96912	0.96358
	0.1	0.02768	0.02035	0.01784	0.01824	0.01724	0.01785	
		0.94523	0.9584	0.96375	0.96143	0.9452	0.96178	
	0.15	0.02831	0.02092	0.01821	0.01856	0.01768	0.01824	
		0.93872	0.95341	0.9601	0.95768	0.96118	0.95842	
	0.2	0.02872	0.02168	0.01848	0.01875	0.01834	0.01868	
		0.9342	0.95199	0.95842	0.9541	0.95748	0.95623	
	(60, 60)	0.05	0.02601	0.01942	0.01654	0.01698	0.01594	0.01743
			0.95246	0.96428	0.96991	0.96628	0.97294	0.96849
0.1		0.02642	0.02018	0.01672	0.01734	0.01682	0.01775	
		0.95042	0.96125	0.96475	0.96025	0.96874	0.94255	
0.15		0.027	0.02052	0.01735	0.01792	0.01753	0.0182	
		0.94735	0.95681	0.96073	0.95884	0.96211	0.9594	
0.2		0.02792	0.02145	0.01801	0.01864	0.01812	0.01828	
		0.9428	0.9547	0.95941	0.9562	0.96387	0.95499	



TABLE 13: Confidence interval of  $p$  with their coverage probability for different  $m$  for  $n$  and  $p$ .

$(n, m)$	$p$	$\tilde{p}^M$	$\tilde{p}^{BS}$	$\tilde{p}^{BLL}$	$\tilde{p}^{BLU}$	$\tilde{p}^{BEL}$	$\tilde{p}^{BEU}$
(40, 20)	0.05	0.02217	0.02088	0.01929	0.01987	0.0192	0.01996
		0.95841	0.96584	0.97415	0.97152	0.975	0.97223
	0.1	0.02258	0.02093	0.0195	0.02027	0.01949	0.02026
		0.95487	0.96428	0.97014	0.96842	0.97122	0.96847
	0.15	0.02287	0.02112	0.02035	0.02076	0.01987	0.02078
		0.95284	0.95874	0.9672	0.96458	0.96845	0.96548
	0.2	0.02292	0.02153	0.02064	0.02099	0.02035	0.02061
		0.94152	0.95699	0.96421	0.962	0.9644	0.96348
(40, 30)	0.05	0.02204	0.02042	0.01906	0.01967	0.01902	0.01954
		0.96284	0.96921	0.97681	0.9742	0.97752	0.97548
	0.1	0.02241	0.02078	0.01928	0.02029	0.01925	0.02027
		0.96084	0.96794	0.97284	0.97084	0.97628	0.97143
	0.15	0.02251	0.02095	0.02008	0.02062	0.0197	0.02067
		0.95524	0.96416	0.96932	0.96758	0.97122	0.96842
	0.2	0.0227	0.0216	0.02068	0.021	0.02017	0.02122
		0.95395	0.95984	0.96524	0.9647	0.96754	0.9652
(40, 40)	0.05	0.02177	0.02026	0.01886	0.01944	0.01875	0.01985
		0.9652	0.97254	0.97928	0.97721	0.97925	0.97688
	0.1	0.02226	0.02056	0.01928	0.01964	0.01944	0.01992
		0.96284	0.96618	0.97542	0.97384	0.97584	0.97425
	0.15	0.02259	0.02093	0.01965	0.01995	0.01976	0.02019
		0.95871	0.963	0.9712	0.97058	0.9735	0.97211
	0.2	0.02286	0.02138	0.0203	0.02046	0.02003	0.02036
		0.95684	0.95942	0.96721	0.96485	0.96941	0.96674
(60, 30)	0.05	0.02194	0.02129	0.02254	0.02062	0.02082	0.02065
		0.96354	0.97124	0.97598	0.97381	0.97622	0.97452
	0.1	0.02187	0.02222	0.02085	0.02251	0.02226	0.02243
		0.96187	0.97015	0.97345	0.97115	0.97425	0.97227
	0.15	0.02148	0.02175	0.02058	0.02107	0.02193	0.02086
		0.95892	0.96842	0.9711	0.96941	0.9723	0.97102
	0.2	0.02112	0.02122	0.02157	0.02193	0.02058	0.02199
		0.95298	0.96587	0.96845	0.9672	0.96942	0.96785
(60, 45)	0.05	0.02152	0.0212	0.02099	0.02249	0.02135	0.02243
		0.96714	0.97548	0.97821	0.97412	0.97972	0.97528
	0.1	0.02112	0.0216	0.02116	0.02211	0.02144	0.02242
		0.9624	0.97284	0.97523	0.97368	0.97686	0.97324
	0.15	0.02226	0.0218	0.02201	0.02249	0.02182	0.02158
		0.95858	0.96823	0.97258	0.97032	0.97315	0.96948
	0.2	0.02093	0.02174	0.02165	0.02169	0.0217	0.02219
		0.95483	0.96341	0.96991	0.96712	0.97021	0.96648
(60, 60)	0.05	0.02092	0.02063	0.02136	0.02096	0.02104	0.02204
		0.97269	0.97884	0.9823	0.97848	0.98486	0.98012
	0.1	0.02198	0.02204	0.02077	0.02089	0.02181	0.02082
		0.97002	0.97629	0.97958	0.9768	0.98045	0.97715
	0.15	0.02083	0.02114	0.02149	0.02122	0.02161	0.02124
		0.96745	0.97142	0.97622	0.97444	0.96845	0.97561
	0.2	0.02185	0.02109	0.02092	0.02162	0.02182	0.02139
		0.96488	0.96897	0.97358	0.9701	0.97524	0.9735

TABLE 14: The observed sample observation based on  $\theta_1 = 1.6, \theta_2 = 1.8, n = 50,$  and  $m = 35$  for different  $p = \{0.05, 0.10, 0.15\}$ .  $(x, c)$  show the  $x^{\text{th}}$  system failed by  $c^{\text{th}}$  cause.

$p$	Sample observations
0.05	(0.025502, 1), (0.045179, 2), (0.059670, 1), (0.197907, 1), (0.212828, 2), (0.236758, 2), (0.277145, 2), (0.347179, 2), (0.364438, 2), (0.421281, 2), (0.426876, 1), (0.446558, 1), (0.468371, 1), (0.525722, 2), (0.634081, 2), (0.651863, 2), (0.698877, 1), (0.738252, 2), (0.774715, 2), (0.783491, 1), (0.816205, 1), (0.874094, 2), (0.911845, 2), (0.979015, 1), (0.983192, 1), (0.986420, 2), (1.010234, 1), (1.032606, 2), (1.040412, 2), (1.041244, 2), (1.109238, 2), (1.139642, 1), (1.149697, 2), (1.360076, 2), (1.402297, 1).
0.1	(0.037048, 2), (0.110138, 1), (0.113047, 2), (0.158316, 1), (0.159671, 1), (0.264439, 1), (0.329658, 2), (0.338978, 2), (0.361539, 2), (0.394643, 2), (0.401278, 2), (0.440678, 2), (0.469238, 1), (0.471437, 2), (0.480524, 2), (0.506564, 1), (0.512345, 1), (0.618062, 1), (0.733344, 2), (0.748629, 1), (0.845750, 1), (0.872206, 2), (0.875464, 2), (1.079641, 2), (1.093948, 1), (1.096268, 1), (1.107178, 2), (1.121729, 1), (1.128656, 2), (1.240465, 2), (1.426567, 1), (1.471565, 2), (1.534641, 2), (1.608148, 1), (1.749865, 2).
0.15	(0.053606, 1), (0.083254, 1), (0.286128, 1), (0.086267, 2), (0.172204, 2), (0.206521, 2), (0.248698, 2), (0.288119, 1), (0.296992, 1), (0.348699, 2), (0.417466, 2), (0.418418, 1), (0.424467, 2), (0.429732, 1), (0.524806, 1), (0.531061, 1), (0.544476, 1), (0.569465, 1), (0.589250, 1), (0.643938, 1), (0.649462, 2), (0.701340, 2), (0.712140, 1), (0.881307, 1), (1.005723, 1), (1.009441, 1), (1.016195, 1), (1.023818, 2), (1.101361, 1), (1.145337, 1), (1.232508, 1), (1.313147, 2), (1.347173, 1), (1.359859, 1), (1.437946, 2).

TABLE 15: ML estimates of parameters and their functions with their length of confidence interval for different  $m$  for  $n$  and  $p$ .

$p$		$\hat{\theta}_1$	$\hat{\theta}_2$	$\hat{\mathcal{C}}_1$	$\hat{\mathcal{C}}_2$	$\hat{R}_1(t)$	$\hat{R}_2(t)$	$\hat{p}$
0.05	Estimate	1.62485	1.82485	0.41782	0.46945	0.53845	0.56014	0.05157
	ACI	0.01854	0.01721	0.00485	0.00415	0.00074	0.00068	0.00007
	Boot-p	0.01946	0.01752	0.00515	0.00502	0.00081	0.00075	0.00008
0.1	Estimate	1.64154	1.84458	0.41845	0.47924	0.54801	0.57234	0.11024
	ACI	0.01894	0.01754	0.00512	0.00482	0.00078	0.00072	0.00014
	Boot-p	0.02048	0.0178	0.00554	0.00529	0.00083	0.00082	0.00015
0.15	Estimate	1.64521	1.8348	0.42549	0.47125	0.54685	0.56173	0.15025
	ACI	0.01924	0.01804	0.00548	0.0049	0.00083	0.00074	0.00045
	Boot-p	0.02077	0.01825	0.00582	0.00541	0.00088	0.00083	0.00051

TABLE 16: Bayes estimates of  $\theta_1$  and  $\theta_2$  with their lengths of CI for different  $m$  for  $n$  and  $p$ .

$p$		$\tilde{\theta}_1^{BS}$	$\tilde{\theta}_1^{BLL}$	$\tilde{\theta}_1^{BLU}$	$\tilde{\theta}_1^{BEL}$	$\tilde{\theta}_1^{BEU}$
0.05	Estimate	1.59492	1.60051	1.61195	1.59581	1.61104
	BCI	0.01521	0.01457	0.01542	0.0149	0.01493
	HPD	0.01552	0.01245	0.01348	0.01374	0.01348
0.10	Estimate	1.60922	1.58826	1.58257	1.59861	1.59421
	BCI	0.01604	0.01479	0.01568	0.01514	0.01521
	HPD	0.01684	0.01304	0.0138	0.01418	0.01384
0.15	Estimate	1.60349	1.62158	1.58599	1.59969	1.60786
	BCI	0.01654	0.01528	0.01608	0.0157	0.0154
	HPD	0.01701	0.0134	0.01485	0.01442	0.01438
$p$		$\tilde{\theta}_2^{BS}$	$\tilde{\theta}_2^{BLL}$	$\tilde{\theta}_2^{BLU}$	$\tilde{\theta}_2^{BEL}$	$\tilde{\theta}_2^{BEU}$
0.05	Estimate	1.79702	1.78983	1.80252	1.81614	1.79501
	BCI	0.01502	0.01324	0.01412	0.01331	0.01405
	HPD	0.01455	0.01242	0.01365	0.01257	0.01344
0.10	Estimate	1.60922	1.58826	1.58257	1.59861	1.59421
	BCI	0.01568	0.01374	0.01462	0.01369	0.0147
	HPD	0.01501	0.01231	0.01387	0.01242	0.01379
0.15	Estimate	1.60349	1.62158	1.58599	1.59969	1.60786
	BCI	0.0159	0.01421	0.0148	0.01438	0.01476
	HPD	0.01534	0.01294	0.01411	0.01333	0.01439

TABLE 17: Bayes estimates of  $R_1(t)$ ,  $R_2(t)$  and  $p$  with their length of CI for different  $m$  for  $n$  and  $p$ .

$p$		$\tilde{R}_1^{BS}(t)$	$\tilde{R}_1^{BLL}(t)$	$\tilde{R}_1^{BLU}(t)$	$\tilde{R}_1^{BEL}(t)$	$\tilde{R}_1^{BEU}(t)$
0.05	Estimate	0.54187	0.53556	0.54057	0.53727	0.53974
	BCI	0.00054	0.00048	0.0005	0.00044	0.00047
	HPD	0.00042	0.00034	0.00038	0.00032	0.00036
0.1	Estimate	0.54242	0.53651	0.54214	0.53828	0.54415
	BCI	0.00059	0.00051	0.00056	0.00049	0.00051
	HPD	0.0005	0.00036	0.00047	0.00035	0.00046
0.15	Estimate	0.54272	0.54215	0.54385	0.54362	0.54434
	BCI	0.00064	0.00057	0.00063	0.00054	0.00057
	HPD	0.00054	0.00042	0.00053	0.0004	0.00049
$p$		$\tilde{R}_2^{BS}(t)$	$\tilde{R}_2^{BLL}(t)$	$\tilde{R}_2^{BLU}(t)$	$\tilde{R}_2^{BEL}(t)$	$\tilde{R}_2^{BEU}(t)$
0.05	Estimate	0.56235	0.5588	0.56499	0.56253	0.55655
	BCI	0.00058	0.00052	0.00055	0.00053	0.00058
	HPD	0.00046	0.0004	0.00043	0.00039	0.00046
0.1	Estimate	0.56389	0.5643	0.56108	0.56481	0.5618
	BCI	0.00064	0.00057	0.00061	0.00059	0.00064
	HPD	0.00053	0.00043	0.00049	0.00046	0.00049
0.15	Estimate	0.55875	0.55775	0.56235	0.56017	0.55555
	BCI	0.00069	0.00064	0.00066	0.00063	0.00071
	HPD	0.00051	0.00048	0.00053	0.0005	0.00054
$p$		$\tilde{p}^{BS}$	$\tilde{p}^{BLL}$	$\tilde{p}^{BLU}$	$\tilde{p}^{BEL}$	$\tilde{p}^{BEU}$
0.05	Estimate	0.05592	0.05552	0.05573	0.05621	0.05617
	BCI	0.00624	0.0052	0.00537	0.00519	0.00542
	HPD	0.00537	0.00438	0.00458	0.00433	0.00449
0.1	Estimate	0.10492	0.10565	0.10297	0.10095	0.09811
	BCI	0.00668	0.00569	0.00586	0.00578	0.00572
	HPD	0.00561	0.00478	0.00493	0.00481	0.00475
0.15	Estimate	0.14797	0.15142	0.15202	0.15261	0.14833
	BCI	0.00712	0.00634	0.00631	0.0063	0.00629
	HPD	0.0062	0.00512	0.0052	0.00517	0.00535

TABLE 18: Bayes estimates of  $\mathfrak{C}_1$  and  $\mathfrak{C}_2$  with their lengths of CI for different  $m$  for  $n$  and  $p$ .

$p$		$\tilde{\mathfrak{C}}_1^{BS}$	$\tilde{\mathfrak{C}}_1^{BLL}$	$\tilde{\mathfrak{C}}_1^{BLU}$	$\tilde{\mathfrak{C}}_1^{BEL}$	$\tilde{\mathfrak{C}}_1^{BEU}$
0.05	Estimate	0.4298	0.4269	0.42062	0.42358	0.42785
	BCI	0.00425	0.00384	0.00412	0.00375	0.0041
	HPD	0.00354	0.00297	0.00312	0.00302	0.00307
0.1	Estimate	0.43953	0.43434	0.42116	0.42547	0.43374
	BCI	0.00461	0.0041	0.00458	0.00408	0.00442
	HPD	0.0037	0.00328	0.00392	0.00342	0.00411
0.15	Estimate	0.42835	0.42641	0.42691	0.42371	0.4205
	BCI	0.00482	0.00445	0.00494	0.00439	0.00501
	HPD	0.00396	0.00388	0.00418	0.00375	0.00425
$p$		$\tilde{\mathfrak{C}}_2^{BS}$	$\tilde{\mathfrak{C}}_2^{BLL}$	$\tilde{\mathfrak{C}}_2^{BLU}$	$\tilde{\mathfrak{C}}_2^{BEL}$	$\tilde{\mathfrak{C}}_2^{BEU}$
0.05	Estimate	0.46751	0.469	0.47247	0.46846	0.46885
	BCI	0.00394	0.00342	0.00387	0.00339	0.00385
	HPD	0.00324	0.00278	0.00346	0.00269	0.00352
0.1	Estimate	0.47491	0.47209	0.4704	0.46683	0.47224
	BCI	0.00454	0.00388	0.00412	0.00375	0.00399
	HPD	0.00384	0.00345	0.00393	0.00338	0.00393
0.15	Estimate	0.47005	0.46978	0.471	0.4705	0.46869
	BCI	0.00497	0.00443	0.00474	0.00438	0.00491
	HPD	0.00421	0.00333	0.00409	0.00342	0.00423

TABLE 19: The survival times of mice exposed to a fixed dose of radiation.

$p$	Sample observations after with type-II PCWBRR
0.05	(40, 2), (42, 2), (51, 2), (62, 2), (159, 1), (179, 2), (189, 1), (191, 1), (198, 1), (200, 1), (206, 2), (207, 1), (220, 1), (222, 2), (228, 2), (235, 1), (245, 1), (250, 1), (252, 2), (256, 1), (261, 1), (265, 1), (266, 1), (280, 1), (282, 2), (324, 2), (333, 2), (341, 2), (343, 1), (350, 1), (383, 1), (385, 2), (403, 1), (407, 2), (414, 1), (420, 2), (428, 1), (431, 2), (461, 2), (462, 2), (517, 2), (524, 2), (564, 2), (567, 2), (586, 2), (619, 2), (620, 2), (621, 2).
0.1	(40, 2), (42, 2), (51, 2), (62, 2), (159, 1), (163, 2), (179, 2), (189, 1), (191, 1), (198, 1), (200, 1), (206, 2), (207, 1), (220, 1), (228, 2), (245, 1), (250, 1), (252, 2), (256, 1), (259, 2), (266, 1), (280, 1), (282, 2), (324, 2), (333, 2), (341, 2), (350, 1), (383, 1), (366, 2), (385, 2), (403, 1), (414, 1), (420, 2), (428, 1), (431, 2), (432, 1), (441, 2), (462, 2), (482, 2), (517, 2), (524, 2), (567, 2), (586, 2), (619, 2), (620, 2), (621, 2), (622, 2), (651, 2), (686, 2).

TABLE 20: ML estimates of parameters and related function with their CIs for different  $m$  of  $n$  and  $p$  for real data.

$p$		$\hat{\theta}_1$	$\hat{\theta}_2$	$\hat{\mathcal{C}}_1$	$\hat{\mathcal{C}}_2$	$\hat{R}_1$	$\hat{R}_2$	$\hat{P}$
0.05	Estimate	0.01425	0.00966	0.38124	0.41457	0.49824	0.52472	0.04972
	ACI	0.00086	0.00247	0.04032	0.03485	0.01548	0.01475	0.02485
	Boot-p	0.00103	0.00291	0.04251	0.03652	0.01864	0.01655	0.02574
0.10	Estimate	0.01419	0.01024	0.38421	0.42364	0.48748	0.51482	0.10248
	ACI	0.00092	0.00269	0.04128	0.03485	0.01596	0.01511	0.02524
	Boot-p	0.0011	0.00312	0.04358	0.03754	0.01911	0.01694	0.02623

TABLE 21: Bayes estimate of parameter and parametric function with their confidence intervals.

$p$		$\tilde{\theta}_1^{BS}$	$\tilde{\theta}_1^{BLL}$	$\tilde{\theta}_1^{BLU}$	$\tilde{\theta}_1^{BEL}$	$\tilde{\theta}_1^{BEU}$
0.05	Estimate	0.0151	0.01485	0.01444	0.01473	0.01438
	BCI	0.00072	0.00065	0.00067	0.00063	0.00069
	HPD	0.00087	0.0007	0.00071	0.00069	0.00073
0.1	Estimate	0.01519	0.01411	0.01428	0.01428	0.01411
	BCI	0.00093	0.00072	0.00075	0.00073	0.00077
	HPD	0.00079	0.00068	0.0007	0.00071	0.00072
0.05		$\tilde{\theta}_2^{BS}$	$\tilde{\theta}_2^{BLL}$	$\tilde{\theta}_2^{BLU}$	$\tilde{\theta}_2^{BEL}$	$\tilde{\theta}_2^{BEU}$
	Estimate	0.00923	0.00929	0.00935	0.00927	0.00942
	BCI	0.00221	0.00203	0.0021	0.00201	0.00213
0.10	HPD	0.00214	0.00188	0.00202	0.00192	0.002
	Estimate	0.00948	0.00943	0.00944	0.00947	0.00938
	BCI	0.00245	0.00209	0.00213	0.00207	0.00214
	HPD	0.0022	0.00192	0.00205	0.00198	0.00203

TABLE 22: Bayes estimate of parameter and parametric function with their confidence intervals.

$p$		$\tilde{\mathcal{C}}_2^{BS}$	$\tilde{\mathcal{C}}_2^{BLL}$	$\tilde{\mathcal{C}}_2^{BLU}$	$\tilde{\mathcal{C}}_2^{BEL}$	$\tilde{\mathcal{C}}_2^{BEU}$
0.05	Estimate	0.38155	0.38421	0.39729	0.38384	0.39685
	BCI	0.03547	0.02975	0.03145	0.03012	0.03247
	HPD	0.02845	0.02384	0.02473	0.02421	0.02524
0.10	Estimate	0.38284	0.38407	0.38476	0.39752	0.39245
	BCI	0.03604	0.03028	0.03289	0.03087	0.03352
	HPD	0.02911	0.02429	0.02594	0.02514	0.02585
0.05		$\tilde{\mathcal{C}}_2^{BS}$	$\tilde{\mathcal{C}}_2^{BLL}$	$\tilde{\mathcal{C}}_2^{BLU}$	$\tilde{\mathcal{C}}_2^{BEL}$	$\tilde{\mathcal{C}}_2^{BEU}$
	Estimate	0.42485	0.41458	0.42945	0.42476	0.41578
	BCI	0.03045	0.02745	0.02824	0.02721	0.02958
0.10	HPD	0.02584	0.02184	0.02237	0.02097	0.02199
	Estimate	0.41865	0.41474	0.42847	0.42384	0.41423
	BCI	0.03485	0.02834	0.03214	0.02958	0.03054
	HPD	0.03754	0.02245	0.02318	0.02154	0.02274

TABLE 22: Continued.

$p$		$\tilde{\mathcal{C}}_2^{BS}$	$\tilde{\mathcal{C}}_2^{BLL}$	$\tilde{\mathcal{C}}_2^{BLU}$	$\tilde{\mathcal{C}}_2^{BEL}$	$\tilde{\mathcal{C}}_2^{BEU}$
$p$		$\tilde{R}_1^{BS}$	$\tilde{R}_1^{BLL}$	$\tilde{R}_1^{BLU}$	$\tilde{R}_1^{BEL}$	$\tilde{R}_1^{BEU}$
0.05	Estimate	0.48658	0.49547	0.49394	0.48485	0.49361
	BCI	0.00945	0.00865	0.00912	0.00859	0.0092
	HPD	0.00789	0.00638	0.00676	0.00642	0.00682
0.10	Estimate	0.49587	0.49235	0.48458	0.48695	0.49054
	BCI	0.00983	0.00877	0.00926	0.0088	0.00932
	HPD	0.00811	0.00676	0.00691	0.00669	0.00711
$p$		$\tilde{R}_2^{BS}$	$\tilde{R}_2^{BLL}$	$\tilde{R}_2^{BLU}$	$\tilde{R}_2^{BEL}$	$\tilde{R}_2^{BEU}$
0.05	Estimate	0.51845	0.52065	0.51874	0.5174	0.52483
	BCI	0.01184	0.01042	0.01098	0.01032	0.01068
	HPD	0.00948	0.00948	0.00997	0.00955	0.00989
0.10	Estimate	0.51005	0.51487	0.52546	0.52485	0.52054
	BCI	0.01245	0.01138	0.01187	0.01101	0.01117
	HPD	0.01010	0.00994	0.01024	0.01019	0.01038
$p$		$\tilde{p}^{BS}$	$\tilde{p}^{BLL}$	$\tilde{p}^{BLU}$	$\tilde{p}^{BEL}$	$\tilde{p}^{BEU}$
0.05	Estimate	0.04928	0.0494	0.04824	0.0494	0.04824
	BCI	0.01384	0.01074	0.0114	0.01011	0.0114
	HPD	0.01022	0.0092	0.00988	0.00931	0.00988
0.10	Estimate	0.10948	0.10941	0.11213	0.10497	0.10513
	BCI	0.01422	0.01122	0.01183	0.01089	0.01183
	HPD	0.01058	0.00984	0.01019	0.00971	0.01019

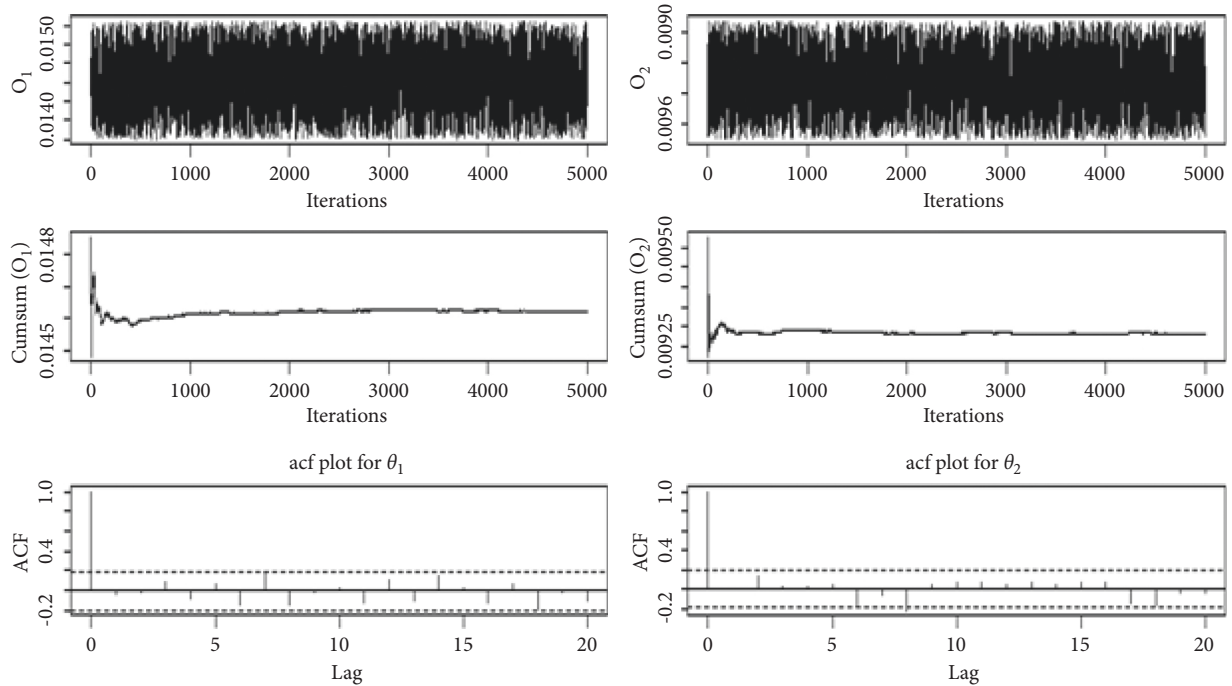


FIGURE 1: The iteration Cusum and acf plot for  $\theta_1$  and  $\theta_2$  of MCMC-generated samples.

cumulative incidence function obtain at the given time  $t_0 = 300$ .

### 7. Conclusion

We studied the competing risks model under progressive type-II censored with binomial removals. We considered the lifetimes of objects follow the Akshaya subdistributions with

unknown parameters. Also, the number of items or individuals removed at every failure time follows the Binomial distribution. The classical and Bayesian approaches are used to account for the point and interval estimation procedures for parameters and parametric functions. The Bayes estimate is obtained by using the Markov Chain Monte Carlo (MCMC) method under symmetric and asymmetric loss functions. So, the Metropolis–Hasting algorithm is applied

to generate Markov Chain Monte Carlo (MCMC) samples from the posterior density function. A simulated data set is applied to diagnose the performance of the given technique applied here. The ML and Bayes estimates with their respected length of confidence intervals are presented. Also, the component reliability and cumulative incidence functions are obtained by using simulated data set and real data set. We can guarantee more accurate results rather than any other model can achieve which is not appropriate for the system and can achieve which is not appropriate for the system. Overview of the analysis of survival competing risk:

- (i) Cumulative incidence functions (CIFs) should be used to estimate the likelihood of each type of competing risk.
- (ii) Researchers must decide whether the research goal is to answer etiologic questions or to estimate incidence or predict prognosis.
- (iii) When estimating incidence or predicting prognosis in the presence of competing risks, use the Fine-Gray subdistribution hazard model.
- (iv) When addressing etiologic questions, use the cause-specific hazard model.
- (v) In some cases, both types of regression models should be estimated for each competing risk in order to fully understand the effect of covariates on the incidence and rate of occurrence of each outcome.

The results for all competing causes, as well as cause-specific and subdistribution hazard functions, must be presented. This method allows for a more comprehensive understanding of not just the effects of prognostic factors but also the absolute risks associated with the various results in the study sample. It is difficult for decision makers to consider all hazards while making clinical decisions. Due to the availability of software, analyzing the cumulative incidence function has become increasingly popular and widely reported in recent years. Biases can occur when using the Kaplan–Meier estimator to estimate the cumulative incidence of the event of interest, as well as when using a proportional hazards model to estimate the effects of covariates on the cumulative incidence function when using a proportional hazards model for the cause-specific hazard function. The impact of incorrectly treating competing events as censoring events has practical implications in these analyses. In general, the more competing events there are, the more probable it is that competing events will be treated as censoring events. When the percentage of competing events is larger than 10%, the scientific objectives of the analysis, as well as the suitable choice of end point and technique of analysis, must be carefully considered.

In our case study, we demonstrated that a variable can have an effect on the incidence of an outcome that differs from its effect on the outcome's cause-specific hazard. This emphasises the importance of investigating the impact of both incidences and cause-specific hazard functions of all event types in order to develop a comprehensive

understanding of the various competing events. Competing risks are events that prevent the occurrence of the desired outcome. In some cases, more clarity may be required before proceeding with the analysis to determine what constitutes a competing risk. For example, if a person develops one type of heart disease, can he or she later develop another type of heart disease, or are the two conditions mutually exclusive, precluding the later second disease? Such clinical issues must be addressed during the design phase before conducting the statistical analysis. For more reading, see Abushal [61, 62].

In conclusion, competing risks are common in survival research. We encourage analysts to fully utilise the variety of statistical methods developed in the statistical literature for the analysis of survival data. Investigators must be aware of competing risks and their potential impact on statistical analyses. Researchers must choose the best method to address the study objectives and ensure that the analysis results are correctly interpreted.

## 8. Discussion and Scope of Future Research

A set of statistical probability distributions used in reliability engineering and lifespan data analysis is referred to as parametric survival regression models. Serial coupling with identical binomial or exponential components is no longer a requirement for system lifetime distributions. Survival analysis data are more difficult to work with since they are characterized by uncertainty, risk, and complexity. This highlights the importance of establishing a development risk structure, methodology, and approach. The suggested family's promise has been proved by fitting it to a real-world data set, and statistical analysis demonstrates that it is a better fit. We plan to investigate a number of issues regarding the analysis of various forms of data using a masked model with independent and dependent failure causes. The most important outcomes of this study are in the fields of media and electronic equipment.

### Data Availability

The document contains all of the data that are accessible.

### Conflicts of Interest

The authors warrant that they do not have any conflicts of interest to disclose.

### Acknowledgments

The authors would like to thank the Deanship of Scientific Research at Umm Al-Qura University for supporting this work by Grant Code 22UQU4310063DSR04.

### References

- [1] D. G. Hoel, "A Representation of Mortality Data by Competing Risks," *Biometrics*, vol. 28, no. 2, pp. 475–488, 1972.
- [2] J. W. Boag, "Maximum likelihood estimates of the proportion of patients cured by cancer therapy," *Journal of the Royal*

- Statistical Society: Series B (Methodological)*, vol. 11, no. 1, pp. 15–44, 1949.
- [3] A. M. Sarhan, A. I. El-Gohary, A. Mustafa, and A. H. Tolba, “Statistical analysis of regression competing risks model with covariates using Weibull sub-distributions,” *International Journal of Reliability and Applications*, vol. 20, no. 2, pp. 73–88, 2019.
  - [4] T. A. Abushal, “Parametric inference of Akash distribution for Type-II censoring with analyzing of relief times of patients,” *Aims Mathematics*, vol. 6, no. 10, pp. 10789–10801, 2021.
  - [5] T. A. Abushal, “Bayesian estimation of the reliability characteristic of shanker distribution,” *Journal of the Egyptian Mathematical Society*, vol. 27, no. 1, pp. 30–15, 2019.
  - [6] Z. Tan, “Estimation of component failure probability from masked binomial system testing data,” *Reliability Engineering & System Safety*, vol. 88, no. 3, pp. 301–309, 2005.
  - [7] A. M. Sarhan, F. M. Guess, and J. S. Usher, “Estimators for reliability measures in geometric distribution model using dependent masked system life test data,” *IEEE Transactions on Reliability*, vol. 56, no. 2, pp. 312–320, 2007.
  - [8] A. M. Sarhan and D. Kundu, “Bayes estimators for reliability measures in geometric distribution model using masked system life test data,” *Computational Statistics & Data Analysis*, vol. 52, no. 4, pp. 1821–1836, 2008.
  - [9] H.-Y. Jiang, “Parameter estimation of the Poisson shock model using masked data,” *International Journal of Pure and Applied Mathematics*, vol. 71, no. 4, pp. 559–569, 2011.
  - [10] A. M. Almarashi, A. Algarni, A. M. Daghistani, G. A. Abd-Elmougod, S. Abdel-Khalek, and M. Z. Raqab, “Inferences for joint hybrid progressive censored exponential lifetimes under competing risk model,” *Mathematical Problems in Engineering*, vol. 2021, Article ID 3380467, 12 pages, 2021.
  - [11] S. J. Almalki, T. A. Abushal, M. D. Alsulami, and G. A. Abd-Elmougod, “Analysis of Type-II censored competing risks’ data under reduced new modified Weibull distribution,” *Complexity*, vol. 2021, Article ID 9932840, 13 pages, 2021.
  - [12] T. A. Abushal, A. A. Soliman, and G. A. Abd-Elmougod, “Statistical inferences of burr xii lifetime models under joint type-1 competing risks samples,” *Journal of Mathematics*, vol. 2021, Article ID 9553617, 16 pages, 2021.
  - [13] M. Miyakawa, “Analysis of incomplete data in competing risks model,” *IEEE Transactions on Reliability*, vol. R-33, no. 4, pp. 293–296, 1984.
  - [14] M. J. Crowder, *Classical Competing Risks*, CRC Press, Boca Raton, FL, USA, 2001.
  - [15] N. Balakrishnan, N. Kannan, C. T. Lin, and H. K. T. Ng, “Point and interval estimation for Gaussian distribution, based on progressively type-ii censored samples,” *IEEE Transactions on Reliability*, vol. 52, no. 1, pp. 90–95, 2003.
  - [16] A. M. Sarhan, M. Alameri, and I. Al-Wasel, “Analysis of progressive censoring competing risks data with binomial removals,” *International Journal of Mathematics Analysis*, vol. 2, no. 20, pp. 965–976, 2008.
  - [17] J. Kumar, M. Panwar, and S. Tomer, “Bayesian estimation of component reliability using progressively censored masked system lifetime data from Rayleigh distribution,” *Journal of Reliability and Statistical Studies*, vol. 7, no. 2, pp. 37–52, 2014.
  - [18] H. A. David and M. L. Moeschberger, *The Theory of Competing Risks*, Griffin, London, UK, 1978.
  - [19] A. M. Sarhan, A. I. E. Gohary, and A. H. Tolba, “Statistical analysis of a competing risks model with Weibull sub-distributions,” *Applied Mathematics*, vol. 08, no. 11, pp. 1671–1683, 2017.
  - [20] R. Shankar, “Akshaya distribution and its application,” *American Journal of Mathematics and Statistics*, vol. 7, no. 2, pp. 51–59, 2017.
  - [21] A. T. Ramadan, A. H. Tolba, and B. S. El-Desouky, “Generalized power Akshaya distribution and its applications,” *Open Journal of Modelling and Simulation*, vol. 9, no. 4, pp. 323–338, 2021.
  - [22] A. C. Cohen, “Progressively censored samples in life testing,” *Technometrics*, vol. 5, no. 3, pp. 327–339, 1963.
  - [23] J.-I. Seo, S.-B. Kang, and H.-Y. Kim, “New approach for analysis of progressive type-ii censored data from the pareto distribution,” *Communications for Statistical Applications and Methods*, vol. 25, no. 5, pp. 569–575, 2018.
  - [24] R. Kishan and J. Kumar, “Bayesian estimation for the Lindley distribution under progressive type-ii censoring with binomial removals,” *International Journal of Agricultural & Statistical Sciences*, vol. 15, no. 1, pp. 361–369, 2019.
  - [25] M. M. Salah, “On progressive type-ii censored samples from alpha power exponential distribution,” *Journal of Mathematics*, vol. 2020, Article ID 2584184, 8 pages, 2020.
  - [26] S. Li and W. Gui, “Bayesian survival analysis for generalized pareto distribution under progressively type ii censored data,” *International Journal of Reliability, Quality and Safety Engineering*, vol. 27, no. 1, Article ID 2050001, 2020.
  - [27] N. Balakrishnan and R. Aggarwala, *Progressive Censoring: Theory, Methods, and Applications*, Springer Science & Business Media, Berlin, Heidelberg, Germany, 2000.
  - [28] B. Pradhan and D. Kundu, “Inference and optimal censoring schemes for progressively censored Birnbaum-Saunders distribution,” *Journal of Statistical Planning and Inference*, vol. 143, no. 6, pp. 1098–1108, 2013.
  - [29] Y. Du and W. Gui, “Statistical inference of adaptive type ii progressive hybrid censored data with dependent competing risks under bivariate exponential distribution,” *Journal of Applied Statistics*, pp. 1–21, 2021.
  - [30] Z. Mahmood, T. M. Jawa, N. Sayed-Ahmed, E. M. Khalil, A. H. Muse, and A. H. Tolba, “An extended cosine generalized family of distributions for reliability modeling: characteristics and applications with simulation study,” *Mathematical Problems in Engineering*, vol. 2022, Article ID 3634698, 20 pages, 2022.
  - [31] A. H. Muse, A. H. Tolba, E. Fayad, O. A. Abu Ali, M. Nagy, and M. Yusuf, “Modelling the COVID-19 mortality rate with a new versatile modification of the log-logistic distribution,” *Computational Intelligence and Neuroscience*, vol. 2021, Article ID 8640794, 14 pages, 2021.
  - [32] A. H. Muse, S. M. Mwalili, and O. Ngesa, “On the log-logistic distribution and its generalizations: a survey,” *International Journal of Statistics and Probability*, vol. 10, no. 3, p. 93, 2021.
  - [33] M. H. Tahir and S. Nadarajah, “Parameter induction in continuous univariate distributions: well-established g families,” *Anais da Academia Brasileira de Ciências*, vol. 87, no. 2, pp. 539–568, 2015.
  - [34] M. H. Tahir and G. M. Cordeiro, “Compounding of distributions: a survey and new generalized classes,” *Journal of Statistical Distributions and Applications*, vol. 3, no. 1, pp. 13–35, 2016.
  - [35] A. H. Tolba, E. M. Almetwally, and D. A. Ramadan, “Bayesian estimation of a one parameter Akshaya distribution with progressively type ii censored data,” *Journal of Statistics Applications Probability An International Journal*, vol. 11, pp. 565–579, 2022.

- [36] D. Kundu, N. Kannan, and N. Balakrishnan, "Analysis of progressively censored competing risks data," *Handbook of Statistics*, vol. 23, pp. 331–348, 2003.
- [37] B. Pareek, D. Kundu, and S. Kumar, "On progressively censored competing risks data for Weibull distributions," *Computational Statistics & Data Analysis*, vol. 53, no. 12, pp. 4083–4094, 2009.
- [38] D. Kundu and B. Pradhan, "Bayesian analysis of progressively censored competing risks data," *Sankhya B*, vol. 73, no. 2, pp. 276–296, 2011.
- [39] R. Bundel, H. Pokhriyal, and S. K. Panwar, "Modeling competing risks for progressively censored data using inverse Lindley distribution," *Applied Mathematics*, vol. 1, no. 2, pp. 1–11, 2016.
- [40] A. K. Dey, A. Jha, and S. Dey, "Bayesian analysis of modified Weibull distribution under progressively censored competing risk model," 2016, <https://arxiv.org/abs/1605.06585>.
- [41] L. Wang, "Inference of progressively censored competing risks data from Kumaraswamy distributions," *Journal of Computational and Applied Mathematics*, vol. 343, pp. 719–736, 2018.
- [42] H. Liao and W. Gui, "Statistical inference of the Rayleigh distribution based on progressively type ii censored competing risks data," *Symmetry*, vol. 11, no. 7, p. 898, 2019.
- [43] M. Chacko and R. Mohan, "Bayesian analysis of Weibull distribution based on progressive type-ii censored competing risks data with binomial removals," *Computational Statistics*, vol. 34, no. 1, pp. 233–252, 2019.
- [44] E. A. Ahmed, Z. Ali Alhussain, M. M. Salah, H. Haj Ahmed, and M. S. Eliwa, "Inference of progressively type-ii censored competing risks data from chen distribution with an application," *Journal of Applied Statistics*, vol. 47, no. 13–15, pp. 2492–2524, 2020.
- [45] F. Azizi, F. Haghighi, and N. Tabibi Gilani, "Statistical inference for competing risks model under progressive interval censored Weibull data," *Communications in Statistics - Simulation and Computation*, vol. 49, no. 7, pp. 1931–1944, 2020.
- [46] S. Liu and W. Gui, "Estimating the parameters of the two-parameter Rayleigh distribution based on adaptive type ii progressive hybrid censored data with competing risks," *Mathematics*, vol. 8, no. 10, p. 1783, 2020.
- [47] C. Lodhi, Y. M. Tripathi, and R. Bhattacharya, "On a progressively censored competing risks data from Gompertz distribution," *Communications in Statistics - Simulation and Computation*, pp. 1–22, 2021.
- [48] A. E.-R. M. Abd El-Raheem, M. Hosny, M. H. Abu-Moussa, and M. H. Abu-Moussa, "On progressive censored competing risks data: real data application and simulation study," *Mathematics*, vol. 9, no. 15, p. 1805, 2021.
- [49] A. K. Mahto, C. Lodhi, Y. M. Tripathi, and L. Wang, "Inference for partially observed competing risks model for Kumaraswamy distribution under generalized progressive hybrid censoring," *Journal of Applied Statistics*, vol. 49, no. 8, pp. 2064–2092, 2021.
- [50] Y. Du and W. Gui, "Statistical inference of burr-xii distribution under adaptive type ii progressive censored schemes with competing risks," *Results in Mathematics*, vol. 77, no. 2, pp. 81–49, 2022.
- [51] Q. Lv, R. Hua, and W. Gui, "Statistical inference of Gompertz distribution under general progressive type ii censored competing risks sample," *Communications in Statistics-Simulation and Computation*, pp. 1–20, 2022.
- [52] B. Efron and R. J. Tibshirani, *An Introduction to the Bootstrap*, CRC Press, Boca Raton, FL, USA, 1994.
- [53] J. Albert, *Bayesian Computation with R*, Springer Science & Business Media, Berlin, Heidelberg, Germany, 2009.
- [54] A. H. Muse, S. Mwalili, O. Ngesa, S. J. Almalki, and G. A. Abd-Elmougod, "Bayesian and classical inference for the generalized log-logistic distribution with applications to survival data," *Computational Intelligence and Neuroscience*, vol. 2021, Article ID 5820435, 24 pages, 2021.
- [55] R. M. El-Sagheer, A. H. Tolba, T. M. Jawa, and N. Sayed-Ahmed, "Inferences for stress-strength reliability model in the presence of partially accelerated life test to its strength variable," *Computational Intelligence and Neuroscience*, vol. 2022, Article ID 4710536, 13 pages, 2022.
- [56] A. H. Muse, S. Mwalili, O. Ngesa, H. M. Alshambari, S. K. Khosa, and E. Hussam, "Bayesian and frequentist approach for the generalized log-logistic accelerated failure time model with applications to larynx-cancer patients," *Alexandria Engineering Journal*, vol. 61, no. 10, pp. 7953–7978, 2022.
- [57] D. A. Ramadan, E. M. Almetwally, and A. H. Tolba, "Statistical inference to the parameter of the Akshaya distribution under competing risks data with application HIV infection to aids," *Annals of Data Science*, pp. 1–27, 2022.
- [58] S. Geman and D. Geman, "Stochastic relaxation, Gibbs distributions and the Bayesian restoration of images," *Journal of Applied Statistics*, vol. 20, no. 5–6, pp. 25–62, 1993.
- [59] A. Azzalini, *Statistical Inference Based on the Likelihood*, CRC Press, Boca Raton, FL, USA, 1996.
- [60] M.-H. Chen, Q.-M. Shao, and J. G. Ibrahim, *Monte Carlo Methods in Bayesian Computation*, Springer Science & Business Media, Berlin, Heidelberg, Germany, 2012.
- [61] M. Kilai, G. A. Waititu, W. A. Kibira, M. M. Abd El-Raouf, and T. A. Abushal, "A new versatile modification of the Rayleigh distribution for modeling COVID-19 mortality rates," *Results in Physics*, vol. 35, Article ID 105260, 2022.
- [62] T. A. Abushal, A. A. Soliman, and G. A. Abd-Elmougod, "Inference of partially observed causes for failure of Lomax competing risks model under type-II generalized hybrid censoring scheme," *Alexandria Engineering Journal*, vol. 61, no. 7, pp. 5427–5439, 2022.



## Research Article

# On Extended Neoteric Ranked Set Sampling Plan: Likelihood Function Derivation and Parameter Estimation

Fathy H. Riad,<sup>1,2</sup> Mohamed A. Sabry ,<sup>2</sup> Ehab M. Almetwally ,<sup>3,4</sup> Ramy Aldallal ,<sup>5</sup> Randa Alharbi ,<sup>6</sup> and Md. Moyazzem Hossain <sup>7</sup>

<sup>1</sup>Mathematics Department, College of Science, Jouf University, P. O.Box 2014, Sakaka, Saudi Arabia

<sup>2</sup>Department of Mathematics, Faculty of Science, Minia University, Minia 61519, Egypt

<sup>3</sup>Department of Mathematical Statistics, Faculty of Graduate Studies for Statistical Research, Cairo University, Cairo, Egypt

<sup>4</sup>Faculty of Business Administration, Delta University of Science and Technology, Gamasa, Egypt

<sup>5</sup>College of Business Administration in Hotat Bani Tamim, Prince Sattam Bin Abdulaziz University, Al-Kharj, Saudi Arabia

<sup>6</sup>Department of Statistics, Faculty of Science, University of Tabuk, Tabuk, Saudi Arabia

<sup>7</sup>Department of Statistics, Jahangirnagar University, Savar, Dhaka 1342, Bangladesh

Correspondence should be addressed to Mohamed A. Sabry; mohusss@cu.edu.eg and Md. Moyazzem Hossain; hossainmm@juniv.edu

Received 16 November 2021; Revised 13 April 2022; Accepted 21 April 2022; Published 2 June 2022

Academic Editor: M. M. El-Dessoky

Copyright © 2022 Fathy H. Riad et al. This is an open access article distributed under the Creative Commons Attribution License, which permits unrestricted use, distribution, and reproduction in any medium, provided the original work is properly cited.

The extended neoteric ranked set sampling (ENRSS) plan proposed by Taconeli and Cabral has proven to outperform many one stages and two stages ranked set sampling plans when estimating the mean and the variance for different populations. Therefore, in this paper, the likelihood function based on ENRSS is proposed and used for estimation of the parameters of the inverted Nadarajah–Haghighi distribution. An extensive Monte Carlo simulation study is conducted to assess the performance of the proposed likelihood function, and the efficiency of the estimated parameters based on ENRSS is compared with the well-known ranked set sampling (RSS) plan and some of its modifications. These modifications include the extended ranked set sampling (ERSS) plan and the neoteric ranked set sampling (NRSS) plan. The results as foreseeable were very satisfactory and gave similar results to Taconeli and Cabral's 2019 results.

## 1. Introduction

Ranked set sampling (RSS) plans were proposed to provide estimators that are more efficient than those derived under simple random sampling (SRS) plans. RSS plans were first proposed by McIntyre in 1952, to find efficient estimates of the mean pasture yields. These plans assume that there are no errors in ranking the units concerning the variable of interest. In most practical applications, imperfect ranking exists and there will be an efficiency loss in the estimators [1]. To reduce such losses, several modifications to the RSS procedure were proposed. The main purpose was to allow for the achievement of higher statistical efficiency and probably a lower operating effort. The first modification of RSS was the extreme ranked set sampling (ERSS) plan introduced by Samwai et al. [2]. Muttlak [3] proposed the median ranked

set sampling (MRSS) plan, Al-Odat and Al-Saleh [4] proposed the moving extreme ranked set sampling (MERSS) plan, Al-Saleh and Al-Omari [5] proposed the multistage ranked set sampling (MSRSS), and others proposed the multistage ranked set sampling (MSRSS). Recently, Zamanzade E, Al-Omari [1] proposed a new ranked set sampling plan based on a dependent scheme, namely, the neoteric ranked set sampling (NRSS) plan which showed relative improvement in the efficiency of the population mean and variance estimates. Moreover, Taconeli and Cabral [6] proposed several modifications to the NRSS plan. One of these plans is the extended neoteric ranked set sampling (ENRSS) plan. They showed that the ENRSS plan is superior to NRSS and other plans. Unlike RSS and ERSS plans, NRSS and ENRSS are classified as dependent RSS plans as the resulting samples have a dependence structure.

In 2020, Sabry and Shabaan proposed the likelihood function of the NRSS plan and used it to estimate the parameters of the inverse Weibull distribution. Chen et al. [7] obtained RSS for efficient estimation of a population proportion. Terpstra and Liudahl [8] constructed concomitant-based rank set sampling proportion estimates. Mahdizadeh [9] discussed entropy-based test of exponentiality in ranked set sampling. Mahdizadeh and Strzalkowska-Kominiak [10] discussed resampling-based inference for a distribution function using censored ranked set samples. Akhter et al. [11] discussed RSS for generalized Bilal distribution. Strzalkowska-Kominiak and Mahdizadeh [12] discussed Kaplan–Meier estimator based on ranked set samples. Aljohani et al. [13] discussed ranked set sampling with an application of modified Kies exponential distribution. Sabry et al. [14] used a hybrid approach to evaluate the performance of some ranked set sampling strategies. Sabry and Almetwally [15] used under-ranked and double-ranked set sampling designs to estimate the parameters of the exponential Pareto distribution. The results showed similar results to Zamanzade and Al-Omari [16] and Taconeli and Cabral [6] results when estimating the population means and variance.

This paper aims to compute the joint order distribution of an ENRSS sample and consequently propose the associated likelihood function. Also, to use the proposed likelihood function to estimate the parameters of the inverted Nadarajah–Haghighi distribution and to conduct Monte Carlo simulations to assess the performance of the ENRSS plan and compare the results with RSS, ERSS, and NRSS plans.

The inverted Nadarajah–Haghighi [INH( $\lambda, \alpha$ )] distribution was proposed by Taher and co-authors (2018). The cumulative distribution function (CDF), probability density function (PDF), and quantile function used are as follows:

$$F(x; \lambda, \alpha) = \exp\{1 - (1 + \lambda x^{-1})^\alpha\} \quad x > 0, \quad (1)$$

$$f(x; \lambda, \alpha) = \lambda \alpha x^{-2} (1 + \lambda x^{-1})^{\alpha-1} \exp\{1 - (1 + \lambda x^{-1})^\alpha\}, \quad (2)$$

$$x = \lambda \left[ (1 - \ln u)^{1/\alpha} - 1 \right]^{-1}, \quad (3)$$

where  $\lambda, \alpha > 0$ , and  $u$  have a uniform  $U(0, 1)$  distribution. Figure 1 illustrates different PDF plots for the INH distribution.

The remainder of the paper is laid out as follows: the second section is devoted to a brief overview of the various RSS plans discussed in this study. In Section 3, maximum likelihood analysis for the INH distribution is considered for all plans, and in Section 4, an extensive simulation study is conducted and the different plans are compared and the results are reported. Finally, in Section 5, the paper is concluded.

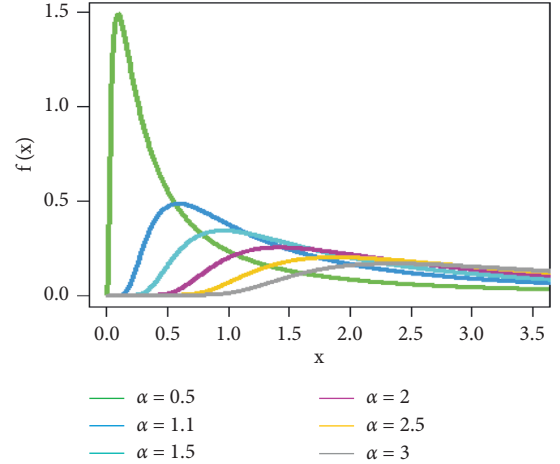


FIGURE 1: Different PDF plot for INH distribution when scale parameter  $\lambda = 1$ .

## 2. Ranked Set Sampling Designs

The ranked set sampling plans covered in this study are discussed in this section, with the number of cycles of the RSS plans assumed to be one for simplicity.

*2.1. RSS Design.* The RSS design according to Wolfe [17] can be described as follows:

Step 1: select  $m^2$  units randomly from the target population with CDF  $F(x; \theta)$  and PDF  $f(x; \theta)$

Step 2: allocate the  $m^2$  selected units as randomly as possible into  $m$  sets, each of size  $m$

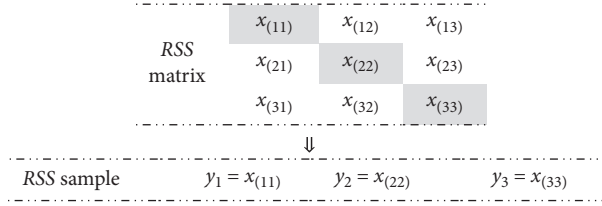
Step 3: rank the units within each set without yet knowing any values for a variable of interest

Step 4: choose a sample for real quantification by selecting the smallest ranked unit from the first set, the second smallest ranked unit from the second set, and so on until the largest ranked unit from the last set is chosen

Step 5: to get a sample of size  $n = mr$ , repeat steps 1 through 4 for  $r$  cycles

Figure 2 describes the process for choosing an RSS sample from one cycle where  $X_{(11)}$  is the lowest observation in the first row,  $X_{(22)}$  is the second-lowest observation from the second row, and finally the greatest observation from the previous row is  $X_{(mm)}$ .

Let  $\{y_{is}, i = 1, 2, \dots, m, s = 1, 2, \dots, r \text{ and } -\infty < x_{(i)} < \infty\}$  denote a ranked set sample derived from a distribution with PDF  $f(x; \theta)$  and CDF  $F(x; \theta)$ , where  $m$  denotes the set size,  $r$  denotes the number of cycles, and  $\theta$  is the parameter space. The probability function for this design is as follows:

FIGURE 2: Display of  $m^2$  observations in one cycle and the selected RSS sample of size  $m = 3$ .

$$L_R(\theta; y) = \prod_{s=1}^r \prod_{i=1}^m \frac{m!}{(i-1)!(m-i)!} f(y_{is}; \theta) [F(y_{is}; \theta)]^{i-1} [1 - F(y_{is}; \theta)]^{m-i}. \quad (4)$$

**2.2. ERSS Design.** It is the first variation of RSS proposed by Samawi et al. [2] which only uses a maximum or minimum ranked unit from each set to determine the population mean. The following approach is used to estimate based on ERSS.

Step 1: repeat Steps 1 through 3 in the RSS design.

Step 2: the selection mechanism can be altered depending on whether the set size is even or odd. Select the lowest-ranked unit of each set from the first  $m/2$  sets and the highest-ranked unit of each set from the

other  $m/2$  sets if the set size  $m$  is even. If the number of units in the set is odd, choose the lowest-ranked unit from the first  $m - 1/2$  sets, the highest-ranked unit from the second  $m - 1/2$  sets, and the median from the remaining set.

Step 3: to get a sample of size  $n = mr$ , repeat the previous procedures  $r$  times.

The process for one cycle, as well as the cases of  $m = 4$  and  $m = 5$ , is as shown in Figure 3.

Let  $\{z_i, i = 1, 2, \dots, m\}$  be a ranked set sample (RSS) generated from a distribution with pdf  $g(x; \theta)$  and cdf  $G(x; \theta)$ , where the set size is  $m$  and the parameter space is  $\theta$ . Let  $g = m/2$ ,  $h = m - 1/2$ , and  $u_i = m - i + 1$ , then the likelihood function of the ERSS sample is given by

*Case 1.  $m$  odd:*

$$\begin{aligned} L_{E_o}(\theta; z) &= \left( \prod_{i=1}^h [g_{1:m}(z_i; \theta) g_{m:m}(z_{u_i}; \theta)] \right) (g_{h+1:m}(z_{h+1}; \theta)) \\ &= \prod_{i=1}^h \left[ m g(z_i; \theta) [1 - G(z_i; \theta)]^{m-1} \times m g(z_{u_i}; \theta) [G(z_{u_i}; \theta)]^{m-1} \right] \times \frac{m!}{(h!)^2} g(z_{h+1}; \theta) (G(z_{h+1}; \theta) (1 - G(z_{h+1}; \theta)))^h. \end{aligned} \quad (5)$$

*Case 2.  $m$  even:*

$$\begin{aligned} L_{E_e}(\theta; z) &= \prod_{i=1}^g g_{1:m}(z_i; \theta) g_{m:m}(z_{u_i}; \theta), \\ &= \prod_{i=1}^g \left( m g(z_i; \theta) [1 - G(z_i; \theta)]^{m-1} \right) \left( m g(z_{u_i}; \theta) [G(z_{u_i}; \theta)]^{m-1} \right). \end{aligned} \quad (6)$$

**2.3. Neoteric Ranked Set Sampling (NRSS) Design.** The NRSS sampling plan presented by Zamanzade E and Al-Omari [1] is described in the following steps:

Step 1: select  $m^2$  random units from the target population.

Step 2: rank the  $m^2$  sample units according to some predetermined criteria.

Step 3: for  $i = 1, \dots, m$ , choose the sample unit rated  $[(i-1)m + l]^{\text{th}}$  for the final sample.  $l =$

$$\begin{cases} m + 1/2 & m \text{ is odd} \\ m + 1/2 & m \text{ is even} \end{cases} \quad \text{and} \quad \text{while} \quad l = \begin{cases} m + 2/2 & i \text{ is odd} \\ m/2 & i \text{ is even} \end{cases}.$$

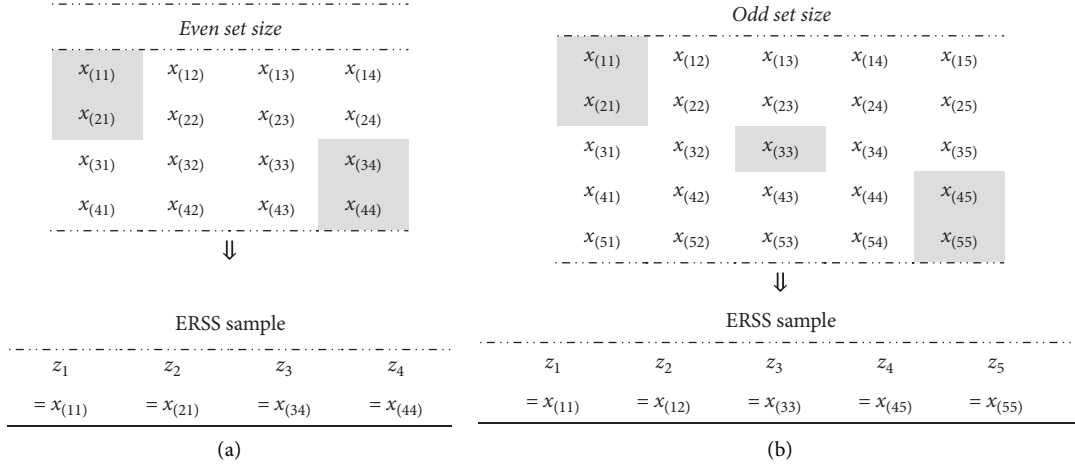


FIGURE 3: Display of  $m^2$  observations in one cycle and the selected ERSS sample of size: (a)  $m = 4$  and (b)  $m = 5$ .

Step 4: to obtain a final sample of size  $n = mr$ , repeat steps 1–3r times.

Figure 4 displays the step for establishing an NRSS sample in one cycle when  $m = 3$

**Lemma 1.** Let  $\{u_i, i = 1, 2, \dots, n\}$  be a neoteric ranked set sample obtained from a distribution with PDF  $h(u; \theta)$  and

CDF  $H(u; \theta)$ , and let  $\{u_{(k_i)_s}, i = 1, 2, \dots, m, s = 1, 2, \dots, r\}$  be a random sample of size  $n$  from a continuous population, where  $m$  is the set size,  $r$  is the number of cycles,  $\theta$  is the parameter space, and  $n = mr$ . Then, the likelihood function of NRSS samples is given by

$$L(\theta) = \frac{m^2!}{\prod_{i=1}^{m+1} (k_i - k_{i-1} - 1)!} \prod_{s=1}^r \prod_{i=1}^m h(u_{(k_i)_s}) \prod_{i=1}^{m+1} \left[ H(u_{(k_i)_s}) - H(u_{(k_{i-1})_s}) \right]^{(k_i - k_{i-1} - 1)}, \quad (7)$$

where

$$k_i = \begin{cases} \frac{m+1}{2} + (i-1)m, & m \text{ odd,} \\ \frac{m}{2} + (i-1)m, & m \text{ even, } i \text{ even,} \\ \frac{m+2}{2} + (i-1)m, & m \text{ even, } i \text{ odd,} \end{cases} \quad (8)$$

and  $k_0 = 0$ ,  $k_{m+1} = m^2 + 1$ , and  $u_{(k_0)} = -\infty$ ,  $u_{(k_{m+1})} = \infty$

*Proof.* (see Sabry and Shabaan [18]).  $\square$

#### 2.4. Extended Neoteric Ranked Set Sampling (ENRSS) Plan.

In ENRSS, Taconeli and Cabral's [6] proposal is based on a single ranking stage, where  $m^3$  sample units are observed instead  $m^2$  sample units as in all one-stage ranked set sampling designs. These  $m^3$  sample units are arranged in a single set and ordered utilizing some inexpensive ranking criteria. The units that will make up the final sample must next be chosen from (almost) evenly spaced spots. The ENRSS technique is described in the steps as follows:

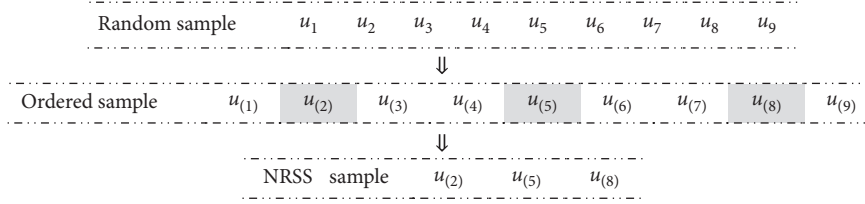
Step 1: choose  $m^3$  elements from the target population and combine them into a single ranking set.

Step 2: for  $i = 1, 2, \dots, m$ , choose the  $[m^2 + 1/2 + (i-1)m^2]^{\text{th}}$  ranked unit to compose the final sample if  $m$  is odd. If  $m$  is even, choose the  $[l + (i-1)m^2]^{\text{th}}$  ranked unit, where  $l = m^2/2$  represents even  $i$  and  $l = m^2 + 2/2$  represents odd  $i$ .

Step 3: to obtain a sample of size  $n = mr$ , repeat steps 1–2r times.

To pick an ENRSS sample with a set size of  $m = 3$ , a single set of  $m^3 = 27$  sample units should be taken, and the sample units ranked in positions 5, 14, and 23 should be chosen to create the final sample. If you want a sample of set size  $m = 4$ , use  $m^3 = 64$ , and the desired ENRSS sample will constitute the ranked units in positions 9, 24, 41, and 56 (see [6]).

**Lemma 2.** Let  $\{v_i, i = 1, 2, \dots, n\}$  be a random sample of size  $n$  from a continuous population and let  $\{v_{(i)_s}, t = 1, 2, \dots, m, s = 1, 2, \dots, r\}$  be an extended neoteric ranked set samples drawn from a model with PDF  $w(v; \theta)$  and CDF  $W(v; \theta)$ , where  $m$  is the set size,  $r$  is the number of cycles,  $\theta$  is the parameter space, and  $n = mr$ . Then, the likelihood function of an ENRSS sample is given by

FIGURE 4: Display of  $m^2$  observations in one cycle and the selected NRSS sample of size  $m = 3$ .

$$L_{EN}(\boldsymbol{\theta}) = \frac{m^3!}{\prod_{i=1}^{m+1} (i_t - i_{t-1} - 1)!} \prod_{s=1}^r \prod_{t=1}^m \omega(v_{(i_t)_s}) \prod_{i=1}^{m+1} [W(v_{(i_t)_s}) - W(v_{(i_{t-1})_s})]^{(i_t - i_{t-1} - 1)}, \quad (9)$$

where

$$i_t = \begin{cases} \frac{m^2 + 1}{2} + (i-1)m^2, & m \text{ odd,} \\ \frac{m^2}{2} + (i-1)m^2, & m \text{ even, } i \text{ even,} \\ \frac{m^2 + 2}{2} + (i-1)m^2, & m \text{ even, } i \text{ odd,} \end{cases} \quad (10)$$

and  $k_0 = 0$ ,  $k_{m+1} = m^3 + 1$ , and  $v_{(k_0)} = -\infty$ ,  $v_{(k_{m+1})} = \infty$ . See Figure 5 which shows  $m^3$  observations in one cycle and the selected ENRSS sample of size  $m = 3$ .

*Proof.* Let  $\{x_i, i = 1, 2, \dots, n\}$  be a random sample from a continuous distribution with order statistics  $\{x_{(i)}, i = 1, 2, \dots, n\}$ . Let  $\{x_{(i_j)}, i = 1, 2, \dots, n\}$  be a subset of the order statistics corresponding to  $\{x_i\}$ . Then, the joint PDF of  $\{X_{(i_j)}\}$  according to [8] and [9] is given by

$$f^{(k)}(x_{(i_1)}, x_{(i_2)}, \dots, x_{(i_k)}) = \frac{n!}{\prod_{j=1}^{k+1} (i_j - i_{j-1} - 1)!} \prod_{j=1}^k f(x_{(i_j)}) \prod_{j=1}^{k+1} [F(x_{(i_j)}) - F(x_{(i_{j-1})})]^{(i_j - i_{j-1} - 1)}, \quad (11)$$

where  $i_0 = 0$  and  $i_{k+1} = n + 1$  (see Figure 6).

Since to get an ENRSS sample  $\{X_{(i_j)}\}$  of size  $m$ ,  $m^3$  units are selected and ranked (ordered). Therefore and according

to [9], the joint PDF of an ENRSS sample of size  $m$  is given by

$$f^{(k)}(v_{(i_1)}, v_{(i_2)}, \dots, v_{(i_m)}) = \frac{m^3!}{\prod_{t=1}^{m+1} (i_t - i_{t-1} - 1)!} \prod_{t=1}^m \omega(v_{(i_t)}) \prod_{i=1}^{m+1} [W(v_{(i_t)}) - W(v_{(i_{t-1})})]^{|i_t - i_{t-1} - 1|. \quad (12)$$

If the ENRSS design is repeated  $r$  time to get a sample of size  $mr$ , the likelihood function of an ENRSS sample with set size  $m$  and number of cycles  $r$  will be given by

$$L_{EN}(\boldsymbol{\theta}) = \frac{m^3!}{\prod_{i=1}^{m+1} (i_t - i_{t-1} - 1)!} \prod_{s=1}^r \prod_{t=1}^m \omega(v_{(i_t)_s}) \prod_{i=1}^{m+1} [W(v_{(i_t)_s}) - W(v_{(i_{t-1})_s})]^{(i_t - i_{t-1} - 1)}, \quad (13)$$

Ordered sample	$z_{(1)}$	$v_{(2)}$	$v_{(3)}$	$v_{(4)}$	$v_{(5)}$	$v_{(6)}$	$v_{(7)}$	$v_{(8)}$	$v_{(9)}$
	$v_{(10)}$	$v_{(11)}$	$v_{(12)}$	$v_{(13)}$	$v_{(14)}$	$v_{(15)}$	$v_{(16)}$	$v_{(17)}$	$v_{(18)}$
	$v_{(19)}$	$v_{(20)}$	$v_{(21)}$	$v_{(22)}$	$v_{(23)}$	$v_{(24)}$	$v_{(25)}$	$v_{(26)}$	$v_{(27)}$
	↓								
	ENRSS sample				$v_{(5)}$	$v_{(14)}$	$v_{(23)}$		

FIGURE 5: Display of  $m^3$  observations in one cycle and the selected ENRSS sample of size  $m = 3$ .

where  $i_0 = 0, i_{m+1} = m + 1, v_{(i_0)} = -\infty, v_{(i_{m+1})} = \infty$  and  $i_t$  is defined in (8). This completes the proof. For more elaborations, we can see in Figure 6.  $\square$

### 3. Estimation of the Inverted Nadarajah–Haghighi Distribution Parameters

The parameters of INH  $(\lambda, \alpha)$  distribution are estimated using the maximum likelihood estimation (MLE) method. The estimation process is taking place when samples are drawn according to SRS, RSS, ERSS, NRSS, and ERSS sampling plans as illustrated in section 2.

**3.1. Estimation Based on SRS.** Let  $(x_i, i = 1, 2, \dots, m)$  be a SRS with CDF and PDF given in (1) and (2), respectively, the likelihood function of the SRS samples from INH  $(\lambda, \alpha)$  distribution is

$$\begin{aligned}
 L(\lambda, \alpha; x) &= \prod_{i=1}^m f(x_i; \lambda, \alpha) \\
 &= \prod_{i=1}^m \lambda \alpha x_i^{-2} (1 + \lambda x_i^{-1})^{\alpha-1} e^{1-(1+\lambda x_i^{-1})^\alpha} \\
 &= \lambda^m \alpha^m e^{m - \sum_{i=1}^m (1+\lambda x_i^{-1})^\alpha} \prod_{i=1}^m x_i^{-2} (1 + \lambda x_i^{-1})^{\alpha-1}.
 \end{aligned} \tag{14}$$

The log-likelihood function is thus given by

$$\begin{aligned}
 \ell(\lambda, \alpha) &= m \log \lambda + m \log \alpha + m - \sum_{i=1}^m (1 + \lambda x_i^{-1})^\alpha \\
 &\quad + \sum_{i=1}^m \log x_i^{-2},
 \end{aligned} \tag{15}$$

and the associated likelihood equations are therefore identified as

$$\frac{\partial \ell}{\partial \lambda} = \frac{m}{\lambda} - \alpha \sum_{i=1}^m x_i^{-1} (1 + \lambda x_i^{-1})^{\alpha-1}, \tag{16}$$

$$\frac{\partial \ell}{\partial \alpha} = \frac{m}{\alpha} - \sum_{i=1}^m (1 + \lambda x_i^{-1})^\alpha \log (1 + \lambda x_i^{-1})^\alpha = 0.$$

**3.2. Estimation Based on RSS.** Let  $\{y_{is}, i = 1, 2, \dots, m; s = 1, 2, \dots, r\}$  be a ranked set sample with the CDF and PDF provided in (1) and (2), respectively, where  $m$  is the set size,  $r$  is the number of cycles, and  $n = mr$ . Assuming  $r = 1$  and according to (4), the likelihood function of the RSS samples from INH  $(\lambda, \alpha)$  distribution is given by

$$\begin{aligned}
 L_R(\lambda, \alpha; y) &= \prod_{i=1}^m C_i \lambda \alpha y_i^{-2} (1 + \lambda y_i^{-1})^{\alpha-1} e^{1-(1+\lambda y_i^{-1})^\alpha} \left[ e^{1-(1+\lambda y_i^{-1})^\alpha} \right]^{i-1} \left[ 1 - e^{1-(1+\lambda y_i^{-1})^\alpha} \right]^{m-i}, \\
 &\propto \lambda^m \alpha^m \prod_{i=1}^m (1 + \lambda y_i^{-1})^{\alpha-1} e^{m(m+1)/2 - \sum_{i=1}^m i(1+\lambda y_i^{-1})^\alpha} \prod_{i=1}^m \left[ 1 - e^{1-(1+\lambda y_i^{-1})^\alpha} \right]^{m-i},
 \end{aligned} \tag{17}$$

where  $C_i = n!/(i-1)!(n-i)!$ . The following is a direct derivation of the associated log-likelihood function:

$$\ell_R(\lambda, \alpha) \propto m \log \lambda + m \log \alpha + (\alpha - 1) \sum_{i=1}^m \log(1 + \lambda y_i^{-1}) + \alpha \sum_{i=1}^m i(1 + \lambda y_i^{-1}) + (m - i) \sum_{i=1}^m \log\left(1 - e^{1-(1+\lambda y_i^{-1})^\alpha}\right), \tag{18}$$

and the normal likelihood equations is as follows:

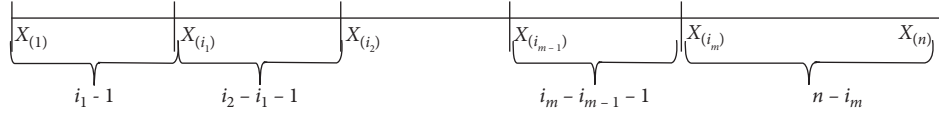


FIGURE 6: Order statistics of a subset of complete order statistics corresponding to the random sample  $\{x_i, i = 1, 2, \dots, n\}$ .

$$\frac{\partial \ell_R}{\partial \lambda} = \frac{m}{\lambda} + (\alpha - 1) \sum_{i=1}^m \frac{y_i^{-1}}{1 + \lambda y_i^{-1}} + \alpha \sum_{i=1}^m i y_i^{-1} - (m - i) \sum_{i=1}^m \frac{\alpha y_i^{-1} (1 + \lambda y_i^{-1})^{\alpha-1} e^{1-(1+\lambda y_i^{-1})^\alpha}}{1 - e^{1-(1+\lambda y_i^{-1})^\alpha}}, \quad (19)$$

$$\frac{\partial \ell_R}{\partial \alpha} = \frac{m}{\lambda \alpha} + \sum_{i=1}^m \log(1 + \lambda y_i^{-1}) + \sum_{i=1}^m i (1 + \lambda y_i^{-1}) - (m - i) \sum_{i=1}^m \frac{(1 + \lambda y_i^{-1})^\alpha \log(1 + \lambda y_i^{-1}) e^{1-(1+\lambda y_i^{-1})^\alpha}}{1 - e^{1-(1+\lambda y_i^{-1})^\alpha}}.$$

3.3. *Estimation Based on ERSS.* Let  $\{z_i, i = 1, 2, \dots, m\}$  be a ERSS drawn from a distribution with CDF and PDF as in (1) and (2), respectively, where  $m$  is the set size. Let  $g = m/2$ ,  $h = m - 1/2$ , and  $u_i = m - i + 1$ , then the likelihood function

of the ERSS representative sample from INH  $(\lambda, \alpha)$  according to (3) and (4) is given by

Case 1.  $m$  odd:

$$\begin{aligned} L_{E_o}(\lambda, \alpha; z) &= \prod_{i=1}^h \left[ \left( m \lambda \alpha z_i^{-2} (1 + \lambda z_i^{-1})^{\alpha-1} e^{1-(1+\lambda z_i^{-1})^\alpha} \left[ 1 - e^{1-(1+\lambda z_i^{-1})^\alpha} \right]^{m-1} \right) \right. \\ &\quad \times \left. \left( m \lambda \alpha z_{u_i}^{-2} (1 + \lambda z_{u_i}^{-1})^{\alpha-1} e^{1-(1+\lambda z_{u_i}^{-1})^\alpha} \left[ e^{1-(1+\lambda z_{u_i}^{-1})^\alpha} \right]^{m-1} \right) \right] \\ &\quad \times \frac{m!}{(h!)^2} \lambda \alpha z_{h+1}^{-2} (1 + \lambda z_{h+1}^{-1})^{\alpha-1} e^{1-(1+\lambda z_{h+1}^{-1})^\alpha} \left( e^{1-(1+\lambda z_{h+1}^{-1})^\alpha} \left( 1 - e^{1-(1+\lambda z_{h+1}^{-1})^\alpha} \right) \right)^h \\ &\propto \lambda^{2h+1} \alpha^{2h+1} (1 + \lambda z_{h+1}^{-1})^{\alpha-1} e^{-\sum_{i=1}^h [(1+\lambda z_i^{-1})^\alpha + (1+\lambda z_{u_i}^{-1})^\alpha]} - (m-1) \sum_{i=1}^h (1+\lambda z_{u_i}^{-1})^\alpha e^{-(1+\lambda z_{h+1}^{-1})^\alpha} \\ &\quad \times \left( e^{1-(1+\lambda z_{h+1}^{-1})^\alpha} \left( 1 - e^{1-(1+\lambda z_{h+1}^{-1})^\alpha} \right) \right)^h \prod_{i=1}^h (1 + \lambda z_i^{-1})^{\alpha-1} (1 + \lambda z_{u_i}^{-1})^{\alpha-1} \left[ 1 - e^{1-(1+\lambda z_i^{-1})^\alpha} \right]^{m-1}. \end{aligned} \quad (20)$$

The log-likelihood function follows directly as

$$\begin{aligned} \ell_{E_o}(\lambda, \alpha) &\propto (2h + 1) \log \lambda + (2h + 1) \log \alpha + (\alpha - 1) \log(1 + \lambda z_{h+1}^{-1}) - \sum_{i=1}^h \left[ (1 + \lambda z_i^{-1})^\alpha + (1 + \lambda z_{u_i}^{-1})^\alpha \right] \\ &\quad - (m - 1) \sum_{i=1}^h (1 + \lambda z_{u_i}^{-1})^\alpha - (1 + h) (1 + \lambda z_{h+1}^{-1})^\alpha \\ &\quad + h \log \left( 1 - e^{1-(1+\lambda z_{h+1}^{-1})^\alpha} \right) + (\alpha - 1) \sum_{i=1}^h \log(1 + \lambda z_i^{-1}) \\ &\quad + (\alpha - 1) \sum_{i=1}^h \log(1 + \lambda z_{u_i}^{-1}) + (m - 1) \sum_{i=1}^h \log \left[ 1 - e^{1-(1+\lambda z_i^{-1})^\alpha} \right]. \end{aligned} \quad (21)$$

Therefore, the associated likelihood normal equations will be

$$\begin{aligned}
\frac{\partial \ell_{E_o}}{\partial \lambda} &= \frac{2h+1}{\lambda} + \frac{(\alpha-1)z_{h+1}^{-1}}{1+\lambda z_{h+1}^{-1}} - \alpha \sum_{i=1}^h \left[ z_i^{-1} (1+\lambda z_i^{-1})^{\alpha-1} + z_{u_i}^{-1} (1+\lambda z_{u_i}^{-1})^{\alpha-1} \right] - \alpha (1+h) z_{h+1}^{-1} (1+\lambda z_{h+1}^{-1})^{\alpha-1} \\
&\quad - \alpha (m-1) \sum_{i=1}^h z_{u_i}^{-1} (1+\lambda z_{u_i}^{-1})^{\alpha-1} - \frac{\alpha h z_{h+1}^{-1} (1+\lambda z_{h+1}^{-1})^{\alpha-1} h e^{1-(1+\lambda z_{h+1}^{-1})^\alpha}}{1 - e^{1-(1+\lambda z_{h+1}^{-1})^\alpha}} + (\alpha-1) \sum_{i=1}^h \frac{z_i^{-1}}{1+\lambda z_i^{-1}} \\
&\quad + (\alpha-1) \sum_{i=1}^h \frac{z_{u_i}^{-1}}{1+\lambda z_{u_i}^{-1}} - (m-1) \sum_{i=1}^h \frac{\alpha z_i^{-1} (1+\lambda z_i^{-1})^{\alpha-1} e^{1-(1+\lambda z_i^{-1})^\alpha}}{1 - e^{1-(1+\lambda z_i^{-1})^\alpha}}, \\
\frac{\partial \ell_{E_o}}{\partial \alpha} &= \frac{2h+1}{\alpha} + \log(1+\lambda z_{h+1}^{-1}) - \sum_{i=1}^h \left[ (1+\lambda z_i^{-1})^\alpha \log(1+\lambda z_i^{-1}) + (1+\lambda z_{u_i}^{-1})^\alpha \log(1+\lambda z_{u_i}^{-1}) \right] \\
&\quad - (m-1) \sum_{i=1}^h (1+\lambda z_{u_i}^{-1})^\alpha \log(1+\lambda z_{u_i}^{-1}) - (1+h) (1+\lambda z_{h+1}^{-1})^\alpha \log(1+\lambda z_{h+1}^{-1}) \\
&\quad + \sum_{i=1}^h \log(1+\lambda z_i^{-1}) + \sum_{i=1}^h \log(1+\lambda z_{u_i}^{-1}) - \frac{h (1+\lambda z_{h+1}^{-1})^\alpha \log(1+\lambda z_{h+1}^{-1}) e^{1-(1+\lambda z_{h+1}^{-1})^\alpha}}{1 - e^{1-(1+\lambda z_{h+1}^{-1})^\alpha}} \\
&\quad - (m-1) \sum_{i=1}^h \frac{(1+\lambda z_i^{-1})^\alpha \log(1+\lambda z_i^{-1}) e^{1-(1+\lambda z_i^{-1})^\alpha}}{1 - e^{1-(1+\lambda z_i^{-1})^\alpha}}.
\end{aligned} \tag{22}$$

Case 2.  $m$  even:

$$\begin{aligned}
L_{E_c}(\lambda, \alpha; z) &= \prod_{i=1}^g \left[ \left( m \lambda \alpha z_i^{-2} (1+\lambda z_i^{-1})^{\alpha-1} e^{1-(1+\lambda z_i^{-1})^\alpha} \left[ 1 - e^{1-(1+\lambda z_i^{-1})^\alpha} \right]^{m-1} \right) \right. \\
&\quad \left. \times \left( m \lambda \alpha z_{u_i}^{-2} (1+\lambda z_{u_i}^{-1})^{\alpha-1} e^{1-(1+\lambda z_{u_i}^{-1})^\alpha} \left[ e^{1-(1+\lambda z_{u_i}^{-1})^\alpha} \right]^{m-1} \right) \right] \\
&\propto \lambda^{2g} \alpha^{2g} e^{-\sum_{i=1}^h \left[ (1+\lambda z_i^{-1})^\alpha + (1+\lambda z_{u_i}^{-1})^\alpha \right] - (m-1) \sum_{i=1}^h (1+\lambda z_{u_i}^{-1})^\alpha} \times \prod_{i=1}^g (1+\lambda z_i^{-1})^{\alpha-1} (1+\lambda z_{u_i}^{-1})^{\alpha-1} \left[ 1 - e^{1-(1+\lambda z_i^{-1})^\alpha} \right]^{m-1}.
\end{aligned} \tag{23}$$

Similarly, the log-likelihood function is given directly as

$$\begin{aligned}
\ell_{E_c}(\lambda, \alpha) &\propto 2g \log \lambda + 2g \log \alpha - \sum_{i=1}^g \left[ (1+\lambda z_i^{-1})^\alpha + (1+\lambda z_{u_i}^{-1})^\alpha \right] - (m-1) \sum_{i=1}^g (1+\lambda z_{u_i}^{-1})^\alpha \\
&\quad + (\alpha-1) \sum_{i=1}^g \left[ \log(1+\lambda z_i^{-1}) + \log(1+\lambda z_{u_i}^{-1}) \right] + (m-1) \sum_{i=1}^g \log \left[ 1 - e^{1-(1+\lambda z_i^{-1})^\alpha} \right].
\end{aligned} \tag{24}$$

Thus, the associated likelihood normal equations will be given as



$$\begin{aligned}
\frac{\partial \ell_{E_e}}{\partial \lambda} &= \frac{2g}{\lambda} - \alpha \sum_{i=1}^h \left[ z_i^{-1} (1 + \lambda z_i^{-1})^{\alpha-1} + z_{u_i}^{-1} (1 + \lambda z_{u_i}^{-1})^{\alpha-1} \right] - \alpha(m-1) \sum_{i=1}^h z_{u_i}^{-1} (1 + \lambda z_{u_i}^{-1})^{\alpha-1} + (\alpha-1) \sum_{i=1}^h \left[ \frac{z_i^{-1}}{1 + \lambda z_i^{-1}} + \frac{z_{u_i}^{-1}}{1 + \lambda z_{u_i}^{-1}} \right] \\
&\quad - \alpha(m-1) \sum_{i=1}^h \frac{z_i^{-1} (1 + \lambda z_i^{-1})^{\alpha-1} e^{1-(1+\lambda z_i^{-1})^\alpha}}{1 - e^{1-(1+\lambda z_i^{-1})^\alpha}}, \\
\frac{\partial \ell_{E_e}}{\partial \alpha} &= \frac{2g}{\alpha} - \sum_{i=1}^h \left[ (1 + \lambda z_i^{-1})^\alpha \log(1 + \lambda z_i^{-1}) + (1 + \lambda z_{u_i}^{-1})^\alpha \log(1 + \lambda z_{u_i}^{-1}) \right] - (m-1) \sum_{i=1}^h (1 + \lambda z_{u_i}^{-1})^\alpha \log(1 + \lambda z_{u_i}^{-1}) \\
&\quad + \sum_{i=1}^h \left[ \log(1 + \lambda z_i^{-1}) + \log(1 + \lambda z_{u_i}^{-1}) \right] - (m-1) \sum_{i=1}^g \frac{(1 + \lambda z_i^{-1})^\alpha \log(1 + \lambda z_i^{-1}) e^{1-(1+\lambda z_i^{-1})^\alpha}}{1 - e^{1-(1+\lambda z_i^{-1})^\alpha}}.
\end{aligned} \tag{25}$$

3.4. *Estimation Based on NRSS.* Assume  $\{u_{(k_i)}, i = 1, 2, \dots, m$  and  $k_i$  is defined as in (6)} be a neoteric ranked set sample, where  $m$  is the set size. According to (5),

the likelihood function of NRSS samples drawn from INH  $(\lambda, \alpha)$  for one cycle is given by

$$\begin{aligned}
L_N(\lambda, \alpha; u) &\propto \prod_{i=1}^m \lambda \alpha \left(1 + \lambda u_{(k_i)}^{-1}\right)^{\alpha-1} e^{1-(1+\lambda u_{(k_i)}^{-1})^\alpha} \prod_{i=1}^{m+1} \left[ e^{1-(1+\lambda u_{(-1/(k_i)))}^\alpha} - e^{1-(1+\lambda u_{(-1/(k_i))}^\alpha} \right]^{(k_i - k_{i-1} - 1)}, \\
&\propto \lambda^m \alpha^m \prod_{i=1}^m \left(1 + \lambda u_{(k_i)}^{-1}\right)^{\alpha-1} \prod_{i=1}^{m+1} \left[ e^{1-(1+\lambda u_{(-1/(k_i))}^\alpha} - e^{1-(1+\lambda u_{(-1/(k_{i-1}))}^\alpha} \right]^{(k_i - k_{i-1} - 1)}, \\
&\propto \lambda^m \alpha^m \prod_{i=1}^m \left(1 + \lambda u_{(k_i)}^{-1}\right)^{\alpha-1} \left[ e^{-(1+\lambda u_{(-1/(k_i))}^\alpha} - e^{-(1+\lambda u_{(-1/(k_{i-1}))}^\alpha} \right]^{(k_i - k_{i-1} - 1)}.
\end{aligned} \tag{26}$$

The log-likelihood associated with this design is then given by

$$\begin{aligned}
\ell_N(\lambda, \alpha) &\propto m \log \lambda + m \log \alpha + (\alpha-1) \sum_{i=1}^m \log \left(1 + \lambda u_{(k_i)}^{-1}\right) \\
&\quad + \sum_{i=1}^{m+1} (k_i - k_{i-1} - 1) \log \left[ e^{1-(1+\lambda u_{(-1/(i))}^\alpha} - e^{1-(1+\lambda u_{(-1/(i-1))}^\alpha} \right],
\end{aligned} \tag{27}$$

where  $k_0 = 0$ ,  $k_{m+1} = m^2 + 1$ , and  $u_{(k_0)} = -\infty$ ,  $u_{(k_{m+1})} = \infty$ . The associated normal equations are directly derived as

$$\begin{aligned}
\frac{\partial \ell_N}{\partial \lambda} &= \frac{m}{\lambda} + (\alpha-1) \sum_{i=1}^m \frac{u_{(k_i)}^{-1}}{1 + \lambda u_{(k_i)}^{-1}} + \alpha \sum_{i=1}^{m+1} (k_i - k_{i-1} - 1) \frac{u_{(k_{i-1})}^{-1} (1 + \lambda u_{(k_{i-1})}^{-1})^{\alpha-1} e^{1-(1+\lambda u_{(-1/(i-1))}^\alpha}}{e^{1-(1+\lambda u_{(-1/(i))}^\alpha} - e^{1-(1+\lambda u_{(-1/(i-1))}^\alpha}} \\
&\quad - \alpha \sum_{i=1}^{m+1} (k_i - k_{i-1} - 1) \frac{u_{(k_i)}^{-1} (1 + \lambda u_{(k_i)}^{-1})^{\alpha-1} e^{1-(1+\lambda u_{(-1/(i))}^\alpha}}{e^{1-(1+\lambda u_{(-1/(i))}^\alpha} - e^{1-(1+\lambda u_{(-1/(i-1))}^\alpha}},
\end{aligned}$$

$$\begin{aligned} \frac{\partial \ell_{EN}}{\partial \alpha} &= \frac{m}{\alpha} + \sum_{i=1}^m \log\left(1 + \lambda u_{(k_i)}^{-1}\right) + \sum_{i=1}^{m+1} \frac{(k_i - k_{i-1} - 1) \left(1 + \lambda u_{(k_{i-1})}^{-1}\right)^\alpha \log\left(1 + \lambda u_{(k_{i-1})}^{-1}\right) e^{1-(1+\lambda u_{(i-1)})^\alpha}}{e^{1-(1+\lambda u_{(i)})^\alpha} - e^{1-(1+\lambda u_{(i-1)})^\alpha}} \\ &\quad - \sum_{i=1}^{m+1} \frac{(k_i - k_{i-1} - 1) \left(1 + \lambda u_{(k_i)}^{-1}\right)^\alpha \log\left(1 + \lambda u_{(k_i)}^{-1}\right) e^{1-(1+\lambda u_{(i)})^\alpha}}{e^{1-(1+\lambda u_{(i)})^\alpha} - e^{1-(1+\lambda u_{(i-1)})^\alpha}}. \end{aligned} \quad (28)$$

3.5. *Estimation Based on ENRSS.* Let  $\{v_{(i)}, t = 1, 2, \dots, m$  and  $i_t$  is defined as in (10)} be a random sample of size  $n$  from a continuous population and let  $\{z_{(i)}, t = 1, 2, \dots, m\}$  be an

extended neuter ranked set sample. Therefore, the likelihood function of the INH  $(\lambda, \alpha)$  distribution for one cycle based on (7) is computed as

$$\begin{aligned} L_{EN}(\lambda, \alpha; v) &\propto \prod_{t=1}^m \lambda \beta \left(1 + \lambda v_{(i_t)}^{-1}\right)^{\alpha-1} e^{1-(1+\lambda v_{(i_t)})^\alpha} \prod_{t=1}^{m+1} \left[ e^{1-(1+\lambda v_{(i)})^\alpha} - e^{1-(1+\lambda v_{(i-1)})^\alpha} \right]^{(i_t - i_{t-1} - 1)}, \\ &\propto \lambda^m \alpha^m \prod_{t=1}^m \left(1 + \lambda v_{(i_t)}^{-1}\right)^{\alpha-1} e^{m - \sum_{t=1}^m (1+\lambda v_{(i_t)})^\alpha} \prod_{t=1}^{m+1} \left[ e^{-(1+\lambda v_{(i)})^\alpha} - e^{-(1+\lambda v_{(i-1)})^\alpha} \right]^{(i_t - i_{t-1} - 1)}, \end{aligned} \quad (29)$$

where  $i_0 = 0, i_{m+1} = m^3 + 1$ , and  $v_{(i_0)} = -\infty, v_{(i_{m+1})} = \infty$ . The log-likelihood associated with this design is then given by

The associated normal equations are directly derived as

$$\begin{aligned} \ell_{EN}(\lambda, \alpha) &\propto m \log \lambda + m \log \alpha + (\alpha - 1) \sum_{i=1}^m \log\left(1 + \lambda v_{(i)}^{-1}\right), \\ &\quad + \sum_{i=1}^{m+1} (i_t - i_{t-1} - 1) \log \left[ e^{-(1+\lambda v_{(i)})^\alpha} - e^{-(1+\lambda v_{(i-1)})^\alpha} \right]. \end{aligned} \quad (30)$$

$$\begin{aligned} \frac{\partial \ell_{EN}}{\partial \lambda} &= \frac{m}{\lambda} + (\alpha - 1) \sum_{i=1}^m \frac{v_{(i)}^{-1}}{1 + \lambda v_{(i)}^{-1}} + \alpha \sum_{t=1}^{m+1} (i_t - i_{t-1} - 1) \frac{v_{(i_{t-1})}^{-1} \left(1 + \lambda v_{(i_{t-1})}^{-1}\right)^{\alpha-1} e^{1-(1+\lambda v_{(i_{t-1})})^\alpha}}{e^{1-(1+\lambda v_{(i)})^\alpha} - e^{1-(1+\lambda v_{(i-1)})^\alpha}} \\ &\quad - \alpha \sum_{t=1}^{m+1} (i_t - i_{t-1} - 1) \frac{v_{(k_i)}^{-1} \left(1 + \lambda v_{(i)}^{-1}\right)^{\alpha-1} e^{1-(1+\lambda v_{(i)})^\alpha}}{e^{1-(1+\lambda v_{(i)})^\alpha} - e^{1-(1+\lambda v_{(i-1)})^\alpha}}, \end{aligned} \quad (31)$$

$$\begin{aligned} \frac{\partial \ell_{EN}}{\partial \alpha} &= \frac{m}{\alpha} + \sum_{i=1}^m \log\left(1 + \lambda v_{(i)}^{-1}\right) + \sum_{t=1}^{m+1} \frac{(i_t - i_{t-1} - 1) \left(1 + \lambda v_{(i_{t-1})}^{-1}\right)^\alpha \log\left(1 + \lambda v_{(i_{t-1})}^{-1}\right) e^{1-(1+\lambda v_{(i-1)})^\alpha}}{e^{1-(1+\lambda v_{(i)})^\alpha} - e^{1-(1+\lambda v_{(i-1)})^\alpha}} \\ &\quad - \sum_{t=1}^{m+1} \frac{(i_t - i_{t-1} - 1) \left(1 + \lambda v_{(i)}^{-1}\right)^\alpha \log\left(1 + \lambda v_{(i)}^{-1}\right) e^{1-(1+\lambda v_{(i)})^\alpha}}{e^{1-(1+\lambda v_{(i)})^\alpha} - e^{1-(1+\lambda v_{(i+1)})^\alpha}}. \end{aligned}$$

The equations presented in this section are nonlinear and complex to be solved analytically; therefore, a numerical solution will be addressed in the next section by the use of simulation algorithm.

#### 4. Simulation Study and Results

We use a Monte Carlo simulation to compare the performance of the various ranked set sample designs in this

TABLE 1: Relative efficiency for RSS-based estimators for different sampling plans and INH distribution with scale parameter  $\lambda = 1$ .

$\alpha$	$m$	$\text{eff}(\alpha_{(\text{RSS-based})}, \alpha_{\text{SRS}})$				$\text{eff}(\lambda_{(\text{RSS-based})}, \lambda_{\text{SRS}})$			
		RSS	ERSS	NRSS	ENRSS	RSS	ERSS	NRSS	ENRSS
0.4	3	1.50	1.80	2.40	6.30	1.28	1.59	2.07	5.59
	6	1.95	2.34	3.12	8.58	1.66	2.07	2.69	7.27
	9	2.80	3.36	4.48	12.04	2.38	2.98	3.87	10.44
	12	3.20	3.84	5.12	14.40	2.72	3.40	4.42	11.93
	15	3.91	4.69	6.26	19.55	3.32	4.15	5.40	14.58
	20	4.32	5.18	6.91	22.03	3.67	4.59	5.97	16.11
1.1	3	1.65	1.98	2.64	6.93	1.40	1.75	2.28	6.15
	6	2.02	2.42	3.23	8.89	1.72	2.15	2.79	7.53
	9	2.57	3.08	4.11	11.05	2.18	2.73	3.55	9.58
	12	3.18	3.82	5.09	14.31	2.70	3.38	4.39	11.86
	15	4.05	4.86	6.48	20.25	3.44	4.30	5.59	15.10
	20	4.61	5.53	7.38	23.51	3.92	4.90	6.37	17.19
1.5	3	1.58	1.90	2.53	6.64	1.34	1.68	2.18	5.89
	6	1.97	2.36	3.15	8.67	1.67	2.09	2.72	7.35
	9	2.31	2.77	3.70	9.93	1.96	2.45	3.19	8.61
	12	3.01	3.61	4.82	13.55	2.56	3.20	4.16	11.23
	15	3.53	4.24	5.65	17.65	3.00	3.75	4.88	13.16
	20	4.19	5.03	6.70	21.37	3.56	4.45	5.79	15.63
2.0	3	1.63	1.96	2.61	6.85	1.39	1.73	2.25	6.08
	6	2.15	2.58	3.44	9.46	1.83	2.28	2.97	8.02
	9	2.58	3.10	4.13	11.09	2.19	2.74	3.56	9.62
	12	2.91	3.49	4.66	13.10	2.47	3.09	4.02	10.85
	15	3.35	4.02	5.36	16.75	2.85	3.56	4.63	12.49
	20	4.11	4.93	6.58	20.96	3.49	4.37	5.68	15.33
2.5	3	1.79	2.15	2.87	7.53	1.52	1.90	2.47	6.68
	6	2.37	2.84	3.78	10.41	2.01	2.52	3.27	8.84
	9	2.84	3.41	4.54	12.20	2.41	3.02	3.92	10.59
	12	3.20	3.84	5.12	14.40	2.72	3.40	4.42	11.93
	15	3.69	4.42	5.90	18.43	3.14	3.92	5.10	13.76
	20	4.52	5.43	7.23	23.06	3.84	4.80	6.24	16.86
3.0	3	1.88	2.26	3.01	7.91	1.60	2.00	2.60	7.01
	6	2.48	2.98	3.97	10.93	2.11	2.64	3.43	9.25
	9	2.98	3.58	4.77	12.81	2.53	3.17	4.12	11.11
	12	3.36	4.03	5.38	15.12	2.86	3.57	4.64	12.53
	15	3.87	4.64	6.19	19.35	3.29	4.11	5.35	14.43
	20	4.75	5.70	7.60	24.21	4.04	5.05	6.56	17.71

section. The information was derived and generated from INH distribution with scale parameter  $\lambda = 1$  and shape parameter  $\alpha = 0.4, 1.1, 1.5, 2, 2.5,$  and  $3$  for different sample sizes ( $m = 3, 6, 9, 15$  and  $20$ ). The simulation algorithm is as follows.

For SRS,

- (1) With 50,000 replicates, generate  $m$  random samples from the INH distribution using the quantile function specified in (3)
- (2) Obtain the MLEs for both scale and shape parameters

For different ranked set samples,

- (1) Use the different RSS designs discussed in Section 2 to simulate different RSS designs samples and generate sample using the quantile function defined in (3) with 50,000 replicates
- (2) Obtain the MLEs for RSS, NRSS, and ENRSS plans

- (3) Calculate the relative bias (RB), mean squared error (MSE), and relative efficiency (RE) of the different RSS estimators compared with the SRS estimators where the relative bias and MSE of an estimator  $\hat{\theta}$  of a parameter  $\theta$  are defined, respectively, as

$$\text{RB} = \sum_{l=1}^{50,000} \frac{\hat{\lambda}_l - \Phi_l}{\Phi_l}, \quad (32)$$

$$\text{MSE} = \frac{1}{50,000} \sum_{l=1}^{50,000} (\hat{\Phi}_l - \Phi_l)^2,$$

and the RE of the estimator  $\hat{\theta}_2$  compared with the estimator  $\hat{\theta}_1$  is defined as

$$\text{eff}(\text{SRS}, \text{Ranked}) = \frac{\text{MSE}(\hat{\Phi}_l)_{\text{SRS}}}{\text{MSE}(\hat{\Phi}_l)_{\text{Ranked}}}. \quad (33)$$

TABLE 2: Relative bias for RSS-based estimators for different sampling plans and INH distribution with scale parameter  $\lambda = 1$ .

$\alpha$	m	RB ( $\hat{\alpha}_{\text{RSS-based}}$ )				RB ( $\hat{\lambda}_{\text{RSS-based}}$ )			
		RSS	ERSS	NRSS	ENRSS	RSS	ERSS	NRSS	ENRSS
0.4	3	0.00115	0.00092	0.00064	0.00032	0.00173	0.00138	0.00097	0.00048
	6	0.00213	0.0017	0.00119	0.0006	0.0032	0.00256	0.00179	0.00089
	9	0.00107	0.00086	0.0006	0.0003	0.00161	0.00128	0.0009	0.00045
	12	0.00112	0.0009	0.00063	0.00031	0.00168	0.00134	0.00094	0.00047
	15	0.00101	0.00081	0.00057	0.00028	0.00152	0.00121	0.00085	0.00042
	20	0.00099	0.00079	0.00055	0.00028	0.00149	0.00119	0.00083	0.00042
1.1	3	0.00098	0.00078	0.00055	0.00027	0.00113	0.0009	0.00063	0.00032
	6	0.00181	0.00145	0.00101	0.00051	0.00209	0.00167	0.00117	0.00059
	9	0.00091	0.00073	0.00051	0.00025	0.00105	0.00084	0.00059	0.00029
	12	0.00095	0.00076	0.00053	0.00027	0.0011	0.00088	0.00062	0.00031
	15	0.00086	0.00069	0.00048	0.00024	0.00099	0.00079	0.00056	0.00028
	20	0.00084	0.00067	0.00047	0.00024	0.00097	0.00078	0.00054	0.00027
1.5	3	0.00083	0.00066	0.00047	0.00023	0.00096	0.00077	0.00054	0.00027
	6	0.00154	0.00123	0.00086	0.00043	0.00178	0.00142	0.001	0.0005
	9	0.00077	0.00062	0.00043	0.00022	0.00089	0.00071	0.0005	0.00025
	12	0.00081	0.00065	0.00045	0.00023	0.00094	0.00075	0.00052	0.00026
	15	0.00073	0.00058	0.00041	0.0002	0.00084	0.00067	0.00047	0.00024
	20	0.00072	0.00057	0.0004	0.0002	0.00083	0.00066	0.00046	0.00023
2	3	0.00056	0.00045	0.00031	0.00016	0.00064	0.00051	0.00036	0.00018
	6	0.00103	0.00082	0.00058	0.00029	0.00119	0.00095	0.00067	0.00033
	9	0.00052	0.00041	0.00029	0.00015	0.0006	0.00048	0.00034	0.00017
	12	0.00054	0.00043	0.0003	0.00015	0.00063	0.0005	0.00035	0.00018
	15	0.00049	0.00039	0.00027	0.00014	0.00057	0.00045	0.00032	0.00016
	20	0.00048	0.00038	0.00027	0.00013	0.00055	0.00044	0.00031	0.00016
2.5	3	0.00031	0.00024	0.00017	0.00009	0.00035	0.00028	0.0002	0.0001
	6	0.00057	0.00045	0.00032	0.00016	0.00065	0.00052	0.00037	0.00018
	9	0.00028	0.00023	0.00016	0.00008	0.00033	0.00026	0.00018	0.00009
	12	0.0003	0.00024	0.00017	0.00008	0.00034	0.00027	0.00019	0.0001
	15	0.00027	0.00021	0.00015	0.00008	0.00031	0.00025	0.00017	0.00009
	20	0.00026	0.00021	0.00015	0.00007	0.0003	0.00024	0.00017	0.00009
3	3	0.00012	0.0001	0.00007	0.00003	0.00014	0.00011	0.00008	0.00004
	6	0.00023	0.00018	0.00013	0.00006	0.00026	0.00021	0.00015	0.00007
	9	0.00011	0.00009	0.00006	0.00003	0.00013	0.0001	0.00007	0.00004
	12	0.00012	0.0001	0.00007	0.00003	0.00014	0.00011	0.00008	0.00004
	15	0.00011	0.00009	0.00006	0.00003	0.00012	0.0001	0.00007	0.00003
	20	0.00011	0.00008	0.00006	0.00003	0.00012	0.0001	0.00007	0.00003

The results of the simulation study are reported in Tables 1 and 2. From the table, some important conclusions can be observed from the results.

As expected, the efficiency of all RSS-based designs increases as the sample size increases and as the shape of the distribution is near symmetry.

- (i) It is clear that the proposed likelihood function for the ENRSS plan is working effectively and provides efficient estimators similar to the results reported by Taconeli and Cabral [6]
- (ii) The ENRSS plan estimators outperform the one-stage RSS plans when the process does not include ranking errors
- (iii) The NRSS plan estimators outperform the one-stage ERSS and RSS and SRS plans
- (iv) The RSS plan estimators outperform the one-stage SRS plans

(v) Biases are almost negligible when the shape of the distribution is near symmetry

### 5. Conclusion

Different sampling designs have been discussed. The likelihood function for the INH distribution was studied based on SRS, RSS, ERSS, NRSS, and ENRSS. By Monte Carlo simulation, the different sampling designs have been compared. It is clear from the simulation results that the likelihood function used to estimate the parameters of the INH distribution based on ENRSS showed relatively efficient estimates compared with SRS, RSS, ERSS, and NRSS estimators. During parameter estimation of an INH distribution based on different sampling designs, the authors advocate employing ENRSS and other two-stage RSS designs as ranked sampling methods. For future research on this topic, the author plans to start a more general study regarding most of the important one-stage RSS plans in both perfect and

imperfect ranking cases and study their performance when making parameter estimations for several symmetric and asymmetric distributions [19–21].

## Data Availability

All data are included in the paper.

## Conflicts of Interest

The authors declare that they have no conflicts of interest.

## Acknowledgments

This study was supported by Princess Nourah bint Abdulrahman University Researchers Supporting Project number (PNURSP2022R299), Princess Nourah bint Abdulrahman University, Riyadh, Saudi Arabia.

## References

- [1] A. I. Al-Omari, "Improvement in estimating the population mean in double extreme ranked set sampling," *International Mathematical Forum*, vol. 26, pp. 1265–1275, 2010.
- [2] H. M. Samawi, M. S. Ahmed, and W. A. Abu-Dayyeh, "Estimating the population mean using extreme ranked set sampling," *Biometrical Journal*, vol. 38, no. 5, pp. 577–586, 1996.
- [3] H. A. Muttalak, "Median ranked set sampling," *Journal of Applied Statistics Sciences*, vol. 6, 1997.
- [4] M. T. Al-Odat and M. F. Al-Saleh, "A variation of ranked set sampling," *Journal of Applied Statistical Science*, vol. 10, no. 2, pp. 137–146, 2001.
- [5] M. F. Al-Saleh and A. I. Al-Omari, "Multistage ranked set sampling," *Journal of Statistical Planning and Inference*, vol. 102, no. 2, pp. 273–286, 2002.
- [6] C. A. Taconeli and A. d. S. Cabral, "New two-stage sampling designs based on neoteric ranked set sampling," *Journal of Statistical Computation and Simulation*, vol. 89, no. 2, pp. 232–248, 2019.
- [7] H. Chen, E. A. Stasny, and D. A. Wolfe, "Ranked set sampling for efficient estimation of a population proportion," *Statistics in Medicine*, vol. 24, no. 21, pp. 3319–3329, 2005.
- [8] J. T. Terpstra and L. A. Liudahl, "Concomitant-based rank set sampling proportion estimates," *Statistics in Medicine*, vol. 23, no. 13, pp. 2061–2070, 2004.
- [9] M. Mahdizadeh, "On entropy based test of exponentiality in ranked set sampling," *Communications in Statistics - Simulation and Computation*, vol. 44, no. 4, pp. 979–995, 2015.
- [10] M. Mahdizadeh and E. Strzalkowska-Kominiak, "Resampling based inference for a distribution function using censored ranked set samples," *Computational Statistics*, vol. 32, no. 4, pp. 1285–1308, 2017.
- [11] Z. Akhter, E. M. Almetwally, and C. Chesneau, "On the generalized bilal distribution some properties and estimation under ranked set sampling," *Axioms*, vol. 11, no. 4, p. 173, 2022.
- [12] E. Strzalkowska-Kominiak and M. Mahdizadeh, "On the Kaplan-Meier estimator based on ranked set samples," *Journal of Statistical Computation and Simulation*, vol. 84, no. 12, pp. 2577–2591, 2014.
- [13] H. M. Aljohani, E. M. Almetwally, A. S. Alghamdi, and E. H. Hafez, "Ranked set sampling with application of modified Kies exponential distribution," *Alexandria Engineering Journal*, vol. 60, no. 4, pp. 4041–4046, 2021.
- [14] M. A. H. Sabry, E. M. Almetwally, H. M. Almongy, and G. M. Ibrahim, "Assessing the performance of some ranked set sampling designs using hybrid approach," *Computers, Materials & Continua*, vol. 68, no. 3, pp. 3737–3753, 2021.
- [15] M. H. Sabry and E. M. Almetwally, "Estimation of the exponential Pareto distribution's parameters under ranked and double ranked set sampling designs," *Pakistan Journal of Statistics and Operation Research*, vol. 17, no. 1, pp. 169–184, 2021.
- [16] E. Zamanzade and A. I. Al-Omari, "New ranked set sampling for estimating the population mean and variance," *Hacettepe Journal of Mathematics and Statistics*, vol. 46, no. 92, pp. 1891–1905, 2015.
- [17] D. A. Wolfe, "Ranked set sampling: an approach to more efficient data collection," *Statistical Science*, vol. 19, no. 4, pp. 636–643, 2004.
- [18] M. A. Sabry and M. Shaaban, "A dependent ranked set sampling designs for estimation of distribution parameters with applications," *Ann Data Sci*, 2020.
- [19] N. Balakrishnan and A. C. Cohen, *Order Statistics and Inference: Estimation Methods*, Academic Press, Boston, MA, 1991.
- [20] G. A. McIntyre, "A method for unbiased selective sampling, using ranked sets," *Australian Journal of Agricultural Research*, vol. 3, no. 4, pp. 385–390, 1952.
- [21] M. H. Tahir, G. M. Cordeiro, S. Ali, and A. Manzoor, "The inverted Nadarajah–Haghighi distribution: estimation methods and applications," *Journal of Statistical Computation and Simulation*, vol. 88, no. 14, pp. 2775–2798, 2018.

## Research Article

# Constructing Multiple-Objective Portfolio Selection for Green Innovation and Dominating Green Innovation Indexes

Meng Li <sup>1</sup>, Kezhi Liao <sup>2</sup>, Yue Qi <sup>3</sup>, and Tongyang Liu <sup>4</sup>

<sup>1</sup>Department of Finance and Accounting, Xi'an University of Technology, 58 Yanxiang Road, Xi'an 710054, China

<sup>2</sup>Department of Accounting, Zhejiang University of Technology, 18 Chaowang Road, Hangzhou 310014, China

<sup>3</sup>China Academy of Corporate Governance & Department of Financial Management, Business School, Nankai University, 94 Weijin Road, Tianjin 300071, China

<sup>4</sup>Department of Financial Management, Nankai University, 94 Weijin Road, Tianjin 300071, China

Correspondence should be addressed to Yue Qi; [yorkche@nankai.edu.cn](mailto:yorkche@nankai.edu.cn)

Received 20 August 2021; Revised 13 March 2022; Accepted 3 April 2022; Published 29 May 2022

Academic Editor: Yingqian Zhang

Copyright © 2022 Meng Li et al. This is an open access article distributed under the Creative Commons Attribution License, which permits unrestricted use, distribution, and reproduction in any medium, provided the original work is properly cited.

Green innovation investments have rapidly grown since 2000. Green innovation indexes play important roles and are typically constructed by screening and indexing. However, Nobel Laureate Markowitz emphasizes portfolio selection instead of security selection and accentuates that “A good portfolio is more than a long list of good stocks.” Moreover, the screening-indexing strategies ignore that investors can take green innovation as an additional objective and thus gain additional utility. We consequently construct 3-objective portfolio selection for green innovation in addition to variance and expected return. An efficient frontier of portfolio selection then extends to an efficient surface which is a panorama of the optimal variance, expected return, and expected green innovation. Investors thus fully envisage the trade-offs and enjoy the freedom of choosing preferred portfolios on the surface. In contrast, the screening-indexing strategies inflexibly leave investors with only one point (i.e., the green innovation index). As the originality, we prove in a theorem that there typically exists a curve on the efficient surface so all portfolios on the curve dominate the green innovation index. We test the dominance by component stocks of China Securities Index 300 and obtain affirmative results out of sample. The results still hold in robustness tests. At last, we classify green innovation into categories, further model the categories by general  $k$ -objective portfolio selection, and still illustrate the dominance. Consequently, investors can consider and control each category.

## 1. Introduction

*1.1. Green Innovation Investments.* As the COVID-19 pandemic unleashes crises of health and environment, environment and green are becoming more critical issues. Reference [1], p.310, defines green innovation as innovation mechanisms to improve environment. Green innovation investments have rapidly grown since 2000. As [2], p.631, contends sustainability as a driver of green innovation, the Global Sustainable Investment Review reports that global sustainable-investments assets reached \$30.7 trillion in 2018 with a 34% increase from 2016.

Green innovation investments are typically fulfilled by screening-indexing strategies. Screening essentially means that investors exclude stocks of potentially socially questionable firms (e.g., gambling or tobacco). Indexing means that investors replicate a capital-market index (as documented by [3], p.341). For example, Morgan Stanley Capital International Inc. (MSCI) deploys the screening-indexing strategies for MSCI KLD 400 Social Index. The Forum of Sustainable and Responsible Investment and the Principles for Responsible Investment Association harness similar strategies.

On one side, the screening-indexing strategies are highly practical and thus substantially expedite green innovation

investments. However on the other side, the strategies suffer from the following weakness:

- (1) The strategies build portfolios by a list of good stocks and thus ignore portfolio completeness, because [4], p.3, emphasizes portfolio selection rather than security selection and stresses portfolio wholeness.
- (2) The strategies ignore that investors can take green innovation as an additional objective and thus gain additional utility. Reference [5], p.683, deduces that investors obtain utility from social responsibility. Reference [6], p.2, highlights society objectives and the urge to balance them with risk and return.
- (3) The strategies inflexibly prescribe an index for most investors and disregard investor difference. Screening out some kinds of stocks is appropriate for some investors but inappropriate for others. References [7], p.5, and [8], pp.27&28, contend that investors are fairly different.

*1.2. Portfolio Selection.* Reference [4], p.6, discovers that investors mind both risk and return. Therefore, [9], p.83, formulates portfolio selection as the following 2-objective optimization:

$$\begin{aligned} \min\{z_1 = \mathbf{x}^T \boldsymbol{\Sigma} \mathbf{x}\}, \text{risk,} \\ \max\{z_2 = \mathbf{x}^T \boldsymbol{\mu}\}, \text{return,} \\ \text{s.t. } \mathbf{x} \in S, \text{feasible region.} \end{aligned} \quad (1)$$

For  $n$  stocks:

- $\boldsymbol{\mu}$  is a vector of stock expected returns,
- superscript  $T$  denotes transposition,
- $\boldsymbol{\Sigma}$  is a covariance matrix of stock returns,
- $\mathbf{x}$  is a portfolio-weight vector,
- $z_1$  measures the variance of the return of portfolio  $\mathbf{x}$ ,
- $z_2$  measures the expectation of the return of portfolio  $\mathbf{x}$ ,
- $S$  is a feasible region in  $\mathbb{R}^n$ ,
- $Z = \{(z_1, z_2) | \mathbf{x} \in S\}$  is the feasible region in  $(z_1, z_2)$  space.

Reference [9] calls the optimal solutions in  $(z_1, z_2)$  space as an efficient frontier. References [10, 11] fully describe multiple-objective optimization. For notations, normal symbols (e.g.,  $n$ ) denote scalars; bold-face symbols (e.g.,  $\mathbf{x}$  or  $\boldsymbol{\Sigma}$ ) denote vectors or matrices.

Mathematically, (1) maps  $S$  to  $Z$ . For instance, we depict  $\mathbf{x}_1 \dots \mathbf{x}_3$  to  $\mathbf{z}_1 \dots \mathbf{z}_3$  by three arrows in the upper part of Figure 1. We also depict  $S$  and  $Z$  as shaded regions and depict the efficient frontier as a thick curve.

*1.3. Multiple-Objective Portfolio Selection.* Reference [12], pp.471&476, later discovers additional objectives (in addition to the variance and expectation). Reference [13] also realizes additional objectives and incorporates them into a utility function. References [14], pp.445–447, [15], pp.62–63,

and [16], pp.1081–1082, emphasize multiple factors for asset pricing and further propose the factors' risks as objectives. Reference [17], p.182, advocates expressive benefits (e.g., social responsibility) as objectives.

References [14, 18–21] and [22] formulate additional objectives by multiple-objective portfolio selection as follows:

$$\begin{aligned} \min\{z_1 = \mathbf{x}^T \boldsymbol{\Sigma} \mathbf{x}\}, \text{risk} \\ \max\{z_2 = \mathbf{x}^T \boldsymbol{\mu}\}, \text{return} \\ \max\{z_3 = \mathbf{x}^T \boldsymbol{\mu}_3\}, \text{general objective 1} \\ \vdots \\ \max\{z_k = \mathbf{x}^T \boldsymbol{\mu}_k\}, \text{general objective } k - 2 \\ \text{s.t. } \mathbf{x} \in S, \text{feasible region,} \end{aligned} \quad (2)$$

where

- $\boldsymbol{\mu}_3 \dots \boldsymbol{\mu}_k$  are vectors of general stock expected objectives (e.g., expected R&D and liquidity),
- $z_3 \dots z_k$  measure the general portfolio expected objectives,
- $Z = \{(z_1, \dots, z_k) | \mathbf{x} \in S\}$  is the feasible region in  $(z_1, \dots, z_k)$  space.

Mathematically, (2) maps  $S$  to  $Z$ . For instance, we depict  $\mathbf{x}_1 \dots \mathbf{x}_3$  to  $\mathbf{z}_1 \dots \mathbf{z}_3$  by three arrows in the lower part of Figure 1. We also depict  $S$  and  $Z$  as shaded regions. The  $S$  of (1) and of (2) remains the same. The  $Z$  of (1) extends to a high-dimensional set for (2). The efficient frontier of (1) also extends to a high-dimensional efficient surface for (2) (denoted as  $N$ ). The surface is the optimal solutions of (2) in  $(z_1, \dots, z_k)$  space.

#### 1.4. Originality for Green Innovation Investments

*1.4.1. Formulation Originality: 3-Objective Portfolio Selection for Green Innovation.* We originate the following 3-objective model for green innovation by taking  $\boldsymbol{\mu}_3$  as a vector of stock expected green innovations and taking  $z_3$  as the portfolio expected green innovation:

$$\begin{aligned} \min\{z_1 = \mathbf{x}^T \boldsymbol{\Sigma} \mathbf{x}\}, \text{risk} \\ \max\{z_2 = \mathbf{x}^T \boldsymbol{\mu}\}, \text{return} \\ \max\{z_3 = \mathbf{x}^T \boldsymbol{\mu}_3\}, \text{green innovation} \\ \text{s.t. } \mathbf{A}^T \mathbf{x} = \mathbf{b}, \text{constraints,} \end{aligned} \quad (3)$$

where

- $\mathbf{A}$  is an  $n \times m$  constraint matrix,
- $\mathbf{b}$  is an  $m$ -vector for the right hand side.

Equation (3) can overcome the weakness of the screening-indexing strategies as follows:

First (3) hinges on portfolio selection and thus enjoys portfolio completeness. Second, (3) explicitly operates green innovation as an additional objective and reserves rooms for the utility. Last, (3) prescribes a whole efficient surface for investors.

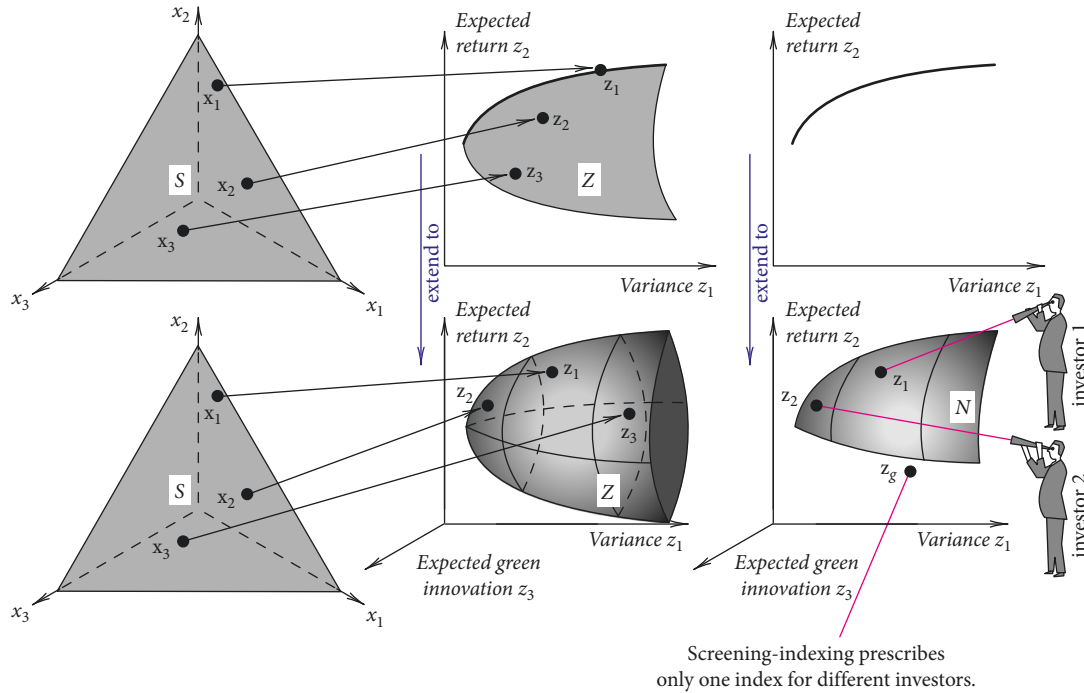


FIGURE 1: Portfolio selection (the upper part) and multiple-objective portfolio selection and its advantage (the lower part).

With the sheer amount of portfolios on the surface, different investors can pick distinctive portfolios. For instance, investor 1 prefers portfolio  $\mathbf{z}_1$ , while investor 2 prefers portfolio  $\mathbf{z}_2$  (as depicted in the lower part of Figure 1). In contrast, the screening-indexing strategies invariably prescribe only one index for vastly different investors. The index is denoted as  $\mathbf{z}_g$  (as depicted in the lower part of Figure 1).

**1.4.2. Formulation Advantage: Dominating Green Innovation Indexes.** Moreover, investors can exploit the efficient surface and harvest portfolios which dominate the green innovation index  $\mathbf{z}_g$ . As the originality, we will prove in a theorem that there exist portfolios which

- (1) enjoy both better expected return and better expected green innovation than the green innovation index does;
- (2) possess the same variance as that of the green innovation index.

The portfolios are depicted as the thickest curve from  $\mathbf{z}_{d2}$  to  $\mathbf{z}_{d3}$  in the right part of Figure 2. The figure will be deliberated later.

**1.5. Paper Structure.** The rest of this paper is organized as follows: We review theoretical background in the next section. Then in the next section, we prove the existence of dominating portfolios by a theorem and propose hypotheses for the out-of-sample dominance. Then in the next section, we measure green innovation on the basis of patent-citation numbers, set up (3), compute the dominance, test the hypotheses by component stocks of China Securities Index 300,

and obtain affirmative results. Then in the next section, we divide green innovation into categories, further formulate the categories as objectives, extend (3) into general  $k$ -objective portfolio selection, and still demonstrate the dominance. We conclude this paper in the last section.

## 2. Literature Review: Green Innovation Investments and Multiple-Objective Portfolio Selection

We briefly review green innovation measurement and green innovation investments, summarize multiple-objective portfolio selection, and display quantitative results.

**2.1. Overall Research for Green Innovation.** A large body of green innovation research focuses on

- (1) the driving force behind green innovation;
- (2) the impact of green innovation on corporations or society.

For research line 1, for example, [23] proposes regulation and pressure as the driving force and verifies the proposition by environment-related patents. Reference [24] proposes political capital as the driving force. Reference [25] proposes green supplier involvement.

For research line 2, for example, [26] contends that green innovation is positively correlated to corporate competitive advantage. Reference [27] reports positive correlations between green innovation and green core competence. Reference [1] concludes that green innovation has positive effects on organizational performance.



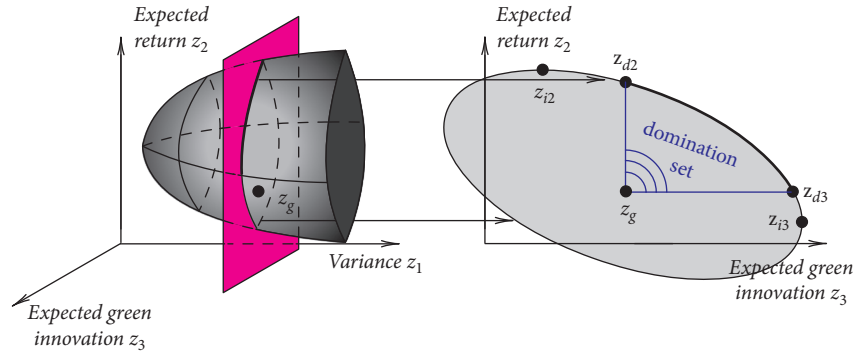


FIGURE 2: The plane passing through the green innovation index  $z_g$ , intersection between the plane and feasible region  $Z$ , and portfolios which dominate the index (on the thickest curve from  $z_{d2}$  to  $z_{d3}$ ).

## 2.2. ESG Measurement and Green Innovation Measurement

**2.2.1. ESG Measurement.** Overall, ESG is a well-dissected but still evolving area. References [28, 29] review more than 2000 ESG studies, advocate future directions, and discover that the studies mainly focus on Europe and US. Reference [30] detects relatively slow ESG developments in Asia and deduces the reason as the lack of reliable ESG measurement. Reference [31] maneuvers rough-set approaches and forecasts ESG ratios by corporate financial performance variables. Several scholars further highlight the following weakness in ESG measurement.

First, scholars naturally instigate all kinds of ESG measurement. While financial measures are definite, environmental measures are relatively vague. To make things more diverse, there are more than 600 ESG-rating agencies with dissimilar measurement themes. References [32, 33] uncover inconsistent measurement results among key rating agencies (e.g., MSCI, Thomson Reuters, and GES).

Second, ESG measures heavily rely on corporate voluntary disclosures, but the disclosures are typically unaudited. Therefore, some corporations tend to manipulate their disclosures. References [34, 35] investigate such manipulation motivations. Reference [36] validates that some firms may exaggerate environmental performance for better images. Reference [37] further designs mechanisms to deter such exaggerations.

**2.2.2. Green Innovation Measurement.** In contrast, scholars sponsor relatively concentrated measurement for green innovation. Moreover, green innovation can be objectively measured by patent-citation numbers. The numbers are issued by independent third parties (e.g., World Intellectual Property Organization). Therefore, in contrast to the lack of reliable ESG measurement in Asia, green innovation can be relatively reliably measured in Asia. References [38, 39] survey green innovation development, recommend future directions, and endorse the patent-citation measurement.

In the early stage of green innovation development, scholars (e.g., [26, 40]) do not have sufficient patent-information support and thus typically utilize surveys to measure green innovation. Later, [23], pp.897–898, questions the potential insight of the surveys, emphasizes the

potential survey bias, and proposes the total number of citations received by the patents as the measure. Similarly, [41], p.637, acknowledges patent-citation numbers and executes Citations/RD (RD as R&D). Reference [42], pp.2249–2250, also acknowledges patent-citation numbers and employs natural logarithms of one plus the numbers.

**2.3. Green Innovation Investments.** Reference [43] stresses the gigantic volume of green innovation investments, underscores the importance of portfolio selection, and inaugurates their models. Reference [29] surveys 463 articles and books for green innovation investments and reviews the following two major methods:

First, investors readily deploy the screening-indexing strategies. For example, [44] utilizes the strategies and reports some positive risk-adjusted performance. Reference [45] utilizes the strategies, compares green innovation investments against passive investments, and finds mixed results. Reference [46] utilizes the strategies and emphasizes opportunity costs for screening. Reference [47] picks the top 100 CSR companies in the world by Forbes, assembles market-capitalization-index portfolios, and locates significant abnormal returns. During the COVID-19 pandemic, [48] attests investor preference for ESG indexes and validates the outperformance. Reference [49] concentrates on the component stocks of S&P 500 Index, executes the screening-indexing strategies, and portrays confirmatory results. In contrast, [50] surveys main-stream investment organizations and finds the strategies relatively ineffective.

Second, mutual-fund companies structure funds by the screening-indexing strategies. For example, [51, 52] and [53] compare green innovation funds' returns against conventional mutual funds' returns but reveal the two groups of returns as typically identical. By further considering crisis and normal periods, [54] discovers that the two groups of returns are typically identical in crisis periods but the green innovation funds underperform the conventional mutual funds in normal periods. Reference [55] exposes that the risk-adjusted returns of funds with high green innovation measures equal those of funds with low green innovation measures. During the COVID-19 pandemic, [56] unveils that investors deliberate ESG risk and that low-ESG-risk funds outperform high-ESG-risk funds.

*2.4. Multiple-Objective Portfolio Selection for Green Innovation and for Other Objectives.* Reference [51], p.1723, concludes that SRI investors are willing to sacrifice financial performance for social objectives. The conclusion can be explained by multiple-objective portfolio selection for green innovation. That is, investors accept some optimal portfolios in  $(z_1, z_2, z_3)$  space of (3), although the portfolios are not optimal in  $(z_1, z_2)$  space of (1). Moreover, [57] considers the traditional financial goal and an ethical goal for utility functions and optimizes the 2-goal model. Reference [58] analyzes social responsibility by multiple-objective portfolio selection and studies the maximum-Sharpe-ratio portfolio and maximum-Delta-ratio portfolio.

For other objectives, [59] studies skewness. Reference [60], pp.119–120, reports that investors compute several risk measures in practice. Reference [61] studies two risk measures: variance and CVaR. Reference [62] analyzes tracking error. Reference [63] studies liquidity. Reference [64] studies R&D. References [65–69] and [70] offer surveys.

#### 2.5. Multiple-Objective Portfolio Optimization with Equality Constraints Only

*2.5.1. A Fundamental Model (4) for Portfolio Selection and Asset Pricing.* References [71], pp.57–62, and [72] inspect the following model:

$$\begin{aligned} \min\{z_1 = \mathbf{x}^T \boldsymbol{\Sigma} \mathbf{x}\} \\ \max\{z_2 = \mathbf{x}^T \boldsymbol{\mu}\} \\ \text{s.t. } \mathbf{1}^T \mathbf{x} = 1. \end{aligned} \quad (4)$$

$\mathbf{1}$  is a vector of ones. Reference [72] analytically derives the minimum-variance frontier and proves the frontier as a parabola. The frontier is the boundary of the feasible region  $Z$  of (4) and is depicted as a curve in the upper part of Figure 1. Although unlimited portfolio weights are allowed, (4) enjoys analytical tractability and thus is widely deployed in portfolio selection and asset pricing (as acclaimed by [73], p.60).

*2.5.2. Extending (4) by Adding an Objective.* Reference [21] extends (4) by adding an objective as follows:

$$\begin{aligned} \min\{z_1 = \mathbf{x}^T \boldsymbol{\Sigma} \mathbf{x}\} \\ \max\{z_2 = \mathbf{x}^T \boldsymbol{\mu}\} \\ \max\{z_3 = \mathbf{x}^T \boldsymbol{\mu}_3\} \\ \text{s.t. } \mathbf{1}^T \mathbf{x} = 1, \end{aligned} \quad (5)$$

where  $z_3$  is a general objective. Reference [21] also analytically derives the result.

*2.5.3. Further Extending (4) by Adding Objectives and Constraints.* Reference [22] further extends (4) by adding objectives and constraints as follows:

$$\begin{aligned} \min\{z_1 = \mathbf{x}^T \boldsymbol{\Sigma} \mathbf{x}\} \\ \max\{z_2 = \mathbf{x}^T \boldsymbol{\mu}\} \\ \max\{z_3 = \mathbf{x}^T \boldsymbol{\mu}_3\} \\ \vdots \\ \max\{z_k = \mathbf{x}^T \boldsymbol{\mu}_k\} \\ \text{s.t. } \mathbf{A}^T \mathbf{x} = \mathbf{b}. \end{aligned} \quad (6)$$

They embrace the following assumptions.

*Assumption 1.* Covariance matrix  $\boldsymbol{\Sigma}$  is positive definite and thus invertible.

*Assumption 2.* Vectors  $\boldsymbol{\mu}$  and  $\boldsymbol{\mu}_3 \dots \boldsymbol{\mu}_k$  and all columns of  $\mathbf{A}$  (altogether  $k - 1 + m$  vectors) are linearly independent.

Reference [22] commands an  $e$ -constraint method (as described by [10], pp.202–206) to (6) as follows:

$$\begin{aligned} \min\{z_1 = \mathbf{x}^T \boldsymbol{\Sigma} \mathbf{x}\} \\ \text{s.t. } \mathbf{x}^T \boldsymbol{\mu} = e_2 \\ \vdots \\ \mathbf{x}^T \boldsymbol{\mu}_k = e_k \\ \mathbf{A}^T \mathbf{x} = \mathbf{b}. \end{aligned} \quad (7)$$

$e_2 \dots e_k$  are the method parameters. As  $e_2 \dots e_k$  vary, the set of all  $(z_1, \dots, z_k)$  vectors of the optimal solutions of (7) forms a minimum-variance surface of (6). As an extension of the minimum-variance frontier of (4), the surface is the boundary of the feasible region  $Z$  of (6) and is depicted as a surface in the lower part of Figure 1. Reference [22], pp.527–528, proves the surface as a paraboloid and analytically derives the surface as follows:

$$z_1 = [z_2 \dots z_k \mathbf{b}^T] (\mathbf{M}^T \boldsymbol{\Sigma}^{-1} \mathbf{M})^{-1} \begin{bmatrix} z_2 \\ \vdots \\ z_k \\ \mathbf{b} \end{bmatrix}, \quad (8)$$

where  $\mathbf{M}$  is introduced as follows:

$$\mathbf{M} = [\boldsymbol{\mu} \ \boldsymbol{\mu}_3 \ \dots \ \boldsymbol{\mu}_k \ \mathbf{A}]_{n \times (k-1+m)}. \quad (9)$$

For a portfolio on the surface with given  $z_2 \dots z_k$ , [22], p.526, computes the portfolio-weight vector  $\mathbf{x}$  as follows:

$$\mathbf{x} = \boldsymbol{\Sigma}^{-1} \mathbf{M} (\mathbf{M}^T \boldsymbol{\Sigma}^{-1} \mathbf{M})^{-1} \begin{bmatrix} z_2 \\ \vdots \\ z_k \\ \mathbf{b} \end{bmatrix}. \quad (10)$$

Moreover, [22], pp.529–531, derives the  $\mathbf{x}$  set of the efficient surface of (6) as follows:

$$\{\mathbf{x} \in \mathbb{R}^n | \mathbf{x} = \mathbf{x}_{mv} + \lambda_2 \mathbf{g}_2 + \dots + \lambda_k \mathbf{g}_k, \lambda_2 \dots \lambda_k \geq 0\}, \quad (11)$$

where  $\mathbf{x}_{mv}$  and  $\mathbf{g}_2 \dots \mathbf{g}_k$  are computed as follows:

$$\begin{aligned} \mathbf{x}_{mv} &= \Sigma^{-1} \mathbf{A} (\mathbf{A}^T \Sigma^{-1} \mathbf{A})^{-1} \mathbf{b} \\ [\mathbf{g}_2 \dots \mathbf{g}_k] &= \frac{1}{2} \Sigma^{-1} \left( \mathbf{I}_n - \mathbf{A} (\mathbf{A}^T \Sigma^{-1} \mathbf{A})^{-1} \mathbf{A}^T \Sigma^{-1} \right) \\ &\quad \cdot [\boldsymbol{\mu} \ \boldsymbol{\mu}_3 \ \dots \ \boldsymbol{\mu}_k], \end{aligned} \quad (12)$$

with  $\mathbf{I}_n$  as an  $n \times n$  identity matrix. The efficient surface is obtained by substituting (11) into (6).

We will compare methods for general multiple-objective portfolio optimization in the next section.

### 3. Dominating Green Innovation Indexes and Testing the Dominance by Hypotheses

As an advantage of (3), the efficient surface precisely and completely demonstrates the trade-offs among optimal variance, expected return, and expected green innovation. Therefore, investors can study the surface, envisage the trade-offs, and pinpoint preferred portfolios on the surface. Moreover, we prove that investors can obtain surface portfolios which dominate the green innovation index. We justify (3), present a graphical interpretation, validate the dominance by a theorem, and propose hypotheses for the out-of-sample dominance.

*3.1. Justifying (3).* We accentuate that (3) can overpower the weakness of the screening-indexing strategies as follows:

First, (3) hinges on portfolio selection and thus enjoys portfolio completeness. For an  $n \times n$  covariance matrix  $\Sigma$ , the screening-indexing strategies exploit only the  $n$  variance elements as individual stock risks, but portfolio selection and (3) additionally exploit the  $n^2 - n/2$  overwhelmingly more covariance elements as stock corisks. Moreover, the screening-indexing strategies implement relatively simplistic indexing, while portfolio selection and (3) implement forceful optimization methodologies. Reference [74] features the scarcity of optimization methodologies in green innovation investments and endorses portfolio selection. Reference [75] also features the scarcity and commences all-underlying-functionality models. Reference [76] scans reasons of the screening-indexing strategies' relatively unsatisfactory performance and urges rudimentary linear regression models. Reference [77] engineers ESG portfolios by utility-based nonparametric models.

Second, (3) explicitly utilizes green innovation as an additional objective and reserves rooms for the utility. References [5], p.683, and [6], p.2, hint investors' such motives. Reference [78] implies that investors balance financial objectives versus ESG objectives and even relatively sacrifice financial objectives to enrich ESG objectives. Reference [79] surveys household preferences for ESG investments and also implies that investors relatively sacrifice financial objectives to enrich ESG objectives. Reference [80] substantiates that international institutional investors care about both financial objectives and social objectives.

Third, (3) prescribes a whole efficient surface for investors. Consequently, investors perceive the efficient surface as a panorama of the optimal variance, expected return, and expected green innovation and thus enjoy the freedom of choosing preferred portfolios on the surface. Different investors can pick distinctive surface portfolios. References [7], p.5, and [8], pp.27&28, feature investor difference. Reference [50] globally surveys ESG information and recounts information-usage difference in motivation, demand, product strategy, and ethical considerations. Reference [81] probes investors' political ideology and fashions portfolio-selection models for a unique group of investors. Reference [43] further explores three types of investors: ESG-unaware investors, ESG-aware investors, and ESG-motivated investors.

Last, we scrutinize green innovation (instead of ESG) in China for (3), because green innovation can be objectively measured by patent-citation numbers.

*3.2. Graphical Interpretation.* For (3), let  $\mathbf{z}_g = (z_{g1}, z_{g2}, z_{g3})$  denote the green innovation index in  $(z_1, z_2, z_3)$  space with  $z_{g1}$ ,  $z_{g2}$ , and  $z_{g3}$  as the variance, expected return, and expected green innovation of the index, respectively. Let  $\mathbf{x}_g$  denote the portfolio-weight vector of the index. By screening,  $\mathbf{x}_g$  bears some zero elements and thus is typically inefficient, because efficient portfolio-weight vectors (11) basically bear few zero elements. Therefore,  $\mathbf{z}_g$  is typically not on the efficient surface.

In the left part of Figure 2, we draw a plane which passes through  $\mathbf{z}_g$  and is parallel to  $(z_2, z_3)$  subspace. The plane is as follows:

$$z_1 = z_{g1}. \quad (13)$$

The plane intersects the feasible region  $Z$  of (3). Because every portfolio on the intersection shares the same  $z_1$  (i.e.,  $z_1 = z_{g1}$ ), we need to focus on just  $(z_2, z_3)$  elements of the intersection in the right part of Figure 2. The intersection is depicted as shaded in the right part. Because [22] proves the minimum-variance surface as a paraboloid (8) and the surface is the boundary of the feasible region  $Z$ , the boundary of the intersection is an ellipse. By (8) with  $k = 3$  and (13), the ellipse is as follows:

$$[z_2 \dots z_k \ \mathbf{b}^T] (\mathbf{M}^T \Sigma^{-1} \mathbf{M})^{-1} \begin{bmatrix} z_2 \\ \vdots \\ z_k \\ \mathbf{b} \end{bmatrix} = z_{g1}. \quad (14)$$

Specifically, the plane intersects the efficient surface at a thicker curve in the right part of Figure 2. The intersection is depicted as a thicker curve from  $\mathbf{z}_{i2}$  to  $\mathbf{z}_{i3}$ .

We utilize the domination-set method of [10], pp.150–154, and draw a domination set at  $\mathbf{z}_g$  in blue color. Every portfolio in the set (except  $\mathbf{z}_g$  itself) dominates  $\mathbf{z}_g$ . The set finally touches the ellipse at the thickest curve from  $\mathbf{z}_{d2}$  to  $\mathbf{z}_{d3}$ ;  $\mathbf{z}_{d2}$  and  $\mathbf{z}_{d3}$  are depicted in the right part of Figure 2. By the method, all the portfolios on the thickest curve dominate  $\mathbf{z}_g$  the most.

3.3. *Proving the Dominance by a Theorem.* We reiterate the graphical interpretation in the following theorem.

**Theorem 1.** *In  $(z_1, z_2, z_3)$  space of (3), there exists a plane passing through  $\mathbf{z}_g$  and being parallel to  $(z_2, z_3)$  subspace unless  $\mathbf{z}_g$  is efficient. The plane intersects the efficient surface and feasible region  $Z$  of (3). On the intersection of the plane and efficient surface, there exists a whole range of portfolios which dominate  $\mathbf{z}_g$ . That is,*

*the portfolios' variances are identical to the variance of  $\mathbf{z}_g$ ,*

*the portfolios' expected returns are greater than or equal to the expected return of  $\mathbf{z}_g$ ,*

*the portfolios' expected green innovations are greater than or equal to the expected green innovation of  $\mathbf{z}_g$ ,*

*at least one of the two "greater than or equal to" relationships is "greater than."*

*Proof.* The plane (13) intersects the  $Z$  of (3). Because all portfolios on the intersection share the same  $z_1$  (i.e.,  $z_1 = z_{g1}$ ) and the efficient surface is the optimal portfolios of (3), the optimal solutions of the intersection are the thicker curve from  $\mathbf{z}_{i2} = (z_{g1}, z_{i2,2}, z_{i2,3})$  to  $\mathbf{z}_{i3} = (z_{g1}, z_{i3,2}, z_{i3,3})$  in the right part of Figure 2. Investors calculate  $\mathbf{z}_{i2}$  and  $\mathbf{z}_{i3}$  by (8) and (11).

If  $\mathbf{z}_g$  is to the right of  $\mathbf{z}_{i2}$  (i.e.,  $z_{g3} \geq z_{i2,3}$  as depicted in the right part of Figure 2), investors compute  $\mathbf{z}_{d2} = (z_{g1}, z_{d2,2}, z_{g3})$  by substituting  $z_3 = z_{g3}$  into (14), calculating the two roots, and taking  $z_{d2,2}$  as the bigger root. Otherwise (i.e., to the left of  $\mathbf{z}_{i2}$ ,  $z_{g3} < z_{i2,3}$  as depicted in the upper left part of Figure 3), investors just take  $\mathbf{z}_{d2} = \mathbf{z}_{i2}$ .

Similarly, if  $\mathbf{z}_g$  is above  $\mathbf{z}_{i3}$  (i.e.,  $z_{g2} \geq z_{i3,2}$  as depicted in the right part of Figure 2), investors compute  $\mathbf{z}_{d3} = (z_{g1}, z_{g2}, z_{d3,3})$  by substituting  $z_2 = z_{g2}$  into (14), calculating the two roots, and taking  $z_{d3,3}$  as the bigger root. Otherwise (i.e., below  $\mathbf{z}_{i3}$ ,  $z_{g2} < z_{i3,2}$  as depicted in the upper right part of Figure 3), investors just take  $\mathbf{z}_{d3} = \mathbf{z}_{i3}$ .

In summary, there are four exhaustively exclusive cases as follows:

- (1)  $z_{g3} \geq z_{i2,3}$  and  $z_{g2} \geq z_{i3,2}$  (right part of Figure 2),
- (2)  $z_{g3} \geq z_{i2,3}$  and  $z_{g2} < z_{i3,2}$  (upper right part of Figure 3),
- (3)  $z_{g3} < z_{i2,3}$  and  $z_{g2} \geq z_{i3,2}$  (upper left part of Figure 3),
- (4)  $z_{g3} < z_{i2,3}$  and  $z_{g2} < z_{i3,2}$  (lower left part of Figure 3).

For the four cases, investors exploit the domination-set method at  $\mathbf{z}_g$ . Every portfolio in the set dominates  $\mathbf{z}_g$ . Specifically, all the portfolios on the thickest curve from  $\mathbf{z}_{d2}$  to  $\mathbf{z}_{d3}$  dominate  $\mathbf{z}_g$  the most. The portfolio-weight vectors can be computed on the basis of (10).  $\square$

3.4. *Testing Hypotheses for the Out-of-Sample Dominance.* By Theorem 1, we can choose a portfolio on the thickest curve from  $\mathbf{z}_{d2}$  to  $\mathbf{z}_{d3}$ , collect out-of-sample data, compute the returns and green innovations of the portfolio and of the

green innovation index  $\mathbf{z}_g$ , and test the following hypotheses:

$$H_0: \text{variance of the portfolio} = \text{variance of } \mathbf{z}_g, \quad (15)$$

$$H_a: \text{variance of the portfolio} \neq \text{variance of } \mathbf{z}_g,$$

$$H_0: \text{expected return of the portfolio} = \text{expected return of } \mathbf{z}_g, \quad (16)$$

$$H_a: \text{expected return of the portfolio} > \text{expected return of } \mathbf{z}_g$$

$$H_0: \text{expected green innovation of the portfolio} = \text{expected green innovation of } \mathbf{z}_g$$

$$H_a: \text{expected green innovation of the portfolio} > \text{expected green innovation of } \mathbf{z}_g.$$

(17)

Reference [82], pp.497–499 & 454–457, describes standard test statistics.

3.5. *Portfolio Selection and Its Out-of-Sample Performance.* Several researchers (e.g., [83–85] and [86]) criticize portfolio selection for its weak out-of-sample performance. However, the researchers' arguments can be reconciled in the following aspects.

First, [9] seminally quantitatively formulates portfolio risk and return rather than focusing on out-of-sample performance (as proclaimed by [87], p.1041). Therefore, portfolio selection is universally described in classic textbooks (e.g., those of [3, 88–90] and [91]).

Second, strong out-of-sample performance implicitly requires that the out-of-sample is preferably large and comes from the same independent and identical distribution as the in-sample distribution. However in reality, financial markets instantly react to all kinds of information; corporations prosper and decline over time. Therefore, the requirement is rarely satisfied. Consequently, weak out-of-sample performance can be caused by the sample distribution.

Last, investors subjectively hope to consistently beat markets without extra cost. However, objectively, such financial perpetual-motion machines violate fundamental finance-theory laws (e.g., efficient-market hypotheses) and thus barely exist.

In this paper, in sample, we extend portfolio selection, instigate 3-objective portfolio selection for green innovation, and prove the existence of dominating portfolios in a theorem. We will launch both theoretical and practical implications in the conclusion.

3.6. *Contrasting Methods of Multiple-Objective Portfolio Optimization.* We briefly contrast different methods for general multiple-objective portfolio optimization.

3.6.1. *Analytical Methods.* Analytical methods are conducted in the form of formulae on the basis of calculus and linear algebra and are thus understandable. We have already

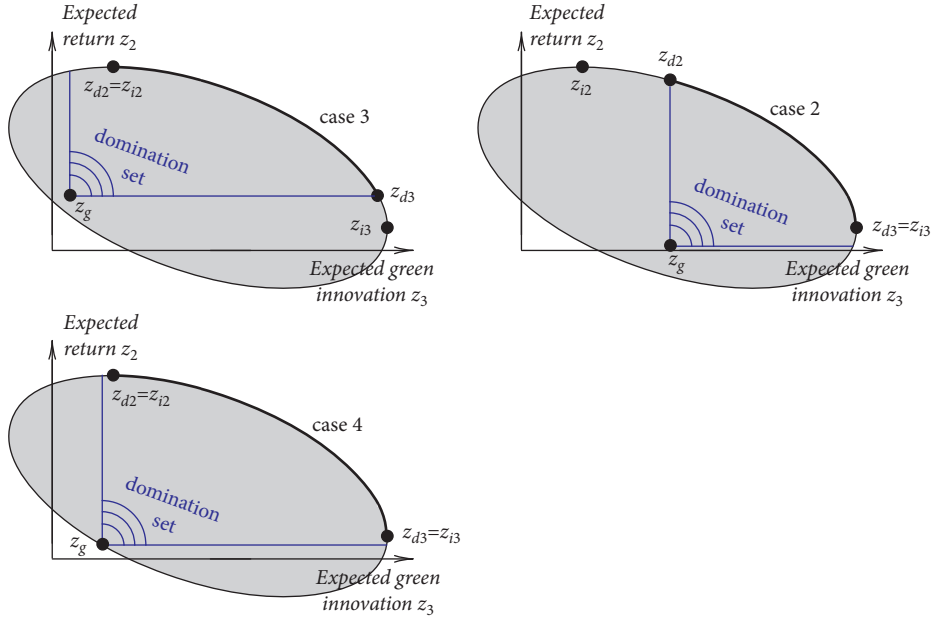


FIGURE 3: The three other cases of the relationship between  $\mathbf{z}_g$  and  $\mathbf{z}_{i2}$  and between  $\mathbf{z}_g$  and  $\mathbf{z}_{i3}$  for Theorem 1.

reviewed analytical methods in the previous section. We optimize (20) by analytical methods (8)–(11). Analytical methods' computational advantage is to readily reckon the efficient surface and dominating portfolios.

However, analytical methods decipher models with equality constraints only. Nevertheless with almost all results in formulae, analytical methods liberate researchers from mathematical programming. Therefore, researchers can enjoy the analytical tractability and empirical implications (as highlighted by [73], p.60).

**3.6.2. Parametric Quadratic Programming.** Parametric quadratic programming is an advanced form of quadratic programming with parameters in the formulation. References [92, 93] describe the topic in detail. Parametric quadratic programming can handle both equality constraints and inequality constraints. Particularly, inequality constraints can prescribe the following conditions:

- some lower bound (floor) of  $\mathbf{x}$  (e.g.,  $\mathbf{x} \geq 0$  to restrict short sales),
- some lower bound and upper bound (ceiling) of an industry to regulate the industry exposure,
- transaction cost.

To solve (1), [94, 95] deploy parametric quadratic programming and propose a *critical-line algorithm*. Reference [95], p.176, proves that the efficient frontier is piece-wisely made up by connected parabolic segments.

Reference [96] calculates the whole efficient surface of (2) with  $k = 3$  and suggests that the surface is piece-wisely made up by connected paraboloidal segments. For example, a surface consists of two segments in the left part of Figure 4. The upper segment is a portion of paraboloid

$z_1 = z_2^2 + 2z_3^2 + 3z_2z_3 + 4z_2 + 4z_3 + 9$ ; the lower segment is a portion of paraboloid  $z_1 = z_2^2 + 5z_3^2 + 6z_2z_3 + 8z_2 + 9z_3 + 8$ . The two segments connect at a thick curve. Reference [97] also exploits parametric quadratic programming and resolves (2).

However, parametric quadratic programming is much more convoluted than quadratic programming and thus rarely commanded. Moreover, parametric quadratic programming suffers from the following obstacles.

First, neither the shape nor the property of the feasible region  $Z = \{(z_1, \dots, z_k) | \mathbf{x} \in S\}$  of (2) is comprehensible. Investors can follow the method depicted in Figure 2 but can not envision the intersection between the plane  $z_1 = z_{g1}$  (13) and  $Z$ . For example, the boundary of the intersection is unknown and depicted as broken curves in the right part of Figure 4. Therefore, the intersection is unknown either. With a green innovation index  $\mathbf{z}_g$  near a corner, investors can obtain eccentric results by operating the domination-set method. In contrast, for (3), investors fully comprehend that the  $Z$  is a paraboloidal set by (8). Therefore, investors fully comprehend that the intersection between the plane (13) and  $Z$  is an elliptical area (as depicted in Figures 2 and 3).

Second, [96], p.181, proclaims that efficient surfaces of (2) with  $k = 3$  and with  $n = 102$  can be made up by 7994 connected paraboloidal segments. For the simplest only-1-segment efficient surface of (3), investors encounter 4 cases of the relationship between  $\mathbf{z}_g$  and  $\mathbf{z}_{i2}$  and between  $\mathbf{z}_g$  and  $\mathbf{z}_{i3}$  (as depicted in Figures 2 and 3). For the simplistic 2-segment efficient surface depicted in Figure 4, investors can encounter  $2 \times 4 = 8$  cases of the relationship between  $\mathbf{z}_g$  and  $\mathbf{z}_{i2}$  and between  $\mathbf{z}_g$  and  $\mathbf{z}_{i3}$  and between  $\mathbf{z}_g$  and  $\mathbf{z}_{i4}$ . For the 7994-segment efficient surfaces, investors will be perplexed by the case number.

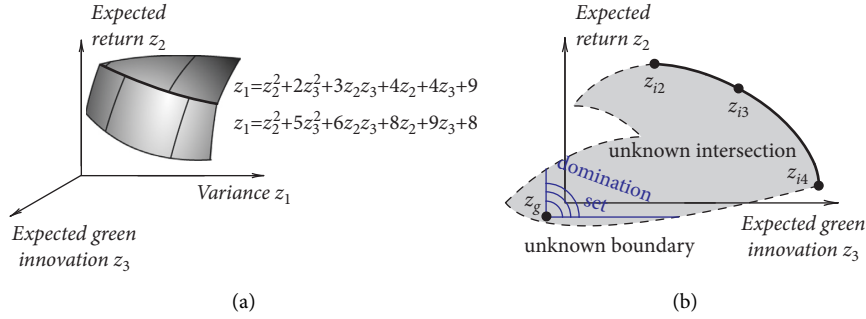


FIGURE 4: For (2) by parametric quadratic programming, an efficient surface with two segments (a) and the intersection between the plane  $z_1 = z_{g1}$  (13) and the unknown feasible region  $Z$  (b).

Last, there is no public-domain software for (2) yet. Although [96] inaugurates and codes their algorithm, they do not publicly release their software.

**3.6.3. Repetitive Quadratic Programming.** Repetitive quadratic programming can handle both equality constraints and inequality constraints. Reference [10], pp.165–183&202–206, elucidates weighted-sums methods and  $\epsilon$ -constraint methods to transform multiple-objective optimization into (ordinary) 1-objective optimization. Investors can channel the methods for (2) as follows:

$$\min \{ \mathbf{x}^T \Sigma \mathbf{x} - \lambda_2 \mathbf{x}^T \boldsymbol{\mu} - \lambda_3 \mathbf{x}^T \boldsymbol{\mu}_3 - \dots - \lambda_k \mathbf{x}^T \boldsymbol{\mu}_k \} \quad (18)$$

s.t.  $\mathbf{x} \in S$ , feasible region.

$$\begin{aligned} \min \{ z_1 = \mathbf{x}^T \Sigma \mathbf{x} \}, \\ \text{s.t. } \mathbf{x}^T \boldsymbol{\mu} = e_2, \\ \mathbf{x}^T \boldsymbol{\mu}_3 = e_3, \\ \vdots \\ \mathbf{x}^T \boldsymbol{\mu}_k = e_k, \\ \mathbf{x} \in S, \end{aligned} \quad (19)$$

where

$\lambda_2 \dots \lambda_k$  are coefficients for weighted-sums methods,  
 $e_2 \dots e_k$  are coefficients for  $\epsilon$ -constraint methods.

Investors preset a group of  $\lambda_2 \dots \lambda_k$  and a group of  $e_2 \dots e_k$ , repetitively solve (18) for each  $\lambda_2 \dots \lambda_k$ , and repetitively solve (19) for each  $e_2 \dots e_k$ . The optimal solutions are actually discrete versions of the efficient surface of (2). We depict some optimal solutions as isolated points in the left part of Figure 5. The isolated points are much less informative than the whole efficient surface depicted in the left part of Figure 4.

Repetitive quadratic programming is easy to understand and thus described in classic textbooks (e.g., Chapter 7 of [3]). Several computational software (e.g., Microsoft Excel and Matlab) can offer quadratic-programming solvers. However, repetitive quadratic programming suffers from the following obstacles:

First, the isolated points can cluster in small parts of the efficient surface instead of uniformly dispersing around the surface (as underlined by [98]).

Second, repetitive quadratic programming can not reveal the paraboloidal-segment structure. For instance, investors perceive just a bunch of isolated points in Figure 5.

Last, investors obtain also isolated points on the intersection and hardly execute the domination-set method for the points. We depict the situation in the right part of Figure 5.

**3.6.4. Genetic Algorithms and Other Heuristic Methods.** As important and popular tools, genetic algorithms and other heuristic methods can handle equality constraints, inequality constraints, and even special conditions (e.g., integer variables). Reference [99] systematically exhibits genetic algorithms. References [100, 101] and [102] employ genetic algorithms for multiple-objective portfolio selection. Reference [103] offers surveys for genetic algorithms.

However, heuristic methods inherently provide suboptimal solutions. For example, we depict some isolated points as suboptimal solutions in the left part of Figure 6. The points are below the efficient surface depicted in the left part of Figure 4. Moreover, the methods also suffer from the obstacles of repetitive quadratic programming. We depict some obstacles in the right part of Figure 6.

## 4. Empirical Tests by Component Stocks of China Securities Index 300

We sample the 300 component stocks of China Securities Index 300 from 2009 to 2018, measure the green innovation, gauge the dominating portfolios, test hypotheses for the out-of-sample dominance, implement robustness tests, and obtain supportive results. We report key computations and omit long calculations (e.g.,  $152 \times 152$  matrices). We have deposited all the data, codes, and results in Mendeley Data <https://data.mendeley.com/>. Please see [104] in the references.

**4.1. Modeling.** Specially, we develop the following model on the basis of (3):

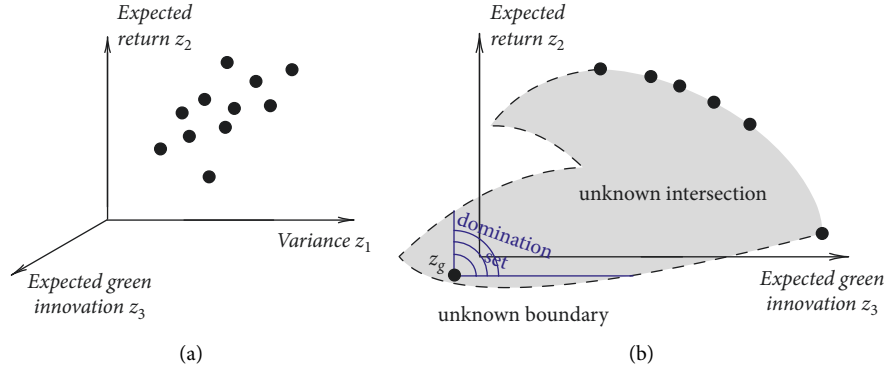


FIGURE 5: For (2) by repetitive quadratic programming, isolated points as discrete versions of the efficient surface (a) and the intersection between the plane  $z_1 = z_{g1}$  (13) and the unknown feasible region  $Z$  (b).

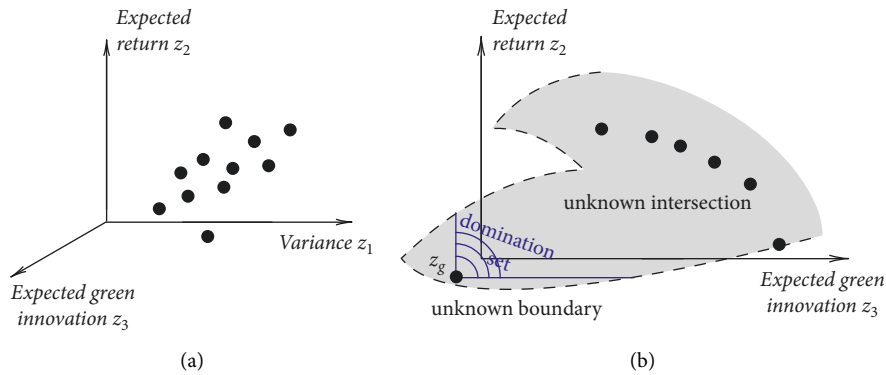


FIGURE 6: For (2) by genetic algorithms, isolated points to approximate the efficient surface (a) and the intersection between the plane  $z_1 = z_{g1}$  (13) and the unknown feasible region  $Z$  (b).

$$\begin{aligned}
 & \min\{z_1 = \mathbf{x}^T \Sigma \mathbf{x}\}, \\
 & \max\{z_2 = \mathbf{x}^T \boldsymbol{\mu}\}, \\
 & \max\{z_3 = \mathbf{x}^T \boldsymbol{\mu}_3\}, \\
 & \text{s.t. } \mathbf{1}^T \mathbf{x} = 1, \\
 & \mathbf{d}^T \mathbf{x} = \bar{d},
 \end{aligned} \tag{20}$$

$\mathbf{d}$  is a vector of stock expected dividend yields (dividend/price);  $\bar{d}$  is a target expected dividend yield and taken as the average of  $\mathbf{d}$ .

Dividend stands as an important constraint. In theory, [105] proposes a theory of dividend by tax clienteles and concludes that corporations attract institutions by paying dividend. Reference [106] suggests a dividend-catering theory and contends that corporations cater to investors by paying dividend. Reference [107] contemplates discrete dividends and solves the corresponding portfolio-optimization model. Reference [108] demonstrates new evidence of dividend-catering theory in the emerging market. In practice, [109], p.71, assumes dividend as an important intrinsic-value factor.

*4.2. Measuring Green Innovation of the Component Stocks by Patent-Citation Numbers.* We follow [41, 42] and explicitly measure green innovation in the following steps:

- (1) We also acknowledge patent-citation numbers.
- (2) We sample all the 300 component stocks of China Securities Index 300 (data source: <http://www.csindex.com.cn/en/indices/index-detail/000300>, May 24, 2020). We follow empirical-test traditions to disregard finance-industry stocks and traditions with incomplete observations. We then obtain  $n = 152$  component stocks with complete monthly returns from January 1, 2009, to December 31, 2018.
- (3) For the 152 component stocks, we obtain the patent information (including international patent classification number) from 2009 to 2018 from State Intellectual Property Office of China (SIPO) (data source: <http://pss-system.cnipa.gov.cn/sipopublicsearch/portal/uiIndex.shtml>, May 29, 2020).
- (4) We check the patent information for green innovation of World Intellectual Property Organization (WIPO) (data source: [https://www.wipo.int/classifications/ipc/en/green\\_inventory/](https://www.wipo.int/classifications/ipc/en/green_inventory/), June 5, 2020).
- (5) We match the patent information of SIPO with that of WIPO by international patent classification number and finally obtain 6154 patents.
- (6) We check Google Patent and obtain 39839 patent citations of the 6154 patents (data source: <https://patents.google.com/patent/>, June 21, 2020).

- (7) Because [110], p.394, and [41], p.637, suggest considering patent-citation numbers in the previous years when they treat patent-citation numbers in this year, we accordingly measure green innovation of stock  $i$  in year  $t$  as follows:

$$G_{i,t} = \sum_{j=0}^5 \sum_{f_{t-j}=1}^{F_{t-j}} C_{i,n_{t-j}}, \quad (21)$$

where  $F_{t-j}$  is total number of patents granted to stock  $i$  in year  $t-j$  which are cited in year  $t$ ;  $f_{t-j}$  is a counter with  $f_{t-j} = 1 \dots F_{t-j}$ ; and  $C_{i,n_{t-j}}$  is the patent-citation number in year  $t$  by patent  $f_{t-j}$  which is granted to stock  $i$  in year  $t-j$ .

- (8) Because researchers (e.g., [42], pp.2249–2250) demonstrate that patent-citation numbers are typically large and skewed, we accordingly take the natural logarithm as follows:

$$G_{i,t} = \log \left( 1 + \sum_{j=0}^5 \sum_{f_{t-j}=1}^{F_{t-j}} C_{i,n_{t-j}} \right). \quad (22)$$

We will describe summary statistics in the next subsection.

We do try to update the component stocks' green innovations to year 2019, but basically all the major Internet search or communication engines (e.g., Google, Yahoo, YouTube, Facebook, Instagram, and Twitter) are unavailable in our location. Moreover, numerous websites are implicitly linked to the engines and thus unreachable. However, we try to sufficiently exploit the existing sample (from 2009 to 2018) by varyingly partitioning the sample period for the robustness tests. We will report the result in a later subsection.

It is promising that [31] maneuvers rough-set approaches and forecasts ESG ratios by corporate financial performance variables. We will try to duplicate their research methods for green innovation.

**4.3. Sampling Returns and Dividend Yields and Summary Statistics from 2009 to 2018.** For the 152 component stocks of China Securities Index 300, we sample the stocks' monthly returns, annual dividend yields, and annual market capitalizations from January 1, 2009, to December 31, 2018 (data source: China Stock Market & Accounting Research Database, <http://www.gtarsc.com>, July 6, 2021). For each component stock, we compute its time-series sample means of annual green innovations, monthly returns, and annual dividend yields. For the 152 component stocks, we document the summary statistics of the cross section sample means in Table 1. For example, for the sample means of green innovations in the second column, the standard deviation is 0.7772. Particularly, the 25th percentile and median are both 0, but the 75th percentile is 0.1637. Therefore, the sample means of green innovations are skewed. Many corporations barely participate in green innovations. We will

further dissect the issue and illuminate the number of participating stocks in a later subsection.

We separate January 1, 2009, to December 31, 2018, into the following subperiods:

- (1) From January 1, 2009, to December 31, 2013, as an in-sample subperiod, we sample the data, estimate  $\Sigma$  and  $\mu$  and  $\mu_3$  for (20), set up (20), compute  $\mathbf{z}_g$ , and calculate the thickest curve from  $\mathbf{z}_{d2}$  to  $\mathbf{z}_{d3}$  of Theorem 1.
- (2) From January 1, 2014, to December 31, 2018, as an out-of-sample subperiod, we select some portfolios on the thickest curve and test hypotheses (15)-(17).
- (3) Reference [111], pp.103–104&142–143&149–150, frequently explicates designs of 5-year in-sample subperiods and next-5-year out-of-sample subperiods. References [112], p.1680, and [113], p.439, accordingly implement the designs. Consequently, we similarly implement the designs. Moreover, we will unequally partition the sample period (January 1, 2009, to December 31, 2018) for robustness tests in a later subsection.

#### 4.4. Estimating $\Sigma$ , $\mu$ , $\mu_3$ , and $\mathbf{d}$ by the Data from 2009 to 2013.

In order to estimate portfolio-selection parameters, we follow [111], p.87, and compute the sample covariance matrix and sample mean vector of the 152 component stocks' monthly returns from January 1, 2009, to December 31, 2013. We next annualize the matrix and vector by following [3], pp.123&133. Because the sample covariance matrix is singular but invertible covariance matrices are required for this paper, we add 0.1 to the diagonal elements. We then assume the matrix and vector as  $\Sigma$  and  $\mu$ , respectively.

Similarly, we compute the sample mean vectors of the annual green innovations and annual dividend yields from 2009 to 2013 and then assume them as  $\mu_3$  and  $\mathbf{d}$ , respectively.

#### 4.5. Optimizing (20) and Dominating the Index by the Data from 2009 to 2013.

Among the 152 component stocks, we follow the screening strategies and drop the stocks whose green innovations from 2009 to 2018 are continually zero. Among the remaining component stocks, we follow [111], p.21, and calculate the market-capitalization-weighted index  $\mathbf{x}_g$ .

We substitute  $\mathbf{x}_g$  into (20) and obtain the green innovation index in  $(z_1, z_2, z_3)$  space as follows:

$$\mathbf{z}_g = \begin{bmatrix} z_{g1} \\ z_{g2} \\ z_{g3} \end{bmatrix} = \begin{bmatrix} (\mathbf{x}_g)^T \Sigma \mathbf{x}_g \\ (\mathbf{x}_g)^T \mu \\ (\mathbf{x}_g)^T \mu_3 \end{bmatrix} = \begin{bmatrix} 0.0456 \\ 0.0634 \\ 2.6962 \end{bmatrix}. \quad (23)$$

With  $z_{g1} = 0.0456$ , the plane passing through  $\mathbf{z}_g$  and being parallel to  $(z_2, z_3)$  subspace is as follows:

$$z_1 = 0.0456. \quad (24)$$



TABLE 1: Descriptive statistics.

	Green innovation	Return (in %)	Dividend yield (in %)
Mean	0.2887	0.2267	1.3393
Standard deviation	0.7772	0.1795	1.0861
25th percentile	0	0.0918	0.5577
Median	0	0.2179	1.081
75th percentile	0.1637	0.3418	1.7864
Minimum	0	-0.2024	0
Maximum	5.9491	0.716	5.1259

We compute the minimum-variance surface (8) as follows:

$$z_1 = 0.0394z_2^2 + 0.0014z_3^2 + 0.0006z_2z_3 - 0.0121z_2 - 0.0009z_3 + 0.0107. \quad (25)$$

The plane intersects the feasible region  $Z$  of (20). The intersection is depicted as shaded in Figure 7. By (24)–(25), we compute the boundary of the intersection as an ellipse as follows:

$$0.0456 = 0.0394z_2^2 + 0.0014z_3^2 + 0.0006z_2z_3 - 0.0121z_2 - 0.0009z_3 + 0.0107. \quad (26)$$

By solving (11) and (26), we locate  $\mathbf{z}_{i2}$  and  $\mathbf{z}_{i3}$  as follows:

$$\begin{aligned} \mathbf{z}_{i2} &= (0.0456, 1.1022, 0.6407). \\ \mathbf{z}_{i3} &= (0.0456, 0.1254, 5.2810). \end{aligned} \quad (27)$$

Although Figure 7 depicts  $(z_2, z_3)$  subspace, we still label points in  $(z_1, z_2, z_3)$  format (e.g.,  $\mathbf{z}_{i2} = (0.0456, 1.1022, 0.6407)$ ). The plane (24) intersects the efficient surface of (20) at a thicker curve from  $\mathbf{z}_{i2}$  to  $\mathbf{z}_{i3}$  in Figure 7. By comparing  $\mathbf{z}_g$  vs. both  $\mathbf{z}_{i2}$  and  $\mathbf{z}_{i3}$ , we know that Case 2 of the four cases of Theorem 1 happens. We accordingly compute  $\mathbf{z}_{d2}$  and  $\mathbf{z}_{d3}$  as follows:

$$\begin{aligned} \mathbf{z}_{d2} &= (0.0456, 0.9712, 2.6962), \\ \mathbf{z}_{d3} &= (0.0456, 0.1254, 5.2810). \end{aligned} \quad (28)$$

The thickest curve from  $\mathbf{z}_{d2}$  to  $\mathbf{z}_{d3}$  in Figure 7 dominates the green innovation index  $\mathbf{z}_g$  the most. We choose  $\mathbf{z}_{d4} \dots \mathbf{z}_{d7}$  which are evenly spaced on the curve. We label  $\mathbf{z}_{d2} \dots \mathbf{z}_{d7}$  in Figure 7, substitute them into (10), and obtain their portfolio-weight vectors  $\mathbf{x}_{d2} \dots \mathbf{x}_{d7}$ .

**4.6. Testing Hypotheses for the Out-of-Sample Dominance by the Data from 2014 to 2018.** By the historical returns and green innovations from 2014 to 2018 and  $\mathbf{x}_{d2} \dots \mathbf{x}_{d7}$  and  $\mathbf{x}_g$ , we compute the historical returns and green innovations of the portfolios  $\mathbf{z}_{d2} \dots \mathbf{z}_{d7}$  and  $\mathbf{z}_g$  from 2014 to 2018.

We then take  $\mathbf{z}_{d2}$  vs.  $\mathbf{z}_g$ ,  $\dots$ ,  $\mathbf{z}_{d7}$  vs.  $\mathbf{z}_g$  for hypotheses (15)–(17) and report the result in Table 2. The first row lists  $\mathbf{z}_{d2}$  vs.  $\mathbf{z}_g$ ,  $\dots$ ,  $\mathbf{z}_{d7}$  vs.  $\mathbf{z}_g$ . For hypothesis (15), the second to fourth rows list the test statistic (as described by [82], pp.497–499),  $p$ -value, and decision. For hypothesis (16), the 5th to 7th rows list the test statistic (as described by [82], pp.454–457),  $p$ -value, and decision. For hypothesis (17), the

8th to 10th rows list the test statistic (as described by [82], pp.454–457),  $p$ -value, and decision. The last row lists whether the dominance holds. We universally set the level of significance as 0.10. For example for  $\mathbf{z}_{d2}$  vs.  $\mathbf{z}_g$  in the second column, the statistic,  $p$ -value, and decision for (15) are 0.0562,  $p > 0.10$ , and “accept  $H_0$ ”. On the basis of accepting  $H_0$  of (15), accepting  $H_0$  of (16), and accepting  $H_0$  of (17), we conclude that the dominance does not hold (i.e., portfolio  $\mathbf{z}_{d2}$  does not dominate the green innovation index  $\mathbf{z}_g$ ). In the same format, portfolios  $\mathbf{z}_{d3} \dots \mathbf{z}_{d7}$  dominate the green innovation index  $\mathbf{z}_g$ .

**4.7. Detecting the Number of Stocks of the Dominating Portfolios  $\mathbf{z}_{d2}$  to  $\mathbf{z}_{d7}$ .** On the basis of (20) and  $n = 152$ , we further operationalize (10) as follows:

$$\mathbf{x} = \Sigma_{152 \times 152}^{-1} [\boldsymbol{\mu}_2 \ \boldsymbol{\mu}_3 \ \mathbf{1} \ \mathbf{d}]_{152 \times 4} \cdot \left( \begin{bmatrix} \boldsymbol{\mu}_2^T \\ \boldsymbol{\mu}_3^T \\ \mathbf{1}^T \\ \mathbf{d}^T \end{bmatrix} \Sigma^{-1} [\boldsymbol{\mu}_2 \ \boldsymbol{\mu}_3 \ \mathbf{1} \ \mathbf{d}] \right)_{4 \times 4}^{-1} \begin{bmatrix} z_2 \\ z_3 \\ 1 \\ \bar{d} \end{bmatrix}_{4 \times 1}. \quad (29)$$

We filter the nonzero elements of  $\mathbf{x}$  (29) and count the nonzero element number as a diversification measure. We notice that  $\mathbf{z}_{d2} \dots \mathbf{z}_{d7}$  and  $\mathbf{z}_{d8} \dots \mathbf{z}_{d11}$  all consist of 152 stocks (i.e., complete diversification).

We also filter the nonzero elements of  $\boldsymbol{\mu}_3$  due to its skewness (as reported in Table 1). We match the nonzero elements of  $\mathbf{x}$  and  $\boldsymbol{\mu}_3$ , count the number, and thus obtain the number of stocks which are engaged in green innovation. For example, we list the following  $\mathbf{x}$  and  $\boldsymbol{\mu}_3$  of  $n = 4$  for simplicity:

$$\begin{aligned} \mathbf{x} &= [0.1 \ 0 \ 0.3 \ 0.6]^T, \\ \boldsymbol{\mu}_3 &= [1.0 \ 2.0 \ 0 \ 4.0]^T. \end{aligned} \quad (30)$$

The number of engaged stocks is two.

For the sample with  $n = 152$ , the numbers of engaged stocks of  $\mathbf{z}_{d2} \dots \mathbf{z}_{d7}$  are all 45. For the next subsection, the numbers of engaged stocks of  $\mathbf{z}_{d8} \dots \mathbf{z}_{d11}$  are all 45 as well.

**4.8. Robustness Tests for  $\mathbf{z}_{d4}$  to  $\mathbf{z}_{d7}$ .** To check the robustness of the research methodology, we choose  $\mathbf{z}_{d8} \dots \mathbf{z}_{d11}$  instead of  $\mathbf{z}_{d4} \dots \mathbf{z}_{d7}$  on the curve from  $\mathbf{z}_{d2}$  to  $\mathbf{z}_{d3}$ . We express  $\mathbf{z}_{d8} \dots \mathbf{z}_{d11}$  in Table 3 (e.g.,  $\mathbf{z}_{d8} = (0.0456, 0.9048, 3.2131)$  in the second column).

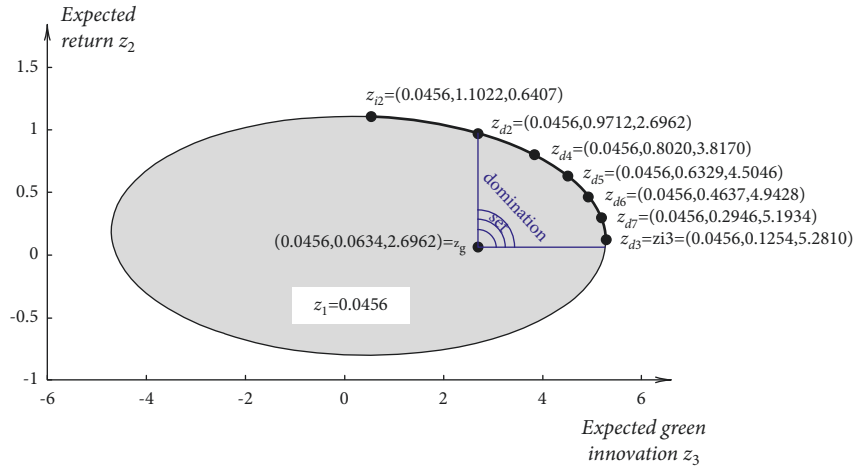


FIGURE 7: The green innovation index  $\mathbf{z}_g$  and dominating portfolios  $\mathbf{z}_{d2}$  to  $\mathbf{z}_{d7}$  on the intersection for the 152 component stocks of China Securities Index 300.

TABLE 2: Testing hypotheses (15)–(17) for  $\mathbf{z}_{d2}$  vs.  $\mathbf{z}_g$ , ...,  $\mathbf{z}_{d7}$  vs.  $\mathbf{z}_g$ .

	$\mathbf{z}_{d2}$ vs. $\mathbf{z}_g$	$\mathbf{z}_{d4}$ vs. $\mathbf{z}_g$	$\mathbf{z}_{d5}$ vs. $\mathbf{z}_g$	$\mathbf{z}_{d6}$ vs. $\mathbf{z}_g$	$\mathbf{z}_{d7}$ vs. $\mathbf{z}_g$	$\mathbf{z}_{d3}$ vs. $\mathbf{z}_g$
For (15), statistic	0.0562	0.0549	0.0470	0.0443	0.0470	0.0679
For (15), $p$ -value	$p > 0.10$	$p > 0.10$	$p > 0.10$	$p > 0.10$	$p > 0.10$	$p > 0.10$
For (15), decision	Accept $H_0$	Accept $H_0$	Accept $H_0$	Accept $H_0$	Accept $H_0$	Accept $H_0$
For (16), statistic	-0.1862	-0.0152	-0.0684	-0.1163	-0.1573	0.0425
For (16), $p$ -value	$p > 0.10$	$p > 0.10$	$p > 0.10$	$p > 0.10$	$p > 0.10$	$p > 0.10$
For (16), decision	Accept $H_0$	Accept $H_0$	Accept $H_0$	Accept $H_0$	Accept $H_0$	Accept $H_0$
For (17), statistic	3.9421	7.2135	6.8907	6.3193	5.4176	7.3204
For (17), $p$ -value	$p > 0.10$	$p < 0.10$	$p < 0.10$	$p < 0.10$	$p < 0.10$	$p < 0.10$
For (17), decision	Accept $H_0$	Reject $H_0$	Reject $H_0$	Reject $H_0$	Reject $H_0$	Reject $H_0$
Dominate?	No	Yes	Yes	Yes	Yes	Yes

TABLE 3: Choosing  $\mathbf{z}_{d8}$  ...  $\mathbf{z}_{d11}$  instead of  $\mathbf{z}_{d4}$  ...  $\mathbf{z}_{d7}$ .

	$\mathbf{z}_{d8}$	$\mathbf{z}_{d9}$	$\mathbf{z}_{d10}$	$\mathbf{z}_{d11}$
$z_1$	0.0456	0.0456	0.0456	0.0456
$z_2$	0.9048	0.8189	0.7052	0.5427
$z_3$	3.2131	3.7301	4.2470	4.7640

TABLE 4: Testing hypotheses (15)–(17) for  $\mathbf{z}_{d8}$  vs.  $\mathbf{z}_g$ , ...,  $\mathbf{z}_{d11}$  vs.  $\mathbf{z}_g$  for robustness tests.

	$\mathbf{z}_{d2}$ vs. $\mathbf{z}_g$	$\mathbf{z}_{d8}$ vs. $\mathbf{z}_g$	$\mathbf{z}_{d9}$ vs. $\mathbf{z}_g$	$\mathbf{z}_{d10}$ vs. $\mathbf{z}_g$	$\mathbf{z}_{d11}$ vs. $\mathbf{z}_g$	$\mathbf{z}_{d3}$ vs. $\mathbf{z}_g$
For (15), statistic	0.0562	0.0517	0.0476	0.0448	0.0451	0.0679
For (15), $p$ -value	$p > 0.10$	$p > 0.10$	$p > 0.10$	$p > 0.10$	$p > 0.10$	$p > 0.10$
For (15), decision	Accept $H_0$	Accept $H_0$	Accept $H_0$	Accept $H_0$	Accept $H_0$	Accept $H_0$
For (16), statistic	-0.1862	-0.1770	-0.1608	-0.1348	-0.0915	0.0425
For (16), $p$ -value	$p > 0.10$	$p > 0.10$	$p > 0.10$	$p > 0.10$	$p > 0.10$	$p > 0.10$
For (16), decision	Accept $H_0$	Accept $H_0$	Accept $H_0$	Accept $H_0$	Accept $H_0$	Accept $H_0$
For (17), statistic	3.9421	4.6233	5.3035	5.9821	6.6581	7.3204
For (17), $p$ -value	$p > 0.10$	$p < 0.10$	$p < 0.10$	$p < 0.10$	$p < 0.10$	$p < 0.10$
For (17), decision	Accept $H_0$	Reject $H_0$	Reject $H_0$	Reject $H_0$	Reject $H_0$	Reject $H_0$
Dominate?	No	Yes	Yes	Yes	Yes	Yes

We then take  $\mathbf{z}_{d8}$  vs.  $\mathbf{z}_g$ , ...,  $\mathbf{z}_{d11}$  vs.  $\mathbf{z}_g$  for hypotheses (15)–(17) and report the result in Table 4. Portfolios  $\mathbf{z}_{d3}$  and  $\mathbf{z}_{d8}$  ...  $\mathbf{z}_{d11}$  dominate the green innovation index  $\mathbf{z}_g$ . Overall, the results of Tables 2 and 4 are similar. The robustness of the research methodology can be verified.

As a comment, scholars typically obtain insignificant results in testing portfolios' returns against indexes' returns due to the volatile nature of stock returns. For example, [114], p.1936, [58], p.1181, [115], p.257, and [116], p.509, report similar insignificant results.

4.9. *Robustness Tests with Different Sample Partitions.* We also unequally partition the sample period (January 1, 2009, to December 31, 2018) as follows:

from January 1, 2009, to December 31, 2014, as an in-sample subperiod and from January 1, 2015, to December 31, 2018, as an out-of-sample subperiod;

from January 1, 2009, to December 31, 2015, as an in-sample subperiod and from January 1, 2016, to December 31, 2018, as an out-of-sample subperiod.

For both partitions, we obtain results similar to those reported in Tables 2–4. For all the equal and unequal partitions, we have deposited all the data, codes, and results in Mendeley Data <https://data.mendeley.com/>. Please see [104] in the references.

## 5. Further Formulating Green Innovation by General $k$ -Objective Portfolio Selection

In this section, we divide green innovation into categories, further formulate each category as an objective, construct general  $k$ -objective portfolio selection, and demonstrate the existence of portfolios which dominate green innovation indexes. The advantage of this further formulation is that investors can consider and control each category.

### 5.1. Dividing Green Innovation into Categories (Green Technology Innovation and Green Management Innovation) and Formulating

5.1.1. *Formulating the Categories by a 4-Objective Model.* Reference [117], p.463, divides green innovation into two categories: green technology innovation and green management innovation. Therefore, we follow the division and further formulate each category as an objective in the following model:

$$\begin{aligned} & \min\{z_1 = \mathbf{x}^T \boldsymbol{\Sigma} \mathbf{x}\}, \text{risk} \\ & \max\{z_2 = \mathbf{x}^T \boldsymbol{\mu}\}, \text{return} \\ & \max\{z_3 = \mathbf{x}^T \boldsymbol{\mu}_3\}, \text{green technology innovation} \\ & \max\{z_4 = \mathbf{x}^T \boldsymbol{\mu}_4\}, \text{green management innovation} \\ & \text{s.t. } \mathbf{A}^T \mathbf{x} = \mathbf{b}, \end{aligned} \quad (31)$$

where

$\boldsymbol{\mu}_3$  is a vector of stock expected green technology innovations,

$\boldsymbol{\mu}_4$  is a vector of stock expected green management innovations,

$z_3$  measures the portfolio expected green technology innovation,

$z_4$  measures the portfolio expected green management innovation.

5.1.2. *Still Dominating the Green Innovation Index by (31).* By the analytical result for (6), we can extend the computations of (13)–(17) and extend Theorem 1 for (31). To save space, the detailed computations are skipped; we just present the key computation and extend Figure 2 to Figure 8. In  $(z_1, \dots, z_4)$  space, we suppose the minimum-variance surface of (31) as follows:

$$\begin{aligned} z_1 = & p_1 z_2^2 + p_2 z_3^2 + p_3 z_4^2 + p_4 z_2 z_3 + p_5 z_2 z_4 + p_6 z_3 z_4 \\ & + p_7 z_2 + p_8 z_3 + p_9 z_4 + p_{10}, \end{aligned} \quad (32)$$

where  $p_1 \dots p_{10}$  are the coefficients. We draw a plane passing through  $\mathbf{z}_g$  and being parallel to  $(z_2, z_3, z_4)$  subspace. The plane is as follows:

$$z_1 = z_{g1}. \quad (33)$$

The plane intersects the feasible region  $Z$  of (31). Because every portfolio on the intersection shares the same  $z_1$  (i.e.,  $z_1 = z_{g1}$ ), we need to focus on just  $(z_2, z_3, z_4)$  elements of the intersection. The intersection is depicted in the lower left part of Figure 8. Because [22] proves the minimum-variance surface as a paraboloid and the surface is the boundary of the feasible region, the boundary of the intersection is an ellipsoid as follows:

$$\begin{aligned} z_{g1} = & p_1 z_2^2 + p_2 z_3^2 + p_3 z_4^2 + p_4 z_2 z_3 + p_5 z_2 z_4 + p_6 z_3 z_4 \\ & + p_7 z_2 + p_8 z_3 + p_9 z_4 + p_{10}. \end{aligned} \quad (34)$$

Moreover, we can select a portion of the ellipsoid, so every portfolio on the portion dominates the green innovation index. The portion is depicted in the lower right part of Figure 8.

5.2. *Further Dividing Green Innovation and Formulating.* World Intellectual Property Organization divides green innovation into seven categories (data source: [https://www.wipo.int/classifications/ipc/en/green\\_inventory/](https://www.wipo.int/classifications/ipc/en/green_inventory/), July 8, 2020). We formulate them in the following model:

$$\begin{aligned} & \min\{z_1 = \mathbf{x}^T \boldsymbol{\Sigma} \mathbf{x}\}, \text{risk} \\ & \max\{z_2 = \mathbf{x}^T \boldsymbol{\mu}\}, \text{return} \\ & \max\{z_3 = \mathbf{x}^T \boldsymbol{\mu}_3\}, \text{regulatory or design aspects} \\ & \max\{z_4 = \mathbf{x}^T \boldsymbol{\mu}_4\}, \text{agriculture or forestry} \\ & \max\{z_5 = \mathbf{x}^T \boldsymbol{\mu}_5\}, \text{alternative energy production} \\ & \max\{z_6 = \mathbf{x}^T \boldsymbol{\mu}_6\}, \text{energy conservation} \\ & \max\{z_7 = \mathbf{x}^T \boldsymbol{\mu}_7\}, \text{nuclear power generation} \\ & \max\{z_8 = \mathbf{x}^T \boldsymbol{\mu}_8\}, \text{transportation} \\ & \max\{z_9 = \mathbf{x}^T \boldsymbol{\mu}_9\}, \text{waste management} \\ & \text{s.t. } \mathbf{A}^T \mathbf{x} = \mathbf{b}, \end{aligned} \quad (35)$$

where

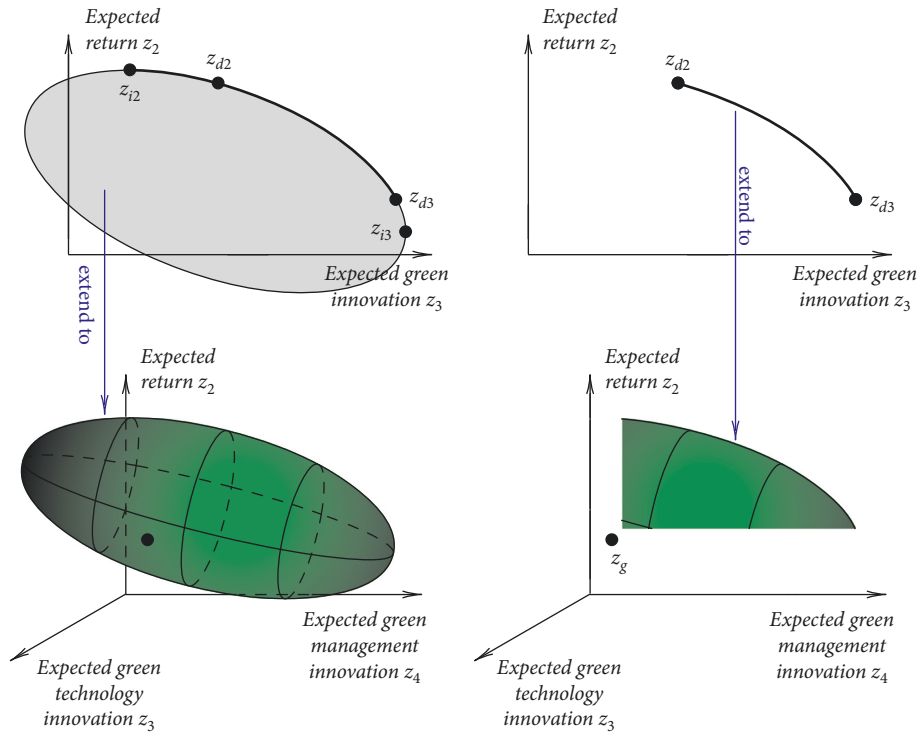


FIGURE 8: Extending (3) in the upper part to (31) in the lower part, the intersection between the plane and feasible region, and the ellipsoid's portion which dominates the index  $z_g$ .

$\mu_3 \dots \mu_9$  are vectors of stock expected categories,  
 $z_3 \dots z_9$  measure the portfolio expected categories.

Furthermore, researchers propose different divisions. Reference [1], p.318, divides green innovation into green product innovation and green process innovation. Reference [118], pp.1829–1830, extracts and classifies green patents on the basis of the division of World Intellectual Property Organization. Overall, we can follow the divisions, treat them as objectives, formulate them by multiple-objective portfolio selection, and compute the dominating portfolios by (6).

## 6. Conclusions

**6.1. Positive Methodology vs. Normative Methodology.** On the basis of (4), Nobel laureate [119], pp.433–434, assumes investor homogeneity and proposes his profound CAPM (capital asset pricing model). Although (4) and investor homogeneity are too simplistic and even unrealistic, [119], p.434, justifies his methodology by arguing for the CAPM's insights. References [119], p.425, and [120], p.99, call this methodology of simplistic assumptions but profound insights as positive methodology.

In contrast, [94, 95] propose a general portfolio-selection model (1) which incorporates kinds of practical constraints. They deploy parametric quadratic programming to solve (1). References [119], p.426, and [120], p.99, call this general-model methodology as normative methodology. It could be a pity that [9, 94] may totally concentrate on the model and optimization rather than contemplating simplistic but profound insights.

We principally pursue positive methodology by assuming simplistic constraints but trying to unveil dominating-portfolio strategies.

**6.2. Theoretical Implications.** Armed with multiple-objective portfolio selection for green innovation, investors can substantially enrich green innovation investments. Particularly, investors can upgrade security selection to portfolio selection, take green innovation as objectives, obtain the efficient surface, and select portfolios which dominate green innovation indexes.

In the sample,  $z_{d2} \dots z_{d7}$  and  $z_{d8} \dots z_{d11}$  all consist of 152 stocks, enjoy complete diversification, and contain 45 stocks which are engaged in green innovation. Investors can naturally increase sample size to check this status of being both efficient and diversified.

Reference [73], p.61, clarifies the consistency between portfolio selection and maximizing-expected-utility approaches. Consequently for (3), investors can naturally extend the traditional utility function and probe the extended utility function for green innovation.

**6.3. Practical Implications.** Instead of the traditionally passive screening-indexing tool, investors perceive a new instrument to actively construct portfolios for risk, return, and green innovation.

Because portfolio selection carries mixed results of out-of-sample performances, investors should not be too fascinated by the formulation (3) and should put (3) into more rigorous tests.

In the more rigorous tests, investors can install kinds of actual constraints (e.g., bounds of  $\mathbf{x}$ , industry restrictions, and transaction costs). For the optimization to charter the unknown territory depicted in Figures 4–6, investors can channel genetic algorithms and even fuzzy-number methods (as commenced by [101, 102]).

**6.4. Concluding Remarks.** Instigating green innovation as multiple objectives opens new opportunities for portfolio selection and green innovation investments. New areas which may not be previously contemplated are now brought to the theoretical and practical forefront.

## Data Availability

The authors have deposited all the data, codes, and results in Mendeley Data <https://doi.org/10.17632/rcwggcsxnh.1>. Please see [104] in the references.

## Conflicts of Interest

The authors declare that there are no conflicts of interest regarding the publication of this paper.

## Acknowledgments

Yue Qi thanks Professor Ralph Steuer in the Department of Finance at the University of Georgia, USA, for his constant support. Yue Qi also thanks Steve Lydenberg, cofounder of MSCI KLD 400 Social Index and cofounder and CEO of The Investment Integration Project <https://www.tiiproject.com>, for his inspiration. This research and publication are supported by the National Social Science Fund of China 2018 [Grant no. 18BGL063].

## References

- [1] J.-W. Huang and Y.-H. Li, “Green innovation and performance: the view of organizational capability and social reciprocity,” *Journal of Business Ethics*, vol. 145, no. 2, pp. 309–324, 2017.
- [2] M. Saunila, J. Ukko, and T. Rantala, “Sustainability as a driver of green innovation investment and exploitation,” *Journal of Cleaner Production*, vol. 179, no. 1, pp. 631–641, 2018.
- [3] Z. Bodie, A. Kane, and A. J. Marcus, *Investments*, McGraw-Hill Education, New York, New York, USA, 11th edition, 2018.
- [4] H. M. Markowitz, *Portfolio Selection: Efficient Diversification In Investments*, John Wiley & Sons, New York, New York, USA, 1st edition, 1959.
- [5] N. P. B. Bollen, “Mutual fund attributes and investor behavior,” *Journal of Financial and Quantitative Analysis*, vol. 42, no. 3, pp. 683–708, 2007.
- [6] C. Louche and S. Lydenberg, *Dilemmas in Responsible Investment*, Greenleaf Publishing Limited, Sheffield, UK, 2011.
- [7] M. Hood, J. Nofsinger, and A. Varma, “Conservation, discrimination, and salvation: investors’ social concerns in the stock market,” *Journal of Financial Services Research*, vol. 45, no. 1, pp. 5–37, 2014.
- [8] A. C. T. Borgers and R. A. J. Pownall, “Attitudes towards socially and environmentally responsible investment,” *Journal of Behavioral and Experimental Finance*, vol. 1, pp. 27–44, 2014.
- [9] H. M. Markowitz, “Portfolio selection,” *The Journal of Finance*, vol. 7, no. 1, pp. 77–91, 1952.
- [10] R. E. Steuer, *Multiple Criteria Optimization: Theory, Computation, and Application*, John Wiley & Sons, New York, New York, USA, 1986.
- [11] G. W. Evans, *Multiple Criteria Decision Analysis for Industrial Engineering: Methodology and Applications*, CRC Press, Boca Raton, Florida, USA, 2017.
- [12] H. M. Markowitz, “Foundations of portfolio theory,” *The Journal of Finance*, vol. 46, no. 2, pp. 469–477, 1991.
- [13] W. F. Sharpe, “Optimal portfolios without bounds on holdings,” *Graduate School of Business*, [https://web.stanford.edu/wfsharpe/mia/opt/mia\\_opt2.htm](https://web.stanford.edu/wfsharpe/mia/opt/mia_opt2.htm), 2001.
- [14] E. F. Fama, “Multifactor portfolio efficiency and multifactor asset pricing,” *Journal of Financial and Quantitative Analysis*, vol. 31, no. 4, pp. 441–465, 1996.
- [15] J. H. Cochrane, “Portfolio advice for a multifactor world,” *Economic Perspectives*, vol. 233, pp. 59–78, 3rd edition, 1999.
- [16] J. H. Cochrane, “Presidential address: discount rates,” *The Journal of Finance*, vol. 66, no. 4, pp. 1047–1108, 2011.
- [17] M. Statman, *Finance for Normal People: How Investors and Markets Behave*, Oxford University Press, New York, New York, USA, 2017.
- [18] R. E. Steuer, Y. Qi, and M. Hirschberger, “Suitable-portfolio investors, nondominated frontier sensitivity, and the effect of multiple objectives on standard portfolio selection,” *Annals of Operations Research*, vol. 152, no. 1, pp. 297–317, 2007.
- [19] G. Dorfleitner, M. Leidl, and J. Reeder, “Theory of social returns in portfolio choice with application to microfinance,” *Journal of Asset Management*, vol. 13, no. 6, pp. 384–400, 2012.
- [20] S. Utz, M. Wimmer, and R. E. Steuer, “Tri-criterion modeling for constructing more-sustainable mutual funds,” *European Journal of Operational Research*, vol. 246, no. 1, pp. 331–338, 2015.
- [21] Y. Qi, R. E. Steuer, and M. Wimmer, “An analytical derivation of the efficient surface in portfolio selection with three criteria,” *Annals of Operations Research*, vol. 251, no. 1–2, pp. 161–177, 2017.
- [22] Y. Qi and R. E. Steuer, “On the analytical derivation of efficient sets in quad-and-higher criterion portfolio selection,” *Annals of Operations Research*, vol. 293, no. 2, pp. 521–538, 2020.
- [23] B. Pascual, A. Fosfuri, L. Gelabert, and L. R. Gomez-Mejia, “Necessity as the mother of ‘green’ inventions: institutional pressures and environmental innovations,” *Strategic Management Journal*, vol. 34, no. 8, pp. 891–909, 2013.
- [24] L. He, S. Zeng, H. Ma, G. Qi, and V. W. Y. Tam, “Can political capital drive corporate green innovation? Lessons from China,” *Journal of Cleaner Production*, vol. 64, no. 2, pp. 63–72, 2014.
- [25] C. C. J. Cheng, “Sustainability orientation, green supplier involvement, and green innovation performance: evidence from diversifying green entrants,” *Journal of Business Ethics*, vol. 161, no. 2, pp. 1–22, 2020.
- [26] Y.-S. Chen, S.-B. Lai, and C.-T. Wen, “The influence of green innovation performance on corporate advantage in Taiwan,” *Journal of Business Ethics*, vol. 67, no. 4, pp. 331–339, 2006.

- [27] Y.-S. Chen, "The driver of green innovation and green image - green core competence," *Journal of Business Ethics*, vol. 81, no. 3, pp. 531–543, 2008.
- [28] G. Friede, T. Busch, and A. Bassen, "ESG and financial performance: aggregated evidence from more than 2000 empirical studies," *Journal of Sustainable Finance & Investment*, vol. 5, no. 4, pp. 210–233, 2015.
- [29] D. Daugaard, "Emerging new themes in environmental, social and governance investing: a systematic literature review," *Accounting and Finance*, vol. 60, no. 2, pp. 1501–1530, 2020.
- [30] M. F. Yen, Y. M. Shiu, and C. F. Wang, "Socially responsible investment returns and news: evidence from Asia," *Corporate Social Responsibility and Environmental Management*, vol. 26, no. 6, pp. 1565–1578, 2019.
- [31] F. García, J. González-Bueno, F. Guijarro, and J. Oliver, "Forecasting the environmental, social, and governance rating of firms by using corporate financial performance variables: a rough set approach," *Sustainability*, vol. 12, no. 8, pp. 1–18, Article ID 3324, 2020.
- [32] N. Semenova and L. G. Hassel, "On the validity of environmental performance metrics," *Journal of Business Ethics*, vol. 132, no. 2, pp. 249–258, 2015.
- [33] A. K. Chatterji, R. Durand, D. I. Levine, and S. Touboul, "Do ratings of firms converge? Implications for managers, investors and strategy researchers," *Strategic Management Journal*, vol. 37, no. 8, pp. 1597–1614, 2016.
- [34] C. Marquis, M. W. Toffel, and Y. Zhou, "Scrutiny, norms, and selective disclosure: a global study of greenwashing," *Organization Science*, vol. 27, no. 2, pp. 483–504, 2017.
- [35] B. Pascual, A. Fosfuri, and L. Gelabert, "Does greenwashing pay off? Understanding the relationship between environmental actions and environmental legitimacy," *Journal of Business Ethics*, vol. 144, no. 2, pp. 363–379, 2017.
- [36] C. Radu and C. Francoeur, "Does innovation drive environmental disclosure? A new insight into sustainable development," *Business Strategy and the Environment*, vol. 26, no. 7, pp. 893–911, 2017.
- [37] E. Pei-yi Yu, B. Van Luu, and C. H. Chen, "Greenwashing in environmental, social and governance disclosures," *Research in International Business and Finance*, vol. 52, no. April, pp. 1–23, Article ID 101192, 2020.
- [38] J. Yin, L. Gong, and S. Wang, "Large-scale assessment of global green innovation research trends from 1981 to 2016: a bibliometric study," *Journal of Cleaner Production*, vol. 197, no. 1, pp. 827–841, 2018.
- [39] S. Karimi Takalo, H. Sayyadi Tooranloo, and Z. Shahabaldini Parizi, "Green innovation: a systematic literature review," *Journal of Cleaner Production*, vol. 279, no. 1, pp. 1–22, Article ID 122474, 2021.
- [40] C.-H. Chang, "The influence of corporate environmental ethics on competitive advantage: the mediation role of green innovation," *Journal of Business Ethics*, vol. 104, no. 3, pp. 361–370, 2011.
- [41] D. Hirshleifer, P.-H. Hsu, and D. Li, "Innovative efficiency and stock returns," *Journal of Financial Economics*, vol. 107, no. 3, pp. 632–654, 2013.
- [42] Y. Chu, X. Tian, and W. Wang, "Corporate innovation along the supply chain," *Management Science*, vol. 65, no. 6, pp. 2445–2466, 2019.
- [43] L. H. Pedersen, S. Fitzgibbons, and L. Pomorski, "Responsible investing: the ESG-efficient frontier," *Journal of Financial Economics*, vol. 142, no. 2, pp. 572–597, 2021.
- [44] P. Bertrand and V. Lapointe, "How performance of risk-based strategies is modified by socially responsible investment universe?" *International Review of Financial Analysis*, vol. 38, no. 3, pp. 175–190, 2015.
- [45] B. R. Auer, "Do socially responsible investment policies add or destroy European stock portfolio value?" *Journal of Business Ethics*, vol. 135, no. 2, pp. 381–397, 2016.
- [46] P. Jan Trinks and B. Scholtens, "The opportunity cost of negative screening in socially responsible investing," *Journal of Business Ethics*, vol. 140, no. 2, pp. 193–208, 2017.
- [47] Z. Li, D. B. Minor, J. Wang, and Y. Chong, "A learning curve of the market: chasing alpha of socially responsible firms," *Journal of Economic Dynamics and Control*, vol. 109, pp. 1–17, Article ID 103772, 2019.
- [48] A. Singh, "COVID-19 and safer investment bets," *Finance Research Letters*, vol. 36, pp. 1–7, Article ID 101729, 2020.
- [49] V. Díaz, D. Ibrushi, and J. Zhao, "Reconsidering systematic factors during the COVID-19 pandemic-the rising importance of ESG," *Finance Research Letters*, vol. 38, pp. 1–6, Article ID 101870, 2021.
- [50] A. Amel-Zadeh and G. Serafeim, "Why and how investors use ESG information: evidence from a global survey," *Financial Analysts Journal*, vol. 74, no. 3, pp. 87–103, 2018.
- [51] L. Renneboog, J. Ter Horst, and J. Ter Horst, "Socially responsible investments: institutional aspects, performance, and investor behavior," *Journal of Banking & Finance*, vol. 32, no. 9, pp. 1723–1742, 2008.
- [52] F. Climent and P. Soriano, "Green and good? The investment performance of US environmental mutual funds," *Journal of Business Ethics*, vol. 103, no. 2, pp. 275–287, 2011.
- [53] Gunther Capelle-Blancard and S. Monjon, "The performance of socially responsible funds: does the screening process matter?" *European Financial Management*, vol. 20, no. 3, pp. 494–520, 2014.
- [54] F. Muñoz, M. Vargas, and I. Marco, "Environmental mutual funds: financial performance and managerial abilities," *Journal of Business Ethics*, vol. 124, no. 4, pp. 551–569, 2014.
- [55] S. Dolvin, J. Fulkerson, and A. Krukover, "Do "good guys" finish last? The relationship between Morningstar sustainability ratings and mutual fund performance," *Journal of Investing*, vol. 28, no. 2, pp. 77–91, 2019.
- [56] F. Ferriani and F. Natoli, "ESG risks in times of COVID-19," *Applied Economics Letters*, vol. 28, no. 18, pp. 1537–1541, 2021.
- [57] E. Ballester, M. Bravo, B. Pérez-Gladish, M. Arenas-Parra, and D. Plà-Santamaria, "Socially responsible investment: a multicriteria approach to portfolio selection combining ethical and financial objectives," *European Journal of Operational Research*, vol. 216, no. 2, pp. 487–494, 2012.
- [58] M. Stephan, S. M. Gasser, M. Rammerstorfer, and S. K. Weinmayer, "Markowitz revisited: social portfolio engineering," *European Journal of Operational Research*, vol. 258, no. 3, pp. 1181–1190, 2017.
- [59] R. H. Campbell, M. W. Liechty, and P. Müller, "Portfolio selection with higher moments," *Quantitative Finance*, vol. 10, no. 5, pp. 469–485, 2010.
- [60] F. J. Fabozzi, S. Focardi, and C. Jonas, "Trends in quantitative equity management: survey results," *Quantitative Finance*, vol. 7, no. 2, pp. 115–122, 2007.
- [61] D. Roman, K. Darby-Dowman, and G. Mitra, "Mean-risk models using two risk measures: a multi-objective approach," *Quantitative Finance*, vol. 7, no. 4, pp. 443–458, 2007.

- [62] P. Jorion, "Portfolio optimization with tracking-error constraints," *Financial Analysts Journal*, vol. 59, no. 5, pp. 70–82, 2003.
- [63] A. W. Lo, C. Petrov, and M. Wierzbicki, "It's 11pm – do you know where your liquidity is? The mean-variance-liquidity Frontier," *Journal of Investment Management*, vol. 1, no. 1, pp. 55–93, 2003.
- [64] J. B. Guerard and A. Mark, "The optimization of efficient portfolios: the case for an R&D quadratic term," *Research in Finance*, vol. 20, pp. 217–247, 2003.
- [65] J. Spronk and W. G. Hallerbach, "Financial modelling: where to go? With an illustration for portfolio management," *European Journal of Operational Research*, vol. 99, no. 1, pp. 113–127, 1997.
- [66] C. A. B. e Costa and J. O. Soares, "Multicriteria approaches for portfolio selection: an overview," *Review of Financial Markets*, vol. 4, no. 1, pp. 19–26, 2001.
- [67] R. E. Steuer and N. Paul, "Multiple criteria decision making combined with finance: a categorized bibliography," *European Journal of Operational Research*, vol. 150, no. 3, pp. 496–515, 2003.
- [68] C. Zopounidis, E. Galariotis, M. Doumpos, S. Sarri, and K. Andriospoulos, "Multiple criteria decision aiding for finance: an updated bibliographic survey," *European Journal of Operational Research*, vol. 247, no. 2, pp. 339–348, 2015.
- [69] M. Masmoudi and F. Ben Abdelaziz, "Portfolio selection problem: a review of deterministic and stochastic multiple objective programming models," *Annals of Operations Research*, vol. 267, no. 1-2, pp. 335–352, 2018.
- [70] B. Aouni, Michael Doumpos, B. Pérez-Gladish, and R. E. Steuer, "On the increasing importance of multiple criteria decision aid methods for portfolio selection," *Journal of the Operational Research Society*, vol. 69, no. 10, pp. 1525–1542, 2018.
- [71] F. W. Sharpe, *Portfolio Theory And Capital Markets*, McGraw-Hill, New York, New York, USA, 1st edition, 1970.
- [72] R. C. Merton, "An analytical derivation of the efficient portfolio Frontier," *Journal of Financial and Quantitative Analysis*, vol. 7, no. 4, pp. 1851–1872, 1972.
- [73] C.-F. Huang and R. H. Litzenberger, *Foundations for Financial Economics*, Prentice-Hall, Englewood Cliffs, New Jersey, USA, 1988.
- [74] I. Oikonomou, E. Platanakis, and C. Sutcliffe, "Socially responsible investment portfolios: does the optimization process matter?" *The British Accounting Review*, vol. 50, no. 4, pp. 379–401, 2018.
- [75] K. Liagkouras, K. Metaxiotis, and G. Tsihrintzis, "Incorporating environmental and social considerations into the portfolio optimization process," *Annals of Operations Research*, vol. 2021, 2021.
- [76] B. H. Taljaard and E. Maré, "Why has the equal weight portfolio underperformed and what can we do about it?" *Quantitative Finance*, vol. 21, no. 11, pp. 1855–1868, 2021.
- [77] T. K. Do, "Socially responsible investing portfolio: an almost stochastic dominance approach," *International Journal of Finance & Economics*, vol. 26, no. 1, pp. 1122–1132, 2021.
- [78] A. Riedl and Paul Smeets, "Why do investors hold socially responsible mutual funds?" *The Journal of Finance*, vol. 72, no. 6, pp. 2505–2550, 2017.
- [79] M. Rossi, D. Sansone, Arthur van Soest, and C. Torricelli, "Household preferences for socially responsible investments," *Journal of Banking & Finance*, vol. 105, no. 8, pp. 107–120, 2019.
- [80] Alexander Dyck, K. V. Lins, L. Roth, and H. F. Wagner, "Do institutional investors drive corporate social responsibility? International evidence," *Journal of Financial Economics*, vol. 131, no. 3, pp. 693–714, 2019.
- [81] A. L. Aiken, J. A. Ellis, and M. Kang, "Do politicians "put their money where their mouth is?" ideology and portfolio choice," *Management Science*, vol. 66, no. 1, pp. 376–396, 2019.
- [82] D. R. Anderson, D. J. Sweeney, T. A. Williams, J. D. Camm, and J. J. Cochran, *Statistics for Business and Economics*, Cengage Learning, Boston, Massachusetts, USA, 13th edition, 2018.
- [83] J. D. Jobson and R. M. Korkie, "Putting Markowitz theory to work," *Journal of Portfolio Management*, vol. 7, no. 4, pp. 70–74, 1981.
- [84] R. O. Michaud, "The Markowitz optimization enigma: is 'optimized' optimal?" *Financial Analysts Journal*, vol. 45, no. 1, pp. 31–42, 1989.
- [85] R. Jagannathan and T. Ma, "Risk reduction in large portfolios: why imposing the wrong constraints helps," *The Journal of Finance*, vol. 58, no. 4, pp. 1651–1684, 2003.
- [86] V. DeMiguel, L. Garlappi, F. J. Nogales, and U. Raman, "A generalized approach to portfolio optimization: improving performance by constraining portfolio norms," *Management Science*, vol. 55, no. 5, pp. 798–812, 2009.
- [87] M. Rubinstein, "Markowitz's "portfolio selection": a fifty-year retrospective," *The Journal of Finance*, vol. 57, no. 3, pp. 1041–1045, 2002.
- [88] R. W. Ross, R. W. Westerfield, J. Jaffe, and B. Jordan, *Corporate Finance*, McGraw-Hill Education, New York, New York, USA, 11th edition, 2016.
- [89] K. E. Back, *Asset Pricing And Portfolio Choice Theory*, Oxford University Press, New York, New York, USA, 2nd edition, 2017.
- [90] J. Y. Campbell, *Financial Decisions and Markets: A Course in Asset Pricing*, Princeton University Press, Princeton, New Jersey, USA, 1st edition, 2018.
- [91] R. A. Brealey, S. C. Myers, and F. Allen, *Principles of Corporate Finance*, McGraw-Hill Education, New York, New York, USA, 13th edition, 2020.
- [92] B. Bank, J. Guddat, D. Klatt, B. Kummer, and K. Tammer, *Non-Linear Parametric Optimization*, Birkhäuser Verlag, Basel, 1983.
- [93] E. N. Pistikopoulos, N. A. Dangelakis, and R. Oberdieck, *Multi-parametric Optimization and Control*, John Wiley & Sons, Hoboken, New Jersey, USA, 1st edition, 2021.
- [94] H. M. Markowitz, "The optimization of a quadratic function subject to linear constraints," *Naval Research Logistics Quarterly*, vol. 3, no. 1-2, pp. 111–133, 1956.
- [95] H. M. Markowitz and G. Peter Todd, *Mean-Variance Analysis in Portfolio Choice and Capital Markets*, Frank J. Fabozzi Associates, New Hope, Pennsylvania, USA, 2000.
- [96] M. Hirschberger, R. E. Steuer, S. Utz, M. Wimmer, and Y. Qi, "Computing the nondominated surface in tri-criterion portfolio selection," *Operations Research*, vol. 61, no. 1, pp. 169–183, 2013.
- [97] P. L. W. Jayasekara, N. Adelgren, and W. W. Wiecek, "On convex multiobjective programs with application to portfolio optimization," *Journal of Multi-Criteria Decision Analysis*, vol. 27, no. 3-4, pp. 189–202, 2019.
- [98] Y. Qi, M. Hirschberger, and R. E. Steuer, "Dotted representations of mean-variance efficient frontiers and their computation," *INFOR: Information Systems and Operational Research*, vol. 47, no. 1, pp. 15–22, 2009.

- [99] K. Deb, *Multi-Objective Optimization Using Evolutionary Algorithms*, John Wiley & Sons, New York, New York, USA, 2001.
- [100] M. Ehrgott, K. Klamroth, and C. Schwehm, "An MCDM approach to portfolio optimization," *European Journal of Operational Research*, vol. 155, no. 3, pp. 752–770, 2004.
- [101] F. García, J. González-Bueno, F. Guijarro, and J. Oliver, "A multiobjective credibilistic portfolio selection model. empirical study in the Latin American integrated market," *Entrepreneurship and Sustainability Issues*, vol. 8, no. 2, pp. 1027–1046, 2020.
- [102] F. García, J. González-Bueno, F. Guijarro, J. Oliver, and R. Tamošiūnienė, "Multiobjective approach to portfolio optimization in the light of the credibility theory," *Technological and Economic Development of Economy*, vol. 26, no. 6, pp. 1165–1186, 2020.
- [103] K. Metaxiotis and K. Liagkouras, "Multiobjective evolutionary algorithms for portfolio management: a comprehensive literature review," *Expert Systems with Applications*, vol. 39, no. 14, pp. 11685–11698, 2012.
- [104] Y. Qi, "Data for "constructing multiple-objective portfolio selection for green innovation and dominating green-innovation indexes"," *Mendeley Data*, 2020.
- [105] F. Allen, A. E. Bernardo, and I. Welch, "A theory of dividends based on tax clienteles," *The Journal of Finance*, vol. 55, no. 6, pp. 2499–2536, 2000.
- [106] M. Baker and J. Wurgler, "A catering theory of dividends," *The Journal of Finance*, vol. 59, no. 3, pp. 1125–1165, 2004.
- [107] S. Desmettre, S. Grün, and R. Korn, "Portfolio optimization with early announced discrete dividends," *Operations Research Letters*, vol. 46, no. 5, pp. 548–552, 2018.
- [108] H. Bilel and K. Mondher, "What can explain catering of dividend? environment information and investor sentiment," *Journal of Economics and Finance*, vol. 45, pp. 428–450, 2021.
- [109] B. Graham and D. L. Dodd, *Security Analysis*, McGraw-Hill, New York, New York, USA, 6th edition, 2009.
- [110] F. Gu, "Innovation, future earnings, and market efficiency," *Journal of Accounting, Auditing and Finance*, vol. 20, no. 4, pp. 385–418, 2005.
- [111] E. J. Elton, M. J. Gruber, S. J. Brown, and W. N. Goetzmann, *Modern Portfolio Theory and Investment Analysis*, John Wiley & Sons, New York, New York, USA, 9th edition, 2014.
- [112] Y. Qi, "Parametrically computing efficient frontiers of portfolio selection and reporting and utilizing the piecewise-segment structure," *Journal of the Operational Research Society*, vol. 71, no. 10, pp. 1675–1690, 2020.
- [113] Y. Qi, Y. Zhang, and S. Ma, "Parametrically computing efficient frontiers and reanalyzing efficiency-diversification discrepancies and naive diversification," *INFOR: Information Systems and Operational Research*, vol. 57, no. 3, pp. 430–453, 2019.
- [114] V. DeMiguel, L. Garlappi, and U. Raman, "Optimal versus naive diversification: how inefficient is the 1/N portfolio strategy?" *Review of Financial Studies*, vol. 22, no. 5, pp. 1915–1953, 2009.
- [115] P.-H. Hsu, Q. Han, W. Wu, and Z. Cao, "Asset allocation strategies, data snooping, and the 1/N rule," *Journal of Banking & Finance*, vol. 97, no. 12, pp. 257–269, 2018.
- [116] Y. Qi, "On outperforming social-screening-indexing by multiple-objective portfolio selection," *Annals of Operations Research*, vol. 267, no. 1-2, pp. 493–513, 2018.
- [117] D. Li, Y. Zhao, L. Zhang, X. Chen, and C. Cao, "Impact of quality management on green innovation," *Journal of Cleaner Production*, vol. 170, no. 2, pp. 462–470, 2018.
- [118] Grazia Cecere, N. Corrocher, C. Gossart, and M. Ozman, "Technological pervasiveness and variety of innovators in green ICT: a patent-based analysis," *Research Policy*, vol. 43, no. 10, pp. 1827–1839, 2014.
- [119] W. F. Sharpe, "Capital asset prices: a theory of market equilibrium," *The Journal of Finance*, vol. 19, no. 3, pp. 425–442, 1964.
- [120] H. M. Markowitz, "Normative portfolio analysis: past, present, and future," *Journal of Economics and Business*, vol. 42, pp. 99–103, 1990.



## Research Article

# The Impact of Internet Use on Corporate Tax Avoidance: Evidence from Chinese Enterprises

Gaoyi Lin <sup>1</sup>, Yanyan Zhao <sup>2</sup>, Wanmin Liu <sup>2</sup>, and Jianjun Zhou <sup>3</sup>

<sup>1</sup>School of Economics and Trade, Guangdong University of Foreign Studies, Guangdong 510006, China

<sup>2</sup>School of Public Finance and Taxation, Central University of Finance and Economics, Beijing 100081, China

<sup>3</sup>School of Economics, Central University of Finance and Economics, Beijing 100081, China

Correspondence should be addressed to Yanyan Zhao; 2019110018@email.cufe.edu.cn

Received 19 October 2021; Revised 24 April 2022; Accepted 26 April 2022; Published 17 May 2022

Academic Editor: M. M. El-Dessoky

Copyright © 2022 Gaoyi Lin et al. This is an open access article distributed under the Creative Commons Attribution License, which permits unrestricted use, distribution, and reproduction in any medium, provided the original work is properly cited.

Based on the data of Chinese industrial enterprises from 2004 to 2009, a fixed-effect model is adopted in this paper to analyze the effect and the mechanism of the enterprises using the Internet on tax avoidance. The result shows that using the Internet will produce the peer effect, which enables enterprises to learn tax avoidance strategies on the Internet and makes the degree of tax avoidance between enterprises and other enterprises in the same industry converge. At the same time, using the Internet has a network effect, and the more the enterprises access the Internet, the higher the degree of tax avoidance for enterprises is. In addition, the effect of the Internet on tax avoidance is influenced by the intensity of tax collection and the nature of enterprises. With a further examination, it has been found that enterprises not only acquire the two tax avoidance strategies of underreporting profits and underpaying taxes through the Internet but also master the planning strategy.

## 1. Introduction

By January 2021, the global Internet population had reached 4.66 billion, and the global Internet penetration rate had reached 59.5 percent, according to the Digital 2021 Global Overview Report. The actual number of Internet users is likely to be bigger as COVID-19 has had some impact on the report. As to the market capitalization of companies, Internet companies are rising rapidly. By December 31, 2018, the world's top 30 listed Internet companies had created a total of 3.5 trillion US dollars, as reported by the China Academy of Information and Communication Technology (CAICT) in 2019 in the China Internet Industry Development Trend and Boom Index Report. In terms of economy, the digital economy among 47 countries measured in 2020 had reached \$32.6 trillion, according to the CAICT's White Paper on the Global Digital Economy (2021), which accounts for 43.7% of GDP and has become an important part of economic development and reconstructed a new map of the global economy. The Internet is showing its great influence and potential for individuals, enterprises, and

society. Also, people are witnessing the subversive economic development and social transformation in the network era.

With the development of the Internet, more and more scholars focus on the impact of the Internet on taxation. Gnanon [1] proved that the increase in Internet use in developing countries has a higher positive impact on tax reform, compared with other countries. Based on information such as tax returns and census data, Lediga [2] studied whether Internet access in South Africa could help intervene in the administration of electronic tax filing services. The result shows that when the percentage of households with Internet access increases by 10%, the percentage of enterprises filing tax returns increases by 1.86%. Although the Internet plays a decisive role in promoting the modernization of tax administration and improving the efficiency of tax collection, it will also cause adverse effects such as aggravating the degree of tax avoidance by enterprises. For example, at the macro-level, by analyzing 152 countries' data from 1999 to 2007, Elgin [3] found that Internet penetration increases online transaction behavior, which makes it easier for enterprises and

households to evade taxes, thereby expanding the size of the shadow economy. At the micro-level, Goolsbee and Bruce et al. found that the online transaction behavior of the Internet makes it easier for consumers to avoid paying consumption tax [4, 5]. Argilés-Bosch et al. found that e-commerce has an impact on companies' labor tax avoidance [6]. Specifically, the French e-commerce business can use more favorable employment agreements to circumvent social insurance premiums.

Although some valuable results have been achieved, there are still deficiencies. Existing studies mainly regard the Internet as a means or a tool for tax avoidance. They believe that the Internet can facilitate tax evasion for existing income sources, or that the taxes on the income gained through the Internet are easy to evade [7]. People ignore the role of the Internet in the dissemination of information. As an online platform for instant communication, the Internet has broken the geographical limitations of traditional communication platforms, which makes it easier for enterprises and individuals to share and master effective tax avoidance strategies, thus influencing the tax avoidance behaviors of enterprises and individuals. An essay closely related to this study is about the influence of Internet forums on the tax avoidance behaviors of Uber drivers [8]. It finds that the forums were flooded with tax-related contents such as tax returns, income definitions, and expense deductions by analyzing interactions in three Internet forums. These contents affect the willingness and behaviors of drivers to comply with tax payments. In this study, we try to explore the impact of the Internet as a communication tool on corporate tax avoidance.

Compared with previous studies, here is the marginal contribution of this article. Firstly, existing literature on the Internet and tax avoidance mainly regards the Internet as a means or tool for tax avoidance and pays less attention to its role in information dissemination. This study regards the use of the Internet by enterprises as a way for enterprises to build social networks. We examine the impact of enterprises' use of the Internet as an information exchange tool on corporate tax avoidance from the perspective of social network connection. It enriches the empirical literature on the intersection of the Internet and the economy as well as deepens the understanding of the economic effects of the Internet. Secondly, compared with Oei and Ring, the authors conduct a deep analysis of the mechanism of the Internet on corporate tax avoidance. Based on that, it is found that the Internet has an impact on corporate tax avoidance through peer effect and network effect, which deepens the understanding of the knowledge transfer mechanism of the Internet. Thirdly, the authors also find that the Internet has taught companies not only tax avoidance strategies of underpaying taxes and underreporting profits but also planning strategies. This finding is of great significance for the government to promote the implementation of tax and fee reduction policies. It requires dialectical treatment and correct guidance for helping enterprises to use the Internet.

The main work of this paper is as follows: using the data from China Industrial Enterprise Database between 2004 and 2009, we measure enterprise Internet use in terms of

whether enterprises report their web address (Web) and e-mail address (e-mail). The result shows that enterprises acquire tax avoidance strategies after using the Internet, which significantly intensifies their tax avoidance behaviors. Through the mechanism analysis, this article finds that the Internet will produce a peer effect, that is, the degree of tax avoidance of enterprises using the Internet is affected by the degree of tax avoidance of other enterprises in the network. In addition, the Internet also produces a network effect. That means the more the enterprises use the Internet, the greater the impact it has on the degree of tax avoidance. Further research shows that the effect of the Internet on the degree of tax avoidance is influenced by the intensity of tax administration and the nature of enterprises.

The rest of this paper is arranged as follows. Section 2 presents the literature review and theoretical analysis. Section 3 gives the theoretical model. Section 4 presents the research design, including the measurement model and the description of the data indicators. Section 5 gives the empirical results and discussion. Section 6 presents further discussion, including other evidence of corporate tax avoidance, heterogeneity analysis, and the evidence of corporate mastery of tax planning strategies. Section 7 gives the conclusions and policy implications.

## 2. Literature Review and Theoretical Analysis

*2.1. The Impact of Social Networking on Tax Avoidance.* The tax avoidance of enterprises is affected by many factors, such as executive characteristics, corporate reputation, official language, corporate debt, and so on [9–13]. Among them, the social network connection is a factor that cannot be ignored. As is known to all, the tax avoidance strategy and experience are private and hidden topics. Enterprises will only share the tax avoidance strategies and experience in their specific social networks. As a result, enterprises can tap into new tax avoidance strategies and experience with the help of their social networks. Once companies learn that other companies in shared networks succeed in avoiding taxes through some tax avoidance strategies and experience, they are likely to copy and refer to that tax avoidance strategy for tax avoidance purposes [14]. Social networking among enterprises has been shown to influence various enterprise strategies, including the use of tax avoidance [15–17]. Among them, the directors' network connection is a variable that is relatively easy to see in the corporate social network connection [18]. Brown and Drake suggest that board ties can promote the sharing of corporate tax avoidance knowledge among firms [14]. Their results indicate that firms have lower effective tax rate when directors on their boards also serve on the boards of other companies with low tax rates. On top of that, previous studies have also looked at employees and families, audit firms, affiliates, government-enterprise relationships, and other types of social network contact on corporate tax avoidance behavior [19–26]. The use of the Internet represents one of the ways in which companies build social networks. With the rapid development of information technology, a large amount of information and data is transmitted on the Internet [27].

Enterprises can obtain the knowledge and strategy of production and operation on the Internet. Most importantly, enterprises will build Internet-based social networks that break down geographic barriers and allow new knowledge, strategies, and ideas to spread faster and more widely. They help enterprises obtain strategies and experience from each other through the Internet. Here is a hypothesis.

*Hypothesis 1.* Companies using the Internet can obtain more strategies and experience from the Internet to raise their tax avoidance.

*2.2. The Peer Effect of the Internet.* The peer effect means that when an enterprise faces a market choice, rather than making an optimal decision in face of a single market, the enterprise will be influenced by the surrounding enterprises of the same status, thus changing its own behaviors and results. For example, Gao et al. [28] concluded that firms in the same region exhibit similar financial decisions. Matray [29] studied the peer effect of technological innovation of firms and found that technological innovation of a single firm promotes technological innovation of geographically adjacent firms. This is mainly because enterprises in the same area are geographically close. Also, there are more opportunities to build social networks and valuable connections. Therefore, there will be more opportunities for communication to form the imitation of communicative learning. Different from the social network composed of traditional social relations, the social network constructed by enterprises through the Internet breaks the geographical barriers so that the communication between enterprises is no longer limited to the adjacent areas. This new type of social network connection enables enterprises to observe and imitate the behaviors of other enterprises when making production and operation decisions and can also provide a reference for other enterprises' decision making so that the tax avoidance strategies of enterprises in Internet organizations tend to be consistent. Therefore, the authors propose Hypothesis 2 based on the above analysis.

*Hypothesis 2.* The Internet has a peer effect, and the tax avoidance of enterprises using the Internet is affected by the tax avoidance of other enterprises using the Internet.

*2.3. The Network Effect of the Internet.* The network effect is that the utility that each user gets from using a product is positively related to the total number of users. The more users there are, the higher the utility each user gets, and the value of each person in the network is proportional to the number of others in the network. This means that the increase in the number of network users will lead to a geometric increase in the total utility of users. In telecommunication systems, for example, there is no value in personally installing phones when people do not use them. The more widespread the telephone is, the more valuable it is to install the telephone [30]. The network effect is common in fields such as e-commerce, transportation, and finance [31–33]. As an interactive and shared

platform, the Internet can help to bring together cross-regional and cross-domain enterprises, resources, and demands and realize multilateral interaction in a low-cost and efficient way. In this process, enterprises can not only learn tax avoidance strategies from other subjects through the Internet but also share and disseminate their own experience to achieve the integration and penetration of information. Therefore, the Internet has a network effect. The more enterprises that access the Internet and the richer the information exchanged on the Internet, the more likely it is for enterprises to obtain effective tax avoidance strategies, thereby increasing the space for tax avoidance. The following hypothesis is therefore made based on the above analysis.

*Hypothesis 3.* The Internet has a network effect. The more the enterprises are on the Internet, the more the tax avoidance of enterprises is after accessing the Internet.

Figure 1 shows the impact path of Internet use by enterprises to increase tax avoidance. The enterprises have peer effect and network effect when using the Internet, which enable enterprises to learn tax avoidance strategies and enhance tax avoidance degree.

### 3. Theoretical Model

This paper adds the factor of enterprises' use of the Internet to the traditional A-S tax evasion model and analyzes the impact mechanism of enterprises' use of the Internet on enterprises' tax evasion behavior. According to the theoretical analysis, the impact of using the Internet on enterprise tax avoidance can be divided into the peer effect and network effect. The peer group effect of the Internet is that the tax avoidance behavior of enterprises will be influenced not only by the incentive of their own interests but also by other enterprises in the same industry in the social network. Enterprises can form social network connections through the Internet so that they can have a larger platform to exchange their tax avoidance experience. Enterprises are not only acquiring experience but also sharing experience, that is, enterprises can communicate and learn tax avoidance (tax planning) means through the Internet. The network effect is that as more enterprises in the same industry access the Internet, the more the tax avoidance experience they share and the larger the knowledge base they build, thus rendering it easier for enterprises to achieve the goal of tax avoidance.

*3.1. Traditional A-S Model.* In the traditional A-S model,  $w$  is all the actual income that taxpayers earn in a certain period and  $w > 0$ .  $x$  is the taxable income actually declared by the taxpayer to the tax department and  $x \geq 0$ . Due to the information asymmetry between taxpayers and tax departments, taxpayers will deliberately understate to evade tax, which will widen the gap between  $w$  and  $x$ .  $\theta$  is the tax rate. In this model, it is assumed to be a fixed tax rate and  $\theta > 0$ .  $p$  is the probability that the taxpayer's tax evasion behavior is discovered by the tax authority.  $\pi$  refers to the proportion of

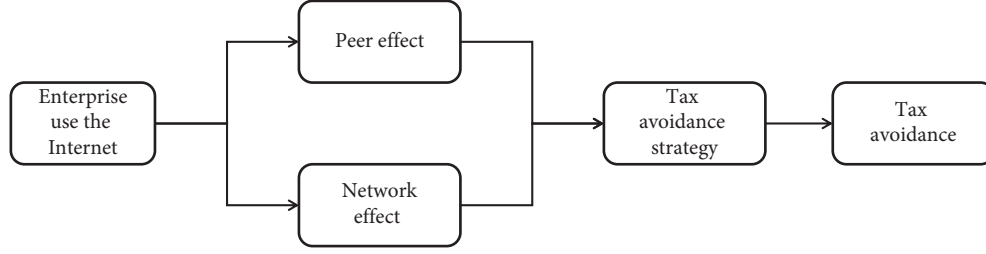


FIGURE 1: The impact path of Internet use by enterprises to increase tax avoidance.

the fines charged by the tax authorities to the undeclared income  $(w - x)$  after the taxpayer's tax evasion is found,  $\pi > 0$ .

$$EU = (1 - p)U(w - \theta x) + pU[w - \theta x - \pi(w - x)]. \quad (1)$$

**3.2. A-S Model of Enterprises Using the Internet.** On the basis of the traditional A-S model, we can add two assumptions to the original model to reflect the impact of corporate Internet use on tax avoidance. There are two main factors affecting enterprises' use of the Internet. One is  $p$ . Enterprises can learn more tax avoidance strategies through the Internet and make it more difficult for tax authorities to find tax avoidance. The other is  $x$ . Enterprises have better tax avoidance strategies so they can declare lower taxable income.

The influence factor of the Internet network effect on  $p$  is defined as  $a$  ( $0 < a < 1$ ). The influence factor on  $x$  is defined as  $b$  ( $0 < b < 1$ ). A new formula consisting of  $p$  and  $x$  is built as follows:

$$\begin{aligned} p &= f(a) = e^{-a}p, \\ p &= f(b) = e^{-b}p. \end{aligned} \quad (2)$$

The A-S model of enterprises using the Internet is

$$\begin{aligned} EU &= (1 - e^{-\alpha}p)U(w - \theta e^{-b}x) \\ &+ e^{-\alpha}pU[w - \theta e^{-b}x - \pi(w - e^{-b}x)]. \end{aligned} \quad (3)$$

In order to analyze conveniently, suppose  $Y = w - \theta e^{-b}x$ ,  $Z = w - \theta e^{-b}x - \pi(w - e^{-b}x)$ , and the simple expression of the model is

$$EU = (1 - e^{-\alpha}p)U(Y) + e^{-\alpha}pU(Z). \quad (4)$$

Taxpayer enterprises can achieve the purpose of tax evasion by limiting the amount of declared income so as to maximize their expected utility. Therefore, equation (5) needs to meet the conditions that the first derivative is equal to 0 and the second derivative is less than 0. This condition is proved below.

The first-order condition is

$$\begin{aligned} \frac{dE(U)}{dx} &= (e^{-\alpha}p - 1)\theta e^{-b}U'(Y) \\ &+ e^{-\alpha}p(\pi e^{-b} - \theta e^{-b})U'(Z) = 0. \end{aligned} \quad (5)$$

The second-order condition is

$$\begin{aligned} \frac{d^2E(U)}{dx^2} &= (1 - e^{-\alpha}p)\theta^2 e^{-2b}U''(Y) \\ &+ e^{-\alpha}p(\pi e^{-b} - \theta e^{-b})^2 U''(Z) < 0. \end{aligned} \quad (6)$$

When the second-order condition is permitted, there is a maximum value of the expected utility of the taxpayer enterprise. At this time,  $x$  can be obtained by means of the first-order condition, which corresponds to the maximum expected utility  $E(U)$ .

Taxpayers often prioritize lower risk tax avoidance strategies for risk aversion purpose. In information economics, the utility function of the risk averter is generally assumed to be concave. The utility increases with the increase of monetary return while the increase rate decreases. The second derivative of the utility function is smaller than zero.

The utility curve of the risk-averse subject meets  $U(\cdot) > 0$ ,  $U'(\cdot) > 0$ ,  $U''(\cdot) < 0$ . Given  $\alpha \geq 0$ ,  $b \geq 0$ ,  $0 < p < 1$ ,  $1 - e^{-\alpha}p > 0$ ,  $\theta^2 e^{-2b} > 0$ ,  $U''(Y) < 0$ ,  $e^{-\alpha}p > 0$ ,  $(\pi e^{-b} - \theta e^{-b})^2 > 0$ ,  $U''(Z) < 0$ , we can get  $d^2E(U)/dx^2 < 0$ , so the second-order condition is permitted. The maximum value can be obtained from equation (6). The taxpayer can maximize the utility by selecting the appropriate declaration amount  $x$ .

Then, we calculate the following equation:

$$\begin{aligned} \frac{\partial x}{\partial b} &= \frac{dE(U)/db}{dE(U)/dx} \\ &= \frac{(1 - e^{-\alpha}p)\theta x e^{-b}U'(Y) + e^{-\alpha}p(\theta - \pi)x e^{-b}U'(Z)}{(e^{-\alpha}p - 1)\theta e^{-b}U'(Y) + e^{-\alpha}p(\pi - \theta)e^{-b}U'(Z)}. \end{aligned} \quad (7)$$

By integrating  $1 - e^{-\alpha}p$  and  $\theta - \pi$  in the numerator and  $e^{-\alpha}p - 1$  and  $\pi - \theta$  in the denominator,  $\partial x/\partial b < 0$  can be obtained.

$$\frac{\partial p}{\partial a} = \frac{dE(U)/da}{dE(U)/dp} = \frac{e^{-\alpha}pU(Y) - e^{-\alpha}pU(Z)}{-e^{-\alpha}U(Y) + e^{-\alpha}U(Z)}. \quad (8)$$

By integrating the numerator and denominator,  $\partial p/\partial a = -p$  can be obtained. Since  $p \geq 0$ ,  $-p \leq 0$ , it can be seen that  $\partial p/\partial a < 0$ .

From the above analysis, it can be seen that the use of the Internet by enterprises will lead to the decline of  $x$  and  $p$ . The more the enterprises use the Internet, the less taxable income they declare, and the lower the probability that enterprises' tax avoidance behavior will be found by the tax authorities.

3.3. *Analysis of Model Results.* Allingham and Sandmo [34] proved that

$$\frac{\partial x}{\partial p} > 0, \frac{\partial x}{\partial \pi} > 0. \quad (9)$$

According to the previous proof,

$$\frac{\partial x}{\partial b} < 0, \frac{\partial p}{\partial a} < 0. \quad (10)$$

Combined with the two conclusions above,  $\partial x/\partial b < 0$ , if an enterprise uses the Internet, its declared taxable income  $x$  will decrease, and so will the actual tax amount of the enterprise.

In other words, if  $\partial p/\partial a < 0$ , when enterprises use the Internet, the probability  $p$  of corporate tax avoidance detected by tax authorities will decrease. From  $\partial x/\partial p > 0$ , it can be seen that the decline of  $p$  will also cause the decline of the taxable income  $x$ , that is, the decrease of  $P$  will increase the tax evasion behavior of enterprises. Through recursion, it can be obtained that the use of the Internet by enterprises will promote the tax evasion behavior of enterprises and reflect the peer effect of the Internet. The more the enterprises use the Internet, the more  $p$  and  $x$  decline and the more radical the tax avoidance behavior of enterprises is. This reflects the network effect of the Internet.

## 4. Data Description, Measurement Model, and Typical Facts

4.1. *Data Description.* This paper is written based on the Chinese industrial enterprise database. We use these data for three reasons. Firstly, to ensure that the research sample matches the research question: the existing Internet research studies mainly use the data of Chinese industrial enterprises or the data of Chinese listed enterprises. In comparison, the former sample is larger, and the latter data are updated. The Ministry of Industry and Information Technology of the PRC revealed at the 2021 China Internet Conference that the number of 5G connections in China has exceeded 365 million, accounting for 80% of the world. The number of netizens has increased to 989 million, and the Internet penetration rate has reached 70.4%. This means that most enterprises are already using the Internet. The main purpose of this study is to compare the differences in tax avoidance between using the Internet and not using the Internet. Thus, if we use the latest enterprise data, all we can find is that only a very small percentage of the sample does not use the Internet. This will affect the estimation conclusion. In addition, the research conclusions obtained from this data have important policy reference significance for countries and regions where the current Internet penetration rate remains low. Secondly, to ensure the applicability of the research findings: the data samples are from state-owned industrial enterprises and non-state-owned industrial enterprises above the designated size. The statistical caliber of “industry” here includes “mining industry,” “manufacturing industry,” and “production and supply industry of electric power, gas, and water” in the “industrial classification of the national

economy,” mainly the manufacturing industry (accounting for more than 90%). Manufacturing enterprises are considered the core of economic development in many countries and regions. The study of Internet use in China has even more important implications for other developing countries and regions. Thirdly, the limitation of data: the data of Chinese industrial enterprises are from 1998 to 2014. The database began counting enterprises with official web pages in 2004 and stopped counting them in 2010 and beyond. Because of this limitation, we can only use data from 2004 to 2009.

The “above scale” here requires the annual mean business income (i.e., sales) of the enterprise to be 5 million yuan or more. In fact, the industrial enterprise database is the most comprehensive database. The database includes two types of enterprise information: one is the basic information of the enterprise and the other refers to the financial data of the enterprise. The basic information of the enterprise includes legal person code, enterprise name, legal representative, contact telephone number, postal code, specific address, year of operation, number of employees, and other variables. The financial data of the enterprise include current assets, accounts receivable, long-term investment, fixed assets, accumulated depreciation, intangible assets, current liabilities, long-term liabilities, main business income, main business costs, operating expenses, management expenses, financial expenses, total profit and tax of operating profits, advertising expenses, research and development expenses, total wages, value-added tax, and other variables.

We filter them and eliminate the unqualified abnormal observations in the database, including the missing values of key variables such as total assets, opening time, total profit, sales revenue, number of employees, and paid-in capital; illogical observed values such as the accumulated depreciation that is less than the depreciation of the current year and the total assets that are less than current assets; the data with wrong records or abnormal indicators, such as the establishment time earlier than 1949, the number of employees smaller than 8, and the sales revenue less than 5 million yuan; and the observed value of the effective tax rate that is greater than 1 or smaller than 0. Based on the availability of enterprise Internet indicators, the sample interval is 2004–2009.

4.2. *Econometric Model.* This paper aims to study the impact of enterprises’ use of the Internet on their tax avoidance degree. A least square regression measurement model is built as follows:

$$\text{Rate1}_{it} = \alpha_0 + \alpha_1 \text{Web}_{it} + \sum_{j=2} \alpha_j X_{it} + V_i + V_t + \mu_{it}. \quad (11)$$

Among them,  $i$  and  $t$  represent the enterprise and the year, respectively, and  $\text{Rate1}_{it}$  represents the difference between the nominal tax rate and the effective tax rate of the enterprise and measures the tax avoidance degree of the enterprise.  $\text{Web}_{it}$  is used to identify whether the enterprise uses the Internet. When the Internet is used,  $\text{Web}_{it} = 1$ ; otherwise,  $\text{Web}_{it} = 0$ . Due to the certain cost of using the

Internet, the authors believe that once the enterprise reports the relevant information of the web page, it will continue to use it later, so it is set that there will be a long duration after using the Internet.  $X_{it}$  represents a series of control variables that affect the explained variables and core explanatory variables. Ignoring these control variables may lead to biased model estimation results. In addition,  $V_i$  is an enterprise's fixed effect, which is used to control factors that the enterprise does not change over time.  $V_t$  is a time-fixed effect, which is used to control the time trend.  $\mu_{it}$  represents the random error term.

### 4.3. Variable Setting

**4.3.1. Measurement of the Internet Use by Enterprises.** Referring to the existing research, e-mails (e-mail) or official web pages (Web) are usually used as the proxy variable for enterprises to use the Internet [35, 36]. In reality, web pages have a stronger role in communication and diffusion, and e-mail is more used for daily communication. Therefore, in this paper, the official web page is selected as the main index to identify whether enterprises use the Internet with e-mail and both as the verification methods.

The selection of proxy variables may bring about some doubts. First of all, enterprises may fill them in statistics rather than using web pages or e-mail, which may falsely increase the degree of Internet use, but the authors believe that enterprises have no reasonable motives to make any false reports. Based on the assumption of economic man, if an enterprise fails to fill in the information truthfully, it is simply to obtain the inflow of economic benefits such as subsidies or reduce the outflow of economic benefits such as taxes. However, there are neither preferential policies for the use of the Internet nor regulations on whether to use the Internet as a direct basis for fund collection. At the same time, the use of the Internet will not be directly linked to variables affecting tax, such as reducing income or increasing expenditure. Therefore, it is nearly impossible to misreport in this form. Even if it exists, it is a relatively random small probability event, which has little impact on the results. Admittedly, there are some enterprises whose Internet is idle, unused, or rarely used. Even if it is similar to the above situation, it also underestimates the role of the Internet, so this is a minimum value. In other words, it will underestimate the extent to which enterprises use the Internet. If we can still get the significant relationship between the research objects when the using Internet is systematically underestimated, we can consider our estimate as a lower limit, that is, using the Internet will at least have an effect on corporate tax avoidance. Finally, the proxy variable in this paper can only judge whether enterprises "own" rather than "actually use" the Internet. It is undeniable that there are some enterprises whose Internet is idle or rarely used, similar to the previous situation, which also underestimates the role of the Internet, so this paper obtains a minimum value. In conclusion, setting web pages or e-mail as proxy variables cannot accurately measure the degree of Internet use by enterprises, but the grasp of the trend is more accurate and is a more reliable data source available at present.

Information about enterprises using e-mail addresses or official websites is available through the Chinese industrial enterprise database. Since the database has counted the situation of enterprises having official web pages since 2004 and will not be counted in 2010 and beyond, the final period selected in this paper is 2004–2009. In the case of setting the binary dummy variable, if the enterprise has a web page, it will be assigned the value of 1; otherwise, it will be 0 (the statistics on the web only include the information filled in, including "www," "www," "com," "com," "CN," "CN," "HTTP," and "HTTP." The statistical results show that the processed web accounts for about 12.59% of the cases without space, and the processed e-mail accounts for about 15.76% of the cases without space). In addition, because there are certain costs for enterprises to use the Internet, in this paper, it is believed that once they fill in the relevant information about the web page in the data survey of industrial enterprises, it will have a long duration after the Internet is started by default.

**4.3.2. Measurement of Enterprise Tax Avoidance.** The existing literature mainly uses the effective tax rate (effective tax rate = income tax payable/total profit) to measure the degree of tax avoidance [37, 38]. In order to eliminate the influence of the nominal tax rate, we adjust the effective tax rate appropriately and use the difference between the nominal tax rate and the effective tax rate as a measure of the degree of corporate tax avoidance. The greater the difference between the nominal tax rate and the effective tax rate is, the higher the degree of tax avoidance will rise. In the robustness test, we change the measurement method of tax avoidance degree, including the effective tax rate, the difference between the average effective tax rate of the industry in the province where the enterprise belongs, and the book-tax difference (BTD).

**4.3.3. Setting of Control Variables.** Considering that many factors affect tax avoidance, we draw on existing literature and add several controls into the model [39–41]: (1) enterprise scale: measured by the natural logarithm of total enterprise assets; (2) enterprise age: measured by the natural logarithm of the difference between the surveyed year and the year of operation; (3) net profit margin of total assets: measured by the ratio of the difference between total profit and income tax payable to total assets; (4) enterprise management cost: expressed as the proportion of management expenses in the sales revenue of main business products; (5) growth rate of total liabilities: calculated by the ratio of the increase of total liabilities to the base period; (6) proportion of current assets in total assets; and (7) annual average number of employees of the enterprise. In addition, this paper also introduces the industry trend item and provincial trend item and controls the time-fixed effect and individual-fixed effect. Besides, the number of letters per capita in each province in the early days of the founding of new China is set as a tool variable in order to control the endogenous problem. The main variables and descriptive statistics used in this paper are shown in Tables 1 and 2.

TABLE 1: Variable measurement.

Variable type	Variable	Variable description
Internet usage indicators	Web	The use of official web pages represents the use of the Internet by enterprises
	E-mail	The use of e-mail represents the use of the Internet by enterprises
	Both	The use of official web pages or e-mail indicates that enterprises use the Internet
Enterprise tax burden	Rate 1	Difference between nominal tax rate and effective tax rate
	Rate 2	Difference between the average tax burden of the province and the effective tax rate of the enterprise
	Etr	Effective tax rate (income tax payable/total profit)
	Btd	Book-tax difference (total profit – taxable income)/total assets
Control variables	Lasset	Natural logarithm of enterprise scale
	Lage	Natural logarithm of enterprise age
	Roa	Net profit/total assets
	Cost	Management cost/total assets
	Lev	Growth rate of total liabilities
	Ratio	Current assets/total assets
	Labor	Annual average number of employees

TABLE 2: Descriptive statistics.

Variable	Mean	Sd	Min	Max
Web	0.126	0.332	0.000	1.000
E-mail	0.156	0.364	0.000	1.000
Both	0.183	0.386	0.000	1.000
Rate 1	0.117	0.161	-0.542	0.330
Rate 2	0.097	0.164	-0.642	0.330
Etr	0.183	0.159	0.000	0.792
Btd	0.044	0.108	-1.440	4.984
Lasset	9.782	1.367	7.313	13.971
Lage	1.894	0.773	0.000	3.871
Roa	0.119	0.174	0.000	0.902
Cost	0.051	0.053	0.001	0.305
Lev	0.061	0.068	0.000	0.365
Ratio	0.574	0.242	0.052	0.983
Labor	4.613	1.059	2.485	7.748

#### 4.4. Typical Facts

**4.4.1. Changes in Tax Burden Difference of Various Industries in the First Year When Enterprises Use the Internet.** In order to observe the change in tax burden before and after enterprises use the Internet, the authors distinguish different industries according to the classification standard of industry categories in the industrial enterprise database (GB/T 4754-2002) and calculate the average change of the difference between the nominal tax rate and the actual tax burden of enterprises in the industry in the early year of Internet compared with the previous year. The results are shown in Table 3. It can be seen that the tax burden difference of all industries in the year of using the Internet has increased compared with the previous year. Moreover, the tax burden difference of most industries exceeds 0.1, which indicates that there is likely to be a correlation between enterprises' use of the Internet and the actual tax burden.

**4.4.2. Comparison of Financial Indicators of Whether Enterprises Use the Internet or Not.** Table 4 shows the statistics of total asset net profit margin ((total profit-income tax payable)/total assets) and enterprise management cost (management expense/sales revenue of main products)

corresponding to whether the enterprise uses the Internet or not. From the analysis of the net profit margin of total assets, which reflects the profitability of enterprises, the ratio of enterprises using the Internet is lower than that of enterprises not using the Internet. The lower the index, the lower the asset utilization efficiency and the operation and management level of the enterprise, that is, the operation and management level of the enterprise using the Internet is relatively lower. From the analysis of enterprise management cost, Internet enterprises are significantly higher than enterprises that do not use the Internet. Based on the available literature, Abouzeedan et al. believe that the use of the Internet by enterprises is an innovation in organizational management, which can strengthen the ability to obtain resources required for operation, production, innovation, and other activities and enhance the ability to save relevant expenses [42, 43]. If the data reported by enterprises are accurate, the phenomenon of low management level and high management cost reflected in the statistical results is contrary to the positive effect described in the literature. Therefore, in this paper, a negative effect may exist in using the Internet and the reported data of enterprises may not be true, or it may be a result of tax avoidance. Thus, it is highly necessary to study the relationship and mechanism between Internet use and tax avoidance.

## 5. Results and Discussion

**5.1. Benchmark Model Regression.** The regression of the benchmark model is based on equation (1). OLS regression is based on the data from 2004 to 2009. The regression results are shown in Table 5. Both individual and time-fixed effects were added to the baseline regression. Column (1) in the table examines the relationship between the virtual variables characterizing the use of the Internet by enterprises and the degree of tax avoidance by enterprises without controlling other variables; in order to reduce the influence of missing factors varying with time at the enterprise level on the regression results, the time-varying control variables at the enterprise level are added in column (2) of the table; column (3) still adds industry and provincial trend items.

TABLE 3: Statistics of changes in the average tax burden of each industry in the first year of using the Internet.

Industry	Change in the industry average tax burden difference	Industry	Change in the industry average tax burden difference
Coal mining and washing industry	0.077	Cultural, educational, and sporting goods manufacturing industry	0.112
Oil and gas extraction industry	0.101	Petroleum processing, coking, and nuclear fuel processing industry	0.125
Ferrous metal mining and dressing industry	0.083	Chemical raw materials and chemical product manufacturing	0.122
Non-ferrous metal mining and dressing industry	0.122	Pharmaceutical manufacturing	0.146
Non-metallic ore mining and dressing industry	0.126	Chemical fiber manufacturing	0.150
Production and supply of electricity and heat	0.106	Rubber product industry	0.115
Gas production and supply industry	0.141	Plastic product industry	0.107
Water production and supply	0.092	Non-metallic mineral product industry	0.124
Agricultural and sideline food processing industry	0.161	Ferrous metal smelting and rolling processing industry	0.115
Food manufacturing	0.128	Non-ferrous metal smelting and rolling processing industry	0.131
Beverage manufacturing	0.136	Metal product industry	0.097
Tobacco product industry	0.048	General equipment manufacturing	0.094
Textile industry	0.110	Special equipment manufacturing	0.111
Textile and garment, shoe, and hat manufacturing	0.127	Transportation equipment manufacturing	0.112
Leather, Fur, feather, and its products industry	0.099	Electrical machinery and equipment manufacturing	0.106
Wood processing and wood, bamboo, rattan, palm, and grass products	0.137	Communication equipment, computers, and other electronic equipment manufacturing	0.164
Furniture manufacturing	0.116	Instrument, culture, and office machinery manufacturing	0.121
Papermaking and paper product industry	0.128	Arts and crafts and other manufacturing industries	0.110
Reproduction of printing and recording media	0.098	Waste resources and waste material recycling and processing industry	0.091

TABLE 4: Statistics of enterprise financial indicators from 2004 to 2009.

Year	Net profit margin of total assets		Enterprise management cost	
	Use the Internet (%)	Do not use the Internet (%)	Use the Internet (%)	Do not use the Internet (%)
2004	6.76	9.08	7.21	5.50
2005	6.97	10.49	6.83	5.02
2006	7.09	11.03	6.77	4.85
2007	7.69	12.56	6.71	4.75
2008	8.81	14.44	6.66	4.83
2009	8.83	14.89	6.80	4.68

The results show that in these three situations, the core explanatory variable of the study—enterprises using the Internet, i.e., having official web pages, has a significant positive impact on the degree of tax avoidance. Also, they can all pass the significance level test of 1%. Among them, the results of only controlling the individual and time-fixed effects show that the tax avoidance degree of enterprises using the Internet is about 0.06 higher than that of

TABLE 5: Benchmark regression.

Variable	(1) Rate 1	(2) Rate 1	(3) Rate 1
Web	0.006*** (0.001)	0.012*** (0.001)	0.012*** (0.001)
Constant	0.132*** (0.000)	-0.006 (0.005)	5.122*** (2.535)
Observations	1,417,428	1,065,563	1,065,563
R-squared	0.541	0.568	0.569
Control variable	NO	YES	YES
Industry trend	NO	NO	YES
Province trend	NO	NO	YES
Individual FE	YES	YES	YES
Time FE	YES	YES	YES

Note. \*, \*\*, and \*\*\* are significant at the levels of 10%, 5%, and 1%, respectively. The values in brackets are enterprise-level clustering standard errors.

enterprises not using the Internet. After controlling the variables at the enterprise level, the difference in tax avoidance does not change significantly and the coefficient



TABLE 6: Robustness test.

Variables	Replace the Internet identification method			Samples with effective tax rate greater than 1 will not be deleted	Change the measurement method of dependent variable			
	(1)	(2)	(3)		(4)	(5)	(6)	(7)
	Rate 1	Rate 1	Rate 1		Rate 1	Etr	Btd	Rate 2
E-mail	0.004*** (0.001)							
Both		0.007*** (0.001)						
P_web			0.003*** (0.001)					
Web				-0.012*** (0.001)	-0.012*** (0.001)	0.012*** (0.001)	0.008*** (0.001)	
Constant	5.045*** (2.535)	5.057*** (2.536)	5.060*** (2.534)	-5.953** (2.606)	-4.821* (2.535)	6.227 (1.066)	4.107* (2.159)	
Observations	1,065,563	1,065,563	1,065,563	1,066,722	1,065,563	1416,671	1,416,671	
R-squared	0.568	0.569	0.568	0.559	0.561	0.698	0.533	
Control variables	YES	YES	YES	YES	YES	YES	YES	
Industry trend	YES	YES	YES	YES	YES	YES	YES	
Province trend	YES	YES	YES	YES	YES	YES	YES	
Individual FE	YES	YES	YES	YES	YES	YES	YES	
Time FE	YES	YES	YES	YES	YES	YES	YES	

Note. \*\*\*, \*\*, and \* indicate the significance level of 1%, 5%, and 10%, respectively, and the *t* statistic value is in parentheses. The results of other control variables are not displayed in the table.

increases. The trendy items of industries and provinces are further added, and the coefficient reached 0.012. From the descriptive statistics in Table 2, it can be seen that the average tax avoidance of the sample is 0.17. On average, when enterprises use the Internet, their tax avoidance will increase by 10 percent. This shows that the use of the Internet by enterprises will indeed significantly aggravate the degree of tax avoidance and exaggerate the gap between nominal tax rate and effective tax rate, and this positive correlation is very significant in both statistical and economic sense. In conclusion, the results of the benchmark regression in this paper preliminarily show that after using the Internet, enterprises will significantly improve the degree of tax avoidance represented by the difference between the nominal tax rate and effective tax rate.

**5.2. Robustness Check.** Based on the previous verification that using the Internet will increase the degree of tax avoidance, an empirical test is made again by changing the measurement method of core variables in this part. Firstly, set the dummy variables e-mail and both to indicate that only the mailbox and both the mailbox together with the web page are used by the enterprise, respectively. The estimation results in columns (1) and (2) in Table 6 are significantly positive, which verifies the above hypothesis again. Secondly, the definition standard of whether an enterprise uses the Internet is changed. It is assumed that only the characteristic fields contained in the information reported in the current year are regarded as using the Internet, and it needs to be reidentified in subsequent years, thus generating variable P\_web. It can be seen from column (3) of Table 6 that the result is also significantly positive, which is consistent with the expectation. Column

(4) shows that the effective tax rate is not deleted when it is larger than 1. Thirdly, the measurement method of tax avoidance degree is changed in columns (5) to (7); the robust tests are performed with the actual tax burden of the enterprise, the profit difference of accounting tax, and the difference between the provincial average tax burden and the enterprise's effective tax rate, respectively. The results are still found stable. This supports the hypothesis that enterprises' use of the Internet will aggravate the degree of tax avoidance because enterprises can communicate with each other more easily and conveniently after using the Internet. There are more ways to learn, copy, disseminate, and improve tax avoidance methods and acquire new strategies and integrate new ideas in mutual communication.

### 5.3. Endogenous Test

**5.3.1. Instrumental Variable.** In this paper, instrumental variables are used to solve the endogenous problems caused by measurement errors and omitted variables. Based on the correlation and exogenous requirements of instrumental variables, the selected instrumental variables should be related only to whether the enterprise uses the Internet and have no direct correlation with other uncontrolled factors in the model, that is, the determined instrumental variables should affect the tax avoidance degree of the enterprise through whether the sample enterprise uses the Internet.

In this paper, the data of letters per capital in each province are selected as the instrumental variable in the early days of new China. Since this variable does not change with time and will be absorbed by the individual-

TABLE 7: Endogeneity test.

Variables	(1) First: Web	(2) Second: Rate 1	(3) Second: Rate 1
Letter_year	0.000** (0.000)		
Web		0.764* (0.433)	2.457*** (0.660)
Constant	-0.032 (0.066)		
Observations	964,238	964,238	585,073
Control variables	YES	YES	YES
Division of labor of enterprises	NO	NO	YES
Individual FE	YES	YES	YES
Time FE	YES	YES	YES

Note. \*\*\*, \*\*, and \* indicate the significance level of 1%, 5%, and 10%, respectively, and the  $t$  statistic value is in parentheses.

fixed effect, an instrumental variable that changes with time based on the interaction between letters per capital and year is built up in this paper. This is because letters are a common way of communication between different subjects in the early days of the founding of the People's Republic of China. The number of letters per capital can reflect people's demand and use of traditional communication methods, and the communication demand is relatively stable or growing steadily, which will affect the acceptance of enterprises for the emerging communication method of the Internet in the sample period. Generally speaking, the higher the demand for communication is, the more likely the current enterprise is to use new tools such as the Internet. At the same time, as a tool for communication in people's daily life, letters will not have a direct impact on the tax avoidance of enterprises. Therefore, in the early days of new China, the average data of the letters per person in each province can meet the two criteria of instrumental variables better, so the endogenous problem can be solved.

The result of these two-stage regression instrumental variables is shown in Table 7. Columns (1) and (2) confirm that the selected variables meet the correlation conditions. There is no problem with weak instrumental variables, and they play a significant role in improving the degree of tax avoidance, which confirms the robustness and reliability of the conclusion further in this paper. Notably, letter can promote the division of labor of enterprises, which means that letter will not only affect enterprises' tax avoidance by affecting their use of the Internet but also affect enterprises' tax avoidance by affecting the degree of division of labor. In order to eliminate the interference of this problem with the results, the division of labor of enterprises is controlled in column (3) of this paper, and the results are still robust.

**5.3.2. Placebo Test.** As mentioned above, we control variables by adding forms at the enterprise level, individual-fixed effect, and time-fixed effect to alleviate the impact of missing

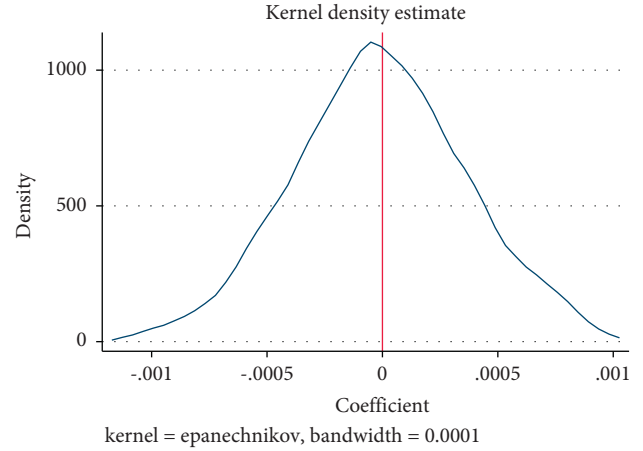


FIGURE 2: Distribution of  $\hat{\alpha}_1^{\text{random}}$  after randomization (placebo test).

variables. However, due to the limitations of data and other factors, there may still be some unobtainable factors, which lead to the deviation of the estimated results. Therefore, referring to the method of Ferrara et al. [44], we indirectly test whether the unobtainable factors will affect the estimation results. According to the benchmark equation (1), the expression of the coefficient  $\alpha_1$  of  $\text{Web}_{it}$  is shown in the following equation:

$$\hat{\alpha}_1 = \alpha_1 + \tau \frac{\text{cov}(\text{web}_{it}, \mu_{it} | \omega)}{\text{var}(\text{web}_{it} | \omega)}, \quad (12)$$

where  $\omega$  represents all control variables involved. If  $\tau = 0$ , the non-observational factors will not bias the estimation, that is,  $\hat{\alpha}_1$  is unbiased. However, the difficulty is that we cannot directly test whether  $\tau$  is zero.

On the premise of using a variable that will not actually affect the corresponding  $\text{Rate1}_{it}$  in theory (that is,  $\alpha_1 = 0$ ) to replace  $\text{Web}_{it}$ , if  $\hat{\alpha}_1 = 0$  is estimated, we can deduce  $\tau = 0$ .

Therefore, we make it completely random for each business to use the Internet and repeat the random process 500 times. This process ensures that  $\text{Rate1}_{it}$  will not be affected by whether a business uses the Internet or not. That is,  $\alpha_1^{\text{random}} = 0$ . In addition, we can estimate the mean value of  $\hat{\alpha}_1^{\text{random}}$ . Figure 2 shows the distribution of  $\hat{\alpha}_1^{\text{random}}$  obtained by 500 random processes, which are concentrated near zero. Therefore,  $\tau = 0$  can be deduced, which proves that the influence of the unobservable factors is well controlled in the study, and the estimation result is robust.

**5.4. Test Peer Effect of the Internet.** It has been proved that the Internet is an effective channel and carrier for communication between enterprises. It helps to improve the speed and breadth of information transmission, provides objective external conditions for enterprises to share tax avoidance strategies and experience to a certain extent, and affects enterprises' tax behavior.

In this paper, the peer effect of the Internet is tested in two methods. Firstly, examine whether the degree of tax

TABLE 8: Peer effect test.

Variables	Classified by medium category		Classified by small category	
	(1)	(2)	(3)	(4)
	Rate 1	Sdrate	Rate 1	Sdrate
Peer	0.720*** (0.021)		0.665*** (0.032)	
Indx		-0.025*** (0.009)		
Indz				-0.034*** (0.012)
Constant	-9.773 (6.967)	0.165*** (0.002)	-8.816 (6.996)	0.167*** (0.002)
Observations	163,224	2,825	163,224	1,078
R-squared	0.576	0.185	0.573	0.330
Control variables	YES	NO	YES	NO
Time trend	YES	NO	YES	NO
Province trend	YES	NO	YES	NO
Individual FE	YES	NO	YES	NO
Time FE	YES	YES	YES	YES

Note. \*\*\*, \*\*, and \* indicate the significance level of 1%, 5%, and 10%, respectively, and the  $t$  statistic value is in parentheses.

avoidance of Internet enterprises is affected by the degree of tax avoidance of other Internet enterprises in the same industry by referring to the practice of corporate cohort effect literature [45]. Therefore, the sample is limited to enterprises using the Internet, and the explanatory variable peer is constructed to represent the average tax avoidance degree of other enterprises using the Internet in the industry except for this enterprise. Then, the degree of corporate tax avoidance Rate 1 is used as the explanatory variable for regression. From the results of columns (1) and (3) in Table 8, it can be seen that the peer constructed based on the industry category or industry sub-category in the industrial enterprise database (GB/T 4754-2002) is significantly positive, which indicates that the tax avoidance degree of Internet enterprises is affected by the tax avoidance degree of other Internet enterprises in the industry, which proves the existence of the peer effect.

The second method is to test whether the standard deviation of the tax avoidance degree of the industry is reduced with the increase of Internet enterprises in the industry. Before using the Internet, limited by space and time barriers, enterprises cannot master more tax avoidance strategies while they can break the above barriers, enrich the tax avoidance experience of members in the group, and make the tax avoidance strategies in the group converge with the help of the peer effect. Some enterprises with a low degree of tax avoidance in the industry have greatly improved their degree of tax avoidance after using the Internet. However, for some enterprises with a high degree of tax avoidance, because they have mastered a certain degree of tax avoidance strategies, the use of the Internet has less impact on their degree of tax avoidance. This means that with the increase

of Internet companies in the industry, there will be less volatility in the extent of tax avoidance within the industry. Therefore, the regression analysis is carried out in the full sample with the standard deviation of the tax avoidance degree of the industry as the explained variable and the proportion of enterprises using the Internet in the industry (the total number of enterprises using the Internet in the industry/the total number of enterprises in the industry) as the explanatory variable for regression. From the results in columns (2) and (4) in Table 8, it can be seen that with the increase in the number of Internet enterprises in the industry, the standard deviation of the tax burden in the industry is narrowing, which once again proves that the peer effect exists in using the Internet.

*5.5. Test Network Effect of the Internet.* As a resource allocation platform, the Internet provides space for enterprises to query, communicate, and disseminate tax avoidance and planning strategies. The more the enterprises access the platform, the more extensive the information can be integrated. Also, enterprises can get a greater probability to learn about tax avoidance strategies to achieve the network effect. However, unlike the general production and operation strategies, tax avoidance methods are targeted. Different industries have specific business contents and scope of business activities. Strategies other than those in this industry may not bring practical effects to enterprises. Therefore, this part is only about the impact of changes in the number of enterprises using the Internet in their industry. Based on the industry category and industry sub-category, we calculate the proportion of Internet using enterprises in each industry every year (the total number of the Internet using enterprises in the industry/total number of enterprises in the industry). We use this ratio to measure the number of enterprises using the Internet and add the interaction term between this ratio and the Web into the benchmark model for regression.

As is shown in Table 9, Indz and Indx represent the proportion of enterprises using the Internet in the industry category and industry sub-category. Web represents whether enterprises use official web pages. The interaction terms are significantly positive, indicating that the more the enterprises in the industry that use the Internet, the higher the degree of tax avoidance after enterprises use the Internet. This confirms the existence of the Internet network effect. The positive externality of the network can provide a convenient way for enterprises to exchange experience in tax avoidance. The network effect will greatly reduce the information search cost and exchange cost of enterprises as well as promote the tax avoidance behaviors of enterprises. The results in Table 9 verify research Hypothesis 3.

The findings on peer and network effects complement research on the economic effects of the Internet. This reflects that the Internet is not just a tool or means of tax avoidance [4, 5] but also a new type of social networking connection

TABLE 9: Network effect test.

Variables	(1) Rate 1	(2) Rate 1
Web	0.008*** (0.002)	0.009*** (0.002)
Indx	0.071*** (0.010)	
Indx * Web	0.022* (0.012)	
Indz		0.094*** (0.013)
Indz * Web		0.022* (0.014)
Constant	5.062*** (2.535)	4.997*** (2.535)
Observations	1,065,563	1,065,563
R-squared	0.569	0.569
Control variables	YES	YES
Time trend	YES	YES
Province trend	YES	YES
Individual FE	YES	YES
Time FE	YES	YES

Note. \*\*\*, \*\*, and \* indicate the significance level of 1%, 5%, and 10%, respectively, and the  $t$  statistic value is in parentheses.

that allows enterprises to master and understand more advice on tax avoidance.

## 6. Further Discussion

**6.1. Further Evidence of Tax Avoidance.** In order to further verify that the use of the Internet will aggravate the tax avoidance degree of enterprises, the tax avoidance strategies of enterprises are discussed in this paper. In the current accounting tax system, the tax avoidance strategy of enterprises can be divided into two modes. The first is to underreport profits. According to document No. 101 issued by the State Administration of Taxation in 2008, the calculation of taxable profit needs to deduct operating costs and non-operating expenses from the enterprise's operating income so that the enterprise can achieve the purpose of underreporting profits by under recording operating income and overstating period expenses. The second is to pay fewer taxes. It is usually achieved by striving for non-taxable income and tax-free income and increasing various deduction items. The difference between the nominal tax rate and the effective tax rate has been used as the dependent variable, which proves that enterprises can learn the second tax avoidance mode by using the Internet, i.e., the strategy of paying fewer taxes. Can the use of the Internet provide the strategy of the first mode and make it possible for enterprises to avoid taxes?

Based on the treatment method of Cai and Liu [46], we use the income method of national income accounting to calculate the imputed profit of book income. Then, we use the approach degree of imputed profit and reported profit to reflect on whether the enterprise uses the first mode for tax avoidance.

$$\text{Impro}_{it} = Y_{it} - \text{MED}_{it} - \text{FC}_{it} - \text{WAGE}_{it} - \text{DEP}_{it} - \text{VAT}_{it}. \quad (13)$$

Among them,  $\text{Impro}_{it}$  is the imputed profit of the enterprise.  $Y_{it}$  is the total industrial output value.  $\text{MED}_{it}$  is the intermediate input, and  $\text{FC}_{it}$  is the financial expenses.  $\text{WAGE}_{it}$  represents the total wages.  $\text{DEP}_{it}$  is the depreciation of the current period, and  $\text{VAT}_{it}$  is the value-added tax. The imputed profit is not equal to the real profit, so it cannot be directly used as the proxy variable of the real profit, but in theory, the two are positively correlated.

$$\pi_{it} = \rho_{it} + \text{Impro}_{it} + \theta_{it}. \quad (14)$$

Among them,  $\pi_{it}$  is the tax profit of the enterprise.  $\rho_{it}$  is an unknown parameter, which reflects the inherent differences in profit calculation by using national income accounting and accounting standards for each enterprise, and  $\theta_{it}$  is the random disturbance term with an expected value of 0. When the reported profit of an enterprise is  $\text{Rpro}_{it}$ , the relationship between the reported profit and the real profit is

$$\text{Rpro}_{it} = d_{it}\pi_{it} + \delta_{it} + \theta_{it}, \quad (15)$$

where  $0 < d_{it} < 1$  represents the degree of tax avoidance of the enterprise. The smaller  $d_{it}$  is, the more the enterprise understates its profits and the more serious the enterprise's tax avoidance is; the closer  $d_{it}$  is to 1, the closer the reported profit is to the imputed profit and the smaller the degree of tax avoidance of the enterprise is. We substitute (12) and (13) into (14) to obtain the relationship between reported profit and imputed profit as follows:

$$\text{Rpro}_{it} = d_{it}\text{Impro}_{it} + d_{it}\rho_{it} + e_{it} + \theta_{it}, \quad (16)$$

where  $d_{it}$  reflects the degree of convergence between imputed profits and reported profits. Therefore, the more serious the tax avoidance, the lower the sensitivity between the imputed profit and the reported profit, and  $d_{it}$  is smaller. It is worth noting that all factors affecting tax avoidance are reflected in  $d_{it}$ , such as the time of establishment, the characteristics of the enterprise, the industry, and so on. Of course, the impact of enterprises' use of the Internet on enterprise tax avoidance is also included, so we expand based on equation (14) and use the following equation for regression:

$$\begin{aligned} \text{Rpro}_{it} = & \left( \beta_0 + \beta_1 \text{Web}_{it} + \sum_{j=2} \beta_j X_{it} \right) \text{Impro}_{it} \\ & + \sum_{j=2} \beta_j X_{it} + v_i + v_t + \mu_{it}. \end{aligned} \quad (17)$$

Among them,  $\text{Rpro}_{it}$  is the reported profit of the enterprise, which directly selects the total profit in the database, and it is also the taxable income that is declared by the enterprise to the tax authorities.  $\text{Impro}_{it}$  is the imputed profit of an enterprise.  $\text{Web}_{it}$  is the dummy variable of whether the enterprise uses the Internet, and  $\beta_1$  measures the impact of the enterprise's use of the Internet on the reported

TABLE 10: Evidence of enterprises' acquisition of tax avoidance strategies.

Variables	(1) Rpro	(2) Rpro	(3) Rpro	(4) Rpro
Impro * Web	-0.008*** (0.001)	-0.004*** (0.001)	-0.006*** (0.001)	-0.007*** (0.001)
Constant	-5.463*** (0.824)	-4.945*** (0.835)	-3.619*** (0.601)	-7.292*** (1.156)
Observations	633,244	457,068	751,344	382,252
R-squared	0.986	0.988	0.988	0.987
Control variables	YES	YES	YES	YES
Industry trend	YES	YES	YES	YES
Province trend	YES	YES	YES	YES
Individual FE	YES	YES	YES	YES
Time FE	YES	YES	YES	YES

Note. \*\*\*, \*\*, and \* indicate the significance level of 1%, 5%, and 10%, respectively, and the  $t$  statistic value is in parentheses.

profit. If the empirical results show that  $\beta_1$  is significantly less than 0, it indicates that after using the Internet, the gap between reported profits and imputed profits is widened, and the degree of tax avoidance is more serious.  $X_{it}$  is a control variable, including enterprise size, enterprise age, net profit margin of total assets, enterprise management cost, and asset-liability ratio.  $V_i$  and  $V_t$  represent individual and time-fixed effects, respectively. Since the intermediate input in 2008 and 2009 is not counted in the database, the time is limited between 2004 and 2007. The asset standardization treatment is carried out for the reported profit and the imputed profit, respectively, referring to the practice of Desai and Dharmapala [47].

The regression result is shown in Table 10. Column (1) shows that the total profit in the excluded sample is less than or equal to 0. Column (2) shows that the reported profit in the excluded sample is greater than the imputed profit. Columns (3) and (4), respectively, show that neither item is excluded and both items are excluded. The regression coefficients are significantly negative, which indicates that the reported profits of enterprises using the Internet have decreased significantly, that is, the total profit reported by enterprises cannot truly reflect the operating income and the enterprises may underreport profits. It shows that enterprises have acquired the tax avoidance strategy of underreporting profits and paying fewer taxes through the use of the Internet.

**6.2. Heterogeneity Analysis.** It is worth noting that since enterprises can learn tax avoidance strategies from the Internet and the tax authorities can also learn about the tax avoidance policies of enterprises, the Internet may not have an impact on the degree of tax avoidance of enterprises. However, certain studies have found that the collection and management intensity of tax authorities is affected by the economic motivation, collection, and management discretion of local governments, which may enable tax authorities to improve the collection and management level with the help of the Internet but did not improve the collection and management intensity.

In order to test this hypothesis, we refer to the method of Xu et al. [48], which constructs the index of regional tax collection and management intensity by using the ratio of actual tax revenue to expected available income and divides the sample into high collection and management intensity group and low collection and management intensity group according to the mean value of collection and management intensity. According to columns (1) and (2) of Table 11, it can be seen that there are differences in the impact of enterprises' use of the Internet on the degree of tax avoidance in regions with different collection and management intensities. In areas with low collection and management intensity, the Internet has a greater impact on the degree of tax avoidance.

In addition, the identification method of collection and management intensity is changed in this paper. China's tax system was divided into the State Taxation Bureau and the Local Taxation Bureau before 2002. The State Taxation Bureau was mainly responsible for collecting the income tax of central enterprises and foreign-funded enterprises. The income tax of other enterprises was collected and managed by the local taxation bureau. In the case of imperfect accounting systems and asymmetric information, local governments inevitably manipulate tax preference or abuse tax flexibility in the process of law enforcement due to the motivation of tax competition in order to attract capital inflows. In addition, the collection and management level of the sample period is relatively low, which is difficult for the State Administration of Taxation to check. This provides a large space for enterprises to avoid tax. In 2002, the income tax sharing reform required that the tax collection and management organization should be changed from the Local Taxation Bureau to the State Taxation Bureau, but it was difficult to connect the two systems back then. In order to maintain the independence of the Local Taxation Bureau and the State Taxation Bureau, the enterprises established before 2002 were collected and managed by the Local Taxation Bureau while the later enterprises were collected and managed by the State Taxation Bureau. Due to the policy, the enterprises founded at different times face different tax enforcements. The results in columns (3) and (4) show that the Web coefficients are significantly positive at the level of 1%, indicating that the tax avoidance degree of enterprises collected and managed by the Local Taxation Bureau and the State Taxation Bureau is improved because enterprises use the Internet. The coefficient difference between groups is significant, suggesting that compared with the collection and management of the State Taxation Bureau, the tax avoidance degree of enterprises collected and managed by the Local Tax Bureau is higher, which further indicates that the tax authorities may improve the collection and management level with the help of the Internet but do not enhance the collection and management intensity.

Lastly, based on the ownership nature of enterprises, a heterogeneity analysis is made in this paper. First of all, the ownership of corporate tax profits determines that private enterprises have stronger tax avoidance motivation, more radical tax avoidance concepts, and more flexible tax avoidance methods than state-owned enterprises [49, 50].

TABLE 11: Heterogeneity analysis.

Variables	(1) High degree Rate 1	(2) Low degree Rate 1	(3) Local taxation Rate 1	(4) State taxation Rate 1	(5) State owned Rate 1	(6) Non-state owned Rate 1
Web	0.010*** (0.002)	0.012*** (0.002)	0.011*** (0.001)	0.010*** (0.003)	-0.002 (0.006)	0.013*** (0.001)
Constant	-3.777 (5.583)	9.968*** (3.829)	4.398 (2.957)	9.081*** (4.766)	-9.459 (8.040)	7.360*** (2.669)
Observations	374,599	444,347	747,377	318,186	56,617	1,004,487
R-squared	0.599	0.597	0.555	0.603	0.592	0.570
Control variables	YES	YES	YES	YES	YES	YES
Industry trend	YES	YES	YES	YES	YES	YES
Province trend	YES	YES	YES	YES	YES	YES
Individual FE	YES	YES	YES	YES	YES	YES
Time FE	YES	YES	YES	YES	YES	YES
Dif (P value)	-0.007***		0.004*		0.012***	

Note. \*\*\*, \*\*, and \* indicate the significance level of 1%, 5%, and 10%, respectively, and the *t* statistic value is in parentheses.

Next, the amount of tax generated by the management of state-owned enterprises may play a positive role in promoting their promotion, which will encourage the management of state-owned enterprises to pay more taxes to the Chinese government. For example, Minh et al. [51] suggest that firms with high state ownership often have little or no tax avoidance but still have a negative impact on firm value. According to the results in columns (5) and (6), the use of the Internet significantly improves the tax avoidance degree of non-state-owned holding enterprises but has no significant impact on the tax avoidance degree of state-owned holding enterprises.

**6.3. Can Enterprises Acquire Planning Strategies by Using the Internet?** Generally speaking, on the premise of stable policy factors, the reduction of enterprise tax burden may be caused by tax avoidance or tax planning. Based on the verification that enterprises have tax avoidance strategies such as underreporting profits and underpaying taxes, whether enterprises can acquire planning strategies while acquiring tax avoidance strategies after using the Internet will be further explored in this part.

Compared with income tax, the value-added tax (VAT) voucher deduction mechanism makes its tax avoidance cost and illegal cost higher. In order to avoid risks, enterprises usually rely on tax planning rather than using radical tax avoidance means to reduce the value-added tax burden. Therefore, if the value-added tax burden of enterprises decreases significantly after using the Internet, it is likely to be due to the acquisition of planning strategies. Therefore, in this paper, the benchmark regression model is adopted to replace the explanatory variable with the value-added tax burden (value-added tax payable/sales revenue of main business products) to observe whether enterprises can learn planning strategies through the Internet.

The results in Table 12 show that the Web coefficients are significantly negative at the 1% level, indicating that the value-added tax burden has decreased significantly after enterprises use the Internet, which proves the above

TABLE 12: Evidence of acquisition planning strategies.

Variables	(1) VAT	(2) VAT	(3) VAT
Web	-0.001*** (0.000)	-0.001*** (0.000)	-0.001*** (0.000)
Constant	0.034*** (0.000)	0.013*** (0.001)	0.133 (0.446)
Observations	1,417,428	1,065,563	1,065,563
R-squared	0.676	0.700	0.700
Control variables	NO	YES	YES
Industry trend	NO	NO	YES
Provincial trend	NO	NO	YES
Individual FE	YES	YES	YES
Time FE	YES	YES	YES

Note. \*\*\*, \*\*, and \* indicate the significance level of 1%, 5%, and 10%, respectively, and the *t* statistic value is in parentheses.

conjecture. That is, using the Internet can not only enable enterprises to learn tax avoidance strategies but also enable enterprises to contact the idea of planning and apply it so as to achieve the effect of tax reduction.

## 7. Conclusions and Suggestions

With the development of information technology, Internet has been used in an ever-expanding range and has gradually penetrated the operation and management of enterprises in various fields, reducing the cost of information exchange as well as improving the efficiency of resource dissemination. It has a far-reaching influence on the production and operation of enterprises. Based on the micro-data of Chinese industrial enterprises from 2004 to 2009, the authors explore the impact of enterprises' use of the Internet on tax avoidance from the perspective of social networks. In conclusion, the use of the Internet by enterprises significantly increases the degree of tax avoidance, and the core conclusion is still very robust when the key variables are changed and endogenous issues are taken into account.

The enterprises have a peer effect when using the Internet. The degree of tax avoidance of enterprises is affected by the degree of tax avoidance of other enterprises using the Internet in the industry. The Internet has a network effect. The more the enterprises in the industry use the Internet, the higher the degree of tax avoidance is after enterprises use the Internet. A further test shows that enterprises can learn the strategies of underreporting profits and underpaying taxes at the same time. In addition, it proves that the tax authorities have improved the level of tax collection and management through the Internet but not the intensity of tax collection and management. The heterogeneity analysis shows that the use of the Internet significantly improves the tax avoidance degree of private enterprises but has no significant impact on the tax avoidance degree of state-owned enterprises. Finally, it is found that the enterprises' VAT burden has been significantly reduced, which proves that enterprises have acquired both tax avoidance strategies and planning strategies after using the Internet. The discovery of this paper is a supplement to the research on the Internet's economic effect. It shows that the Internet is not only a tool or means of tax avoidance [4, 5] but also a new type of social network connection. Oei and Ring [8] conducted research from the social network perspective of the Internet based on personal data. They found that personal use of the Internet has an effect on personal tax avoidance. Our research is based on enterprise data. Both studies prove that as a new social tool, the social network connection built by the Internet will have an impact on the tax avoidance of micro-individuals. More importantly, with a deep analysis of the mechanism of the Internet on corporate tax avoidance, the authors find that the Internet has an impact on corporate tax avoidance through the peer effect and network effect. It deepens the understanding of the knowledge transfer mechanism of the Internet.

The findings of this study have certain policy references for countries and regions that have popularized the Internet, are popularizing the Internet, and will popularize the Internet. Firstly, to encourage and guide enterprises to make rational use of the Internet: for countries with high Internet penetration rates such as China, the "Internet plus" strategy has laid a huge user base and brought about profound changes in enterprise information interaction and operation management. The Internet has built a new type of social network connection for enterprises, enabling enterprises to have more channels to master more preferential tax information, obtain tax planning experience, and optimize tax burden according to their own conditions. Clearly, the Internet is an effective vehicle for the "last mile" of tax reduction and fee reduction. However, at the same time, enterprises should be guided to use the Internet reasonably to avoid tax risks and industrial chaos caused by radical tax avoidance. Secondly, to strengthen tax collection and administration: the use of the Internet has given a certain impetus to the information technology level of both the tax collector and the payer. Enterprises can learn from the Internet not only about tax subsidies but also about tax avoidance. In fact, tax avoidance is to make use of loopholes in the law to achieve the goal of tax evasion, which distorts

the intention of tax policy and damages the fairness and effectiveness of the market. On the one hand, the tax authorities should rely on big data to strengthen precise supervision and tax audit capabilities. On the other hand, the tax authorities should determine the optimal intensity of tax collection and management according to the policy objectives, the tax cost, and other factors to maintain tax fairness and efficiency. The third phase of the Golden Tax project completed by the Chinese government and the fourth phase of the Golden Tax project under construction are examples of the comprehensive use of the Internet and big data for tax collection and administration. Thirdly, to step up publicity and set up reward and punishment mechanisms to enhance enterprises' sense of social responsibility: in particular, it is necessary to strengthen the publicity and guidance of private enterprises to achieve positive interaction between taxation and enterprises. The government should create an excellent Internet cultural environment, guide enterprises to fully exploit and utilize the advantages of the Internet, and give full play to the positive role of the Internet.

### Data Availability

The data used to support the findings of this study are available from the first and corresponding authors upon request.

### Conflicts of Interest

The authors declare that they have no conflicts of interest.

### Acknowledgments

This research was funded by the Research Project of Guangdong University of Foreign Studies (grant no. 2022RC040).

### References

- [1] S. K. Gnanon, "Internet and tax reform in developing countries," *Information Economics and Policy*, vol. 51, Article ID 100850, 2020.
- [2] C. Lediga, *The Impact of Internet Penetration on Corporate Income Tax Filing in South Africa*, Ruhr Economic Papers, Bochum, Germany, 2020.
- [3] C. Elgin, "Internet usage and the shadow economy: evidence from panel data," *Economic Systems*, vol. 37, no. 1, pp. 111–121, 2013.
- [4] A. Goolsbee, "In a world without borders: the impact of taxes on internet commerce," *Quarterly Journal of Economics*, vol. 115, no. 2, pp. 561–576, 2000.
- [5] D. Bruce, W. Fox, and M. Murray, "To tax or not to tax? The case of electronic commerce," *Contemporary Economic Policy*, vol. 21, no. 1, pp. 25–40, 2003.
- [6] D. Aguilar, A. Agüero, and R. Barrantes, "Network effects in mobile telecommunications markets: a comparative analysis of consumers' preferences in five Latin American countries," *Telecommunications Policy*, vol. 44, no. 5, Article ID 101972, 2020.
- [7] M. J. Bridges and P. Green, "Tax evasion and the internet," *Journal of Money Laundering Control*, vol. 2, no. 2, pp. 105–114, 1998.

- [8] S. Y. Oei and D. M. Ring, "The tax lives of uber drivers: evidence from internet discussion forums," *Columbia Journal of Transnational Law*, vol. 8, no. 2, pp. 56–112, 2017.
- [9] O. J. Ilaboya and E. Aronmwan, "Overconfident CEOs and corporate tax avoidance," *Journal of Accounting and Management*, vol. 11, no. 2, pp. 70–80, 2021.
- [10] L. Gao, "Accountant CFOs and corporate tax avoidance," *Journal of Corporate Accounting & Finance*, vol. 33, no. 1, pp. 164–184, 2022.
- [11] J. R. Graham, M. Hanlon, and T. Shevlin, "Incentives for tax planning and avoidance: evidence from the field," *The Accounting Review*, vol. 89, no. 3, pp. 991–1023, 2014.
- [12] K. Na and W. Yan, "Languages and corporate tax avoidance," *Review of Accounting Studies*, vol. 27, pp. 148–184, 2022.
- [13] M. Salehi and S. Salami, "Corporate tax aggression and debt in Iran," *Journal of Islamic Accounting and Business Research*, vol. 11, no. 1, pp. 257–271, 2020.
- [14] J. L. Brown and K. D. Drake, "Network ties among low-tax firms," *The Accounting Review*, vol. 89, no. 2, pp. 483–510, 2014.
- [15] P. S. Adler and S. W. Kwon, "Social capital: prospects for a new concept," *Academy of Management Review*, vol. 27, no. 1, pp. 17–40, 2002.
- [16] L. Argote, B. McEvily, and R. Reagans, "Managing knowledge in organizations: an integrative framework and review of emerging themes," *Management Science*, vol. 49, no. 4, pp. 571–582, 2003.
- [17] R. Reagans and B. McEvily, "Network structure and knowledge transfer: the effects of cohesion and range," *Administrative Science Quarterly*, vol. 48, no. 2, pp. 240–267, 2003.
- [18] D. Strang and S. A. Soule, "Diffusion in organizations and social movements: from hybrid corn to poison pills," *Annual Review of Sociology*, vol. 24, no. 1, pp. 265–290, 1998.
- [19] J. Paetzold and H. Winner, "Taking the high road? Compliance with commuter tax allowances and the role of evasion spillovers," *Journal of Public Economics*, vol. 143, pp. 1–14, 2016.
- [20] A. Bohne and J. S. Nimczik, *Information frictions and learning dynamics: evidence from tax avoidance in Ecuador*, Institute of Labor Economics (IZA), Bonn, Germany, 2018.
- [21] W. Frimmel, M. Halla, and J. Paetzold, "The intergenerational causal effect of tax evasion: evidence from the commuter tax allowance in Austria," *Journal of the European Economic Association*, vol. 17, no. 6, pp. 1843–1880, 2019.
- [22] A. Alstadsaeter, W. Kopczuk, and K. Telle, "Social networks and tax avoidance: evidence from a well-defined Norwegian tax shelter," *International Tax and Public Finance*, vol. 26, no. 6, pp. 1291–1328, 2019.
- [23] F. Akbari, M. Salehi, and M. A. B. Vlashani, "The effect of managerial ability on tax avoidance by classical and Bayesian econometrics in multilevel models: evidence of Iran," *International Journal of Emerging Markets*, vol. 13, no. 6, pp. 1656–1678, 2018.
- [24] D. Pomeranz, "No taxation without information: deterrence and self-enforcement in the value-added tax," *The American Economic Review*, vol. 105, no. 8, pp. 2539–2569, 2015.
- [25] W. C. Boning, J. Guyton, and R. Hodge, "Heard it through the grapevine: the direct and network effects of a tax enforcement field experiment on firms," *Journal of Public Economics*, vol. 190, Article ID 104261, 2020.
- [26] C. Kim and L. Zhang, "Corporate political connections and tax aggressiveness," *Contemporary Accounting Research*, vol. 33, no. 1, pp. 78–114, 2016.
- [27] M. R. Abbaszadeh, M. Salehi, and S. M. Faiz, "Association of information technology and internal controls of Iranian state agencies," *International Journal of Law and Management*, vol. 61, no. 1, pp. 133–150, 2019.
- [28] W. Gao, L. Ng, and Q. Wang, "Does corporate headquarters location matter for firm capital structure?" *Financial Management*, vol. 40, no. 1, pp. 113–138, 2011.
- [29] A. Matray, "The local innovation spillovers of listed firms," *Journal of Financial Economics*, vol. 141, no. 2, pp. 395–412, 2021.
- [30] M. L. Katz and C. Shapiro, "Network externalities, competition, and compatibility," *The American Economic Review*, vol. 75, no. 3, pp. 424–440, 1985.
- [31] J. Chu and P. Manchanda, "Quantifying cross and direct network effects in online consumer-to-consumer platforms," *Marketing Science*, vol. 35, no. 6, pp. 870–893, 2016.
- [32] J. J. Laird, J. Nellthorp, and P. J. Mackie, "Network effects and total economic impact in transport appraisal," *Transport Policy*, vol. 12, no. 6, pp. 537–544, 2005.
- [33] F. Thies, M. Wessel, and A. Benlian, "Network effects on crowdfunding platforms: exploring the implications of relaxing input control," *Information Systems Journal*, vol. 28, no. 6, pp. 1239–1262, 2018.
- [34] M. G. Allingham and A. Sandmo, "Income tax evasion: a theoretical analysis," *Journal of Public Economics*, vol. 1, pp. 323–338, 1972.
- [35] L. A. Ricci and F. Trionfetti, "Productivity, networks, and export performance: evidence from a cross-country firm dataset," *Review of International Economics*, vol. 20, no. 3, pp. 552–562, 2012.
- [36] N. Yadav, "The role of internet use on international trade: evidence from Asian and Sub-Saharan African enterprises," *Global Economy Journal*, vol. 14, no. 2, pp. 189–214, 2014.
- [37] O. Z. Li, H. Liu, and C. Ni, "Controlling shareholders' incentive and corporate tax avoidance: a natural experiment in China," *Journal of Business Finance & Accounting*, vol. 44, no. 5–6, pp. 697–727, 2017.
- [38] F. Wang, S. Xu, and J. Sun, "Corporate tax avoidance: a literature review and research agenda," *Journal of Economic Surveys*, vol. 34, no. 4, pp. 793–811, 2020.
- [39] T. Tang, P. L. L. Mo, and K. H. Chan, "Tax collector or tax avoider? An investigation of intergovernmental agency conflicts," *The Accounting Review*, vol. 92, no. 2, pp. 247–270, 2017.
- [40] J. A. Chyz, F. B. Gaertner, and A. Kausar, "Overconfidence and corporate tax policy," *Review of Accounting Studies*, vol. 24, no. 3, pp. 1114–1145, 2019.
- [41] W. Wen, H. Cui, and Y. Ke, "Directors with foreign experience and corporate tax avoidance," *Journal of Corporate Finance*, vol. 62, Article ID 101624, 2020.
- [42] A. Abouzeedan and M. Busler, "Internetization management' the way to run the strategic alliances in the E-globalization age," *Global Business Review*, vol. 8, no. 2, pp. 303–321, 2007.
- [43] A. Abouzeedan, M. Klofsten, and T. Hedner, "Internetization management as a facilitator for managing innovation in high-technology smaller firms," *Global Business Review*, vol. 14, no. 1, pp. 121–136, 2013.
- [44] E. L. Ferrara, A. Chong, and S. Duryea, "Soap operas and fertility: evidence from Brazil," *American Economic Journal: Applied Economics*, vol. 4, no. 4, pp. 1–31, 2012.
- [45] M. T. Leary and M. R. Roberts, "Do peer firms affect corporate financial policy?" *The Journal of Finance*, vol. 69, no. 1, pp. 139–178, 2014.



- [46] H. Cai and Q. Liu, "Competition and corporate tax avoidance: evidence from Chinese industrial firms," *The Economic Journal*, vol. 119, no. 537, pp. 764–795, 2009.
- [47] M. A. Desai and D. Dharmapala, "Corporate tax avoidance and high-powered incentives," *Journal of Financial Economics*, vol. 79, no. 1, pp. 145–179, 2006.
- [48] W. Xu, Y. Zeng, and J. Zhang, "Tax enforcement as a corporate governance mechanism: empirical evidence from China," *Corporate Governance: An International Review*, vol. 19, no. 1, pp. 25–40, 2011.
- [49] K. H. Chan, P. L. L. Mo, and A. Y. Zhou, "Government ownership, corporate governance and tax aggressiveness: evidence from China," *Accounting and Finance*, vol. 53, no. 4, pp. 1029–1051, 2013.
- [50] H. A. Annuar, I. A. Salihu, and S. N. S. Obid, "Corporate ownership, governance and tax avoidance: an interactive effects," *Procedia-Social and Behavioral Sciences*, vol. 164, pp. 150–160, 2014.
- [51] H. N. Minh, A. P. Tuan, and X. G. Yue, "The impact of tax avoidance on the value of listed firms in Vietnam," *Cogent Business & Management*, vol. 8, no. 1, Article ID 1930870, 2021.

## Research Article

# On Statistical Properties of a New Bivariate Modified Lindley Distribution with an Application to Financial Data

Ahmed Elhassanein <sup>1,2</sup>

<sup>1</sup>Department of Mathematics, College of Science, University of Bisha, Bisha, Saudi Arabia

<sup>2</sup>Department of Mathematics, Faculty of Science, Damanhour University, Damanhour, Egypt

Correspondence should be addressed to Ahmed Elhassanein; [el\\_hassanein@yahoo.com](mailto:el_hassanein@yahoo.com)

Received 24 October 2021; Revised 24 December 2021; Accepted 9 March 2022; Published 12 May 2022

Academic Editor: S.S. Askar

Copyright © 2022 Ahmed Elhassanein. This is an open access article distributed under the Creative Commons Attribution License, which permits unrestricted use, distribution, and reproduction in any medium, provided the original work is properly cited.

There is an increasing interest in expanding the one-parameter Lindley distribution to two-parameter, three-parameter, and five-parameter. The univariate one-parameter Lindley distribution is still one of the most applicable distributions in data analysis especially in lifetime data. Modeling dependent random quantities required bivariate parametric probability distributions. This study presents a new bivariate three-parameter probability distribution called bivariate modified Lindley distribution. The one-parameter modified Lindley distribution is used as a base line to construct the new model. Its statistical properties including cumulative function, density function, marginals, moments, conditional distributions, and copula are discussed. Simulation is constructed to declare theoretical properties, to show the flexibility of the new model and to investigate the goodness of fit. Two sets of real data, financial data and UEFA Champion's League data, are used to show the applicability of the proposed model for different types of data.

## 1. Introduction

Parametric probability distributions are very powerful tools for data analysis. The improvement of such distributions had a great attention [1–6]. Lindley [7] introduced the one-parameter Lindley distribution as a developed version of the exponential distribution. He considered the probability density function and cumulative function in the form

$$f(x; \theta) = \frac{\theta^2}{1 + \theta} (1 + x)e^{-\theta x}, \theta, x > 0, \quad (1)$$

$$F(x; \theta) = 1 - \left[ 1 + \frac{\theta x}{1 + \theta} e^{-\theta x} \right]. \quad (2)$$

Recently, Lindley distribution and its modified forms have been applied in different fields such as engineering, physics, medicine, and finance. Ghitany et al. [8] studied

statistical properties of the Lindley distribution. They proved the applicability of the distribution for the waiting times before service of the bank customers and its superiority in comparison with the exponential distribution, see also [9–21]. Shankar and Mishra [22] developed a two-parameter version of the one-parameter Lindley distribution. The probability density function and cumulative function were formulated from (1) and (2) in the form

$$f(x; \alpha; \theta) = \frac{\theta^2}{1 + \alpha\theta} (\alpha + x)e^{-\theta x}, \alpha, \theta, x > 0, \quad (3)$$

$$F(x; \alpha; \theta) = 1 - \left[ \frac{1 + (\alpha + x)\theta}{1 + \alpha\theta} e^{-\theta x} \right]. \quad (4)$$

For  $\alpha = 1$ , the one-parameter Lindley distribution is obtained. Shanker et al. [23] constructed a new three-parameter Lindley distribution with probability density function and cumulative function:

$$f(x; \alpha; \theta; \beta) = \frac{\theta^2}{\beta + \alpha\theta} (\alpha + \beta x) e^{-\theta x}, \alpha\theta + \beta, \theta, \beta, x > 0, \quad (5)$$

$$F(x; \alpha; \theta; \beta) = 1 - \left[ 1 + \frac{\alpha + \theta\beta x}{\beta + \alpha\theta} \right] e^{-\theta x}. \quad (6)$$

The model was used to analyze lifetime data. Asgharzadeh et al. [24] pursued the method by Gupta and Kundu [25], to introduce a weighted Lindley (NWL) distribution. Wongrin and Bodhisuwan [26] modeled a count data using a new modified Lindley distribution called Poisson-generalised Lindley distribution. Maurya et al. [27] analyzed survival times' data via a new three-parameter Lindley distribution formulated following the work of Cordeiro and De Castro [28]. Mota et al. [29] discussed mathematical properties of a reparameterized version of the weighted Lindley that can be used for data with bathtub-shaped or increasing hazard rate function distribution. Rather and Özel [30] propose a new weighted power Lindley distribution for modeling lifetime data. Elbatal et al. [31] extended the power Lindley distribution to a new five-parameter lifetime model named the exponentiated Kumaraswamy power-Lindley distribution. Chesneau et al. [32] derived a new inverted modified Lindley distribution. Diandarma et al. [33] formulated a discrete version of the Lindley distribution and conducted simulation to show that it has unimodal, right skew, high fluidity, and overdispersion.

Dependent random data appear in many fields as reliability, survival analysis, queueing analysis, insurance risk analysis, life insurance, and finance. For example, in lifetime data analysis, the lifetimes of organisms or items are most often dependent. Carriere [34] reported a high positive correlation between the times of deaths of coupled lives. Jagger and Sutton [35] discussed the significantly increase of the risk of mortality after the marital bereavement. Bivariate parametric probability distributions play a fundamental role in analyzing dependent data. There is an increasing interest in generating new bivariate models. Common ideas for generating bivariate distribution introduced by Balakrishnan and Lai [36] and Kundu and Gupta [37, 38] are employed by many researchers to introduce new distribution based on different marginals [39–43]. Although this method suits lifetime data, it is not applicable for a lot of other types of data. Maximum likelihood estimators cannot be obtained in the closed form. The joint pdf can take different shapes and it has a singular part. The bivariate modeling is still a challenge issue. Vaidyanathan and Varghese [44] proposed a new bivariate Lindley distribution using Morgenstern approach which can be used for analyzing bivariate lifetime data. Thomas and Jose [45] considered a marginal Rayleigh distribution and impound it with the pdf of an extended form of Lindley distribution to generate a new bivariate distribution.

In this study, we employed the idea discussed in [46, 47], to construct a new simple bivariate modified Lindley distribution based on the one-parameter modified Lindley distribution. The new distribution is flexible; its statistical quantities are available in explicit forms. The joint

probability density function is absolutely continuous. The maximum likelihood function can be obtained. It is applicable for lifetime data, financial data, and other types of data including heavy-tailed data and approximately symmetric data. Its hazard function gives various shapes according to the parameters.

The reset of the study is organized as follows. The new distribution is formulated in Section 2. Statistical properties are discussed in Section 3. Maximum likelihood estimators are derived in Section 4. Simulation is presented in Section 5. Real financial data are used to apply the new model in Section 6. Conclusion and remarks are given in Section 7.

## 2. Model Description

Recently, Chesneau et al. [32] introduced a new distribution named modified Lindley (ML) distribution that depends on only one parameter, and its cumulative distribution function is given by

$$F(x) = 1 - \left[ 1 + \frac{\theta x}{1 + \theta} e^{-\theta x} \right] e^{-\theta x}, x > 0. \quad (7)$$

The cdf (7) will be used as a base line distribution to generate a bivariate modified Lindley distribution following Alzaatreh et al. [48] and Ganji et al. [49]. Let  $(X, Y)$  be a random vector with joint probability density function  $h_{X,Y}(x, y)$ , where  $x \in [\alpha_1, \beta_1]$ ,  $y \in [\alpha_2, \beta_2]$ ,  $-\infty < \alpha_1 < \beta_1 < \infty$ , and  $-\infty < \alpha_2 < \beta_2 < \infty$ . Let  $(\Psi, \Omega)$  be a random vectors with marginals  $H_\Psi(\psi)$  and  $H_\Omega(\omega)$ , respectively, and let  $F_\Psi(H_\Psi(\psi))$  and  $F_\Omega(H_\Omega(\omega))$  be functions such that  $F_\Psi(H_\Psi(\psi))$  and  $F_\Omega(H_\Omega(\omega)) \in [\alpha_2, \beta_2]$  and  $F_\Psi(H_\Psi(\psi))$  and  $F_\Omega(H_\Omega(\omega))$  are differentiable and monotonically nondecreasing functions and  $F_\Psi(H_\Psi(\psi)) \rightarrow \alpha_1$  as  $\psi \rightarrow -\infty$ ,  $F_\Psi(H_\Psi(\psi)) \rightarrow \beta_1$  as  $\psi \rightarrow \infty$ ,  $F_\Omega(H_\Omega(\omega)) \rightarrow \alpha_2$  as  $\omega \rightarrow -\infty$ , and  $F_\Omega(H_\Omega(\omega)) \rightarrow \beta_2$  as  $\omega \rightarrow \infty$ . Then, the cdf of random variable  $(\Psi, \Omega)$  is given by  $F_{\Psi,\Omega}(F_\Psi(H_\Psi(\psi)), F_\Omega(H_\Omega(\omega))) = \int_{\alpha_1}^{F_\Psi(H_\Psi(\psi))} \int_{\alpha_2}^{F_\Omega(H_\Omega(\omega))} h_{X,Y}(x, y) dx dy$ .

Suppose the transformation function  $h_{X,Y}(x, y) = 1 + \xi_1(1-x) + \xi_2(1-y) + 2\xi_3(1-x-y)$ , where  $x, y \in [0, 1]$ ,  $\xi_1, \xi_2, \xi_3 \in [-1, 1]$ ,  $-1 \leq \xi_1 + \xi_3 \leq 1$ , and  $-1 \leq \xi_2 + \xi_3 \leq 1$ . Then, the cumulative function of the modified Lindley random vector  $(\Psi, \Omega)$  is given by

$$\begin{aligned} G_{\Psi,\Omega}(\psi, \omega) &= \left( 1 - \left[ 1 + \frac{\theta\psi}{1 + \theta} e^{-\theta\psi} \right] e^{-\theta(\psi)} \right) \left( 1 - \left[ 1 + \frac{\theta\omega}{1 + \theta} e^{-\theta\omega} \right] e^{-\theta\omega} \right) \\ &\quad \times \left\{ 1 + (\xi_1 + \xi_3) \left[ 1 + \frac{\theta\psi}{1 + \theta} e^{-\theta\psi} \right] e^{-\theta\psi} \right. \\ &\quad \left. + (\xi_2 + \xi_3) \left[ 1 + \frac{\theta\omega}{1 + \theta} e^{-\theta\omega} \right] e^{-\theta\omega} \right\}, \end{aligned} \quad (8)$$

where  $\theta > 0$ ,  $\psi > 0$ , and  $\omega > 0$ .

*Definition 1.* A random vector  $(\Psi, \Omega)$  is said to have a modified Lindley distribution with parameter  $(\theta, \xi_1, \xi_2, \xi_3)$ , where  $\theta > 0$ ,  $-1 < \xi_1 + \xi_3 < 1$ ,  $-1 < \xi_2 + \xi_3 < 1$ , if its

cumulative function is given by (8) for  $\psi > 0$  and  $\omega > 0$  and will be denoted by  $(\Psi, \Omega) \sim BIML(\theta, \xi_1, \xi_2, \xi_3)$ .

**Lemma 1.** Let  $(\Psi, \Omega) \sim BIML(\theta, \xi_1, \xi_2, \xi_3)$ . Then, its probability density function is given by

### 3. Statistical Properties

In this section, statistical properties of the new distribution are discussed.

$$\begin{aligned} g_{\Psi, \Omega}(\psi, \omega) &= \theta^2 e^{-\theta(\psi+\omega)} \left(1 - \frac{1-2\theta\psi}{1+\theta} e^{-\theta\psi}\right) \left(1 - \frac{1-2\theta\omega}{1+\theta} e^{-\theta\omega}\right) \\ &\times \left\{1 + (\xi_1 + \xi_3) \left(2 \left[1 + \frac{\theta\psi}{1+\theta} e^{-\theta\psi}\right] e^{-\theta\psi} - 1\right)\right. \\ &\left. + (\xi_2 + \xi_3) \left(2 \left[1 + \frac{\theta\omega}{1+\theta} e^{-\theta\omega}\right] e^{-\theta\omega} - 1\right)\right\}. \end{aligned} \quad (9)$$

**Lemma 2.** Let  $(\Psi, \Omega) \sim BIML(\theta, \xi_1, \xi_2, \xi_3)$ . Then, its marginals are given by

$$\begin{aligned} G_{\Psi}(\psi) &= \left(1 - \left[1 + \frac{\theta\psi}{1+\theta} e^{-\theta\psi}\right] e^{-\theta\psi}\right) \\ &\times \left\{1 + (\xi_1 + \xi_3) \left[1 + \frac{\theta\psi}{1+\theta} e^{-\theta\psi}\right] e^{-\theta\psi}\right\}, \\ G_{\Omega}(\omega) &= \left(1 - \left[1 + \frac{\theta\omega}{1+\theta} e^{-\theta\omega}\right] e^{-\theta\omega}\right) \\ &\times \left\{1 + (\xi_2 + \xi_3) \left[1 + \frac{\theta\omega}{1+\theta} e^{-\theta\omega}\right] e^{-\theta\omega}\right\}, \end{aligned} \quad (10)$$

$$\begin{aligned} g_{\Psi}(\psi) &= \theta e^{-\theta\psi} \left(1 - \frac{1-2\theta\psi}{1+\theta} e^{-\theta\psi}\right) \\ &\left\{1 + (\xi_1 + \xi_3) \left(2 \left[1 + \frac{\theta\psi}{1+\theta} e^{-\theta\psi}\right] e^{-\theta\psi} - 1\right)\right\}, \\ g_{\Omega}(\omega) &= \theta e^{-\theta\omega} \left(1 - \frac{1-2\theta\omega}{1+\theta} e^{-\theta\omega}\right) \\ &\left\{1 + (\xi_2 + \xi_3) \left(2 \left[1 + \frac{\theta\omega}{1+\theta} e^{-\theta\omega}\right] e^{-\theta\omega} - 1\right)\right\}. \end{aligned} \quad (11)$$

**Lemma 3.** Let  $(\Psi, \Omega) \sim BIML(\theta, \xi_1, \xi_2, \xi_3)$ . Then,

$$g_{\Psi/\Omega}(\psi/\omega) = \theta e^{-\theta\psi} \left(1 - \frac{1-2\theta\psi}{1+\theta} e^{-\theta\psi}\right) \left(1 + \frac{\Delta(\xi_1, \psi)}{1 + \Delta(\xi_2, \omega)}\right), \quad (12)$$

$$g_{\Omega/\Psi}(\omega/\psi) = \theta e^{-\theta\omega} \left(1 - \frac{1-2\theta\omega}{1+\theta} e^{-\theta\omega}\right) \left(1 + \frac{\Delta(\xi_2, \omega)}{1 + \Delta(\xi_1, \psi)}\right), \quad (13)$$

where

$$\Delta(\xi, z) = (\xi + \xi_3) \left( \left[1 + \frac{\theta z}{1+\theta} e^{-\theta z}\right] e^{-\theta z} - 1 \right). \quad (14)$$

**Lemma 4.** Let  $(\Psi, \Omega) \sim BIML(\theta, \xi_1, \xi_2, \xi_3)$ . Then,

$$\begin{aligned}
\mu_{\Psi/\Omega}^r(\omega) &= E(\Psi^r/\Omega = \omega) = \left(1 + \frac{\xi_1 + \xi_3}{1 + \Delta(\xi_2, \omega)}\right) \left( \left(1 - \frac{1}{2^{r+1}} \frac{1}{1 + \theta}\right) \frac{\Gamma(r+1)}{\theta^r} + \frac{1}{2^{r+1}} \frac{1}{1 + \theta} \frac{\Gamma(r+2)}{\theta^r} \right) \\
&\quad - \frac{2(\xi_1 + \xi_3)}{1 + \Delta(\xi_2, \omega)} \left\{ \left(1 - \frac{1}{2^{r+1}} \frac{\theta + 2}{1 + \theta} + \frac{1}{3^{r+1}} \frac{1}{1 + \theta}\right) \frac{\Gamma(r+1)}{\theta^r} \right. \\
&\quad \left. + \left( \frac{1}{2^{r+1}} \frac{1}{1 + \theta} - \frac{1}{3^{r+1}} \frac{1}{1 + \theta} + \frac{1}{4^{r+2}} \frac{1}{(1 + \theta)^2} \right) \frac{\Gamma(r+2)}{\theta^r} \right. \\
&\quad \left. - \frac{1}{2^{2r+5}} \frac{1}{(1 + \theta)^2} \frac{\Gamma(r+3)}{\theta^r} \right\}, \tag{15}
\end{aligned}$$

$$\begin{aligned}
\mu_{\Omega/\Psi}^r(\psi) &= E(\Omega^r/\Psi = \psi) = \left(1 + \frac{\xi_2 + \xi_3}{1 + \Delta(\xi_1, \psi)}\right) \left( \left(1 - \frac{1}{2^{r+1}} \frac{1}{1 + \theta}\right) \frac{\Gamma(r+1)}{\theta^r} + \frac{1}{2^{r+1}} \frac{1}{1 + \theta} \frac{\Gamma(r+2)}{\theta^r} \right) \\
&\quad - \frac{2(\xi_2 + \xi_3)}{1 + \Delta(\xi_1, \psi)} \left\{ \left(1 - \frac{1}{2^{r+1}} \frac{\theta + 2}{1 + \theta} + \frac{1}{3^{r+1}} \frac{1}{1 + \theta}\right) \frac{\Gamma(r+1)}{\theta^r} \right. \\
&\quad \left. + \left( \frac{1}{2^{r+1}} \frac{1}{1 + \theta} - \frac{1}{3^{r+1}} \frac{1}{1 + \theta} + \frac{1}{4^{r+2}} \frac{1}{(1 + \theta)^2} \right) \frac{\Gamma(r+2)}{\theta^r} \right. \\
&\quad \left. - \frac{1}{2^{2r+5}} \frac{1}{(1 + \theta)^2} \frac{\Gamma(r+3)}{\theta^r} \right\}. \tag{16}
\end{aligned}$$

**Lemma 5.** Let  $(\Psi, \Omega) \sim \text{BIML}(\theta, \xi_1, \xi_2, \xi_3)$ . Then,

$$\begin{aligned}
\mu_{r,s} &= E(\Psi^r \Omega^s) = (1 + \xi_1 + \xi_2 + 2\xi_3) \\
&\quad \times \left( \left(1 - \frac{1}{2^{r+1}} \frac{1}{1 + \theta}\right) \frac{\Gamma(r+1)}{\theta^r} + \frac{1}{2^{r+1}} \frac{1}{1 + \theta} \frac{\Gamma(r+2)}{\theta^r} \right) \\
&\quad \times \left( \left(1 - \frac{1}{2^{s+1}} \frac{1}{1 + \theta}\right) \frac{\Gamma(s+1)}{\theta^s} + \frac{1}{2^{s+1}} \frac{1}{1 + \theta} \frac{\Gamma(s+2)}{\theta^s} \right) \\
&\quad - 2 \left\{ (\xi_1 + \xi_3) \left( \left(1 - \frac{1}{2^{s+1}} \frac{1}{1 + \theta}\right) \frac{\Gamma(s+1)}{\theta^s} + \frac{1}{2^{s+1}} \frac{1}{1 + \theta} \frac{\Gamma(s+2)}{\theta^s} \right) \right. \\
&\quad \times \left[ 1 - \frac{1}{2^{r+1}} \frac{\theta + 2}{1 + \theta} + \frac{1}{3^{r+1}} \frac{1}{1 + \theta} \frac{\Gamma(r+1)}{\theta^r} + \left( \frac{1}{2^{r+1}} \frac{1}{1 + \theta} - \frac{1}{3^{r+1}} \frac{1}{1 + \theta} + \frac{1}{4^{r+2}} \frac{1}{(1 + \theta)^2} \right) \frac{\Gamma(r+2)}{\theta^r} - \frac{1}{4^{r+3}} \frac{2}{(1 + \theta)^2} \frac{\Gamma(r+3)}{\theta^r} \right] \\
&\quad \left. + (\xi_2 + \xi_3) \left( \left(1 - \frac{1}{2^{r+1}} \frac{1}{1 + \theta}\right) \frac{\Gamma(r+1)}{\theta^r} + \frac{1}{2^{r+1}} \frac{1}{1 + \theta} \frac{\Gamma(r+2)}{\theta^r} \right) \right. \\
&\quad \left. \times \left[ 1 - \frac{1}{2^{s+1}} \frac{\theta + 2}{1 + \theta} + \frac{1}{3^{s+1}} \frac{1}{1 + \theta} \frac{\Gamma(s+1)}{\theta^s} + \left( \frac{1}{2^{s+1}} \frac{1}{1 + \theta} - \frac{1}{3^{s+1}} \frac{1}{1 + \theta} + \frac{1}{4^{s+2}} \frac{1}{(1 + \theta)^2} \right) \frac{\Gamma(s+2)}{\theta^s} - \frac{1}{4^{s+3}} \frac{2}{(1 + \theta)^2} \frac{\Gamma(s+3)}{\theta^s} \right] \right\}. \tag{17}
\end{aligned}$$

**Lemma 6.** Let  $(\Psi, \Omega) \sim BIML(\theta, \xi_1, \xi_2, \xi_3)$ . Then, the bivariate reliability function is given by

$$\begin{aligned}
R(\psi, \omega) &= 1 - \left( 1 - \left[ 1 + \frac{\theta\psi}{1+\theta} e^{-\theta\psi} \right] e^{-\theta\psi} \right) \\
&\quad \times \left\{ 1 + (\xi_1 + \xi_3) \left[ 1 + \frac{\theta\psi}{1+\theta} e^{-\theta\psi} \right] e^{-\theta\psi} \right\} \\
&\quad - \left( 1 - \left[ 1 + \frac{\theta\omega}{1+\theta} e^{-\theta\omega} \right] e^{-\theta\omega} \right) \\
&\quad \times \left\{ 1 + (\xi_2 + \xi_3) \left[ 1 + \frac{\theta\omega}{1+\theta} e^{-\theta\omega} \right] e^{-\theta\omega} \right\} \\
&\quad + e^{-\theta(\psi+\omega)} \left( 1 - \left[ 1 + \frac{\theta\psi}{1+\theta} e^{-\theta\psi} \right] \right) \left( 1 - \left[ 1 + \frac{\theta\omega}{1+\theta} e^{-\theta\omega} \right] \right) \\
&\quad \times \left\{ 1 + (\xi_1 + \xi_3) \left[ 1 + \frac{\theta\psi}{1+\theta} e^{-\theta\psi} \right] + (\xi_2 + \xi_3) \left[ 1 + \frac{\theta\omega}{1+\theta} e^{-\theta\omega} \right] \right\}.
\end{aligned} \tag{18}$$

**Lemma 7.** Let  $(\Psi, \Omega) \sim BIML(\theta, \xi_1, \xi_2, \xi_3)$ . Then, the bivariate hazard rate function is given by

$$\begin{aligned}
h(\psi, \omega) &= \theta^2 e^{-\theta(\psi+\omega)} \left( 1 - \frac{1-2\theta\psi}{1+\theta} e^{-\theta\psi} \right) \left( 1 - \frac{1-2\theta\omega}{1+\theta} e^{-\theta\omega} \right) \\
&\quad \times \left\{ 1 + (\xi_1 + \xi_3) \left( 2 \left[ 1 + \frac{\theta\psi}{1+\theta} e^{-\theta\psi} \right] e^{-\theta\psi} - 1 \right) \right. \\
&\quad \left. + (\xi_2 + \xi_3) \left( 2 \left[ 1 + \frac{\theta\omega}{1+\theta} e^{-\theta\omega} \right] e^{-\theta\omega} - 1 \right) \right\} \\
&\quad \times \left[ 1 - \left( 1 - \left[ 1 + \frac{\theta\psi}{1+\theta} e^{-\theta\psi} \right] e^{-\theta\psi} \right) \right. \\
&\quad \times \left\{ 1 + (\xi_1 + \xi_3) \left[ 1 + \frac{\theta\psi}{1+\theta} e^{-\theta\psi} \right] e^{-\theta\psi} \right\} \\
&\quad \left. - \left( 1 - \left[ 1 + \frac{\theta\omega}{1+\theta} e^{-\theta\omega} \right] e^{-\theta\omega} \right) \right. \\
&\quad \times \left\{ 1 + (\xi_2 + \xi_3) \left[ 1 + \frac{\theta\omega}{1+\theta} e^{-\theta\omega} \right] e^{-\theta\omega} \right\} \\
&\quad \left. + \left( 1 - \left[ 1 + \frac{\theta\psi}{1+\theta} e^{-\theta\psi} \right] e^{-\theta\psi} \right) \left( 1 - \left[ 1 + \frac{\theta\omega}{1+\theta} e^{-\theta\omega} \right] e^{-\theta\omega} \right) \right. \\
&\quad \left. \times \left\{ 1 + (\xi_1 + \xi_3) \left[ 1 + \frac{\theta\psi}{1+\theta} e^{-\theta\psi} \right] + (\xi_2 + \xi_3) \left[ 1 + \frac{\theta\omega}{1+\theta} e^{-\theta\omega} \right] \right\} \right]^{-1}.
\end{aligned} \tag{19}$$

The Copula function is of the most important quantities that is used to describe the stochastic dependence between

continuous random variables. Let  $(\Psi, \Omega) \sim BML(\theta)$ ; since  $G_{\Psi, \Omega}(\psi, \omega) = P(\Psi \leq \psi, \Omega \leq \omega)$ ,  $G_{\Psi}(\psi) = P(\Psi \leq \psi)$ , and

$G_\Omega(\omega) = P(\Omega \leq \omega)$ , then its copula function can be defined as  $G_{\Psi, \Omega}(\psi, \omega) \triangleq C(u, v)$ , where  $u = G_\Psi(\psi)$ ,  $v = G_\Omega(\omega)$ , and  $u, v \in (0, 1)$  [50–52].

**Lemma 8.** Let  $(\Psi, \Omega) \sim BIML(\theta, \xi_1, \xi_2, \xi_3)$ . Then, its copula function  $c(u, v) = \partial^2 C(u, v) / \partial u \partial v$  is given by

$$c(u, v) = \frac{1 + \Delta(\xi_1, \psi) + \Delta(\xi_2, \omega)}{(1 + \Delta(\xi_1, \psi))(1 + \Delta(\xi_2, \omega))}, \quad (20)$$

where  $\Delta(\xi, z)$  is given by (14).

#### 4. Estimation

Considering a random sample  $(\psi_1, \omega_1), (\psi_2, \omega_2), \dots, (\psi_n, \omega_n)$  from the bivariate modified Lindley random

variable  $(\Psi, \Omega) \sim BIML(\theta, \xi_1, \xi_2, \xi_3)$ , the maximum log-likelihood function for the unknown parameters  $\Xi = (\theta, \xi_1, \xi_2, \xi_3)'$  is given by

$$\begin{aligned} L(\Xi) = & 2n \ln \theta - \theta \sum_{i=1}^n (\psi_i + \omega_i) + \sum_{i=1}^n \ln \left( 1 - \frac{1 - 2\theta \psi_i e^{-\theta \psi_i}}{1 + \theta} \right) \\ & + \sum_{i=1}^n \ln \left( 1 - \frac{1 - 2\theta \omega_i e^{-\theta \omega_i}}{1 + \theta} \right) \\ & + \sum_{i=1}^n \left\{ \ln \left[ 1 + (\xi_1 + \xi_3) \left( 2 \left[ 1 + \frac{\theta \psi_i}{1 + \theta} e^{-\theta \psi_i} \right] e^{-\theta \psi_i} - 1 \right) \right. \right. \\ & \left. \left. + (\xi_2 + \xi_3) \left( 2 \left[ 1 + \frac{\theta \omega_i}{1 + \theta} e^{-\theta \omega_i} \right] e^{-\theta \omega_i} - 1 \right) \right] \right\}. \end{aligned} \quad (21)$$

The score vector  $\Xi = (\Xi_\theta, \Xi_{\xi_1}, \Xi_{\xi_2}, \Xi_{\xi_3})'$  is given by

$$\begin{aligned} \Xi_\theta = & \frac{2n}{\theta} - \sum_{i=1}^n (\psi_i + \omega_i) \\ & + \sum_{i=1}^n \frac{e^{-\theta \psi_i} (1 + (3 + \theta) \psi_i - 2\theta(1 + \theta) \psi_i^2)}{(1 + \theta)(1 + \theta + (2\theta \psi_i - 1) e^{-\theta \psi_i})} \\ & + \sum_{i=1}^n \frac{e^{-\theta \omega_i} (1 + (3 + \theta) \omega_i - 2\theta(1 + \theta) \omega_i^2)}{(1 + \theta)(1 + \theta + (2\theta \omega_i - 1) e^{-\theta \omega_i})} \\ & - 2(\xi_1 + \xi_3) \sum_{i=1}^n \frac{\psi_i e^{-\theta \psi_i} (1 - (1 - 2\theta(1 + \theta) \psi_i / (1 + \theta)^2) e^{-\theta \psi_i})}{1 + \Delta(\xi_1, \psi_i) + \Delta(\xi_2, \omega_i)} \\ & - 2(\xi_2 + \xi_3) \sum_{i=1}^n \frac{\omega_i e^{-\theta \omega_i} (1 - (1 - 2\theta(1 + \theta) \omega_i / (1 + \theta)^2) e^{-\theta \omega_i})}{1 + \Delta(\xi_1, \psi_i) + \Delta(\xi_2, \omega_i)}, \\ \Xi_{\xi_1} = & \sum_{i=1}^n \frac{2 \left[ 1 + (\theta \psi_i / (1 + \theta)) e^{-\theta \psi_i} \right] e^{-\theta \psi_i} - 1}{1 + \Delta(\xi_1, \psi_i) + \Delta(\xi_2, \omega_i)}, \\ \Xi_{\xi_2} = & \sum_{i=1}^n \frac{2 \left[ 1 + (\theta \psi_i / (1 + \theta)) e^{-\theta \psi_i} \right] e^{-\theta \psi_i} - 1}{1 + \Delta(\xi_1, \psi_i) + \Delta(\xi_2, \omega_i)}, \\ \Xi_{\xi_3} = & \sum_{i=1}^n \frac{2 \left[ 1 + (\theta \psi_i / (1 + \theta)) e^{-\theta \psi_i} \right] e^{-\theta \psi_i} - 1}{1 + \Delta(\xi_1, \psi_i) + \Delta(\xi_2, \omega_i)} + \sum_{i=1}^n \frac{2 \left[ 1 + (\theta \psi_i / (1 + \theta)) e^{-\theta \psi_i} \right] e^{-\theta \psi_i} - 1}{1 + \Delta(\xi_1, \psi_i) + \Delta(\xi_2, \omega_i)}, \end{aligned} \quad (22)$$

where  $\Delta(\xi, z)$  is given by (14).

#### 5. Simulation

In this section, three sets of parameters are used to discuss the behaviour of the new bivariate distribution, to show its flexibility and to investigate the goodness of fit: the set I,  $(\theta, \xi_1, \xi_2, \xi_3) = (0.9, 0.5, 0.4, 0.1)$ , the set II,  $(\theta, \xi_1, \xi_2, \xi_3) = (0.4, 0.1, -0.4, 0.6)$ , and the set III,  $(\theta, \xi_1, \xi_2, \xi_3) = (2, 0.8, 0.7, -0.4)$ . For the set I, we can observe the heavy tail and unimodality of the joint probability density

function (Figure 1(a)). The marginal densities are unimodal with right tail (Figures 1(f) and 1(h)). The joint cumulative function approaches 1 for small values  $(\psi, \omega)$  (Figure 1(b)). It is also the case for the cumulative marginals (Figures 1(g) and 1(i)). The hazard function is approximately constant, see Figure 1(c). The level of independence increases with the increase of the value of  $(u, v)$ , see Figures 1(d) and 1(e). For the set II, the density function loses heavy tail property (Figure 2(a)). The marginal densities still have right tail (Figures 2(f) and 2(h)). The joint cumulative function and cumulative marginals converge the maximum value slowly

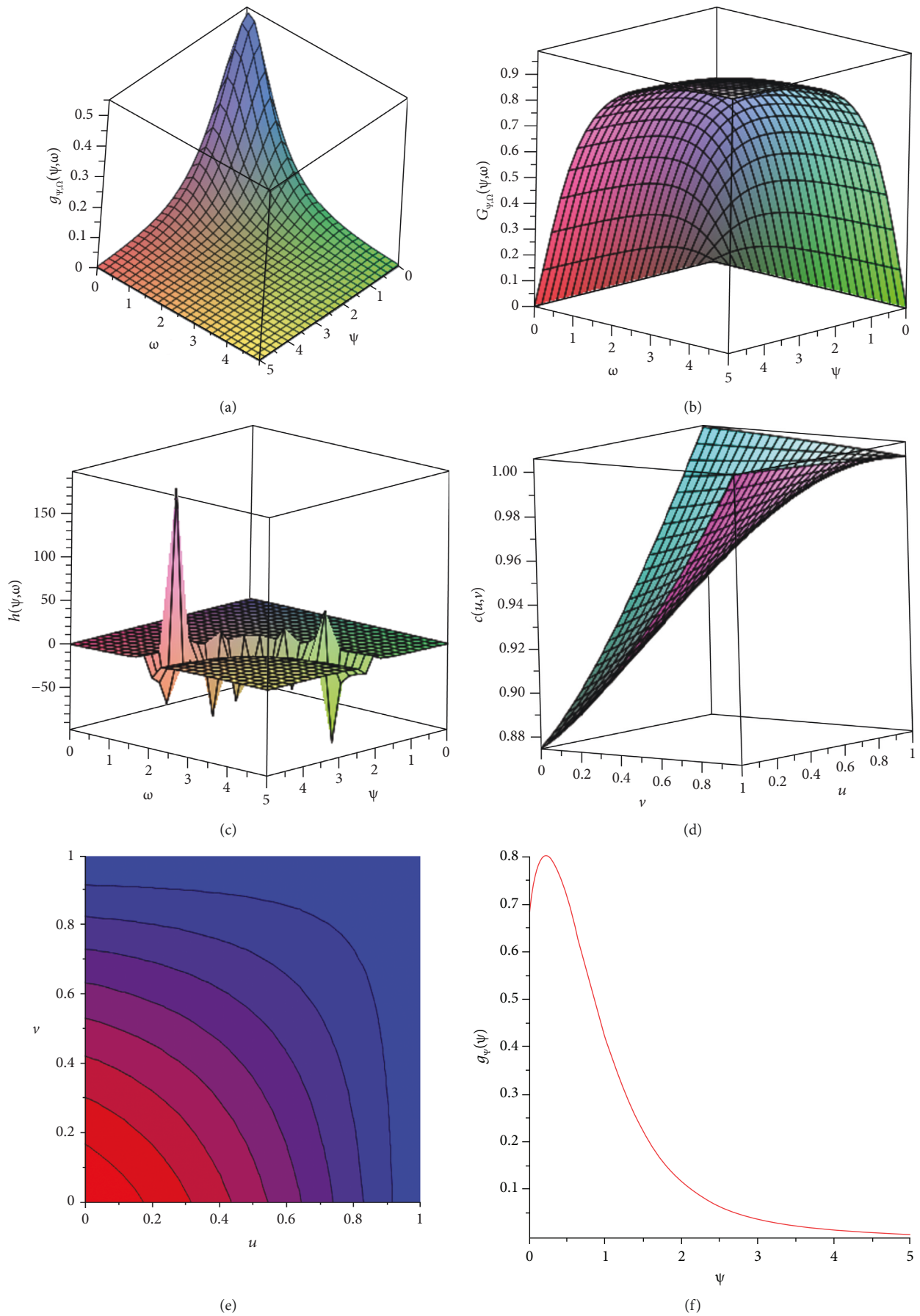


FIGURE 1: Continued.



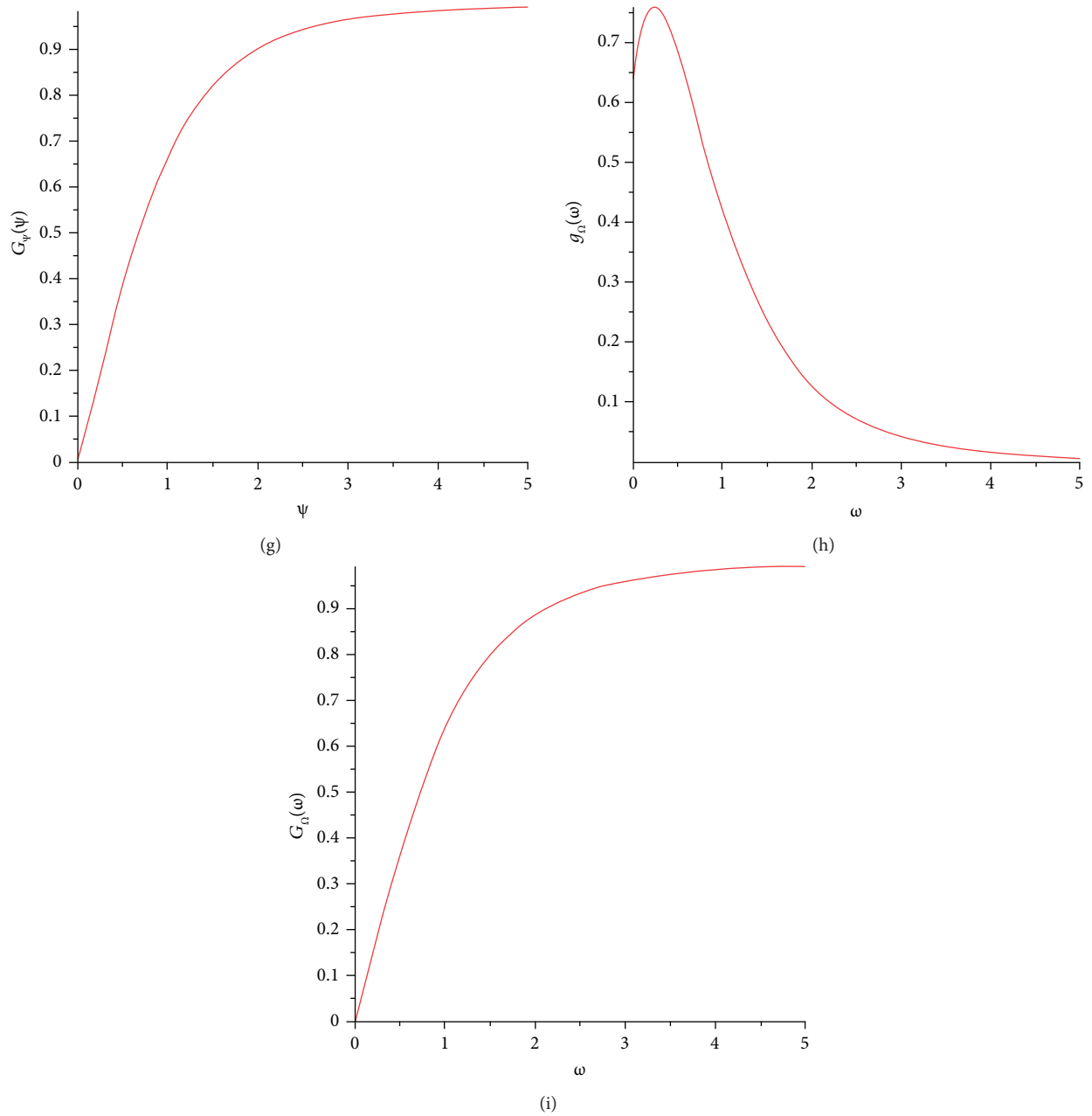


FIGURE 1: Statistical quantities for the set I of parameters,  $(\theta, \xi_1, \xi_2, \xi_3) = (0.9, 0.5, 0.4, 0.1)$ .

in comparison with the set I, see Figures 2(b), 2(g), and 2(i). The hazard function is an increasing function (Figure 2(c)). The independence structure of the two random variables can be observed in Figures 2(d) and 2(e). For the set III, the joint probability density function and marginals have heavy tail

and unimodal (Figures 3(a), 3(f), and 3(h)). The joint cumulative function and cumulative marginals approach the maximum value fast in comparison with that for set I (Figures 3(b), 3(g), and 3(i)). The hazard function changes its behaviour from increasing to decreasing (Figure 3(c)). We

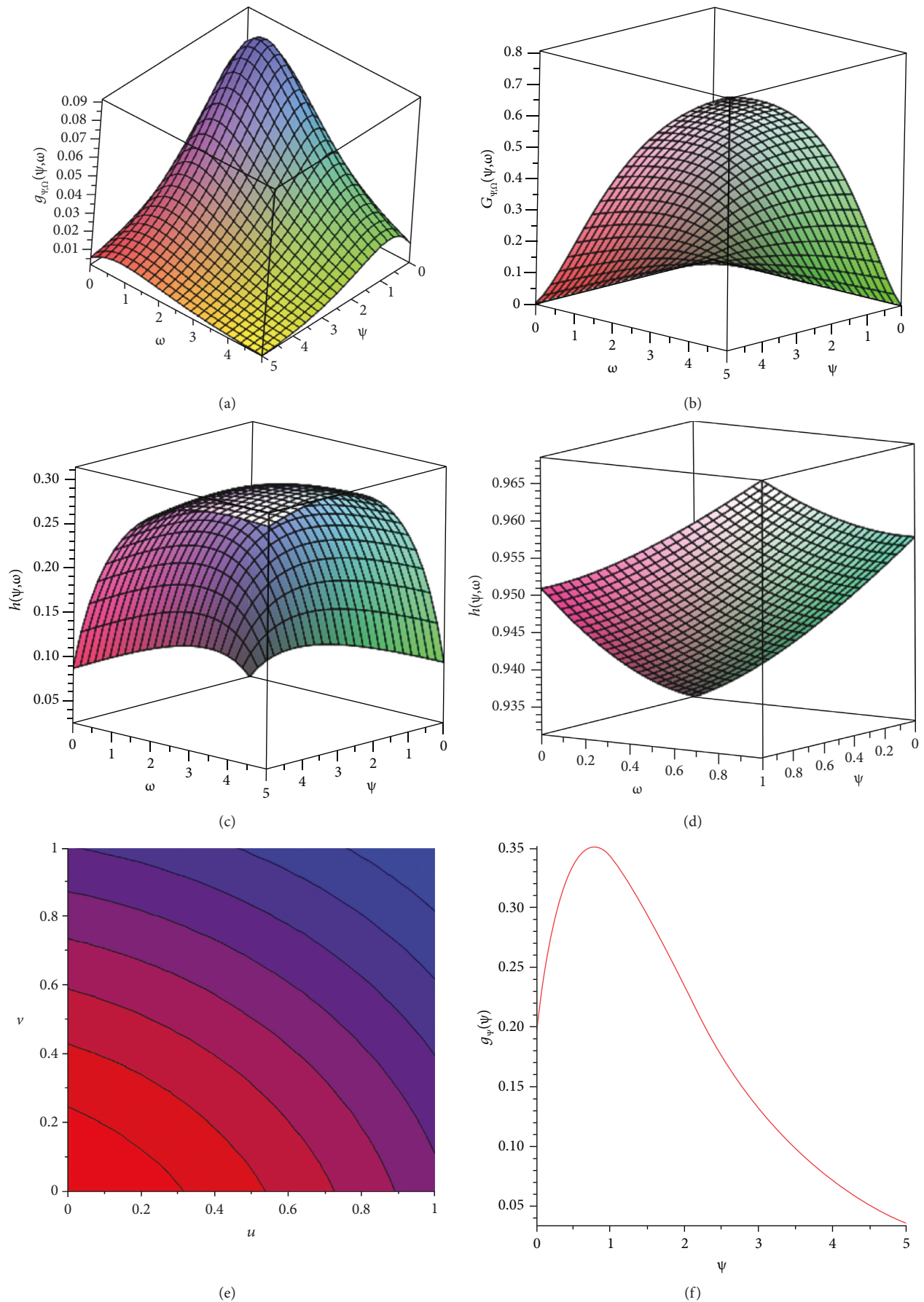


FIGURE 2: Continued.

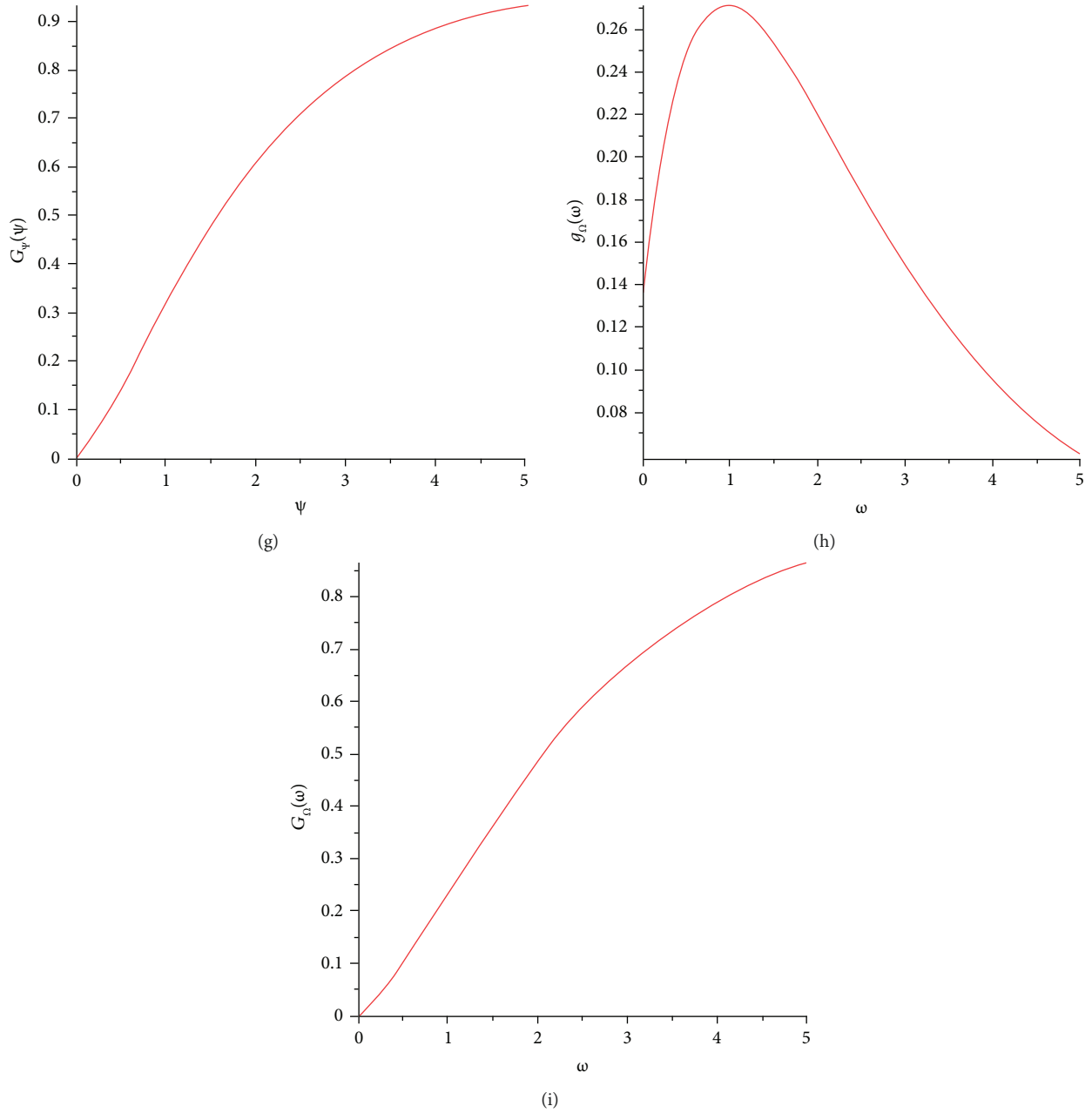
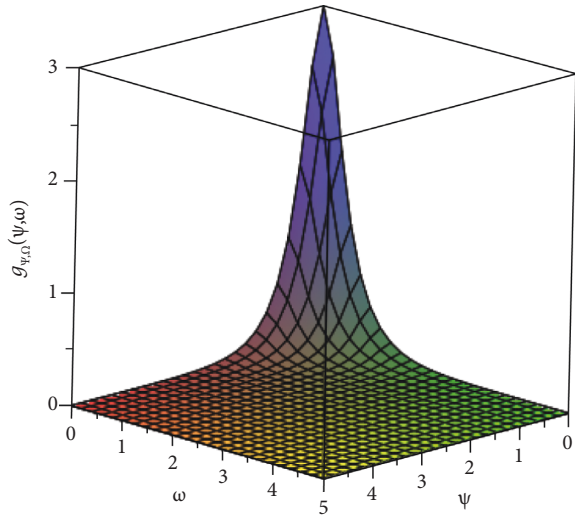


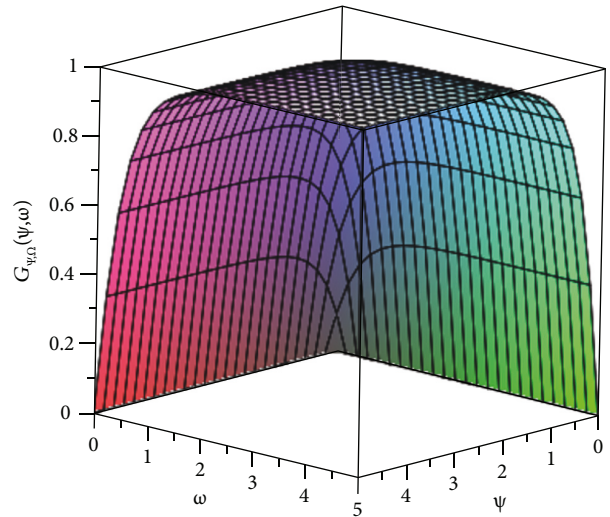
FIGURE 2: Statistical quantities for the set II of parameters,  $(\theta, \xi_1, \xi_2, \xi_3) = (0.4, 0.1, -0.4, 0.6)$ .

can observe the increase of the copula function with the increase of  $(u, v)$  (Figures 3(d) and 3(e)). It is clear that the model has different properties for different values of parameters and the hazard function has different shapes. To

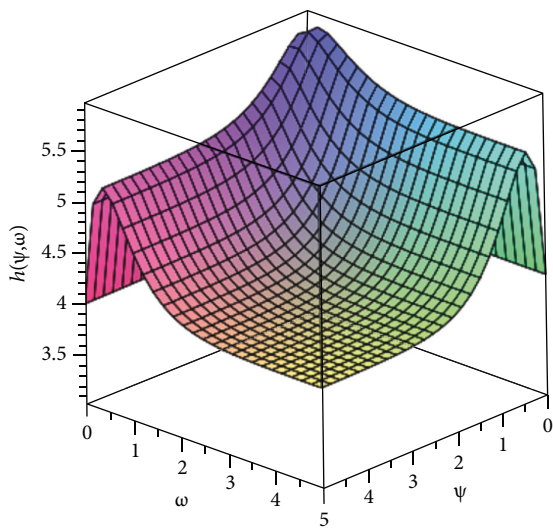
investigate the applicability, the performance of the maximum likelihood method, and the goodness of fit, Monte Carlo simulation is performed to generate samples for the three sets of parameters (I, II, III) in addition to two other



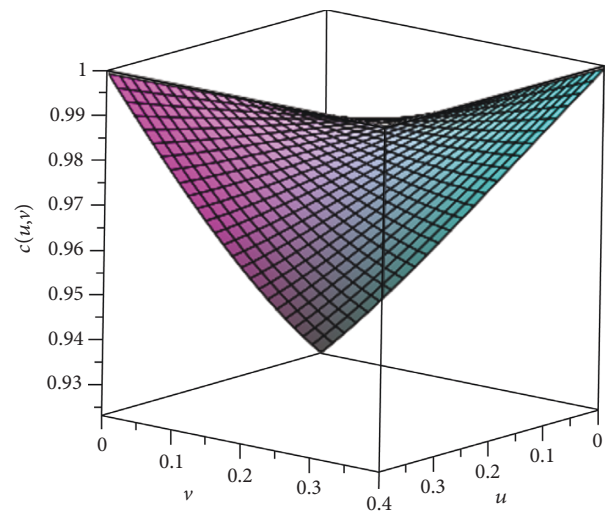
(a)



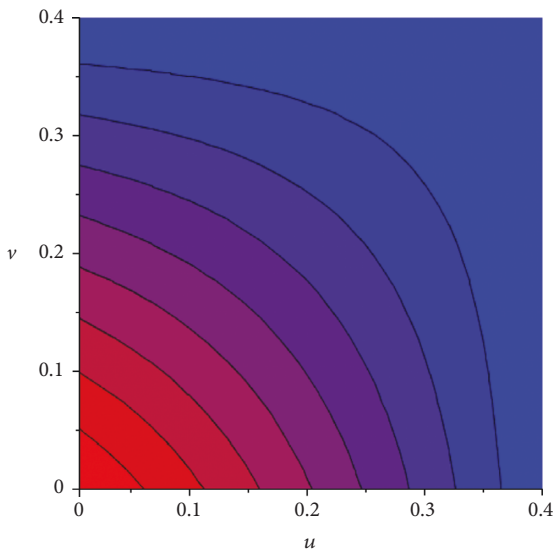
(b)



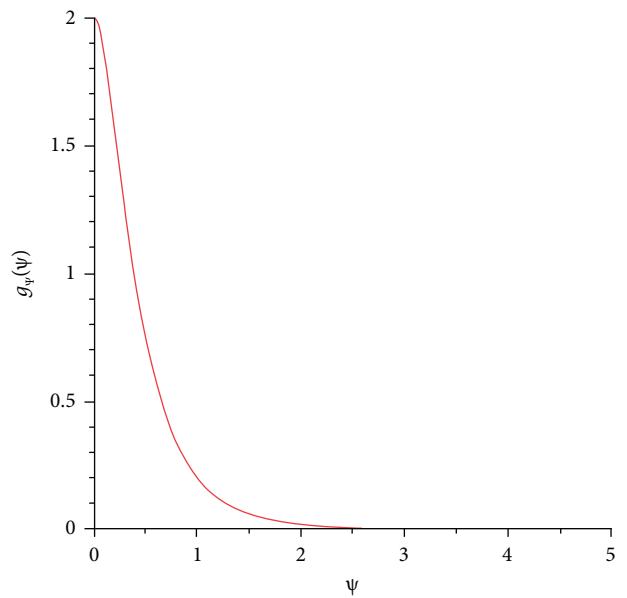
(c)



(d)



(e)



(f)

FIGURE 3: Continued.

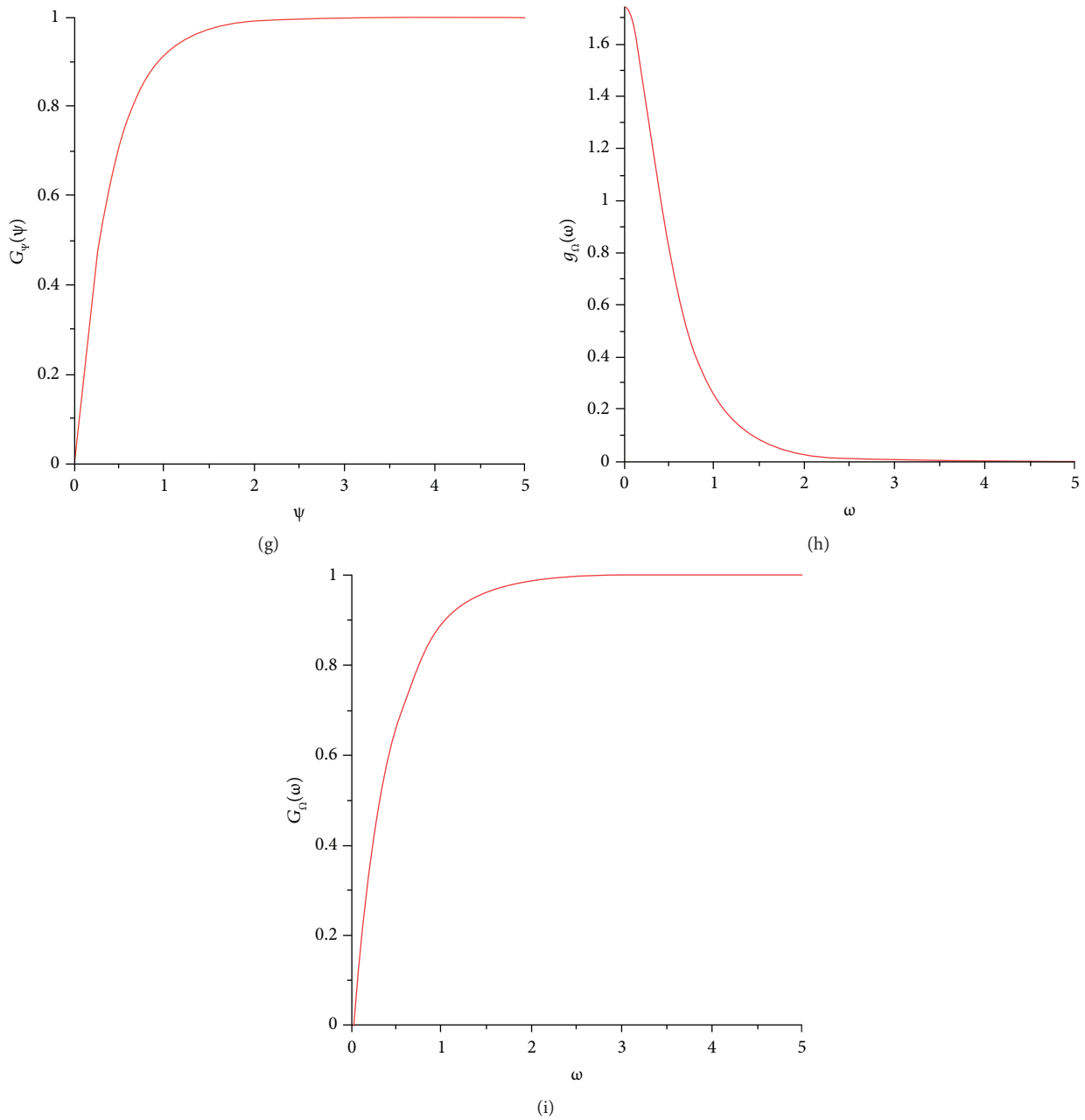


FIGURE 3: Statistical quantities for the set III of parameters,  $(\theta, \xi_1, \xi_2, \xi_3) = (2, -0.7, -0.9, 1.2)$ .

sets IV and V, where IV  $(\theta, \xi_1, \xi_2, \xi_3) = (0.5, -0.8, -0.4, 0.6)$  and V  $(\theta, \xi_1, \xi_2, \xi_3) = (1.5, -0.8, 0.4, 0.3)$ . The sizes of the samples are different ( $n = 20, 50, 100$ ). The parameters  $\xi_1, \xi_2$ , and  $\xi_3$  are treated as chosen parameters. The maximum likelihood method is used to estimate the unknown parameter  $\theta$ ; the results are given in Table 1. We note that the bias and the standard error decrease with the increase of the

sample size. The maximum likelihood method gives good estimates for the unknown parameter.

### 6. Real-Data Application

In this section, two data sets are used to apply the new model,  $BIML(\theta, \xi_1, \xi_2, \xi_3)$ .

TABLE 1: The average estimates for the parameter  $\theta$ , for sets of data I, II, and III, with bias and standard error.

Set of data	Sample size	Average estimate	Bias	SE
I	$n = 20$	0.8461	-0.0539	0.0348
	$n = 50$	0.8626	-0.3074	0.0219
	$n = 100$	0.8200	-0.0800	0.0180
II	$n = 20$	0.3810	-0.0190	0.0149
	$n = 50$	0.3836	-0.0164	0.0110
	$n = 100$	0.3885	-0.0115	0.00740
III	$n = 20$	1.9182	-0.0818	0.0529
	$n = 50$	1.9746	-0.0254	0.0524
	$n = 100$	1.9912	-0.0088	0.0378
IV	$n = 20$	0.47298	-0.02702	0.0290
	$n = 50$	0.46070	-0.0393	0.00620
	$n = 100$	0.4786	-0.0214	0.00809
V	$n = 20$	1.3483	-0.1517	0.0250
	$n = 50$	1.3536	-0.1464	0.0318
	$n = 100$	1.4036	-0.0964	0.0252

TABLE 2: Estimated parameters for the financial data with AIC and BIC.

Parameter	Estimate	AIC	BIC
$\theta$	1.4191778		
$\xi_1$	0.3844708	697.7194	711.8687
$\xi_2$	-0.1507097		
$\xi_3$	-0.5212492		

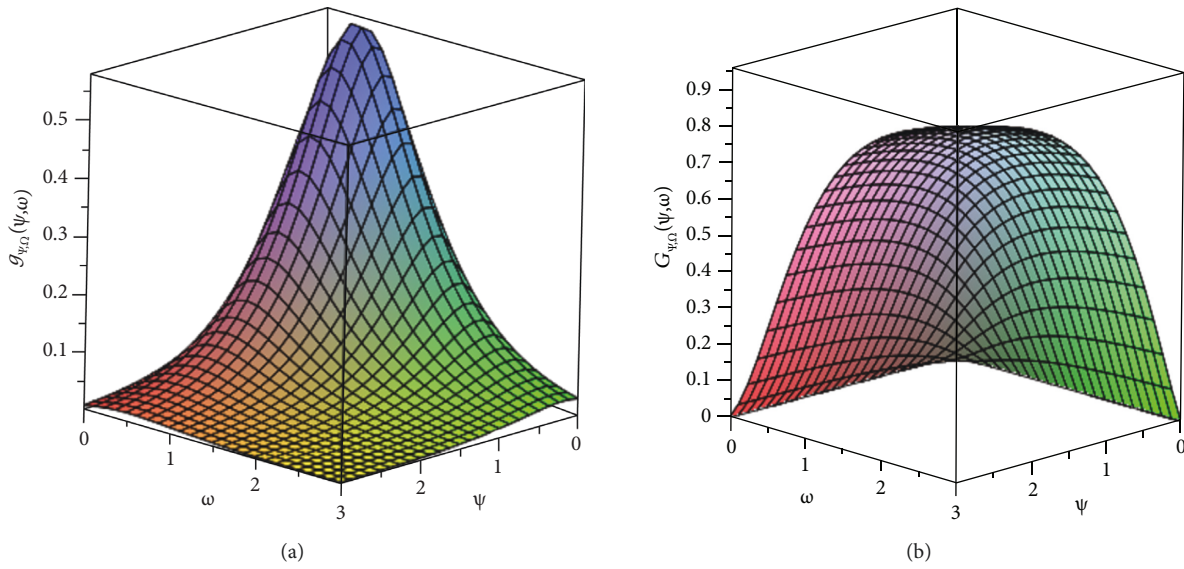
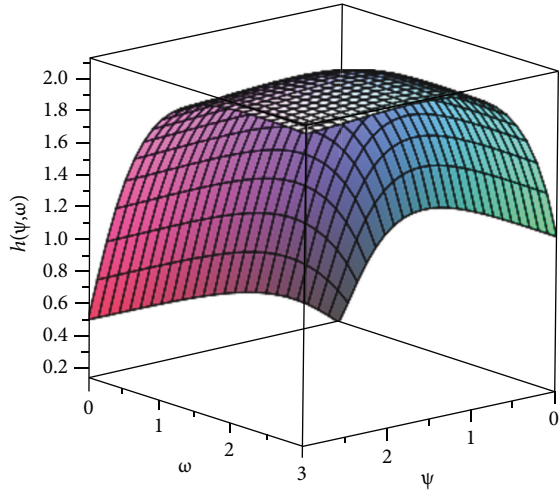
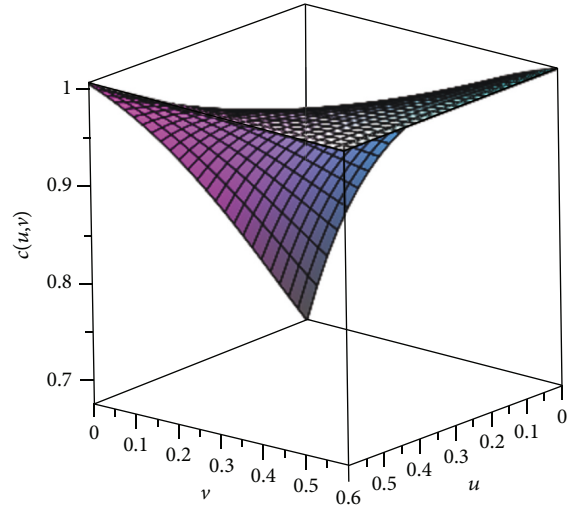


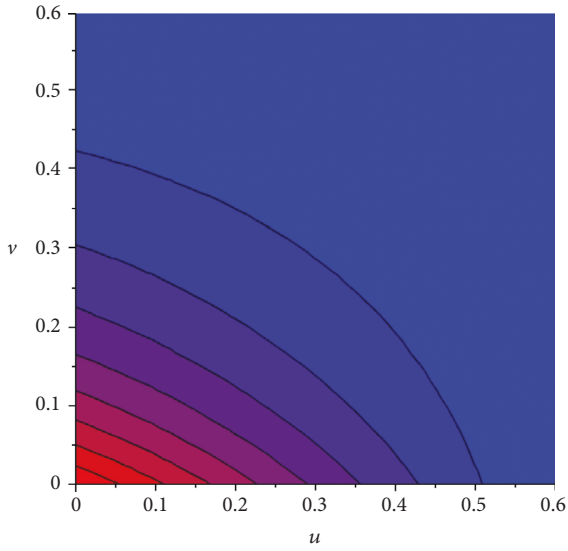
FIGURE 4: Continued.



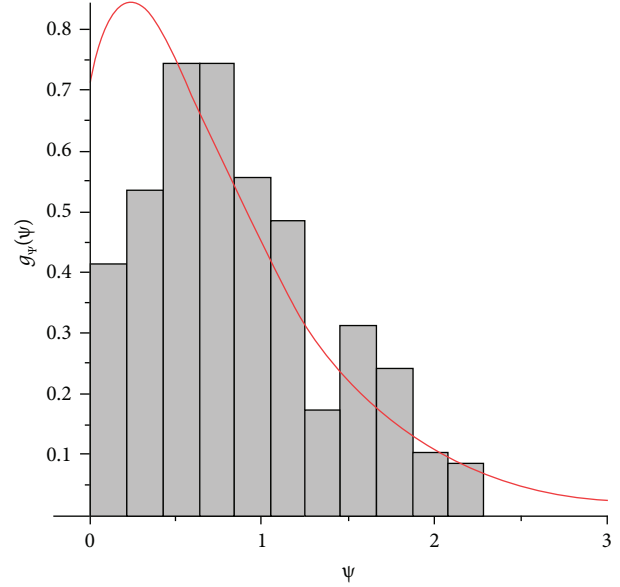
(c)



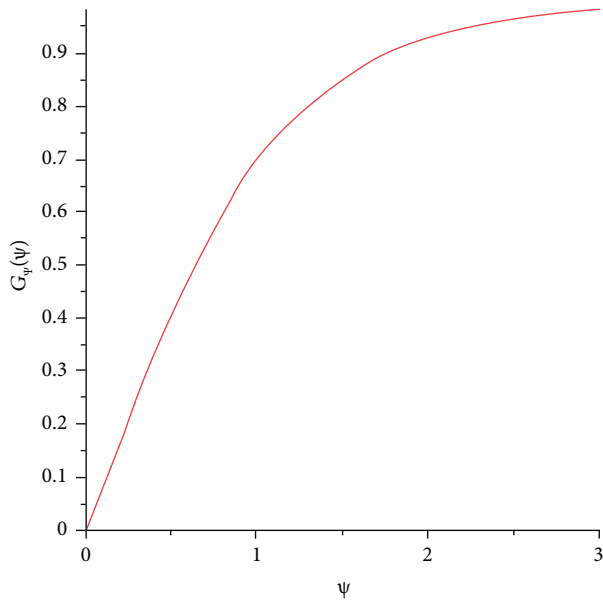
(d)



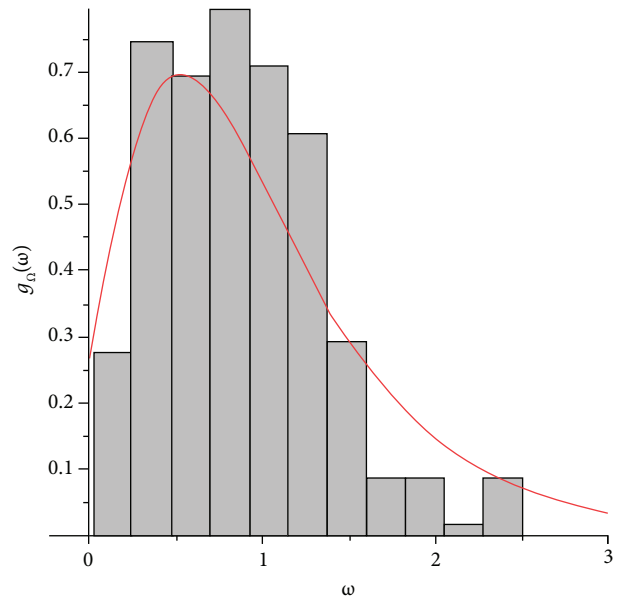
(e)



(f)



(g)

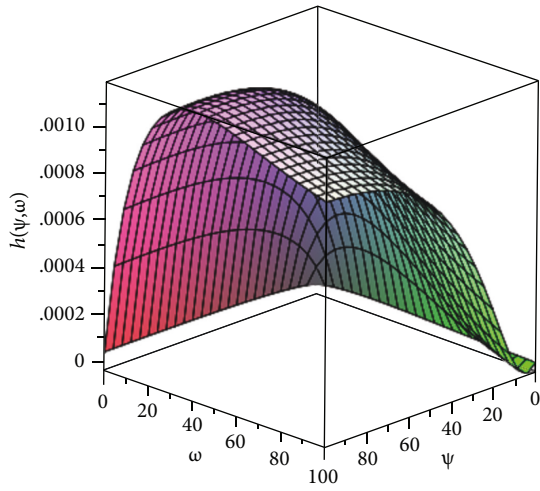


(h)

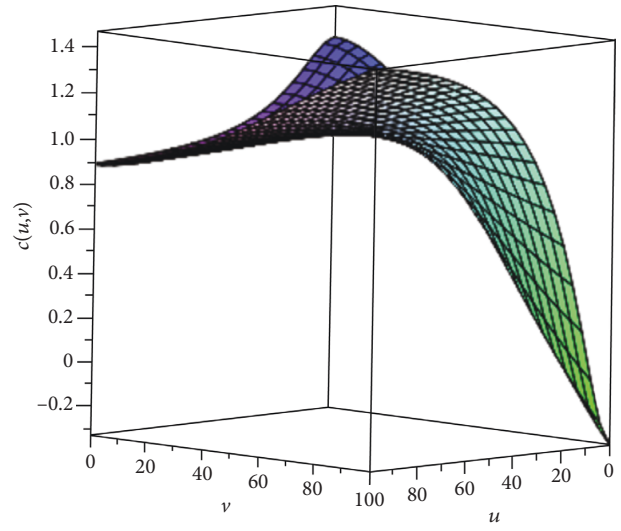
FIGURE 4: Continued.



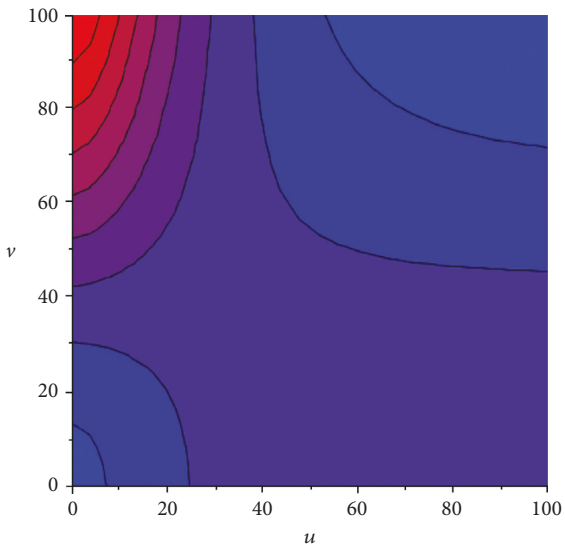




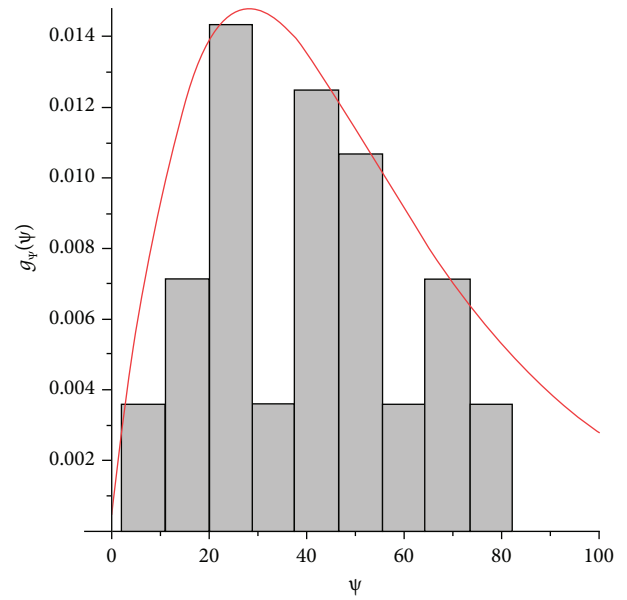
(c)



(d)



(e)



(f)

FIGURE 5: Continued.

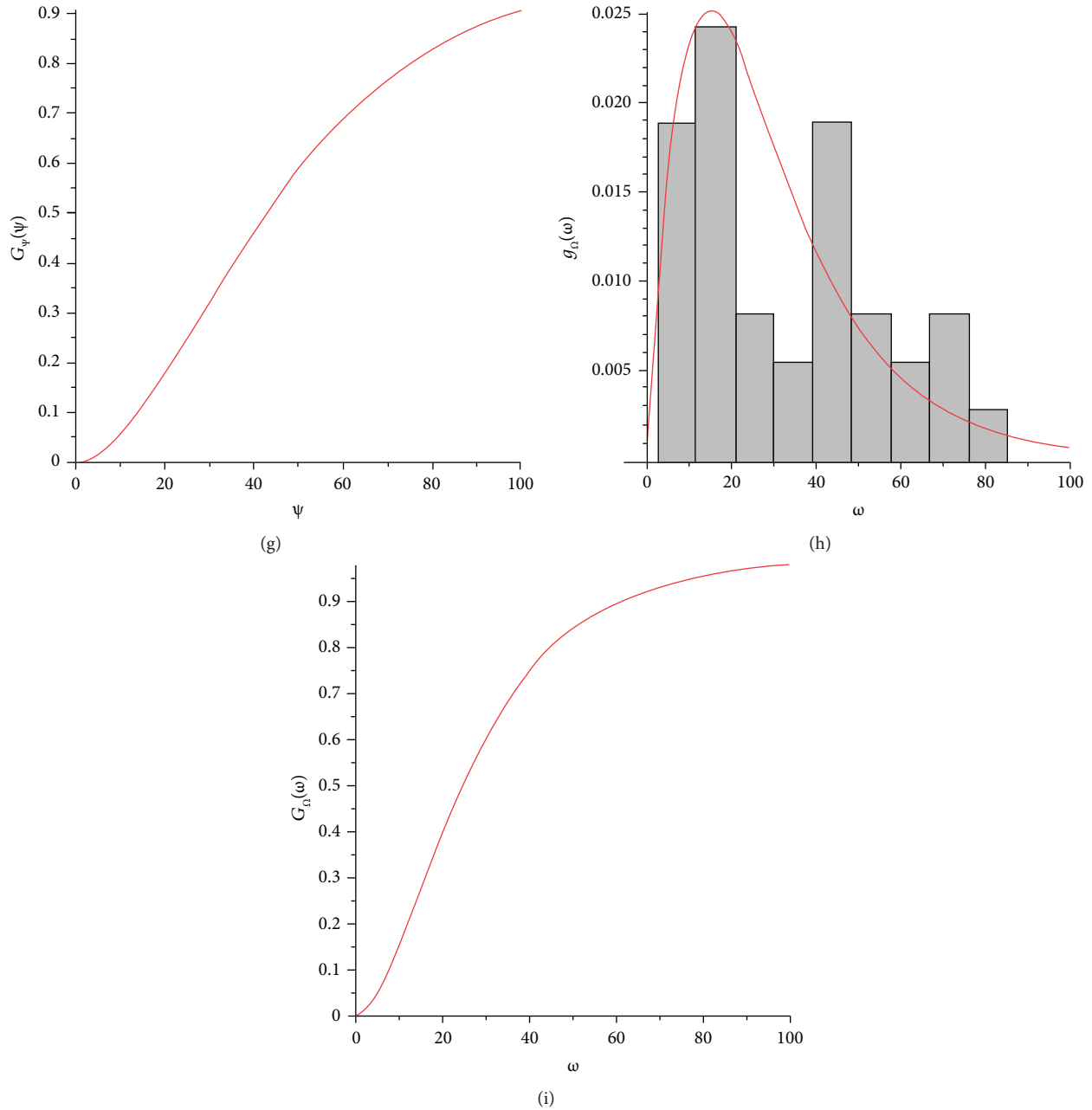


FIGURE 5: Statistical functions fitted for the dataset: (a) joint density function, (b) cumulative function, (c) hazard function, (d) copula function, (e) contour plot of copula function, and (f)–(i) marginals.

**6.1. Financial Data.** In this section, we apply  $BIML(\theta, \xi_1, \xi_2, \xi_3)$  to a bivariate financial dataset. The dataset consists of the absolute normalization of the daily closing prices of NASDAQ Composite index and the Microsoft Corporation share price between 1 January 2020 and 31 December 2020. The data are available at <https://finance.yahoo.com/>. Fung and Seneta [53] analyzed the returns of the daily closing prices of NASDAQ Composite index and the Microsoft Corporation share price between 1 January 1996 and 31 December 2005 as a bivariate set. The maximum likelihood estimates with Akaike's information criterion (AIC) and Bayesian

information criterion (BIC) are given in Table 2. The statistical functions related to the fitted distribution are presented in Figure 4.

**6.2. UEFA Champion's League Data.** In this section, the UEFA Champion's League data obtained from [54] have been analyzed to show the applicability of the new model and the performance of the maximum likelihood method for different types of data. The estimated parameters with AIC and BIC are in Table 3. The statistical functions related to the fitted distribution are presented in Figure 5.

## 7. Conclusion

The univariate one-parameter Lindley model is a simple probability distribution that has a lot of preferable properties and various applications. This study presented a new bivariate parametric probability distribution using the one-parameter modified Lindley model as a base line distribution, named bivariate modified Lindley (BIML) distribution. Statistical quantities of the new model have been derived in explicit forms. That strongly supports the usefulness of the new model from theoretical and also practical point of view. The new proposed model has absolutely continuous probability density function that changes according to parameters. The hazard function presented different shapes. The flexibility and applicability of the new model have been shown via simulation. The maximum likelihood estimators have been introduced. The method presented good performance via Monte Carlo simulation. The new model has been applied for two different types of data.

## Data Availability

The data used to support the findings of the study are included within the article.

## Conflicts of Interest

The author declares no conflicts of interest.

## References

- [1] G. Aryal and I. Elbatal, "Kumaraswamy modified inverse Weibull distribution: theory and application," *Applied Mathematics & Information Sciences*, vol. 9, no. 2, p. 651, 2015.
- [2] A. Z. Afify, M. Alizadeh, E. Altun, and G. Ö. Kadilar, "The odd Exponentiated half-logistic-G family: properties, characterizations and applications," *Chilean Journal of Statistics*, vol. 8, pp. 65–91, 2017.
- [3] A. S. Hassan and S. G. Nassr, "The inverse weibull generator of distributions, properties and applications," *Journal of Data Science*, vol. 16, pp. 723–742, 2018.
- [4] J. Farrukh, F. Jamal, M. A. Nasir, G. Elgarhy, and N. Khan, "Generalized inverted kumaraswamy generated family of distributions: theory and applications," *Journal of Applied Statistics*, vol. 46, 2018.
- [5] Q. Ramzan, M. Amin, M. Amin, A. Elhassanein, and M. Ikram, "The extended generalized inverted Kumaraswamy Weibull distribution: properties and applications," *AIMS Mathematics*, vol. 6, no. 9, pp. 9955–9980, 2021.
- [6] Q. Ramzan, S. Qamar, M. Amin, H. Alshambari, A. Nazeer, and A. Elhassanein, "On the Extended Generalized Inverted Kumaraswamy Distribution," *Computational Intelligence and Neuroscience*, vol. 2022, Article ID 1612959, 2022.
- [7] D. V. Lindley, "Fiducial distributions and bayes' theorem," *Journal of the Royal Statistical Society: Series B*, vol. 20, no. 1, pp. 102–107, 1958.
- [8] M. E. Ghitany, B. Atieh, and S. Nadarajah, "Lindley distribution and its application," *Mathematics and Computers in Simulation*, vol. 78, no. 4, pp. 493–506, 2008.
- [9] H. Zakerzadeh and A. Dolati, "Generalized Lindley distribution," *Journal of Mathematical Extension*, vol. 3, pp. 13–25, 2009.
- [10] M. E. Ghitany, F. Alqallaf, D. K. Al-Mutairi, and H. A. Husain, "A two-parameter weighted Lindley distribution and its applications to survival data," *Mathematics and Computers in Simulation*, vol. 81, no. 6, pp. 1190–1201, 2011.
- [11] H. S. Bakouch, B. M. Al-Zahrani, A. A. Al-Shomrani, V. A. A. Marchi, and F. Louzada, "An extended Lindley distribution," *Journal of the Korean Surgical Society*, vol. 41, no. 1, pp. 75–85, 2012.
- [12] S. Ali, "On the bayesian estimation of the weighted Lindley distribution," *Journal of Statistical Computation and Simulation*, vol. 85, no. 5, pp. 855–880, 2015.
- [13] P. L. Ramos and F. Louzada, "The generalized weighted Lindley distribution: properties, estimation, and applications," *Cogent Mathematics*, vol. 3, no. 1, Article ID 1256022, 2016.
- [14] P. L. Ramos, F. Louzada, and V. G. Cancho, "Maximum likelihood estimation for the weighted Lindley distribution parameter under different types of censoring," *Revista Brasileira de Biometria/Biometric Brazilian Journal*, vol. 35, no. 1, pp. 115–131, 2017.
- [15] F. Louzada and P. L. Ramos, "A new long-term survival distribution," *Biostatistics and Biometrics Open Access Journal*, vol. 1, no. 5, pp. 104–109, 2017.
- [16] S. A. Kemaloglu and M. Yilmaz, "Transmuted two-parameter Lindley distribution," *Communications in Statistics - Theory and Methods*, vol. 46, no. 23, pp. 11866–11879, 2017.
- [17] A. Asgharzadeh, S. Nadarajah, and F. Sharafi, "Weibull Lindley distribution," *REVSTAT Statistical Journal*, vol. 16, pp. 87–113, 2018.
- [18] P. L. Ramos, M. P. Almeida, V. L. D. Tomazella, and F. Louzada, "Improved bayes estimators and prediction for the wilson-hilferty distribution," *Anais da Academia Brasileira de Ciencias*, vol. 91, no. 3, Article ID e20190002, 2019.
- [19] R. Shanker, K. K. Shukla, and T. A. Leonida, "Weighted quasi Lindley distribution with properties and applications," *International Journal of Statistics and Applications*, vol. 9, no. 1, pp. 8–20, 2019.
- [20] A. Z. Afify, M. Nassar, G. M. Cordeiro, and D. Kumar, "The Weibull Marshall-Olkin Lindley distribution: properties and estimation," *Journal of Taibah University for Science*, vol. 14, no. 1, pp. 192–204, 2020.
- [21] D. Hamed and A. Alzagal, "New class of Lindley distributions: properties and applications," *Journal of Statistical Distributions and Applications*, vol. 811 pages, 2021.
- [22] R. Shanker and A. Mishra, "A quasi Lindley distribution," *African Journal of Mathematics and Computer Science Research*, vol. 6, no. 4, pp. 64–71, 2013.
- [23] R. Shanker, K. K. Shukla, R. Shanker, and T. A. Leonida, "A three-parameter Lindley distribution," *American Journal of Mathematics and Statistics*, vol. 7, no. 1, pp. 15–26, 2017.
- [24] A. Asgharzadeh, H. S. Bakouch, S. Nadarajah, and F. Sharafi, "A new weighted Lindley distribution with application," *Brazilian Journal of Probability and Statistics*, vol. 30, no. 1, pp. 1–27, 2016.
- [25] R. D. Gupta and D. Kundu, "A new class of weighted exponential distributions," *Statistics*, vol. 43, no. 6, pp. 621–634, Article ID MR2588273, 2009.
- [26] W. Wongrin and W. Bodhisuwan, "The Poisson-generalised Lindley distribution and its applications," *Songklanakarin Journal of Science and Technology*, vol. 38, no. 6, pp. 645–656, 2016.
- [27] S. K. Maurya, D. Kumar, P. Kumar, S. K. Singh, and U. Singh, "A new extension of Lindley distribution and its application," *Journal of Scientific Research*, vol. 64, no. 2, pp. 366–373, 2020.

- [28] G. M. Cordeiro and M. De Castro, "A new family of generalized distributions," *Journal of Statistical Computation and Simulation*, vol. 81, no. 7, pp. 883–898, 2011.
- [29] A. L. Mota, P. Ramos, P. H. Ferreira, V. L. D. Tomazella, and F. Louzada, "A reparameterized weighted Lindley distribution: properties, estimation and applications," *Revista Colombiana de Estadística - Applied Statistics*, vol. 44, no. 1, pp. 65–90, 2021.
- [30] A. A. Rather and G. Özel, "The weighted power Lindley distribution with applications on the life time data," *Pakistan Journal of Statistics and Operation Research*, vol. 16, no. 2, pp. 225–237, 2020.
- [31] I. Elbatal, Y. M. El Gebaly, and E. A. Amin, "An extended power Lindley distribution and its application," *Afrika Statistika*, vol. 11, no. 2, pp. 1075–1094, 2016.
- [32] C. Chesneau, L. Tomy, and J. Gillariose, "A new modified Lindley distribution with properties and applications," *Journal of Statistics and Management Systems*, vol. 24, no. 7, pp. 1383–1403, 2021.
- [33] R. Diandarma, S. Nurrohmah, and I. Fithriani, "Discrete Lindley distribution," *Proceedings of the 5Th International Symposium on Current Progress in Mathematics and Sciences (Iscpms2019)*, vol. 2242, Article ID 030024, 2020.
- [34] J. F. Carriere, "Bivariate survival models for coupled lives," *Scandinavian Actuarial Journal*, vol. 2000, no. 1, pp. 17–32, 2000.
- [35] C. Jagger and C. J. Sutton, "Death after marital bereavement-is the risk increased?" *Statistics in Medicine*, vol. 10, no. 3, pp. 395–404, 1991.
- [36] N. Balakrishnan and C. Lai, *Continuous Bivariate Distributions*, Springer, Berlin, Germany, 2 edition, 2009.
- [37] D. Kundu and R. D. Gupta, "Bivariate generalized exponential distribution," *Journal of Multivariate Analysis*, vol. 100, no. 4, pp. 581–593, 2009.
- [38] D. Kundu and R. D. Gupta, "A class of bivariate models with proportional reversed hazard marginals," *Sankhya B*, vol. 72, no. 2, pp. 236–253, 2010.
- [39] D. Kundu and A. Gupta, "On bivariate inverse weibull distribution," *Brazilian Journal of Probability and Statistics*, vol. 31, no. 2, pp. 275–302, 2017.
- [40] H. Z. Muhammed, "Bivariate generalized burr and related distributions: properties and estimation," *Journal of Data Science*, vol. 17, no. 3, pp. 532–548, 2019.
- [41] A. S. Al-Moisheer, "Bivariate mixture of inverse Weibull distribution: properties and estimation," *Mathematical Problems in Engineering*, vol. 2020, Article ID 5234601, 2020.
- [42] H. Z. Muhammed, "Bivariate dagum distribution," *Int. J. Reliab. Appl.* vol. 18, no. 2, pp. 65–82, 2017.
- [43] S. Mondal and D. Kundu, "A bivariate inverse Weibull distribution and its applications in complementary risks models," *Journal of Applied Statistics*, vol. 47, no. 6, pp. 1084–1108, 2021.
- [44] V. S. Vaidyanathan and A. S. Varghese, "Morgenstern type bivariate Lindley distribution," *Stat. Optim. Inf. Comput.* vol. 4, pp. 132–146, 2016.
- [45] P. Y. Thomas and J. Jose, "A new bivariate distribution with Rayleigh and Lindley distributions as marginals," *Journal of Statistical Theory and Practice*, vol. 14, no. 2, p. 28, 2020.
- [46] J. A. Darwish, L. I. Al turk, and M. Q. Shahbaz, "Bivariate transmuted Burr distribution: properties and applications," *Pak.j.stat.oper.res.* vol. 17, no. 1, pp. 15–24, 2021.
- [47] M. Ragab and A. Elhassanein, "A new bivariate extended generalized inverted Kumaraswamy Weibull distribution," *Advances in Mathematical Physics*, vol. 2022, Article ID 1243018, 2022.
- [48] A. Alzaatreh, C. Lee, and F. Famoye, "A new method for generating families of continuous distributions," *Metron*, vol. 71, no. 1, pp. 63–79, 2013.
- [49] M. Ganji, H. Bevrani, and N. Hami, "A new method for generating continuous bivariate families," *Journal of the Iranian Statistical Society*, vol. 17, no. 1, pp. 109–129, 2018.
- [50] T. S. Durrani and X. Zeng, "Copulas for bivariate probability distributions," *Electronics Letters*, vol. 43, no. 4, 2007.
- [51] J. Navarro, "Characterizations using the bivariate failure rate function," *Statistics & Probability Letters*, vol. 78, no. 12, p. 1349, 2010.
- [52] M. V. de Oliveira Peres, J. A. Achcar, and E. Z. Martinez, "Bivariate lifetime models in presence of cure fraction: a comparative study with many different copula functions," *Heliyon*, vol. 6, no. 6, Article ID e03961, 2020.
- [53] T. Fung and E. Seneta, "Modelling and estimation for bivariate financial returns," *International Statistical Review*, vol. 78, no. 1, pp. 117–133, 2010.
- [54] S. G. Meintanis, "Test of fit for Marshall-Olkin distributions with applications," *Journal of Statistical Planning and Inference*, vol. 137, no. 12, pp. 3954–3963, 2007.

## Research Article

# Economic Policy Uncertainty and Sectoral Trading Volume in the U.S. Stock Market: Evidence from the COVID-19 Crisis

Dohyun Pak and Sun-Yong Choi 

*Department of Financial Mathematics, Gachon University, Gyeonggi 13120, Republic of Korea*

Correspondence should be addressed to Sun-Yong Choi; [sunyongchoi@gachon.ac.kr](mailto:sunyongchoi@gachon.ac.kr)

Received 26 May 2021; Accepted 22 March 2022; Published 25 April 2022

Academic Editor: Sameh S. Askar

Copyright © 2022 Dohyun Pak and Sun-Yong Choi. This is an open access article distributed under the Creative Commons Attribution License, which permits unrestricted use, distribution, and reproduction in any medium, provided the original work is properly cited.

We empirically analyze the impact of economic uncertainty due to the COVID-19 pandemic on the trading volume of each sector in the S&P 500 index. Wavelet coherence analysis is carried out using economic policy uncertainty data and the trading volume of each sector in the S&P 500 index from July 2004 to September 2020. Furthermore, we apply multifractal detrended fluctuation (MF-DFA) analysis to the trading volume series of all sectors. The wavelet coherence analysis shows that the COVID-19 pandemic has substantially influenced trading volume in all sectors. However, the impact of the pandemic is different from that during the global financial crisis in some sectors, such as information technology, consumer discretionary, and communication services. Because of the lockdown taken to suppress COVID-19, increased remote working and remote learning are the main reasons for these results. Additionally, according to the MF-DFA analysis, the trading volume of all the sectors has clear multifractal characteristics, and they are all nonpersistent. Specifically, trading volumes of the real estate and materials sector are highly correlated, whereas the trading volumes of industry and information technology sectors are comparatively less correlated.

## 1. Introduction

Trading volume has long been a major concern in finance. For example, many studies have reported that trading volume has a relationship with returns and the absolute value of returns (Crouch [1]; Copeland [2]; Karpoff [3]; Jones et al. [4]; Foster [5]; Kramer [6]; Wang and Yau [7]; Chen et al. [8]; Gagnon and Karolyi [9]; Lin [10]; Wang et al. [11]). According to these studies, there is a positive relationship between trading volume and stock returns. Similarly, the trading volume has also been investigated in terms of volatility (Karpoff [3]; Foster [5]; Lee and Rui [12]; Güner and Önder [13]; Li and Wu [14]; Wen and Yang [15]; Rossi and De Magistris [16]; Darolles et al. [17]; Clements and Neda [18]; Ftiti et al. [19]; Kao et al. [20]; Khuntia and Pattanayak [21]). One of the important motivations of these studies is that the volume of transactions represents the scale and rate of information flow to the stock market (Wang and Yau [7]; Clements and Neda [18]; Ftiti et al. [19]). That is, the trading volume captures the most important information

about market participants' trading activities. Recently, several studies have investigated the relationship between changes in trading volume and uncertainty (Choi [22]; Rehse et al. [23]; Nagar et al. [24]; Chen et al. [25]; Chiah and Zhong [26]). In particular, Chiah and Zhong [26] and Chen et al. [25] examined how changes in the financial markets caused by the coronavirus disease 2019 (COVID-19) pandemic affect the trading volume. Meanwhile, numerous mathematical models are also used to investigate and control the COVID-19 pandemic. First, many studies describe the main features of the COVID-19 pandemic using the susceptible-infected-removed (SIR) models (Colombo et al. [27]; Tian et al. [28]; Alshomrani et al. [29]; Leung et al. [30]; Read et al. [31]; Wu et al. [32]; Yang et al. [33]). In these studies, the SIR-type models are fitted to the actual data, and the reproductive number was estimated (Read et al. [31]). Furthermore, the COVID-19 pandemic peaks and sizes are predicted based on the SIR-type models (Yang et al. [33]). Second, agent-based models have been used to capture the interaction structure of the underlying populations for the

COVID-19 pandemic (Adiga et al. [34]). For example, Agrawal et al. [35] build an agent-based simulator to study the impact of various nonpharmaceutical interventions in the COVID-19 pandemic and demonstrate the ability of simulators through several case studies. Gharakhanlou and Hooshangi [36] develop an agent-based model that simulates the spatio-temporal outbreak of COVID-19. Additionally, they simulate the transmission of COVID-19 between human agents based on one of the SIR-type models. Third, there are studies on developing new mathematical models for COVID-19. For example, Matouk [37] suggests a susceptible-infected model with a multi-drug resistance, called SIMDR. They also investigated the dynamic behavior of the SIMDR model for the COVID-19 pandemic. Mohammed et al. [38] examine the dynamic behavior of COVID-19 using Lotka–Volterra-based models. Particularly, their proposed models contain fractional derivatives, which present a more sufficient and realistic description of the COVID-19 phenomena. In this study, we examine the impact of economic uncertainty on the trading volume of the U.S. stock market. We employ the U.S. daily news-based economic policy uncertainty (EPU) index to measure economic uncertainty. To do that, we calculate industry-specific trading volume and investigate the relationship between the trading volume of each industry and EPU. Furthermore, we investigate the multifractal nature of the industry-specific trading volume. Based on this investigation, we analyze the fluctuations of trading volumes. Industry-specific trading volume is defined based on the trading volume of 11 S&P 500 index sectors. We apply wavelet coherence analysis to estimate the interdependence and causality between EPU and each sector's trading volume from January 2008 to September 2020. Furthermore, we examine the relationship between them in terms of several events during the sample period such as the global financial crisis (GFC) and COVID-19 pandemic. Recently, many studies have investigated the relationship between EPU and volatility of various financial assets, such as the stock market (Ko and Lee [39]; Liu and Zhang [40]; Li et al. [41]; Choi [42], oil Mei et al. [43]; Ma et al. [44]; Wen et al. [45], foreign exchange Juhro and Phan [46]; Bartsch [47]; Chen et al. [48], and cryptocurrency Demir et al. [49]; Wang et al. [50]; Cheng and Yen [51]). Unlike the previous literature, studies of the relationship between the trading volume and EPU are relatively scarce. To the best of our knowledge, this is the first report on the relationship between EPU and trading volume. Furthermore, we employ the multifractal detrended fluctuation analysis (MF-DFA) approach introduced by Kantelhardt et al. [52] to investigate long-range autocorrelations and describe the multifractal properties of the trading volume. Several studies show that stock markets are multifractal (Bacry et al. [53]; Kwapien et al. [54]; Zunino et al. [55]; Wang et al. [56]; Machado [57]; Choi [58]). The contributions of this study are threefold: first, it adds to the flourishing strand of the literature on the impact of COVID-19 on the U.S. stock market (Mazur et al. [59]; Sharif et al. [60]; Hanke et al. [61]; Smales [62]; Baker et al. [63]). Second, our study extends the literature by examining the change in trading volume at the industry level following extreme

events. In particular, while some studies have examined the relationship between the effect of the COVID-19 pandemic and trading volume of individual stocks or the stock market in each country (Ortmann et al. [64]; Chiah and Zhong [26]), no studies have addressed the trading volume of each sector. Third, we inspect whether the trading volumes for all sectors have multifractal characters. The investigation of the multifunctional nature of the trading volume at the industrial level is also not adequately explored in the existing literature. The remainder of this study is organized as follows: Section 2 describes the data and reviews the wavelet coherence analysis and MF-DFA approaches. Section 3 presents the main findings. Finally, concluding remarks are provided in Section 4.

## 2. Data Description and Methodology

*2.1. Data Description.* The time series of EPU is obtained from <https://www.policyuncertainty.com>. This website presents data on the news-based EPU index proposed by Baker et al. [65]. The sample period runs from July 2004 to September 2020. The index measures EPU using information from keyword searches in 10 large newspapers and is normalized to the volume of news articles discussing EPU.

Figure 1 shows the monthly time series of EPU and total trading volume (the sum of the trading volume of all the shares included in the S&P 500 index) during the sample period and several events that shocked the market such as the Lehman bankruptcy, debt-ceiling crisis, trading tensions between the United States and China, and the COVID-19 pandemic. As can be seen, the EPU index during the pandemic is significantly higher than in other events. In addition, changes in total trading volume tend to be similar to changes in EPU. About 500 companies in the U.S. stock market are used to define the S&P 500 index, which has 11 sectors in total (we use the global industry classification standard). The market cap of the S&P 500 is 70–80% of total U.S. stock market capitalization. Consequently, the sectors of the index naturally become a classification criterion for the U.S. economy. To calculate the trading volume of each sector, we first define the daily average sectoral trading volume of the  $i$ -th sector at time  $t$  as follows:

$$r_{i,t} = \frac{1}{N(t)} \sum_{j=1}^{N(t)} V_{j,t}, \quad (1)$$

where  $N(t)$  is the total number of stocks (the total number of shares ( $N$ ) changes as the incorporated stock in the  $i$ -th sector changes) in the sector at time  $t$  and  $V_{j,t}$  is the trading volume of the  $j$ -th stock in the  $i$ -th sector at time  $t$ . Because the EPU is calculated monthly, we define the monthly average trading volume (MATV)  $\bar{r}_{i,m}$  for  $m, \{m = \text{July 2004, August 2004, } \dots \text{ September 2020}\}$  as the sum of average daily trading volume in each month. Table 1 presents the summary statistics of MATV. In addition, the MATV in each sector is shown in Figure 2. According to Table 1 and Figure 2, the MATV of the IT and financial industries is large and the fluctuation of MATV is also large. On the contrary, the MATV of the utilities and real estate

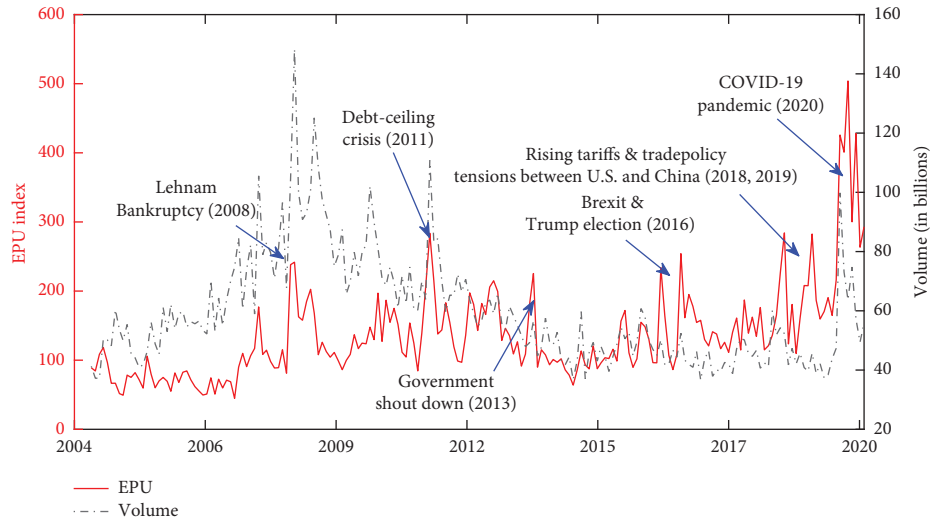


FIGURE 1: The monthly EPU index from July 2004 to September 2020. The events are based on those presented on the website.

TABLE 1: Summary statistics of MATV in the S&P 500 index. Here, the statistics are obtained based on scale-adjusted MATV (divided by 10 million).

Sectors	Observed	Mean	Maximum	Minimum	Standard deviation	Skewness	Kurtosis
Communication services	195	19.4914	33.7481	12.1475	3.8021	0.4977	0.4525
Consumer discretionary	195	10.9942	23.6278	6.5459	3.8239	1.1698	0.5081
Consumer staples	195	9.9723	24.7695	5.9175	2.8209	1.5751	3.8429
Energy	195	14.023	39.8828	7.8626	4.5355	2.1723	8.1248
Financial	195	13.3954	53.8857	3.5619	8.5303	1.9237	5.1907
Health care	195	8.1234	17.7929	4.5768	2.2544	1.2121	1.6574
Industrials	195	7.6887	23.1635	4.3141	3.0851	1.9966	5.0637
Information technology	195	33.5651	108.5334	11.6259	18.1847	0.8331	0.5104
Materials	195	6.8426	20.1044	3.0459	2.5255	1.509	4.2935
Real estate	195	3.8818	13.2393	1.0849	1.8127	1.7786	6.2873
Utilities	195	5.3573	10.6955	2.4811	1.3121	0.3104	1.9175

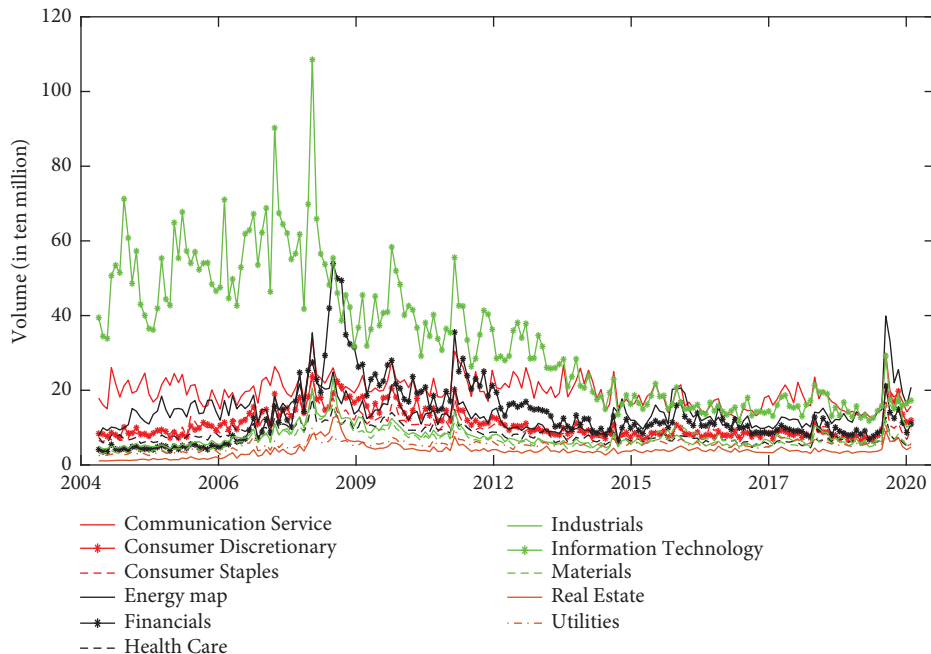


FIGURE 2: MATV ( $\{\bar{r}_{i,m}, i = 1, 2, \dots, 11\}$ ) from July 2004 to September 2020.

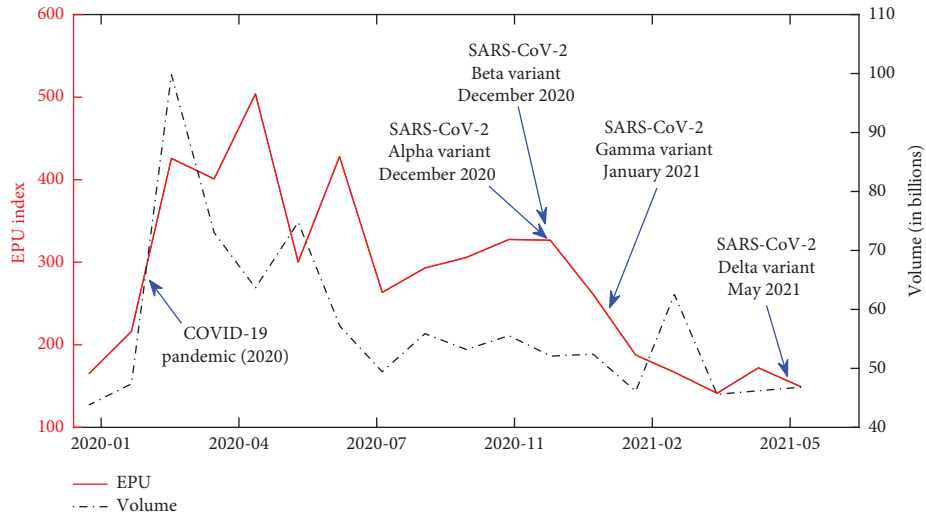


FIGURE 3: The monthly EPU index and total volume from January 2020 to July 2021.

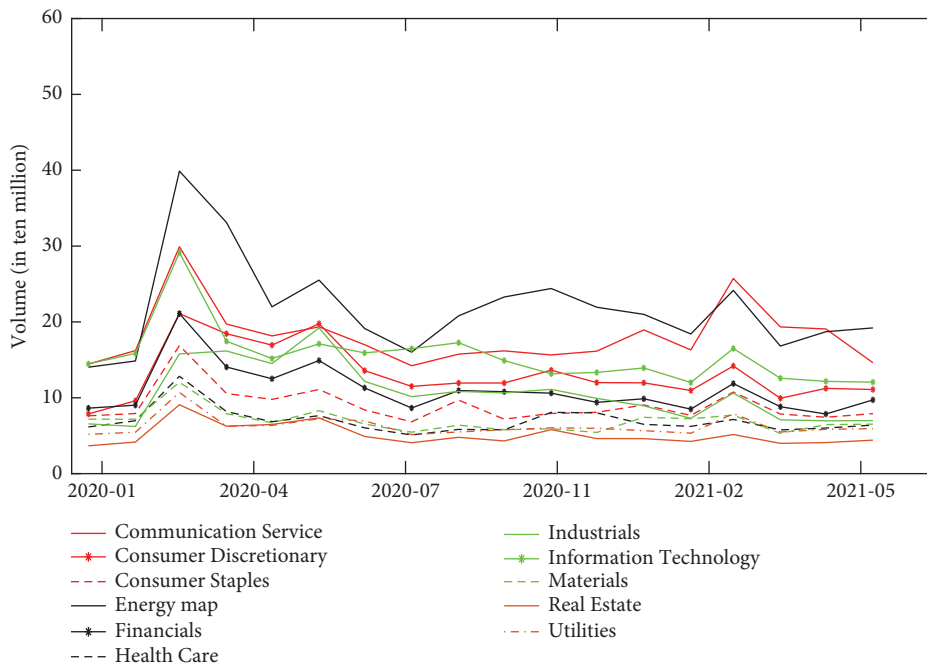


FIGURE 4: The MATV for 11 sectors from January 2020 to July 2021.

sectors is smaller than those of the other industries and their changes are also small. Furthermore, during both the GFC and the COVID-19 pandemic, there is a considerable change in trading volume in all sectors. According to the World Health Organization (WHO) (“Tracking SARS-CoV-2 variants” <https://www.who.int/en/activities/tracking-SARS-CoV-2-variants>), several COVID-19 variants have been observed, namely, alpha, beta, gamma, and delta. As they were all officially designated after December 2020, our sample data do not include the impact of the new COVID-19 variants on the EPU and the MATV. Therefore, we provide the extended EPU and MATV, that is, from January 2020 to June 2021, in Figures 3 and 4. In Figure 3, the designation date of COVID-19 variances is indicated. When looking at

the plots, the EPU and the volume do not seem to have been significantly affected by the occurrence of COVID-19 variances. Furthermore, MATVs in all sectors do not appear to be significantly related to the COVID-19 variants. However, it is noteworthy that the MATV of the energy sector from January 2020, except for a few periods, is the largest among the MATVs of all sectors. This is largely different from the MATV results before 2020 in Figure 2. We use monthly EPU and the monthly sample data during the COVID-19 pandemic are not enough to apply to the wavelet coherency analysis. To solve this problem, a short-term sample data set is needed, such as weekly or daily data. Additionally, a longer study period may capture the impact of the new COVID-19 variants. These are opportunities for future studies.



## 2.2. Methodology

**2.2.1. Wavelet Coherence Analysis.** Using wavelet coherence analysis with the Morlet specification, we investigate the causality and interdependence between the EPU and trading volume. Based on this analysis, we make inferences in a time-frequency frame. From several studies (Ko and Lee [39]; Kristoufek [66]; Pal and Mitra [67]; Sharif et al. [60]), this can be briefly explained as follows: For time series  $x(t)$ , the continuous wavelet transform is given by the following equation:

$$W_x(\tau, s) = \int_{-\infty}^{\infty} x(t) \tilde{\psi}_{\tau, s}^*(t) dt, \quad (2)$$

where  $s$  is the scaling factor adjusting the length of the wavelet and  $\tau$  is the translation parameter adjusting the wavelet location in time.  $\tilde{\psi}_{\tau, s}^*(t)$  is the complex conjugate function of  $\psi_{\tau, s}^*(t)$ . In addition,  $\tilde{\psi}$  is found by scaling and shifting the mother wavelet  $\psi$ . According to Soares et al. [68], we choose the Morlet wavelet suggested by Goupillaud et al. [69] as the mother wavelet  $\psi$ :

$$\psi_{\tau, s}^*(t) = \frac{1}{\sqrt{|s|}} \psi\left(\frac{t - \tau}{s}\right), \quad s, \tau \in \mathbb{R}, s \neq 0. \quad (3)$$

For the  $x(t)$  and  $y(t)$  time series, the cross-wavelet transform is defined as follows:

$$W_{xy}(\tau, s) = W_x(\tau, s) W_y^*(\tau, s). \quad (4)$$

From the cross-wavelet transform, the wavelet coherence between two series,  $x(t)$  and  $y(t)$ , is given by Torrence and Webster [70]:

$$R^2(\tau, s) = \frac{|S(1/s W_{xy}(\tau, s))|^2}{S(1/s |W_x(\tau, s)|^2) S(1/s |W_y(\tau, s)|^2)}, \quad (5)$$

where  $S$  is the smooth operator in time and scale.  $R^2(\tau, s)$  is a squared correlation localized in time frequency and  $0 \leq R^2(\tau, s) \leq 1$ . Based on Bloomfield et al. [71], the phase difference from the phase angle obtained by the cross-wavelet transform is as follows:

$$\rho_{xy}(\tau, s) = \tan^{-1} \left( \frac{\text{Im}[S(1/s W_{xy}(\tau, s))]}{\text{Re}[S(1/s W_{xy}(\tau, s))]} \right), \quad (6)$$

where  $\rho_{xy} \in [-\pi, \pi]$ ,

where  $\text{Re}$  and  $\text{Im}$  are the real and imaginary parts of the smooth cross-wavelet transform, respectively.  $\rho_{xy}(\tau, s)$  can explain the interdependence and causality between the two time series,  $x(t)$  and  $y(t)$ , while the squared wavelet coherence does not know the direction of the relationship. Based on several studies (Flor and Klarl [72]; Cai et al. [73]; Funashima [74]), we can determine the connection between the two time series,  $x(t)$  and  $y(t)$ , by understanding the scale of the phase difference,  $\rho_{xy}$ . If  $\rho_{xy} \in (0, \pi/2)$ ,  $x(t)$  and  $y(t)$  have positive relations, and  $x(t)$  leads  $y(t)$ . If  $\rho_{xy} \in (-\pi/2, 0)$ ,  $x(t)$  lags  $y(t)$ . For  $\rho_{xy} \in (\pi/2, \pi)$ ,  $x(t)$  and  $y(t)$  have negative relations, but  $x(t)$  lags  $y(t)$ . If  $\rho_{xy} \in (-\pi, -\pi/2)$ , the two time series also have negative relations, with  $x(t)$  leading  $y(t)$ .

**2.2.2. Multifractal Detrended Fluctuation Analysis.** The MF-DFA method represents the multifractal properties of a financial time series. According to Kantelhardt et al. [52], the MF-DFA procedure consists of the following five steps (Wang et al. [75]). Let  $\{x_k, k = 1, \dots, N\}$  be a time series, where  $N$  is the length of the series:

(i) Step 1. Determine the profile

$$Y(i) (i = 1, 2, \dots, N) \cdot Y(i) = \sum_{k=1}^i (x(k) - \bar{x}), \quad (7)$$

where

$$\bar{x} = \sum_{k=1}^N x \frac{(k)}{N}. \quad (8)$$

(ii) Step 2. Divide the profile  $\{Y(i)\} (i = 1, 2, \dots, N)$  into  $N_s \equiv \text{int}(N/s)$  nonoverlapping segments of equal length  $s$ . To cover the whole sample, repeat the same procedure from the end of the sample. In this way,  $2N_s$  segments are obtained altogether:

$$\begin{aligned} & \{Y[(\nu - 1)s + i]\}_{i=1}^s, \quad \nu = 1, 2, \dots, N_s, \\ & \{Y[N - (\nu - N_s)s + i]\}_{i=1}^s, \quad \nu = N_s + 1, N_s + 2, \dots, 2N_s. \end{aligned} \quad (9)$$

(iii) Step 3. Calculate the local trend for each of the  $2N_s$  segments. For every segment, the local trend is estimated by a least-square fitting polynomial. Consequently, the variance is determined as follows:

$$F^2(s, \nu) = \begin{cases} \frac{1}{s} \sum_{i=1}^s \{Y[(\nu - 1)s + i] - \hat{Y}_\nu^m(i)\}^2, & \nu = 1, 2, \dots, N_s, \\ \frac{1}{s} \sum_{i=1}^s \{Y[N - (\nu - N_s)s + i] - \hat{Y}_\nu^m(i)\}^2, & \nu = N_s + 1, N_s + 2, \dots, 2N_s. \end{cases} \quad (10)$$

Here,  $\hat{Y}_\nu^m(i)$  is the fitting polynomial with order  $m$  in segment  $\nu$ . In this study, we adopt a linear polynomial ( $m = 1$ ) to prevent overfitting and facilitate the calculation (Lashermes et al. [76]; Ning et al. [77]).

- (iv) Step 4. Average over all the segments. Then, we obtain the  $q$ -th order fluctuation function:

$$F_q(s) = \begin{cases} \left[ \frac{1}{2N_s} \sum_{\nu=1}^{2N_s} (F^2(s, \nu))^{q/2} \right]^{1/q}, & q \neq 0, \\ \exp \left[ \frac{1}{4N_s} \sum_{\nu=1}^{2N_s} \ln(F^2(s, \nu)) \right], & q = 0. \end{cases} \quad (11)$$

- (v) Step 5. Determine the scaling behavior of the fluctuation functions. Compare the log-log plots  $F_q(s)$  with  $s$  for each value of  $q$ . If the series are long-range power-law correlated,  $F_q(s)$  increases for high values of  $s$ . The power law is expressed as follows:

$$F_q(s) \propto s^{h(q)}, \quad (12)$$

where  $h(q)$  represents the generalized Hurst exponent. Equation (12) can be written as  $F_q(s) = a \cdot s^{h(q)} + b$ . After taking the logarithms of both sides,

$$\log(F_q(s)) = h(q) \cdot \log(s) + c, \quad (13)$$

where  $c$  is a constant.

The exponent  $h(q)$  depends on  $q$ . The time series is monofractal when  $h(q)$  does not depend on  $q$ ; otherwise, it is multifractal. For  $q = 2$ ,  $h(2)$  is identical to the Hurst exponent Calvet and Fisher [78]. Thus, the function  $h(q)$  is called a generalized Hurst exponent. If  $h(2) = 0.5$ , the time series are not correlated, and it follows a random-walk process. When  $0.5 < h(2)$ , the time series is long-range dependent, and an increase (decrease) is more likely to be followed by another increase (decrease).  $h(2) < 0.5$  means a nonpersistent series; that is, an increase (decrease) is more likely to be followed by a decrease (increase). According to Kantelhardt et al. [52],  $h(q)$  relates to the multifractal scaling exponents  $\tau(q)$  as follows:

$$\tau(q) = qh(q) - 1. \quad (14)$$

To estimate multifractality, we transform  $q$  and  $\tau(q)$  to  $\alpha$  and  $f(\alpha)$  using a Legendre transform with the following equations:

$$\begin{aligned} \alpha &= \frac{d}{dq} \tau(q), f(\alpha) \\ &= \alpha(q)q - \tau(q), \end{aligned} \quad (15)$$

where  $f(\alpha)$  is the multifractal spectrum or singularity spectrum, and  $\alpha$  is the singularity strength. Furthermore,

we define the degree of multifractality  $\Delta h$  as follows (Yuan et al. [79]; Ant3nio et al. [80]; Ruan et al. [81]):

$$\Delta h = \max(h(q)) - \min(h(q)). \quad (16)$$

In addition, we define the width of the multifractal spectrum  $\Delta\alpha$  as follows (Wang et al. [82]; Ant3nio et al. [80]; Ruan et al. [81]):

$$\Delta\alpha = \max(\alpha) - \min(\alpha). \quad (17)$$

A larger  $\Delta h$  value indicates a stronger degree of multifractality and a wider multifractal spectrum, implying a stronger degree of multifractality. As another important feature of the multifractal spectrum (Drozdź and Oświcimka [83]; Maiorino et al. [84]; Drozdź et al. [85]; W3torek et al. [86]), we define the asymmetric parameter as follows:

$$\Theta = \frac{\Delta\alpha_L - \Delta\alpha_R}{\Delta\alpha_L + \Delta\alpha_R}, \quad (18)$$

where  $\Delta\alpha_L = \alpha_0 - \alpha_{\min}$ ,  $\Delta\alpha_R = \alpha_{\max} - \alpha_0$ . Here,  $\alpha_0$  is the  $\alpha$  value at the maximum of  $f(\alpha)$ . The asymmetric parameter estimates the asymmetry of the spectrum and determines the dominance of small and large fluctuations for the multifractal spectrum. When the asymmetric parameter  $\Theta = 0$ , both large and small fluctuations lead fairly to multifractality. In addition,  $\Theta > 0$  exhibits left-sided asymmetry, which implies that subsets of large fluctuations contribute substantially to the multifractal spectrum. Conversely,  $\Theta < 0$  exhibits right-sided asymmetry in the spectrum, thus indicating that smaller fluctuations constitute a dominant multifractality source.

### 3. Empirical Analysis

**3.1. Wavelet Analysis.** In this subsection, we provide the wavelet coherence between EPU and MATV for each sector to investigate the interdependence between them. Figures 5 and 6 present the estimated wavelet coherence and relative phasing of the two series represented by arrows. An explanation for wavelet coherence analysis is provided in previous studies (Torrence and Webster [70]; Tiwari [87]; Lu et al. [88]; Pal and Mitra [67]). Based on the wavelet coherence analysis results, our main findings are summarized as follows: first, in the figures, the red areas are mainly observed in the GFC and COVID-19 pandemic periods, which indicates strong interdependence between EPU and MATV. In other words, during the GFC and COVID-19 pandemic periods, the EPU and sectoral trading volume have noteworthy interdependence in most sectors. In times other than these two events, while several sectors display a common strong interconnection, the heavy linkage is short. Second, during the pandemic, in most sectors, the MATV has a different relationship with EPU than during the GFC. In particular, the red area in the consumer discretionary, energy, and utility industries is larger during the pandemic than in the GFC. Therefore, the pandemic has a greater influence on the MATV of industries than the GFC. Third, on the contrary, in the communication services, consumer staples, information technology, and materials sectors, the

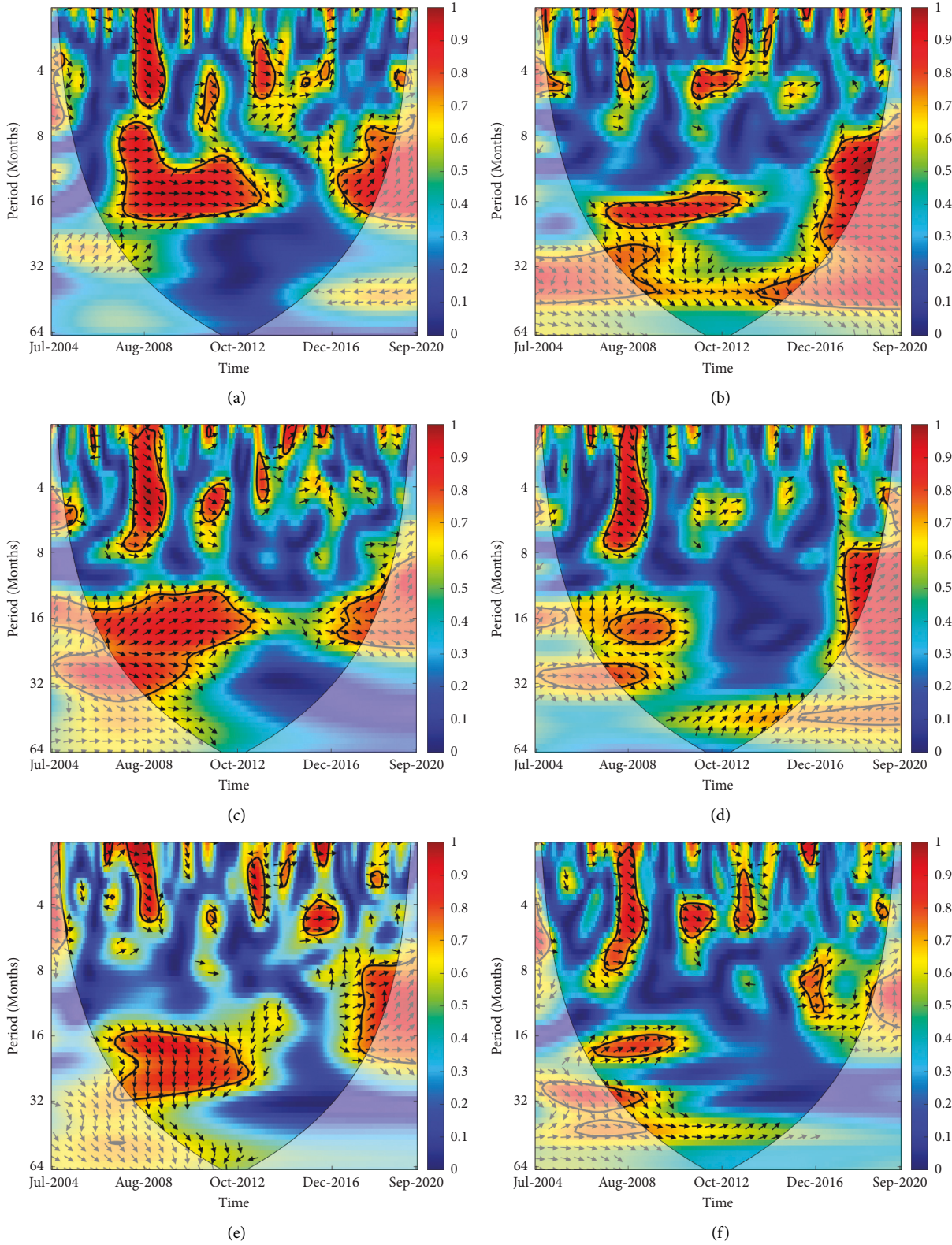


FIGURE 5: The wavelet coherence and phase plots between the EPU index and MATV for six sectors (communication services, consumer discretionary, consumer staples, energy, financial, and health care). (a) EPU and communication services. (b) EPU and consumer discretionary. (c) EPU and consumer staples. (d) EPU and energy. (e) EPU and financial. (f) EPU and health care.

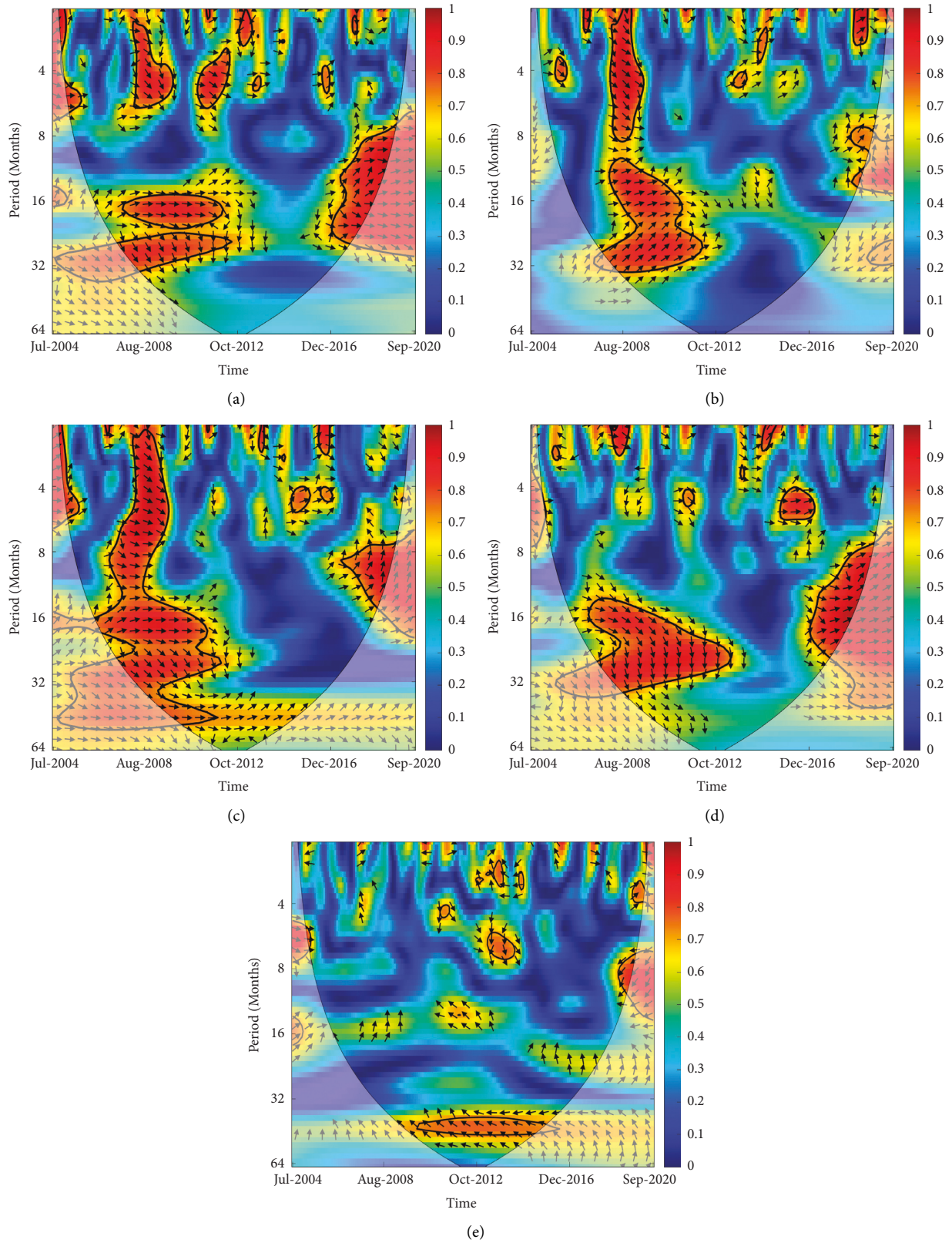


FIGURE 6: The wavelet coherence and phase plots between the +EPU index and MATV for five sectors (industrials, information technology, materials, real estate, and utilities). (a) EPU and industrials. (b) EPU and information technology. (c) EPU and materials. (d) EPU and real estate. (e) EPU and utilities.

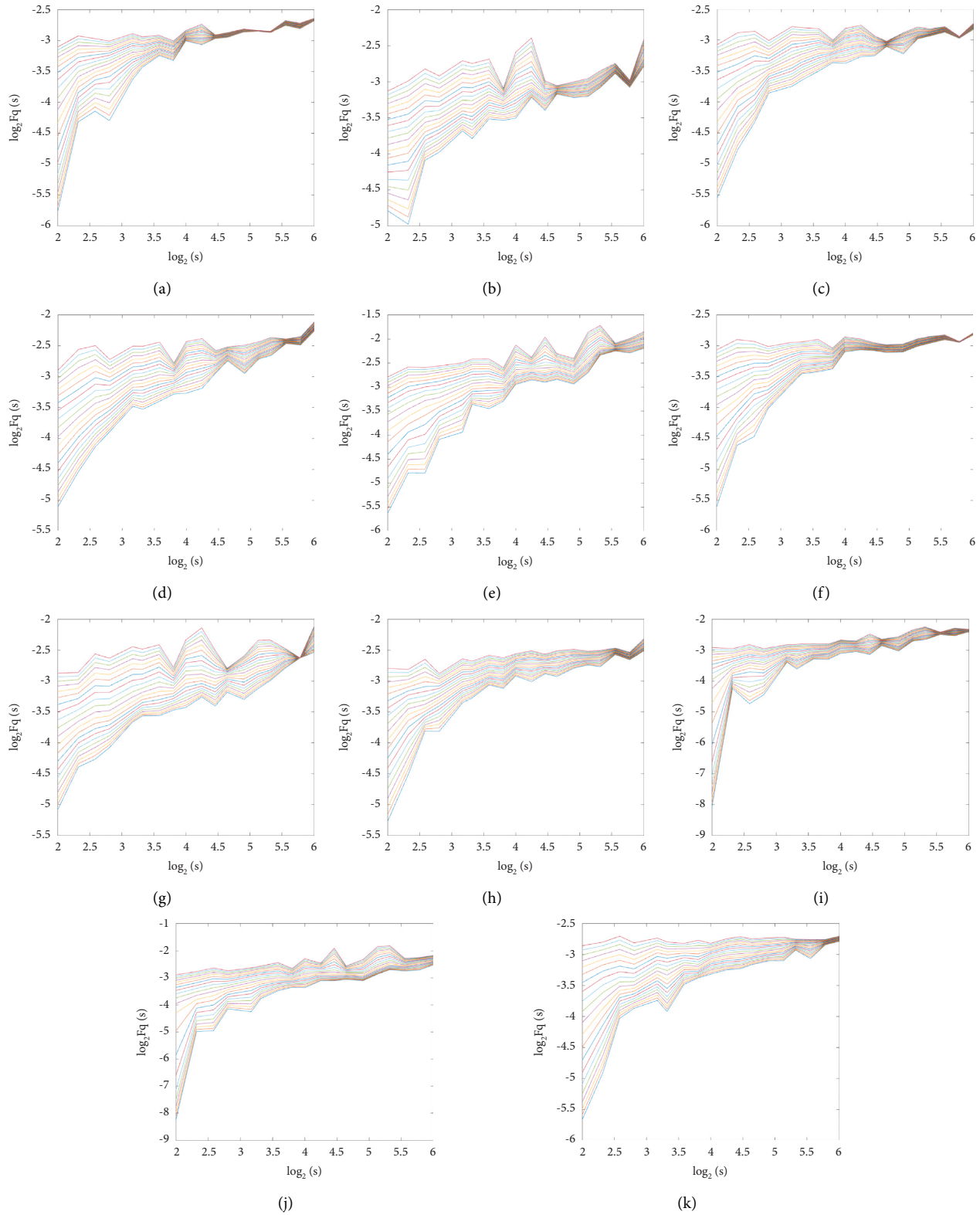


FIGURE 7: The curve of the multifractal fluctuation function  $F_q(s)$  compared to  $s$  in a log-log plot of the MATV series for all the sectors during the GFC. (a) Communication service. (b) Consumer discretionary. (c) Consumer staples. (d) Energy. (e) Financials. (f) Health care. (g) Industrials. (h) Information technology. (i) Materials. (j) Real estate. (k) Utilities.

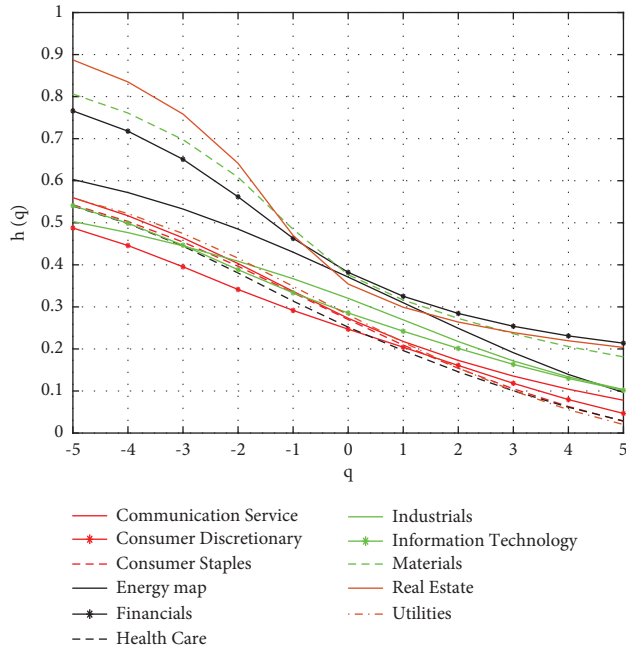


FIGURE 8: Generalized Hurst exponents  $h(q)$  of the MATV series.

impact of the GFC on trading volume is greater. One of the reasons may be that some sectors such as technology and e-commerce are more profitable than before because of the pandemic (“Winners from the pandemic Big tech’s covid-19 opportunity,” *The Economist*, <https://www.economist.com/leaders/2020/04/04/big-techscovid-19-opportunity>).

**3.2. Multifractal Analysis.** In this subsection, we apply MF-DFA to the MATV series to investigate the fractal nature of the MATV series, based on the degree of multifractality ( $\Delta h$ ) and the width of the multifractal spectrum ( $\Delta \alpha$ ). First, we display the log-log plots of  $F_q(s)$  compared to  $s$  for all the MATV series for  $q = -5, -4.5, \dots, 4.5, 5$ , corresponding to the curve from the bottom to the top when the polynomial order  $m = 1$  in Figure 7. According to the plots, we obtain the presence of different scaling laws and exponents.

Second, we further show the generalized Hurst exponents of the MATV series, as shown in Figure 8. As shown in Figure 8, the generalized Hurst exponent of the MATV series decreases as  $q$  increases from  $-5$  to  $5$  in all sectors. This implies that the MATV of all sectors has obvious multifractal features. Additionally, all sectors’ Hurst exponents ( $= h(2)$ ) are smaller than  $0.5$ . This indicates that the MATV series of all sectors are nonpersistent.

Third, Figure 9 and Table 2 illustrate the multifractal spectra and the degree of multifractality and width of the multifractal spectra of all the MATV series, respectively. Regarding the degrees of multifractality ( $\Delta \alpha$  and  $\Delta h$ ) given in Table 2, the real estate and materials sectors have the first and second-largest degrees of multifractality, respectively. Meanwhile, the industry and information technology sectors have the first and second smallest degree of multifractality, respectively. This implies that the MATV of the real estate and materials sectors is more highly correlated, whereas the

MATV of the industry and information technology sectors is less correlated. Finally, all MATV series have negative asymmetric parameters  $\Theta$ . In other words, the small fluctuations in MATV are more leading multifractality sources than the large fluctuations in the MATV series of all sectors.

#### 4. Concluding remarks

We present empirical evidence on the relationship between economic uncertainty about the COVID-19 pandemic and trading volume at the sector level. Furthermore, we compare the effect of this pandemic with the impact of the GFC in the United States. We employ the wavelet coherence analysis to measure the interrelation and causality between EPU and trading volume of each sector. According to the MF-DFA analysis, we examine the multifractality of the trading volume for all sectors. The empirical results provide a number of interesting conclusions. First, we find a strong positive correlation between EPU and MATV in all sectors in the middle term during the pandemic. In addition, the phase patterns indicate that EPU leads MATV in all sectors. Second, in terms of the impact of the market shock, some industries show different characteristics during the pandemic compared with the GFC. For example, in industries based on Internet technology such as the IT and communication services sectors, the impact of EPU is relatively small. Third, the impact of COVID-19 on the trading volume of the consumer discretionary and material sectors is longer and shorter than that during the GFC, respectively. According to an article (“Consumer discretionary and IT stocks are “egregiously expensive,” strategist says,” *CNBC*, <https://www.cnbc.com/2020/12/04/avoid-expensive-consumer-discretionary-and-it-stocks-strategist-says.html>), IT and consumer discretionary stocks have performed strongly since the outbreak of the COVID-19 pandemic, with more people working remotely and spending time at home due to lockdown restrictions. In particular, the MSCI World Consumer Discretionary Price Index has rocketed by 85% since mid-March 2020, while the MSCI World Information Technology Price Index has soared by over 75%. On the contrary, unlike during the GFC, there has been no sharp drop in housing prices during the pandemic; rather, housing prices have risen because of the Federal Reserve’s unprecedented monetary easing (Zhao [89]). Moreover, the materials sector is generally affected by the housing market. Therefore, these factors seem to have caused the difference in the materials sector. Finally, based on the MF-DFA results, the MATV of all the sectors has obvious multifractal features, and the small fluctuations in the MATV are a more dominant multifractality source. In addition, the MATV of the real estate and materials sectors is more highly correlated; meanwhile, the MATV of the industry and information technology sectors is less correlated. Our study contributes insights into the influence of the COVID-19 pandemic on the trading volume of the sectors in the U.S. stock market. The findings demonstrate that overall COVID-19 has affected trading volume considerably. However, some industries are not affected to the same degree as during the GFC. The reason for this difference could be

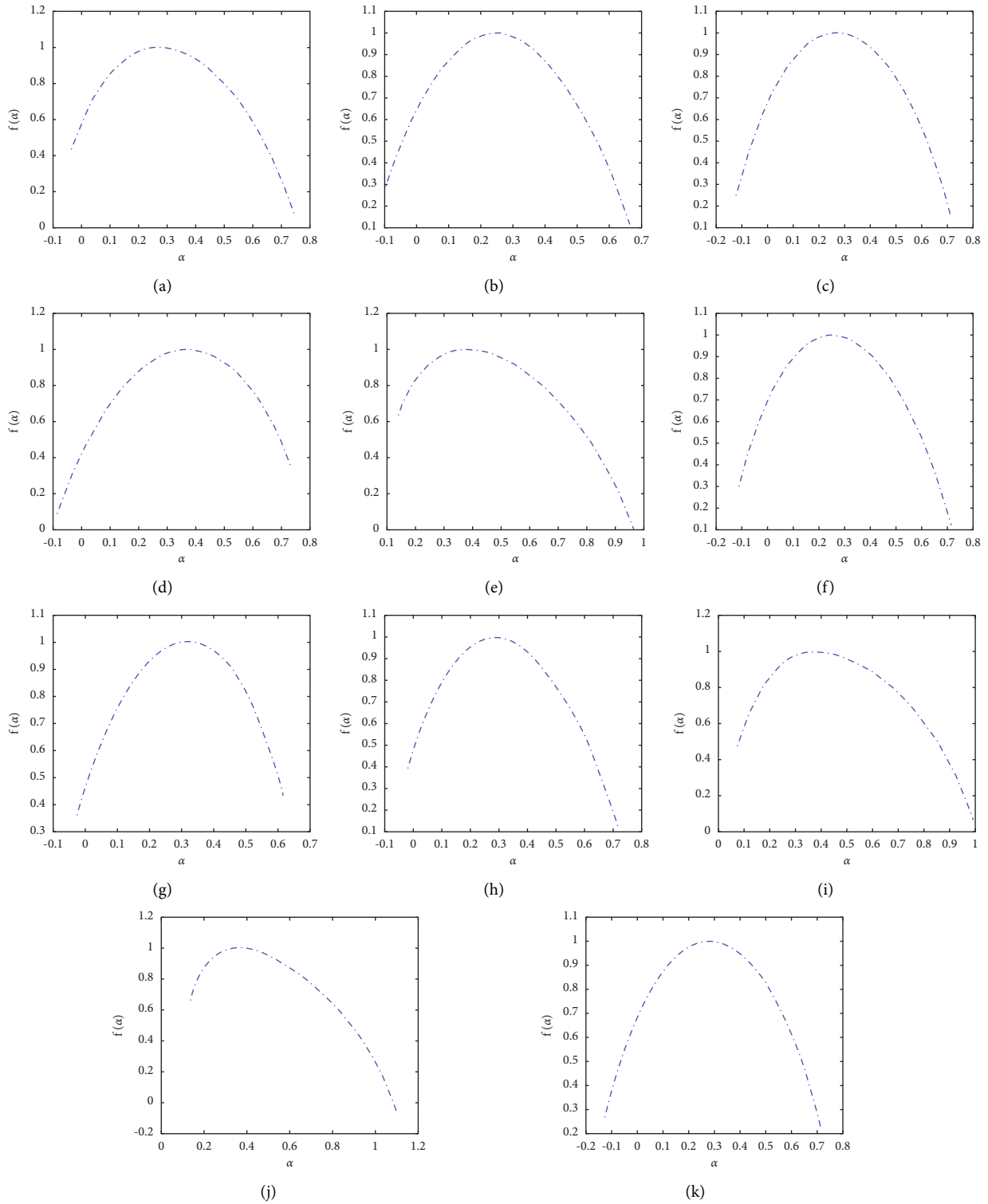


FIGURE 9: The multifractal spectra of each MATV series for all the sectors. (a) Communication service. (b) Consumer discretionary. (c) Consumer staples. (d) Energy. (e) Financials. (f) Health care. (g) Industrials. (h) Information technology. (i) Materials. (j) Real estate. (k) Utilities.

the lockdown taken to prevent the spread of COVID-19 as well as the implementation of a 0% interest rate and unlimited quantitative easing (Donthu and Gustafsson [90]; Zhang et al. [91]). Moreover, our findings show that the

trading volume series for all sectors has a multifractal nature. Compared to the existing literature that mainly conducted multifractal analysis on the trading volume of the financial market (Bolgorian and Raei [92]; Stosic et al. [93]; Zhang

TABLE 2: The width of the multifractal spectrum  $\Delta\alpha$  in equation (17) and degree of multifractality  $\Delta h$  for the MATV for all the sectors.

Sector	$\alpha_{\max}$	$\alpha_{\min}$	$\alpha_0$	$\Delta\alpha$	$\Delta h$	$\Theta$
Communication service	0.7323	-0.027	0.2179	0.7593	0.4818	-0.355
Consumer discretionary	0.6544	-0.0853	0.2041	0.7398	0.441	-0.2175
Consumer staples	0.7014	-0.1123	0.2092	0.8138	0.5147	-0.2098
Energy	0.7278	-0.0745	0.3099	0.8023	0.5065	-0.0419
Financials	0.9589	0.1443	0.3252	0.8146	0.5524	-0.5558
Health care	0.7071	-0.1023	0.1961	0.8094	0.5112	-0.2628
Industrials	0.6086	-0.0174	0.2692	0.626	0.3997	-0.0843
Information technology	0.7078	-0.0115	0.2422	0.7193	0.4391	-0.2948
Materials	0.9872	0.0828	0.3163	0.9044	0.6251	-0.4836
Real estate	1.0968	0.14	0.2992	0.9567	0.6838	-0.6673
Utilities	0.706	-0.1207	0.216	0.8267	0.5385	-0.1854

et al. [94]), this study has another contribution to examining the multifractal nature of the trading volume at the industry level. Finally, we mention a few directions for future research. First, as the COVID-19 pandemic has not been officially terminated, the data used in this study cannot reflect all the effects of the COVID-19 pandemic on the trading volume. Therefore, with the official closure of the COVID-19 pandemic, it is necessary to conduct a study on the entire COVID-19 pandemic period. If so, we can inspect the effect of the new variants of COVID-19 on the trading volume. Second, here, the multiplicity properties of the trading volume of sectors were investigated. According to the previous literature (Ané and Ureche-Rangau [95]; Cheng et al. [96]; Boudt and Petitjean [97]; Ong [98]; Ma et al. [99]; Ftiti et al. [100]), the trading volume is known to be highly related to the price and volatility of stocks. Future studies should examine the fractal relationship between trading volume and stock price or volatility based on an industrial level. Finally, as another measure for complexity, the entropy measure might be applied to the trading volume. The entropy measure properly describes the chaotic structure of the time series and it has been broadly used for financial data (Maasoumi and Racine [101]; Bentes and Menezes [102]; Stosic et al. [103]; Ahn et al. [104]; Machado [57]). Therefore, a study on the entropy measure for the trading volume can enhance our findings.

### Data Availability

The data used to support the findings of this study are available from the corresponding author upon request.

### Conflicts of Interest

The authors declare that they have no conflicts of interest.

### Acknowledgments

The work of S.-Y. Choi was supported by the National Research Foundation of Korea (NRF) grant funded by the Korean government (MSIT) (no. 2019R1G1A1010278).

### References

- [1] R. L. Crouch, "The volume of transactions and price changes on the New York stock exchange," *Financial Analysts Journal*, vol. 26, no. 4, pp. 104–109, 1970.
- [2] T. E. Copeland, "A model of asset trading under the assumption of sequential information arrival," *The Journal of Finance*, vol. 31, no. 4, pp. 1149–1168, 1976.
- [3] J. M. Karpoff, "The relation between price changes and trading volume: a survey," *Journal of Financial and Quantitative Analysis*, vol. 22, pp. 109–126, 1987.
- [4] C. M. Jones, G. Kaul, and M. L. Lipson, "Transactions, volume, and volatility," *Review of Financial Studies*, vol. 7, no. 4, pp. 631–651, 1994.
- [5] A. J. Foster, "Volumevolatility relationships for crude oil futures markets," *Journal of Futures Markets*, vol. 15, no. 18, p. 929, 1995.
- [6] C. Kramer, "Noise trading, transaction costs, and the relationship of stock returns and trading volume," *International Review of Economics & Finance*, vol. 8, no. 4, pp. 343–362, 1999.
- [7] G. H. Wang and J. Yau, "Trading volume, bid–ask spread, and price volatility in futures markets," *Journal of Futures Markets: Futures, Options, and Other Derivative Products*, vol. 20, no. 10, pp. 943–970, 2000.
- [8] G.-m. Chen, M. Firth, and O. M. Rui, "The dynamic relation between stock returns, trading volume, and volatility," *The Financial Review*, vol. 36, no. 3, pp. 153–174, 2001.
- [9] L. Gagnon and G. A. Karolyi, "Information, trading volume, and international stock return comovements: evidence from cross-listed stocks," *Journal of Financial and Quantitative Analysis*, vol. 44, pp. 953–986, 2009.
- [10] H.-Y. Lin, "Dynamic stock return–volume relation: evidence from emerging asian markets," *Bulletin of Economic Research*, vol. 65, no. 2, pp. 178–193, 2013.
- [11] Z. Wang, Y. Qian, and S. Wang, "Dynamic trading volume and stock return relation: does it hold out of sample?" *International Review of Financial Analysis*, vol. 58, pp. 195–210, 2018.
- [12] C. F. Lee and O. M. Rui, "Does trading volume contain information to predict stock returns? evidence from China's stock markets," *Review of Quantitative Finance and Accounting*, vol. 14, no. 4, pp. 341–360, 2000.
- [13] N. Güner and Z. Önder, "Information and volatility: evidence from an emerging market," *Emerging Markets Finance and Trade*, vol. 38, 2002.
- [14] J. Li and C. Wu, "Daily return volatility, bid–ask spreads, and information flow: analyzing the information content of



- volume,” *Journal of Business*, vol. 79, no. 5, pp. 2697–2739, 2006.
- [15] F. Wen and X. Yang, “Empirical study on relationship between persistence-free trading volume and stock return volatility,” *Global Finance Journal*, vol. 20, no. 2, pp. 119–127, 2009.
- [16] E. Rossi and P. S. De Magistris, “Long memory and tail dependence in trading volume and volatility,” *Journal of Empirical Finance*, vol. 22, pp. 94–112, 2013.
- [17] S. Darolles, G. Le Fol, and G. Mero, “Measuring the liquidity part of volume,” *Journal of Banking & Finance*, vol. 50, pp. 92–105, 2015.
- [18] A. E. Clements and T. Neda, “Information flow, trading activity and commodity futures volatility,” *Journal of Futures Markets*, vol. 36, no. 1, pp. 88–104, 2016.
- [19] Z. Ftiti, F. Jawadi, and W. Louhichi, “Modelling the relationship between future energy intraday volatility and trading volume with wavelet,” *Applied Economics*, vol. 49, no. 20, pp. 1981–1993, 2017.
- [20] Y.-S. Kao, H.-L. Chuang, and Yu.-C. Ku, “The empirical linkages among market returns, return volatility, and trading volume: evidence from the s&p 500 vix futures,” *The North American Journal of Economics and Finance*, vol. 54, Article ID 100871, 2019.
- [21] S. Khuntia and J. K. Pattanayak, “Adaptive long memory in volatility of intra-day bitcoin returns and the impact of trading volume,” *Finance Research Letters*, vol. 32, Article ID 101077, 2020.
- [22] H. M. Choi, “Market uncertainty and trading volume around earnings announcements,” *Finance Research Letters*, vol. 30, pp. 14–22, 2019.
- [23] D. Rehse, R. Ryan, N. Rottke, and J. Zietz, “The effects of uncertainty on market liquidity: evidence from hurricane sandy,” *Journal of Financial Economics*, vol. 134, no. 2, pp. 318–332, 2019.
- [24] V. Nagar, S. Jordan, and L. Wellman, “The effect of economic policy uncertainty on investor information asymmetry and management disclosures,” *Journal of Accounting and Economics*, vol. 67, no. 1, pp. 36–57, 2019.
- [25] C. Chen, L. Liu, and N. Zhao, “Fear sentiment, uncertainty, and bitcoin price dynamics: the case of covid-19,” *Emerging Markets Finance and Trade*, vol. 56, no. 10, pp. 2298–2309, 2020a.
- [26] M. Chiah and A. Zhong, “Trading from home: the impact of covid-19 on trading volume around the world,” *Finance Research Letters*, vol. 37, Article ID 101784, 2020.
- [27] R. M. Colombo, M. Garavello, F. Marcellini, and E. Rossi, “An age and space structured sir model describing the covid-19 pandemic,” *Journal of mathematics in industry*, vol. 10, no. 1, pp. 1–20, 2020.
- [28] H. Tian, Y. Liu, Y. Li et al., “An investigation of transmission control measures during the first 50 days of the covid-19 epidemic in China,” *Science*, vol. 368, no. 6491, pp. 638–642, 2020.
- [29] A. S. Alshomrani, M. Z. Ullah, and B. Dumitru, “Caputo sir model for covid-19 under optimized fractional order,” *Advances in Difference Equations*, vol. 2021, no. 1, pp. 1–17, 2021.
- [30] K. Leung, J. T. Wu, Di Liu, and G. M. Leung, “First-wave covid-19 transmissibility and severity in China outside hubei after control measures, and second-wave scenario planning: a modelling impact assessment,” *The Lancet*, vol. 395, no. 10233, pp. 1382–1393, 2020.
- [31] J. M. Read, J. R. Bridgen, D. A. Cummings, A. Ho, and C. P. Jewell, “Novel coronavirus 2019-nCoV (COVID-19): early estimation of epidemiological parameters and epidemic size estimates B,” *Philosophical Transactions of the Royal Society*, vol. 376, p. 1829, 2020.
- [32] J. T. Wu, K. Leung, and G. M. Leung, “Nowcasting and forecasting the potential domestic and international spread of the 2019-ncov outbreak originating in wuhan, China: a modelling study,” *The Lancet*, vol. 395, no. 10225, pp. 689–697, 2020.
- [33] Z. Yang, Z. Zeng, Ke Wang et al. “Modified seir and ai prediction of the epidemics trend of covid-19 in China under public health interventions,” *Journal of Thoracic Disease*, vol. 12, no. 3, p. 165, 2020.
- [34] A. Adiga, D. Dubhashi, B. Lewis, M. Marathe, V. Srinivasan, and A. Vullikanti, “Mathematical models for covid-19 pandemic: a comparative analysis,” *Journal of the Indian Institute of Science*, vol. 1–15, 2020.
- [35] S. Agrawal, S. Bhandari, A. Bhattacharjee et al., “City-scale agent-based simulators for the study of non-pharmaceutical interventions in the context of the covid-19 epidemic,” *Journal of the Indian Institute of Science*, vol. 1–39, 2020.
- [36] N. M. Gharakhanlou and N. Hooshangi, “Spatio-temporal simulation of the novel coronavirus (covid-19) outbreak using the agent-based modeling approach (case study: urmia, Iran),” *Informatics in Medicine Unlocked*, vol. 20, Article ID 100403, 2020.
- [37] A. E. Matouk, “Complex dynamics in susceptible-infected models for covid-19 with multi-drug resistance,” *Chaos, Solitons & Fractals*, vol. 140, Article ID 110257, 2020.
- [38] W. W. Mohammed, E. S. Aly, A. E. Matouk, S. Albosaily, and E. M. Elabbasy, “An analytical study of the dynamic behavior of lotka-volterra based models of covid-19,” *Results in Physics*, vol. 26, Article ID 104432, 2021.
- [39] J.-H. Ko and C.-M. Lee, “International economic policy uncertainty and stock prices: wavelet approach,” *Economics Letters*, vol. 134, pp. 118–122, 2015.
- [40] Li Liu and T. Zhang, “Economic policy uncertainty and stock market volatility,” *Finance Research Letters*, vol. 15, pp. 99–105, 2015.
- [41] T. Li, F. Ma, X. Zhang, and Y. Zhang, “Economic policy uncertainty and the Chinese stock market volatility: novel evidence,” *Economic Modelling*, vol. 87, pp. 24–33, 2020.
- [42] S.-Y. Choi, “Industry volatility and economic uncertainty due to the covid-19 pandemic: evidence from wavelet coherence analysis,” *Finance Research Letters*, vol. 37, p. 101783, 2020.
- [43] D. Mei, Q. Zeng, X. Cao, and X. Diao, “Uncertainty and oil volatility: new evidence,” *Physica A: Statistical Mechanics and Its Applications*, vol. 525, pp. 155–163, 2019.
- [44] R. Ma, C. Zhou, H. Cai, and C. Deng, “The forecasting power of epu for crude oil return volatility,” *Energy Reports*, vol. 5, pp. 866–873, 2019.
- [45] F. Wen, Y. Zhao, M. Zhang, and C. Hu, “Forecasting realized volatility of crude oil futures with equity market uncertainty,” *Applied Economics*, vol. 51, no. 59, pp. 6411–6427, 2019.
- [46] S. M. Juhro and D. H. B. Phan, “Can economic policy uncertainty predict exchange rate and its volatility? evidence from asean countries,” *Buletin Ekonomi Moneter dan Perbankan*, vol. 21, no. 2, pp. 251–268, 2018.
- [47] Z. Bartsch, “Economic policy uncertainty and dollar-pound exchange rate return volatility,” *Journal of International Money and Finance*, vol. 98, Article ID 102067, 2019.

- [48] L. Chen, Z. Du, and Z. Hu, "Impact of economic policy uncertainty on exchange rate volatility of China," *Finance Research Letters*, vol. 32, Article ID 101266, 2020b.
- [49] E. Demir, G. Gozgor, C. K. M. Lau, and S. A. Vigne, "Does economic policy uncertainty predict the bitcoin returns? an empirical investigation," *Finance Research Letters*, vol. 26, pp. 145–149, 2018.
- [50] G.-J. Wang, C. Xie, D. Wen, and L. Zhao, "When bitcoin meets economic policy uncertainty (epu): measuring risk spillover effect from epu to bitcoin," *Finance Research Letters*, vol. 31, 2019b.
- [51] H.-P. Cheng and K.-C. Yen, "The relationship between the economic policy uncertainty and the cryptocurrency market," *Finance Research Letters*, vol. 35, Article ID 101308, 2020.
- [52] J. W. Kantelhardt, S. A. Zschiegner, E. Koscielny-Bunde, S. Havlin, A. Bunde, and H. E. Stanley, "Multifractal detrended fluctuation analysis of nonstationary time series," *Physica A: Statistical Mechanics and Its Applications*, vol. 316, no. 1-4, pp. 87–114, 2002.
- [53] E. Bacry, D. Jean, and M. Jean-François, "Modelling financial time series using multifractal random walks," *Physica A: Statistical Mechanics and Its Applications*, vol. 299, no. 1-2, pp. 84–92, 2001.
- [54] J. Kwapien, P. Oświmka, and S. Drożdż, "Components of multifractality in high-frequency stock returns," *Physica A: Statistical Mechanics and Its Applications*, vol. 350, no. 2-4, pp. 466–474.
- [55] L. Zunino, A. Figliola, B. M. Tabak, D. G. Pérez, M. Garavaglia, and O. A. Rosso, "Multifractal structure in Latin-american market indices," *Chaos, Solitons & Fractals*, vol. 41, no. 5, pp. 2331–2340, 2009.
- [56] Y. Wang, L. Liu, and R. Gu, "Analysis of efficiency for shenzhen stock market based on multifractal detrended fluctuation analysis," *International Review of Financial Analysis*, vol. 18, no. 5, pp. 271–276, 2009.
- [57] J. A. T. Machado, "Fractal and entropy analysis of the dow jones index using multidimensional scaling," *Entropy*, vol. 22, no. 10, p. 1138, 2020.
- [58] S.-Y. Choi, "Analysis of stock market efficiency during crisis periods in the us stock market: differences between the global financial crisis and covid-19 pandemic," *Physica A: Statistical Mechanics and Its Applications*, vol. 574, Article ID 125988, 2021.
- [59] M. Mazur, M. Dang, and M. Vega, "Covid-19 and the march 2020 stock market crash. evidence from s&p1500," *Finance Research Letters*, Article ID 101690, 2020.
- [60] A. Sharif, C. Aloui, and L. Yarovaya, "Covid-19 pandemic, oil prices, stock market, geopolitical risk and policy uncertainty nexus in the us economy: fresh evidence from the wavelet-based approach," *International Review of Financial Analysis*, vol. 70, Article ID 101496, 2020.
- [61] M. Hanke, M. Kosolapova, and A. Weissensteiner, "Covid-19 and market expectations: evidence from option-implied densities," *Economics Letters*, vol. 195, Article ID 109441, 2020.
- [62] L. A. Smales, "Investor attention and the response of us stock market sectors to the covid-19 crisis," *Review of Behavioral Finance*, 2020.
- [63] B. S. R. Baker, N. Bloom, S. J. Davis, K. Kost, M. Sammon, and T. Viratyosin, "The unprecedented stock market reaction to covid-19," *The Review of Asset Pricing Studies*, vol. 10, no. 4, pp. 742–758, 2020.
- [64] R. Ortman, M. Pelster, and S. Tobias Wengerek, "Covid-19 and investor behavior," *Finance Research Letters*, vol. 37, Article ID 101717, 2020.
- [65] B. S. R. Baker, N. Bloom, and S. J. Davis, "Measuring economic policy uncertainty," *Quarterly Journal of Economics*, vol. 131, no. 4, pp. 1593–1636, 2016.
- [66] L. Kristoufek, "What are the main drivers of the bitcoin price? evidence from wavelet coherence analysis," *PLoS One*, vol. 10, no. 4, Article ID e0123923, 2015.
- [67] D. Pal and S. K. Mitra, "Oil price and automobile stock return co-movement: a wavelet coherence analysis," *Economic Modelling*, vol. 76, pp. 172–181, 2019.
- [68] M. J. Soares and M. J. Soares, "Business cycle synchronization and the euro: a wavelet analysis," *Journal of Macroeconomics*, vol. 33, no. 3, pp. 477–489, 2011.
- [69] P. Goupillaud, A. Grossmann, and J. Morlet, "Cycle-octave and related transforms in seismic signal analysis," *Geophysical Research Letters*, vol. 23, no. 1, pp. 85–102, 1984.
- [70] C. Torrence and P. J. Webster, "Interdecadal changes in the enso-monsoon system," *Journal of Climate*, vol. 12, no. 8, pp. 2679–2690, 1999.
- [71] D. S. Bloomfield, R. T. J. McAtter, B. W. Lites, P. G. Judge, M. Mathioudakis, and F. P. Keenan, "Wavelet phase coherence analysis: application to a quiet-sun magnetic element," *The Astrophysical Journal*, vol. 617, no. 1, pp. 623–632, 2004.
- [72] M. A. Flor and T. Klarl, "On the cyclicity of regional house prices: new evidence for us metropolitan statistical areas," *Journal of Economic Dynamics and Control*, vol. 77, pp. 134–156, 2017.
- [73] X. J. Cai, S. Tian, N. Yuan, and S. Hamori, "Interdependence between oil and east asian stock markets: evidence from wavelet coherence analysis," *Journal of International Financial Markets, Institutions and Money*, vol. 48, pp. 206–223, 2017.
- [74] Y. Funashima, "Time-varying leads and lags across frequencies using a continuous wavelet transform approach," *Economic Modelling*, vol. 60, pp. 24–28, 2017.
- [75] F. Wang, X. Ye, and C. Wu, "Multifractal characteristics analysis of crude oil futures prices fluctuation in China," *Physica A: Statistical Mechanics and Its Applications*, vol. 533, Article ID 122021, 2019a.
- [76] B. Lashermes, P. Abry, and P. Chainais, "New insights into the estimation of scaling exponents," *International Journal of Wavelets, Multiresolution and Information Processing*, vol. 2, no. 04, pp. 497–523, 2004.
- [77] Y. Ning, Y. Wang, and C.-w. Su, "How did China's foreign exchange reform affect the efficiency of foreign exchange market?" *Physica A: Statistical Mechanics and Its Applications*, vol. 483, pp. 219–226, 2017.
- [78] L. Calvet and A. Fisher, "Multifractality in asset returns: theory and evidence," *The Review of Economics and Statistics*, vol. 84, no. 3, pp. 381–406, 2002.
- [79] Y. Yuan, X.-t. Zhuang, and X. Jin, "Measuring multifractality of stock price fluctuation using multifractal detrended fluctuation analysis," *Physica A: Statistical Mechanics and Its Applications*, vol. 388, no. 11, pp. 2189–2197, 2009.
- [80] C. d. S. F. Ant6nio, D. M. Nat6lia, and E. Fonseca de Almeida, "Multifractal analysis of bitcoin market," *Physica A: Statistical Mechanics and Its Applications*, vol. 512, pp. 954–967, 2018.
- [81] Q. Ruan, S. Zhang, D. Lv, and X. Lu, "Financial liberalization and stock market cross-correlation: mf-dcca analysis based on shanghai-Hong Kong stock connect," *Physica A:*

- Statistical Mechanics and Its Applications*, vol. 491, pp. 779–791, 2018.
- [82] Y. Wang, C. Wu, and Z. Pan, “Multifractal detrending moving average analysis on the us dollar exchange rates,” *Physica A: Statistical Mechanics and Its Applications*, vol. 390, no. 20, pp. 3512–3523, 2011.
- [83] S. Drożdż and P. Oświczka, “Detecting and interpreting distortions in hierarchical organization of complex time series,” *Physical Review*, vol. 91, no. 3, Article ID 030902, 2015.
- [84] E. Maiorino, F. Maria Bianchi, L. Livi, A. Rizzi, and A. Sadeghian, “Data-driven detrending of nonstationary fractal time series with echo state networks,” *Information Sciences*, vol. 382, pp. 359–373, 2017.
- [85] S. Drożdż, R. Kowalski, P. Oświczka, R. Rak, and R. Gbarowski, “Dynamical variety of shapes in financial multifractality,” *Complexity*, vol. 2018, Article ID 7015721, 13 pages, 2018.
- [86] M. Wątopek, S. Drożdż, P. Oświczka, and M. Stanuszek, “Multifractal cross-correlations between the world oil and other financial markets in 2012–2017,” *Energy Economics*, vol. 81, pp. 874–885, 2019.
- [87] A. K. Tiwari, “Oil prices and the macroeconomy reconsideration for Germany: using continuous wavelet,” *Economic Modelling*, vol. 30, pp. 636–642, 2013.
- [88] Y. Lu, X. J. Cai, and S. Hamori, “Does the crude oil price influence the exchange rates of oil-importing and oil-exporting countries differently? a wavelet coherence analysis,” *International Review of Economics & Finance*, vol. 49, pp. 536–547, 2017.
- [89] “US housing market during COVID-19: aggregate and distributional evidence,” *COVID Economics*, vol. 50, pp. 113–154, 2020.
- [90] N. Donthu and A. Gustafsson, “Effects of covid-19 on business and research,” *Journal of Business Research*, vol. 117, p. 284, 2020.
- [91] D. Zhang, M. Hu, and Q. Ji, “Financial markets under the global pandemic of covid-19,” *Finance Research Letters*, vol. 36, Article ID 101528, 2020.
- [92] M. Bolgorian and R. Raei, “A multifractal detrended fluctuation analysis of trading behavior of individual and institutional traders in tehran stock market,” *Physica A: Statistical Mechanics and Its Applications*, vol. 390, no. 21–22, pp. 3815–3825, 2011.
- [93] D. Stosic, D. Stosic, T. B. Luderemir, and T. Stosic, “Multifractal behavior of price and volume changes in the cryptocurrency market,” *Physica A: Statistical Mechanics and Its Applications*, vol. 520, pp. 54–61, 2019.
- [94] X. Zhang, L. Yang, and Y. Zhu, “Analysis of multifractal characterization of bitcoin market based on multifractal detrended fluctuation analysis,” *Physica A: Statistical Mechanics and Its Applications*, vol. 523, pp. 973–983, 2019.
- [95] T. Ané and L. Ureche-Rangau, “Does trading volume really explain stock returns volatility?” *Journal of International Financial Markets, Institutions and Money*, vol. 18, no. 3, pp. 216–235, 2008.
- [96] H. Cheng, J.-b. Huang, Y.-q. Guo, and X.-h. Zhu, “Long memory of price-volume correlation in metal futures market based on fractal features,” *Transactions of Nonferrous Metals Society of China*, vol. 23, no. 10, pp. 3145–3152, 2013.
- [97] K. Boudt and M. Petitjean, “Intraday liquidity dynamics and news releases around price jumps: evidence from the djia stocks,” *Journal of Financial Markets*, vol. 17, pp. 121–149, 2014.
- [98] M. A. Ong, “An information theoretic analysis of stock returns, volatility and trading volumes,” *Applied Economics*, vol. 47, no. 36, pp. 3891–3906, 2015.
- [99] R. Ma, H. D. Anderson, and B. R. Marshall, “Stock market liquidity and trading activity: is China different?” *International Review of Financial Analysis*, vol. 56, pp. 32–51, 2018.
- [100] Z. Ftiti, F. Jawadi, W. Louhichi, and M. A. Madani, “On the relationship between energy returns and trading volume: a multifractal analysis,” *Applied Economics*, vol. 51, no. 29, pp. 3122–3136, 2019.
- [101] E. Maasoumi and J. Racine, “Entropy and predictability of stock market returns,” *Journal of Econometrics*, vol. 107, no. 1–2, pp. 291–312, 2002.
- [102] S. R. Bentes and R. Menezes, “Entropy: a new measure of stock market volatility?” in *Journal of Physics: Conference Series* vol. 394, IOP Publishing, Article ID 012033, 2012.
- [103] D. Stosic, D. Stosic, Teresa Luderemir, Wilson de Oliveira, and T. Stosic, “Foreign exchange rate entropy evolution during financial crises,” *Physica A: Statistical Mechanics and Its Applications*, vol. 449, pp. 233–239, 2016.
- [104] K. Ahn, D. Lee, S. Sohn, and B. Yang, “Stock market uncertainty and economic fundamentals: an entropy-based approach,” *Quantitative Finance*, vol. 19, no. 7, pp. 1151–1163, 2019.

## Research Article

# On the Dynamics of Cournot Duopoly Game with Governmental Taxes

S. S. Askar 

*Department of Statistics and Operations Research, College of Science, King Saud University, P. O. Box 2455, Riyadh 11451, Saudi Arabia*

Correspondence should be addressed to S. S. Askar; [saskar@ksu.edu.sa](mailto:saskar@ksu.edu.sa)

Received 12 October 2021; Revised 9 February 2022; Accepted 5 March 2022; Published 14 April 2022

Academic Editor: Atila Bueno

Copyright © 2022 S. S. Askar. This is an open access article distributed under the Creative Commons Attribution License, which permits unrestricted use, distribution, and reproduction in any medium, provided the original work is properly cited.

A quadratic utility function is introduced in this paper to study the dynamic characteristics of Cournot duopoly game. Based on the bounded rationality mechanism, a discrete dynamical map that describes the game's dynamic is obtained. The map possesses only one equilibrium point which is Nash point. The stability conditions for this point are analyzed. These conditions show that the point becomes unstable due to two bifurcation types that are flip and Neimark–Sacker. The synchronization property for that map is studied. Through local and global analysis, some dynamics of attracting sets are investigated. This analysis gives some insights on the basis of those sets and the shape of the critical curves. It also shows some lobes found in those attracting sets which are constructed due to the origin focal point.

## 1. Introduction

The Cournot duopoly game as described in literature consists of two players (or two competing firms), each wants to seek the optimal quantity of his/her production. Many scholars in literature have studied the dynamic of such games which have been described by discrete maps ([1–5]). The Nash equilibrium point of such games and its stability conditions were the core of study by scholars. Different types of bifurcations have been reported in literature as causes for the equilibrium point to be unstable. In addition, many utility functions have been adopted to model such games. Of which are Cobb–Douglas, constant elasticity of substitution (CES) and others. Interested readers are advised to see some applications of those utility functions and their properties in literature ([1–10]).

The present paper introduces a simple quadratic utility function. This function gives under Lagrangian function and its first-order condition price functions same as given by Cobb–Douglas. Our introduced utility function may be considered as a special case of Singh and Vives function [1]; however, the later does not give linear prices as reported in literature [6] if one apply Lagrangian function and its first-

order conditions on it. Anyway, we highlight here some important works that have studied such kind of games. For instance, in [11], a Cournot–Bertrand duopoly game whose products are considered to be differentiated has been studied. Few useful investigations on such games and their optimality have been reported in the following studies ([12–14]). In [15], Tremblay et al. have analyzed the differentiated products in a Cournot–Bertrand duopoly game. They have focused on studying the static game and the stability/instability conditions of the game's Nash equilibrium point. In [8], a theoretical framework of a Cournot–Bertrand game has been introduced. Based on a two-dimensional discrete linear map, Naimzada et al. [16] have analyzed a model of Cournot–Bertrand and studied its dynamic characteristics. Naimzada et al. have adopted different mechanisms such as the best response and adaptive adjustment to introduce the model which has been used to describe the dynamic of the game.

When studying such games, different types of adjustment mechanisms have been used in the modelling process. The modelling process means introducing the discrete map that describes the dynamic of game at discrete time steps. The most popular mechanism that has been used in the

modelling process of such games is the bounded rationality approach. It has been considered as a gradient-based approach. Other mechanisms that has been used in few studies in literature are the naive mechanism, the tit-for-tat approach, and the approximation of local monopolistic or LMA mechanism. Information about those mechanisms and their properties can be founded in literature ([17–21]). Other interesting works on the extensions of those mechanisms and their applications have been reported ([22–26]).

The present paper belongs to the category of Cournot duopoly game on which both competing firms adopt the bounded rationality approach and want to seek the optimal quantities of production in order to achieve the profit maximization. The current game differs from those in literature [27], on which we introduce a new utility function that has not been adopted before. In this paper, local and global analyses are performed to investigate the game's dynamics. This includes the investigation of multiple stable attractors and analyzes the attractive basins for some attracting sets. The main results in such study focus on analyzing the dynamics of the unique Nash equilibrium of the map's game. This includes investigating the types of bifurcations by which the equilibrium point may be unstable. The obtained results show that there are two types of bifurcations by which the Nash point becomes unstable. These types are flip and Neimark–Sacker bifurcations. In addition, the form of the game's map possesses a focal point that is the origin which gives rise to some lobes affecting on the shape of the attractive basins of some attracting sets. Furthermore, the synchronization property is studied. Moreover, the critical curves are calculated and show that the phase plane of the game's map belongs to  $Z_1 - Z_3$  type.

The structure of paper is given as follows. The quadratic utility function and the discrete dynamic map describing the game are introduced in Section 2. This section includes also the stability investigation of the Nash equilibrium point and the route to chaos due to two different types of bifurcations. In addition, local and global analyses including the synchronization property are discussed in this section. Furthermore, the critical curves that divide the phase plane of the game's map into  $Z_1$  and  $Z_3$  regions are calculated. Finally, Section 3 concludes our obtained results and suggests some future works.

## 2. The Model with Tax

Let us first assume the following quadratic utility function:

$$\begin{aligned} U &= Q - Q^2 \\ &= q_1 + q_2 - (q_1 + q_2)^2, \end{aligned} \quad (1)$$

where  $Q = q_1 + q_2$  and  $q_i, i = 1, 2$  denotes the quantity produced by the player (firm)  $i$ . Our suggested model in this manuscript consists of two competing firms whose decision variables are the quantities produced by them. It is simple to see that the utility given in (1) is convex which economically means that the good  $q_i, i = 1, 2$  has an increasing marginal utility. Furthermore, the marginal utility of the good  $q_1$  does not depend on the good  $q_2$  (as  $(\partial^2 U / \partial q_1 q_2) = -2 \neq 0$ ). In

addition, this utility is homogeneous. Assuming the budget constraint  $p_1 q_1 + p_2 q_2 = m, m > 0$ , then we get the following maximization problem:

$$\begin{aligned} \text{Max } U(q_1, q_2), \\ \text{s.t } p_1 q_1 + p_2 q_2 = m, \end{aligned} \quad (2)$$

where  $p_i > 0, i = 1, 2$  represents the price of good  $q_i, i = 1, 2$ . Solving (2), we get (see Appendix A)

$$\begin{aligned} p_i &= \frac{1}{Q} \\ &= \frac{1}{q_1 + q_2}. \end{aligned} \quad (3)$$

Now, we assume that both firms detect the optimum according to maximizing their profits as follows:

$$\max_{(q_1, q_2)} \begin{cases} \pi_1(q_1, q_2) = p_1 q_1 - C(q_1) - \text{Tax}(q_1), \\ \pi_2(q_1, q_2) = p_2 q_2 - C(q_2) - \text{Tax}(q_2), \end{cases} \quad (4)$$

where  $C_i(q_i)$  represents the cost of the quantity  $q_i, i = 1, 2$  and is taken as a linear cost  $C_i(q_i) = c_i q_i$  where  $(\partial C_i(q_i) / \partial q_i) = c_i$  denotes a constant marginal cost. We assume also that the government has imposed a tax on each quantity as  $\text{Tax}(q_i) = r_i q_i, i = 1, 2$  and  $r_i \in (0, 1)$ . Now, (4) can be represented by

$$\begin{aligned} \pi_1(q_1, q_2) &= \frac{q_1}{Q} - (c_1 + r_1)q_1, \\ \pi_2(q_1, q_2) &= \frac{q_2}{Q} - (c_2 + r_2)q_2. \end{aligned} \quad (5)$$

Recalling the mechanism of bounded rationality [8], both firms can update their outputs as follows:

$$\begin{aligned} q_1(t+1) &= q_1(t) + k_1 q_1(t) \frac{\partial \pi_1(q_1(t), q_2(t))}{\partial q_1(t)}, \\ q_2(t+1) &= q_2(t) + k_2 q_2(t) \frac{\partial \pi_2(q_1(t), q_2(t))}{\partial q_2}, \end{aligned} \quad (6)$$

where  $t = 0, 1, 2, \dots$ . Using (5) in (6), we get the two-dimensional discrete dynamic map that describes the current game.

$$T(q_1, q_2): \begin{cases} q_1(t+1) = q_1(t) + k_1 q_1(t) \left[ \frac{q_2}{Q^2} - c_1 - r_1 \right], \\ q_2(t+1) = q_2(t) + k_2 q_2(t) \left[ \frac{q_1}{Q^2} - c_2 - r_2 \right]. \end{cases} \quad (7)$$

Now, we discuss the dynamic characteristics of the equilibrium point of map (7) in the next section.

**2.1. The Equilibrium Point and Its Stability.** The equilibrium point of the above map is a unique Nash equilibrium point

and is obtained by setting  $q_1(t+1) = q_1(t) = \bar{q}_1$  and  $q_2(t+1) = q_2(t) = \bar{q}_2$ . It has the following form:

$$O = (\bar{q}_1, \bar{q}_2) = \left( \frac{c_2 + r_2}{(c_1 + c_2 + r_1 + r_2)^2}, \frac{c_1 + r_1}{(c_1 + c_2 + r_1 + r_2)^2} \right), \quad (8)$$

which is a positive point. We should highlight here that the equilibrium point (8) is the same as the one given in [28] but when the model has free taxes ( $r_1 = r_2 = 0$ ). The following propositions are used in the sequel to classify the type of the point  $O$ .

**Proposition 1.** *Let the Jacobian matrix the map (7) at any equilibrium point possesses two eigenvalues  $\lambda_1$  and  $\lambda_2$ . Then, this equilibrium point can be classified according to the following:*

- (i) *If  $|\lambda_{1,2}| < 1$ , then it becomes an attracting node and it is stable*
- (ii) *If  $|\lambda_{1,2}| > 1$ , then it is an unstable repelling node*
- (iii) *If  $|\lambda_1| < 1$  and  $|\lambda_2| > 1$ , (or  $|\lambda_1| > 1$  and  $|\lambda_2| < 1$ ) then it is an unstable saddle point*
- (iv) *It is a nonhyperbolic point if  $|\lambda_1| = 1$  and  $|\lambda_2| \neq 1$  (or  $|\lambda_1| \neq 1$  and  $|\lambda_2| = 1$ )*

*In case, the eigenvalues have a complicated analytical form, we use the following proposition.*

$$J_O = \begin{pmatrix} 1 - \frac{2(c_1 + r_1)(c_2 + r_2)k_1}{c_1 + r_1 + c_2 + r_2} & \frac{-(c_2 + r_2)(c_1 + r_1 - c_2 - r_2)k_1}{c_1 + r_1 + c_2 + r_2} \\ \frac{(c_1 + r_1)(c_1 + r_1 - c_2 - r_2)k_2}{c_1 + r_1 + c_2 + r_2} & 1 - \frac{2(c_1 + r_1)(c_2 + r_2)k_2}{c_1 + r_1 + c_2 + r_2} \end{pmatrix}. \quad (10)$$

*And its eigenvalues are*

$$\lambda_{1,2} = 1 - \frac{(c_1 + r_1)(c_2 + r_2)(k_1 + k_2)}{(c_1 + r_1 + c_2 + r_2)} \pm \frac{2(c_1 + r_1)(c_2 + r_2)}{(c_1 + r_1 + c_2 + r_2)} \sqrt{k_1^2 + k_2^2 - \frac{(c_1^2 + r_1^2 + c_2^2 + r_2^2 + 2c_1r_1 + 2c_2r_2)k_1k_2}{(c_1 + r_1)(c_2 + r_2)}}. \quad (11)$$

**Proposition 3.** *The equilibrium point  $O$  is locally asymptotically stable if the following conditions are satisfied:*

**Proposition 2.** *Let  $\tau$  and  $\delta$  be the trace and determinant of the Jacobian matrix of (7), and suppose the following*

$$\begin{aligned} g(1) &= 1 - \tau + \delta, \\ g(-1) &= 1 + \tau + \delta, \\ \Omega &= 1 - \delta. \end{aligned} \quad (9)$$

*Then, we have the following properties:*

- (i) *The equilibrium point is locally asymptotically stable if  $g(1) > 0$ ,  $g(-1) > 0$ , and  $\Omega > 0$ .*
- (ii) *The equilibrium point becomes unstable through a flip bifurcation if  $g(1) > 0$ ,  $g(-1) = 0$ , and  $\Omega > 0$ . In this case, the two eigenvalues are real and pass through  $-1$ .*
- (iii) *The equilibrium point becomes unstable through a transcritical or fold bifurcation if  $g(1) > 0$ ,  $g(-1) > 0$ , and  $\Omega > 0$ . In this case, the two eigenvalues are real and pass through  $1$ .*
- (iv) *The equilibrium point becomes unstable through Neimark–Sacker if  $g(1) > 0$ ,  $g(-1) > 0$ , and  $\Omega < 0$ . In this case, the two eigenvalues are complex and their modulus passes through  $1$ .*

*The Jacobian matrix for the map (7) at the equilibrium point  $O$  becomes*

$$(c_1 + r_1)(c_2 + r_2)k_1k_2 - \frac{4(c_1 + r_1)(c_2 + r_2)}{c_1 + r_1 + c_2 + r_2}(k_1 + k_2) + 4 > 0, \quad (12)$$

$$\frac{2(c_1 + r_1)(c_2 + r_2)}{c_1 + r_1 + c_2 + r_2}(k_1 + k_2) - (c_1 + r_1)(c_2 + r_2)k_1k_2 > 0.$$

*Proof.* Simple calculations show that  $\tau$  and  $\delta$  for the Jacobian given in (10) become

$$\tau = 2 \left( 1 - \frac{(c_1 + r_1)(c_2 + r_2)(k_1 + k_2)}{(c_1 + r_1 + c_2 + r_2)} \right),$$

$$\delta = 1 - \frac{2(c_1 + r_1)(c_2 + r_2)(k_1 + k_2)}{(c_1 + r_1 + c_2 + r_2)} + (c_1 + r_1)(c_2 + r_2)k_1k_2. \quad (13)$$

Substituting (13) in (9), we get  $g(1) = (c_1 + r_1)(c_2 + r_2)k_1k_2$  which is always positive since  $c_i, r_i$  and  $k_i, i = 1, 2$  are positive parameters. Simplifying the other two conditions completes the proof.  $\square$

**Proposition 4.** *The equilibrium point  $O$  may be destabilized due to*

- (i) flip bifurcation if  $k_1k_2 < (4/((c_1 + r_1)(c_2 + r_2)))$
- (ii) Neimark-Sacker bifurcation  $k_1 + k_2 < (4(c_1 + r_1 + c_2 + r_2)/((c_1 + r_1)(c_2 + r_2)))$

*Proof.* Substituting (13) in  $g(-1)$  and  $\Omega$  then taking  $g(-1) = 0$ , we get

$$(c_1 + r_1)(c_2 + r_2)k_1k_2 = \frac{4(c_1 + r_1)(c_2 + r_2)(k_1 + k_2)}{(c_1 + r_1 + c_2 + r_2)}. \quad (14)$$

Substituting (14) in  $\Omega > 0$  completes the proof of (i). For the part (ii), we put  $\Omega = 0$ , and then we get

$$(c_1 + r_1)(c_2 + r_2)k_1k_2 = \frac{8(c_1 + r_1)(c_2 + r_2)(k_1 + k_2)}{(c_1 + r_1 + c_2 + r_2)}. \quad (15)$$

Then substituting (15) in  $g(-1) > 0$  completes the proof of (ii).  $\square$

**2.2. The Synchronization Property.** Synchronized trajectories in such game is an important property that may give more information about the dynamic of the model's game. Indeed, such property may be occurred and there may be a transversely stable orbit on the diagonal  $\Delta = \{(q_1, q_2) : q_1 = q_2\}$ . In case, such dynamics exist due to nonsynchronizing trajectories, and it would be important to detect the initial conditions leading to synchronization property. The possibility of such property arises when an invariant one-dimensional submanifold of  $\mathbb{R}^2$  exists. This means that the synchronized trajectories are described by

$$(q_1(t), q_2(t)) = \{T^t : (q_1(0), q_2(0)) | q_1(t) = q_2(t) \forall t \geq 0\}. \quad (16)$$

These trajectories given in (16) are regularized by the restriction of the map  $T$  on the invariant submanifold by which synchronized dynamics occur and are described by the one-dimensional map:

$$T|_{\Delta} \Delta \longrightarrow \Delta. \quad (17)$$

For trajectories beginning outside the map given in (17) are said to be synchronized ones if  $|q_1(t) - q_2(t)| \longrightarrow 0$  as  $t \longrightarrow \infty$ . Our map given in (7) possesses the six parameters,  $k_1, k_2, c_1, c_2, r_1$ , and  $r_2$ . Now, we assume the following:

$$k_1 = k_2 = k, \quad (18)$$

$$c_1 = c_2 = c \text{ and } r_1 = r_2 = r.$$

Under this assumption, the map (7) becomes

$$T_s(q_1, q_2): \begin{cases} q_1(t+1) = q_1(t) + kq_1(t) \left[ \frac{q_2}{Q^2} - c - r \right], \\ q_2(t+1) = q_2(t) + kq_2(t) \left[ \frac{q_1}{Q^2} - c - r \right]. \end{cases} \quad (19)$$

The restriction  $T_{s|\Delta} \Delta \longrightarrow \Delta$  conjugates the following one-dimensional map:

$$q' = q + kq \left[ \frac{1}{4q} - c - r \right]. \quad (20)$$

Studying the transverse stability of the synchronized attractors of the system (19) requires to calculate its Jacobian at the equilibrium point  $O_s = ((1/4)(c+r), (1/4)(c+r))$  as follows:

$$J_{T_s}(q_1, q_2) = \begin{pmatrix} 1 - k(c+r) & 0 \\ 0 & 1 - k(c+r) \end{pmatrix}, \quad (21)$$

Whose eigenvalues are  $\lambda_1 = \lambda_2 = 1 - k(c+r)$ . It is simple to see that  $|\lambda_{1,2}| < 1$  if  $k < (2/c+r)$ , and hence  $O_s$  is an attracting stable node.

**2.3. Local Analysis.** In this section, we give some numerical experiments to validate the above results. As in [6], we assume the following values,  $c_1 = 2, c_2 = 1.5, r_1 = 0.13, r_2 = 0.15, k_1 = 0.2$ , and  $k_2 = 0.1$ . The Jacobian (10) at these values becomes

$$J_O \approx \begin{pmatrix} 0.6281 & -0.4191 \\ 0.0271 & 0.8141 \end{pmatrix}, \quad (22)$$

whose eigenvalues are real and equal  $\lambda_1 \approx 0.6344$  and  $\lambda_2 \approx 0.8077$ . One can see that  $|\lambda_{1,2}| < 1$ , and hence the

equilibrium point  $O = (0.2194787379, 0.1508916323)$  is the local stable point. Any increase in the parameters  $r_1, r_2, k_1$ , and  $k_2$  leads to unstable equilibrium point through flip bifurcation. In Figure 1(a), we take the parameter  $k_1$  as the bifurcation parameter and fix the other parameters' values to  $c_1 = 2, c_2 = 1.5, r_1 = 0.13, r_2 = 0.15$ , and  $k_2 = 0.1$ . As it can be seen that the point  $O$  is locally stable for all the values of  $k_1$  till this parameter reaches the point of cycle of period two and it becomes unstable. As  $k_1$  increases further, higher periodic cycles are born, then the map enters the chaos area, and then becomes chaotic (as confirmed in the Largest Lyapunov exponent (LLE) given in Figure 1(c)). We should highlight here that the governmental taxes are different with 13% imposed on the quantity produced by the first firm while the tax imposed on the second firm is 15%. Numerical experiments show that higher governmental taxes imposed lead to shrinking of the stability region as will be discussed in the global analysis later on. Figure 1(b) shows that the impact on the parameter  $k_1$  is slightly different on the quantities produced by both firms. This may be due to the cost of productions and taxes imposed that are slightly different. The same discussions are for the impact of the parameter  $k_2$  when it is taken as the bifurcation diagram. Figures 1(d)–1(f) show the bifurcation diagram with respect to  $k_2$  and the corresponding LLE at the parameters' values,  $c_1 = 2, c_2 = 1.5, r_1 = 0.13, r_2 = 0.15$ , and  $k_1 = 0.2$ . On the other hand, we give in Figure 1(g)–1(l) the taxation impact on the equilibrium point and the corresponding LLE. Figure 1(g) shows that at the parameters' values  $c_1 = 2, c_2 = 1.5, k_1 = 1.1, k_2 = 0.9$ , and  $r_2 = 0.15$ , the equilibrium point is stable at taxation rate  $r_1 < 37\%$ ; then, it becomes unstable through Neimark–Sacker bifurcation. As  $r_1$  increases further, a closed ring is born that is followed by a cycle of period 7 and then the map enters the chaotic region. The same discussion and observations are for the other taxation parameter  $r_2$  on where its effect is given in Figures 1(j) and 1(k). The Figures 1(j) and 1(k) show the impact of  $r_2$  on the quantity  $q_2$ . Simulation shows that in the interval  $[0.256756, 0.26667]$ , the quantity  $q_2$  bifurcates into two chaotic bands not period 2-cycle, and this is observed in the corresponding Lyapunov exponent given in Figure 1(l).

Now, we assume the set of parameters' values ( $r_1 > r_2$ ),  $c_1 = 2, c_2 = 1.5, r_1 = 0.25, r_2 = 0.20, k_1 = 1$ , and  $k_2 = 1$ . The Jacobian [10] at these values becomes

$$J_O \approx \begin{pmatrix} -0.93671 & -0.23671 \\ 0.31329 & -0.93671 \end{pmatrix}, \quad (23)$$

Whose eigenvalues are complex and equal  $\lambda_{1,2} \approx -0.93671 \pm 0.27232i$ . One can see that  $|\lambda_{1,2}| < 1$ , and hence the equilibrium point  $O = (0.1089568979, 0.1442076590)$  is local stable point. Any increase in the parameters  $r_1, r_2, k_1$ , and  $k_2$  leads to unstable equilibrium point through Neimark–Sacker (N-S) bifurcation. In Figures 2(a) and 2(b), we take the parameter  $k_1$  as the bifurcation parameter and fix the other parameters' values to  $c_1 = 2, c_2 = 1.5, r_1 = 0.25, r_2 = 0.20$ , and  $k_2 = 1$ . It is clear that the equilibrium point loses its stability through N-S bifurcation. The same observations are obtained when we

take the parameters  $r_1, r_2$ , and  $k_2$  as the bifurcation's parameter. The Figures 2(c)–2(h) give the N-S bifurcations for those parameters.

**2.4. Global Analysis.** The above local analysis regarding the bifurcation diagrams does not permit further understanding about the future evolution of the map (7). For this reason, some complex behaviors and their basins of attraction are given here. As said before, the map (7) depends on the parameters  $k_1, k_2, c_1, c_2, r_1$ , and  $r_2$ . Let us first investigate the influences of the parameters  $k_1$  and  $k_2$  by assuming the following parameters values,  $c_1 = 2, c_2 = 1.5, r_1 = 0.13, r_2 = 0.15$ . This set of parameters values gives the two-dimensional bifurcation diagram in the  $(k_1, k_2)$  – plane presented by Figure 3(a). It is clear that this plane is divided into different periods by different colors besides the stability region. The figure shows that the system behaves chaotically when the speed of adjustment parameters  $k_1$  and  $k_2$  are all high. Any changing in those two parameters while keeping the other parameters fixed makes the system enter the chaotic region through Flip and Neimark Sacker bifurcation. The system's attractors and multistability have been investigated by many scholars in literature ([4, 6, 16]). Such investigations have shown one of the important conditions of chaos which is the sensitivity to the initial conditions. In economic market, different strategies by decision makers may lead to different directions to the development of the firm's direction. Consequently, adopting a good way of choosing initial conditions is very important which in turn gives an indication of whether the firm will behave well or not in the future. This includes the coexistence of multiple attractors and their influences on the stability of the equilibrium point. The basins of attraction can help in investigating such attractors. It can be used to analyze the convergence of system after a series of iterations (games) based on certain initial conditions. It helps the firm's decision makers to choose a range of initial values by which the firm can develop better. For instance, let us assume the following initial set:  $c_1 = 2, c_2 = 1.5, r_1 = 0.13, r_2 = 0.15, k_1 = 1.39422$ , and  $k_2 = 0.66044$ . This set gives rise to a period of 3-cycle with its basins of attraction plotted in Figure 3(b). In Figure 3(b), the gray color characterizes the divergence (or the unfeasible trajectories), while the other colors represent the attractive basin of the equilibrium point  $O$  and the basin of attraction of period 3-cycle coexisting with  $O$ . The peculiar shape of the basin of attraction given in Figure 3(b) will be because of the origin point as will be discussed in the next section. Figure 3(c) gives a chaotic situation of the system around the equilibrium point as  $k_1$  increases to 1.26, and the other parameters values are fixed to  $c_1 = 2, c_2 = 1.5, r_1 = 0.13, r_2 = 0.15, k_2 = 0.1$ . Increasing the taxes and the speed of adjustment parameters gives rise to instability situation of the equilibrium point due to Neimark–Sacker bifurcation. For instance, the parameter values  $c_1 = 2, c_2 = 1.5, r_1 = 0.25, r_2 = 0.20, k_1 = 1.027$ , and  $k_2 = 0.1$  present a quasiperiodic dynamic possessing an attracting invariant closed ring around the equilibrium



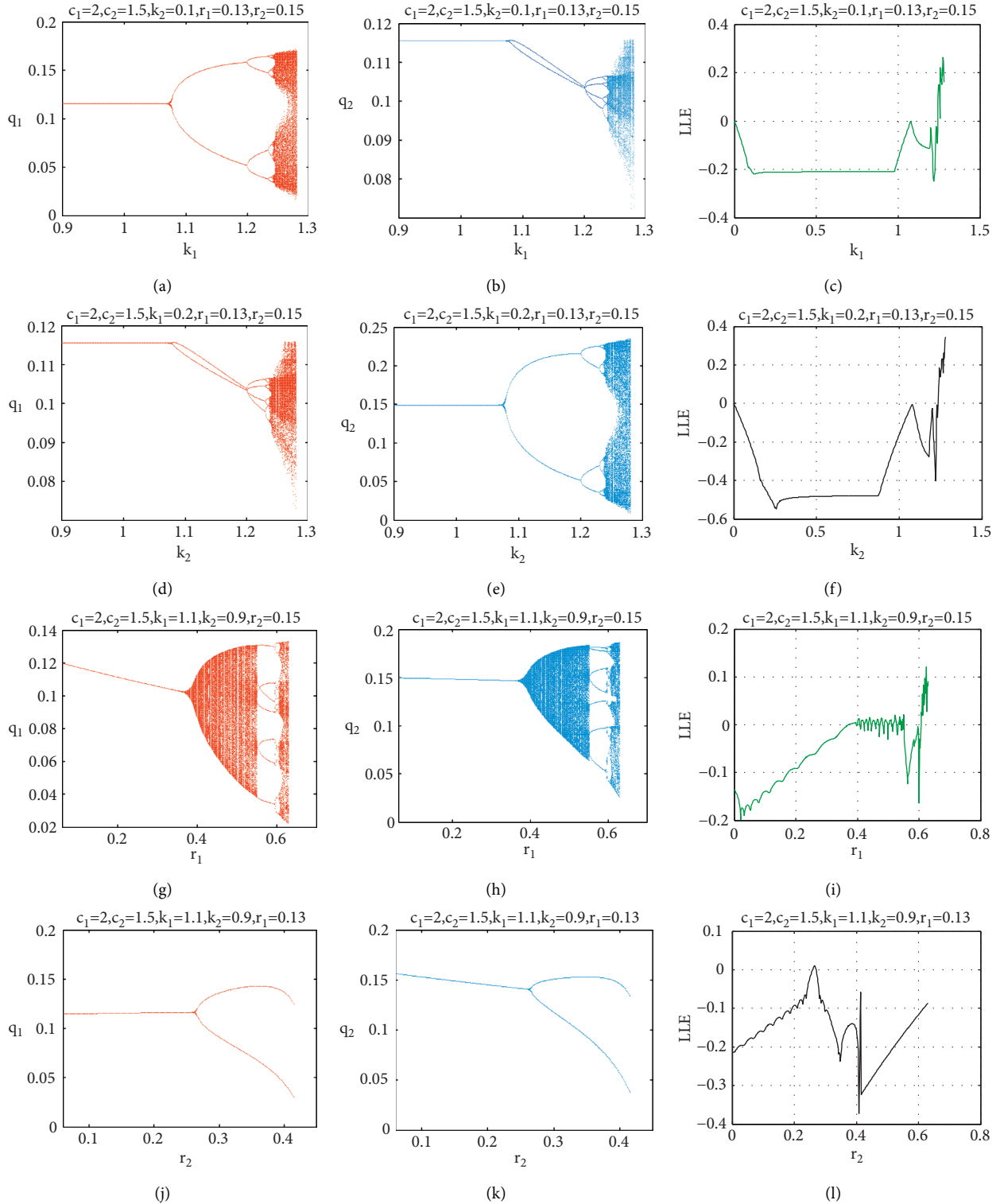


FIGURE 1: (a–l) Different types of bifurcation diagrams with respect to the parameters  $r_1, r_2, k_1$ , and  $k_2$  when  $r_1 < r_2$  and their corresponding Lyapunov exponents. Each figure is plotted at some parameters values given in the text and within the figure itself.

point. Other closed invariant curve is given when increasing the speed of adjustment parameter  $k_1$  to 1.1. As shown previously, the stability conditions depend on the tax parameters and any changes in those parameters give rise to instability of the equilibrium point. For this reason,

the two-dimensional bifurcation diagram in the  $(r_1, r_2)$ –plane is depicted in Figure 3(f). We finish this section by giving in Figure 4, an example of period 2-cycle at fixing the parameters values:  $c_1 = 2, c_2 = 1.5, r_1 = 0.027, r_2 = 0.448, k_1 = 1.1$ , and  $k_2 = 0.9$ .

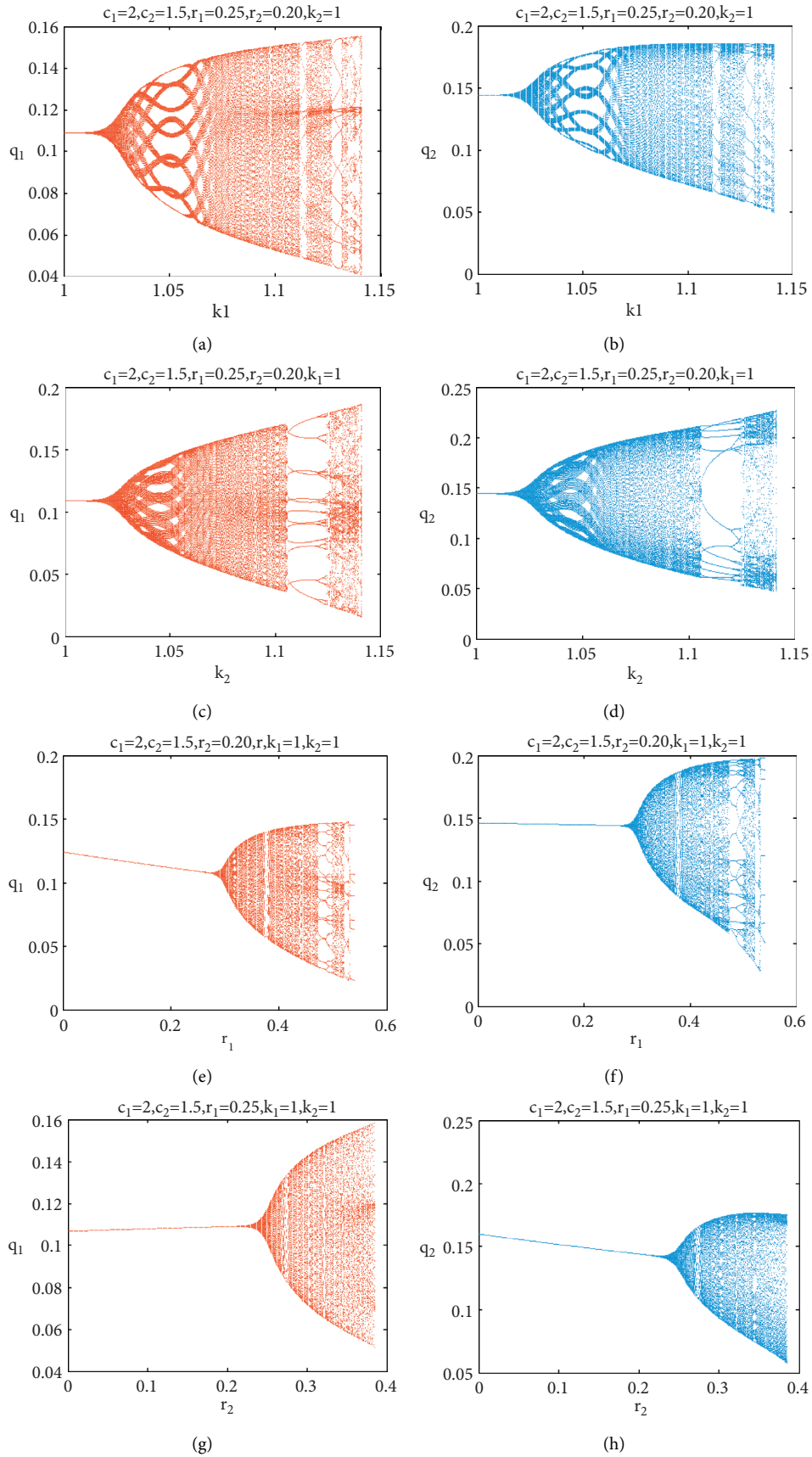


FIGURE 2: (a–h) The N-S bifurcation diagrams with respect to the parameters  $r_1, r_2, k_1$ , and  $k_2$  when  $r_1 > r_2$ . Each figure is plotted at some parameters values given in the text and within the figure itself.

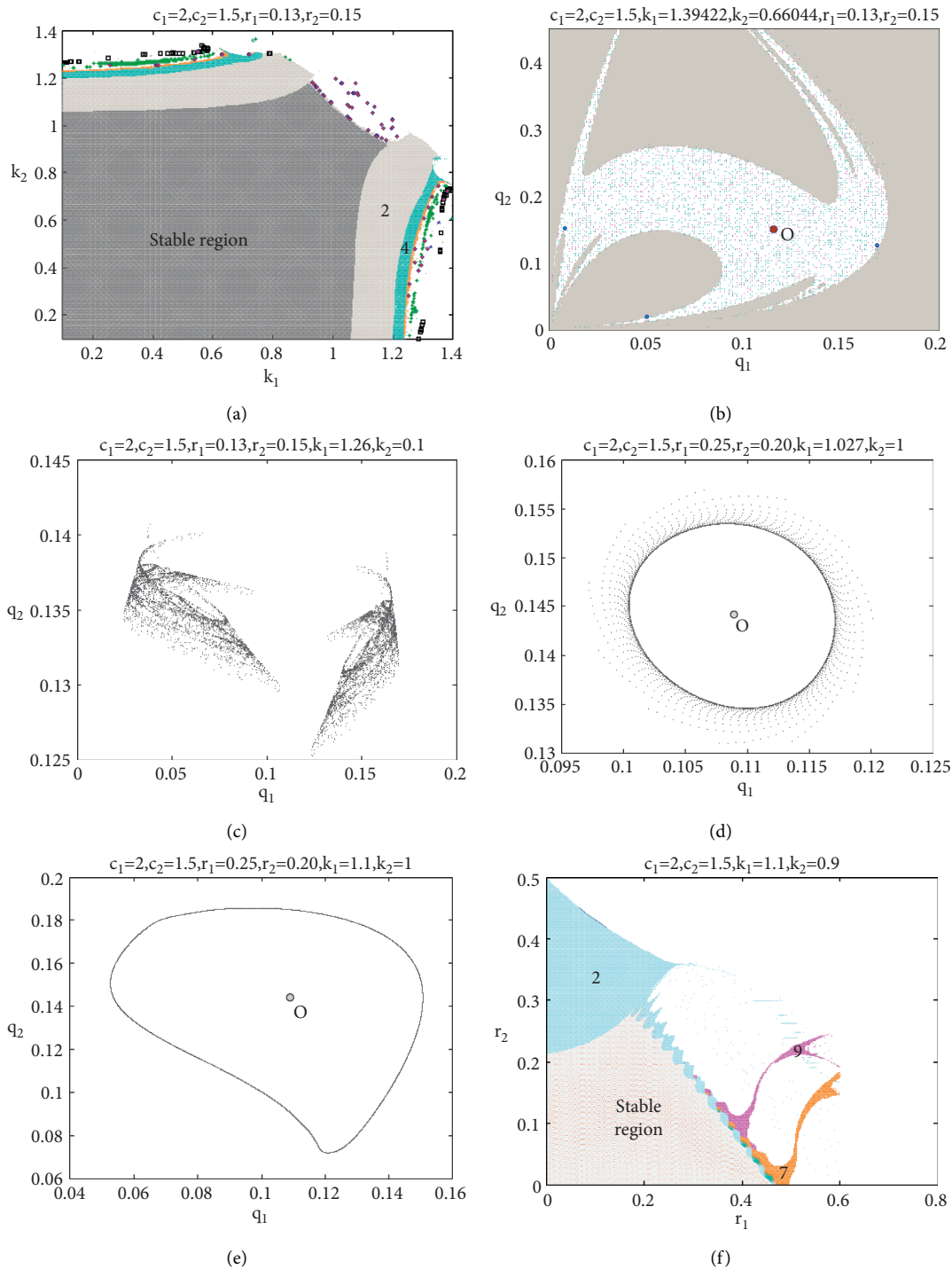


FIGURE 3: (a) 2D-bifurcation diagram at  $c_1 = 2, c_2 = 1.5, r_1 = 0.13, r_2 = 0.15$ . (b) The period of 3-cycle at  $c_1 = 2, c_2 = 1.5, r_1 = 0.13, r_2 = 0.15, k_1 = 1.39422$ , and  $k_2 = 0.66044$ . (c) Chaotic dynamic behavior at  $c_1 = 2, c_2 = 1.5, r_1 = 0.13, r_2 = 0.15, k_1 = 1.26, k_2 = 0.1$ . (d) Closed invariant curve at  $c_1 = 2, c_2 = 1.5, r_1 = 0.25, r_2 = 0.20, k_1 = 1.027, k_2 = 0.1$ . (e) Closed ring at  $c_1 = 2, c_2 = 1.5, r_1 = 0.25, r_2 = 0.20, k_1 = 1.1, k_2 = 0.1$ . (f) 2D-bifurcation diagram at  $c_1 = 2, c_2 = 1.5, k_1 = 1.1, k_2 = 0.9$ .

**2.5. Critical Curves and Preimage Zones.** The phase plane of the map (7) at any sets of parameters' values possesses some important characteristics. Looking at this map, one can observe that at  $q_1(t) = 0$  or  $q_2(t) = 0$ , one gets  $q_1(t+1) = 0$  or  $q_2(t+1) = 0$ , respectively. This means that the origin point  $(0, 0)$  traps the map (7), and therefore, it is important

to start with this point in order to calculate the boundaries of the attractive basins for any attracting set for that map. To do that, we set  $q_1(t+1) = q_1$  and  $q_2(t+1) = q_2$  in (7) where 'indicates time evolution. This means that the map's time evolution is attained by the iteration of  $T: (q_1, q_2) \rightarrow (q_1, q_2)$  as follows:

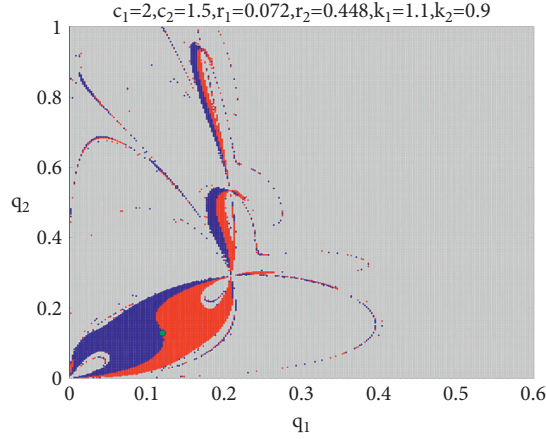


FIGURE 4: The period of 2-cycle at  $c_1 = 2$ ,  $c_2 = 1.5$ ,  $r_1 = 0.072$ ,  $r_2 = 0.448$ ,  $k_1 = 1.1$ , and  $k_2 = 0.9$ .

$$T: \begin{cases} \dot{q}_1 = q_1 + k_1 q_1 \left[ \frac{q_2}{Q^2} - c_1 - r_1 \right], \\ \dot{q}_2 = q_2 + k_2 q_2 \left[ \frac{q_1}{Q^2} - c_2 - r_2 \right]. \end{cases} \quad (24)$$

If the inverse map  $T^{-1}: (q_1, q_2) \rightarrow (q_1, q_2)$  is existed and gets unique values in each point in the range, then the map is called invertible. Hence, the point  $(q_1, q_2) \in \mathbb{R}^2$  is called a rank-1 image while  $(q_1, q_2)$  is called rank-1 preimages. If for an image  $(q_1, q_2)$ , there are at least two rank-1

preimages and we call  $T$  a noninvertible map. The following proposition shows that the point  $(0, 0)$  has two real rank-1 preimages, and hence, the map is noninvertible.

**Proposition 5.** *The origin point  $(0, 0)$  has two real rank-1 preimages.*

*Proof.* Setting  $\dot{q}_1 = 0$  and  $\dot{q}_2 = 0$  in (23), one gets a system of algebraic equations whose solutions are the two preimages as follows:

$$\begin{aligned} O_{-1}^{(0)} &= (0, 0), \\ O_{-1}^{(1)} &= \left( \frac{k_1^2 k_2 (c_2 k_2 + r_2 k_2 - 1)}{[k_1 k_2 (c_1 + c_2 + r_1 + r_2) - k_1 - k_2]^2}, \frac{k_1 k_2^2 (c_1 k_1 + r_1 k_1 - 1)}{[k_1 k_2 (c_1 + c_2 + r_1 + r_2) - k_1 - k_2]^2} \right). \end{aligned} \quad (25)$$

This completes the proof.

Figure 5 shows that phase plane of the map is divided by the two regions that are  $Z_1$  and  $Z_3$ , and hence, the map (7) is

of type  $Z_1 - Z_3$ . These two regions are calculated by the critical curves  $LC$  and  $LC_{-1}$ . The later can be calculated by vanishing the Jacobian of (7) which gives

$$\begin{aligned} \ell_1 \ell_2 q_2^3 + \ell_1 \ell_2 q_1^3 + k_2 \ell_1 q_1^2 + k_1 \ell_2 q_2^2 + 3\ell_1 \ell_2 q_1 q_2^2 + 3\ell_1 \ell_2 q_1^2 q_2 + \ell_3 q_1 q_2 &= 0, \\ \ell_i &= (1 - c_i k_i - r_i k_i); i = 1, 2 \\ \ell_3 &= k_1 k_2 (c_1 + c_2 + r_1 + r_2) - k_1 - k_2. \end{aligned} \quad (26)$$

Because  $LC$  is calculated from the relation  $LC = T(LC_{-1})$ , and (26) contains many parameters, it is plotted at the parameter values  $c_1 = 2$ ,  $c_2 = 1.5$ ,  $r_1 = 0.13$ ,  $r_2 = 0.15$ ,  $k_1 = 1$ ,  $k_2 = 0.9$ . It is important to highlight that the map (7) is defined at any point in the phase plane except the line  $q_2 = -q_1$  and its preimages of any order. Particularly, there is point in the phase

plane where the map (7) takes the form  $(0/0)$ . This point is called a focal point, and in our case, it is the origin point  $(0, 0)$ . It is responsible for constructing the lobes found in the basins of attraction of any attracting set. These lobes have been discussed in detail in [28]. Such lobes appear in Figure 3(b), and we highlight them in Figure 6.  $\square$

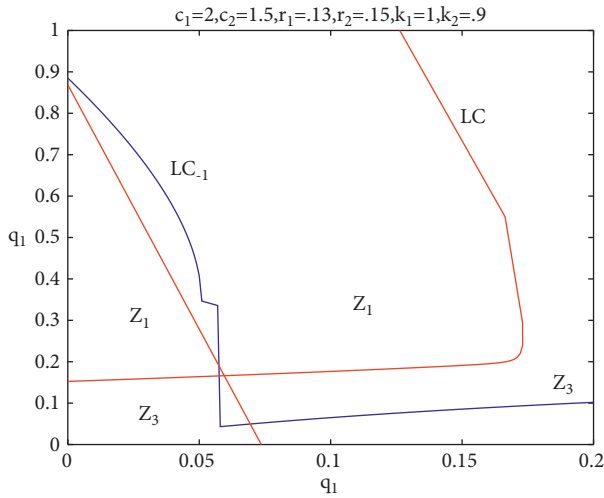


FIGURE 5: The critical curves  $LC$  and  $LC_{-1}$  and the region  $Z_i, i = 1, 3$  at the set of parameters:  $c_1 = 2, c_2 = 1.5, r_1 = 0.13, r_2 = 0.15, k_1 = 1, k_2 = 0.9$ .

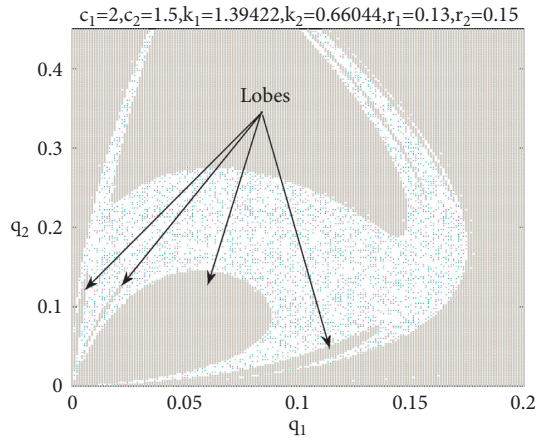


FIGURE 6: The Lobes constructed with period of 3-cycle at:  $c_1 = 2, c_2 = 1.5, r_1 = 0.13, r_2 = 0.15, k_1 = 1.39422$  and  $k_2 = 0.66044$ .

### 3. Conclusion

In the present paper, we have introduced a Cournot duopoly game whose players are rational and seek the optimality of quantity production in order to achieve profit maximization. The utility function introduced in this paper may be considered as a special case of the Singh and Vives function [1]. Our utility function has given inverse demand functions which are the same as those obtained from Cobb–Douglas utility. The map's game possesses a unique equilibrium point which is Nash point which loses its stability through flip and Neimark–Sacker bifurcation. As shown in the obtained results, increasing the tax parameters gives rise to Neimark–Sacker bifurcation, then route to chaos is obtained, and then unpredictable behaviors for the dynamics of the game are arisen. It has been observed that the high values for the tax parameters affect the stability region. The region has decreased for high values of the taxes and the speed of adjustment parameters. Furthermore, the attractive basins

for some attracting sets have been presented. The shapes of those basins are peculiar because they have contained some lobes due to the origin focal point. Future study directions will focus on the application of the introduced utility in economic models of public enterprises with consumer surplus.

## Appendix

### A. The Lagrangian Function can be Described as Follows:

$$L(q_1, q_2, \lambda) = U(q_1, q_2) + \lambda(m - p_1 q_1 - p_2 q_2). \quad (\text{A.1})$$

So, the first-order conditions are given by

$$\begin{aligned} \frac{\partial L}{\partial q_1} &= \frac{\partial U}{\partial q_1} - \lambda p_1 \\ &= 0, \end{aligned}$$

$$\begin{aligned} \frac{\partial L}{\partial q_2} &= \frac{\partial U}{\partial q_2} - \lambda p_2 \\ &= 0, \end{aligned} \quad (\text{A.2})$$

$$\frac{\partial L}{\partial \lambda} = m - \sum_{i=1}^2 p_i q_i.$$

Using (1) in the first two equations of (A.2), one can get (3).

### Data Availability

No data were used to support this study.

### Conflicts of Interest

The authors declare that they have no conflicts of interest.

### Acknowledgments

This work was supported and funded by Research Supporting Project (number RSP-2022/167), King Saud University, Riyadh, Saudi Arabia.

### References

- [1] N. Singh and X. Vives, "Price and quantity competition in a differentiated duopoly," *The RAND Journal of Economics*, vol. 15, no. 4, pp. 546–554, 1984.
- [2] A. A. Elsadany, "Dynamics of a Cournot duopoly game with bounded rationality based on relative profit maximization," *Applied Mathematics and Computation*, vol. 294, pp. 253–263, 2017.
- [3] J. Tuinstra, *A price adjustment process in a model of monopolistic competition*. *International Game Theory Review*, vol. 6, no. 3, pp. 417–442, 2004.

- [4] A. K. Naimzada and R. Raimondo, "Chaotic congestion games," *Applied Mathematics and Computation*, vol. 321, pp. 333–348, 2018.
- [5] M. Ueda, "Effect of information asymmetry in Cournot duopoly game with bounded rationality," *Applied Mathematics and Computation*, vol. 362, Article ID 124535, 2019.
- [6] T. Puu, "Chaos in duopoly pricing," *Chaos, Solitons & Fractals*, vol. 1, no. 6, pp. 573–581, 1991.
- [7] S. S. Askar and A. Al-khedhairi, "Dynamic investigations in a duopoly game with price competition based on relative profit and profit maximization," *Journal of Computational and Applied Mathematics*, vol. 367, Article ID 112464, 2020.
- [8] S. S. Askar, "On Cournot-Bertrand competition with differentiated products," *Annals of Operations Research*, vol. 223, no. 1, pp. 81–93, 2014.
- [9] S. S. Askar, "Triopoly Stackelberg game model: one leader versus two followers," *Applied Mathematics and Computation*, vol. 328, pp. 301–311, 2018.
- [10] S. S. Askar and A. Al-Khedhairi, "Analysis of nonlinear duopoly games with product differentiation: Stability, Global Dynamics, and Control," *Discrete Dynamics in Nature and Society*, vol. 2017, Article ID 2585708, 13 pages, 2017.
- [11] S. Bylka and J. Komar, "Cournot-Bertrand mixed oligopolies," in *Warsaw Fall Seminars in Mathematical Economics 1975*, M. Łoś, J. Łoś, and A. Wieczorek, Eds., vol. 133, Berlin, Heidelberg, Springer, 1976 Lecture Notes in Economics and Mathematical Systems.
- [12] J. Häckner, "A note on price and quantity competition in differentiated oligopolies," *Journal of Economic Theory*, vol. 93, no. 2, pp. 233–239, 2000.
- [13] P. Zanchettin, "Differentiated duopoly with asymmetric costs," *Journal of Economics and Management Strategy*, vol. 15, no. 4, pp. 999–1015, 2006.
- [14] A. Arya, B. Mittendorf, and D. E. M. Sappington, "Outsourcing, vertical integration, and price vs. quantity competition," *International Journal of Industrial Organization*, vol. 26, no. 1, pp. 1–16, 2008.
- [15] C. H. Tremblay and V. J. Tremblay, "The Cournot-Bertrand model and the degree of product differentiation," *Economics Letters*, vol. 111, no. 3, pp. 233–235, 2011.
- [16] A. K. Naimzada and F. Tramontana, "Dynamic properties of a Cournot-Bertrand duopoly game with differentiated products," *Economic Modelling*, vol. 29, no. 4, pp. 1436–1439, 2012.
- [17] J. Ma, L. Sun, S. Hou, and X. Zhan, "Complexity study on the Cournot-Bertrand mixed duopoly game model with market share preference," *Chaos: An Interdisciplinary Journal of Nonlinear Science*, vol. 28, no. 2, Article ID 023101, 2018.
- [18] E. Ahmed, A. S. Hegazi, M. F. Elettrey, and S. S. Askar, "On multi-team games," *Physica A: Statistical Mechanics and Its Applications*, vol. 369, no. 2, pp. 809–816, 2006.
- [19] E. Ahmed and M. F. Elettrey, "Controls of the complex dynamics of a multi-market Cournot model," *Economic Modelling*, vol. 37, pp. 251–254, 2014.
- [20] Y. Peng and Q. Lu, "Complex dynamics analysis for a duopoly Stackelberg game model with bounded rationality," *Applied Mathematics and Computation*, vol. 271, pp. 259–268, 2015.
- [21] F. Tramontana, "Heterogeneous duopoly with isoelastic demand function," *Economic Modelling*, vol. 27, no. 1, pp. 350–357, 2010.
- [22] J. Tanimoto, *Evolutionary Games with Sociophysics*, Springer, Berlin, Heidelberg, 2019.
- [23] J. Tanimoto, *Fundamentals of Evolutionary Game Theory and its Applications*, Springer, Berlin, Heidelberg, 2015.
- [24] J. Tanimoto, *Mathematical Analysis of Environmental System*, Springer, Berlin, Heidelberg, 2014.
- [25] W. Zhong, S. Kokubo, and J. Tanimoto, "How is the equilibrium of continuous strategy game different from that of discrete strategy game?" *Biosystems*, vol. 107, no. 2, pp. 88–94, 2012.
- [26] S. Kokubo, Z. Wang, and J. Tanimoto, "Spatial reciprocity for discrete, continuous and mixed strategy setups," *Applied Mathematics and Computation*, vol. 259, pp. 552–568, 2015.
- [27] H. Wang and J. Ma, "Complexity analysis of a Cournot-Bertrand duopoly game model with limited information," *Discrete Dynamics in Nature and Society*, vol. 2013, Article ID 287371, 6 pages, 2013.
- [28] F. Cavalli, A. Naimzada, and F. Tramontana, "Nonlinear dynamics and global analysis of a heterogeneous Cournot duopoly with a local monopolistic approach versus a gradient rule with endogenous reactivity," *Communications in Nonlinear Science and Numerical Simulation*, vol. 23, no. 1-3, pp. 245–262, 2015.

## Research Article

# Mathematical and Statistical Models with Applications of Spread of Private Tutoring in Saudi Arabia

Alanazi Talal Abdulrahman <sup>1</sup> and Adel A. Attiya <sup>1,2</sup>

<sup>1</sup>Department of Mathematics, College of Science, University of Ha'il, Hail, Saudi Arabia

<sup>2</sup>Department of Mathematics, Faculty of Science, Mansoura University, Mansoura 35516, Egypt

Correspondence should be addressed to Adel A. Attiya; [aattiy@mans.edu.eg](mailto:aattiy@mans.edu.eg)

Received 19 August 2021; Revised 8 December 2021; Accepted 10 February 2022; Published 6 April 2022

Academic Editor: Sameh S. Askar

Copyright © 2022 Alanazi Talal Abdulrahman and Adel A. Attiya. This is an open access article distributed under the Creative Commons Attribution License, which permits unrestricted use, distribution, and reproduction in any medium, provided the original work is properly cited.

Over the past century, private tutoring (PT) in many countries has increased dramatically. Moreover, the main disadvantage of PT is that has a byproduct and a characteristic on the educational system in developing countries in terms of contributing to conditions such as large class sizes, low public expenditures, and an inadequate number of universities. In Saudi Arabia, the spread of PT at school and university levels has yet to be addressed by researchers. One goal of this examination was to research the spread of PT in relation to mathematics being taught at school and university levels. This investigation used quantitative data of the questionnaire to determine the reasons for the spread. A total of 1000 students responded from University of Ha'il. The edge plans given results that are associated and like the assessment that is performed with the whole data. The current study found that a good family financial situation and lack of parental supervision of the children were significant factors underlying the spread of private tutoring at school and university levels.

## 1. Introduction

Over the past century, private tutoring (PT) in many countries has increased dramatically. Private coaching is a far-reaching marvel in numerous nations. Moreover, the main disadvantage of PT is that has a byproduct and a characteristic on the educational system in developing countries in terms of contributing to conditions such as large class sizes, low public expenditures, and an inadequate number of universities. In Saudi Arabia, the spread of PT at school and university levels has yet to be addressed by researchers. There is evidence that PT plays important role in Saudi Arabia's educational systems and private mentoring influences numerous subjects in the Saudi instructive educational programs, albeit certain subjects take a lot of consideration. PT has become a threat to the skills and methods of students and teachers (Ikediashi et al. [1]). One goal of this examination was to research the spread of PT in relation to mathematics being taught at school and university levels. To achieve this goal, this investigation used

quantitative data of the questionnaire to determine the reasons for the spread. This paper begins, however, by reviewing the previous research on the spread of PT in Saudi Arabia.

Many published studies (e.g., Kwok [2] and Bray [3]) describe PT as "shadow education." According to Kwok, in many created nations (for example, Canada and USA) the interest for private mentoring has expanded. Surveys such as the one conducted by Tansel and Bircan [4] have shown that PT is an educational form that lies outside the formal tutoring framework. These surveys also connect PT to a motivation for financial gain. They note that understudies who take private mentoring trust that their odds of effectively traveling through the instructive framework will be expanded. The findings of Nyandara [5] were that students take on private educational costs because they need to get high marks on examinations. The students enrolling in private education paid Ksh 2000 per term. The private education helped enhance their scholarly performance. Manzoor [6] studied the reasons for and necessity of PT in

English for Bangla medium primary school students in Bangladesh. As part of this examination, thirty-five respondents were surveyed using written questionnaire. In addition, classroom monitoring was done to identify failures, if any, in English education. The discoveries from the overview demonstrate that a large portion of the essential dimension students get private coaching and they are happy with the English exercise given by their private mentor as opposed to their teacher. Ali studied private tutoring in Jordan. The study concluded that the causes of the spread of private tutoring are to get high grade in request to enroll at colleges and in specific specializations and influenced the commonness of private mentoring is the sort of scholarly branch. Ghounane [7] conducted a study titled "Private Tutoring and Public Schools in Algeria: Issues and Reflections. The study concluded, «parents send their children to private sessions for several reasons among which the poor teaching level in mainstream schooling in addition to the competitive nature that is based on the idea of prestige».

Nusseibeh in Al-Fattal [8] examined the reasons for the spread of private lessons from the point of view of managers, teachers, students, and parents and ways to reduce this spread in Syria. The study concluded the reasons of the spread of this wonder return to the superintendent initially, and to the understudy, thirdly to the family, at that point to the educator. Hamid et al [9] argued that understudies may depend on PT not because of its demonstrated viability but since of their declining confidence in school English instructing. Rima and Saji in Ahmed [10] discussed the prevalence of private tutoring in Deir Al Balah and the reasons for its emergence. The study concluded that non-self-reliance and lack of interest to explain the teacher are the reasons of the spread private tutoring. The study of Tansel and Bircan Bodur [11] was the first of many investigators to demonstrate PT, particularly to get ready for the focused college selection test, is a significant, across the board marvel in Turkey. The examination of Yung (2015) researched the learning knowledge and impressions of 14 Chinese students who had gotten English private coaching (PT) during their auxiliary instruction in Hong Kong. Every member finished a foundation survey and partook in a one-to-one semi organized meeting. The examination uncovered members' conflicted and dumbfounding dispositions toward PT. Despite the fact that they considered PT key for auxiliary instruction, they did not see it as a compelling method to build their English capability in light of its exorbitant spotlight on assessment aptitudes rather than the utilization of English as a language of worldwide correspondence. A longitudinal study of PT by Bray [12] reports that PT has for quite some time been a noteworthy wonder in parts of East Asia, including Japan, Hong Kong, South Korea and Taiwan. Lately it has developed significantly in different pieces of Asia and in Africa, Europe and North America. The elements basic the development of private mentoring fluctuate, yet in all settings, it has real ramifications for learning and business. Families with the important assets can verify more noteworthy amounts as well as better characteristics of private coaching. Kids getting such coaching are then ready to perform better in school, and over the long haul to

improve their lifetime income. Conversely, offspring of low-income families who do not get such advantages will most likely be unable to stay aware of their friends and may drop out of school at a prior age.

Three main types of PT occur in our application in Saudi Arabia: the first is individual tutoring in which student goes to the teacher's home, this kind of PT is very expensive and costs much than other types of PT. The second kind is group tutoring in which the students go to the teacher's home, this kind of PT does not cost as much as individual tutoring. The third kind of PT is provided by school administrations, usually after school hours.

## 2. Procedures

Approach is an assortment of practices, techniques, and rules utilized by the individuals who work in an order or on the other hand take part in a request or research. Technique is a progression of decisions:

- (1) Decisions about what data and information to accumulate
- (2) Decisions about how to examine the data and information that you assemble
- (3) Other methodological decisions

*2.1. Research Design.* Two main types of study design of data collection were used to identify the spread of PT at school and university levels in Saudi Arabia. The first method involved conducting surveys regarding the spread of PT and then analyzing the survey results. The questionnaire questions contain 16 questions to find out the reasons that led to the spread of the problem of private lessons, where the study takes into account the different factors that relate to the student, teacher or university professor and educational administration, family, school or university. The questions asked the participants to assess how strongly they agreed with each statement in the questionnaires (see Table 1).

*2.2. Participants.* Two primary techniques to gather genuine information were utilized: (1) the math scores for the last tests were gathered from the everyday schedule and (2) understudy polls were directed by scattering 16-question surveys to understudies. These are results rather than methods. Also, consider providing detail on the scores collected and on the students surveyed and on how the surveys were distributed and collected, as well as including a sample questionnaire with this paper. The target population comprised 1,000 students from University of Ha'il. We could then calculate the achievement levels for the targeted student using the suitable sample. These levels are displayed in Table 1, which presents the data collected. A questionnaire was given to the students to find out the reasons that led to the spread of the problem of private lesson. The questionnaire questions contain 16 questions to find out the reasons that led to the spread of the problem of private lessons. The questions asked the participants to assess how strongly they



TABLE 1: Notes to be considered about the data tables.

X	Factor	Signal	Description
$X_1$	Lake of achievement	+	Yes
		-	No
$X_2$	Frequent absence from school or university	+	Yes
		-	No
$X_3$	Obtain a high mark	+	Yes
		-	No
$X_4$	Explain the behavior of the student during the lesson	+	Yes
		-	No
$X_5$	The culture of the tradition of classmates	+	Yes
		-	No
$X_6$	Lack of self-reliance	+	YES
		-	NO
$X_7$	Inadequate knowledge of the educational material	+	YES
		-	NO
$X_8$	A poor economic situation	+	YES
		-	NO
$X_9$	Unsuitable work environments	+	YES
		-	NO
$X_{10}$	Financial situation	+	YES
		-	NO
$X_{11}$	Lack of parental supervision of the children	+	YES
		-	NO
$X_{12}$	Lack of incentives for teachers	+	YES
		-	NO
$X_{13}$	Lack of supervision and follow-up of teachers or university professors	+	YES
		-	NO
$X_{14}$	The lack of counseling for teachers regarding enrolling in training courses on modern teaching methods	+	YES
		-	NO
$X_{15}$	Large number of students in classroom	+	YES
		-	NO
$X_{16}$	Students are not aware of the good use and communication of tutoring	+	YES
		-	NO
	Y (response)	Grades	First term exams math in 2018 in

agreed with each statement in the questionnaires. The respondents were asked to the mathematics scores for the final tests. The open finished inquiries gave the respondents extension to communicate their assessments about private tutoring in Mathematics.

### 2.3. Instruments

**2.3.1. Edge Designs Analysis.** Elster and Neumaier [13] presented the edge plan. The edge relies upon a model independent test that can be utilized for dynamic factors. To know the dynamic factors, the estimations are master-minded into a gathering of E sets. In this methodology, the estimations vary in just a single part. It is exceptionally normal in screening tests and infers that practically all distinctions

$$z_{i,j} = y_i - y_j, \quad (i, j) \in E, \quad (1)$$

comprise commotion as it were. In case it is expected that the commotion in the information is added substance, ordinarily conveyed with zero mean and fluctuation  $\sigma$ , the  $n - p$  of the  $z_{i,j}$  are regularly appropriated with zero mean and change  $2\sigma$ . In view of the obscure number of exceptions, the

change should be assessed heartily. For instance, the accompanying middle gauge can be utilized:

$$\sigma = \left| \frac{\text{med}\{z_{i,j} : (i, j) \in E\}}{0.675\sqrt{2}} \right|. \quad (2)$$

A preplan comprising of six elements and twelve preliminaries is chosen that shown down (Table 2).

More details about the edge design can be referred to Abdulrahman, Alanazi and Alamri, and Alanazi Talal Abdulrahman.

**2.3.2. Regression Analysis.** Consider modeling between dependent and independent variables. The dependent is First term Exams Math in 2018, and independent variables are the reasons for the spread. An analysis of the data using linear regression with the software package SPSS with equation model, mean and standard deviation.

The plan picked in the past advance is dissected utilizing the edges and regression strategies. On the off chance that the elements that we get from the edge plan strategy are equivalent to the regression technique, these components are the genuine reasons that prompted the spread of PT.

TABLE 2: Edge design of six factors and twelve runs.

Run	$x_1$	$x_2$	$x_3$	$x_4$	$x_5$	$x_6$
1	1	1	-1	1	1	1
2	-1	1	1	1	1	1
3	1	-1	1	1	1	1
4	-1	-1	-1	1	-1	1
5	-1	-1	-1	1	1	-1
6	-1	-1	-1	-1	1	1
7	-1	1	-1	1	1	1
8	-1	-1	1	1	1	1
9	1	-1	-1	1	1	1
10	-1	-1	-1	-1	-1	1
11	-1	-1	-1	1	-1	-1
12	-1	-1	-1	-1	1	-1

### 3. Result

The gathered information were inspected utilizing the edge plan procedure and regression examination, which was performed utilizing SPSS programming to decide the central driver of spread of private exercises at school and college levels in Saudi Arabia.

Utilizing a few models, we show the utilization and examination of these two strategies for one repeat for the information gathered from schools and college.

*Example 1.* Let  $n = 6$  and obtain a high mark  $X_3$ , the behavior of the student during the lesson explain  $X_4$ , the culture of the tradition of classmates  $X_5$ , no reliance on self  $X_6$ , inadequate knowledge of the educational material  $X_7$ , a poor economic situation  $X_8$ . Analyzing the data in Table 3 using edge design is the following. To begin with, we observe to be all of the six contrasts of the response  $y$  over the edges and the absolute regard, as given in Table 4. Second, we figure the center to anticipate the number  $p$  as powerful parts. Third, we find  $(\sigma)$  and learn  $w(p)$  and  $k \times 20.5 \sigma$ . Finally, if the  $w(p)$  is more critical than  $p$  for some hypothesis  $p$ , we stop the method and track down the unique factor. Table 5 exhibits the results; we have  $w(5) = \text{zero}$ , which suggests there are no unique parts.

An examination of the information in Table 3 (utilizing direct relapse) with the product bundle.

SPSS uncovered there is no dynamic variable and gave an expected straight model

$$Y = 82.5 + \varepsilon, \quad (3)$$

with

$$R - sg = 70.9\%, \quad (4)$$

of mean 84.75 and standard deviation  $\sigma = 16.42$ . Additionally, from the outcome, the leftover is typical in light of the fact that  $p$ -esteem (0.200) is more than 0.05.

From the above, I observe that the robust edge design method shows no active factors and the regression analysis method shows no active factor reward. Therefore, I conclude that there is no active factor with linear contributions.

*Example 2.* Let  $n = 6$  and the behavior of the student during the lesson explain  $X_4$ , the culture of the tradition of

TABLE 3: One replicate for Example 1.

Run	$X_3$	$X_4$	$X_5$	$X_6$	$X_7$	$X_8$	Y	Response number
1	1	1	-1	1	1	1	62	46
2	-1	1	1	1	1	1	100	17
3	1	-1	1	1	1	1	98	25
4	-1	-1	-1	1	-1	1	96	61
5	-1	-1	-1	1	1	-1	90	87
6	-1	-1	-1	-1	1	1	70	310
7	-1	1	-1	1	1	1	80	98
8	-1	-1	1	1	1	1	96	65
9	1	-1	-1	1	1	1	81	30
10	-1	-1	-1	-1	-1	1	50	41
11	-1	-1	-1	1	-1	-1	97	15
12	-1	-1	-1	-1	1	-1	97	116

TABLE 4: Model-free checks with edge plan in Table 3.

$X_3$	$X_4$	$X_5$	$X_6$	$X_7$	$X_8$
-18	4	17	46	-7	-27
18	4	17	46	7	27

classmates  $X_5$ , no reliance on self  $X_6$ , inadequate knowledge of the educational material  $X_7$ , a poor economic situation  $X_8$  and unsuitable work environments  $X_9$ . Dissecting the information in Table 6 as described previously. The results are shown in Tables 7 and 8. Therefore, we have  $(5) = 4$  active factors: the behavior of the student during the lesson explain, the culture of the tradition of classmates, inadequate knowledge of the educational material, and unsuitable work environments. An analysis of the data in Table 6 (using linear regression) with the software package SPSS revealed there is no active variable and gave an estimated linear model

$$Y = 82.33 + \varepsilon, \quad (5)$$

with

$$R - sg = 62.2\%, \quad (6)$$

of mean 78.58 and standard deviation  $\sigma = 13.85$ . Also from the result, the residual is normal because  $p$ -value (0.095) is more than 0.05.

From the above, we observe that the robust edge design method shows four active factors—the behavior of the student during the lesson explain, the culture of the tradition of

TABLE 5: step estimations for the investigation with the edge plan.

$p$	Median	$\sigma(p)$ e	$k \times 2^{0.5} \sigma(p)$	$\omega(p)$	$\omega(p) < p?$
0	17.5	18.33	25.92	2	No
1	17	17.80	25.18	2	No
2	12	12.57	17.77	3	No
3	7	7.33	10.37	4	No
4	5.5	5.76	8.14	4	No
5	4	4.19	5.92	5	No

TABLE 6: One replicate for Example 2.

Run	$X_4$	$X_5$	$X_6$	$X_7$	$X_8$	$X_9$	Y	Response number
1	1	1	-1	1	1	1	75	21
2	-1	1	1	1	1	1	98	25
3	1	-1	1	1	1	1	62	46
4	-1	-1	-1	1	-1	1	98	10
5	-1	-1	-1	1	1	-1	70	3
6	-1	-1	-1	-1	1	1	70	6
7	-1	1	-1	1	1	1	88	583
8	-1	-1	1	1	1	1	80	29
9	1	-1	-1	1	1	1	58	108
10	-1	-1	-1	-1	-1	1	85	8
11	-1	-1	-1	1	-1	-1	66	37
12	-1	-1	-1	-1	1	-1	93	121

TABLE 7: Model-free checks with edge plan in Table 6.

$X_4$	$X_5$	$X_6$	$X_7$	$X_8$	$X_9$
-13	18	4	13	4	-23
13	18	4	13	4	23

TABLE 8: step estimations for the investigation with the edge plan.

$p$	Median	$\sigma(p)$ e	$k \times 2^{0.5} \sigma(p)$	$\omega(p)$	$\omega(p) < p?$
0	13	13.61	19.25	1	No
1	13	13.61	19.25	1	No
2	8.5	8.90	12.59	4	No
3	4	4.19	5.92	4	No
4	4	4.19	5.92	4	No
5	4	4.19	5.92	4	No

classmates, inadequate knowledge of the educational material, and unsuitable work environments—and the regression analysis method shows no active factor. We consequently infer that there is no dynamic factor with a direct commitment.

*Example 3.* Let  $n=6$  and the culture of the tradition of classmates  $X_5$ , no reliance on self  $X_6$ , inadequate knowledge of the educational material  $X_7$ , a poor economic situation  $X_8$ , unsuitable work environments  $X_9$ , and good financial situation for family  $X_{10}$ .

Analyzing the data in Table 9 as described previously, the outcomes are displayed in Table 10 and 11. We along these lines have  $w(2)$ =one dynamic factor good financial situation for family. An investigation of the information in Table 9 (utilizing straight regression) with the product bundle SPSS uncovered there is no dynamic variable and gave an expected direct model

TABLE 9: One replicate for Example 3.

Run	$X_5$	$X_6$	$X_7$	$X_8$	$X_9$	$X_{10}$	Y	Response number
1	1	1	-1	1	1	1	97.5	62
2	-1	1	1	1	1	1	81	30
3	1	-1	1	1	1	1	75	21
4	-1	-1	-1	1	-1	1	93	121
5	-1	-1	-1	1	1	-1	50	41
6	-1	-1	-1	-1	1	1	50	36
7	-1	1	-1	1	1	1	81	20
8	-1	-1	1	1	1	1	58	108
9	1	-1	-1	1	1	1	95	139
10	-1	-1	-1	-1	-1	1	86	33
11	-1	-1	-1	1	-1	-1	70	144
12	-1	-1	-1	-1	1	-1	85	8

TABLE 10: Model-free checks with edge plan in Table 9.

$X_5$	$X_6$	$X_7$	$X_8$	$X_9$	$X_{10}$
16.5	23	-20	7	-20	-35
16.5	23	20	7	20	35

TABLE 11: step estimations for the investigation with the edge plan.

$p$	Median	$\sigma(p)$ e	$k \times 2^{0.5} \sigma(p)$	$\omega(p)$	$\omega(p) < p?$
0	20	20.95	29.62	1	No
1	20	20.95	29.62	1	No
2	18.5	19.11	27.03	1	Yes

$$Y = 93.66 + \varepsilon, \quad (7)$$

with

$$R - sg = 60.8\% \quad (8)$$

of mean 76.79 and standard deviation  $\sigma = 16.64$ . Also from the result, the residual is normal because  $p$ -value (0.200) is more than 0.05.

From the above, we observe that the robust edge design method shows one active factor—good financial situation for family—and the regression analysis method shows no active factor. We thus conclude that there was no active factor with a linear contribution.

*Example 4.* Let  $n=6$  and inadequate knowledge of the educational material  $X_7$ , a poor economic situation  $X_8$ , unsuitable work environments  $X_9$ , good financial situation for family  $X_{10}$ , lack of parental supervision of the children  $X_{11}$  and lack of incentives for teachers  $X_{12}$ .

Analyzing the data in Table 12 as described previously. The results are shown in Table 13 and 14. I thus have  $w(5) = 0$  active factors. An investigation of the information in Table 9 (regression analysis) with the product bundle SPSS uncovered there is a functioning variable. SPSS uncovered there is a functioning variable: inadequate knowledge of the educational material and gave an expected straight model

$$Y = 75 - 12.80 \cdot X_7 + \varepsilon, \quad (9)$$

with

TABLE 12: One replicate for Example 4.

Run	$X_7$	$X_8$	$X_9$	$X_{10}$	$X_{11}$	$X_{12}$	Y	Response number
1	1	1	-1	1	1	1	70	3
2	-1	1	1	1	1	1	81	20
3	1	-1	1	1	1	1	50	50
4	-1	-1	-1	1	-1	1	100	395
5	-1	-1	-1	1	1	-1	89	47
6	-1	-1	-1	-1	1	1	72	54
7	-1	1	-1	1	1	1	95	45
8	-1	-1	1	1	1	1	90	18
9	1	-1	-1	1	1	1	70	14
10	-1	-1	-1	-1	-1	1	99	88
11	-1	-1	-1	1	-1	-1	86	33
12	-1	-1	-1	-1	1	-1	97	15

TABLE 13: : Model-free checks with edge plan in Table 12.

$X_7$	$X_8$	$X_9$	$X_{10}$	$X_{11}$	$X_{12}$
-25	-9	-20	1	3	-25
25	9	20	1	3	25

$$R - sg = 75\%, \quad (10)$$

of mean 83.25 and standard deviation  $\sigma = 15.16$ .

Also from the result, the residual is normal because  $p$ -value (0.200) is more than 0.05. From the above, we observe that the robust edge design method shows no active factor, and the regression analysis method shows one active factor: inadequate knowledge of the educational material. We thus conclude that there was no active factor with a linear contribution.

*Example 5.* Let  $n = 6$  and a poor economic situation  $X_8$ , unsuitable work environments  $X_9$ , good financial situation for family  $X_{10}$ , lack of parental supervision of the children  $X_{11}$ , lack of incentives for teachers  $X_{12}$ , and lack of supervision and follow-up of teachers or university professors  $X_{13}$ .

Analyzing the data in Table 15 as described previously. The results are shown in Tables 16 and 17. We thus have  $w(5) = 3$  active factors: a poor economic situation, good financial situation for family, and lack of parental supervision of the children. An investigation of the information in Table 15 (regression analysis) with the product bundle SPSS uncovered four dynamic factors: unsuitable work environments, good financial situation for family, lack of supervision, and follow-up of teachers or university professors and lack of incentives for teachers, and gave an expected straight model

$$Y = 39.5 - 15.7 \cdot X_9 - 19.95 \cdot X_{10} + 14.3 \cdot X_{11} + 12.3 \cdot X_{12} + \varepsilon, \quad (11)$$

with

$$R - sg = 87.5\%, \quad (12)$$

of mean 78.75 and standard deviation  $\sigma = 17.41$ . Also from the result, the residual is normal because  $p$ -value (0.095) is more than 0.05.

TABLE 14: step estimations for the investigation with the edge plan.

$p$	Median	$\sigma(p)$	$e$	$k \times 2^{0.5} \sigma(p)$	$\omega(p)$	$\omega(p) < p?$
0	14.5	15.18		21.48	2	No
1	9	9.42		13.33	3	No
2	6	6.28		8.88	4	No
3	3	3.14		4.44	4	No
4	2	2.09		2.96	5	No
5	1	1.047		1.48	5	No

TABLE 15: One replicate for Example 5.

Run	$X_8$	$X_9$	$X_{10}$	$X_{11}$	$X_{12}$	$X_{13}$	Y	Response number
1	1	1	-1	1	1	1	58	19
2	-1	1	1	1	1	1	50	50
3	1	-1	1	1	1	1	70	3
4	-1	-1	-1	1	-1	1	95	7
5	-1	-1	-1	1	1	-1	98	5
6	-1	-1	-1	-1	1	1	93	24
7	-1	-1	-1	1	1	1	95	90
8	-1	-1	1	1	1	1	70	14
9	1	-1	-1	1	1	1	100	129
10	-1	-1	-1	-1	-1	1	60	31
11	-1	-1	-1	1	-1	-1	81	99
12	-1	-1	-1	-1	1	-1	75	285

TABLE 16: Model-free checks with edge plan in Table 15.

$X_8$	$X_9$	$X_{10}$	$X_{11}$	$X_{12}$	$X_{13}$
-37	-20	-30	35	17	18
37	20	30	35	17	18

From the above, we observe that the robust edge design method shows these active factors—a poor economic situation, good financial situation for family, and lack of parental supervision of the children—and the regression analysis method showed these active factors: unsuitable work environments, good financial situation for family, lack of supervision of children, and lack of incentives for teachers. We thus conclude that there are two active factors—good financial situation for family and lack of parental supervision of the children—with a linear contribution.

*Example 6.* Let  $n = 6$  and unsuitable work environments  $X_9$ , good financial situation for family  $X_{10}$ , lack of parental supervision of the children  $X_{11}$ , lack of incentives for teachers  $X_{12}$ , lack of supervision and follow-up of teachers or university professors  $X_{13}$ , and the lack of counseling for teachers regarding enrolling in training courses on modern teaching methods  $X_{14}$ .

Analyzing the data in Table 18 as described previously. The results are shown in Tables 19 and 20. We thus have  $w(5) = 4$  active factors: unsuitable work environments, good financial situation for family, lack of parental supervision of the children, and lack of incentives for teachers. An analysis of the data in Table 18 (using linear regression) with the software package SPSS revealed there was one active variable—good financial situation for family—and gave an estimated linear model

TABLE 17: step estimations for the investigation with the edge plan.

$p$	Median	$\sigma(p) e$	$k \times 2^{0.5} \sigma(p)$	$\omega(p)$	$\omega(p) < p$ ?
0	25	26.18	37.03	0	No
1	20	20.95	29.62	3	No
2	19	19.90	28.14	3	No
3	18	18.85	26.66	3	No
4	17.5	18.33	25.92	3	Yes

TABLE 18: One replicate for Example 6.

Run	$X_9$	$X_{10}$	$X_{11}$	$X_{12}$	$X_{13}$	$X_{14}$	Y	Response number
1	1	1	-1	1	1	1	100	16
2	-1	1	1	1	1	1	70	3
3	1	-1	1	1	1	1	58	19
4	-1	-1	-1	1	-1	1	75	549
5	-1	-1	-1	1	1	-1	70	34
6	-1	-1	-1	1	1	1	60	31
7	-1	1	-1	1	1	1	89	130
8	-1	-1	1	1	1	1	60	28
9	1	-1	-1	1	1	1	85	8
10	-1	-1	-1	-1	-1	1	90	69
11	-1	-1	-1	1	-1	-1	75	285
12	-1	-1	-1	-1	1	-1	65	66

TABLE 19: Model-free checks with edge plan in Table 18.

$X_9$	$X_{10}$	$X_{11}$	$X_{12}$	$X_{13}$	$X_{14}$
11	10	-27	-15	-5	-5
11	10	27	15	5	5

TABLE 20: step estimations for the investigation with the edge plan.

$p$	Median	$\sigma(p) e$	$k \times 2^{0.5} \sigma(p)$	$\omega(p)$	$\omega(p) < p$ ?
0	10.5	10.99	15.55	1	No
1	10	10.47	14.81	2	No
2	7.5	7.85	11.11	2	No
3	5	5.23	7.40	4	No
4	5	5.23	7.40	4	No
5	5	5.23	7.40	4	Yes

$$y = 97.50 + 9.25 \cdot X_{10} + \varepsilon, \quad (13)$$

with

$$R - sg = 83.4\%, \quad (14)$$

of mean 74.75 and standard deviation  $\sigma = 13.59$ . Also from the result, the residual is normal because  $p$ -value (0.200) is more than 0.05.

From the above, we observe that the robust edge design method shows four active factors—unsuitable work

environments, good financial situation for family, lack of parental supervision of the children, and lack of incentives for teachers—and the regression analysis method shows one active factor: good financial situation for family. We thus conclude that there was one active factor—good financial situation for family—with a linear contribution.

In summary, experimental results are shown in the following table that compares all examples with two methods (Table 21).

TABLE 21: Experimental results with two methods.

Example	Edge design analysis	Regression analysis	Experimental results of active factors
Example 1	No active factors	No active factors	No active factors
Example 2	The behavior of the student during the lesson explains the culture of the tradition of classmates, inadequate knowledge of the educational material, and unsuitable work environment.	No active factors	No active factors
Example 3	Good financial situation for family	No active factors	No active factors
Example 4	No active factors	Inadequate knowledge of the educational material	No active factors
Example 5	A poor economic situation, good financial situation for family, and lack of parental supervision of the children	Unsuitable work environments, good financial situation for family, lack of supervision, and follow-up of teachers or university professors and lack of incentives for teachers	Good financial situation for family, and lack of parental supervision of the children
Example 6	Unsuitable work environments, good financial situation for family, lack of parental supervision of the children, and lack of incentives for teachers	Good financial situation for family	Good financial situation for family

#### 4. Conclusion

The current study examined and described the spread of private tutoring? in general and university education in Saudi Arabia. One of the aims of this paper was to study significant factors underlying the spread of PT at school and university levels. In reviewing the literature, no data was found on the association between the edge designs analysis and regression analysis. Therefore, there were two main types of analysis study design used to identify the actual reasons for the spread of PT: the edge plans assessment and backslide examination. We can say that the examination with the edge plans given results that are associated and like the assessment that is performed with the whole data. The current study found that a good family financial situation and lack of parental supervision of the children were significant factors underlying the spread of private tutoring at school and university levels. In future examinations, it very well may be feasible for information to utilize supersaturated plans, where many variables are explored utilizing a couple of trial runs. [14–18].

#### Data Availability

The data that support the findings of this study are available on request from the corresponding author.

#### Conflicts of Interest

The authors declare that there are no conflicts of interest.

#### References

- [1] D. I. Ikediashi, S. O. Ogunlana, and A. Alotaibi, "Analysis of project failure factors for infrastructure projects in Saudi Arabia: a multivariate approach," *Journal of Construction in Developing Countries*, vol. 19, no. 1, p. 35, 2014.
- [2] P. Kwok, "Examination-oriented knowledge and value transformation in East Asian cram schools," *Asia Pacific Education Review*, vol. 5, no. 1, pp. 64–75, 2004.
- [3] M. Bray, "Researching shadow education: methodological challenges and directions," *Asia Pacific Education Review*, vol. 11, no. 1, pp. 3–13, 2010.
- [4] A. Tansel and F. Bircan, "Demand for education in Turkey: a tobit analysis of private tutoring expenditures," *Economics of Education Review*, vol. 25, no. 3, pp. 303–313, 2006.
- [5] F. O. Nyandara, *Determining the Effects of Strategic Plan Implementation One the Performance of South Nyanza Sugar Company Limited, Kenya*, PhD Thesis, Kisii University, Kisii, Kenya, 2017.
- [6] S. Manzoor, *Reasons and Necessity of Private Tutoring in English for Bangla Medium Primary School Students in Bangladesh*, PhD Thesis, BRAC University, Dhaka, Bangladesh, 2013.
- [7] N. Ghounane, "Private tutoring and public schools in Algeria: Issues and reflections," *Global Journal of Human-Social Science Research*, 2018.
- [8] A. Al-Fattal, *Understanding Student Choice of university and Marketing Strategies in Syrian Private Higher Education*, University of Leeds, Leeds, England, 2010.
- [9] M. O. Hamid, A. Khan, and M. M. Islam, "The spread of private tutoring in English in developing societies: exploring students' perceptions," *Discourse: Studies in the Cultural Politics of Education*, vol. 39, no. 6, pp. 868–886, 2018.
- [10] M. E. H. Ahmed, *Community Service & Continuing Education Deanship Community Development Institute*, PhD Thesis, The Islamic University of Gaza, Gaza, Palestine, 2016.
- [11] A. Tansel, F. Bircan, and K. W.-H. Yung, "Learning English in the shadows: understanding Chinese learners' experiences of private tutoring," *Tesol Quarterly*, vol. 49, no. 4, pp. 707–732, 2015.
- [12] M. Bray, "Private supplementary tutoring: comparative perspectives on patterns and implications," *Compare: A Journal of Comparative and International Education*, vol. 36, no. 4, pp. 515–530, 2006.
- [13] C. Elster and A. Neumaier, "Screening by conference designs," *Biometrika*, vol. 82, no. 3, pp. 589–602, 1995.

- [14] T. Alanazi, S. D. Georgiou, and S. Stylianou, "Construction and analysis of edge designs from skew-symmetric supplementary difference sets," *Communications in Statistics - Theory and Methods*, vol. 47, no. 20, pp. 5064–5076, 2018.
- [15] Y. A. Ali, "Private tutoring in Jordan: underpinning factors and impacts," *International Journal of Humanities and Social Science*, vol. 3, no. 13, pp. 109–114, 2013.
- [16] T. A. Alanazi, "Application of edge designs to study the spread of diabetes. JP Journal of Biostatistics," *JP Journal of Biostatistics*, vol. 18, no. 2, pp. 187–198, 2021.
- [17] T. A. Alanazi and O. Alamri, "Robust estimation methods used to study the reasons behind increasing divorce cases in Saudi society," *Mathematical Problems in Engineering*, vol. 2021, Article ID 4027599, 6 pages, 2021.
- [18] A. T. Abdulrahman, "Application edge designs to study the actual causes that led to the frequent traffic accidents," *Civil Engineering and Architecture*, vol. 9, no. 4, pp. 1057–1063, 2021.

## Research Article

# The Catastrophe Analysis of Shanghai Crude Oil Futures Price from the Perspective of Volatility Factors

Weifeng Gong <sup>1,2</sup>, Yahui Li <sup>3</sup>, Chuanhui Wang <sup>1</sup>, Haixia Zhang <sup>1</sup>, and Zhengjie Zhai<sup>1</sup>

<sup>1</sup>School of Economics, Qufu Normal University, Rizhao 276826, China

<sup>2</sup>School of Economics and Management, Nanjing University of Aeronautics and Astronautics, Nanjing 211006, China

<sup>3</sup>Liaocheng Municipal Tax Service, State Taxation Administration, Liaocheng 252000, China

Correspondence should be addressed to Chuanhui Wang; [chhwang001@163.com](mailto:chhwang001@163.com)

Received 15 August 2021; Revised 12 November 2021; Accepted 4 February 2022; Published 21 March 2022

Academic Editor: M. M. El-Dessoky

Copyright © 2022 Weifeng Gong et al. This is an open access article distributed under the Creative Commons Attribution License, which permits unrestricted use, distribution, and reproduction in any medium, provided the original work is properly cited.

The volatility of Shanghai crude oil futures prices is researched in this paper. The cusp catastrophe analysis of Shanghai crude oil futures price is based on the perspective of volatility influencing factors. Some important factors are selected based on commodity attributes and financial attributes, including certain China's macrofactors, such as producer price index and macroeconomic prosperity index. The principal component analysis is used to process the factors. The control variables of the cusp catastrophe model are extracted. The discriminant of the cusp catastrophe model and the principal component analysis are combined to determine the month of mutation. The three-dimensional renderings and plane projections of Shanghai crude oil futures price mutations in 2018 and 2019 are presented. The model is tested by comparing the time points of price sudden change nodes and emergencies. The results show that only nine factors can be used to roughly determine whether the Shanghai crude oil futures price has a sudden change. During the analysis period, the mutation months are May 2018, December 2018, February 2019, June 2019, and September 2019. It can be proved that the established model has certain feasibility and accuracy.

## 1. Introduction

Shanghai crude oil futures are currently China's first and only crude oil futures, and they are also the first product opened to the outside world in China's futures industry. The official listing of Shanghai crude oil futures marks the start of the internationalization of China's futures market, which means that an important step has been taken in the internationalization of the renminbi, and it also means that China has formally joined the competition for crude oil pricing power in the Asia-Pacific region. In recent years, oil prices have experienced roller coaster-like ups and downs, and some unexpected events have also caused shocks in crude oil prices, thereby affecting the trend of crude oil futures. Sudden changes in prices belong to the evolution of the economic and financial category, which is manifested in the economic and financial aspects, mainly due to the sharp rise and fall of some financial instruments such as stocks, futures, and foreign exchange or the impact of some "black swan events" on the economic and financial markets.

Since its inception, catastrophe theory has been well applied in the fields of physics and engineering, but its application in the fields of social and behavioral sciences is not very extensive, and there are relatively few studies on economics. In the existing literature, the research part adopts the method of structural mutation. For example, a structural mutation phenomenon could be verified using the volatility of the financial market [1, 2]. The mutation inflection point of the economic interval was clarified range using the structural mutation theory [3]. Ewing and Malik [4] introduced the GARCH model to study the volatility of financial markets. Zeng and Yin [5] combined Bayesian statistical methods to analyze the stock market. Zhang [6] tested the operability of structural mutations introduced in the time series model. Gong and Lin [7] combined the HAR model to study the crude oil futures market [7]. Some scholars also focus on method improvement. Wang [8] used latent state variables and the irreversible hidden Markov chain method. Zhang [9] used the PPM mutation point and Hurst index method.



There are some pieces of literature on economic issues using the cusp catastrophe model. Wang and Sun [10] combined the model with the supply chain financial ecosystem to evaluate the stability of the system. Wang et al. [11] focused on the early warning of sudden changes in the economic system. The former mainly integrates a variety of theories such as catastrophe theory, grey number theory, and grey prediction theory, while the latter researches the cusp catastrophe warning of generalized virtual assets with real estate as the representative. Qiu and Yang [12] and Li [13] combined the cusp catastrophe model with other theories. The former combines the dissipative structure theory to analyze the entropy change of the financial system, and the latter combines the random theory to establish a catastrophe model based on the Shanghai Stock Exchange Index and the Shenzhen Stock Exchange Index in China. Li and Shi [14] used the cusp catastrophe model to analyze the general characteristics of securities returns. In the paper, the cusp catastrophe model is used to study the abrupt changes in crude oil futures prices.

A study on the mutation of Shanghai crude oil futures prices is helpful to comprehensively understand and grasp the development status and inherent characteristics of the oil futures market and can make up for China's shortcomings in oil futures. Understanding the reasons for the changes in oil futures prices and grasping the laws of oil futures price fluctuations are conducive to the further development and improvement of China's oil futures market, further reflecting the price guiding role of oil futures and thus enhancing the voice and power of China's crude oil futures market in the international market. In the paper, the cusp catastrophe model would be adopted. Use influencing factors to reflect the mutation in price fluctuations so as to research the fluctuations of Shanghai crude oil futures prices.

## 2. Methodology

The catastrophe theory was founded by the French mathematician Rene Thom in 1972 in the book "Stable Structure and Morphogenesis." This book systematically expounds the catastrophe theory. For the discontinuous mutations that exist in nature and social life, various forms and structures have been studied in the catastrophe theory.

When dealing with the phenomenon of continuous gradual change, the classic calculus method is usually used. However, when encountering a sudden change, the state space of the system becomes nondifferentiable. We cannot use calculus. In this case, the catastrophe theory was born. Catastrophe theory is a mathematical theory specially used to deal with discontinuous and jumping phenomena. The volatility of Shanghai crude oil futures prices has seen skyrocketing and slumping phenomena, which is a sudden change in the economic and financial aspects. It has mutation characteristics and can be studied using mutation models.

**2.1. Catastrophe Theory.** The mathematical foundation of catastrophe theory mainly involves three aspects. One is the singularity theory of smooth mapping. The second is the

bifurcation set theory of power system. The third is stability theory. Among the more basic concepts are potential, singularity, bifurcation, and stability.

Potential can express the state variables and external parameters of the system to describe the behavior of the system. The degenerate stationary point is a singularity. The stationary point is the point where the potential derivative of the smoothing function is zero. Stationary points are classified according to different conditions. Bifurcation is a change phenomenon in a parameter-containing system, which is mainly manifested in the sudden change of qualitative properties such as the equilibrium state of the system and the number and stability of periodic motion when the parameters in the system change or pass certain critical values. Stability mainly refers to the ability of things to resist interference. When the system continues to appear in a certain state, external interference may cause the system to deviate from this state and become unstable. But when the interference is eliminated, it returns to its original state and continues to remain stable. A set of parameters can be used to describe the state of a system. When the parameter takes a unique extreme value, the system is in a stable state. When the parameter changes within a certain range, it means that there is more than one extreme value. Then the system is in an unstable state.

The catastrophe theory is based on differential equations and functions to classify the singularities of the system. When the number of state variables does not exceed two and the number of control variables does not exceed four, there are at most seven types of elementary mutations. The type of each elementary mutation is determined by a potential energy function, where  $y$  and  $x$  are state variables and  $t, w, v,$  and  $u$  are control variables. The first derivative of the potential energy function is zero, or the set of all points where the first partial derivative is zero is called a balanced surface, which can be used to describe the whole process of a certain type of sudden change.

**2.2. The Cusp Catastrophe Model.** In mutation theory, the definition of the catastrophe model gives the potential function equation. The determination of the potential function equation is judged by the number of state variables and control variables, and different numbers determine different potential functions. According to the perspective of this study, the appropriate potential function and mutation model are selected.

The potential function equation of the cusp catastrophe model is shown as follows:

$$V(x) = x^4 + ux^2 + vx, \quad (1)$$

where  $x$  is the state variable and  $u$  and  $v$  are the control variables. This function presents the phase point in the three-dimensional space with  $(x, u, v)$  as the coordinate, which represents the state of the system. In addition,  $x$  also represents the influence factor of Shanghai crude oil futures price fluctuation. Through the data processing of the influence factors, two new variables representing the commodity attributes and financial attributes are extracted,

namely,  $u$  and  $v$ . In this way, the potential function of the catastrophe model can be combined with the economic problem being studied.

When  $V'(x)$  is equal to zero, equilibrium surface equation of potential function  $M$  is shown as follows:

$$4x^3 + 2ux + v = 0. \quad (2)$$

When  $V''(x)$  is equal to zero, singularity set  $S$  of potential function is shown as follows:

$$12x^2 + 2u = 0. \quad (3)$$

The equilibrium surface equation  $M$  and the singularity set equation  $S$  are established jointly. The forked set  $B$  is obtained.

$$8u^3 + 27v^2. \quad (4)$$

According to the balance surface equation of the potential function, the balance surface is the set of all critical points of the potential function. From the singular point set equation of the potential function, it is known that the singular point set is the set of all points with vertical tangents on the balance surface. It can be seen from the bifurcation set equation that the bifurcation set is a projection on the plane of the control variable. It is a collection of points of the control variable and represents all the points that make the state variable jump.

As shown in Figure 1, the curved surface in the curved surface graph is the abrupt manifold of the cusp catastrophe model (in Figure 1), which represents the change of the potential function at different positions. The balance surface is composed of three layers, upper leaf, lower leaf, and middle leaf, which are three possible balance positions. The upper and lower leaves represent a stable balance and are smooth curved surfaces. The middle leaf represents an unstable balance and is the middle fold. The bifurcation set is the projection of the middle lobe on the plane where the control variable is located, which represents the critical position where the system changes suddenly. If the control variables  $u$  and  $v$  do not cross the bifurcation set, then the behavior of the system changes gradually from the initial state to the end state. If the control variable crosses the bifurcation set, it will cause nonstationary and discontinuous changes in the state variable, and it may fall from the upper leaf of the curved surface to the lower leaf or jump from the lower leaf to the upper leaf of the curved surface. The instability of this state can be considered a sudden change.

The balance surface equation of the cusp catastrophe model is a one-dimensional cubic equation about  $x$ ,  $4x^3 + 2ux + v = 0$  (i.e., formula (2)). According to the Kaldan formula, the number of real roots of the equation can be determined by the sign of the discriminant  $\Delta = 8u^3 + 27v^2$  (i.e., formula (4)). When  $\Delta = 0$ , it means the projection on the control variable plane, that is, the bifurcation set. At the same time, the bifurcation set divides the plane of the control variable into two regions. As shown in Figure 2, the point above the bifurcation set curve indicates  $\Delta > 0$ , and the point below the bifurcation set curve indicates  $\Delta < 0$ . The point on the bifurcation set curve indicates  $\Delta = 0$ .

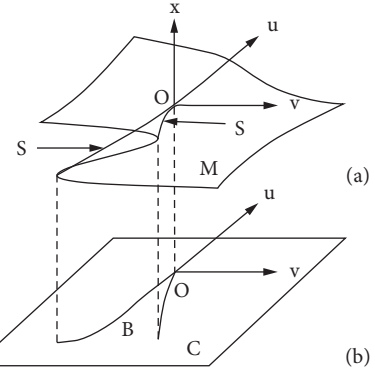


FIGURE 1: Cusp catastrophe model surface map.

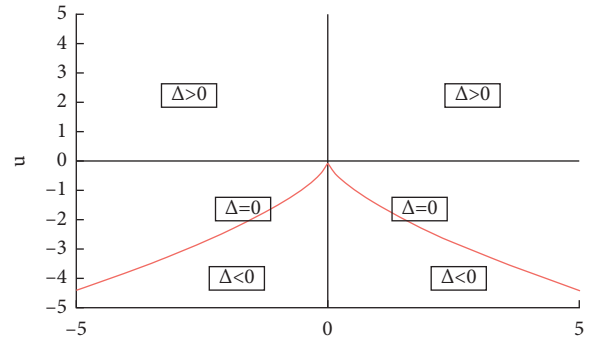


FIGURE 2: Bifurcation set curve.

### 3. Volatility Factors

The Shanghai crude oil futures price is essentially a CIF price, which is different from Brent crude oil futures and WTI crude oil futures. Therefore, the factors affecting the price fluctuation of Shanghai crude oil futures are slightly different from those of other crude oil markets. For obtaining a price that more closely matches the market, one of the meanings and functions of Shanghai crude oil futures is to reflect the changes in the supply and demand structure of China's crude oil market. Therefore, the prices generated by the market during trading will refer more to the current fundamentals of China's crude oil market.

**3.1. Selection of Impact Factors.** Although crude oil futures are derivative financial instruments relying on crude oil prices, they are closely related to crude oil. The influencing factors involve not only the category of crude oil but also the characteristics of crude oil futures themselves. On the one hand, as an indispensable strategic resource for national survival and development, crude oil is endowed with dual attributes by the market, including its own commodity attributes and derivative financial attributes. Crude oil not only occupies a very important position in global trade but also is closely related to the political, financial, and economic aspects of countries around the world. On the other hand,

both Shanghai crude oil futures and crude oil futures in other markets have commodity and financial attributes. Therefore, there will be some of the same influencing factors, such as fundamental factors, geopolitical factors, macro-factors, and capital factors. Therefore, this paper is mainly based on the commodity and financial attributes of crude oil futures to explore the factors affecting the price of Shanghai crude oil futures.

*3.1.1. Commodity Attributes.* The so-called commodity attributes are related to the microinfluencing factors of crude oil futures products, the most important of which is the supply and demand relationship of crude oil. Shanghai crude oil futures reflect the supply and demand of China's coastal crude oil market. On the one hand, it has maintained a good linkage with international oil prices for a long time. On the other hand, when emergencies occur in the region, they can respond more directly and quickly. Especially in the face of emergencies, the price of Shanghai crude oil futures can quickly rise or fall to meet market supply and demand requirements and support prices. Not only is it friendly to market participants in terms of hedging risks, but also in terms of optimizing resource allocation, the Shanghai crude oil futures market provides industrial customers with new resource allocation channels. Market participants commented that Shanghai crude oil futures prices are reasonable and meaningful not only to the buyers and sellers involved in the transaction but also to producers and end consumers. Therefore, in view of the crude oil commodity attributes reflected in Shanghai crude oil futures, China's crude oil production volume and crude oil import volume indicators are used as the supply of crude oil futures.

Since the Shanghai crude oil futures price is essentially a CIF price, it is relatively more able to reflect changes in refinery processing costs. In the case of large fluctuations in the freight market, changes in overseas crude oil prices, which represent the shipping port price, generally do not reflect this difference. However, the fluctuation of the Shanghai crude oil futures price, which represents the arrival price, includes freight fluctuations. In contrast, because it can better reflect the changes in refinery processing costs, it can attract more resource countries, producers, international oil companies, and traders to make quotations based on Shanghai crude oil futures. Considering this reason, crude oil futures demand uses crude oil processed volume and crude oil apparent consumption indicators.

*3.1.2. Financial Attributes.* Crude oil futures are traded with crude oil as the subject matter and play a role in providing risk management tools. The standardized contracts, margin systems, and settlement systems of futures all reveal the inherent financial attributes of futures. The financial attributes are mostly related to macroinfluencing factors, such as exchange rates, politics, and economics. Therefore, when studying the factors affecting the price of Shanghai crude oil futures, the trading volume and open interest indicators can be used.

International crude oil futures, such as Brent crude oil futures, WTI crude oil futures, and Dubai/Oman crude oil futures, are all priced and settled in US dollars. However, China's crude oil futures are priced and settled in RMB. Therefore, under normal circumstances, changes in China's monetary policy and the value of RMB will have an impact on the price and operation of China's crude oil futures. Although the RMB has not yet achieved internationalization, there are still many restrictions on cross-border flows. However, when studying the influencing factors of Shanghai crude oil futures, the RMB exchange rate is still indispensable.

According to the relevant announcement of the Shanghai International Energy Exchange, the subject of the Shanghai crude oil futures contract is intermediate sour crude oil. Deliverable oil types include UAE Dubai crude oil, Upper Zakum crude oil, Oman crude oil, Qatar offshore oil, Yemen Masira crude oil, Iraqi Basra light oil, and China Victory crude oil. Among the international crude oil futures, Dubai crude oil and Oman crude oil are sour intermediate crude oils. Brent crude oil can be used as a representative of the benchmark crude oil in the west region, while Dubai crude oil can be used as a representative of the benchmark crude oil in the East region. Among the three major crude oil futures, from the perspective of distance, the physical resources corresponding to WTI and Brent crude oil futures will arrive in China much longer than the actual delivery of Oman crude oil futures. In terms of oil quality, the quality of WTI, Brent crude oil, and Oman crude oil is also very different. Therefore, when it comes to cross-regional arbitrage, it is obvious that there is no need to set aside short distances and correlate Shanghai crude oil futures prices with WTI and Brent. Similarly, when studying influencing factors, the Oman crude oil price index can be used.

From a macroperspective, changes in China's economic data will be more intuitively reflected in changes in oil prices. The impact of this change on Shanghai crude oil futures prices is obvious to all. This paper uses the producer price index of the petroleum industry and the macroeconomic prosperity index to represent the impact of China's macrolevel on crude oil futures.

*3.2. Impact Factor Index Construction.* The factors affecting the price fluctuation of Shanghai crude oil futures are discussed from the perspective of commodity attributes and financial attributes. The construction of its indicators also starts from these two aspects. According to the analysis and selection of influencing factors, when considering the commodity attributes based on supply and demand, China's crude oil production and crude oil imports are used as the supply of crude oil futures. Since China's crude oil production is very small and basically depends on imports, the combined crude oil production and crude oil imports are two indicators of crude oil supply. The demand for crude oil futures uses crude oil processed volume and crude oil apparent consumption indicators. When considering financial attributes, it uses crude oil futures' own trading volume and open interest indicators, as well as the RMB exchange rate

and Oman crude oil prices. In addition, the producer price index of the petroleum industry and the macroeconomic prosperity index represent the impact of China's macrolevel on crude oil futures. The influencing factors of Shanghai crude oil futures price fluctuation mentioned above are shown in (Table 1).

## 4. Empirical Analysis

**4.1. Principal Component Analysis.** Through the above analysis, nine indicators are selected from the influencing factors of Shanghai crude oil futures, and the principal components are extracted based on the principal component model. Since Shanghai crude oil futures were listed on March 26, 2018, the time period for selecting data began in April 2018. Due to the statistical delay of certain macro-indicators, the data are as of December 2019. The data come from the Central Economics database and the CSMAR database. The reported data were used to support this study and are available at <https://www.cei.cn/> and <https://www.gtafe.com/>.

This paper uses SPSS software for principal component analysis. Standardize the original indicators to eliminate the influence of variables on the level and dimension. Then KMO and Bartlett sphericity tests were performed, and the test passed. The method of determining the number of principal components is based on the number of eigenvalues greater than 1. As shown in Table 2, all variables have extracted 70% or more of the information; that is, most of

the information of all variables can be explained by the principal components, and the variable information is less lost. Therefore, it is determined that there are two principal components in this principal component extraction, and the overall effect is relatively ideal.

As shown in Table 3, the score coefficient matrix of the principal components after normalization is obtained.  $F_i = k_1X_1 + k_2X_2 + \dots + k_8X_8$ ,  $i = 1, 2$ . The coefficients in the formula are shown in Table 3.

**4.2. Application of Cusp Mutation Model.** The catastrophe model type can be judged according to the number of state variables and the number of control variables. The two extracted principal components can be used as control variables of the catastrophe model. The price of Shanghai crude oil futures can be used as the state variable of the mutation model. Therefore, the cusp catastrophe model was used according to two control variables and one state variable. A three-dimensional image of the equilibrium surface equation of the cusp catastrophe model can be made. As shown in Figure 3, the projection on the control variable plane is the bifurcation set. The red line is the left bifurcation set, and the blue line is the right bifurcation set.

Through the results of principal component analysis, the two extracted principal components are used as the control variables  $u(t)$  and  $v(t)$  of the mutation model. The mutation model is established as follows:

$$\begin{aligned} u(t) &= 0.282x_1(t) + 0.270x_2(t) - 0.016x_3(t) + 0.257x_4(t) - 0.031x_5(t) \\ &\quad - 0.107x_6(t) - 0.312x_7(t) - 0.252x_8(t) - 0.139x_9(t), \\ v(t) &= -0.125x_1(t) - 0.104x_2(t) + 0.270x_3(t) - 0.493x_4(t) + 0.281x_5(t) \\ &\quad + 0.357x_6(t) + 0.193x_7(t) + 0.095x_8(t) - 0.074x_9(t). \end{aligned} \quad (5)$$

Two principal components can be calculated by combining the historical data of nine indicators, including crude oil supply, crude oil apparent consumption, crude oil processing volume, trading volume, position, RMB exchange rate, Oman crude oil price, producer price index, and macroeconomic climate index. Since the equilibrium surface equation of the cusp mutation model is  $4x^3 + 2ux + v = 0$ ,  $4x^3(t)$  can also be calculated based on the actual historical data. The nonlinear regression is transformed into multiple linear regression, and the equilibrium surface equation of the abrupt transition model is fitted. The regression model is expressed as follows:

$$4x^3(t) + 11.838u(t)x(t) - 2.815v(t) + 2.434 = 0. \quad (6)$$

Therefore, the standard cusp catastrophe model balance surface equation is constructed as follows:  $4X^3(t) + 2U(t)X(t) + V(t) = 0$ .

Then,  $X(t) = x(t)$ ,  $U(t) = 5.919u(t)$ , and  $V(t) = -2.815v(t) + 2.434$ .

According to the equilibrium surface equation of the cusp mutation model, it can be seen that  $\Delta = 8u^3(t) + 27v^2(t)$ .

When  $\Delta > 0$ , the balance surface equation of the cusp catastrophe model has only one real root, so the corresponding potential function curve has only one minimum value. In this case, the smooth change of  $(u, v)$  makes  $x$  change smoothly, indicating that the system is stable.

When  $\Delta < 0$ , the balance surface equation of the cusp catastrophe model will have three different real roots. Therefore, the corresponding potential function curve will have two minimum values. In this case, the system has three balance points. One is in an unstable state, and two are in a stable state. The system changes smoothly between states, a process of slow change. A sudden change occurs only when the system passes or reaches the boundary of the equilibrium state, at which time the system is in an unstable state.

When  $\Delta = 0$ , the equilibrium surface equation of the cusp catastrophe model has three real roots. When  $u$  and  $v$  are not zero, two of the three real roots are the same. In this

TABLE 1: Influencing factors of Shanghai crude oil futures price changes.

Dependent variable	Main type	Influencing factors
Shanghai crude oil futures prices	Commodity attributes	Crude oil supply $X_1$ Apparent crude oil consumption $X_2$ Crude oil processing volume $X_3$ Trading volume $X_4$
	Financial attributes	Open interest $X_5$ RMB exchange rate $X_6$ Oman crude oil prices $X_7$ Producer price index $X_8$ Macroeconomic sentiment index $X_9$

TABLE 2: Explanation of total variance.

Ingredient	Initial eigenvalue			Rotating load sum of squares		
	Total	Percentage of variance	Accumulation %	Total	Percentage of variance	Accumulation %
1	5.657	62.851	62.851	4.065	45.169	45.169
2	1.198	13.314	76.165	2.790	30.996	76.165
3	0.756	8.400	84.565			
4	0.641	7.123	91.688			
5	0.426	4.735	96.424			
6	0.175	1.942	98.365			

TABLE 3: Component score coefficient matrix.

Influencing factors	The coefficient of component 1	The coefficient of component 2
Crude oil supply $X_1$	0.282	-0.125
Apparent crude oil consumption $X_2$	0.270	-0.104
Crude oil processing volume $X_3$	-0.016	0.270
Trading volume $X_4$	0.257	-0.493
Open interest $X_5$	-0.031	0.281
RMB exchange rate $X_6$	-0.107	0.357
Oman crude oil prices $X_7$	-0.312	0.193
Producer price index $X_8$	-0.252	0.095
Macroeconomic sentiment index $X_9$	-0.139	-0.074

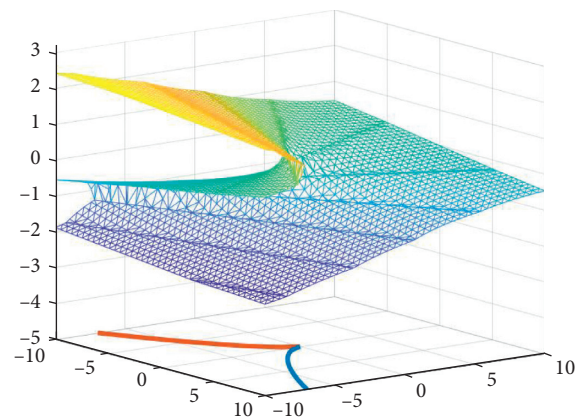


FIGURE 3: Cusp catastrophe model balance surface equation 3D diagram.

case, the system is in two critically stable states. If a slight disturbance occurs, the system will jump from a critical state to a stable equilibrium state, that is, a sudden change. If  $u = v = 0$ , there are three equal real roots, all at the zero point,

and there is only one minimum value for the corresponding potential function curve. Although the system jumps over the state of zero point, because the state before and after the jump is the same, there is no sudden change.

The selected data are from 2018 to 2019 in this paper. Therefore, the monthly data frequency is used to divide the time according to the year, and the annual Shanghai crude oil futures price fluctuations are analyzed. The first time period is from April 2018 to December 2018, and the second time period is from January 2019 to December 2019. The 2018 data has nine months, and the 2019 data has twelve months. Therefore, first conduct a static analysis with three months as a partial range to determine the situation of  $\Delta = 8u^3(t) + 27v^2(t)$ , and then perform an integrated full-range analysis and judgment, which can more accurately represent the sudden change of crude oil futures.

**4.2.1. Empirical Analysis in 2018.** The analysis is divided into three months, which are from April to June, July to September, and October to December. First, according to the monthly distribution, the principal component analysis is performed in turn, and the number of principal component analyses is determined to be three times. Then calculate the control variables  $u(t)$  and  $v(t)$  of the catastrophe model. Finally, the judgment result of  $\Delta$  is output according to the formula  $\Delta = 8u^3(t) + 27v^2(t)$ . The results are integrated as shown in Table 4, which is the analysis result table in 2018.

It can be seen from Table 4 that the months with  $\Delta < 0$  are May and December. They are  $-0.32709$  and  $-7.09259$ . Three-dimensional renderings of sudden changes in Shanghai crude oil futures prices in 2018 are shown in Figure 4.

When a three-dimensional map is presented in a two-dimensional state, some months cannot be fully displayed. Therefore, the U-V coordinates in the three-dimensional image are projected into a plane. The bifurcation curve to judge the sudden price change of Shanghai crude oil futures in 2018 is shown in Figure 5.

It can be seen from Figure 5 that the months in the  $\Delta < 0$  area are May and December. It shows that the price of Shanghai crude oil futures fluctuated greatly from April to May, May to June, and November to December 2018 and was in an unstable situation. In Figure 5, the coordinates in May are  $(u, v) = (-1.097, -0.3591)$ . At this time, the system passes through the boundary of the equilibrium state and is in an unstable state, indicating that a sudden change will occur. The coordinates in December are  $(u, v) = (-1.017, 0.5472)$ . The system reaches the boundary of the equilibrium state and is also in an unstable state, and there is also the possibility of sudden changes.

**4.2.2. Empirical Analysis in 2019.** The analysis is based on a partial range of three months, which can be divided into January to March, April to June, July to September, and October to December. First, the principal component analysis is carried out based on the distribution of the month. The results determine that the number of principal component analyses is four. Then, the control variables  $u(t)$  and  $v(t)$  of the catastrophe model are calculated. Finally, the judgment result of  $\Delta$  is output according to the formula and graphically through Matlab software. Because of the original data from October to December, there is a variable with zero

TABLE 4: The principal component analysis in 2018.

	$u(t)$	$v(t)$	$\Delta$	Judge symbol
April	0.98227	0.60702	17.53076	$\Delta > 0$
May	-1.01683	0.54717	-0.32709	$\Delta < 0$
June	0.03456	-1.15418	35.96788	$\Delta > 0$
July	-0.879	-0.74879	9.70532	$\Delta > 0$
August	-0.20897	1.13563	34.74769	$\Delta > 0$
September	1.08797	-0.38684	14.34288	$\Delta > 0$
October	0.23774	1.12996	34.58136	$\Delta > 0$
November	0.8597	-0.77087	21.12762	$\Delta > 0$
December	-1.09745	-0.35909	-7.09259	$\Delta < 0$

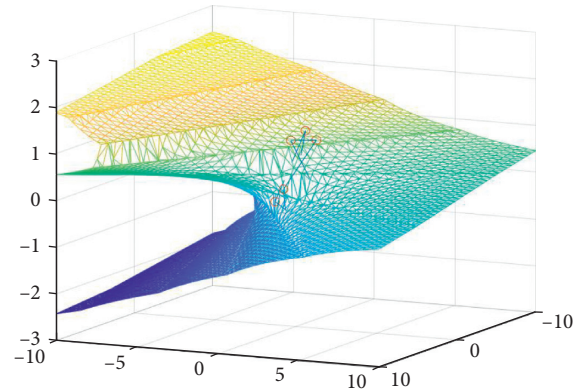


FIGURE 4: Three-dimensional renderings of sudden changes in Shanghai crude oil futures prices in 2018.

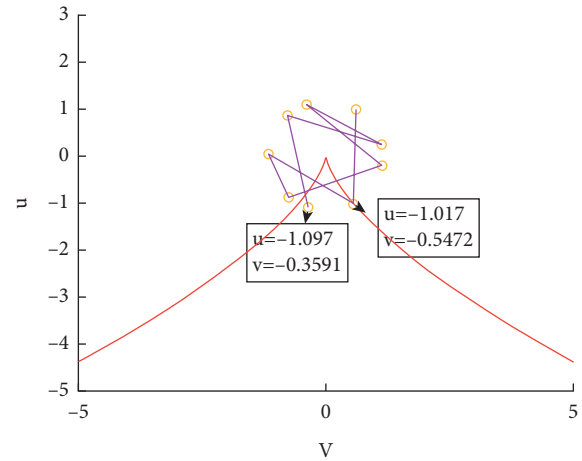


FIGURE 5: Plane projection chart of Shanghai crude oil futures price sudden change in 2018.

variance. Therefore, the principal component analysis cannot be performed in these three months, so the time is combined and analyzed; that is, the principal component analysis is performed from July to December 2019. The analysis results are shown in Table 5.

It can be seen from Table 5 that the months with  $\Delta < 0$  are February, June, and September. They are  $-0.09986$ ,  $-12.31665$ , and  $-8.28517$ . The three-dimensional graph is drawn, and the results from January to December 2019 in the graph are marked in Figure 6.

TABLE 5: The principal component analysis in 2019.

	$u(t)$	$v(t)$	$\Delta$	Judge symbol
January	0.98542	-0.6019	17.43681	$\Delta > 0$
February	-1.01397	-0.55244	-0.09986	$\Delta < 0$
March	0.02856	1.15435	35.97833	$\Delta > 0$
April	0.57539	1.00113	28.58503	$\Delta > 0$
May	0.57931	-0.99886	28.49381	$\Delta > 0$
June	-1.1547	-0.00227	-12.31665	$\Delta < 0$
July	1.04845	-1.43844	65.08601	$\Delta > 0$
August	-0.67867	-0.8712	17.99199	$\Delta > 0$
September	-1.05655	-0.2064	-8.28517	$\Delta < 0$
October	-0.75572	0.83452	15.35063	$\Delta > 0$
November	0.12442	0.743	14.92073	$\Delta > 0$
December	1.31806	0.93852	42.10087	$\Delta > 0$

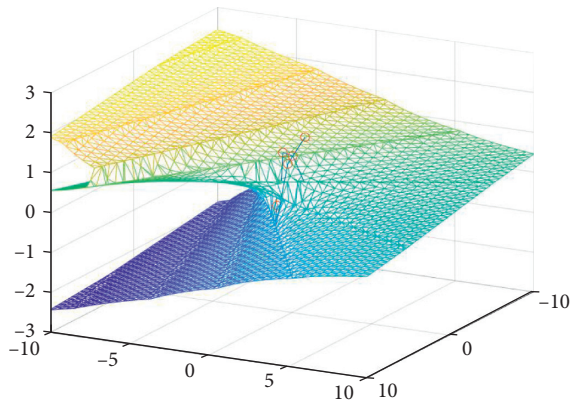


FIGURE 6: Three-dimensional renderings of sudden changes in Shanghai crude oil futures prices in 2019.

When a three-dimensional map is presented in a two-dimensional state, some months cannot be fully displayed. Therefore, the  $U$ - $V$  coordinates in the three-dimensional image are projected into a plane. The bifurcation curve to judge the sudden price change of Shanghai crude oil futures in 2019 is shown in Figure 7.

It can be seen from Figure 7 that the months in the  $\Delta < 0$  area are February, June, and September. It shows that Shanghai crude oil futures prices fluctuated greatly around February, June, and September and were in an unstable situation. According to Figure 7, the coordinates in June are  $(u, v) = (-1.155, -0.00227)$ , and the coordinates in September are  $(u, v) = (-1.057, -0.2064)$ . At this time, the system passes through the boundary of the equilibrium state and is in an unstable state, indicating that a sudden change will occur. The coordinates in February are  $(u, v) = (-1.014, -0.5524)$ . The system reaches the boundary of the equilibrium state and is also in an unstable state, and there is also the possibility of sudden changes.

**4.3. Model Test.** Utilizing the cusp catastrophe model, the volatility and sudden change of Shanghai crude oil futures prices from April 2018 to December 2019 are applied and analyzed. The months of sudden change were May and December 2018 and February, June, and September 2019. In order to verify the feasibility and accuracy of the cusp

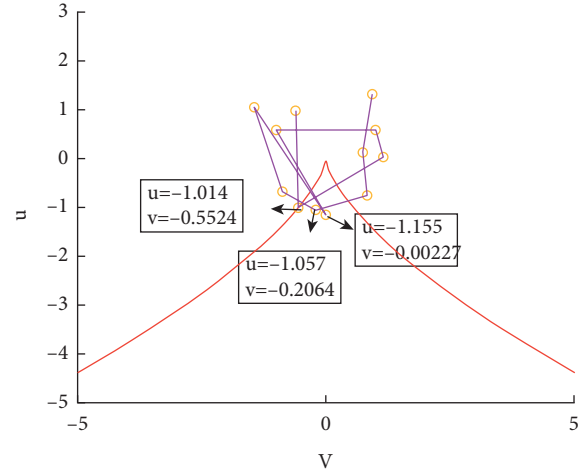


FIGURE 7: Plane projection of sudden changes in Shanghai crude oil futures prices in 2019.

catapult model, it can be compared with the real situation of Shanghai crude oil futures prices, and it can also be analyzed in conjunction with the actual international or domestic geopolitical events and emergencies. In this way, the cusp catastrophe model was tested.

In Figure 8, the real price curve of Shanghai crude oil futures trading from April 2018 to December 2019 is obtained. The daily price limit of Shanghai crude oil futures is 8%, but as the contract settlement day approaches, on the third to last trading day, the price limit will be adjusted to 10%. The Shanghai crude oil futures price standard line is set to 500, and the maximum fluctuation range is selected. Combined with the changing law of the graph, fluctuations in which the price difference is greater than or equal to 50 points can be regarded as a sudden change. The several obvious mutation months, namely, May and December 2018 and June 2019, can be directly observed.

Since March 2018, the Sino-US trade war has had a certain impact on crude oil futures prices, which intensified price fluctuations. On May 7, the Ministry of Ecology and Environment of our country passed the "Environmental Pollution Compulsory Liability Insurance Management Measures (Draft)," which included oil and natural gas exploitation, basic chemical raw material manufacturing, synthetic material manufacturing, and chemical raw material drug manufacturing into the scope of compulsory insurance. The price of crude oil futures was negatively affected. Therefore, Shanghai crude oil futures prices showed a sudden downward trend in May. In December 2018, the US's crude oil and fuel exports exceeded imports for the first time in history, and it became a net oil exporter for the first time, demonstrating the influence of US shale oil on the global energy landscape. As American oil continuously enters the world oil market, the rebalancing of global oil is a long way off. On December 7, OPEC and its allies finally decided to reduce production by 1.2 million barrels per day. OPEC member states pledged to reduce their production by 800,000 barrels from January for a period of 6 months. At the same time, Russia and other partners also pledged to reduce

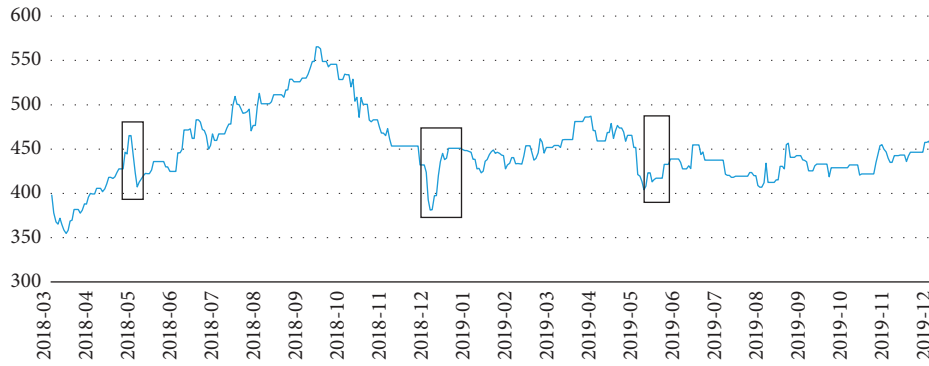


FIGURE 8: Shanghai crude oil futures real price chart.

production by an additional 400,000 barrels of oil a day. On December 12, the number of high-yield oil wells was born with the frequent success of China's oil exploration front. China National Petroleum Corporation announced that it would strongly promote China's continental shale oil revolution. Therefore, in December 2018, the Shanghai crude oil futures price experienced a sudden drop followed by a sudden rise.

On June 13, 2019, the Oman Sea was maliciously attacked, and a tanker explosion occurred. On June 20, 2019, Basra, an important oil production base in southern Iraq, was attacked by rockets. On September 14, 2019, two oil facilities of the Saudi Arabian National Petroleum Corporation (Aramco) were attacked by drones. Therefore, crude oil futures prices fluctuate due to geopolitical emergencies.

From what has been discussed above, the sudden change month of Shanghai crude oil futures price obtained by the cusp catastrophe model is basically consistent with the actual situation, which has certain significance for the study of its price fluctuation.

## 5. Predictive Analysis

**5.1. Principal Component Variable Prediction.** Through principal component analysis, it can be known that the variables of the first principal component, namely, the demand-oriented principal component, include crude oil supply, apparent crude oil consumption, Oman crude oil price, producer ex-factory price index, and macroeconomic prosperity index. The variables of the second principal component, namely, the transactional principal component, include crude oil processing volume, transaction volume, open interest, and RMB exchange rate. Discrete variables can be predicted using the grey GM (1, 1) model. Continuous variables can be predicted using the ARIMA model.

Taking crude oil supply as an example, the forecasting process of discrete variables is illustrated. Firstly, the original sequence is processed as follows.

Then, the grey model development coefficient  $a$  and grey action volume  $b$  need to be calculated.

$$\begin{aligned} a &= -0.007, \\ b &= 5255.312. \end{aligned} \quad (7)$$

Finally, the average simulation relative error is calculated.

The average simulated relative error is 3.331%. From the above steps, the forecast data for the next period in the future can be obtained, and the forecast value is 6107.806.

Taking Oman crude oil price as an example, the prediction process of continuous variables is shown as follows:

The unit root test of the Oman crude oil price is a nonstationary time series. Differential processing on it is performed, as shown in Table 7. After two differences, the  $t$ -statistic is  $-6.062284$ , which is less than the significance level of 1% ( $-3.857386$ ), 5% ( $-3.040391$ ), and 10% ( $-2.660551$ ). Therefore, it can be determined that  $d=2$  in the ARIMA ( $p, d, q$ ) model (Table 7).

By processing the indicator of Oman crude oil price, the nonstationary time series is differentiated into a stationary time series. Using ACF and PACF functions to draw autocorrelation graphs and partial autocorrelation graphs, the  $p$  and  $q$  values of the ARIMA ( $p, d, q$ ) model can be determined. As shown in Figure 9, it can be roughly judged that the model established for the indicator of Oman crude oil price is ARIMA (1, 2, 0).

The forecast function can be used to forecast the Oman crude oil price in the next period. That is to predict January 2020. The result is 65.41127. The predicted values of all variables in the next period are shown in Table 8.

The forecasted value with the data of the last quarter of 2019 for principal component analysis is combined. Then, the control variables  $u(t)$  and  $v(t)$  of the catastrophe model are calculated. Finally, the judgment result of  $\Delta$  according to the formula  $\Delta = 8u^3(t) + 27v^2(t)$  is shown in Table 9. The sudden change in the price of Shanghai crude oil futures in the next period can be predicted.

The U-V coordinates of the three-dimensional image into a plane are projected. It can be seen from Figure 10 that the month in the  $\Delta < 0$  area is January 2020. The coordinates are  $(u, v) = (-1.28446, -0.63602)$ . The forecast results show that the status has changed from December 2019 to January 2020 and from January 2020 to February 2020. The price of Shanghai crude oil futures fluctuates greatly and is in an unstable situation. Sudden changes will occur.

In order to verify the feasibility and accuracy of the forecast model, an empirical comparison and analysis of the real situation of Shanghai crude oil futures prices can be



TABLE 6: Crude oil supply original sequence processing.

	Original sequence	1-AGO sequence	Immediate mean value
1	5497.1	5497.1	8248.1
2	5502	10999.1	13508.7
3	5019.2	16018.3	18612.0
4	5187.4	21205.7	23924.55
5	5437.7	26643.4	29262.85
6	5238.9	31882.3	34726.7
7	5688.8	37571.1	40491.4
8	5840.6	43411.7	46417.45
9	6011.5	49423.2	52320.35
10	5794.3	55217.5	57946.45
11	5457.9	60675.4	63469.45
12	5588.1	66263.5	69235.55
13	5944.1	72207.6	75030.5
14	5645.8	77853.4	80637.35
15	5567.9	83421.3	86287.4
16	5732.2	89153.5	92071.3
17	5835.6	94989.1	97833.3
18	5688.4	100677.5	103758.7
19	6162.4	106839.9	109899.95,
20	6120.1	112960.0	116037.4
21	6154.8	119114.8	

TABLE 7: ADF inspection of Oman crude oil prices.

		<i>t</i> -statistic	Prob.*
Augmented dickey-fuller test statistic		-6.062284	0.0001
Test critical values	1% level	-3.857386	
	5% level	-3.040391	
	10% level	-2.660551	

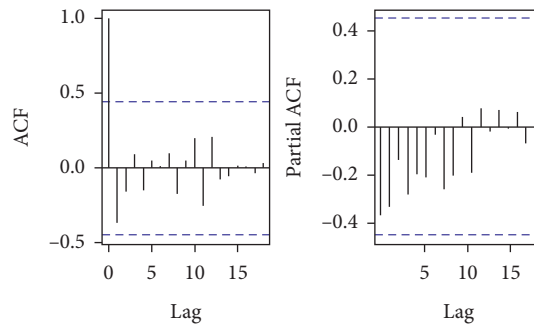


FIGURE 9: Autocorrelation graph and partial autocorrelation graph of Oman crude oil price difference series.

TABLE 8: Index prediction value.

Index	Crude oil supply	Apparent crude oil consumption	Crude oil processing volume
Predictive value	6107.806	6115.305	5691.642
Index	Producer price index	Macroeconomic sentiment index	Trading volume
Predictive value	87.603	95.304	1.063356
Index	Open interest	RMB exchange rate	Oman crude oil prices
Predictive value	40.94751	7.007294	65.41127

TABLE 9: Predictive analysis result table.

$u(t)$	$v(t)$	$\Delta$	Judge symbol
1.09003	-0.34749	13.62131856	$\Delta > 0$
0.3647	-0.50602	7.301577059	$\Delta > 0$
-0.17027	1.48952	59.86459385	$\Delta > 0$
-1.28446	-0.63602	-6.031123225	$\Delta < 0$

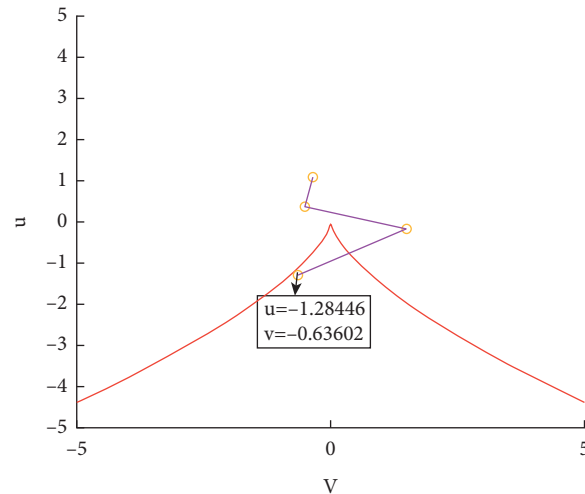


FIGURE 10: Plane projection chart of Shanghai crude oil futures price sudden change forecast.



FIGURE 11: Shanghai crude oil futures real price trend chart.

carried out. It can also be analyzed in conjunction with geopolitical events and emergencies which have occurred internationally or domestically. As shown in Figure 11, the real prices of Shanghai crude oil futures in January and February 2020 are compared and analyzed.

The US-Iran dispute in early January 2020 triggered market concerns about crude oil supply. Crude oil prices were strongly supported. During the continuous fermentation of the event, crude oil prices quickly rushed to the highest point since September 2019. However, as the event subsided and the global economy did not fully improve, crude oil prices fell rapidly.

During the Spring Festival, an epidemic in China occurred, and many provinces initiated the first-level response to major public health emergencies, especially Hubei Province, which was completely closed at the end of January. The market is expected to have a certain impact on China and the global economy, suppressing the rise of crude oil. China's crude oil demand accounts for 14%-15% of the world's total. The decline in China's demand for crude oil is also one of the reasons why crude oil prices have hit a new low. The results predicted in the paper are consistent with actual price trends and real sudden events.

## 6. Conclusions

Taking the factors related to domestic crude oil into account in the price fluctuations of China's market and expanding to foreign markets through the futures trading mechanism will help strengthen China's position in the international futures market pricing. In the paper, nine influencing factors are selected as the entry point (including China's crude oil supply, China's apparent crude oil consumption, China's crude oil processing volume, Shanghai crude oil futures trading volume, open interest, RMB exchange rate, Oman crude oil price, China's oil industry producer price index, and China's macroeconomic prosperity index). A principal component analysis to process factors is used. Then, two principal components as the control variables of the cusp catastrophe model are extracted. A standard cusp catastrophe model balance surface equation is constructed to analyze the Shanghai crude oil futures price catastrophe. Judging the sudden change in the price of crude oil futures is conducive to locking in the fluctuation range of crude oil prices and giving greater play to the hedging function of futures, thereby reducing the market risk of China's oil companies and avoiding China's passive position in

international competition. Judging the sudden change based on the data factor and the sign of the discriminant can greatly simplify the calculation and make it more specific. Combining with the visualization of Matlab software is more conducive to China's oil companies and other market participants to obtain the volatility of futures market prices, thereby avoiding risks.

Through analyzing actual price fluctuations and actual sudden changes, it can be concluded that May and December 2018 and June 2019 are the sudden change months. The comparative analysis shows that the cusp catastrophe model has certain feasibility and accuracy. The model predicts a sudden change in January 2020 and compares the actual price trend with the real sudden change event to test the forecast results. It is found that the predicted results are more accurate and consistent with the facts. The research on the sudden change and forecast of Shanghai crude oil futures prices will help to fully understand and grasp the development status and inherent characteristics of the oil futures market and can make up for China's shortcomings in oil futures.

Many macrovariables in China are involved in the volatility factors. Limited by the statistics of macrovariables, the smallest scope of this paper can only be months. Therefore, the analysis of price changes in the Shanghai crude oil futures market can only be limited to months. The future research direction can shorten the research period from one month to one day and analyze the mutation in more detail.

### Data Availability

Previously reported data were used to support this study and are available at <https://www.cei.cn/>, <https://www.gtafe.com/>.

### Conflicts of Interest

The authors declare that they have no conflicts of interest.

### Authors' Contributions

Weifeng Gong conceptualized the study, developed methodology, wrote the original paper, and responsible for funding acquisition. Yahui Li investigated the study and was responsible for project administration. Chuanhui Wang contributed to formal analysis and reviewed and edited the paper. Haixia Zhang and Zhengjie Zhai contributed to formal analysis and edited the paper.

### Acknowledgments

This paper benefited from years of thinking about these issues and the discussion with many colleagues related to economics at that time. This research was supported by the National Natural Science Foundation of China under grant number 71804089, Humanities and Social Sciences Youth Foundation of Ministry of Education of China under grant numbers 18YJCZH034 and 19YJC790128, and Jiangsu Postdoctoral Research Funding Plan under grant number 2018K195C. This research was also supported by the

Graduate Education Quality Improvement Project of Shandong Province, China, under grant numbers SDYKC19180 and SDYAL19180, "the Quality Course in Financial Statistics" (Project no. SDYKC19180), and the "Financial literacy Oriented Teaching Case Library of Derivative Financial Instruments" (Project no. SDYAL19180).

### References

- [1] S. Hammoudeh and H. Li, "Sudden changes in volatility in emerging markets: The case of Gulf Arab stock markets," *International Review of Financial Analysis*, vol. 17, no. 1, pp. 47–63, 2008.
- [2] W. Mensi, S. Hammoudeh, and S.-M. Yoon, "Structural breaks, dynamic correlations, asymmetric volatility transmission, and hedging strategies for petroleum prices and USD exchange rate," *Energy Economics*, vol. 48, pp. 46–60, 2015.
- [3] Q. Pan and T. C. Han, "Structural mutation and sustained economic growth—based on panel data analysis of 157 countries," *Journal of Tsinghua University (Philosophy and Social Sciences)*, vol. 34, no. 3, pp. 168–179, 2019.
- [4] B. T. Ewing and F. Malik, "Volatility transmission between gold and oil futures under structural breaks," *International Review of Economics & Finance*, vol. 25, pp. 113–121, 2013.
- [5] Z. F. Zeng and S. Y. Yin, "Research on structural abrupt change of stock market based on bayesian statistics," *Statistics & Decisions*, no. 13, pp. 160–162, 2016.
- [6] H. Zhang, "Geopolitics, financial crisis and global crude oil price system—empirical study based on endogenous structural breaks," *Chinese Review of Financial Studies*, no. 3, pp. 21–46, 2017.
- [7] X. Gong and B. Q. Lin, "Jump risk, structural breaks and forecasting crude oil futures volatility," *Chinese Journal of Management Science*, vol. 26, no. 11, pp. 11–21, 2018.
- [8] X. G. Wang, "Simultaneous detection approach in multi-structural breaks based on latent state variable," *Statistics & Decisions*, vol. 34, no. 3, pp. 14–19, 2018.
- [9] Y. S. Zhang, "International crude oil futures prices' mutation point identification research: Based on PPM change point Analysis and Hurst index analysis," *Statistics & Information Forum*, vol. 31, no. 8, pp. 78–84, 2016.
- [10] J. Wang and Y. Q. Sun, "Use cusp catastrophe model to examine the stability of financial ecosystem," *Finance and Accounting Monthly*, vol. 27, pp. 86–87, 2010.
- [11] C. H. Wang, Z. G. Fang, and Y. Q. Guo, "Research on the grey sharp point catastrophe warning model for the generalized virtual assets," *Research on The Generalized Fictitious Economy*, vol. 5, no. 2, pp. 72–79, 2014.
- [12] Y. K. Qiu and X. L. Yang, "The Judge of financial system stability based on entropy and catastrophe theory," *Journal of Technical Economics & Management*, no. 5, pp. 100–104, 2014.
- [13] L. Lin, "Stochastic cusp catastrophe model for Chinese stock market," *Journal of Systems Engineering*, vol. 31, no. 1, pp. 55–65, 2016.
- [14] Z. M. Li and K. Shi, "The cusp catastrophe model of securities return," *Journal of Xinjiang University (Natural Science Edition)*, vol. 20, no. 2, pp. 125–129, 2003.

## Research Article

# A Novel Modeling Technique for the Forecasting of Multiple-Asset Trading Volumes: Innovative Initial-Value-Problem Differential Equation Algorithms for Reinforcement Machine Learning

Mazin A. M. Al Janabi 

Full Professor of Finance & Banking and Financial Engineering, Tecnológico de Monterrey, EGADE Business School, Santa Fe Campus, Mexico, Mexico

Correspondence should be addressed to Mazin A. M. Al Janabi; [mazinaljanabi@gmail.com](mailto:mazinaljanabi@gmail.com)

Received 29 May 2021; Accepted 7 January 2022; Published 17 March 2022

Academic Editor: Sameh S. Askar

Copyright © 2022 Mazin A. M. Al Janabi. This is an open access article distributed under the Creative Commons Attribution License, which permits unrestricted use, distribution, and reproduction in any medium, provided the original work is properly cited.

Liquidity risk arises from the inability to unwind or hedge trading positions at the prevailing market prices. The risk of liquidity is a wide and complex topic as it depends on several factors and causes. While much has been written on the subject, there exists no clear-cut mathematical description of the phenomena and typical market risk modeling methods fail to identify the effect of illiquidity risk. In this paper, we do not propose a definitive one either, but we attempt to derive novel mathematical algorithms for the dynamic modeling of trading volumes during the closeout period from the perspective of multiple-asset portfolio(s), as well as for financial entities with different subsidiary firms and multiple agents. The robust modeling techniques are based on the application of initial-value-problem differential equations technique for portfolio selection and risk management purposes. This paper provides some crucial parameters for the assessment of the trading volumes of multiple-asset portfolio(s) during the closeout period, where the mathematical proofs for each theorem and corollary are provided. Based on the new developed econophysics theory, this paper presents for the first time a closed-form solution for key parameters for the estimation of trading volumes and liquidity risk, such as the unwinding constant, half-life, and mean lifetime and discusses how these novel parameters can be estimated and incorporated into the proposed techniques. The developed modeling algorithms are appealing in terms of theory and are promising for practical econophysics applications, particularly in developing dynamic and robust portfolio management algorithms in light of the 2007–2009 global financial crunch. In addition, they can be applied to artificial intelligence and machine learning for the policymaking process, reinforcement machine learning techniques for the Internet of Things (IoT) data analytics, expert systems in finance, FinTech, and within big data ecosystems.

## 1. Introduction

Liquidity risk measures and the illiquidity of assets and trading volumes, in both financial and commodity markets, have been a subject of much debate, interest, and controversy in the last few decades. There is a longstanding Wall Street saying that “*it takes trading volume to make prices move.*” Thus, there are plentiful empirical conclusions to reinforce the impact of trading volume on absolute value of price changes, conditional volatility, and the illiquidity of multiple trading assets during the closeout period [1–9].

In an earlier strand of research papers, Jain and Joh [1] investigate the dependence between hourly prices and trading volume and provide evidence on the joint features of hourly common stock trading volume and returns on the New York Stock Exchange. Their study shows that the average volume traded displays substantial changes across trading hours of the day (i.e., average trading volumes across six trading hours of the day) and across days of the week, while the average returns deviate across hours of the day and, to a certain extent, across days of the week. In addition, the relation between trading volume absolute returns is significantly more different for positive returns than for

nonpositive returns. In a similar vein, the dynamics between stock returns, trading volume, and volatility in nine key national stock markets (i.e., index returns and trading volume from USA, Japan, UK, France, Canada, Italy, Switzerland, Netherlands, and Hong Kong) are examined by Chen et al. [2]. Their empirical outcomes indicate a positive correlation between trading volume and the absolute value of the stock price change, as well as persistence in volatility, and indicate that trading volume provides certain information to the returns process.

The 2007–2009 global financial crisis (GFC) has stressed the necessity for more efficient liquidity measures and management tools, in both normal and stressed market conditions, and placed the market microstructure of liquidity risk measures and trading volumes [1, 2] at the forefront agenda for research and development, particularly in emerging and illiquid markets [3–6]. One of the raising concerns in the wake of the GFC is that typical Value-at-Risk (VaR) market risk measures omit a key component, the risk associated with illiquidity of trading assets. As a result, financial markets and institutions would like to implement robust models and optimization algorithms that can place a cost not only for market risk but also for liquidity risk [4, 7]. In addition, the 2007–2009 financial meltdown has underlined the deficiencies of the Value-at-Risk (VaR) risk measures for the computation of market risk because such metrics do not integrate liquidity risk into the total risk process [3]. Furthermore, the GFC stressed the fact that illiquidity risk is challenging to quantify as it relies on multiple market microstructure parameters and that scenario testing is critical to any contemporary liquidity risk modeling process. Thus, robust liquidity modeling techniques and appropriate scenario identification risk processes have become major issues for the financial community to address. In fact, very little is written about why modeling the dynamics of the trading volume is important in measuring liquidity risk. To that end, the connection of the trading volume modeling under consideration to illiquidity risk is the key motivation of this paper.

The notion of illiquidity refers to the aptitude to convert in timely manner trading assets into cash at the prevailing market prices with little or no cost, risk, or disruption and without affecting its asset price [4]. Thus, liquidity risk is synonymous with both the necessary time to liquidate trading assets and the cost of liquidation, a trade-off that is a key feature in modeling market liquidity risk. The market liquidity risk depends on quite a few parameters and grounds. For instance, certain trading assets, such as highly traded equities, are integrally more liquid than other assets. In addition, the position size is a significant parameter and plays a key role in liquidity risk since it refers to ability of the financial trading entity to unwind into the financial markets, in one trading day, the aggregate number of shares compared with that day's total trading volume. Nevertheless, under stressed market conditions, liquidity can drop drastically, as financial markets' participants generally tend to be more risk-averse. In this case, the financial trading entity may be involuntary obliged to retain its assets positions for a much longer period, thereby intensifying liquidity risk [6].

Market liquidity risk has currently gained a great deal of consideration in light of the aftermath of the 2007–2009 GFC. During the past few years, quite a few research papers were written on the consideration of illiquidity risk in the VaR methodology. While a great deal has been written on the topic, the notions of liquidity risk, position size and traded volume, and the unwinding of assets during the closeout periods lack clear definitions, let alone the risk processes themselves.

Yet, despite this widespread acknowledgment of the phenomena, there exists no specific mathematical description of illiquidity risk and conventional VaR methods fail to identify the effect of illiquidity risk. In this paper, we do not propose a complete one either, but we propose novel modeling algorithms of some classes of illiquidity risk which are helpful for complementing the description of market risk and for forecasting dynamic trading volumes declines (or decays) during the closeout horizon under illiquid and stressed market circumstances and within a multivariate context. Undeniably, the reinforcement machine learning processes of the liquidity modeling algorithms proposed in this paper do not integrate all the microstructure features of the illiquidity risk measures (machine learning, which has been identified as a technology with significant impacts for portfolio construction and risk management, can enable the development of far more accurate risk-return forecasting techniques by identifying sophisticated, multifaceted, and stochastic trends in big data among all types of investments [10–13]. The categorization of machine learning approaches encompasses a wide range of methodologies and technologies that convey a shared goal from many perspectives. In this way, machine learning approaches may be classified using quite diverse metrics and conventions depending on the type of learning desired. As a result, the authors direct readers to [10–13] for some of the most recent research on machine learning, big data, and expert systems in finance for modern portfolio optimization and management. Furthermore, some literature addressed the genuine concerns of big data and associated green challenges and applications, while others examined the notion of information and communication technologies (ICT) for sustainable development goals (SDG). For further insights on these two important topics, the authors refer the readers to [14, 15].). However, it is useful as a tool for estimating dynamic trading volumes and liquidity risk when the influence of liquidity of certain financial assets is substantial.

A range of liquidity risk modeling techniques have been suggested in the academic literature. For convenience, and to be faithful to the literature, we focus on some contemporary challenges to tackle the issue of illiquidity risk and liquidity-adjusted VaR (LVaR) with special emphasis on merely the recent attempts and literature.

In effect, previous researchers have endeavored to study the notion of illiquidity risk but not fundamentally within the perception of multiple-asset portfolios (for other relevant literature on liquidity risk, internal risk modeling techniques, asset pricing, and portfolio choice and diversification, one can refer as well to Al Janabi [12]; Ruozi and Ferrari [16]; Grillini et al. (2019); Roch and Soner [17]; Al

Janabi et al. [6]; Weiß and Supper [8]; Al Janabi, Ferrer, and Shahzad [7]; Madoroba and Kruger [18]; Madhavan et al. [19]; Takahashi and Alexander [20]; Cochrane (2005); and Meucci [21]; among others). Their main motivation, in fact, was on examining transaction costs (i.e., the expanding of the bid-ask spreads); however, the special impacts of undesirable market prices with distinct dependence measures have not been researched systematically, yet Hung et al. [3], Weiß and Supper [8], Al Janabi et al. [6], and Al Janabi et al. [7] are exemptions. In their research study, Weiß and Supper [8] propose a multivariate model for evaluating liquidity-adjusted intraday VaR based on vine copulas and the attained research outcomes validate that the recommended method functions adequately in forecasting possible intraday liquidity-adjusted portfolio shortfalls. Al Janabi et al. [7] and Al Janabi et al. [6] used a modified version of Al Janabi model for liquidity risk management [18] combined with different copula function and presented an endogenous liquidity adjusted VaR method, which measured the liquidity risk triggered by illiquid  $t$  holdings and difficult supply-demand imbalances. Al Janabi et al. [6] present a portfolio optimization model based on the integration of dynamic conditional correlation  $t$ -copula and LVaR algorithms. In a similar vein, Al Janabi, Ferrer, and Shahzad [7] examine a robust portfolio optimization approach based on vine-copula and LVaR modeling algorithm. While Al Janabi et al. [6] study a portfolio that consists of nine assets (i.e., G-7 stock market indexes, crude oil, and gold commodities), [7] a research paper substitutes oil by a general commodity index and it incorporates Bitcoin as an additional asset. Among the conclusions therein is the fact that the presence of liquidity dimension in market risk is feasible to improve the robustness of market risk computations.

On another front, Hung et al. [3] study the influence of illiquidity on calculating VaR predictions using multivariate GARCH- $t$  and GJR-GARCH- $t$  models for portfolios with unlike liquidity strengths. The obtained conclusions show that calculating portfolio VaR predictions with multivariate techniques outperform the univariate techniques for full and subsample cycles in terms of precision and estimations of effectiveness. Allaj [5] presented a general framework of a one period risk measurement technique that incorporates illiquidity risk into standard risk measures. These risk techniques are decomposed into two terms, one determining the risk of the future value of a given position in an asset or a portfolio of assets and the other the initial cost of that position. Finally, Careta and Jaimungal [9] examined an optimal execution policy for an investor seeking to complete a large order using limit and market orders. They demonstrated that the different considered strategies outperform the Almgren and Chriss [22] modeling technique because those strategies benefited from the optimal mix of limit orders.

In this backdrop, though many attempts in liquidity risk modeling focused on transaction costs and VaR measures, it is well known that traditional risk measures such as VaR models are incoherent [23] and can lead to regulatory arbitrage to reduce capital requirements. As such, conventional VaR methods cannot satisfy the subadditivity

requirement to be classified as coherent measures like other popular measures such as Expected Shortfall (ES). The lack of subadditivity in a risk measure can be manipulated to form regulatory arbitrage as financial institutions can establish different subsidiary firms to save regulatory capital. This is where this research study comes in as we attempt to make clear the fundamental nature of illiquidity risk measures and propose novel modeling techniques and robust algorithms to tackle the problem of illiquidity risk and trading volumes during the closeout (or unwinding) period for multiple-asset portfolios within the same financial entity, as well as for financial holding enterprises with different subsidiary firms and multiple agents.

Despite the large amount of research on liquidity risk, our special interest in introducing the trading volume, as a key factor for a multiagent dynamic model of trading activities and then in modeling the dynamics of the trading volume during the closeout period (i.e., the liquidation or unwinding horizon), rests on the lack of research studies that apply trading volume in an attempt to boost the forecasting of risk measures. Our study contributes to the understanding of liquidity risk and the dynamic modeling of trading volume during the closeout period in several ways. First, this paper is the first econophysics attempt, to the best of my knowledge, to develop a novel modeling technique and robust techniques for the estimation of trading volumes and illiquidity risk during the closeout period and within the context of multiple-asset portfolios, as well as for financial holding entities with different subsidiary firms and multiple agents. Second, in contrast to all known models for liquidity risk, this paper implements an innovative dynamic modeling technique in deriving the liquidity risk process and trading volume using initial-value-problem differential equations algorithms, as other authors have done heretofore. The proposed robust modeling techniques can resolve some of the main drawbacks of the traditional VaR method of being incoherent because of its lack of subadditivity and its tendency to lead to a form of regulatory arbitrage [23]. Third, this paper provides some new important parameters, which are the first of their kind to the best of the author's knowledge, for the assessment of the trading volumes of multiple-asset portfolios during the closeout period, where the mathematical proofs for each theorem and corollary are provided. Based on the new developed econophysics theory, this paper presents for the first time a closed-form solution for key parameters for the estimation of trading volumes and liquidity risk, such as the unwinding constant, half-life, and mean lifetime, and discusses how these novel parameters can be estimated and incorporated into the recommended techniques. Fourth, we examine potential reinforcement machine learning algorithms for the implementation of the proposed novel econophysics modeling techniques to risk forecasting and multiple-asset portfolio selection practices. To that end, in line with Al Janabi et al. [7] and Al Janabi [12], we define a modified dynamic process of Al Janabi model [18] for multiple-asset portfolio selection and risk forecasting and combine it with the innovative initial-value-problem differential equations algorithms. As a result, the alternative reinforcement machine learning algorithms can

address some of the drawbacks of the traditional mean-variance VaR technique, presenting robust generalizations and meaningful improvements on Markowitz's [24] mean-variance solution. Fifth, the developed modeling techniques are appealing in terms of theory and are promising for likely real-world applications, particularly in developing dynamic and robust portfolio management algorithms that financial markets and institutions could put into effect in the wake of the 2007–2009 global financial meltdown. In addition, it can be applied to artificial intelligence and machine learning for the policymaking process, reinforcement machine learning techniques for the Internet of Things (IoT) data analytics, expert systems in finance, FinTech, and within big data ecosystems.

The remainder of the paper is organized as follows. In Section 2, we provide details of mathematical definition and derivation of the modeling algorithms and liquidity risk process using initial-value-problem differential equations techniques. Section 3 provides expansion of the modeling algorithms to multiple-asset portfolios. Section 4 examines portfolio selection and risk management practices and highlights certain reinforcement machine learning issues. In addition, in this section, we present one potential reinforcement machine learning algorithm for the possible implementation of the proposed modeling techniques to multiple-asset portfolio selection and risk management practices, and we discuss the overall reinforcement machine learning process with the aid of an operational flowchart. Section 5 concludes the paper and provides future directions for research on the topic and the possible applications of the proposed novel modeling techniques and robust algorithms.

## 2. The Model

We define the dynamic process of continuous changes in the trading volume of any portfolio of multiple assets as an initial-value-problem differential equation of the form

$$\frac{dV(H)}{dH} = -\mu V(H) + V_N(H), \quad (1)$$

where  $V(H)$  is the current trading volume of a multiple-asset portfolio, whose domain consists of all nonnegative real numbers ( $\mathbb{R}^+$ ); that is,  $V(H) \geq 0$ ;  $V_N(H)$  is the rate of incorporation of “new” trading volume of multiple assets to the current trading portfolio, whose domain consists of all nonnegative real numbers ( $\mathbb{R}^+$ ); that is,  $V_N(H) \geq 0$ ;  $H$  is the closeout period (i.e., unwinding horizon or holding period), which can take nonnegative real numbers that are above or equal to 1.0 ( $\mathbb{R}_{\geq 1.0}^+$ ) only during the unwinding process to convert trading assets into cash at the prevailing market prices; that is,  $H \geq 1.0$ ; and  $\mu =$  is a constant of proportionality that we can label as the “unwinding constant.” This unwinding constant can be defined as the probability per unit time that the current trading volume of any portfolio of multiple assets will undergo a decline (or a decay) in its holding assets, given that multiples of trading assets will be sold (i.e., unwound) during the closeout period  $H$ .

In fact, the first term on the right-hand side of (1) denotes the rate of decline (or the rate of the decay process) of the current trading volume of the existing multiple-asset portfolio, whereas the second term indicates the rate of incorporating (i.e., the rate of the “production” or “creation” process) new multiple-asset trading volume to the existing portfolio. Certainly, the above statements are rather ambiguous and, hence, we need to explain the economic foundations in some mathematically and financially meaningful means. To begin, we need some means to explain the rationality and usefulness of the proposed dynamic trading volume model and to link its assumptions to market dynamics.

There are multiple rationalities behind the mathematical foundation and the financial dentition of the proposed differential equation model. To that end, and in line with other liquidity risk research papers discussed earlier, which usually make many ad hoc assumptions, we attempt to typically link in some way the proper economic foundation and assumptions to market dynamics and provide full justification, detailed as follows:

- (1) In our modeling technique, we are attempting to explain both terms of (1) as the rate of decline (or decay) process of trading volume and the rate of the incorporation process (i.e., the rate of the “production” or “creation” process) of new trading volume. This is because there are some resemblances in our econophysics modeling technique and other physical science and social science processes, such as the decay and production of radionuclides and the process of the decline in the population of nations and the simultaneous process of the incorporation of new immigrants to those nations.
- (2) Portfolio managers and their respective markets' traders (i.e., multiple agents) can unwind certain assets and add new multiple assets to the current trading portfolio on a daily basis. This is because the decline in the trading volume of certain multiple assets is accompanied by the incorporation (i.e., “production” or “creation”) of new trading volume by other multiple agents inside the same financial entity or within multiple agents of different subsidiaries of the principal financial holding firm. In addition, in our model, multiple agents are provided with various trading volumes that are for a limited time only associated with their particular circumstances and the market conditions and, as such, we propose a dynamic multiagent model with agent-dependent and time-dependent trading volumes.
- (3) The level and depth of public and private information available to the different portfolio managers and traders are imbalanced (i.e., asymmetric levels of different news, statistical datasets, figures and facts, communications, and lines of evidence are accessible and available to the contrasting market participants). This assumption is quite relevant as it allows the expansion of the proposed dynamic trading volume

model from the perspective of a single multiple-asset portfolio to multiple-asset portfolios. It also permits financial holding entities, with different subsidiary firms and multiple agents, to consider different trading volumes and closeout horizons for all multiple-asset portfolios.

- (4) Within a large pool of markets' traders, the activities, behaviors, and actions of the individual traders are uncorrelated in many instances, even though these traders are engaging and executing buying-selling market orders of multiple-asset portfolios inside the same financial entity or within multiple agents of different subsidiaries of the primary financial holding company.
- (5) One key assumption that we make in our proposed model is that the trading positions of multiple-asset portfolio(s) are unwound only at the quoted or prevailing market prices. As such, the quantity (or position size) to liquidate each day into the markets is limited to a preset fraction of that day's trading volume. Thus, in our suggested modeling technique, the multiple-asset trading positions will be unwound into the markets at that fraction of trading volume over each time period until the overall trading positions are completely liquidated, and the income from the unwinding process is settled into cash.
- (6) The rooted effects of the "call option-like" embedded incentives given to traders to induce them to undertake additional risk as the potential upside rewards are quite appealing, whereas the downside impacts and consequences are very limited for their irrational and/or exorbitant risk-takings.
- (7) In fact, some of these rational assumptions embedded in our econophysics differential equation model can contradict some traditional market theories and perhaps disappoint fully devoted believers in efficient markets hypothesis. However, the actual realities on the ground of how financial markets work, as evidenced by the latest severe financial crises and meltdowns besides the scandalous events of several rogue traders and trading entities, have placed efficient market hypothesis on the edge of rationality and judgment to questioning its assumptions and validity. Based on our particular working experiences in diverse financial markets and institutions, the authors of this paper fundamentally believe that some financial markets (probably in the western hemisphere) are more efficient than other markets. As such, the authors are strong believers that the large bulks of emerging markets are considerably less efficient than their western counterparts.

In this backdrop, rearranging (1) yields

$$\frac{dV(H)}{dH} + \mu V(H) = V_N(H). \quad (2)$$

Indeed, (2) is a part of a general differential equation of the form

$$\frac{dy}{dx} + r(x)y = q(x). \quad (3)$$

In fact, the algebraic step to solve (3) does not separate variables. However, it does remove the  $y$  variable from the right side of the equation and at the same time sets up the left side for multiplication by an "integrating factor" trailed by a vital use of the "product rule" for differentiation.

**Theorem 1.** Assume that  $r(x)$  and  $q(x)$  are continuous functions and let  $R(x)$  be any antiderivative of  $r(x)$ . The general solution of the differential equation  $dy/dx + r(x)y = q(x)$  is then

$$y(x) = e^{-R(x)} \int e^{R(x)} q(x) dx + C e^{-R(x)}, \quad (4)$$

where  $C$  is an arbitrary constant.

*Proof of Theorem 1.* The existence of both  $dy/dx$  and  $y(x)$  in the sum on the left side of (3) instructs us to contemplate the "product rule" for differentiation. If  $u$  is a function of  $x$  that is never 0, then we have the following:

$$\begin{aligned} \frac{d}{dx} (uy) &= u \frac{dy}{dx} + \left( \frac{du}{dx} \right) y \\ &= u \left( \frac{dy}{dx} + \frac{1}{u} \left( \frac{du}{dx} \right) y \right). \end{aligned} \quad (5)$$

The notion is to obtain a function  $u$  so that the factor of  $y$  on the right side of the former equation matches the factor of  $y$  in (3). Namely, we seek to find a function  $u$  such that

$$\frac{1}{u(x)} \left( \frac{du}{dx} \right) = r(x). \quad (6)$$

This separable differential equation can be solved by rewriting it as

$$\int \frac{1}{u} du = \int r(x) dx. \quad (7)$$

Given that  $R(x)$  is an antiderivative of  $r(x)$ , the universal solution of the prior equation is  $\ln(|u|) = R(x) + C_0$ , where  $C_0$  is a constant of integration. Further, since any specific solution  $u$  will help in achieving our purpose, we can streamline the algebra by selecting a solution  $u$  with  $u(x) > 0$  and  $C_0 = 0$ . With these selections, we can obtain the following  $\ln(u) = R(x)$ , or  $u(x) = e^{R(x)}$  which is our integrating factor. Now, on multiplying both sides of (3) by  $e^{R(x)}$ , we can get

$$r(x)e^{R(x)} \cdot y + e^{R(x)} \frac{dy}{dx} = e^{R(x)} q(x). \quad (8)$$

Therefore,



$$\begin{aligned}
\frac{d}{dx}(e^{R(x)} \cdot y) &= \left( \frac{d}{dx} e^{R(x)} \right) \cdot y + e^{R(x)} \frac{dy}{dx} \\
&= R'(x) e^{R(x)} \cdot y + e^{R(x)} \frac{dy}{dx} \\
&= r(x) e^{R(x)} \cdot y + e^{R(x)} \frac{dy}{dx} \\
&= e^{R(x)} q(x).
\end{aligned} \tag{9}$$

In other words,  $e^{R(x)} \cdot y$  is an antiderivative of  $e^{R(x)} q(x)$ , such that

$$e^{R(x)} \cdot y = \int e^{R(x)} q(x) dx + C. \tag{10}$$

To that end, formula (4) can be obtained on dividing each side of (10) by  $e^{R(x)}$ . Thus, the Proof of Theorem 1 is completed.

Set against this background, linear equations [such as in the case of (1) and/or (2)] with constant coefficients arise frequently in practical applications, such as in the case of the trading volume of multiple-asset portfolio posed in this paper. In general terms, these differential equations have the form  $dy(t)/dt + \theta y(t) = \alpha$ . We can realize that by rewriting this equation in the form  $dy(t)/dt = -\theta y(t) + \alpha$ , which is a separable linear differential equation. Though this equation may be solved using other mathematical techniques, we can simplify the calculations by implementing Theorem 1.  $\square$

**Theorem 2.** Assume that  $\theta$  and  $\alpha$  are constants with  $\theta \neq 0$ ; then the linear differential equation is

$$\frac{dy(t)}{dt} + \theta y(t) = \alpha. \tag{11}$$

It has a general solution:

$$y(t) = \frac{\alpha}{\theta} + C e^{-\theta t}. \tag{12}$$

As a result, the initial-value-problem

$$\frac{dy(t)}{dt} + \theta y(t) = \alpha, \quad y(0) = y_0, \tag{13}$$

has the following unique single solution:

$$y(t) = \frac{\alpha}{\theta} + \left( y_0 - \frac{\alpha}{\theta} \right) e^{-\theta t}. \tag{14}$$

*Proof of Theorem 2.* In fact, (11) is the special case of (3) that arises from placing  $q(t) = \alpha$  and  $r(t) = \theta$ . Given that  $R(t) = \theta t$  is an antiderivative of  $r(t)$ , (4) states that (11) has the following solution:

$$y(t) = e^{-\theta t} \int e^{\theta t} \alpha dt + C e^{-\theta t} = \frac{\alpha}{\theta} + C e^{-\theta t}. \tag{15}$$

This proves (12). However, if  $y(0) = y_0$ , then  $\alpha/\theta + C e^{-\theta \cdot 0} = y_0$ , or  $C = y_0 - \alpha/\theta$ .

After substituting the above obtained value of  $C$  into (12), one can obtain formula (14); that is,  $y(t) = \alpha/\theta + (y_0 - \alpha/\theta) e^{-\theta t}$  and, hence, it finalizes the proof of Theorem 2.

In this backdrop, we can now apply the above theorems to the case of portfolio management with structural asset allocations, specifically for the assessment of trading volume of multiple-asset portfolios at different closeout periods.  $\square$

**Corollary 1.** As denoted earlier, the closeout period ( $H$ ) can take nonnegative real numbers that are above or equal to 1.0 ( $\mathbb{R}_{\geq 1.0}^+$ ) only during the unwinding process to convert trading assets into cash at the prevailing market prices; that is,  $H \geq 1.0$ . However, to simplify the solution of the initial-value-problem differential equation at the beginning of the trading process and before the initiation of the actual liquidation process of any asset, we are assuming here that the notion of  $H \geq 1.0$  is still valid before the acquisition of any multiple assets at the initial conditions of the trading process (i.e., when  $t = 0$ ).

In a similar vein and following the differential equations process of the above two theorems and their respective proofs, for the singular case of an initial-value-problem of a multiple-asset trading portfolio at which  $V(0) = V_0$  (when  $t = 0$ , at the start of the trading process) and  $V_N(H) = V_N$  (for the special case of a constant rate for the incorporation of new volumes of the further multiple assets to the existing trading portfolio), the solution to (2) is easily obtained as

$$V(H) = V_0 e^{-\mu H} + \left( \frac{V_N}{\mu} \right) (1 - e^{-\mu H}). \tag{16}$$

In addition, for the exceptional case when  $V_0 = 0$  at  $t = 0$ , (16) is confined to

$$V(H) = \left( \frac{V_N}{\mu} \right) (1 - e^{-\mu H}). \tag{17}$$

Furthermore, for the special case in which there is not any incorporation of new volumes of multiple assets to the existing trading portfolio during the closeout horizon (i.e.,  $V_N = 0$ ), the solution of (2) via (16) can be reduced to

$$V(H) = V_0 e^{-\mu H}. \tag{18}$$

*Proof of Corollary 1.* Equation (2), that is,  $dV(H)/dH + \mu V(H) = V_N(H)$ , has the following general solution, where  $C$  is an arbitrary constant:

$$V(H) = \frac{V_N(H)}{\mu} + C e^{-\mu H}. \tag{19}$$

The initial-value-problem can be structured when  $t = 0$  at the start of the trading process, such that

$$\frac{dV(H)}{dH} + \mu V(H) = V_N(H), \tag{20}$$

$$V(0) = V_0, \quad \text{for } t = 0,$$

and indeed, when  $V_N(H) = V_N$  for the easiest case when the incorporation or “generation rate” is constant in time (i.e., the special case of a constant rate for the incorporation of new volumes of multiple assets to the existing trading portfolio during the closeout horizon), (20) can be evaluated analytically to give a unique solution:

$$V(H) = \left(\frac{V_N}{\mu}\right) + \left[V_0 - \left(\frac{V_N}{\mu}\right)\right] e^{-\mu H}. \quad (21)$$

Further, (21) can be written as

$$V(H) = V_0 e^{-\mu H} + \left(\frac{V_N}{\mu}\right) (1 - e^{-\mu H}). \quad (22)$$

For the special case when  $V_0 = 0$  at  $t = 0$ , (22) is reduced to

$$V(H) = \left(\frac{V_N}{\mu}\right) (1 - e^{-\mu H}). \quad (23)$$

As a result, (23) is the same as (17) and, for the exceptional case in which there is not any addition of new trading volume to the trading portfolio (i.e.,  $V_N = 0$ ), the solution of (2) via (22) can be reduced to

$$V(H) = V_0 e^{-\mu H}. \quad (24)$$

This establishes (18) and ends the proof of Corollary 1.

Set against this background, we can now proceed to determine the required parameters for solving (16) and/or its special case (18), detailed as follows.  $\square$

**Corollary 2.** *Using the special case formula  $V(H) = V_0 e^{-\mu H}$  as discussed earlier in (24) and Corollary 1 along with its proof, it is not difficult to show that the half-life ( $H_{1/2}$ ) and the mean lifetime ( $\bar{H}$ ) for a multiple-asset portfolio to unwind its assets throughout the closeout period ( $H$ ) can be expressed as*

$$H_{1/2} = \frac{\ln 2}{\mu} \cong \frac{0.693}{\mu}. \quad (25)$$

$$\bar{H} = \frac{1}{\mu} = 1.44 H_{1/2}. \quad (26)$$

*Proof of Corollary 2.* The unwinding of a multiple-asset portfolio holding is a statistical random or stochastic process.

It is not possible to foresee whether or not a single asset can be sold out (closed out) in a given time period along the unwinding horizon  $H$ . Nevertheless, we can forecast the probable or typical closing-out performance of sizeable multiple-asset portfolios. We can contemplate a sample portfolio comprising sizeable volume  $V$  of assets. In a very small holding period interval  $\Delta H$ ,  $\Delta V$  of the assets can be sold into the market. The probability that the holding assets are being sold into the market in  $\Delta H$  is thus  $\Delta V/V$ . Clearly as  $\Delta H$  becomes smaller, so will the probably of unwinding of particular assets within the trading portfolio  $\Delta V/V$ . However, as  $\Delta H$  gets smaller, the statistical variation in the

unwinding rate of trading volume would turn out to be apparent and the determined unwinding probability per unit time would have higher statistical variations. As a result, the statistically averaged unwinding probability per unit time, in the limit of infinitely small  $\Delta H$ , comes close to a constant  $\mu$ ; that is, we can express

$$\mu \equiv \lim_{\Delta H \rightarrow 0} \left(\frac{\Delta V/V}{\Delta H}\right). \quad (27)$$

Indeed, each trading portfolio has its distinguishing unwinding constant  $\mu$ , which, for the above characterization, is the probability a particular trading volume unwinds in a unit time for an infinitesimal time period (i.e., holding horizon). The same concept can be applied to individual assets within the trading portfolio, or in other words we can generalize the case of trading volume of a multiple-asset portfolio to its constituent’s assets. In this sense, each trading asset within the large portfolio can have its own unwinding constant, namely,  $\mu_i$ . In fact, the smaller  $\mu$  is, the more slowly the trading volume can be sold to financial markets. Certainly, for stable multiple-asset portfolios, which is indeed a rare case in practical asset management norms,  $\mu = 0$ .

We can now consider a sample multiple-asset portfolio constituted of a considerable number of assets with unwinding constant  $\mu$ . With a sizable volume portfolio ( $V \gg 1$ ), we can apply continuous mathematics to define an intrinsically discrete process. Thus,  $V(H)$  can be understood as the average or expected trading volume (a continuous quantity) of all assets at time  $H$ . Therefore, the probability that holding assets are being sold (or unwound) in an interval  $dH$  is  $\mu dH$ , and the expected number of declines (diminishes) in the trading volume that happen in  $dH$  at time  $H$  is  $\mu dH V(H)$ . In essence, this must be equivalent to the decline,  $dH$ , in the number of multiple assets in the sample portfolio (i.e., which is also equal to the decrease in the number of unsold assets in time  $dH$ ); that is,

$$-dV = \mu V(H) dH \quad (28)$$

or

$$\frac{dV(H)}{dH} = -\mu V(H). \quad (29)$$

This differential equation can be integrated to obtain the exponential variation with time formula, which governs the behavior of a process characterized by a constant rate of change, as follows:

Dividing by  $V(H)$ , we may integrate (29) from time zero to time  $H$  to obtain

$$\int_{V(0)}^{V(H)} \frac{dV(H)}{V(H)} = -\mu \int_0^H dH, \quad (30)$$

where  $V(0) = V_0$  is the initial trading volume of multiple assets at the launching of the trading process at  $t = 0$ . Noting that  $dV(H)/V(H) = d \ln(V(H))$ , (30) becomes

$$\ln[V(H)/V(0)] = -\mu H. \quad (31)$$

The characteristic exponential rate of declining of a multiple-asset portfolio trading volume is yielded.

$$V(H) = V_0 e^{-\mu H}. \quad (32)$$

This dynamic process, which is governed by exponential decline of portfolio holding assets, has a notable characteristic. The necessary time it takes for the multiple-asset portfolio to diminish to one-half the original volume,  $H_{1/2}$ , is a constant termed half-life. In other words, the half-life is a more intuitive measure of the time during which the trading activity of unwinding of assets falls by a factor of two. From (32), we can get

$$\begin{aligned} V(H_{1/2}) &\equiv \frac{V_0}{2} \\ &= V_0 e^{-\mu H_{1/2}}. \end{aligned} \quad (33)$$

Solving for  $H_{1/2}$  yields

$$H_{1/2} = \frac{\ln 2}{\mu} \cong \frac{0.693}{\mu}. \quad (34)$$

It is essential to note that the half-life is independent from the holding-horizon time  $H$ . Therefore, after  $n$  half-lives, the original trading volume has reduced by a multiplicative parameter of  $1/2^n$ ; that is,

$$V(nH_{1/2}) = \frac{1}{2^n} V_0. \quad (35)$$

The number of half-lives  $n$  required for any given multiple-asset portfolio to diminish to a fraction  $\omega$  of its original volume is obtained as

$$\omega \equiv \frac{V(nH_{1/2})}{V_0} = \frac{1}{2^n}. \quad (36)$$

Upon solving for  $n$ , it gives

$$n = -\frac{\ln \omega}{\ln 2} \cong -1.44 \ln \omega. \quad (37)$$

On the other hand, the exponential decline of portfolio holding assets of (32) could be stated by means of half-life in this way:

$$V(H) = V_0 \left(\frac{1}{2}\right)^{H/H_{1/2}}. \quad (38)$$

From the exponential decline of portfolio holding assets, we can define some suitable probabilities and averages. If we start by having a portfolio trading volume of  $V_0$  at  $t=0$ , we can expect to have  $V_0 e^{-\mu H}$  trading assets after a period of time  $H$ . Accordingly, the probability  $\hat{P}$  that the holding assets do not diminish in value (i.e., are not being sold as yet) in a time horizon  $H$  can be deduced as

$$\begin{aligned} \hat{P}(H) &= \frac{V(H)}{V(0)} \\ &= e^{-\mu H}. \end{aligned} \quad (39)$$

The probability  $P$  that trading assets do diminish (i.e., are being unwound or sold) in a time interval  $H$  is

$$\begin{aligned} P(H) &= 1 - \hat{P}(H) \\ &= 1 - e^{-\mu H}. \end{aligned} \quad (40)$$

As the time interval turns out to be small, that is,  $H \rightarrow \Delta H \ll 1$ , we can observe that

$$\begin{aligned} P(\Delta H) &= 1 - e^{-\mu \Delta H} \\ &= 1 - \left[ 1 - \mu \Delta H + \left(\frac{1}{2}\right)(\mu \Delta H)^2 - \left(\frac{1}{6}\right)(\mu \Delta H)^3 + \dots \right], \\ &\cong \mu \Delta H. \end{aligned} \quad (41)$$

This approximate solution is in line  $t$  with our former clarification of the unwinding constant  $\mu$  as being the decline probability per infinitesimal unwinding time horizon.

Given the above outcomes, we are now able to get the probability distribution function for when a trading volume declines in value. Explicitly, let  $p(H)dH$  be the probability that a trading volume that exists at  $t=0$  declines in value in the time period between  $H$  and  $H+dH$ . Evidently,

$$\begin{aligned} p(H)dH &= \{\text{Prob} \cdot \text{it does not decline in value}(0, H)\} \\ &\quad \times \{\text{Prob} \cdot \text{it declines in value in the next } dH \text{ time interval}\} \\ &= \{\hat{P}(H)\} \{P(H)\} \\ &= \{e^{-\mu H}\} \{\mu dH\} \\ &= \mu e^{-\mu H} dH. \end{aligned} \quad (42)$$

The same results of (42) can be obtained if we consider a sample multiple-asset portfolio with an initial volume of  $V_0$  at time  $t=0$ . In view of (32), there will be  $V_0 e^{-\mu H}$  trading volume remaining after  $H$  time interval. The fraction of the original volume which has not declined in value is therefore  $e^{-\mu H}$ . This fraction can also be viewed as the probability that the portfolio trading volume will not decline in value in the time interval from  $t=0$  to  $t=H$ . Now let  $p(H)dH$  be the probability that the trading volume declines in value in the time  $dH$  between  $H$  and  $H+dH$ . This is evidently equal to the probability that the trading volume has not declined in value up to time  $H$  times the probability that it does in fact decline in value in the additional time  $dH$ . It follows therefore that  $p(H)dH = e^{-\mu H} \times \mu dH = \mu e^{-\mu H} dH$ , which is the same as (42).

If (42) is integrated over all  $H$ , it is obtained that

$$\begin{aligned} \int_0^{\infty} p(H)dH &= \mu \int_0^{\infty} e^{-\mu H} dH \\ &= 1. \end{aligned} \quad (43)$$

This shows that the probability that a particular trading volume eventually declines in value (i.e., unwinds throughout the holding horizon  $H$ ) is equal to unity, as would be expected.

In a large sample multiple-asset portfolio, trading assets can be sold (i.e., always unwound). From (32), we see that a large time period (probably an infinite time) is needed to unwind all multiple assets within the portfolio. However, as time escalates, less trading assets can be sold into the financial markets. In fact, we can calculate the mean lifetime

( $\bar{H}$ ) for a multiple-asset portfolio to unwind its assets throughout the closeout period ( $H$ ) by using the decline probability distribution  $p(H)dH$  of (42). The average or mean lifetime can now be determined by finding the average value of  $H$  over the probability distribution  $p(H)$ . Denoting the mean lifetime by  $\bar{H}$ ,

$$\begin{aligned}\bar{H} &= \int_0^{\infty} H p(H) dH = \int_0^{\infty} H \mu e^{-\mu H} dH \\ &= \frac{1}{\mu}.\end{aligned}\quad (44)$$

Moreover, the mean lifetime of (44) can be obtained by defining  $\bar{H}$  as the average time that a particular trading volume is likely to survive before it is being sold into the market. The trading volume that survives to time  $H$  is just  $V(H)$ , and the volume that declines in value between  $H$  and  $H + dH$  is  $|dV/dH|dH$ . The mean lifetime is then

$$\bar{H} = \frac{\int_0^{\infty} H |dV/dH| dH}{\int_0^{\infty} |dV/dH| dH}, \quad (45)$$

where the denominator gives the total number of declines in trading volume. Evaluating the integrals of (45) gives  $\bar{H} = 1/\mu$ . Thus, the mean lifetime is the inverse of the unwinding constant.

In view of (34), the mean lifetime can also be written as

$$\begin{aligned}\bar{H} &= \frac{H_{1/2}}{0.693} \\ &= 1.44H_{1/2}.\end{aligned}\quad (46)$$

This confirms (26) and finalizes the proof of Corollary 2.  $\square$

### 3. Expansion to Multiple-Asset Portfolios

While in the previous section we looked at the dynamic model of trading volume from the perspective of a single multiple-asset portfolio, we can now expand and generalize differential (2) to multiple-asset portfolios, as well as, for financial holding entities, with different subsidiary firms and multiple agents, by considering different trading volumes and closeout horizons for all multiple-asset portfolios, as follows:

$$\begin{aligned}\sum_{i=1}^k \frac{dV_i(H_i)}{dH_i} &= \sum_{i=1}^k -\mu_i V_i(H_i) + V_{N_i}(H_i); \\ \forall i &= 1, 2, \dots, k.\end{aligned}\quad (47)$$

The solution of the differential equation for each trading asset within the multiple-asset portfolio of (47) can be obtained via (16) to yield

$$V_i(H_i) = V_{0_i} e^{-\mu_i H_i} + \left( \frac{V_{N_i}}{\mu_i} \right) (1 - e^{-\mu_i H_i}). \quad (48)$$

Furthermore, for the exceptional case when  $V_{0_i} = 0$  at  $t_i = 0$  (i.e., at the initiation of the trading process), (48) is restricted to

$$V_i(H_i) = \left( \frac{V_{N_i}}{\mu_i} \right) (1 - e^{-\mu_i H_i}). \quad (49)$$

Likewise, for the special case in which there is not any buildup of new volume of some assets (i.e.,  $V_{N_i} = 0$ ), the solution of the above differential equation can be reduced to yield

$$V_i(H_i) = V_{0_i} e^{-\mu_i H_i}. \quad (50)$$

Therefore, we can now define the variation in the total portfolio trading volume ( $V$ ) throughout the closeout period ( $H$ ) as

$$\begin{aligned}V(H) &= \sum_{i=1}^k V_i(H_i) \\ &= \sum_{i=1}^k \left[ V_{0_i} e^{-\mu_i H_i} + \left( \frac{V_{N_i}}{\mu_i} \right) (1 - e^{-\mu_i H_i}) \right];\end{aligned}\quad (51)$$

$$\forall i = 1, 2, \dots, k.$$

The above equation can be reduced for the special case in which there is not any addition of new volumes for all assets during the unwinding horizon (i.e.,  $\sum_{i=1}^k V_{N_i} = 0$ ;  $\forall i = 1, 2, \dots, k$ ) to yield

$$\begin{aligned}V(H) &= \sum_{i=1}^k V_i(H_i) \\ &= \sum_{i=1}^k V_{0_i} e^{-\mu_i H_i}; \\ \forall i &= 1, 2, \dots, k.\end{aligned}\quad (52)$$

Finally, in order to solve for the unwinding constant for multiple-asset portfolios, we can determine  $\mu_i$  for each trading asset via a trial-and-error process along the individual closeout horizons of all assets. For instance, if traders can determine  $H_i$  (i.e., the necessary number of trading days to completely unwind any particular asset),  $V_i(H_i)$ ,  $V_{N_i}$ ,  $V_{0_i}$  then one can solve for the unwinding constants ( $\mu_i$ ;  $\forall i = 1, 2, \dots, k$ ) for the different multiple assets under consideration in a given portfolio as follows.

In real-world practices, the overnight trading volume of multiple assets is appraised as the average volume over certain time horizon, usually a month of trading operations. In typical operations, the overnight trading volume of multiple assets can be viewed as the average overnight volume that can be unwound during unfavorable market conditions. On the contrary, the trading volume during a crisis period can be roughly approximated as the average daily trading volume minus a few standard deviations. While this alternate tactic is relatively unpretentious, it is still fairly unbiased approach. Furthermore, it is relatively

straightforward to assemble the needed datasets to implement the required unwinding events.

In fact, the liquidation days  $H_i$  required to completely unwind any particular asset are associated with the selection of the unwinding threshold. Nevertheless, the magnitude of this threshold is expected to alter under stressed ecosystems. In reality, the selection of the unwinding period (i.e., the closeout horizon) can be projected from the overall trading volume and the overnight volume that can be unwound into the financial markets without substantially interrupting

multiple-asset values. To that end, in real-world applications, the absolute values of the different closeout periods are generally estimated as

$$H_i = \left\lceil \frac{\text{Total Trading Position Size of Asset}_i}{\text{Daily Trading Volume of Asset}_i} \right\rceil, \quad (53)$$

s.t.  $H_i \geq 1.0$ .

Equation (53) can also be written as

$$H_i = \left\lceil \frac{\text{Total Number of Asset}_i \text{ in Trading Portfolio} \times \text{Price of Asset}_i}{\text{Daily Number of Asset}_i \text{ to Unwind from Trading Portfolio} \times \text{Price of Asset}_i} \right\rceil, \quad (54)$$

s.t.  $H_i \geq 1.0$ .

Accordingly, if for instance we determine that it is necessary to have  $H_i = 4.0$  days to unwind  $V_i$  (4.0) of volume of any particular asset  $i$  and at the same time  $V_{N_i}$  and  $V_0$  are known data at that specific time horizon, then one can solve for  $\mu_i$  by a trial-and-error process or by using a numerical procedure such as the iterative process of the Newton-Raphson method, yielding (The Newton-Raphson (NR) procedure is an iteration process. This NR method involves the process of iterating (or repeating) technique in which repetition of a sequence of operations yields outcomes uninterruptedly closer to a preferred outcome. To that end, Newton-Raphson method is intended to resolve an equation of the kind  $f(x) = 0$ . It begins with an estimation of the solution:  $x = x_0$ . It then yields sequentially improved guesses of the solution:  $x = x_1, x = x_2, x = x_3, \dots$  using the formula  $x_{i+1} = x_i - f(x_i)/f'(x_i)$ . Typically,  $x_2$  is very close to the factual answer.)

$$V_i(4.0) = V_0 e^{-\mu_i 4.0} + \left( \frac{V_{N_i}}{\mu_i} \right) (1 - e^{-\mu_i 4.0}). \quad (55)$$

Similarly, for the special case in which there is not any new addition of volume of this particular asset (i.e.,  $V_{N_i} = 0$ ), (55) can be shortened to

$$V_i(4.0) = V_0 e^{-\mu_i 4.0}. \quad (56)$$

Thus, once the various unwinding (or decay) constants (i.e.,  $\mu_i; \forall i = 1, 2, \dots, k$ ) for the different multiple assets under consideration are computed, we can now apply the statistics of the decay constants in (51) to solve for the various characteristics of the total trading volumes (i.e.,  $V(H) = \sum_{i=1}^k V_i(H_i); \forall i = 1, 2, \dots, k$ ) by using different closeout periods (i.e.,  $H_i; \forall i = 1, 2, \dots, k$ ).

#### 4. Portfolio Selection and Risk Management Practices with a Reinforcement Machine Learning Process

In this backdrop, we present one potential reinforcement machine learning algorithm for the implementation of the

proposed econophysics techniques to risk assessment and multiple-asset portfolio selection practices, detailed as follows.

In line with Al Janabi et al. [7] and Al Janabi [12], we can define the following multiple-asset portfolio selection and risk assessment process:

Stage 1: liquidity-adjusted value-at-risk (LVaR) model and multiple-asset portfolio algorithm:

- (1) Formally, the Value-at-Risk (VaR) for any individual trading asset  $i$  can be computed in this way:

$$VaR_i = |(E(R_i) - \Phi * \sigma_i)(Asset_i * Fx_i)|, \quad (57)$$

where  $E(R_i)$  is the expected return,  $\Phi$  is the confidence level,  $\sigma_i$  is the conditional risk factor (volatility),  $Asset_i$  denotes the mark-to-market value, and  $Fx_i$  is the foreign exchange unit for any trading asset.

- (2) To get the global VaR of a multiple-asset portfolio, the correlations parameters  $[\rho_{i,j}]$  among the diverse assets are considered and the computational process can be presented in terms of matrices; thus,

$$VaR_p = \sqrt{\sum_{i=1}^k \sum_{j=1}^k VaR_i VaR_j \rho_{i,j}} = \sqrt{[VaR]^T [\rho] [VaR]}. \quad (58)$$

It is feasible that the risk engine and objective function can include the special impacts of non-linearity and nonnormality of assets returns in the optimization process. This can be achieved by employing Kendall's tau algorithm (or any other copula-based modeling methods) as a yardstick to evaluate the degree of nonlinear dependence and to be used instead of the linear Pearson's correlation factors. Similarly, Cornish-Fisher expansion as a yardstick of nonnormality can simply be tailored to solve the problem of nonnormality in multiple-asset returns.

- (3) As in the work of Al Janabi et al. [6], the LVaR algorithm for the computation of multiple-asset portfolios for any closeout period  $H_i$  can be expressed as

$$LVaR_{i_{adj}} = VaR_i \left( \sqrt{\frac{(2H_i + 1)(H_i + 1)}{6H_i}} \right), \quad (59)$$

where the closeout period can be estimated using (53) or (54) above. In order to compute the LVaR for the entire multiple-asset portfolio (i.e.,  $LVaR_{P_{adj}}$ ), the next model, which is an extension of (58), can be used:

$$\begin{aligned} LVaR_{P_{adj}} &= \sqrt{\sum_{i=1}^k \sum_{j=1}^k LVaR_{i_{adj}} LVaR_{j_{adj}} \rho_{i,j}} \\ &= \sqrt{[LVaR_{adj}]^T [\rho] [LVaR_{adj}]}. \end{aligned} \quad (60)$$

- (4) The simulation experiments for this first stage can be conducted as follows:
- (i) From the obtained multiple-asset datasets, the distribution parameters are estimated (i.e., the vector of expected returns and variance/covariance matrices or the association matrices of any other dependence measures)
  - (ii) Next, these parameters are used to produce samples of independent identically distributed random vectors from multivariate elliptical distributions or any other selected distributions
  - (iii) The forecasting returns distribution is obtained using time series modeling techniques
  - (iv) Each trading asset's expected return and conditional risk parameters are computed and sample of  $k$  observations is generated

Stage 2: portfolio optimization algorithm and financial and operational constraints:

- (1) The portfolio optimization problem and the procedures of solving the proposed modeling algorithm are formulated as follows:

$$\begin{aligned} \text{Min: } LVaR_{P_{adj}} &= \sqrt{\sum_{i=1}^k \sum_{j=1}^k LVaR_{i_{adj}} LVaR_{j_{adj}} \rho_{i,j}} \\ &= \sqrt{[LVaR_{adj}]^T [\rho] [LVaR_{adj}]}. \end{aligned} \quad (61)$$

- (2) The risk objective function of (61) could be minimized dependent on complying with the following operational and financial constraints:

$$\sum_{i=1}^k E(R_i)x_i = E(R_p); \quad l_i \leq x_i \leq u_i; \quad i = 1, 2, \dots, k, \quad (62)$$

$$\sum_{i=1}^k x_i = 1.0; \quad l_i \leq x_i \leq u_i; \quad i = 1, 2, \dots, k, \quad (63)$$

$$\sum_{i=1}^k V_i(H_i) = V(H) \quad i = 1, 2, \dots, k, \quad (64)$$

$$[LRF] \geq 1.0; \quad \forall i = 1, 2, \dots, k, \quad (65)$$

where  $LRF$  is the liquidation risk factor that is expressed for any particular asset  $i$  as

$$LRF_i = \left[ \sqrt{\frac{(2H_i + 1)(H_i + 1)}{6H_i}} \right] \geq 1.0; \quad i = 1, 2, \dots, k. \quad (66)$$

In (62)–(66) above,  $E(R_p)$  and  $V(H)$  symbolize the target portfolio expected return and the total volume of the multiple-asset portfolio, respectively, and  $x_i$  is the fraction (i.e., the weights) for every trading asset. The values  $l_i$  and  $u_i$ , for  $i = 1, 2, \dots, k$  in (62)–(63), stand for the lower and upper limits for the portfolio weights  $x_i$ . Moreover,  $[LRF]$  denotes a  $(k \times 1)$  vector of the closeout periods for each trading asset of the multiple-asset portfolio. Therefore, as indicated earlier, the various unwinding constants (i.e.,  $\mu_i; \forall i = 1, 2, \dots, k$ ) for the different multiple assets under consideration can be computed using the procedure discussed in (51)–(56). Next, we can use the statistics of the decay constants in (51) to solve for the various characteristics of the total trading volumes (i.e.,  $V(H) = \sum_{i=1}^k V_i(H_i); \forall i = 1, 2, \dots, k$ ) by applying different closeout periods (i.e.,  $H_i; \forall i = 1, 2, \dots, k$ ). Thereafter, the obtained individual trading volumes for each of the multiple assets (i.e.,  $V_i(H_i); \forall i = 1, 2, \dots, k$ ) can be used in an iteration process to recompute the specific closeout periods,  $H_i$ , using (53) or (54). Finally, the obtained total trading volume (i.e.,  $V(H)$ ) can be integrated into the optimization process as a constraint in line with (64).

- (3) The simulation experiments for this second stage can be implemented as follows:

- (i) For each modeling technique, the related optimization problems are solved to structure the different efficient frontiers of the multiple-asset portfolios and the related asset allocation is determined

- (ii) Out-of-sample features of the attained portfolios are computed applying the factual factors of the underlying distribution
- (iii) The above two steps are reiterated several times to calculate more steady assessment of out-of-sample traits  $s$  of the chosen portfolios and structure the corresponding efficient frontiers

Stage 3: construction of efficient frontiers, comparison, and validation with the mean-variance method:

- (1) Solve the modeling algorithm in (61)–(66) by using a quadratic programming (QP) technique to obtain the best allocation weights of each trading asset and then construct the equivalent efficient frontiers for multiple-asset portfolios.
- (2) In this final stage, construct different efficient frontiers of the LVaR proposed algorithm versus the traditional mean-variance method [24], using (53)–(66).
- (3) Validate and compare the output results of the multiple-asset portfolio(s) obtained in Stage (2) with the optimum portfolio(s) defined in Stage (1).
- (4) Repeat the optimization process until another convergence to meaningful portfolio(s) is accomplished. These portfolios should comply with the optimization parameters and budget restrictions defined above.
- (5) At this final phase of the operational method validation process, new meaningful portfolio(s) with coherent asset-allocations, which conform to the constraints' settings stated in Stage (2), are satisfied consistently.
- (6) Finally, repeat the process to compute more steady valuation of the characteristics of the out-of-sample designated portfolios.

Indeed, this extension to multiple-asset portfolios, as well as for financial holding entities with different subsidiary firms and multiple agents, can resolve some of the main drawbacks of the incoherence of traditional VaR models due to its lack of subadditivity [23]. In fact, the conventional VaR measure is not coherent because it does not comply with the subadditivity restriction, which is a clear requirement for any coherent risk measure; otherwise, there would be no risk advantage in combining uncorrelated multiple assets into trading portfolios. Artzner et al. [23] described the following set of rational criteria that a measure of risk,  $\Omega(X)$ , where  $X$  is a set of outcomes, should comply with the following requirements: Subadditivity can be defined to satisfy this condition:  $\Omega(X + Y) \leq \Omega(X) + \Omega(Y)$ . Thus, by adding two multiple-asset portfolios together, the overall risk cannot get any worse than combining the two risks independently because of diversification effects that reduce the total risk substantially. As such, the conventional VaR measure is not coherent, since it does not satisfy the subadditivity specification. For instance, if we have two multiple-asset portfolios  $X$  and  $Y$ , then this diversification benefit can be

defined as  $\Omega(X) + \Omega(Y) - \Omega(X + Y)$ , which according to the subadditivity condition can only take nonnegative values. In fact, the nonexistence of subadditivity in a risk measure can be exploited to structure a regulatory arbitrage since a financial entity can create different subsidiary firms, in an opposite procedure of the above example two multiple-asset portfolios, to avert and/or save regulatory capital cushion. Thus, with a coherent measure of risk (e.g., Expected Shortfall (ES) risk measure), explicitly due to its subadditivity, one can easily incorporate risks of separate multiple-asset portfolios to obtain moderate assessments of the aggregate risk.

In this backdrop and to capitalize on its usefulness as a risk management and portfolio selection tool, we have structured the portfolio management modeling algorithms such that the suggested risk engine and robust optimization modeling techniques can be used for computer programming and machine learning objectives, machine learning for the policymaking process, and reinforcement machine learning techniques for the IoT data analytics. To that end, the graphical flowchart in Figure 1 demonstrates a succinct framework of the different computational steps of the overall market and liquidity risk modeling algorithms and their association for computer programming and reinforcement machine learning objectives.

The above robust modeling techniques and algorithms can be applied to reinforcement machine learning processes for portfolio selection and risk management to determine the most suitable risk-return profiles and assets allocation. Given the iterative nature of the above novel modeling algorithms, it can be applied to reinforcement machine learning processes for portfolio optimization and risk management conditional on using credible operational and financial constraints. Moreover, it can be of interest to machine learning for the policymaking process, reinforcement machine learning techniques for the Internet of Things (IoT) data analytics, financial engineering, FinTech, and within big data ecosystems.

As an extension to this work, we aspire in another research study to use the proposed modeling algorithms to the case of multiple asset portfolios and to examine the impact of adverse prices on the global market and illiquidity risk profiles. To that end, the following natural step in this research is to choose certain emerging markets or a particular region and strive to apply the proposed modeling techniques and algorithms to specific multiple-asset portfolios and then to compute the effect of market and illiquidity risks on the global potential risk exposure. In addition, it is quite feasible to apply the novel econophysics modeling techniques and algorithms to the case of selected developed, emerging, and commodity markets. In this case, the proposed robust reinforcement machine learning processes and modeling algorithms can be applied to multiple securities trading and/or asset management portfolios to examine the effect of unfavorable price impact on the total market and liquidity risk potential exposures. Our aim would be to demonstrate different experiments and to test empirically our proposed approach by simulations using real market datasets and to

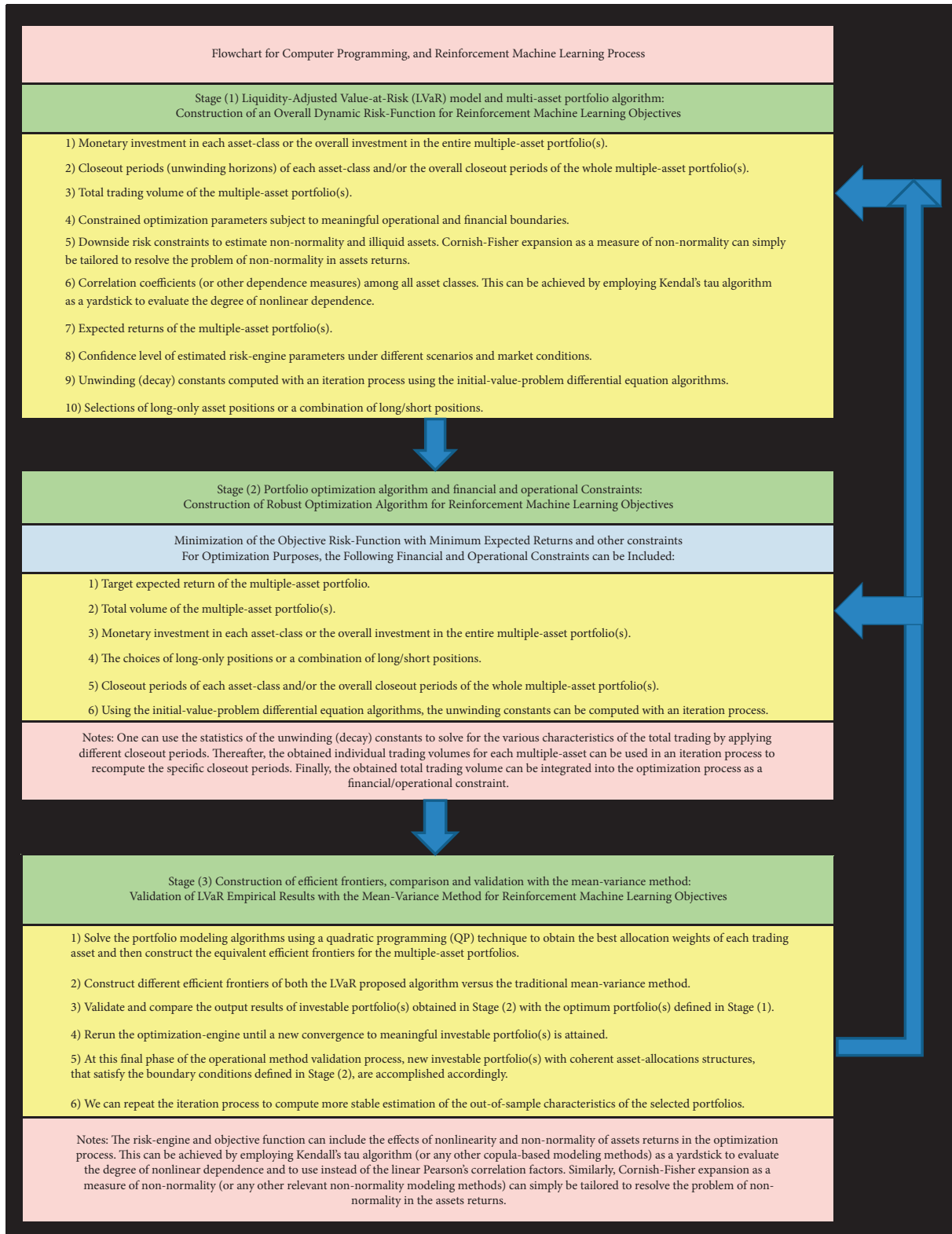


FIGURE 1: A graphical flowchart of the operational stages of the proposed modeling algorithm.

examine the impact of adverse prices on the global market/ and illiquidity risk profiles by implementing realistic operational and financial constraints.

The flowchart in Figure 1 represents a summarized view of the three stages of the proposed modeling algorithms and the connections among the different phases. This flowchart



can be very useful for computer programming, comprehending the indispensable input factors for the risk-engine, constrained optimization procedure, and reinforcement machine learning. The figure is designed by the author.

## 5. Conclusion and Future Directions

Liquidity as the ease of trading of assets has recently acquired a great deal of attention in the academic literature and in market practices. Illiquidity risk grows with the size of the holding positions and refers to the inability to unwind trading assets at the prevailing market conditions without incurring additional costs. Illiquidity happens over some short term but disappears over a longer horizon. However, unlike other risk factors, liquidity risk cannot be diversified or hedged. Furthermore, the liquidity risk depends on several factors and causes and, thus, there are not any standard methods or techniques for its estimation and control.

In this paper, after a concise review of certain contemporary literature on liquidity risk, we propose a novel econophysics mathematical technique and robust algorithms for the modeling of trading volumes and illiquidity risk during the closeout period for multiple-asset portfolios, as well as for financial holding entities with different subsidiary firms and multiple agents.

Liquidity risk should be quantified in a dynamic setting, accounting directly or indirectly for the influence of the multiple market risk factors, including the term structure of the time-varying volatility. In this paper and in contrast to most of the previous works on market illiquidity, we put in perspective the analytical components to modeling the impact of liquidity risk with the use of daily trading volumes of multiple-asset portfolios.

The contributions of this paper to the academic literature, in this specific field of quantitative methods for financial markets applications, are severalfold. As such, this paper is the first attempt, to the best of my knowledge, to develop a novel econophysics modeling technique and robust algorithms for the estimation of trading volumes and illiquidity risk during the closeout period and within the context of multiple-asset portfolios, as well as for financial holding entities with different subsidiary firms and multiple agents, using initial-value-problem differential equations algorithms. Furthermore, this paper provides some new important parameters, which are the first of their kind to the best of my knowledge, for the assessment of the trading volumes of multiple-asset portfolios during the closeout period, where the mathematical proofs for each theorem and corollary are provided. Based on the new developed econophysics theory, this paper presents for the first time a closed-form solution for key parameters for the estimation of trading volumes and liquidity risk, such as the unwinding constant, half-life, and mean lifetime, and discusses how these novel parameters can be estimated and incorporated into the recommended modeling techniques. Finally, in this backdrop, the robust reinforcement machine learning modeling techniques and algorithms are promising and interesting in terms of theory as well as for possible real-

world uses for multiple-asset portfolios and can have a variety of applications in financial markets and institutions, predominantly in light of the 2007–2009 global financial crunch. In addition, the proposed novel techniques and risk computation algorithms can contribute to improving risk management and portfolio optimization and selection processes in emerging, developed, and commodity markets, especially in the wake of the 2007–2009 financial crunch. Furthermore, the proposed modeling processes could have fundamental uses and applications for expert systems in finance, financial technology (FinTech), machine learning for the policymaking process, Internet of Things (IoT), and within big data environments.

Several venues are still open for future research in this specific econophysics field. To that end, for further directions on trading volume and liquidity risk, we recommend the following:

- (1) The constant of proportionality,  $\mu$ , that we have denoted earlier as the “*unwinding constant*” and defined as being the decline (or the decay) probability per infinitesimal unwinding time horizon can be possibly expanded to multiple unwinding constants using decline or decay chains by competing processes. The trading volumes of some multiple assets will decline by more than one operational process (or mode) and the market impact of trading on multiple-asset prices may well not be one time but possibly will cause second-phase impacts. As a result, every decay form (or mode) is differentiated by its specific unwinding constant  $\mu_i$ . To obtain the relevant unwinding constant when the decline process has  $n$  participating decay modes, we need to rewrite the differential equation in slightly different form by expressing the unwinding constant of the  $i$ th mode by  $\mu_i$  and solving for the overall unwinding constant, namely,  $\mu = \sum_{i=1}^n \mu_i$ . Nevertheless, for general decay chain processes, the structure of the differential equations can become rather complex and would require the use of the so-called Bateman equation(s) with the set of initial conditions to find a general solution for the coefficients using the Laplace transform. In a similar fashion, we can now determine the half-life and mean lifetime during each decay mode and then find the effective or overall half-life and mean lifetime when the decline process has  $n$  participating decay modes.
- (2) A general solution to the above posed issue can be given by the Bateman equation(s) in which the activity of the  $i$ th mode of the chain is given in terms of the unwinding constants of all preceding modes. The Bateman equations can be derived using the Laplace transform. Thus, the system of differential equations for all decline or decay modes may be transformed to a system of linear equations by taking the Laplace transform. Next, using the notion that the Laplace transform of a derivative is achieved by integration by parts, the Laplace transform of the first derivatives can be obtained. Now, these equations may be solved

successively, and a solution can be obtained for the specific coefficients using the inverse transform and that will yield the Bateman equation(s). These simple properties of the Laplace transform make it a very convenient tool for solving systems of first-order linear differential equations, such as the differential equations posed in this paper. They allow these differential equations to be treated as if they were systems of simple transformed linear equations without derivatives.

- (3) Although our proposed robust modeling techniques clearly reflect liquidity risk with the use of trading volumes of multiple-asset portfolios, we did not explore the time-varying characteristics of market liquidity and the dynamic relationships between trading operations and the movements in assets prices with respect to market's spreads. A potential next step would be to examine the dynamics of market impact by employing time-series techniques. Likewise, the market impact of trading on multiple-asset prices might not be a unique event; rather it could initiate second phase outcomes. Moreover, since the motivating strengths on the back of the tick-by-tick markets price movements are related to not only trading actions but also the influx of fresh information and statistics, recognition of these factors would be crucial to comprehending intraday price changes in a dynamic framework.
- (4) One of the key issues for liquidity risk measures is the handling of delay risk since the dynamics of delay and its relation to the price dynamics are yet indistinct in times of stressed market conditions and crises. The incorporation of delay risk and how to measure and forecast delay are still unresolved research topics and, thus, further intuitions into when and under which conditions delay arises can aid to evolve this line of reasoning.
- (5) As discussed earlier, the risk of illiquidity should be quantified in a dynamic framework. One alternate measure of liquidation risk and cost can be accomplished with the application of a piecewise linear function that models trading volume discounting, as the larger the trading position size, the lower the liquidation price. For this purpose, Laplace transform, which is a more generalized transform, as well as Fourier transform, can be used to solve piecewise linear functions. In fact, the Fourier transform, which is a subset of Laplace transform, is the extension of the Fourier series to nonperiodic signals (e.g., the Fourier transform of triangle and rectangular pulse functions). To that end, the Fourier transform is used largely for steady-state signal analysis, while Laplace transform is used for transient signal analysis. Therefore, the Laplace transform is useful at looking for the response to pulses, step-functions, and delta-functions, while the Fourier transform is beneficial for continuous signals. However, it is important to emphasize that one

of the main drawbacks of the Fourier transform is that it can be clearly defined merely for stable systems, whereas Laplace transform can be defined for both stable and unstable systems. Nevertheless, it is possible to convert Laplace transform to Fourier transform and vice versa.

- (6) In a similar fashion to the piecewise linear function discussed above, it is also possible to model liquidation risk and cost with the application of pulse function (i.e., the pulse-transfer function), which are commonly used in control systems and signal processes via the Laplace transform, where the Z-transform (i.e., the discrete Laplace transform) is the most suitable for the analytical study of the linear pulse control systems. As a result, the pulse control system in which the control is accomplished by pulses (i.e., signals of short-durations) produced at preset times can be explained as a system of finite differences equations.

### Data Availability

Data sharing is not applicable to this article as no datasets were generated or analyzed during the current study and the article describes entirely theoretical research.

### Additional Points

A novel modeling technique for forecasting trading volumes is proposed. The modeling techniques are based on initial-value-problem differential equations. We develop algorithms for optimizing multiple-asset portfolios with liquidity constraints. We propose operational stages for computer programming and reinforcement machine learning.

### Conflicts of Interest

The author declares that there are no conflicts of interest.

### References

- [1] P. C. Jain and G.-H. Joh, "The dependence between hourly prices and trading volume," *Journal of Financial and Quantitative Analysis*, vol. 23, no. 3, pp. 269–283, 1988.
- [2] G.-M. Chen, M. Firth, and O. M. Rui, "The dynamic relation between stock returns, trading volume, and volatility," *The Financial Review*, vol. 36, no. 3, pp. 153–174, 2001.
- [3] J.-C. Hung, J.-B. Su, M. C. Chang, and Y.-H. Wang, "The impact of liquidity on portfolio value-at-risk forecasts," *Applied Economics*, vol. 52, no. 3, pp. 242–259, 2020.
- [4] G. Morelli, "Liquidity drops," *Annals of Operations Research*, vol. 299, no. 1, 2019.
- [5] E. Allaj, "Risk measuring under liquidity risk," *Applied Mathematical Finance*, vol. 24, no. 3, pp. 246–279, 2017.
- [6] M. A. M. Al Janabi, J. Arreola Hernandez, T. Berger, and D. K. Nguyen, "Multivariate dependence and portfolio optimization algorithms under illiquid market scenarios," *European Journal of Operational Research*, vol. 259, no. 3, pp. 1121–1131, 2017.
- [7] M. A. M. Al Janabi, R. Ferrer, and S. J. H. Shahzad, "Liquidity-adjusted value-at-risk optimization of a multi-asset portfolio

- using a vine copula approach,” *Physica A: Statistical Mechanics and Its Applications*, vol. 536, Article ID 122579, 2019.
- [8] G. N. F. Weiß and H. Supper, “Forecasting liquidity-adjusted intraday Value-at-Risk with vine copulas,” *Journal of Banking & Finance*, vol. 37, no. 9, pp. 3334–3350, 2013.
- [9] Á. Cartea and S. Jaimungal, “Optimal execution with limit and market orders,” *Quantitative Finance*, vol. 15, no. 8, pp. 1279–1291, 2015.
- [10] C. B. Kalayci, O. Ertenlice, and M. A. Akbay, “A comprehensive review of deterministic models and applications for mean-variance portfolio optimization,” *Expert Systems with Applications*, vol. 125, pp. 345–368, 2019.
- [11] G.-Y. Ban, N. El Karoui, and A. E. B. Lim, “Machine learning and portfolio optimization,” *Management Science*, vol. 64, no. 3, pp. 1136–1154, 2018.
- [12] M. A. M. A. Janabi, “Is optimum always optimal? A revisit of the mean-variance method under nonlinear measures of dependence and non-normal liquidity constraints,” *Journal of Forecasting*, vol. 40, no. 3, pp. 387–415, 2021.
- [13] F. D. Paiva, R. T. N. Cardoso, G. P. Hanaoka, and W. M. Duarte, “Decision-making for financial trading: a fusion approach of machine learning and portfolio selection,” *Expert Systems with Applications*, vol. 115, pp. 635–655, 2019.
- [14] J. Wu, S. Guo, J. Li, and D. Zeng, “Big data meet green challenges: greening big data,” *IEEE Systems Journal*, vol. 10, no. 3, pp. 873–887, 2016.
- [15] J. Wu, S. Guo, H. Huang, W. Liu, and Y. Xiang, “Information and communications technologies for sustainable development goals: state-of-the-art, needs and perspectives,” *IEEE Communications Surveys & Tutorials*, vol. 20, no. 3, pp. 2389–2406, 2018.
- [16] R. Ruozi and P. Ferrari, “Liquidity risk management in banks: economic and regulatory issues,” *Springer Briefs in Finance*, Springer, Berlin, Germany, 2013.
- [17] A. Roch and H. M. Soner, “Resilient price impact of trading and the cost of illiquidity,” *International Journal of Theoretical and Applied Finance*, vol. 16, no. 6, pp. 1–27, 2013.
- [18] S. B. Walter Madoroba and J. W. Kruger, “Liquidity effects on value-at-risk limits: construction of a new VaR model,” *The Journal of Risk Model Validation*, vol. 8, no. 4, pp. 19–46, 2014.
- [19] A. Madhavan, M. Richardson, and M. Roomans, “Why do security prices change? A transaction-level analysis of nyse stocks,” *Review of Financial Studies*, vol. 10, no. 4, pp. 1035–1064, 1997.
- [20] D. Takahashi and S. Alexander, “Illiquid alternative asset fund modeling,” *Journal of Portfolio Management*, vol. 28, no. 2, pp. 90–100, 2002.
- [21] A. Meucci, “Managing diversification,” *Risk*, vol. 22, no. 5, pp. 74–79, 2009.
- [22] R. Almgren and N. Chriss, “Optimal execution of portfolio transactions,” *Journal of Risk*, vol. 3, no. 2, pp. 5–39, 2001.
- [23] P. Artzner, F. Delbaen, J.-M. Eber, and D. Heath, “Thinking coherently,” *Risk magazine*, vol. 10, no. 11, pp. 68–72, 1997.
- [24] H. Markowitz, *Portfolio selection: efficient diversification of investments*, John Wiley, New York, USA, 1959.

## Research Article

# A Combined Prediction Model for Hog Futures Prices Based on WOA-LightGBM-CEEMDAN

Xiang Wang <sup>1</sup>, Shen Gao,<sup>2</sup> Yibin Guo,<sup>1</sup> Shiyu Zhou,<sup>3</sup> Yonghui Duan,<sup>2</sup> and Daqing Wu<sup>4</sup>

<sup>1</sup>Department of Civil Engineering, Zhengzhou University of Aeronautics, No. 15, Wenyuan West Road, Zhengdong New District, Zhengzhou 450015, China

<sup>2</sup>Department of Civil Engineering, Henan University of Technology, No. 100, Lianhua Street, Gaoxin District, Zhengzhou 450001, China

<sup>3</sup>Department of Management, Shanghai University, No. 99 Shangda Road, Baoshan District, Shanghai 200444, China

<sup>4</sup>Department of Economics and Management, Shanghai Ocean University, No. 999, Huchenghuan Road, Pudong New District, Shanghai 201306, China

Correspondence should be addressed to Xiang Wang; [shanghaiwx1976@126.com](mailto:shanghaiwx1976@126.com)

Received 8 September 2021; Revised 14 January 2022; Accepted 3 February 2022; Published 27 February 2022

Academic Editor: Ning Cai

Copyright © 2022 Xiang Wang et al. This is an open access article distributed under the Creative Commons Attribution License, which permits unrestricted use, distribution, and reproduction in any medium, provided the original work is properly cited.

An integrated hog futures price forecasting model based on whale optimization algorithm (WOA), LightGBM, and Complete Ensemble Empirical Mode Decomposition with Adaptive Noise (CEEMDAN) is proposed to overcome the limitations of a single machine learning model with low prediction accuracy and insufficient model stability. The simulation process begins with a grey correlation analysis of the hog futures price index system in order to identify influencing factors; after that, the WOA-LightGBM model is developed, and the WOA algorithm is used to optimize the LightGBM model parameters; and, finally, the residual sequence is decomposed and corrected by using the CEEMDAN method to build a combined WOA-LightGBM-CEEMDAN model. Furthermore, it is used for comparison experiments to check the validity of the model by using data from CSI 300 stock index futures. Based on all experimental results, the proposed combined model shows the highest prediction accuracy, surpassing the comparative model. The model proposed in this study is accurate enough to meet the forecasting accuracy requirements and provides an effective method for forecasting future prices.

## 1. Introduction

China's futures market has grown rapidly in recent years. A commodity future is a contract in which a certain number of commodities will be delivered by an exchange at a future time. As a form of risky investment and risky return, futures trading is also a very important investment tool for investors. Meanwhile, the futures market can reasonably use and gather a vast amount of social idle capital, which is valuable to China's market economy. For both companies and investors, an accurate prediction of prices in the futures market is a key guide. Due to the fact that commodity futures are influenced by a variety of factors, which can cause large fluctuations in price, it is difficult to achieve accurate price

control. Therefore, the accurate prediction of futures prices has become a hot research topic.

In the research on price forecasting in futures markets, traditional econometric models are used along with machine learning models. Futures prices are used as time series in most econometric models, which employ statistical methods to make linear forecasts. Common methods include autoregressive integrated moving average (ARIMA) [1, 2] and generalized autoregressive conditional heteroscedasticity (GARCH) [3, 4]. In contrast, the prices in the futures market are often influenced by a variety of factors along with the characteristics of nonstationarity, nonlinearity, and high complexity, which can lead to large errors when only making linear forecast [5, 6].

By contrast with econometric models, machine learning models are effective in mining and retaining the valuable information in the data and in dealing with nonlinear data effectively [7]. Artificial neural network (ANN) [8, 9], support vector machine (SVM) [10, 11], long short-term memory (LSTM) [12], and ensemble learning models are some of the common models. Ensemble learning models can effectively combine the results of multiple base learners to achieve secondary learning of the problem with high generalizability. The ensemble learning model uses boosting to train the base learner by serial learning. This strategy reduces the prediction bias of the model and improves the algorithm's ability to fit. Zhang and Hamori [13] used extreme gradient boosting (XGBoost) as an experimental model for crude oil futures price forecasting, and the results showed that the XGBoost model was able to achieve an accuracy rate of 86%. Deng et al. [14] used XGBoost model to predict the price of apple futures, and bagging ensemble learning was used to further integrate and optimize the model in order to reduce overfitting. To predict the LME nickel settlement price, Gu et al. [5] employed the empirical wavelet transform (EWT) and gradient boosting decision tree (GBDT). Luo et al. [15] used genetic algorithm (GA) to optimize the parameters of their GBDT model and predict copper and soybean futures prices in China, which proved to be superior to BP neural network and SVM models. In spite of the above boosting algorithm's advantages, there are some problems; for example, the GBDT model takes too long to diagnose when processing the data of complex samples, resulting in low prediction efficiency [16]; the XGBoost model still traverses the data set during the node splitting process, increasing the computational burden. LightGBM is an improved version of the GBDT model using a unique leaf-wise growth strategy based on the maximum depth limit, which can reduce more errors and get better accuracy while using the same number of splits. While the histogram algorithm of the LightGBM can improve model running efficiency while reducing memory footprint, it has not been applied to the futures price forecasting problem as it has been used in several fields [17–19].

In order to further improve machine learning models' accuracy, most studies focus on the models themselves or data but ignore the valuable information hidden in the sequence of prediction residuals. The information from these hidden residual sequences can significantly enhance the final prediction [20]. Usually, residual series resulting from forecasting are a kind of time series with nonpure randomness and autocorrelation, and the decomposition-individual forecasting-ensemble method is a desirable way to handle such characteristics. The existing studies include many decomposition methods, including variational mode decomposition (VMD) [21, 22], wavelet transform (WT) [23], and empirical mode decomposition (EMD). Among them, the EMD method can decompose data into multiple intrinsic mode functions (IMF) according to the data characteristics, which has a better ability to decompose for nonlinear and nonsmooth data and can effectively extract the characteristics of the data at different frequency scales [24]. EMD, however, is prone to the phenomenon of modal

mixing during decomposition, which affects its decomposition performance. Wu [25] proposed ensemble empirical mode decomposition (EEMD) to improve the EMD, which can effectively solve the modal mixing problem by adding Gaussian white noise to the original signal, but there is still residual Gaussian white noise in the decomposed IMFs, resulting in incorrect reconstruction. To improve EEMD, Torres proposed the CEEMDAN method [26]. CEEMDAN adds adaptive white noise at each stage, which effectively overcomes EEMD's large reconstruction error. CEEMDAN has been used in several areas of forecasting because of its advantages. Zhang et al. [27] applied the CEEMDAN method to decompose wind speed series and used a neural network model to predict each IMF component, and finally the prediction results of each component were combined, and the experimental results showed that the method could effectively improve forecast accuracy. Wang et al. [28] combined CEEMDAN decomposition method and GRU neural network to predict natural gas price. The CEEMDAN decomposition method was used by Zhao and Chen [29] to decompose the carbon price, and the extreme learning machine (ELM) model was optimized with the improved sparrow algorithm to forecast each IMF component, and the results showed that the combined approach can effectively improve the forecasting accuracy. In their study, Cao et al. [30] established an EMD-LSTM model and a CEEMDAN-LSTM model to forecast stock market prices, and, based on empirical analysis, the CEEMDAN-LSTM model had more accurate predictions.

Following the above analysis, this paper uses the LightGBM model to forecast the futures price and the whale optimization algorithm (WOA) to select the hyperparameters of the model. For further improvement of the model prediction results, the CEEMDAN decomposition method is used to decompose the residual series of the predictions of LightGBM. As the support vector regression (SVR) model has better nonlinear fitting and generalization ability, it is used to predict each component generated by CEEMDAN, and the results are combined after the prediction is completed, resulting in a combined WOA-LightGBM-CEEMDAN model. A combined forecasting model is used to forecast the price of hog futures in China. We selected hog futures prices as the subject of this paper for two main reasons. Firstly, hogs are one of the most important agricultural products in China, and they provide a significant percentage of the country's meat consumption. According to data published by the National Bureau of Statistics, pork accounted for more than 75% of China's total meat consumption from 2013 to 2019 [31]. In any case, the dramatic fluctuations in the price of pork have had a significant impact on both the balance of supply and demand on the market as well as on both farmers and consumers. In the futures market, there are functions of price discovery and hedge, which can mitigate the economic loss caused by price fluctuation, bring income to investors, and help farmers to adjust the scale of pig breeding appropriately so that economic benefits are maximized. As a result, it is imperative to produce accurate forecasts for hog futures prices in order to stabilize

hog market prices and maintain a balance between supply and demand. Furthermore, in comparison to other types of price data, the price of hog futures is influenced to a greater degree by market supply and demand and is relatively less influenced by government macrocontrol, while the price data is to some degree influenced by the cycle. Finally, on January 8, 2021, hog futures will be listed and traded in mainland China. Currently, there is less discussion on predicting hog futures, and the model in this study is used to predict hog futures prices in China, which has some significance for future research of the same type.

The following are the main steps in this paper for forecasting the hog futures price. To begin with, we establish a system of hog futures price indexes and employ a grey correlation analysis to identify the main factors affecting the futures price of hogs, thereby improving the model's prediction accuracy. Additionally, LightGBM is used to establish a hog futures price forecasting model, and WOA is used to optimize model parameters in order to eliminate forecasting errors caused by the parameter settings of LightGBM. Furthermore, in order to improve the model prediction accuracy, the CEEMDAN method is used to correct the residual series of LightGBM prediction results in order to construct a combined WOA-LightGBM-CEEMDAN model.

The remainder of this paper is organized as follows. The second section provides an introduction to the LightGBM model, WOA, and CEEMDAN, followed by a description of the implementation steps of the combination model in this paper. In Section 3, we describe the prediction index system and data used in this paper and provide the parameter settings for the model. Our experimental analysis and discussion of hog futures prices are presented in Section 4. In Section 5, we summarize some conclusions and suggest directions for future research.

## 2. Materials and Methods

**2.1. LightGBM.** The LightGBM model, developed by Microsoft, is an open-source gradient boosting model based on decision trees. The LightGBM model is also capable of parallel learning, similar to the XGBoost model. LightGBM, however, has the advantage of a faster training rate and less memory consumption compared to XGBoost [32].

Consider a set of data sets  $M = \{x_i, y_i\}_1^N$ , in which  $x = \{x_1, \dots, x_n\}$  is the input to the model and  $y$  is the prediction label. The model function is  $F(x)$  and the loss function is  $L(y, F(x))$ . In gradient boosting, the negative gradient of the loss function  $L$  is used instead of the residuals to determine the value of the current model function  $F(x)$ . Taking  $g_{ij}$  as the negative gradient of the  $j$ th iteration, we obtain

$$g_{ij} = - \left[ \frac{\partial L(y_i, F(x_i))}{\partial F(x_i)} \right]_{F(x)=F_{j-1}(x)}. \quad (1)$$

If  $h(x)$  is the weak learner, then  $h(x)$  should be used to fit the negative gradient of the loss function to find the best fit value as follows:

$$g_j = \arg \min_g L(y_i, F_{j-1}(x_i) + gh_j(x_i)). \quad (2)$$

The model update formula is defined as follows:

$$F_j(x) = F_{j-1}(x) + g_j h_j(x). \quad (3)$$

In the above approach, gradient boosting is updated iteratively; one weak learner is trained at a time. After the iterations are completed, the weak learners are added together to obtain the strong learner.

To accelerate the training of the gradient boosting framework model without compromising accuracy, the LightGBM model uses a number of optimization methods, the most prominent of which is the histogram algorithm as well as the leaf-wise growth strategy with depth constraints.

In the LightGBM model, the histogram algorithm is a method of discretizing data, which reduces the computational cost and memory consumption, thus improving its efficiency.

The decision tree growth strategy used in the traditional gradient boosting framework model is a very inefficient layer-by-layer growth strategy, since it treats the subleaves of the same layer in an indiscriminate way, causing unnecessary model runs and thus increasing the burden on the model. Leaf-wise growth strategy with depth limit finds the leaf with the highest splitting gain from all the current leaves, then splits, and so forth. With the same number of splits as the layer-by-layer growth strategy, the leaf-wise growth strategy can effectively reduce errors and increase prediction accuracy. In addition, LightGBM includes a maximum depth limit that enables the model to achieve maximum prediction accuracy while preventing overfitting.

**2.2. Whale Optimization Algorithm.** The whale optimization algorithm [33] (WOA) is a population intelligence algorithm developed by Australian scientist Mirjalili and Lewis in 2016. The purpose of the algorithm is to determine optimal target parameters by simulating the feeding behavior of humpback whales. In the WOA algorithm, the location of each humpback whale represents a viable solution for a set of parameters, and changes in location are made in three different ways: encircling prey, spiral search, and random search.

**2.2.1. Encircling Prey.** The whales first share the information about the location of the searched prey as a group, with the location of the prey or the closest whale to the prey regarded as the optimal solution, and then they approach the whale that is currently closest to the prey's location, thus contracting its encirclement. This behavior is defined as follows:

$$\begin{cases} X(t+1) = X^*(t) - A \cdot D, \\ D = |C \cdot X^*(t) - X(t)|. \end{cases} \quad (4)$$

The position of the killer whale is  $X$ ;  $X^*(t)$  is the current optimal position of the whale;  $t$  is the current number of iterations;  $A$  and  $C$  are the coefficient matrices, and the expressions are

$$\begin{cases} A = 2a \cdot r_1 - a, \\ C = 2r_2, \\ a = 2 - \frac{2t}{t_{\max}}. \end{cases} \quad (5)$$

There are two random numbers,  $r_1$  and  $r_2$ , taking values ranging from 0 to 1;  $a$  is the convergence factor, linearly decreasing from 2 to 0; and  $t_{\max}$  is the global maximum number of iterations.

**2.2.2. Spiral Search.** In the search phase, the whale approaches its prey along an ascending spiral, and the mathematical expression for this phase is

$$\begin{cases} X(t+1) = X^*(t) + D \cdot e^{bl} \cos(2\pi l), \\ D = |C \cdot X^*(t) - X(t)|. \end{cases} \quad (6)$$

In this scenario,  $b$  is a constant parameter determining the shape of the spiral, and  $l$  is a uniformly distributed random number varying from  $-1$  to  $1$ .

During rotational search, the whale contracts its envelope to approach its prey. By assuming that each has a 50% probability of rotational search and envelope contraction, the expression can be defined as follows:

$$X(t+1) = \begin{cases} X^*(t) - A \cdot D, & p < 0.5, \\ X^*(t) + D \cdot e^{bl} \cos(2\pi l), & p \geq 0.5, \end{cases} \quad (7)$$

where  $p$  is a random number with values ranging from 0 to 1.

**2.2.3. Random Search.** For the purpose of enhancing the global search capability of the whale, WOA has also developed a random search algorithm to further increase the search range. When  $|A| \geq 1$ , the whale is outside the envelope and the whale moves away from the current optimal solution and performs a random search. Conversely, when  $|A| < 1$ , a spiral search is used to update the position. The expressions can be defined as follows:

$$\begin{cases} X(t+1) = X_{\text{rand}}(t) - A \cdot D^*, \\ D^* = |CX_{\text{rand}}(t) - X(t)|, \end{cases} \quad (8)$$

where  $X_{\text{rand}}(t)$  is the random position of the whale.

**2.3. WOA-LightGBM.** Model parameters have a considerable influence on model prediction effects, and there are many parameters in the LightGBM model which affect the model in different ways. Therefore, this paper borrows from the previous study [34] to set the LightGBM parameters to be searched for, that is, the number of boosted trees to fit ( $n_{\text{estimators}}$ ), the learning rate ( $\text{learning\_rate}$ ), maximum tree depth for base learners ( $\text{max\_depth}$ ), and maximum tree leaves for base learners ( $\text{num\_leaves}$ ). By using the parameters of the LightGBM model as the position vectors of each whale, the WOA seeks the global optimal position in

the algorithm through iterative search and outputs it as the final parameters of the LightGBM model. The specific processes are as follows:

Step 1: Initialize the whale optimization algorithm. Set the number of whale populations, the maximum number of iterations, and the whale search area boundaries for the WOA algorithm.

Step 2: Set up the fitness function. In the WOA algorithm, first, the position of the current population is randomly initialized within the boundary range, then the fitness function is used to calculate the fitness value for each whale in the current population, and then the whale with the smallest fitness value is chosen as the global optimal solution for the current population. In the LightGBM model, the fitness function is selected as the mean square error function, and the specific expression is as follows:

$$f(x_i) = \frac{1}{n} \sum_{j=1}^n (\theta_{i,j} - \hat{\theta}_{i,j})^2, \quad (9)$$

where  $x_i$  is the location of the  $i$ th individual whale,  $\theta_{i,j}$  is the corresponding  $j$ th true value in the  $i$ th individual, and  $\hat{\theta}_{i,j}$  is the predicted value derived from the LightGBM model based on the parameters set for  $x_i$ .

Step 3: Maintain the position of individual whales according to the three methods of encircling prey, spiral search, and random search within the WOA, and control all whales within a predetermined boundary.

Step 4: Upon completion of the position update, the whale position is input into the fitness function in order to calculate the fitness result, and the optimal whale position is selected as the current global optimal solution.

Step 5: Repeat Step 3 and Step 4 until the algorithm has reached the maximum number of iterations.

Step 6: Output the final WOA algorithm search results and integrate them into the LightGBM model for modeling predictions.

The flow chart of the above steps is depicted in Figure 1.

**2.4. CEEMDAN Residual Correction Model.** Despite the fact that the LightGBM model for hog futures price forecasting can utilize historical time data to obtain better results, there are still a number of residual series that display nonlinearity and large degrees of randomness. Therefore, a method for forecasting and correcting the residual series is needed to improve the model's forecasting accuracy.

EMD is a technique for decomposing nonlinear, non-smooth sequences into IMFs components with different fluctuation scales; however, it is susceptible to modal mixing when decomposing the signals, which interferes with the decomposition process. EEMD can effectively resolve the modal mixing phenomenon by adding Gaussian white noise to the original signal; however, there is still Gaussian white noise present in the components of the IMF decomposed by

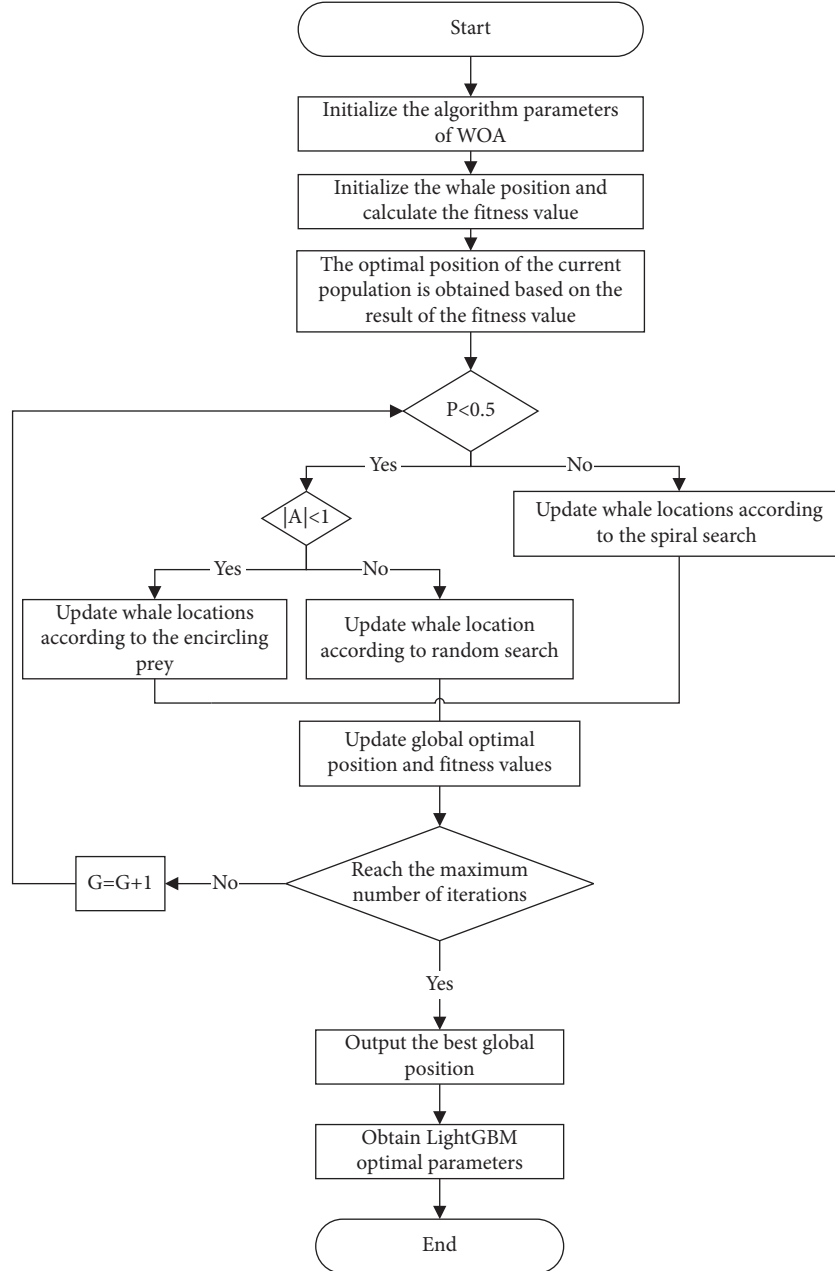


FIGURE 1: Flow chart of WOA-LightGBM model pred.

the EEMD method, which can lead to errors during reconstruction. Due to this, the CEEMDAN [26] method proposed by Torres incorporates adaptive white noise at each stage in order to overcome the large reconstruction error of the EEMD method. Therefore, the CEEMDAN method is employed in this study in order to decompose the residual series and predict each IMFs component as well as the trend term component separately.

CEEMDAN can be decomposed into the following steps:

Step 1: Obtain the residual series. The WOA-LightGBM model is used to model and forecast the hog futures price, and the residual series is obtained by calculating

the difference between the forecast results and the true values:

$$y(t) = Y_{\text{real}} - Y_{pr}, \quad (10)$$

where  $y(t)$  symbolizes the residual series;  $Y_{\text{real}}$  is the true value of hog futures; and  $Y_{pr}$  is the forecast value derived by the WOA-LightGBM model.

Step 2: An adaptive Gaussian white noise sequence is added to the original sequence to obtain the new sequence with noise:

$$\bar{y}_i(t) = y(t) + \sigma n_i(t), \quad i = 1, 2, \dots, N. \quad (11)$$



$y(t)$  represents the original residual sequence;  $\bar{y}_i(t)$  represents the new sequence with white noise added to it;  $n_i(t)$  denotes the white noise added to the original data;  $\sigma$  denotes the adaptive coefficient.

Step 3: On the new sequence  $M$ , the EMD decomposition is applied after the addition of white noise to obtain  $N$  IMFs, and the first IMF of CEEMDAN can be derived by averaging the  $N$  modal components as follows:

$$\text{imf}_1(t) = \frac{1}{N} \sum_{i=1}^N \text{imf}_{1i}(t). \quad (12)$$

Hence,  $R_1(t)$  is the residual component at this point:

$$R_1(t) = \bar{y}_i(t) - \text{imf}'_1(t). \quad (13)$$

Step 4: The adaptive white noise sequence  $\sigma n_i(t)$  is added to  $R_1(t)$  to form a new sequence with noise  $R_1(t) + \sigma E_1(n_i(t))$ , where  $E_j(\bullet)$  is the  $j$ th eigenmodal component obtained from the EMD decomposition. By decomposing the new series with the EMD and averaging, the second IMF and the residual component are obtained.

$$\text{imf}_2(t) = \frac{1}{N} \sum_{i=1}^N E_1(R_1(t) + \sigma_1 E_1(n_i(t))), \quad (14)$$

$$R_2(t) = R_1(t) - \text{imf}'_2(t).$$

Step 5: Repeat the three preceding steps in order to obtain the  $j+1$ th IMF and the  $j$ th residual component.

$$\text{imf}_{j+1}(t) = \frac{1}{N} \sum_{i=1}^N E_1(R_j(t) + \sigma_j E_j(n_i(t))), \quad (15)$$

$$R_j(t) = R_{j-1}(t) - \text{imf}'_j(t).$$

Step 6: This procedure is repeated until the CEEMDAN is terminated when the remaining components cannot be decomposed by EMD, and, finally, the original sequence  $y(t)$  is decomposed into multiple IMFs and a residual component.

$$y(t) = \sum \text{imf}(t) + R_{es}(t). \quad (16)$$

Once CEEMDAN has decomposed the original series, all IMFs and residual components are predicted separately using appropriate prediction models, and then the individual predictions are linearly combined to determine the final residual prediction. With regard to prediction methods, SVR is an algorithm used for regression modeling by SVM, which has a strong ability to generalize to data that are nonlinear and have stochastic fluctuations [35]. Therefore, in this study, SVR is used to predict each IMF as well as the residual components generated by CEEMDAN separately.

2.5. *WOA-LightGBM-CEEMDAN*. The aim of this study is to improve the forecasting performance of the hog futures price by combining WOA, LightGBM, and CEEMDAN models to formulate the WOA-LightGBM-CEEMDAN model. Here are the specific steps for implementation:

Step 1: Data preprocessing. Preprocess the data and divide it into training sets and testing sets.

Step 2: Obtain the preliminary fitted values. Establish the LightGBM model for forecasting the hog futures price, employ the WOA algorithm to determine the parameters of the model, and then use the optimized model to estimate the preliminary price of the hog futures and obtain the preliminary fitted value.

Step 3: Obtain the residual series. The preliminary fitted value results are compared with the original data, and residual series are derived. The specific formula is as follows:

$$\Delta(t_i) = y_{\text{real}}(t_i) - \hat{y}_{\text{LGB}}(t_i), \quad i = 1, 2, \dots, N, \quad (17)$$

where  $\Delta(t_i)$  represents the residual series value;  $y_{\text{real}}(t_i)$  represents the true value; and  $\hat{y}_{\text{LGB}}(t_i)$  represents the prediction result of the WOA-LightGBM model.

Step 4: The residual series are brought into CEEMDAN for modal decomposition in order to obtain the IMF components of different frequencies with number  $n$ , as well as a trend component.

Step 5: The SVR model is used to predict each component of CEEMDAN separately, and the results are combined to obtain the final residual prediction value  $\Delta(t_i)$  after the prediction has been completed.

Step 6: Residual correction is performed on the WOA-LightGBM model. After combining the residual prediction results from the WOA-LightGBM model and the preliminary fitting results obtained from the WOA-LightGBM model, we obtain residual correction results for the combined final model:

$$\hat{y}(t_i) = \Delta(t_i) + \hat{y}_{\text{LGB}}(t_i), \quad i = 1, 2, \dots, N. \quad (18)$$

An intuitive implementation flow chart is shown in Figure 2.

### 3. Data Description

3.1. *Impact Factors of Hog Futures*. Hog futures prices are influenced by a variety of factors. The purpose of this paper is to identify primary indicators of hog futures price from three perspectives: supply, demand, and futures market.

Among the supply factors, the price of piglets is an important input before pig slaughtering, and changes in piglet prices will directly affect the cost of production of pigs. The price of sows directly influences the number and price of piglets, which impacts the cost of pig breeding. Feed is another important input for hog production, and changes in feed prices will have an impact on the size of production.

At the level of demand factors, when the price of pork exceeds consumers' psychological expectations, they will

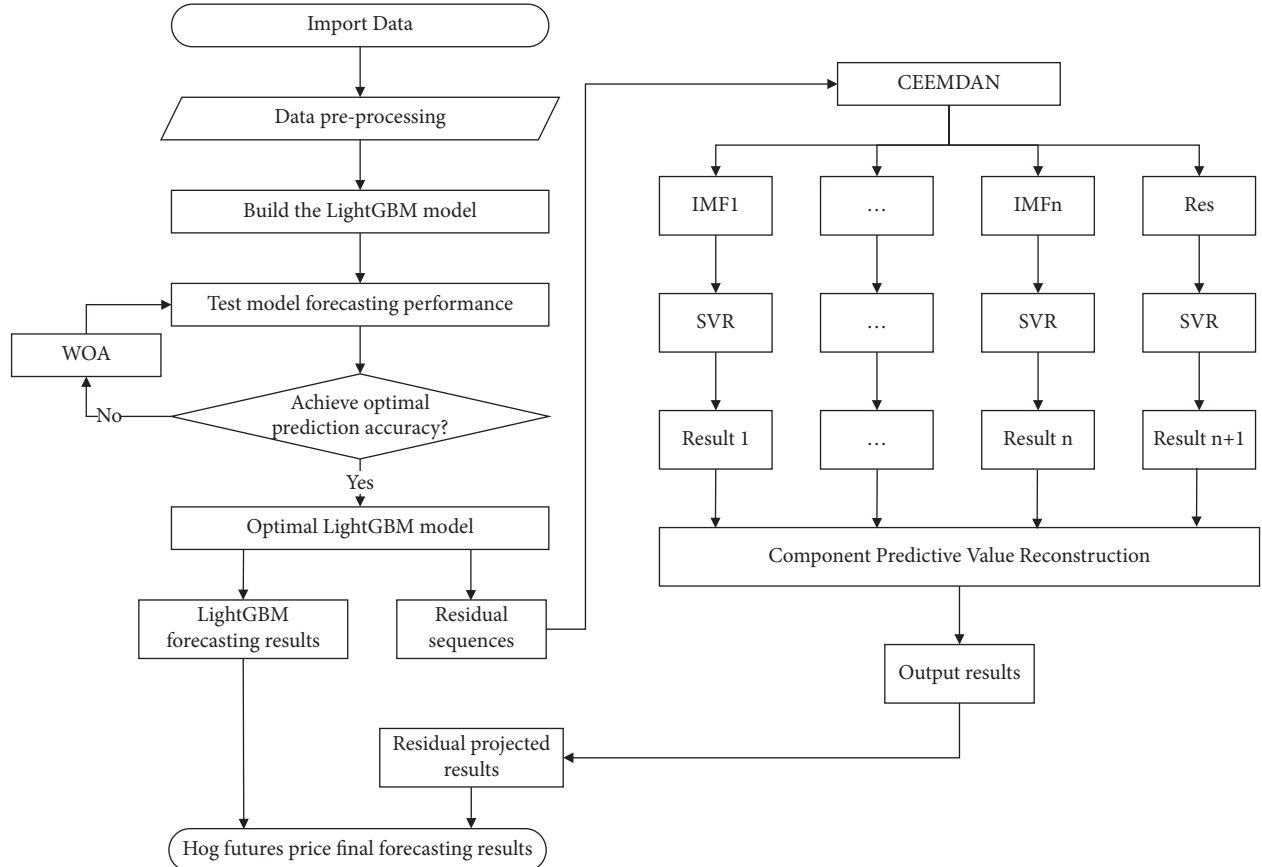


FIGURE 2: Structure flow chart of WOA-LightGBM-CEEMDAN.

prefer alternatives with lower prices, so the price of alternatives will directly affect the consumption of pork and therefore the price of hogs.

At the level of futures market factors, volume and open interest can accurately reflect the relationship between supply and demand as well as the volatility of the futures market, while providing helpful information in predicting the overall trend of the market. Basis is the difference between the spot price and the futures price and is a dynamic indicator of the actual change between the two prices; basis changes directly impact the effectiveness of the hedge. The spot price is the foundation of the futures price. The spot price always appears prior to the futures price, while, at the same time, the delivery price of the futures price is always based on the spot transaction price.

The sow price considered in this study is the national binary 50 kg sow price; the corn and soybean meal prices are used to represent feed prices; and the beef price and lamb price are used to represent alternative prices. Table 1 provides detailed indicators for each classification.

**3.2. Grey Relation Analysis.** Grey relation analysis (GRA) is used to further screen the indicators in order to improve their accuracy and reduce their error. The GRA [36] method measures the degree of association between the reference and comparison series through grey correlation. The specific calculation process is as follows:

Step 1: Take the hog futures price data  $Y_i = \{y_{i1}, y_{i2}, \dots, y_{in}\}$  ( $i = 1, 2, \dots, n$ ) as the reference series and the influencing factors  $X_j = \{x_{j1}, x_{j2}, \dots, x_{jn}\}$  ( $j = 1, 2, \dots, n$ ) in Table 1 as the comparison series.

Step 2: Calculate the grey correlation coefficients for each reference sequence and comparison sequence. The calculation formula is

$$\xi_{ij}(k) = \frac{\min_i \min_k |x_j(k) - y_i(k)| + \rho \cdot \max_i \max_k |x_j(k) - y_i(k)|}{|x_j(k) - y_i(k)| + \rho \cdot \max_i \max_k |x_j(k) - y_i(k)|}. \quad (19)$$

$\rho$  is a resolution factor that takes values between 0 and 1. For this paper, we take  $\rho = 0.5$ ;  $i = 1, 2, \dots, n$ ,  $j = 1, 2, \dots, n$ ;  $k = 1, 2, \dots, n$ .

Step 3: Calculate the correlation:

$$r_{ij} = \frac{1}{n} \sum_{k=1}^n \xi_{ij}(k). \quad (20)$$

$r_{ij}$  is the correlation index value between the reference series and the comparison series. An index value close to 1 indicates a higher degree of correlation between the comparison series and the reference series.

Table 2 shows the GRA results for hog futures price influencing factors. Among the many indicators, the factors with grey correlations less than 0.7 were removed in this paper, and the ultimate hog futures price influencing factors indicator system is shown in Table 3.

**3.3. Data Source.** This paper forecasts hog futures prices and establishes the influencing factors from three perspectives: supply, demand, and futures markets. Since hog futures are listed and traded on the Dalian Commodity Exchange on January 8, 2021, the data time points are all selected as daily data from January 8, 2021, to July 22, 2021, for a total of 129 samples for simulation experiments. In the experiments, 70% of the data are used as training data and 30% as testing data. Among them, except for lamb price and beef price from Wind database, other indicators are published on Huarong Rongda data analyst website (<https://dt.hrrdqh.com/>). Based on the above data, piglet price and sow price are weekly data, which were converted into daily data by using the EVIEWS software. Table 4 presents descriptive statistics for each indicator.

### 3.4. Experiment Preparation

**3.4.1. Model Evaluation.** The mean square error (MSE), the mean absolute error (MAE), the root mean square percentage error (RMSPE), the mean absolute percentage error (MAPE),  $R$ -square ( $R^2$ ), and directional accuracy (DA) [37] are selected as the model evaluation functions. In general, when the values of MSE, MAE, RMSPE, and MAPE indicators are smaller and the values of  $R^2$  and DA indicators are larger, the model predicts better and vice versa. Here is the formula for the functions:

$$\begin{aligned}
 \text{MSE} &= \frac{1}{n} \sum_{i=1}^n (y_i - \hat{y}_i)^2, \\
 \text{MAE} &= \frac{1}{n} \sum_{i=1}^n |y_i - \hat{y}_i|, \\
 \text{RMSPE} &= \sqrt{\frac{1}{n} \sum_{i=1}^n \left| \frac{y_i - \hat{y}_i}{y_i} \right|^2} * 100\%, \\
 \text{MAPE} &= \frac{1}{n} \sum_{i=1}^n \left| \frac{y_i - \hat{y}_i}{y_i} \right| * 100\%, \\
 R^2 &= 1 - \frac{\sum_{i=1}^n (y_i - \hat{y}_i)^2}{\sum_{i=1}^n (y_i - \bar{y}_i)^2}, \\
 \text{DA} &= \frac{1}{N} \sum_{i=1}^N a(i) \times 100\%.
 \end{aligned} \tag{21}$$

In the above formula,  $N$  denotes the number of samples in the test set;  $y_i$  is the true value;  $\hat{y}_i$  is the forecasting result; when  $(y(i+1) - y(i))(\hat{y}(i+1) - y(i)) \geq 0$ ,  $a(i) = 1$ ; otherwise,  $a(i) = 0$ .

**3.4.2. Data Preprocessing.** Based on the descriptive statistics shown in Table 4, it appears that the order of magnitude of the factors varies due to the different units. To avoid prediction errors due to the order of magnitude of the data, all predicted data are normalized by using the following equation:

$$x^* = \frac{x - x_{\min}}{x_{\max} - x_{\min}}, \tag{22}$$

where  $x^*$  is the normalized data value;  $x$  is the input data, and  $x_{\min}$  and  $x_{\max}$  are the minimum and maximum values of the input data.

**3.4.3. Model Parameters Setting.** To analyze and compare the model prediction performance, multiple algorithms were used to measure the prediction effect of the WOA-LightGBM-CEEMDAN model. For the single model, SVR, BPNN, extreme learning machine (ELM), GBDT, and XGBoost models are selected to compare and analyze the prediction performance of LightGBM. In terms of WOA algorithm performance, the grey wolf optimization (GWO) algorithm is selected to optimize the LightGBM model (GWO-LightGBM) to analyze and compare the WOA-LightGBM. As to the prediction effect of the residual correction combination model, WOA-LightGBM-EEMD, which uses EEMD method to decompose the residual series, and WOA-LightGBM-SVR, which directly performs SVR model prediction without decomposing the residual series first, are used as comparative analysis models.

For the above model, given that GBDT and XGBoost have many parameters, the model parameters selection of literature [34] is used to select parameter values. We select the number of boosting stages to perform ( $n_{\text{estimators}}$ ), boosting learning rate ( $\text{learning\_rate}$ ), the minimum number of samples required to split an internal node ( $\text{min\_samples\_split}$ ), and the minimum number of samples required to be at a leaf node ( $\text{min\_samples\_leaf}$ ) in the GBDT model as the parameters to be searched for. In the XGBoost model, number of gradient boosted trees ( $n_{\text{estimators}}$ ), boosting learning rate ( $\text{learning\_rate}$ ), maximum tree depth for base learners ( $\text{max\_depth}$ ), subsample ratio of the training instance ( $\text{subsample}$ ), and subsample ratio of columns when constructing each tree ( $\text{colsample\_bytree}$ ) are selected as the parameters to be searched for.

The specific parameters of each model are shown in Table 5.

## 4. Results Discussion

**4.1. Analysis of the Preliminary Fitting Performance of WOA-LightGBM.** Figure 3 illustrates WOA-LightGBM's preliminary performance on the testing set for predicting hog futures prices. Figure 3 illustrates the fact that while the WOA-LightGBM model can predict the trend of hog futures prices reasonably well, it cannot predict the exact futures prices, and there are still a series of residuals. Therefore, CEEMDAN is used to decompose the residual series generated by WOA-LightGBM.

TABLE 1: Primary indicator system for hog futures prices.

Category	Indicators
Supply	Piglet price
	Sow price
	Corn price
	Soybean meal price
Demand	Lamb price
	Beef price
Futures market	Open interest
	Volume
	Basis
	Spot price
	Previous closing price

TABLE 2: Results of GRA.

Category	Indicators	GRA
Supply	Piglet price	0.85
	Sow price	0.81
	Corn price	0.76
	Soybean meal price	0.64
Demand	Lamb price	0.81
	Beef price	0.77
Futures market	Open interest	0.64
	Volume	0.73
	Basis	0.69
	Spot price	0.79
	Previous closing price	0.96

TABLE 3: Final indicators of hog futures price impact factors.

Category	Indicators
Supply	Piglet price
	Sow price
	Corn price
Demand	Lamb price
	Beef price
Futures market	Volume
	Spot price
	Previous closing price

The specific methods of CEEMDAN are as follows:

Step 1: The WOA-LightGBM model is predicted separately for the training and testing sets to obtain the prediction results for the entire sample length.

Step 2: The WOA-LightGBM model predictions are subtracted from the true value series to obtain the model residual series, and CEEMDAN is used to decompose the residual series into IMFs and residual components.

Step 3: For each component, the SVR model is trained using 70% of the residual series, and the remaining 30% is used for prediction.

Step 4: The prediction results of the SVR model for each component are summed to obtain the final residual prediction results for the test set.

Figure 4 displays the results of the CEEMDAN decomposition of the total sample length, with a total of four IMFs and one residual component.

4.2. *Analysis of Model Prediction Performance.* Figure 5 and Table 6 illustrate the fitting curves of each model for the hog futures prices in the testing set sample and the prediction performance for the six evaluation indicators, respectively. This analysis leads to the following conclusions.

The WOA-LightGBM model is optimal for one-model prediction, which can be attributed primarily to the following factors. Firstly, SVR, ELM, and BPNN models relate to a single machine learning algorithm, while LightGBM belongs to a boosting ensemble learning framework, which can effectively improve the prediction accuracy and generalization ability of the model by combining the predictions of multiple base learner algorithms. Secondly, compared with GBDT and XGBoost, which are part of the decision tree framework, LightGBM's unique leaf-wise subleaf growth strategy may effectively improve the prediction efficiency of the algorithm, while the depth limit may effectively prevent the overfitting problem of the model.

As for the optimization performance of the WOA, the prediction results of the GWO-LightGBM model and the WOA-LightGBM model can be analyzed, and it can be seen that the prediction accuracy of the WOA-LightGBM model is improved by 37.24%, 19.42%, 20.54%, 19.31%, 0.28%, and 5.71% for MSE, MAE, RMSPE, MAPE,  $R^2$ , and DA, respectively. Under the same parameter setting, as compared to GWO algorithm, WOA can lock the optimal parameters of the LightGBM model more quickly and improve the accuracy of the prediction.

In terms of the combined algorithm, all combined models have better prediction results than single models, and the WOA-LightGBM-CEEMDAN model has the highest prediction accuracy. The results demonstrate that the CEEMDAN residual correction combination model proposed in this paper can further improve the prediction accuracy of the WOA-LightGBM model, thereby improving the accuracy of forecasting the price of hog futures.

4.3. *Analysis of Model Prediction Errors for WOA-LightGBM-CEEMDAN.* Further analysis of the prediction performance of the WOA-LightGBM-CEEMDAN model is conducted by examining prediction errors between the prediction results and the real values for the WOA-LightGBM-CEEMDAN, WOA-LightGBM-EEMD, WOA-LightGBM-SVR, and WOA-LightGBM models. The prediction errors of the four models are presented in Table 7 and Figure 6. In the forecasting performance analysis of the testing set in Table 7, WOA-LightGBM-CEEMDAN has the best prediction results, with an average error of  $-1.35$  yuan/ton, while the WOA-LightGBM model without residual correction has the largest error in prediction, reaching an average of  $71.65$  yuan/ton. This can be attributed primarily to the following factors: (a) Because residual sequences of a single machine learning model may contain valuable information that can boost the final prediction effect, the WOA-LightGBM model

TABLE 4: Descriptive statistics of hog futures price data.

	Count	Mean	Std	Min	25%	50%	75%	Max
Futures price	128.0	24439.2	3760.8	16735.0	20167.5	25412.5	27297.5	29380.0
Piglet price	128.0	251.1	101.5	91.8	154.9	264.0	340.9	382.6
Sow price	128.0	769.3	132.8	469.9	781.8	825.6	851.8	887.2
Corn price	128.0	2822.8	57.3	2527.8	2797.2	2835.6	2862.8	2908.7
Lamb price	128.0	75992.9	1632.1	71930.0	75450.0	76180.0	77280.0	78420.0
Beef price	128.0	77580.5	668.7	76200.0	77087.5	77635.0	78155.0	78930.0
Volume	128.0	12669.2	13361.3	1601.0	3684.0	7750.5	16896.8	91056.0
Spot price	128.0	23209.6	6988.9	12440.0	16405.0	23020.0	28195.0	36390.0
Previous closing price	128.0	24502.2	3731.9	16735.0	20533.8	25500.0	27297.5	29380.0

TABLE 5: Parameters setting.

Model	Parameters setting
CEEMDAN	Trials = 100; epsilon = 0.005
EEMD	Trials = 100; noise_width = 0.05
WOA-LightGBM	n_estimators = 18; learning_rate = 0.027; max_depth = 10; num_leaves = 9
WOA-XGBoost	n_estimators = 38; learning_rate = 0.064; colsample_bytree = 0.3015; max_depth = 54; subsample = 0.2258
WOA-GBDT	n_estimators = 10; learning_rate = 0.1002; min_samples_leaf = 10; max_depth = 12; min_samples_split = 4
ELM	Number of nodes in the hidden layer: 10
BPNN	Number of nodes in the hidden layer: 8
SVR	C = 40; gamma = 36
WOA	Number of iterations: 100; population size: 10
GWO	Number of iterations: 100; population size: 10

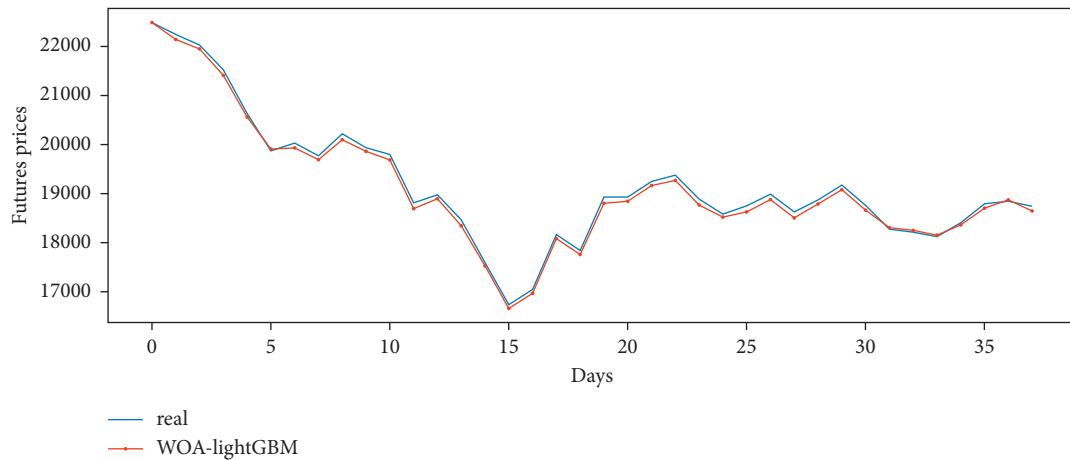


FIGURE 3: Preliminary fitting curve of WOA-LightGBM model.

has the largest prediction error in Table 7. (b) The modal decomposition algorithm allows the signal to be decomposed in accordance with the residual series' own time scale, which holds a significant advantage in dealing with non-linear and nonstationary data. Thus, the residual correction models predicted after the CEEMDAN and EEMD decomposition in the table are all superior to the residual correction models predicted directly using the SVR model. (c) Using the modal decomposition algorithm, it is further demonstrated that the CEEMDAN method by adding adaptive white noise can reduce the reconstruction error generated during the decomposition process and, as a result, improve the prediction accuracy by comparing the residual correction effects of CEEMDAN and EEMD.

**4.4. Experiments in Other Financial Data.** In order to test the predictive power of this paper's model in other areas, the daily trading data of the CSI 300 stock index futures are used. The data was obtained from the Wind database. The data selected spans from January 4, 2016, to July 21, 2021, with a total of 1,351 transactions. It is specifically selected as the forecast target, and the opening price, high price, low price, volume, raising limit price, and limit down price are taken as the influencing factors for the prediction. 70% of the data will be used as a training set and 30% as a testing set. Table 8 provides the calculation results of the six indicators for the model in this paper and the comparison models.

The results of the indicator analysis in Table 8 lead to the following conclusions. First of all, among the single machine

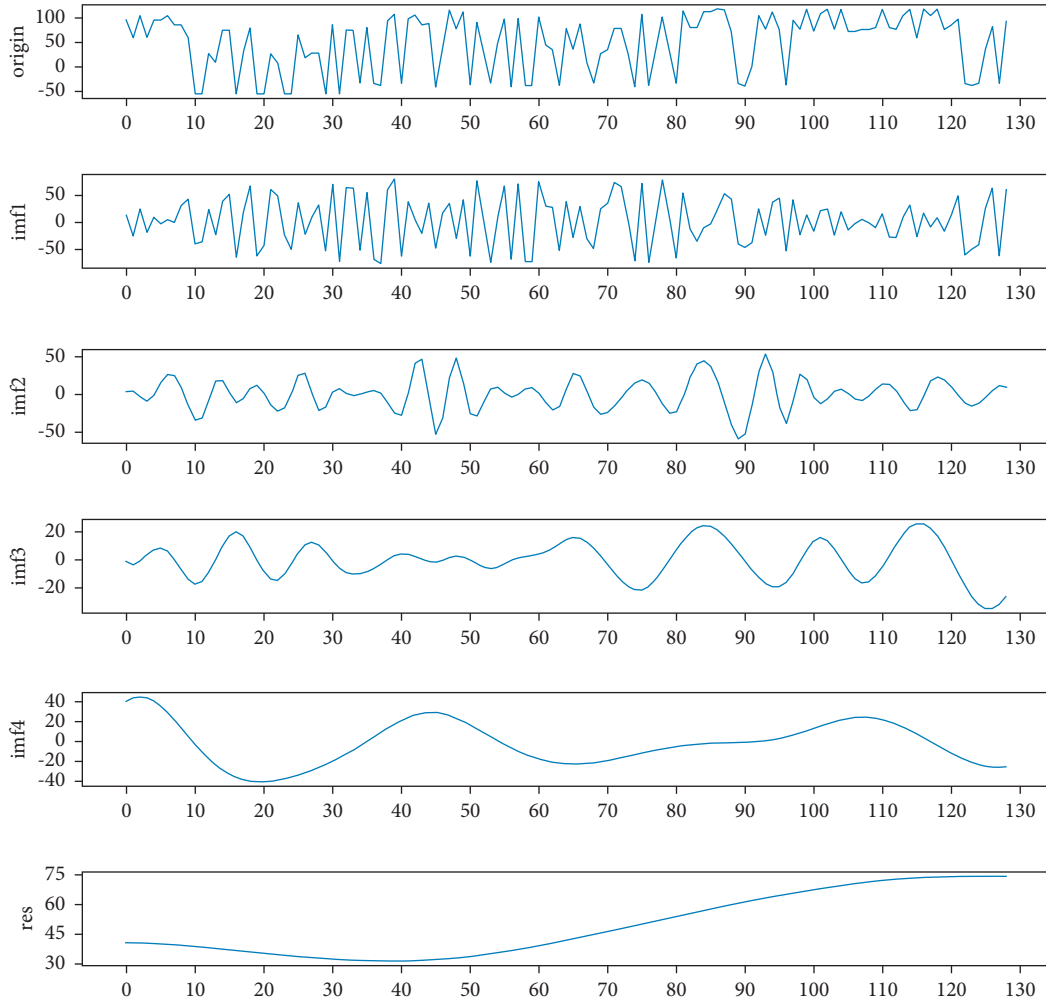


FIGURE 4: CEEMDAN decomposition of WOA-LightGBM prediction residuals.

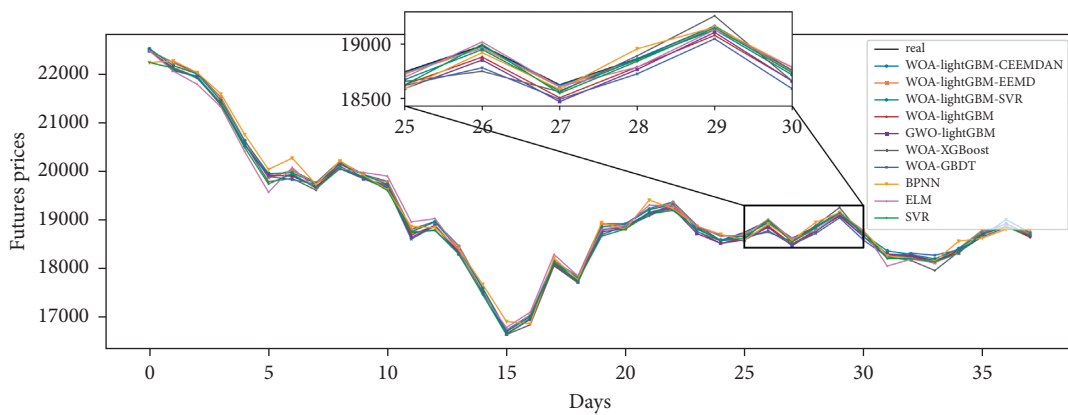


FIGURE 5: Predicted performance of the test set.

learning models, the LightGBM model optimized by the WOA algorithm has the best accuracy. In addition, its prediction metrics of MSE, MAE, RMSPE, MAPE,  $R^2$ , and DA improved by 34.89%, 22.46%, 19.82%, 23.01%, 0.01%, and 0.52%, respectively, compared with the GWO-

LightGBM model, which ranked second among the single models. Second, all three residual correction combinations outperform the single machine learning model, suggesting that further forecasting of the residual series and the extraction of information may enhance the prediction

TABLE 6: Forecast accuracy table for hog futures.

	MSE	MAE	RMSPE (%)	MAPE (%)	R <sup>2</sup>	DA
WOA-LightGBM-CEEMDAN	<b>58.3171</b>	<b>5.2654</b>	<b>0.0407</b>	<b>0.0277</b>	<b>99.9964e-02</b>	<b>0.9737</b>
WOA-LightGBM-EEMD	154.3967	11.3160	0.0653	0.0595	99.9905e-02	<b>0.9737</b>
WOA-LightGBM-SVR	2540.5649	42.5720	0.2638	0.2223	99.8432e-02	0.9474
WOA-LightGBM	7465.1947	81.1565	0.4512	0.4246	99.5393e-02	<b>0.9737</b>
GWO-LightGBM	11895.0375	100.7162	0.5678	0.5262	99.2659e-02	0.9211
WOA-XGBoost	11987.5541	95.6370	0.5793	0.5036	99.2602e-02	0.9211
WOA-GBDT	14009.2782	100.5755	0.6179	0.5251	99.1353e-02	0.8947
BPNN	12584.6199	88.6895	0.5844	0.4641	99.2233e-02	0.9474
ELM	13074.8747	89.1647	0.5781	0.4580	99.1931e-02	<b>0.9737</b>
SVR	13390.6722	89.7970	0.5905	0.4616	99.1736e-02	0.9474

Bold shows the best predicted results in the classification of each indicator.

TABLE 7: Fitting error analysis of the four models.

Date	Real	CEEMDAN		EEMD		SVR		WOA-LightGBM	
		Fitted value	Error	Fitted value	Error	Fitted value	Error	Fitted value	Error
2021/5/28	22485	22489.67	-4.67	22484.88	0.12	22530.28	-45.28	22485	0
2021/5/31	22245	22242.76	2.24	22237.85	7.15	22180.4	64.60	22140.26	104.74
2021/6/1	22025	22015.68	9.32	22008.5	16.50	22011.98	13.02	21948.65	76.35
2021/6/2	21525	21523.93	1.07	21518.05	6.95	21463.73	61.27	21412.14	112.86
2021/6/3	20640	20642.38	-2.38	20637.71	2.29	20630.58	9.42	20563.5	76.50
2021/6/4	19870	19883.66	-13.66	19878.53	-8.53	19960.14	-90.14	19908.5	-38.50
2021/6/7	20025	20024.6	0.40	20017.03	7.97	19974.63	50.37	19929.61	95.39
2021/6/8	19770	19767.81	2.19	19759.64	10.36	19752.83	17.17	19693.65	76.35
2021/6/9	20215	20211.61	3.39	20201.77	13.23	20148.2	66.80	20096.61	118.39
2021/6/10	19935	19932.91	2.09	19921.95	13.05	19932.15	2.86	19862.48	72.52
...	...	...	...	...	...	...	...	...	...
2021/7/8	18865	18862.46	2.54	18849.55	15.45	18858.18	6.82	18788.5	76.50
2021/7/9	19165	19164.54	0.46	19151.03	13.97	19131.55	33.45	19079.9	85.10
2021/7/12	18760	18758.54	1.46	18748.36	11.64	18717.02	42.98	18662.11	97.89
2021/7/13	18270	18284.68	-14.68	18272.09	-2.09	18364.79	-94.79	18304.53	-34.53
2021/7/14	18210	18225.68	-15.68	18216.4	-6.40	18292.82	-82.82	18248.5	-38.50
2021/7/15	18120	18137.65	-17.65	18128.5	-8.50	18199.54	-79.53	18154.53	-34.53
2021/7/16	18400	18415.71	-15.71	18408.92	-8.92	18407.64	-7.64	18363.31	36.69
2021/7/19	18785	18793.16	-8.16	18786.45	-1.45	18743.8	41.20	18702.32	82.68
2021/7/20	18840	18862.93	-22.93	18855.92	-15.92	18928.48	-88.48	18874.53	-34.53
2021/7/21	18740	18743.18	-3.18	18735.75	4.25	18691.71	48.29	18647.38	92.62
Average error		-1.35		8.59		16.28		71.65	

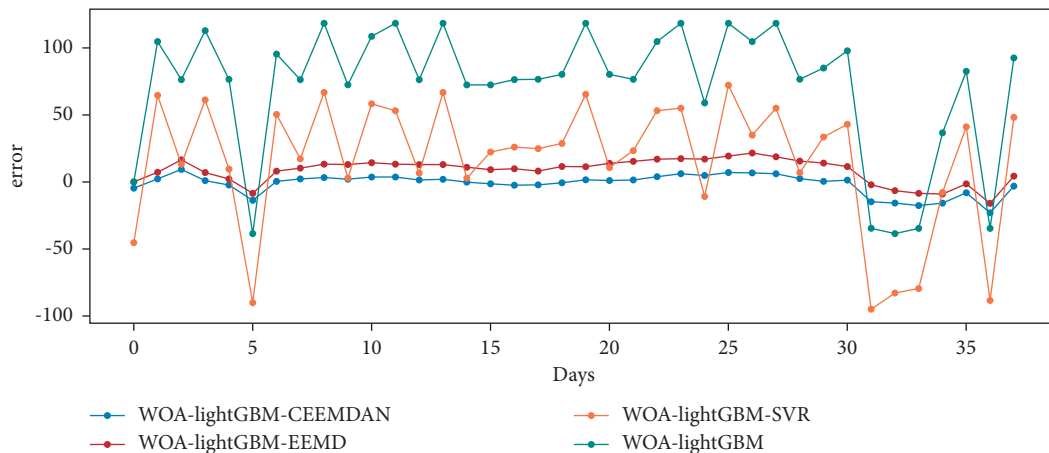


FIGURE 6: Model prediction error analysis.

TABLE 8: Forecast accuracy table of CSI 300 stock index futures.

	MSE	MAE	RMSPE (%)	MAPE (%)	R <sup>2</sup>	DA
WOA-LightGBM-CEEMDAN	<b>9.5274</b>	<b>2.3375</b>	<b>0.0668</b>	<b>0.0509</b>	<b>99.9971e-02</b>	<b>0.9753</b>
WOA-LightGBM-EEMD	13.7575	2.7583	0.0793	0.0595	99.9958e-02	0.9704
WOA-LightGBM-SVR	28.9593	3.9951	0.1187	0.0872	99.9911e-02	0.9580
WOA-LightGBM	56.6955	4.9665	0.1610	0.1064	99.9827e-02	0.9432
GWO-LightGBM	87.0789	6.4052	0.2008	0.1382	99.9734e-02	0.9383
WOA-XGBoost	103.8484	7.9996	0.2242	0.1759	99.9682e-02	0.9333
WOA-GBDT	197.0538	10.3638	0.3015	0.2249	99.9397e-02	0.9259
ELM	166.7355	9.0973	0.2846	0.1994	99.9489e-02	0.9358
BPNN	264.4969	11.5221	0.3634	0.2512	99.9191e-02	0.9037
SVR	354.7475	10.4587	0.4366	0.2356	99.8915e-02	0.9136

Bold shows the best predicted results in the classification of each indicator.

TABLE 9: Ranking the features importance of hog futures prices.

LightGBM		XGBoost		GBDT	
Features	Score	Features	Score	Features	Score
Volume	0.354167	Sow price	0.203349	Sow price	0.205162
Sow price	0.270833	Lamb price	0.129648	Volume	0.204963
Previous closing price	0.229167	Beef price	0.12844	Corn price	0.189453
Piglet price	0.0625	Spot price	0.121461	Spot price	0.167043
Spot price	0.0625	Piglet price	0.115235	Piglet price	0.109867
Lamb price	0.020833	Corn price	0.114087	Previous closing price	0.065497
Corn price	0	Previous closing price	0.104195	Lamb price	0.035748
Beef price	0	Volume	0.083584	Beef price	0.022267

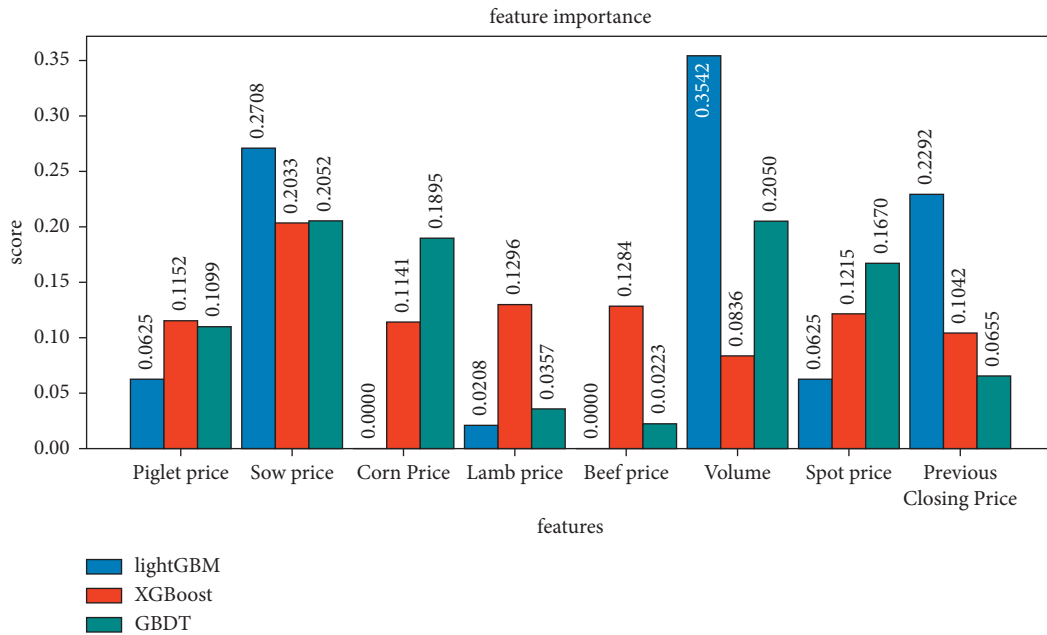


FIGURE 7: Histogram of feature importance.

accuracy of the model. Last but not least, in the three combined prediction models, WOA-LightGBM-CEEMDAN showed the best prediction results. Compared to the second-ranked WOA-LightGBM-EEMD model, the calculation results of the six prediction indexes were improved by 30.75%, 15.26%, 15.7%, 14.45%, 0.001%, and 0.50%,

respectively, indicating that the correction method of decomposition-individual forecasting-ensemble residual series by CEEMDAN, which is applied in this study, can be effective in extracting valuable information from prediction residuals of LightGBM model, improving the model's predictions.



**4.5. Analysis of Feature Importance.** In order to determine the most influential factors in hog futures price forecasting, the WOA-LightGBM, WOA-XGBoost, and WOA-GBDT models are used to analyze the feature importance. Table 9 and Figure 7 provide the results of the feature importance ranking for each model. The preliminary observations indicate that the results of the feature ranking in the three models are not exactly the same. The further analysis of the feature rankings in Table 9 reveals that the sow price, piglet price, and spot price are ranked in the top five out of the three models that are essential in forecasting hog futures prices. Specifically, first of all, the change in sow price reflects the market's current replenishment sentiment and influences the number of hogs that will be slaughtered after six months. A high sow price indicates positive market sentiment and a high pig slaughter volume after six months. At the same time, the price of sows is also an important part of the cost of hog farming. Secondly, the piglet price change can also reflect the market's eagerness for replenishment, reflecting the scale of pig slaughter in the past four months, and the piglet price with a lag of four months has a direct correlation with the current hog price. Finally, spot prices are inherently correlated with futures prices, particularly when they are close to delivery.

## 5. Conclusions

In this paper, a combined forecasting model of hog futures prices is developed by using WOA-LightGBM and CEEMDAN, which addresses the shortcomings of single machine learning models in terms of forecasting accuracy and model stability. In the first place, we define the index system of hog futures price influencing factors from three perspectives: supply, demand, and futures market, and we use grey correlation analysis to screen the indexes. Secondly, we decompose and correct the prediction residual series of the WOA-LightGBM model using the CEEMDAN method in order to construct a combined WOA-LightGBM-CEEMDAN prediction model. The following conclusions were reached as a result of simulation experiments on hog futures price data.

Firstly, the decomposition and correction of the residual sequences generated by the WOA-LightGBM model using the CEEMDAN method can enhance the prediction accuracy of the model compared to a single machine learning model. In addition, the CEEMDAN method can extract the effective information of residual series at different frequency scales in the residual correction combination model compared with the EEMD and SVR models, thus improving the model prediction accuracy. Secondly, by applying this paper's model to the prediction problem of CSI 300 stock index futures prices, it is discovered that the combined model presented in this paper offers the highest level of prediction accuracy when compared with the comparison algorithm, indicating the applicability of this paper's model to other prediction problems. Finally, we used three machine learning models, LightGBM, XGBoost, and GBDT, to model and perform feature importance analyses on hog futures prices separately and found that sow price, piglet price, and

spot price are the most influential factors when predicting hog futures prices.

In light of the above research conclusions and the methods recommended in this paper, the following suggestions are made. To begin with, the CEEMDAN method employs the concept of "decomposition-individual forecasting-ensemble" to correct the residual series, which has the potential to improve the prediction accuracy of the model and establish a new method for researchers to use in future research projects on the prediction of financial data such as futures and stocks. Secondly, the combined model proposed in this paper can more accurately predict the future price trend compared with the single machine learning model, and investors are able to receive reference support for future investment decisions based on the forecasting results of the model. Finally, the LightGBM model is able to rank the features of the model as a function of the prediction process, thereby determining the most influential factors in the model's performance. Thus, for market regulators, the feature importance analysis of the LightGBM model can be used to adjust prices of factors that have the greatest influence on futures prices, thus achieving a regulation of futures prices.

It is important to note, however, that, in this paper, the time span of the hog futures prices examined is short, and the data sample is small, so the time series information of the hog futures prices is not fully utilized in building the model. Also, due to the short time span of the selected data, the cycle effect of hog futures prices was not taken into account when the data was processed. As such, future research should consider the cycle effects of hog futures prices, and the time series information should also be integrated into the forecasting process of the model in order to improve its forecasting performance.

## Data Availability

The data used to support the findings of this study are available from the corresponding author upon request.

## Conflicts of Interest

The authors declare no conflicts of interest.

## Acknowledgments

This research was funded by the National Natural Science Foundation of China (Grant no. 81973791).

## References

- [1] C. G. Sheng, G. Y. Wang, Y. D. Geng, and L. R. Chen, "The correlation analysis of futures pricing mechanism in China's carbon financial market," *Sustainability*, vol. 20, no. 18, 2020.
- [2] C. Y. Wang, "Forecast on price of agricultural futures in China based on arima model," *Asian Agricultural Research*, vol. 8, no. 11, pp. 9–12, 2016.
- [3] A. Trujillo-barrera, P. Garcia, and M. L. Mallory, "Short-term price density forecasts in the lean hog futures market,"

- European Review of Agricultural Economics*, vol. 45, no. 1, pp. 121–142, 2018.
- [4] O. V. De la torre-torres, D. Aguila-socho-montoya, and M. D. del rio-rama, “A two-regime markov-switching garch active trading algorithm for coffee, cocoa, and sugar futures,” *Mathematics*, vol. 8, no. 6, 2020.
  - [5] Q. H. Gu, Y. X. Chang, N. X. Xiong, and L. Chen, “Forecasting nickel futures price based on the empirical wavelet transform and gradient boosting decision trees,” *Applied Soft Computing*, vol. 109, 2021.
  - [6] J. Chai, Y. Wang, S. Wang, and Y. Wang, “A decomposition-integration model with dynamic fuzzy reconstruction for crude oil price prediction and the implications for sustainable development,” *Journal of Cleaner Production*, vol. 229, pp. 775–786, 2019.
  - [7] X. Wang, S. Gao, S. Y. Zhou, Y. B. Guo, Y. H. Duan, and D. Q. Wu, “Prediction of house price index based on bagging integrated WOA-SVR model,” *Mathematical Problems in Engineering*, vol. 2021, Article ID 3744320, 15 pages, 2021.
  - [8] W. P. Liu, C. Z. Wang, Y. G. Li, Y. S. Liu, and K. K. Huang, “Ensemble forecasting for product futures prices using variational mode decomposition and artificial neural networks,” *Chaos, Solitons & Fractals*, vol. 146, 2021.
  - [9] J. Manickavasagam, S. Visalakshmi, and N. Apergis, “A novel hybrid approach to forecast crude oil futures using intraday data,” *Technological Forecasting and Social Change*, vol. 158, Article ID 120126, 2020.
  - [10] J. H. Chen, S. F. Ma, and Y. Wu, “International carbon financial market prediction using particle swarm optimization and support vector machine,” *Journal of Ambient Intelligence and Humanized Computing*, vol. 2021, pp. 1–15, 2021.
  - [11] R. Y. Chen, B. Pan, and X. D. Lin, “Chinese stock index futures price fluctuation analysis and prediction based on complementary ensemble empirical mode decomposition,” *Mathematical Problems in Engineering*, vol. 2016, Article ID 3791504, 13 pages, 2016.
  - [12] J. Wang, J. Wang, and N. Zhang, “A new hybrid forecasting model based on SW-LSTM and wavelet packet decomposition: a case study of oil futures prices,” *Computational Intelligence and Neuroscience*, vol. 2021, Article ID 7653091, 22 pages, 2021.
  - [13] Y. L. Zhang and S. Hamori, “Forecasting crude oil market crashes using machine learning technologies,” *Energies*, vol. 13, no. 10, 2020.
  - [14] S. K. Deng, X. R. Huang, Z. H. Qin, F. Zhe, and T. X. Yang, “A novel hybrid method for direction forecasting and trading of apple futures,” *Applied Soft Computing*, vol. 110, 2021.
  - [15] G. H. Luo, J. Chen, and X. M. Ke, “Research on the simulation of futures commodity transaction price forecast,” *Computer Simulation*, vol. 35, no. 9, pp. 421–426, 2018.
  - [16] Y. Zhang, J. Chen, X. F. Wang, and F. Liu, “Application of xgboost to fault diagnosis of rolling bearings,” *Noise and Vibration Control*, vol. 37, no. 4, pp. 166–170, 2017.
  - [17] D. Li, J. Peng, and D. He, “Aero-engine exhaust gas temperature prediction based on lightgbm optimized by improved bat algorithm,” *Thermal Science*, vol. 22, no. 1, 2021.
  - [18] J. Yan, Y. T. Xu, Q. Cheng et al., “Lightgbm: accelerated genomically designed crop breeding through ensemble learning,” *Genome Biology*, vol. 22, no. 1, 2021.
  - [19] Y. Ju, G. Sun, Q. Chen, M. Zhang, H. Zhu, and M. U. Rehman, “A model combining convolutional neural network and lightgbm algorithm for ultra-short-term wind power forecasting,” *IEEE Access*, vol. 7, pp. 28309–28318, 2019.
  - [20] L. Zhang, Y. Dong, and J. Wang, “Wind speed forecasting using a two-stage forecasting system with an error correcting and nonlinear ensemble strategy,” *IEEE Access*, vol. 7, pp. 176000–176023, 2019.
  - [21] Y. Li, Z. J. Qian, W. Deng, D. Z. Zhang, H. H. Lu, and S. H. Wang, “Forecasting crude oil prices based on variational mode decomposition and random sparse bayesian learning,” *Applied Soft Computing*, vol. 113, 2021.
  - [22] M. Niu, Y. Hu, S. Sun, and Y. Liu, “A novel hybrid decomposition-ensemble model based on VMD and HGWO for container throughput forecasting,” *Applied Mathematical Modelling*, vol. 57, pp. 163–178, 2018.
  - [23] H. Liu and L. Shen, “Forecasting carbon price using empirical wavelet transform and gated recurrent unit neural network,” *Carbon Management*, vol. 11, no. 1, pp. 25–37, 2020.
  - [24] N. E. Huang, Z. Shen, S. R. Long et al., “The Empirical Mode Decomposition and the Hilbert Spectrum for Nonlinear and Non-stationary Time Series Analysis,” *Proceedings: Mathematical, Physical and Engineering Sciences*, vol. 454, no. 1971, pp. 903–995, 1998.
  - [25] Z. H. Wu and N. E. Huang, “Ensemble empirical mode decomposition: A noise — assisted data analysis method,” *Advances in Adaptive Data Analysis*, vol. 1, no. 1, pp. 1–41, 2009.
  - [26] M. E. Torres and M. A. Colominas, “A complete ensemble empirical mode decomposition with adaptive noise,” in *Proceedings of the 2011 IEEE International Conference on Acoustics, Speech and Signal Processing (ICASSP)*, pp. 4144–4147, Prague, Czech Republic, May 2011.
  - [27] W. Zhang, Z. Qu, K. Zhang, W. Mao, Y. Ma, and X. Fan, “A combined model based on CEEMDAN and modified flower pollination algorithm for wind speed forecasting,” *Energy Conversion and Management*, vol. 136, pp. 439–451, 2017.
  - [28] J. Wang, J. X. Cao, S. Yuan, and M. Cheng, “Short-term forecasting of natural gas prices by using a novel hybrid method based on a combination of the CEEMDAN-SE and the PSO-ALS-optimized GRU network,” *Energy*, vol. 233, 2021.
  - [29] J. Zhou and D. Chen, “Carbon price forecasting based on improved CEEMDAN and extreme learning machine optimized by sparrow search algorithm,” *Sustainability*, vol. 13, no. 9, 2021.
  - [30] J. Cao, Z. Li, and J. Li, “Financial time series forecasting model based on CEEMDAN and LSTM,” *Physica A: Statistical Mechanics and Its Applications*, vol. 519, pp. 127–139, 2019.
  - [31] CBS, *China Statistical Yearbook*, China Statistics Press, Beijing, China, 2020.
  - [32] A. Sharma and B. Singh, “AE-LGBM: Sequence-based novel approach to detect interacting protein pairs via ensemble of autoencoder and LightGBM,” *Computers in Biology and Medicine*, vol. 125, 2020.
  - [33] S. Mirjalili and A. Lewis, “The whale optimization algorithm,” *Advances in Engineering Software*, vol. 95, pp. 51–67, 2016.
  - [34] W. Z. Liang, S. Z. Luo, G. Y. Zhao, and H. Wu, “Predicting hard rock pillar stability using GBDT, XGBoost, and LightGBM algorithms,” *Mathematics*, vol. 8, no. 5, 2020.
  - [35] H. B. Luo and D. M. You, “Integrated prediction on stock index series based on main trend identification and intelligent error correction,” *Systems Engineering*, vol. 33, no. 2, pp. 24–30, 2015.
  - [36] Y. S. Zhu, W. H. Wang, and B. T. Han, “Grey correlative degree analysis of factors affecting demands in the real estate market,” *Transactions of Beijing Institute of Technology*, vol. 6, pp. 782–785, 2002.
  - [37] Y. Zhao, J. Li, and L. Yu, “A deep learning ensemble approach for crude oil price forecasting,” *Energy Economics*, vol. 66, pp. 9–16, 2016.

## Research Article

# Prediction and Classification of Financial Criteria of Management Control System in Manufactories Using Deep Interaction Neural Network (DINN) and Machine Learning

Amir Yousefpour  and Hamid Mazidabadi Farahani

*School of Civil Engineering, Iran University of Science and Technology, Tehran, Iran*

Correspondence should be addressed to Amir Yousefpour; [amir\\_yousefpour@cmps2.iust.ac.ir](mailto:amir_yousefpour@cmps2.iust.ac.ir)

Received 6 September 2021; Accepted 27 December 2021; Published 27 February 2022

Academic Editor: Sameh S. Askar

Copyright © 2022 Amir Yousefpour and Hamid Mazidabadi Farahani. This is an open access article distributed under the Creative Commons Attribution License, which permits unrestricted use, distribution, and reproduction in any medium, provided the original work is properly cited.

The management control system aids administrators in guiding a business toward its organizational plans; as a result, management control is primarily concerned with the execution of the plan and plans. Financial and nonfinancial criteria are used to create management control systems. The financial element focuses on net income, earnings, and other financial metrics. The two components of leadership strategy in this study are cost and differentiation, which highlight the strategy of differentiation in attaining higher quality due to the robust strategy's attention on a particular area of the company. In this study, we presented a novel method named deep interaction neural network to predict the performance of the manufacturing companies based on their leading competitors using features cost leadership and differentiation strategies. Moreover, the management control system is classified into two financial and nonfinancial factors based on machine learning methods. Based on the results, the presented factors can accurately estimate the company's performance based on management control criteria with a 93.48% R-square. Moreover, it can be seen that the DT method is presented with higher classification performance values.

## 1. Introduction

Companies' procedures and processes to succeed in executing strategies are referred to as management control systems. Coherence, incentive, decision support, intended outcomes, assessment, and other management control systems are all aided by management control systems. In a broader sense, a management control system is intended to adjust the business to the operating area to protect partners' interests. To put it another way, the management control system's objective is to provide a secure network for delivering valuable data for decision-making, planning, and evaluation processes [1]. Like other functional units, this system is expected to interact with the scenarios of the external structure, which are referred to as features. As a result, one of the significant management policies is the management control system and its connection with considerations, particularly the type of corporate objectives [2].

Leadership and management control systems have been the subject of practical empirical studies globally since the early 1980s [1, 3, 4]. All such studies focused primarily only on financial report control systems. However, the study led by Merchant and Otley [1] progressively discovered the limitations of this strategy with the need to consider other control dimensions and eventually developed a control package that combined different control mechanisms. Businesses utilize a collection of linked control mechanisms to realign actions with strategic mission, by this viewpoint [5]. There are several methods for the application of machine learning, optimization, and programming in control systems [6–9]. These processes combine to produce the management control system. It is impossible to have a correct understanding of it without considering their connection and interaction. In recent decades, there has been a modest improvement in investigating the phenomena of “control” because of this fact and technique. However, most research

linked to the design and construction of management control packages has focused solely on the efficacy of each control mechanism. For more than two decades, these processes have been ignored combined in many situations, such as the organization's strategy to attain successful control results after forming the closed approach. It has not yet been used perhaps and adequately in research. The management control system gathers and analyzes data to assess the performance of different business assets, such as personnel, technical, and financial resources, and the organization while taking organizational plans into account. Finally, the attitude of organizational resources to developing the conceptual framework is influenced by the management control system [10]. The management control system aids managers in guiding an organization toward its critical planning; as a result, management control is primarily concerned with the execution of the plan and plans [11, 12]. Financial and nonfinancial factors are used to create management control systems. The financial element focuses on net income, earnings, and other financial metrics. Nevertheless, nonfinancial purposes such as quality products, customer happiness, sales involvement, timely submission, and staff ethics apply to all organizational subcategories. Based on financial and nonfinancial aspects, management control systems are divided into two subgroups. We introduced a unique approach called deep interaction neural network in this study to forecast the operating efficiency of firms based on their top rivals' cost leadership and differentiation tactics. Furthermore, using machine learning approaches, management control systems are divided into two groups depending on financial and nonfinancial aspects. The outcomes are shown in the following sections.

## 2. Literature Review

Malm and Brown [4] state that their approach is based on a survey of 40 years of control research. They present five control typologies that, together with the second structure, were given by Merchant and Van der Stede [13]; the most widely used control schema in academia [13]. Abadi et al. [14] have optimized the scheduling of nurses for the healthcare system [15]. Ahmadi et al. [15] have used a new model for selecting users with Q-reinforcement learning and machine learning methods [15]. Huang et al. [16] studied performance goals, community affiliation, and online collaboration ability to reflect connections. They for reach out to their destination using a deep learning method have used [16]. Wu et al. [17] have designed a new machine learning model for combining techniques to improve high-impact bug report forecasting [17]. He et al. [6] have analyzed multideep learning to classify users in the centric network [18]. Ahmadi et al. [19] and Taghizadeh et al. [20] have designed a new model from machine learning that is regarding genetic algorithm for forecasting the GDP with ARDL bound test [19, 20]. Liu et al. [21] have analyzed an unsupervised approach for area flexibility in heterogeneous industries [21]. Dong et al. [22] have examined unsupervised

feature training with learning aggregation-induced suitability vision [22]. Zhou et al. [23] have analyzed a new model for coding optimization. They have used a machine learning model in AVS2 [23]. Lv et al. [24] investigated spatial public goods games using PSO. The result shows that the proposed model has high accuracy [24]. Sharifi et al. [25] have studied the application of machine learning and digital style on control systems in the industry [25]. Ghorbani et al. [26] have analyzed risk hedging for call options in investments. Also, in another research, Ghorbani et al. [27] have studied on-call and put option pricing in investments [27]. Ahmadi [14] has evaluated a new economic growth model using a computational approach and fuzzy MCDM [14]. Prasad et al. [28] have used a surface technique and machine learning methods for methylene blue removal in the industry [28]. Ghorbani [29] has analyzed option pricing with investment using the random rate [29]. Korzeniowski et al. [30] have used put options using a linear programming for hull-white investment [30]. Zhang et al. [31] have investigated an optimization model for E-healthcare systems. The result shows that the proposed model is applied in the industry [31]. Ahmadi et al. [32] have studied a new hybrid approach for predicting GDP using machine learning approaches [32]. Artin et al. [33] have learned a new method for predicting traffic using ensemble learning and machine learning [33]. Merchant and Van der Stede [13] proposed a taxonomy of organizational control mechanisms that are based on the topic of administration and divide different forms of control into three fundamental classifications: (1) centers for financial responsibility, (2) incentive compensation mechanisms, and (3) financial management control methods, such as control of outcomes, activities, employees, and society, according to Merchant [2]. In human resources, behavioral outcomes such as work satisfaction have been critical. Some people consider providing a positive work activity to enhance employee welfare or job satisfaction to be a good aim in and of itself. Furthermore, it is reasonable to assume that employees who are content with their occupations would identify with organizational goals and perform more successfully, and all other factors are equal. Self-assessment procedures, in which employees offer an estimate of their performance or organizational unit across a range of potentially relevant management activities or goals, have dominated organizational outcomes in the contingency-based study [34]. More advanced technology, established operational processes, high levels of experts, and job norms were all part of administrative control. According to employers, employees were thought to have a high amount of authority and engagement in defining standards, and they spent more time budgeting [34] (see Table 1).

It is crucial to evaluate accounting information as part of a set of methods of control in order to describe how the financial report control system method conforms to the organizational framework of the company, one of the most significant of which is tactic; in those other words, it is supposed that companies, cash flows, and other control methods are meaningfully developed and built together [13]. Moradi et al. [44] investigated the influence of

TABLE 1: Principles and a review of objective research for management control systems.

Management control mechanisms	Definition	Relationships	Empirical evidence
<i>Financial control scheme</i>			
Diagnostic control	Observes events by looking for breaches from present criteria.	Defense (+) Aggressive (-)	Simons [35]
Interactive control	Principles that make significant of the subgroup to talk, communicate, educate, and try to find ways.	Defense (-) Aggressive (+)	Simons [36]
Financial control intensity	Accountability for meeting well before performance objectives, which may or may not be stringent.	Defense (+) Aggressive (-, +)	Simons [37]
Variety of criteria	Requirements for effectiveness: restricted to broad	Defense (-) Offensive (+)	Merchant [38] Simons [37]
<i>Motivational control scheme</i>			
Motivational payments	There is a monetary incentive for motivating staff.	Defense (-) Offensive (+)	Simons [39]
How to determine motivational factors	Regarding management evaluations (perception and intellectual) or present (objective) formulae	Defense (+) Aggressive (-)	Govindarajan and Fisher [40] Simmons [41]
<i>Structural control scheme</i>			
Type of organizational structure	Human authority, decision-making, and interaction patterns	Defense (-) Aggressive (+)	Langfield-Smith [42]
<i>Cultural control scheme</i>			
Recruitment and selection control	To match personal views with the interest of the company, use recruitment, and instructional strategies.	Defense (-) Aggressive (+)	Abernethy [43]

transformational leaders' style and management control systems on cooperative and private company management performance. The route analytical framework was utilized to evaluate the data. The Sobel test was employed to assess the control variables. The findings revealed that transformational leadership and three different approaches to developing management control systems could have a direct and indirect positive impact on management efficiency. The Sobel test technique was used to study the role of the mediator variable, which revealed that the robust performance assessment system, reward system, and BSA system all play a mediating role in connection to factors.

According to the concept of appropriateness, no one management control system matches all companies and their textural features. According to this idea, the features of each organization determine the particular properties of an application system. This concept aims to compare organizational features and procedures. In East Java, Indonesia, Riyadi et al. [45] investigated the impact of supply networks and management control systems on production businesses' efficiency and profitability. With rising competition, it is necessary to develop an integrated system in order to achieve corporate profitability. The study's significant result is that businesses should be aware of the social environment produced as part of the supply chain since it can potentially diminish the value of a company's profitability if not built properly and precisely. Dana et al. [46] present an analysis of the literature in management control systems and the intellectual capital accounting method in logistics and how these concepts connect to business performance durability. Intellectual capital is one of the most significant aspects of the value chain in the direction of value creation. Quantifying and presenting

intellectual capital allows managers and stakeholders to be successful in running the company. Feder and Weissenberger [47] investigate the factors that lead to establishing such a CSR-related management controller and the resulting performance impacts of German businesses. It claims that the perceived significance of CSR, stakeholder expectations, and proactiveness of top-level management impact the presence of CSR-related formal and informal regulations, based on legitimacy theory. The article concludes that firms should have a favorable attitude toward CSR and should aggressively integrate comparable features into their internal control systems based on the findings. Companies may also direct their CSR-related actions and create good performance impacts by incorporating CSR-related features into their management control systems, including formal and informal controls. Owolabi et al. [48] aimed to look at the link between the design and usage of performance measuring innovations and organizational results across Nigerian listed companies. It suggests that utilizing performance measuring technologies in a diagnostic approach creates a bad picture of the client, but this is not the case when used interactively.

### 3. Methods and Materials

Management control systems have been classified in several ways in finance literature. These subcategories are formal and informal controls, experience and control outcomes, and poor financial and nonfinancial regulations [35, 42]. The contrast between financial and nonfinancial controls has been considered in these several categories, which have been used to investigate the link between the management control system and plan [49, 50]. As a result, it has been claimed that

in order to better link management control systems to the present competitive climate, nonfinancial analysis, in addition to short-sighted economic information, is required [51]. Simon utilized controls, diagnosis, and confrontation as a framework for analyzing the differences among financial and nonfinancial management control systems. Identification control has a backward and intraorganizational strategy and is connected with financial management control systems; mutual administration, on the other hand, is linked with nonfinancial management control systems and moves forward externally. In business planning, financial and nonfinancial factors are essential; as a result, the management control system is divided into two main types in this study: financial and nonfinancial. Suppose such an examination allows for a more comprehensive assessment of the management control system's connection in businesses. According to [34], there is a pressing need for research into the nonfinancial aspects of management control systems. Such interactive types of control can improve managers' capacity to foresee and handle unpredictable upcoming scenarios, particularly changing events in a competitive corporate environment [52]. As a result, nonfinancial control is also considered while dealing with these financial investigations.

The following financial management control system aspects have been studied in the literature:

- (i) Cost norms
- (ii) Deviation evaluation
- (iii) Financial management
- (iv) Recruitment expenses
- (v) Overhead expenses
- (vi) Cost-benefit analysis

The following are nonfinancial management control system aspects that have been studied in management control system publications:

- (i) Customer appreciation
- (ii) Timely and dependable delivery
- (iii) Key product activity measures
- (iv) Quality
- (v) Testing (a continual process of comparing product, service, and assignments and responsibilities to that of rivals)
- (vi) Employee-based solutions
- (vii) Organizational strategies

Each theoretical model serves as a foundation for research by determining the required factors and their interactions. In other aspects, the conceptual model, also known as a mind map or analytical tool, is ideally used to initiate and conduct research. If predicted, the factors, connections, and interactions between them were evaluated and tested during the study's deployment. As needed, modifications were made, and some of them were decreased or increased. In essence, Porter's triple model is referred to as Porter's generic strategies model, depicted in Figure 1 under three approaches.

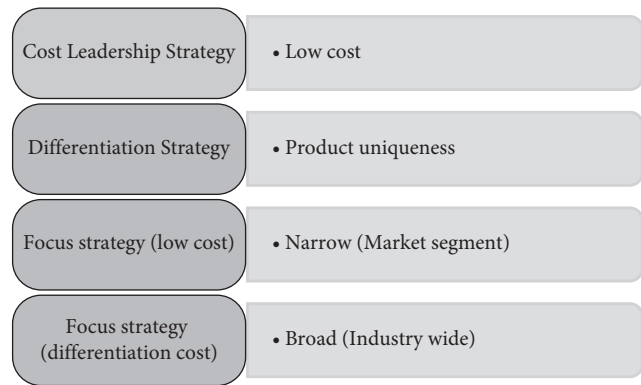


FIGURE 1: Porter's generic three strategies' methods.

The two factors of leadership strategy in this investigation are cost and differentiation, which highlight the strategy of differentiation in attaining higher quality due to the focus strategy's attention on a specific industry area. Wherever feasible, the leadership approach stresses cost minimization. Figure 2 lists the features of each of these different sorts of tactics.

The financial and nonfinancial management control systems, on the other hand, are both relevant when it comes to the strategic plan; thus, the management control system is separated into financial and nonfinancial subgroups in this research since these analyzes allow for a broad assessment of management control system's partnership in businesses. Cost norms, analysis reports, financial management, recruiting cost and variable cost, and overhead evaluation are some of the financial management control system aspects addressed in management control studies. Studies have demonstrated that accepting a specific corporate strategy may enhance performance through timely and dependable delivery, measurements linked to crucial productivity tasks, quality, comparability, employee-based measures, and strategy development [53, 54].

Firms seeking a differentiation strategy are less likely to prioritize planning. In contrast, those pursuing a cost leadership approach are more likely to stress capital budgeting assessment [40]. Financial control has resulted in higher performance indicators for a low-cost tactic; however, controls based on nonfinancial or social processes have resulted in higher effectiveness for a differentiation strategy. Differentiation strategy involves nonfinancial elements to inspire innovation and creativity [42] (Porter, 1980). The observations of a recent study back up previous reports that firms with low costs significantly outperformed when they used financial controls and companies with higher differentiation performed much better when they used nonfinancial factors [42]; thus, the nonfinancial management control system is coherent with a differentiation strategy, while the financial management control system is coherent with a differentiation strategy (see Figure 2).

## 4. Results and Discussion

*4.1. Data Collection and Questionnaire.* Questions regarding management control systems first introduce the notion of

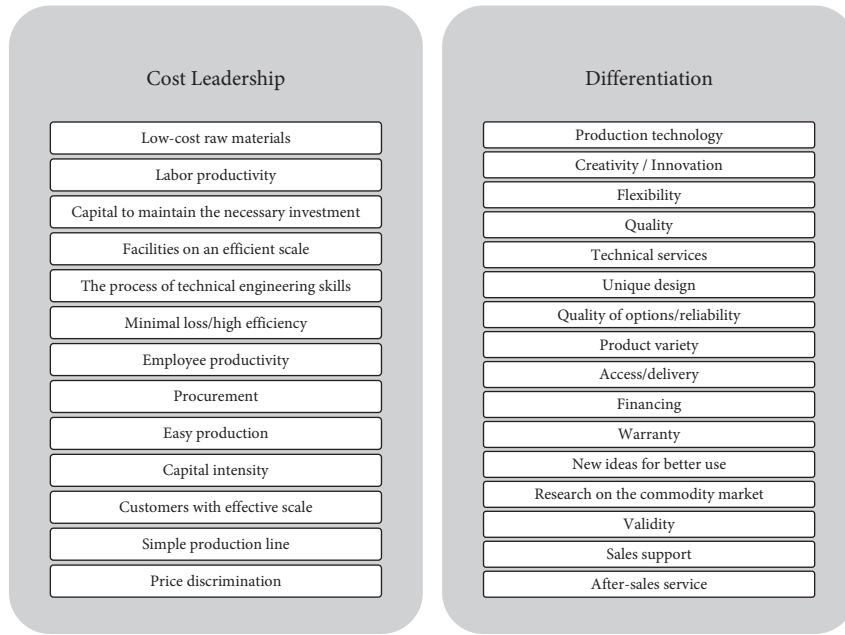


FIGURE 2: Cost leadership and differentiation strategy characteristics.

management control systems to provide responders greater transparency. After that, concerns about management control systems based on financial and nonfinancial aspects are given in two parts. It has 13 nonfinancial factors questions and 16 financial factors questions on a scale of 1 to 9. For an indefinitely large population, Cochran’s formula is employed. The statistical population is likely to have a sample size of SD2, which is defined by the degree of dispersion or variation between items and surveys.

4.2. *The Presented Method of Financial Assessment of Management Control System.* This study is made up of five factors, one of which is the company’s plan. First, the company’s management control system is also investigated, which is an adjusting factor. Next, the company’s productivity is assessed, which is the research’s regression coefficient. The management control system is separated into two factors: financial factors-based management control and nonfinancial factors-based management control, using the following four estimation methods (see Figure 3).

All factors are contained in regressors, which are used to verify the specific hypothesis and included as follows:

- (1) P: the performance of the business is equivalent to that of its main rival
- (2) CLS: the level to which a company’s strategy conforms to a cost-cutting plan
- (3) DS: how well a company’s strategy aligns with its differentiation strategy
- (4) FMCS: financial management control system (FMCS) conformance
- (5) NFMCS: nonfinancial control management system (NFMCS) conformance

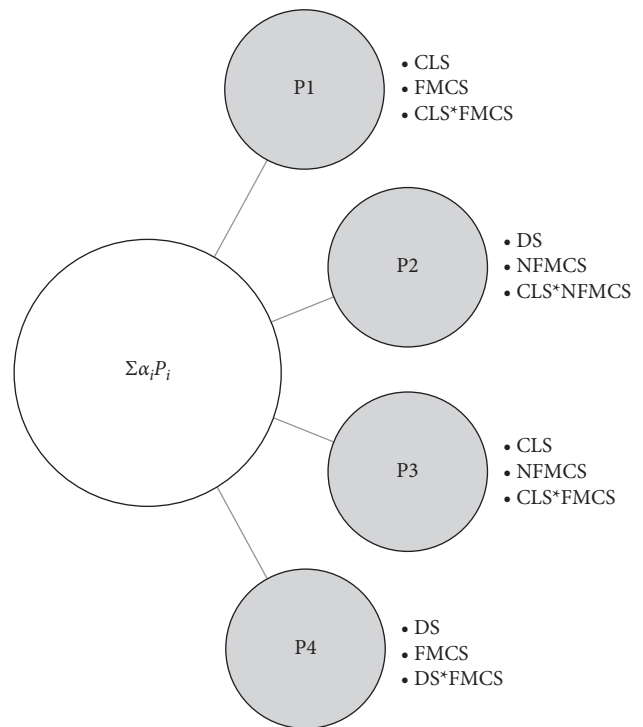


FIGURE 3: The primary equation system of the research.

A questionnaire achieves it with a value ranging from 1 to 9. Other factors in this study and the performance assessment as a dependent variable will serve as independent and control variables, depending on the hypothesis investigated. They will also serve as moderator factors in the case of financial and nonfinancial management control system factors.

Figure 4 shows the DINN that has been provided. It is a type of artificial neural network feedforward technique. It

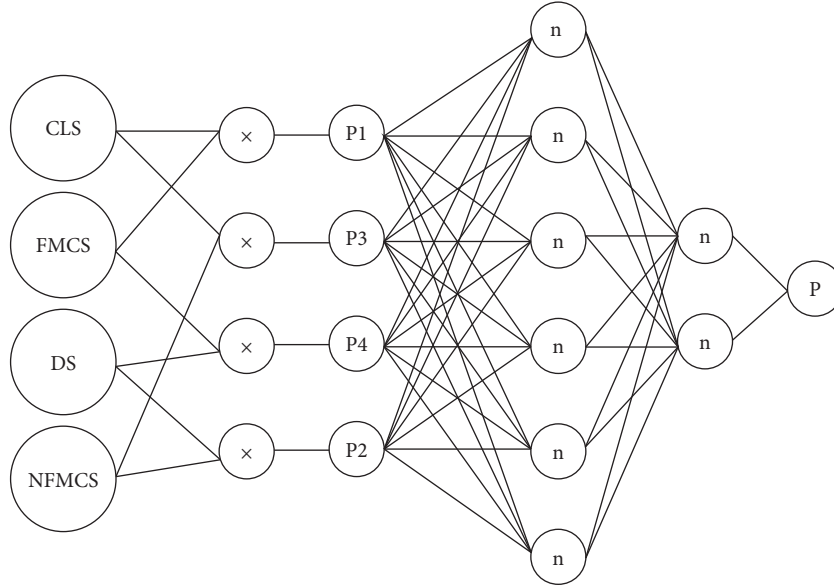


FIGURE 4: The architecture of deep interaction neural network.

has at least five levels, including an input layer that contains the problem's input variables. Based on the governing research problem, the interaction layer is the second layer (see Figure 4). Input and interaction characteristics are included in the third layer, which is the secondary variable layer. The hidden layer of the ANN method includes neurons and weights of each feature in the governing issue in the fourth layer (layers). The last layer is the output layer, which is the goal or dependent variable. Any hidden layers may be reduced to a two-layer input-output system if a DINN has a linear activation function in all neurons; that is, a linear function maps the weighted inputs to the output of each neuron. Some neurons in DINN employ a multilayer perceptron created to simulate the frequency of actual neurons' nerve impulses. The most frequent activation function is sigmoid, which is defined as follows:

$$\log \text{Sig}(v_i) = (1 + e^{-v_i})^{-1}. \quad (1)$$

After each input item is processed, the perceptron learns by adjusting connection weights based on the degree of inaccuracy in the output relative to the predicted result with a learning rate of  $10^{-5}$ . Backpropagation, a refinement of the least mean squares method in the linear activation functions, is used in supervised methods.

**4.3. Results of Prediction Using Presented DINN.** The main feature of the study for performance analysis of management control systems is presented in Figure 2. It contains two categories such as cost leadership with 16 features and differentiation including 13 features. The values of each feature are extracted from the questionnaire based on a rate from 1–9. The lower value means the lower importance of each feature. Moreover, it is separated into two financial and nonfinancial features used in the study's classification section. The input and output features of the presented DINN method are as follows (see Figure 1):

- (i) (x1): MCLS: the mean value of the degree to which a company's strategy adapts to the cost leadership strategy
- (ii) (x2): MDS: the mean value of the degree to which a company's strategy adapts to the differentiation strategy
- (iii) (x3): FMCS: the mean value of the compliance with the financial management control system
- (iv) (x4): NFMCS: the mean value of the compliance with the nonfinancial control management system
- (v) (x5): x1.x3: the interaction between x1 and x3
- (vi) (x6): x1.x4: the interaction between x1 and x4
- (vii) (x7): x2.x3: the interaction between x2 and x3
- (viii) (x8): x2.x4: the interaction between x2 and x4
- (ix) (y) P: the performance of the company is comparable to its leading competitor

In this study, the novel ANN architecture is presented based on the interaction of the input variables. DINN architecture is illustrated in Figure 4. It contains six layers that consist of input layer with 4 variables of  $X = \{x1, \dots, x4\}$  and four interaction layers as  $X_{in} = \{x5, \dots, x8\}$ . The third layer is the secondary variable layer includes input and interaction feature  $X = \{x1, \dots, x8\}$ . The 4<sup>th</sup> and 5<sup>th</sup> layers are hidden layers of the DINN approach that includes 20 and 10 neurons, respectively, in the governing architecture. Finally, the last layer is the output layer which is the target or dependent variable of Y.

The results of prediction using the presented DINN method are presented in Figures 5 and 6. Based on the training process with 7000 epochs, the output results are presented with 93.48% R-square. Moreover, the absolute mean square error is 0.655 which is illustrated in Figure 5. The output value is connected to the target value with the expression of  $Y_{\text{predicted}} = 0.86 Y_{\text{Target}} + 0.73$ .



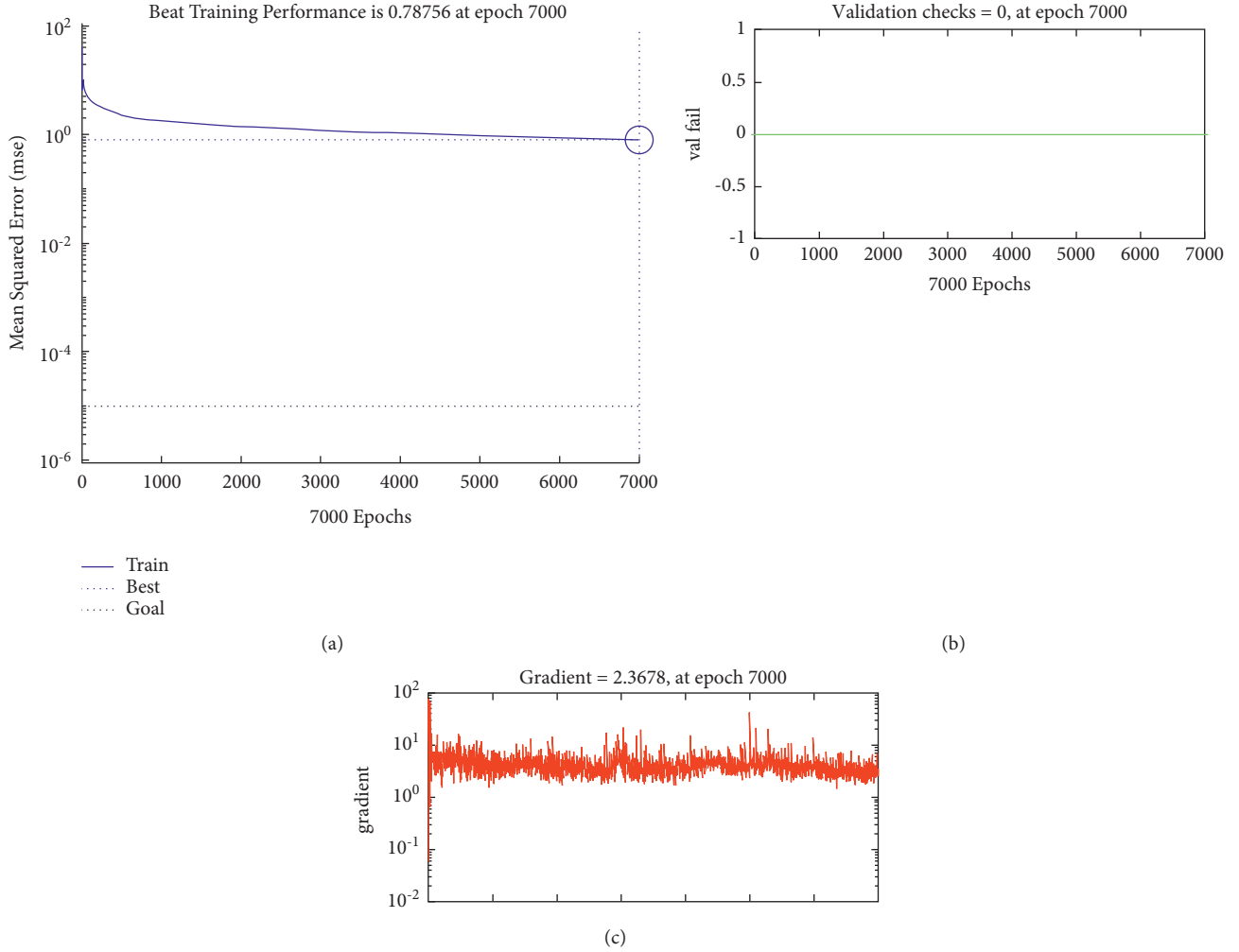


FIGURE 5: Results of the DINN method for performance prediction. (a) Error value in the training process, (b) failure value in the training process, and (c) the value of the gradient of the target and model value.

#### 4.4. The Results of Classification Using Machine Learning.

In this study, participants rate each feature based on a 1–9 importance scale. Finally, it is computed that each one emphasizes of financial criteria of the nonfinancial control system. Based on the input variables of the last section as  $X = \{x1, \dots, x8\}$  and categorical variable of financial (1) and nonfinancial (0) class, the classification is done. Therefore, this study used five machine learning methods to diagnose and classify the participants' financial and nonfinancial comments. The methods include K-nearest neighbor (KNN), support vector machine (SVM), linear discrimination analysis (LDA), Naïve Bayesian (NB), and decision tree (DT).

The sensitivity and specificity of the two indicators' statistics are utilized to evaluate the binary classification result (duality). The accuracy of the findings of a test that divides the information into these two categories may be measured and described using sensitivity and attribute indicators when the data can be separated into positive and negative groups. Sensitivity refers to the percentage of affirmative situations that are accurately identified as such. The fraction of negative

situations that are accurately identified as negative is referred to as specificity.

- (i) True positive (TP): the financial comment is detected correctly.
- (ii) False positive (FP): the nonfinancial comment is detected with mistakes.
- (iii) True negative (TN): the nonfinancial comment is detected correctly.
- (iv) False negative (FN): the financial comment is detected with mistakes.

The sensitivity of splitting the number of true-positive instances into the sum of true-positive and false-negative cases in mathematical language is as follows:

$$\text{sensitivity} = \frac{TP}{TP + FN} \quad (2)$$

Similarly, specificity causes genuine negative cases to be divided into false-positive and true-negative cases.

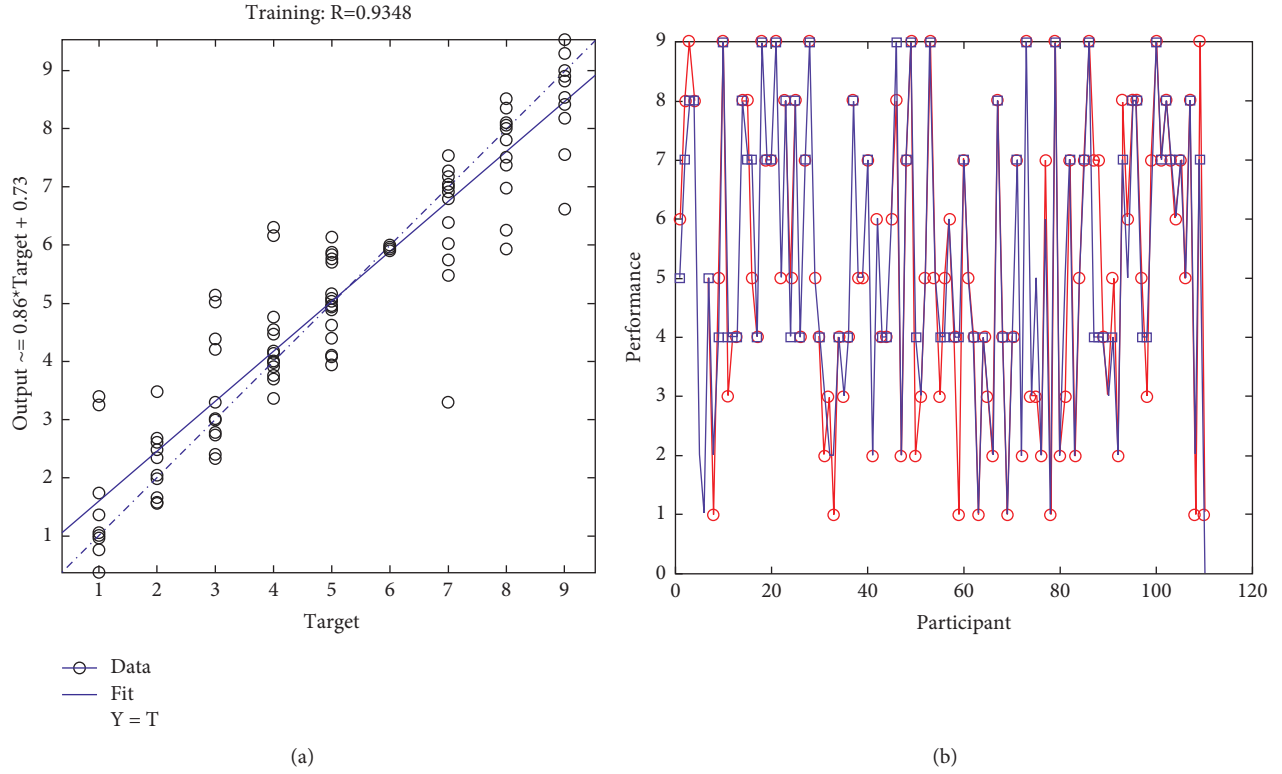


FIGURE 6: Results of the DINN method for performance prediction. (a) Scatter plot of the performance and (b) the observation plot of the performance of management control system.

$$\text{specificity} = \frac{\text{TN}}{\text{TN} + \text{FP}}, \quad (3)$$

$$\text{precision} = \frac{\text{TP}}{\text{TP} + \text{FP}}, \quad (4)$$

$$\text{accuracy} = \frac{\text{TN} + \text{TP}}{\text{TN} + \text{TN} + \text{FP} + \text{FN}}. \quad (5)$$

The test's nature and kind determine the sensitivity and specificity of a test. The outcome of a test, on the other hand, cannot be evaluated only based on sensitivity and specificity. The confusion matrix is a representation of the operation of algorithms in AI technology. This example is most commonly employed in supervised learning algorithms, although it may also be utilized in unsupervised learning. The anticipated value is shown in each matrix row if each column has a valid (true) case.

The results of confusion matrixes in the classification process are illustrated in Figures 7 and 9. Of 110 participants, 47 emphasized positive (financial) orientation, and 63 focused on negative (nonfinancial) class. Regarding the results of the KNN method in Figure 7, 96.8% are diagnosed correctly from financial comments. Moreover, from the nonfinancial group, 46 (97.9%) are located in the negative category. Therefore, the sensitivity and specificity of the KNN are 96.8% and 97.9%, respectively. Moreover, the precision of the KNN is 98.4%. In other words, from all the detected financial comments, 98.4% are correct. Finally, the accuracy of the KNN classifier is 97.3%.

Based on the results of the SVM method in Figure 7, from financial comments, 62 (98.4%) are diagnosed correctly. Moreover, from the nonfinancial group, 46 (97.9%) are located in the negative category. Therefore, the sensitivity and specificity of the SVM are 98.4% and 97.9%, respectively. Moreover, the precision of the SVM is 98.4%, and the accuracy of the SVM classifier is 98.2%. The false detection has occurred in two of the participants.

Regarding the results of the LDA approach in Figure 8, from the financial participant, 53 (84.1%) are detected correctly. Also, from the nonfinancial class, 43 (91.5%) are detected in the nonfinancial group. Therefore, the sensitivity and specificity of the LDA are 84.1% and 91.5%, respectively. Moreover, the precision of the LDA is 93.0%. In other words, from all the detected financial comments, 93.0% are correct. Moreover, the accuracy of the LDA classifier is 87.3%. Also, the finding of the NB method is presented in Figure 8; from 63 financial comments, 60 (95.2%) are found correctly. Also, from 47 nonfinancial groups, 44 (93.6%) are located in the negative class. Thus, the sensitivity and specificity of the NB are 95.2% and 93.6%, respectively. Moreover, the precision and accuracy of the NB are 95.2% and 94.5%, respectively. The final method is DT presented in Figure 9 that TP, FP, TN, and FN are 63, 0, 46, and 1, respectively. Therefore, the sensitivity and specificity of the DT are 100% and 97.9%, respectively. Moreover, the precision of the DT is 98.4%, with an accuracy of 99.1%. The ROC curve is also presented in Figure 10 to illustrate the classifier scores and performance well. The ROC curve is plotted based on the FP rate versus the TP rate. Based on the results, a lower FP rate with a higher TP rate is desirable.

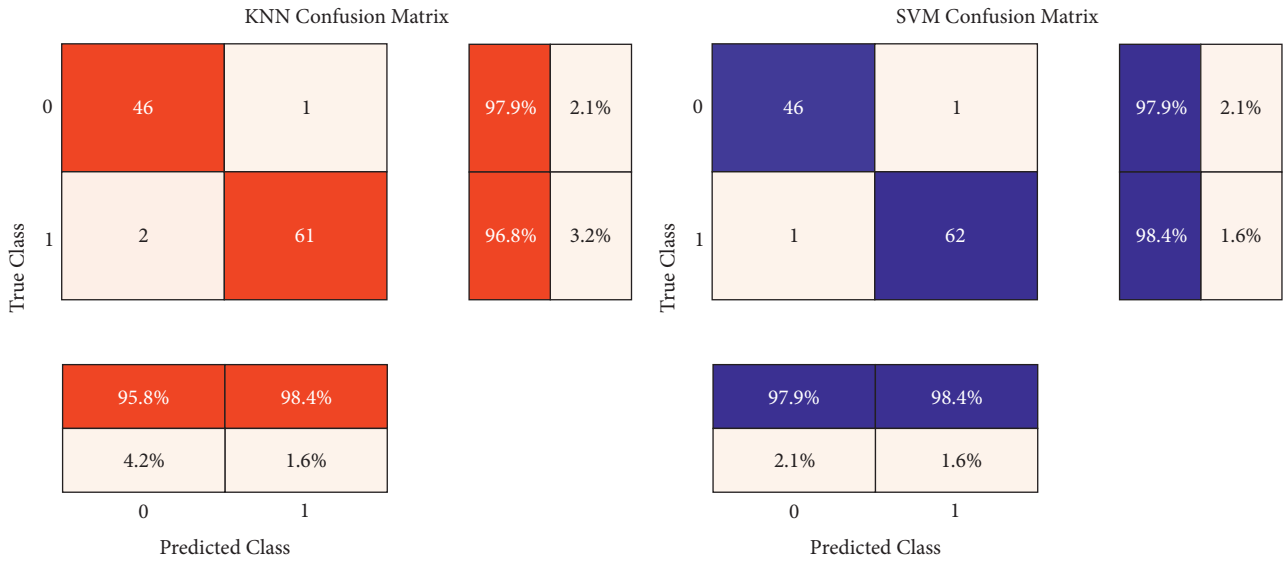


FIGURE 7: Confusion matrix of KNN and SVM methods.

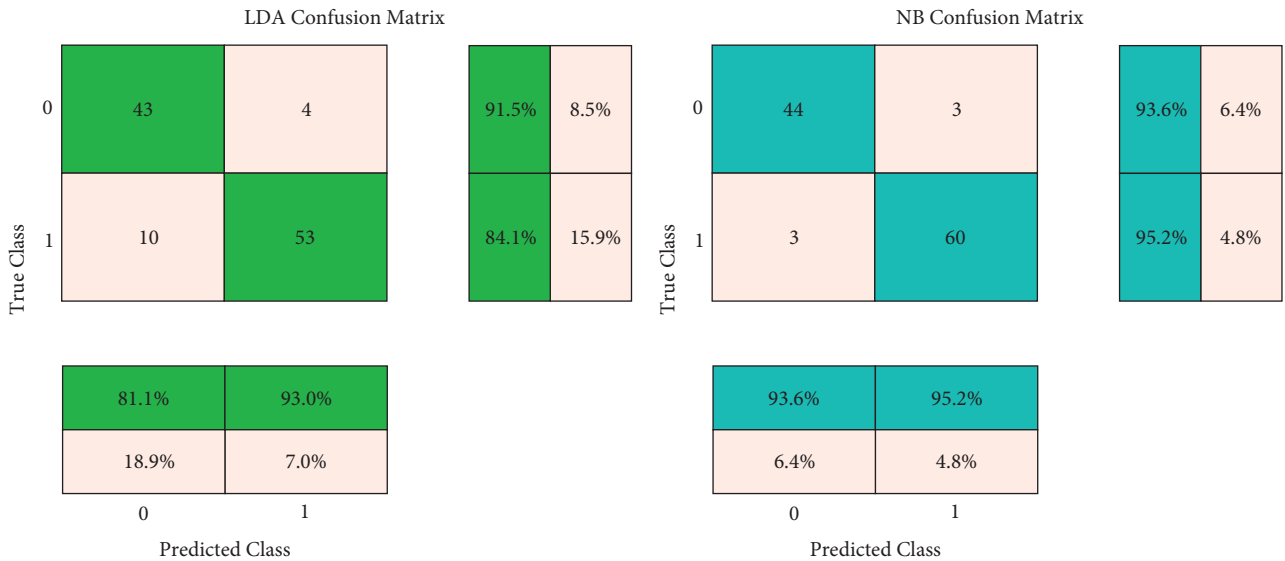


FIGURE 8: Confusion matrix of LDA and NB methods.

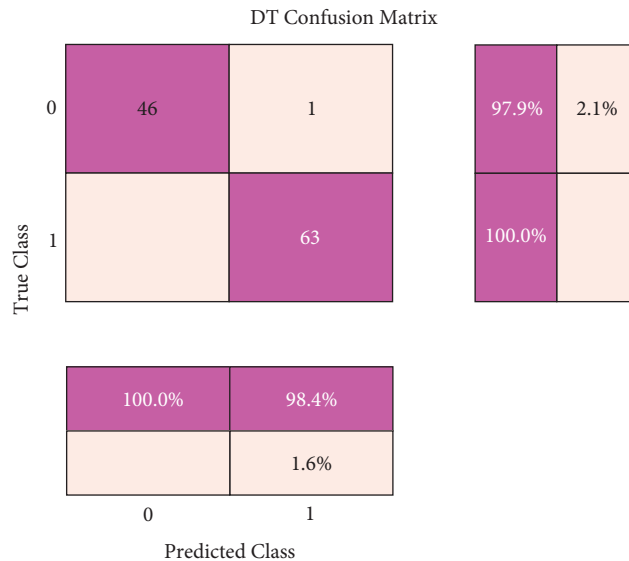


FIGURE 9: Confusion matrix of DT method.

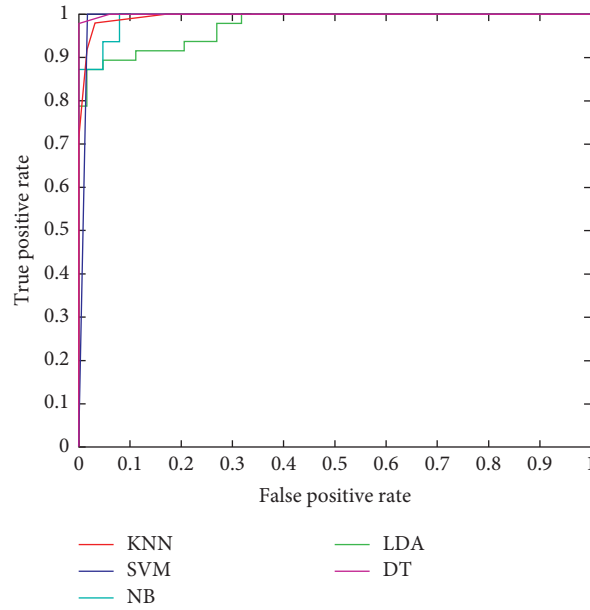


FIGURE 10: The ROC curve for the presented classifiers.

TABLE 2: The comparison between the presented machine learning classifiers.

Method	Sensitivity (%)	Specificity (%)	Precision (%)	AUC (%)	Accuracy (%)
KNN	96.8	97.9	98.4	99.46	97.3
SVM	98.4	97.9	98.4	99.16	98.2
LDA	84.1	91.5	93.0	97.26	87.3
NB	95.2	93.6	95.2	99.19	94.5
DT	100	97.9	98.4	99.93	99.1

Based on the comparison between the presented machine learning classifiers to detect financial and nonfinancial control management systems in Table 2, it can be seen that the DT method is presented with higher classification performance values. Based on the results, the higher accuracy belongs to DT with 99.1% with 100% sensitivity. Moreover, AUC is the area under the ROC curve to illustrate the performance of the classifiers. The higher value of AUC also belongs to the DT classifier.

## 5. Conclusion

It is essential to evaluate each of the elements in terms of causality to comprehend the efficacy of factors in research with the nature of causal circumstances. Each case will have its own set of criteria for determining the need and sufficiency of causative circumstances. Factors that interact with one another have an interaction impact, increasing or diminishing the desired outcome. The two categories of leadership strategy in this study are cost and differentiation, which highlight the strategy of differentiation in attaining higher quality due to the focus strategy's attention on a specific industry area. Wherever feasible, the leadership approach stresses cost minimization. The financial and nonfinancial management control systems, on the other hand, are both critical when it comes to company strategy;

thus, the management control system is split into financial and nonfinancial categories in this study since such analysis allows for an influence society of management control program's connection in industries. The results of prediction using the presented DINN and classification using machine learning methods are as follows. Based on the training process with 7000 epochs, the output results are presented with 93.48% R-square. Moreover, the mean square error is 0.655. Regarding the results of the KNN method, the sensitivity and specificity of the KNN are 96.8% and 97.9%, respectively. Moreover, the precision of the KNN is 98.4%. In other words, from all the detected financial comments, 98.4% are correct. Finally, the accuracy of the KNN classifier is 97.3%. Moreover, in the SVM from the nonfinancial group, 46 (97.9%) are located in the negative category. From financial comments, 62 (98.4%) are diagnosed correctly. Also, the precision of the LDA is 93.0%. In other words, from all the detected financial comments, 93.0% are correct. Moreover, the accuracy of the LDA classifier is 87.3%. Furthermore, the sensitivity and specificity of the NB are 95.2% and 93.6%, respectively. It can be seen that the DT method is presented with higher classification performance values. Based on the results, the higher accuracy belongs to DT with 99.1% with 100% sensitivity in comparison with other classifiers. For the future of the presented work, it can be suggested that the researchers focused on classification

and performance analysis of the other aspects of the Merchant theory for analysis of the manufactories and production companies.

## Data Availability

Article data were collected through a questionnaire.

## Conflicts of Interest

The authors declare no conflicts of interest.

## References

- [1] K. A. Merchant and D. T. Otley, "A review of the literature on control and accountability," *Handbook of Management Accounting Research*, vol. 2, pp. 785–802, 2007.
- [2] K. A. Merchant, *Control in Business Organizations*, Ballinger, Cambridge, England, 1985.
- [3] D. T. Otley, "The contingency theory of management accounting: achievement and prognosis," *Accounting, Organizations and Society*, vol. 5, no. 4, pp. 413–428, 1980.
- [4] T. Malmi and D. A. Brown, "Management control systems as a package—Opportunities, challenges and research directions," *Management Accounting Research*, vol. 19, no. 4, pp. 287–300, 2008.
- [5] D. S. Bedford, T. Malmi, and M. Sandelin, "Management control effectiveness and strategy: an empirical analysis of packages and systems," *Accounting, Organizations and Society*, vol. 51, pp. 12–28, 2016.
- [6] S. He, F. Guo, Q. Zou, and HuiDing, "MRMD2.0: a Python tool for machine learning with feature ranking and reduction," *Current Bioinformatics*, vol. 15, no. 10, pp. 1213–1221, 2021.
- [7] M. Ahmadi and M. Qaisari Hasan Abadi, "A review of using object-orientation properties of C++ for designing expert system in strategic planning," *Computer Science Review*, vol. 37, Article ID 100282, 2020.
- [8] A. Ala, F. E. Alsaadi, M. Ahmadi, and S. Mirjalili, "Optimization of an appointment scheduling problem for healthcare systems based on the quality of fairness service using whale optimization algorithm and NSGA-II," *Scientific Reports*, vol. 11, no. 1, pp. 19816–19819, 2021.
- [9] G. Briganti, M. Scutari, and P. Linkowski, "A machine learning approach to relationships among alexithymia components," *Psychiatria Danubina*, vol. 32, pp. 180–187, 2020.
- [10] D. T. Otley and A. J. Berry, "Control, organisation and accounting," *Accounting, Organizations and Society*, vol. 5, no. 2, pp. 231–244, 1980.
- [11] P. M. Collier, "Entrepreneurial control and the construction of a relevant accounting," *Management Accounting Research*, vol. 16, no. 3, pp. 321–339, 2005.
- [12] Z.-X. Zhang, P. S. Hempel, Y.-L. Han, and D. Tjosvold, "Transactive memory system links work team characteristics and performance," *Journal of Applied Psychology*, vol. 92, no. 6, pp. 1722–1730, 2007.
- [13] K. A. Merchant and W. A. Van der Stede, *Management Control Systems: Performance Measurement, Evaluation and Incentives*, Pearson Education, London, England, 2007.
- [14] M. Ahmadi, "A computational approach to uncovering economic growth factors," *Computational Economics*, vol. 58, no. 4, pp. 1051–1076, 2021a.
- [15] M. Ahmadi, T. Ali, D. Javaheri, A. Masoumian, S. J. Ghousechi, and Y. Pourasad, "DQRE-SCnet: a novel hybrid approach for selecting users in federated learning with deep-Q-reinforcement learning based on spectral clustering," *Journal of King Saud University-Computer and Information Sciences*, 2021.
- [16] C. Huang, X. Wu, X. Wang, T. He, F. Jiang, and J. Yu, "Exploring the relationships between achievement goals, community identification and online collaborative reflection: a deep learning and bayesian approach," *Educational Technology & Society*, vol. 24, no. 3, pp. 210–223, 2021.
- [17] X. Wu, W. Zheng, X. Chen, Y. Zhao, T. Yu, and D. Mu, "Improving high-impact bug report prediction with combination of interactive machine learning and active learning," *Information and Software Technology*, vol. 133, Article ID 106530, 2021.
- [18] Y. He, L. Dai, and H. Zhang, "Multi-branch deep residual learning for clustering and beamforming in user-centric network," *IEEE Communications Letters*, vol. 24, no. 10, pp. 2221–2225, 2020.
- [19] M. Ahmadi and R. Taghizadeh, "A gene expression programming model for economy growth using knowledge-based economy indicators: a comparison of GEP model and ARDL bounds testing approach," *Journal of Modelling in Management*, vol. 14, 2019.
- [20] R. Taghizadeh and M. Ahmadi, "Statistical and econometrical analysis of knowledge-based economy indicators affecting economic growth in Iran: the new evidence of principal component analysis—tukey and ARDL bound test," *Preprint: January*, vol. 10, 2019.
- [21] F. Liu, G. Zhang, and J. Lu, "Heterogeneous domain adaptation: an unsupervised approach," *IEEE Transactions on Neural Networks and Learning Systems*, vol. 31, no. 12, pp. 5588–5602, 2020.
- [22] J. Dong, Y. Cong, G. Sun, Z. Fang, and Z. Ding, "Where and how to transfer: knowledge aggregation-induced transferability perception for unsupervised domain adaptation," *IEEE Transactions on Pattern Analysis and Machine Intelligence*, vol. 1, p. 1, 2021.
- [23] Y. Zhou, G. Xu, K. Tang, L. Tian, and Y. Sun, "Video coding optimization in AVS2," *Information Processing & Management*, vol. 59, no. 2, Article ID 102808, 2022.
- [24] S. Lv and F. Song, "Particle swarm intelligence and the evolution of cooperation in the spatial public goods game with punishment," *Applied Mathematics and Computation*, vol. 412, Article ID 126586, 2022.
- [25] A. Sharifi, M. Ahmadi, and A. Ala, "The impact of artificial intelligence and digital style on industry and energy post-COVID-19 pandemic," *Environmental Science and Pollution Research*, vol. 28, no. 34, pp. 46964–46984, 2021.
- [26] N. Ghorbani and A. Korzeniowski, "Adaptive risk hedging for call options under cox-ingersoll-ross interest rates," *Journal of Mathematical Finance*, vol. 10, no. 4, pp. 697–704, 2020.
- [27] N. Ghorbani and A. Korzeniowski, "Call and put option pricing with discrete linear investment strategy," 2021, <https://arxiv.org/ftp/arxiv/papers/2110/2110.04676.pdf>.
- [28] R. Prasad and K. D. Yadav, "Use of response surface methodology and artificial neural network approach for methylene blue removal by adsorption onto water hyacinth," *Water Conservation and Management*, vol. 4, no. 2, pp. 83–89, 2021.
- [29] N. Ghorbani, *Option pricing with investment strategy under stochastic interest rates*, The University of Texas at Arlington, PhD diss., 2021b.
- [30] A. Korzeniowski and N. Ghorbani, "Put options with linear investment for hull-white interest rates," *Journal of Mathematical Finance*, vol. 11, no. 1, pp. 152–162, 2021.

- [31] M. Zhang, Y. Chen, and W. Susilo, "PPO-CPQ: a privacy-preserving optimization of clinical pathway query for E-healthcare systems," *IEEE Internet of Things Journal*, vol. 7, no. 10, pp. 10660–10672, 2020.
- [32] M. Ahmadi, S. Jafarzadeh-Ghoushchi, R. Taghizadeh, and A. Sharifi, "Presentation of a new hybrid approach for forecasting economic growth using artificial intelligence approaches," *Neural Computing & Applications*, vol. 31, no. 12, pp. 8661–8680, 2019.
- [33] J. Artin, V. Amin, M. Ahmadi, S. A. P. Kumar, and A. Sharifi, "Presentation of a novel method for prediction of traffic with climate condition based on ensemble learning of neural architecture search (NAS) and linear regression," *Complexity*, vol. 2021, Article ID 8500572, 13 pages, 2021.
- [34] R. H. Chenhall, "Management control systems design within its organizational context: findings from contingency-based research and directions for the future," *Accounting, Organizations and Society*, vol. 28, no. 2-3, pp. 127–168, 2003.
- [35] R. Simons, "Strategic orientation and top management attention to control systems," *Strategic Management Journal*, vol. 12, no. 1, pp. 49–62, 1991.
- [36] R. Simons, *Performance Measurement and Control Systems for Implementing Strategies*, Prentice-Hall, Upper Saddle River, 2000.
- [37] R. Simons, *Levers of Control: How Managers Use Innovative Control Systems to Drive Strategic Renewal*, Harvard Business School Press, Boston, Massachusetts, 1995.
- [38] K. A. Merchant, "Influences on departmental budgeting: an empirical examination of a contingency model," *Accounting, Organizations and Society*, vol. 9, no. 3-4, pp. 291–307, 1984.
- [39] R. Simons, "How new top managers use control systems as levers of strategic renewal," *Strategic Management Journal*, vol. 15, no. 3, pp. 169–189, 1994.
- [40] V. Govindarajan and J. Fisher, "Strategy, control systems, and resource sharing: effects on business-unit performance," *Academy of Management Journal*, vol. 33, no. 2, pp. 259–285, 1990.
- [41] R. Simons, *Levers of Control*, Harvard Business School Press, Boston, Massachusetts, 1995.
- [42] K. Langfield-Smith, "Management control systems and strategy: a critical review," *Accounting, Organizations and Society*, vol. 22, no. 2, pp. 207–232, 1997.
- [43] M. A. Abernethy and W. F. Chua, "A field study of control system "redesign": the impact of institutional processes on strategic choice," *Contemporary Accounting Research*, vol. 13, no. 2, pp. 569–606, 1996.
- [44] D. Moradi, R. Zandipak, and S. Ghazvineh, "The impact of transformational leadership style and management control system on management performance of Co-operative and private companies in malayer," *Co-Operation and Agriculture*, vol. 9, no. 33, pp. 15–59, 2020.
- [45] S. Riyadi, M. Nugroho, and D. Arif, "The effect of supply network and management control system on the efficiency and profitability of manufacturing companies," *Uncertain Supply Chain Management*, vol. 9, no. 4, pp. 963–972, 2021.
- [46] L.-P. Dana, M. M. Rounaghi, M. Mahdi Rounaghi, and G. Enayati, "Increasing productivity and sustainability of corporate performance by using management control systems and intellectual capital accounting approach," *Green Finance*, vol. 3, no. 1, pp. 1–14, 2021.
- [47] M. Feder and B. E. Weißenberger, "Towards a holistic view of CSR-related management control systems in German companies: determinants and corporate performance effects," *Journal of Cleaner Production*, vol. 294, Article ID 126084, 2021.
- [48] F. Owolabi, S. Ajibolade, and U. Uwuigbe, "The design and use of performance measurement innovations and organizational outcomes in Nigerian listed companies," *Problems and Perspectives in Management*, vol. 19, no. 2, pp. 91–103, 2021.
- [49] H. T. Johnson and R. S. Kaplan, *Relevance Lost: The Rise and Fall of Management Accounting*, Harvard Business School Press, Boston, Massachusetts, 1987.
- [50] R. S. Kaplan and D. P. Norton, "The balanced scorecard—measures that drive performance," *Harvard Business Review*, vol. 70, pp. 71–79, 1992.
- [51] R. H. Chenhall, "Integrative strategic performance measurement systems, strategic alignment of manufacturing, learning and strategic outcomes: an exploratory study," *Accounting, Organizations and Society*, vol. 30, no. 5, pp. 395–422, 2005.
- [52] S. K. Widener, "An empirical analysis of the levers of control framework," *Accounting, Organizations and Society*, vol. 32, no. 7-8, pp. 757–788, 2007.
- [53] R. Simons, "Accounting control systems and business strategy: an empirical analysis," *Accounting, Organizations and Society*, vol. 12, no. 4, pp. 357–374, 1987.
- [54] R. Simons, "The role of management control systems in creating competitive advantage: new perspectives," *Accounting, Organizations and Society*, vol. 15, no. 1-2, pp. 127–143, 1990.

## Research Article

# Multifactor Stock Selection Strategy Based on Machine Learning: Evidence from China

Jieying Gao , Huan Guo , and Xin Xu 

*School of Finance, Capital University of Economics and Business, Beijing 100070, China*

Correspondence should be addressed to Xin Xu; [xuxin@cueb.edu.cn](mailto:xuxin@cueb.edu.cn)

Received 20 August 2021; Accepted 30 December 2021; Published 3 February 2022

Academic Editor: Sameh S. Askar

Copyright © 2022 Jieying Gao et al. This is an open access article distributed under the Creative Commons Attribution License, which permits unrestricted use, distribution, and reproduction in any medium, provided the original work is properly cited.

Machine learning methods have been used in multifactor stock strategy for years. This paper uses three machine learning methods and linear regression method to find the most appropriate approach. First, a framework is established and 10 style factors and 30 industry factors are chosen. Second, four methods are used to forecast portfolio returns and compared by predicting returns, successful rate, and Sharpe ratio. Finally, this paper draws conclusion. The main findings are as follows: the support vector regression has the most stable successful rate for predicting, while ridge regression and linear regression have the most unstable successful rate with more extreme cases; algorithm of support vector regression fitting higher-degree polynomials in Chinese A-share market is optimized, compared with the traditional linear regression both in terms of stock return and retracement control; the results of support vector regression significantly outperforming the CSI 500 index prove further.

## 1. Introduction

Quantitative trading in securities market usually adopts CTA (commodities trading adviser) strategy, intraday high-frequency strategy, and multifactor quantitative strategy. The multifactor models are widely used in the stock market, including Fama–French three-factor asset pricing model [1], Carhart four-factor model [2], and the further improved five-factor and six-factor models. Scholars have found hundreds of market anomalies which might provide excess returns and created a “factor zoo”. Bridgewater Associates, Renaissance Technologies, and AQR Capital Management, the top hedge funds by assets in the world, trade in global financial markets achieving exceptional returns for their investors by strictly adhering to quantitative strategies. The vast majority of nonquantitative stock funds also introduce the multifactor model to analyze and allocate their securities positions to a certain extent.

The traditional factor strategies are usually used to forecast stock returns by scoring factor exposures, and linear regression methods commonly used are time series regression, cross-sectional regression, Fama and MacBeth [3] regression, and Hansen GMM regression [4]. However, the relationship

between the factor value and the return of individual stocks in the actual stock market is often nonlinear which leads to linear regression that cannot well fit in many cases. In addition, Green et al [5] and Hou et al [6] studies have shown that out-of-sample testing finds that most factors cannot consistently provide excess returns. One of the reasons for the disappearance of excess returns is the increasing convergence of prediction and trading models using traditional methods in the security market, which leads to failure. With the development of artificial intelligence technology, Mullainathan and Spiess [7], Kleinberg et al [8] show data mining, machine learning, and other technical methods are applied to the field of economics and management research. Major financial institutions have also adopted new technologies and methods to improve quantitative trading strategies in security market transactions.

The finance analytical method is improved by introducing machine learning methods, which make the empirical research paradigm expand from linear to nonlinear, from focusing on parameter significance to the model structure and dynamic feature. Appropriate and robust models are built to capture the effective characteristics of financial data and to interpret economic meaning, making great efforts to improve prediction accuracy.

Liu et al. [9] use a support vector machine (SVM) to classify forecasting stock price index and find that support vector function can accurately reflect the variation trend and improve the prediction accuracy. On the basis of the multifactor stock selection model, Wang et al. [10] verify the predictive performance of the random forest algorithm in China's stock market by using it to predict the rise and fall of stocks and analyze the returns of selected stocks. Xie et al. [11] use LASSO regression and elastic net in the process of factor screening to select factors and determine the weight and find that the factors screened by this method could obtain excess returns. Gu et al. [12] test the performance of machine learning algorithms in the US market and find that machine learning models can effectively outperform traditional linear regression models. Wang and Li [13] use the gcForest algorithm to classify individual stocks and predict the probability of rise and fall of stocks. They build an investment portfolio and a back test shows that the portfolio could achieve significant excess returns. They compare the back-test results of SVM and random forest algorithm and find that the gcForest algorithm has obvious advantages over other algorithms in both stable and rising period in the stock market from a comprehensive analysis of various technical indicators.

Although machine learning methods have been used in return forecasts in the security market in recent years, there are still questions about which method is the best or most appropriate for the emerging stock market? Security markets are more volatile in developing countries and have their own features. Based on the Chinese stock market, this study aims to establish a forecasting framework to predict the relationship between abnormal factors and excess returns with different methods, conducting a systematic test and evaluating which method is best. Therefore, this study puts forward three research questions:

- (1) Is the machine learning model superior to the traditional predictive model? To verify the first observation, a traditional linear regression model and three machine learning algorithm models are selected in this study. Rapach et al. [14] show traditional linear regression has been used in financial forecasting and achieved good results.
- (2) If the prediction model  $f(\cdot)$  adopts linear function form, whether the performance of the nonlinear model is better than that of the linear regression model. To verify the second observation, traditional regression and linear ridge machine learning models are used to compare with random forest and support vector machine models. Ridge regression is chosen because it can solve the problem of the sparse model as Hastie et al. [15] research, and random forest and support vector machine algorithms are chosen because both of them are the core algorithms according to machine learning theory and have achieved good results in many tasks as Fernández-Delgado et al. research [16].
- (3) If the predictive model  $f(\cdot)$  adopts the machine learning methods, which performance is best among the three machine learning models and why?

## 2. Factor Variable Selection and Model Selection

The task of multifactor model forecasting is a standard supervised learning and regression task, that is, to explore the following functional form:

$$R_{t+1,j} = f(x_{t,j}; \theta) + \varepsilon_{t,j}, \quad (1)$$

where  $X_{t,j}$  is the factor, the explanatory variable selected by the researcher in advance that has an influence on the return rate of the stock  $j$  at time  $t$ . The function  $f(\cdot)$  can take any form and represents all the possible ways in which  $x$  can act on  $y$  that the researcher can imagine. The residual term  $\varepsilon$  represents other possible influence factors beyond control. Compared with the traditional factor regression model, formula (1) does not require that the number of variables in  $X$  is smaller than the number of samples and allows  $x$  to take effect on  $y$  of almost any form. Under specific sample conditions with the traditional econometric analysis framework, researchers can estimate  $f(\cdot)$  by the reduced phenomenon regression model and nonparametric methods. But in the reduced linear regression model, the explanatory variable  $x_j$  is easily correlated with the residual term  $\varepsilon_j$ . In addition, when the sample size is limited and  $x$  contains many variables, traditional nonparametric estimation is difficult to overcome technical obstacles, and how to select variables has not been solved as showed by Henderson et al. [17].

*2.1. Factors Selection.* The essence of the multifactor model is to build an optimal asset portfolio through factor selection. Therefore, factors should be selected as many as possible to explain the return of stocks, so as to minimize the residual of the regression model which represents the return of stocks that cannot be explained by factors. The selection of individual stocks is based on the results of portfolio earnings of the forecasting model. The characteristics of samples, that is, the independent variables in the model, are determined by researchers on account of their market experience. At present, the common practice in the investment industry is to divide factors into industry factors and style factors. The industry factor is a dummy variable, if the individual stock belongs to a certain industry, the corresponding factor value is 1, and the factor value of other industries is 0. Style factors are selected by investors' study and comprehension of the market. The number of style factors excavated by quantitative institutions and the ability to interpret alpha of the stock manifest academic competence of financial institutions, and different institutions may choose different style factors.

Based on the situation of China's A-share stock market, twelve primary factors from four categories are selected: the valuation factor which includes price-to-earnings ratio, price-to-book, total market capitalization, the financial factor which includes price-to-cash-flow ratio and price-to-sales ratio, the momentum factor which includes turnover rate, turnover, yield, the length of the cylinder, and the closing price, and technical factor which includes the length



of upper wick and length of lower wick. Technical factors are improved because few researches have paid attention to the length of the wick, but it shows the trading mood which has a great effect on stock price, especially in emerging security markets.

The primary factors are back-tested with the stratified method, and the results are sorted in descending order listed in Table 1. Group a buys the top 20% stocks with the largest factor value ranking in each cross-sectional period each week, while group e buys the stocks with the last 20% factor value ranking in each cross-sectional period each week. The frequency of position adjustment is weekly. At the same time, stocks with an absolute weekly return of more than 15% were removed, which account for less than 2% of the number of stocks, in order to eliminate the impact of stocks with a consecutive daily limit up and daily limit down.

The results of long-short portfolios of the stratified back test show that the net value of four factors, namely, length of wick, length of the lower shadow, price-cash flow ratio, and price-sales ratio, is low, indicating these factors are not correlated with the stock return rate strongly. Considering the net value curve of the long-short portfolio and the stratified back test, two financial factors, price-cash-flow ratio and price-sales ratio, are filtered out, and ten style factors are selected. Combining with 30 industry factors, now 40 factors are selected for the return forecasting model as shown in Table 2.

**2.2. Model Selection.** Machine learning is a collection of many forms of predictive functions  $f(\cdot)$  and all kinds of algorithms. As stock return prediction is a supervised learning regression task, theoretically, all machine learning algorithms adapted to regression task can be used to build stock return prediction models. In this study, three machine learning regression algorithms (ridge regression, random forest regression, and support vector regression) are used to predict the returns of individual stocks. Based on the predicted returns of individual stocks, the investment portfolio is constructed for back test, and the efficiency of the machine learning algorithm is analyzed.

**2.2.1. Ridge Regression Model.** In the traditional linear regression model, the parameter estimation is generally obtained by minimizing the loss function. The formula of the loss function is as follows:

$$\text{Loss}_{\text{OLS}}(\beta) = \|Y - X\beta\|^2, \quad (2)$$

where  $\text{LOSS}$  is the loss function,  $X$  and  $Y$  are data matrix and outcome variable, respectively, and  $\beta$  is regression coefficient vector. In contrast to  $\text{OLS}$  estimates, Hoerl and Kennard [18] propose to add a constant  $\lambda$  to the principal diagonal of the  $X'X$  matrix to ensure the matrix  $(X'X + \lambda I)$  is invertible and alleviate the multicollinearity problem. In order to obtain the unique solution of the parameter vector  $\beta$ , the paper regularizes it to limit its data range. The penalty term is introduced into the loss function for penalized regression.

$$\text{Loss}(\beta) = (y - X\beta)'(y - X\beta) + \lambda\|\beta\|_2^2, \quad (3)$$

where the first term of (3) is the sum of squares of residuals. The second term is the penalty term, and  $\lambda$  is the adjustment parameter to control the penalty intensity. The optimal solution of parameter  $\beta$  in the ridge regression model  $\hat{\beta}_{\text{ridge}}(\lambda) = (X'X + \lambda I)^{-1}X'y$  can be obtained when the loss function is minimum. The choice of parameter  $\lambda$  determines the degree to which the regression coefficient is compressed. Different values of  $\lambda$  will generate different results. A common method in machine learning proposed by McNeish and Daniel [19] is  $K$ -fold cross-validation. The cross-test error is as follows:

$$\begin{aligned} \text{CV}(\lambda) &= \overline{\text{MSE}}_{\lambda} \\ &= \frac{1}{K} \sum_{k=1}^K \frac{1}{n_k} \sum_{i \in \text{fold}_k} [y_i - \hat{y}_i(\lambda)]^2. \end{aligned} \quad (4)$$

The cross-validation error  $\text{CV}(\lambda)$  is a function of  $\lambda$ , and  $\lambda$  is optimal when  $\text{CV}(\lambda)$  is the smallest.

**2.2.2. Random Forest.** Random forest is also a combined prediction model, belonging to a Bagging algorithm variation in the family of integrated algorithms. It is a tree-based integrated learning model proposed by Breiman [20] and widely used to solve classification and regression.

The paper uses random forest algorithm of Bagging, using bootstrapping to generate random training samples  $n$  from the initial dataset. The probability of each sample being selected is  $1/n$ , and the probability of each sample not being collected  $k$  times is  $\lim_{k \rightarrow \infty} (1 - (1/n))^k \rightarrow (1/e) \approx 0.368$ . The 36.8% dataset that did not participate in the training model composes the out-of-bag sample, which can be used to evaluate the out-of-bag error.  $D_t$  is used to represent the training sample set actually used by  $h_t$ , and  $H^{\text{ob}}(x)$  represents the out-of-bag sample prediction of sample  $x$ , whose formula is

$$H^{\text{ob}}(x) = \arg \max_{y \in Y} \sum_{t=1}^T II(h_t(x) = y) * II(x \notin D_t), \quad (5)$$

and the out-of-bag estimation of the generalization error of the Bagging algorithm is

$$\epsilon^{\text{ob}} = \frac{1}{|D|} \sum_{(x,y) \in D} II(H^{\text{ob}}(x) \neq y). \quad (6)$$

Cawley et al. [21] use the above results as the criteria for model pruning and overfitting to reduce the risk of overfitting.

The random forest method is similar to the bagging method both of which rely on initial data and use the bootstrap method to build the training set. Random forest also introduces a random attribute selection in the training process of the decision tree. In other words, in random forest generation, a subset containing  $j$  attributes are randomly selected from the attribute set of each node of each decision

TABLE 1: Net value of factor stratified back-test and long-short portfolio.

		a	b	c	d	e	Long-short portfolio
Valuation factors	PE (price/earnings)	1.15	1.75	2.30	2.58	2.32	1.43
	PB(price/book value)	1.07	1.78	2.29	2.36	2.81	2.01
	Market value	1.05	1.06	1.27	2.05	10.05	10.64
Financial factors	Price/cash flow	1.40	2.01	2.61	2.57	1.60	1.10
	Price/sales	1.38	1.93	2.11	2.21	2.47	1.43
	Turnover	0.29	0.77	2.03	4.43	14.89	47.62
Momentum factors	Turnover rate	0.34	1.91	2.94	3.75	4.08	7.58
	Yield	0.35	1.72	3.45	4.16	3.51	10.08
	Length of wick	1.25	2.18	2.61	2.33	1.88	1.35
Technical factors	Closing price	0.53	1.29	2.24	3.15	6.39	10.78
	Length of lower shadow	1.43	2.83	2.65	2.10	1.39	1.06
	Length of upper shadow	0.59	2.38	2.88	2.76	2.77	3.74

TABLE 2: 40 selected factors.

Style factors		Industry factors	
PE	Petroleum and petrochemical	Electrical equipment and new energy	Banking
PB	Coal industry	National defense and military industry	Nonbank finance
Market value	Nonferrous industry	Auto industry	Real estate
Turnover	Electricity and utilities	Trade and retail	Comprehensive finance
Turnover rate	Steel	Consumer service	Transportation
Yield	Basic chemical engineering	Home appliance	Electron
Length of wick	Architectural industry	Textile and garment	Communication
Closing price	Architectural material industry	Pharmaceutical industry	Computer
Length of lower shadow	Light manufacturing	Food and beverage industry	Media industry
Length of upper shadow	Machinery industry	Agriculture, forestry, animal husbandry, and fishery	Comprehensive industry

tree, and then, an optimal attribute is selected from this  $j$  subset for partitioning after random selection. The more machine learners there are, the better the random forest learns. In the study, the method of the weighted mean for regression is adopted in the integrated strategy of random forest, and its formula can be expressed as

$$H(x) = \frac{1}{T} \sum_{i=1}^T \omega_i h_i(x). \quad (7)$$

**2.2.3. Support Vector Machines.** The support vector machine algorithm, first proposed by Vapnik and Vladimir [22], is to maximize the interval among training samples of different categories in the sample space so as to achieve optimal classification. For the nonlinear samples applied in the study, the feature space can be mapped into a higher-dimensional space, and all samples can be correctly classified by a mapping function. The sample space partition in the hyperplane can be expressed by the following linear equation.

$$\omega^T x + b = 0, \quad (8)$$

where  $\omega$  is the normal vector that determines the direction of the hyperplane, and  $b$  is the displacement term that determines the distance between the hyperplane and the origin point. Thus, the distance from any point  $x$  in the sample space to the hyperplane ( $\omega, b$ ) can be obtained as follows:

$$r = \frac{|\omega^T x + b|}{\omega}. \quad (9)$$

Assuming that any point  $(x_i, y_i) \in D$ , the sample space points are classified as

$$\begin{cases} \omega^T x_i + b \geq +1, & y_i = +1, \\ \omega^T x_i + b \leq -1, & y_i = -1. \end{cases} \quad (10)$$

It can be seen from the above formula that in order to find the partition hyperplane with the maximum interval, it is necessary to find the parameters  $\omega$  and  $b$  which satisfy the constraints in (10) so that the sum of the distances from the two heterogeneous support vectors to the hyperplane can be maximized. The constraint conditions can be obtained as

$$\begin{cases} \min_{\omega, b} \frac{1}{2} \omega^2, \\ \text{s.t. } y_i (\omega^T x_i + b) \geq 1, \quad i = 1, 2, \dots, m. \end{cases} \quad (11)$$

For nonlinear classifiers, the support vector machine has several kernel functions to realize hyperplane partition, including polynomial kernel, Gaussian radial basis kernel, Laplacian kernel, and Sigmoid kernel. These nonlinear kernel functions mainly transform the original feature space into a higher-dimensional feature space and are separated by a hyperplane. In this paper, the Gaussian radial basis is

chosen as the kernel function to establish the support vector machine model.

### 3. Data Preprocessing and Training Model

Predicting the returns of individual stocks is the most important part of the multifactor stock selection strategy, and the alpha of the strategy usually comes from stocks selected. Value of factor of individual stocks is taken as the characteristics of the data (independent variable) and the return rate of individual stocks in the next period as the label of the data (dependent variable). After using the data from  $t-24$  to  $t-1$  period as the model training set, the factor data of individual stocks in the  $t$  period are used to predict the return rate of  $t+1$  period. The period of stock portfolio transfer selected in the paper is weekly, so the corresponding training set is the data of 24 weeks from the forecast day to the week 24 weeks before.

**3.1. Data Preprocessing.** Because the dimensions of each factor are not consistent, it is necessary to standardize the factors so as to compare and regress. Before data standardization, in order to avoid interference caused by the estimation of the correlation between a few extreme value data factors and the rate of return, the extreme data are excluded first.

Figure 1 shows the probability density comparison of factor data of stock market value before and after the de-extreme operation. It can be seen that the de-extreme method effectively reduces the impact of extreme values on the prediction results.

After the market value factor data of stock is de-extreme, the distribution before and after standardization is compared in Figure 2. Figure 2(a) shows the data distribution before standardization, and Figure 2(b) shows the data distribution after standardization. It can be seen that the dimensions of the normalized data are adjusted.

**3.2. Model Training.** After deleting extremes and standardization of all factor loading data, four algorithms including linear regression, ridge regression, random forest regression, and support vector regression are used, respectively, to predict the returns of individual stocks. In the ridge regression algorithm, the penalty parameter alpha is set to 90. In the random forest regression, 500 trees are selected to test with regression tree as the base learner. In the support vector machine algorithm, radial basis function is used, the radial kernel gamma parameter is set to 0.5, and penalty parameter is set to 100.

There are 40 sample features including the 10 style factors and 30 industry factors in the model. The label of the sample is the return rate of individual stocks in the next cross-sectional period. The sample characteristics and labels of 24 weeks before the prediction are selected as the training set, and rolling prediction is carried out. Finally, the forecasting value of the weekly return of all stocks in the security market from July 9, 2010, to November 15, 2019, is obtained for the construction of the investment portfolio. The data

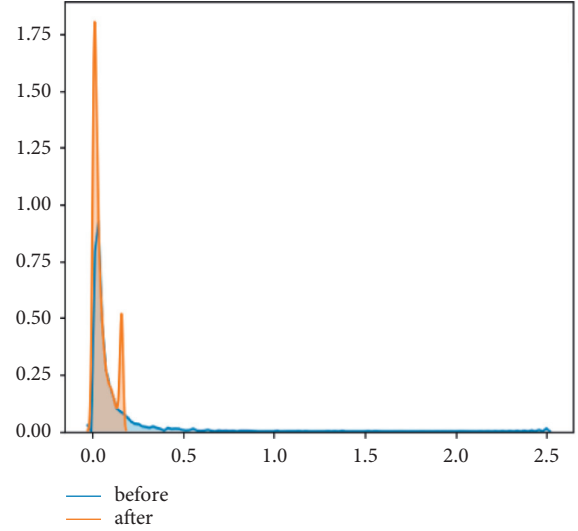


FIGURE 1: Distribution of samples de-extreme.

come from the Chinese A-stock market, obtained from CSMAR (China Stock Market & Accounting Research Database) and WIND Information Financial Terminal Market Sequence.

## 4. Prediction Results and Analysis

**4.1. Mean Square Error Comparison.** Mean square error (MSE) is the sum of squares of the difference between the true value and the predicted value of the test set divided by the number of samples in the test set. In a linear regression model, it refers to the loss function. Generally, the MSE index can intuitively reflect the deviation between the model prediction results and the real results and indicates the generalization ability of the model to the new data in the test set.

$$\frac{1}{m} \sum_{i=1}^m (y_i - \hat{y}_i)^2. \quad (12)$$

Figure 3 shows the MSE statistical results of the four algorithms in each back-test section period.

It can be seen that the MSE indexes of the four algorithms are very close, indicating that for all stocks in the security market, the generalization ability of the four algorithms is close to each other. Compared with the trend of turnover of Shanghai and Shenzhen stock exchanges in Figure 4, the deviation of the model forecast result is greater as the turnover of the market magnifies. The characteristic is in line with the actual situation of the Chinese A-share market, for market sentiment often being hot and retail investors entering the market in a concentrated way when the transaction volume is enlarged, which corresponds to the two highest transaction volumes in Figure 4 of 2015 and early 2019. At these times, irrational investors increase in the market, and market efficiency decreases, which are reflected in the price deviation of individual stocks. In this case, historical data usually cannot accurately predict the future, so the prediction deviation of the corresponding model increases.

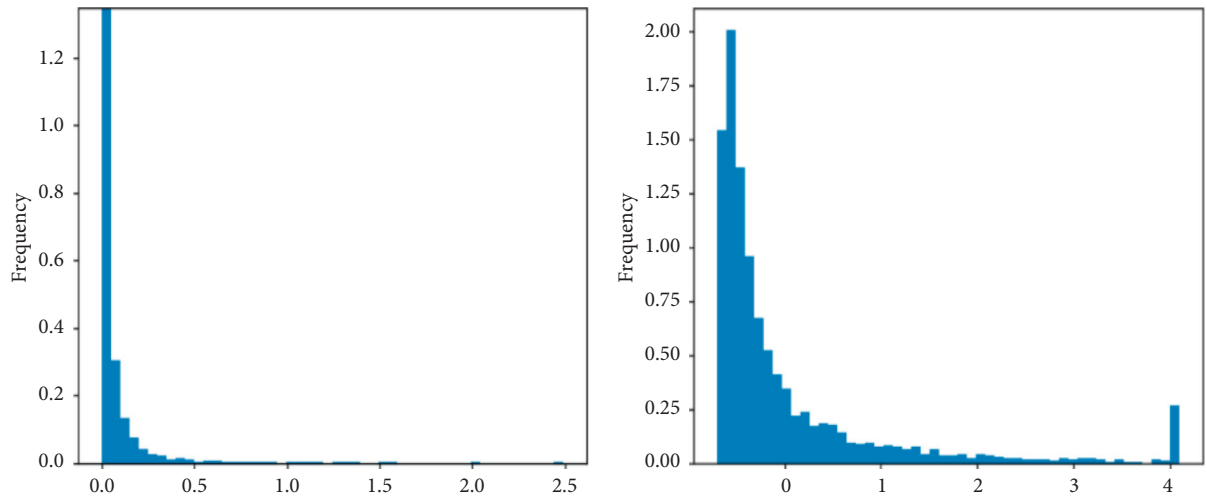


FIGURE 2: Distribution of samples before (a) and after (b) standardization. Note: the unit of the X-axis in (a) is 1 billion, and the unit of the X-axis in (b) is 1.

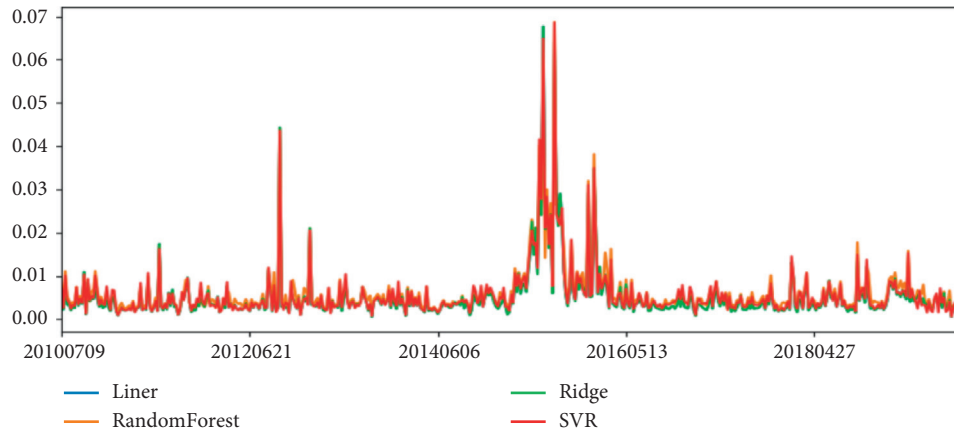


FIGURE 3: MSE indexes of four algorithms.

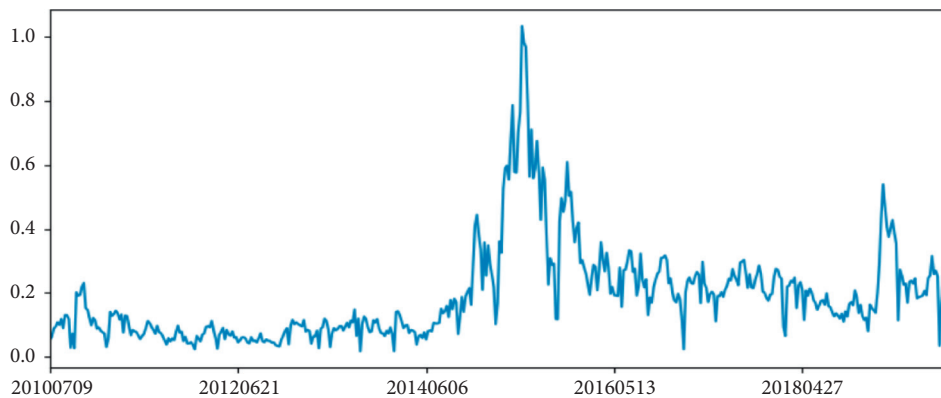


FIGURE 4: Turnover trend of the Chinese A-share market in the same period.

4.2. *Success Rate of Forecast.* In the multifactor stock selection model, the deviation between the forecast return and the actual return often cannot completely determine the merits of the strategy. The deviation can be divided into two

kinds: one is the actual return of the selected stock being higher than the forecast return, and the other is the actual return of the selected stock being lower than the forecast return. Obviously, the first bias is favorable for investors,

while the second bias is an adverse result that should be avoided as far as possible. Therefore, some other indicators are used to help evaluate the model, such as predicting success rate.

The success rate of forecast refers to the probability that the actual return of the stock which the model predicts is positive, that is, the accuracy of the model to predict the rise of the stock. In many cases, the absolute value of the prediction results of the model is not high. For example, although the model predicts a 3% return on individual stocks, the actual stock rise of 2% or 4% is acceptable. Because if the actual return falls in the end, the forecast will cause a loss on the investment. Therefore, the success rate is also an important index of model evaluation.

Figure 5 shows the probability density distributions of the four algorithms for predicting the success rate during the back test.

Except for SVR, the distributions of the other three algorithms all have two peaks, among which linear regression and ridge have the most unstable success rate, with the two peaks close to 0 and 1, respectively, and the peak near 0 is higher. Random forest is slightly better than the two algorithms, but many extreme values of the prediction of the success rate still exist. Therefore, from the perspective of prediction success rate, SVR is the most stable, followed by random forest regression, while ridge regression and traditional linear regression are very unstable and have many extreme values as shown in Table 3.

**4.3. Model Comparison and Analysis.** Figure 6 shows the net value curves of the investment portfolio constructed using the corresponding earnings forecast results of the four algorithms. Linear regression corresponds to linear regression, random forest corresponds to random forest regression, ridge corresponds to ridge regression, SVR corresponds to support vector regression, and benchmark corresponds to CSI 500 index trend.

The back-test results show the following.

**4.3.1. SVR Is Superior to the Traditional Linear Regression Algorithm.** Compared with the traditional linear regression, the return of the portfolio constructed by the SVR is significantly improved from the perspective of return rate and retracement control. The traditional linear regression is not suitable for high-dimensional data, the number of independent variables of high-dimensional data is greater than the sample size, and the rank of matrix  $X$  is less than the number of rows, which will lead to the matrix  $X$  is not full rank, and the unique solution cannot be obtained.

In addition, even if there is no problem of high-dimensional data, approximate (incomplete) multicollinearity which means the high correlation between characteristic variables often appears in the traditional linear regression model. The matrix becomes almost irreversible under multicollinearity, magnifying the variance and underestimating the significance of OLS estimation.

The back-test results show that SVR has a better prediction effect on the return of stocks than linear regression,

and the algorithm fits the characteristics of higher-degree polynomial and is more suitable for the stock market. For example, it can be seen from the results of the stratified back test in the primary factor chosen part that the style factors with better effects in the model have fluctuated to a certain degree since 2018, such as factors of market value and turnover rate. In 2017, China's stock market saw a record number of IPOs, and the regulator cracked down on high increasing the number of common shares and other subject speculation, and there was a big shift in market style such as the market's small-cap effect changed significantly. For this kind of nonlinear behavior, the machine learning algorithm is relatively well adapted. Compared with the CSI small-cap 500 index of the Chinese stock market, Sharpe [23] ratio calculated is 0.27, which means at the same risk, the portfolio gains more than CSI 500.

However, the result of SVR has got a large retracement since 2018, which may be caused by the increasing use of machine learning algorithms by quantitative institutions in China's A-share market. That is, the increase of funds in the market for return prediction using the SVR algorithm reduces the alpha of the algorithm itself.

**4.3.2. The Results of Linear Regression Are Similar.** The back-test results show that the trend of ridge regression is very close to that of linear regression, which is determined by the two algorithms themselves. Ridge regression only adds a penalty term to the linear regression; in this study, the penalty term is rather big which leads to similar results. Although ridge regression and linear regression algorithms had relatively high returns before 2018, they began to plunge after 2018, which reflecting the distribution of the success rate of linear regression prediction was unstable. Analysis of the forecast results shows the successful rate distributions of ridge regression and linear regression are extreme, and Xu et al. [24] find that stocks with high return asymmetry exhibit low expected returns. In the market, if the forecast successful rate is unstable, it will have a negative impact on the net value.

The advantage of ridge regression over classical linear regression models lies in its tradeoff between prediction error and variance. With the increase of  $\lambda$ , the smoothness of the fitting of ridge regression decreases, although the variance decreases, but the deviation increases. In general, when the relationship between the response variable and the prediction variable is approximately linear, the least squares estimate will have a low bias but a large variance, which means that small changes in the training data may lead to large changes in the least squares regression coefficient. When the number of variables and the number of observations are close, the variance of the least squares estimation will be larger, and when the number of variables is greater than the number of observations, the least squares have no unique solution. Ridge regression method can still get a large decrease of variance by a small increase of deviation, and a better fitting effect can be obtained by using this tradeoff. The back-test results show that the ridge regression fitting trend effect is very close to that of the ordinary linear regression,

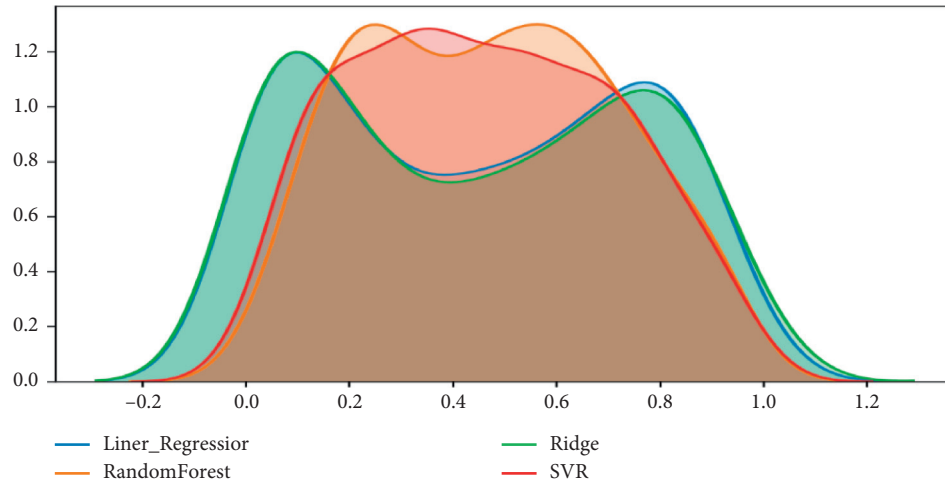


FIGURE 5: Distributions of the success rate of forecast earnings.

TABLE 3: Back-test results of different algorithms.

Algorithm	Annualized return	Maximum retracement rate (%)	Sharpe ratio weekly
Linear regression	-5.38%	94.73	---
Ridge regression	-6.61	95.56	---
Random forest regression	-4.74	83.43	---
Support vector regression (SVR)	70.12%	58.63	0.27

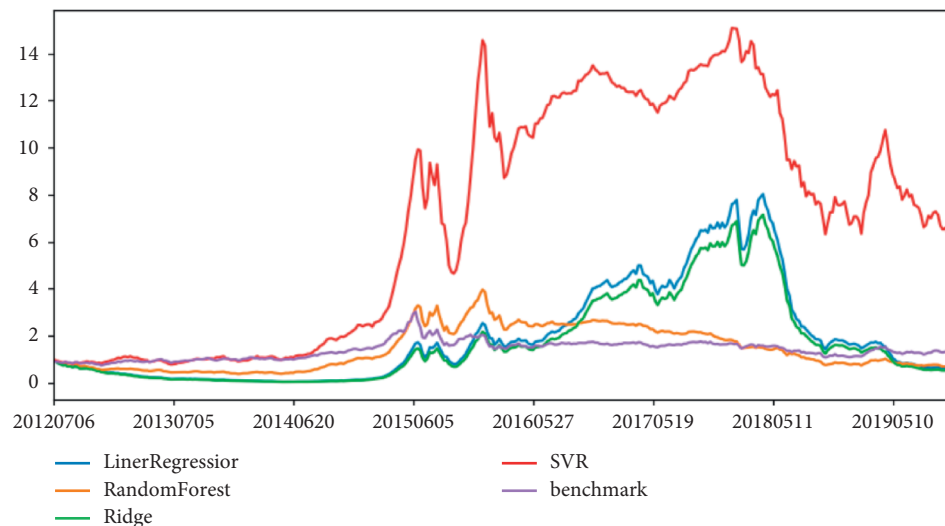


FIGURE 6: Net value curves of back test.

which also reflects from another side that the variance of the least square estimation is not large.

*4.3.3. Stochastic Forest Regression Is Insignificant in the Sample.* Random forest only uses some node variables in the decision tree. Because different nodes are forced to split with different variables, the correlation between different decision trees can be reduced, thus reducing the variance. Therefore, in the tradeoff between variance and bias, random forest

sacrifices a small amount of bias for a smaller variance, so as to reduce the mean square error. Since all characteristic variables are used for splitting in this study, even though the deviation is small, the correlation between different decision trees is strong, resulting in a large variance. So, the portfolio constructed by the stochastic forest regression algorithm does not generate significant excess returns, and this algorithm has no obvious advantage over the traditional linear regression algorithm in the construction of the multifactor stock selection model.

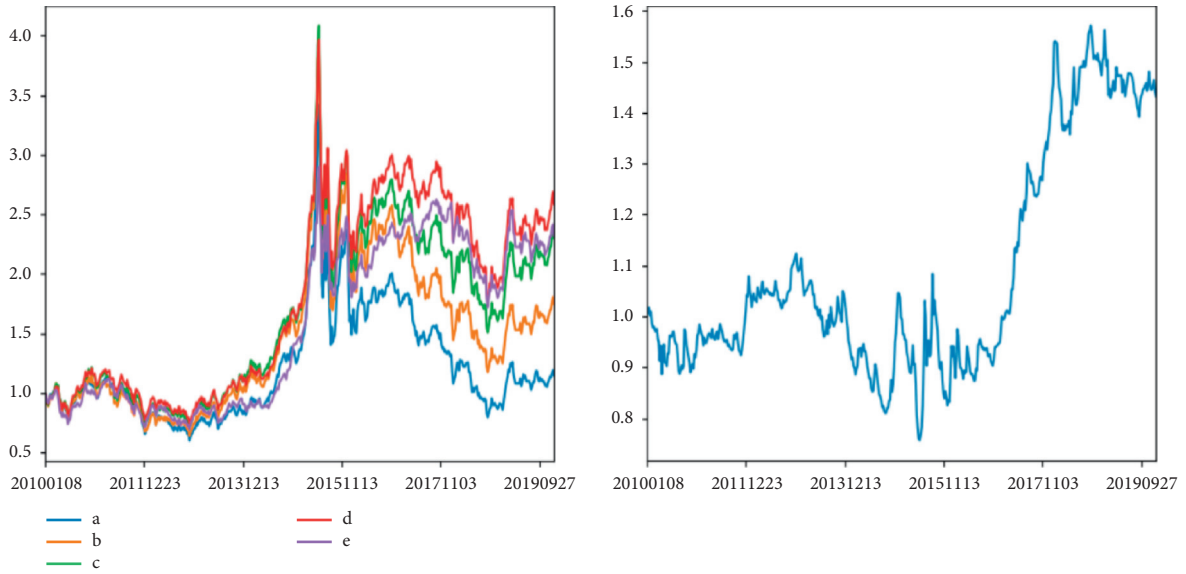


FIGURE 7: Stratified back test of price/earnings factor (a) and net value curve of long-short portfolio (b).

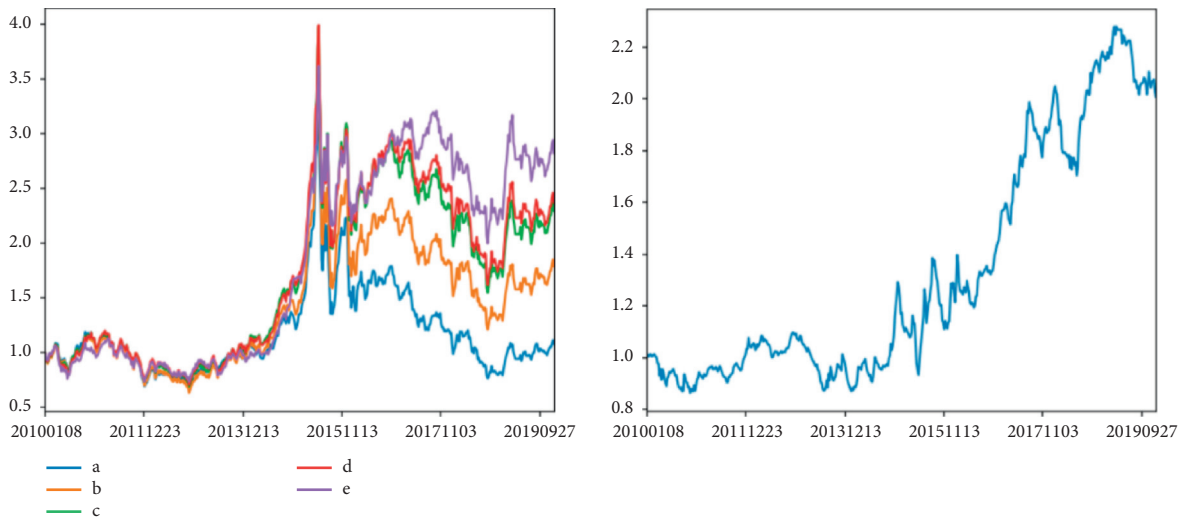


FIGURE 8: Stratified back test of price/book value factor (a) and net value curve of long-short portfolio (b).

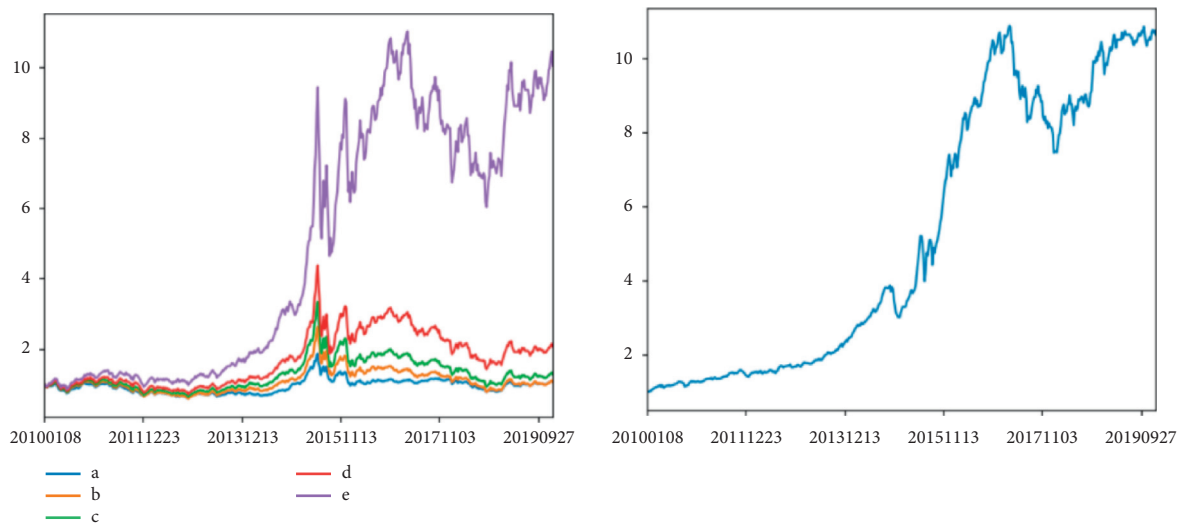


FIGURE 9: Stratified back test of market value factor (a) and net value curve of long-short portfolio (b).

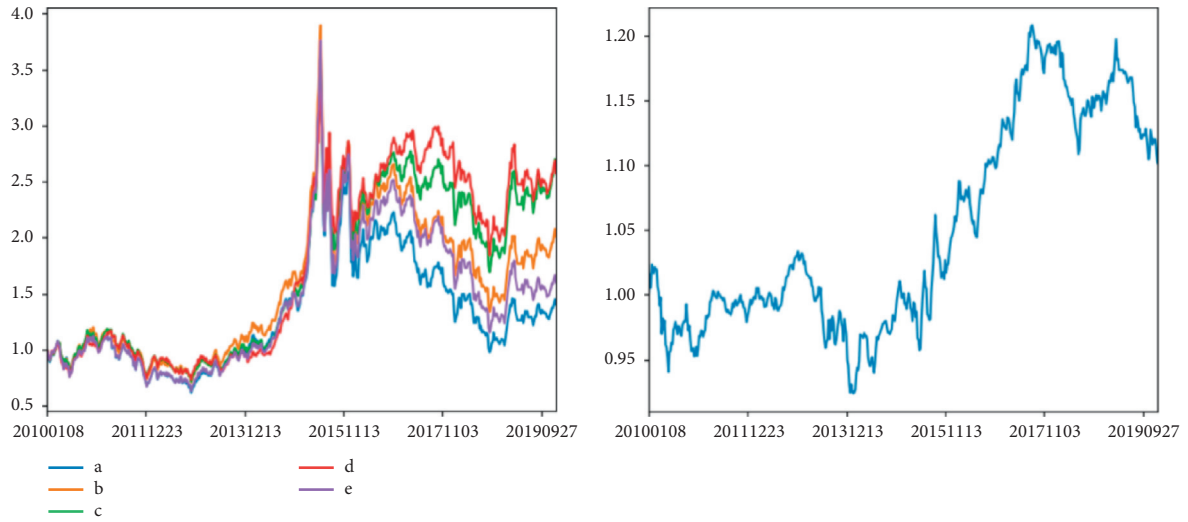


FIGURE 10: Stratified back test of price/cash flow factor (a) and net value curve of long-short portfolio (b).

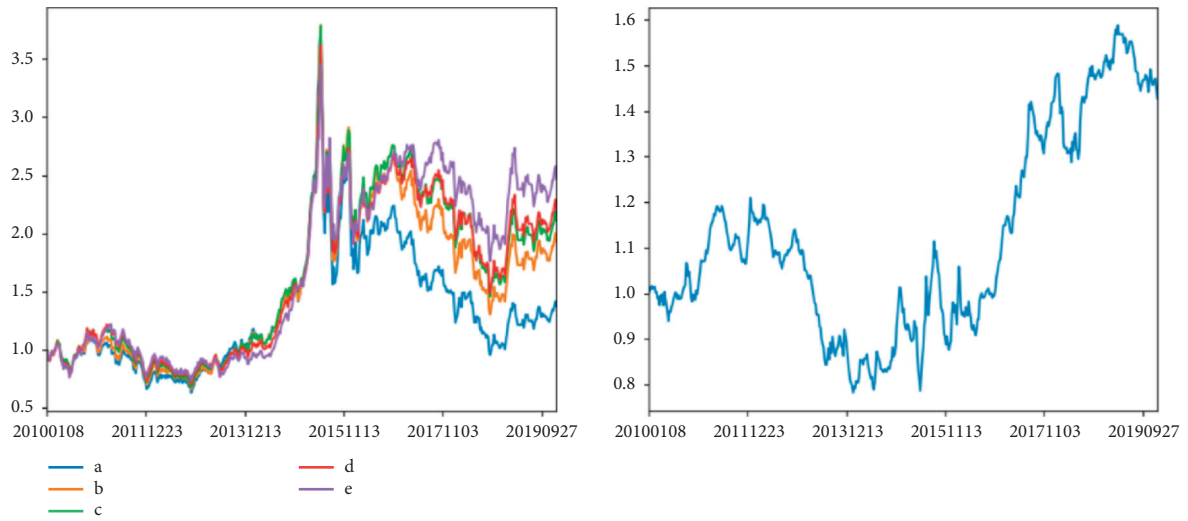


FIGURE 11: Stratified back test of price/sales factor (a) and net value curve of long-short portfolio (b).

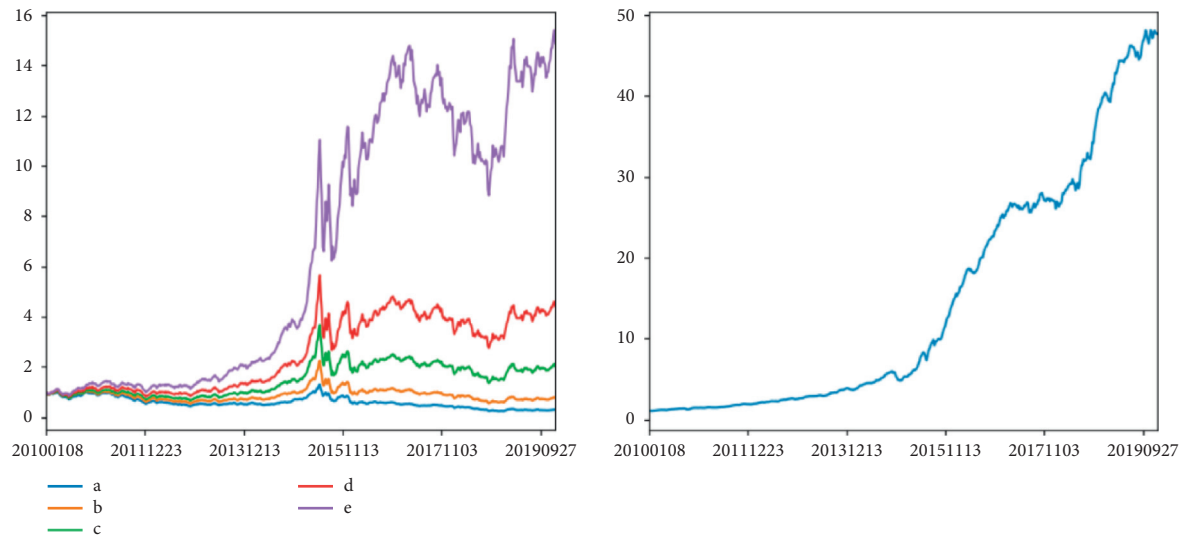


FIGURE 12: Stratified back test of turnover factor (a) and net value curve of long-short portfolio (b).



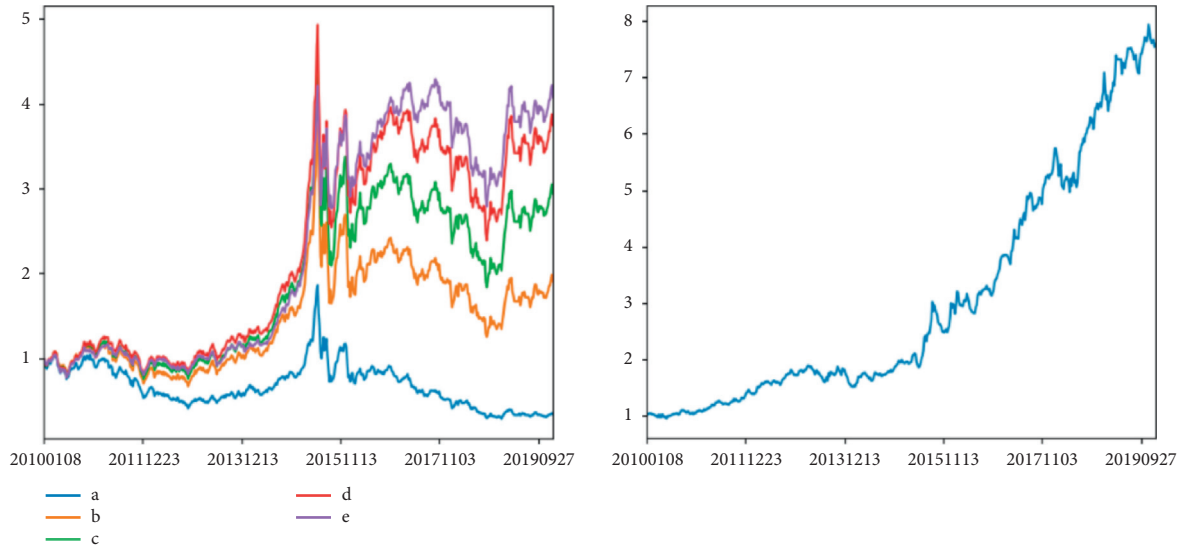


FIGURE 13: Stratified back test of turnover rate factor (a) and net value curve of long-short portfolio (b).

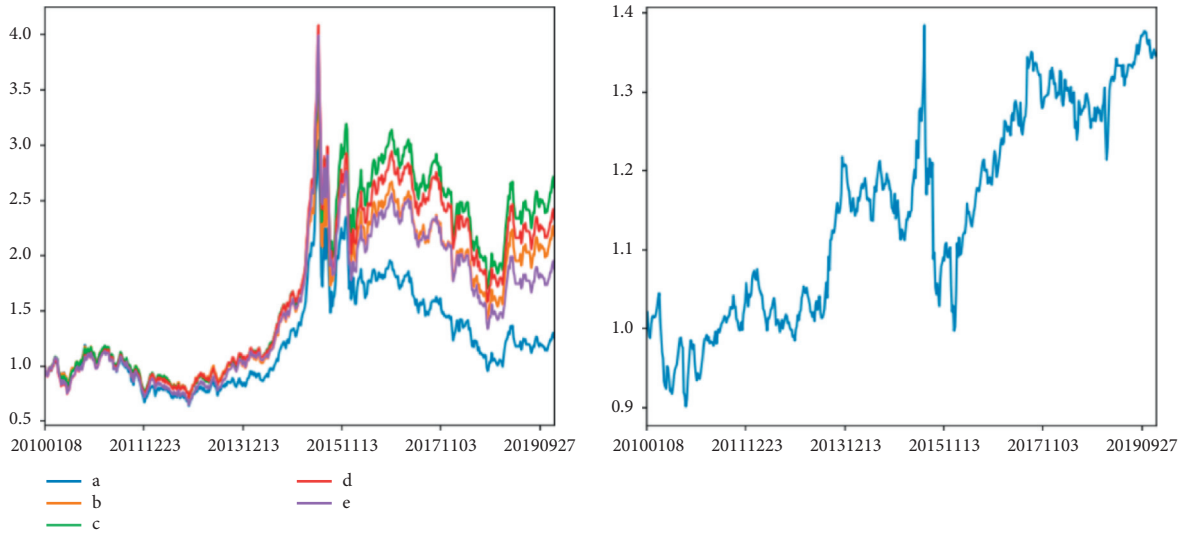


FIGURE 14: Stratified back test of length of wick factor (a) and net value curve of long-short portfolio (b).

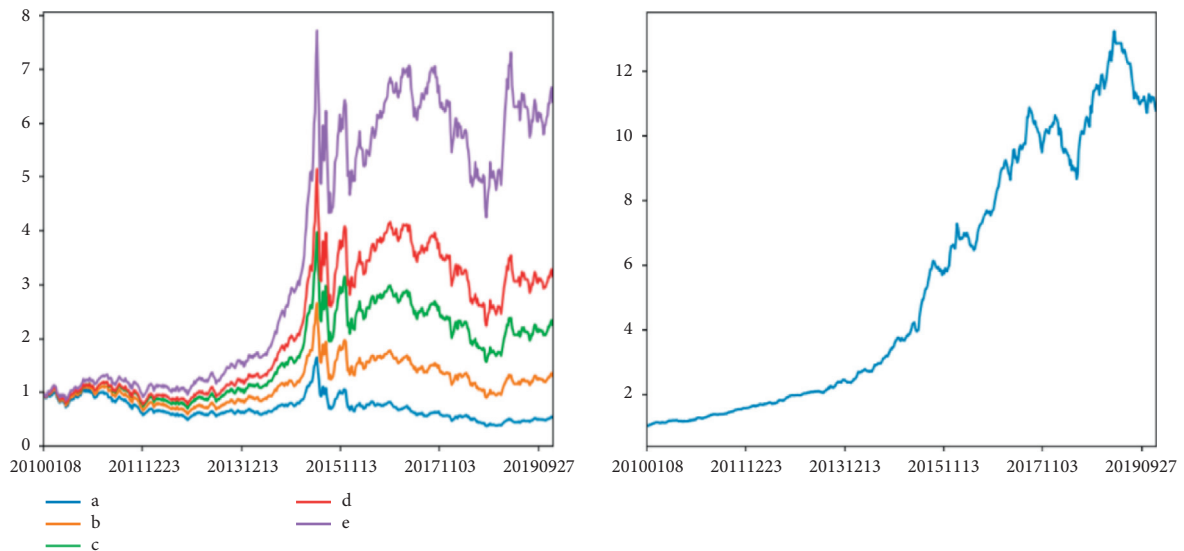


FIGURE 15: Stratified back test of closing price factor (a) and net value curve of long-short portfolio (b).

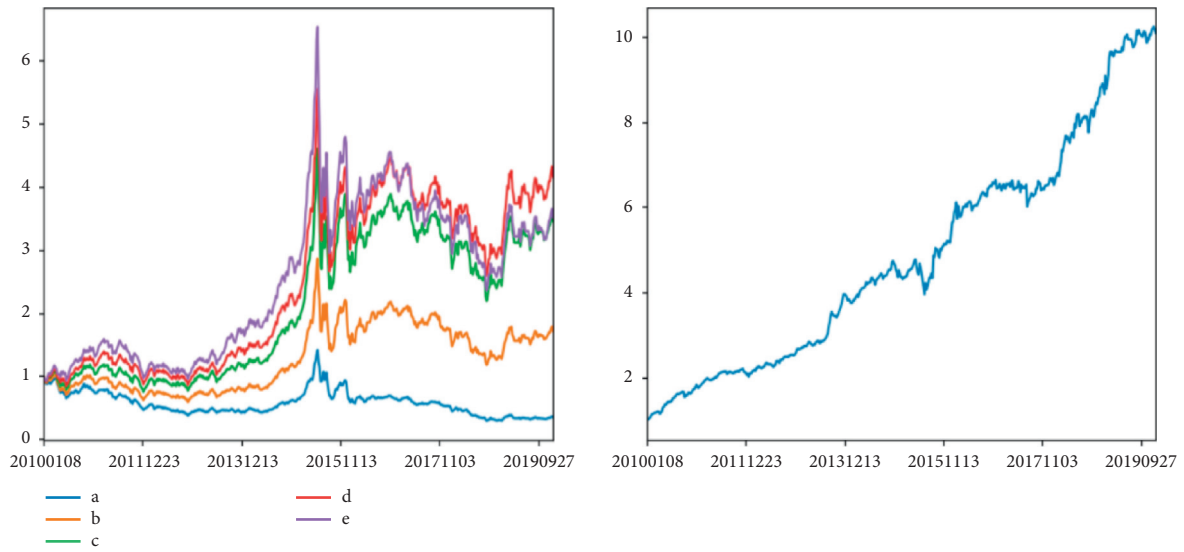


FIGURE 16: Stratified back test of yield factor (a) and net value curve of long-short portfolio (b).

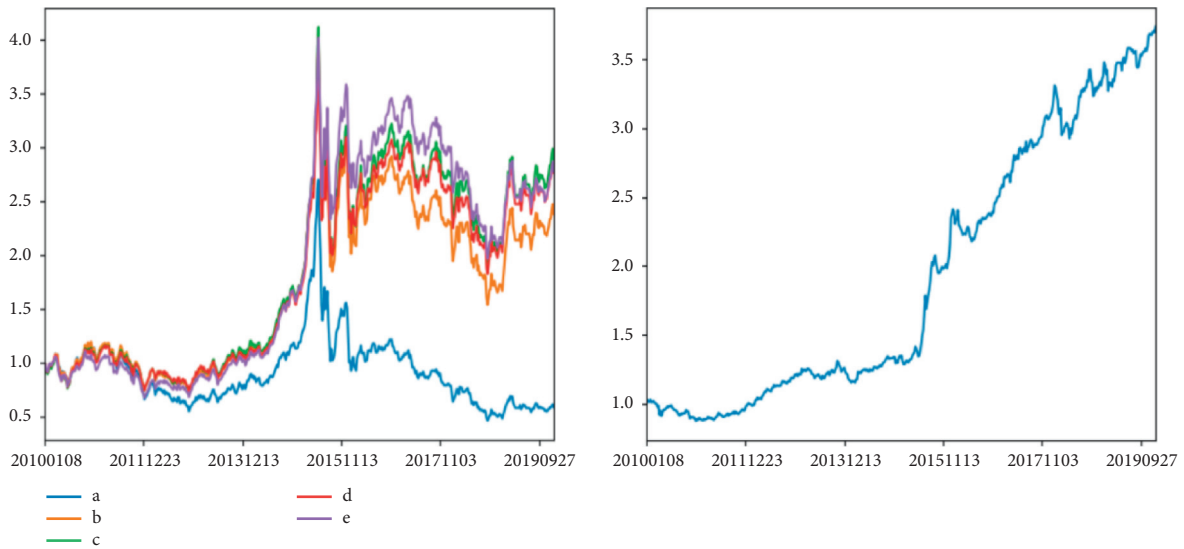


FIGURE 17: Stratified back test of length of upper shadow factor (a) and net value curve of long-short portfolio (b).

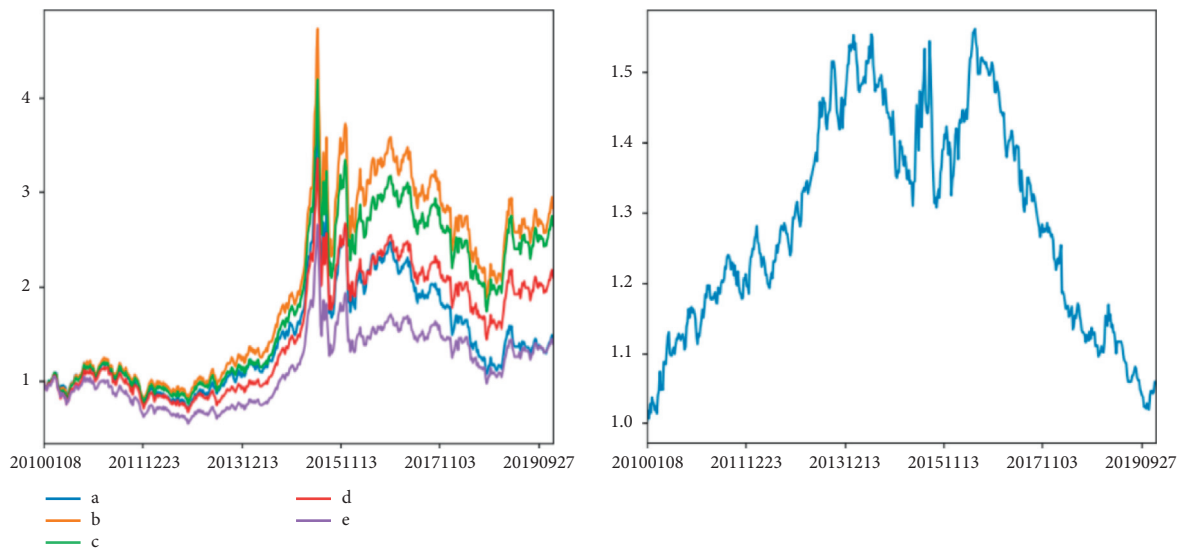


FIGURE 18: Stratified back test of length of lower shadow factor (a) and net value curve of long-short portfolio (b).

## 5. Conclusion and Prospect

*5.1. Conclusion.* This study aims to study the application of machine learning algorithm in multifactor selection strategy.

First, according to results of the stratified back-test and long-short portfolio, the price-to-sales ratio and price-to-cash-flow ratio factors which are not strongly correlated with the return rate of stocks are removed. The remaining 10 style factors and 30 industry factors constitute the independent variables in the return forecast model.

Next, four algorithms, including linear regression and three machine learning regression, are used, respectively, to predict the return of stocks. The deviation of the forecast results increases when the stock market turnover is enlarged, indicating that the prediction effect of the model will weaken when the market sentiment is high and the irrational pricing of investors increases. Among the four algorithms, the support vector regression has the most stable successful rate for predicting stocks return, while the ridge regression algorithm and linear regression algorithm have the most unstable successful rate for predicting with more extreme cases.

Finally, portfolios are built of which the position weight of individual stocks is determined by the weighted average of expected returns, and the forecast results of the four algorithms are back-tested. It is found that the support vector regression has a significant improvement compared with the traditional linear regression, both in terms of return and retracement control. The result can significantly outperform the CSI 500 index, indicating that the support vector regression algorithm in machine learning has a better effect in predicting returns in the multifactor stock selection strategy.

In conclusion, support vector regression can be used to fit higher-degree polynomials in the Chinese A-share market, and its applicability is strong.

*5.2. Prospect.* Multifactor stock selection model can help investors not only to make more efficient and accurate decisions in investment but also have a clearer understanding of the huge and intricate security market and price fluctuation to seize trade opportunity. With the advent of the Internet of things, the acceleration of the development of big data and cloud computing, and the continuous innovation of data mining algorithms, more and more reasonable algorithms will be explored and used in the Chinese equity market to gain an excess return.

From the perspective of the data relationship, the nonlinear relationship between the prediction excess return rate variable and the anomaly factor maybe not very strong, which leads to the prediction effect of some machine learning algorithms used in this study is not as good as that of the traditional linear regression model. On the other hand, it is also limited by the problems of the algorithm itself. Although the ridge regression model can solve the  $X'X$  irreversible problem in the linear regression model, the cost paid is to “compress” the regression coefficients, thereby making the model more stable and reliable. Since the penalty term is the quadratic function of the regression coefficient  $\beta$ ,

when seeking the minimum value of the objective function, its partial derivative always retains the independent variable itself. So, sometimes ridge regression cannot realize the choice of variables in a true sense. Although the results of SVM model performance are sometimes excellent, its biggest disadvantage is that when the data scale is large, the operating cost is relatively high. Therefore, future work can be further studied from the following two aspects: if the real data do have sparse problems, LASSO regression can be considered to achieve better results; and if the correlation between decision trees is strong, the prediction accuracy can be further improved by using AdaBoost algorithm.

## Appendix

### Figure interpretation

Figures 7–18 show the results of stratified back test of primary factors and net value curve of long-short portfolio, which is used for factor screening.

### Python code

The models are implemented in Python 3.7.3, and back-test part program code is listed below.

```
import pandas as pd
import matplotlib.pyplot as plt
import math
import numpy as np
import os

def get_hundred (arr):
    temp = []
    for i in arr:
        if i == 0:
            temp.append( 0)
        else:
            temp.append(math.floor(i / 100) * 100)
    return temp

def get_net_value(day):
    """
    get net value
    : param day: back test date
    : return: net value
    """

    global position
    nv = money
    for symbol, quantity in position.items():
        if pd.isnull(df_close[symbol][day]):
            print('stock without price : {} , use the nearest
            price {}'.format(symbol))
            nv = nv + price[symbol] * quantity
        continue
```

```

else :
    nv = nv + df_close[symbol][day] * quantity
    price[symbol] = df_close[symbol][day]
return nv
def judge(day, next_day):
    """
    : param day: back test date
    : return: record word of position change :
    change_quantity
    """
    global change_quantity
    new_nv = get_net_value(day)
    df_judge = pd.DataFrame({'new_weight': df_weight
    [next_day]},
    index=df_weight.index)
    df_judge[ 'new_symbol_mv' ] = df_judge[ 'new_
    weight' ] * new_nv
    df_judge[ 'price' ] = df_close.loc[day, :]
    df_judge = df_judge[df_judge[ 'price' ] > 0]
    df_judge[ 'new_symbol_quantity' ] = df_judge
    [ 'new_symbol_mv' ] / (df_judge[ 'price' ] * ((1000 +
    trade_fee) / 1000))
    df_judge = df_judge.fillna( 0)
    # df_judge = df_judge.sort_va
    lues(by='new_symbol_mv', ascending=False)
    df_judge[ 'new_symbol_quantity' ] = get_hun
    dred(df_judge[ 'new_symbol_quantity' ])
    df_old_quantity = pd.DataFrame([position], index=
    [ 'old_quantity' ])
    df_old_quantity = df_old_quantity.T
    df_judge[ 'old_quantity' ] = df_old_quantity
    [ 'old_quantity' ]
    df_judge = df_judge.fillna( 0)
    df_judge[ 'change_quantity' ] = df_judge[ 'new_s
    ymbol_quantity' ] - df_judge[ 'old_quantity' ]
    change_ = df_judge[ 'change_quantity' ][df_judge
    [ 'change_quantity' ] != 0]
    return change_
def buy(symbol, quantity, cost):
    global position, money
    if symbol in position:
        position[symbol] = position[symbol] + quantity
    else:
        position[symbol] = quantity
    money = money - cost
def sell(symbol, quantity, cost):
    global position, money
    position[symbol] = position[symbol] - quantity
    if position[symbol] == 0:
        del position[symbol]
    money = money + cost
def trade(day):
    """
    trade according to position change
    :param day: back test date
    :return:
    """
    stop_trade = []
    for symbol in change_quantity.index:
        if df_close[symbol][day] == 0:
            print('{}suspended , can not trade'.-
            format(symbol, day))
            stop_trade.append(symbol)
    for symbol in change_quantity.index: # sale
        if change_quantity[symbol] < 0:
            if symbol in stop_trade: # judge if suspended
                print('{}suspended , can not sell'.-
                format(symbol, day))
                continue
            if df_ret[symbol][day] > -0.09: # judge if limit
            down
                if position[symbol] >= abs(change_quantity
                [symbol]): # judge if amount of stocks arrive to the
                number to sell
                    trade_money = abs(change_quantity
                    [symbol]) * df_close[symbol][day] * (1000 - trade_fee)
                    / 1000
                    sell(symbol=symbol, quantity=
                    abs(change_quantity[symbol]), cost=trade_money)
                else: # see all
                    trade_money = position[symbol] *
                    df_close[symbol][day] * (1000 - trade_fee) / 1000
                    print('{}number not enough{} , sell all
                    {}'.format(day, symbol, abs(change_quantity[symbol]),
                    position[symbol]))
                    sell( symbol=symbol, quantity=position
                    [symbol], cost=trade_money)
                else:
                    print('{}litmit down, can not sell'.-
                    format(day, symbol))
                    continue
            else :
                continue
    for symbol in change_quantity.index: # buy
        if change_quantity[symbol] > 0:
            if symbol in stop_trade: # judge if suspended
                print('{}suspende , can not buy'.-
                format(symbol, day))

```

```

        continue
    if money < 10000: # cash below 10000 give up
        buying
        print('{} ash below 10000,give up buying
        {}'.format(day, symbol))
        continue
    if df_ret[symbol][day] < 0.09: # if Limit Up
        trade_money = abs(change_quantity[symbol])
        * df_close[symbol][day] * (1000 + trade_fee) / 1000
        if money > trade_money: # cash enough
            trade_money = change_quantity[symbol] *
            df_close[symbol][day] * (1000 + trade_fee) / 1000
            buy(symbol, change_quantity[symbol],
            trade_money)
        else: # cash not enough, buy as can
            trade_quantity = 100 * math.floor(money /
            (df_close[symbol][day] * 100 * ((1000 + trade_fee) /
            1000)))
            if trade_quantity > 0:
                trade_money = trade_quantity * df_close
                [symbol][day] * (1000 + trade_fee) / 1000
                buy(symbol, trade_quantity,
                trade_money)
                print('cash is not enough , {} 买 {}buy as it
                can{}'.format(day, symbol, trade_quantity))
            if trade_quantity < 0:
                print('error , {} 买 {}buy number is neg-
                ative'.format(day, symbol))
            else: # skip if limit down
                print('{} 买,{}limit up,can not buy'.format(day,
                symbol))
            continue
        else :
            continue
def get_account(day):
    """
    get the account information for program debugging
    : param day:
    : return: account information of today, back csv file
    """
    symbol_list = []
    quantity_list = []
    price_list = []
    mv_list = []
    for symbol, quantity in position.items():
        symbol_list.append(symbol)
        quantity_list.append(quantity)
        price_list.append(price[symbol])
        mv_list.append(quantity * price[symbol])

```

```

    df_account = pd.DataFrame({'symbol': symbol_list,
    'quantity': quantity_list, 'price': price_list, 'mv':
    mv_list})
    df_account[ 'money' ] = money df_close =
    pd.read_csv # matrix of closing price
    df_close[df_close.columns[0]] = list(map(lambda x:
    str(x),
    df_close[df_close.columns[0]]))
    df_close = df_close.set_index(df_close.columns[ 0])
    df_ret = pd.read_csv
    df_ret[df_ret.columns[ 0]] = list(map(lambda x: str(x),
    df_ret[df_ret.columns[0]]))
    df_ret = df_ret.set_index(df_ret.columns[ 0])
    df_sum = pd.DataFrame()
    df_change_rate = pd.DataFrame()
    model_name = os.listdir
    for m_name in model_name:
        bug_record = []
        position = {}
        price = {}
        money = 500_0000
        origin_money = 500_0000
        net_value = []
        change_rate = []
        long_short = []
        money_record = []
        trade_fee = 9
        df_weight = pd.read_csv.format(m_name))
        df_weight = df_weight.set_index(df_weight.columns[0])
        start_day = '20120706'
        all_time_interval = list(df_weight.columns)
        back_test_interval = all_time_interval[all_ti-
        me_interval.index(start_day): -1]
        for date in back_test_interval:
            next_date = list(df_weight.columns)[1 +
            list(df_weight.columns).index(date)]
            change_quantity = judge(date, next_date)
            trade(date)
            # get_account(date)
            net_value.append(get_net_value(date) /
            origin_money)
            if date == start_day:
                print('{}net value change{}%'.format(date,
                0))
            change_rate.append( 0)
            money_record.append(money)
        else:

```

```

# print((get_net_value(date) /
1_000_000_000 - net_value[-2]) * 100 / net_value[-1])
print('{}net value{}'.format(m_name.split('_')[1], date, round(net_value[-1],
6)))
print('{}net value{}'.format(m_name.split('_')[1], date, round(net_value[-1] /
net_value[-2] - 1, 6)))
money_record.append(money)
change_rate.append( round(net_value[-1] /
net_value[-2] - 1, 6))
df_result = pd.DataFrame({'net_value': net_value,
'change_rate': change_rate},
index=back_test_interval)
df_sum[ '{}.format(m_name[:-4]) ] = df_result
['net_value']
df_change_rate[ '{}.format(m_name[:-4]) ] =
df_result['change_rate']
df_result.to_csv.format(m_name))
df_sum[ 'index' ] = df_result.index
df_sum = df_sum.set_index( 'index' )
df_sum.plot.line()
plt.show()
df_change_rate[ 'index' ] = df_change_rate.index
df_change_rate = df_change_rate.set_index( 'index' )
df_change_rate.plot.line()
plt.show().

```

## Data Availability

The data generated and analyzed in this manuscript are available from the CSMAR (China Stock Market & Accounting Research Database) and WIND Information Financial Terminal Market Sequence.

## Conflicts of Interest

The authors declare that they have no conflicts of interest.

## Acknowledgments

This study was supported by the “Great Wall Scholar Training Program” for the Construction of High-level Teachers in Universities of Beijing and the Planning Project of Beijing Social Science Fund (grant no. 20SRB010) and Cultivation of Major Research Projects of CUEB: Study on the mechanism, measurement, early warning and prevention of systemic financial risk contagion in China.

## References

- [1] F. Eugene and K. French, “The cross-section of expected stock returns,” *The Journal of Finance*, vol. 47, no. 2, pp. 427–465, 1992.
- [2] M. M. Carhart, “On persistence in mutual fund performance,” *The Journal of Finance*, vol. 52, no. 1, pp. 57–82, 1997.
- [3] E. F. Fama and J. D. MacBeth, “Risk, return, and equilibrium: empirical tests,” *Journal of Political Economy*, vol. 81, no. 3, pp. 607–636, 1973.
- [4] L. P. Hansen, “Large sample properties of generalized method of moments estimators,” *Econometrica*, vol. 50, no. 4, pp. 1029–1054, 1982.
- [5] J. Green, J. R. M. Hand, and X. F. Zhang, “The characteristics that provide independent information about average U.S. Monthly stock returns,” *Review of Financial Studies*, vol. 30, no. 12, pp. 4389–4436, 2017.
- [6] K. Hou, C. Xue, and L. Zhang, “Replicating anomalies,” *Review of Financial Studies*, vol. 33, no. 5, pp. 2019–2133, 2020.
- [7] S. Mullainathan and J. Spiess, “Machine learning: an applied econometric approach,” *The Journal of Economic Perspectives*, vol. 31, no. 2, pp. 87–106, 2017.
- [8] J. Kleinberg, H. Lakkaraju, J. Leskovec, J. Ludwig, and S. Mullainathan, “Human decisions and machine predictions,” *Quarterly Journal of Economics*, vol. 133, no. 1, pp. 237–293, 2018.
- [9] D. W. Liu, “Modeling and forecasting stock price Index based on support vector machine,” *Statistics and Decision making*, vol. 2, p. 3, 2013.
- [10] S. Y. Wang, Z. F. Cao, and M. Z. Chen, “Research on application of random forests in the quantitative stock selection model,” *Operations Research and Management Science*, vol. 3, pp. 163–168, 2016.
- [11] H. L. Xie and H. U. Di, “The application of multi-factor quantization model in portfolio: the comparative research on LASSO and elastic net,” *Statistics & Information Forum*, vol. 32, no. 10, pp. 36–42, 2017.
- [12] S. Gu, B. T. Kelly, and D. Xiu, *Empirical Asset Pricing via Machine Learning (No. w25398)*, National Bureau of Economic Research, Cambridge, MA, USA, 2018.
- [13] L. Wang and L. Li, “Multi-factor quantitative stock selection strategy based on gcForest,” *Computer Engineering and Applications*, vol. 56, no. 15, pp. 86–91, 2020.
- [14] D. E. Rapach, J. K. Strauss, and G. Zhou, “Out-of-sample equity premium prediction: combination forecasts and links to the real economy,” *Review of Financial Studies*, vol. 23, no. 2, pp. 821–862, 2010.
- [15] J. H. Friedman, *The Elements of Statistical Learning: Data Mining, Inference, and Prediction*, Springer open, New York, NY, USA, 2017.
- [16] M. Fernández-Delgado, E. Cernadas, S. Barro, and D. Amorim, “Do we need hundreds of classifiers to solve real world classification problems?” *Journal of Machine Learning Research*, vol. 15, no. 1, pp. 3133–3181, 2014.
- [17] D. J. Henderson, C. Papageorgiou, and C. F. Parmeter, “Growth empirics without parameters,” *The Economic Journal*, vol. 122, no. 559, pp. 125–154, 2011.
- [18] A. E. Hoerl and R. W. Kennard, “Ridge regression: biased estimation for nonorthogonal problems,” *Technometrics*, vol. 12, no. 1, pp. 55–67, 1970.
- [19] D. M. McNeish and M. Daniel, “Using lasso for predictor selection and to assuage overfitting: a method long overlooked in behavioral sciences,” *Multivariate Behavioral Research*, vol. 50, no. 5, pp. 471–484, 2015.
- [20] L. Breiman, “Random forests,” *Machine Learning*, vol. 45, no. 1, pp. 5–32, 2001.
- [21] G. C. Cawley and N. L. C. Talbot, “On over-fitting in model selection and subsequent selection bias in performance evaluation,” *Journal of Machine Learning Research*, vol. 11, no. 1, pp. 2079–2107, 2010.

- [22] V. N. Vapnik, *The Nature of Statistical Learning Theory*-Springer, New York, NY, USA, 1995.
- [23] W. F. Sharpe, "Capital asset prices: a theory OF market equilibrium under conditions OF risk\*," *The Journal of Finance*, vol. 19, no. 3, pp. 425–442, 1964.
- [24] Z. Xu, T. Chevapatrakul, and X. Li, "Return asymmetry and the cross section of stock returns," *Journal of International Money and Finance*, vol. 97, no. OCT, pp. 93–110, 2019.

## Research Article

# A Composite Index for Measuring Stock Market Inefficiency

Raffaele Mattera <sup>1</sup>, Fabrizio Di Scorio <sup>2</sup>, and Juan E. Trinidad-Segovia <sup>2</sup>

<sup>1</sup>Department of Economics and Statistics, University of Naples Federico II, Naples, Italy

<sup>2</sup>Department of Economics and Business, University of Almeria, Almeria, Spain

Correspondence should be addressed to Juan E. Trinidad-Segovia; [jetrini@ual.es](mailto:jetrini@ual.es)

Received 28 August 2021; Revised 2 January 2022; Accepted 5 January 2022; Published 24 January 2022

Academic Editor: Sameh S. Askar

Copyright © 2022 Raffaele Mattera et al. This is an open access article distributed under the Creative Commons Attribution License, which permits unrestricted use, distribution, and reproduction in any medium, provided the original work is properly cited.

Market inefficiency is a latent concept, and it is difficult to be measured by means of a single indicator. In this paper, following both the adaptive market hypothesis (AMH) and the fractal market hypothesis (FMH), we develop a new time-varying measure of stock market inefficiency. The proposed measure, called composite efficiency index (CEI), is estimated as the synthesis of the most common efficiency measures such as the returns' autocorrelation, liquidity, volatility, and a new measure based on the Hurst exponent, called the Hurst efficiency index (HEI). To empirically validate the indicator, we compare different European stock markets in terms of efficiency over time.

## 1. Introduction

From Malkiel and Fama [1] seminal work, there have been several papers that studied the market efficiency. The efficient market hypothesis (EMH) is based on many unrealistic assumptions such as serial independence, returns' normality, homoscedasticity, and absence of long memory. Nowadays, it is well accepted that stock returns share some statistical properties, called stylized facts (see Cont [2]), which suggest strong deviation from the EMH. Various methods have been proposed to test the efficient market hypothesis (EMH), but the empirical evidence varies according to the specific markets, periods of time, and the selected approaches implemented to measure the efficiency.

EMH considers that the investor is generic. An investor is anyone who wants to buy, sell, or hold a security because of the available information, and it is rational price-taker. This generic approach, where information and investors are general cases, implies that financial markets are "informationally efficient." However, it is easy to see that extreme market reactions occur more frequently than as expected by the EMH, and noise traders operate to provide the necessary liquidity for the rational investors. Proposed by Peters (1994) on Mandelbrot's' previous work, the fractal market

hypothesis (FMH) arrives to provide a new framework to model the turbulence in financial markets. The FMH is based on the concept of market liquidity, and how the information that arrives to the market is interpreted by different agents. So, the market is stable when there are investors operating in a large number of investment horizons on the market is provided of wide liquidity. When information has the same impact on all investors, the market liquidity will decrease, and the market will be unstable. The FMH considers that the market collapses when one-horizon traders are market dominants placing many sell orders that the rest of agents cannot absorb.

As the EMH, APT, and CAPM are equilibrium models, it is expected that work properly when markets are stable, but not under turbulences. Weron and Weron [3] remarked that the purpose of the FMH is to give a model of investor behavior and market price movements that fits our observations. The key is that, under the FMH, the market is stable when it has no characteristic timescale or investment horizon.

Market efficiency is surely a latent concept, and it is difficult to be measured by means of a single indicator. Nevertheless, it has been measured in different ways. Moreover, from Lo [4], we know that market efficiency



changes over the time. This is the main idea underlying the adaptive market hypothesis (AMH). As a consequence, a good measure of efficiency has to be time-varying.

Among the several approaches for measuring market efficiency, the most common is based on returns' autocorrelation (e.g., Ito et al. [5, 6], Noda [7], and Tran and Leirvik [8]). The degree of returns' autocorrelation is an index of market efficiency because, if present, it reflects a deviation from the random walk hypothesis. In particular, Ito et al. [5, 6] measured time-varying efficiency by considering the autocorrelation in stock monthly returns estimated with a time-variant autoregressive (TV-AR) model. Tran and Leirvik [8] improved the measure of Ito et al. [5, 6] for high-frequency data and for a large number of autocorrelations.

Furthermore, from a historical perspective, volatility has been proved to be a good proxy of market efficiency as well (Földvári and Van Leeuwen [9]). In this direction, Lo and MacKinlay [10] proposed a test statistic based on the ratio of variances which is still nowadays commonly used in testing for market efficiency. More recently, Liu and Chen [11] studied market efficiency by means of ARMA-GARCH forecasts in order to account the heteroscedastic nature of stock returns.

Another type of market efficiency measure is related to the market liquidity (e.g., Sukpitak and Hengpunya [12]). With this respect, Chordia et al. [13] found that predictability is lower in the market with narrower bid-ask spreads and that prices were closer to random walk in more liquid markets. Similarly, Chung and Hrazdil [14] showed that the more liquid in a market, the higher is its efficiency. There are several ways of measuring liquidity (for a review, see Gabrielsen et al. [15]), but one of the most recognized and used was proposed by Amihud [16].

A fourth approach and, perhaps, the most discussed (e.g., Kristoufek and Vosvrda [17, 18], Sensoy and Tabak [19], and Kristoufek and Vosvrda [20, 21]) is based on the analysis of markets' long-range dependence, also defined as long memory. The long memory property describes if and how much past events influence the future evolution of the process (Asuloos et al. [22]). There are several researchers who studied the long memory of financial markets (e.g., Lillo and Farmer [23], Jiang et al. [24], Ferreira and Dionisio [25], Barviera et al. [26], Sánchez Granero et al. [27], and Dimitrova et al. [28]).

The long memory is commonly studied through the Hurst exponent, previously introduced by Hurst [29] and lately developed by Mandelbrot and Van Ness [30], which represents the rate of decay of the autocorrelation function of a time series. If  $h > 1/2$ , we say that the time series shows persistent behavior; if  $h < 1/2$ , we define the time series as antipersistent. Bianchi et al. [31] claimed that different values of the Hurst exponent  $h$  are related to different regimes: "bull" and "bear" periods and the mean reversion.

Overall, the Hurst exponent is closely related to market efficiency, and several authors (e.g., Bianchi [32], Sánchez Granero et al. [27], and Dimitrova et al. [28]) showed that a value of  $h = 0.5$  reflects an efficient market. Therefore, in constructing a measure of inefficiency, the deviations of  $h$  from the value  $h = 0.5$  have to be computed (Kristoufek and

Vosvrda [17]). However, a time-invariant Hurst exponent explicitly contradicts the adaptive market hypothesis (AMH). To overcome this limitation, we consider a new efficiency measure based on a time-varying Hurst exponent that is computed by assuming that stock prices follow a multifractional Brownian motion (mBm).

However, each of the aforementioned approaches only considers one aspect of efficiency. Composite indicators are used in several domains of science to summarise in a meaningful way the information coming from different sources. Starting from the fact that efficiency is a difficult concept to measure by means of a single indicator, in this paper, we construct a new composite indicator, called composite efficiency index (CEI), of financial market efficiency by combining all the aforementioned different measures.

Building composite indicators is a complex task that involves several steps: (1) selection of the theoretical framework, (2) the selection of the subindicators, and (3) the aggregation method (i.e., how the single indicators are combined). The theoretical framework of the proposed CEI is obviously represented by the financial market efficiency. Regarding the selection of the subindicators, we consider each of the aforementioned approaches of measuring market efficiency. Regarding the last step, our approach consists in estimating a factor model where the composite index is the latent common factor. Then, the composite index is obtained by the principal component estimator (see Bai and Ng [33]).

As an empirical application, we study the efficiency of different European stock markets by considering also the effects of the COVID-19 pandemic by means of this new composite index. More in detail, we consider the Netherlands, Austria, Belgium, France, Germany, Spain, and Switzerland stock markets and construct country-specific composite indicators. Then, we proceed to estimate the inefficiency of the market during the reference period and investigate the deterministic or random nature of this phenomenon. Moreover, the properties of the efficiency process are studied from a statistical point of view through the stationarity test (Dickey–Fuller test) and the analysis of the (partial) autocorrelation function.

The rest of this paper is organized as follows. In the next sections, the remaining three steps required for the construction of the composite efficiency index (CEI) are discussed in detail. In particular, in Sections 2 and 3, the information set is presented (i.e., the set of the considered subindicators), while in Section 4, the employed methodology (i.e., the aggregation method) is discussed. In particular, Section 3 discusses in detail a new Hurst-based inefficiency measure. In Section 5, we apply the proposed methodology to European stock market data, while some final remarks are discussed in the conclusions.

## 2. Measuring Market Efficiency

In the following, we discuss in detail the subindices considered for the construction of the composite efficiency index (CEI). The classical single indicators are the returns' autocorrelation, volatility, and liquidity. Moreover, we also

construct a new efficiency measure based on the time-varying Hurst exponent that is used as an additional sub-index, which is discussed in more detail in Section 3 of this paper.

**2.1. Autocorrelation.** The proposed index exploits several aspects of the efficiency for its construction. First of all, the returns' autocorrelation: we consider the fact that, according to the EMH, an autoregressive process of any order  $p$  cannot explain the dynamics of the returns  $r_t$ . Hence, we consider the following AR( $p$ ) process:

$$r_t = \alpha + \beta_1 r_{t-1} + \beta_2 r_{t-2} + \dots + \beta_p r_{t-p} + \varepsilon_t. \quad (1)$$

Let  $\widehat{\beta} = (\widehat{\beta}_1, \widehat{\beta}_2, \dots, \widehat{\beta}_p)$  be the vector of the estimated  $\beta$  coefficients in (1). If the market is efficient, the vector  $\beta$  should contain all values very close to zero. Following Noda [7], we consider the magnitude market inefficiency (MIM):

$$\text{MIM}_t = \left| \frac{\sum_{j=1}^p \widehat{\beta}_{j,t}}{1 + \sum_{j=1}^p \widehat{\beta}_{j,t}} \right|, \quad (2)$$

where absolute values are used to get rid of sign effects. For this index, deviations from zero represent inefficient markets. Clearly, this measure is not rid of weaknesses. For example, the market efficiency computed in this way, as any model-based approach, depends on the sampling errors. Nevertheless, (2) represents the first of the subindicator's set.

**2.2. Volatility.** Another important proxy for stock market inefficiency that we consider is volatility. Even if there are several ways of computing volatility, Földvári and Van Leeuwen [9] showed that GARCH models provide a good way for appropriately reconstructing volatility. Therefore, as volatility measure, we consider the in-sample predictions obtained by a  $t$ -GARCH(1, 1) model of Bollerslev [34]:

$$\begin{aligned} r_t &= \mu_t + \varepsilon_t, & \varepsilon_t &= \sigma_t z_t \\ \sigma_t^2 &= \omega + \alpha z_{t-1}^2 + \beta \sigma_{t-1}^2, \end{aligned} \quad (3)$$

where the innovation term contained in  $(z_t; t \geq 0)$  is assumed to be a stochastic process with i.i.d.  $t$ -student realizations in order to account for stock returns fat tails (e.g., Cerqueti et al. [35]).

**2.3. Liquidity.** Measuring market liquidity is important as well. Indeed, we know that illiquid markets are very inefficient. Despite there are several ways of measuring liquidity (for a review, see Gabrielsen et al. [15]), we consider the illiquidity measure developed by Amihud [16], which is one of the most recognized since it can be computed by using only prices and volumes. Moreover, it is also used by policy makers to estimate liquidity in financial markets. The Amihud [16] illiquidity measure is obtained with the following equation:

$$\text{ILL}_t = \frac{1}{T} \sum_{t=1}^T \frac{|r_t|}{v_t}, \quad (4)$$

where  $r_{t,T}^i$  is the return at time  $t$  and  $v_t$  is the volume. (4) is a realized measure of illiquidity since it can be computed on a yearly basis, monthly as the average of the daily ratios within each month, or daily as the average of the intradaily ratios. A rough daily measure can be obtained by simply considering the daily ratio in (4). Despite the fact that the Amihud [16] index is a measure of the price impact, differently from the bid-ask spread, its main advantage is based on the simplicity of calculation and the easy availability of the data.

### 3. A New Hurst-Based Efficiency Measure

At the end, we consider a very promising measure of market efficiency based on the fractal market hypothesis (FMH). Exploring efficiency by the FMH requires the estimation of the Hurst exponent. Indeed, nowadays, the Hurst-based inefficiency measures are well established (e.g., Kristoufek and Vosvrda [17, 18], Sensoy and Tabak [19], and Kristoufek and Vosvrda [20, 21]).

Nevertheless, there are some relevant questions regarding the usage of the Hurst exponent in finance. First of all, the way which the Hurst exponent is computed is crucial. Indeed, even if different approaches to calculate the Hurst exponent have been proposed in the last decades (see López-García and Requena [36] for an interesting review), several authors (e.g., Lo [37], Sánchez Granero et al. [27], and Weron [38]) claimed that the Hurst exponent estimation using classical methodologies presents a lack of preciseness when the length of the series is not large enough. In addition, Mercik et al. [39], Fernández-Martínez et al. [40], and Sánchez et al. [41] proved that most of the classical algorithms used to calculate the Hurst exponent are valid only for fractional Brownian motions and do not work properly for another kind of distributions such as stable ones.

Another important issue lies on the fact that assuming a constant value for the Hurst exponent  $h$  is unrealistic (e.g., see Bianchi [32], Bianchi et al. [31], and Mattera and Sciorio [42]) and explicitly contradicts the adaptive market hypothesis (AMH). To overcome this limitation, we consider an additional efficiency measure based on a time-varying Hurst exponent.

The mathematical representation of a fractal market is based on the fractional Brownian motion (fBm) and assumes a value of Hurst that can be  $h \neq 0.5$ . A very useful generalization of the fractional Brownian motion that is consistent with the adaptive market hypothesis is represented by the multifractional Brownian motion (mBm).

The multifractional Brownian motion (mBm) was introduced to replace the real  $h$  by a function  $t \rightarrow h_t$  ranging in  $[0, 1]$ . The function  $h_t$  is the regularity function of mBm.

Corlay et al. [43] started from the definition of a fractional Brownian field. Let  $(\Omega, F, P)$  be a probability space. A fractional Brownian field on  $R \times (0, 1)$  is a Gaussian field, noted  $(W(t, h))_{(t,h) \in R \times [0,1]}$ , such that, for every  $h$  in  $[0, 1]$ , the defined process is a fractional Brownian motion with Hurst parameter  $h$ .

A multifractional Brownian motion is simply a "path" traced on a fractional Brownian field. More precisely, it is defined as follows.

Let  $h: R \rightarrow [0, 1]$  be a deterministic continuous function and  $W$  be a fractional Brownian field. A mBm on  $W$  with functional parameter  $h$  is the Gaussian process defined by  $W_t^h: = W(t, h_t)$  for all  $t \in R$ .

The multifractional Brownian motion can be represented by the following formulation (Bianchi [32]):

$$W_{h_t}(t) = KV_{h_t} \int_{\mathcal{R}} |t-s|^{h_t-(1/2)} - |s|^{h_t-(1/2)} dW(s), \quad (5)$$

where the normalizing factor  $V_{h_t}$  is equal to

$$V_{h_t} = \frac{\sqrt{\Gamma(2h_t+1)\sin(\pi h_t)}}{\Gamma(h_t+(1/2))}, \quad (6)$$

and its covariance is given by

$$E[W_{h_t}(t)W_{h_s}(s)] = K^2 D(h_t, h_s) (t^{h_t+h_s} + s^{h_t+h_s} - |t-s|^{h_t+h_s}), \quad (7)$$

where

$$D(h_t, h_s) = \frac{\sqrt{\Gamma(2h_t+1)\Gamma(2h_s+1)\sin(\pi h_t)\sin(\pi h_s)}}{2\Gamma(2h_t+h_s+1)\sin[(\pi(h_t+h_s))/2]}. \quad (8)$$

In the mBm, a time-varying Hurst exponent  $h_t$  is related to the idea of long memory instead of a static one. Higher values than 0.5 for the Hurst exponent indicate the persistence of the time series, while lower values indicate antipersistence. Under efficient markets, we have a geometric Brownian motion (gBm) process, and the Hurst index assumes a value of 0.5.

We then introduce a new time-varying measure of market inefficiency, called Hurst-based efficiency index (HEI), given by the absolute deviation of the empirical (time-varying) Hurst exponent from its theoretical value of 0.5 under efficient markets:

$$HEI_t = |0.5 - h_t|. \quad (9)$$

In this paper, we propose to estimate  $h_t$  with the AMBE method of Bianchi et al. [31] and Bianchi and Pianese [44] that works as follows.

Considering a time series  $X_{h_t,t}$  follows a multifractional Brownian motion (5), the author assumes a discrete version  $\{X_{i,n}\}_{i=1,\dots,n-1}$ , which, for  $j = i - \delta, \dots, i - q$ ,  $i = \delta + 1, \dots, n$ , and  $q = 1, \dots, \delta$ , locally behaves like a fractional Brownian motion with a given exponent  $h$  within a window of proper length  $\delta$ . Then, Bianchi [32] derived the following estimator:

$$\hat{h}_t = -\frac{\log(\sqrt{\pi}) \mathcal{S}^k / (2^{k/2} \Gamma(k+1/2) K^k)}{k \log((n+1)/q)} \quad (10)$$

with  $\mathcal{S}^k$ :

$$\mathcal{S}^k = \frac{1}{\delta - q + 1} \sum_{j=i-\delta}^{i-q} |X_{j+q,n} - X_{j,n}|^k, \quad i = \delta + 1, \dots, n. \quad (11)$$

In order to apply estimator (9), the parameters  $q$ ,  $k$ , and  $\delta$  have to be chosen. According to Bianchi [32], the best choice for  $q = 1$ . About  $k$ , since it affects the estimator's variance,

the choice should be made with a variance-minimization criterion. The optimal choice is  $k = 2$  (see Bianchi [32] for the estimator's variance formula). In the end, about the parameter  $\delta$ , the author suggests a value of  $\delta = 30$  for the financial application.

Therefore, the Hurst-based efficiency index (HEI) is obtained by replacing  $h_t$  estimated with (9) within (8).

## 4. Methodology

The last step required for building composite indicators is based on the aggregation/synthesis of the subindices. With this respect, several authors (e.g., Becker et al. [45] and Karagiannis [46]) agree that one of the most critical aspects in the definition of a composite index is this last step because the weighting procedures reflect the relevance of each indicator in determining the overall composite index.

Different schemes have been proposed in the literature, but no one is free from weaknesses (for an overview, see Greco et al. [47]).

The first approach is to consider an equal weighting scheme. This scheme is commonly employed when it is assumed that each indicator has the same informative power with respect to the phenomenon under investigation. Despite its simplicity, the equal weighting does not take into account both the variability of different indicators and their relationship structure.

To avoid equal weighting, the literature considered specific statistical methods. Some popular approaches are based on the correlation analysis and linear regression.

According to the correlation analysis, it is possible to determine the weights by considering the correlation between each indicator and a selected benchmark (Kantiray [48]) such that the stronger is the correlation of a given subindex, and the higher is its weight. The main drawbacks of the correlation-based approach rely on the fact that correlations may be statistically not significant and do not necessarily imply causation, only taking into account if different indicators move or not in the same direction.

Regression analysis, instead, allows exploring the causal linkage between the individual indicators and a benchmark. Indicators' weights are retrieved by estimating the linear model. However, even if regression analysis exploits causal relationships in weighting subindicators, as in correlation analysis, the choice of an appropriate endogenous variable is required.

This aspect is problematic since most of the times, a composite indicator is built with the aim of measuring a latent concept. This is the case of well-being (e.g., Slottje [49] and Haq and Zia [50]), but another interesting example is the financial market inefficiency, where several proxies exist (e.g., volatility and market liquidity) but a single measure does not.

Therefore, a third approach for constructing composite indicators is based on factorial analysis and principal component analysis (PCA). In these cases, no benchmark has to be chosen, and the composite indicator is obtained as the synthesis of a set of subindices that roughly explain the phenomenon. The composite indicator proposed in this paper falls within this last class of approaches.

More in detail, we start by considering a factor model structure. Factor models have been widely applied in both theoretical and empirical finance. An important distinction which has to be done is between observed and latent factor models. Observed factors are known and based on outside information. On the contrary, latent factors are unknown and need to be estimated.

Let  $T$  and  $N$  denote the sample size in the time series and number of subindices, respectively. For  $i = 1, \dots, N$  and  $t = 1, \dots, T$ , the observation  $X_{i,t}$  has a factor structure represented as

$$X_{i,t} = \lambda_i' F_t + e_{i,t}. \quad (12)$$

The factor model (11) can be written in the matrix form as follows:

$$\mathbf{X} = \mathbf{F}\mathbf{\Lambda}' + \mathbf{e}, \quad (13)$$

where  $\mathbf{F} = (F_1, F_2, \dots, F_T)'$  is the  $T \times r$  matrix of factors and  $\mathbf{\Lambda} = (\lambda_1, \lambda_2, \dots, \lambda_N)'$  is the  $N \times r$  matrix of factor loadings. Our objective is to estimate both  $F$  and  $\Lambda$ . The most common approach for estimating the static latent factor is through the principal component estimator (e.g., Stock and Watson [51] and Bai and Ng [33]).

By choosing the normalizations  $F'F/T = I_r$  and diagonal  $\mathbf{\Lambda}'\mathbf{\Lambda}$ , we consider the following objective function minimization:

$$\text{tr}[(\mathbf{X} - \mathbf{F}\mathbf{\Lambda}')'(\mathbf{X} - \mathbf{F}\mathbf{\Lambda}')], \quad (14)$$

where  $\text{tr}(\cdot)$  denotes the matrix trace. The estimator for  $\mathbf{F}$ , denoted by  $\hat{\mathbf{F}}$ , is a  $T \times r$  matrix consisting of  $r$  unitary eigenvectors associated with the  $r$  largest eigenvalues of the matrix  $X'X/(TN)$  in the decreasing order. Then,  $\hat{\mathbf{\Lambda}} = X'\hat{\mathbf{F}}$  is an  $N \times r$  matrix of estimated factor loadings. Stock and Watson [51] showed that the sample eigenvector of  $X'X$  asymptotically behaves like those of  $\mathbf{\Lambda}'F'F\mathbf{\Lambda}$ , and then, use these eigenvectors to consistently estimate  $\hat{\mathbf{F}}$ .

We consider the composite efficiency index (CEI) as the  $r = 1$  estimated factor. The choice of single common factor is reasonable because in the empirical application, we find that the first factor explains most of the total variance. Indeed, it is important to highlight that if the first factor accounts for at least 65% of the total variance, the latent concept is usually considered unidimensional, and the first factor is assumed to be the composite indicator (see Nardo et al. [52]). Moreover, by employing the Bai and Ng [53] procedure, we find that only one latent factor (i.e.,  $r = 1$ ) can be used to describe market efficiency for all the considered stock markets. Alternatively, also, the Kaiser rule can be applied to identify the number of factors (The Kaiser rule suggests to drop factors with eigenvalues below 1. The motivation is that it makes no sense to add a factor explaining less variability than just one indicator.), but the use of Bai and Ng [53] procedure is more appropriate when dealing with factor models. The Bai and Ng procedure works for both strict and approximate factor models. In approximate factor models, some correlation in the idiosyncratic components is allowed, and thus is more general than the strict factor model where the idiosyncratic components are uncorrelated. Their procedure can also be

applied for the definition of the optimal number of factors for strict factor models.

Factor model and PCA are inevitably related concepts. However, differently from PCA, the first involves the estimation of a model where some observable variables are determined by both common factors and unique factors. Moreover, a factor model has its own covariance structure such that the total data variability can be decomposed into that accounted for by common factors and that due to unique factors. Nevertheless, PCA is commonly used to estimate the common latent factors.

## 5. Application to European Stock Markets

**5.1. Data and Subindices.** To show the usefulness of the proposed index, we provide an application to the major European stock markets. In detail, we consider the prices and volume time series for the stock exchange index of the Netherlands (AEX), Austria (ATX), Belgium (BEL20), France (CAC40), Germany (DAX30), Spain (IBEX35), and Switzerland (SMI). For each time series, we consider the daily data from January 1, 2003, to August 1, 2021. For some market indices (i.e., ATX and IBEX), we have shorter time series because of data availability. However, different time series length is not an issue for our application. The time series of the log returns are shown in Figure 1.

The ingredients needed for the computation of the composite indicator are those described in Section 2 of the paper. To compute the MIM (2), the indicator of market efficiency based on the returns' autocorrelation structure has been obtained by considering a time-varying AR process (TV-AR) as in [7]. In particular, following a rolling-window approach, we consider an estimation window equal to  $M = 252$ , hence, of 1 year of daily observations, which is updated day by day. Therefore, given a  $T$ -length time series, we obtain, for each market, a MIM time series of length  $T - M$ . Figure 2 shows the evolution over time of the MIM for each of the considered stock market indices. The higher the MIM value, the higher the market inefficiency.

Then, another indicator of market efficiency that we consider is based on the estimated conditional volatility. In this paper, following authors such as Földvári and Van Leeuwen [9] and Liu and Chen [11], we consider in-sample predictions from a  $t$ -GARCH(1, 1) model (3). Figure 3 reports the evolution over time of the estimated conditional volatility.

It is clear from Figure 3 that volatility increases during the period of crisis. Market liquidity is another important measure of market efficiency since, as we have seen, a liquid market is more efficient than an illiquid one. In the paper, we consider the illiquidity measure of Amihud [16] in (4). As in the case of the MIM index, to compute the ILL index, we used a rolling-window approach with the estimation window  $m = 252$ , i.e., one year of observation. Since the ILL index is a realized measure, we compute the market illiquidity over the last year by updating the indicator daily. The results for the considered sample of market returns are shown in Figure 4.

In the end, we have the new measure of market inefficiency based on the time-varying Hurst exponent. As

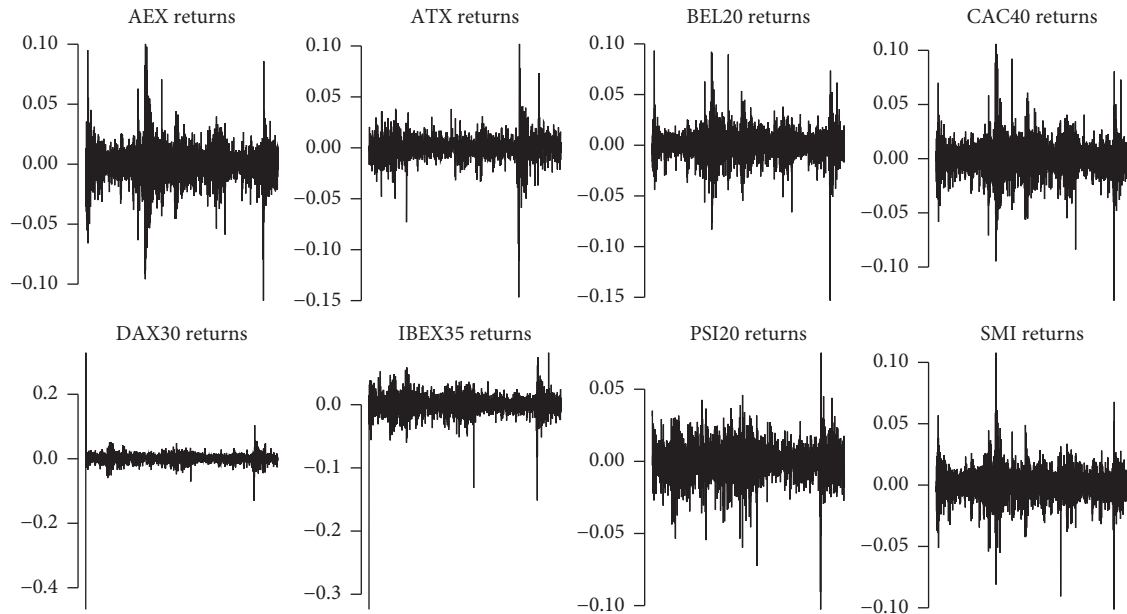


FIGURE 1: Daily returns of the considered stock market indices.

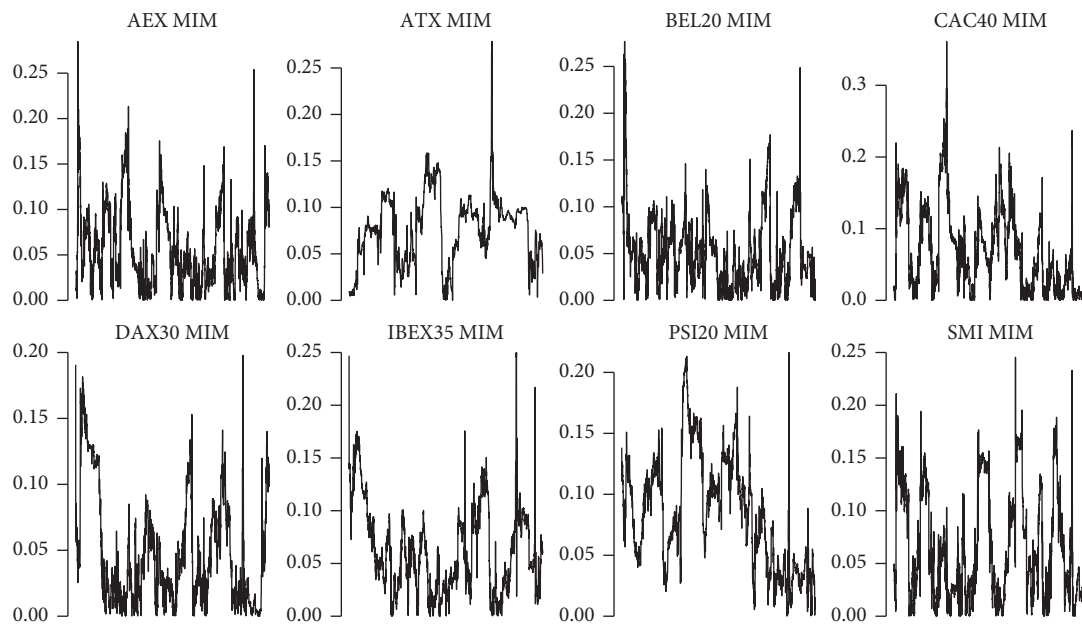


FIGURE 2: Daily estimated MIM for each of the considered stock market indices.

explained in Section 2 of the paper, the Hurst exponent is computed with the AMBE method proposed by Bianchi [32] and Bianchi et al. [31]. The Hurst estimates are shown in Figure 5.

Figure 5 somehow validates the adaptive market hypothesis (AMH) since we observe many deviations from the value of  $h = 0.5$ , under which the market should be efficient. Moreover, the degree of efficiency changes over time as well, and the severity of the deviation is not constant over the time. Indeed, while, in some time periods, we observe strongly persistent behaviors (i.e.,  $h_t > 0.5$ ), in others, the markets seem to be antipersistent.

Nevertheless, any deviation from  $h = 0.5$  represents a deviation from the hypothesis of efficient market. Therefore, we derive the Hurst-based efficiency index (HEI) as the absolute deviations of the Hurst exponent in Figure 5 from the value  $h_t = 0.5$ , as shown in (8).

The resulting time series are shown in Figure 6.

A value of  $HEI_t = 0$  means that the market is somehow efficient, and the bigger the HEI value, the higher the degree of market inefficiency. We observe huge spikes in the HEI time series in the presence of crisis. In particular, by considering Figures 2–6 together, we can see that the time periods with picks in the HEI index are associated to picks in

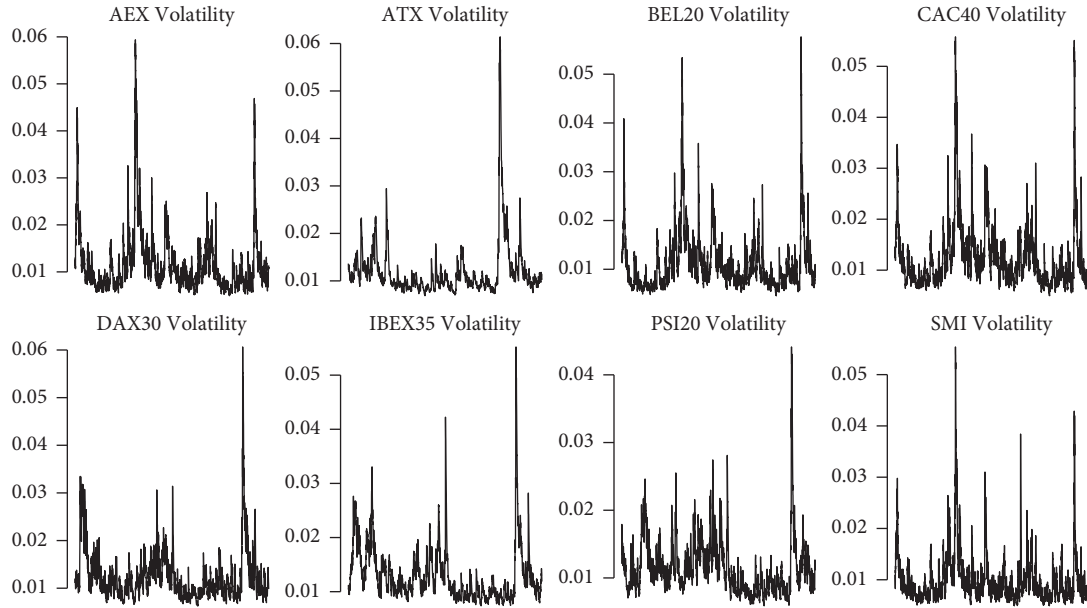


FIGURE 3: Daily estimated conditional volatility for each of the considered stock market indices.

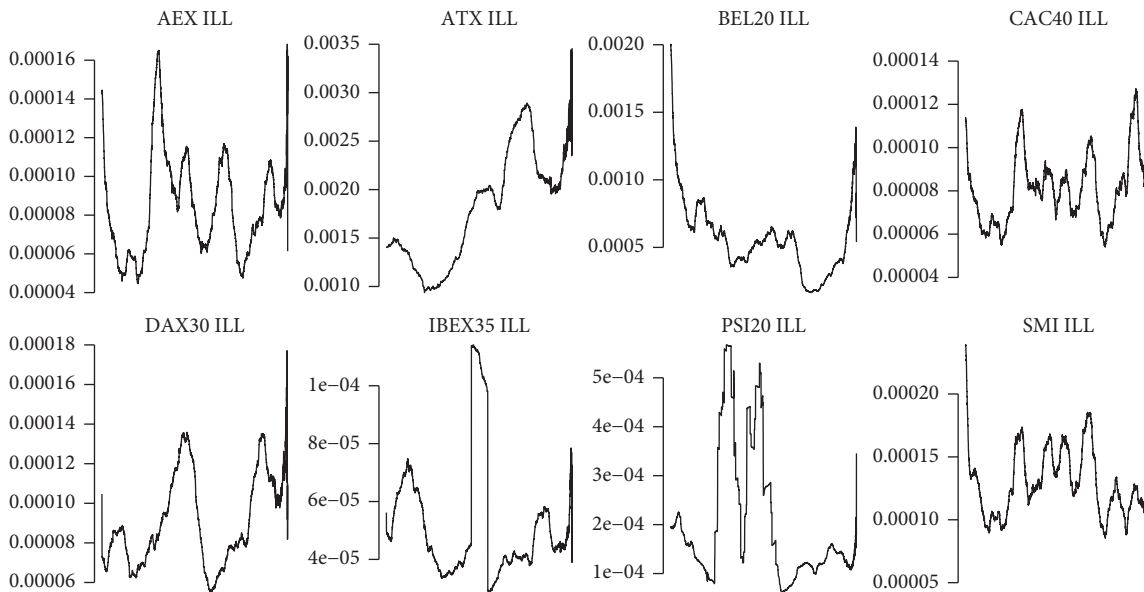


FIGURE 4: Daily estimated illiquidity index of Amihud [16] for each of the considered stock market indices.

the other inefficiency measures, i.e., MIM, ILL, and volatility. Therefore, all the indices increase with increasing inefficiency, and therefore, the HEI index gets higher values when the market becomes more illiquid and highly volatile.

Nonetheless, we aim to measure the complexity of financial market by considering a single index that incorporates all these information. To this aim, we developed the composite efficiency index by following the methodology explained in Section 3.

**5.2. Composite Efficiency Index: In-Sample Analysis.** In the following, we aim to describe the in-sample dynamics of the developed CEI. As previously explained, the CEI is

computed as the latent factor underlying the movements of the aforementioned subindices. Such a latent factor is consistently estimated with the principal component (PC) estimator. The CEI time series, for each stock market, is shown in Figure 7.

Clearly, different markets show very different behaviors of the index. This fact depends on different importance of each single subcomponent in being the main driving force of inefficiency across different markets.

As a consequence, while some markets present trends in efficiency levels (e.g., ATX and PSI markets), others show more random behaviors around their mean. This fact rises the problem of efficiency predictability. With a predictable market efficiency, policy makers would be able to identify

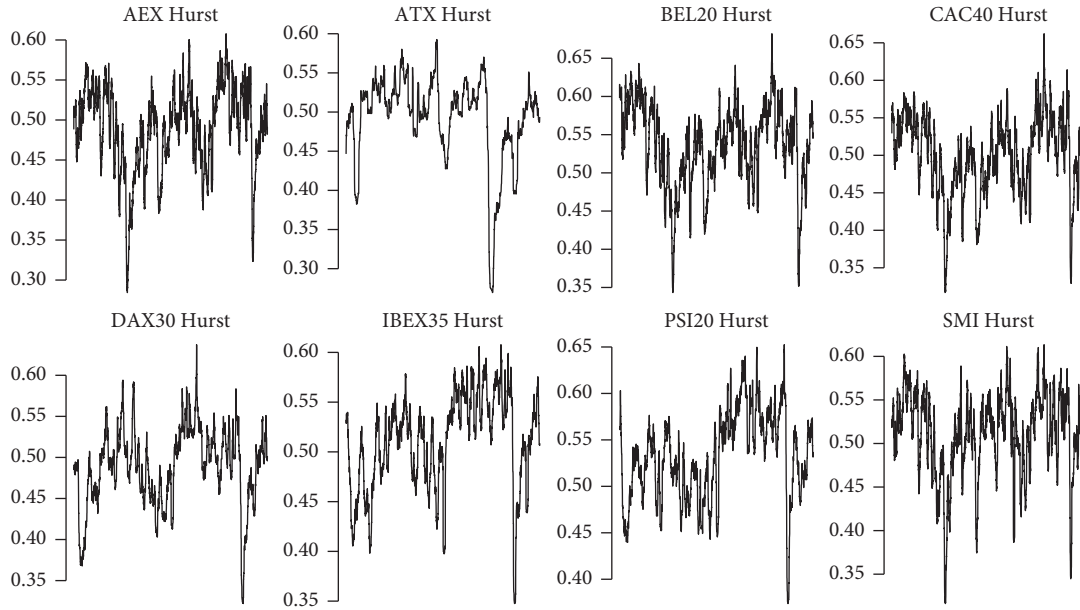


FIGURE 5: Daily estimated Hurst exponent for each of the considered stock market indices.

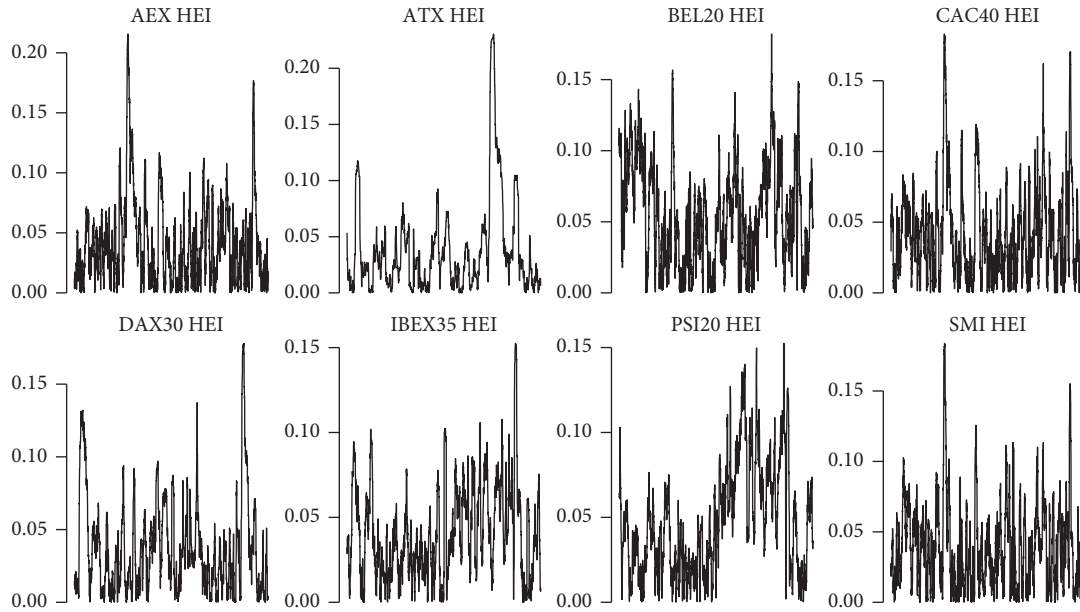


FIGURE 6: Daily estimated Hurst-based efficiency index (HEI) for each of the considered stock market indices.

appropriate policies with the aim of making markets more efficient in the near future. Similarly, stock traders would adjust their investment strategies accordingly.

Figure 8 shows the autocorrelation structure of the CEI for the sample of stock markets.

Figure 8 highlights a very strong autocorrelation structure for the CEI across all the considered markets. Hence, the CEI shows a very persistent behavior. This evidence suggests a possibly strong predictability. To get further evidence, we test if the CEIs are random walk (RW) or not. In doing so, we perform the Ljung–Box [54] test on the CEI's first different ( $\Delta CEI_t$ ). Ljung–Box [54], usually used to test for the white noise hypothesis, is based on the following test statistic:

$$Q = T(T+2) \sum_{k=1}^h (T-k)^{-1} \rho_k^2, \quad (15)$$

where  $T$  is the length of the time series,  $\rho_k$  is the  $k$ th autocorrelation coefficient, and  $h$  is the number of lags used for testing. Hyndman and Athanasopoulos [55] recommended using  $h = 10$  for nonseasonal data. Autocorrelations at different lags  $k$  are computed with the usual estimator:

$$\hat{\rho}_k = \frac{\sum_{t=k+1}^T (y_t - \bar{y})(y_{t-k} - \bar{y})}{\sum_{t=1}^T (y_t - \bar{y})^2}, \quad (16)$$

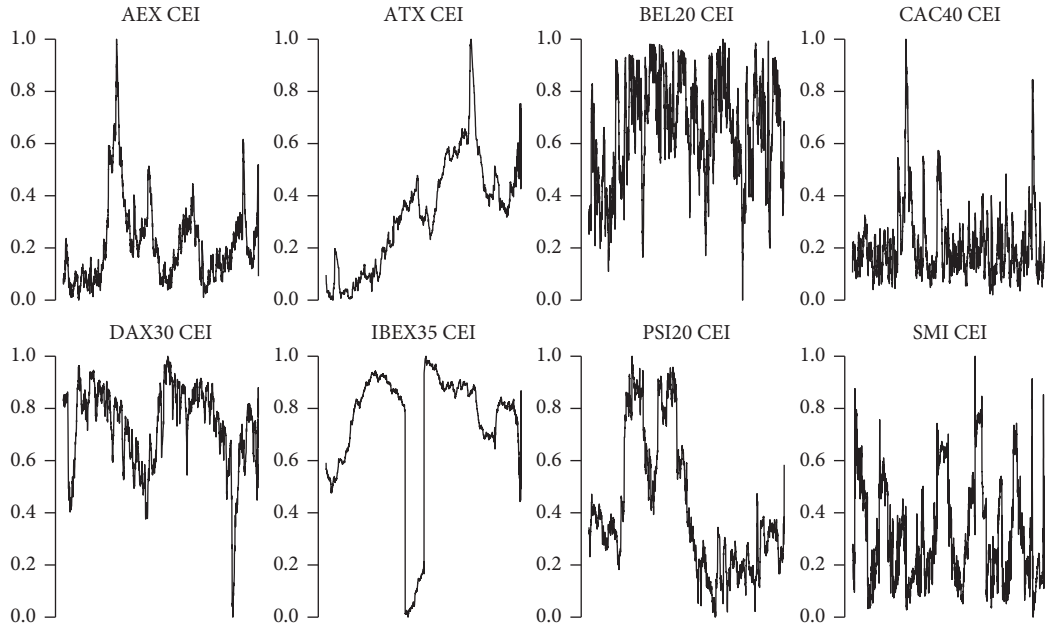


FIGURE 7: Daily composite efficiency index (CEI) for each of the considered stock market indices.

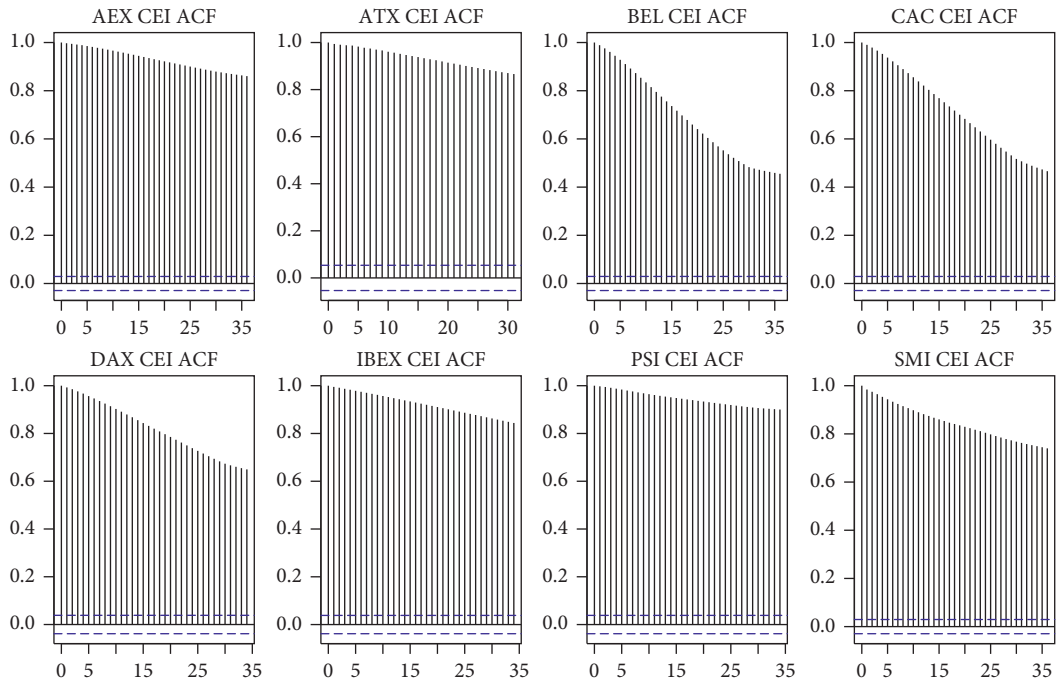


FIGURE 8: ACF of the daily composite efficiency index (CEI) for each of the considered stock market indices.

with  $\bar{y}$  being the sample average over  $T$  of the time series  $y_t$ . A large value of the statistics  $Q$ , which follows a  $\chi^2$  distribution with  $h - K$  degrees of freedom, indicates that there is a significant autocorrelation structure in the time series. Under the null hypothesis, the time series is a white noise. In applying the Ljung–Box test, we exploit the fact that if  $CEI_t$  is random walk, its first difference  $\Delta CEI_t$  must be a white noise process. The results are reported in Table 1.

As Table 1 shows, by rejecting the null hypothesis of white noise for the CEI first differences, we reject the

random walk hypothesis for the CEI time series for all the markets. Therefore, the market efficiency and its variation follow predictable stochastic processes. However, each market has its own data-generating process.

*5.3. Composite Efficiency Index: Out-of-Sample Analysis.* Another important aspect that can be studied is to assess if the market efficiency can be useful for predicting stock returns. In doing so, we conduct an out-of-sample analysis



TABLE 1: Ljung–Box [54] results.

Market	Q	$p$ value
AEX	261.74	$2.2 e^{-16}$
ATX	156.22	$2.2 e^{-16}$
BEL20	105.9	$2.2 e^{-16}$
CAC40	133.23	$2.2 e^{-16}$
DAX30	88.632	$9.992 e^{-15}$
IBEX35	104.09	$2.2 e^{-16}$
PSI20	76.871	$2.055 e^{-12}$
SMI	209.27	$2.2 e^{-16}$

following the empirical approach of the exchange rate predictability literature (e.g., Meese and Rogoff [56], Rossi [57], Molodtsova and Papell [58], and Mattera et al. [59]). Indeed, we compare the forecasts obtained with a random walk without drift model

$$\hat{r}_{i,t} = r_{i,t-1} \quad (17)$$

with those obtained by the following predictive regression:

$$r_{i,t} = \alpha_i + \beta_i \Delta \text{CEI}_{i,t} + \epsilon_{i,t}, \quad (18)$$

where  $\alpha$  is the constant term,  $\beta$  represents the impact of  $\Delta \text{CEI}$  on the returns, and  $\epsilon_t$  is an error term. Note that we use the first difference of the CEI instead of its levels. This is because it is not guaranteed a priori that the composite index is stationary. Stationarity of the composite indicator clearly depends on the stationarity of the subindicators. To see the results, Table 2 contains the results of the augmented Dickey–Fuller test, showing that some of the CEIs present either unit roots or deterministic trends.

This is evident also looking at the indices' autocorrelation structure shown in Figure 8. With first differences, instead, all the indices are stationary, and the consistency of the OLS estimator is guaranteed. Moreover, first difference can be seen as a measure of the CEI variation rate. Hence, we are interested in understanding if inefficiency variation is able to predict variation in prices, i.e., the returns.

In order to evaluate the forecasts' accuracy in out of sample, we split the dataset into a training set used to estimate parameters and to obtain forecasts and a training set with one-third of the observations used for predictive accuracy tests. In particular, we conduct an experiment following a rolling-sample approach. Given a  $T$ -long dataset, we choose an estimation window of length  $M$  equal to two-third of the dataset. Then, in each period  $t$ , starting from  $t = M + 1$ , we use the  $M$  observations to estimate the parameters needed for obtaining the forecasts for  $t + 1$ . This process is repeated  $T - M$  times by adding the return for the next period in the dataset and dropping the earliest one until the end of the dataset is reached. The outcome is, for each strategy, a time series of  $T - M$  out-of-sample forecasts.

Then, for each  $i$ th stock market, we compute the forecasting error as follows:

$$e_{i,t} = \hat{r}_{i,t} - r_{i,t}. \quad (19)$$

In the end, given the forecasting error in (17), we compute the mean square forecast error (MSfE) and use

TABLE 2: Augmented Dickey–Fuller test results.

Market	ADF statistic	$p$ value
AEX CEI	3.48	0.044
ATX CEI	-2.64	0.309
BEL20 CEI	-7.30	0.010
CAC40 CEI	-6.68	0.010
DAX30 CEI	-4.23	0.010
IBEX35 CEI	-2.42	0.399
PSI20 CEI	-2.26	0.466
SMI CEI	-4.20	0.010

TABLE 3: Out-of-sample forecasting accuracy results.

Market	MSfE (16)	MSfE (15)	$p$ value [60]	$p$ value [61]
AEX	0.000113	0.000224	$4.9193 e^{-18}$	$2.296 e^{-13}$
ATX	0.000363	0.000698	$2.7894 e^{-06}$	0.0002241
BEL20	0.000144	0.000272	$1.8871 e^{-10}$	$2.191 e^{-07}$
CAC40	0.000142	0.000277	$6.2007 e^{-14}$	$1.256 e^{-09}$
DAX30	0.000195	0.000406	$2.9687 e^{-12}$	$2.819 e^{-10}$
IBEX35	0.000201	0.000416	$4.3183 e^{-16}$	$5.155 e^{-05}$
PSI20	0.000141	0.000277	$3.3021 e^{-11}$	$8.479 e^{-08}$
SMI	0.000088	0.000182	$1.5224 e^{-13}$	$1.336 e^{-09}$

Clark and West [60] to test whether the forecasts obtained from model (16) are statistically different from those of the benchmark RW model (15). Under the null hypothesis of the Clark and West [60] test, the two competing forecasting models have statistically equal predictive ability. If the MSfE of model (16) is lower and statistically different with respect to the MSfE of model (15), we can argue that the variation of the market efficiency level, measured by the CEI, is a good predictor for stock market returns. Moreover, for sake of robustness, we also consider the results of the Diebold and Mariano test [61] of predictive accuracy. The results of the out-of-sample experiment are shown in Table 3.

According to the Clark and West test [60] for all stock markets, the forecast obtained through regression is statistically different than the random walk benchmark (see columns 3 and 4 of Table 3). Moreover, the MSfE of (16) is always lower than the random walk MSfE, meaning that the CEI is a useful predictor for market returns. This is a generalized result because the forecast error of the two competing models is statistically different, i.e., the observed differences are not sample driven.

## 6. Conclusion

Since the Fama seminal work on the topic, there have been several papers that studied the market efficiency. However, the market efficiency is a latent concept, and it is difficult to be measured by means of a single indicator. Indeed, market efficiency has been investigated by means of various methods. Among the most important, we have the random walk hypothesis, the martingale hypothesis, and the liquidity.

Nevertheless, most of the literature studies are based on the EMH, which lies on several strong assumptions such as independence, normality, and many others, while several empirical studies have proved that stock returns show some

statistical properties that are known as stylized facts. A very important stylized fact is represented by the presence of long-range dependence, also defined as long memory. The long memory property describes if and how much past events influence the future evolution of the process.

The long memory is commonly studied through the Hurst exponent, previously introduced by Hurst [29] and lately developed by Mandelbrot and Wallis [62], which represents the rate of decay of the autocorrelation function of a time series.

The fractal market hypothesis (FMH) claims that the Hurst exponent is related to market efficiency since a value of  $h = 0.5$  reflects efficient market conditions. The mathematical representation of the stock prices under the FMH is given by the fractional Brownian motion (fBm). However, a main drawback of the fBm lies on the fact that the Hurst exponent is assumed to be static and not time-varying. Therefore, constructing an efficiency measure with a static Hurst exponent contradicts the adaptive market hypothesis (AMH).

However, by assuming a multifractional Brownian motion (mBm) for stock prices, we compute a time-varying Hurst exponent that can potentially explain how efficiency changes over time. With this respect, following Bianchi [32], we use a simple measure of market inefficiency, called Hurst-based efficiency index (HEI), computed as the absolute deviation of the time-varying Hurst exponent from 0.5.

Then, to capture, in a more accurate way, all the efficiency dimensions, we computed a composite indicator by using the developed Hurst-based inefficiency measure, conditional volatility, and market liquidity.

We apply the proposed indicator to European stock market indices to study the behavior inefficiency. We find that the proposed index called CEI does not follow a random walk process getting evidence of efficiency predictability. This result could be relevant to both policy makers and traders. We also use the CEI as predictors in a log-return predictive regression problem. We find that the CEI is a relevant predictor for daily stock returns as well.

## Data Availability

All the data can be found in <https://es.finance.yahoo.com>.

## Conflicts of Interest

The authors declare that they have no conflicts of interest.

## Acknowledgments

Juan E. Trinidad-Segovia was supported by the Spanish Ministerio de Ciencia, Project No. PGC2018-101555-B-I00, and Universidad de Almería, project no. UAL18-FQM-B038-A (UAL/CECEU/FEDER).

## References

- [1] B. G. Malkiel and E. F. Fama, "Efficient capital markets: a review of theory and empirical work," *The Journal of Finance*, vol. 25, no. 2, pp. 383–417, 1970.
- [2] R. Cont, *Empirical Properties of Asset Returns: Stylized Facts and Statistical Issues*, Quantitative Finance, New York and Chicago, 2001.
- [3] A. Weron and R. Weron, "Fractal market hypothesis and two power-laws," *Chaos, Solitons & Fractals*, vol. 11, no. 1, pp. 289–296, 2000.
- [4] A. W. Lo, "Reconciling efficient markets with behavioral finance: the adaptive markets hypothesis," *The Journal of Investment Consulting*, vol. 7, no. 2, pp. 21–44, 2005.
- [5] M. Ito, A. Noda, and T. Wada, "International stock market efficiency: a non-bayesian time-varying model approach," *Applied Economics*, vol. 46, no. 23, pp. 2744–2754, 2014.
- [6] M. Ito, A. Noda, and T. Wada, "The evolution of stock market efficiency in the us: a non-bayesian time-varying model approach," *Applied Economics*, vol. 48, no. 7, pp. 621–635, 2016.
- [7] A. Noda, "A test of the adaptive market hypothesis using a time-varying ar model in Japan," *Finance Research Letters*, vol. 17, pp. 66–71, 2016.
- [8] V. L. Tran and T. Leirvik, "A simple but powerful measure of market efficiency," *Finance Research Letters*, vol. 29, pp. 141–151, 2019.
- [9] P. Földvári and B. Van Leeuwen, "What can price volatility tell us about market efficiency? conditional heteroscedasticity in historical commodity price series," *Cliometrica*, vol. 5, no. 2, pp. 165–186, 2011.
- [10] A. W. Lo and A. C. MacKinlay, "Stock market prices do not follow random walks: evidence from a simple specification test," *Review of Financial Studies*, vol. 1, no. 1, pp. 41–66, 1988.
- [11] L. Liu and Q. Chen, "How to compare market efficiency? the sharpe ratio based on the arma-garch forecast," *Financial Innovation*, vol. 6, no. 1, pp. 1–21, 2020.
- [12] J. Sukpitak and V. Hengpunya, "The influence of trading volume on market efficiency: the dcca approach," *Physica A: Statistical Mechanics and Its Applications*, vol. 458, pp. 259–265, 2016.
- [13] T. Chordia, R. Roll, and A. Subrahmanyam, "Liquidity and market efficiency," *Journal of Financial Economics*, vol. 87, no. 2, pp. 249–268, 2008.
- [14] D. Chung and K. Hrazdil, "Liquidity and market efficiency: a large sample study," *Journal of Banking & Finance*, vol. 34, no. 10, pp. 2346–2357, 2010.
- [15] A. Gabrielsen, M. Marzo, and P. Zagaglia, "Measuring Market Liquidity: An Introductory Survey," *SSRN Electronic Journal*, 2011.
- [16] Y. Amihud, "Illiquidity and stock returns: cross-section and time-series effects," *Journal of Financial Markets*, vol. 5, no. 1, pp. 31–56, 2002.
- [17] L. Kristoufek and M. Vosvrda, "Measuring capital market efficiency: long-term memory, fractal dimension and approximate entropy," *The European Physical Journal B*, vol. 87, no. 7, pp. 1–9, 2014.
- [18] L. Kristoufek and M. Vosvrda, "Gold, currencies and market efficiency," *Physica A: Statistical Mechanics and Its Applications*, vol. 449, pp. 27–34, 2016.
- [19] A. Sensoy and B. M. Tabak, "Time-varying long term memory in the European Union stock markets," *Physica A: Statistical Mechanics and Its Applications*, vol. 436, pp. 147–158, 2015.
- [20] L. Kristoufek and M. Vosvrda, "Commodity futures and market efficiency," *Energy Economics*, vol. 42, pp. 50–57, 2014.
- [21] L. Kristoufek, "On Bitcoin markets (in)efficiency and its evolution," *Physica A: Statistical Mechanics and Its Applications*, vol. 503, pp. 257–262, 2018.

- [22] M. Ausloos, R. Cerqueti, and C. Lupi, “Long-range properties and data validity for hydrogeological time series: the case of the paglia river,” *Physica A: Statistical Mechanics and Its Applications*, vol. 470, pp. 39–50, 2017.
- [23] F. Lillo and J. D. Farmer, “The long memory of the efficient market,” *Studies in Nonlinear Dynamics and Econometrics*, vol. 8, no. 3, 2004.
- [24] Y. Jiang, H. Nie, and W. Ruan, “Time-varying long-term memory in bitcoin market,” *Finance Research Letters*, vol. 25, pp. 280–284, 2018.
- [25] P. Ferreira and A. Dionísio, “How long is the memory of the us stock market?” *Physica A: Statistical Mechanics and Its Applications*, vol. 451, pp. 502–506, 2016.
- [26] A. F. Bariviera, M. J. Basgall, W. Hasperu e, and M. Naiouf, “Some stylized facts of the bitcoin market,” *Physica A: Statistical Mechanics and Its Applications*, vol. 484, pp. 82–90, 2017.
- [27] M. A. S anchez Granero, J. E. Trinidad Segovia, and J. Garc ıa P erez, “Some comments on hurst exponent and the long memory processes on capital markets,” *Physica A: Statistical Mechanics and Its Applications*, vol. 387, no. 22, pp. 5543–5551, 2008.
- [28] V. Dimitrova, M. Fern andez-Mart ınez, M. A. S anchez-Granero, and J. E. Trinidad Segovia, “Some comments on Bitcoin market (in)efficiency,” *PLoS One*, vol. 14, no. 7, Article ID e0219243, 2019.
- [29] H. E. Hurst, “Long-term storage capacity of reservoirs,” *Transactions of the American Society of Civil Engineers*, vol. 116, no. 1, pp. 770–799, 1951.
- [30] B. B. Mandelbrot and J. W. Van Ness, “Fractional brownian motions, fractional noises and applications,” *SIAM Review*, vol. 10, no. 4, pp. 422–437, 1968.
- [31] S. Bianchi, A. Pantanella, and A. Pianese, “Modeling stock prices by multifractional brownian motion: an improved estimation of the pointwise regularity,” *Quantitative Finance*, vol. 13, no. 8, pp. 1317–1330, 2013.
- [32] S. Bianchi, “Pathwise identification of the memory function of multifractional brownian motion with application to finance,” *International Journal of Theoretical and Applied Finance*, vol. 8, no. 2, pp. 255–281, 2005.
- [33] J. Bai and S. Ng, “Principal components estimation and identification of static factors,” *Journal of Econometrics*, vol. 176, no. 1, pp. 18–29, 2013.
- [34] T. Bollerslev, “A conditionally heteroskedastic time series model for speculative prices and rates of return,” *The Review of Economics and Statistics*, vol. 69, no. 3, pp. 542–547, 1987.
- [35] R. Cerqueti, M. Giacalone, and R. Mattera, “Skewed non-Gaussian garch models for cryptocurrencies volatility modelling,” *Information Sciences*, vol. 527, no. 1–26, 2020.
- [36] M. Lopez Garcia and J. Requena, “Different methodologies and uses of the hurst exponent in econophysics,” *Estudios de Econom ıa Aplicada*, vol. 1, no. 13, pp. 37–42, 2019.
- [37] A. W. Lo, “Long-term memory in stock market prices,” *Econometrica*, vol. 59, no. 5, pp. 1279–1313, 1991.
- [38] R. Weron, “Estimating long-range dependence: finite sample properties and confidence intervals,” *Physica A: Statistical Mechanics and Its Applications*, vol. 312, no. 1–2, pp. 285–299, 2002.
- [39] S. Mercik, K. Weron, K. Burnecki, and A. Weron, “Enigma of self-similarity of fractional levy stable motions,” *Acta Physica Polonica B*, vol. 34, no. 7, p. 3773, 2003.
- [40] M. Fern andez-Mart ınez, M. A. S anchez-Granero, and J. E. Trinidad Segovia, “Measuring the self-similarity exponent in L evy stable processes of financial time series,” *Physica A: Statistical Mechanics and Its Applications*, vol. 392, no. 21, pp. 5330–5345, 2013.
- [41] M.  . S anchez, J. E. Trinidad, J. Garc ıa, and M. Fern andez, “The effect of the underlying distribution in hurst exponent estimation,” *PLoS One*, vol. 10, no. 5, Article ID e0127824, 2015.
- [42] R. Mattera and F. D. Sciorio, “Option pricing under multifractional process and long-range dependence,” *Fluctuation and Noise Letters*, vol. 20, no. 1, Article ID 2150008, 2021.
- [43] S. Corlay, J. Lebovits, and J. L. V ehel, “Multifractional stochastic volatility models,” *Mathematical Finance*, vol. 24, no. 2, pp. 364–402, 2014.
- [44] S. Bianchi and A. Pianese, “Time-varying hurst-h older exponents and the dynamics of (in)efficiency in stock markets,” *Chaos, Solitons & Fractals*, vol. 109, pp. 64–75, 2018.
- [45] W. Becker, M. Saisana, P. Paruolo, and I. Vandecasteele, “Weights and importance in composite indicators: closing the gap,” *Ecological Indicators*, vol. 80, pp. 12–22, 2017.
- [46] G. Karagiannis, “On aggregate composite indicators,” *Journal of the Operational Research Society*, vol. 68, no. 7, pp. 741–746, 2017.
- [47] S. Greco, A. Ishizaka, M. Tasiou, and G. Torrisi, “On the methodological framework of composite indices: a review of the issues of weighting, aggregation, and robustness,” *Social Indicators Research*, vol. 141, no. 1, pp. 61–94, 2019.
- [48] A. Kantiray, “On the measurement of certain aspects of social development,” *Social Indicators Research*, vol. 21, no. 1, pp. 35–92, 1989.
- [49] D. J. Slotje, “Measuring the quality of life across countries,” *The Review of Economics and Statistics*, vol. 73, no. 4, pp. 684–693, 1991.
- [50] R. Haq and U. Zia, “Multidimensional wellbeing: an index of quality of life in a developing economy,” *Social Indicators Research*, vol. 114, no. 3, pp. 997–1012, 2013.
- [51] J. H. Stock and M. W. Watson, “Forecasting using principal components from a large number of predictors,” *Journal of the American Statistical Association*, vol. 97, no. 460, pp. 1167–1179, 2002.
- [52] M. Nardo, M. Saisana, A. Saltelli, S. Tarantola, A. Hoffman, and E. Giovannini, “Handbook on Constructing Composite Indicators: Methodology and User Guide,” Technical report, OECD Publishing, Paris, France, 2005.
- [53] J. Bai and S. Ng, “Determining the number of factors in approximate factor models,” *Econometrica*, vol. 70, no. 1, pp. 191–221, 2002.
- [54] G. M. Ljung and G. E. P. Box, “On a measure of lack of fit in time series models,” *Biometrika*, vol. 65, no. 2, pp. 297–303, 1978.
- [55] R. J. Hyndman and G. Athanasopoulos, *Forecasting: Principles and Practice*, OTexts, 2018.
- [56] R. A. Meese and K. Rogoff, “Empirical exchange rate models of the seventies: do they fit out of sample?” *Journal of International Economics*, vol. 14, no. 1–2, pp. 3–24, 1983.
- [57] B. Rossi, “Exchange rate predictability,” *Journal of Economic Literature*, vol. 51, no. 4, pp. 1063–1119, 2013.
- [58] T. Molodtsova and D. H. Papell, “Out-of-sample exchange rate predictability with taylor rule fundamentals,” *Journal of International Economics*, vol. 77, no. 2, pp. 167–180, 2009.
- [59] R. Mattera, M. Misuraca, G. Scepti, and M. Spano, “A mixed-frequency approach for exchange rates predictions,” *Electronic Journal of Applied Statistical Analysis*, vol. 14, no. 1, pp. 230–253, 2021.
- [60] T. E. Clark and K. D. West, “Using out-of-sample mean squared prediction errors to test the martingale difference

hypothesis," *Journal of Econometrics*, vol. 135, no. 1-2, pp. 155-186, 2006.

- [61] F. X. Diebold and R. S. Mariano, "Comparing predictive accuracy," *Journal of Business & Economic Statistics*, vol. 20, no. 1, pp. 134-144, 2002.
- [62] B. B. Mandelbrot and J. R. Wallis, "Robustness of the rescaled range  $r/s$  in the measurement of noncyclic long run statistical dependence," *Water Resources Research*, vol. 5, no. 5, pp. 967-988, 1969.

## Research Article

# Jumping Risk Communities in the Energy Industry: An Empirical Analysis Based on Time-Varying Complex Networks

Hui Wang <sup>1</sup>, Lili Jiang <sup>2</sup>, Hongjun Duan <sup>3</sup>, Yifeng Wang <sup>2</sup>, Yichen Jiang <sup>4</sup>,  
and Xiaolei Zhang <sup>1</sup>

<sup>1</sup>Pan-Asia Business School, Yunnan Normal University, Kunming, China

<sup>2</sup>Business School, Suqian College, Suqian, China

<sup>3</sup>Jiangsu Vocational and Technical College of Finance and Economics, Huaian, China

<sup>4</sup>Zhejiang Science and Technology Information Research Institute, Hangzhou, China

Correspondence should be addressed to Lili Jiang; 719821098@qq.com, Yichen Jiang; beaconsy@qq.com, and Xiaolei Zhang; financialmath@163.com

Received 9 May 2021; Revised 7 December 2021; Accepted 16 December 2021; Published 11 January 2022

Academic Editor: M. M. El-Dessoky

Copyright © 2022 Hui Wang et al. This is an open access article distributed under the Creative Commons Attribution License, which permits unrestricted use, distribution, and reproduction in any medium, provided the original work is properly cited.

This paper uses the 5-five-minute high-frequency data of energy-listed companies in China's A-share market to extract the jump of energy stock prices and build a dynamic stock price jump complex network. Then, we analyze the clustering effect of the complex network. The research shows that the energy stock price jump is an important part of stock price volatility, and the complex network of energy stock jump risk has obvious time-varying characteristics. However, the infection problem of stock price jump risks needs specific analysis. China's coal industry has an important influence on the development of China's energy industry. According to the clustering analysis results of the network community, the clustering effect of the network community has time-varying characteristics. After October 2017, the clustering effect of the jumping risk of the coal industry and the new energy industry is obvious. The risk contagion within the new energy industry community is a key point for the development of the new energy industry.

## 1. Introduction

With the acceleration of global economic integration, the energy finance market developed based on the energy industry and relying on the financial market has become an important global financial trading platform. The effective combination of the energy and financial markets has become the key to whether the energy market can meet the growing energy demand in the human economy. At the same time, with the rapid development of energy finance, energy and financial risk management has become the key to the development of the international energy and international financial markets. The energy finance market efficiently allocates resources while spreading the risks of the energy finance market throughout the industry. This paper takes the energy stock price in China's stock market as the research object and uses the realized jump method to measure the

jump risk in the energy financial market. To study the dynamic characteristics of a complex network of energy prices, we use Prim's algorithm to build a complex network of energy price jumping risks.

The main work of our paper is as follows. First, we use the five-minute high-frequency data of the energy stock market to obtain the realized volatility. Second, we use the realized jump method to obtain the jump risk of the energy stock. Third, we build complex networks for all stock price jumps to study the dynamic changes of complex networks. Fourth, the community method is used to study the dynamic changes in the energy stock jump communities. Through our research, the paper draws the following conclusions. (1) The energy stock price jump is an important part of energy stock price volatility. (2) The complex network of the energy company stock price jump has obvious time-varying characteristics. After October

2017, the link between the stock price jump is closer, and the risk of a stock price jump is more likely to occur. (3) The energy stock complex network community has a strong time-varying feature. (4) China's coal industry is the most critical in the complex network of the entire energy industry, and the internal risk management of the coal industry is very important. (5) The risk contagion within the new energy industry community is vital for the development of the new energy industry.

The main contributions of this paper are as follows. (1) This paper takes the jump of the energy industry stock price as the object and studies the jumping risk problem of the energy industry by using the complex network method. (2) This paper analyzes the dynamic characteristics of the complex network of energy stock jump risk. (3) The coal industry occupies a central position in China's energy complex network, and the risk of jumping within the coal industry community and the new energy industry community is worthy of attention.

## 2. Literature Review

Energy finance market risk management has always been a hot issue for many scholars around the world. Many scholars have studied the impact of financial markets on energy and financial markets from the perspectives of the stock, gold, and foreign exchange markets. Kaneko and Lee [1] found a negligible interaction between oil prices and stock returns by studying the relationship between the oil market and the stock market. Basher and Sadorsky [2] used a multifactor risk analysis model to investigate the relationship between oil price risk and emerging stock market returns using conditional regression and unconditional regression. It found that oil price volatility significantly influences stock market returns in emerging markets. The results of Zhang et al. [3] show a significant spillover effect between oil prices and the US dollar exchange rate. Narayan [4] showed a long-term cointegration relationship among international gold prices, future oil prices, and spot prices. The change in oil price affects mainly the price of gold through inflation.

The above studies are based on the analysis of energy market prices, and volatility is an important indicator to measure risk. This paper will use realized volatility and the realized jump method to study the complex network of energy stock price jumps; therefore, it is necessary to review the related research.

With continuous research on volatility, the use of historical standard deviation to study volatility can no longer meet the needs of modern research. The method of extracting realized volatility from high-frequency data has attracted increasing attention from scholars, such as Andersen and Bollerslev [5] and Barndorff-Nielsen and Shephard [6]. It is precise because of the rapid development of realized volatility methods that scholars can use realized methods to separate realized jumps from realized volatility so that they can more accurately study the relevant properties of price jumps. For example, Wang et al. [7], Anderson et al. [8], Zeng and Zuo [9], Xu et al. [10], Wang [7], and Hu et al. [11] do so.

In recent years, an increasing number of scholars have studied the complex network of stock prices. By constructing a complex network of stock prices, scholars can study the risk contagion, price linkage, and return forecasting among stock prices. In the process of constructing complex networks, many scholars have proposed various methods: Mantegna [12] and Zhuang and Jin [13] proposed a minimum spanning tree algorithm. Pothen et al. [14] used Laplacian graph feature values to construct complex networks; Chi et al. [15] and Peron et al. [16] established stock networks by using the relationship between stock prices as the edges between them in the model. Newman [17, 18] proposed the Girvan-Newman (GN) algorithm and fast Newman algorithm to construct complex networks. Zhan et al. [19] proposed the fast unfolding algorithm based on Newman [17, 18].

Some of the literature has used the method of complex networks to study the energy financial market. Xi and An [20] constructed a complex network using the financial indicators of energy stocks. The study found that the threshold value of 0.7 is the sudden change of the network. With the increase in the threshold value, the community's independence is enhanced. Li et al. [21] used the method of complex networks to study the global energy investment structure and found that the vast majority of foreign investment and foreign investment relations are still in the hands of a few countries.

By analyzing the existing research, we can determine the following. First, the existing research mainly focuses on the study of the interaction between the energy market and other markets. There is little research focus on the mutual contagion of stock risk of different energy companies within the energy industry. Second, in the study of the risk of the energy industry, most of the research mainly analyzes the energy price directly. Few articles use the jump of energy stock prices to conduct in-depth analysis. Third, research on applying complex networks to energy finance risk management is scant. Fourth, when using complex networks to study market risk, few scholars study the dynamic characteristics of complex networks.

Based on the existing research, this paper extracts the jump risk of energy stock prices from high-frequency data of energy stock prices and studies the jump risk of energy industry stock prices. This paper applies the method of complex networks to the energy industry and deeply studies the clustering effect of the jump risk of the energy industry. This paper studies the time-varying characteristics of complex networks and communities of energy price jump risk.

## 3. Theoretical Analyses of Realized Jump and Complex Network

We follow the methods of Zhang et al. [3] to research the time-varying complex network of jump risk in the energy industry. This paper uses the realized method to extract jumps from energy stock volatility and uses it to study the complex network clustering effect within the energy industry. According to the following formula,

realized volatility = continuous volatility + realized jump. (1)

Equation (1) shows that when we obtain the realized volatility and continuous volatility, we can calculate the realized jump.

*3.1. Extracting Volatility by Using the Realized Method.*  $p_{t,i}$  is the log price of the  $i$ th underlying asset on the  $t$ -th day. The intraday return  $r_{t,i}$  can be expressed as

$$r_{t,i} = p_{t,i} - p_{t,i-1}. \quad (2)$$

We define  $RD_t$  is the realized variance. The realized variance can be calculated as follows:

$$RD_t = \sum_{i=1}^N r_{t,i}^2. \quad (3)$$

$N$  is the number of returns on  $t$ -th day. By annualizing the realized variance, we can obtain the realized volatility.

$$RV_t = \sqrt{W \cdot RD_t}, \quad (4)$$

where  $RV_t$  is the realized volatility.  $W$  is the number of trading days in a year.

*3.2. Realized Jump.* Early research was based on parametric models to study and estimate jumps by setting specific model

forms. With the widespread use of high-frequency data, the use of realized methods to calculate jumps has been favored by scholars. The realized method is nonparametric. It is model-free, convenient to calculate, and accurate to estimate.

The realized jump method was first proposed by Barndorff-Nielsen et al. [22]. Based on quadratic variation theory, they decompose the total variation into two parts: integral volatility and discrete jump.

When the asset return  $x(t)$  follows the geometric Brownian motion with a jump, the total volatility of the logarithmic return at time  $t$  is not a consistent estimate of the integral volatility. It will be a composite volatility that includes a discrete jump component and continuous volatility components. The quadratic variation of the logarithmic return at time  $t$ ,  $t \in [t, t-1]$  is

$$QV_t = [r, r]_t = \int_{t-1}^t \sigma_s^2 ds + \sum_{t-1 \leq s \leq t} \kappa_s^2, \quad t \in [t, t-1]. \quad (5)$$

According to quadratic variation theory, at time  $t$ ,  $t \in [t, t-1]$ , the total change in the logarithmic return consists of a continuous integral volatility  $\int_{t-1}^t \sigma_s^2 ds$  ( $\int_{t-1}^t \sigma_s^2 ds < \infty$ ) and a discrete jump part  $\sum_{t-1 \leq s \leq t} \kappa_s^2$ .

Anderson and Bollerslev [5] showed that when the frequency of intraday discrete samples is sufficiently large, the quadratic variation consistently estimates the actual volatility. At  $t \in [0, T]$ ,

$$RV_t = \sum_{i=1}^n r_{t,i}^2 \xrightarrow{n \rightarrow \infty} QV_t = [r, r]_t = \int_{t-1}^t \sigma_s^2 ds + \sum_{t-1 \leq s \leq t} \kappa_s^2, \quad t \in [0, T]. \quad (6)$$

The integral volatility under a continuous path can be estimated from the realized bipower variation (RBV). When the sample is large enough, that is,  $n \rightarrow \infty$ , the RBV is achieved as a consistent estimate of the integral volatility (IV). The RBV is a consistent estimator of integral volatility.

$$RBV_t = u_1^{-2} \left( \frac{n}{n-2} \right) \sum_{j=3}^n |r_{t,j-2}| |r_{t,j}|, \quad t \in [0, T]. \quad (7)$$

$u_a = E[|Z|^a] = 2^{a/2} [\Gamma((a+1)/2)\Gamma(1/2)]^{-1}$ .  $\Gamma$  is the Gamma function.  $Z \sim N(0, 1)$ . When  $a=1$ ,  $u_1 = E[|Z|] = \sqrt{\pi/2}$ .  $n/n-2$  is the correction for the sample space.

*3.3. Constructing the Complex Network Based on Prim's Algorithm.* There are many different methods to construct a complex network, such as the Kruskal algorithm and the Prim algorithm. After comparing different algorithms, we think that the Prim algorithm has the advantages of stability and simplicity. This paper uses the Prim algorithm to construct the time-varying complex network of

the jump of the energy stock prices, which can make the complex network more robust. The closeness to the center is used to analyze the importance of different nodes:

$$C_c(v_i) = \frac{(N-1)}{\left[ \sum_{i=1, j \neq 1}^N d_{ij} \right]}. \quad (8)$$

Suppose there are  $N$  nodes in a complex network.  $C_c(v_i)$  is the degree of closeness to the center for each node. We use  $d_{ij}$  to represent the minimum number of edges between two nodes  $i$  and  $j$ , which belong to  $[1, N]$ . The greater the degree of closeness of the node, the more importance it has in the network.

*3.4. The Community of the Complex Network.* After constructing the complex network of the jump of the Chinese energy stock price, we need to further analyze which stock price jump is relatively closely related in the entire complex network. The community is used to study the clustering problem of complex networks. When dividing communities, the fast unfolding algorithm is used to classify the communities of the stocks.

The modular  $Q$  function is a good way to divide the number of communities. The communities can be calculated as follows:

$$\frac{\sum_{i,j} a_{ij} \delta(\sigma_i, \sigma_j)}{\sum_{i,j} a_{ij}} = \frac{\sum_{i,j} a_{ij} \delta(\sigma_i, \sigma_j)}{2M}. \quad (9)$$

In the modular  $Q$  function, we use the community number to distinguish whether two different nodes are in the same community. If the community labels of the two nodes are the same, we consider that the two nodes belong to the same communities.  $\sigma_i$  represents the community label of node  $v_i$ . If  $v_i$  and  $v_j$  are connected, then  $a_{ij} = 1$ . If  $v_i$  and  $v_j$  are not connected, then  $a_{ij} = 0$ . If  $v_i$  and  $v_j$  belong to the same community,  $\delta(\sigma_i, \sigma_j) = 1$ . If they do not belong to the same community,  $\delta(\sigma_i, \sigma_j) = 0$ .  $M$  represents the number of all interconnected edges in the complex network, and  $M = \sum a_{ij}$ .

The Modular  $Q$  function is

$$Q = \frac{1}{2M} \sum_{i,j} \left[ \left( a_{ij} - \frac{k_i k_j}{2M} \delta(\sigma_i, \sigma_j) \right) \right]. \quad (10)$$

The  $i$  and  $j$  represent the  $i$ th and  $j$ th nodes.  $K_i$  and  $k_j$  represent the weight of the edge connected to node  $i$  and node  $j$ , respectively. The larger the value of  $Q$  is, the better the result of community division is. The fast unfolding algorithm is simple and efficient; thus, we use it to divide the network into communities. The reduction formula of the Modular  $Q$  function is

$$Q = \frac{\sum \text{in}}{2M} - \left( \frac{\sum \text{tot}}{2M} \right)^2, \quad (11)$$

where  $\sum \text{in}$  represents the sum of the number of connected edges of all nodes in the same community, and  $\sum \text{tot}$  is the number of edges connected to nodes of the same community.

## 4. Empirical Analyses

**4.1. Data.** This paper takes all energy stocks listed on China A-Share from October 10, 2016, to October 10, 2018, as an empirical study. We handle the data as follows. (1) Remove the missing values. (2) Use five-minute high-frequency data for the empirical analysis. (3) Assume that the stock price jump is 0 during the suspension period. (4) The data is from the Wind database.

**4.2. The Empirical Results of Realized Volatility and Jump of Energy Stock Price.** Taking China Petroleum (601857.SH) as an example, the time series of the return of China Petroleum (601857.SH) is shown in Figure 1.

Figure 1 shows that starting from 2018, the yield fluctuated 601857.SH increased. The volatility and jump risk can be predicted as 601857.SH will increase significantly starting from 2018. To further explain the basic statistical characteristics of the sample data, Table 1 shows the statistical characteristics of the six stocks.

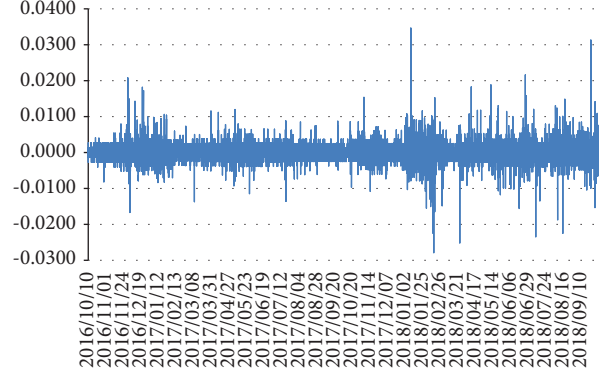


FIGURE 1: 601857.SH 5-minute high-frequency return.

Figure 2 shows the results of the realized volatility and jumps.

Figure 2 shows that the stock price jump is a common phenomenon and an important part of volatility. The trend of 601857.SH in Figure 2 verifies the previous prediction. Beginning in 2018, the realized volatility of 601857.SH becomes larger, and the frequency and intensity of the jump increase. Figure 2 shows that the stock price jumps in different periods are not completely consistent, and there are certain differences in the frequency and intensity of stock jumps in different time periods. This difference inspires us to study the time-varying characteristics of stock jump risk. For this article, we need to study the time-varying characteristics of complex networks of the energy industry. The statistical properties of the realized volatility and the realized jump are shown in Tables 2 and 3.

**4.3. Empirical Results of Time-Varying Complex Network.** To study the time-varying characteristics of the complex network of energy stock price jumps, this paper divides the sample interval into four time periods, which are from October 10, 2016, to April 10, 2017; April 11, 2017, to October 10, 2017; October 11, 2017, to April 10, 2018; and April 11, 2018, to October 10, 2018.

**4.3.1. Correlation Coefficient Matrix and Distance Matrix of the Energy Stock Jump.** Table 4 shows the correlation coefficient matrix for some energy stock price jumps from October 2016 to April 2017.

We use the following formula to transfer the jump correlation coefficient  $\rho_{ij}(\Delta t)$  to the corresponding distance  $d(i, j)$ :

$$d(i, j) = \sqrt{2[1 - \rho_{ij}(\Delta t)]}. \quad (12)$$

The smaller the distance  $d(i, j)$  is, the stronger the correlation between stocks (Table 5).

**4.3.2. Using a Distance Matrix to Build an Energy Stock Jump Complex Network.** As shown in Figures 3–6, this paper constructs the complex networks of energy stock jumps in four different time periods. Each complex network diagram



TABLE 1: Statistical characteristic of the sample.

Stock code	Mean	Maximum	Minimum	Standard deviation	Skewness	Kurtosis	ADF ( <i>P</i> value)
601857.SH	$-8.47E-06$	0.0602	-0.0753	0.0030	0.0880	41.8161	0.0001
601898.SH	$-1.44E-05$	0.0641	-0.0904	0.0032	0.1365	67.4181	0.0001
601918.SH	$-2.69E-05$	0.0892	-0.0870	0.0039	1.7818	79.0994	0.0001
...	...	...	...	...	...	...	...
000059.SZ	$1.18E-05$	0.0346	-0.0279	0.0020	0.3518	21.4666	0.0001
000096.SZ	$-2.52E-06$	0.0577	-0.0392	0.0028	0.4606	24.8307	0.0001
000159.SZ	$-1.29E-06$	0.0719	-0.0458	0.0033	0.9072	26.7503	0.0001

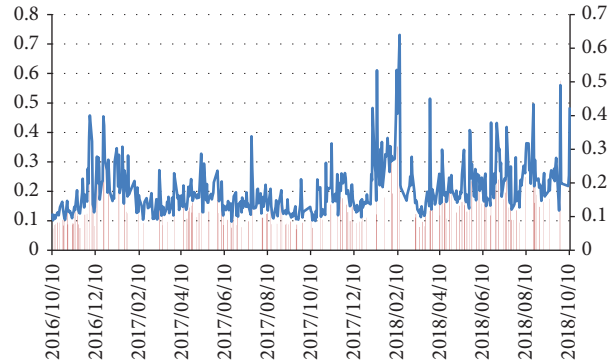


FIGURE 2: Realized volatility and realized jump of 601857.SH.

TABLE 2: Statistical properties of realized volatility for some energy stocks.

Stock code	Mean	Maximum	Minimum	Standard deviation	Skewness	Kurtosis	ADF ( <i>P</i> value)
601857.SH	0.2028	0.7310	$6.17E-05$	0.0851	1.9145	8.8743	$\leq 0.0000$
601898.SH	0.2793	1.0872	0.0001	0.1155	2.5710	13.5124	$\leq 0.0000$
601918.SH	0.3438	1.2864	0.0000	0.1426	1.9979	9.3526	$\leq 0.0000$
...	...	...	...	...	...	...	...
000059.SZ	0.2990	1.4772	0.0002	0.1411	2.8378	17.5631	$\leq 0.0000$
000096.SZ	0.3120	1.6058	0.0004	0.1690	2.7712	14.7394	$\leq 0.0000$
000159.SZ	0.3668	1.7750	0.0002	0.2311	2.8914	13.5160	$\leq 0.0000$

TABLE 3: Statistical properties of realized jumps for some energy stocks.

Stock code	Mean	Maximum	Minimum	Standard deviation	Skewness	Kurtosis	ADF ( <i>P</i> value)
601857.SH	0.0471	0.5721	0.0000	0.0824	2.3704	10.6442	$\leq 0.0000$
601898.SH	0.0604	0.7949	0.0000	0.1051	2.6145	13.6347	$\leq 0.0000$
601918.SH	0.0823	1.0694	0.0000	0.1354	2.3204	11.7368	$\leq 0.0000$
...	...	...	...	...	...	...	...
000059.SZ	0.0488	1.1677	0.0000	0.1179	4.0722	27.6676	$\leq 0.0000$
000096.SZ	0.0861	1.4636	0.0000	0.1526	3.4660	22.6176	$\leq 0.0000$
000159.SZ	0.0993	1.5125	0.0000	0.2004	3.3232	17.1421	$\leq 0.0000$

TABLE 4: Jump correlation coefficient matrix from October 2016 to April 2017.

	601857.SH	601898.SH	601918.SH	...	000059.SZ	000096.SZ	000159.SZ
601857.SH	1.0000	0.3860	0.2683	...	0.4625	0.3234	0.3725
601898.SH	0.3860	1.0000	0.2589	...	0.2664	0.2192	0.4458
601918.SH	0.2683	0.2589	1.0000	...	0.1162	0.0752	0.0973
...	...	...	...	...	...	...	...
000059.SZ	0.4625	0.3234	0.3725	...	1.0000	0.2631	0.2270
000096.SZ	0.2664	0.2192	0.4458	...	0.2631	1.0000	0.1187
000159.SZ	0.1162	0.0752	0.0973	...	0.2270	0.1187	1.0000

TABLE 5: Jump distance matrix from October 2016 to April 2017.

	601857.SH	601898.SH	601918.SH	...	000059.SZ	000096.SZ	000159.SZ
601857.SH	0.0000	1.1081	1.2097	...	1.0369	1.2113	1.3295
601898.SH	1.1081	0.0000	1.2175	...	1.1632	1.2497	1.3600
601918.SH	1.2097	1.2175	0.0000	...	1.1203	1.0528	1.3436
...	...	...	...	...	...	...	...
000059.SZ	1.0369	1.1632	1.1203	...	0.0000	1.2140	1.2434
000096.SZ	1.2113	1.2497	1.0528	...	1.2140	0.0000	1.3277
000159.SZ	1.3295	1.3600	1.3436	...	1.2434	1.3277	0.0000

has 62 nodes, which represent the jump of 62 energy sample stock prices. In complex network diagrams, the number of interconnected nodes and the length of the distance between nodes are used to represent complex network relationships. The more nodes that are connected to each other, the greater the stock price jumps directly when the node's energy stock price jumps. The distance between the nodes represents the weight between the nodes. If the distance between the two nodes is shorter, then the correlation between the jumps of the stock price is stronger. If the node does not appear in the complex network diagram, then there is no correlation between the jump of the energy stock price and other stock prices.

We can draw the following conclusions. (1) China's energy stock prices directly or indirectly affect one another. Figures 3–6 show that the 62 sample points in this paper all appear in the complex network diagram. They will be directly or indirectly linked, indicating that the jump risk of China's energy stock price is ubiquitous and can be influenced by each node. (2) In the complex network diagram, the influence of different energy stock price jumps is inconsistent. For example, in Figure 3, node 55 is directly connected to multiple stocks. When the stock price of this node jumps, it will cause node 13. The stock prices on 15, 15, 22, 32, and 37 jumped, but the stocks directly connected to nodes 6 and 36 were fewer. The results show that in the energy stock industry, the contagion of risks in different stocks is inconsistent. (3) The infectious power of the energy stock jump risk will change with time. Comparing node 55 in Figure 3 with node 31 in Figure 5 shows that there are 6 nodes in Figure 3. Nodes 55 are connected, but only one node in Figure 5 is connected to node 55. In Figure 5, a total of 8 nodes are connected to node 31, indicating that the risk-infecting ability of the same source-only stock changes over time in the entire network diagram. (4) The shape of the complex network changes with time, indicating that the energy stock price jumps the complex network relationship over time. Figures 3 and 4 show the complex network of energy stock hopping before October 2017, showing a "banded" distribution. There are fewer nodes directly adjacent to each node, indicating that the energy stock price jumps on a certain node. It is not easy to directly cause a large jump in the energy stock price of the entire network. However, Figures 5 and 6 show that the complex network of energy stock hopping after October 2017 tends to be "grouped", and the nodes directly adjacent to each node increase, indicating that the energy stock price occurs on a certain node. Jumping will directly cause more energy stock

prices to jump. The results show that starting from October 2017, the correlation between stock market jump risks in the energy industry is stronger, and the risk contagion between energy stocks is stronger.

*4.3.3. Analysis of the Importance of Network Nodes.* This study uses closeness centrality to analyze the importance of the nodes. Table 6 shows that the energy stocks with the highest centrality value in the complex network diagrams of four different time periods are 300157. SZ, 000059. SZ, 000059. SZ, and 000968. SZ, respectively.

Table 6 shows the following. (1) The role of each node in the complex network on the stability and invulnerability of the network is inconsistent. In the period of October 2016 to April 2017, 300157.SZ is most important to the stability of the network. (2) The importance of nodes in complex networks is time-varying. In different time periods, according to the results of the closeness centrality, the top five energy stock codes are not completely consistent. (3) For the Chinese energy market, the coal industry is the most important throughout the network tree. The analysis shows that in these four time periods, more than 50% of the stocks are coal stocks, and after October 2017, the proportion of coal stocks increased. The results show that the stability of the coal industry is very important for the development of China's energy industry. The reason is that China is a large country in coal production and consumption. In China's energy consumption structure, coal energy consumption stands at more than 65%. Therefore, at present, the coal industry is at the core of China's energy finance complex network.

*4.3.4. Complex Network Dynamic Cluster Analysis.* The previous analysis shows that the time-varying characteristics of the complex network of energy stock jumps are obvious. To further explain the dynamic clustering characteristics of energy stock jumping complex networks, a fast unfolding algorithm is used.

The results of the community-based Q-based community classification in Table 7 show that from October 2016 to October 2018, the optimal number of community divisions is gradually reduced, indicating that more energy stock price jumps are included in the same community. The clustering characteristics within the community are more obvious, and the results further confirm that after October 2017, the contagion of the risk of jumping between energy stocks becomes stronger. The clustering analysis results of complex

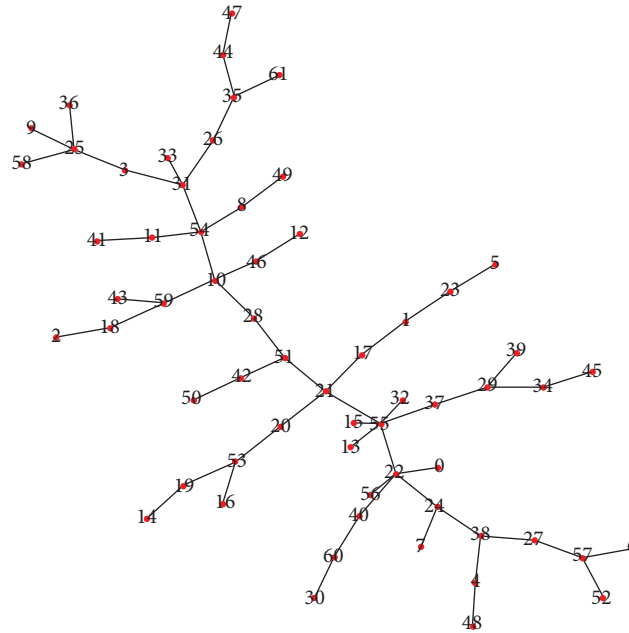


FIGURE 3: Energy stock jump complex network from October 2016 to April 2017.

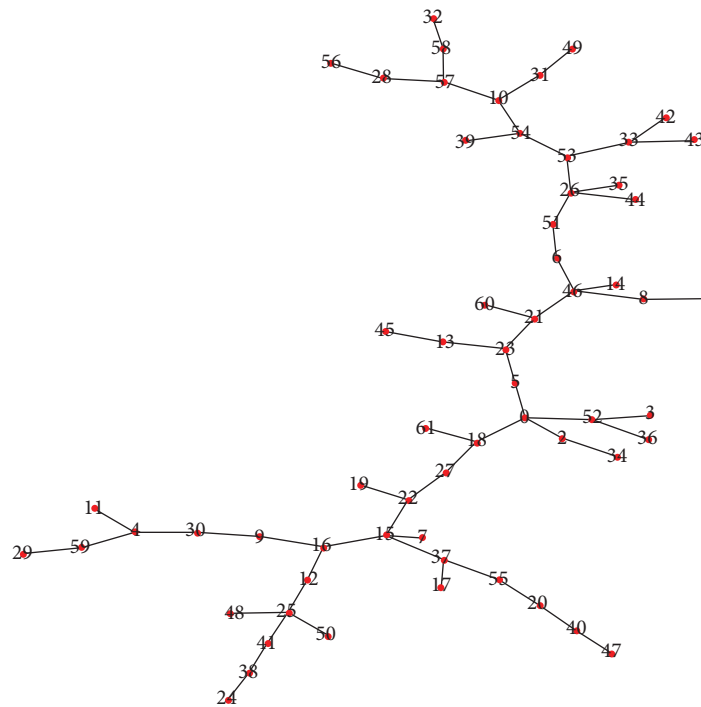


FIGURE 4: Energy stock jump complex network from April 2017 to October 2017.

networks in different time periods are reported in Figures 7–10. The different colors in Figures 7–10 represent different communities. The jump correlation between communities is shown in Table 8.

The analysis of the average correlation coefficient of the communities in different time periods reported in Table 8 shows that the energy enterprises with the highest average correlation coefficient in different time periods are

inconsistent, and the time-varying characteristic is obvious. Prior to October 2017, most of the energy stocks in the communities with the highest average correlation coefficient were energy mining equipment manufacturers, but after October 2017, most of the energy stocks in the communities with the highest average correlation coefficient were coal companies and new energy companies. The empirical results show that the degree of risk contagion of

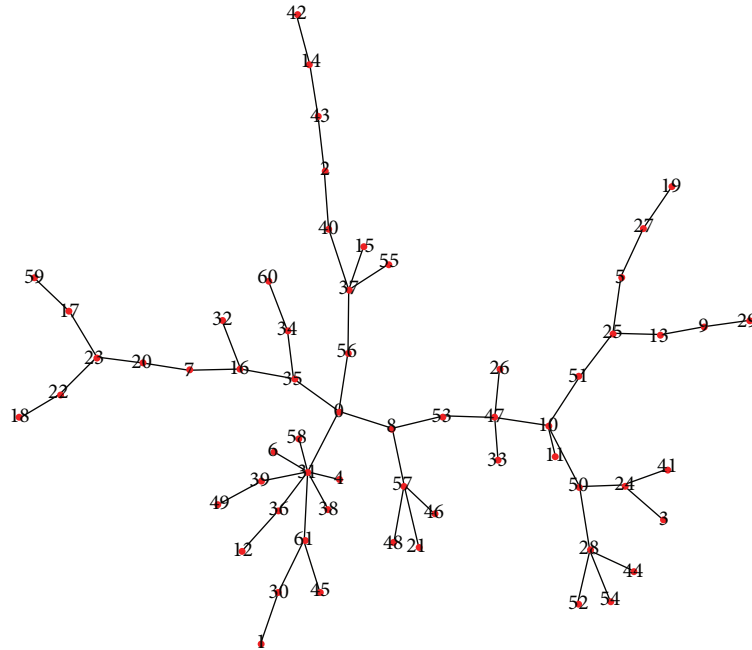


FIGURE 5: Energy stock jump complex network from October 2017 to April 2018.

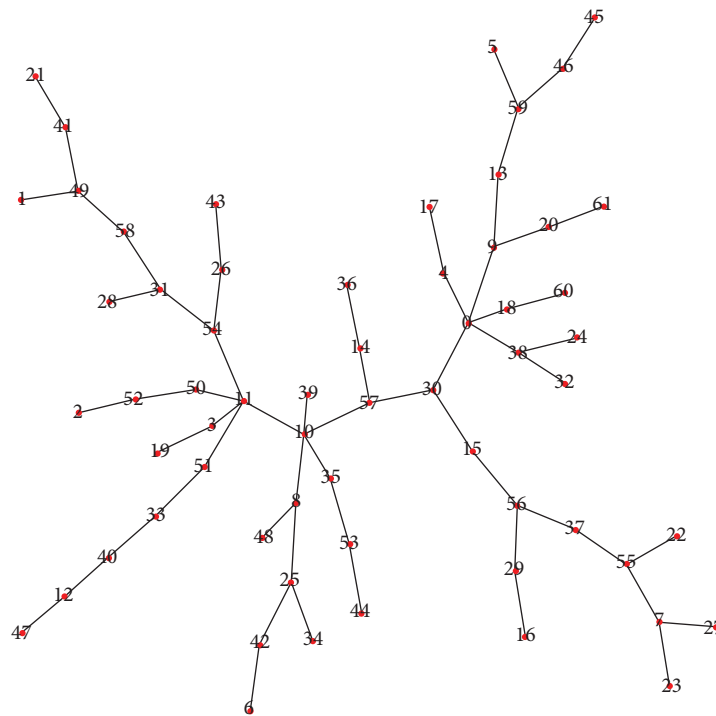


FIGURE 6: Energy stock jump complex network from April 2018 to October 2018.

different types of energy companies is inconsistent at different time periods. China must pay attention to the risk contagion within the coal industry and the new energy industry. China's coal stock jump risk is highly correlated and prone to risk contagion within the coal industry. Once the risk accumulates within the coal industry, it is likely to affect the entire energy industry in China. China also needs

to pay attention to the risk contagion problem within new energy enterprises. At present, many enterprises in China develop mainly new energy focused on electricity, solar energy, wind energy, and so on. These enterprises have similar development paths and are prone to systemic risks, which hinder the development of the new energy industry in China.

TABLE 6: Importance analysis of complex network nodes based on closeness centrality.

Ranking	2016.10-2017.04	2017.04-2017.10	2017.10-2018.04	2018.04-2018.10
1	300157.SZ	000059.SZ	000059.SZ	000968.SZ
2	601101.SH	000723.SZ	000937.SZ	601898.SH
3	601808.SH	002629.SZ	601666.SH	600339.SH
4	600188.SH	300191.SZ	600348.SH	002128.SZ
5	000983.SZ	600157.SH	600508.SH	000059.SZ

TABLE 7: Modular Q statistics.

Period	Optimal number of communities	Modular Q value
2016.10-2017.04	10	0.7846
2017.04-2017.10	9	0.7698
2017.10-2018.04	8	0.7802
2018.04-2018.10	7	0.7740

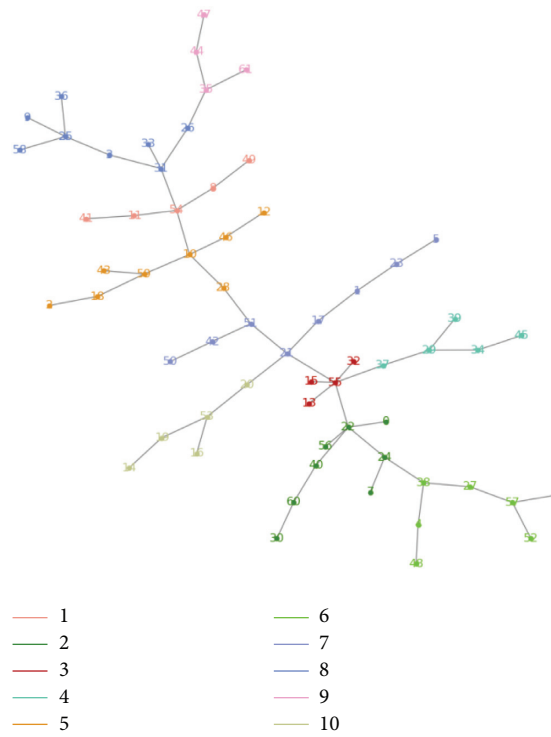


FIGURE 7: The community of energy stock price jump from October 2016 to April 2017.

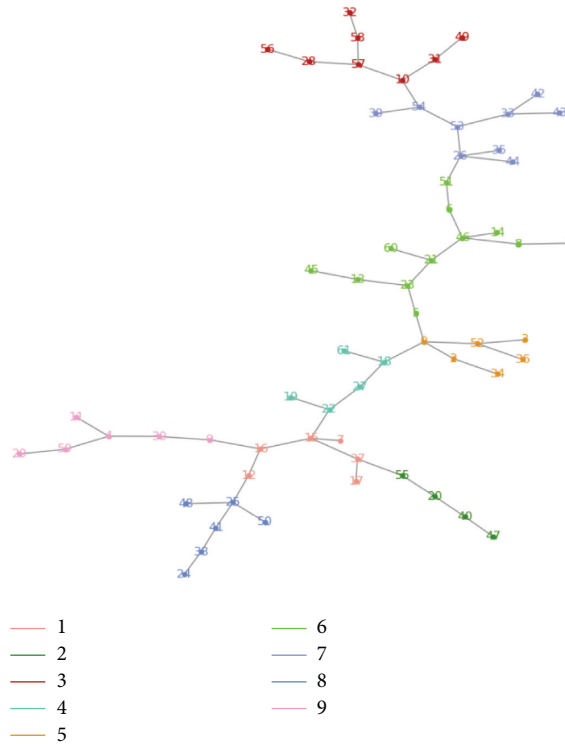


FIGURE 8: The community of energy stock price jump from April 2017 to October 2017.

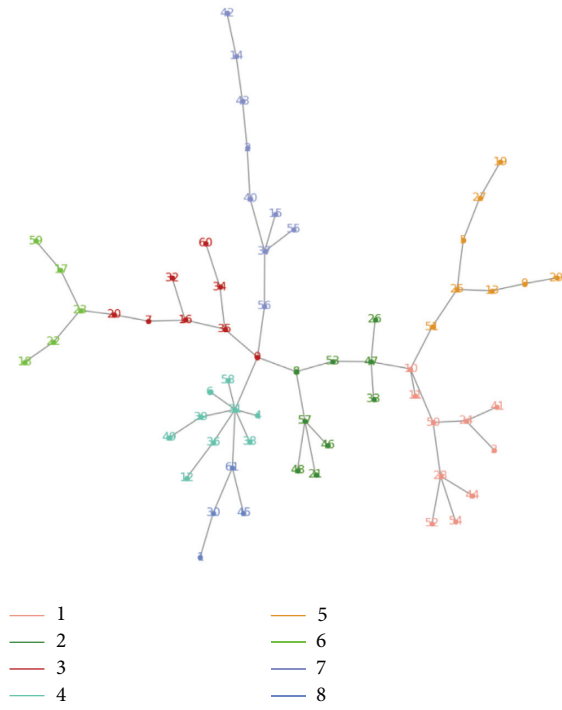


FIGURE 9: The community of energy stock price jump from October 2017 to April 2018.

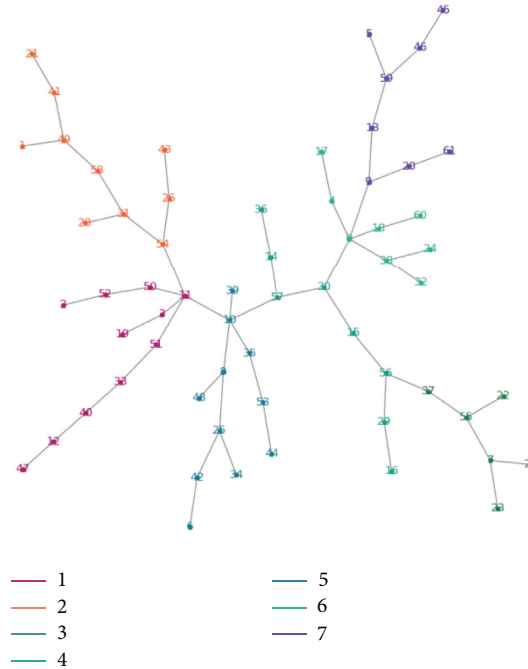


FIGURE 10: The community of energy stock price jump from April 2018 to October 2018.

TABLE 8: Communities with the strongest correlation coefficient at different time periods.

Period	Stock code	Average correlation coefficient
2016.10-2017.04	600387.SH, 002353.SZ, 002267.SZ, 601808.SH	0.4855
2017.04-2017.10	600583.SH, 000852.SZ, 002221.SZ, 002353.SZ, 002490.SZ, 002554.SZ	0.4038
2017.10-2018.04	000552.SZ, 600777.SH, 000983.SZ, 002128.SZ, 600971.SH, 601088.SH, 601225.SH, 601699.SH, 600028.SH, 600188.SH	0.6198
2018.04-2018.10	000096.SZ, 601918.SH, 600856.SH, 601015.SH, 300157.SZ, 601699.SH, 600123.SH, 600188.SH, 600348.SH	0.5152

## 5. Conclusions

This paper systematically studies the clustering problem of dynamic complex networks of stock jumping risk of energy-listed companies. Based on the research of this paper, we conclude the following. (1) The jump of the stock price is an important component of volatility. (2) The complex network of stock price jumps of energy enterprises has obvious time-varying characteristics. After October 2017, the risk contagion of the stock price jump is more likely to occur. (3) The community of the energy stock price complex network also has strong time-varying characteristics. (4) The coal industry is the most critical in the complex network of the entire energy industry, and the internal risk of the coal industry is highly contagious. (5) The risk contagion within the new energy industry community is key for the development of the new energy industry.

Based on the above conclusions, we believe that in the field of energy finance, the following points should be considered. (1) The energy stock price jump is a common phenomenon, but the infection problem of stock price jump risks needs specific analysis. (2) The issue of energy financial risk management should be viewed holistically. (3) There are

different ways to jump risk contagion in the energy industry. We need to systematically analyze the clustering results of the energy industry, penetrate specific industries according to the results, and adopt appropriate methods for risk management. (4) China needs to take measures to protect the jumping risk of the coal industry.

## Data Availability

All data used to support the finding of the study are available from the corresponding author upon request.

## Conflicts of Interest

The authors declare that they have no conflicts of interest.

## Acknowledgments

This paper was supported by the 2020 Suqian Science and Technology Planning Project (Social Development): "Research on Science and Technology Finance Boosting the Development of Science and Technology SMEs in Suqian under the Background of the Epidemic" (S202005), the

Zhejiang Science and Technology Information Research Institute R&D Project: “A Data Processing Method for Intelligent Mining and Text Anomaly Monitoring” (R2021D001), and Doctoral Research Initiation Project Fund (2019BSXM11).

## References

- [1] T. Kaneko and B. S. Lee, “Relative importance of economic factors in the U.S. And Japanese stock markets,” *Journal of the Japanese and International Economies*, vol. 9, no. 3, pp. 290–307, 1995.
- [2] S. A. Basher and P. Sadorsky, “Oil price risk and emerging stock markets,” *International Finance*, vol. 17, no. 2, pp. 224–251, 2004.
- [3] Y. J. Zhang, Y. Fan, H. T. Tsai, and Y. M. Wei, “Spillover effect of US dollar exchange rate on oil prices,” *Journal of Policy Modeling*, vol. 30, no. 6, pp. 973–991, 2008.
- [4] P. K. Narayan, S. Narayan, and X. Zheng, “Gold and oil futures market: are markets efficient?” *Applied Energy*, vol. 87, no. 10, pp. 3299–3303, 2010.
- [5] T. G. Andersen and T. Bollerslev, “Deutsche mark-dollar volatility: intraday activity patterns, macroeconomic announcements, and longer run dependencies,” *The Journal of Finance*, vol. 53, no. 1, pp. 219–265, 1998.
- [6] O. E. Barndorff-Nielsen and N. Shephard, “Econometric analysis of realized Co-variation: high frequency based covariance, regression, and correlation in financial economics,” *Econometrica*, vol. 72, no. 3, pp. 885–925, 2004.
- [7] C. F. Wang, Y. Ning, Z. M. Fang, and Y. Li, “An empirical research on jump behavior of realized volatility in Chinese stock markets,” *Systems Engineering*, vol. 26, no. 2, pp. 1–6, 2008.
- [8] T. G. Andersen, T. Bollerslev, and X. Huang, “A reduced form framework for modeling volatility of speculative prices based on realized variation measures,” *Journal of Econometrics*, vol. 160, no. 1, pp. 176–189, 2011.
- [9] Z. F. Zeng and J. Zuo, “Research on relationship of jump and volatility spillover between shanghai and Hong Kong stock market returns —based on SVCJ model by MCMC algorithm,” *Chinese Journal of Management Science*, vol. 21, no. S1, pp. 334–340, 2013.
- [10] W. J. Xu, F. Ma, and Y. Wei, “Investigating the performance of the high-frequency volatility models using the nonparametric jump tests,” *Systems Engineering*, vol. 34, no. 12, pp. 10–16, 2016.
- [11] S. Hu, Z. Gu, Y. Wang, and X. Zhang, “An analysis of the clustering effect of a jump risk complex network in the Chinese stock market,” *Physica A: Statistical Mechanics and its Applications*, vol. 523, pp. 622–630, 2019.
- [12] R. N. Mantegna, “Hierarchical structure in financial markets,” *The European Physical Journal B - Condensed Matter and Complex Systems*, vol. 11, no. 1, pp. 193–197, 1999.
- [13] X. W. Zhuang and X. Jin, “The research of correlation between network topological index and volatility of shanghai stock market,” *Journal of Donghua University*, vol. 36, no. 3, pp. 453–456, 2015.
- [14] A. Pothen, H. D. Simon, and K. P. Liou, “Partitioning sparse matrices with eigenvectors of graphs,” *SIAM Journal on Matrix Analysis and Applications*, vol. 11, no. 3, pp. 430–452, 1990.
- [15] K. T. Chi, J. Liu, and F. C. M. Lau, “A network perspective of the stock market,” *Journal of Empirical Finance*, vol. 17, no. 4, pp. 659–667, 2010.
- [16] T. K. Peron, L. F. Costa, and F. A. Rodrigues, “The structure and resilience of financial market networks,” *Chaos An Interdisciplinary Journal of Nonlinear Science*, vol. 22, no. 1, p. 193, 2012.
- [17] M. E. J. Newman, “Fast algorithm for detecting community structure in networks,” *Physical Review E-Statistical, Nonlinear and Soft Matter Physics*, vol. 69, no. 6, Article ID 066133, 2003.
- [18] M. E. J. Newman and M. Girvan, “Finding and evaluating community structure in networks,” *Physical Review E-Statistical, Nonlinear and Soft Matter Physics*, vol. 69, no. 2, Article ID 026113, 2004.
- [19] W. W. Zhan, J. L. Xi, and Z. X. Wang, “Hierarchical agglomerative community detection algorithm based on similarity modularity,” *Journal of System Simulation*, vol. 29, no. 5, pp. 1028–1040, 2017.
- [20] X. Xi and H. An, “Research on Energy Stock Market Associated Network Structure Based on Financial indicators,” *Physica A Statistical Mechanics and its Applications*, vol. 490, pp. 1309–1323, 2018.
- [21] H. Li, H. An, F. Wei, Y. Wang, W. Zhong, and L. Yan, “Global energy investment structure from the energy stock market perspective based on a Heterogeneous Complex Network Model,” *Applied Energy*, vol. 194, pp. 648–657, Article ID S0306261916306596, 2016.
- [22] O. E. Barndorff-Nielsen, B. Nielsen, N. Shephard, and C. Ysusi, “Measuring and Forecasting Financial Variability Using Realised Variance,” *State Space and Unobserved Component Models*, pp. 205–235, 2004.



## Research Article

# Workforce Participation, Ageing, and Economic Welfare: New Empirical Evidence on Complex Patterns across the European Union

Mirela S. Cristea <sup>1</sup>, Marilen G. Pirtea <sup>2</sup>, Marta C. Suciuc <sup>3</sup> and Gratiela G. Noja <sup>4</sup>

<sup>1</sup>Department of Finance, Banking and Economic Analysis, Faculty of Economics and Business Administration, University of Craiova, 200585 Craiova, Romania

<sup>2</sup>Department of Finance, Faculty of Economics and Business Administration, West University of Timisoara, 300115 Timisoara, Romania

<sup>3</sup>Department of Economics and Economic Policies, Faculty of Theoretical and Applied Economics, The Bucharest University of Economic Studies, 010374 Bucharest, Romania

<sup>4</sup>Department of Marketing and International Economic Relations, Faculty of Economics and Business Administration, West University of Timisoara, 300115 Timisoara, Romania

Correspondence should be addressed to Gratiela G. Noja; [gratiela.noja@e-uvt.ro](mailto:gratiela.noja@e-uvt.ro)

Received 17 November 2021; Accepted 24 December 2021; Published 6 January 2022

Academic Editor: S.S. Askar

Copyright © 2022 Mirela S. Cristea et al. This is an open access article distributed under the Creative Commons Attribution License, which permits unrestricted use, distribution, and reproduction in any medium, provided the original work is properly cited.

The ageing population has become one of the major issues, with manifold consequences upon the economic welfare and elderly living standards satisfaction. This paper grasps an in-depth assessment framework of the ageing phenomenon in connection with the labor market, with significant implications upon economic welfare, across the European Union (EU-27). We configure our research on four distinctive groups of the EU-27 countries based on the Active Ageing Index mapping, during 1995–2018, by acknowledging the different intensities of ageing implications on economic well-being from one group of countries to another. The methodological endeavor is based on Structural Equation Modelling. Empirical results highlight that the ageing dimensions and labor market productivity notably shape the socioeconomic development of EU countries, visibly distinguished across the four panels. The economic development induced remarkable positive spillover effects on the welfare of older people, under the influence of the ageing credentials and dynamic shaping factors. Our research advances the literature underpinnings on this multifaceted topic by investigation made on specific groups of the EU countries and distinctive strategies proposed for each group of countries, as effective results for improving the well-being of older people. Constant policy rethinking and adequate strategies should be a top priority for each specific group of EU countries, to further sustain the ageing phenomenon, with positive implications mostly on elderly welfare.

## 1. Introduction

In all countries all over the world, the demographic studies entail that a series of societal challenges have emerged, where elderly cohorts are increasing at a steady pace and are expected to continue growing over the following decades [1]. Thus, the ageing population, which means the increasing of life expectancy and decreasing of birth rates, has become a major issue, affecting the labor market equilibrium and, also, the welfare of older people, mainly, due to a weak viability

and sustainability of the pension funds [2], health deterioration, or lower social involvement [3–6].

As a result of these tendencies, the population composition has changed and, in the coming years, even more notable mutations are expected to occur, from *the pyramid-shaped frame*, with the basis of people aged 0–16 years, more numerous than the people aged over 65, representing upper segments, to a representation of “*a rectangular pattern*” [7] (p. 4) [8]. As regards Europe, which becomes the oldest continent in the world, the European Union (EU) has

registered the highest old-age dependency ratio (65+/ (15–64)), representing 31% in 2019, compared to 13.95% at the worldwide level [9], being projected to increase at 57% in 2100 [10]. As much, against the background of a declining active labor force (15–64 years), the implications of demographic ageing on economic and social well-being are more and more visible within all countries, but with different intensities [5, 11–15]. This requires an accurate and specific analysis by distinct groups of countries with similar characteristics.

Therefore, the ageing phenomenon and socioeconomic welfare approaches at the EU level have been highly debated previously within the literature, but their integrative impact has been less considered, as far as we know especially for the four specific groups of the EU Member States (MS).

In front of these facts and challenges, the main aim of our paper is to assess the ageing phenomenon in connection with the labor market implications in terms of socioeconomic welfare within the EU–27 MS, widened with an in-depth analysis for the four distinctive EU–27 MS groups. We have excluded the United Kingdom (UK), due to the Brexit final outcomes. The analyzed groups (panels) are mapped according to the *United Nations Economic Commission for Europe (UNECE)/European Commission (EC)* [16], considering the *Active Ageing Index (AAI)*. We have accounted for the four panels of EU MS in our investigation (that correspond to the groups/clusters marked by the UNECE/EC [16] with blue, green, red, and yellow colours), in order to propose a mix of specific policies and strategies for each group of countries, as Walker and Zaidi [17] also recommended as effective results. In our research, we applied *Structural Equation Modelling (SEM)* for an integrative measurement approach (direct, indirect, and total) of the interlinkages between the ageing phenomenon and labor market factors (under the influence of specific selected economic and social variables) upon economic development and poverty alleviation of older people (65+). The analyzed period is 1995–2018.

The paper is organized as follows: after a concise introduction on the subject, centered on the importance of the ageing phenomenon within the economic and social framework at the level of the EU and, more specific, for the four groups of MS considered in the empirical analysis, a synthesized brief literature review is accomplished. This section is split in two parts: the main policies adopted, particularly within the EU area, at regional and local levels, and state of the art on the ageing phenomenon and labor market integration within the economic welfare context. Thereafter, we present the selected data for the empirical investigation, the research methodology applied, and the scientific hypotheses. Discussions of the obtained results follow further, which are summarized within the concluding remarks. Extensive information regarding the empirical evidence is enclosed within Appendix.

## 2. Literature Review: Theoretical Framework

*2.1. Ageing Phenomenon and Key Policies to Promote Active Ageing Management Support.* All around the world, there are numerous notices and recommendations regarding the

awareness of ageing implications in all facets of life (health, life satisfaction, financial support, social involvement, and education). Thus, as World Health Organization (WTO) [8] (p. 6) underlines, population ageing “*is one of humanity’s greatest triumphs,*” which entails its awareness and support by policymakers, promoting healthy and active ageing management strategies as an important requirement among all countries.

The *Organization for Economic Cooperation and Development (OECD)* proposes as recommendations, even since 2006, the need to introduce “*age-friendly*” policies, as “*part of a broader strategy for responding to the challenges of population ageing*” [1] (p. 13). Due to significant increases in life expectancy that exceed the birth rate, the older workforce (aged 55–64) is greater than the previous years, but the age of exit of the labor market became lower than in the past [18]. Therefore, the main goals of the policymakers, proposed by the OECD, should underline the importance of working ageing support, striving towards offering elderly individuals a higher degree of opportunities and options in regard to working environments [1, 18].

At the level of the EU, as a response to the ageing phenomenon, a series of the MS have started to adopt and implement measures that are in line with the OECD stated goals of continuous employment of elderly workers, enclosed within 55–64 years’ cohort. Thus, starting with the year 2012, the EU pays a particular attention to *active ageing* management strategies, through specific policies and measures addressed to all MS.

These strategies and policies are designed such as to better hinder the negative implications upon older people’s life satisfaction and welfare. In this vein, as one of the policy tools or instruments, “the Active Ageing Index (AAI)” was built and tested to discover and evaluate the unexploited potential for older people’s well-being [3, 19, 20]. The AAI represents a composite index that comprises 22 indicators, based on evaluation of the four life dimensions of older people’s integration, namely: (i) “*the employment field,*” which follows the employment rate of people aged between 55 and 75 years; (ii) the ways of “*participation in society*” voluntary, care to their younger relatives or other people in need, and political activities; (iii) “*independent, healthy, and secure living*” field that follows physical training and security, the way of benefit by health services, income level, poverty risk, and lifelong learning motivation and participation; and (iv) “*capacity to actively age,*” revealed by life expectancy, healthy life, adapting to the digital society, and education [3]. The AAI was determined starting with the year 2010, at every two years. The latest available report is for the year 2018 [16], whose results were grouped in four clusters of countries, marked with different colours, as follows: *cluster 1*, green, that comprises ten Central and Mediterranean EU MS; *cluster 2*, red, which encloses six Continental and Mediterranean EU MS; *cluster 3*, blue, comprising seven EU MS, geographically dispersed; and *cluster 4*, yellow, including five countries, namely, the Nordic States (with the UK). We performed the graphical mapping of the AAI clustering for the countries considered in our empirical analysis (without UK) in Stata 16 (presented in Appendix, Figure A-I).

*Cluster 1* (green) obtained a medium AAI score under the EU average (31.4 compared to 35.8), with the minimum value of the AAI for Greece (28.1) and the maximum one for Spain (34.1). The other three clusters registered higher AAI scores than of the EU average. Thereby, *cluster 2* (red) registered an average of the AAI score upper low to the EU one (36.4 compared to 35.8), with the minimum and maximum AAI scores for Luxembourg (35.3) and France (38.4), respectively. *Cluster 3* (blue) registered a medium score of AAI of 36.6 (upper medium to the EU average, of 35.8). Countries at the extremities of the AAI interval were Lithuania (33.6) and Germany (39.5). *Cluster 4* (yellow) registered a medium value of the AAI of 42.8 (the highest result compared with the EU average), with the highest score for Sweden (46.9) and the lowest one for Finland (40.6) [16] (pp. 24-25). As regards the scores obtained within each cluster for the four life dimensions considered in terms of AAI evaluation, namely, “the employment,” “social participation,” “independent, healthy, and secure living,” and “capacity to actively age,” the results for the year 2018 reveal the following: cluster 1 (red) faces the biggest difficulties with the social participation domain (with over 20% below the EU average for this field, a level of 14.1, compared with 17.9), but also with other three groups of indicators that registered values below the EU average; cluster 2 (red) registered the most challenges only for the employment domain (with over 17% below the EU average, a level of 25.7, compared with 31.1); cluster 3 (blue) are confronting with most challenges for social participation component (with over 15% below the EU average, a level of 15.1, compared with 17.9), but also with independent living and capacity to actively age (being with almost 3% under the EU average for each domain); and the cluster 4 (yellow) registered higher AAI scores for each of the four domains (being over the EU average), but with the lowest implication for the *independent living* component (with more than 5% over the EU average, a level of 75.6, compared with 71.8) [16] (pp. 21, 23). According to these results, specific policies and strategies need to be enhanced for each group of countries.

Important instruments to promote adequate people’s integration on the labor market are *active labor market policies (ALMPs)* and *passive labor market policies (PLMPs)*. According to the European Commission [21], ALMP “covers activation measures for the unemployed and other target groups including the categories of training, job rotation and job sharing, employment incentives, supported employment and rehabilitation, direct job creation, and start-up incentives.” PLMPs “cover out-of-work income maintenance and support (mostly unemployment benefits) and early retirement benefits” [21]. These policies induce positive effects on the labor market, especially in the case of the Danish labor market, the well-known Danish “flexicurity” model, which put together the employment protection and unemployment benefits, “backed with strong activation policies” [22] (p. 14). This model is adapted at the “ageing workforce” (The Eurofound, 2020), by enhancing longer working lives through a lot of incentives especially dedicated for pension funds and reduction of early retirement schemes. ALMPs in Denmark are set up “to improve job matching for older

*unemployed people*” by “senior job schemes” sustained by the centers dedicated for the elder people’s needs [23] (p. 14).

Thus, specific measures, policies, and strategies designed to sustain the ageing phenomenon, healthy, and active ageing management tools are more than necessary at the level of each EU MS, by offering better incentives to encourage longer labor market participation; decreasing benefits through public retirement schemes that incentivize employees to exit the labor market much earlier than expected; providing better tracking and accountability to the use of welfare benefits to ensure that original purposes are met and they do not provide an incentive for workers that are looking to exit the labor market early.

*2.2. State of the Arts on the Ageing Phenomenon and Labor Market Integration within the Economic Welfare Context.* The brief literature review highlights that there are numerous, diverse, and quite complex studies that relate the ageing phenomenon with labor productivity or socioeconomic welfare, but very few were dedicated to specific panel groups of the EU countries.

As regards the macroeconomic impact of ageing, there are “two conceptually different ways: through a higher dependency ratio (i.e., a higher proportion of retirees to workers) and through workforce ageing” [11] (p. 4).

Most studies illustrate that, regarding the demographic changes, the new pattern of the *pyramid-shaped population, of rectangular type* (older people 65+ increasing more than the younger group, 0–19 years), will have an unfavorable influence on productivity and economic growth [7, 24].

As regards working ageing (55–64 aged group of employees) and productivity in Europe, a negative effect is estimated [11]. In order to restrain the unfavorable impact over labor productivity, authors [11] (p. 18) highlighted “the crucial role played by labor market reforms such as increases in active labor market policies on training or increase in the availability of medical inputs” and also older employees’ training and innovation. Cristea et al. [5] deepen the analysis of the influence of employees aged 55–64 years on labor productivity on the four groups of EU countries, according to the AAI scores. Authors [5] showed that, within countries with the lowest AAI results, the ageing workforce (55–64 years) induce a downsized labor productivity, while for the other countries, with higher AAI scores, the effects are favorable.

More specifically, different age groups of employees tend to have varying levels of productive outputs. Thus, with changes brought by population ageing, the average productivity per employee might be affected sometimes to a quite significant extent, due to amassed experience accumulated over the course of active life, devaluation of knowledge and understanding, and also various tendencies manifested mostly in the cases of mental and physical accomplishment [25]. To hinder these trends, “the need to maintain the relevance of older workers’ skills” becomes primary for working ageing support [25] (p. 75). Advocating this assumption, Guest and Shacklock [26] reveal the differences existing between young and old employees. Thus, to

one side, young employees have a higher level of endurance and physical strength, easily adapt to outside stress and influences, bring more intellectual capital, and offer higher cognitive processing. On the other side, older employees are generally seen as more suitable administrators/managers, with more in-depth judgements, being more reliable and thus providing a greater turnover.

When assessing individual level productivity of the working force, a direct correlation can be observed between the level of training and education and overall productive output [27]. As regards elderly cohorts, Feyrer [27] concludes that the accumulated knowledge in the early part of active life may become outdated in time if no actions to update and adapt the existing knowledge base are undertaken on behalf of employees and employers, thus producing a potential amplification of some undesirable effects on innovation and productivity. Von Gaessler and Ziesemer [28] (p. 125) illustrated that, in sixteen OECD countries, “*the optimal response to higher growth of the dependency ratio is more education to enhance productivity.*”

The combination of a series of factors through productive life, including a tapering off in human and intellectual capital investments, the depreciation in mental and physiological factors, and the advent of disrupting technologies, will lead to a decline in productivity after the age of 40 years, until retirement. A series of authors argue that the decline in productivity in the case of elderly employees might affect the levels of innovation and understanding and implementation of new technologies, causing a potential amplification of further disparity between expected production goals and their accomplishments [27, 29]. Jones [30] and Aksoy et al. [31] highlighted that the innovation is strongly influenced by the size of young and middle-aged groups and adversely affected by elderly groups. Therefore, the orientation and preference of people aged over 55 years for a pronounced use of the digital technologies becomes a challenge and necessity, as response to the 4th industrial revolution era [17, 32] and nowadays online shift working, due to SARS-CoV-2 [33].

The implications of demographic ageing on economic growth have long been researched in the literature, highlighting unfavorable implications, but with various intensity for different groups of countries.

Thus, considering the economic and demographic conditions of developed and developing countries, Bloom, Canning, and Fink [12] highlight the fact that these implications are unfavorable, more pronounced in developed countries than in developing ones, but which can be mitigated by appropriate economic and social policies. Thus, by increasing women’s engagement in the labor market (because of lowering the fertility rate) and raising the retirement age, the authors [12] argue that the unfavorable influences of increasing life expectancy and reducing fertility rates on growth economic conditions will attenuate. Unfavorable implications of demographic ageing on GDP per capita are also highlighted by Fougère and Mérette [13] in their analysis designed for seven industrialized countries within OECD countries. However, the authors [13] show that, through investments in the lifelong formation of human

capital, demographic ageing might bring more opportunities for economic growth than threats, results proved also by Kotschy and Sunde [14]. Using a composite indicator for economic dimension, namely, “economic complexity (EC),” based on employment data for Italian regions/provinces, and its connection with fertility rate (TFR), Innocenti, Vignoli, and Lazzeretti [34] (p. 11) proved the positive association between the dimensions, explained by the idea that “provinces characterized by higher levels of EC also had higher levels of TFR.” However, Nagarajan, Teixeira, and Silva [15] show that the problem of population ageing, at present, is not only of the developed countries, but also of developing or less developed ones. In addition to the factors for increasing women’s involvement in the labor market and the lifelong education of the population, also agreed by the authors [15], they stress the role of external support to less developed countries by the international organizations, through assistance health and development, and also by attracting migrants from less developed countries to the developed ones, to alleviate the effects of poverty on the elderly population in these countries.

As a summary, adequate policies and strategies are more than necessary for specific groups of countries with similar characteristic that can hamper the negative effects of old dependency ratio and ageing workforce upon economic welfare.

### 3. Data and Methodology

By reviewing the relevant literature underpinnings, we group the data into three categories of indicators, namely: *welfare variables*, *ageing credentials*, and *labor market and other specific indicators*.

We grouped the EU countries on four panels, following the clustering made by the UNECE/EC [16] (p. 11) according with the AAI scores for the year 2018, as follows: *1<sup>st</sup> panel* (EU-1) comprises the EU MS with AAI scores under the EU average, namely, “Greece, Croatia, Romania, Hungary, Slovenia, Poland, Bulgaria, Slovakia, Italy, and Spain” (from the lowest, Greece, to the highest, Spain); *2<sup>nd</sup> panel* (EU-2) encloses the EU countries with AAI scores upper low of the EU mean, namely, “Luxembourg, Malta, Cyprus, Austria, Belgium, and France”; *3<sup>rd</sup> panel* (EU-3) comprises the EU countries with AAI scores upper medium of the EU average score: “Lithuania, Portugal, Latvia, the Czech Republic, Estonia, Ireland, and Germany”; and *4<sup>th</sup> panel* (EU-4) has countries ranging the highest results for the AAI scores among the other EU MS, namely, “Finland, the Netherlands, Denmark, and Sweden” (except UK, due to final Brexit decision).

More specific, the variables included in our research, compiled separately for the four groups of EU MS, are (Table 1, Appendix Tables A-Ia–A-Id):

- (i) *Welfare Indicators*. Gross Domestic Product (GDP) per capita (*GDP\_C*); at-risk-of-poverty rate, 65+ (*POV\_R\_65*).
- (ii) *Ageing Representative Indicators*. Old dependency ratio (*OD\_65*); life expectancy at birth total population (*LE*); crude birth rate (*BR*).

TABLE 1: Variables comprised in the econometric models.

Acronym	Explanation	Unit of measure	Database
<i>GDP_C</i>	Gross Domestic Product per capita	Constant 2010 USD	The World Bank, World Development Indicators (WDI)
<i>POV_R_65</i>	At-risk-of-poverty rate, 65+, EU statistics on income and living conditions (EU-SILC) and the European Community Household Panel (ECHP) Surveys	%	European Commission, Eurostat
<i>LP</i>	Labor productivity per person employed as percentage from the EU-27 average	% (EU-27 = 100)	European Commission, Eurostat
<i>OD_65</i>	Old dependency ratio (population 65+ to population 15-64 years)	%	European Commission, Eurostat
<i>LE</i>	Life expectancy at birth, total population	Years	European Commission, Eurostat
<i>BR</i>	Crude birth rate	“The ratio of the number of live births per 1000 persons”	European Commission, Eurostat
<i>ER_55_64</i>	Employment rate, 55-64 years aged group or working ageing	% of total population	European Commission, Eurostat
<i>EARN</i>	Annual net earnings for “two-earner married couple, with two children”	Purchasing Power Standard (PPS)	European Commission, Eurostat
<i>ALMP</i>	Active labor market policies	% of GDP	European Commission, Employment, Social Affairs & Inclusion
<i>PLMP</i>	Passive labor market policies	% of GDP	European Commission, Employment, Social Affairs & Inclusion
<i>Edu_acq</i>	Educational attainment of population (upper secondary, postsecondary, nontertiary and tertiary education, levels 3-8) (15-64 years)	% of 15-64 years	European Commission, Eurostat
<i>GERD</i>	Research and development expenditure	% of GDP	European Commission, Eurostat
<i>Active_pop</i>	Active population, 15-64 years' aged group	Thousand persons (annual averages)	European Commission, Eurostat

Source: authors' process.

(iii) *Labor Market and Other Specific Indicators*. Labor productivity per person employed, as percentage from the EU-27 average (*LP*); employment rate, 55-64 years' aged group or ageing workforce (*ER\_55\_64*); total labor force/active population (*Active\_pop*); active labor market policies (*ALMP*); passive labor market policies (*PLMP*); population with secondary, upper, postsecondary, and tertiary education (levels 3-8) (*EDU\_acq*); Research and Development (*R&D*) expenditures (*GERD*); annual net earnings (*EARN*).

The analyzed period is 1995-2018 and the data was collected from Eurostat [35], the Employment, Social Affairs & Inclusion [21], and the World Development Indicators [9] databases. Graphical representation of 2018 data for main indicators is presented below as diagrams (Figures 1-3) and as traditional graphs for an adequate comparison in the Appendix (Figures A-II-A-IV).

The main welfare representative indicators (*GDP\_C* and *POV\_R\_65*) in 2018 highlight important differentials between the EU-27 MS. Most significant outcomes are accounted by the countries enclosed within the old EU-14 group (that adhered to the EU until 1995), namely: Luxembourg, Denmark, Sweden, Netherlands, Austria, and Finland, considering *GDP\_C* (Figure 1(a)); and Slovak

Republic and Hungary (from the new EU group of countries), along with France, Denmark, Netherlands, Greece, and Luxembourg, after *POV\_R\_65* (Figure 1(b)). The highest poverty rates of older people (+65) are in countries from the new EU-13 group (which became EU MS after 2004), namely, Estonia, Latvia, Lithuania, Bulgaria, and Croatia.

With reference to the *ageing selected indicators*, for the year 2018, the highest *birth rate* (Figure 2(a)) was registered in Ireland, France, and Sweden, from the old EU-14 countries, on the one hand, and Estonia, Cyprus, and Czech Republic, from the new EU-13 countries, on the other hand. The highest *life expectancy* (Figure 2(b)) was in the old EU-14 MS, namely, Italy, Spain, France, and Sweden, but also in Malta and Cyprus from the new EU-13 group of countries. The highest *old dependency ratio* (*OD\_65*) was registered in Italy, Greece, Germany, Finland, and Portugal, from the old EU-14 MS, and Bulgaria, from the new EU-13 group (Figure 2(c)).

The main outcome of the labor market, namely, the labor productivity per person employed, was over the average of the EU in Ireland (the highest, almost double the EU average), Luxembourg, France, Austria, Belgium and Denmark, Finland, Germany, Italy, and the Netherlands (Figure 3(a)). Considering the specific policies addressed to





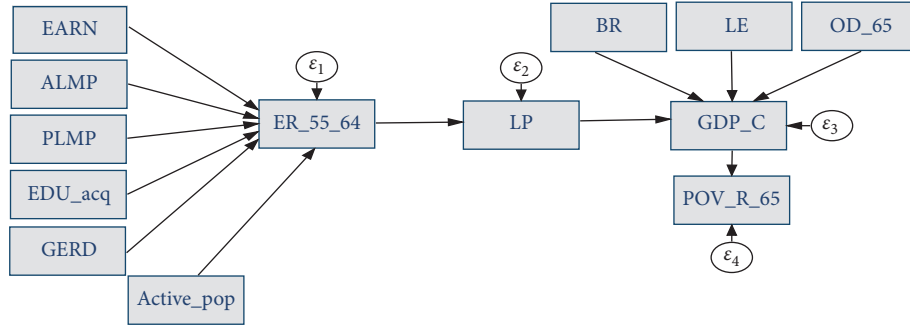


FIGURE 4: General pattern of the SEM model. *Source:* authors' process.

We pursue to verify the following hypotheses ( $H$ ):

- (i)  $H_1$ . The employment rate of the 55–64 years' aged group ("ageing workforce") represents a significant factor of influence of labor market productivity, under the impact of other economic and social factors, with relevant distinctions across the four panels of EU MS.
- (ii)  $H_2$ . Ageing dimensions and labor productivity significantly shape the economic development of the EU countries, visibly distinguished across the four panels of EU MS.
- (iii)  $H_3$ . There are overall (direct indirect, total) significant and diverse implications of economic development upon older people's poverty levels under the influence of the ageing credentials and labor market factors, across the four panels of EU MS.

## 4. Results and Discussion

We have built and processed the SEM models for each distinctive group of EU countries, mapped according to the UNECE/EC [16], based on the AAI. The results obtained are given in Figure 5.

To certify the results obtained, we first verified a series of particular tests, such as the Wald test for each equation (Table 2); the good-fit tests: *likelihood ratio*, *information criteria*, *baseline comparison*, and *size of residuals* which also comprises *the coefficient of determination (CD)* (Table 3) point out over 90% (in case of the EU-1 and EU-2 groups of countries) and 80% (in case of the EU-3 and EU-4 panels), and the older people's poverty level has been shaped by the considered variables. We have also calculated *the Alpha Cronbach tests* per item and per total scale that reveal the Alpha coefficients of over 0.80, for each considered panel, which highlights a very good reliability of the scale (Table 4).

As regards the cumulative effects of the ageing workforce ( $ER_{55\_64}$ ) upon labor market productivity ( $LP$ ), under the influence of considered economic and social factors, a positive impact was induced only for the EU-4 panel (the Nordic States, with the best results considering AAI mapping) (Figure 5(d)) (the estimated coefficient is 0.93). The updated results for the countries with the highest AAI scores are opposite to Cristea et al. [5], which show unfavorable implications of older workforce insertion upon labor

productivity. Regarding the other panels, a negative influence of  $ER_{55\_64}$  upon  $LP$  was entailed for the EU-3 panel (Figure 5(c)), namely, countries with upper medium AAI results, above the EU average (the estimated coefficient is  $-0.315$ ), while for the EU-1 and EU-2 panels (Figures 5(a) and 5(b)), the results are favorable. These cumulative effects were accounted under the influence of  $EARN$  (positive estimated coefficients, at the highest levels for the EU-3 and EU-4 groups of countries) and  $ALMP$  (negative estimated coefficients for the EU-1, EU-2, and EU-3 panels, and a positive coefficient for the EU-4 panel). Also, there are other factors with negative effects on  $ER_{55\_64}$ , namely:  $PLMP$  for the EU-3 and EU-4 group of countries, while for the countries with the lowest AAI results (EU-1 and EU-2), the results are slightly contradictory;  $Edu\_acq$ , for the EU-1 and EU-2 group of countries, while for the countries with the highest AAI scores (EU-3 and EU-4), the educational influence is positive; total labor force ( $Active\_pop$ ) for the EU-1 group (the estimated coefficient is  $-0.0535$ ), which entails the need for increasing the employment rate, while for the EU-3 panel, the influence is favorable (the estimated coefficient is 0.164);  $GERD$ , for the EU-3 group of countries, while for the EU-1 and EU-4, the results are positive.

Thereby, we can evidence that the 1st hypothesis,  $H_1$ : The employment rate of the 55–64 years' aged group ("ageing workforce") represents a significant factor of influence of labor market productivity, under the impact of other economic and social factors, with relevant distinctions across the four panels of EU MS, is fulfilled only for the countries with the highest and upper medium AAI scores.

These impacts can be hindered by increasing the participation on the labor market for the group of people aged 55–64 years with all levels of education, adapted to their abilities; reconsidering the active labor market policies, on the model of the Nordic States and the Netherlands, where the indirect influences upon  $LP$  are favorable (due to the highest  $ALMP$  share in GDP), since "the results of such policies and accurate associated measures have remarkable positive effects upon the well-being on the employees and the overall economic activity" [36] (pp. 735–736); rethinking the  $PLMP$ , since these policies have induced negative influence on  $ER_{55\_64}$ ; for the EU-3 and EU-4 panels, reconsidering the R&D applications ( $GERD$ ) for 55–64 years' jobs creation, adapted to digital transformation and nowadays telework environment, as stated also in [11, 27, 29–31].



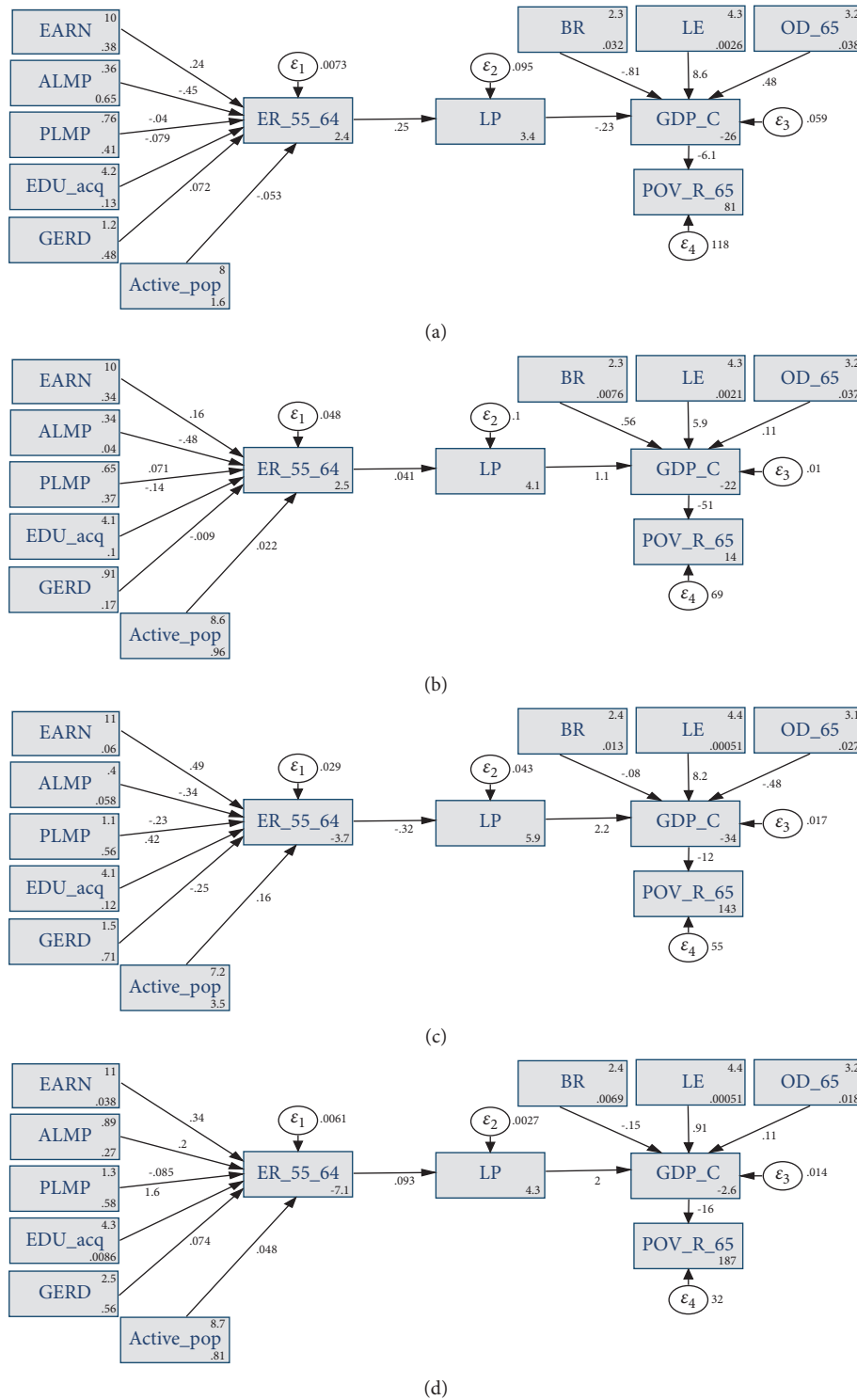


FIGURE 5: SEM models, 1995–2018: (a) EU-1; (b) EU-2; (c) EU-3; (d) EU-4. Source: own process.

Further, the integrative impacts of *LP* (under direct and indirect effects of considered variables) and ageing credentials (*BR*, *LE*, and *OD\_65*) are conducted to an increase in *GDP\_C* for the countries with AAI scores above the EU average (EU-2, EU-3 and EU-4) (the estimated coefficients are 1.055, 2.241, and 1.987, respectively) (reversed of those revealed by Fougère and Mérette [13]), while for the

countries with AAI scores under the EU level, the cumulative effects are unfavorable (the estimated coefficient is  $-0.234$ ), being similar to the results revealed by Bloom, Canning, and Fink [12]. As regards ageing credentials, for the countries with AAI scores under the EU level (EU-1) (Figure 5(a)), birth rate (*BR*) has induced unfavorable impact on *GDP\_C* (opposite of those proved by Innocenti,

TABLE 2: Wald test results for the SEM models, EU-27, 1995–2018.

Variables	EU-1 panel			EU-2 panel			EU-3 panel			EU-4 panel		
	Chi <sup>2</sup>	df	<i>p</i> value	Chi <sup>2</sup>	df	<i>p</i> value	Chi <sup>2</sup>	df	<i>p</i> value	Chi <sup>2</sup>	df	<i>p</i> value
<i>Log_ER_55_64</i>	368.65	6	0.000	80.93	6	0.000	138.21	6	0.000	551.39	6	0.000
<i>Log_LP</i>	1.15	1	0.2840	0.21	1	0.6493	18.46	1	0.000	6.31	1	0.0120
<i>Log_GDP_C</i>	544.83	4	0.000	3981.66	4	0.000	1169.88	4	0.000	83.35	4	0.000
<i>Log_POV_R_65</i>	8.03	1	0.0046	0.20	1	0.0508	63.73	1	0.000	24.86	1	0.000

$H_0$ : All coefficients excluding the intercept are 0. We can thus reject the null hypothesis for each equation, with limitation on LP. Source: authors' process.

TABLE 3: Goodness-of-fit tests for the SEM models, EU-27, 1995–2018.

	EU-1 panel	EU-2 panel	EU-3 panel	EU-4 panel
Likelihood ratio				
Model vs. saturated chi <sup>2</sup> _ms (30)	842.038	847.432	766.993	512.168
<i>p</i> > chi <sup>2</sup>	0.000	0.000	0.000	0.000
Baseline vs. saturated chi <sup>2</sup> _bs (42)	1303.435	1497.824	1156.007	797.052
<i>p</i> > chi <sup>2</sup>	0.000	0.000	0.000	0.000
Population error				
RMSEA (root mean squared error of approximation)	0.394	0.315	0.406	0.360
90% CI, lower bound	0.372	0.297	0.381	0.333
Upper bound	0.418	0.334	0.431	0.388
Pclose (probability RMSEA ≤ 0.05)	0.000	0.000	0.000	0.000
Information criteria				
AIC (Akaike's information criterion)	496.177	615.809	100.296	-1084.422
BIC (Bayesian information criterion)	730.371	883.450	323.083	-875.127
Baseline comparison				
CFI (comparative fit index)	0.356	0.439	0.338	0.361
TLI (Tucker–Lewis index)	0.099	0.214	0.074	0.106
Size of residuals				
CD (coefficient of determination)	0.947	0.902	0.806	0.862

Source: own research.

TABLE 4: Cronbach's Alpha for the SEM models, EU-27, 1995–2018.

Items	EU-1 panel		EU-2 panel		EU-3 panel		EU-4 panel	
	Item-test correlation	Alpha	Item-test correlation	Alpha	Item-test correlation	Alpha	Item-test correlation	Alpha
<i>Log_EARN</i>	0.6791	0.7651	0.7834	0.8119	0.7293	0.8199	0.1624	0.8246
<i>Log_ALMP</i>	0.7990	0.7545	0.5726	0.8324	0.8508	0.8185	0.5808	0.7895
<i>Log_PLMP</i>	0.7954	0.7561	0.7444	0.8192	0.6355	0.8327	0.3309	0.8089
<i>Log_EDU_acq</i>	0.2780	0.8133	0.4689	0.8373	0.7718	0.8180	0.6840	0.7803
<i>Log_GERD</i>	0.7262	0.7665	0.5298	0.8351	0.8192	0.8112	0.7542	0.7601
<i>Log_Active_pop</i>	0.8369	0.7499	0.4255	0.8438	0.6832	0.8247	0.7033	0.7635
<i>Log_BR</i>	0.0382	0.8318	0.3135	0.8521	0.1252	0.8635	0.6466	0.7756
<i>Log_LE</i>	0.7565	0.7592	0.9170	0.7973	0.4746	0.8460	0.5419	0.7937
<i>Log_OD_65</i>	0.0518	0.8328	0.7088	0.8206	0.7129	0.8235	0.5705	0.7840
<i>Log_ER_55_64</i>	0.3059	0.8112	0.4796	0.8430	0.2736	0.8596	0.6189	0.7836
<i>Log_LP</i>	0.7123	0.7683	0.7285	0.8198	0.6349	0.8302	0.4643	0.7986
<i>Log_GDP_C</i>	0.6883	0.7707	0.8555	0.8044	0.6536	0.8298	0.7251	0.7653
<i>Log_POV_R_65</i>	0.4881	0.7885	0.2255	0.8548	0.5990	0.8339	0.3859	0.8006
Total scale		0.7980		0.8407		0.8434		0.8012

Source: own research.

Vignoli, and Lazzeretti [34] for Italy, which revealed that economic complexity based on employment data and fertility rate is favorable, while life expectancy (*LE*) and old dependency ratio (*OD\_65*) positively influenced *GDP\_C*. The direct implications of population dimensions (*BR* and *LE*) have generated beneficial impacts upon economic

welfare for the EU-2 countries (the estimated coefficients are positive). For the EU-3 panel, *LE* was positively associated with *GDP\_C* (the estimated coefficient is 8.192), while *OD\_65* has induced unfavorable impact on economic development, which suggest that the population over 65 is not very well supported by the working force (aged 15–64 years).

For the EU-4 panel, none of the ageing credentials is not relevant from the statistical point of view (due to low data enclosed into this panel, with only 4 countries). Hereby, we can substantiate that the 2nd hypothesis,  $H_2$ : *Ageing dimensions and labor productivity significantly shape the economic development of the EU countries, visibly distinguished across the four panels of EU MS*, is fulfilled.

Finally, the overall integrative results unveil that the economic welfare, reflected by the  $GDP\_C$ , under direct and indirect influences of ageing credentials and labor market factors, positively influenced older people poverty ( $POV\_R\_65$ ), in EU-1, EU-3, and EU-4 panels (Figures 5(a), 5(c), and 5(d)) (the estimated coefficients are negative, -6.087, -11.75, and -15.98, respectively). For the EU-2 panel, the results are not relevant from the statistical point of view. Thereby, linked with the previous results from the literature, our findings are supported by the ones obtained by Cristea et al. [5] (p. 1367), which attested that “poverty is diminished for all considered EU panels under the sheer implications of selected factors,” namely, labor productivity and ageing dimensions. Moreover, as regards the life expectancy, there are findings that proved that “the poor tend to die much earlier than the rich (. . .) This enormous gap translates into a difference in life expectancy of more than 13 years between the lowest and highest income quintiles” [37] (p. 1). Therefore, our 3rd hypothesis,  $H_3$ : *There are overall (direct, indirect, total) significant and diverse implications of economic development upon older people’s poverty levels under the influence of the ageing credentials and labor market factors, across the four panels of EU MS*, is fulfilled.

To put in a nutshell, in countries with the lowest AAI ranks (EU-1), the economic development ( $GDP\_C$ ) requires proper policies and strategies in terms of birth rate encouraging, sustaining life expectancy by active and healthy ageing strategies, a better engagement on the labor market of the 55–64 years aged people, and long life learning programs for ensuring updating skills and competencies for the ageing workforce.

Similar results had been highlighted by other authors, as Nagarajan, Teixeira, and Silva [15] and Kotschy and Sunde [14] also proved. These policies and strategies should be clearly drawn for each of the four groups of the EU countries (clustered according to AAI scores).

## 5. Concluding Remarks

Given the significance of the ageing support around the world within the framework of an increased life expectancy and a decreased birth rate, our general objective is to appraise the ageing dimensions and labor market credentials in conjunction with economic welfare (measured by GDP per capita and older people’s poverty) within the EU-27 MS, deepened on four distinctive panels, mapped by the UNECE/EC [16] according to the active and healthy ageing strategies (AAI scores). The research endeavor consisted in testing three hypotheses, by applying *structural equations modelling*, for each specific group of the EU MS (below the EU average, medium low and upper EU average, and the highest scores).

Thereby, for the 1st group of countries that comprises the EU MS with AAI scores below the EU average (Greece, Croatia, Romania, Hungary, Slovenia, Poland, Bulgaria, Slovakia, Italy, and Spain), related to each hypothesis and the results obtained, we propose specific strategies and policies. As regards the favorable implication of the employment rate of the 55–64 years’ aged group (*ageing workforce*) on labor productivity under the influence of other economic and social factors ( $H_1$ ), we propose the following measures: further improving earnings level, especially pension income in Bulgaria and Romania, as Walker and Zaidi [17] mention; a keen need for accurate measures designed to a massive rethinking of active labor market policies, such as training programs, job placement, and centers for career counselling (since total labor force stock and active labor market policies generated negative impacts on older workforce integration), extending the good practices of these policies applied in Denmark and Sweden (significant share in GDP, the highest implications revealed by SEM applied for panel EU-4); sustained R&D expenditures, especially for the workplace of people aged 55–64 years; adequate job creation for the elderly workforce in order to enhance labor productivity, namely, “by introducing age-friendly work environments” [17] (p. 43); and rethinking of the educational attainment by lifelong educational programs for specific skills enhancement of older workers. As regards ageing dimensions and labor productivity impacts upon economic development of these countries ( $H_2$ ), we propose the following policies: reconsideration for sustaining the birth/fertility rate, “more associated with an area’s typical specialization (agriculture, industry, or services)” of a country, as Innocenti, Vignoli, and Lazzarotti [34] suggested for Italian provinces; improving labor productivity under the impact of digital transformation, external benefits [38], and all of the considered economic and social factors. Regarding the overall implications of economic development in these countries upon older people’s poverty under the influence of the ageing credentials and labor market factors in these countries ( $H_3$ ), which were favorable, further sustaining of these dimensions jointly with independent and healthy living dimension of the AAI [16] (poverty credentials being considered for this domain by the UNECE/EC) is more than necessary, especially on the fact that the majority of the countries from this group registered the higher poverty rate of older people (Figure 1(b)).

As for the 2nd group of countries that comprises the EU countries with AAI scores upper low of the EU average (Luxembourg, Malta, Cyprus, Austria, Belgium, and France), related to ageing workforce on labor productivity under the influence of other economic and social factors ( $H_1$ ), there is a keen need for policies and strategies that also account for a reconsideration of the educational programs, along with active labor market policies, such as career advice for older workforce, training, incentives, and better workplace capable of providing a higher employers flexibility (to straighten their negative effects). Also, we acknowledge that, for this group of countries, among the four domains of the AAI, the employment component of older people presented the highest challenges [16] (p. 23). As regards the ageing

dimensions and labor productivity impacts upon economic development ( $H_2$ ) and, overall, upon older people's poverty ( $H_3$ ), we note that a further support of the active ageing dimensions and labor productivity is required (the results for these hypotheses were favorable).

The strategies and policies addressed to *the 3rd group of countries* that comprises the EU countries with AAI scores upper medium of the EU average (Lithuania, Portugal, Latvia, the Czech Republic, Estonia, Ireland, and Germany), related to ageing workforce on labor productivity under the influence of other economic and social factors ( $H_1$ ), are the following: better incentives to encourage longer labor market participation, especially for the 55–64 years' group of people with all levels of education (active labor market policies rethinking), decreasing benefits through public retirement schemes that incentivize employees to exit the labor market much earlier than expected (passive labor market policies reconsideration due to negative implications), along with targeting the R&D applications for 55–64 years' adequate job creation and specific skills reorientation. These measures will also induce spillover effects to hinder the older dependency ratio effects on economic development ( $H_2$ ) and to sustain their overall implications upon lessening older people's poverty ( $H_3$ ) (the results for this hypothesis were favorable).

As regards *the 4th group of countries*, which encloses countries with the highest results of AAI scores among EU MS (Finland, the Netherlands, Denmark, and Sweden), the keen focus on strategies and policies is not as considerable as for the other panels, since the results of the considered hypotheses were favorable. Still, since the results for PLMPs implications on the employment rate of older people ( $H_1$ ) were unfavorable, these countries must center on a reconsideration of the passive labor market policies to improve ageing workforce and an active insertion on the labor market.

Overall, in the case of almost all panels (except the 2nd one as regards the statistical significance), the economic development induced positive effects on the welfare levels of older people, reflected by a lessening of elderly poverty (65+ years).

*The main limitations of our research* consisted in missing data and/or a relatively reduced data availability for some variables and, in some situations, a lower degree of statistical significance of the estimated coefficients. Moreover, the results are under the foreseen implications of SARS-CoV-2 pandemic on the ageing dimensions (especially, life expectancy). Other limitations may rely on the differences among countries (as regards their economies) included in each panel by the UNECE/EC [16], according with AAI clustering, especially for the 1st group (with Central and Eastern European Countries, CEEC, together with Italy and Spain that have different historical, socioeconomic, and demographic backgrounds, such as the longest life expectancy) and the 3rd group of countries (being included heterogeneous countries as regards their economy). Therefore, the policies and measures proposed may be influenced by this grouping. We acknowledge that *further research* will have to focus on the integrative index of active

ageing analysis for each EU country, making a differentiation between life expectancy and healthy life expectancy at the level of each EU MS, in order to set distinctive policies. Also, we will consider the gender implications and the effects induced by COVID-19 infections.

## Data Availability

The data used to support the findings of this study are available from the corresponding author upon request.

## Conflicts of Interest

The authors declare that there are no conflicts of interest regarding the publication of this paper.

## Supplementary Materials

Table A-Ia: Summary statistics, EU-1 panel, 1995–2018. Table A-Ib: Summary statistics, EU-2 panel, 1995–2018. Table A-Ic: Summary statistics, EU-3 panel, 1995–2018. Table A-Id: Summary statistics, EU-4 panel, 1995–2018. Figure A-I: Graphical mapping of AAI clustering for the countries considered in the empirical analysis, EU-27 Member States, 2018. Figure A-II: The welfare indicators, EU-27, 2018: (a) *GDP\_C*. (b) *POV\_R\_65*. Figure A-III: The ageing indicators, EU-27, 2018: (a) BR. (b) LE. (c) OD\_65. Figure A-IV: The main labor market indicators, EU-27, 2018: (a) LP. (b) ALMP. (c) PLMP. (*Supplementary Materials*)

## References

- [1] OECD, *Live Longer, Work Longer. Ageing and Employment Policies*, OECD Publishing, Paris, France, 2006.
- [2] M. Cristea and A. Mitrică, "Global ageing: do privately managed pension funds represent a long term alternative for the romanian pension system? empirical research," *Romanian Journal of Political Science*, vol. 16, no. 1, pp. 63–106, 2016.
- [3] European Commission, "Ready for the demographic revolution? measuring active ageing," 2016, <https://ec.europa.eu/social/main.jsp?langId=en&catId=752&furtherNews=yes&newsId=2430#navItem-1>.
- [4] M. Káčerová and J. Mládek, "Population ageing as generation substitutions: economic and social aspects," *Ekonomický časopis*, vol. 60, no. 3, pp. 259–276, 2012.
- [5] M. Cristea, G. G. Noja, D. E. Dăncăciă, and P. Ștefea, "Population ageing, labour productivity and economic welfare in the european union," *Economic Research-Ekonomska Istraživanja*, vol. 33, no. 1, pp. 1354–1376, 2020.
- [6] J. Song and D. Ryu, "Ageing effects on consumption risk-sharing channels in european countries," *Zbornik Radova Ekonomskog Fakulteta U Rijeci: Časopis za Ekonomsku Teoriju i Praksu*, vol. 36, no. 2, pp. 585–617, 2018.
- [7] K. Kinsella and D. R. Phillips, "Global ageing: the challenge of success," *Population Bulletin*, vol. 60, no. 1, pp. 3–40, 2005.
- [8] WTO, "Active ageing: a policy framework," World Health Organization, Geneva, Switzerland, WHO/NMH/NPH/02.8, 2002.
- [9] The World Bank, "World development indicators," 2020, <https://databank.worldbank.org/reports.aspx?source=world-development-indicators>.

- [10] European Commission and Eurostat Products Eurostat News, “Old-age dependency ratio increasing in the eu,” 2020.
- [11] S. S. Aiyar and C. Ebeke, *The Impact of Workforce Aging on European Productivity*, International Monetary Fund, Washington, DC, USA, 2016.
- [12] D. E. Bloom, D. Canning, and G. Fink, “Implications of population ageing for economic growth,” *Oxford Review of Economic Policy*, vol. 26, no. 4, pp. 583–612, 2010.
- [13] M. Fougère and M. Mérette, “Population ageing and economic growth in seven OECD countries,” *Economic Modelling*, vol. 16, no. 3, pp. 411–427, 1999.
- [14] R. Kotschy and U. Sunde, “Can education compensate the effect of population ageing on macroeconomic performance?” *Economic Policy*, vol. 33, no. 96, pp. 587–634, 2018.
- [15] N. R. Nagarajan, A. A. C. Teixeira, and S. T. Silva, “Ageing population: identifying the determinants of ageing in the least developed countries,” *Population Research and Policy Review*, vol. 40, pp. 187–210, 2020.
- [16] UNECE/European Commission, *2018 Active Ageing Index: Analytical Report*, United Nations, New York, NY, USA, 2018, [https://www.unecce.org/fileadmin/DAM/pau/age/Active\\_Ageing\\_Index/Stakeholder\\_Meeting/ACTIVE\\_AGEING\\_INDEX\\_TRENDS\\_2008-2016\\_web\\_cover\\_reduced.pdf](https://www.unecce.org/fileadmin/DAM/pau/age/Active_Ageing_Index/Stakeholder_Meeting/ACTIVE_AGEING_INDEX_TRENDS_2008-2016_web_cover_reduced.pdf).
- [17] A. Walker and A. Zaidi, “Strategies of active ageing in europe,” in *The Future of Ageing in Europe*, A. Walker, Ed., Palgrave Macmillan, Singapore, pp. 29–52, 2019.
- [18] OECD, *Working Better with Age, Ageing and Employment Policies*, OECD Publishing, Paris, France, 2019.
- [19] European Commission, *Active Ageing Index at the Local Level. Peer Review in Social protection and Social Inclusion 2015–2016*, Directorate-General for Employment, Social Affairs and Inclusion, Population Unit of the UNECE and the European Centre for Social Welfare Policy and Research in Vienna, Berlin, Germany, 2016.
- [20] A. Zaidi, *Active Ageing Index: a Legacy of the European Year 2012 for Active Ageing and Solidarity Between Generations*, European Centre (Policy Brief 4), Vienna, Austria, 2015.
- [21] European Commission, “Employment, social affairs & inclusion. statistical data,” 2020, <https://ec.europa.eu/social/main.jsp?catId=1143&intPageId=3227&langId=en>.
- [22] OECD, *Ageing and Employment Policies: Denmark 2015: Working Better with Age*, OECD Publishing, Paris, France, 2015.
- [23] The European Foundation for the Improvement of Living and Working Conditions (Eurofound), “Ageing workforce,” 2020, <https://www.eurofound.europa.eu/topic/ageing-workforce>.
- [24] P. Johnson, “The impact of ageing: the supply of labour and human capital,” in *Economic Policy for Aging Societies*, S. Horst, Ed., Springer, Berlin, Germany, 2002.
- [25] S. Dixon, “Implications of population ageing for the labor market,” *Labour Market Trends*, vol. 111, no. 2, pp. 67–76, 2003.
- [26] R. Guest and K. Shacklock, “The impending shift to an older mix of workers: perspectives from the management and economics literatures,” *International Journal of Organisational Behaviour*, vol. 10, no. 3, pp. 713–728, 2005.
- [27] J. Feyrer, “Aggregate evidence on the link between age structure and productivity,” *Population and Development Review*, vol. 34, pp. 78–99, 2008.
- [28] A. E. Von Gaessler and T. Ziesemer, “Optimal education in times of ageing: the dependency ratio in the Uzawa-Lucas growth model,” *The Journal of the Economics of Ageing*, vol. 7, pp. 125–142, 2016.
- [29] A. Börsch-Supan and M. Weiss, “Productivity and age: evidence from work teams at the assembly line,” *Journal of the Economics of Ageing*, vol. 7, pp. 30–42, 2016.
- [30] B. F. Jones, “Age and great invention,” *The Review of Economics and Statistics*, vol. 92, no. 1, pp. 1–14, 2010.
- [31] Y. Aksoy, H. S. Basso, T. Grasl, and R. P. Smith, *Demographic Structure and Macroeconomic Trends*, Banco de Espana Birkbeck Working Papers in Economics and Finance 1501, Madrid, Spain, 2015.
- [32] P. A. Balland and R. Boschma, “Mapping the potentials of regions in europe to contribute to new knowledge production in industry 4.0 technologies,” *Regional Studies*, vol. 55, pp. 1–15, 2021.
- [33] E. Forsythe, L. B. Kahn, F. Lange, and D. Wiczer, “Labor demand in the time of COVID-19: evidence from vacancy postings and ui claims,” *Journal of Public Economics*, vol. 189, Article ID 104238, 2020.
- [34] N. Innocenti, D. Vignoli, and L. Lazzeretti, “Economic complexity and fertility: insights from a low fertility country,” *Regional Studies*, vol. 55, pp. 1–15, 2021.
- [35] European Commission, “Eurostat, database,” 2020, <https://ec.europa.eu/eurostat/data/database>.
- [36] G. G. Noja and M. Cristea, “Working conditions and flexicurity measures as key drivers of economic growth: empirical evidence for europe,” *Ekonomický Časopis*, vol. 66, no. 7, pp. 719–749, 2018.
- [37] V. Kufenko, K. Prettnner, and A. Sousa-Poza, “The economics of ageing and inequality: introduction to the special issue,” *Journal of the Economics of Ageing*, vol. 14, pp. 1–4, 2019.
- [38] C. M. Barbu and S. Ponea, “Professional motivation and satisfaction. case study at Prexi com ltd,” *Journal of Advanced Research in Management*, vol. 10, no. 2, pp. 85–97, 2019.

## Research Article

# A Novel Approach to Improving E-Government Performance from Budget Challenges in Complex Financial Systems

Enkeleda Lulaj <sup>1</sup>, Ismat Zarin <sup>2</sup> and Shawkat Rahman <sup>3</sup>

<sup>1</sup>Faculty of Management in Tourism, Hospitality and Environment, “Haxhi Zeka” University, Eliot Engel 30.000, Peja, Kosovo

<sup>2</sup>Department of English, University of Asia Pacific, Dhaka, Bangladesh

<sup>3</sup>School of Business, University of Liberal Arts, Dhaka, Bangladesh

Correspondence should be addressed to Ismat Zarin; [ismatzarin@uap-bd.edu](mailto:ismatzarin@uap-bd.edu)

Received 27 October 2021; Revised 26 November 2021; Accepted 29 November 2021; Published 4 January 2022

Academic Editor: S.S. Askar

Copyright © 2022 Enkeleda Lulaj et al. This is an open access article distributed under the Creative Commons Attribution License, which permits unrestricted use, distribution, and reproduction in any medium, provided the original work is properly cited.

Today, the risk management of budget challenges throughout the budget process is greater than ever. The process of change has been driven by new information and communication technologies, resulting in e-government. The purpose of this scientific paper is to see whether budgetary challenges have an effect on the performance of e-government in complex financial systems based on factors F1, F2, F3, F4, and F5: lack of information, lack of cooperation, lack of resources and reduction of focus, lack of budget experts and financial stability, and shortcomings and inconsistencies during the budget process. Therefore, this study aims to advance the understanding of how to manage risks from budgetary challenges by focusing on a novel approach to improve e-government performance in complex financial systems. Empirical research was based on three key issues: an approach to e-government, analyzing which variables need more attention to risk, and learning how to meet budgetary challenges to improve performance during governance. For this study, the data were conducted by Kosovo’s public institutions, more specifically at the central level (Ministry of Finance) and at the local level (38 municipalities of Kosovo). A total of 38 questionnaires were analyzed and divided into three sessions, which were analyzed through three analyses, such as factor analysis, data reliability analysis, and multiple regression analysis, using SPSS version 23.0 for Windows. The research was conducted over the years 2017, 2018, 2019, and 2020, while the analysis involved several processes, where some of the factors were removed in order to make the model acceptable. In this case, 21 variables were tested and divided into 5 factors. The results showed that special attention should be paid to these factors to reduce budgetary challenges and increase the performance of e-government in complex financial systems, such as (a) lack of resources (staff, funds, infrastructure, tools, etc.), (b) increasing the focus on risk management even after the transfer of funds from the ministry to the municipality, (c) the selection of programs based on priorities and not on the basis of wishes and policies, (d) having political stability, rule of law, and more control, and (e) having regulations and guidelines from the practices of developed countries as well as taking into account the opinions of budget experts. The implications of this paper have to do with only a considerable number of variables, which were taken in the study as well as only in the municipalities of Kosovo. In this case, for other analyses by other researchers, other variables can be analyzed in other countries by making comparisons.

## 1. Introduction

Risk management is becoming a more and more important tool for budget cuts. Therefore, budget cuts not only reduce the level of resources available to carry out the mission of institutions but also create uncertainty by undermining the ability of institutions to make sound decisions. Effects on institutions include the retirement of key people or budget experts and investments based on judgements and projects,

not priorities. Hence, risk management is essential so that unintended events do not occur [1]. Public finances are a historical category, the consideration of which is placed within analytical frameworks based on efficiency, effectiveness, equity, and economy. According to [2], risk management is a requirement of organizations to meet and exceed financial expectations. The performance of an institution requires in some way the acceptance of risks, but if it takes a risky strategy, it will send the institution into failure. Each

institution faces different types of risks, internal, external, and strategic. This approach is based on the new successful framework supported by the Financial Reporting Council [3]. The budget has been talked about since the time of human existence until now. At every stage, the importance and role of the budget and public money have influenced financial reforms, whether increasing or decreasing performance during budget governance. So, during the interest in the public budget by budget policymakers, there is a need to know many budget theories and analyses, which help to better see the challenges during the budget process and to find the best results for evaluating and improving budget performance in the complex financial systems [4]. The need for effective risk management in government institutions, whether central or local, and the consequences of a failure to adequately address risk are becoming increasingly apparent [5]. The Kosovo budget is prepared by the Ministry of Finance (MoF) in coordination with budget organizations and is approved at the end of the year by the Kosovo Assembly. The budget for next year is prepared in the current year through a chain action known as the budgetary process. Until getting a final form as a draft bill for budget and before presentation for approval in the Parliament, the budget process usually is placed between the Ministry of Finance and budget organizations. The latter conform to instructions from the Ministry of Finance and send their proposals for budget according to the plans and objectives set with the work plan. According to the Law on Public Financial Management and Accountability, "budgetary organization means an authority or public enterprise that directly receives an appropriation." In the process of drafting the budget, the Ministry of Finance and budget organizations act between them in two directions: bottom-up: when budgetary organizations have the freedom of the design of costs and budget requirements depending on their plans; top-down: when budget organizations were allocated a budget taking into account the budget and expenditures of the organization during the previous year, not taking into account the needs for the budget of organizations. As in many countries, Kosovo applies a mixed form of both directions, meaning that budgetary organizations prepare or propose their budget for expenditure during one year (bottom-up direction) but also are limited in this preparation as a result of a budgetary ceiling as recognized in this field (top-down direction) [6]. Analysis of risk management activities and budget cycles reveal that budgeting generally serves as a facilitator and catalyst for risk and disaster management in government institutions [7]. According to [8], in order to avoid the risk in the local budget, they analyzed the participation of citizens in the budget process. Therefore, in order to have fewer budget challenges, it is recommended to increase the number of citizens and advisory committees during the budget process. The classical analysis is often based on combining probability and impact, either using a probability-impact diagram or multiplying both terms to obtain what is called risk critique [9]. Moreover, when risks to budgetary challenges are modeled as independent, it is impossible to properly assess the consequences of indirect complexity on institutions [10]. The local government risk assessment system can provide

signaling guidance and policy references for finance to anticipate the risks of budgetary challenges, to regulate the priority order of debt repayment within the relevant directorates at both levels of government, to optimize the structure of fiscal revenues and expenditures, and so on [11]. A challenge to be considered, according to [12], is local government debt as a major problem in China's financial operations for a long time, and it has also become a key problem that seriously affects the financial risk of governments in any country. The construction of the local government debt risk assessment system should be based on the analysis of the government debt situation, and the risk assessment results should reflect the level of local government debt risk and help the local government to find and resolve risks in a timely manner [13]. According to [14], it is concluded that e-government directly affects the participation of citizens in budget documents and indirectly affects the increase of control, transparency, and accountability. International organizations such as the World Bank and the United Nations define e-government as the adoption and integration of information technologies (Internet, computer, telephone, and other useful networks) within government institutions, transforming relationships with their various clients (citizens, businesses, other government agencies, etc.) [15]. According to [16], the use of machine learning algorithms in complex government decision-making was analyzed, so it is emphasized that decision-makers need to update policies and legislation to ensure whether decisions need to be reapproved. Systematic financial risk is an important challenge in the economy and financial systems that must be managed in order to avoid unforeseen occurrences [17]. According to [18], potential risks in structured financial networks were analyzed through the use of network analysis and machine algorithms. They stressed that this model helps policymakers and investors to use the financial network as a useful tool to improve portfolio selection as risk-free as possible. The model based on sociopolitical development known as the model of maturity is also important in e-government [19]. To manage the risk to prevent budgetary challenges, the e-government framework is important, which describes complex relationships at different stages such as information, communication, transactions, integrations, and participation in e-government. As government evolves through these stages, data collection and privacy risks increase for all types of e-governments. The types of risks from e-government are government that provides services to citizens, government that provides services to individuals as policymakers, government that provides services to businesses, government that provides services to employees, and so on [20]. According to [21], they reported that Asia-Pacific Governments are only in the early stages of adopting technology and communication to improve information and financial reporting, improve government distribution service, improve communication with citizens, and serve as a catalyst for empowering citizens to interact with the government. Therefore, in their paper, they found that the step has been slower in the public sector than in the private sector. Also included are innovative e-government trends, issues, and practices, as well as challenges and opportunities for

e-government development [22]. E-government initiatives are widespread and constitute an important part of the government investment portfolio in almost all countries of the world [23]. In general, the various descriptive models represent linear progress of stages to increase knowledge about risk management through e-government [24]. The use of information and communication technology in public administration is often presented as a multifaceted reform with strong transformative potential to prevent risks from budgetary challenges [25]. E-government during the budget process has been a hot topic in the public administration research community for some time [26]. The literature reports experiences with e-government initiatives during the budget process as chaotic and uncontrollable, despite numerous recent initiatives at various levels of government and academic and practical conferences on e-government [27]. Good e-governance during the budget process refers to the management of public resources by governing authorities [28]. While democratic online engagement is a slowly evolving process, initial steps are being taken by governments that enable e-participation to shape democratic reform [29]. Extensive use of e-government during the budget process can increase government transparency through citizen participation in documents published on institutions' websites. However, beyond this, e-government can be dysfunctional if operational capacity is reduced during the budget process leading to budgetary challenges, in which case there is a need to develop theories, models, and training to help institutions address this challenge [30]. According to [31], in development policy circles, corruption has become an urgent global issue. However, the contemporary relationship between corruption and development is complex and affects budgetary challenges [32]. The disappointing performance of conventional public sector reforms during the budget process in developing countries has led to the emergence of "new" approaches seeking to overcome traditional bureaucratic barriers to change: leadership-focused interventions such as the African Governance Initiative (AGI); accountability-focused initiatives such as the Open Government Partnership (OGP); and adaptation-focused models such as those of the African Power and Politics (APP). Beyond new implementation tactics, however, there is a need for new strategies to manage the risk of budgetary challenges [33]. Does democratization mean faster growth, less corruption, and less inefficiency? Past studies provide unclear results on the effects of democracy on budget performance and economic growth [34]. A more direct relationship between citizens and policymakers in e-government will promote democracy and accountability during the budget process [35]. Data openness has been praised for improving transparency and providing a window into government functioning. Although this relationship is intuitively obvious, it is in fact complex and simply opening the data may not bring transparency during the budget process but may bring new budget challenges [36]. According to [37], they aimed to illustrate the role of e-government in modern management by researching some developed and some developing countries, so the findings show that there is an increase in e-government in developing countries. However, whether e-government will undoubtedly

lead to a more transparent, interactive, open, and consequently accountable government remains a central issue. As the overall levels of accountability increase, the accountability gap between different national bureaucracies often remains intact as web-based technologies typically maintain or reinforce existing practices [38]. Fiscal transparency and citizen participation in budgeting processes are widely promoted as tools towards the goals of accountability and democratic response in the distribution and use of public funds [39]. Financial responsibilities, openness, and transparency initiatives aim to make government controlled by citizens [40]. Some international research has highlighted the consequences of corruption in public services, which affects another budgetary challenge [41]. International construction is complex and involves high risks. However, with the development of technological innovation, Building Information Modeling (BIM) emerged and seemed to be able to address some risks. Understanding BIM applications in international construction risk management requires a more advanced review by governing institutions during the budget process [42]. Compared to traditional e-government, the government has taken a qualitative step in the degree of control automation, service and decision-making intelligence, remote support capability, and the spatial-temporal extent that government can control. Finally, through testing, the government case management system has good stability; there is no overload and delay when many users enter the system, so the speed of response and efficiency of the system essentially meet the requirements of citizens to review the public budget and other financial-budget reports [43]. But in developing countries, financial management and risk assessment skills are insufficient to adapt to the rapidly evolving new environment [44]. E-government provides an opportunity for citizens to have access to budget documents, but not all institutions have published reports and budget documents, which is mismanagement and a budget challenge that needs to be improved [45]. The feedback system and the neighborhood effect are the essential elements that influence the e-government response during the budget cycle [46]. Equal treatment of all citizens is one of the basic principles of good administrative practice. However, there are a growing number of media and scientific reports on unequal treatment by the public administration. Therefore, through a survey conducted with citizens, it turns out that there is discrimination and unequal treatment by government institutions in the unfair distribution of budget projects according to priorities, but the projects are divided based on political beliefs. Governing institutions through e-government need to manage risks from various budgetary challenges by bringing approaches to improve performance in complex financial systems.

Figures 1 and 2 show the e-government chains during the budget process at both levels (central and local). The financial reporting chain at the central level during the budget process starts from the bottom-up, e.g., The Minister of Finance reports to the Government. The Government reports to the Assembly of Kosovo. However, the Assembly reports to the citizens on the performance during the e-government. Again the financial reporting chain during the budget process at the



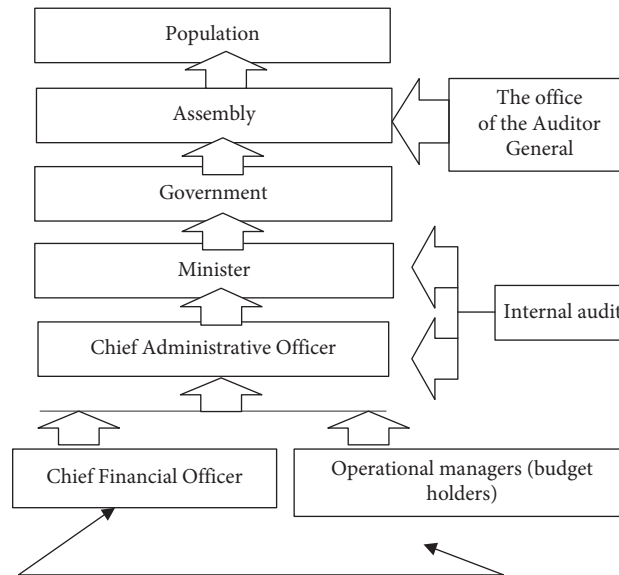


FIGURE 1: The chain of e-government during the budget process at the central level.

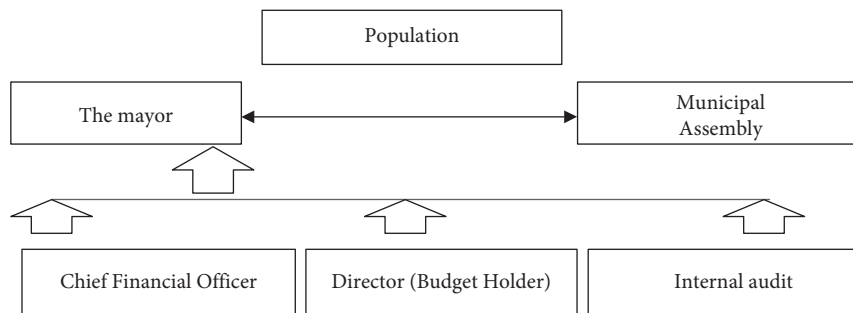


FIGURE 2: The chain of e-government during the budget process at the local level.

local level starts from the bottom-up, for example, internal auditor, finance director, and financial officer, and they report to the Mayor. The Mayor together with the Municipal Assembly reports to the citizens. If there is transparency in financial-budget reporting, then the budget challenges will be smaller, and at the same time, the performance of the Municipality in complex financial systems will increase.

## 2. Methods and Materials

**2.1. The Purpose of the Paper.** A research on a new approach to improving e-government performance from budget challenges to complex financial systems in all Kosovo municipalities has not been conducted earlier; therefore, the purpose of this scientific paper is to see if budgetary challenges have an effect on the performance of e-government in complex financial systems based on factors F1, F2, F3, F4, and F5, lack of information, lack of cooperation, lack of resources and reduction of focus, lack of budget experts and financial stability, and shortcomings and inconsistencies during the budget process. Through this goal, based on the factors taken in the study, the hypotheses will be validated. Therefore, this research will (a) bring an approach to e-government, (b) analyze how to manage risk from budget

challenges, in which variables need more attention to risks, and (c) learn something special about how to meet budget challenges to improve e-government performance in complex financial systems.

**2.2. Methods.** For this study, data were collected from public institutions in the State of Kosovo, more specifically at the central level (Ministry of Finance) and at the local level (38 municipalities of Kosovo). So, the State of Kosovo has 38 municipalities, and the questionnaire was conducted in all municipalities through primary data (questionnaire conducted with mayors, budget directors, financial-budget officials, and treasury officials). All municipalities expressed their willingness to cooperate, and the sample was statistically verified through secondary data (financial-budget reports) and control of each website of Kosovo municipalities looking at the performance of e-government in complex financial systems. A total of 38 questionnaires were analyzed and divided into three sessions, which were analyzed through three analyses, such as factor analysis, data reliability analysis, and multiple regression analysis, using SPSS version 23.0 for Windows. The research was conducted over the years 2017, 2018, 2019, and 2020. The analysis involved

several processes where some of the factors were deleted in order to make the model acceptable, in which case, as stated in the conceptual model, the purpose of these analyses is to obtain reliable data (KMO over the value 0.600, Alpha over the value 0.700, and  $R^2$  over the value 0.800). In this case, 21 variables were tested, which were divided into 5 factors.

**2.2.1. Instrument.** As stated in the introduction, the main purpose and objective of this research is to find an approach to improve e-governance in the complex financial system through risk management from budget challenges. Are these factors related to each other and do they affect the performance of institutions? Based on these issues, the findings from the econometric models will provide recommendations for Kosovo's institutions.

**2.2.2. Data Collection.** Data collection was performed from the results of factorial analysis and reliability analysis (KMO, Bartlett test, Sig., Alpha, etc.) as well as regression analysis ( $R$ ,  $R^2$ , Adjusted  $R^2$ , Std. error of the estimate, F, Sig. F, Durbin-Watson, and ANOCA), which assessed the budget challenges in Kosovo's institutions.

**2.2.3. Data Analysis.** Research data related to risk management from budget challenges were analyzed through the three analyses mentioned previously.

Hypotheses:

$H_0$ : budget challenges do not have a negative effect on e-government performance in complex financial systems.

$H_A$ : budget challenges have a negative effect on e-government performance in complex financial systems

$$\beta_0 + \beta_1 (F1) + \beta_2 (F2) + \beta_3 (F3) + \beta_4 (F4) + \beta_5 (F5) + \mu \quad (1)$$

Factors:

Factor 1 (F1): lack of accurate information and ineffective decision-making for risk management during the budget process as a budget challenge to improving e-government performance in the complex financial system.

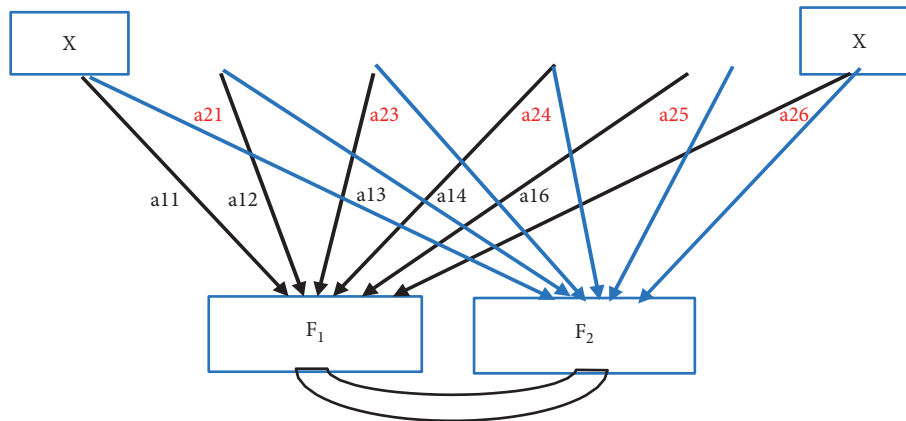
Factor 2 (F2): lack of cooperation for risk management during the budget process as a budget challenge to improving e-government performance in the complex financial system.

Factor 3 (F3): lack of resources and reduction of focus (cooperation) for risk management during the budget process as a budget challenge to improving e-government performance in the complex financial system.

Factor 4 (F4): lack of budget experts and stability for risk management during the budget process as a budget challenge to improving e-government performance in the complex financial system.

Factor 5 (F5): shortcomings and inconsistencies during the budget process as a budget challenge to improving e-government performance in the complex financial system.

**2.3. Materials.** Analyses are factorial analysis, reliability analysis, and multiple regression analysis.



From original  $n$ -variables  $x_1, x_2, x_3, \dots, x_k$ ,  $k$  new variables  $F_1, F_2, \dots, F_k$  were obtained:

$$\begin{aligned} F_1 &= \alpha_{11}x_1 + \alpha_{12}x_2 + \alpha_{1k}x_k, \\ F_2 &= \alpha_{21}x_1 + \alpha_{22}x_2 + \alpha_{2k}x_k, \\ F_k &= \alpha_{k1}x_1 + \alpha_{k2}x_2 + \alpha_{kk}x_k, \end{aligned} \quad (2)$$

where  $F1$  indicates as much variance as possible to the budgetary budget challenges and  $F2$  indicates the remaining variance, using  $k$  for each of the predictor variables on how to manage risk from budget challenges for  $x_1, x_2$ , and  $x_3$ , for each level ( $n$ ). Then,  $X_{ij}$  represents levels  $i$  and  $j$  for the predicted variables of  $X_j$ . Observations  $Y_1, Y_2, \dots, Y_n$ , for each  $n$  level are presented through the following equation to e-government in complex financial systems:

$$\begin{aligned}
Y_1 &= \beta_0 + \beta_1 x_{11} + \beta_2 x_{12} \cdots + \beta_k x_{1k} + \mu_1, \\
Y_2 &= \beta_0 + \beta_1 x_{21} + \beta_2 x_{22} \cdots + \beta_k x_{2k} + \mu_2, \\
Y_i &= \beta_0 + \beta_1 x_{i1} + \beta_2 x_{i2} \cdots + \beta_k x_{ik} + \mu_i, \\
Y_n &= \beta_0 + \beta_1 x_{n1} + \beta_2 x_{n2} \cdots + \beta_k x_{nk} + \mu_n.
\end{aligned} \tag{3}$$

The system of equations  $n$  presented above is represented by the matrix symbol, as in the following equation risk management from budget challenges [47]:

$$Y = x\beta + \mu,$$

$$Y = \begin{bmatrix} Y_1 \\ Y_2 \\ Y_3 \\ \cdot \\ \cdot \\ Y_n \end{bmatrix} x = \begin{bmatrix} 1 & x_{11} & x_{12} & \cdots & x_{1n} \\ 1 & x_{21} & x_{22} & \cdots & x_{2n} \\ 1 & x_{31} & x_{32} & \cdots & x_{3n} \\ \cdot & \cdot & \cdot & \cdots & \cdot \\ \cdot & \cdot & \cdot & \cdots & \cdot \\ 1 & x_{n1} & x_{n2} & \cdots & x_{nm} \end{bmatrix} \beta = \begin{bmatrix} \beta_1 \\ \beta_2 \\ \beta_3 \\ \cdot \\ \cdot \\ \beta_n \end{bmatrix} \mu = \begin{bmatrix} \mu_1 \\ \mu_2 \\ \mu_3 \\ \cdot \\ \cdot \\ \mu_n \end{bmatrix}. \tag{4}$$

The mathematical equation explains the division of analysis factors into 6 factors, where each of these factors has of great importance in managing the risk of budgetary challenges to bring performance to governing institutions.

### 3. Result and Discussion

In this research, as discussed in the methodology, three econometric analyses are included: factorial analysis, data reliability analysis, and multiple regression analysis.

**3.1. Results from Factorial Analysis and Reliability Analysis.** Through data processing from 21 variables, five factors (F1, F2, F3, F4, and F5) and their subfactors were obtained as follows:

**Factor 1 (F1):** lack of accurate information and ineffective decision-making for risk management during the budget process as a budget challenge to improving e-government performance in the complex financial system.

#### 3.1.1. Variables

**Subfactor F1.1.** Unrealistic and inaccurate information:

- (i) Q1. Do unclear policy budgeting programs for public expenditures and revenues make it difficult to determine budget performance? (Q1F1.1).
- (ii) Q2. The lack of accurate and timely data in monthly, quarterly, semiannual, and annual reports to serve as input during the budget process has reduced the performance (Q2F1.1).
- (iii) Q3. Poor performance stems from ineffective decision-making from planning to budget implementation as well as to inadequate financing of operations, poor control, unpredictable expenditures, and so on (Q3F1.1).

- (iv) Q4. Financial reforms are unsustainable and political (Q4F1.1).

**Subfactor F1.2.** Ineffective decision-making during the budget process:

- (i) Q5. Lack of resources (staff, funds, infrastructure, tools, etc.) a challenge to pay attention to? (Q5F1.2).
- (ii) Q6. Poor management and inefficient decision-making during the budget process affect performance (Q6F1.2).
- (iii) Q7. Providing unrealistic and inaccurate information during the budget process is a challenge that affects performance (Q7F1.2).

**Factor 2 (F2):** lack of cooperation for risk management during the budget process as a budget challenge to improving e-government performance in the complex financial system.

#### 3.1.2. Variables

**Subfactor F2.1.** Lack of cooperation during the budget process:

- (i) Q12. Discrepancies between the local budget of the respective directorates make it difficult to assess budget performance (Q12F2.1).
- (ii) Q10. If there is no budget performance, there will be consequences for programs, intensive monitoring, budget reduction, and so on (Q10F2.1).
- (iii) Q14. Are risk management austerity measures applied in case of budget challenges? (Q14F2.1).
- (iv) Q19. Poor performance results from ineffective decision-making throughout the budget process regarding inadequate financing of operations, poor control, unpredictable expenditures, and so on (Q19F2.1).
- (v) Q20. After the budget is allowed by the Ministry for the Municipality, does the focus decrease on increasing performance and transparency during governance? (Q20F2.1).

**Subfactor F2.2.** Lack of supervision:

- (i) Q18. Lack of oversight during the budget process affects inefficiency in public revenues and expenditures (Q18F2.2).

**Factor 3 (F3):** lack of resources and reduction of focus (cooperation) for risk management during the budget process as a budget challenge to improving e-government performance in the complex financial system.

#### 3.1.3. Variables

**Subfactor F3.1.** Lack of resources and reduction of focus (collaboration) during the budget process:

- (i) Q11. Risk of reduction performance due to lack of resources and poor cooperation (Q11F3.1).
- (ii) Q6. Poor management and inefficient decision-making during the budget process affect performance (Q6F3.1).
- (iii) Q12. Discrepancies between the local budget of the respective directorates make it difficult to assess budget performance (Q12F3.1).
- (iv) Q8. After the budget is allowed by the Municipality for the Directorate, does the focus decrease on increasing performance and transparency during governance? (Q8F3.1).
- (v) Q9. The selection of funding programs based on bias rather than priorities has reduced performance and transparency (Q9F3.1).

**Factor 4 (F4):** lack of budget experts and stability for risk management during the budget process as a budget challenge to improving e-government performance in the complex financial system.

*Subfactor F4.1.* Budget experts and stability for risk management.

#### 3.1.4. Variables

- (i) Q15. Qualified budget staff affects the increase of budget performance. Is the number of qualified employees dedicated to the budget sufficient? (Q15F4.1).
- (ii) Q13. The lack of positive government results in budget and grant management has reduced performance (Q13F4.1).
- (iii) Q16. Does accountability, political stability, effectiveness, rule of law, and control affect budget performance during governance? (Q16F4.1).

**Factor 5 (F5):** shortcomings and inconsistencies during the budget process as a budget challenge to improving e-government performance in the complex financial system.

*Subfactor F5.1.* Shortcomings and inconsistencies.

#### 3.1.5. Variables

- (i) Q7. Providing unrealistic and inaccurate information during the budget process is a challenge that affects performance (Q7F5.1).
- (ii) Q17. Discrepancies between the central and local budgets (expenditures, revenues) make it difficult to assess the performance (Q17F5.1).
- (iii) Q21. Lack of regulations, guidelines, funds, budgetary practices has reduced performance during governance (Q21F5.1).

The first factor (F1) has contributed to OECD [48], which made analysis in the countries that are members of the OECD regarding how information is used in budget

decision-making. So according to the findings, it was emphasized that most countries are engaged in providing information to inform and not determining budget allocation, and nonuse of information is the lack of a method to integrate it in the budget process. The second factor (F2) has contributed to OECD [49], which pointed out cooperation during the budget process is an active approach that can help the budget process by creating better budget documents and that will increase performance. The third factor (F3) has contributed to OECD [50], which stressed that governments continue to “provide” services although it is clear to the population or service users that they lack the means to do so and, as a result, coverage is dependent and the quality of services is poor. Therefore, this overexpansion of human and financial resources is one of the main causes of government failure in developing countries. The fourth factor (F4) has contributed to OECD [51], which stressed that it should increase the performance in EU countries for the functioning of the budget through public accountability as well as through increasing confidence in the allocation of budget funds. Regarding the fifth factor (F5), government budgets are based on revenue and expenditure forecasts. These forecasts are subject to stochastic error and strategic manipulation during governance. According to [52], in their analysis, they pointed out that circumstantial evidence in the budget literature and popular media suggests that government officials routinely circumvent budget-based forecasts. In the countries in which they analyzed budgets, they were systematically pessimistic, revenues were underestimated, and expenditures were overestimated.

Table 1 shows data from the KMO test for factors F1, F2, F3, F4, and F5 (0.719, 0.718, 0.801, 0.815, and 0.754 > 0.50, Sig. 0.000) and also data from Alpha coefficients (0.854, 0.820, 0.815, 0.887, and 0.867  $\leq \alpha \leq 1.00$ ). The first factor (F1) includes two subfactors (F1.1 and F1.2). In the first factor, the subfactor Q1F1 has the highest value Q1F1 = 0.893 (Do unclear policy budgeting programs for public expenditures and revenues make it difficult to determine budget performance), while the subfactor Q4F1 has the lowest value Q4F1 = 0.642 (Financial reforms are unsustainable and political). The second factor (F2) includes two subfactors (F2.1 and F2.2). In the second factor, the subfactor Q12F2.1 has the highest value Q12F2.1 = 0.909 (Discrepancies between the local budget of the respective directorates make it difficult to assess budget performance), while the subfactor Q20F2.1 has the lowest value Q20F2.1 (After the budget is allowed by the Ministry for the Municipality, does the focus decrease on increasing performance and transparency during governance). The third factor (F3) includes a subfactor. The subfactor Q11F3.1 has the highest value Q11F3.1 = 0.813 (Risk of reduction performance due to lack of resources and poor cooperation), while the subfactor Q9F3.1 has the lowest value Q9F3.1 = 0.698 (The selection of funding programs based on bias rather than priorities has reduced performance and transparency). The fourth factor (F4) includes a subfactor. The subfactor Q15F4.1 has the highest value Q15F4.1 = 0.856 (Qualified budget staff affects the increase of budget performance. Is the number of qualified employees dedicated to the budget sufficient?),



TABLE 1: Continued.

KMO and Bartlett's test		Factor analysis		Rotated component matrix	Reliability analysis
		Factor 3		Subfactor 3.1	Cronbach's alpha
Denominations	Results	Lack of resources and reduction of focus (cooperation) for risk management during the budget process as a budget challenge to improving of e-government performance in the complex financial system		Lack of resources and reduction of focus (collaboration) during the budget process	Results
KMO	<b>0.801</b>	Var	<b>Q11F3.1</b>	<b>0.813</b>	<b>0.815</b>
Bartlett's test	<b>63.727</b>	Var	<b>Q6F3.1</b>	<b>0.809</b>	
		Var	<b>Q12F3.1</b>	<b>0.752</b>	
df	<b>10</b>	Var	<b>Q8F3.1</b>	<b>0.720</b>	
Sig.	<b>0.000</b>	Var	<b>Q9F3.1</b>	<b>0.698</b>	
		Factor 4		Sub-factor 4.1	Results
Denominations	Results	Lack of budget experts and stability for risk management during the budget process as a budget challenge to improving of e-government performance in the complex financial system		Budget experts and stability for risk management	
KMO	<b>0.815</b>	Var	<b>Q15F4.1</b>	<b>0.856</b>	<b>0.887</b>
Bartlett's Test	<b>17.246</b>	Var	<b>Q13F4.1</b>	<b>0.811</b>	
		Var	<b>Q16F4.1</b>	<b>0.680</b>	
df	<b>3</b>				
Sig.	<b>0.001</b>				
		Factor 5		Subfactor 5.1	Results
Denominations	Results	Shortcomings and inconsistencies during the budget process as a budget challenge to improving of e-government performance in the complex financial system		Shortcomings and inconsistencies	
KMO	<b>0.754</b>	Var	<b>Q7F5.1</b>	<b>0.881</b>	<b>0.867</b>
Bartlett's test	<b>17.487</b>	Var	<b>Q17F5.1</b>	<b>0.781</b>	
		Var	<b>Q21F.1</b>	<b>0.652</b>	
df	<b>3</b>				
Sig.	<b>0.001</b>				

Values that are presented in bold are values that confirm the importance of the test. Example: (i) The KMO test to be accepted must have a value above 0.50. All factors have a value higher than 0.50 (data are suitable for factor analysis); (ii) Reliability analysis (alpha test must be above 0.60 to be accepted). And so on. Therefore, all the results made in bold are important and confirm the model. Those that have not been verified have been further processed through other tests or removed from the model indicating their irrelevance.

TABLE 2: Multiple regression analysis.

Multiple regression analysis										
Model	Model summary					Change statistics (ANOVA)				
	R	R <sup>2</sup>	Adj. R <sup>2</sup>	Std. error	R sq.	F	df 1	df 2	Sig.	Durbin-Watson
1	0.991	0.987	0.983	0.07517	0.987	367.736	5	28	0.000	1.209

TABLE 3: Coefficients table and proof of hypotheses.

Coefficients table							Proof of hypotheses	
		Model						
		Constant	F1	F2	F3	F4		
Unstandardized coefficient	B	<b>0.135</b>	<b>0.415</b>	<b>0.326</b>	<b>0.335</b>	<b>0.242</b>	<b>0.192</b>	$\hat{y} = \alpha_0 + \beta_1 (F1) + \beta_2 (F2) + \beta_3 (F3) + \beta_4 (F4) + \beta_5 (F5)$ $= 0.135 + 0.415x_1 + 0.326x_2 + 0.335x_3 + 0.242x_4 + 0.19x_5 + 0.01\mu$ Reliability interval 95% (Sig.2-tailed), $p \leq 0.01$ , $p$ value is less than the level of importance 5%. In this case, rejected $H_0$ and accepted $H_A$ $(\beta_1, \beta_2, \beta_3, \beta_4, \beta_5 \neq 0)$
Standardized coefficient	Beta		0.407	0.192	0.246	0.314	0.018	
t		2.175	10.182	6.764	10.972	10.078	0.070	
Sig.		<b>0.000</b>	<b>0.000</b>	<b>0.000</b>	<b>0.000</b>	<b>0.000</b>	<b>0.000</b>	
95.0% confidence interval for B	Lower bound	0.010	0.252	0.137	0.158	0.193	0.064	
	Upper bound	0.339	0.378	0.256	0.231	0.291	0.060	
Collinearity statistics	Tolerance		<b>0.335</b>	<b>0.290</b>	<b>0.547</b>	<b>0.492</b>	<b>0.236</b>	
	VIF		<b>0.983</b>	<b>0.448</b>	<b>0.830</b>	<b>0.931</b>	<b>0.630</b>	

Values written in bold are important to the model as explained in the results of this table.

while the subfactor Q16F4.1 has the lowest value  $Q16F4.1 = 0.680$  (Does accountability, political stability, effectiveness, rule of law, and control affect budget performance during governance). The fifth factor (F5) includes a subfactor. The subfactor Q7F5.1 has the highest value  $Q7F5.1 = 0.881$  (Providing unrealistic and inaccurate information during the budget process, a challenge that affects performance), while the subfactor Q21F5.1 has the lowest value  $Q21F5.1$  (Lack of regulations, guidelines, funds, and budgetary practices have reduced performance during governance). All of these factors need to be considered to manage the risk of budgetary challenges as an approach to improving e-government performance in complex financial systems. The Alpha coefficient has very high reliability for all factors (F1, F2, F3, F4, and F5), which means that the variables of these factors need to be improved as emphasized in the factor analysis.

3.2. Result from Multiple Regression Analysis. Through data processed from 21 variables for 5 factors from the two previous analyzes, the findings resulted as follows.

Table 2 shows that 99% ( $R^2 = 0.987$ , Sig. = 000, and  $F = 367.736$ ) for risk management from budget challenges depends on independent variables F1 (lack of accurate information and ineffective decision-making), F2 (lack of cooperation), F3 (lack of resources and reduction of focus), F4 (lack of budget experts), and F5 (deficiencies and inconsistencies), while 1% depends on other variables outside this model by random error. Adjusted R Sq. at a value of 0.983 indicates that 98% of the variables are related to the model, while according to the D-W test (1.209), the model is

significant and the autocorrelation is negative, which means that the standard error of the coefficient  $b$  is very small.

Table 3 shows the parameter values of the predicted model results and the  $t$  values by analyzing them for each variable at the 5% significance level. The constant in the value of 0.135 indicates that if the budget challenges during the budget process based on F1, F2, F3, F4, F5 are zero, their accuracy is 14%. If the approach to improve the performance of e-government in complex financial systems is done in accordance with independent variables, the accuracy will be 152%, which means that if the risk from budgetary challenges is managed as lack of accurate information and ineffective decision-making = 42%, lack of cooperation = 33%, lack of resources and reduction of focus = 34%, lack of budget experts = 24%, and shortcomings and inconsistencies = 19%, performance during the budget process will increase. The Beta coefficient indicates that all independent variables are significant in the model, but the most important variable is  $F1 = 42\%$ . Collinearity statistics, including tolerance values and VIF ( $0.335 = 0.983$ ,  $0.290 = 0.448$ ,  $0.547 = 0.830$ ,  $0.492 = 0.931$ , and  $0.236 = 0.630$ ), are important in the model because it does not make the problem of multiple relationships between independent variables.

Figure 3 shows that the scatterplot for the first factor (F1) includes two subfactors (F1.1 and F1.2); according to these subfactors, it is emphasized that unclear income and expenditure programs as well as unstable financial and political reforms hamper performance in complex systems financial ( $Q1F1 = 0.893$ ;  $Q4F1 = 0.642$ ).

Figure 4 shows that the scatterplot for subfactor (F1.1) includes variables Q1F1.1, Q2F1.1, Q3F1.1, and Q4F1.1; according to these variables, it is emphasized that there is a

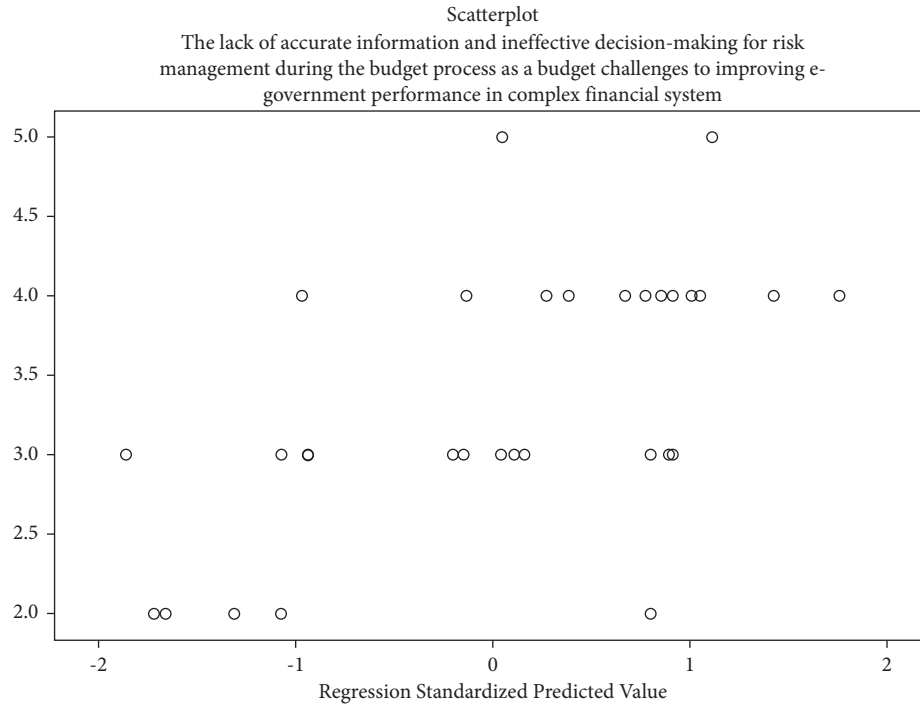


FIGURE 3: Factor 1: lack of accurate information and ineffective decision-making for risk management during the budget process as a budget challenge to improving e-government performance in the complex financial system.

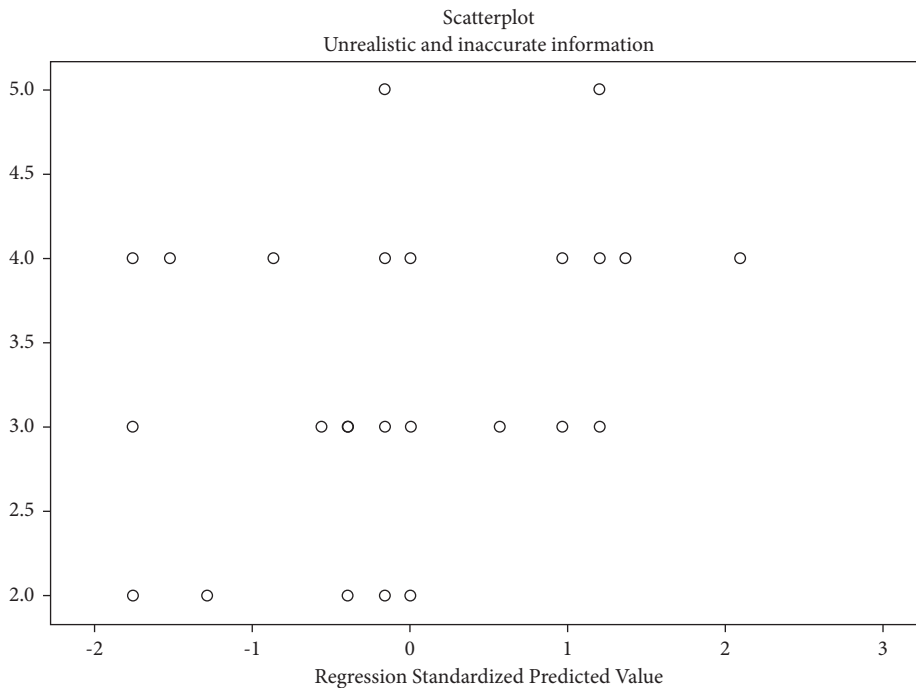


FIGURE 4: The first subfactor of the first factor: unrealistic and inaccurate information.

lack of accurate and timely data in all financial reports, there is ineffective decision-making, budget control is weak, spending is often unpredictable, and reforms are unstable and political. All of these variables need to be considered for performance in complex financial systems.

Figure 5 shows that the scatterplot for subfactor (F1.2) includes variables Q5F1.2, Q6F1.2, and Q7F1.2; according to these variables, it is emphasized that attention should be paid to the lack of resources (staff, funds, infrastructure, tools, etc.) as well as poor and inefficient management; also



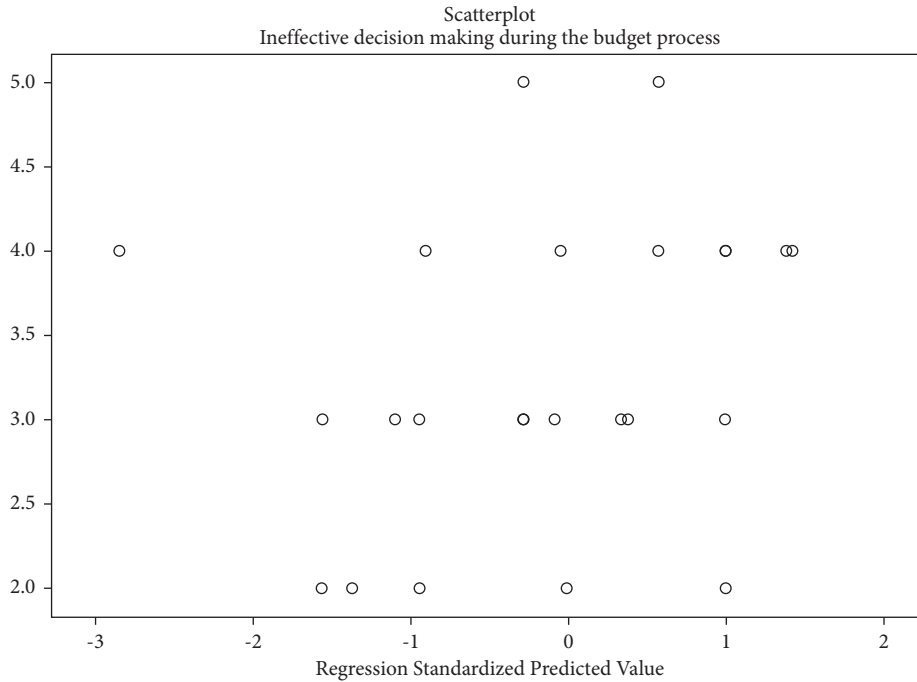


FIGURE 5: The second subfactor of the first factor: ineffective decision-making during the budget process.

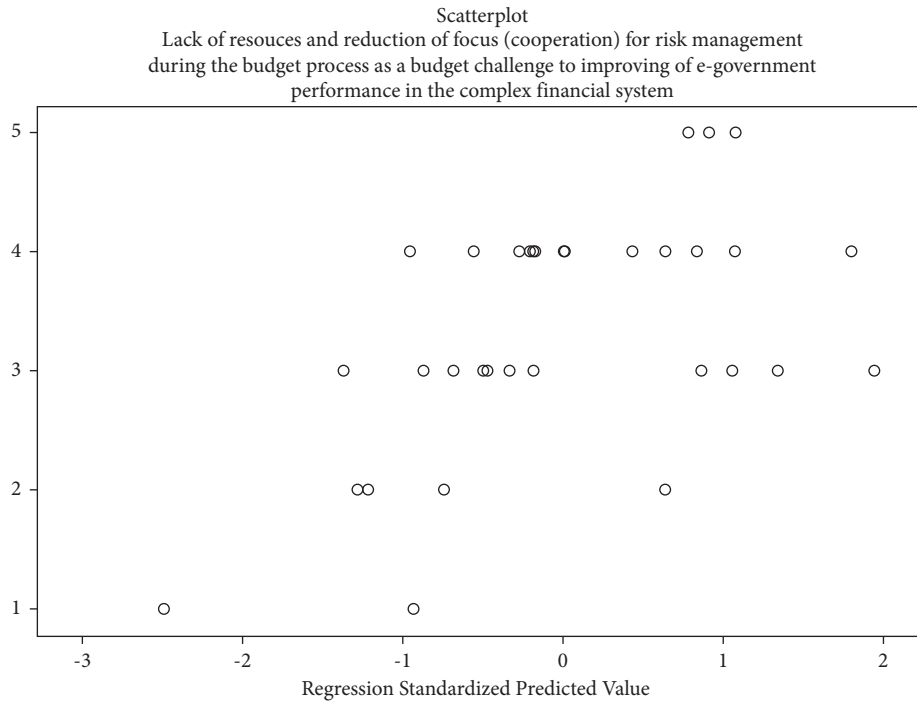


FIGURE 6: Factor 2: lack of cooperation for risk management during the budget process as a budget challenge to improving e-government performance in the complex financial system.

accurate information must be provided during the budget process. All of these variables need to be considered for performance in complex financial systems.

Figure 6 shows that the scatterplot for the second factor (F2) includes two subfactors (F2.1 and F2.2); according to these

subfactors, it is emphasized that budget inconsistencies in the relevant directorates within municipalities and the reduction of focus after the budget are transferred from the Ministry of Finance to the Municipality; they reduce performance in complex financial systems (Q12F2.1 and Q20F2.1).

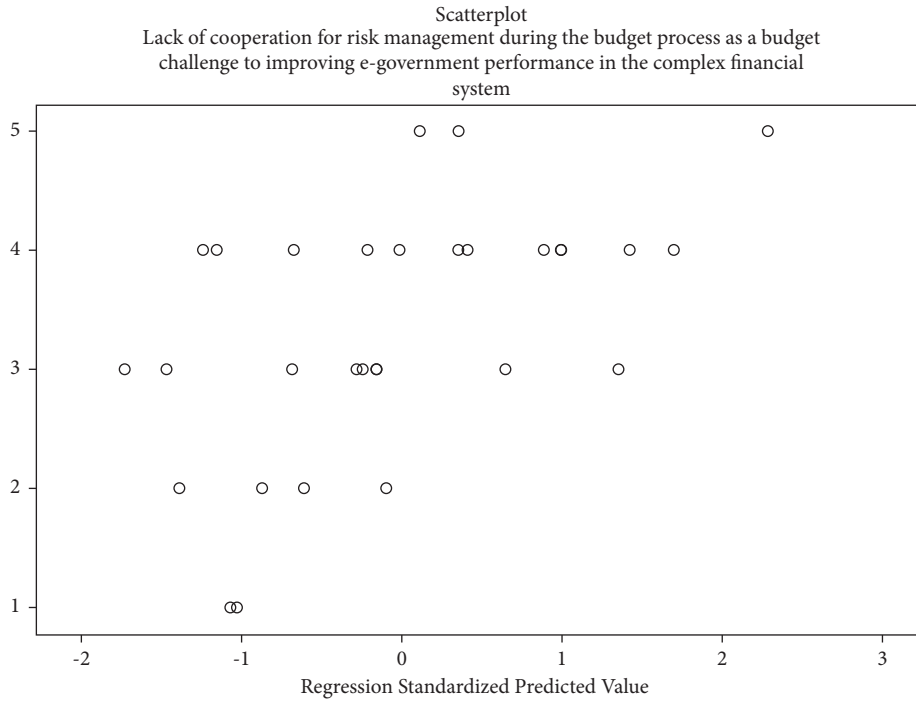


FIGURE 7: Factor 3: lack of resources and reduction of focus (cooperation) for risk management during the budget process as a budget challenge to improving e-government performance in the complex financial system.



FIGURE 8: Factor 4: lack of resources and reduction of focus (cooperation) for risk management during the budget process as a budget challenge to improving e-government performance in the complex financial system.

Figure 7 shows that the scatterplot for the third factor (F3) includes a subfactor (F3.1); according to this subfactor, it is emphasized that poor cooperation and lack of resources,

as well as the selection of programs based on preferences and not on priorities, reduce performance in complex financial systems (Q11F3.1 and Q9F3.1).

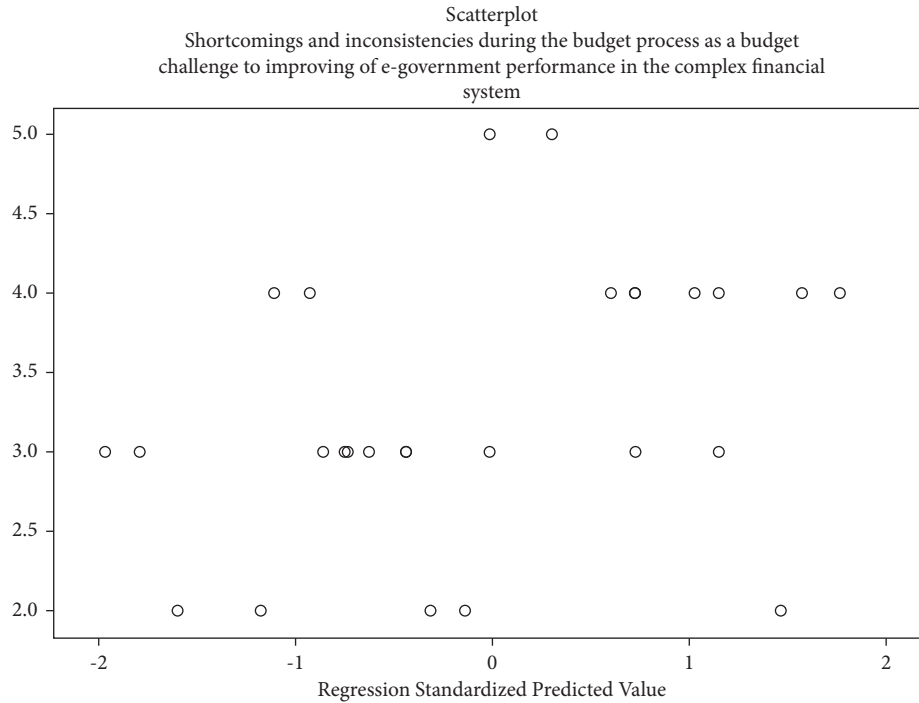


FIGURE 9: Factor 5: shortcomings and inconsistencies during the budget process as a budget challenge to improving e-government performance in the complex financial system.

Figure 8 shows that the scatterplot for the fourth factor (F4) includes a subfactor (F4.1); according to this subfactor, it is emphasized that an insufficient number of staff, poor accountability, nonpolitical stability, inefficiency, not the rule of law, and noncontrol reduce performance in complex financial systems (Q15F4.1 and Q16F4.1).

Figure 9 shows that the scatterplot for the fifth factor (F5) includes a subfactor (F5.1); according to this subfactor, it is emphasized that the lack of regulations, guidelines, practices, funds, and accurate information during the budget process reduce performance in complex financial systems (Q7F5.1 and Q21F5.1).

#### 4. Conclusion

The budget is increasingly becoming the main tool for the financial management of the country as a whole. Therefore, risk management contributes significantly to the performance of e-government in complex financial systems, especially in the case of risk management from budgetary challenges to Kosovo institutions, where the magnitude of the risk of a challenge may jeopardize the health or performance of a Municipality or Ministry. The main goals of risk management from the main challenges are fewer execution rules and more coordination and focus rules. Therefore, the results of this research are easy to understand and apply. The main originality of this research was to combine the conceptual methodology with the managerial one in order for Kosovos' institutions to benefit from their advantages through the results from factorial analysis, reliability analysis and multiple

regression analysis in Tables 1–3 and in Figures 1–9 which provide an approach to managing risk from budgetary challenges as well as to improve government performance in complex financial systems. Hence, a novel has been proposed to improve performance and decide which variables should be taken into account by local levels of government in Kosovo, such as F1, lack of information and ineffective decision-making; F2, lack of cooperation; F3, lack of resources and reduced focus; F4, lack of budget experts; F5, shortcomings and inconsistencies. In perspective, risk management skills from budget challenges bring positive value to institutions. But, other techniques, methodologies, and philosophies exist from other researches to apply the principles of e-government in complex financial systems. Given the main goals mentioned in the methodology part, which variables need to be managed more carefully to manage the risk to bring budget performance? Hence, it was concluded that the variables Q5F1, Q20F2.1, Q9F3.1, Q16F4.1, and Q21F5.1 should be improved by the institutions in Kosovo. Another perspective for e-government is the implementation of applications that help manage risks from budget challenges, as well as finally modeling the interdependence between more than two risks from budget challenges; for example, if the institution combines two risks, then these two risks may bring a third. As general recommendations for Kosovo's public institutions that have resulted from this research are as follows: (a) improve the lack of resources (staff, funds, infrastructure, tools, etc.), (b) not to reduce the focus on performance enhancement and risk management, after the budget is transferred from the ministry to the municipality, (c) the selection of programs to be funded

should not be based in prejudices but in priorities, (d) there should be political stability, rule of law, and control in order to avoid risks from budgetary challenges and increase performance, and (e) have more regulations and guidelines from the practices of developed countries, and take into account the opinions of experts budget on how to overcome challenges to e-government. The implications of this paper are that only a considerable number of variables are taken into the study and only the municipalities in Kosovo. In this case, for other analyses by other researchers, other variables can be analyzed.

## Data Availability

The data used to support and prove the findings of this study are available from the corresponding author upon request.

## Conflicts of Interest

The authors declare that there are no conflicts of interest regarding the publication of this paper.

## References

- [1] A. Halachmi and D. Greiling, "Transparency e-government and accountability: some issues and considerations," *Public Performance & Management Review*, vol. 36, no. 4, pp. 562–584, 2013.
- [2] A. Ray, "Implications of the future use of machine learning in complex government decision-making in Australia," *ANU Journal of Law and Technology*, vol. 1, no. 1, pp. 5–14, 2020.
- [3] A. Samitas, E. Kampouris, and D. Kenourgios, "Machine learning as an early warning system to predict financial crisis," *International Review of Financial Analysis*, vol. 71, Article ID 101507, 2020.
- [4] A. Savoldelli, C. Codagnone, and G. Misuraca, "Understanding the e-government paradox: learning from literature and practice on barriers to adoption," *Government Information Quarterly*, vol. 31, pp. 63–71, 2014.
- [5] B. W. Wirtz and P. Daiser, *E-government: Strategy Process Instruments*, Deutsche Universität für Verwaltungswissenschaften Speyer, Speyer, Germany, 2015.
- [6] B. W. Wirtz and P. Daiser, *E-Government: Strategy Process Instruments*, German University of Administrative Sciences Speyer, Chair for Information and Communication Management, Speyer, Germany, 2nd edition, 2017.
- [7] C. G. Wescott, "E-government in the asia-pacific region," *Asian Journal of Political Science*, vol. 9, no. 2, pp. 1–24, 2010.
- [8] D. J. Calista and J. Melitski, "E-government and e-governance: converging constructs of public sector information and communications technologies," *Public Administration Quarterly*, vol. 31, no. 1/2, pp. 87–120, 2007, <http://www.jstor.org/stable/41288283>.
- [9] K. Callahan, "The utilization and effectiveness of citizen advisory committees in the budget process of local governments," *Journal of Public Budgeting, Accounting & Financial Management*, vol. 14, no. 2, pp. 295–319, 2002.
- [10] D. P. Moynihan, "Managing for results in state government: evaluating a decade of reform," *Public Administration Review*, vol. 66, no. 1, pp. 77–89, 2006.
- [11] D. Chen, "Risk assessment of government debt based on machine learning algorithm," *Complexity*, vol. 2021, Article ID 3686692, 12 pages, 2021.
- [12] D. W. Webster and T. H. Stanton, *Improving Government Decision Making through Enterprise Risk Management*, IBM Center for the Business Government, Washington, WA, USA, 2015.
- [13] F. Marle, "An assistance to project risk management based on complex systems theory and agile project management," *Complexity*, vol. 2020, Article ID 3739129, 20 pages, 2020.
- [14] G. Abels, "Citizen involvement in public policy-making: does it improve democratic legitimacy and accountability? The case of PTA," *Interdisciplinary Information Sciences*, vol. 13, no. 1, pp. 103–116, 2007.
- [15] G. D. Bona, A. Silvestri, A. Forcina, and A. Petrillo, "Total efficient risk priority number (TERPN): a new method for risk assessment," *Journal of Risk Research*, vol. 21, no. 11, pp. 1384–1408, 2017.
- [16] G. Grant and D. Chau, "Developing a generic framework for e-government," *Journal of Global Information Management (JGIM)*, vol. 13, no. 1, p. 30, 2006.
- [17] G. Jansson, "Local values and e-government-continuity and change in public administration," *Implementing Public E-Services in Two Swedish Municipalities*, pp. 1–119, Linköping University Electronic Press, Linköping, Sweden, 2011.
- [18] G. Kou, X. Chao, Y. Peng, F. E. Alsaadi, and V. E. Herrera, "Machine learning methods for systemic risk analysis in financial sectors," *Technological and Economic Development of Economy*, vol. 25, no. 5, pp. 716–742, 2019.
- [19] H. Liu and G. Tian, "Building engineering safety risk assessment and early warning mechanism construction based on distributed machine learning algorithm," *Safety Science*, vol. 120, pp. 764–771, 2019.
- [20] H. Mohtadi and T. L. Roe, "Democracy rent seeking public spending and growth," *Journal of Public Economics*, vol. 87, no. 3–4, pp. 445–466, 2003.
- [21] G. A. Tularam and G. Attili, "Importance of Risk Analysis and Management – the Case of Australian Real Estate Market," *Risk Management - Current Issues And Challenges*, intechopen, London, UK, 2012.
- [22] J. B. Justice, J. Melitski, and D. L. Smith, "E-government as an instrument of fiscal accountability and responsiveness: do the best practitioners employ the best practices?" *The American Review of Public Administration*, vol. 36, no. 3, pp. 301–322, 2006.
- [23] J. Freeman and S. Quirke, "Understanding E-democracy government-led initiatives for democratic reform," *JeDEM-e Journal of eDemocracy and Open Government*, vol. 5, no. 2, pp. 141–154, 2013.
- [24] J. S. Hiller and F. Bélanger, *Privacy Strategies for Electronic Government*, pp. 162–198, E-government, Lanham, MD, USA, 2001.
- [25] J. Sangki, "Vision of future e-government via new e-government maturity model: based on Korea's e-government practices," *Telecommunications Policy*, vol. 42, no. 10, pp. 860–871, 2018.
- [26] J. Manzoni and S. I. Cheshire, *Management of Risk in Government*, England, 2017, <https://www.gov.uk/government/publications/management-of-risk-in-government-framework>.
- [27] K. Layne and J. Lee, "Developing fully functional E-government: a four-stage model," *Government Information Quarterly*, vol. 18, no. 2, pp. 122–136, 2001.
- [28] X. Chen and J. Si, "Design and research of a government affairs office platform," *Mobile Information Systems*, vol. 2021, Article ID 1775663, 8 pages, 2021.
- [29] E. Lulaj, "The impact and effects of financial reporting in the public accounting econometric analysis model: revenue and

- expenditures for period 2007-2017,” *European Journal of Economics and Business Studie*, vol. 5, no. 1, p. 46, 2019.
- [30] E. Lulaj, “Accounting, reforms and budget responsibilities in the financial statements,” *Finance And Taxation*, vol. 1, no. 91, pp. 61–69, 2021.
- [31] M. Bauhr, “Need or greed? Conditions for collective action against corruption,” *Governance*, vol. 30, no. 4, pp. 561–581, 2017.
- [32] M. Vintar, M. Kunstelj, M. Dečman, and B. Berčič, “Development of e-government in Slovenia,” *Information Polity*, vol. 8, no. 3, pp. 133–149, 2003.
- [33] M. Qi and J. Wang, “Using the internet of things E-government platform to optimize the administrative management mode,” *Wireless Communications and Mobile Computing*, vol. 2021, Article ID 2224957, 11 pages, 2021.
- [34] N. Charron, V. Lapuente, and P. Annoni, “Measuring quality of government in EU regions across space and time,” *Papers in Regional Science*, vol. 98, no. 5, pp. 1925–1953, 2019.
- [35] P. Yanguas and B. Bukenya, ““New” approaches confront “old” challenges in African public sector reform,” *Third World Quarterly*, vol. 37, no. 1, pp. 136–152, 2016.
- [36] Q. Qu, C. Liu, and X. Bao, “E-commerce enterprise supply chain financing risk assessment based on linked data mining and edge computing,” *Mobile Information Systems*, vol. 2021, Article ID 9938325, 9 pages, 2021.
- [37] R. L. Tampis and J. D. Urrutia, “Regression analysis of the economic factors of the gross domestic product in the Philippines,” *Journal of Fundamental and Applied Sciences*, vol. 9, pp. 190–291, 2017, <http://www.jfas.info>.
- [38] W. Wong and E. Welch, “Does e-government promote accountability? a comparative analysis of website openness and government accountability,” *Governance, Governance*, vol. 17, no. 2, pp. 275–297, 2004.
- [39] S. Grohs, C. Adam, and C. Knill, “Are some citizens more equal than others? Evidence from a field experiment,” *Public Administration Review*, vol. 76, no. 1, pp. 155–164, 2016.
- [40] V. Pina, L. Torres, and B. Acerete, “Are ICTs promoting government accountability? a comparative analysis of e-governance developments in 19 OECD countries,” *Critical Perspectives on Accounting*, vol. 18, no. 5, pp. 583–602, 2007.
- [41] S. M. William and M. Rafferty, “From development and grand corruption to governance,” *International Journal for Crime, Justice and Social Democracy*, vol. 6, no. 4, p. 12, 2017.
- [42] S. Esselimani, M. Sagsan, and S. Kiral, “E-government effect on participatory democracy in the maghreb: indirect effect and government-led participation,” *Discrete Dynamics in Nature and Society*, vol. 2021, Article ID 6642998, 13 pages, 2021.
- [43] S. Thomas, “Risk management and the dynamics of budget cuts,” in *Managing Risk and Performance*, Wiley, Hoboken, NJ, USA, 2014.
- [44] S. Tian, R. He, C. Huang, Q. Feng, and F. Jiang, “A SCI analysis model: research on influencing factors of local E-government responsiveness in China,” *Discrete Dynamics in Nature and Society*, vol. 2021, Article ID 6654354, 10 pages, 2021.
- [45] T. Wang, S. Zhao, G. Zhu, and H. Zheng, “A machine learning-based early warning system for systemic banking crises,” *Applied Economics*, vol. 53, no. 26, pp. 2974–2992, 2021.
- [46] G. Tsenguun, H. Y. Chong, P. C. Liao, and Y. D. Wu, “A bibliometric review on risk management and building information modeling for international construction,” *Advances in Civil Engineering*, vol. 2018, Article ID 8351679, 13 pages, 2018.
- [47] U. Nations, *E-government for the Future We Want*, United Nations E-Government Survey, 2014, <https://www.ipa.government.bg/>.
- [48] T. Curristine, “Performance information in the budget process: results of the OECD 2005 questionnaire,” *OECD Journal on Budgeting*, vol. 5, pp. 88–113, 2005, <https://www.oecd.org/>.
- [49] M. V. Roestel, *A collaborative approach to budgeting and the impact on the budgeting process: a case study*, Walden University, Minneapolis, Minnesota, Ph.D., 2016.
- [50] F. Fozzard, *The Basic Budgeting Problem, Approaches to Resource Allocation in the Public Sector and Their Implications for Pro-poor Budgeting*, Overseas Development Institute, London UK, 2001.
- [51] R. Downes, D. Moretti and S. Nicol, “Budgeting and performance in the European Union: a review by the OECD in the context of EU budget focused on results,” *OECD Journal on Budgeting*, vol. 17, pp. 1–60, 2017.
- [52] P. D. Larkey and R. A. Smith, “Bias in the formulation of local government budget problems,” *Policy Sciences*, vol. 22, no. 2, pp. 123–166, 1989, <http://www.jstor.org/stable/4532165>.

## Research Article

# Local Asymptotic Normality Complexity Arising in a Parametric Statistical Lévy Model

Wissem Jedidi 

Department of Statistics and OR, King Saud University, P.O. Box 2455, Riyadh 11451, Saudi Arabia

Correspondence should be addressed to Wissem Jedidi; wissem\_jedidi@yahoo.fr

Received 27 August 2021; Accepted 9 November 2021; Published 29 December 2021

Academic Editor: Ning Cai

Copyright © 2021 Wissem Jedidi. This is an open access article distributed under the Creative Commons Attribution License, which permits unrestricted use, distribution, and reproduction in any medium, provided the original work is properly cited.

We consider statistical experiments associated with a Lévy process  $X = (X_t)_{t \geq 0}$  observed along a deterministic scheme  $(iu_n, 1 \leq i \leq n)$ . We assume that under a probability  $\mathbb{P}_\theta$ , the r.v.  $X_t, t > 0$ , has a probability density function  $\varphi_\theta$ , which is regular enough relative to a parameter  $\theta \in (0, \infty)$ . We prove that the sequence of the associated statistical models has the LAN property at each  $\theta$ , and we investigate the case when  $X$  is the product of an unknown parameter  $\theta$  by another Lévy process  $Y$  with known characteristics. We illustrate the last results by the case where  $Y$  is attracted by a stable process.

## 1. Introduction

This work is a part of an ambitious program consisting in the estimation of the parameter  $\theta$  intervening in the stochastic differential equation driven by a known Lévy process  $Y$ :

$$dX_t = b(\theta, X)dt + a(\theta, X)dY_t, \quad (1)$$

These kinds of models are motivated by mathematical finance problems ([1]). In this context, the property of local asymptotic normality property (LAN) has become an important issue [2]. The LAN property is described as follows: a sequence of families of probabilities  $(\mathbb{P}_\theta^n)_{\theta \in \Theta}$  indexed by an open set  $\Theta \subset \mathbb{R}$  is said to have the LAN property at each point  $\theta_0 \in \Theta$  with speed  $\sqrt{n}$ , if the sequence of probabilities localized around  $\theta_0$ ,

$$\left(\mathbb{P}_{\theta_0 + n^{-1/2}\theta}^n\right)_{\theta \in \{(\xi / (\theta_0 + n^{-1/2})) \mid \xi \in \Theta\}}, \quad (2)$$

converges, in the sense of weak convergence of the associated likelihood processes, to a Gaussian shift  $(\mathbb{P}_\theta)_{\theta \in \mathbb{R}}$ ; see Section 2 for a precise definition. The LAN property allows to recover the so-called asymptotic Fisher information quantity  $I(\theta_0)$ . This quantity is crucial in any estimation procedure, since  $1/I(\theta_0)$  provides the lower bound of the variance of any estimator of  $\theta_0$ .

The LAN property was investigated by Akritas [3] in models associated with Lévy processes  $X$  observed continuously in time over the interval  $[0, n]$ ,  $n \rightarrow \infty$ . He obtained the property under the assumption of differentiability, according to the parameter  $\theta$ , of the characteristics  $(b_\theta, c_\theta, \nu_\theta)$  of  $X$ . With the same asymptotic, Luschgy [4] obtained the local asymptotic mixed normality (LAMN) property on models associated with semimartingales. As a notion, LAMN property is more general than the LAN because it allows the Fisher information quantity to be random. With the asymptotic  $[0, n]$ ,  $n \rightarrow \infty$ , the estimation methods do not seem to be feasible in practice, for this reason, several recent works focused on discretized schemes, i.e., observations of the process  $X$  along the discrete scheme

$$X_{iu_n}, \quad 1 \leq i \leq n, n \rightarrow \infty. \quad (3)$$

In practice, the most interesting case of the discretization path  $u_n = 1/n$  turns out to be relatively difficult. The classical case of a Brownian motion  $Y$  in (1) has been widely treated [5]. Clément and Gloter [6] studied the LAN for the model in (1), in the case where  $Y$  is a Lévy process attracted by a symmetric stable process with index  $\alpha \in (1, 2]$ . Aït-Sahalia and Jacod [7], Masuda [8], and Kawai and Masuda [9, 10]

studied LAN property for the model in (1) in case of constant coefficients, i.e.,

$$dX_t = \theta_1 dt + \theta_2 dY_t, \quad (4)$$

Our investigation goes to same direction of Aït-Sahalia and Jacod [11], who studied the LAN property and the problem of estimation of the parameter  $(\theta_1, \theta_2)$  involved in the model of a log-asset price  $X$ , solution of (3) with  $Y$  being a standard symmetric stable process with index  $\alpha \in (0, 2]$ . Section 4 completes their situation in case where  $Y$  is a general stable process, eventually mixed. The last direction was initiated Rammeh [12] with observations according to random schemes  $(T(i, n), 1 \leq i \leq n)$  for the scale model:

$$X = \theta Y, \quad (5)$$

where  $\theta$  is a real unknown real parameter, and  $Y$  is a symmetrical standard  $\alpha$ -stable process. Rammeh showed that the LAN property always occurs, and his main arguments strongly rely to the linearity in  $\theta$  to the fact that stable processes have the temporal scaling property and to the asymptotic behavior of the stable densities. Theorem 2 generalizes Rammeh's results in the context of deterministic discrete scheme  $T(i, n) = iu_n$ .

Because of the intricacy of the case (1), we first focus on the following model, which contains (5) and intercepts (1): we assume that for all  $\theta \in \Theta$ , under  $\mathbb{P}_\theta$ ,  $X$  is a Lévy process, null at  $t = 0$ , such that its Lévy exponent is given by the so-called Lévy-Khintchine formula:

$$\begin{aligned} \mathbb{E}_{\mathbb{P}_\theta} [e^{iuX_t}] &= e^{t\varphi_\theta(u)}, \quad \varphi_\theta(u) = iub_\theta - \frac{c_\theta^2 u^2}{2} \\ &+ \int_{\mathbb{R}} (e^{iuy} - 1 - iuy1_{|y| \leq 1}) \mu_\theta(dy), \end{aligned} \quad (6)$$

where  $b_\theta \in \mathbb{R}$ ,  $c_\theta \in \mathbb{R}_+$ , and  $\mu_\theta$  is a positive measure on  $\mathbb{R}$  which integrates  $\min(y^2, 1)$ .

For sake of clarity, we take  $\Theta$  is the open interval  $\mathbb{R}$ . As in the precited literature, we will assume the following.

- (i) The existence of densities  $g_t^\theta$ , such that  $\theta \mapsto g_t^\theta$  is regular enough,
- (ii) The convergence, as  $n \rightarrow \infty$ , of some integrals depending on  $g_{u_n}^\theta$ .

Theorem 1 and Corollary 1 provide conditions ensuring the LAN property for the model (6), when the process  $X$  is observed along the discrete scheme (3). Denoting  $\bar{g}_{u_n}^\theta$ , the logarithmic derivative of  $g_{u_n}^\theta$  relative to  $\theta$ , the asymptotic Fisher information quantity at each  $\theta$  should satisfy

$$I(\theta) = \lim_{n \rightarrow \infty} \int (\bar{g}_{u_n}^\theta)^2(x) g_{u_n}^\theta(x) dx \in (0, \infty). \quad (7)$$

It is difficult to find Lévy processes fulfilling (7), and the reasons are numerous, for instance, the existence of the densities  $g_t^\theta$ , the fact that they are not explicit in general, and their degeneracy as  $t \rightarrow 0$ . For these reasons, Corollary 1 focuses on the linear dependance (4) of the characteristics relative to  $\theta$ . In this case, we may assume, without loss of generality, that  $\Theta$  contains a reference value, 1 for example,

and the value 0 is excluded in order to avoid trivialities. In this case, we only need to assume some regularities of the function  $g_{u_n}^\theta(x)$  and conditions of the kind (7) for  $\theta = 1$ . Let  $h_n := g_{u_n}^1$  and  $\bar{h}_n$  be the logarithmic derivatives of  $h_n(x)$ . The asymptotic Fisher information quantity should then satisfy

$$I(\theta) = \frac{1}{\theta^2} \lim_{n \rightarrow \infty} \int (1 + x\bar{h}_n(x))^2 h_n(x) dx \in (0, \infty). \quad (8)$$

The case of the discretization with constant path  $u_n = u \in (0, \infty)$  is quite obvious since the scale model (5) becomes a regular i.i.d. one, that is, to say  $I(\theta)$  is finite and nonnull. If  $u_n \rightarrow 0$ , the situation is more intricate because  $h_n$  degenerates when  $n \rightarrow \infty$ . It turns out that even the linear model (5) is falsely simple to handle. Intuitively, one looks at special Lévy processes  $Y$  attracted by stable processes on the sense of (10). The price to pay is to exhibit refined controls on the probability density function of  $Y_t$ ,  $t > 0$ . In a second step, we restrict our attention to the scale model (5). For simplicity's sake, it is easier in this case to express the probabilities  $(\mathbb{P}_\theta)_{\theta \in \Theta}$  in the form (5) rather than considering them as solutions of martingale problems associated with the family of characteristics  $(b_\theta, c_\theta, \mu_\theta)_{\theta \in \Theta}$  because of the intricacy inherent in the truncation functions [13]. Generic examples of Lévy processes are stable processes. They characterized Lévy exponent as follows. Let  $(\alpha, \beta, \gamma, \delta) \in A = (0, 2] \times [-1, 1] \times (0, +\infty) \times \mathbb{R}$  and

$$\begin{aligned} K(\alpha) &= \alpha 1_{(0,1]}(\alpha) + (\alpha - 2) 1_{(1,2]}(\alpha), \\ \bar{K}(\alpha) &= \frac{K(\alpha)}{\alpha}. \end{aligned} \quad (9)$$

A stable process, with parameters  $(\alpha, \beta, \gamma, \delta)$ , is a Lévy process  $X = (S_t^{\alpha, \beta, \gamma, \delta})_{t \geq 0}$ , such that the corresponding Lévy exponent is given by

$$\varphi(u) = \begin{cases} i\delta u - \gamma|u|^\alpha \exp(-i\pi\beta K(\alpha)\text{Sign}((u)/2)), & \text{if } \alpha \neq 1, \\ i\delta u - \gamma|u|(1 + i2\beta \log|u|\text{Sign}(u)/\pi), & \text{if } \alpha = 1. \end{cases} \quad (10)$$

The parameter  $\alpha$  is the stability coefficient,  $\beta$  is the skewness coefficient,  $\gamma$  is the scale coefficient, and  $\delta$  is the drift parameter. The corresponding triplet  $(b, c, \mu)$  of characteristics is given by

$$b = \delta + \gamma \sin(\pi\beta K((\alpha)/2)) 1_{\alpha \neq 1},$$

$$c = \sqrt{2}\gamma 1_{\alpha=2},$$

$$\mu(dx) = (C(\alpha, \beta, \gamma) 1_{x>0} + C(\alpha, -\beta, \gamma) 1_{x<0}) |x|^{-(\alpha+1)} dx 1_{\alpha < 2},$$

$$C(\alpha, \beta, \gamma) = \frac{\gamma}{\pi} \Gamma(\alpha + 1) \begin{cases} \sin\left(\frac{\pi}{2} \alpha (1 + \bar{K}(\alpha)\beta)\right), & \text{if } \alpha \neq 1, \\ 1 + \beta, & \text{if } \alpha = 1. \end{cases} \quad (11)$$

See [14]. In model (6), a candidate for the unknown parameter  $\theta$  could be any the parameters  $\alpha, \beta, \gamma$ , or  $\delta$ . Since

stable processes enjoy the scaling property, with  $\delta(\alpha, t) := t[\delta + (2\beta/\pi)\gamma \log(\gamma)1l_{\alpha=1}]$ ,

$$\left(\mathcal{S}_t^{\alpha,\beta,\gamma,\delta}\right)_{t \geq 0} \stackrel{d}{=} \gamma^{1/\alpha} \left(\delta(\alpha, t) + \mathcal{S}_t^{\alpha,\beta,1,0}\right)_{t \geq 0}, \quad (12)$$

then a candidate for the unknown parameter in the model (5) is clearly the parameter  $\theta = \gamma^{1/\alpha}$ . For more account on Lévy processes, the reader is referred to [13] or [15] and for stable distributions, we suggest [16] and also [17]. Section 4 provides nontrivial examples of LAN models associated with Lévy processes  $Y$  attracted by stable ones. That means that there exist measurable functions  $b(t) \in \mathbb{R}$ ,  $a(t) > 0$  and a nondegenerate distribution  $\nu$ , such that

$$\widehat{Y}_t = \frac{Y_t - b(t)}{a(t)} \xrightarrow{d} \nu, \quad \text{as } t \rightarrow 0 \text{ or as } t \rightarrow \infty. \quad (13)$$

In [18], Far focused on the LAMN property for the model (5) discretized along the scheme  $iu_n = (i/n)$ ,  $1 \leq i \leq n$ , when the process  $Y$  is of the form  $Y = W + N$ , the sum of a standard Brownian motion and an independent compound Poisson process. She obtained LAMN property under the condition that the Lévy measure  $\nu$  of  $N$  has no diffuse singular part and that if  $\nu$  is absolutely continuous, then the model has the LAN property. Our development in Section 5 constitutes a complement to Corollary 1 for the scale model (5) and also to Far's work [18] and illustrates how to build a LAN scale model from another LAN scale model.

## 2. Definition of the LAN Property

In Section 3, we provide some theoretical results on models associated with observations, at times  $iu_n$ ,  $u_n > 0$ , of the process  $X$ , and to illustrate by some examples. To this end, we consider the sequence of i.i.d. random variables and the family of  $\sigma$ -fields:

$$\begin{aligned} X_j^n &= X_{(j+1)u_n} - X_{ju_n}, \\ \mathcal{E}_i^n &= \sigma(X_j^n, \quad 0 \leq j \leq i-1) = \sigma(ju_n, \quad 0 \leq j \leq i). \end{aligned} \quad (14)$$

Denoting  $\mathcal{H}^n = \mathcal{E}_n^n$  and  $\mathcal{H}_t^n = \mathcal{E}_{[nt]}^n$ ,  $t \in [0, 1]$ , we introduce the sequence of filtered statistical models:

$$E^n = \left(\Omega, \mathcal{H}^n, (\mathcal{H}_t^n)_{t \in [0,1]}, (\mathbb{P}_\theta^n)_{\theta \in \Theta}\right). \quad (15)$$

For any fixed  $\theta_0 \in \Theta$ , we denote

$$\begin{aligned} \Theta_n &= \left\{ \theta \in \mathbb{R}: \quad \theta_0 + \frac{\theta}{\sqrt{n}} \in \Theta \right\}, \\ [\theta]_n &= \theta_0 + \frac{\theta}{\sqrt{n}}, \end{aligned} \quad (16)$$

$$\mathbb{P}_{[\theta]_n}^n = \mathbb{P}_{[\theta]_n} | \mathcal{H}^n,$$

and we introduce the statistical experiments localized around  $\theta_0$ :

$$\begin{aligned} \mathcal{E}^n(\theta_0) &= \left(\Omega, \mathcal{H}^n, (\mathcal{H}_t^n)_{t \in [0,1]}, (\mathbb{P}_\theta^n)_{\theta \in \Theta_n}\right), \\ \mathcal{E}'(\theta_0) &= \left(\Omega', \mathcal{F}', (\mathcal{F}'_t)_{t \in [0,1]}, (\mathbb{P}'_\theta)_{\theta \in \mathbb{R}}\right), \end{aligned} \quad (17)$$

where the last statistical experiment is a Gaussian Shift. By a Gaussian shift, we mean, that for all  $\theta \in \mathbb{R}$ ,  $\mathbb{P}'_\theta$  is the unique probability on  $(\Omega', \mathcal{F}')$  equivalent to  $\mathbb{P}'_0$  on each  $\mathcal{F}'_t$  and that its associated likelihood process is the geometric Brownian motion defined by

$$Z_t'^\theta = \frac{d\mathbb{P}'_\theta | \mathcal{F}'_t}{d\mathbb{P}'_0 | \mathcal{F}'_t} = \exp \left\{ \theta \sqrt{I(\theta_0)} X'_t - \frac{\theta^2}{2} I(\theta_0) t \right\}, \quad t \in [0, 1], \quad (18)$$

where  $(X'_t)_{t \in [0,1]}$  is a Wiener process, and then, under  $\mathbb{P}'_0$ , the process  $(X'_t - t\theta\sqrt{I(\theta_0)})_{t \geq 0}$  is again a Wiener process. The quantity  $I(\theta_0)$  is called the asymptotic Fisher information quantity; it is a positive constant related to the sequence of statistical experiments  $\mathcal{E}^n(\theta_0)$  in (17) and has to be determined. The asymptotic Fisher information quantity is crucial in any estimation procedure. Indeed, under the LAN property,  $1/I(\theta_0)$  is the lower bound of the variance of any estimator  $\vartheta_n$  of  $\theta_0$ . More precisely, HAJEK's asymptotic convolution theorem says that if  $\vartheta_n$  satisfies

$$\mathcal{L}aw \left( \sqrt{n} \left( \vartheta_n - \left( \theta_0 + \frac{\theta}{\sqrt{n}} \right) \right) | \mathbb{P}'_\theta \right) \rightarrow \mathcal{L}_{\theta_0}, \quad \text{as } n \rightarrow \infty, \quad (19)$$

then the distribution  $\mathcal{L}_{\theta_0}$  is the convolution product  $\mathcal{L}_{\theta_0} = \mathcal{L}_{\theta_0}^1 * \mathcal{L}_{\theta_0}^2$ , where  $\mathcal{L}_{\theta_0}^0 = \text{normal}(0, I(\theta_0)^{-1})$  and  $\mathcal{L}_{\theta_0}^2$  is a probability measure on  $\mathbb{R}$ . See [19] for more.

Local asymptotic normality of the sequence of models  $E^n$  in (17), in a value  $\theta_0 \in \Theta$ , is actually equivalent to the weak functional convergence in time of the sequence of statistical experiments  $\mathcal{E}^n(\theta_0)$  to the Gaussian shift  $\mathcal{E}'(\theta_0)$  in (17). This fact is explained as follows: let  $Z_t'^{\eta,\xi}$  and  $Z_t^{n,\eta,\xi}$  be the likelihood processes defined, for all  $\eta, \xi \in \Theta_n$  and at each time  $t \in [0, 1]$ , by

$$Z_t'^{\eta,\xi} = \frac{d\mathbb{P}'_\eta | \mathcal{F}'_t}{d\mathbb{P}'_\xi | \mathcal{F}'_t} = \mathbb{E}_{\mathbb{P}'_\xi} \left[ \frac{d\mathbb{P}'_\eta}{d\mathbb{P}'_\xi} | \mathcal{F}'_t \right] = \frac{Z_t'^\eta}{Z_t'^\xi}, \quad (20)$$

$$Z_t^{n,\eta,\xi} = \frac{d\mathbb{P}_\eta^n | \mathcal{H}_t^n}{d\mathbb{P}_\xi^n | \mathcal{H}_t^n} = \mathbb{E}_{\mathbb{P}_\xi^n} \left[ \frac{d\mathbb{P}_\eta^n}{d\mathbb{P}_\xi^n} | \mathcal{H}_t^n \right],$$

with the convention  $(a/0) = 0$ , if  $a \in (0, +\infty)$ . According to [5], the likelihood process  $Z_t^{n,\eta,\xi}$  of the statistical experiment  $\mathcal{E}^n(\theta_0)$  is represented by

$$Z_t^{n,\eta,\xi} = \prod_{j=1}^{[nt]} \frac{g_{u_n}^\eta}{g_{u_n}^\xi}(X_j^n). \quad (21)$$

The notion of weak functional convergence in time was introduced by Lecam [2] and developed by Strasser [19] and Jacod [20]. It is expressed as follows: for every finite subset  $J$  of  $\mathbb{R} = \cup_{n \geq 1} \Theta_n$ , and every  $\xi \in \Theta$ , we have

$$\mathcal{L}aw \left( (Z_t^{n,\eta,\xi})_{\eta \in J} | \mathbb{P}_{[\xi]_n}^n \right) \rightarrow \mathcal{L}aw \left( (Z_t'^{\eta,\xi})_{\eta \in J} | \mathbb{P}'_\xi \right), \quad \text{as } n \rightarrow +\infty, \quad (22)$$



in the sense of the weak convergence for the Skorohod topology.

### 3. When Does LAN Property Hold for Lévy Models?

Our aim is to give sufficient conditions on the p.d.f.  $g_t$  of  $X_t$  under  $\mathbb{P}_\theta$ , ensuring the LAN property for the sequence of filtered statistical models  $E^n$ .

$$\left[ d_\theta t, \infty \text{ (respectively, } (-\infty, d_\theta t]), \text{ with } d_\theta = b_\theta - \int_{\mathbb{R}} y 1_{|y| \leq 1} \mu_\theta(dy). \right. \quad (23)$$

In all other cases, the distribution of  $X_t$  has a support equal to  $\mathbb{R}$ . There are many situations in which for all  $t > 0$ ,  $X_t$  has a probability p.d.f.  $g_t^\theta(x)$  which is infinitely differentiable in  $x$ . For instance, the latter holds if

$$c_\theta > 0, \quad (24)$$

or if  $\int_{|y| \leq \varepsilon} \min(y^2, 1) \mu_\theta(dy) \geq K_\theta \varepsilon^\alpha,$

3.1. LAN Property for the Model (6). In this section, we will consider the model (6). If  $c_\theta = 0$ ,  $\mu_\theta$  integrates  $|y| \wedge 1$ , and  $\mu_\theta(0, \infty) = 0$  (respectively,  $\mu_\theta(-\infty, 0) = 0$ ), then the support of the distribution of  $X_t$  is

for any  $\varepsilon \in [0, 1]$  and for some  $K_\theta > 0$  and some  $\alpha \in (0, 2)$ , see [21]. Later on, we may assume the following:

$$(H0): \text{ for all } \theta \in \Theta \text{ and } t > 0, \text{ under } \mathbb{P}_\theta, \text{ the support of the law of } X_t \text{ is an interval } K_t, \text{ independent from } \theta, \text{ of the form } K_t = \mathbb{R} \text{ or } (-\infty, dt) \text{ and } X_t \text{ has a p.d.f. } x \mapsto g_t^\theta(x) \text{ which is of class } C^2, \text{ relative to } \theta. \quad (25)$$

We denote  $\mathcal{K}_n = K_{u_n}$  and we define, on the interior of  $\mathcal{K}_n$ , the following functions:

$$\begin{aligned} h_n^\theta &= g_{u_n}^\theta, \\ \bar{h}_n^\theta &= \frac{\partial}{\partial \theta} \log h_n^\theta, \\ \ddot{h}_n^\theta &= \frac{\partial^2}{\partial \theta^2} h_n^\theta, \\ \dot{h}_n^\theta &= h_n^\theta \left| \bar{h}_n^\theta \right|^2 \\ \ddot{h}_n^\theta &= \dot{h}_n^\theta + \left| \ddot{h}_n^\theta \right|. \end{aligned} \quad (26)$$

When the number  $\chi > 0$  appears, it is always understood that  $n$  is big enough so that  $\chi$  and  $-\chi$  are in  $\Theta_n$ . For all  $\theta \in \Theta, \rho \in (0, 1)$ , and  $\rho' = 1 - \rho$ , we denote

$$\begin{aligned} I_n^\theta &:= \int_{\mathcal{K}_n} i_n^\theta(x) dx, \\ \tilde{I}_n(\chi) &= \sup_{|\varepsilon| \leq \chi} I_n^{[\varepsilon]}, \\ \tilde{J}_n^\rho(\chi) &:= \sup_{|\zeta|, |\varepsilon| \leq \chi} \int_{\mathcal{K}_n} \frac{j_n^{[\zeta]}(x) j_n^{[\varepsilon]}(x)}{(h_n^{[\zeta]}(x))^\rho (h_n^{[\varepsilon]}(x))^{\rho'}} dx = \tilde{J}_n^{\rho'}(\chi). \end{aligned} \quad (27)$$

$$(28)$$

For statisticians,  $I_n^{\theta_0}$  is a familiar quantity and corresponds to the Fisher information quantity at stage  $n$ . The quantity  $\tilde{J}_n^\rho(\chi)$  is less intuitive; it is a localized quantity around the true value  $\theta_0$  and corresponds to the rest of Taylor approximations at the order 1 of Hellinger integrals of the model.

We are now able to state our first result, that is, the LAN property for the model (6).

**Theorem 1.** Assume (H0) and the following conditions:

$$(H1): \lim_{n \rightarrow +\infty} I_n^{\theta_0} = I(\theta_0) \in (0, \infty) \text{ and for all } \chi > 0, \limsup_{n \rightarrow +\infty} \bar{I}_n(\chi) < +\infty,$$

$$(H2): \text{There exists } a \in (0, (1/2)) \text{ such that for all } \chi > 0, \text{ one has} \quad (29)$$

$$\lim_{n \rightarrow +\infty} \frac{\bar{J}_n^\rho(\chi)}{n} = 0 \quad \text{for } \rho \in \{(1/2), a, 1-a\}.$$

Then, the sequence of sequence of filtered statistical models  $E^n$  (15), corresponding to (6), has the LAN property at  $\theta_0$  with the speed  $\sqrt{n}$  and the asymptotic Fisher information quantity  $I(\theta_0)$ .

*Remark 1*

- (i) Cauchy–Schwarz inequality gives  $I_n^\theta \leq [\bar{J}_n^{1/2}(|\theta|)]^{1/2}$ , and both conditions (H1) and (H2) are implied by

$$(H3): \lim_{n \rightarrow +\infty} I_n^{\theta_0} = I(\theta_0) \text{ and there exists } a \in (0, (1/2)), \text{ such that for all } \chi > 0, \text{ one has} \quad (30)$$

$$\limsup_{n \rightarrow +\infty} \bar{J}_n^\rho(\chi) < +\infty \quad \text{for } \rho \in \{(1/2), a, 1-a\}.$$

- (ii) Under different conditions and a different proof, Masuda obtained ([8], Theorem 2.12) the same conclusion as in Theorem 1.

Genon-Catalot and Jacod [5] exhibited discretized models according to random sampling schemes  $(T(i, n), 1 \leq i \leq n)$  associated with a diffusion process  $X$  driven by Brownian motions (with coefficients dependent on  $\theta$  and by an homogeneous way on  $X$ ) and proved the LAMN property under conditions similar to (H0), that is, differentiability to the third order relative to  $\theta$  and integrability of the densities of the processes. Their proofs have a general vocation in the sense that they only use the Markovian property of the processes and are based on a method of approximation of the log-likelihood. Because of the intricate form 16 of the likelihood processes, we show the weak functional convergence of  $\mathcal{E}^n(\theta_0)$  to  $\mathcal{E}'(\theta_0)$  via the convergence of the Hellinger processes, and with a tool, one can find in [20].

*Proof of Theorem 1.* Fix  $\theta_0$ . The Hellinger process of order  $\rho \in (0, 1)$  between  $\mathbb{P}'_\eta$  and  $\mathbb{P}'_\xi$ , relative to  $(\mathcal{F}'_t)_{t \in [0, 1]}$ , is deterministic and has the form

$$\mathcal{H}^{\eta, \xi}(\rho)_t = \rho(1-\rho)(\eta - \xi)^2 I(\theta_0) \left(\frac{t}{2}\right). \quad (31)$$

According to ([20], Theorem 5.3), it is enough to show that the Hellinger processes  $\mathcal{H}^{\eta, \xi}(\rho)$  between  $\mathbb{P}^n_\eta$  and  $\mathbb{P}^n_\xi$ , relative to  $(\mathcal{G}^n_t)_{t \in [0, 1]}$ , satisfy the following: there exists  $a \in (0, (1/2))$ , such that for every  $\forall \eta, \xi \in \mathbb{R}$ ,  $\rho \in \{(1/2), a, 1-a\}$ , and  $t \in [0, 1]$ , and the convergence in law

$$\mathcal{H}^{\eta, \xi}(\rho)_t \xrightarrow{\mathbb{P}^n_\xi} \mathcal{H}^{\eta, \xi}(\rho)_t, \quad \text{as } n \rightarrow \infty, \quad (32)$$

holds. We will use this method because in our framework, the processes  $\mathcal{H}^{\eta, \xi}$  are also deterministic and have the

following quite simple form one can find in [5]: with  $[nt]$  being the integer part of  $nt$ , we have

$$\mathcal{H}^{\eta, \xi}(\rho)_t = [nt] \left( 1 - \int_{\mathcal{X}_n} (h_n^{[\eta]_n})^\rho (h_n^{[\xi]_n})^{1-\rho}(y) dy \right). \quad (33)$$

- (1) For  $\rho \in (0, 1)$ ,  $\rho' = 1 - \rho$ , take  $\Phi_\rho(u, v) = \rho u + \rho' v - u^\rho v^{\rho'}$ ,  $u, v \geq 0$ , and observe that

$$\mathcal{H}^{\eta, \xi}(\rho)_1 = \int_{\mathcal{X}_n} \Phi_\rho(h_n^{[\eta]_n}, h_n^{[\xi]_n})(y) dy. \quad (34)$$

According to (32) and (33), it is enough to show that  $\forall \eta, \xi \in \mathbb{R}$ , and  $\rho \in \{(1/2), a, 1-a\}$ , and we have

$$\lim_{n \rightarrow \infty} n \int_{\mathcal{X}_n} \Phi_\rho(h_n^{[\eta]_n}, h_n^{[\xi]_n})(y) dy = \frac{\rho \rho'}{2} (\eta - \xi)^2 I(\theta_0). \quad (35)$$

- (2) Assume (H0), (H1), and (H2) for a fixed  $a \in (0, (1/2))$ . Applying Taylor expansion at the first order of  $\theta \mapsto (h_n^\theta)^\rho$  for  $\eta \in \mathbb{R}$  and  $n$  big enough, we get for  $\eta \in \Theta_n$ , the representation of  $(h_n^{[\eta]_n})^\rho$  on  $\mathcal{X}_n$ :

$$(h_n^{[\eta]_n})^\rho = (h_n^{\theta_0})^\rho + \frac{\rho \eta}{\sqrt{n}} k_n^{\theta_0, \rho} + \frac{\rho \eta}{\sqrt{n}} V_n^{\eta, \rho}, \quad (36)$$

where for all  $\theta \in \Theta$ , the functions

$$\begin{aligned} k_n^{\theta, \rho} &= \bar{h}_n^\theta (h_n^\theta)^\rho, \quad \dot{k}_n^{\theta, \rho} = (h_n^\theta)^\rho \left[ \frac{\partial}{\partial \theta} \bar{h}_n^\theta + \rho \left( \bar{h}_n^\theta \right)^2 \right] \\ &= (h_n^\theta)^\rho \left[ \frac{\dot{h}_n^\theta}{h_n^\theta} - \rho' \left( \bar{h}_n^\theta \right)^2 \right], \end{aligned} \quad (37)$$

$$V_n^{\eta, \rho} = \int_0^1 [k_n^{[\eta r]_n, \rho} - k_n^{\theta_0, \rho}] dr = \frac{\eta}{\sqrt{n}} \int_0^1 (1-r) \dot{k}_n^{[\eta r]_n, \rho} dr, \quad (38)$$

are defined on the interior of  $\mathcal{X}_n$ . Also, observe the following relations:

$$\begin{aligned} k_n^{\theta,\rho} (h_n^\theta)^{\rho'} &= k_n^{\theta,\rho'} (h_n^\theta)^\rho = k_n^{\theta,1}, \\ k_n^{\theta,\rho} k_n^{\theta,\rho'} &= i_n^\theta, \\ \dot{k}_n^{\theta,\rho} (h_n^\theta)^{\rho'} &= \dot{k}_n^{\theta,1} - \rho' i_n^\theta. \end{aligned} \quad (39)$$

Because of (38) and (39), one has

$$\begin{aligned} V_n^{\eta,1} - (h_n^{\theta_0})^{\rho'} V_n^{\eta,\rho} &= \frac{\eta}{\sqrt{n}} \int_0^1 (1-r) \left[ \dot{k}_n^{[\eta r]_n,1} - (h_n^{\theta_0})^{\rho'} \dot{k}_n^{[\eta r]_n,\rho} \right] dr \\ &= \frac{\eta}{\sqrt{n}} \int_0^1 (1-r) \dot{k}_n^{[\eta r]_n,\rho} \left[ (h_n^{[\eta r]_n})^{\rho'} - (h_n^{\theta_0})^{\rho'} \right] dr + \frac{\eta \rho'}{\sqrt{n}} \int_0^1 (1-r) i_n^{[\eta r]_n} dr. \end{aligned} \quad (40)$$

Using (36), finally write

$$V_n^{\eta,1} - (h_n^{\theta_0})^{\rho'} V_n^{\eta,\rho} = \frac{\eta^2 \rho'}{n} \int_0^1 (1-r) \dot{k}_n^{[\eta r]_n,\rho} \left[ k_n^{\theta_0,\rho'} + V_n^{\eta r,\rho'} \right] dr + \frac{\eta \rho'}{\sqrt{n}} \int_0^1 (1-r) i_n^{[\eta r]_n} dr. \quad (41)$$

(3) For all  $\eta, \xi \in \mathbb{R}$  and  $n$  large enough, so that  $\eta, \xi \in \Theta_n$ , write

$$\begin{aligned} \Phi_\rho(h_n^{[\eta]_n}, h_n^{[\xi]_n}) &= \rho \left[ h_n^{\theta_0} + \frac{\eta}{\sqrt{n}} k_n^{\theta_0,1} + \frac{\eta}{\sqrt{n}} V_n^{\eta,1} \right] + \rho' \left[ h_n^{\theta_0} + \frac{\xi}{\sqrt{n}} k_n^{\theta_0,1} + \frac{\xi}{\sqrt{n}} V_n^{\xi,1} \right] \\ &\quad - \left[ (h_n^{\theta_0})^\rho + \frac{\rho \eta}{\sqrt{n}} k_n^{\theta_0,\rho} + \frac{\rho \eta}{\sqrt{n}} V_n^{\eta,\rho} \right] \left[ (h_n^{\theta_0})^{\rho'} + \frac{\rho' \xi}{\sqrt{n}} k_n^{\theta_0,\rho'} + \frac{\rho' \xi}{\sqrt{n}} V_n^{\xi,\rho'} \right]. \end{aligned} \quad (42)$$

Then, use (39) and obtain

$$\begin{aligned} n\Phi_\rho(h_n^{[\eta]_n}, h_n^{[\xi]_n}) &= \sqrt{n}\rho\eta \left[ V_n^{\eta,1} - (h_n^{\theta_0})^{\rho'} V_n^{\eta,\rho} \right] + \sqrt{n}\rho'\xi \left[ V_n^{\xi,1} - (h_n^{\theta_0})^{\rho'} V_n^{\xi,\rho'} \right] \\ &\quad - \rho\rho'\eta\xi \left[ i_n^{\theta_0} + V_n^{\eta,\rho} V_n^{\xi,\rho'} + k_n^{\theta_0,\rho} V_n^{\xi,\rho'} + k_n^{\theta_0,\rho'} V_n^{\eta,\rho} \right]. \end{aligned} \quad (43)$$

According to (41), we have

$$n\Phi_\rho(h_n^{[\eta]_n}, h_n^{[\xi]_n}) = \rho\rho' \left[ A_n^{\eta,\xi} + B_n^{\eta,\xi} \right], \quad (44)$$

where

$$\begin{aligned} A_n^{\eta,\xi} &= \eta^2 \int_0^1 (1-r) i_n^{[\eta r]_n} dr + \xi^2 \int_0^1 (1-r) i_n^{[\xi r]_n} dr - \eta\xi i_n^{\theta_0}, \\ B_n^{\eta,\xi} &= \frac{\eta^3}{\sqrt{n}} \int_0^1 (1-r) \dot{k}_n^{[\eta r]_n,\rho} \left[ k_n^{\theta_0,\rho'} + V_n^{\eta r,\rho'} \right] dr + \frac{\xi^3}{\sqrt{n}} \int_0^1 (1-r) \dot{k}_n^{[\xi r]_n,\rho'} \left[ k_n^{\theta_0,\rho} + V_n^{\xi r,\rho} \right] dr, \\ &\quad - \eta\xi \left[ k_n^{\theta_0,\rho} V_n^{\xi,\rho'} + k_n^{\theta_0,\rho'} V_n^{\eta,\rho} + V_n^{\eta,\rho} V_n^{\xi,\rho'} \right]. \end{aligned} \quad (45)$$

(4a) We will now prove the following convergence that will imply (35): for all  $\eta, \xi \in \mathbb{R}$ ,

$$\lim_{n \rightarrow \infty} \int_{\mathcal{X}_n} A_n^{\eta, \xi}(x) dx = \frac{1}{2}(\eta - \xi)^2 I(\theta_0), \quad (46)$$

$$\lim_{n \rightarrow \infty} \int_{\mathcal{X}_n} B_n^{\eta, \xi}(x) dx = 0. \quad (47)$$

(4b). To prove (46), we use both (26) and (37), and for all  $\rho \in (0, 1)$  and  $\theta \in \Theta$ , we have the representation and the control.

$$\begin{aligned} |k_n^{\theta, \rho}| &= \sqrt{i_n^\theta (h_n^\theta)^{\rho - (1/2)}}, \\ |\dot{k}_n^{\theta, \rho}| &\leq \frac{j_n^\theta}{(h_n^\theta)^\rho}. \end{aligned} \quad (48)$$

Let  $\eta, \xi \in \mathbb{R}$ , and let  $\chi = |\eta| \vee |\xi|$ . Using (26), (37), and Taylor expansion at the first order of  $\theta \mapsto (k_n^{\theta, (1/2)})^2$ , we obtain the galloping control, valid for all  $r \in [0, 1]$ :

$$\begin{aligned} I_n^{[\eta r]_n} - I_n^{\theta_0} &= \int_{\mathcal{X}_n} \left[ k_n^{[\eta r]_n, (1/2)}(x)^2 - k_n^{\theta_0, (1/2)}(x)^2 \right] dx \\ &= \frac{2\eta r}{\sqrt{n}} \int_0^1 k_n^{[\eta r s]_n, (1/2)}(x) \dot{k}_n^{[\eta r s]_n, (1/2)}(x) ds dx. \end{aligned} \quad (49)$$

Taking  $\rho = 1/2$  in (48), applying Cauchy–Schwarz inequality and assuming (H1) and (H2), we obtain

$$\sup_{r \in [0, 1]} |I_n^{[\eta r]_n} - I_n^{\theta_0}| \leq 2|\eta| \bar{I}_n(\chi) \left( \frac{\bar{J}_n^{1/2}(\chi)}{n} \right)^{1/2} \rightarrow 0 \quad \text{as } n \rightarrow \infty. \quad (50)$$

We then can write

$$\begin{aligned} \int_{\mathcal{X}_n} A_n^{\eta, \xi}(x) dx &= \eta^2 \int_0^1 (1-r) I_n^{[\eta r]_n} dr + \xi^2 \int_0^1 (1-r) I_n^{[\xi r]_n} dr - \eta \xi I_n^{\theta_0} \\ &= \eta^2 \int_0^1 (1-r) (I_n^{[\eta r]_n} - I_n^{\theta_0}) dr + \xi^2 \int_0^1 (1-r) (I_n^{[\xi r]_n} - I_n^{\theta_0}) dr + \frac{1}{2}(\eta^2 + \xi^2 - 2\eta\xi) I_n^{\theta_0}, \end{aligned} \quad (51)$$

and clearly (50) implies (46).

(4c). To prove (47), we use same the same arguments as in (4b), the Taylor expansion at the first order of  $\theta \mapsto k_n^{\theta, (1/2)}$ , and the representation

$$\begin{aligned} \dot{k}_n^{[\eta r]_n, \rho} k_n^{\theta_0, \rho'} &= \dot{k}_n^{[\eta r]_n, \rho} k_n^{[\eta r]_n, \rho'} - \frac{\eta r}{\sqrt{n}} \int_0^1 \dot{k}_n^{[\eta r]_n, \rho} \dot{k}_n^{[\eta r s]_n, \rho'} ds, \\ \rho &\in (0, 1), r \in [0, 1]. \end{aligned} \quad (52)$$

By (48) and Cauchy–Schwarz inequality, we have the following control, valid for all  $r \in [0, 1]$ :

$$\begin{aligned} \int_{\mathcal{X}_n} \left| \dot{k}_n^{[\eta r]_n, \rho}(x) k_n^{\theta_0, \rho'}(x) \right| dx \\ \leq \int_{\mathcal{X}_n} \sqrt{i_n^{[\eta r]_n}(x)} \frac{j_n^{[\eta r]_n}(x)}{\sqrt{h_n^{[\eta r]_n}(x)}} dx + \frac{|\eta| r}{\sqrt{n}} \bar{J}_n^\rho(\chi). \end{aligned} \quad (53)$$

The latter implies

$$\begin{aligned} \sup_{r \in [0, 1]} \int_{\mathcal{X}_n} \left| \dot{k}_n^{[\eta r]_n, \rho}(x) k_n^{\theta_0, \rho'}(x) \right| dx \\ \leq \sqrt{\bar{I}_n(\chi) \bar{J}_n^{1/2}(\chi)} + \frac{\chi}{\sqrt{n}} \bar{J}_n^\rho(\chi) := \delta_n^\rho(\chi) = \delta_n^{\rho'}(\chi). \end{aligned} \quad (54)$$

Using (48), we also have

$$\int_{\mathcal{X}_n} \left| \dot{k}_n^{[\eta r]_n, \rho}(x) V_n^{\eta r, \rho'}(x) \right| dx \leq \frac{|\eta| r}{\sqrt{n}} \int_0^1 (1-s) \int_{\mathcal{X}_n} \left| \dot{k}_n^{[\eta r]_n, \rho}(x) \dot{k}_n^{[\eta r s]_n, \rho'}(x) \right| dx ds, \quad (55)$$

and reproducing the method, we used to get (54), and we obtain

$$\sup_{r \in [0, 1]} \int_{\mathcal{X}_n} \left| \dot{k}_n^{[\eta r]_n, \rho}(x) V_n^{\eta r, \rho'}(x) \right| dx \leq \delta_n^\rho(\chi). \quad (56)$$

According to (38) and (54), we also have

$$\int_{\mathcal{X}_n} |k_n^{\theta_0, \rho'}(x) V_n^{\eta, \rho'}(x)| dx \leq \frac{|\eta|}{\sqrt{n}} \int_0^1 (1-r) \int_{\mathcal{X}_n} |k_n^{[\eta r]_n, \rho'}(x) k_n^{\theta_0, \rho'}(x)| dx dr \leq \frac{\chi}{\sqrt{n}} \delta_n^{\rho'}(\chi). \quad (57)$$

Furthermore, (38), (48), and Cauchy–Schwarz inequality imply

$$\int_{\mathcal{X}_n} |V_n^{\eta, \rho'}(x) V_n^{\xi, \rho'}(x)| dx \leq \frac{|\eta \xi|}{n} \int_0^1 \int_0^1 (1-r)(1-s) \int \frac{j_n^{[\eta r]_n}(x) j_n^{[\xi s]_n}(x)}{h_n^{[\eta r]_n}(x)^{\rho'} h_n^{[\xi s]_n}(x)^{\rho}} dx ds dr \leq \frac{|\chi|}{\sqrt{n}} \delta_n^{\rho'}(\chi). \quad (58)$$

Finally, according to (45), (54), (56)–(58), we obtain the control

$$\int_{\mathcal{X}_n} B_n^{\eta, \xi}(x) dx \leq 7\chi^3 \frac{\delta_n^{\rho'}(\chi)}{\sqrt{n}} = 7\chi^3 \left[ \left( \tilde{I}_n(\chi) \frac{\tilde{J}_n^{(1/2)}(\chi)}{n} \right)^{(1/2)} + \chi \frac{\tilde{J}_n^{\rho'}(\chi)}{n} \right], \quad (59)$$

and we conclude with the fact that assumptions (H1) and (H2) imply (47).  $\square$

**3.2. LAN Property for the Scale Model (5).** As a consequence of Theorem 1, we obtain a result for the scale model (5). The main argument is that the r.v.  $X_t$ ,  $t > 0$  has a p.d.f  $g_t^1$  under  $\mathbb{P}_1$  if and only if  $X_t$  has the p.d.f.  $g_t^\theta(x) = g_t^1(x/\theta)/\theta$  under  $\mathbb{P}_\theta$ . From now on, the functions  $h_n, h'_n$ , and  $h''_n$  denote, respectively,  $h_n^1$ , the p.d.f. of  $X_{u_n}$  under  $\mathbb{P}_1$ , the first and the second derivatives of  $h_n$ . For  $\theta \in \Theta$  and  $n \geq 1$ , we have the expression

$$h_n^\theta(x) = \frac{1}{\theta} h_n\left(\frac{x}{\theta}\right), \quad \frac{x}{\theta} \in \mathcal{X}_n := \text{support}(h_n). \quad (60)$$

Therefore, if we want (H0) to be satisfied, we need to impose  $K = \mathcal{X}_n = \mathbb{R}$  or  $\mathbb{R}_+$  or  $\mathbb{R}_-$ . Then, for all  $x \in K$ , we have

$$\begin{aligned} i_n^\theta(x) &= \frac{1}{\theta^3} i_n\left(\frac{x}{\theta}\right), \\ j_n^\theta(x) &= \frac{1}{\theta^3} j_n\left(\frac{x}{\theta}\right), \end{aligned} \quad (61)$$

where the functions  $i_n := i_n^1$  and  $j_n := j_n^1$  are given by

$$i_n(x) = \left| 1 + x \frac{h'_n(x)}{h_n(x)} \right|^2 h_n(x), \quad (62)$$

$$j_n(x) = i_n(x) + \left| 2 + 4x \frac{h'_n(x)}{h_n(x)} + x^2 \frac{h''_n(x)}{h_n(x)} \right| h_n(x).$$

Making a change of variables, we see that the quantities  $I_n^\theta$  and  $\tilde{I}_n(\chi)$ , defined in (27), satisfy

$$I_n^\theta = \frac{1}{\theta^2} \int_K i_n(x) dx = \frac{I_n}{\theta^2}, \quad (63)$$

$$\tilde{I}_n(\chi) = \sup_{|\zeta| \leq \chi} \frac{I_n}{(|\zeta|_n)^2} \leq \frac{I_n}{(|\theta_0| - (\chi/\sqrt{n}))^2}.$$

Using Cauchy–Schwarz inequality and again a change of variables, we obtain the following: for all  $\chi > 0$ , the quantities  $\tilde{J}_n^\rho(\chi)$ ,  $\rho \in (0, 1)$ , defined in (28), satisfy

$$\begin{aligned} \tilde{J}_n^\rho(\chi) &\leq \sup_{|\zeta|, |\varepsilon| \leq \chi} \left[ \int_K \frac{j_n^{[\zeta]_n}(x)^2}{h_n^{[\zeta]_n}(x)^{2\rho}} dx \right]^{1/2} \left[ \int_K \frac{j_n^{[\varepsilon]_n}(x)^2}{h_n^{[\varepsilon]_n}(x)^{2\rho'}} dx \right]^{1/2} \\ &= \sup_{|\zeta|, |\varepsilon| \leq \chi} \left[ \frac{1}{(|\zeta|_n|^{5-2\rho} |\varepsilon|_n|^{5-2\rho'})} \int_K \frac{j_n(x)^2}{h_n(x)^{2\rho}} dx \int_K \frac{j_n(x)^2}{h_n(x)^{2\rho'}} dx \right]^{1/2} \\ &\leq \left| |\theta_0| - \frac{\chi}{\sqrt{n}} \right|^{4\rho-10} [J_n(\rho) J_n(\rho')]^{1/2}, \quad J_n(r) := \int_K \frac{j_n(x)^2}{h_n(x)^{2r}} dx. \end{aligned} \quad (64)$$

**Corollary 1.** For the scale model (5), the sequence of statistical models  $E^n$  has the LAN property with speed  $\sqrt{n}$  at each  $\theta \in \Theta$  if the following conditions are satisfied:

(C0): under  $\mathbb{P}_1$ , the support  $K$  of the law of  $X_1$  is either  $\mathbb{R}$  or  $\mathbb{R}_+$  or  $\mathbb{R}_-$ . For all

$t > 0$ , the r.v.  $X_t$  has a p.d.f.  $g_t^1(x)$  which is of class  $C^2$  on the interior of  $K$ .

(C1): the sequence  $I_n := \int_K i_n(x) dx$  satisfies  $\lim_{n \rightarrow +\infty} I_n = I \in (0, \infty)$ , (65)

(C2): there exists  $a \in \left(0, \frac{1}{2}\right)$  such that  $\lim_{n \rightarrow \infty} \frac{1}{n} J_n(\rho) = 0$  for  $\rho \in \left\{\frac{1}{2}, a, 1-a\right\}$ .

In this case, the asymptotic Fisher information quantity is  $I(\theta) = I/\theta^2$ .

*Proof.* It is immediate that (C0) implies (H0). Representation (63) shows that (C1) implies (H1) and (64) shows that (C2) implies (H2).  $\square$

*Remark 2.* Since  $h_n$  is the p.d.f. of  $X_{u_n}$ , then we should be aware that the discretization path  $u_n$  intervene in the assumptions (C1) and (C2). In Theorem 2, we will see that in some favorable cases, the effect of the path  $u_n$  has a quite negligible effect. In general, the LAN property depends strongly on the asymptotic of  $u_n$ .

#### 4. Examples of LAN Property for Lévy Processes Attracted by Stable Processes

In this section, we provide some examples of Lévy processes  $X$  satisfying the conditions of Corollary 1. This corollary provides the LAN property for the scale model (5),  $X = \theta Y$ , under regularity and integrability conditions on the p.d.f. of  $Y_t$ ,  $t > 0$ . Unfortunately, these p.d.f., if they exist, are not explicit in general; for this reason, we focus on processes  $Y$  which belong to the domain of attraction of stable processes.

We recall that a process  $S^{\alpha, \beta, \gamma, \delta}$  is stable, if it is a Lévy process with Lévy exponent given in (10). In the case

$\alpha \in (0, 1)$  and  $\delta \geq 0$ , the process  $S^{\alpha, 1, \gamma, \delta}$  is a subordinator, i.e., a positive increasing the Lévy process, and the distribution of  $S_t^{\alpha, 1, \gamma, \delta}$ ,  $t > 0$ , has a support equal to  $[\delta t, \infty)$ . In all cases,  $S_t^{\alpha, 1, \gamma, \delta}$ ,  $t > 0$ , has a p.d.f.  $G_t^{\alpha, \beta, \gamma, \delta}$  which is infinitely differentiable and is explicit only for the particular values  $(\alpha, \beta) = ((1/2), 1), (1, 0), (2, 0)$ . These values correspond, respectively, to the first passage times of the Brownian motion, the Cauchy process, and the Brownian Motion. Otherwise,  $G_t^{\alpha, \beta, \gamma, \delta}$  is expressed only as the inverse Fourier transform of  $\exp \phi(u)$ . As announced, the introduction, we focus in this section on the case where the Lévy processes  $Y$ , in the scale model (5), is attracted by a stable process, i.e., satisfying (13). Bertoin and Doney [22] showed that if (10) holds, then the process  $Y$  is attracted by a stable one, and then, the following holds:

- (i) There exists  $b \in \mathbb{R}$ ,  $\alpha \in (0, 2]$ , and a slowly varying function  $l(t)$  (i.e., a function satisfying  $(l(\lambda t)/l(t)) \rightarrow 1, \forall \lambda > 0$ ), such that  $b(t) = bt$  and  $a(t) = t^{1/\alpha} l(t)$
- (ii)  $\nu(dx) = G(x) dx$ , where  $G$  is the p.d.f. of some stable r.v.  $S_1^{\alpha, \beta, \gamma, 0}$ ,  $\beta \in [-1, 1], \gamma > 0$ ;
- (iii) The p.d.f.  $G_t$  of  $\tilde{Y}_t$ ,  $t > 0$ , is infinitely differentiable and satisfies

$$(G_t)^{(k)}(x) \rightarrow G^{(k)}(x), \quad \text{uniformly in } x \in \text{Support}(G), t \rightarrow 0 \text{ or } t \rightarrow \infty, k \in \mathbb{N}. \quad (66)$$

- (iv) The convergence in (13) can be entirely expressed with the behavior of the tail of the Lévy measure of  $Y$  or by the existence of a Brownian component.

Observe that the p.d.f.  $h_n$  of  $Y_{u_n}$  is represented by

$$h(x) = G_{u_n} \left( \frac{x - b(u_n)}{a(u_n)}, x \in \mathbb{R} \right) \quad (67)$$

As in (8), let us denote by  $\bar{G}_{u_n}$  and  $\bar{G}$  the logarithmic derivative of  $G_{u_n}$  and  $\log G$ , respectively. After the change of

variable  $x \mapsto a(u_n)x + b(u_n)$ , the asymptotic Fisher information quantity in (63) takes the form

$$I(\theta) = \frac{I}{\theta^2}, \quad I = \lim_{n \rightarrow \infty} \int \left[ 1 + \left( x + \frac{b(u_n)}{a(u_n)} \right) \bar{G}_{u_n}(x) \right]^2 G_{u_n}(x) dx. \quad (68)$$

The convergence (66) does not ensure that  $I(\theta)$  is finite and nonnull; it only ensures that if it happens, then

$$l = \lim_{n \rightarrow \infty} \left( \frac{b(u_n)}{a(u_n)} \right) \text{ exists,} \quad (69)$$

$$I = \int [1 + (x+l)\overline{G}(x)]^2 G(x) dx \in (0, \infty).$$

The stronger control

$$\limsup_{|x| \rightarrow \infty, n \rightarrow \infty} |x\overline{G}_{u_n}(x)| < \infty, \quad (70)$$

is sufficient to prove (69), but it is hard to obtain. In [14, 17], we provided controls for the p.d.f.  $G_t(x)$  in the space variable  $x$  and uniformly in small or big time  $t$ , the processes

$$Y = \sum_{i=k}^N S^{a_k, b_k, c_k, d_k}, \quad (71)$$

$$\text{or } Y = S^{\alpha, \beta, 1, 0} \circ Z,$$

where the coefficients  $(a_k, b_k, c_k, d_k)$  vary in a set  $\mathcal{D}_N$ , the processes  $S^{a_k, b_k, c_k, d_k}$  are independent, and  $S^{\alpha, \beta, 1}$  is independent of the subordinator  $Z$ . We emphasize that in (71),  $Y$  satisfies (13) and does not enjoy the scaling property (12) anymore.

- (i) If  $Y = \sum_{i=k}^N S^{a_k, b_k, c_k, d_k}$  and the stability coefficients  $a_k$  are pairwise different, we have an asymptotic scaling property; if  $i_\wedge = \text{Arg min}\{\alpha_i, 1 \leq i \leq N\}$  and  $i_\vee = \text{Arg max}\{\alpha_i, 1 \leq i \leq N\}$  and  $i = i_\vee$  (respectively,  $i_\wedge$ ), then

$$\frac{Y_t - \sum_{k=1}^N \delta_{t, a_k}}{(\gamma t)^{1/a_i}} \xrightarrow{d} S_1^{a_i, b_i, 1, 0}, \quad \text{as } t \rightarrow 0 \text{ (respectively, } t \rightarrow \infty). \quad (72)$$

The last property will be useful in Subsection 4.2 when taking the path  $u_n \rightarrow 0$  (respectively,  $u_n \rightarrow \infty$ ).

- (ii) If  $Y = S^{\alpha, \beta, 1, 0} \circ Z$ , we assume that the subordinator  $Z$  is itself attracted by a stable subordinator: for some  $0 < \varepsilon < 1$  and some (deterministic) speed  $r_t$ ,

$$\frac{Z_t}{r_t} \xrightarrow{d} S_1^{\varepsilon, 1, 1, 0}, \quad \text{as } t \rightarrow 0 \text{ (respectively, as } \infty). \quad (73)$$

The function  $t \mapsto r_t$  is necessarily a regularly varying function of order  $1/\varepsilon$  at 0 (respectively,  $\infty$ ):  $r_t = t^{1/\varepsilon} l(t)$  and  $l$  is slowly varying, i.e.,  $(l(\lambda t)/l(t)) \rightarrow 1, \forall \lambda > 0$ . Then, there exist  $\beta \in (-1, 1)$  and  $\gamma' > 0$ , such that

$$\frac{Y_t}{r_t^{1/\alpha}} \xrightarrow{d} S_1^{\varepsilon \alpha, \beta', \gamma', 0}, \quad \text{as } t \rightarrow 0 \text{ (respectively, } t \rightarrow \infty). \quad (74)$$

**4.1. The Scale Models Associated with Stable Processes Have the LAN Property.** The following result is a first application of Corollary 1.

**Theorem 2.** For the scale model (5), assume  $Y = S^{\alpha, \beta, \gamma, \delta}$  is a stable process, such that  $\delta = 0$  is null if  $\alpha < 1$  and  $|\beta| = 1$ . Recall  $\delta_{t, \alpha}$  is defined in (12). Let the path  $u_n$  satisfy  $l_n = (\gamma u_n)^{-1/\alpha} \delta_{u_n, \alpha} \rightarrow l \in \mathbb{R}$  and one of the following conditions:

- (i)  $u_n \rightarrow L \in (0, \infty)$
- (ii)  $u_n \rightarrow L = 0$  and  $n^R u_n \rightarrow \infty$ , for some  $R > 0$
- (iii)  $u_n \rightarrow L = +\infty$  and  $n^{-S} u_n \rightarrow 0$ , for some  $S > 0$

Then, the sequence of sequence of filtered statistical scale models  $E^n$  (15) have the LAN property with speed  $\sqrt{n}$  at each  $\theta \in \Theta$ . The asymptotic Fisher information quantity is given by

$$I(\theta) = \frac{1}{\theta^2} \left[ \int (y+l)^2 \frac{G'(y)^2}{G(y)} dy - 1 \right], \quad (75)$$

where  $G$  is the p.d.f. of  $S_1^{\alpha, \beta, 1, 0}$ .

**Remark 3.** If  $\alpha \in (0, 1)$ , then support of the law of  $S_1^{\alpha, \beta, \gamma, \delta}$  is  $[\delta, \infty)$  (respectively,  $(-\infty, \delta]$ ) if  $\beta = 1$  (respectively,  $\beta = -1$ ); otherwise, the support is whole  $\mathbb{R}$ . The assumption  $\delta = 0$  ensures that the support of the law of  $S_1^{\alpha, \beta, \gamma, \delta}$  satisfies the condition (C0) of Corollary 1. We are aware that the cases  $u_n \rightarrow 0$  and  $u_n \rightarrow \infty$  are not very realistic by the statistical point of view. The most interesting cases are as follows:

- (a)  $u_n = u \in (0, \infty)$ , then  $L = u$ , and the assumptions of Theorem 2 are satisfied. This is an essentially trivial result because we treat then a regular i.i.d. model.
- (b)  $u_n = (u/n), u \in (0, \infty)$ , then  $L = 0$ , and the assumptions of Theorem 2 are satisfied if and only if one of the following holds:
  - (i)  $\alpha < 1, \delta = 0$ , and then,  $l = 0$ ;
  - (ii)  $\alpha = 1, \beta = 0$ , and then,  $l = \delta/\gamma$ ;
  - (iii)  $\alpha > 1$ , and then,  $l = 0$ .

*Proof.* of Theorem 2. (1a) Recall that  $h_n$  denotes the infinitely differentiable p.d.f of  $S_{u_n}^{\alpha, \beta, \gamma, \delta}$ . Due to the scaling property (12), we have the following representations: for all  $k \in \mathbb{N}$  and  $x \in \text{support}(h_n)$ ,

$$(h_n)^{(k)}(x) = \frac{1}{(\gamma u_n)^{(k+1)/\alpha}} (G_1^{\alpha, \beta, 1, 0})^{(k)} \left( \frac{x - \delta_{u_n, \alpha}}{(\gamma u_n)^{1/\alpha}} \right), \quad (76)$$

where

$$\text{Support}(h_n) = \begin{cases} \mathbb{R}_+, & \text{if } 0 < \alpha < 1, \beta = 1, \\ \mathbb{R}_-, & \text{if } 0 < \alpha < 1, \beta = -1, \\ \mathbb{R}, & \text{otherwise.} \end{cases} \quad (77)$$

(1b) In [14, 17], we provided several properties of the p.d.f.  $G = G_1^{\alpha, \beta, 1, 0}$ . For instance, there exist positive constants  $A, B, C, D$  that depend explicitly on  $\alpha, \beta$ , such that

$$G(x) \begin{cases} \underset{0+}{\sim} \left( \text{respectively, } \underset{0-}{\sim} \right) \xi(x), & \text{if } \beta = 1 \text{ (respectively, } -1) \text{ and } 0 < \alpha < 1, \\ \underset{+\infty}{\sim} \left( \text{respectively, } \underset{-\infty}{\sim} \right) \chi(x), & \text{if } \beta \neq -1 \text{ (respectively, } 1) \text{ and } 0 < \alpha < 2, \\ \underset{+\infty}{\sim} \left( \text{respectively, } \underset{-\infty}{\sim} \right) \eta(x), & \text{if } \beta = -1 \text{ (respectively, } 1) \text{ and } \alpha = 1, \\ \underset{+\infty}{\sim} \left( \text{respectively, } \underset{-\infty}{\sim} \right) \xi(x), & \text{if } \beta = -1 \text{ (respectively, } 1) \text{ and } 1 < \alpha \leq 2. \end{cases} \quad (78)$$

where

$$\begin{aligned} \chi(x) &:= \frac{D}{|x|^{\alpha+1}}, \\ \xi(x) &:= B|x|^{(2-\alpha)/2(\alpha-1)} e^{-A|x|^{\alpha/(\alpha-1)}}, \\ \eta(x) &= C \exp\left(-e^{\pi|x|/2} + \frac{\pi|x|}{4}\right), \end{aligned} \quad (79)$$

and  $f(x) \underset{l}{\sim} g(x)$  means  $\lim_{x \rightarrow l} (f(x)/g(x)) = 1$ . Furthermore, with the convention  $(0/0) = 0$ , the functions

$$F_k(x) := \left| \frac{G^{(k)}(x)}{G(x)} \right|, \quad k \in \mathbb{N}, \quad (80)$$

are continuous on support  $(h_n)$ , given by (77), and there exist positive numbers  $a, b, c$ , depending explicitly on  $\alpha$  and  $\beta$  and  $k$ , such that

$$F_k(x) \begin{cases} \underset{0+}{\sim} \left( \text{respectively, } \underset{0-}{\sim} \right) a|x|^{k/(\alpha-1)}, & \text{if } \beta = 1 \text{ (respectively, } -1) \text{ and } 0 < \alpha < 1, \\ \underset{+\infty}{\sim} \left( \text{respectively, } \underset{-\infty}{\sim} \right) b|x|^{-k}, & \text{if } \beta \neq -1 \text{ (respectively, } 1) \text{ and } 0 < \alpha < 2, \\ \underset{+\infty}{\sim} \left( \text{respectively, } \underset{-\infty}{\sim} \right) c \exp\left(\frac{k\pi|x|}{2}\right), & \text{if } \beta = -1 \text{ (respectively, } 1) \text{ and } \alpha = 1, \\ \underset{+\infty}{\sim} \left( \text{respectively, } \underset{-\infty}{\sim} \right) a|x|^{k/(\alpha-1)}, & \text{if } \beta = -1 \text{ (respectively, } 1) \text{ and } 1 < \alpha \leq 2. \end{cases} \quad (81)$$

From the last equivalences, we see that for any non-negative integer  $s$ , we have the implication

$$0 \leq r \leq k \implies \lim_{|x| \rightarrow \infty} |x|^{2(1-\rho)(1+\alpha)} (|x|^r F_k)^s (G)^{2(1-\rho)} \in [0, \infty). \quad (82)$$

Thus, since  $0 < \rho < 1 - (1/(2(1+\alpha))) \Leftrightarrow 2(1-\rho)(1+\alpha) > 1$ , then

$$0 \leq r \leq k,$$

$$0 < \rho < 1 - \frac{1}{(\alpha+1)} \implies x \mapsto (|x|^r F_k(x))^s G(x)^{2(1-\rho)} \in L^1(dx). \quad (83)$$

(2) We need to verify the assumptions of Corollary 1, i.e., to check (C1):



$$\begin{aligned}
I_n &= \int \left[ 1 + x \frac{h'_n(x)}{h_n(x)} \right]^2 h_n(x) dx \longrightarrow I \\
&= \int (y+l)^2 \frac{(G')^2}{G}(y) dy - 1 \in (0, \infty), \quad \text{as } n \longrightarrow \infty,
\end{aligned} \tag{84}$$

and also (C2); there exists  $a \in (0, (1/2))$ , such that for  $\rho \in \{(1/2), a, 1-a\}$ , one has

$$\begin{aligned}
\frac{1}{n} J_n(\rho) &= \frac{1}{n} \int \frac{(j_n)^2}{(h_n)^{2\rho}}(x) dx \longrightarrow 0, \quad j_n(x) \\
&= \left[ \left| 1 + x \frac{h'_n(x)}{h_n(x)} \right|^2 + \left| 2 + 4x \frac{h'_n(x)}{h_n(x)} + x^2 \frac{h''_n(x)}{h_n(x)} \right| \right] h_n(x).
\end{aligned} \tag{85}$$

(3) The scaling property (76) and the corresponding change of variables give the following representation of the quantity  $I_n$  in (84):

$$I_n = \int \left[ 1 + (y+l_n) \frac{G'(y)}{G(y)} \right]^2 G(y) dy. \tag{86}$$

Using (82) and the fact that  $l_n \longrightarrow l \in \mathbb{R}$ , we obtain

$$x \mapsto \sup_{n \in \mathbb{N}} \left[ 1 + (y+l_n) \frac{G'(y)}{G(y)} \right]^2 G(y) \in L^1(dy), \tag{87}$$

$$\lim_{n \rightarrow \infty} I_n = \int \left[ 1 + (y+l) \frac{G'(y)}{G(y)} \right]^2 G(y) dy.$$

Developing the last expression, integrating by parts and using the fact that  $G(y)$  and  $yG(y)$  both tend to 0 as  $y$  goes to each endpoint of the support (77), we recover (84).

(4) Again, by the change of variables corresponding to (76) and by the representation (85), one has

$$J_n(\rho) = (\gamma u_n)^{(2\rho-1)/\alpha} \int \left[ \left| 1 + (y+l_n) \frac{G'(y)}{G(y)} \right|^2 + \left| 2 + 4(y+l_n) \frac{G'(y)}{G(y)} + (y+l_n)^2 \frac{G''(y)}{G(y)} \right| \right]^2 G(y)^{2(1-\rho)} dy. \tag{88}$$

Thanks to (83) and to the fact that  $l_n \longrightarrow l \in \mathbb{R}$ , and it is clear that if  $\rho \in (0, 1 - 1/2(\alpha + 1))$ , then

$$\sup_{n \in \mathbb{N}} \left[ \left| 1 + (y+l_n) \frac{G'(y)}{G(y)} \right|^2 + \left| 2 + 4(y+l_n) \frac{G'(y)}{G(y)} + \left( y + l_n^2 \frac{G''(y)}{G(y)} \right) \right| \right]^2 G(y)^{2(1-\rho)} \tag{89}$$

is integrable. Let  $\epsilon := (1/2) - (1/(2(\alpha + 1)))$ . To prove the convergence (85), it is enough to have

$$\rho \in \left( 0, \epsilon + \frac{1}{2} \right), \tag{90}$$

$$\lim_{x \rightarrow \infty} \frac{u_n^{(2\rho-1)/\alpha}}{n} = 0. \tag{91}$$

(5) Now, we distinguish between the values of  $L = \lim_{n \rightarrow \infty} u_n$ .

- (a) If  $L = 0$  and if  $\rho \geq (1/2)$ , then (91) is true. By assumptions, we have  $(1/u_n) \leq n^R$ , for large  $n$ . If  $\rho < (1/2)$ , then we have (91) as soon as  $(R(1-2\rho)/\alpha) < 1$ , which is equivalent to  $\rho > (1/2) - (\alpha/(2R))$ . Thus, we only have to choose

$\epsilon' = (\epsilon \wedge \alpha / (4R))$  and  $a = (1/2) - \epsilon'$  to get (90) to obtain (91) for  $\rho \in \{(1/2), a, 1-a\}$ .

- (b) If  $L \in (0, \infty)$ , then (91) is always true.

- (c) If  $L = +\infty$  and if  $\rho \leq (1/2)$ , then (91) is true. As in (5a), we have  $u_n \leq n^S$  for large  $n$ . If  $\rho > (1/2)$  then we have (91) as soon as  $(S(2\rho-1)/\alpha) < 1$ , which is equivalent to  $\rho < (1/2) + (\alpha/(2S))$ . Thus, we only need to choose  $\epsilon'' = (\epsilon \wedge \alpha / (4S))$  and  $a = (1/2) - \epsilon''$  to obtain (90) and (91) for  $\rho \in \{1/2, a, 1-a\}$ .  $\square$

*4.2. The Scale Models Associated with the Sum of Independent Stables Processes Have the LAN Property.* This subsection gives a second example which also generalizes the previous one and achieves the situation (13). Define  $\bar{K}(\alpha) = 1$  if  $\alpha \leq 1$

and  $\bar{K}(\alpha) = (\alpha - 2)/\alpha$  and assume the following restrictions on the skewness parameters:

( $S_{a,b}$ ): we have  $N$  independent stable processes  $S^{a_k, b_k, c_k, 0}$ , such that the parameters satisfy

$$(a) \ a_1 < a_2 < \dots < a_N < 2 \text{ and } \mathcal{D} = \bigcap_{k=1}^N \left[ a_k, \frac{2}{(1 + |b_k \bar{K}(a_k)|)} \right] \neq \emptyset; \quad (92)$$

$$(b) \ b_k = 0 \text{ if } a_k = 1 \text{ and } B = \max \left\{ \frac{|b_k \bar{K}(a_k)|}{\bar{K}(a_N)}, \ 1 \leq k \leq N \right\} < 1.$$

Let  $Y = \sum_{k=1}^N S^{a_k, b_k, c_k, 0}$  and  $Y^i$  be the processes defined by

$$Y_t^i = \frac{Y_t}{t^{1/a_i}}, \quad i = 1 \text{ or } i = N \text{ and } t > 0. \quad (93)$$

The processes  $Y^i$  satisfy the asymptotic scaling property (72). Denote by  $H_t$  the p.d.f of  $Y_t$ ,

$$H_t = G_t^{a_1, b_1, c_1, 0} * \dots * G_t^{a_N, b_N, c_N, 0}, \quad (94)$$

and by  $H_{i,t}$ , the one of  $Y_t^i$ . Then,  $h_n = H_{u_n}$  satisfies

$$(h_n)^{(k)}(x) = (u_n c_i)^{-(k+1)/a_i} (H_{i, u_n})^{(k)}((u_n c_i)^{-1/a_i} x). \quad (95)$$

In [14, 17], we showed that the following functions  $H_0$  and  $H_\infty$  given by

$$H_L := \begin{cases} \lim_{t \rightarrow \infty} H_{1,t}(x) = G_1^{a_1, b_1, 1, 0}(x), & \text{if } L = +\infty, \\ \lim_{t \rightarrow 0^+} H_{N,t}(x) = G_1^{a_N, b_N, 1, 0}(x), & \text{if } L = 0, \end{cases} \quad (96)$$

are well defined, and the above convergence holds uniformly in  $x \in \text{support}(G_1^{a_i, b_i, 1, 0})$  and still hold for the successive derivatives. As one can guess, we are going to exploit identity (95) and state the following result.

**Theorem 3.** *Let  $(u_n)_n$  be a sequence satisfying one of the following conditions:*

- (i)  $u_n \rightarrow L \in (0, \infty)$
- (ii)  $u_n \rightarrow L = 0$ , and there exists  $R > 0$ , such that  $n^R u_n \rightarrow +\infty$ ;
- (iii)  $u_n \rightarrow L = +\infty$ , and there exists  $S > 0$ , such that  $n^{-S} u_n \rightarrow 0$ .

For the scale model (5) with  $Y = \sum_{k=1}^N S^{a_k, b_k, c_k, 0}$ , assume ( $S_{a,b}$ ). Then, the sequence of filtered statistical scale models  $E^n$  (15) have the LAN property with speed  $\sqrt{n}$  at each value  $\theta \in \Theta$ . With  $H_L$  given in (95), the asymptotic Fisher information quantity has the following expression:

$$I(\theta_0) = \frac{I_L}{\theta^2}, \quad (97)$$

$$I_L = \int y^2 \frac{(H_L')^2(y)}{H_L(y)} dy - 1.$$

*Remark 4*

- (i) Let us briefly explain the nature of the assumption in Theorem 3. In [17], conditions of type ( $S_{a,b}$ ) allowed us to show that  $Y_t^i$  is distributed as an  $\alpha$ -stable variable mixed on the skewness and scale parameters by other processes. More precisely, for all  $t > 0$ , we have these identities in distribution: for all  $\alpha$  in the interior of the domain  $\mathcal{D}$  (given in ( $S_{a,b}$ )) and for all  $t > 0$ , there exist a r.v.  $\beta_t^i$  and  $\gamma_t^i$ , such that

$$Y_t^i \stackrel{d}{=} S_1^{\alpha, \beta_t^i, \gamma_t^i, 0} = (\gamma_t^i)^{1/\alpha} S_1^{\alpha, \beta_t^i, 1, 0}. \quad (98)$$

The processes  $\beta$  and  $\gamma^i$  are

$$|\beta_t^i| \leq B, \quad (99)$$

$$\frac{C}{t^{\alpha/a_i}} Z_t \leq \gamma_t^i \leq \frac{D}{t^{\alpha/a_i}} Z_t,$$

Where  $Z_t = \sum_{k=1}^n S_t^{(a_k/\alpha), 1, 1, 0}$  is a sum of independent standard stable subordinators, and the non-negative numbers  $C < D$  depend only on  $(\alpha, a_1, b_1, c_1, \dots, a_N, b_N, c_N)$ . In the case where  $b_k \bar{K}(a_k)$  is a constant for all  $k = 1, \dots, N$ , then  $\beta_t^i = b_1 \bar{K}(a_1)$ ,  $\gamma_t^i$  is distributed as a normalized sum of independent stable subordinators, and the converge in the following distribution holds.

$$(\beta_t^i, \gamma_t^i) \rightarrow \left( \frac{b_i \bar{K}(a_i)}{\bar{K}(\alpha)}, S_1^{(a_i/\alpha), 1, 1, 0} \right),$$

if  $i = 1$  and  $t \rightarrow \infty$ , or if  $i = N$  and  $t \rightarrow 0$ .

$$(100)$$

Furthermore, notice that the assumption  $(\mathbf{S}_{a,b})$  is satisfied in the symmetrical cases

- (ii) In general, when  $\beta, \gamma, \delta$  are r.v.'s lying in the set of admissible parameters and  $\mathcal{F}$  is the  $\sigma$ -field generated by them, we gave in [17] a structure of the  $\mathcal{F}$ -conditional Lévy process to  $(S_r^{\alpha,\beta,\gamma,\delta})_{r \geq 0}$ . See also [13] for the notion of the  $\mathcal{F}$ -conditional Lévy process. If  $\beta$  is deterministic,  $S_1^{\alpha,\beta,\gamma,0}$  is simply distributed as  $\gamma^{1/\alpha} S_1^{\alpha,\beta,1,0}$ , and with our construction, we allow the same identity even if  $\beta$  is random and correlated with  $\gamma$ . We also considered in [17] the densities of some families of mixed stable variables  $(S_1^{\alpha,\beta,\gamma,\delta})_{t \in T}$  and gave several examples when these densities and their derivatives behave like the proper stable densities and this uniformly in  $t \in T$ .
- (iii) It is also possible to state a version of Theorem 3 with stable processes with drifts. It is enough to strengthen the conditions on the asymptotic as done in Theorem 2. We consider that Theorem 3 is far from being exhaustive. It is produced in the aim of illustrating the difficulty of this case. If one wants to reduce the assumption  $(\mathbf{S}_{a,b})$  on the coefficients, then additional controls on the densities are needed.

Before tackling the proof of Theorem 3, we need the following result borrowed from [17].

**Theorem 4** (See [17]). *Controls of the densities of some mixed stable variables  $(S_1^{\alpha,\beta,\gamma,r,0})_{r \in \mathcal{R}}$ . Let  $(\gamma_r)_{r \geq 0}$  be a pure jump subordinator characterized by*

$$\mathbb{E}[e^{-\lambda \gamma_1}] = \exp \int_{(0,\infty)} (e^{-\lambda x} - 1) \nu(dx), \quad \lambda \geq 0. \quad (102)$$

Assume  $\nu(x) = \nu(x, \infty) = x^{-a} L(x)$ , where  $a \in (0, 1)$ , and  $L$  is a slowly varying function. For  $r, x > 0$ , define

$$\begin{aligned} \nu_r &:= \sup \left\{ t > 0 : \nu(t) > \frac{1}{r} \right\}, \\ \nu_r(x) &:= r \nu(x \nu_r, \infty), \\ \bar{\nu}_r &:= \frac{\gamma_r}{\nu_r}. \end{aligned} \quad (103)$$

- (a) *If  $L$  is slowly varying at infinity and  $r \rightarrow \infty$  or if  $L$  is slowly varying at zero, then*

$$\nu_r(x) \rightarrow \frac{1}{x^a}, \quad x > 0, \quad (104)$$

$$\bar{\nu}_r \xrightarrow{d} S_1^{a,1,(\Gamma(1-a)/a),0}, \quad \text{as } r \rightarrow 0+.$$

- (b) *Moreover, assume that there exist  $0 < c \leq a \leq d < 1$  and  $K \geq 1$ , such that*

$$\left( \frac{y}{x} \right)^{a-c} \leq \frac{L(y)}{L(x)} \leq K \left( \frac{y}{x} \right)^{a-d}, \quad 0 < y < x. \quad (105)$$

Let  $R' > R > 0$  and  $(\gamma_r^p)_{t \in R_p}$  denote one of these families:

$R_1 = R_4 = (0, R], R_2 = [R, R'], R_3 = [R, \infty)$ , and  $\gamma_r^1 = \gamma_r^2 = \gamma_r$ ,  $\gamma_r^3 = \bar{\gamma}_r$  with  $L$  slowly varying at  $\infty$ , and  $\gamma_r^4 = \bar{\gamma}_r$ , with  $L$  slowly varying at 0. Let  $\alpha \in (0, 2)$  and  $(\beta_r)_{r \geq 0}$  be any family of r.v.'s, such that  $\sup_{r \geq 0} |\beta_r| \leq B$ , for some  $B \in [0, 1)$ , ( $B = 0$ , if  $\alpha = 1$ ). Then, the p.d.f.  $G_r^p$  of the mixed stable variables  $S_1^{\alpha,\beta_r,\gamma_r^p}$  are infinitely differentiable and satisfy the following: for all  $k \in \mathbb{N}$  and all  $p$ , we have

$$\begin{aligned} 0 &< \liminf_{|x| \rightarrow \infty} \inf_{r \in R_p} |x|^{1+\alpha} {}^d G_r^p(x), \\ \limsup_{|x| \rightarrow \infty} \sup_{r \in R_p} |x|^{1+\alpha c} G_r^p(x) &< \infty, \end{aligned} \quad (106)$$

$$\limsup_{|x| \rightarrow \infty} \sup_{r \in R_p, x \in \mathbb{R}} \frac{|x^k (G_r^p)^{(k)}(x)|}{G_r^p(x)} < \infty.$$

For all  $X > 0, p \neq 1$ , we have

- (c) *If  $(\gamma_r')_{r \geq 0}$  is a family of r.v.'s, such that  $(\gamma_r'/K) \leq \gamma_r' \leq K \gamma_r'$  for some  $K > 1$  and all  $r \geq 0$ , then the controls (106) and (17) remain true for the p.d.f.'s obtained by replacing  $(\gamma_r, \bar{\gamma}_r)$  by  $(\gamma_r', (\gamma_r'/\nu_r'))$ , where  $\nu_r$  is given by (103).*

**Remark 5.** If  $\gamma$  is a pure jump  $a$ -stable subordinator, then  $\nu_r(x) = x^{-a}$ , and the scaling property gives  $\bar{\gamma}_r \stackrel{d}{=} S_1^{a,1,\Gamma(1-a)/a}$ . Furthermore, if  $\beta_r = \beta, r > 0$ , is deterministic, then  $S_1^{\alpha,\beta,\bar{\gamma}_r} \stackrel{d}{=} S_1^{\alpha a, \beta', \gamma'}$ , for some  $\beta' \in (-1, 1), \gamma' > 0$ . The estimates (106) and (17) are an immediate consequence of the behavior of the stable densities given in the Proof of Theorem 2.

**Example 1.** The following are examples of processes satisfying the conditions of Theorem 4. Let  $0 < b, b_1, \dots, b_N < 1$ , and  $c, c_1, \dots, c_N > 0$ . Let  $\gamma^1, \gamma^2$  be pure jump subordinators whose Lévy measures are, respectively, equal to

$$\begin{aligned} \nu_1(dx) &= \sum_{k=1}^N \frac{c_k}{x^{b_k+1}} 1_{x>0} dx, \\ \nu_2(dx) &= \frac{c}{x^{b+1}} 1_{x>0} dx + \delta_1(dx). \end{aligned} \quad (108)$$

The process  $\gamma^1$  is the sum of independent stable subordinators, and  $\gamma^2$  is the independent sum of a stable subordinator and a standard Poisson process. With  $b_\vee = \max b_i$  and  $b_\wedge = \min b_i$ , notice that

$$\nu_1(x) = \frac{L_1^\vee(x)}{x^{b_\vee}} = \frac{L_1^\wedge(x)}{x^{b_\wedge}}, \quad (109)$$

$$\nu_2(x) = \frac{L_2(x)}{x^b},$$

where  $L_1^\vee, L_2$  are slowly varying at 0,  $L_1$  is slowly varying at  $\infty$ , and

$$0 < y < x \implies \left(\frac{y}{x}\right)^{b_\nu - b_\lambda} \leq \frac{L_1^\vee(y)}{L_1^\vee(x)} \leq 1,$$

$$1 \leq \frac{L_1^\wedge(y)}{L_1^\wedge(x)} \leq \left(\frac{y}{x}\right)^{b_\lambda - b_\nu}, \quad (110)$$

$$\left(\frac{y}{x}\right)^{b/2} \leq \frac{L_2(y)}{L_2(x)} \leq 2.$$

The following result is a consequence of Theorem 4.

$$0 \leq r \leq k,$$

$$0 < \rho < 1 - \frac{1}{(a_1 + 1)} \implies \sup_{t \in T_i} (|z|^r F_{i,t}^k(z))^s H_{i,t}(z)^{2(1-\rho)} \text{ is integrable.} \quad (112)$$

*Proof.* By Remark 5, notice that the Lévy measure of subordinator  $Z$  in (99) has the required conditions. According to Theorem 4 (c), these conditions imply that the family  $(H_{1,t})_{t \in T_1}$  behaves like  $(G_r^3)_{r \in \mathbb{R}_3}$  and that  $(H_{N,t})_{t \in T_N}$  behaves like  $(G_r^4)_{r \in \mathbb{R}_4}$  with  $c = a_1/\alpha$  and  $d = a_N/\alpha$ .  $\square$

**Corollary 2.** Assume  $(\mathbf{S}_{a,b})$ . Let  $H_{i,t}$  be the p.d.f of  $Y_t^i$ ,  $i = 1, N, t > 0$ . Let  $T > 0, T_1 = [T, \infty), T_N = [0, T)$ , and

$$F_{i,t}^k(z) = \left| \frac{(H_{i,t})^{(k)}(z)}{H_{i,t}(z)} \right|, \quad k \in \mathbb{N}, z \in \mathbb{R}. \quad (111)$$

Then, for every nonnegative integer  $s$ , we have

*Proof of Theorem 3.* We will check the assumptions of Corollary 1, which consist in the convergence of the integrals

$$I_n = \int \left[ 1 + z \frac{(H_{i,u_n})'}{H_{i,u_n}}(z) \right]^2 H_{i,u_n}(z) dz,$$

$$J_n(\rho) = (\gamma u_n)^{(2\rho-1)/\alpha} \int \left[ \left| 1 + z \frac{(H_{i,u_n})'}{H_{i,u_n}}(z) \right|^2 + \left| 2 + 4z \frac{(H_{i,u_n})'}{H_{i,u_n}}(z) + z^2 \frac{(H_{i,u_n})''}{H_{i,u_n}}(z) \right|^2 \right] H_{i,u_n}(z)^{2(1-\rho)} dz. \quad (113)$$

The latter is guaranteed by Corollary 2, since the functions  $F_{i,t}^k$  satisfy

$$\sup_{n \in \mathbb{N}} (|z|^r F_{i,u_n}^k)^s (H_{i,u_n})^{2(1-\rho)} \in L^1(dz), \quad (114)$$

for  $s \in \{0, 1, 2, 3, 4\}, r \in \{0, 1, \dots, k\}, 0 \leq k \leq 2$ , and  $\rho \leq 1 - (1/(a_1 + 1))$ . The rest is obtained by reproducing the Proof of Theorem 2.  $\square$

*Remark 6.* Notice that the main argument for proving Theorem 3 is the behavior of the densities uniformly in time. Theorem 4 provides many other examples. For example, with the same proof as in Theorem 3, one could state a version with stable processes time changed by any independent “nice” subordinator. The time change process could be the sum of a stable subordinator and a Poisson process (Remark 5). Finally, it appears that more investigation concerning the behavior in small time of p.d.f.’s of Lévy processes attracted by stable processes is crucial for statistical purposes.

## 5. How to Build a LAN Model from Another LAN Model?

In this section, we investigate to which extent the choice of the asymptotic is crucial. Assume we start from a LAN model associated to the observations of a Lévy process  $X$  along a discretization scheme  $i u_n, 1 \leq i \leq n$ . Can we affirm that the model associated to the observations of  $X + \tilde{X}$ , where  $\tilde{X}$  is another independent Lévy process, also enjoys the LAN property with the same discretization scheme? We need some preliminaries and two lemmas to answer the last question.

Consider two independent Lévy processes  $Y$  and  $N$  defined on some probability space  $(\Omega, \mathcal{F}, \mathbb{P})$  with values in the Skorohod space  $\Omega = \mathbb{D}(\mathbb{R}^+, \mathbb{R})$  (when the processes  $Y$  and  $N$  are seen as infinite-dimensional random variables). Assume that  $N$  is a nondrifted compound Poisson process with Lévy measure  $\nu$ , and consider the process  $\tilde{Y} := Y + N$ . Recall that the increment process  $X^n$  of  $X$ , observed along a scheme  $u_n$ , is defined in (14) by

$$X_j^n = X_{(j+1)u_n} - X_{ju_n}, \quad 0 \leq j \leq n-1. \quad (115)$$

For  $\theta \in \Theta$ , suppose we observe  $X^n = \theta Y^n$ ,  $\tilde{X}^n = \theta \tilde{Y}^n$ , and let

$$\begin{aligned} \mathbb{P}_\theta &= \mathcal{L}aw(\theta Y | \bar{\mathbb{P}}), \\ \tilde{\mathbb{P}}_\theta &= \mathcal{L}aw(\theta \tilde{Y} | \bar{\mathbb{P}}). \end{aligned} \quad (116)$$

The probability measure  $\mathbb{P}_\theta^n$  (respectively,  $\tilde{\mathbb{P}}_\theta^n$  and the scale models  $E^n$  (respectively,  $\tilde{E}^n$ ) correspond to  $X$  (respectively,  $\tilde{X}$ ) as in (15) and (16).

Recall that if  $Q, Q'$  are two probability measures on some sample space, then the total variation distance  $\|Q - Q'\|$  is the quantity

$$\|Q - Q'\| = \sup_{\phi \in \Phi} |\mathbb{E}_Q(\phi) - \mathbb{E}_{Q'}(\phi)|, \quad (117)$$

$$\Phi = \{\phi: \Omega \rightarrow [-1, 1], \phi \text{ measurable}\}.$$

Lecam's lemma [2] is as follows:

**Lemma 1.** For every probability measures  $Q, Q', R, R'$ , we have the inequality

$$\int 1 \wedge \left| \frac{dR}{dQ} - \frac{dR'}{dQ'} \right| d(Q + Q') \leq \|Q - Q'\| + 2\|R - R'\| + (2\|Q - Q'\| \|R + R'\|)^{1/2}. \quad (118)$$

We also have the following result.

**Lemma 2.** If  $\lim_{n \rightarrow \infty} nu_n = 0$ , then  $\lim_{n \rightarrow \infty} \sup_{\theta \in \Theta} \|\mathbb{P}_\theta^n - \tilde{\mathbb{P}}_\theta^n\| = 0$ .

*Proof.* Since

$$\bar{\mathbb{P}}(N_{u_n} \in dy) = e^{-\nu(\mathbb{R})u_n} \sum_{k=0}^{\infty} \frac{u_n^k}{k!} \nu^{*k}(dy), \quad (119)$$

$$\bar{\mathbb{P}}(N_{u_n} = 0) \geq e^{-\nu(\mathbb{R})u_n},$$

and since  $N$  has stationary and independent increments, we have

$$\begin{aligned} \|\mathbb{P}_\theta^n - \tilde{\mathbb{P}}_\theta^n\| &= \sup_{\phi \in \Phi} \left| \mathbb{E}_{\mathbb{P}_\theta^n}[\phi(X)] - \mathbb{E}_{\tilde{\mathbb{P}}_\theta^n}[\phi(X)] \right| = \sup_{\phi \in \Phi} \left| \mathbb{E}_{\mathbb{P}_\theta}[\phi(X^n)] - \mathbb{E}_{\tilde{\mathbb{P}}_\theta}[\phi(X^n)] \right| \\ &= \sup_{\phi \in \Phi} \left| \mathbb{E}_{\bar{\mathbb{P}}}[\phi(\theta Y^n)] - \mathbb{E}_{\bar{\mathbb{P}}}[\phi(\theta \tilde{Y}^n)] \right| = \sup_{\phi \in \Phi} \left| \mathbb{E}_{\bar{\mathbb{P}}}[\phi(\theta Y^n)] - \mathbb{E}_{\bar{\mathbb{P}}}[\phi(\theta(Y^n + N^n))] \right| \\ &= \sup_{\phi \in \Phi} \left| \mathbb{E}_{\bar{\mathbb{P}}}[\phi(\theta Y^n)] - \mathbb{E}_{\bar{\mathbb{P}}}[\phi(Y^n + N^n)] \right| = \sup_{\phi \in \Phi} \left| \mathbb{E}_{\bar{\mathbb{P}}}[(\phi(Y^n) - \phi(Y^n + N^n))1_{N^n \equiv 0}] \right| \\ &\leq 2\bar{\mathbb{P}}(N^n \neq 0) = 2(1 - \bar{\mathbb{P}}(N^n \equiv 0)) = 2(1 - \bar{\mathbb{P}}(N_{(j+1)u_n} - N_{ju_n} = 0, \quad \forall 0 \leq j \leq n)) \\ &\leq 2(1 - \bar{\mathbb{P}}(N_{u_n} = 0))^n \leq 2(1 - e^{-\nu(\mathbb{R})nu_n}). \end{aligned} \quad (120)$$

It is now clear that  $\|\mathbb{P}_\theta^n - \tilde{\mathbb{P}}_\theta^n\|$  goes to 0, uniformly in  $\theta$  as  $nu_n \rightarrow 0$ .

Now, we are able to complete Far's problem [18], which treats the case where  $Y$  is a Brownian motion and where the discretization path is  $u_n = 1/n$ , i.e.,  $\lim_{n \rightarrow \infty} nu_n = 1$ .  $\square$

**Theorem 5.** Assume  $\lim_{n \rightarrow \infty} nu_n = 0$ . If the scale model (5)  $E^n$  associated to the process  $X$  has the LAN property with speed  $\sqrt{n}$  in a point  $\theta_0 \in \Theta$ , then so is the scale model  $\tilde{E}^n$  associated to the process  $\tilde{X}$ .

*Proof* of Theorem 5. (1) Fix  $\theta_0 \in \Theta$ , and  $J$  is a finite subset of  $\mathbb{R}$  and  $\xi \in \mathbb{R}$ . We shall prove that the weak functional

convergence (22) of the likelihood processes  $(Z_t^{n,\eta\xi})_{\eta \in J}$  of  $E^n$  yields the one of the likelihood processes  $(\tilde{Z}_t^{n,\eta\xi})_{\eta \in J}$  of  $\tilde{E}^n$ . The expression of the likelihood processes is given by (21), and for more convenience, we denote them from now on by

$$\begin{aligned} \mathbf{Z}_t^n &= \left( Z_k^{n,\eta\xi} \right)_{\eta \in J}, \\ \tilde{\mathbf{Z}}_t^n &= \left( \tilde{Z}_t^{n,\eta\xi} \right)_{\eta \in J}, \\ \mathbf{Z}'_t &= \left( Z'_t{}^{\eta\xi} \right)_{\eta \in J}, \quad t \in [0, 1]. \end{aligned} \quad (121)$$

We need to show the following convergence in laws:

$$\mathcal{L}aw\left(\mathbf{Z}^n | \mathbb{P}'_{[\xi]_n}\right) \longrightarrow \mathcal{L}aw\left(\left(\mathbf{Z}'^{\eta\xi}\right)_{\eta \in J} | \mathbb{P}'_\xi\right) \implies \mathcal{L}aw\left(\tilde{\mathbf{Z}}^n | \bar{\mathbb{P}}'_{[\xi]_n}\right) \longrightarrow \mathcal{L}aw\left(\left(\mathbf{Z}'^{\eta\xi}\right)_{\eta \in J} | \mathbb{P}'_\xi\right), \quad \text{as } n \rightarrow \infty, \quad (122)$$

or equivalently, for every  $K$ -Lipschitz function  $f: \mathbb{D}(\mathbb{R}_+, \mathbb{R}^J) \rightarrow \mathbb{R}$ , bounded by a constant  $C > 0$ , we need to show that

$$\lim_{n \rightarrow \infty} \mathbb{E}_{\mathbb{P}_{[\xi]_n}^n} [f(\mathbf{Z}^n)] = \mathbb{E}_{\mathbb{P}'_\xi} [f(\mathbf{Z}')] \implies \lim_{n \rightarrow \infty} \mathbb{E}_{\tilde{\mathbb{P}}_{[\xi]_n}^n} [f(\tilde{\mathbf{Z}}^n)] = \mathbb{E}_{\mathbb{P}'_\xi} [f(\mathbf{Z}')]. \quad (123)$$

(2) For such functions  $f$ , we will control the difference:

$$\mathbb{E}_{\mathbb{P}_{[\xi]_n}^n} [f(\mathbf{Z}^n)] - \mathbb{E}_{\tilde{\mathbb{P}}_{[\xi]_n}^n} [f(\tilde{\mathbf{Z}}^n)] = \left( \mathbb{E}_{\mathbb{P}_{[\xi]_n}^n} [f(\mathbf{Z}^n)] - \mathbb{E}_{\tilde{\mathbb{P}}_{[\xi]_n}^n} [f(\mathbf{Z}^n)] \right) + \left( \mathbb{E}_{\tilde{\mathbb{P}}_{[\xi]_n}^n} [f(\mathbf{Z}^n)] - \mathbb{E}_{\tilde{\mathbb{P}}_{[\xi]_n}^n} [f(\tilde{\mathbf{Z}}^n)] \right). \quad (124)$$

In virtue of Lemma 2, we have

$$\left| \mathbb{E}_{\mathbb{P}_{[\xi]_n}^n} [f(\mathbf{Z}^n)] - \mathbb{E}_{\tilde{\mathbb{P}}_{[\xi]_n}^n} [f(\tilde{\mathbf{Z}}^n)] \right| \leq C \sup_{\theta \in \Theta} \|\mathbb{P}_\theta^n - \tilde{\mathbb{P}}_\theta^n\| \rightarrow 0, \quad \text{as } n \rightarrow \infty. \quad (125)$$

For every  $\varepsilon > 0$ , we have

$$\begin{aligned} \mathbb{E}_{\tilde{\mathbb{P}}_{[\xi]_n}^n} [f(\mathbf{Z}^n) - f(\tilde{\mathbf{Z}}^n)] &= \mathbb{E}_{\tilde{\mathbb{P}}_{[\xi]_n}^n} \left[ (f(\mathbf{Z}^n) - f(\tilde{\mathbf{Z}}^n)) 1_{|\mathbf{Z}^n - \tilde{\mathbf{Z}}^n| \leq \varepsilon} \right] + \mathbb{E}_{\tilde{\mathbb{P}}_{[\xi]_n}^n} \left[ (f(\mathbf{Z}^n) - f(\tilde{\mathbf{Z}}^n)) 1_{|\mathbf{Z}^n - \tilde{\mathbf{Z}}^n| > \varepsilon} \right] \\ \left| \mathbb{E}_{\tilde{\mathbb{P}}_{[\xi]_n}^n} [f(\mathbf{Z}^n)] - f(\tilde{\mathbf{Z}}^n) \right| &\leq \varepsilon K + 2C \tilde{\mathbb{P}}_{[\xi]_n}^n (|\mathbf{Z}^n - \tilde{\mathbf{Z}}^n| > \varepsilon). \end{aligned} \quad (126)$$

With representation (21), observe that  $\mathbf{Z}^n$  and  $\tilde{\mathbf{Z}}^n$  are a step process, time-dependent, up to  $\lfloor nt \rfloor$ ,  $t \in [0, 1]$ . Then, denoting

$$\tau^n = \inf \left\{ 1 \leq j \leq n \text{ s.t. } |\mathbf{Z}_j^n - \tilde{\mathbf{Z}}_j^n| > \varepsilon, \quad \forall \eta \in J, \xi \in \mathbb{R} \right\}, \quad (127)$$

and using Markov in equality, we obtain

$$\begin{aligned} \tilde{\mathbb{P}}_{[\xi]_n}^n (|\mathbf{Z}^n - \tilde{\mathbf{Z}}^n| > \varepsilon) &= \tilde{\mathbb{P}}_{[\xi]_n}^n (|\mathbf{Z}_{\tau^n}^n - \tilde{\mathbf{Z}}_{\tau^n}^n| > \varepsilon) = \tilde{\mathbb{P}}_{[\xi]_n}^n (|\mathbf{Z}_i^n - \tilde{\mathbf{Z}}_j^n| > \varepsilon, \quad \forall 1 \leq j \leq n) \\ &\leq \frac{1}{\varepsilon} \mathbb{E}_{\tilde{\mathbb{P}}_{[\xi]_n}^n} [1 \wedge |\mathbf{Z}_{\tau^n}^n - \tilde{\mathbf{Z}}_{\tau^n}^n|]. \end{aligned} \quad (128)$$

Applying Lemma 1 with  $R = \mathbb{P}_{[\eta]_n}^n$ ,  $Q = \mathbb{P}_{[\xi]_n}^n$ ,  $R' = \tilde{\mathbb{P}}_{[\eta]_n}^n$ ,  $Q' = \tilde{\mathbb{P}}_{[\xi]_n}^n$ , we obtain

$$\mathbb{E}_{\tilde{\mathbb{P}}_{[\xi]_n}^n} [1 \wedge |\mathbf{Z}_{\tau^n}^n - \tilde{\mathbf{Z}}_{\tau^n}^n|] \leq 2 \sup_{\theta \in \Theta} \left[ 3 \|\mathbb{P}_\theta^n - \tilde{\mathbb{P}}_\theta^n\| + (2 \|\mathbb{P}_\theta^n - \tilde{\mathbb{P}}_\theta^n\|)^{1/2} \right], \quad (129)$$

and then, Lemma 2 gives

$$\lim_{n \rightarrow \infty} \sup_{\eta \in J, \xi \in \mathbb{R}} \tilde{\mathbb{P}}_{[\xi]_n}^n (|\mathbf{Z}^n - \tilde{\mathbf{Z}}^n| > \varepsilon) = 0. \quad (130)$$

The latter, together with (126), allows to conclude that

$$\lim_{n \rightarrow \infty} \mathbb{E}_{\mathbb{P}_{[\xi]_n}^n} [f(\mathbf{Z}^n) - f(\tilde{\mathbf{Z}}^n)] = 0. \quad (131)$$

□

## Data Availability

No data were used to support this study.

## Conflicts of Interest

The author declares that there are no conflicts of interest.

## Acknowledgments

The work was supported by the “Research Supporting Project number (RSP-2021/162), King Saud University, Riyadh, Saudi Arabia.” The author would like to thank the referees for their valuable comments and recommendations that improved the content of the article. The author is also grateful to Jean Jacod who introduced him to the topic of statistic of Lévy processes.

## References

- [1] O. E. Barndorff-Nielsen, T. Mikosch and S. I. Resnick, *Lévy Processes: Theory and Applications* Birkhäuser, Boston, MA, USA, 2001.
- [2] L. Lecam, *Asymptotic Methods in Statistical Decision Theory* Springer, New York, NY, USA, 1986.
- [3] M. G. Akritas, “Asymptotic inference in Lévy processes of the discontinuous type,” *Annals of Statistics*, vol. 9, no. 3, pp. 604–614, 1981.
- [4] H. Luschgy, “Local asymptotic mixed normality for semimartingale experiments,” *Probability Theory and Related Fields*, vol. 92, no. 2, pp. 151–176, 1992.
- [5] V. Genon-Catalot and J. Jacod, “Estimation of the diffusion coefficient for diffusion processes: random sampling,” *Scandinavian Journal of Statistics*, vol. 21, no. 3, pp. 193–221, 1994.
- [6] E. Clément and A. Gloter, “Local asymptotic mixed normality property for discretely observed stochastic differential equations driven by stable Lévy processes,” *Stochastic Processes and their Applications*, vol. 125, no. 6, pp. 2316–2352, 2015.
- [7] Y. Aït-Sahalia and J. Jacod, “Volatility estimators for discretely sampled Lévy processes,” *Annals of Statistics*, vol. 35, no. 1, pp. 355–392, 2007.
- [8] H. Masuda, “Joint estimation of discretely observed stable Lévy processes with symmetric Lévy density,” *Journal of the Japan Statistical Society*, vol. 39, no. 1, pp. 49–75, 2009.
- [9] R. Kawai and H. Masuda, “On the local asymptotic behavior of the likelihood function for Meixner Lévy processes under high-frequency sampling,” *Statistics and Probability Letters*, vol. 81, no. 4, pp. 460–469, 2011.
- [10] R. Kawai and H. Masuda, “Local asymptotic normality for normal inverse Gaussian Lévy processes with high-frequency sampling,” *ESAIM: Probability and Statistics*, vol. 17, pp. 13–32, 2013.
- [11] Y. Aït-Sahalia and J. Jacod, “Fisher’s information for discretely sampled Lévy processes,” *Econometrica*, vol. 76, no. 4, pp. 727–761, 2008.
- [12] H. Rammeh, *LPMA CNRS-UMR 7599*, PhD thesis, University of Paris, Paris, France, 1994.
- [13] J. Jacod and A. N. Shiryaev, *Limit theorems for Stochastic Processes* Springer, Berlin Heidelberg, NY, USA, 1987.
- [14] W. Jedidi, “Stable Processes, Mixing, and Distributional Properties. I,” *Theory of Probability and its Applications*, vol. 52, no. 4, pp. 580–593, 2008.
- [15] P. Protter, *In Stochastic Integration and Differential Equations*, Springer Verlag, Berlin, Heidelberg, Germany, 1990.
- [16] V. M. Zolotarev, *One Dimensional Stable Laws* Transactions of the American Mathematical Society, Providence, RI, USA, 1986.
- [17] W. Jedidi, “Stable Processes, Mixing, and Distributional Properties. II,” *Theory of Probability & Its Applications*, vol. 53, no. 1, pp. 81–105, 2009.
- [18] H. Far, *LPMA CNRS-UMR 7599*, PhD thesis, Paris, France.
- [19] H. Strasser, *Mathematical Theory of Statistics, Statistical Experiment and Asymptotic Decision Theory* Walter de Gruyter., New York, NY, USA, 1985.
- [20] J. Jacod, “Convergence of filtered statistical models and Hellinger processes,” *Stochastic Processes and their Applications*, vol. 32, no. 1, pp. 47–68, 1989.
- [21] J. Picard, “Density in small time for Lévy processes,” *ESAIM: Probability and Statistics*, vol. 1, pp. 357–389, 1997.
- [22] J. Bertoin and R. Doney, “Spitzer’s condition for random walks and Lévy processes,” *Annales de l’Institut Henri Poincaré (B) Probability and Statistics*, vol. 33, no. 2, pp. 167–178, 1997.

## Research Article

# The New Novel Discrete Distribution with Application on COVID-19 Mortality Numbers in Kingdom of Saudi Arabia and Latvia

M. Nagy,<sup>1</sup> Ehab M. Almetwally,<sup>2,3</sup> Ahmed M. Gemeay,<sup>4</sup> Heba S. Mohammed,<sup>5,6</sup> Taghreed M. Jawa,<sup>7</sup> Neveen Sayed-Ahmed,<sup>7</sup> and Abdisalam Hassan Muse <sup>8</sup>

<sup>1</sup>Department of Mathematics, Faculty of Science, Fayoum University, Fayoum, Egypt

<sup>2</sup>Faculty of Business Administration, Delta University of Science and Technology, Gamasa, Egypt

<sup>3</sup>Department of Mathematical Statistics, Faculty of Graduate Studies for Statistical Research, Cairo University, Egypt

<sup>4</sup>Department of Mathematics, Faculty of Science, Tanta University, Tanta 31527, Egypt

<sup>5</sup>Mathematical Sciences Department, College of Science, Princess Nourah Bint Abdulrahman University, Riyadh, Saudi Arabia

<sup>6</sup>Department of Mathematics, Faculty of Science, New Valley University, El Kharga, Egypt

<sup>7</sup>Department of Mathematics, College of Science, Taif University, P.O. Box 11099, Taif 21944, Saudi Arabia

<sup>8</sup>Department of Mathematics (Statistics Option) Program, Pan African University, Institute of Basic Science, Technology and Innovation (PAUST), Nairobi 6200-00200, Kenya

Correspondence should be addressed to Abdisalam Hassan Muse; [abdisalam.hassan@amoud.edu.so](mailto:abdisalam.hassan@amoud.edu.so)

Received 19 September 2021; Accepted 27 November 2021; Published 24 December 2021

Academic Editor: Sameh S. Askar

Copyright © 2021 M. Nagy et al. This is an open access article distributed under the Creative Commons Attribution License, which permits unrestricted use, distribution, and reproduction in any medium, provided the original work is properly cited.

This paper aims to introduce a superior discrete statistical model for the coronavirus disease 2019 (COVID-19) mortality numbers in Saudi Arabia and Latvia. We introduced an optimal and superior statistical model to provide optimal modeling for the death numbers due to the COVID-19 infections. This new statistical model possesses three parameters. This model is formulated by combining both the exponential distribution and extended odd Weibull family to formulate the discrete extended odd Weibull exponential (DEOWE) distribution. We introduced some of statistical properties for the new distribution, such as linear representation and quantile function. The maximum likelihood estimation (MLE) method is applied to estimate the unknown parameters of the DEOWE distribution. Also, we have used three datasets as an application on the COVID-19 mortality data in Saudi Arabia and Latvia. These three real data examples were used for introducing the importance of our distribution for fitting and modeling this kind of discrete data. Also, we provide a graphical plot for the data to ensure our results.

## 1. Introduction

Modeling pandemics is significant in our life as it makes it easier for researchers to understand the behavior of the spread of each virus and its effect on humanity. Nowadays, a new virus has risen on the top of the scene, Severe Acute Respiratory Syndrome coronavirus 2 (SARS-CoV-2), which causes COVID-19. This virus attracts the interest of many researchers who tried many attempts to model daily deaths in the entire world by the effect of COVID-19 infection. As an example of these studies, Al-Babtain et al. [1] introduced a natural discrete Lindley distribution and studied the

mortality numbers in Egypt from 8 March to 30 April 2020. Also, Hasab et al. [2] make a study on the COVID-19 mortality numbers by using the susceptible infected recovered (SIR) epidemic dynamics of COVID-19 pandemic to model COVID-19 infections in Egypt. Algarni et al. [3] discussed type-I half-logistic Burr XG family with application of COVID-19 data. Almetwally [4] discussed the odd Weibull inverse Topp-Leone distribution with applications to COVID-19 data. Almetwally et al. [5] discussed new distribution with applications to the COVID-19 mortality rate in two different countries. El-Morshedy et al. [6] studied a new discrete distribution, called discrete generalized



Lindley, to analyze the counts of the daily COVID-19 cases in Hong Kong and daily new deaths in Iran. Maleki et al. [7] used an autoregressive time-series model regarding the two-scale mixture normal distribution to predict the retrieved and reported COVID-19 occurrences. Nesteruk [8] forecasts the daily new COVID-19 occurrences in China by using the mathematical model SIR. Batista [9] used a logistic growth regression model to estimate the final size and its peak time of the COVID-19 epidemic. Muse et al. [10] discussed modeling the COVID-19 mortality rate with a new versatile modification of the log-logistic distribution. Liu et al. [11] presented a new statistical model called arcsine-modified Weibull distribution for modeling COVID-19 patients' data.

Afify and Mohamed [12] developed the extended odd Weibull exponential (EOWE) distribution for data modeling in many sciences such as architecture, medicine, and reliability. The EOWE distribution is a flexible model offering different density function forms such as left-skewed, symmetrical, right-skewed, and reversed-J; see, the work of Alshenawy et al. [13]. Its hazard rate function (HRF) may provide declining, constant, rising, upside-down bathtub and J-shaped hazard rates, and bathtub and modified bathtub hazard ratings are quite important in terms of durability technologies. For more details, see the work of Alshenawy et al. [13]. Generally speaking, most distributions are used to model such data and can usually take four or five parameters to achieve these hazard rates. DEOWE distribution has three parameters only, and it can be used to analyze censored data due to its easy, closed forms of its HRF and cumulative distribution function (CDF).

The CDF and probability mass function (PMF) of the DEOWE distribution are given, respectively, by

$$F(x; \alpha, \beta, \lambda) = 1 - \{1 + \beta[\exp(\lambda x) - 1]^\alpha\}^{-1/\beta}, \quad (1)$$

$$x > 0, \alpha, \beta, \lambda > 0,$$

and

$$f(x; \alpha, \beta, \lambda) = \alpha \lambda \exp(\alpha \lambda x) [1 - \exp(-\lambda x)]^{\alpha-1} \cdot \{1 + \beta[\exp(\lambda x) - 1]^\alpha\}^{-1/\beta-1}, \quad x > 0, \alpha, \beta, \lambda > 0. \quad (2)$$

Why do we need discrete distributions is a question that any researcher would ask. The reason is that most current continuous distributions do not provide reliable findings for modeling the COVID-19 scenarios. The reason for all of this, as we all know, is that death counts or regular new cases display extreme dispersion.

Many authors have introduced discrete distributions to overcome the deficiencies of the continuous distribution in modeling mortality numbers, such as Para and Jan [14] have introduced discrete Burr-type XII and discrete Lomax distributions. Discrete Lomax (DL) distribution is the discrete distribution which exhibits heavy tails and can be helpful in medical science and other fields, discrete Burr (DB), which is presented by Krishna and Pundir [15], discrete Lindley (DL), which is introduced by Gómez-Déniz and Calderín-Ojeda [16], discrete generalized exponential (DGEx), which is presented by Nekoukhou et al. [17], natural discrete Lindley

(NDL), which is introduced by Al-Babtain et al. [1], and discrete Gompertz Exponential (DGzEx), which is presented by El-Morshedy et al. [6]. Gillariose et al. [18] introduced discrete Weibull Marshall–Olkin family of distributions with properties, characterizations, and applications. Discrete Marshall–Olkin generalized exponential distribution has been presented by Almetwally et al. [19]. Al-Babtain et al. [20] discussed the estimation of the parameters of two discrete models called discrete Poisson–Lindley and discrete Lindley distributions, with some applications.

To convert a continuous distribution to a discrete one, a variety of methods are possible. A survival discretization approach is the most widely used technique for generating discrete distributions. It necessitates the existence of CDF, the existence of a continuous and nonnegative survival function, and the division of period through unit intervals. In Roy [21], the probability mass function (PMF) of a discrete distribution is described as

$$P(X = x) = P(x \leq X < x + 1) = S(x) - S(x + 1); \quad (3)$$

$$x = 0, 1, 2, \dots,$$

where  $S(x) = P(X \geq x) = 1 - F(x; \Theta)$ , where  $F(x; \Theta)$  is a CDF of continuous distribution and  $\Theta$  is a vector of parameters. The random variable  $X$  is said to have the discrete distribution if its CDF is given by  $P(X < x) = F(x + 1; \Theta)$ . The hazard rate is given by  $hr(x) = P(X = x)/(S(x))$ . The reversed failure rate of discrete distribution is given as  $rfr(x) = P(X = x)/(1 - S(x))$ .

The novelty and the motivation to write this paper is to find the best statistical model which can provide the fit for COVID-19 mortality numbers in Saudi Arabia and Latvia by introducing a new discrete model, namely, the DEOWE distribution. The point estimation of the unknown parameters has been discussed by using the MLE method. Also, we make an expectation for the mortality number in each day.

The remainder of this article is organized as follows. In Section 2, we define DEOWE distribution. DEOWE linear representation of its PMF is obtained in Section 3, along with some of its statistical properties. The MLE method is used for parameter estimation in Section 4. In Section 5, we performed a simulation study to study the performance of the distribution relative to the true values of the parameters; also, we evaluated the relative bias (Rbias) and mean square error (MSE) of the estimation method. Two real datasets were used as three real data applications on the mortality numbers in Section 6. These three applications were used to prove that the proposed distribution provides the efficiency of the DEOWE distribution with respect to other distributions by evaluating the information criteria and the  $P$  values and chi-square values for all distributions. Finally, conclusions and the major findings are given in Section 7.

## 2. DEOWE Distribution

In this section, we introduce the DEOWE distribution, the PMF, and the CDF which are obtained. Some figures with

different values of the parameters for the PMF and HRF of the distribution are represented in Figures 1 and 2.

The DEOWE distribution is obtained based on the survival discretization method. Let  $S(x; \vartheta) = 1 - F(x; \vartheta)$  denote the survival function (S) of a baseline model with parameter vector  $\vartheta$ , respectively, so the CDF of the DEOWE distribution is given by

$$F(x; \alpha, \beta, \lambda) = 1 - \left\{ 1 + \beta \left[ e^{\lambda(x+1)} - 1 \right]^\alpha \right\}^{-1/\beta}, \quad (4)$$

$$x = 0, 1, 2, \dots \infty. \alpha, \beta, \lambda > 0.$$

The corresponding PMF of (4) is defined by

$$P(X = x; \alpha, \beta, \lambda) = \left\{ 1 + \beta \left[ e^{\lambda x} - 1 \right]^\alpha \right\}^{-1/\beta} - \left\{ 1 + \beta \left[ e^{\lambda(x+1)} - 1 \right]^\alpha \right\}^{-1/\beta},$$

$$x = 0, 1, 2, \dots \infty. \alpha, \beta, \lambda > 0, \quad (5)$$

where  $\alpha, \beta$ , and  $\lambda$  are positive parameters. The random variable with PMF (5) is denoted by  $X \sim \text{DEOWE}(\alpha, \beta, \lambda)$ ; the corresponding HRF of the DEOWE distribution is defined by

$$h(X = x; \alpha, \beta, \lambda) = \left( \frac{1 + \beta \left[ e^{\lambda x} - 1 \right]^\alpha}{1 + \beta \left[ e^{\lambda(x+1)} - 1 \right]^\alpha} \right)^{-1/\beta} - 1. \quad (6)$$

### 3. Mathematical Properties

This section of the paper introduces the linear representation of the DEOWE distribution with its quantile function.

**3.1. Linear Representation.** In this section, we made a linear representation for the PMF of the proposed distribution. We used linear representation to derive different statistical properties of the proposed model. Unfortunately, we reach a result form which does not follow any statistical model, and it is mathematically difficult to use to derive different statistical properties. In the case of the proposed distribution, we have three different cases for this linear representation.

For  $|x| < 1$ , we have the following expansion:

$$(1+x)^{-n} = \sum_{k=0}^{\infty} (-1)^k \binom{n+k-1}{k} x^k. \quad (7)$$

For  $|x| > 1$ , we have the following expansion:

$$(1+x)^{-n} = \sum_{k=0}^{\infty} (-1)^k \binom{n+k-1}{k} x^{-(k+n)}. \quad (8)$$

*Case 1.* If  $\beta[e^{\lambda x} - 1]^\alpha < 1$  and  $x \neq 0$ , then we have

$$\left\{ 1 + \beta \left[ e^{\lambda x} - 1 \right]^\alpha \right\}^{-1/\beta} = \sum_{k,m,w=0}^{\infty} (-1)^{k+m+w} \binom{1/\beta + k - 1}{k} \cdot \binom{\alpha k}{m} \frac{\beta^k \lambda^w (m - \alpha k)^w}{w!} x^w, \quad (9)$$

and if  $\beta[e^{\lambda(x+1)} - 1]^\alpha < 1$  and  $x \neq 0$ , then we have

$$\left\{ 1 + \beta \left[ e^{\lambda(x+1)} - 1 \right]^\alpha \right\}^{-1/\beta} = \sum_{k,m,w=0}^{\infty} (-1)^{k+m+w} \binom{1/\beta + k - 1}{k} \cdot \binom{\alpha k}{m} \frac{\beta^k \lambda^w (m - \alpha k)^w}{w!} e^{-\lambda(m-\alpha k)} x^w. \quad (10)$$

From equations (7) and (8), we have a linear representation of PMF (5) as the following:

$$P(X = x; \alpha, \beta, \lambda) = \sum_{k,m,w=0}^{\infty} \Phi_{k,m,w} x^w, \quad (11)$$

where  $\Phi_{k,m,w} = \frac{(-1)^{k+m+w} \binom{1/\beta + k - 1}{k} \binom{\alpha k}{m} \beta^k \lambda^w (m - \alpha k)^w / w!}{[1 - e^{-\lambda(m-\alpha k)}]}$ .

*Case 2.* . If  $\beta[e^{\lambda x} - 1]^\alpha > 1$ , then we have

$$\left\{ 1 + \beta \left[ e^{\lambda x} - 1 \right]^\alpha \right\}^{-1/\beta} = \sum_{k,m,w=0}^{\infty} (-1)^{k+m+w} \binom{\frac{1}{\beta} + k - 1}{k} \cdot \binom{\alpha \left( k + \frac{1}{\beta} \right) + m - 1}{m} \times \frac{\beta^{-(k+1/\beta)} \lambda^w [m + \alpha(k + 1/\beta)]^w}{w!} x^w. \quad (12)$$

If  $\beta[e^{\lambda(x+1)} - 1]^\alpha > 1$ , then we have

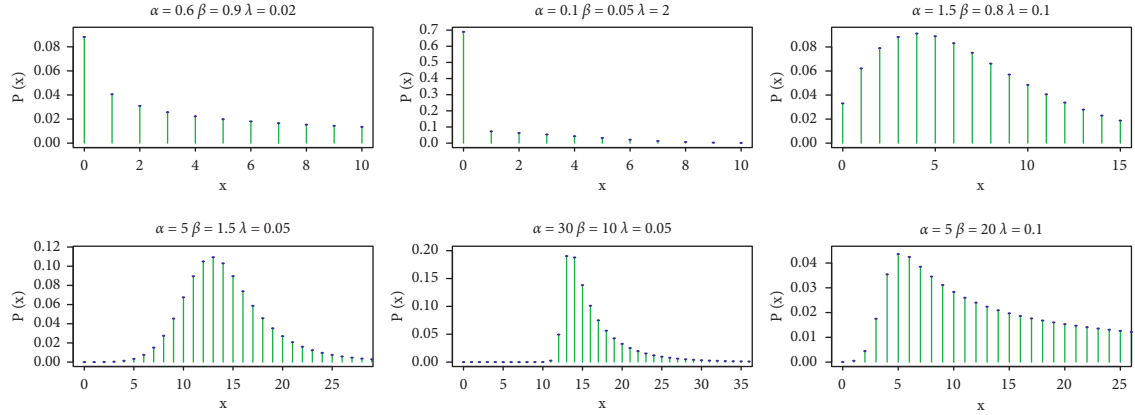


FIGURE 1: Different shapes' PMF of DEOWE distribution by using different values of the parameters. These figures show that the PMF can behave in different shapes.

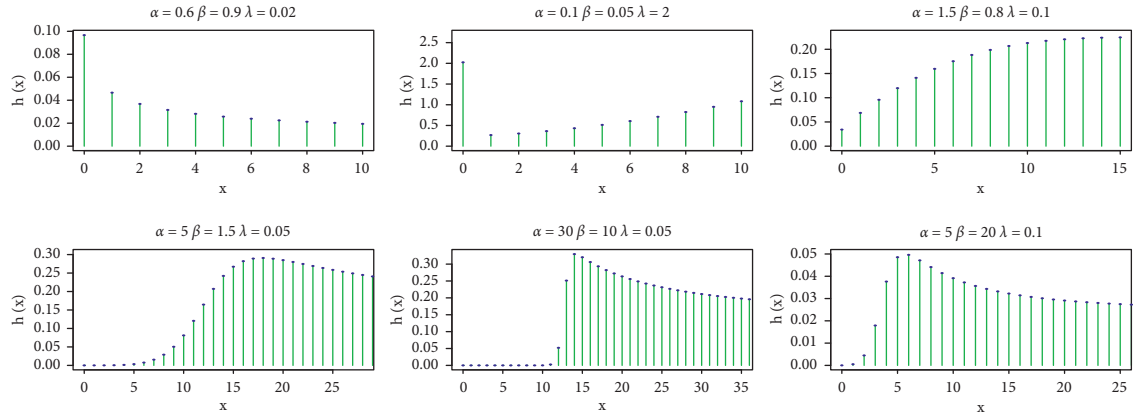


FIGURE 2: Different shapes' HRF of DEOWE distribution by using different values of the parameters. These figures show that the HRF can behave in different shapes.

$$\begin{aligned}
 \{1 + \beta[e^{\lambda(x+1)} - 1]^\alpha\}^{-1/\beta} &= \sum_{k,m,w=0}^{\infty} (-1)^{k+m+w} \binom{\frac{1}{\beta} + k - 1}{k} \\
 &\cdot \binom{\alpha\left(k + \frac{1}{\beta}\right) + m - 1}{m} \\
 &\times \frac{\beta^{-(k+1/\beta)} \lambda^w [m + \alpha(k + 1/\beta)]^w}{w!} \\
 &\cdot e^{-\lambda[m + \alpha(k+1/\beta)]} x^w.
 \end{aligned} \tag{13}$$

From equations (9) and (10), we have a linear representation of PMF (5) as the following:

$$P(X = x; \alpha, \beta, \lambda) = \sum_{k,m,w=0}^{\infty} \Psi_{k,m,w} x^w, \tag{14}$$

where

$$\Psi_{k,m,w} = (-1)^{k+m+w} \binom{\frac{1}{\beta} + k - 1}{k} \binom{\alpha(k + 1/\beta) + m - 1}{m} \beta^{-(k+1/\beta)} \lambda^w [m + \alpha(k + 1/\beta)]^w / w! \{1 - e^{-\lambda[m + \alpha(k+1/\beta)]}\}.$$

Case 3. If  $\beta[e^{\lambda x} - 1]^\alpha < 1$  and  $\beta[e^{\lambda(x+1)} - 1]^\alpha > 1$ , then, from equations (7) and (10), we have a linear representation of PMF (5) as the following:

TABLE 1: Numerical values of mean, variance, BS, and MK of DEOWE distribution.

$\alpha$	$\beta$	$\lambda$	Mean	Variance	BS	MK
0.25	0.5	0.75	2.4448	13.68952	0.7331407	1.41471
0.5	0.75	1.5	0.8347	1.406517	0.4518331	1.297248
0.5	2.5	0.75	4.6491	41.72894	0.4530885	1.265127
2.5	0.5	0.25	2.7052	1.297823	0.04143768	1.251105
1.5	3	2	0.7423	0.9247832	0.3490083	1.446349
2	1.5	0.5	1.7974	1.720525	0.1950339	1.366696
3	0.25	1.5	0.3023	0.2109358	-0.01123612	1.235523
0.75	2	3	0.6083	0.8625574	0.4008665	1.350532
0.03	0.05	3	2.6457	21.2683	0.9999985	2.105148

$$\begin{aligned}
P(X = x; \alpha, \beta, \lambda) &= \sum_{k,m,w=0}^{\infty} (-1)^{k+m+w} \binom{\frac{1}{\beta} + k - 1}{k} \binom{\alpha k}{m} \frac{\beta^k \lambda^w (m - \alpha k)^w}{w!} x^w \\
&- \sum_{k,m,w=0}^{\infty} (-1)^{k+m+w} \binom{\frac{1}{\beta} + k - 1}{k} \binom{\alpha \left(k + \frac{1}{\beta}\right) + m - 1}{m} \\
&\times \frac{\beta^{-(k+1/\beta)} \lambda^w [m + \alpha(k + 1/\beta)]^w}{w!} e^{(-\lambda[m + \alpha(k+1/\beta)])} x^w.
\end{aligned} \tag{15}$$

3.2. *Quantile Function.* The quantile function (QF) of the DEOWE distribution is the inverse function of the CDF, and it is given as follows:

$$x_u = \frac{\log\left(\left((1-p)^{-\beta} - 1/\beta\right)^{1/\alpha} + 1\right)}{\lambda} - 1. \tag{16}$$

The three quarterlies (Q) of the DEOWE distribution can be obtained by setting  $u = 0.25, 0.5,$  and  $0.75$  in equation (11).

Bowley's skewness (BS) and Moor's kurtosis (MK) can be calculated by the QF, respectively, as follows:

$$BS = \frac{Q(1/4) + Q(3/4) - 2Q(1/2)}{Q(3/4) - Q(1/4)} \tag{17}$$

and

$$MK = \frac{Q(7/8) - Q(5/8) + Q(3/8) - Q(1/8)}{Q(6/8) - Q(2/8)}. \tag{18}$$

Table 1 shows the numerical mean, variance, BS, and MK for the distribution using different parameters. These different values are coherent with the plots in Figure 1

#### 4. Parameter Estimation

In this section, we use the MLE method to estimate the unknown parameters of the DEOWE distribution. Assume that  $x_1, \dots, x_n$  represents a random count discrete sample that follows the DEOWE distribution having the parameters,  $\alpha, \beta,$  and  $\lambda$ . So, the log-likelihood function will have the following form:

$$\begin{aligned}
\ell(\Omega) &= \sum_{i=1}^m \ln\left(\left\{1 + \beta\left[e^{\lambda x} - 1\right]^{\alpha}\right\}^{-1/\beta}\right. \\
&\quad \left.- \left\{1 + \beta\left[e^{\lambda(x+1)} - 1\right]^{\alpha}\right\}^{-1/\beta}\right),
\end{aligned} \tag{19}$$

where  $\Omega = (\alpha, \beta, \lambda)$  is a vector of the DEOWE parameters. The MLEs are obtained by solving the following normal equations:

$$\begin{aligned}
\frac{\partial \ell(\Omega)}{\partial \alpha} &= \sum_{i=1}^n \frac{\ln \left[ e^{\widehat{\lambda}(x_{i+1})} - 1 \right] \left[ e^{\widehat{\lambda}(x_{i+1})} - 1 \right]^{\widehat{\alpha}} \left\{ 1 + \widehat{\beta} \left[ e^{\widehat{\lambda}(x_{i+1})} - 1 \right]^{\widehat{\alpha}} \right\}^{-1/\widehat{\beta}-1}}{\left\{ 1 + \widehat{\beta} \left[ e^{\widehat{\lambda}x_i} - 1 \right]^{\widehat{\alpha}} \right\}^{-1/\widehat{\beta}} - \left\{ 1 + \widehat{\beta} \left[ e^{\widehat{\lambda}(x_{i+1})} - 1 \right]^{\widehat{\alpha}} \right\}^{-1/\widehat{\beta}}} \\
&\quad - \frac{\ln \left[ e^{\widehat{\lambda}x_i} - 1 \right] \left[ e^{\widehat{\lambda}x_i} - 1 \right]^{\widehat{\alpha}} \left\{ 1 + \widehat{\beta} \left[ e^{\widehat{\lambda}x_i} - 1 \right]^{\widehat{\alpha}} \right\}^{-1/\widehat{\beta}-1}}{\left\{ 1 + \widehat{\beta} \left[ e^{\widehat{\lambda}x_i} - 1 \right]^{\widehat{\alpha}} \right\}^{-1/\widehat{\beta}} - \left\{ 1 + \widehat{\beta} \left[ e^{\widehat{\lambda}(x_{i+1})} - 1 \right]^{\widehat{\alpha}} \right\}^{-1/\widehat{\beta}}} = 0, \\
\frac{\partial \ell(\Omega)}{\partial \beta} &= \sum_{i=1}^n \frac{\ln \left\{ 1 + \widehat{\beta} \left[ e^{\widehat{\lambda}x_i} - 1 \right]^{\widehat{\alpha}} \right\} \left\{ 1 + \widehat{\beta} \left[ e^{\widehat{\lambda}x_i} - 1 \right]^{\widehat{\alpha}} \right\}^{-1/\widehat{\beta}} - \left[ e^{\widehat{\lambda}x_i} - 1 \right]^{\widehat{\alpha}} \left\{ 1 + \widehat{\beta} \left[ e^{\widehat{\lambda}x_i} - 1 \right]^{\widehat{\alpha}} \right\}^{-1/\widehat{\beta}-1}}{\left\{ 1 + \widehat{\beta} \left[ e^{\widehat{\lambda}x_i} - 1 \right]^{\widehat{\alpha}} \right\}^{-1/\widehat{\beta}} - \left\{ 1 + \widehat{\beta} \left[ e^{\widehat{\lambda}(x_{i+1})} - 1 \right]^{\widehat{\alpha}} \right\}^{-1/\widehat{\beta}}} \\
&\quad - \frac{\ln \left\{ 1 + \widehat{\beta} \left[ e^{\widehat{\lambda}(x_{i+1})} - 1 \right]^{\widehat{\alpha}} \right\} \left\{ 1 + \widehat{\beta} \left[ e^{\widehat{\lambda}(x_{i+1})} - 1 \right]^{\widehat{\alpha}} \right\}^{-1/\widehat{\beta}} - \left[ e^{\widehat{\lambda}(x_{i+1})} - 1 \right]^{\widehat{\alpha}} \left\{ 1 + \widehat{\beta} \left[ e^{\widehat{\lambda}(x_{i+1})} - 1 \right]^{\widehat{\alpha}} \right\}^{-1/\widehat{\beta}-1}}{\left\{ 1 + \widehat{\beta} \left[ e^{\widehat{\lambda}x_i} - 1 \right]^{\widehat{\alpha}} \right\}^{-1/\widehat{\beta}} - \left\{ 1 + \widehat{\beta} \left[ e^{\widehat{\lambda}(x_{i+1})} - 1 \right]^{\widehat{\alpha}} \right\}^{-1/\widehat{\beta}}} = 0,
\end{aligned} \tag{20}$$

and

$$\frac{\partial \ell(\Omega)}{\partial \lambda} = \widehat{\alpha} \sum_{i=1}^n \frac{(x_i + 1)e^{\widehat{\lambda}(x_{i+1})} \left\{ 1 + \widehat{\beta} \left[ e^{\widehat{\lambda}(x_{i+1})} - 1 \right]^{\widehat{\alpha}} \right\}^{-1/\widehat{\beta}-1} - x_i e^{\widehat{\lambda}x_i} \left\{ 1 + \widehat{\beta} \left[ e^{\widehat{\lambda}x_i} - 1 \right]^{\widehat{\alpha}} \right\}^{-1/\widehat{\beta}-1}}{\left\{ 1 + \widehat{\beta} \left[ e^{\widehat{\lambda}x_i} - 1 \right]^{\widehat{\alpha}} \right\}^{-1/\widehat{\beta}} - \left\{ 1 + \widehat{\beta} \left[ e^{\widehat{\lambda}(x_{i+1})} - 1 \right]^{\widehat{\alpha}} \right\}^{-1/\widehat{\beta}}} = 0. \tag{21}$$

These equations cannot be solved explicitly. Hence, a nonlinear optimization algorithm as the Newton–Raphson method is used.

## 5. Simulation Studies

This part of the paper is devoted to make the Monte Carlo simulation procedure. This simulation study is performed for the classical estimation method: MLE for estimating parameters of DEOWE distribution in a lifetime by R language. Monte Carlo experiments are carried out based on data generated from 10 000 random samples from DEOWE distribution, where  $X$  has DEOWE lifetime for different

actual values of parameters and different sample sizes  $n$ : (20, 40, 70, and 100).

We evaluate in every table Rbias and MSE of estimators. Tables 2–4 summarize the simulation results of the point estimation method in this paper. We consider the Rbias and the MSE values to perform the needed comparison between different parameters' values and their effect on point estimation values.

In every table, we fix the  $\beta$  value and increase the values of both  $\lambda$  and  $\alpha$ , and then, we study the effect of increasing and decreasing the values. Concluding remarks are provided at the end of this section to illustrate the impact of the increment and decrements of the parameter's values.

TABLE 2: Rbias and MSE for parameter of DEOWE distribution by using MLE when  $\beta = 0.5$ .

$\beta = 0.5$		$\lambda$	0.01		0.05		0.15	
$\alpha$	$N$		Rbias	MSE	Rbias	MSE	Rbias	MSE
0.5	20	$\alpha$	0.049 4	0.006 33	0.165 8	0.025 4	0.305 3	0.077 3
		$\beta$	-0.009 1	0.000 72	0.002 8	0.089 6	0.061 3	0.485 2
		$\lambda$	0.057 8	0.000 012	0.016 2	0.001 2	-0.026 6	0.008 0
	40	$\alpha$	0.028 8	0.002 63	0.147 6	0.014 4	0.265 6	0.049 2
		$\beta$	0.003 6	0.002 98	0.028 5	0.076 5	0.132 2	0.384 3
		$\lambda$	0.034 3	0.000 005	-0.051 3	0.000 2	-0.047 1	0.006 3
	70	$\alpha$	0.037 0	0.002 01	0.141 7	0.010 2	0.250 7	0.029 9
		$\beta$	-0.002 1	0.000 29	0.072 6	0.076 0	0.132 4	0.260 4
		$\lambda$	0.004 5	0.000 002	-0.041 3	0.000 2	-0.112 9	0.002 3
	100	$\alpha$	0.040 0	0.001 915	0.131 7	0.007 7	0.269 6	0.025 3
		$\beta$	-0.003 0	0.000 031	0.053 6	0.060 1	0.107 3	0.173 4
		$\lambda$	-0.012 7	0.000 002	-0.061 9	0.000 1	-0.080 8	0.002 0
1.5	20	$\alpha$	0.002 0	0.002 674	0.048 2	0.045 5	0.155 6	0.150 5
		$\beta$	-0.005 4	0.001 886	-0.032 1	0.056 7	-0.151 2	0.168 6
		$\lambda$	0.010 6	0.000 002	-0.022 2	0.000 053	-0.100 8	0.000 8
	40	$\alpha$	-0.000 9	0.001 018	0.010 7	0.004 8	0.136 3	0.084 6
		$\beta$	0.001 0	0.000 389	-0.007 9	0.004 5	-0.022 4	0.077 4
		$\lambda$	0.007 7	0.000 001	-0.018 2	0.000 025	-0.103 0	0.000 5
	70	$\alpha$	0.000 3	0.000 052	0.042 5	0.016 5	0.150 8	0.080 0
		$\beta$	-0.000 3	0.000 008	-0.023 1	0.014 5	0.019 1	0.039 5
		$\lambda$	0.004 3	0.000 001	-0.031 4	0.000 018	-0.102 8	0.000 4
	100	$\alpha$	0.000 0	0.000 002	0.024 1	0.007 0	0.102 2	0.037 7
		$\beta$	0.000 0	0.000 002	0.006 5	0.011 0	-0.084 9	0.018 9
		$\lambda$	-0.000 7	0.000 000 4	-0.027 1	0.000 014	-0.102 6	0.000 3
5	20	$\alpha$	-1.18E-06	1.63E-08	-0.000 7	0.024 3	0.002 6	0.004 7
		$\beta$	4.19E-05	1.64E-07	0.007 9	0.009 4	-0.034 9	0.007 6
		$\lambda$	-0.005 13	1.87E-07	-0.031 11	6.91E-06	-0.095 7	0.000 2
	40	$\alpha$	2.48E-09	1.41E-13	0.003 1	0.033 6	0.000 949	7.01E-05
		$\beta$	5.77E-08	1.21E-12	-0.071 1	0.020 4	-0.018 0	0.000 5
		$\lambda$	-0.004 35	1.01E-07	-0.036 06	6.71E-06	-0.092 7	0.000 2
	70	$\alpha$	1.90E-05	5.52E-06	0.003 5	0.013 6	0.026 1	0.119 6
		$\beta$	-0.000 6	6.23E-05	-0.068 2	0.009 5	-0.186 7	0.037 2
		$\lambda$	-0.004 8	5.80E-08	-0.035 98	4.63E-06	-0.101 9	0.000 2
	100	$\alpha$	-3.22E-09	8.23E-13	0.002 1	0.009 0	0.002 4	0.000 5
		$\beta$	2.12E-07	3.87E-12	-0.013 7	0.004 6	-0.046 8	0.002 1
		$\lambda$	-0.005 96	4.22E-08	-0.032 87	3.62E-06	-0.096 5	0.000 2

TABLE 3: Rbias and MSE for parameter of DEOWE distribution by using MLE when  $\beta = 1.5$ .

$\beta = 1.5$		$\lambda$	0.05		0.15		0.5	
$\alpha$	$n$		Rbias	MSE	Rbias	MSE	Rbias	MSE
0.5	20	$\alpha$	0.150 7	0.026 7	0.255 4	0.060 2	0.410 2	0.120 0
		$\beta$	-0.003 2	0.118 2	-0.007 8	0.365 7	-0.086 2	0.656 7
		$\lambda$	0.045 1	0.003 4	-0.021 3	0.012 9	-0.212 8	0.080 8
	40	$\alpha$	0.143 9	0.016 1	0.239 1	0.035 1	0.428 8	0.101 8
		$\beta$	-0.003 7	0.022 8	-0.000 5	0.265 4	-0.018 4	0.530 6
		$\lambda$	-0.051 3	0.000 2	-0.112 8	0.004 7	-0.244 1	0.056 8
	70	$\alpha$	0.142 6	0.010 7	0.236 0	0.024 1	0.415 6	0.066 9
		$\beta$	-0.001 9	0.022 9	0.004 2	0.108 7	-0.016 2	0.215 7
		$\lambda$	-0.082 5	0.000 1	-0.149 5	0.001 4	-0.271 6	0.032 2
	100	$\alpha$	0.136 5	0.008 6	0.231 8	0.021 3	0.422 0	0.069 6
		$\beta$	0.002 7	0.026 1	0.005 1	0.101 9	-0.030 6	0.431 6
		$\lambda$	-0.091 2	0.000 1	-0.162 4	0.001 2	-0.305 6	0.039 7

TABLE 3: Continued.

$\alpha$	$\beta = 1.5$ $n$	$\lambda$	0.05		0.15		0.5	
			Rbias	MSE	Rbias	MSE	Rbias	MSE
1.5	20	$\alpha$	0.050 7	0.053 7	0.188 3	0.213 2	0.510 6	1.600 6
		$\beta$	0.011 9	0.206 2	0.028 4	0.687 5	0.080 0	1.738 6
		$\lambda$	-0.015 4	0.000 10	-0.087 8	0.001 2	-0.282 1	0.023 8
	40	$\alpha$	0.045 1	0.027 0	0.191 2	0.164 4	0.496 8	1.014 6
		$\beta$	-0.002 3	0.051 6	0.050 5	0.326 1	0.079 7	1.076 8
		$\lambda$	-0.030 1	0.000 05	-0.090 9	0.000 7	-0.276 7	0.022 2
	70	$\alpha$	0.024 9	0.007 3	0.173 5	0.104 1	0.495 8	0.835 9
		$\beta$	-0.002 4	0.006 6	0.041 7	0.133 7	0.110 7	0.787 2
		$\lambda$	-0.021 0	0.000 024	-0.093 6	0.000 5	-0.270 1	0.020 2
	100	$\alpha$	0.023 3	0.006 6	0.131 9	0.051 4	0.442 3	0.567 4
		$\beta$	0.000 8	0.014 1	0.009 5	0.057 6	0.066 9	0.397 7
		$\lambda$	-0.028 6	0.000 021	-0.101 4	0.000 4	-0.275 5	0.020 6
5	20	$\alpha$	0.014 0	0.119 5	0.018 6	0.128 6	0.076 2	0.600 5
		$\beta$	-0.048 2	0.079 0	-0.022 9	0.085 8	-0.198 8	0.461 0
		$\lambda$	-0.040 085 6	1.08E-05	-0.100 1	0.000 3	-0.267 6	0.018 6
	40	$\alpha$	-0.000 6	0.024 2	0.013 1	0.046 1	0.052 7	0.128 7
		$\beta$	-0.015 5	0.031 2	-0.053 1	0.041 8	-0.249 8	0.284 4
		$\lambda$	-0.033 310 9	7.45E-06	-0.099 5	0.000 3	-0.269 0	0.018 5
	70	$\alpha$	0.008 4	0.009 9	0.002 5	0.000 7	0.051 2	0.124 7
		$\beta$	-0.041 0	0.021 1	-0.010 5	0.001 2	-0.224 6	0.187 6
		$\lambda$	-0.036 834 2	6.23E-06	-0.096 8	0.000 2	-0.269 7	0.018 4
	100	$\alpha$	0.000 6	0.003 0	0.004 2	0.007 2	0.052 2	0.577 8
		$\beta$	-0.003 4	0.006 2	-0.014 5	0.005 4	-0.160 6	0.173 5
		$\lambda$	-0.034 227 1	4.87E-06	-0.097 6	0.000 23	-0.266 0	0.017 8

TABLE 4: Rbias and MSE for parameter of DEOWE distribution by using MLE when  $\beta = 5$ .

$\alpha$	$\beta = 5$ $n$	$\lambda$	0.15		0.5		1.5	
			Rbias	MSE	Rbias	MSE	Rbias	MSE
0.5	20	$\alpha$	0.252 2	0.083 1	0.418 6	0.189 2	0.950 4	0.588 5
		$\beta$	0.005 1	1.021 8	0.017 1	1.796 8	0.080 2	4.372 6
		$\lambda$	0.189 8	0.043 4	0.073 0	0.179 2	-0.197 0	0.723 0
	40	$\alpha$	0.233 1	0.048 5	0.379 3	0.105 1	0.878 9	0.405 9
		$\beta$	0.011 6	0.756 3	0.009 0	1.020 9	0.091 9	2.799 3
		$\lambda$	-0.023 8	0.010 7	-0.097 0	0.080 2	-0.247 7	0.644 4
	70	$\alpha$	0.234 5	0.031 8	0.399 8	0.080 9	0.874 5	0.332 1
		$\beta$	0.002 1	0.600 4	0.017 4	0.690 8	0.091 3	2.181 8
		$\lambda$	-0.108 8	0.004 7	-0.177 6	0.048 3	-0.301 7	0.517 1
	100	$\alpha$	0.233 7	0.026 0	0.392 9	0.067 6	0.883 6	0.297 9
		$\beta$	0.004 7	0.238 6	0.013 0	0.609 8	0.118 2	1.928 7
		$\lambda$	-0.141 4	0.002 1	-0.202 3	0.037 8	-0.342 3	0.463 8
1.5	20	$\alpha$	0.242 5	0.274 5	0.521 3	1.015 6	0.833 8	2.409 0
		$\beta$	0.042 0	1.460 5	0.072 5	3.340 7	-0.013 7	1.945 9
		$\lambda$	-0.090 8	0.001 6	-0.259 6	0.031 7	-0.427 0	0.669 7
	40	$\alpha$	0.183 0	0.137 5	0.484 2	0.760 1	0.852 9	2.258 9
		$\beta$	0.011 1	0.280 1	0.072 0	2.463 6	-0.035 7	1.429 4
		$\lambda$	-0.102 3	0.001 0	-0.278 3	0.025 4	-0.470 2	0.662 9
	70	$\alpha$	0.179 4	0.125 3	0.468 9	0.701 4	0.847 4	1.938 5
		$\beta$	0.013 6	0.275 8	0.047 4	2.127 6	-0.028 1	1.145 3
		$\lambda$	-0.103 9	0.000 7	-0.274 2	0.021 4	-0.508 4	0.599 1
	100	$\alpha$	0.180 4	0.103 9	0.456 9	0.632 3	0.840 4	1.773 8
		$\beta$	0.012 5	0.257 0	0.019 0	0.749 1	-0.031 4	0.696 5
		$\lambda$	-0.112 0	0.000 7	-0.277 8	0.020 2	-0.514 8	0.607 5

TABLE 4: Continued.

$\alpha$	$\beta = 5$	$\lambda$	0.15		0.5		1.5	
			Rbias	MSE	Rbias	MSE	Rbias	MSE
5	20	$\alpha$	0.0401	0.2775	0.1260	0.6790	0.2727	2.2337
		$\beta$	-0.0166	0.3161	-0.0834	0.5264	-0.3003	2.8737
		$\lambda$	-0.1062	0.0004	-0.2656	0.0191	-0.5253	0.6265
	40	$\alpha$	0.0081	0.0214	0.1563	0.8875	0.2578	1.8989
		$\beta$	-0.0049	0.0144	-0.0913	0.6280	-0.2720	2.1897
		$\lambda$	-0.1004	0.0003	-0.2718	0.0191	-0.5251	0.6231
	70	$\alpha$	0.0608	0.3348	0.1168	0.5326	0.2469	1.8195
		$\beta$	-0.0096	0.3463	-0.0707	0.2366	-0.2301	2.0759
		$\lambda$	-0.1016	0.0003	-0.2648	0.0179	-0.4529	0.6130
	100	$\alpha$	0.0316	0.1140	0.1063	0.5815	0.2388	1.5142
		$\beta$	-0.0099	0.0730	-0.0674	0.4447	-0.2299	1.8351
		$\lambda$	-0.1020	0.0003	-0.2631	0.0177	-0.4153	0.5636

TABLE 5: Descriptive statistics for first data.

$n$	Min	Q1	Median	Mean	Q3	Max	Skewness	Kurtosis
54	2.000	4.000	4.000	5.222	6.000	11.000	0.930	2.855

TABLE 6: MLE and standard error SE for models and goodness-of-fit criteria for each model.

Number of death/day	Death counts	Binom	Pois	DMOGE	DAPL	EDW	DEOWE	Nbinom	Skellam
0	0	0.3694	0.2913	0.0001	0.0035	0.0000	0.0002	0.2991	0.2914
1	0	1.7588	1.5215	0.0873	0.4602	0.0406	0.0507	1.5463	1.5218
2	2	4.2651	3.9728	2.1697	3.3627	2.2269	1.3951	4.0048	3.9734
3	8	7.0205	6.9155	9.1950	8.0609	9.3175	9.9097	6.9283	6.9163
4	19	8.8219	9.0286	13.5320	10.8835	12.8132	15.3291	9.0068	9.0292
5	7	9.0240	9.4299	11.0455	10.4100	10.7873	10.2807	9.3851	9.4300
6	5	7.8249	8.2075	7.0853	7.9878	7.3429	6.0497	8.1650	8.2072
7	3	5.9144	6.1231	4.2590	5.3191	4.5686	3.6739	6.1004	6.1225
8	2	3.9768	3.9970	2.5513	3.2404	2.7459	2.3243	3.9958	3.9964
9	5	2.4158	2.3192	1.5465	1.8725	1.6356	1.5205	2.3309	2.3188
10	2	1.3421	1.2112	0.9493	1.0522	0.9769	1.0210	1.2260	1.2109
11	1	0.6886	0.5750	0.5885	0.5847	0.5882	0.6999	0.5874	0.5748
	$\alpha$	0.2568	5.2222	14.9699	0.0001	0.6768	6.9746	517.0315	5.2220
	SE	0.9118	0.3110	5.4493	0.2356	0.0688	2.1294	3.6558	3.6542
	$\beta$			0.6325	1.6509	85.8710	3.8842	0.9900	0.0002
	SE			0.0919	0.0002	0.0002	1.6734	0.1555	0.0099
	$\theta$			0.2948	0.0002	0.2066	0.1568		
	SE			0.3184		0.0370	0.0110		
	$\chi^2$	22.0856	22.2000	13.9355	16.9089	14.0654	11.5446	22.1640	22.2003
	P value	0.0237	0.0229	0.2366	0.1106	0.2294	0.3988	0.0231	0.0229
	AIC	236.2832	235.7855	230.4802	234.1400	230.8243	229.6866	237.8167	237.7855
	CAIC	236.3601	235.8624	230.9602	234.6200	231.3043	230.1666	238.0520	238.0208
	BIC	238.2722	237.7745	236.4472	240.1069	236.7913	235.6536	241.7946	241.7635
	HQIC	237.0503	236.5526	232.7814	236.4412	233.1255	231.9879	239.3508	239.3197

5.1. *Concluding Remarks on Simulation Results.* In this section of the paper, we introduce the major findings deduced from the simulation tables; we introduced the effect of increasing the sample sizes and the effect of increasing the true values of the parameters used in the simulation study. Also, we will discuss the effect of fixing the value of every two

parameters and increasing the value of the third one. The following points can be noted from Tables 2–4:

- (1) As we can see from the results from Tables 2–4, by increasing the sample size, we can see that the consistent property of MLEs comes true, and the



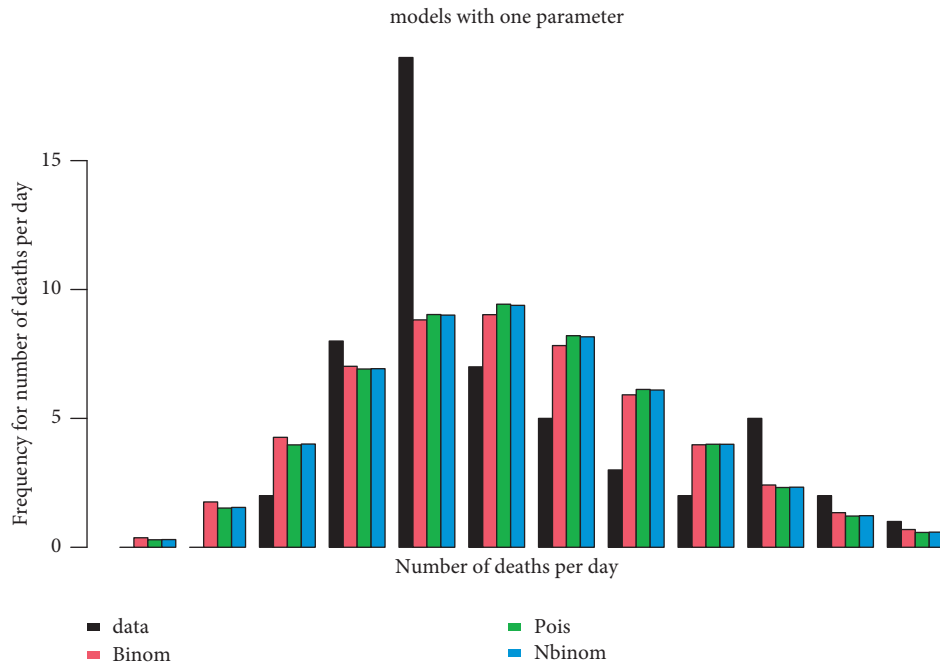


FIGURE 3: Graphical plots for the expected frequencies and the data using the PMF of different one parameter distributions, where the  $x$ -axis represents the number of deaths per day and the  $y$ -axis represents the frequency for this number.

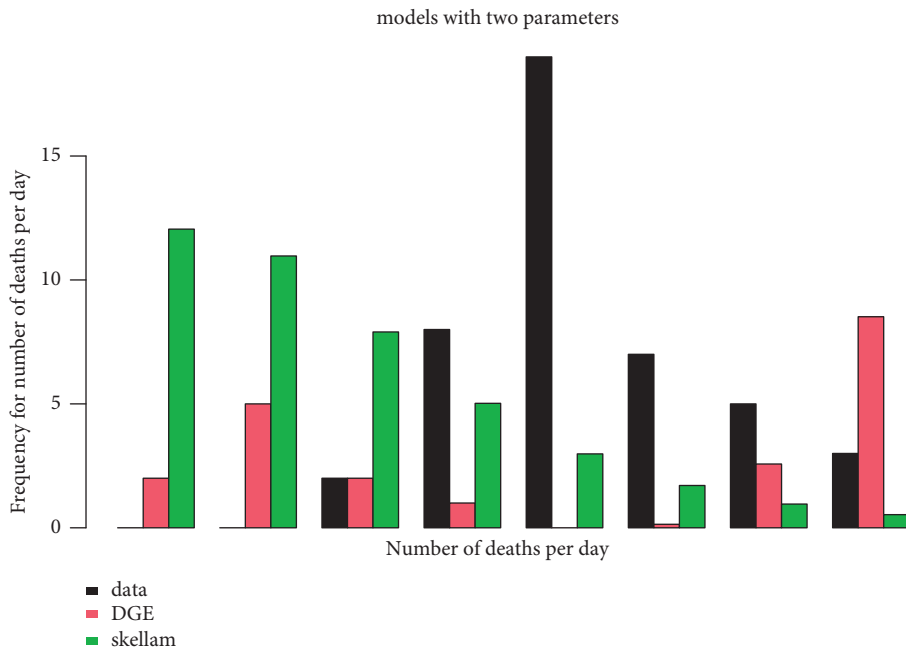


FIGURE 4: Graphical plots for the expected frequencies and the data using the PMF of different two-parameter distributions, where the  $x$ -axis represents the number of deaths per day and the  $y$ -axis represents the frequency for this number.

- Rbias value and MSE values of the three parameters decrease
- (2) Referring to Table 2, by making the value of  $\beta = 0.5$  and for a fixed value of  $\alpha = 0.5, 1.5, 5$  and increasing  $\lambda$  from 0.01 to 0.15, we deduce that the MSE and Rbias of the parameters increase in most cases
- (3) Referring to Table 3 by fixing the value of  $\beta = 1.5$  and for a fixed value of  $\alpha = 0.5, 1.5, 5$  and increasing  $\lambda$  from 0.05 to 0.5, we deduce that the MSE and Rbias of the parameters increase in most cases
- (4) By increasing the value of  $\beta$  from 1.5 to be five as in Table 4 and making the sample size fixed for both

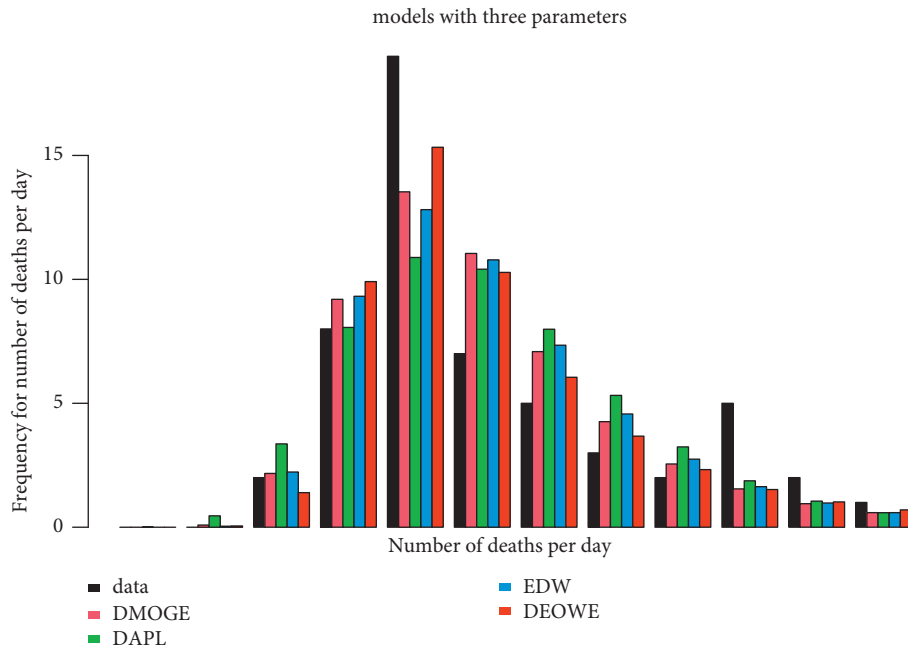


FIGURE 5: Graphical plots for the expected frequencies and the data using the PMF of different three-parameter distributions, where the x-axis represents the number of deaths per day and the y-axis represents the frequency for this number.

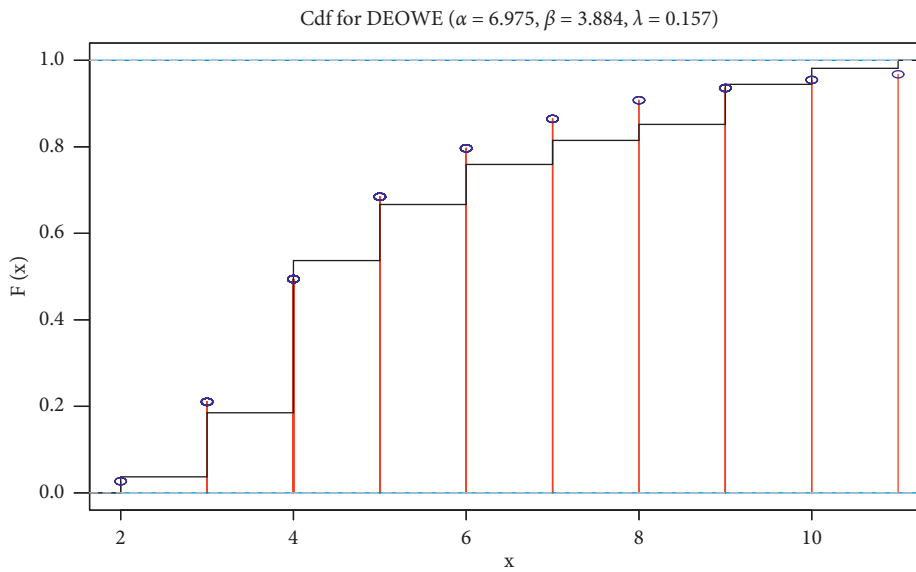


FIGURE 6: Graphical plots of the data and the CDF, as we can see in the plot, is distribution with the random variable with value x, where x is the number of deaths per day.

values of beta, we deduced that the MSE and Rbias of the parameters increase in most cases

### 6. Applications to COVID-19 Data

In this section of the paper, we introduce two real data applications on the COVID-19 mortality numbers in Saudi Arabia, and the third data are outside Saudi Arabia; this third data were for Latvia mortality rate. The first data were an expressed sample on the first wave, while the second sample was an expressed sample on the second wave. The

first application depends on the period from 26 December to 17 February 2021 for the infections in Saudi Arabia. We used this period because recording the infection numbers in this period was accurate as it was the peak of the second wave in Saudi Arabia. As in the earlier months of infection, recording the number of deaths was not accurate, so we choose this period specifically. The second dataset was taken for a period from 30 May 2020 to 20 August 2020. We choose this period because this period was the starting of the outbreak of COVID-19 in Saudi Arabia, and the mortality numbers start to increase also. This period is considered as the peak of the

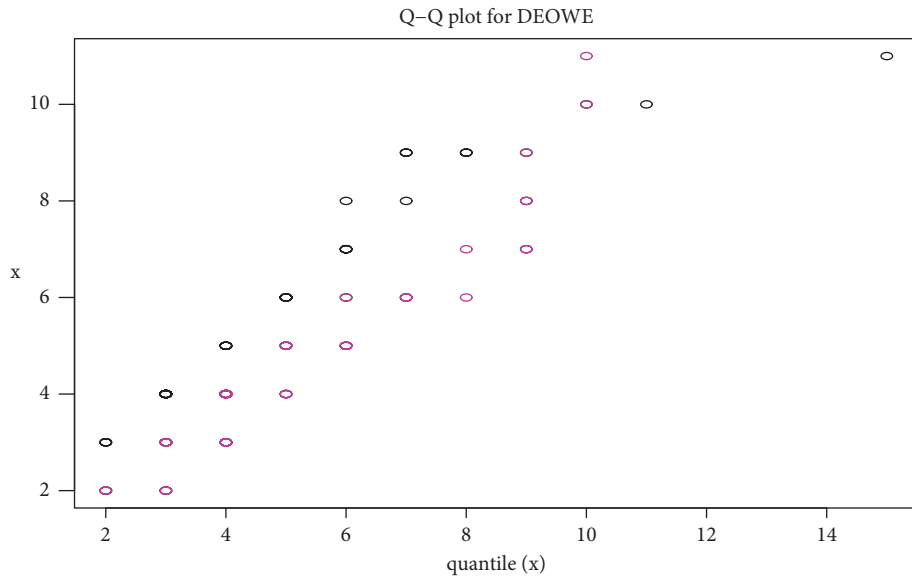


FIGURE 7: Graphical plots of the data and the quantile function as a function of  $(x)$ , where  $x$  is the number of deaths per day.

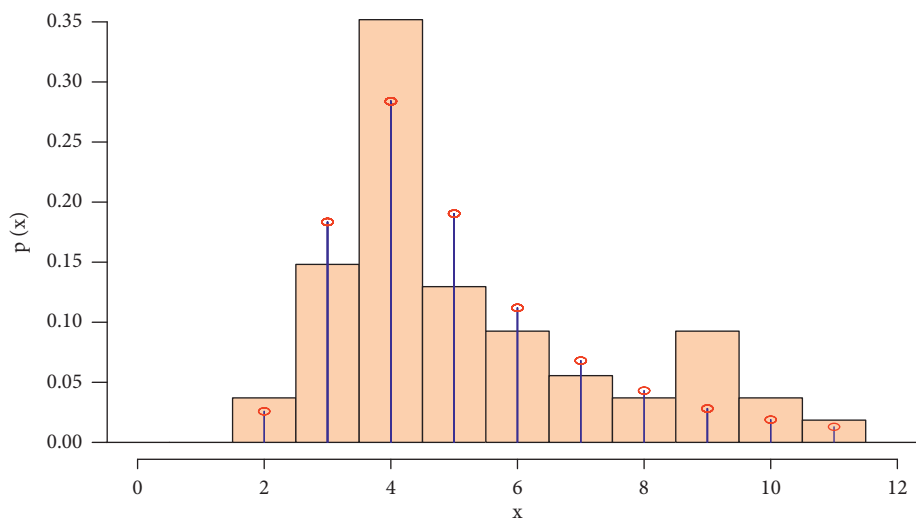


FIGURE 8: Graphical plots of the data and the PMF of the DEOWE distributions, where  $x$  is the number of deaths per day and  $p(x)$  is the probability for each  $x$ .

TABLE 7: Descriptive statistics for the second data.

$n$	Min	Q1	Median	Mean	Q3	Max	Skewness	Kurtosis
83	17.00	32.00	37.00	36.93	41.00	58.00	0.093	3.029

first wave in Saudi Arabia, which is very important to be modeled. We also evaluated the information criteria to introduce the importance of the proposed distribution compared with other competitors.

*6.1. Application 1.* In this section, we introduce a very important real data application for the DEOWE distribution, which the number of deaths due to COVID-19

infection in Saudi Arabia of 54 days of infection. Table 5 contains some information and descriptive statistics for this data, which are recorded from 26 December to 17 February 2021. The data used in this application are as below: 9, 8, 9, 11, 8, 10, 9, 7, 9, 7, 10, 9, 7, 6, 4, 4, 5, 4, 5, 4, 6, 3, 5, 5, 6, 6, 3, 4, 4, 4, 2, 3, 4, 4, 3, 2, 4, 3, 4, 4, 3, 3, 4, 4, 5, 4, 4, 5, 5, 4, 4, 4, 6, 3. This data were collected from the world health organization, and these numbers represent the number of deaths per day. For more information, see the following

TABLE 8: The dataset used in this application associated with the frequency of each death number and the probability of this number.

Number of deaths/day	Death counts for each number	DGE	DMOGE	EDW	DEOWE
17	1	0.058 5	0.178 8	0.196 5	0.225 8
18	0	0.122 0	0.225 4	0.273 3	0.293 7
19	0	0.228 5	0.283 3	0.370 9	0.377 2
20	1	0.389 4	0.355 2	0.492 0	0.478 8
21	1	0.611 7	0.444 2	0.638 6	0.600 9
22	2	0.895 6	0.553 9	0.812 2	0.746 0
23	1	1.232 9	0.688 4	1.013 1	0.916 2
24	2	1.608 7	0.852 0	1.240 2	1.113 4
25	0	2.003 0	1.049 5	1.491 3	1.338 3
26	1	2.393 8	1.285 0	1.762 5	1.590 9
27	2	2.760 0	1.562 0	2.048 1	1.869 4
28	1	3.083 5	1.882 1	2.341 4	2.170 0
29	1	3.351 0	2.243 9	2.634 2	2.486 9
30	4	3.554 2	2.641 8	2.917 5	2.811 4
31	3	3.690 1	3.064 6	3.182 1	3.132 8
32	3	3.759 8	3.494 6	3.418 6	3.437 9
33	0	3.768 0	3.907 9	3.618 4	3.712 2
34	7	3.721 4	4.275 8	3.774 3	3.940 9
35	3	3.628 4	4.568 1	3.880 3	4.110 4
36	6	3.497 9	4.757 8	3.932 9	4.209 7
37	8	3.338 5	4.825 8	3.930 4	4.231 6
38	2	3.158 3	4.765 1	3.873 5	4.174 1
39	6	2.964 7	4.582 0	3.765 4	4.040 6
40	5	2.763 8	4.294 9	3.610 9	3.839 5
41	4	2.560 9	3.930 6	3.416 5	3.583 2
42	3	2.360 3	3.519 1	3.189 9	3.286 6
43	0	2.165 0	3.089 4	2.939 5	2.965 4
44	1	1.977 6	2.665 7	2.673 8	2.634 9
45	2	1.799 8	2.266 0	2.401 1	2.308 2
46	2	1.632 5	1.901 9	2.128 9	1.996 1
47	0	1.476 6	1.579 4	1.864 0	1.706 1
48	2	1.332 1	1.300 0	1.611 8	1.443 2
49	2	1.199 1	1.062 2	1.376 5	1.209 6
50	2	1.077 1	0.862 8	1.161 2	1.005 8
51	1	0.965 9	0.697 4	0.967 6	0.830 6
52	1	0.864 8	0.561 5	0.796 5	0.681 8
53	0	0.773 2	0.450 6	0.647 7	0.557 0
54	1	0.690 5	0.360 8	0.520 3	0.453 1
55	0	0.615 9	0.288 2	0.412 9	0.367 3
56	1	0.548 9	0.229 9	0.323 7	0.297 0
57	0	0.488 8	0.183 1	0.250 6	0.239 6
58	1	0.434 9	0.145 7	0.191 6	0.193 0

TABLE 9: Descriptive statistics for the data of COVID-19 mortality numbers in Latvia.

$n$	Min	Q1	Median	Mean	Q3	Max	Skewness	Kurtosis
33	0	5	8	9	11	18	-0.509 94	0.189 237

link: <https://covid19.who.int/>. This data were used as a real data example for the proposed distribution and its competitor distributions. We compare the fitting results of the binomial (bionm), negative binomial(Nbionm), Poisson (Pois) distributions, see the work of Johnson et al. [22], discrete generalized exponential (DGE) distribution, see the work of Nekoukhou et al. [17], the discrete alpha power inverse Lomax (DAPIL) distribution is introduced by Almetwally and Ibrahim [23], the discrete Marshall–Olkin

Generalized exponential (DMOGE) distribution is introduced by Almetwally et al. [19], and Skellam [24] introduced the Skellam distribution, and the results of these fitting are tabulated in Table 6.

To make the comparison between many distributions, we must make this comparison based on some criteria; one of these analytical measures is called the Akaike information criterion (AIC), see [25]; there are another criteria called Bayesian information criterion (BIC), see [26], for more

TABLE 10: The dataset used in this application associated with the frequency of each death number and the probability of this number.

Value	Count	DGE	DMOGE	EDW	DEOWE
0	1	0.316 4	1.036 6	0.838 9	0.894 1
1	1	1.316 7	1.112 9	1.416 1	1.427 3
2	2	2.221 1	1.402 2	1.763 8	1.759 3
3	3	2.785 1	1.750 8	2.029 3	2.018 3
4	1	3.025 3	2.125 1	2.240 1	2.224 0
5	4	3.023 4	2.481 1	2.403 1	2.380 2
6	2	2.864 1	2.764 1	2.516 9	2.485 7
7	0	2.615 7	2.921 2	2.576 8	2.537 4
8	2	2.327 2	2.919 3	2.576 5	2.532 3
9	3	2.031 0	2.758 5	2.510 9	2.468 0
10	4	1.746 9	2.471 9	2.377 3	2.344 2
11	3	1.486 0	2.111 8	2.178 3	2.163 6
12	3	1.253 2	1.731 9	1.922 2	1.932 0
13	1	1.049 7	1.373 2	1.624 3	1.659 8
14	1	0.874 6	1.060 1	1.305 6	1.361 4
15	0	0.725 6	0.801 5	0.990 7	1.055 0
16	0	0.600 0	0.596 6	0.703 6	0.761 0
17	1	0.494 8	0.438 9	0.463 3	0.500 3
18	1	0.407 1	0.320 1	0.280 1	0.290 1

TABLE 11: MLE and SE for models' parameters and goodness-of-fit criteria for each model.

	DGE	DMOGE	EDW	DEOWE
$\alpha$	2.752 7	0.672 1	3.625 2	1.338 7
SE	0.768 5	1.524 8	0.598 7	0.305 4
$\beta$	0.815 1	0.713 0	0.393 6	0.169 8
SE	0.029 817	0.047 5	0.498 6	0.318 0
$\theta$		23.465 1	0.999 9	0.065 9
SE		3.396 5	0.185 6	0.010 7
$\chi^2$	15.249 3	11.719 0	11.700 8	11.700 5
<i>P</i> value	0.644 8	0.861 4	0.862 3	0.863 1
AIC	199.460 7	196.707 7	195.341 1	195.325 5
CAIC	199.860 7	197.535 3	196.168 7	196.153 1
BIC	202.453 7	201.197 2	199.830 6	199.815 0
HQIC	200.467 8	198.218 3	196.851 7	196.836 1

information, and we can also refer to Hannan–Quinn for more information criterion (HQIC), see [27], for more information, and last criteria are called the consistent Akaike information criterion (CAIC), see [28], for more details; all these criteria were used to compare the goodness of fit of the proposed model with other competing distributions. These measures are as follows.

The AIC is given by

$$AIC = 2k - 2\ell. \tag{22}$$

The CAIC is

$$CAIC = \frac{2nk}{n - k - 1} - 2\ell. \tag{23}$$

The BIC is calculated as follows:

$$BIC = k \log(n) - 2\ell. \tag{24}$$

The HQIC is

$$HQIC = 2k \log(\log(n)) - 2\ell. \tag{25}$$

where  $k$  is the number of model parameters,  $n$  is the sample size, and  $\ell$  refers to the log-likelihood function evaluated at the MLEs. Table 6 provides values of AIC, BIC, CAIC, HQIC and, chi square ( $\chi^2$ ) with a degree of freedom, and its *P* value for all models is fitted based on the real dataset of Saudi Arabia. Figure 3 indicates a comparison between these distributions to get the best distribution; also, Figures 3–5 indicate the graphical plots of the data and the PMF of DEOWE distributions, with the corresponding competitive distributions with various numbers of parameters. As we can see that the plot in Figure 6 is the CDF of the distributions with the random variable  $X$ , while the third graph in Figure 7 is for the quantile function as a function of  $x$ , where  $x$  is the number of deaths per day; Figure 8 shows graphical plots of the data and the PMF of the DEOWE distributions.

*6.2. Application 2.* In this section, the DEOWE distribution is fitted to another set of data of COVID-19 mortality numbers in Saudi Arabia of 83 days of infection, which is recorded from 30 May 2020 to 20 August 2020. Table 7

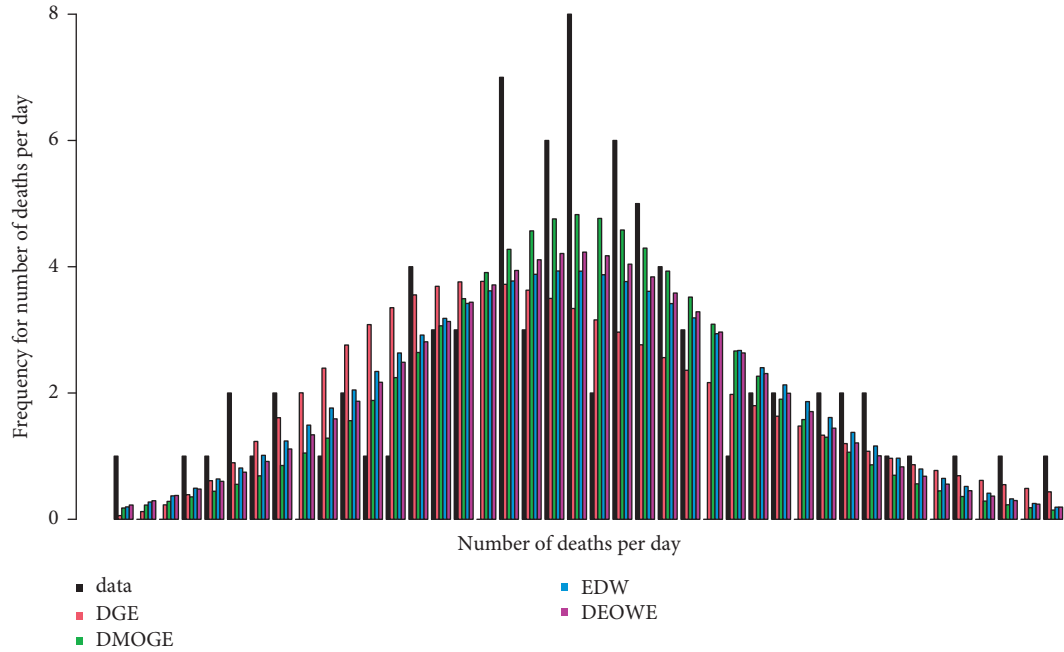


FIGURE 9: Graphical plots for the expected frequencies and the data using the PMF of different parameters distributions, where the  $x$ -axis represents the number of deaths per day and the  $y$ -axis represents the frequency for this number.

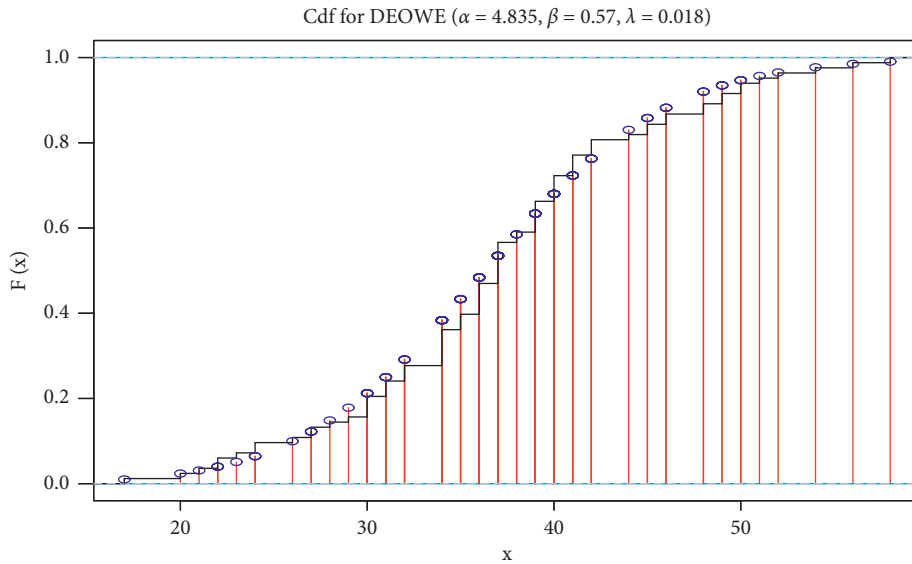


FIGURE 10: Graphical plots of the data and the CDF, as we can see in the plot, the distributions with the random variable with value  $x$ , where  $x$  is the number of deaths per day.

contains some information and descriptive statistics for this data, while Table 8 contains the dataset used in this application associated with the frequency of each death number and the probability of this number; the data are as follows: 17, 22, 23, 22, 24, 30, 32, 31, 34, 36, 34, 37, 36, 38, 36, 39, 40, 39, 41, 39, 48, 45, 46, 37, 40, 39, 41, 41, 46, 37, 40, 48, 50, 49, 54, 50, 56, 58, 52, 49, 42, 41, 51, 30, 42, 20, 40, 42, 45, 37, 40, 39, 37, 34, 44, 34, 37, 31, 30, 27, 29, 27, 26, 24, 21, 30, 32, 35, 36, 35, 38, 37, 37, 32, 34, 36, 34, 35, 31, 39, 28, 34, 36. These

data were collected from the World Health Organization and these numbers represents the number of deaths per day, for more information see the following link: <https://covid19.who.int/>. We compare the fitting results of the discrete generalized exponential (DGE) distribution, see the work of Nekoukhou et al. [17], the discrete Marshall–Olkin generalized exponential (DMOGE) distribution is introduced by Almetwally et al. [19], and exponentiated discrete Weibull (EDW) distribution is introduced by Nekoukhou et al. [29].

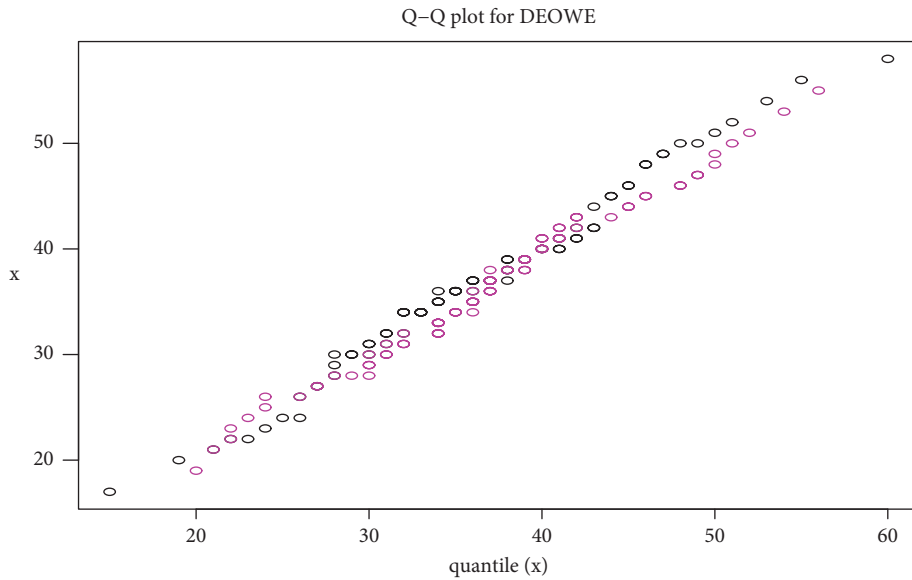


FIGURE 11: Graphical plots of the data and the quantile function as a function of  $(x)$ , where  $x$  is the number of deaths per day.

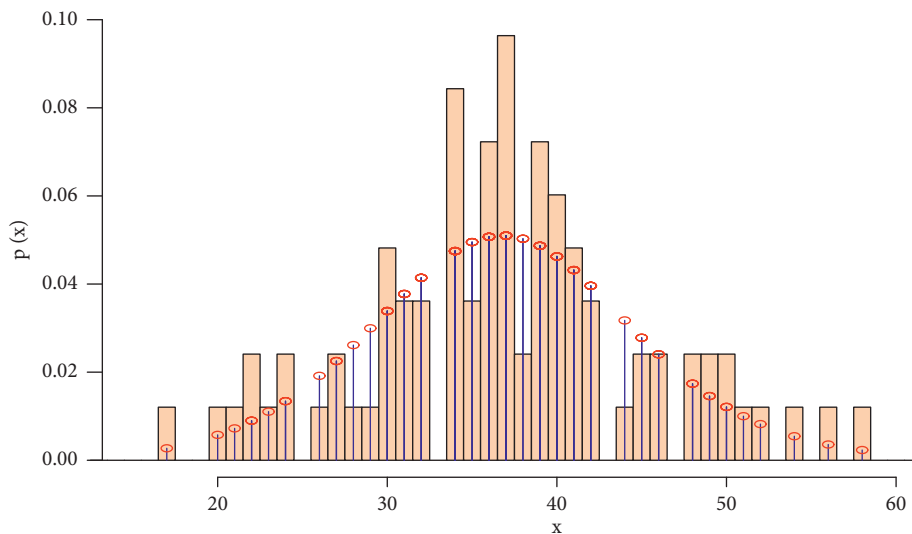


FIGURE 12: Graphical plots of the data and the PMF of the DEOWE distributions, as we can see in the plot is the PMF of the distributions with the random variable with value  $(x)$ , where  $x$  is the number of deaths per day and  $P(x)$  is the probability for  $x$ .

6.3. *Application 3.* In this section, the DEOWE distribution is fitted to another set of data of COVID-19 mortality numbers in Latvia of 33 days of infection, which is recorded from 12 May 2021 to 13 April 2021. We choose this period specifically because it was the peak of the second wave of the COVID-19 infection in Latvia. Table 9 contains some information and descriptive statistics for this data, while Table 10 contains the dataset used in this application associated with the frequency of each death number and the probability of this number, and Table 11 contains the MLE of the parameters and the  $P$  values and chi-square values for the distributions, also the information criteria for each distribution. The data are as follows: 11, 9, 11, 10, 2, 8, 12, 12, 10, 10, 5, 2, 12, 11, 13, 3, 5, 6, 5, 10, 6, 14, 9, 1, 8, 3, 3, 9, 17, 18, 5, 0, 4. These data were collected from the world health

organization, and these numbers represent the number of deaths per day. For more information, see the following link: <https://covid19.who.int/>. We compare the fitting results of the discrete generalized exponential (DGE) distribution, see the work of Nekoukhou et al. [17], the discrete Marshall–Olkin generalized exponential (DMOGE) distribution is introduced by Almetwally et al. [19], and exponentiated discrete Weibull (EDW) distribution is introduced by Nekoukhou et al. [29].

#### 6.4. Concluding Remarks on the Real Data

- (1) By referring to the goodness-of-fit measurements' values in Tables 6 and 12, we deduce that the DEOWE distribution has the lowest chi square, AIC,

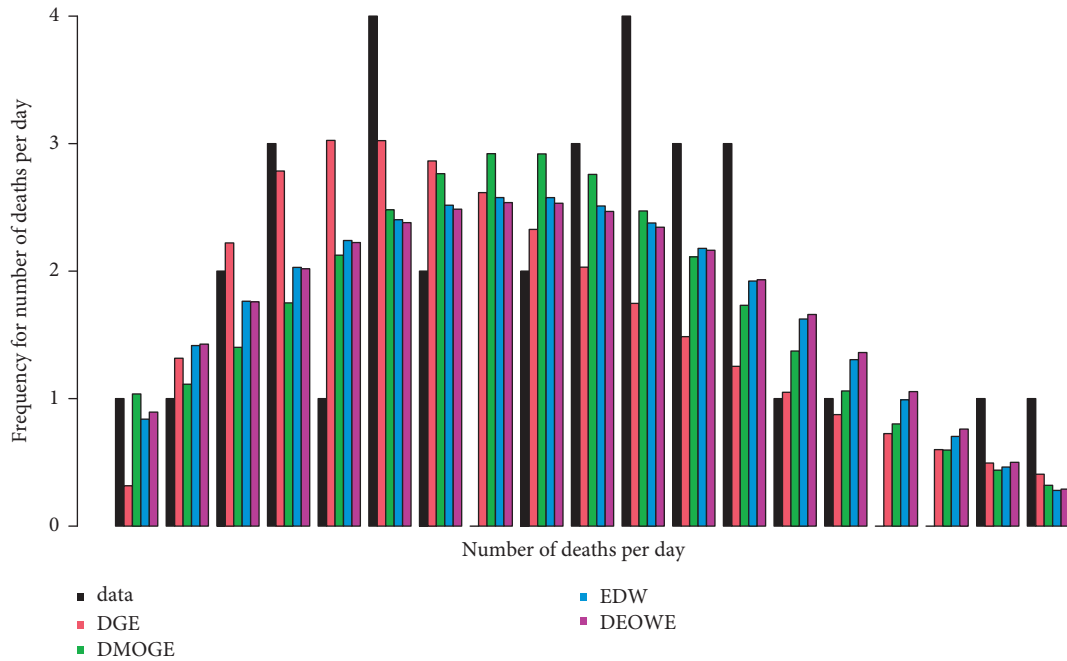


FIGURE 13: Graphical plots for the expected frequencies and the data using the PMF of different parameters' distributions, where the  $x$ -axis represents the number of deaths per day and the  $y$ -axis represents the frequency for this number.

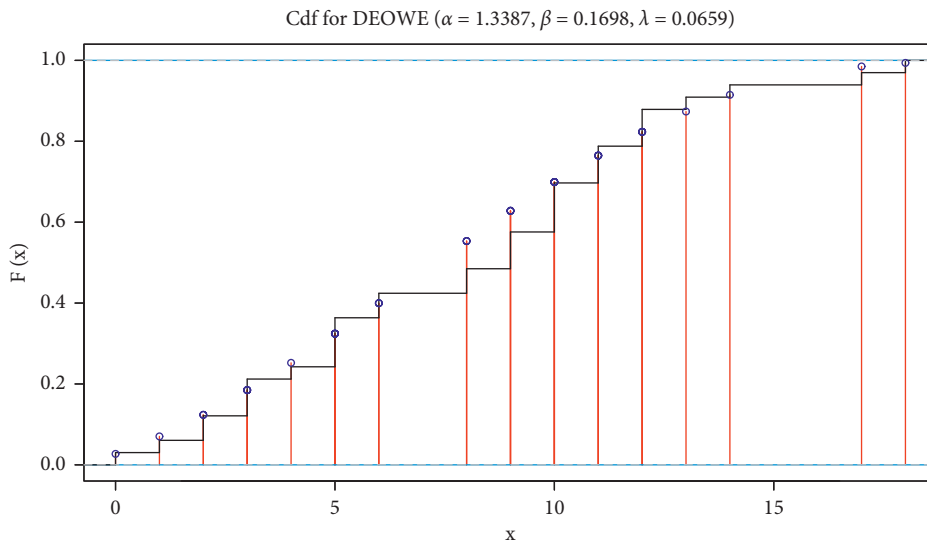


FIGURE 14: Graphical plots of the data and the CDF, as we can see in the plot, is the distributions with the random variable with value  $x$ , where  $x$  is the number of deaths per day.

and CAIC values among all distributions for the three applications.

- (2) By referring to the values of the goodness of fit measurements in Tables 6 and 12, we deduce that the DEOWE distribution has the highest  $P$  value among all of its competitors for the three applications.
- (3) For application one and by referring to Figures 3 and 4, we can see that the one- and two-parameter distributions provide poor fitting for the data. In contrast, the three-parameter DEOWE distribution

in Figure 5 provides better fitting for the data among all its competitors.

- (4) For application two and by referring to Figure 9, we can see that the three-parameter DEOWE distribution in Figure 9 provides better fitting for the data among all its competitors.
- (5) For application two, we can see that the plot in Figure 10 is the CDF of the distributions with the random variable  $X$ , while the graph in Figure 11 is for the quantile function as a function of  $x$ , where  $x$  is the



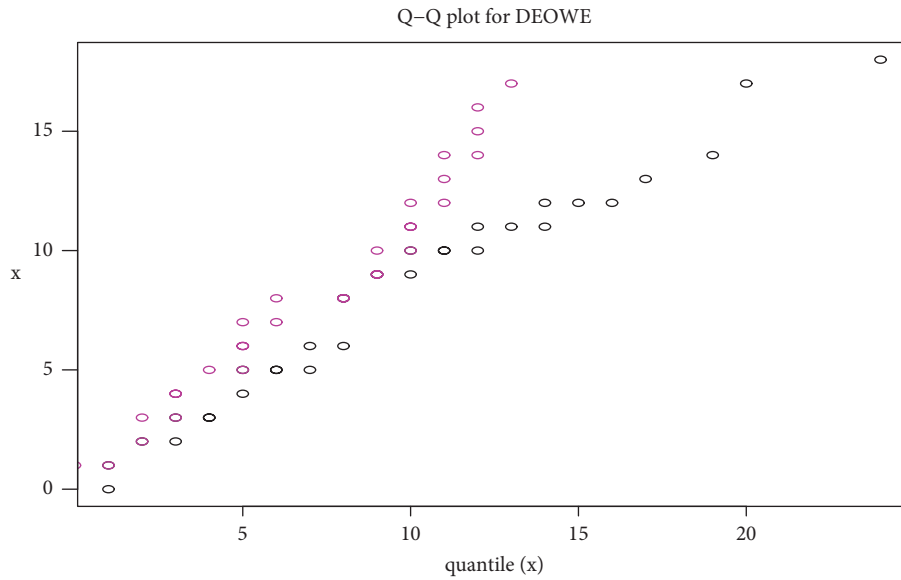


FIGURE 15: Graphical plots of the data and the quantile function as a function of  $x$ , where  $x$  is the number of deaths per day.

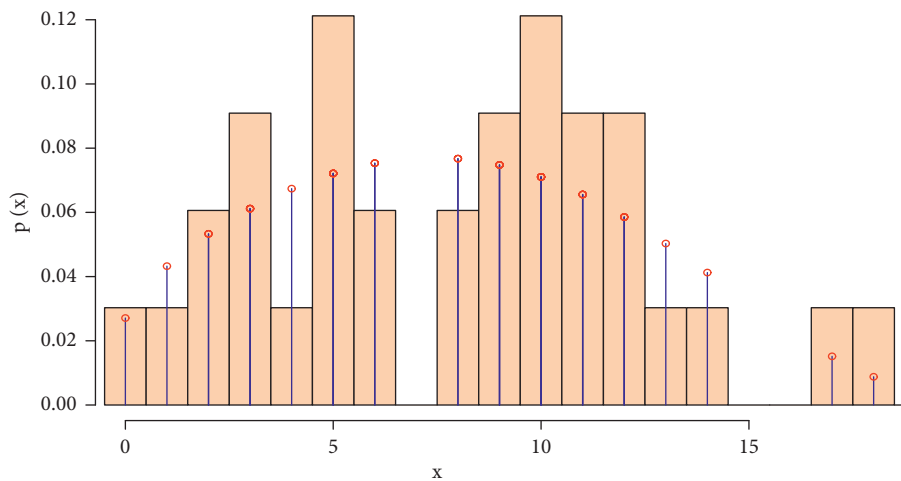


FIGURE 16: Graphical plots of the data and the PMF of the DEOWE distributions, as we can see in the plot which is the PMF of the distributions with the random variable with value  $x$ , where  $x$  is the number of deaths per day and  $P(x)$  is the probability for  $x$ .

number of deaths per day. Figure 12 shows graphical plots of the data and the PMF of the DEOWE distributions

- (6) For application three and by referring to Figure 13, we can see that the three-parameter DEOWE distribution in Figure 13 provides better fitting for the data among all its competitors for more information about the PMF of the other distributions, see the Appendix.
- (7) For application three, we can see that the plot in Figure 14 is the CDF of the distributions with the random variable  $X$ , while the graph in Figure 15 is for the quantile function as a function of  $x$ , where  $x$  is the number of deaths per day. Figure 16 shows graphical plots of the data and the PMF of the DEOWE distributions

### 7. Conclusion

In this paper, we introduced a new distribution, which is called DEOWE distribution the aim to do this work was the lack of flexibility in other distributions. We studied its statistical properties and obtained a linear representation for its PMF and the associated quantile function. We used the MLE method for estimating the distribution parameters  $\alpha, \beta$ , and  $\lambda$ . Also, a real dataset of the mortality numbers in the Kingdom of Saudi Arabia (KSA) was considered to assess the performance of the DEOWE. The distribution fitting for the real dataset was compared with its competitors, and by referring to the values of the goodness of fit measurements, we deduce that the DEOWE distribution has the lowest chi square, AIC, and CAIC for the first dataset, and for the second dataset, we deduce that the DEOWE distribution has the lowest chi square, AIC, CAIC, BIC, and HQIC and the

TABLE 12: MLE and SE for models' parameters and goodness-of-fit criteria for each model.

	DGE	DMOGE	EDW	DEOWE
$\alpha$	0.8847	20.505 0	3.157 6	4.835 5
SE	0.008 9	0.003 9	1.516 5	0.767 1
$\beta$	57.948 8	0.792 6	2.440 6	0.570 4
SE	18.469 4	0.004 0	0.951 5	0.315 7
$\theta$		300.010 0	0.999 8	0.018 1
SE		0.002 7	0.000 5	0.000 7
$\chi^2$	52.624 2	43.500 3	38.782 6	37.463 0
$P$ value	0.105 4	0.365 4	0.569 6	0.628 6
AIC	602.986 2	594.508 2	593.607 3	593.432 5
CAIC	603.136 2	594.812 0	593.911 1	593.736 3
BIC	607.823 8	601.764 7	600.863 9	600.689 1
HQIC	604.929 7	597.423 4	596.522 6	596.347 8

highest  $P$  value among all of its competitors. This result indicates that the DEOWE distribution provides a superior model for fitting the mortality number compared with other competitive distributions. Also, we make a graphical plot for the data using the DEOWE with other competitive distributions, and the plots come in our favor and assure the results of the goodness-of-fit measurements.

## Appendix

The PMF of the compared models is given as the following.

- (i) Binomial distribution:  $P(X = x) = p^x \binom{n}{x} (1-p)^{n-x}$ ,  $x = 0, 1, 2, 3, \dots, n$ .
- (ii) Poisson distribution:  $P(X = x) = e^{-\lambda} \lambda^x / x!$ ,  $x = 0, 1, 2, 3, \dots$
- (iii) Negative binomial distribution:  $P(X = x) = p^n (1-p)^x \binom{n+x-1}{n-1}$ ,  $x = 0, 1, 2, 3, \dots$
- (iv) Skellam distribution:  $P(X = x) = e^{-\mu_1 - \mu_2} (\mu_1/\mu_2)^{x/2} I_k(2\sqrt{\mu_1\mu_2})$ ,  $x = \dots, -3, -2, -1, 0, 1, 2, 3, \dots$
- (v) Discrete alpha power inverse Lomax:  $P(X = x) = (\alpha^{\rho^{1/(1+(\delta/x+1))}} - \alpha^{\rho^{1/(1+(\delta/x+1))}}) / (\alpha - 1)$ ,  $x = 0, 1, 2, 3, \dots$
- (vi) Discrete generalized exponential distribution:  $P(X = x) = (1 - \theta^{x+1})^\alpha - (1 - \theta^x)^\alpha$ ,  $x = 0, 1, 2, 3, \dots$
- (vii) Discrete Marshall–Olkin generalized exponential distribution:  
 $P(X = x) = (\lambda(1 - (1 - \rho^x)^\alpha) / \lambda + (1 - \lambda)(1 - \rho^{x+1})^\alpha) - (\lambda(1 - (1 - \rho^{x+1})^\alpha) / \lambda + (1 - \lambda)(1 - \rho^{x+1})^\alpha) a s^\alpha$ ,  $x = \dots, -3, -2, -1, 0, 1, 2, 3, \dots$
- (viii) Exponentiated discrete Weibull:  
 $P(X = x) = (1 - \rho^{(x+1)^\alpha})^\beta - (1 - \rho^{x^\alpha})^\beta$ ,  $x = \dots, -3, -2, -1, 0, 1, 2, 3, \dots$

For more information about the code used in the paper, see Function "maxLik" of "maxLik" package in the R program which has been used by Pho, K. H., and Nguyen, V. T. (2018) in Comparison of Newton–Raphson algorithm and Maxlik function, *Journal of Advanced Engineering and Computation*, 2(4), 281–292, and Henningsen, A., and

Toomet, O. (2011), maxLik: A package for maximum likelihood estimation in R. *Computational Statistics*, 26(3), 443–458.

## Data Availability

All data links and references are provided within the article.

## Conflicts of Interest

The authors declare no conflicts of interest regarding this paper.

## Authors' Contributions

All authors supervised, validated, visualized, wrote the original draft, and reviewed and edited the manuscript. Editing and replying to reviewers have been done by Dr Taghreed M. Jawa and Neveen Sayed-Ahmed. Proof editing and fixing typos and revising the language have been done by both Dr Taghreed M. Jawa and Dr Neveen Sayed-Ahmed.

## Acknowledgments

This work was supported by Taif University researchers, supporting project no. TURSP-2020/318, Taif University, Taif, Saudi Arabia.

## References

- [1] A. A. Al-Babtain, A. H. N. Ahmed, and A. Z. Afify, "A new discrete analog of the continuous Lindley distribution, with reliability applications," *Entropy*, vol. 22, no. 6, p. 603, 2020.
- [2] A. Hasab, E. El-Ghitany, and N. Ahmed, "Situational analysis and epidemic modeling of COVID-19 in Egypt," *Journal of High Institute of Public Health*, vol. 50, no. 1, pp. 46–51, 2020.
- [3] A. Algarni, A. M. Almarashi, I. Elbatal et al., "Type I half logistic Burr XG family: properties, bayesian, and non-bayesian estimation under censored samples and applications to COVID-19 data," *Mathematical Problems in Engineering*, vol. 2021, Article ID 5461130, 2021.
- [4] E. M. Almetwally, "The odd Weibull inverse topp-leone distribution with applications to COVID-19 data," *Annals of Data Science*, pp. 1–20, 2021, <https://doi.org/10.1007/s40745-021-00329-w>.
- [5] E. Almetwally, R. Alharbi, D. Alnagar, and E. Hafez, "A new inverted topp-leone distribution: applications to the COVID-19 mortality rate in two different countries," *Axioms*, vol. 10, no. 1, p. 25, 2021.
- [6] M. El-Morshedy, E. Altun, and M. S. Eliwa, "A new statistical approach to model the counts of novel coronavirus cases," *Research Square*, 2020.
- [7] M. Maleki, M. R. Mahmoudi, D. Wraith, and K. H. Pho, "Time Series Modelling to Forecast the Confirmed and Recovered Cases of COVID-19," *Travel Medicine and Infectious Disease*, vol. 37, Article ID 101742, 2020.
- [8] I. Nesteruk, "Statistics-based predictions of coronavirus epidemic spreading in mainland China," *Innovative Biosystems and Bioengineering*, vol. 4, no. 1, pp. 13–18, 2020.
- [9] M. Batista, "Estimation of the final size of the COVID-19 epidemic," 2020.
- [10] A. H. Muse, A. H. Tolba, E. Fayad, O. A. Abu Ali, M. Nagy, and M. Yusuf, "Modelling the COVID-19 mortality rate with

- a new versatile modification of the log-logistic distribution," *Computational Intelligence and Neuroscience*, vol. 2021, Article ID 8640794, 2021.
- [11] X. Liu, Z. Ahmad, A. M. Gemeay, A. T. Abdulrahman, E. H. Hafez, and N. Khalil, "Modeling the survival times of the COVID-19 patients with a new statistical model: a case study from China," *PLoS One*, vol. 16, no. 7, Article ID e0254999, 2021.
- [12] A. Z. Afify and O. A. Mohamed, "A new three-parameter exponential distribution with variable shapes for the hazard rate: estimation and applications," *Mathematics*, vol. 8, no. 1, p. 135, 2020.
- [13] R. Alshenawy, A. Al-Alwan, E. M. Almetwally, A. Z. Afify, and H. M. Almongy, "Progressive type-II censoring schemes of extended odd Weibull exponential distribution with applications in medicine and engineering," *Mathematics*, vol. 8, no. 10, p. 1679, 2020.
- [14] B. A. Para and T. R. Jan, "On discrete three parameter Burr type XII and discrete Lomax distributions and their applications to model count data from medical science," *Biometrics and Biostatistics International Journal*, vol. 4, no. 2, pp. 1–15, 2016.
- [15] H. Krishna and P. Singh Pundir, "Discrete Burr and discrete pareto distributions," *Statistical Methodology*, vol. 6, no. 2, pp. 177–188, 2009.
- [16] E. Gómez-Déniz and E. Calderín-Ojeda, "The discrete Lindley distribution: properties and applications," *Journal of Statistical Computation and Simulation*, vol. 81, no. 11, pp. 1405–1416, 2011.
- [17] V. Nekoukhou, M. H. Alamatsaz, and H. Bidram, "Discrete generalized exponential distribution of a second type," *Statistics*, vol. 47, no. 4, pp. 876–887, 2013.
- [18] J. Gillariose, O. S. Balogun, E. M. Almetwally, R. A. K. Sherwani, F. Jamal, and J. Joseph, "On the discrete Weibull marshall-olkin family of distributions: properties, characterizations, and applications," *Axioms*, vol. 10, no. 4, p. 287, 2021.
- [19] E. M. Almetwally, H. M. Almongy, and H. A. Saleh, "Managing risk of spreading" COVID-19" in Egypt: modelling using a discrete marshall-olkin generalized exponential distribution," *International Journal of Probability and Statistics*, vol. 9, no. 2, pp. 33–41, 2020.
- [20] A. A. Al-Babtain, A. M. Gemeay, and A. Z. Afify, "Estimation methods for the discrete poisson lindley and discrete lindley distributions with actuarial measures and applications in medicine," *Journal of King Saud University - Science*, vol. 33, Article ID 101224, 2020.
- [21] D. Roy, "The discrete normal distribution," *Communications in Statistics - Theory and Methods*, vol. 32, no. 10, pp. 1871–1883, 2003.
- [22] N. L. Johnson, A. W. Kemp, and S. Kotz, *Univariate discrete distributions*, Vol. 444, John Wiley & Sons, , Hoboken, New Jersey, 2005.
- [23] E. M. Almetwally and G. M. Ibrahim, "Discrete alpha power inverse Lomax distribution with application of COVID-19 data," *International Journal of Applied Mathematics*, vol. 9, no. 6, pp. 11–22, 2020.
- [24] J. G. Skellam, "The frequency distribution of the difference between two poisson variates belonging to different populations," *Journal of the Royal Statistical Society*, vol. 109, no. 3, p. 296, 1946.
- [25] H. Akaike, "A new look at the statistical model identification," *IEEE Transactions on Automatic Control*, vol. 19, no. 6, pp. 716–723, 1974.
- [26] G. Schwarz, "Estimating the dimension of a model," *Annals of Statistics*, vol. 6, pp. 461–464, 1978.
- [27] E. J. Hannan and B. G. Quinn, "The determination of the order of an autoregression," *Journal of the Royal Statistical Society: Series B Methodological*, vol. 41, no. 2, pp. 190–195, 1979.
- [28] H. Bozdogan, "Model selection and Akaike's Information Criterion (AIC): the general theory and its analytical extensions," *Psychometrika*, vol. 52, no. 3, pp. 345–370, 1987.
- [29] V. Nekoukhou and B. Hamid, "The exponentiated discrete Weibull distribution," *Statistics and Operations Research Transactions*, vol. 39, pp. 127–146, 2015.

## Research Article

# Nonlinear Cointegration and Asymmetric Adjustment in Purchasing Power Parity of the USA, Germany, and Pakistan

**Kashif Ali,<sup>1</sup> Hafsa Hina,<sup>2</sup> Muhammad Ijaz<sup>3</sup> ,<sup>3</sup> and Mahmoud El-Morshedy<sup>4,5</sup> **

<sup>1</sup>Department of Statistics, University of Peshawar, Peshawar, Pakistan

<sup>2</sup>Department of Econometrics and Statistics, PIDE, Islamabad, Pakistan

<sup>3</sup>Department of Mathematics and Statistics, The University of Haripur, Haripur, Pakistan

<sup>4</sup>Department of Mathematics, College of Science and Humanities in Al-Kharj, Prince Sattam Bin Abdulaziz University, Al-Kharj 11942, Saudi Arabia

<sup>5</sup>Department of Mathematics, Faculty of Science, Mansoura University, Mansoura 35516, Egypt

Correspondence should be addressed to Muhammad Ijaz; [ijaz.statistics@gmail.com](mailto:ijaz.statistics@gmail.com)

Received 16 October 2021; Accepted 2 December 2021; Published 21 December 2021

Academic Editor: S.S. Askar

Copyright © 2021 Kashif Ali et al. This is an open access article distributed under the Creative Commons Attribution License, which permits unrestricted use, distribution, and reproduction in any medium, provided the original work is properly cited.

The current study explores nonlinear cointegration as well as asymmetric adjustment to investigate the long-run purchasing power parity in three major trading partners of Pakistan. The ESTAR and LSTAR models were used to investigate the behavior of the nominal exchange rates. The findings declared that series follows the nonlinear exchange rate. The asymmetric behavior of the exchange rate allows the threshold cointegration model to be implemented. In the case of Pakistan-China, the result suggests that long-run PPP holds. As a result, trading will be more profitable if the exchange rate is varied in relation to major trading partners rather than just the US dollar.

## 1. Introduction

Globalization and financial liberalization have significantly increased the role of international finance and trade, whereas small open economies like Pakistan can only creep the benefits of globalization and financial liberalization if they are maintaining a stable exchange rate. The exchange rate volatility has a direct impact on the profitability of multinational corporations and financial institutions. A stable exchange rate may help in reducing the operational risk of enterprise and financial institutions, by guiding the evaluation of the performance of investments, financing, and hedging decision [1]. Instability in the exchange rate is emerged due to poor economic fundamentals, internal and external shocks to the economy, and changes in existing policy structures, which lead to change in the behavior of the exchange rate series from linear to nonlinear.

The purchasing power parity (PPP) can explain the long-run equilibrium of the exchange rate. PPP serves as a standard for calculating exchange rates and determining

whether real exchange shocks diminish over time. The concept of PPP is closely related to the behavior of exchange rates, which often help to detect whether implemented policies are responsible for disequilibrium in an open economy or not. The PPP theory of exchange rate which is originally advanced by Cassel [2] states that, in the floating exchange rates system, where the trade is free and transport, speculative expectations costs and capital flows are absent; the nominal exchange rate is the ratio of that two countries price level.

Aminifard [4] studied the trade relations and long-run purchasing power parity (PPP) between the selected East Asian Countries and Iran, Korea, and the World Economy; Zhao [5] worked on the nonlinear cointegration; Enders [6] and Patel [7] used the cointegration test by Engle and Granger [8], but they fail to accept the validity of long-run PPP. Ahmad and Khan [9] studied the long-run PPP for Pakistan and for some Asian countries and verified the failure of the PPP theory. Basher and Mohsin [10] also test the relative form of PPP using panel cointegration and reject

the PPP hypothesis. The problem at the core of this methodology was that when the data-generating process is nonlinear, then standard unit root tests, as well as cointegration tests, have insufficient power to detect stationarity. Another problem with traditional cointegration tests is that it assumes symmetric adjustment, but it is quite possible that an exchange of country is asymmetric. For more detailed study, we refer to the studies by Abdul Qayyum et al. [11]; Abuaf [12]; Basher and Razzaque [13]; Chumrusphonlert and Enders [14]; Enders [6]; Enders [15]; Franses [16]; Hansen and Seo [17]; Husain [18]; Hylleberg et al. [19]; Liu [20]; Miron and Beaulieu [21]; Sollis [22]; and Tong [23].

Nonlinearity in the exchange rate allows for a more general form of PPP where the adjustments of foreign as well as domestic prices need not be proportional and symmetric to exchange rate. In recent times, the Engle–Granger linear cointegration has been extended into a threshold framework by many researchers such as Johansen’s [24] research allows for threshold short-run dynamics in error-correction models. Balke and Fomby [25] introduce a threshold cointegration model that accommodates for threshold adjustments towards a long-run (LR) equilibrium while Enders and Falk [15] employ a similar model to investigate the purchasing power parity (PPP).

As we discussed above that many researchers test the long-run PPP by the method of Engle–Granger [8] and Johansen and Juselius [26], some of the results in favor of PPP and some of them reject the PPP. After the development of the threshold cointegration technique by Balke and Fomby [25] and Hansen and Seo [27], many researchers such as Chumrusphonlert and Enders [14]; Enders and Siklos [28]; and Henson and Seo [27] had tested the long-run PPP by applying the nonlinear cointegration method. Phiri [29] defined the nonlinear effects in purchasing power parity, Ang et al. [30]; discussed deviations in PPP and exchange rate, Arize et al. [31] discussed the nonlinear ARDL approach and PPP for more than 80 countries, Tipoy et al. [32] worked out the exchange rate misalignment and economic growth using nonlinear panel cointegration, Bahmani-Oskooee et al. [33] explored the asymmetric cointegration approach for the China and its trading partners, Iqbal et al. [34] studied the asymmetric nonlinear cointegration for Pakistan and its other trading partners. Thus, the existence of the long-run PPP is supported by most of the research studies.

In practice, the linear models are preferring to use when the dependent variables are linear in nature. In the current study, the dependent variables, i.e., the exchange rates of Pak-China, Pak-USA, and Pak-Germany were tested by using the STAR model and found nonlinear. Thus, it is allowed us to use the nonlinear cointegration procedure.

The main objective of the research is to evaluate the nominal exchange rate adjustment via PPP theory for the top three trading partners of Pakistan (USA, Germany, and China), instead of assuming linear cointegration as done by many researchers in the case of Pakistan. This study contributes to the existing literature of Pakistan, in the case of Pakistan; no one incorporated the threshold cointegration in

the purchasing power parity hypothesis. In particular, the linear behavior of the nominal exchange rate will examine through exponential smooth threshold autoregressive (ESTAR) and logistic smooth threshold autoregressive (LSTAR) models. Furthermore, the speed adjustment of the exchange rate toward the long-run equilibrium is also being measured through the threshold error-correction model.

*1.1. Novelty and Significance of the Study.* In existing literature, many researchers have treated the exchange rate as a linear model. This study shows that the exchange rate follows a nonlinear model in the case of Pakistan. For this purpose, we have considered the nonlinear cointegration technique so that to delineate the long-run relationship of the exchange rate of Pakistan with that of the toped three trader countries, i.e., USA, China, and Germany. Moreover, the main aim of the study is to analyze the theory of PPP by considering the exchange rate of the top three trading partners of Pakistan.

## 2. Materials and Methodology

*2.1. Data and Variable Description.* This dataset consists of monthly observations covering the period from 1982 to 2013. The nominal exchange rate of Pak rupee is measured against per unit of US dollar, China yuan, and German euro and denoted by  $EX_{p-U}$ ,  $EX_{p-C}$  and  $EX_{p-G}$ .  $p$  is the consumer price index of Pakistan and  $p_U^*$ ,  $p_C^*$ , and  $p_G^*$  are the CPI for USA, China, and Germany. The dataset is taken from the IMF website.

*2.2. Econometric Modeling for PPP.* The advocates of the law of one price claim that PPP holds internationally for the same bundle of goods through the adjustment of the exchange rate. The relative form of PPP is defined by Cassel [2] with the following mathematical form:

$$\Delta e_t = \beta_0 + \beta_1 (\Delta p_t - \Delta p_t^*) + \varepsilon_t, \quad (1)$$

where “ $\Delta$ ” is the first difference of the series;  $p$ ,  $p^*$ , and  $\varepsilon_t$  stand for the natural log of the domestic price, foreign price, and nominal exchange rate, respectively, while  $\varepsilon_t$  is the noise.

*2.3. Unit Root Test of Beaulieu and Miron.* This technique is used to check whether the data under consideration is stationary or nonstationary. The unit root test by Beaulieu and Miron [21] is usually used to detect the nonseasonal and seasonal unit root in monthly data. Beaulieu and Miron [21] proposed an auxiliary regression model for the identification of unit root given as follows:

$$y_{13T} = \alpha + \beta t + \sum_{i=1}^{11} \gamma_i s_i + \sum_{i=1}^{12} \pi_i y_{it-1} + \varepsilon_t, \quad (2)$$

where  $y_t$  is the series of interest; the deterministic part is consisting of any combination of constant ( $\alpha$ ), a linear trend ( $t$ ), and seasonal dummies ( $s_i$ ).  $\varepsilon_t$  is the white noise error term. Table 1 illustrates all possible hypotheses for the monthly nonseasonal and seasonal unit roots.

TABLE 1: Null and alternative hypotheses for monthly unit root test.

Test of unit root at different frequencies	Null and alternative hypotheses
Zero frequency unit root	$H_0^A, \pi_1 = 0$ vs $H_1^A, \pi_1 < 0$
Biannual frequency unit root	$H_0^B, \pi_2 = 0$ vs $H_1^B, \pi_2 < 0$
Seasonal frequency unit root	$H_0^j, \pi_i = \pi_{i+1} = 0$ vs $H_1^j$ , at least one of them is not equal to zero where $j = C, D, E, F, G$ and $i = 3, 4, 5, \dots, 12$

The existence of seasonal unit roots can be tested by  $t$ -statistic in each frequency with the null hypotheses  $H_0 = \pi_i = 0$ , where  $i = 2, 3, \dots, 12$ , or by means of  $F$ -statistic associated with joint hypotheses  $H_0 = \pi_i = \pi_{i+1} = 0$ , where  $i = 3, 5, 7, 9, 11$ .

**2.4. Testing Linearity of Variables.** The STAR model is used to check whether the behavior of series is linear or nonlinear. Initially, the STAR model was proposed by Chan and Tong [35]; Terasvirta [36] and others. STAR model has further two subclasses, i.e., logistic STAR (LSTAR) model, where the function of weights has logistic function and the exponential STAR (ESTAR) model, in which the function of weights has the form of an exponential function.

The LSTAR model is defined by

$$y_t = \partial_0 + \partial_1 y_{t-1} + \dots + \partial_p y_{t-p} + K[\beta_0 + \beta_1 y_{t-1} + \dots + \beta_p y_{t-p}] + \varepsilon_t, \quad (3)$$

where

$$K = [1 + \exp(-\gamma(y_{t-d} - c))]^{-1}. \quad (4)$$

In (4), the parameter  $\gamma$  is called the smoothness parameter, which is responsible for the smoothness of  $G$ , while  $G$  is bounded as  $0 \leq K \leq 1$ .  $c$  is the threshold parameter.  $y_{t-d}$  is called the transition variable ( $d$  is the delay parameter).

The ESTAR is the same as (3), but the value of  $K$  is different as

$$K = 1 - \exp[-\gamma(y_{t-d} - c)^2]. \quad (5)$$

The Lagrange multiplier (LM) test cannot be used directly to test whether a series has LSTAR or ESTAR behavior as the values of parameters in these models are unidentified under the null hypothesis which is that the model is in linear form. As a result, Terasvirta [36] creates a background for determining whether a series is best modelled as an LSTAR or ESTAR process. Terasvirta [36] proposed an auxiliary regression test to detect the presence of LSTAR behavior:

$$e_t = \partial_0 + \partial_1 y_{t-1} + \dots + \partial_p y_{t-p} + \partial_{11} y_{t-1} y_{t-d} + \dots + \partial_{1p} y_{t-p} y_{t-d} + \partial_{21} y_{t-1} y_{t-d}^2 + \dots + \partial_{2p} y_{t-p} y_{t-d}^2 + \partial_{31} y_{t-1} y_{t-d}^3 + \dots + \partial_{3p} y_{t-p} y_{t-d}^3 + \varepsilon_t. \quad (6)$$

For more detail, see [36].

**2.5. Threshold Cointegration and Asymmetric Adjustment.** The Engel–Granger’s [8] methodology for PPP begins by proposing a long-run equilibrium relationship of the form:

$$E_t = \beta_0 + \beta_1 p_t - \beta_2 p_t^* + \mu_t, \quad (7)$$

where  $E_t$  is the log of the nominal exchange rate;  $p_t$  defines the log of the domestic price level;  $p_t^*$  represents the foreign price levels; and  $\mu_t$  is the disturbance term.

After estimating the (7) by OLS methodology, the next step in the Engel–Granger procedure is to test the stationarity of the linear combination of the nominal exchange rate and prices. Residuals of (7) are commonly used to measure the linear combination. Therefore, the stationarity of the residuals series conforms the existence of PPP theory in long run. Stationarity of residual series is tested by applying ADF auxiliary regression, i.e., provided under

$$\Delta \mu_t = \rho \mu_{t-1} + \varepsilon_t. \quad (8)$$

If the hypothesis  $\rho = 0$  is rejected, then the sequence of  $\mu_t$  is stationary. In such a case, the PPP holds the long-run exchange rate.

The standard cointegration test implicitly assumes a symmetric adjustment process. If the exchange rate adjustment is asymmetric, then (8) is unspecified. The errors from (7) are estimated in the form of a threshold autoregressive (TAR) defined by Enders and Siklos [28]. The mathematical form of the TAR model is given by

$$\Delta \mu_t = I_t \rho_1 \mu_{t-1} + (1 - I_t) \rho_2 \mu_{t-1} + \varepsilon_t, \quad (9)$$

where  $I_t$  is the indicator function such that

$$I_t = \begin{cases} 0, & \text{for } \mu_{t-1} < \tau, \\ 1, & \text{for } \mu_{t-1} > \tau, \end{cases} \quad (10)$$

and  $\tau$  is the value of the threshold.

Asymmetric adjustment is held if  $\rho_1 \neq \rho_2$ . When the term  $\mu_{t-1}$  is positive, the value of adjustment is  $\rho_1 \mu_{t-1}$  which is positive, and when the term  $\mu_{t-1}$  is negative, the value of adjustment  $\rho_2 \mu_{t-1}$  is negative. A sufficient but not necessity condition for stationarity is  $\mu_t$  which is  $-2 < (\rho_1, \rho_2) < 0$ . If the variance of  $\mu_t$  is sufficiently large, it is also possible for one value of  $\rho_j$  to be between minus two and zero and for the other value equal to zero [14]. For a nonstandard distribution, the value of  $F$ -statistic with the null hypothesis will be  $\rho_1 = \rho_2 = 0$ ; for this purpose, Enders and Siklos [28] used the expression  $\Phi_\mu$ . If the null hypothesis of  $\rho_1 = \rho_2 = 0$  is not accepted, it is quite possible to test for symmetric adjustment, i.e.,  $\rho_1 = \rho_2$  using a standard procedure of  $F$ -test. If  $\rho_1 = \rho_2$ , the adjustment is symmetric; a special case of the equation is the Engel–Granger test for cointegration (10).

**2.6. Empirical Study.** For empirical study, the dataset is taken from the international monitoring fund (IMA) with

TABLE 2: Unit root test at first difference.

Variable	Model	$\pi_1 = 0$	$\pi_2 = 0$	$\pi_3 = \pi_4 = 0$	$\pi_5 = \pi_6 = 0$	$\pi_7 = \pi_8 = 0$	$\pi_9 = \pi_{10} = 0$	$\pi_{11} = \pi_{12} = 0$	Order of integer
EX <sub>Pak-USA</sub>	C*, t**, d**	-4.65* (-2.82)	-5.32* (-1.89)	23.20* (3.05)	23.121* (3.08)	23.39* (3.14)	25.17* (3.05)	20.23* (3.07)	I(1)
EX <sub>Pak-China</sub>	C*, t**, d**	-4.79* (-2.78)	-4.56* (-1.89)	31.09* (3.05)	25.901* (3.08)	25.05* (3.11)	21.46* (3.05)	22.80* (3.07)	I(1)
EX <sub>Pak-Germany</sub>	C*, t**, d**	-5.85* (-2.78)	-5.99* (-1.89)	27.80* (3.05)	29.12* (3.08)	31.12* (3.14)	26.44* (3.05)	31.82* (3.07)	I(1)
CPI <sub>Germany</sub>	C**, t**, d**	-5.80* (-1.87)	-5.33* (-1.89)	29.29* (3.05)	32.32* (3.11)	31.12* (3.16)	26.00* (3.07)	26.54* (3.08)	I(1)
CPI <sub>Pak</sub>	C*, t**, d**	-3.49* (-2.81)	-5.96* (-2.97)	34.77* (6.35)	27.31* (6.37)	43.99* (6.29)	20.90* (6.36)	24.36* (6.31)	I(1)
CPI <sub>USA</sub>	C*, t**, d**	-4.49* (-2.76)	-6.50* (-2.79)	45.49* (6.35)	45.05* (6.37)	29.85* (6.29)	48.35* (6.36)	16.16* (6.31)	I(1)
CPI <sub>China</sub>	C*, t**, d**	-2.10* (-1.87)	-3.82* (-1.89)	12.17* (3.05)	17.71* (3.11)	11.98* (3.16)	20.40* (3.07)	18.85* (3.08)	I(1)

the URL given at the end of the paper. The foremost and necessary step in the implementation of the cointegration test is to examine the stationarity of individual variables by using the Beaulieu and Miron test. Table 2 reflects the result of the unit root test. The results describe those variables are nonstationary at the level and stationary at first difference.

All variables are in the log form and integrated of order one I (1). The \* indicates significant results at the 5% level of significance while \*\* shows insignificant results. The second column shows the existence of constant ( $c$ ), trend ( $t$ ), and dummies ( $d$ ) in the model. The critical values enclosed in parenthesis are taken from Beaulieu and Miron [21] and recently cited by Philip Hans Franses and Bart Hobijn [37].

The next step is to check whether the behavior of the Pak rupee exchange rate against the US dollar, China yuan, and German euro series is linear or nonlinear; we have considered the STAR model. Furthermore, whether the series behave like ESTAR or LSTAR model, for this purpose, STAR model is used. The identification of linearity vs nonlinearity is carried out through the Akaike information criteria (AIC). Table 3 defines the result.

On the basis of the above analysis (Table 3), it is determined that the exchange rate series shows asymmetric behavior; in this case, linear cointegration procedure is misleading. A proper way to introduce by Enders and Siklos [28] is that the residuals from a linear combination of the exchange rate and prices are estimated in the form of threshold autoregressive (TAR) model. As the threshold, level of  $\hat{\mu}_t$  series is unknown. Therefore, we had followed Chan's [38] methodology for identifying the unknown threshold. Chan [38] illustrated that the consistent estimate of the threshold will be the smallest residual sum of square (RSS). The results of threshold cointegration for the exchange rate of Pakistan against the US dollar, Chinese yuan, and German euro are presented in Table 4.

The critical values with alpha = 10% are taken from Enders and Siklos [28].

Table 4 explicates the estimated values of the speed of adjustment under each regime. The result shows that the

TABLE 3: Linear vs nonlinear behavior of exchange rates.

Variable name	Lag	Linear vs nonlinear	ESTAR vs LSTAR
EX <sub>Pak_USA</sub>	2	Nonlinear	ESTAR
EX <sub>Pak_China</sub>	2	Nonlinear	LSTAR
EX <sub>Pak_Germany</sub>	1	Nonlinear	LSTAR

TABLE 4: Estimated equations using threshold cointegration test and consistent estimates (based country: Pakistan).

Country	$\rho_1$	$\rho_2$	$\rho_1 = \rho_2$	$\phi_\mu$	Lag	Flag	Threshold value
USA	-0031	-0.032	2.432	6.67	2	TAR	0.5991
China	-0.002	-0.081	7.010	6.67	12	TAR	0.00041
Germany	-0.0151	-0.026	1.895	6.67	0	TAR	-0.03257

exchange rates in the case of the USA and Germany do not converge from lower regime to upper regime and indicates the existence of linear cointegration. While in the case of China, it shows convergence from one regime to another and nonlinear cointegration. It is concluded that the linear form of PPP holds in the case of the exchange rate of Pakistan against the USA dollar and German euro while the nonlinear form of PPP holds in the case of China. The consistent estimated values of the threshold are obtained.

To study a long-run equilibrium relationship of variables, one can use an asymmetric error-correction model. In the case of Pakistan and China, the estimated long-run relationship is

$$EX_{\text{Pak\_China}} = -2.0919 + 0.702706p_t - 0.277305p_t^*, \quad (11)$$

St. error: (0.078) (0.014) (0.028).

Using the long-run relationship of the nominal exchange rate and prices in a case of China, the estimated error-correction equation with the consistent estimates is given by

$$\begin{aligned} \Delta EX_{\text{Pak-China}} = & -0.036716ec_{t-1}^+ - 0.065466ec_{t-1}^- + 0.042\Delta P_{t-1} + 0.130\Delta P_{t-2} + 0.238\Delta P_{t-3} - 0.214\Delta P_{t-4} \\ & - 0.052\Delta P_{t-1}^* - 0.134\Delta P_{t-2}^* - 0.029\Delta P_{t-3}^* - 0.014\Delta P_{t-4}^* + 0.093\Delta EX_{t-1} + 0.044\Delta EX_{t-2} \\ & + 0.024\Delta EX_{t-3} + 0.039\Delta EX_{t-4}, \end{aligned} \quad (12)$$

$$\text{Adj} - R^2 = 0.07101,$$

$$\text{Auto}\chi_{(12)}^2 = 0.2143,$$

$$\text{Hetro}\chi_{(12)}^2 = 0.99,$$

where

$$ec_{t-1}^+ = (1 - I_t)(e_t + 2.0919 - 0.702706p_t + 0.277305p_t^*), \quad (13)$$

and  $I_t$  is the indicator function and is defined as

$$I_t = \begin{cases} 1, & \text{if } \Delta\hat{\mu}_{t-1} \geq 0.00041, \\ 0, & \text{if } \Delta\hat{\mu}_{t-1} < 0.00041. \end{cases} \quad (14)$$

The coefficients of  $ec_{t-1}^+$  define the speed adjustment of positive deviations from PPP while  $ec_{t-1}^-$  determines the speed adjustment of negative deviations from PPP. The  $t$ -



statistics 2.52545 and  $-3.30908$  conclude that both coefficients are significant at a 5% level. The point estimates imply that the exchange rate adjusts by 3.67% of a positive gap from long-run PPP and by 6.54% of a negative gap. The point is that positive deviations from PPP are eliminated faster than negative deviations.

### 3. Conclusion and Policy Implication

The goal of the paper is to estimate the long-run relationship in PPP by using threshold cointegration along with an asymmetric adjustment in three major trading partners of Pakistan; these are the United States, China, and Germany. The study used time series monthly data over the period 1982 to 2013. To check the order of integration of variables, we considered a seasonal unit root test. Accordingly, all variables, i.e., nominal exchange rate, domestic price level, and foreign price level are stationary at the first difference for all countries. In order to check whether the behavior of the exchange rate series is linear or nonlinear, we use STAR model and found nonlinear behavior in the case of all exchange rate series. Further, we specify whether the nonlinear behavior of the exchange rate series is according to ESTAR or LSTAR and selected ESTAR behavior in favor of LSTAR for Pak-USA and LSTAR for Pak-China and Pak-Germany exchange rates. The asymmetric behavior of the exchange rates series allowed executing the threshold cointegration suggested by Enders and Siklos [28].

The findings of PPP suggest that it holds between Pakistan and China, while in the case of Pakistan vs USA, it does not hold. Thus, Pakistan needs to increase its exports to China; trade and investment with China will bring advantage to Pakistan. The trade performance of Pakistan can be improved if the policy makers monitor the exchange rate fluctuation in major trading partners. Trading will be more beneficial if the exchange rate varied with respect to major trade partners rather than only with the US dollar.

The research study may be conducted to cover the data during COVID-19 and record the fluctuations in the exchange rate of the top three trade partners of Pakistan. A future research study may be conducted with the nonlinear cointegration technique with the ARDL approach. Similarly, the same study may be extended to add some other trade partners.

### Data Availability

The data used to support this study are available at <https://data.imf.org/?sk=4c514d48-b6ba-49ed-8ab9-52b0c1a0179b&skId=14091512409>.

### Disclosure

This article was submitted to the journal from the thesis of Kashif Ali supervised by Dr. Hafsa Hina at PIDE (Pakistan Institute of Development Economics).

### Conflicts of Interest

The authors declare that they have no conflicts of interest.

### References

- [1] M. A. Khan and A. Qayyum, "Trade, financial and growth nexus in Pakistan (No. 2007, 14)," *Economic Analysis Working Papers*, 2007.
- [2] G. Cassel, "The present situation of the foreign exchanges," *The Economic Journal*, vol. 26, no. 103, pp. 319–323, 1916.
- [3] D. Corbae and S. Ouliaris, "Cointegration and tests of purchasing power parity," *The Review of Economics and Statistics*, vol. 70, no. 3, pp. 508–511, 1988.
- [4] S. K. Aminifard, "Trade relations and long-run purchasing power parity (PPP) between the selected east asian countries and Iran," *Korea and the World Economy*, vol. 12, pp. 327–340, 2011.
- [5] Y. Zhao, *Nonlinear Cointegration: Theory and Application to Purchasing Power Parity*, Dalarna University, Dalarana, Sweden, 2007.
- [6] W. Enders, "Arima and cointegration tests of PPP under fixed and flexible exchange rate regimes," *The Review of Economics and Statistics*, vol. 70, no. 3, pp. 504–508, 1988a.
- [7] J. Patel, "Purchasing power parity as a long-run relation," *Journal of Applied Econometrics*, vol. 5, no. 4, pp. 367–379, 1990.
- [8] C. W. J. Granger and R. F. Engle, "Co-integration and error correction: representation, estimation, and Testing," *Econometrica*, vol. 55, pp. 251–276, 1987.
- [9] E. Ahmad and F. N. Khan, "Test of purchasing power parity based on cointegration technique: the Asian Evidence," *Pakistan Economic and Social Review*, vol. XLIII, no. 2, pp. 167–183, 2005.
- [10] S. A. Basher and M. Mohsin, "PPP tests in cointegrated panels: evidence from Asian developing countries," *Applied Economics Letters*, vol. 11, no. 3, pp. 163–166, 2004.
- [11] Q. Abdul, M. A. Khan, K. U. Zaman, and F. S. Omar, "Exchange rate misalignment in Pakistan: evidence from purchasing power parity theory," *Pakistan Development Review*, vol. 43, no. 4, pp. 721–735, 2004.
- [12] N. Abuaf and P. Jorion, "Purchasing power parity in the long run," *The Journal of Finance*, vol. 45, no. 1, pp. 157–174, 1990.
- [13] R. H. Basher and H. Fazal, "A correct test of purchasing power parity: the case of pak-rupee exchange rates," *Pakistan Development Review*, vol. 35, pp. 671–682, 1996.
- [14] K. Chumrusphonlert and W. Enders, "Threshold cointegration and purchasing power parity," *Applied Economics*, vol. 36, pp. 889–896, 2004.
- [15] W. Enders and B. Falk, "Threshold-autoregressive, median-unbiased, and cointegration tests of purchasing power parity," *International Journal of Forecasting*, vol. 14, no. 2, pp. 171–186, 1998.
- [16] P. H. Franses, "Seasonality, non-stationarity and the forecasting of monthly time series," *International Journal of Forecasting*, vol. 7, no. 2, pp. 199–208, 1991.
- [17] B. E. Hansen and B. Seo, "Testing for two-regime threshold cointegration in vector error-correction models," *Journal of Econometrics*, vol. 110, no. 2, pp. 293–318, 2002.
- [18] R. H. Husain, "A correct test of purchasing power parity: the case of pak-rupee exchange rates," *Pakistan Development Review*, vol. 35, no. 4, pp. 671–682, 1996.
- [19] S. Hylleberg, R. F. Engle, C. W. J. Granger, and B. S. Yoo, "Seasonal integration and cointegration," *Journal of Econometrics*, vol. 44, no. 1–2, pp. 215–238, 1990.
- [20] Y. S. Liu, C. W. Su, and T. Chang, "Purchasing power parity with nonlinear and asymmetric smooth adjustment," *Applied Economics Letters*, vol. 19, no. 6, pp. 575–578, 2012.

- [21] J. A. Miron and J. J. Beaulieu, "Seasonal unit root in aggregate U.S. Data," *Journal of Econometrics*, vol. 55, no. 1-2, 1992.
- [22] R. Sollis, "A simple unit root test against asymmetric STAR nonlinearity with an application to real exchange rates in Nordic countries," *Economic Modelling*, vol. 26, no. 1, pp. 118–125, 2009.
- [23] H. Tong, *Non-linear Time Series: A Dynamical System Approach*, Oxford University Press, Oxford, United Kingdom, 1990.
- [24] S. Johansen, "Statistical analysis of cointegration vectors," *Journal of Economic Dynamics and Control*, vol. 12, no. 2-3, pp. 231–254, 1988.
- [25] N. S. Balke and T. B. Fomby, "Threshold cointegration," *International Economic Review*, vol. 38, 1997.
- [26] Johansen and Juselius, "Maximum likelihood estimation and inference on cointegration with application to the demand for money," *Oxford Bulletin of Economics & Statistics*, vol. 52, pp. 169–210, 1990.
- [27] B. E. Hansen and B. Seo, *Testing for Threshold Cointegration*, University of Wisconsin, Madison, WI, USA, 2000.
- [28] W. Enders and P. L. Siklos, "Cointegration and threshold adjustment," *Journal of Business & Economic Statistics*, vol. 19, no. 2, pp. 166–176, 2001.
- [29] A. Phiri, "Nonlinear adjustment effects in the purchasing power parity (no. 08/2017)," *Journal of Economics and Econometrics*, vol. 60, no. 2, pp. 14–38, 2017.
- [30] A. L. Ang, Y. T. Thum, and S. K. Sek, "Does trade openness explain the deviation of purchasing power parity and exchange rate movement?" *Journal of Physics: Conference Series*, vol. 1988, no. 1, Article ID 012087, 2021.
- [31] A. C. Arize and M. O. Bahmani, "Nonlinear ARDL approach and PPP: evidence from 82 countries," *Global Economy Journal*, vol. 21, pp. 1–17, 2021.
- [32] C. K. Tipoy, M. C. Breitenbach, and M. F. Zerihun, "Exchange rate misalignment and economic growth: evidence from nonlinear panel cointegration and granger causality tests," *Studies in Nonlinear Dynamics & Econometrics*, vol. 22, no. 2, 2018.
- [33] M. O. Bahmani, N. Bose, and Y. Zhang, "Asymmetric cointegration, nonlinear ARDL, and the J-Curve: a bilateral analysis of China and its 21 trading partners," *Emerging Markets Finance and Trade*, vol. 54, no. 13, pp. 3131–3151, 2018.
- [34] J. Iqbal, M. Nosheen, and G. R. Panezai, "Asymmetric cointegration, Non-linear ARDL, and the J-curve: a bilateral analysis of Pakistan and its trading partners," *International Journal of Finance & Economics*, vol. 26, no. 2, pp. 2263–2278, 2021.
- [35] W. S. Chan and H. Tong, "On tests for non-linearity in time series analysis," *Journal of Forecasting*, vol. 5, no. 4, pp. 217–228, 1986.
- [36] T. Terasvirta, "Specification, estimation, and evaluation of smooth transition autoregressive models," *Journal of the American Statistical Association*, vol. 89, no. 425, pp. 208–218, 1994.
- [37] P. H. Franses and B. Hobijn, "Critical values for unit root tests in seasonal time series," *Journal of Applied Statistics*, vol. 24, no. 1, pp. 25–48, 1997.
- [38] K. S. Chan, "Consistency and limiting distribution of the least squares' estimator of a threshold autoregressive model," *Annals of Statistics*, vol. 21, no. 1, pp. 520–533, 1993.

## Research Article

# The Arctan-X Family of Distributions: Properties, Simulation, and Applications to Actuarial Sciences

Ibrahim Alkhairy,<sup>1</sup> M. Nagy,<sup>2</sup> Abdisalam Hassan Muse ,<sup>3</sup> and Eslam Hussam <sup>4</sup>

<sup>1</sup>Department of Mathematics, Al-Qunfudah University College, Umm Al-Qura University, Mecca, Saudi Arabia

<sup>2</sup>Department of Mathematics, Faculty of Science, Fayoum University, Fayoum, Egypt

<sup>3</sup>Department of Mathematics (Statistics Option) Programme, Pan African University, Institute for Basic Science, Technology, and Innovation (PAUSTI), Nairobi, Kenya

<sup>4</sup>Department of Mathematics, Faculty of Science, Helwan University, Cairo, Egypt

Correspondence should be addressed to Abdisalam Hassan Muse; [abdisalam.hassan@amoud.edu.so](mailto:abdisalam.hassan@amoud.edu.so)

Received 12 October 2021; Accepted 3 November 2021; Published 10 December 2021

Academic Editor: Sameh S. Askar

Copyright © 2021 Ibrahim Alkhairy et al. This is an open access article distributed under the Creative Commons Attribution License, which permits unrestricted use, distribution, and reproduction in any medium, provided the original work is properly cited.

The purpose of this paper is to investigate a new family of distributions based on an inverse trigonometric function known as the arctangent function. In the context of actuarial science, heavy-tailed probability distributions are immensely beneficial and play an important role in modelling data sets. Actuaries are committed to finding for such distributions in order to get an excellent fit to complex economic and actuarial data sets. The current research takes a look at a popular method for generating new distributions which are excellent candidates for dealing with heavy-tailed data. The proposed family of distributions is known as the Arctan-X family of distributions and is introduced using an inverse trigonometric function. For the specific purpose of the show of strength, we studied the Arctan-Weibull distribution as a special case of the developed family. To estimate the parameters of the Arctan-Weibull distribution, the frequentist approach, i.e., maximum likelihood estimation, is used. A rigorous Monte Carlo simulation analysis is used to determine the efficiency of the obtained estimators. The Arctan-Weibull model is demonstrated using a real-world insurance data set. The Arctan-Weibull is compared to well-known two-, three-, and four-parameter competitors. Among the competing distributions are Weibull, Kappa, Burr-XII, and beta-Weibull. For model comparison, we used the most precise tests used to know whether the Arctan-Weibull distribution is more useful than competing models.

## 1. Introduction

Numerous disciplines of study have examined heavy-tailed probability distributions, including actuarial science, bio-medical sciences, engineering, risk management, and economics. In recent years, some procedures have been proposed to generate a new class of heavy-tailed probability distributions with adequate description and a high degree of flexibility. Among these techniques, the use of trigonometric functions and their inverses has been at the forefront of the development of new families of probability distributions. One of the really essential functions of financial and actuarial science is the accurate forecasting of large monetary financial losses. Underestimation of such losses exposes the company to serious operational risks, including such bankruptcy and underestimating premium. To mitigate such

circumstances and provide precise forecasts of actuarial science losses, actuaries frequently propose flexible heavy-tailed distributions.

Financial and actuarial data sets are generally heavy-tailed, unimodal-shaped, right-handed, and positive [1, 2]. The complex financial data sets can be better modelled by developing new families of probability distributions [1–5]. The suggested models significantly raise the effectiveness of quantitative analysis methods, and substantial work has been devoted establishing new statistical models. However, a number of basic difficulties with actual data seem to exist that do not really fit into most common statistical models. In order to capture the real-world phenomena, statistical distributions are commonly used. The theory of statistical distributions is widely studied along with the new developments for their usefulness. To describe different real-

world phenomena, several families of distributions are developed. Recent developments in distribution theory and its uses have resulted in the emergence of a number of general families of probability distributions that have successfully been applied to a variety of statistical and probability problems. For more details, see [6–10].

Constructing flexible parametric models for modelling various types of data is a difficult task for applied statisticians. In general, this allows for the discovery of new features of real-world phenomena as well as the provision of advised predictions. Several families of distributions have been created in this regard using various techniques such as (i) inducing shape, skewness, or kurtosis parameter [6]; (ii) compounding of distributions [7]; transformation technique [11–13]; (iv) finite mixture of distributions [14–16]; and (v) composition of two or more distributions [17]. For more information about these techniques, see [6–10].

Unfortunately, the abovementioned generalization techniques for the classical probability distributions may face some constraints, such as (i) Adding more parameters to the probability model enhances its flexibility, and such methods usually result in reparameterization problems. (ii) There is an increase in the number of model parameters, which makes it more difficult to examine the model parameters. (iii) The tractability of the cdf is reduced by several extending approaches, which makes manual calculation of statistical characteristics more difficult to do. (iv) Other generalisation approaches make the pdf more complicated, leading in computing difficulties. The addition of additional extra parameters to existing models enhances the flexibility of the models, which is a desired characteristic. On the other side, it makes it more difficult to draw conclusions, for extra reading see [18, 19].

In order to make the model more flexible, most statistical models proposed in the literature have a large number of parameters. These estimators, according to some authors, are difficult to obtain using numerical resources. However, it is preferable to create models with a small number of parameters but a high degree of flexibility for modelling the data. To achieve this goal, a small group of researchers decided to look for new distributions using trigonometric functions and their inverses (see [18–27]).

The fundamental objective of this research is to present and examine a new family of probability distributions with a small number of parameters but a high degree of flexibility for data modelling. To accomplish this, a group of researchers decided to look for new distributions using trigonometric functions and their inverses. Chesneau et al. [20] developed a new family of distributions called the sine Kumaraswamy-G family of probability distributions. Souza et al. [21] introduced a new family of probability distributions using the sine function. Souza et al. [22] proposed a new family of probability distributions using the tangent function. Souza [28] introduced other families of probability distributions using the cosine and secant functions. Mahmood et al. [27] developed a new family of probability distribution using the sine distribution. Chesneau et al. [23] developed a new family of probability distributions based on sine and cosine functions.

On the other hand, other researchers developed a new family of probability distributions using the inverse

trigonometric functions. Lung et al. [18] developed a new family of probability distributions using the arcsine function. Rahman et al. [29] developed a new family of distributions by using the arcsine distribution. Chesneau et al. [24] developed a new distribution based on the arccosine function. Chaudary [26] introduced the Arctan Lomax distribution using the arctangent distribution. Muse et al. [30] introduced a new versatile log-logistic distribution using the tangent function. Furthermore, other researchers discussed the application of trigonometric functions and their inverses; for more information, see [19, 24, 27, 31–33].

Given the preceding discussion, statisticians are willing to propose new distributions or distribution families based on an easily expressed pdf (probability density function) and a closed and tractable form of cdf (cumulative distribution function). As a result, an effort is being made in this paper to develop a new distribution family that avoids the issues mentioned above while also providing the best fit to financial data sets. The proposed family is known as the Arctan-X family of distributions (abbreviated “AT-X”) and was developed using the arctangent function. The proposed family has a straightforward pdf expression as well as a tractable and closed cdf form.

Here to authors’ knowledge, there is no published study on its mathematical and practical characteristics based on the arctangent function for the purpose of developing a new family of distributions in its whole in the present literature. One of the reasons for writing this paper is to address this unexpected gap. We derive some of the fundamental mathematical and statistical properties of the new family by using the general setting of the Arctan-X class, such as hazard rate function (hrf), survivor function (sf), quantile function (qf), moments and moment generating function (mgf), skewness, kurtosis, and residual life function.

The remainder of the article is arranged as follows: the Arctan-X family and its main mathematical properties are discussed in Section 2. Section 3 presents special cases of the Arctan-X family. The Arctan-Weibull distribution is introduced in Section 4. The Arctan-Weibull distribution mathematical and statistical features are examined in Section 5. Section 6 is used to estimate the Arctan-X family parameters. Section 7 outlines the suggested model’s Monte Carlo simulation. In Section 8, the suggested model’s superiority is shown and explained using a real-world data application. Finally, Section 9 contains final findings and major remarks and the whole work summary.

## 2. Arctan-X Family of Distributions

The AT-X family is provided in detail in this part of the paper. The AT-X family has many merits; one of these merits is that it has a very easily expressed pdf and a tractable and closed cdf form. If we assume that  $X$  is a random variable that belongs to the Arctan-X family, then its cdf can be written as the following expression:

$$F_{\text{arctan}}(x; \theta) = \frac{4}{\pi} \arctan(G(x; \theta)), x \in \mathbb{R}. \quad (1)$$

Here,  $G(x; \theta)$  is considered as the cdf of the baseline (or parent) random variable depending on the parameter vector

$\theta \in \mathbb{R}$ , and if  $G(x)$  has pdf  $g(x)$ , then the pdf of the class is expressed as

$$f_{\arctan}(x; \theta) = \frac{4}{\pi} \frac{g(x; \theta)}{1 + G(x; \theta)^2}, \quad x \in \mathbb{R}. \quad (2)$$

The complementary cdf (or survival function) can be written as below:

$$S_{\arctan}(x; \theta) = 1 - \frac{4}{\pi} \arctan(G(x; \theta)), \quad x \in \mathbb{R}. \quad (3)$$

The instantaneous failure rate (or hazard rate function (hrf)) can be written as below:

$$\begin{aligned} h_{\arctan}(x; \theta) &= \frac{f_{\arctan}(x; \theta)}{S_{\arctan}(x; \theta)} \\ &= \frac{4g(x; \theta)}{\pi - 4 \arctan(G(x; \theta))\{1 + G(x; \theta)^2\}}, \quad x \in \mathbb{R}. \end{aligned} \quad (4)$$

The retro hazard (or reversed hazard rate function) may be expressed in the following manner:

$$\begin{aligned} r_{\arctan}(x; \theta) &= \frac{f_{\arctan}(x; \theta)}{F_{\arctan}(x; \theta)} = \frac{4g(x; \theta)}{\arctan(G(x; \theta))\{1 + G(x; \theta)^2\}}, \\ & \quad x \in \mathbb{R}, \end{aligned} \quad (5)$$

And, the integrated hazard rate (or cumulative hazard rate function) is given by

$$\begin{aligned} H_{\arctan}(x; \theta) &= -\log S_{\arctan}(x; \theta) \\ &= -\log \left\{ 1 - \frac{4}{\pi} \arctan(G(x; \theta)) \right\}, \quad x \in \mathbb{R}. \end{aligned} \quad (6)$$

**2.1. Quantile Function.** The quantile function (also known as the inverse cdf) of the Arctan-X family follows by inverting the Arctan-X distribution function. It may be written as follows in terms of the tangent trigonometric function:

$$x = Q_G(u) = F^{-1}(u) = G^{-1} \left( \tan \left( \frac{\pi}{4} u \right) \right), \quad (7)$$

where  $u \in (0, 1)$ . The quantile function expression may be used to generate random numbers from AT-X distributions.

**2.2. Moments.** In the field of actuarial science and financial science, moments are very important, particularly in applications. It gives the researcher a hand to get the key properties and characteristics of the proposed distribution under consideration. The  $r^{\text{th}}$  moments of the AT-X distribution family are calculated as

$$\mu'_r = \int_{-\infty}^{\infty} x^r f_{\arctan}(x; \theta) dx. \quad (8)$$

Using the pdf of the AT-X family in equation (8), we get

$$\mu'_r = \frac{4}{\pi} \int_{-\infty}^{\infty} x^r \frac{g(x; \theta)}{1 + G(x; \theta)^2} dx. \quad (9)$$

Using the Taylor series, we have

$$\frac{1}{1 + x^2} = \sum_{n=0}^{\infty} \frac{(-1)^n}{2n + 1} x^{2n+1}. \quad (10)$$

Let  $x = G(x; \theta)$ , in equation [10]; we get

$$\frac{1}{1 + G(x; \theta)^2} = \sum_{n=0}^{\infty} \frac{(-1)^n}{2n + 1} G(x; \theta)^{2n+1}. \quad (11)$$

By the aid of equation (7) and substituting in equation (9), we will have the following result:

$$\mu'_r = \frac{4}{\pi} \sum_{n=0}^{\infty} \frac{(-1)^n}{2n + 1} \Psi_{r, 2n+1}, \quad (12)$$

Such that  $\Psi_{r, 2n+1} = \int_{-\infty}^{\infty} x^r g(x; \theta) G(x; \theta)^{2n+1} dx$ .

The moment-generating function for the AT-X family can be expressed in a general form as follows:

$$M_X(t) = \frac{4}{\pi} \sum_{r, n=0}^{\infty} \frac{(-1)^n}{(2n + 1)r!} t^r \Psi_{r, 2n+1}. \quad (13)$$

### 3. Special Cases of the Arctan-X Family

This section discusses certain cases of the intended Arctan-X family of distributions by using different base cumulative distribution functions. In Table 1, we present fifteen special cases of the proposed family including Weibull, Gompertz, log-logistic, Lomax, Kumaraswamy, Pareto, normal, Dagum, Burr-XII, Rayleigh, gamma, Lindley, exponential, Gumbel, and uniform distributions.

As an example, in the case of alternative parametrization, choose cdf  $G(x; \theta)$  of the Weibull distribution and introduce the Arctan-Weibull distribution as follows.

A random variable  $X$  is said to have a Weibull distribution with shape parameter  $\alpha > 0$  and scale parameter  $\lambda > 0$  denoted by  $X \sim \text{Wei}(\alpha, \lambda)$ . Its cdf is defined by the following:

$$F(x; \theta) = 1 - e^{-ax^\lambda}; \quad x \geq 0, \theta > 0. \quad (14)$$

And, the pdf is given by

$$f(x; \theta) = \lambda \alpha (ax)^\lambda \exp\{- (ax)^\lambda\}; \quad x \geq 0, \theta > 0. \quad (15)$$

We can write the reliability (survival) function as below:

$$S(x; \theta) = 1 - F(x; \theta) = e^{-ax^\lambda}; \quad x \geq 0, \theta > 0. \quad (16)$$

The hrf is given by

$$h(x; \theta) = \frac{f(x; \theta)}{S(x; \theta)} = \frac{f(x; \theta)}{1 - F(x; \theta)} = \lambda \alpha (ax)^\lambda; \quad (17)$$

$$x \geq 0, \theta > 0.$$

The retro hazard rate is given by

TABLE 1: New contributed special cases of the Arctan-X family.

No.	Baseline model	cdf	Generated model	Support
1	Weibull	$4/\pi \arctan(1 - e^{-\alpha x^\lambda})$	AT-Weibull	$x \in \mathbb{R}^+$
2	Log-logistic	$4/\pi \arctan(1/1 + (x/\alpha)^{-\lambda})$	AT-Log logistic	$x \in \mathbb{R}^+$
3	Lomax	$4/\pi \arctan(1 - (1 + \alpha x)^{-\lambda})$	AT-Lomax	$x \in \mathbb{R}^+$
4	Dagum	$4/\pi \arctan(\{(1 + (x/\alpha)^{-\lambda})\}^{-p})$	AT-Dagum	$x \in \mathbb{R}^+$
5	Uniform	$4/\pi \arctan(x/\vartheta)$	AT-Uniform	$0 < x < \vartheta, \vartheta > 0$
6	Burr-XII	$4/\pi \arctan(1 - (1 + x^\lambda)^{-\alpha})$	AT-BXII	$x \in \mathbb{R}^+$
7	Gamma	$4/\pi \arctan((1/\Gamma\alpha)\gamma(\alpha, \beta))$	AT-Gamma	$x \in \mathbb{R}^+$
8	Gompertz	$4/\pi \arctan(1 - e^{-\lambda(e^{\beta x} - 1)})$	AT-Gompertz	$x \in \mathbb{R}^+$
9	Gumbel	$4/\pi \arctan(e^{-e^{-(x-\mu)/\alpha}})$	AT-Gumbel	$x \in \mathbb{R}$
10	Lindley	$4/\pi \arctan(1 - (e^{-\lambda x}(1 + \lambda + \lambda x))/1 + \lambda)$	AT-Lindley	$x \in \mathbb{R}^+$
11	Kumaraswamy	$4/\pi \arctan(1 - (1 - x^\lambda)^\alpha)$	AT-Kumaraswamy	$x \in [0, 1]$
12	Pareto	$4/\pi \arctan(1 - (m/x)^\lambda)$	AT-Pareto	$x \in [m, \infty)$
13	Normal	$4/\pi \arctan(\Phi(x - \mu/\sigma))$	AT-Normal	$x \in \mathbb{R}$
14	Rayleigh	$4/\pi \arctan(1 - e^{-\alpha x^2})$	AT-Rayleigh	$x \in \mathbb{R}^+$
15	Exponential	$4/\pi \arctan(1 - e^{-\alpha x^2})$	AT-Exponential	$x \in \mathbb{R}^+$

$$r(x; \boldsymbol{\theta}) = \frac{f(x; \boldsymbol{\theta})}{F(x; \boldsymbol{\theta})} = \frac{[\lambda \alpha (\alpha x)^{\lambda-1} \exp\{-(\alpha x)^\lambda\}]}{[1 - e^{-\alpha x^\lambda}]}; \quad (18)$$

$$x \geq 0, \boldsymbol{\theta} > 0.$$

The integrated hazard rate function is given by

$$H(x) = -\log S(x; \boldsymbol{\theta}) = -\log(e^{-\alpha x^\lambda}) = e^{-\alpha x^\lambda}; \quad x \geq 0, \boldsymbol{\theta} > 0, \quad (19)$$

where  $\boldsymbol{\theta} = (\alpha, \lambda)$  is a vector of unknown parameters.

#### 4. Arctan-Weibull Distribution

The Weibull distribution has a straightforward mathematical definition. It is tractable mathematically. It is also a model that can be used in a variety of situations. The Weibull distribution is regarded as a versatile model for loss modelling in general insurance due to its ability to adequately model data with a high degree of positive skewness, which is a characteristic of claim amounts. Hence, this part of the

paper is devoted to introduce the new proposed distribution which is the AT-W distribution and derive the basic probability functions including the pdf, hrf, cdf, survivor function, integrated hazard function, and the retro hazard. Considering that  $G(x)$  is the cdf of the two-parameter Weibull distribution. The cdf of the AT-W distribution, for  $x > 0$ , can be expressed as

$$F_{AT-W}(x; \boldsymbol{\theta}) = \frac{4}{\pi} \arctan(1 - e^{-\alpha x^\lambda}), \quad x \in \mathbb{R}. \quad (20)$$

The corresponding pdf to the above cdf is given by

$$f_{AT-W}(x; \boldsymbol{\theta}) = \frac{4}{\pi} \frac{\lambda \alpha (\alpha x)^{\lambda-1} \exp\{-(\alpha x)^\lambda\}}{1 + \left\{4/\pi \arctan(1 - e^{-\alpha x^\lambda})\right\}^2}, \quad x \in \mathbb{R}. \quad (21)$$

The sf is expressed as follows:

$$S_{AT-W}(x; \boldsymbol{\theta}) = 1 - \frac{4}{\pi} \arctan(1 - e^{-\alpha x^\lambda}). \quad (22)$$

The hrf is obtained by

$$h_{AT-W}(x; \boldsymbol{\theta}) = \frac{4[\lambda \alpha (\alpha x)^{\lambda-1} \exp\{-(\alpha x)^\lambda\}]}{\pi - 4 \arctan\left(4/\pi \arctan(1 - e^{-\alpha x^\lambda})\right) \left\{1 + \left\{4/\pi \arctan(1 - e^{-\alpha x^\lambda})\right\}^2\right\}}. \quad (23)$$

The inverted hazard rate function is as follows:

$$r_{AT-W}(x; \boldsymbol{\theta}) = \frac{4[\lambda \alpha (\alpha x)^{\lambda-1} \exp\{-(\alpha x)^\lambda\}]}{\arctan\left(4/\pi \arctan(1 - e^{-\alpha x^\lambda})\right) \left\{1 + \left\{4/\pi \arctan(1 - e^{-\alpha x^\lambda})\right\}^2\right\}}. \quad (24)$$

The cumulative hazard function may be denoted by the following:

$$\begin{aligned} H_{AT-W}(x; \theta) &= -\log S_{\text{Tan-LL}}(x; \theta) \\ &= -\log \left[ 1 - 4/\pi \arctan \left( 1 - e^{-\alpha x^\lambda} \right) \right], \end{aligned} \quad (25)$$

such that  $x \geq 0$  and  $\alpha, \lambda > 0$ .  $\theta = (\alpha, \lambda)'$  is the vector parameter in all of the above equations, respectively.

Figures 1, 2, and 3 show some possible shapes of the AT-W distribution's pdf, cdf, and sf functions to explore the behavioural patterns of its density, cdf, and sf functions for different values of the model parameters.

## 5. Properties of the Proposed Model

This section is devoted to use numerical examples to derive some statistical and mathematical properties of the AT-W distribution, such as the quantile function, skewness and kurtosis, moments, and residual and reverse residual life functions.

**5.1. Quantile Function.** The inverse cdf function is mostly employed in theoretical areas of distribution theory, such as the simulations and applicability. The simulation software uses a quantile function to create random samples. The quantile function of the AT-W distribution is denoted by

$$x = Q_G(u) = F^{-1}(u) = G^{-1} \left( \tan \left( \frac{\pi}{4} u \right) \right), \quad (26)$$

where  $u$  is uniformly distributed from zero to one.

The quantile function of the AT-W model as follows:

$$Q_{AT-W}(p, \alpha, \lambda) = \left\{ -\frac{1}{\alpha} \log \left[ 1 - \left[ \tan \left( \frac{\pi}{4} u \right) \right]^{1/\lambda} \right] \right\}. \quad (27)$$

The median, lower quartile, and upper quartile of AT-W distribution can be obtained easily by using the quantile function by setting  $u = 1/2, 1/4,$  and  $3/4,$  respectively.

**5.2. Skewness and Kurtosis.** Galton skewness (or asymmetry) and Moors kurtosis of the AT-W model with two parameters have the following mathematical expression form:

$$\begin{aligned} S_K &= \frac{Q(3/4) + Q(1/4) - 2Q(2/4)}{Q(3/4) - Q(1/4)}, \\ K_M &= \frac{Q(7/8) + Q(3/8) - Q(5/8) - Q(1/8)}{Q(6/8) - Q(2/8)}. \end{aligned} \quad (28)$$

Here,  $Q$  donates the value of the quartile.

The preceding expressions can explicitly form as a function of the AT-W quantile function. These measures have many advantages [34].

**5.3. Moments.** Moments are essential in statistical modelling, particularly in applications. The LLT distribution's  $r$ th moment is defined as

$$\mu'_r = \int_{-\infty}^{\infty} x^r f(x; \alpha, \lambda) dx. \quad (29)$$

In fact, we have

$$\mu'_r = \int_{-\infty}^{\infty} \frac{4}{\pi} \frac{\lambda \alpha (\alpha x)^{\lambda-1} \exp\{-(\alpha x)^\lambda\}}{1 + \left\{ 4/\pi \arctan \left( 1 - e^{-\alpha x^\lambda} \right) \right\}^2} dx. \quad (30)$$

**5.4. Residual Life and Reverse Residual Life.** This can be widely used in actuarial science, survival analysis, and many other fields such as the risk management; for more information, see [35]. The analysis of a device's lifetime after reaching age  $x$  is especially important in reliability and survival analysis. Thus,  $X$  is the original lifetime with survival function  $S(x) = P(X \geq x)$  and the random variable  $X_x = (X - x | X > x)$  is the corresponding residual life after age  $x$  [36].

The distribution of  $X_x$  can be calculated using the conditional probability definition in the following expression:

$$R_{(t)}(x) = \frac{S(x+t)}{S(x)}, \quad x = 0, 1, 2, \dots \quad (31)$$

The residual lifetime is calculated using the following equation of the AT-W random variable (r.v.):

$$\begin{aligned} R_{(t)}(x) &= \frac{S(x+t)}{S(x)}, \\ R_{(t)}(x) &= \frac{1 - 4/\pi \arctan \left( 1 - e^{-\alpha(x+t)^\lambda} \right)}{1 - 4/\pi \arctan \left( 1 - e^{-\alpha x^\lambda} \right)}. \end{aligned} \quad (32)$$

In addition, we can obtain the reverse residual life of the LLT r.v. as follows:

$$\begin{aligned} \hat{R}_{(t)}(x) &= \frac{S(x+t)}{S(x)}, \\ \hat{R}_{(t)}(x) &= \frac{1 - 4/\pi \arctan \left( 1 - e^{-\alpha(x+t)^\lambda} \right)}{1 - 4/\pi \arctan \left( 1 - e^{-\alpha x^\lambda} \right)}. \end{aligned} \quad (33)$$

## 6. Classical Method of Estimation

Using classical methods is very important in the estimation process, so we devoted this section to maximum likelihood technique for estimating the parameters of the AT-X family of distributions from uncensored complete samples. Suppose that we have a random sample denoted as  $X_1, X_2, \dots, X_n$  that represents  $n$  independent random variables drawn from the AT-X family that have the following observations:  $x_1, x_2, \dots, x_n$ , we can write the likelihood function for the AT-X family is defined as follows:

$$L = \prod_{i=1}^n f(x_i, \theta), \quad (34)$$

$$L(x; \alpha, \beta) = \prod_{i=1}^n \left\{ \frac{4}{\pi} \frac{g(x; \theta)}{1 + G(x; \theta)^2} \right\}.$$

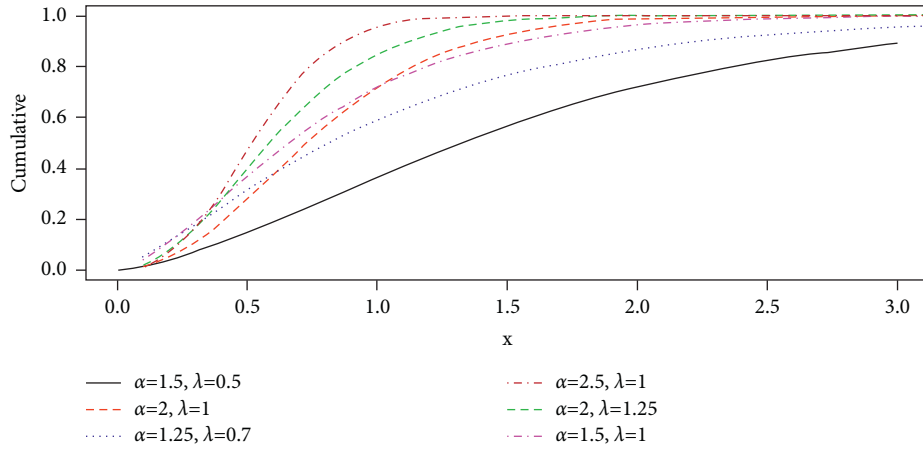


FIGURE 1: Visual representation of the cdf plots of the AT-W distribution for various parameter values.

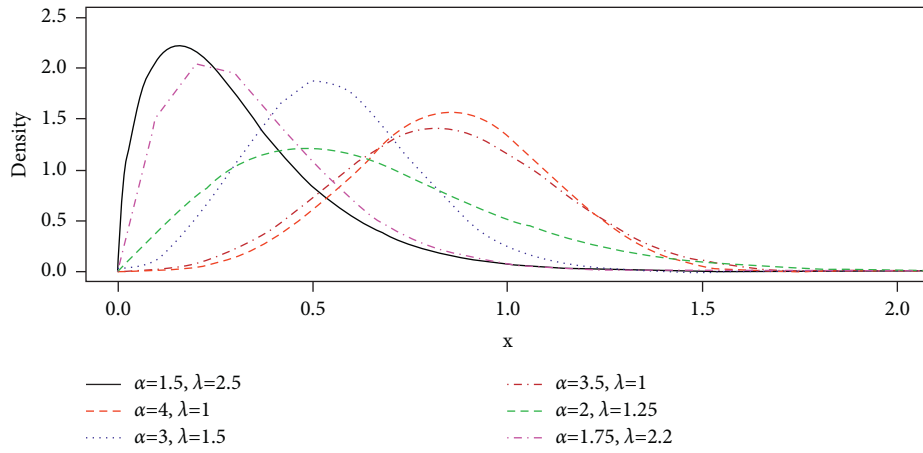


FIGURE 2: Visual representation of the pdf plots of the AT-W distribution for various parameter values.

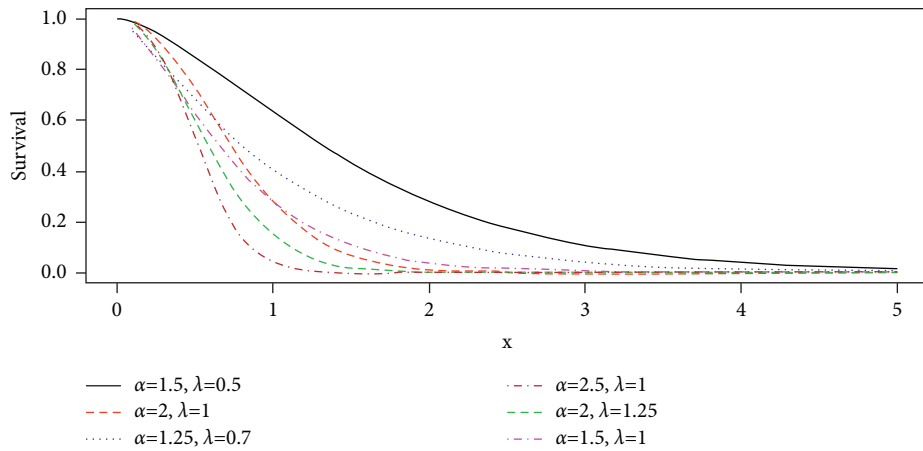


FIGURE 3: Visual representation of the cdf plots of the AT-W distribution for various parameter values.

We can express the log-likelihood function as below:

$$\ell = n \log\left(\frac{4}{\pi}\right) + \sum_{i=1}^n \log g(x_i; \theta) - \sum_{i=1}^n \log[1 + G(x_i; \theta)^2]. \quad (35)$$

Obtaining the partial derivate of the log-likelihood equation, we get

$$\frac{\partial \ell}{\partial \theta} = \sum_{i=1}^n \frac{\partial g(x_i; \theta)/\partial \theta}{g(x_i; \theta)} + \sum_{i=1}^n \frac{G(x_i; \theta)}{[1 + G(x_i; \theta)^2]} \partial g(x_i; \theta)/\partial \theta. \quad (36)$$



By equating the first derivative  $\partial \ell / \partial \theta$  to zero and trying to solve this equation numerically, we get the MLE estimator of  $\theta$ . Now it is very easy to get the values of the estimates of the parameters by the aid of equation (35) for any subcase of the proposed family with pdf and cdf given by  $g(x; \theta)$  and  $G(x; \theta)$  respectively.

We can find the estimates by two methods either by the R program directly (Adequacy Model Package), the OX program (subroutine MaxBFGS), or the SAS (PROX NLMIXED) or indirectly by solving the nonlinear likelihood equations.

## 7. Monte Carlo Simulation Study

We assess the effectiveness of the maximum likelihood estimation (MLE) method for estimating the Arctan-Weibull distribution parameters using Monte Carlo simulation. A numerical evaluation of the performance of MLE of the AT-W model is performed using `nlminb()` R-function with the argument `method = "BFGS"`. The simulation study is conducted to investigate the average bias (AB), root mean square error (RMSE), and mean square error (MSE), for the proposed model's parameters,  $\alpha$  and  $\lambda$ .

We performed the simulation process by various samples and different values for the parameters. We generated the samples used in the simulation process from the quantile function of the AT-W distribution. In order to generate accurate samples and to get perfect estimates, we made 750 iterations using sample sizes  $n = 25, 50, \dots, 750$  and the parameter scenarios  $\alpha = 5.0$  and  $\lambda = 4.0$ , in set I,  $\alpha = 0.8$  and  $\beta = 1.5$  in set II, and  $\alpha = 2.0$ , and  $\lambda = 1.2$ , in set III.

The MLEs are ascertained for each item of simulated data, say  $(\hat{\alpha}_i, \hat{\lambda}_i)$  for  $i = 1, 2, \dots, 750$  and the AB, RMSEs, and MSEs of the parameters were computed by

$$\begin{aligned} AB &= \frac{1}{N} \sum_{i=1}^N (\hat{\theta}_i - \theta), \\ MSE &= \frac{1}{N} \sum_{i=1}^N (\hat{\theta}_i - \theta)^2, \\ RMSE &= \sqrt{\frac{1}{N} \sum_{i=1}^N (\hat{\theta}_i - \theta)^2}, \end{aligned} \quad (37)$$

where  $\theta = \alpha$  and  $\beta$ .

**7.1. Simulation Results.** We explore the MLE method's performance in estimating the AT-W parameters using an MC simulation study with 750 repetitions. We determine the mean of the estimated parameters, the absolute bias, the mean square error (MSE), and the root mean square error (RMSE), and the following steps were followed:

- (i) We generated the samples by inverting the cdf given in [20]
- (ii) Three different sets are taken for different true values of the parameters

- (iii) We used different sample sizes as mentioned in the simulation table

Tables 2–4 summarize the numerical findings of the MC simulation study. The average of the estimated parameters, as well as the AB, MSE, and RMSEs, is evaluated. Based on the results in the simulation tables, it is self-evident that MLEs is effective in estimating unknown parameters and that the resulting estimates are relatively stable and close to actual real values. Furthermore, as the sample size increases, the AB, MSE, and RMSEs decrease and so do the biases, MSE, and RMSE. For visual representation, the MC simulation outcomes are depicted in Figures 4–6. These graphs indicate that increasing the sample size  $n$  results in a decrease in the estimated value of AB, MSEs and RMSEs, and the average MLEs close to their true values.

## 8. Practical Illustration Using the Insurance Data Set

This section will examine a highly correlated real-world data set from the insurance business in order to show the AT-W distribution's value. We compare the proposed distribution's goodness-of-fit test results and some information criterion measures to those of some other well-known competing distributions, such as the Weibull, Kappa, Burr-XII, and beta-Weibull distributions.

The primary attractiveness of the AT-W distribution derivation is its applicability to data analysis problems, which makes it useful in a variety of fields, particularly those concerned with insurance data analysis. Lately, a number of potential distribution families for insurance data sets have been offered. For more information on these, see [4, 5, 18, 19, 34, 35, 38–40].

The cdf of the fitted models is as follows:

- (1) Weibull distribution is

$$F(x, \alpha, \lambda) = 1 - e^{-\alpha x^\lambda}. \quad (38)$$

- (2) Burr-XII distribution is

$$F(x; c, k, s) = 1 - \{1 + (xk)^s\}^{-k}. \quad (39)$$

- (3) Beta-Weibull distribution is

$$F(x; \alpha, \beta, \lambda, \kappa) = I_{(1-e^{-\alpha x^\lambda})}(\beta, \kappa), \quad x \geq 0. \quad (40)$$

- (4) Kappa distribution is

$$F(x, \alpha, \lambda) = \{1 - \alpha(1 - \lambda x)^{1/\lambda}\}^{1/\alpha}. \quad (41)$$

Certain analytical measures are used to identify the best fitting functionalities of the competitive distributions. In this regard, the Akaike Information Criterion (AIC), Hannan–Quinn Information Criterion (HQIC), Corrected Akaike Information Criterion (CAIC), and Bayesian Information Criterion (BIC) values were used to select the most appropriate ones. Apart from discriminating tests, additional goodness-of-fit includes testing, like the

TABLE 2: Monte Carlo simulation results for the AT-W distribution using Set I values ( $\alpha = 5.0$  and  $\lambda = 4.0$ ).

Parameters	$n$	Set I			
		MLE	AB	MSE	RMSE
$\alpha$	25	5.2646	0.2646	0.7854	0.8862
	50	5.1632	0.1632	0.4005	0.6328
	100	5.0704	0.0704	0.1196	0.3458
	200	5.0280	0.0280	0.0701	0.2648
	300	5.0196	0.0196	0.0515	0.2269
	400	5.0145	0.0145	0.0351	0.1873
	500	5.0122	0.0122	0.0285	0.1688
	600	5.0091	0.0091	0.0252	0.1587
$\lambda$	700	5.0072	0.0072	0.0221	0.1487
	25	4.0193	0.0193	0.0329	0.1813
	50	4.0101	0.0101	0.0150	0.1225
	100	4.0069	0.0069	0.0072	0.0848
	200	4.0039	0.0039	0.0038	0.0616
	300	4.0026	0.0026	0.0023	0.0480
	400	4.0017	0.0017	0.0020	0.0447
	500	4.0015	0.0015	0.0015	0.0387
600	4.0013	0.0012	0.0012	0.0346	
700	4.0011	0.0011	0.0011	0.0332	

TABLE 3: Monte Carlo (MC) simulation results for the AT-W distribution using Set II values ( $\alpha = 0.8$  and  $\lambda = 1.5$ ).

Parameters	$n$	Set I			
		MLE	AB	MSE	RMSE
$\alpha$	25	0.8540	0.0540	0.0242	0.1556
	50	0.8231	0.0231	0.0084	0.0916
	100	0.8147	0.0147	0.0040	0.0632
	200	0.8072	0.0072	0.0019	0.0436
	300	0.8034	0.0034	0.0013	0.0361
	400	0.8026	0.0026	0.0007	0.0265
	500	0.8023	0.0023	0.0006	0.0245
	600	0.8020	0.0020	0.0005	0.0223
$\lambda$	700	0.8018	0.0018	0.0004	0.0200
	25	1.6155	0.1155	0.2185	0.4674
	50	1.5485	0.0485	0.0912	0.3020
	100	1.5333	0.0333	0.0450	0.2121
	200	1.5130	0.0130	0.0180	0.1342
	300	1.5081	0.0081	0.0150	0.1225
	400	1.5044	0.0044	0.0084	0.0916
	500	1.5040	0.0040	0.0072	0.0848
600	1.5037	0.0037	0.0058	0.0762	
700	1.5021	0.0021	0.0042	0.0648	

Anderson–Darling ( $A^*$ ) statistic, the Cramer–von Mises ( $W^*$ ) distance value test, and the Kolmogorov–Smirnov (K-S) statistic with associating  $p$  values, as well as the log-likelihood function, are also recorded.

The best model has the lowest values of AIC, BIC, CAIC, and HQIC, as well as the  $A^*$ ,  $W^*$ , and K-S tests. Furthermore, the model with the greatest log-likelihood function value is selected as the best model and  $p$  values for the K-S statistics are applied to compare the competitive distributions. We observed that when compared to other distributions, the AT-W model provided the greatest match and fitting because it has the smallest values of the measured analytical tools.

TABLE 4: Monte Carlo simulation results for the AT-W distribution using Set III values ( $\alpha = 2.0$  and  $\lambda = 1.2$ ).

Parameters	$n$	Set III			
		MLE	AB	MSE	RMSE
$\alpha$	25	2.1311	0.1311	0.1438	0.3792
	50	2.0523	0.0523	0.0523	0.2286
	100	2.0230	0.0230	0.0236	0.1536
	200	2.0092	0.0092	0.0120	0.1095
	300	2.0088	0.0088	0.0086	0.0927
	400	2.0076	0.0076	0.0063	0.0794
	500	2.0048	0.0048	0.0049	0.0700
	600	2.0038	0.0038	0.0042	0.0648
$\lambda$	700	2.0022	0.0022	0.0030	0.0548
	25	1.2255	0.0255	0.0198	0.1407
	50	1.2082	0.0082	0.0086	0.0927
	100	1.2056	0.0056	0.0041	0.0640
	200	1.2046	0.0046	0.0022	0.0469
	300	1.2030	0.0030	0.0013	0.0361
	400	1.2015	0.0015	0.0011	0.0332
	500	1.2005	0.0005	0.0008	0.0283
600	1.2004	0.0004	0.0006	0.0245	
700	1.2003	0.0003	0.0005	0.0223	

The AIC is

$$AIC = 2k - 2l. \tag{42}$$

The BIC is

$$BIC = k \ln(n) - 2l. \tag{43}$$

The CAIC is

$$CAIC = \frac{2nk}{n - k - 1} - 2l. \tag{44}$$

The HQIC is

$$HQIC = 2k \ln(\ln(n)) - 2l. \tag{45}$$

Here,  $l$  is the value of the likelihood function after taking the log for it and by substituting it with the estimates of the MLE,  $n$  is the size of the sample taken in the experiment, and  $k$  is the parameter number in the distribution. The following goodness-of-fit measurements are considered.

We can compute the value of the Anderson–Darling ( $A^*$ ) test statistic by using the following equation:

$$A^* = -n - \frac{1}{n} \sum_{i=1}^n (2i - 1) \times [\ln G(X_i) + \ln\{1 - G(X_{n-i+1})\}]. \tag{46}$$

We can compute the value of the Cramer–von Mises ( $W^*$ ) test statistics by using the following equation:

$$W^* = \frac{1}{12n} + \sum_{i=1}^n \left[ \frac{2i - 1}{2n} + G(X_i) \right]^2. \tag{47}$$

Here,  $x_i$  is the output number  $i$  in the vector of the data. When the data is sorted in ascending order, this  $x_i$  is calculated.

8.1. Data I: Insurance Data Set. This data set includes 58 observations and represents monthly unemployment

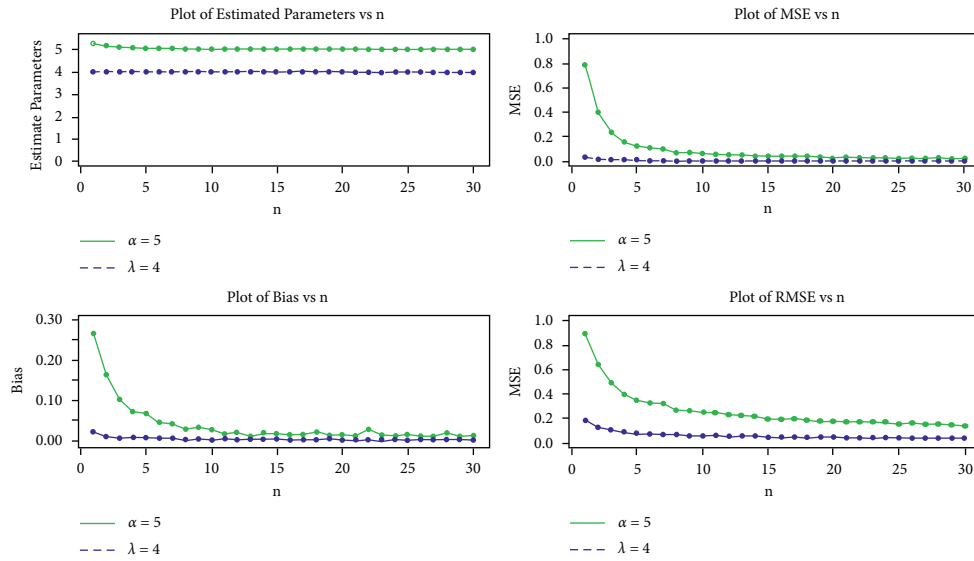


FIGURE 4: Visual representation of the MC simulation outcomes given in Table 2.

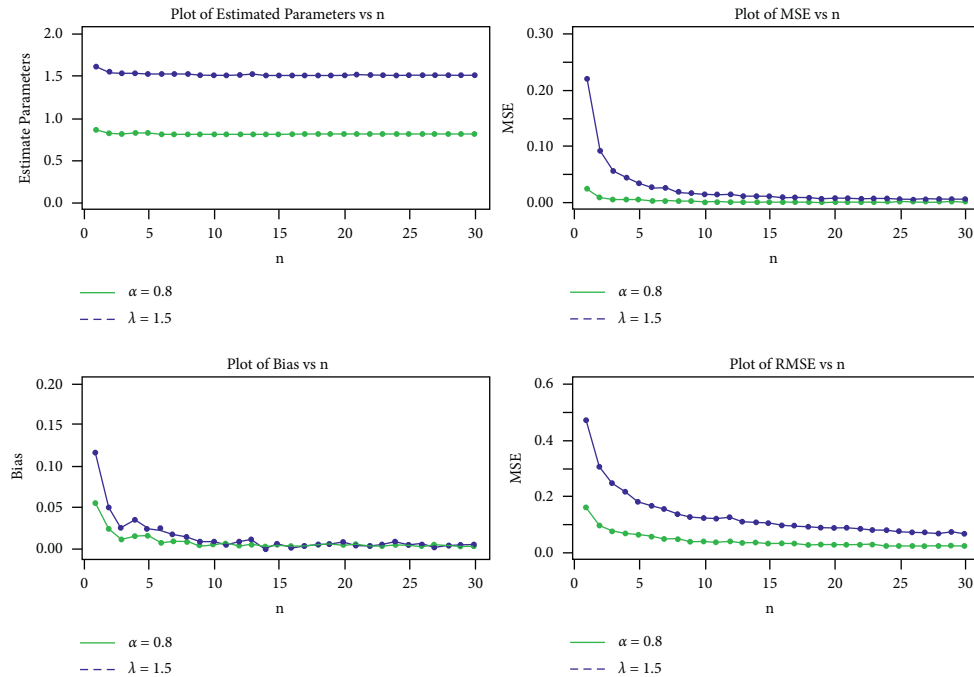


FIGURE 5: Visual representation of the MC simulation outcomes given in Table 3.

insurance metrics from July 2008 to April 2013. It was reported by the Maryland state, USA, Department of Labour, Licensing, and Regulation. The data set contains 21 variables, of which variable number 12 is of particular interest and it is studied by using alpha power-exponentiated exponential distribution to analyse [40]. The data can be found at: [catalog.data.gov/dataset/unemployment-insurance-data-july-2008-to-april-2013](http://catalog.data.gov/dataset/unemployment-insurance-data-july-2008-to-april-2013). The data frame contains the following 58 observations: Table 5

8.2. *Analyses of Exploratory Data.* The basic objective of research is to get information from large amounts of data. In

this paper, we employed four distinct strategies to do exploratory study: (1) descriptive statistics for the data set, particularly our variable of interest; (2) box plot; (3) TTT plot; and (4) histogram.

The total-time-on-test (TTT) plot is a graphical representation of the form of the failure rate curve. Qualitative information regarding the shape of the failure rate function may help in the selection of a specific distribution in a variety of real-world application. The TTT plot for our data set used in this study exists in Figure 7, and it has a form indicative of a rising failure rate that is recommended for using Weibull distribution or its modifications.

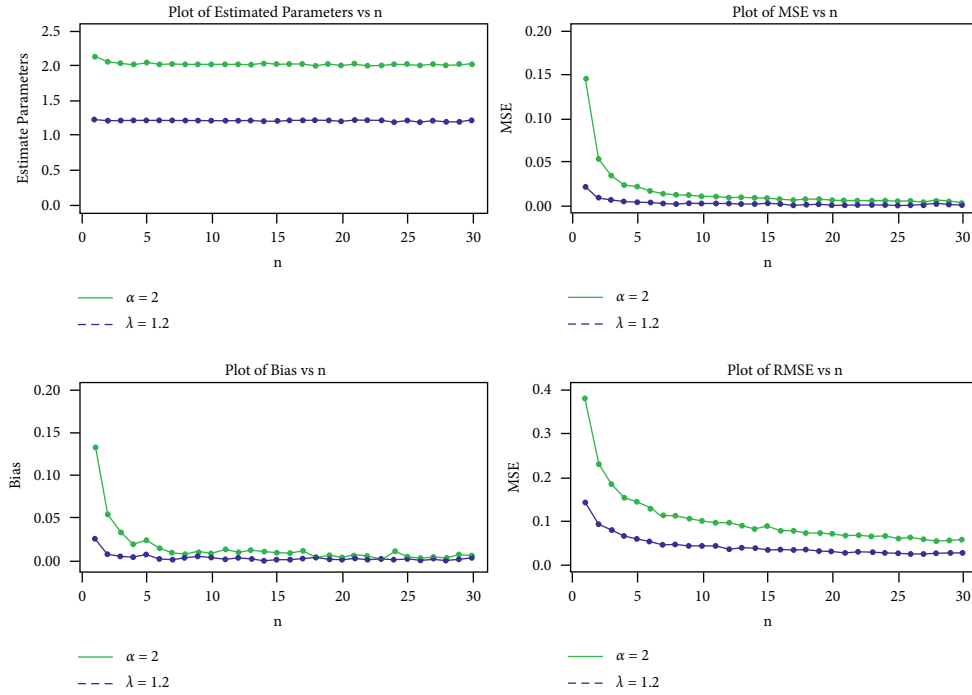


FIGURE 6: Visual representation of the MC simulation outcomes given in Table 4.

TABLE 5

52	33	39	50	29	52	60	32	57	64	61	64	41													
36	50	53	61	68	60	50	64	57	61	59	69	70													
137	170	100	90	222	109	68	63	56	90	74	95	114	133	66	75	72	54	57	52	66	69	83	44	60	80
58	80	80	52	65	73																				

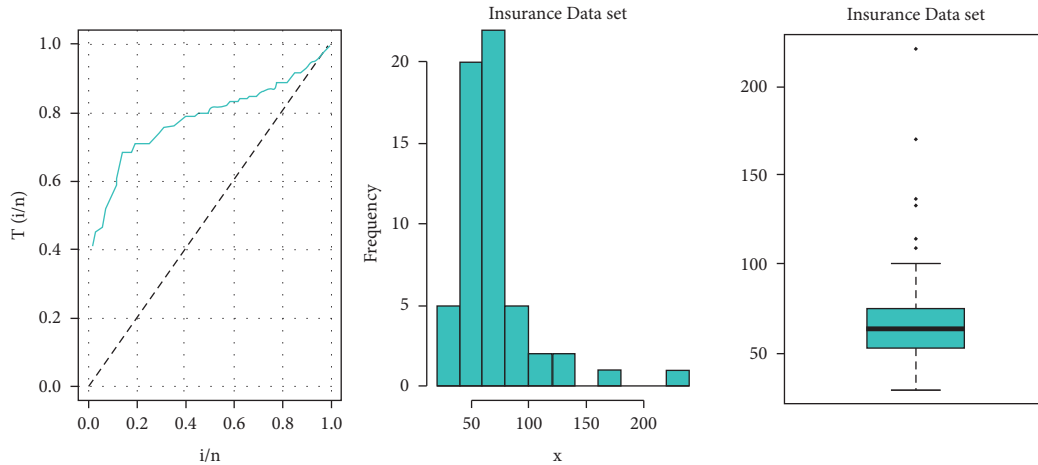


FIGURE 7: TTT plot, histogram, and box plots for the insurance data set.

Table 6 shows us the descriptive statistics of the insurance data set by computing specific aspects of the data (central tendency and spread).

8.3. Analysis of Data Set I. Table 5 contains descriptive statistics for data set I. The subjacent distribution of Data Set I, in particular, is highly skewed data (skewness estimated to

be 2.436) with a heavier tail (kurtosis estimated to be 7.622). The proposed AT-W distribution has the lowest AIC, CAIC, BIC, and HQIC values and the highest log-likelihood values as shown in Table 7, As a result, it is chosen as the best appropriate model among the alternatives evaluated in this paper.

Table 8 shows the parameter estimate and  $p$  value for the Cramer-von Mises ( $W^*$ ), Anderson-Darling ( $A^*$ ), and

TABLE 6: Descriptive measures of the Data Set I.

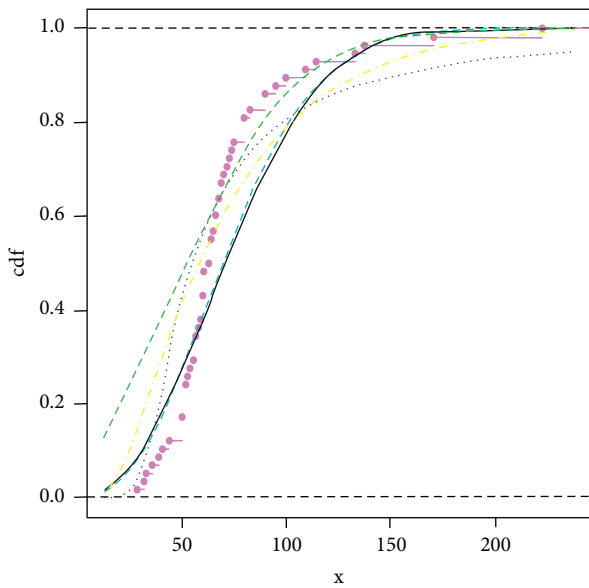
N	Min.	Median	Mode	Variance	Asymmetry	Kurtosis	Mean	Max.	CV	Geo. mean
58	29	63.50	52	1065.698	2.436	7.622	70.67	222	0.462	65.43

TABLE 7: The AIC, BIC, CAIC, HQIC, and likelihood values for the insurance data.

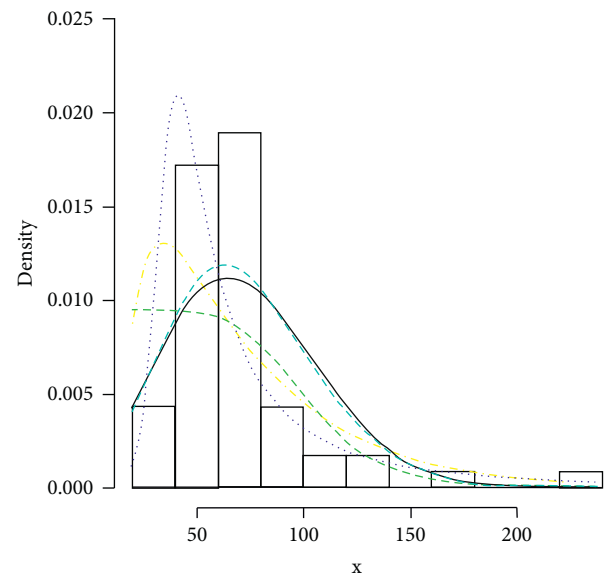
	Distribution				
	$\ell$	AIC	BIC	CAIC	HQIC
AT-W	<b>-277.467</b>	<b>558.934</b>	<b>563.054</b>	<b>559.152</b>	<b>560.539</b>
Weibull	-279.439	562.878	566.483	563.096	564.483
Burr-XII	-278.724	563.449	569.630	563.893	565.856
Beta-W	-282.961	573.922	582.164	574.677	577.132
Kappa	-289.477	582.955	587.076	583.955	584.560

TABLE 8: MLEs of the proposed model parameters, the goodness-of-fit tests, and the  $p$  values (in parenthesis) for Data Set I.

	Distributions			
	Estimates (SEs)	W*	A*	K - S (P value)
AT-W ( $\alpha, \lambda$ )	$\alpha = 2.383 (0.204)$ $\lambda = 0.011 (0.001)$	<b>0.475</b>	<b>2.595</b>	<b>0.187 (0.035)</b>
Weibull ( $\alpha, \lambda$ )	$\alpha = 2.268 (0.196)$ $\beta = 0.012 (0.001)$	0.548	2.987	0.184 (0.039)
Burr-XII ( $\alpha, \beta, \lambda$ )	$\alpha = 7.151 (1.485)$ $\beta = 0.225 (0.062)$ $\lambda = 36.285 (3.870)$	0.228	1.328	0.295 (0.0001)
Beta-Weibull ( $\alpha, \beta, \lambda, \kappa$ )	$\alpha = 6.754 (2.562)$ $\beta = 0.128 (0.024)$ $\beta = 1.164 (0.058)$	0.273	1.467	0.293 (0.0001)
Kappa ( $\alpha, \beta$ )	$\beta = 10.050 (1.051)$ $\alpha = 5.745 (48.933)$ $\beta = 77.672 (0.584)$	0.503	2.754	0.353 (0.032)



— Weibull  
 - - - Kappadis  
 . . . Burr-XII  
 - - - B-W  
 - - - AT-W



— Weibull  
 - - - Kappadis  
 . . . Burr-XII  
 - - - B-W  
 - - - AT-W

FIGURE 8: Visual display for the estimated cdf of the competing models.

FIGURE 9: Visual display for the estimated pdf of the competing models.

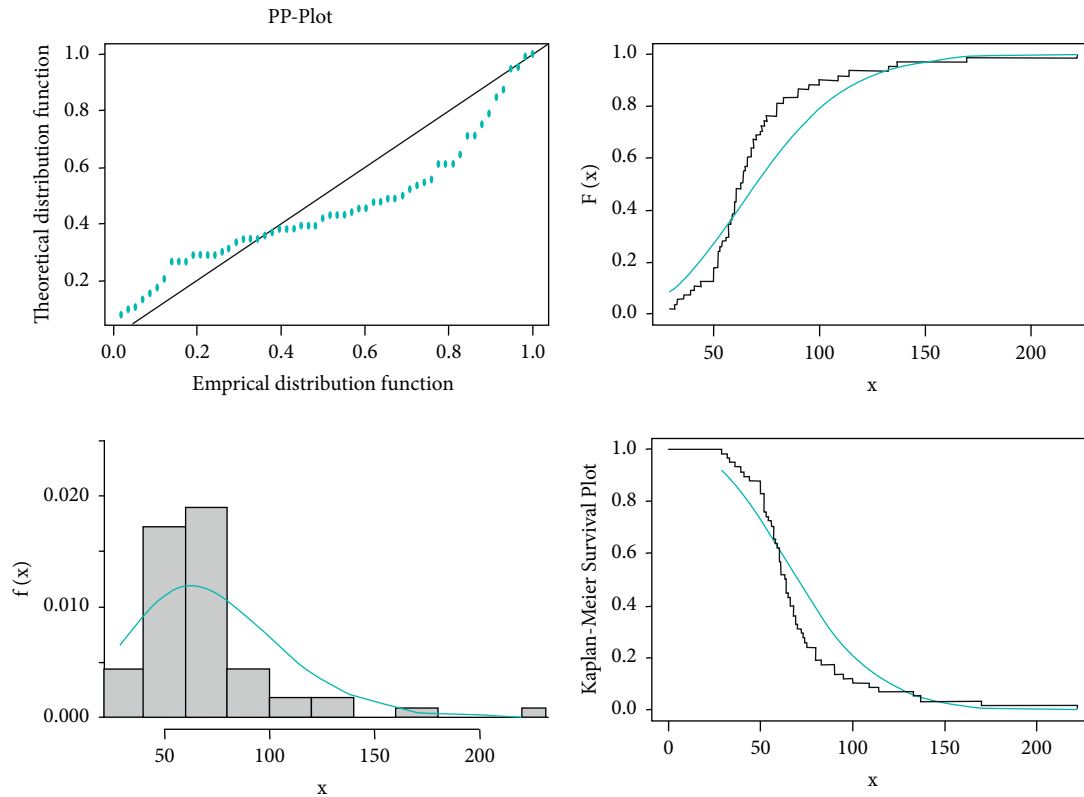


FIGURE 10: Visual display of the estimated PP, cdf, pdf, and Kaplan–Meier plots of the AT-W distribution for the insurance data set.

Kolmogorov–Smirnov (K-S) tests for all competing distributions using the above Data Set I. According to Table 8, the proposed LLT distribution has the lowest values in  $A^*$ ,  $W^*$ , and K-S tests, as well as the highest  $p$  value. As a consequence, the suggested AT-W distribution is selected as the best acceptable model among the competing distributions studied in this research. Also, plots of fitted cdf and pdfs with histogram of the observed data are shown in Figures 8 and 9. In addition, the visual representation of the estimated cdf, pdf, and PP plot in Figure 10 shows Kaplan–Meier plotting of the AT-W distribution for data set I.

## 9. Conclusion

Distribution theory takes uncertainties into account and provides a set of regulations for discussing financial and economic taking decision difficulties. Due to the importance of distribution theory, we were motivated to introduce a new distribution family based on the inverse trigonometric function. We introduced a new superior family which better fits many kinds of data. The AT-X is very intriguing and offers better fit to many kinds of data such as actuarial data financial data and many other related data in such fields. The Arctan-Weibull (AT-W) distribution is defined as a subset of the family. The study developed the fundamental probability functions as well as some statistical properties of the sub-model. The parameters of the AT-W model are estimated using classical inference by the maximum likelihood estimation technique. The proposed distribution is applied to

insurance data set with a high degree of granularity. The AT-W distribution was compared to some well-known competitors, including Weibull, Kappa, Burr-XII, and beta-Weibull distributions. Four information criterion measures (AIC, BIC, CAIC, and HQIC) were used to make comparisons, as well as three goodness-of-fit measures ( $A^*$ ,  $W^*$ , and KS test statistics with corresponding  $p$  values) and the likelihood function. Using these metrics, it is discovered that the AT-W model could be a good fit for analyzing high-dimensional financial data.

This study has a plethora of potential extensions. In practice, the special submodels of Table 1 may be investigated in the future study, for instance. Additionally, a variety of frequentist and Bayesian techniques may be employed to estimate the parameters of these particular submodels. The proposed family could also be extended to study regression analysis as a generalized linear regression model [41] (GLRM).

## Data Availability

The data used to support the findings of this study are included within the article.

## Conflicts of Interest

The authors declare no conflicts of interest regarding this paper.

## References

- [1] Z. Ahmad, E. Mahmoudi, G. G. Hamedani, and O. Kharazmi, "New methods to define heavy-tailed distributions with applications to insurance data," *Journal of Taibah University for Science*, vol. 14, no. 1, pp. 359–382, 2020.
- [2] M. Arif, D. Mohamad Ksahn, S. K. Khosa et al., "Modelling insurance losses with a new family of heavy-tailed distributions," *Computers, Materials & Continua*, vol. 66, no. 1, pp. 537–550, 2021.
- [3] J. Zhao, Z. Ahmad, E. Mahmoudi, E. H. Hafez, and M. M. M. El-Din, "A new class of heavy-tailed distributions: modeling and simulating actuarial measures," *Complexity*, vol. 2021, no. iii, 2021.
- [4] Z. Ahmad, E. Mahmoudi, M. Alizadeh, R. Roozegar, and A. Z. Afify, "The exponential T-X family of distributions: properties and an application to insurance data," *Journal Matematika*, vol. 2021, Article ID 3058170, 18 pages, 2021.
- [5] N. M. Alfaer, A. M. Gemeay, H. M. Aljohani, and A. Z. Afify, "The extended log-logistic distribution: inference and actuarial applications," *Mathematics*, vol. 9, no. 12, p. 1386, 2021.
- [6] M. H. Tahir and S. Nadarajah, "Parameter induction in continuous univariate distributions: well-established G families," *Anais da Academia Brasileira de Ciências*, vol. 87, no. 2, pp. 539–568, 2015.
- [7] M. H. Tahir and G. M. Cordeiro, "Compounding of distributions: a survey and new generalized classes," *Journal of Statistical Distributions and Applications*, vol. 3, no. 1, 2015.
- [8] C. R. De Brito, L. C. Rêgo, W. R. De Oliveira, and F. Gomes-Silva, "Method for generating distributions and classes of probability distributions: the univariate case," *Hacetatepe J. Math. Stat.* vol. 48, no. 3, pp. 897–930, 2019.
- [9] Z. Ahmad, G. G. Hamedani, and N. S. Butt, "Recent developments in distribution theory: a brief survey and some new generalized classes of distributions," *Pakistan Journal of Statistics and Operation Research*, vol. 15, no. 1, pp. 87–110, 2019.
- [10] A. H. Muse, S. M. Mwalili, and O. Ngesa, "On the log-logistic distribution and its generalizations: a survey," *International Journal of Statistics and Probability*, vol. 10, no. 3, pp. 93–121, 2021.
- [11] M. Eling, "Fitting insurance claims to skewed distributions: are the skew-normal and skew-student good models?" *Insurance: Mathematics and Economics*, vol. 51, no. 2, pp. 239–248, 2012.
- [12] R. Kazemi, A. Jalilian, and A. Kohansal, "Fitting skew distributions to Iranian auto insurance claim data," *Appl. Appl. Math. An Int. J.* vol. 12, no. 2, pp. 790–802, 2017.
- [13] M. R. Mahmoud, H. H. El-damrawy, and H. S. Abdalla, *A New Class of Skew Normal Distribution: Tanh-Skew Normal Distribution A New Class of Skew Normal Distribution: Tanh-Skew Normal Distribution and its Properties*, 2021.
- [14] T. Miljkovic and B. Grün, "Modeling loss data using mixtures of distributions," *Insurance: Mathematics and Economics*, vol. 70, pp. 387–396, 2016.
- [15] M. Blostein and T. Miljkovic, "On modeling left-truncated loss data using mixtures of distributions," *Insurance: Mathematics and Economics*, vol. 85, pp. 35–46, 2019.
- [16] H. M. Barakat, "A new method for adding two parameters to a family of distributions with application to the normal and exponential families," *Statistical Methods and Applications*, vol. 24, no. 3, pp. 359–372, 2015.
- [17] S. A. Abu Bakar, N. A. Hamzah, M. Maghsoudi, and S. Nadarajah, "Modeling loss data using composite models," *Insurance: Mathematics and Economics*, vol. 61, pp. 146–154, 2015.
- [18] Y. Liang Tung, Z. Ahmad, and E. Mahmoudi, "The arcsine-X family of distributions with applications to financial sciences," *Computer Systems Science and Engineering*, vol. 39, no. 3, pp. 351–363, 2021.
- [19] W. He, Z. Ahmad, A. Z. Afify, and H. Goual, "The arcsine exponentiated- X family: validation and insurance application," *Complexity*, vol. 2020, no. i, 2020.
- [20] C. Chesneau, F. Jamal, T. H. E. Sine, and K. F. Of, "The sine Kumaraswamy-G family of distributions," *Journal of Mathematical Extension*, 2020.
- [21] L. Souza, W. R. D. O. Juniory, C. C. R. De Britoz, C. Chesneaux, T. A. E. Ferreiray, and L. G. M. Soaresy, "On the Sin-G class of distributions: theory, model and application," *J. Math. Model.* vol. 7, no. 3, pp. 357–379, 2019.
- [22] L. Souza, W. Junior, C. C. R. D. Brito, C. Chesneau, R. L. Fernandes, and T. A. E. Ferreira, "Tan-G class of trigonometric distributions and its applications," *Cubo (Temuco)*, vol. 23, no. 1, pp. 1–20, 2021.
- [23] C. Chesneau, H. S. Bakouch, and T. Hussain, "A new class of probability distributions via cosine and sine functions with applications," *Communications in Statistics - Simulation and Computation*, vol. 48, no. 8, pp. 2287–2300, 2019.
- [24] C. Chesneau, L. Tomy, and J. Gillariose, "On a new distribution based on the arccosine function," *Arabian Journal Mathematics*, vol. 10, 2021.
- [25] M. Ç. Korkmaz, C. Chesneau, and Z. S. Korkmaz, "A new alternative quantile regression model for the bounded response with educational measurements applications of OECD countries," *Journal of Applied Statistics*, vol. 13, no. 1, pp. 1–24, 2021.
- [26] A. K. Chaudhary and V. Kumar, "The ArcTan Lomax distribution with properties and applications," *International Journal of Scientific Research in Science, Engineering and Technology*, vol. 4099, pp. 117–125, 2021.
- [27] Z. Mahmood, C. Chesneau, and M. H. Tahir, "A new sine-G family of distributions: properties and applications," *Bulletin Computational Applied Mathematics*, vol. 7, no. 1, pp. 53–81, 2019.
- [28] L. Souza, "New trigonometric classes of probabilistic distributions," Thesis, Universidade Federal Rural de Pernambuco, Brazil, 2015.
- [29] S. E. E. Profile: Arcsine-G Family of Distributions, 2021, [https://scholar.google.com/citations?view\\_op=view\\_citation&hl=en&user=GpJsqPoAAAAJ&citation\\_for\\_view=GpJsqPoAAAAJ:70eg2SAEIzsc](https://scholar.google.com/citations?view_op=view_citation&hl=en&user=GpJsqPoAAAAJ&citation_for_view=GpJsqPoAAAAJ:70eg2SAEIzsc).
- [30] A. H. Muse, A. H. Tolba, E. Fayad, O. A. Abu Ali, M. Nagy, and M. Yusuf, "Modelling the COVID-19 mortality rate with a new versatile modification of the log-logistic distribution," *Computational Intelligence and Neuroscience*, vol. 2021, Article ID 8640794, 14 pages, 2021.
- [31] Z. Ahmad, "The hyperbolic sine Rayleigh distribution with application to bladder cancer susceptibility," *Annals of Data Science*, vol. 6, no. 2, pp. 211–222, 2019.
- [32] M. Muhammad, R. A. R. Bantan, L. Liu et al., "A new extended cosine-G distributions for lifetime studies," *Mathematics*, vol. 9, no. 21, p. 2758, 2021.
- [33] M. Muhammad, H. M. Alshabari, A. R. A. Alanzi et al., "A new generator of probability models: the exponentiated sine-G family for lifetime studies," *Entropy*, vol. 23, no. 11, p. 1394, 2021.
- [34] A. H. Muse, S. Mwalili, O. Ngesa, S. J. Almalki, and G. A. Abdelmougod, "Bayesian and classical inference for the

- generalized log-logistic distribution with applications to survival data,” *Computational Intelligence and Neuroscience*, vol. 2021, Article ID 5820435, 4 pages, 2021.
- [35] Z. Ahmad, E. Mahmoudi, and O. Kharazmi, “On modeling the earthquake insurance data via a new member of the T- X family,” *Computational Intelligence and Neuroscience*, vol. 2020, Article ID 7632495, 20 pages, 2020.
- [36] R. E. Melchers and A. T. Beck, “Structural Reliability Analysis and Prediction,” *John Wiley & Sons*, Hoboken, NJ, USA, 2018.
- [37] A. A. Al-Babtain, I. Elbatal, C. Chesneau, and M. Elgarhy, “Sine Topp-Leone-G family of distributions: theory and applications,” *Open Physics*, vol. 18, no. 1, pp. 574–593, 2020.
- [38] W. Zhao, S. K. Khosa, Z. Ahmad, M. Aslam, and A. Z. Afify, “Type-I heavy tailed family with applications in medicine, engineering and insurance,” *PLoS One*, vol. 15, Article ID e0237462, 2020.
- [39] Z. A. Ahmad, E. M. Mahmoudi, and G. G. Hamedani, “A family of loss distributions with an application to the vehicle insurance loss data,” *Pakistan Journal of Statistics and Operation Research*, vol. 15, no. 3, pp. 731–744, 2019.
- [40] A. Z. Afify, A. M. Gemeay, and N. A. Ibrahim, “The heavy-tailed exponential distribution: risk measures, estimation, and application to actuarial data,” *Mathematics*, vol. 8, no. 8, 2020.
- [41] F. Jamal, C. Chesneau, D. L. Bouali, and M. U. Hassan, “Beyond the Sin-G family: the transformed SinG family,” *PLoS One*, vol. 16, 2021.



## Research Article

# The Traditional Influence on Increasing Acceptance of Commercial Smartphone Applications in Specific Regions of the Arabic World

Adel A. Bahaddad 

*Faculty of Computing and IT, King Abdulaziz University, Jeddah, Saudi Arabia*

Correspondence should be addressed to Adel A. Bahaddad; [dbabahaddad10@kau.edu.sa](mailto:dbabahaddad10@kau.edu.sa)

Received 16 August 2021; Accepted 9 November 2021; Published 8 December 2021

Academic Editor: Sameh S. Askar

Copyright © 2021 Adel A. Bahaddad. This is an open access article distributed under the Creative Commons Attribution License, which permits unrestricted use, distribution, and reproduction in any medium, provided the original work is properly cited.

The consumer sector represents one of the key players in the diffusion of M-commerce in contemporary societies. Consumers' traditionalism has a significant impact in determining the appropriate products to offer electronically, as well as in determining the functions and information that should be offered to enable them to make the right decisions at the right time. Many characteristics and requirements in general-use commercial applications cannot be acceptable for more targeted release if they are not compatible with the target population's traditional requirements, and therefore, the M-commerce applications go to complexity level in design because of the socio-technical systems. This study is conducted in three GCC countries, Saudi Arabia, the United Arab Emirates, and Qatar on 799 participant consumers. This study focuses to determine the basic requirements for smartphones' commercial applications, including the requirements affected by different traditionalism in the studied communities.

## 1. Introduction

Smartphone commercial applications represent one type of digital revolution. This revolution is occurring as mobile communications shift from electronic application systems to smart devices that work in intelligent environments. One of the most important and successful areas of commercial applications is the consumer sector where there is increasing use of mobile commerce (M-commerce) applications by consumers. The consumer represents a fundamental role in the distribution and success of M-commerce applications in current societies [1]. Knowledge of consumer traditional and habits significantly helps to determine the direction of application development in order to provide consumers with the application tools and information that enable them to make the right decisions at the right time [2].

Several reports discuss increases in electronic purchasing (e-purchasing) through M-commerce applications in the current decade. The widespread use of smart devices in the Arabic Gulf region indicates important possibilities in this

region for e-purchasing services through M-commerce applications [3–5]. However, despite the growing number of smart phones, M-commerce is still limited in the Arabic Gulf countries compared to the size of their economies and their level of per capita income [5].

Many contemporary studies have focused on the importance of M-commerce applications in specific geographical areas for several reasons. M-commerce offers possibilities for delivering services to consumers more safely and for providing essential products of interest to consumers in specific geographical areas. Application requirements are important to analyse for specific consumer communities in order to design applications for increased consumer acceptance and easy, convenient use [6, 7]. Application design that meets specific consumer service requirements represents a better option than a unified generic application for different geographical areas with various traditions [8]. Characteristics of M-commerce applications may not be accepted if they are not compatible with the requirements of users—whether sellers or buyers—in a specific target population [8, 9].

The study presented in this paper was conducted in three countries: Saudi Arabia, the United Arab Emirates, and Qatar. These three countries represent the top three Arabic states in the Gulf Cooperation Council (GCC) that are using smartphone devices according to numbers reported in recent country publications [4]. This study focused on identifying the features that should be provided in M-commerce applications in order to increase their acceptance based on user perspectives in target populations in Arabic Gulf countries. This paper will help M-commerce application developers deliver the required and optional features desired by the target audience in the GCC for commercial applications.

## 2. Literature Review

The literature review informing this study and development focused on four key topics that collectively helped identify further research that needed to be completed for this study. Further details on these four topics are presented in the following sections.

*2.1. M-Commerce Defined.* M-commerce is the business of buying and selling goods and services via smartphones and other handheld devices. It is based on the Wireless Application Protocol (WAP), which has greatly advanced this technology, gaining acceptance in many developed countries in Europe and America [10]. M-commerce represents one of the main e-commerce submodels as a result of two main factors:

- (1) The growing demand for service applications that are compatible with smartphone operating systems (OS), such as Internet browsers
- (2) The ability to adopt and activate many security, trust, and organisational frameworks that have helped overcome many e-commerce issues over a short period of time, such as protection and security within a wireless network environment [11].

As with e-commerce, there is no specific definition of M-commerce. In fact, many definitions correspond significantly with the broad and varied ones mentioned in the context of e-commerce. Some examples of M-commerce definitions explain the general boundaries of this activity. Lehman Brothers Holdings Inc. defines M-commerce as using mobile devices to communicate, inform, and entertain by using text and data through public or private networks [2]. Ovum concentrates on the essence of M-commerce, which is using a mobile phone or personal digital assistant (PDA) on a public telephone network to conduct transactions that lead to the transfer of money or to obtain particular information, services, or properties [12]. As defined by Mobilicity Inc., M-commerce uses wireless technology to provide a variety of personal services, such as location information, to customers, employees, and partners [11].

This paper focuses on the following definitions with respect to M-commerce. Both Morgan and Humphreys define M-commerce as conducting online procurement

and selling via smartphones and other handheld devices, while Morgan adds that it should be between businesses and consumers (Morgan and Humphreys; 1999 cited in [13]). In summary, the M-commerce definition for this research involves online trading via smartphones and tablet devices for a wide range of products and services, with the ability to pay for the same by electronic means. Once the transaction is completed, these products and services can be sent to the consumer simply and conveniently.

*2.2. Evaluation of M-Commerce Applications.* Many studies assessing M-commerce applications have been published over the last decade. Some of them have emphasised the M-commerce framework before the spread of smartphones. For example, many studies focused on the ten most important principles that should be adopted in the commercial application of mobile telephony. These principles include the following: using graphics carefully, avoiding long lists, making significant options visible, providing helpful and meaningful error messages, avoiding dead ends, formatting and presenting content appropriately, offering consistency in navigation map and menu options, providing sufficient and prompt channels to users, minimising user input, and structuring tasks to assist application users in interactions with the system [14, 15]. Al-Naimat's study with others has highlighted specific M-commerce applications, such as hotel bookings, ticket sales, and location services. This study stresses the importance of appropriate design in M-commerce applications providing location services and identifies the basic requirements for mobile applications of this type [16].

Using the M-commerce platform with smartphones is the outcome of two main factors: adopting current research on e-commerce websites to M-commerce and developing the research results on traditional M-commerce to work in the smartphone environment. According to some researchers in this field, the design of M-commerce interfaces is divided into seven main aspects:

- (1) Context: the importance of the smoothness and efficiency of mobile applications [14]
- (2) Content: the display of application interfaces in the form of multimedia combinations that enable interactions with the user [15]
- (3) Community: the reputation of and feedback on a specific product or vendor through electronic communication with other members of the interested community
- (4) Customisation: personalisation of mobile setting features to provide special user mobile interfaces [14, 15]
- (5) Communication: dialogue between applications and users using interactive tools and live broadcasts [17]
- (6) Connection: the importance of providing connections with other applications or websites to offer a flexible M-commerce environment [15, 17]

- (7) Commerce: trade-related aspects, such as interfaces for sales of goods and services [14, 17]

In addition, studies such as those of Gera's and others [18] and Venkatesh et al. [15, 19, 20] have focused on usability as one of the main complex aspects in M-commerce applications. They indicate that correctly designed commercial applications will help their users find what they are looking for and successfully conduct transactions via mobile phones. From a variety of angles, these four studies discuss the main usage requirements in M-commerce for the target segments. Gera's and others (2021) and AlQahtani and others (2020) [14, 18] point out the context of information displayed in M-commerce applications and the importance of specific standards such as the Attraction of Users' Attention, applications that deal with various devices such as handheld gadgets, and the Security of Information stored in these applications that will help provide the appropriate capability to use these applications in any circumstances. Venkatesh and others note that the success of web usability in commercial websites does not necessarily yield the same result in M-commerce applications because of the differences between two fields' characteristics and properties. Thus, a reexamination of usability in M-commerce applications for smartphones is required in order to meet the requisite level of consumer acceptance [19, 21]. Furthermore, it is vital to provide some useful features such as turn on or off (since some mobile features depend on the places and personal choices) and a small number of relevant ads, as well as to reduce the size of web pages to fit into mobile phones and tablet devices [19, 21, 22]. Bruschi and Rappel [20] stress the significance of ensuring the quality of commercial applications related to User Tasks, Content, Search, and Navigation Systems. Moreover, they point out the constraints that could be imposed by the design requirements with respect to these functions. Furthermore, Hsu and Yeh added three main categories to determine the M-commerce user requirements which are Functionality, Profitability, and Credibility. The Functionality contains Simplicity, Usability, Flexibility, Interface, Speed, and Accessibility. The profitability includes the added value, options of payment, price, and individualization. The credibility is divided into safety and correction of the system [15, 20].

*2.3. Design Indicators That Increase the Effectiveness of M-Commerce Applications.* Many issues are closely related to the acceptance, adoption, and diffusion of online trading via electronic applications in e-commerce or M-commerce [23]. A number of studies have examined some of both e-commerce and M-commerce issues in order to understand and design appropriate frameworks to correct imbalances and deficiencies, as well as to fill the gaps (e.g., [21, 23–25]). This solution is important because it forces communities and societies to understand the boundaries and requirements that should be tested for compliance with current and future requirements to arrive at a new maturity level in the work environment. Work on the maturity level should take place at the institutional level, applying to companies and the integration of their working system with the electronic

environment, and also at the production and distribution levels, including knowledge of the requirements to make the right decision at the right time, in order to reach greater maturity in addressing the target segment's needs [15, 26]. Many indicators should be considered when designing M-commerce applications, which will change based on traditional requirements of communities. These indicators can be divided into six fundamental parts: *Appearance, Content, Organisation, Interaction, Customer-Focus, and Assurance* [15, 26–29] (see Figure 1). Each part also encompasses different subaspects and indicators. The following paragraphs provide details of these indicators, clarifying the requirements of M-commerce applications relating to the needs of key stakeholders (such as consumers and sellers dealing with M-commerce applications via smartphones), and discuss how such applications can be designed to meet stakeholder needs.

*2.3.1. Appearance (AP).* The exterior design of smartphone applications related to M-commerce might be one of the most notable ways to entice new customers in the future, as many studies have confirmed. Customers see an application's attractive appearance as interesting and are encouraged by its adoption of online approaches for their different needs [8, 13, 26, 29, 30]. The appearance indicator can be summarized as following points:

- AP01.* Innovation and new design format are fundamental
- AP02.* Beauty of design is an important criterion for dealing with M-commerce application
- AP03.* Achieving a general balance among colours, images, and texts, ensuring these are included
- AP04.* Coordinate the colours used in the screen interface, making certain that no colour dominates the others
- AP05.* Use expressive images rather than text links only
- AP06.* Use light colours with a dark background, and vice versa
- AP07.* Use no more than four different colours per screen
- AP08.* Use a particular font type to ensure the text format is consistent and readable
- AP09.* Provide display options of several font sizes (e.g., small, medium, and large) to accommodate readers' individual requirements
- AP010.* Use no more than one headline per screen
- AP011.* Avoid using capital letters extensively in normal text in the English language

*2.3.2. Content (CO).* Evaluating mobile applications involves the assessment of information update procedures, across the applications overall and for specific application screens [8, 29–32]. The content indicators are divided into the following aspects:

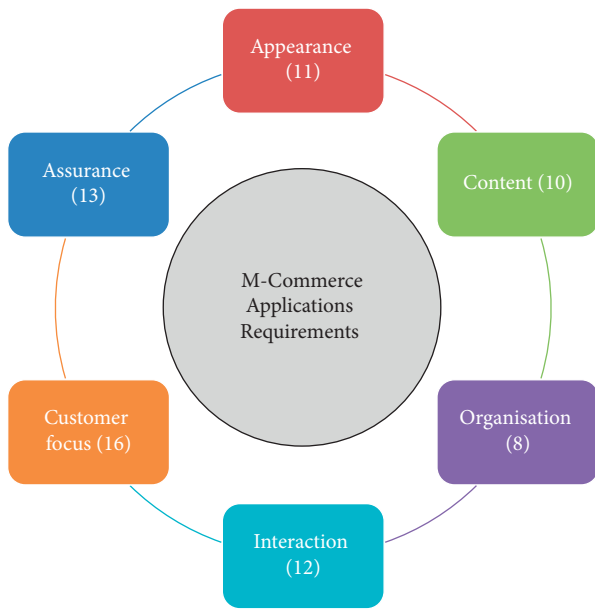


FIGURE 1: Summary of M-commerce application requirements.

*CO01.* Use a mechanism to update the screen content and application version generally

*CO02.* Regularly update all application items such as products and the dates they were added

*CO03.* Show the date and time of update of each item

*CO04.* Provide information about the company application's goals

*CO05.* Mention pertinent facts about the company's history, including its services and activities

*CO06.* Present information about the products and services offered by the application

*CO07.* Provide accurate content that is free of spelling and grammatical errors

*CO08.* Present the information about policy and legislation

*CO09.* Applications should be available to target customers in a specific area

*CO010.* Application languages should be tailored to the target population

**2.3.3. Organization (OR).** Good organization of mobile applications helps increase quality and performance levels and assists easy, smooth access to application content and internal links [22, 30, 33]. This part can be divided into the following parts:

*OR01.* The application name should be meaningful and easy to remember

*OR02.* The company logo should be displayed prominently in the application

*OR03.* The application should contain a map menu to facilitate navigability between the application screens and services

*OR04.* It should explicitly display the current page title

*OR05.* The application should be structured and consistent in planning and design

*OR06.* The application should be structured and consistent in sending alert messages, especially in communicating messages about input, process, and output

*OR07.* It should contain fixed buttons of fundamental functions in most or all of the application's basic screens

*OR08.* The fundamental functions should be available and accessible from anywhere in the application

**2.3.4. Interaction (IN).** Interaction in smartphone applications focuses on aspects that help increase the user's attention to these applications across multiple means of display, such as text, audio, video, and images [34, 35]. This interaction is measured through the following aspects:

*IN01.* Use multimedia elements such as images, video, and audio should be included as alternative options for any unexpected error

*IN02.* Use the previous elements effectively and offer more than one option in each place

*IN03.* Adopt these elements effectively, so as not to affect download time

*IN04.* The user is able to change or rearrange the application's interface options and sort products on the display screen

*IN05.* Search results can be displayed horizontally or vertically

*IN06.* Search results can be customised by filtering products and services, for instance

*IN07.* The user can choose special displays such as different colours in the application background

*IN08.* The messages tailor the products offered to customers' personal interests, which will make them want to visit the application periodically

*IN09.* Messages and recommendations to customers that would encourage them to buy a particular product

*IN010.* Personalised advertisements reach customers via their personal accounts, such as e-mail and personal accounts in social networking sites.

*IN011.* It should use auditory stimuli such as ring tones and musical files with actions or events

*IN012.* Use audio symbols to play audio files when received any information or offers

**2.3.5. Customer-Focus (CF).** This section focuses on the provision of mechanisms for communicating with customers and discovering their reactions to an application. It also discusses client feedback via mobile applications, which is helpful for building appropriate systems and raising the performance level in both mobile application acceptance and sales, which will influence the company's future plans

[3, 8, 12, 34–37]. The customer-focus indicators can be summarized as follows:

- CF01.* The application should include communication channels for complaints
- CF02.* The application should include communication channels for suggestions
- CF03.* The application should include communication channels for customer reviews of company services and products
- CF04.* New customers should receive new membership rewards for joining
- CF05.* Customers who contribute to improving company products and services should receive e-gifts or e-coupon via company application
- CF06.* Customers with repeat visits and purchases via the application should receive gifts
- CF07.* It should provide assistance through channels such as online chat and free hotlines
- CF08.* It should offer internal search capabilities in various application features
- CF09.* It should have a list of FAQs
- CF010.* It should provide “how to” information in a variety of formats, such as video, audio, and documents
- CF011.* The company should organise and present its refund and exchange policies for products
- CF012.* The company should design a feature to let customers follow up on or track their order until it is received
- CF013.* The application should design and provide e-receipts, which should be PDF files or mobile messages
- CF014.* The company should implement policies to handle disputes, allowing the customer to submit complaints at different stages of the procurement process
- CF015.* Offer several versions of company mobile application that are compatible with various smartphone OS
- CF016.* Ensure customer service availability in 24 hours a day and 7 days a week, if possible

**2.3.6. Assurance (AS).** Providing guarantees to customers significantly increases the maturity level of smartphone applications. This section emphasises the considerable assurance that should be provided to customers to increase their confidence in the M-commerce field [12, 35, 38–41]. The assurance indicators can be summarized as follows:

- AS01.* Provide a variety of safe m-payment methods
- AS02.* Increase customer awareness by briefly describing the main threats in m-shopping, and show customers how to address these risks through safe and logical solutions

*AS03.* The security certificates and legitimacy should be presented clearly in the application

*AS04.* It should display the security policy clearly according to countries’ legislation

*AS05.* It should present the application’s pass certification tests from OS companies

*AS06.* Special passwords for m-shopping applications should be developed

*AS07.* It should show customers a certificate that their information recorded in the application is confidential

*AS08.* It should display a privacy policy clearly according to government privacy legislation

*AS09.* It should ensure that customer data is not reserved via temporary files such as cookies files

*AS010.* Provide information about the company or employees who can communicate with customers in case there are any questions or concerns

*AS011.* Implement a copyright policy to deter criminals from setting up an imitation application and deceiving customers into using it

*AS012.* Increase the credibility of the application’s content by providing alternative supporting sources, such as e-mail address and SMS facilities

Figure 1 presents a representation of the model and its aspects described in the following.

**2.4. Using Traditional Requirements to Moderate the Effectiveness of M-Commerce Applications.** Based on the foregoing discussion, IT is not traditionally neutral. So, traditional and social background aspects of the society are likely to have a significant influence on M-commerce development and design. The key is for these differences to be accurately determined for different communities and countries. In 2006, the eBay commerce website was refused in China for several reasons, including the payment method process; the issue relates to the differences between Chinese and American cultures [14, 21]. Thus, Sarkar and others indicated that “higher uncertainty avoidance will reinforce the positive effect of citizen trust on intentions to engage in e-government” [42]. Moreover, the display specifications for websites are influenced by traditional requirements, according to the High-Context Communication (HCC) and Low-Context Communication (LCC) theory which has five dimensions that are used to measure the differences between societies (see more details in Appendix B) [7]. Other studies have determined this perspective and the importance of traditional aspects in adopting technology decisions in different countries. An example of these studies is that of Khan and others (2021), which included three countries: Japan, Switzerland, and the US. The results indicate that the Technology Acceptance Models (TAMs) for both the USA and Switzerland are positive, but not for Japan, suggesting that the TAM may not predict the use of technology in different opinions of traditions [43]. Another example is Gera and others’ study (2021), which made a comparison of

wireless communication infrastructure among similar countries traditionally. For some countries such as the UK and South Korea, the study emphasised that outcomes of M-commerce adoption cannot be matched, because the traditional dimensions of the societies are different. Moreover, understanding these dimensions will help develop M-commerce services and set realistic goals to be approved appropriately [42]. Other studies have focused on different factors that affect the degree of acceptance of technology, as well as indicators that are associated with traditions [43, 44].

The standpoint of the author is that traditions of specific society represents one of the main indicators that will guide the acceptance or rejection of any technological framework such as M-commerce, including its processes, appearance, and the content of M-commerce applications [39, 45]. Therefore, these indicators should be tested to ensure the indicators that are more applicable in a particular community in the GCC region. It is also worth mentioning that it is important for traditions to be considered for M-commerce studies in other countries so it is reusable or generalizable. Accordingly, it is beneficial to determine the different indicators to be used correctly and appropriately in various communities in GCC, to find out their views based on their society's traditional. These differences could be one of the key factors in making appropriate decisions for specific communities [39, 43]. For this reason, traditions will be measured by calculating the differences between the indicators to identify the level of importance for each sample in this study. It will be helpful in determining this study sample's needs and opinions in order to accept the study indicators [12].

### 3. Methodology

The study focuses on the consumer segment that already has skills in e-commerce and has previously completed online purchases. Thus, it focuses on the participants' knowledge and perspectives to determine the different requirements between the target audience in Arabic communities. It is would be beneficial to increase the level of acceptance by identifying the particular target requirements and identifying the differences between the Arabic communities to increase their confidence to use smartphone M-commerce applications by providing exactly what the target audience wants in their M-commerce application frameworks. The six groups of indicators are tested in this study to identify the differences between the communities. Choosing an electronic questionnaire is the best option for data gathering for two main reasons. Firstly, the online questionnaire can be distributed to a widespread geographical area. Secondly, because there are a large number of indicators, this means a consequently large survey. Online surveys can reach a large potential audience to allow a sufficient number of participants to provide complete data [28, 46].

There are logical procedures to be used when conducting the online data collection stage. The condition questions are applied to ensure the data gathering is coming from the right sample, initial part of the questionnaire contains an explanation of the purpose of the questionnaire, and contact

information for the research team, in case any of the participants had questions about the questionnaire [46]. Furthermore, there are three conditional questions which were helpful to ensure the participants are the right sample for this study.

The number of completed surveys is 408, 175, and 252 from Saudi Arabia, Qatar, and the United Arab Emirates, respectively, and their total is 799. The required number of completed surveys to create a statistically significant sample population is calculated according to number of sample size, confidence level, and acceptable margin of error which are presented in Table 1. As a result, the numbers of each different segment will be obtained based on the numbers listed in Table 1, which were calculated based on the Raosoft statistical base [47].

### 4. Analysis

The analysis contains some statistical tests to calculate some main numbers which would be valuable for this study. The statistical tests include the standard deviations (SDs), standard errors (SEs), and mean tests.

*4.1. Assessment of Standard Deviations and Standard Errors.* Standard deviation (SD) is a measurement for the similarity of data and their distance from the middle of the bell curve. The standard error of the mean (SE) is a variance from the sample mean and defined as the indicator of the representation level of a particular population sample [48]. If the SD is large, it indicates the samples are widely scattered around the mean; in contrast, a small SD has less scattered data. If the SE value is large, it refers to a lot of variation between the means of different samples. A small value of SE represents that most of the sample means are identical, thus representing an accurate reflection of the demographics in the study. In contrast, if the SE is large, then the sample is too weak to represent the target population. The values of SD and SE in all indicators in this study are relatively small compared to the means of each indicator (see Appendix A); therefore, the value of the mean can be considered representative for each indicator in the data. In addition, the small SE values demonstrate that the sample used was sufficiently representative of the target population segment.

*4.2. Preliminary Findings.* As presented in previous sections, the SD and SE for all indicators are small and are bounded between 1.19–0.42 and 0.09–0.02, respectively. As a result, it was determined that the mean of previous indicators could represent adequately for entire indicators. This section focuses on the assessment of the values of the means in the study's indicators, which are presented in Appendix A. The Likert scales are used to measure levels of agreement of participants with a proposed statement. So, 5 is the highest level of agreement and 1 is the lowest level of agreement (or highest level of disagreement) The participants' attitudes towards each construct and each indicator were determined based on the means of each indicator's constructs (see Appendix A) or depend on the average of each construct as

TABLE 1: Calculated sample sizes of the study.

	KSA	QAT	UAE	Total
Number of populations	30,770,375	2288927	8264000	40533672
Mobile user rate	72.8%	73%	73.8%	73.2%
Actual	22400833	1670916.71	6098832	29595693
Confidence level	95	95	95	99
Margin of error you can accept	7.5	7.5	7.5	5
Sample size	171	171	171	644
Actual participants	408	177	252	837
Extra	237	6	81	193

Source: QSAa, 2015; CDSI, 2015; UAE STATISTICS, 2016; Raosoft, 2016.

presented in Table 2. The beginning and ending numbers of each period of the Likert scale have been calculated based on 4 periods divided by 5 numbers (1 to 5 = 0.80). Periods of beginning and ending each option in the Likert scale are presented in Table 3.

*4.2.1. Indicators Influencing Commercial Mobile Application Design.* It is important to present the respondents' attitudes toward the assessment questions regarding the commercial smartphones' application design to ensure that gaps in the research questions are filled. These represent the fundamental aspects of design that these e-commerce applications should include based, in this case, on the perspective of Arabic traditional influence. The indicators focused on consumers' opinions, because they are the target population for shopping via smartphones. Table 2 shows that the overall means are significant numbers which range between 4.2141 and 4.6896 in all countries' samples. Most of the averages of these constructs' indicators have indicated "strongly agree," and this reflects the importance of the inclusion of these indicators in the commercial applications for smartphone target segment. The means of other constructs appeared slightly less than of the prior constructs. All of these constructs appeared in the "agree" section which means they continue to be important segments, but less so than the rest of the others. For example, the **appearance constructs** presented in the initial means analysis of Qatar samples was 4.1760. Also, the mean of the interactive construct for Saudi Arabia and Qatar were 4.1876 and 4.1559, respectively. This gives an initial indication that appearance and interactivity are factors that do not have the level of importance similar to other constructs (content, organization, customer focus, and assurance) in online commerce of smartphones.

Their construct mean in the Saudi Arabia sample was between 4.0328 and 4.6896. In Qatar, the sample mean was between 4.0702 and 4.6745, while in the United Arab Emirates, the sample mean was between 4.5989 and 4.0976. In these constructs, the means indicate that their importance varies depending on the participants' differing opinions in the samples. This indicates the importance of obtaining more details for these constructs, which are covered later in the discussion part.

*4.2.2. Level of Indicators Constituting Commercial Application Requirements.* Table 2 shows respondents' views about their requirements for smartphone business applications, of

which availability should be tailored to the Arabic traditions in general and in particular to the countries in the study (Saudi Arabia, Qatar, and the United Arab Emirates). The requirements of commercial applications can be categorised into six constructs: (1) appearance, (2) organization, (3) content, (4) interactivity, (5) customer focus, and (6) assurance. In the appearance construct, there are four questions that received a "strongly agree" response in the mean in all samples, with values between 4.26 and 4.51. There were three indicators that have response "agree", and their means range between 4.14 and 3.92 in the same samples. These indicators focus on the colour of numbers in the screen, use of image links instead of text links, and the avoidance of using capital letters extensively in normal text in the English language. The content construct was an important construct because it tested the necessary information that might be important to be available in all display screens for customers' smartphone applications. Therefore, values of means for 9 content questions had importance ratios between 4.46 and 4.72. However, three values showed a lower level, and their importance was between 4.10 and 3.87 in all samples. This indicator was the importance of providing information about the companies' electronic activities.

Furthermore, the organization construct showed a high level for all responses, with the value of the mean ranging between 4.52 and 4.78. This demonstrates the importance of all these factors for participants in the countries included in the study. The interactive construct presented a high level as well, from IN01 and IN04 to IN06, with their mean values ranging between 4.54 and 4.75. By contrast, the remaining five elements did not register responses of a greater level than "agree." The customer-focus construct had the largest number of questions (16). This construct focused on the communication mechanisms with customers and determines their reactions on the commercial application uses. In the statistical stage, the constructs that showed 15 of the 16 indicators have the "strongly agree" attitude in the mean value, which ranged between 4.42 and 4.86, while one question, the importance of providing a channel for customer complaints, earned a mean of 3.92, indicating that the electronic complaint channels do not have the same level of importance as, for example, a voice call. Finally, the assurance construct, which focused on the methods that help increase customer confidence in online shopping via mobile applications contained 13 questions, with a "strongly agree" attitude in all. It emphasises the importance of these

TABLE 2: Summary of frequency and attitude of all constructs depending on each country.

Name of constructs	No. of items	Saudi Arabia			Qatar			Emirates		
		Mean	Std. deviation	Attitude	Mean	Std. deviation	Attitude	Mean	Std. deviation	Attitude
AP	11	4.2141	0.41966	Strongly agree	4.1760	0.45733	Agree	4.2450	0.43152	Strongly agree
CO	10	4.3669	0.37636	Strongly agree	4.3797	0.41960	Strongly agree	4.3752	0.38660	Strongly agree
OR	8	4.4787	0.37290	Strongly agree	4.5120	0.39244	Strongly agree	4.5230	0.39504	Strongly agree
IN	12	4.1876	0.45280	Agree	4.1559	0.44424	Agree	4.2666	0.42974	Agree
CF	16	4.5389	0.38660	Strongly agree	4.5654	0.37774	Strongly agree	4.5427	0.40056	Strongly agree
AS	13	4.6722	0.41675	Strongly agree	4.6572	0.38191	Strongly agree	4.6545	0.41315	Strongly agree

TABLE 3: Weighted mean based on the Likert scale.

Weight	Level (opinion)	Weighted mean	
		From	To
1	Strongly disagree	1	1.79
2	Disagree	1.80	2.59
3	Neutral	2.60	3.39
4	Agree	3.40	4.19
5	Strongly agree	4.20	5

constructs indicators for participants and customers significantly. The mean values of these indicators were recorded between 4.70 and 4.96.

## 5. Discussion

In order to increase the acceptance level of commercial applications, it is important to determine the basic requirements of the consumer and what the consumer wants in commercial applications for smartphones. Increased consumer acceptance will help increase the sales volume and the number of regular consumers. The use of commercial applications cannot easily be studied in a large geographical region but can be studied at smaller state levels [7]. There are various unions between Arabic Gulf countries that correspond to similar traditional characteristics and commercial application requirements. However, some indicators show differences in community requirements in this region. The analysis of indicator differences is important in determining the requirements of individual communities. The availability of these consumer requirements in M-commerce applications will affect application acceptance and use. The following indicators showed differences in one participating community or more based on the previous six indicator groups that are presented in Section 2.3 previously.

*5.1. Special and Unique Requirements for Arabic Environments.* As noted in Hofstede's cultural dimensions' theory, special parameters can be set for specific communities to define particular audience characteristics. This section focuses on the practical requirements for

commercial smartphone applications in GCCs. Some differences do exist in the study samples, particularly in the traditional moderators. This led to the identification of special technical requirements that might be applied in specific communities.

Notably, the difference between the interest levels in study samples where some indicators are important to specific segments does not necessarily mean they are important to other segments. Therefore, it is important to highlight the indicators that present clear differences in the study segments (see Table 4 and Figures 2 and 3). These are divided into three user requirement groups: Systems Quality, Information Quality, and Service Quality. These indicators are listed by showing the scores that deviate from the others by less than or more than 10%.

*5.1.1. Appearance Functions.* In this group, four indicators, all in the subset of appearance constructs, present different results. The sample from Qatar also has one additional result that differs from that found in Saudi Arabia and UAE. These functions are summarized as follows:

- (1) AP04: presenting diversity in colours on the screen; do not use a particular colour more than others. In the Qatar sample, 72% identified this as important; in Saudi Arabia and the UAE, 88.7% and 88.6% did, respectively (increased).
- (2) AP05: using expressive images instead of using texts in overall services of application. In the Qatar sample, 81.3% identified this as important; in Saudi Arabia and the UAE, 73.6% and 67.5% did, respectively (decreased).
- (3) AP08: using specific type of Arabic or English fonts to ensure readability. In the Qatar sample, 83.6% identified this as important; in Saudi Arabia and the UAE, 73.8% and 67.1% did, respectively (decreased).
- (4) AP09: font size selection, which should be appropriate for readers of a smartphone screen. In Qatar sample, the result shows 93.6%, while in SA and the UAE, 86.3% and 85.8% were seen, respectively (decreased).



TABLE 4: The indicators that show different rates between the participants sampling results.

Indicators code	KSA		Qatar		UAE	
	L. of I.	Rate %	L. of I.	Rate %	L. of I.	Rate %
AP04	H	88.6	L	72	H	88.7
AP05	L	73.6	H	81.3	L	67.5
AP08	L	73.8	H	83.6	L	67.1
AP09	L	86.3	H	93.6	L	85.8
CO04	H	92	L	77.2	H	93.1
CO05	H	81.7	L	67.2	H	80
CO07	L	86.8	H	97.1	L	84.9
IN02	H	91.4	L	82.4	H	91.1
IN03	H	86.5	L	98.2	H	83.3
IN05	H	93.5	L	87.1	H	93.9
IN07	H	91.5	L	72.5	H	95.1
IN09	H	82.1	L	68.4	H	82.5
IN12	L	62.7	H	71.9	L	58.5
AS10	L	89.6	H	98.2	L	91.1
AS12	L	77.2	H	94.1	H	94.3
CF03	H	97.7	L	91.2	H	97.1
CF08	L	85.5	H	94.2	L	87
CF09	L	41.2	H	92.4	H	94.7

L: low ; H: high; L. of I.: level of importance.



FIGURE 2: The mean curve of all construct indicators.

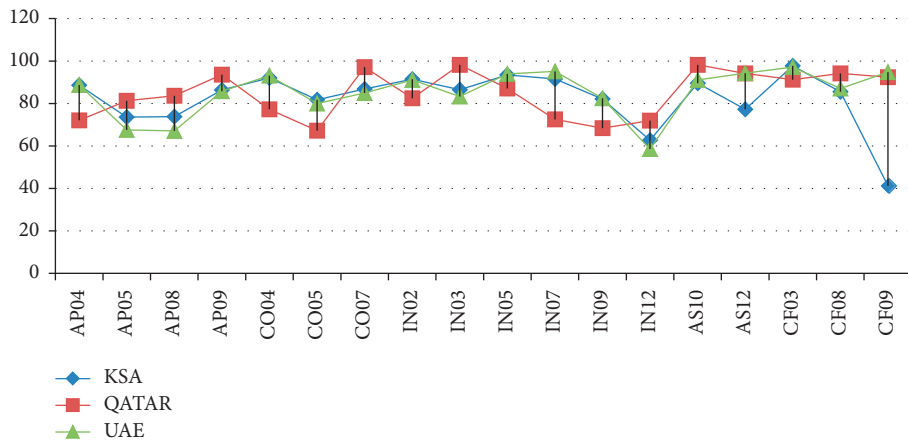


FIGURE 3: Graph of indicators that show different rates depending on the sampling results.

*5.1.2. Content Indicators.* There are three indicators in content constructs in which obvious differences appear, and all of these differences appeared in the Qatar sample which can be summarized as follows:

- (1) CO04: providing information about the company's objectives and the application. In the Qatar sample, 77.2% considered this important; in Saudi Arabia and the UAE, 92% and 93.1% did, respectively (increased).
- (2) CO05: providing information about the company's activities and services. In the Qatar sample, 67.2% considered this important; in Saudi Arabia and the UAE, 80% and 81.7% did, respectively (increased).
- (3) CO07: ensuring the application information content is free from spelling and grammatical errors. In the Qatar sample, 97.1% considered this important; in Saudi Arabia and the UAE, 86.8% and 84.9% did, respectively (decreased).

*5.1.3. Interactive Indicators.* In the interactive constructs, there are six indicators which have differences, and all of them appear in the Qatar sample.

- (1) IN02: using a variety of options to display the product information. In the Qatar sample, 82.4% considered this important; in Saudi Arabia and the UAE, 91.4% and 91.1% did, respectively (increased).
- (2) IN03: ensuring multimedia elements are built professionally for ease of download in the "check the description" screen. In the Qatar sample, 97.1% considered this important; in Saudi Arabia and the UAE, 86.8% and 84.9% did, respectively (decreased).
- (3) IN05: the ability to display search results horizontally or vertically. In the Qatar sample, 87.1% considered this important; in both Saudi Arabia and the UAE, 93.5% did (increased).
- (4) IN07: providing the possibility of choosing private display methods such as using different colours in the background of application. In the Qatar sample, 72.5% considered this important; in Saudi Arabia and the UAE, 91.5% and 95.1% did, respectively (increased).
- (5) IN09: sending promotions and vouchers via e-mail for consumers to invite them to purchase particular products regularly. In the Qatar sample, 68.4% considered this important; in Saudi Arabia and the UAE, 82.1% and 82.5% did, respectively (increased).
- (6) IN12: using symbols/icons to run audio files or visual features so users can choose between reading, listening to, or watching their news. In the Qatar sample, 71.9% considered this important; in Saudi Arabia and the UAE, 62.7% and 58.5% did, respectively (decreased).

*5.1.4. Assurance Indicators.* In the assurance construct, there are two indicators with different results among the study samples (one sample from Qatar and one from Saudi Arabia):

- (1) AS10: display privacy policy to customers for information saved in the application to explain that it is confidential. In the Qatar sample, 98.2% considered this important; in Saudi Arabia and the UAE, 89.6% and 91.1% did, respectively (decreased).
- (2) AS12: highlighting the copyright policy to prevent imposters from deceiving customers. In the Saudi Arabia sample, 77.2% considered this important; in Qatar and the UAE, 94.1% and 94.3% did, respectively (increased).

*5.1.5. Customer-Focus Functions.* In the customer-focus constructs, results are different for three indicators, two from Qatar and one from Saudi Arabia.

- (1) CF03: providing direct communication channels to obtain customers' opinions about company services and products. In the Qatar sample, 91.2% considered this important; in Saudi Arabia and the UAE, 97.8% and 97.1% did, respectively (increased).
  - (2) CF08: providing an application map to help the user find and search the internal features of the application. In the Qatar sample, 94.2% considered this important; in Saudi Arabia and the UAE, 85.5% and 87% did, respectively (decreased) (see Figure 3 to present all differences).
  - (3) CF09: providing a list of frequently asked questions (FAQ) and their answers. In the Saudi Arabia sample, 41.2% considered this important; in Qatar and the UAE, 92.4% and 94.7% did, respectively (increased).
- (1) 18 indicators show different results among the three samples in total. The rate distribution for which country was experiencing the difference is Qatar, 94.45%; Saudi Arabia, 5.5%; and nothing has been different in UAE. The rate of indicators distributed on the constructs are 22.2% of AP, 16.67% of CO, 33.33% of IN, 11.11% of AS, and 22.2% of CF.
- (2) The results in Qatar were clearly somewhat different from those in the other two samples. This does not necessarily mean that the difference in interest in M-commerce is significant (it is not, in this case); but, it may mean that the target audience for commercial smartphone applications in Qatar is somewhat different than in the other two countries, assuming the samples are representative.
- (3) Figure 4 shows the level of difference in the results between the three participants' samples; these have been addressed previously. These indicators do not have a great significance in determining level of interest in M-commerce in instances where there is a difference of greater than or equal to 10% among some of three study samples with respect to participants' views. When considering in the application design stage, seeing the functional links to the indicators and the target audience might be important. Therefore, these functions can be considered as

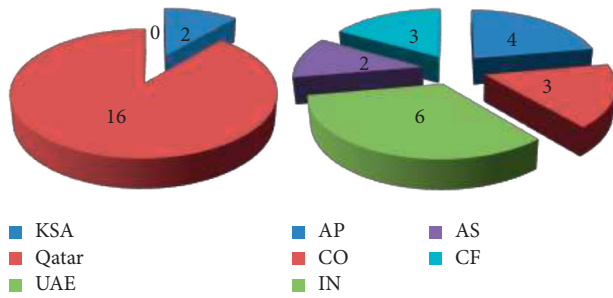


FIGURE 4: Rate of different indicators of M-commerce application construct requirements.

optional functions that are usable given an interested target audience or can alternately be dispensed of. Moreover, it can help to use the location service in the smartphone to determine where the user will be living and predominantly using the phone; then, it can be redesigned to include features automatically depending on the importance or lack thereof of specific indicators. For example, if the application is used in Qatar, indicators that tested as being important in this country should appear, while others should be disabled. Furthermore, the applications and functionalities that appear can also be tailored by location service and then modified manually in the application by the user if need be.

- (4) This part of the study leads us to reexamine these indicators for any country that has not been studied recently, particularly the rest of the GCC. Finding out how these countries view these indicators would be important before fully redesigning current smartphone applications tailored to these communities.

Through evaluating the reactions of the sample populations to the functions displayed previously, clear differences between the study's various segments were identified. The rates of difference among the samples' viewpoints were quantified. Furthermore, suggestions have been made to help determine what functions should be enabled and disabled in smartphones depending on location of the user. Functions that were not different among the samples could be treated the same way in smartphones across all three sample countries.

## 6. Implication, Limitations, and Motivation

- (1) The results, shown in Table 4, relate to the statistical relationship between indicators of AP, CO, IN, CF, and AS, which have significant relationships in all statistical sampling. These relationships emphasize the greater importance of particular indicators in previous five groups of commercial smartphone applications [49]. It might be the beliefs about systems and information quality in the context of diffusing and spreading M-commerce being more important than service quality, which is important for the support of User Satisfaction and the Intention

to Use smartphone commercial applications in the future. This means that achieving a sustainable competitive advantage in the electronic market will be very important if system and information quality are available. The importance of service quality, which was statistically significant in some segments, was helpful in determining the basic parameters of target segment requirements in online purchases made through smartphones. Consequently, it was determined that service quality requirements are harder for competitors to achieve the information and system quality requirements because these requirements vary and are different from one segment to another [29, 50]. These experiments confirm that the multidimensional analysis and coherent approach help manage the situation and place the focus on different aspects of the IS Success system, which includes system, information, and services quality; the other requirements in the model focus on the benefits of system success, which include User Satisfaction, Intention to Use, and Net Benefits regarding commercial smartphone applications.

- (2) Growing development in electronic systems for the conduction of e-commerce and growth of IS Success and acceptance of various models in commercial applications has been a good way to understand the various dimensions of net benefits and other outcomes of these approaches; this is particularly true of GCC states, which have shown a growing interest in smartphone devices. It has also increased online business in these countries in the past decade to appropriate levels that will create strategies for improving incomplete success variables that affect GCC societies in particular [12, 51].
- (3) Finally, achieving leadership in the M-commerce field requires a broader range of measurements to assess and monitor changes in the importance level of M-commerce success indicators [50, 52]. This study provided appropriate measures, which were statistically tested to measure these indicators so they could be part of the CIO M-commerce system to measure variables of successful levels carefully and to take the necessary corrective actions for improvement.

Many of the limitations found in this study can be addressed in future research. They include the following:

- (4) The M-commerce research approaches are relatively the new model in GCC. Their results and effects on different types of e-commerce in previous studies targeted many consumer groups around the world and in the GCC region. This study was conducted in three countries of the GCC: Saudi Arabia, Qatar, and the United Arab Emirates. Thus, the results of this study are limited to the GCC traditions because of the convergence between these countries in their overall traditional aspects and their preservation level of religious values. However, it would be interesting in future research to prepare a similar study

TABLE 5: Descriptive statistics of all indicators.

			KSA	QAT			UAE						KSA	Qatar			UAE		
Descriptive statistics of content indicator constructs										Descriptive statistics of appearance indicator constructs									
VD	Mean	SD	SE	Mean	SD	SE	Mean	SD	SE	VD	Mean	SD	SE	Mean	SD	SE	Mean	SD	SE
CO01	3.987	0.79	0.04	4.368	0.68	0.05	4.016	0.87	0.06	AP01	4.518	0.58	0.03	4.444	0.59	0.04	4.508	0.60	0.04
CO02	4.376	0.62	0.03	4.538	0.63	0.05	4.386	0.69	0.04	AP02	4.412	0.55	0.03	4.439	0.58	0.04	4.435	0.61	0.04
CO03	4.617	0.57	0.03	4.374	0.67	0.05	4.557	0.60	0.04	AP03	4.402	0.58	0.03	4.263	0.66	0.05	4.447	0.62	0.04
CO04	4.355	0.65	0.03	4.029	0.79	0.06	4.451	0.70	0.04	AP04	4.272	0.68	0.03	3.959	0.85	0.06	4.358	0.69	0.04
CO05	4.091	0.75	0.04	3.877	0.86	0.07	4.102	0.80	0.05	AP05	4.008	0.79	0.04	4.146	0.84	0.06	3.955	0.86	0.06
CO06	4.023	0.74	0.04	4.216	0.84	0.06	4.085	0.78	0.05	AP06	4.184	0.74	0.04	4.047	0.81	0.06	4.285	0.81	0.05
CO07	4.262	0.75	0.04	4.655	0.53	0.04	4.276	0.79	0.05	AP07	3.997	0.81	0.04	4.018	0.88	0.07	3.988	0.85	0.05
CO08	4.668	0.53	0.03	4.298	0.71	0.05	4.711	0.49	0.03	AP08	4.026	0.82	0.04	4.246	0.81	0.06	3.992	0.91	0.06
CO09	4.306	0.71	0.04	4.398	0.71	0.05	4.362	0.70	0.04	AP09	4.264	0.76	0.04	4.439	0.65	0.05	4.301	0.81	0.05
CO10	4.536	0.70	0.04	4.532	0.61	0.05	4.455	0.73	0.05	AP10	4.443	0.70	0.04	4.006	0.90	0.07	4.443	0.72	0.05
Descriptive statistics of interactive indicator constructs										Descriptive statistics of organization indicator constructs									
VD	Mean	SD	SE	Mean	SD	SE	Mean	SD	SE	VD	Mean	SD	SE	Mean	SD	SE	Mean	SD	SE
IN01	4.648	0.57	0.03	4.351	0.67	0.05	4.63	0.58	0.04	VD	Mean	SD	SE	Mean	SD	SE	Mean	SD	SE
IN02	4.295	0.63	0.03	4.152	0.73	0.06	4.435	0.68	0.04	OR01	4.681	0.59	0.03	4.667	0.50	0.04	4.691	0.63	0.04
IN03	4.213	0.70	0.04	4.714	0.49	0.04	4.179	0.76	0.05	OR02	4.614	0.58	0.03	4.322	0.74	0.06	4.618	0.57	0.04
IN04	4.725	0.50	0.03	4.532	0.64	0.05	4.736	0.48	0.03	OR03	4.244	0.76	0.04	4.409	0.68	0.05	4.272	0.79	0.05
IN05	4.542	0.66	0.03	4.339	0.74	0.06	4.488	0.65	0.04	OR04	4.350	0.64	0.03	4.444	0.56	0.04	4.451	0.65	0.04
IN06	4.308	0.67	0.03	4.491	0.62	0.05	4.398	0.69	0.04	OR05	4.383	0.58	0.03	4.491	0.56	0.04	4.468	0.60	0.04
IN07	4.329	0.63	0.03	4.047	0.89	0.07	4.476	0.60	0.04	OR06	4.386	0.57	0.03	4.421	0.62	0.05	4.524	0.55	0.04
IN08	4.054	0.78	0.04	4.082	0.79	0.06	4.089	0.80	0.05	OR07	4.358	0.63	0.03	4.544	0.61	0.05	4.415	0.69	0.04
IN09	4.132	0.74	0.04	3.860	0.84	0.06	4.187	0.75	0.05	OR08	4.609	0.57	0.03	4.690	0.50	0.04	4.585	0.57	0.04
IN10	3.902	0.79	0.04	3.772	0.89	0.07	3.959	0.83	0.05	OR09	4.687	0.53	0.03	4.620	0.57	0.04	4.683	0.50	0.03
IN11	3.816	0.81	0.04	3.684	0.83	0.06	3.850	0.83	0.05										
IN12	3.780	0.76	0.04	3.848	0.76	0.06	3.772	0.80	0.05										
Descriptive statistics of assurance indicator constructs										Descriptive statistics of customer-focus indicator constructs									
VD	Mean	SD	SE	Mean	SD	SE	Mean	SD	SE	VD	Mean	SD	SE	Mean	SD	SE	Mean	SD	SE
AS01	4.707	0.52	0.03	4.912	0.30	0.02	4.65	0.58	0.04	CF01	3.987	0.73	0.04	4.696	0.55	0.04	3.927	0.81	0.05
AS02	4.850	0.41	0.02	4.696	0.57	0.04	4.833	0.42	0.03	CF02	4.736	0.54	0.03	4.620	0.53	0.04	4.687	0.61	0.04
AS03	4.671	0.59	0.03	4.684	0.54	0.04	4.667	0.57	0.04	CF03	4.668	0.54	0.03	4.561	0.67	0.05	4.606	0.60	0.04
AS04	4.637	0.57	0.03	4.632	0.55	0.04	4.585	0.60	0.04	CF04	4.593	0.64	0.03	4.503	0.67	0.05	4.606	0.62	0.04
AS05	4.611	0.59	0.03	4.708	0.51	0.04	4.565	0.63	0.04	CF05	4.477	0.77	0.04	4.591	0.65	0.05	4.411	0.82	0.05
AS06	4.681	0.55	0.03	4.684	0.51	0.04	4.646	0.61	0.04	CF06	4.601	0.68	0.03	4.532	0.65	0.05	4.626	0.69	0.04
AS07	4.674	0.56	0.03	4.702	0.54	0.04	4.667	0.60	0.04	CF07	4.544	0.72	0.04	4.246	0.70	0.05	4.520	0.75	0.05
AS08	4.681	0.57	0.03	4.667	0.57	0.04	4.707	0.57	0.04	CF08	4.228	0.74	0.04	4.380	0.60	0.05	4.350	0.77	0.05
AS09	4.643	0.63	0.03	4.380	0.84	0.06	4.618	0.65	0.04	CF09	4.340	0.62	0.03	4.328	0.61	0.05	4.459	0.63	0.04
AS10	4.549	0.74	0.04	4.714	0.49	0.04	4.557	0.71	0.05	CF10	4.288	0.65	0.03	4.503	0.58	0.04	4.390	0.72	0.05
AS11	4.785	0.58	0.03	4.661	0.61	0.05	4.748	0.54	0.03	CF11	4.611	0.57	0.03	4.637	0.55	0.04	4.589	0.58	0.04
AS12	4.687	0.62	0.03	4.538	0.63	0.05	4.663	0.64	0.04	CF12	4.697	0.55	0.03	4.573	0.58	0.04	4.687	0.57	0.04
AS13	4.650	0.59	0.03	4.567	0.58	0.04	4.602	0.64	0.04	CF13	4.668	0.59	0.03	4.795	0.43	0.03	4.626	0.60	0.04
										CF14	4.801	0.45	0.02	4.766	0.49	0.04	4.801	0.46	0.03
										CF15	4.749	0.53	0.03	4.673	0.53	0.04	4.768	0.53	0.03
										CF16	4.671	0.57	0.03	4.643	0.55	0.04	4.63	0.61	0.04

TABLE 6: The high-context communication (HCC) and low-context communication (LCC) theory.

Parameter	Tendency in HCC cultures	Tendency in LCC cultures
Animation	High use of animation, especially in connection with images of moving people	Lower use of animation, mainly reserved for highlighting effects, e.g., of text
Promotion of values	Images promote values characteristic of collectivist societies	Images promote values characteristic of individualistic societies
Individuals separate or together with the product	Featured images depict products and merchandise in use by individuals	Images portray lifestyles of individuals, with or without a direct emphasis on the use of products or merchandise
Level of transparency	Links promote an exploratory approach to navigation on the website; process-oriented	Clear and redundant cues in connection with navigation on a website; goal-oriented
Linear vs. parallel navigation on the website	Many sidebars and menus; opening of new browser windows for each new page	Few sidebars and menus; constant opening in the same browser window

Source: [7].

to validate the model in different traditional contexts of Arabic communities, because the ratification of diverse traditions and using a large sample collected in a variety of places would help the circulation of the proposed model in various Arabic communities [2, 9, 53].

- (5) The cumulative visions of previous studies support the determination of the net benefit for its importance in many aspects of this study [8, 54]. Thus, identifying the standards of the net benefit might lead to knowing the specific net benefits sought in various types of M-commerce systems. Determining net benefits requires critical thinking and empirical research, especially on those factors that vary from one community to another.
- (6) This was a preliminary study of an IS Success model in M-commerce, which focused on one side of the stakeholders, the customer. M-commerce systems success models can be developed using other stakeholders and levels of analysis to increase accuracy and power levels in the results of future research [2, 9, 53].

One of the main obstacles in many electronic systems is acceptance by the right target segment. Sociotechnical systems, therefore, represent one of the most sensitive aspects in many theoretical frameworks, as well as digital transformation processes associated with traditional systems and the extent of audience acceptance by the target segment. This is because acceptance depends on the level of interest of the target segment and the extent of the systems' requirements, which can be applied to a specific segment and within a specific scope. Complexity thus appears during the construction of specialized electronic systems, which includes the requirements of the target segment. Care must be taken not to harm the spirit of the general requirements for the applications of the approach, in this case, for example, commercial applications on smartphones. Many characteristics of a society, together with its acceptance of technical aspects, depend on traditions and the appropriate way of accommodating them; the same is true for many influencing and key contributing factors that have been presented in this paper. Complexity and change in systems' characteristics are widely seen in global companies and organizations that operate on a diverse geographical scale. One example is McDonald's, which has many outlets worldwide. The products it offers depend on community traditions, and they appear on its website according to the users' location. As a result, McDonald's seeks to reach the largest possible segment by diversifying many aspects to its commercial applications or websites and by studying different societies and translating their requirements into technical requirements that can be implemented through various technical tools [55]. Thus, complexity helps to expand the characteristics of applications, which leads to an increase in the acceptance of diverse applications or systems by multisocieties, including commercial applications. To summarize, based on the sociotechnical systems approach, complexity is one of the

most important aspects in the success of commercial applications. This is due to complexity's ability in providing technical, specialized requirements for commercial applications, as well as the requirements that help target segments accept these applications in accordance with the vision and goal of M-commerce applications.

## 7. Conclusion

This study focused on identifying consumer requirements of commercial applications. Accurate user requirement analysis is important in the development of M-commerce applications that are accepted by current societies. This study focused on the analysis of consumer traditions and habits to determine the trends associated with acceptance of specific products, as well as the features that help consumers with effective decision-making ability. This study has shown the importance of identifying target population characteristics for widespread commercial application success which can be focused on in future studies.

Traditional characteristics and consumer habits represent important factors to understand increasing commercial application acceptance and use. This study identified important differences in consumer requirements among the communities that participated in the study. The differences in community requirements should be considered when designing applications for wider geographical areas. This study also identified similarities in many consumer indicators that help determine general M-commerce application requirements. The optional features that have been highlighted in the discussion section represent important functionality for specific communities that can help them be successful using smartphone commercial applications.

## Appendix

### A. Descriptive Statistics of All Indicators

This presents all indicators that have been conducted in the study. It includes the indicators that are related to content, interactive, assurance, appearance, organization, and customer-focus. The separate results have been included for KSA, UAE, and Qatar. The results also contained the mean, standard deviation (SD), and standard error (SE), as shown in Table 5.

### B. The High-Context Communication (HCC) and Low-Context Communication (LCC) Theory

These include five dimensions that are used to measure the differences between societies. The main parameters of HCC and LCC (animation, promotion of values, individuals separate or together with the product, level of transparency, and linear vs. parallel navigation on the website) are given in Table 6 [56–60].

## Data Availability

King Abdulaziz University has a warehouse facility which is designed to store important information for their researchers. The questionnaires' responses were stored directly in this data warehouse. The data is also stored in two further locations in online share folders that may be accessed by the readers from anywhere and at any time. The link for data is <https://drive.google.com/drive/folders/1xIOND3wTkZQ4Ykvwou4j7uSOgi0yLglh?usp=sharing>.

## Conflicts of Interest

The author declares no conflicts of interest.

## Acknowledgments

This project was funded by the Deanship of Scientific Research (DSR) at King Abdulaziz University, Jeddah, under Grant no. FP-145-43. The author, therefore, acknowledges the DSR's technical and financial support.

## Supplementary Materials

The supplementary material includes a questionnaire which represents one of the main research tools for this study. The questionnaire survey was carried out during 2019-2020, the period of the coronavirus pandemic. Various means of communication, such as e-mails and WhatsApp groups, and various methods of social distance were used for data gathering. s. (*Supplementary Materials*)

## References

- [1] eMarketer, "Smartphones, tablets spread across the Middle East and Africa," 2015, <http://www.emarketer.com/Article/Smartphones-Tablets-Spread-Across-Middle-East-Africa/1012989>.
- [2] A. A. Bahaddad, "Evaluating M-commerce systems success: measurement and validation of the DeLone and McLean model of IS success in Arabic society (GCC case study)," *Journal of Business Theory and Practice*, vol. 5, no. 3, p. 156, 2017a.
- [3] H. Khan, F. Talib, and M. N. Faisal, "An analysis of the barriers to the proliferation of M-commerce in Qatar," *Journal of Systems and Information Technology*, vol. 17, no. 1, pp. 54–81, 2015.
- [4] eMarketer, "Smartphones, mobile commerce roundup," 2015a, [https://www.emarketer.com/public\\_media/docs/eMarketer\\_Mobile\\_Commerce\\_Roundup.pdf](https://www.emarketer.com/public_media/docs/eMarketer_Mobile_Commerce_Roundup.pdf).
- [5] Statista, "Number of apps available in leading app stores as of July 2015," 2015, <http://www.statista.com/statistics/276623/number-of-apps-available-in-leading-app-stores/>.
- [6] Icfal, "eBay's Problems in China," 2008, <http://www.icmrindia.org/casestudies/catalogue/Business%20Strategy/BSTR278.htm>.
- [7] E. Würtz, "A cross-cultural analysis of websites from high-context cultures and low-context cultures," *Journal of Computer-Mediated Communication*, vol. 11, no. 1, pp. 1–23, 2005.
- [8] G. McLean, K. Osei-Frimpong, K. Al-Nabhani, and H. Marriott, "Examining consumer attitudes towards retailers' m-commerce mobile applications - an initial adoption vs. continuous use perspective," *Journal of Business Research*, vol. 106, pp. 139–157, 2020.
- [9] A. A. Bahaddad, "The role of community characteristics in determining target audiences in Arabic Gulf countries interested in online purchasing through commercial smartphone applications," *International Journal of Computer Application*, vol. 168, no. 2, 2017b.
- [10] D. Kumar and N. Goyal, "Security issues in M-commerce for online transaction," in *Proceedings of the 2016 5th International Conference on Reliability, Infocom Technologies and Optimization (Trends and Future Directions)(ICRITO)*, pp. 409–414, IEEE, Noida, India, September 2016.
- [11] L. Abbott, *What Is M-Commerce?*, 2001, <http://www.mobileinfo.com/Mcommerce/>.
- [12] R. S. Alotaibi, "Understanding customer loyalty of M-commerce applications in Saudi Arabia," *International Transaction Journal of Engineering, Management, & Applied Sciences & Technologies*, vol. 12, no. 6, pp. 1–12, 2021.
- [13] A. Salameh, S. Hassan, J. Alekam, and A. Alkafagi, "Assessing the effect of service quality and information quality on customers' overall perceived service quality in M-commerce," *Australian Journal of Basic and Applied Sciences the Effect of Service Quality and Information Quality*, 2015.
- [14] Y. AlQahtani, N. Beloff, and M. White, "A novel model of adoption of M-commerce in Saudi Arabia," *Position Papers of the 2020 Federated Conference on Computer Science and Information Systems*, vol. 22, pp. 25–34, 2020.
- [15] C. W. Hsu and C. C. Yeh, "Understanding the critical factors for successful M-commerce adoption," *International Journal of Mobile Communications*, vol. 16, no. 1, pp. 50–62, 2018.
- [16] A. Al-Naimat, M. A. Alnuaimi, A. M. Abdulaal, and M. Z. Almuqit, "Determinants of m-commerce usage in the Jordanian hospitality industry," *Journal of Theoretical and Applied Information Technology*, vol. 98, no. 23, pp. 3834–3842, 2020.
- [17] C. Ermiş, *Social Influencers in the Digital Environment: The Effect of Social media Influencer's Gender and Age on Credibility and purchase Intention*, Master's thesis, University of Twente, Enschede, Netherlands, 2021.
- [18] R. Gera, P. Chadha, and V. Ahuja, "Mobile shopping apps adoption: a systematic literature review," *International Journal of Electronic Business*, vol. 16, no. 3, pp. 239–261, 2021.
- [19] V. Venkatesh, V. Ramesh, and A. P. Massey, "Understanding usability in mobile commerce," *Communications of the ACM*, vol. 46, no. 12, pp. 53–56, 2003.
- [20] I. Bruschi and N. Rappel, "Exploring the acceptance of instant shopping—An empirical analysis of the determinants of user intention," *Journal of Retailing and Consumer Services*, vol. 54, Article ID 101936, 2020.
- [21] V. Marinković and Z. Kalinić, "Understanding consumers' continuance intention and word of mouth in mobile commerce based on extended UTAUT model," in *Impact of Mobile Services on Business Development and E-Commerce*, pp. 108–125, IGI Global, Pennsylvania, United States, 2020.
- [22] M. J. Noh and K. T. Lee, "An analysis of the relationship between quality and user acceptance in smartphone apps," *Information Systems and E-Business Management*, vol. 14, no. 2, pp. 273–291, 2015.
- [23] B. Taneja, *The Digital Edge for M-Commerce to Replace E-Commerce. In Emerging Challenges, Solutions, and Best Practices for Digital Enterprise Transformation*, IGI Global, Hershey, PA, USA, pp. 299–318, 2021.
- [24] S. Pandey and D. Chawla, "Exploring factors that drive adoption of various categories of m-commerce: an emerging

- market study,” *Global Business Review*, vol. 21, no. 2, pp. 526–546, 2020.
- [25] K. Im, K. Nam, and H. Cho, “Towards successful business model management with analytic network process-based feasibility evaluation and portfolio management,” *Electronic Markets*, vol. 30, no. 3, pp. 509–523, 2020.
- [26] A. Tarhini, A. A. Alalwan, A. B. Shammout, and A. Al-Badi, “An analysis of the factors affecting mobile commerce adoption in developing countries: towards an integrated model,” *Review of International Business and Strategy*, vol. 29, no. 3, 2019.
- [27] T. Iqbal, “Investigating logistics issues in service quality of SMEs in Saudi Arabia,” *Uncertain Supply Chain Management*, vol. 8, no. 4, pp. 875–886, 2020.
- [28] M. Legesse, *The Impact of mobile Banking Service Quality on Customers Satisfaction (The Case of Commercial Bank of Ethiopia in Selected branch*, Doctoral dissertation, St. Mary’s University, Twickenham, London, 2020.
- [29] N. S. Bhati, “Validation of customers’ perceived e-service quality determinants: a confirmatory factor analysis approach,” *International Journal of Services, Economics and Management*, vol. 11, no. 2, pp. 97–118, 2020.
- [30] M. Y. Alduaij, “An exploratory study of m-commerce key benefits and barriers among actual users, intentional users and non-intentional users,” *Innovation*, vol. 20, no. 3, pp. 260–276, 2018.
- [31] F. Talib and M. Faisal, “An analysis of the barriers to the proliferation of M-commerce in Qatar,” *Journal of Systems and Information Technology*, vol. 17, no. 1, pp. 54–81, 2015.
- [32] P. Zambonini, “Payments innovations and trends in the Gulf cooperation Council,” *Journal of Payments Strategy & Systems*, vol. 9, no. 1, pp. 59–78, 2015.
- [33] M. L. Tan, R. Prasanna, K. Stock, E. E. Doyle, G. Leonard, and D. Johnston, “Usability factors influencing the continuance intention of disaster apps: a mixed-methods study,” *International Journal of Disaster Risk Reduction*, vol. 50, Article ID 101874, 2020.
- [34] A. Macarthy, “500 social media marketing tips: essential advice, hints and strategy for business: facebook, twitter, pinterest, Google+, YouTube, instagram, LinkedIn, and mor,” 2021, <https://pdfroom.com/books/500-social-media-marketing-tips-essential-advice-hints-and-strategy-for-business-facebook-twitter-pinterest-google-youtube-instagram-linkedin-and-more/wW5mwnnwgyo>.
- [35] K. Pousttchi, D. Tilson, K. Lyytinen, and Y. Hufenbach, “Introduction to the special issue on mobile commerce: mobile commerce research yesterday, today, tomorrow-what remains to be done?” *International Journal of Electronic Commerce*, vol. 19, no. 4, pp. 1–20, 2015.
- [36] R. AlGhamdi, O. A. Alfarraj, and A. A. Bahaddad, “How retailers at different stages of Ecommerce maturity evaluate their entry to Ecommerce activities?” 2015, <https://arxiv.org/abs/1503.05172>.
- [37] M.-T. Lu, S.-K. Hu, L.-H. Huang, and G.-H. Tzeng, “Evaluating the implementation of business-to-business m-commerce by SMEs based on a new hybrid MADM model,” *Management Decision*, vol. 53, no. 2, pp. 290–317, 2015.
- [38] I. Mohamed and D. Patel, “Android vs iOS security: a comparative study,” in *Proceedings of the 2015 12th International Conference on Information Technology-New Generations (ITNG)*, pp. 725–730, IEEE, Las Vegas, NV, USA, April 2015.
- [39] C. Perri, C. Giglio, and V. Corvello, “Smart users for smart technologies: investigating the intention to adopt smart energy consumption behaviors,” *Technological Forecasting and Social Change*, vol. 155, Article ID 119991, 2020.
- [40] M. A. Salem and K. M. Nor, “The effect of COVID-19 on consumer behaviour in Saudi Arabia: switching from brick and mortar stores to E-Commerce,” *International Journal of Scientific & Technology Research*, vol. 9, no. 07, pp. 15–28, 2020.
- [41] M. Zheng, H. Xue, Y. Zhang, T. Wei, and J. C. Lui, “Enpublic apps: security threats using iOS enterprise and developer certificates,” in *Proceedings of the 10th ACM Symposium on Information, Computer and Communications Security*, pp. 463–474, ACM, New York, NY, United States, April 2015.
- [42] S. Sarkar, S. Chauhan, and A. Khare, “A meta-analysis of antecedents and consequences of trust in mobile commerce,” *International Journal of Information Management*, vol. 50, pp. 286–301, 2020.
- [43] I. U. Khan, Z. Hameed, S. N. Khan, S. U. Khan, and M. T. Khan, “Exploring the effects of culture on acceptance of online banking: a comparative study of Pakistan and Turkey by using the extended UTAUT model,” *Journal of Internet Commerce*, pp. 1–34, 2021.
- [44] P. Y. K. Chau, M. Cole, A. P. Massey, M. Montoya-Weiss, and R. M. O’Keefe, “Cultural differences in the online behavior of consumers,” *Communications of the ACM*, vol. 45, no. 10, pp. 138–143, 2002.
- [45] H. Alqahtani and M. Kavakli-Thorne, “Factors affecting acceptance of a mobile augmented reality application for cybersecurity awareness,” in *Proceedings of the 2020 4th International Conference on Virtual and Augmented Reality Simulations*, pp. 18–26, New York, NY, United States, February 2020.
- [46] J. W. Creswell, *Educational Research: Planning, Conducting, and Evaluating Quantitative and Qualitative Research*, Pearson/Merrill Prentice Hall, Hoboken, New Jersey, 2008.
- [47] Raosoft, “Sample size calculator,” 2021, <http://www.raosoft.com/samplesize.html>.
- [48] A. Field, *Discovering Statistics Using SPSS*, SAGE Publications, London, 2005.
- [49] W. H. DeLone and E. R. McLean, “Measuring e-commerce success: applying the DeLone & McLean information systems success model,” *International Journal of Electronic Commerce*, vol. 9, no. 1, pp. 31–47, 2004.
- [50] A. Bahaddad, R. AlGhamdi, S. M. Buhari, M. O. Alassafi, and A. Alzahrani, “A conceptual framework for successful E-commerce smartphone applications: the context of GCC,” 2019, <https://arxiv.org/abs/1908.06350>.
- [51] Alpen Capital, *GCC Retail Industry*, 2011, [http://www.alpencapital.com/downloads/GCC%20Retail%20Industry%20Report%202011\\_1%20November%202011.pdf](http://www.alpencapital.com/downloads/GCC%20Retail%20Industry%20Report%202011_1%20November%202011.pdf).
- [52] S. Omar, K. Mohsen, G. Tsimonis, A. Oozeerally, and J. H. Hsu, “M-commerce: the nexus between mobile shopping service quality and loyalty,” *Journal of Retailing and Consumer Services*, vol. 60, Article ID 102468, 2021.
- [53] A. Bahaddad, “Fundamental requirements for smartphone commercial applications development for Arabic societies: evidence from three Gulf cooperation Council states,” *International Journal of Computing Sciences Research*, vol. 1, no. 1, pp. 30–51, 2017c.
- [54] R. Agarwal and A. Mehrotra, “SEM approach to understanding m-commerce use in a developing country,” *International Journal of Business and Globalisation*, vol. 27, no. 3, pp. 403–423, 2021.
- [55] Y. H. Lee, “Study of GUI design appearing in fast food restaurant DID-focused on lotteria, McDonald’s, burger king

- and mom's touch," *Journal of the Korea Convergence Society*, vol. 10, no. 11, pp. 253–262, 2019, p.
- [56] Cdsi, "Statistical summary of teaching adm. & tec. Staff by agency-2010," 2016, [https://docs.google.com/viewerng/viewer?url=http://www.stats.gov.sa/sites/default/files/ar-edu0000-01-2014\\_0.xls](https://docs.google.com/viewerng/viewer?url=http://www.stats.gov.sa/sites/default/files/ar-edu0000-01-2014_0.xls).
- [57] I. Dumanska, L. Hrytsyna, O. Kharun, and O. Matviiets, "E-commerce and M-commerce as global trends of international trade caused by the covid-19 pandemic," *WSEAS Transactions on Environment and Development*, vol. 17, pp. 386–397, 2021.
- [58] S. Mouakket, "Investigating the role of mobile payment quality characteristics in the United Arab Emirates: implications for emerging economies," *International Journal of Bank Marketing*, vol. 38, no. 7, pp. 1465–1490, 2020.
- [59] QSAa, "Ministry of development planning and statistics – Statistics sector," 2015, <http://www.qsa.gov.qa/Eng/index.htm>.
- [60] Uae Statistics, "Federal competitiveness and statistics authority," 2016, <http://www.fcsa.gov.ae/Home/ReportDetails1/tabid/90/Default.aspx?ItemId=2399&PTID=129&MenuId=1>.



## Research Article

# Inferences for Generalized Pareto Distribution Based on Progressive First-Failure Censoring Scheme

Rashad M. El-Sagheer,<sup>1</sup> Taghreed M. Jawa,<sup>2</sup> and Neveen Sayed-Ahmed <sup>2</sup>

<sup>1</sup>Mathematics Department, Faculty of Science, Al-Azhar University, Nasr City 11884, Cairo, Egypt

<sup>2</sup>Department of Mathematics and Statistics, College of Science, P.O. Box 11099, Taif University, Taif 21944, Saudi Arabia

Correspondence should be addressed to Neveen Sayed-Ahmed; nevensayd@yahoo.com

Received 22 October 2021; Accepted 15 November 2021; Published 7 December 2021

Academic Editor: Sameh S. Askar

Copyright © 2021 Rashad M. El-Sagheer et al. This is an open access article distributed under the Creative Commons Attribution License, which permits unrestricted use, distribution, and reproduction in any medium, provided the original work is properly cited.

In this article, we consider estimation of the parameters of a generalized Pareto distribution and some lifetime indices such as those relating to reliability and hazard rate functions when the failure data are progressive first-failure censored. Both classical and Bayesian techniques are obtained. In the Bayesian framework, the point estimations of unknown parameters under both symmetric and asymmetric loss functions are discussed, after having been estimated using the conjugate gamma and discrete priors for the shape and scale parameters, respectively. In addition, both exact and approximate confidence intervals as well as the exact confidence region for the estimators are constructed. A practical example using a simulated data set is analyzed. Finally, the performance of Bayes estimates is compared with that of maximum likelihood estimates through a Monte Carlo simulation study.

## 1. Introduction

In life testing and reliability analysis, some units can be lost or withdrawn from the experiment before failure occurs. One of the major reasons for removal of the experimental units is to save the working experimental units for future use, thereby conserving the cost and time associated with testing. This leads us to use the censoring schemes. The type-II censoring can be considered a common type of censored scheme. Many authors have studied the statistical inference for different probability distributions using progressive type-II censoring, including Balakrishnan and Sandhu [1, 2], Cohen [3], Mann [4], Ng [5], Balakrishnan et al. [6], Gibbons and Vance [7], Yuen and Tse [8], Ng et al. [9], Balakrishnan [10], Soliman [11, 12], Madi and Raqab [13], Mahmoud et al. [14], Mahmoud et al. [15], Soliman et al. [16], El-Sagheer [17–19], Mahmoud et al. [20], El-Sagheer and Hasaballah [21], El-Sagheer et al. [22], and Soliman et al. [23]. Recently, Zhang and Gui [24] studied the statistical inference for the lifetime performance index of Pareto distribution based on progressive type-II censored sample.

On the other hand, Viveros and Balakrishnan [25] have described a life test in which the experimenter can decide to divide the items being tested into several groups and then run all the items at the same time until occurrence of the first failure in each group. Such a censoring scheme is called first-failure censoring. For more details about statistical inference using first-failure censoring, it is recommended that the reader refers to Wu and Yu [26], Wu et al. [27], Lee et al. [28], and Wu et al. [29]. However, using this censoring scheme does not enable the experimenter to remove experimental units from the test until the first failure is observed. For this reason, Wu and Kuş [30] introduced a life testing scheme, which combines first-failure censoring with a progressive type-II censoring called a progressive first-failure censoring (Pro-F-F-C) scheme. Many previous studies have discussed inference under a Pro-F-F-C scheme for different lifetime distributions, for example, Weibull by Wu and Kuş [30], Burr Type XII by Soliman et al. [31, 32], Gompertz by Soliman et al. [33], Lomax by Mahmoud et al. [34], Compound Rayleigh by Abushal [35], Generalized Inverted Exponential by Ahmed [36], the Mixture of Weibull and Lomax

by Mahmoud et al. [37], and exponentiated Frechet by Soliman et al. [38]. Recently, Cai and Gui [39] discussed the classical and Bayesian inference for a Pro-F-F-C left-truncated normal distribution.

Generalized Pareto distribution (GPD) is a significant continuous lifetime distribution. It plays a key role in statistical inference studies and reliability problems. It is also well known for being a distribution that has decreasing failure rate property. The pdf and cdf of a random variable  $X$  have a GPD given, respectively, as

$$f_X(x; \alpha, \beta) = \alpha\beta^\alpha (x + \beta)^{-(\alpha+1)}, x > 0, \alpha, \beta > 0, \quad (1)$$

$$F_X(x; \alpha, \beta) = 1 - \beta^\alpha (x + \beta)^{-\alpha}, x > 0, \alpha, \beta > 0, \quad (2)$$

where  $\alpha$  and  $\beta$  are the shape and scale parameters, respectively. The survival and hazard rate functions of GPD at mission time  $t$  are given by the following expressions:

$$s(t) = \beta^\alpha (t + \beta)^{-\alpha}, t > 0, \quad (3)$$

$$h(t) = \alpha (t + \beta)^{-1}, t > 0. \quad (4)$$

For more details about GPD, its properties, and applications, see Kremer [40]. In this article, we obtain the Bayes estimates and MLEs for the unknown quantities of the GPD using a Pro-F-F-C scheme. The approximate confidence intervals (ACIs) for  $\alpha$  and  $\beta$  are constructed based on the asymptotic normality of MLEs. In the Bayesian framework, the point estimates of unknown parameters under squared error (SE), linear-exponential (LINEX), and general entropy (GE) showing loss functions are discussed. The process is done using the conjugate gamma prior for the shape parameter and discrete prior for the scale parameter  $\beta$ . The exact confidence interval and exact confidence region for the estimators are then derived. To evaluate and compare the performance of these proposed inference procedures, a simulation study with different parameter values is undertaken. Additionally, a numerical example using simulated data set is studied to show the practicality and usefulness of these proposed methods.

The rest of the paper is arranged as follows. Section 2 deals with the classical method of estimation. Bayes estimators relative to different loss functions are considered in Section 3. In Section 4, the ACIs, exact confidence intervals, and exact confidence regions for the parameters are discussed. In Section 5, the proposed procedures obtained in the previous sections are investigated using simulated data. A simulation study is conducted to compare the proposed procedures in Section 6. Finally, a conclusion is provided in Section 7.

## 2. Maximum Likelihood Estimation

Let  $x_i = x_{i:m:n:k}^R$ ,  $i = 1, 2, \dots, m$ , be a Pro-F-F-C order statistics from the GPD with the progressive censoring scheme  $R = (R_1, R_2, \dots, R_m)$ . According to Wu and Kuş [30], the joint probability density function can be written as

$$f_{1,2,\dots,m}(x_{1:m:n:k}^R, \dots, x_{m:m:n:k}^R) \propto k^m \prod_{j=1}^m f(x_{j:m:n:k}^R) \quad (5)$$

$$(1 - F(x_{j:m:n:k}^R))^{k(R_j+1)-1}.$$

From (1), (2), and (5), the likelihood function  $L(\underline{x}; \alpha, \beta)$  is given by

$$L(\underline{x}; \alpha, \beta) \propto k^m \alpha^m \prod_{i=1}^m \beta^{\alpha k(R_i+1)} (x_i + \beta)^{-(\alpha k(R_i+1)+1)}. \quad (6)$$

Thus, the log-likelihood function  $\ell(\underline{x}; \alpha, \beta)$  is

$$\ell(\underline{x}; \alpha, \beta) \propto m \log k + m \log \alpha + \sum_{i=1}^m \alpha k(R_i + 1) \log \beta \quad (7)$$

$$- \sum_{i=1}^m (\alpha k(R_i + 1) + 1) \log(x_i + \beta).$$

By equating each result of the first-order derivatives of log-likelihood function with respect to  $\alpha$  and  $\beta$ , to zero, we obtain

$$\frac{\partial \ell(\underline{x}; \alpha, \beta)}{\partial \alpha} = \frac{m}{\alpha} + \sum_{i=1}^m k(R_i + 1) \log \beta \quad (8)$$

$$- \sum_{i=1}^m k(R_i + 1) \log(x_i + \beta) = 0,$$

$$\frac{\partial \ell(\underline{x}; \alpha, \beta)}{\partial \beta} = \sum_{i=1}^m \frac{\alpha k(R_i + 1)}{\beta} - \sum_{i=1}^m \frac{(\alpha k(R_i + 1) + 1)}{(x_i + \beta)} = 0. \quad (9)$$

Hence,

$$\hat{\alpha} = m \left( \sum_{i=1}^m k(R_i + 1) \log(x_i + \hat{\beta}) - \sum_{i=1}^m k(R_i + 1) \log \hat{\beta} \right)^{-1}, \quad (10)$$

and  $\hat{\beta}$  the solution of

$$\sum_{i=1}^m \frac{\hat{\alpha} k(R_i + 1)}{\hat{\beta}} - \sum_{i=1}^m \frac{(\hat{\alpha} k(R_i + 1) + 1)}{(x_i + \hat{\beta})} = 0. \quad (11)$$

Since there is no closed form of the solution to the above equations, the Newton-Raphson method (NRM) is widely used to obtain the desired MLEs in such situations. Once MLEs of  $\alpha$  and  $\beta$  are obtained, the MLEs of  $s(t)$  and  $h(t)$  for given  $t$  can be obtained by the invariant property of the MLEs as

$$\hat{s}(t) = \hat{\beta}^{\hat{\alpha}} (t + \hat{\beta})^{-\hat{\alpha}}, t > 0, \quad (12)$$

$$\hat{h}(t) = \hat{\alpha} (t + \hat{\beta})^{-1}, t > 0. \quad (13)$$

## 3. Bayesian Estimation

Bayes estimation is quite different from the MLE method because it takes into consideration both the information from observed sample data and the prior information. Bayes'

theorem is completely dependent on the parameter estimation through calculation of the posterior distribution. As calculating the posterior distribution is conditional on the data, this requires explicit specification of the prior distribution model parameters. Furthermore, in order to gain the best estimate of the unknown parameter, it is necessary to determine the appropriate loss functions.

The next step is to take into account different loss functions. First, we consider the square error (SE) loss function which is widely used in the literature. Because of the symmetry nature of this function, it gives equal weight to overestimation as well as underestimation. Under SE, the Bayesian estimate (BE) of any function of parameters, say  $\psi(\Theta) = u(\alpha, \beta, s, h)$ , is the unconditional posterior mean which is given as

$$\hat{\psi}_{BS}(\Theta) = E(\psi(\Theta)) = \int_{\Theta} \psi(\Theta) \pi^*(\Theta) d\Theta. \quad (14)$$

However, in many situations, the parameter may be overestimated or show serious consequences of underestimation, or vice versa. In such cases, an asymmetric loss function, which associates greater importance to overestimation or underestimation, can be taken into consideration for parameters estimation. A beneficial asymmetric loss function is the LINEX loss as follows:

$$L_{LINEX}(\hat{\psi}(\Theta), \psi(\Theta)) = e^{a(\hat{\psi}(\Theta) - \psi(\Theta))} - a(\hat{\psi}(\Theta) - \psi(\Theta)) - 1, \quad (15)$$

where  $a$  is a shape parameter whose sign refers to the direction and its magnitude represents the degree of symmetry. Moreover, for  $a$  figure close to zero, the LINEX loss more or less becomes a SE loss. Thus, the BE of  $\psi(\Theta)$  under this loss function is given by

$$\begin{aligned} \hat{\psi}_{BL}(\Theta) &= -\frac{1}{a} \log \left[ E(e^{-a\psi(\Theta)}) \right] \\ &= -\frac{1}{a} \log \int_{\Theta} e^{-a\psi(\Theta)} \pi^*(\Theta) d\Theta. \end{aligned} \quad (16)$$

Next, we consider the GE loss function as follows:

$$L_{GE}(\hat{\psi}(\Theta), \psi(\Theta)) = \left( \frac{\hat{\psi}(\Theta)}{\psi(\Theta)} \right)^q - q \log \left( \frac{\hat{\psi}(\Theta)}{\psi(\Theta)} \right) - 1, \quad (17)$$

where  $q$  is a shape parameter which represents departure from symmetry. Subsequently, based on the GE loss functions, the BE of  $\psi(\Theta)$  is obtained as

$$\hat{\psi}_{BG}(\Theta) = [E(\psi(\Theta)^{-q})]^{-1/q} = \left[ \int_{\Theta} (\psi(\Theta)^{-q}) \pi^*(\Theta) d\Theta \right]^{-1/q}. \quad (18)$$

It is remarked that for  $q = -1$ , the BE of  $\psi(\Theta)$  concurs with the BE under SE loss function.

**3.1. Posterior Analysis.** In this subsection, we consider that the parameter  $\beta$  a discrete prior and  $\alpha$  has a conjugate gamma prior. Suppose that  $\beta = \beta_j$ ,  $j = 1, 2, \dots, N$ , then

$$\pi(\beta) = \Pr(\beta = \beta_j) = \eta_j, \quad (19)$$

where  $0 \leq \eta_j \leq 1$  and  $\sum_{j=1}^N \eta_j = 1$ . Further,  $\alpha$  has

$$\pi(\alpha | \beta = \beta_j) = \frac{a_j^{b_j}}{\Gamma(b_j)} \alpha^{b_j-1} \exp(-a_j \alpha), \quad \alpha, a_j, b_j > 0. \quad (20)$$

Then, the posterior distribution of  $\alpha$  takes the form as follows:

$$\pi^*(\alpha | \beta = \beta_j; T_j) = \frac{(T_j + a_j)^{(b_j+m)}}{\Gamma(b_j + m)} \alpha^{b_j+m-1} \exp(-\alpha(T_j + a_j)), \quad (21)$$

where

$$T_j = \sum_{i=1}^m k(R_i + 1) [\log(x_i + \beta_j) - \log \beta_j]. \quad (22)$$

The joint posterior of  $\alpha$  and  $\beta_j$  using (6), (19), and (20) is

$$\pi^*(\alpha, \beta = \beta_j; T_j) = \frac{a_j^{b_j} v_j \eta_j}{k_2 \Gamma(b_j)} \alpha^{b_j+m-1} \exp(-\alpha(T_j + a_j)), \quad (23)$$

where

$$k_2 = \sum_{j=1}^N \frac{a_j^{b_j} v_j \eta_j \Gamma(b_j + m)}{\Gamma(b_j) (T_j + a_j)^{(b_j+m)},} \quad (24)$$

$$v_j = \prod_{i=1}^m (x_i + \beta_j)^{-1}.$$

By using the Bayes theorem for discrete variables, the marginal posterior probability of  $\beta$  is

$$P_j = \Pr(\beta = \beta_j | T_j) = \frac{a_j^{b_j} v_j \eta_j \Gamma(b_j + m)}{k_2 \Gamma(b_j) (T_j + a_j)^{(b_j+m)},} \quad (25)$$

where  $k_2$  and  $v_j$  are given in (24); the marginal posterior probability of  $\alpha$  is

$$\pi^*(\alpha | T_j) = \sum_{j=1}^m \pi^*(\alpha | \beta = \beta_j, T_j). \quad (26)$$

**3.2. BE under SE Loss.** In this subsection, we obtain the BE of  $\alpha$ ,  $\beta$ ,  $s(t)$ , and  $h(t)$  under SE loss function. By using (14), (21), and (25), the BEs  $\tilde{\alpha}_{BS}$ ,  $\tilde{\beta}_{BS}$ ,  $\tilde{s}_{BS}(t)$ , and  $\tilde{h}_{BS}(t)$  are given by

$$\tilde{\alpha}_{BS} = \int_0^\infty \sum_{j=1}^N \alpha P_j \pi^*(\alpha | \beta = \beta_j, T_j) d\alpha = \sum_{j=1}^N P_j \frac{(b_j + m)}{(T_j + a_j)}, \tilde{\beta}_{BS} = E_\beta(\beta | \underline{x}) = \sum_{j=1}^N \beta_j P_j, \tilde{s}_{BS}(t) = \sum_{j=1}^N P_j \left[ 1 + \frac{\log(1 + (t/\beta_j))}{(T_j + a_j)} \right]^{(b_j+m)}, \quad (27)$$

$$\tilde{h}_{BS}(t) = \sum_{j=1}^N \frac{P_j (b_j + m)}{(t + \beta_j)(T_j + a_j)}. \quad (28)$$

3.3. *BE under LINEX Loss.* Based on (16), (21), and (25), the BEs  $\tilde{\beta}_{BL}$ ,  $\tilde{\alpha}_{BL}$ ,  $\tilde{s}_{BL}(t)$ , and  $\tilde{h}_{BL}(t)$  are

$$\begin{aligned} \tilde{\beta}_{BL} &= -\frac{1}{a} \log \left[ \sum_{j=1}^N P_j \exp(-a\beta_j) \right], \\ \tilde{\alpha}_{BL} &= -\frac{1}{a} \log \left[ \sum_{j=1}^N P_j \left( 1 + \frac{a}{(T_j + a_j)} \right)^{-(b_j+m)} \right], \\ \tilde{s}_{BL}(t) &= -\frac{1}{a} \log \left[ \sum_{j=1}^N \sum_{\epsilon=1}^{\infty} \frac{(-a)^\epsilon}{\epsilon!} P_j \left( 1 + \frac{\epsilon \log(1 + t/\beta_j)}{(T_j + a_j)} \right)^{-(b_j+m)} \right], \end{aligned} \quad (29)$$

$$\tilde{h}_{BL}(t) = -\frac{1}{a} \log \left[ \sum_{j=1}^N P_j \left( 1 + \frac{a}{(t + \beta_j)(T_j + a_j)} \right)^{-(b_j+m)} \right]. \quad (30)$$

3.4. *BE under GE Loss.* From (18), (21), and (25), the BEs  $\tilde{\beta}_{BG}$ ,  $\tilde{\alpha}_{BG}$ ,  $\tilde{s}_{BG}(t)$ , and  $\tilde{h}_{BG}(t)$  are, respectively,

$$\begin{aligned} \tilde{\beta}_{BG} &= \left[ \sum_{j=1}^N \beta_j^{-q} P_j \right]^{(-1/q)}, \\ \tilde{\alpha}_{BG} &= \left[ \sum_{j=1}^N P_j \frac{(T_j + a_j)^q \Gamma(b_j + m - q)}{\Gamma(b_j + m)} \right]^{(-1/q)}, \\ \tilde{s}_{BG}(t) &= \left[ \sum_{j=1}^N P_j \left( 1 - \frac{q \log(1 + (t/\beta_j))}{(T_j + a_j)} \right)^{-(b_j+m)} \right]^{(-1/q)}, \\ \tilde{h}_{BG}(t) &= \left[ \sum_{j=1}^N P_j (t + \beta_j)^q \times \frac{(T_j + a_j)^q \Gamma(b_j + m - q)}{\Gamma(b_j + m)} \right]^{(-1/q)}. \end{aligned} \quad (31)$$

$$\tilde{h}_{BG}(t) = \left[ \sum_{j=1}^N P_j (t + \beta_j)^q \times \frac{(T_j + a_j)^q \Gamma(b_j + m - q)}{\Gamma(b_j + m)} \right]^{(-1/q)}. \quad (32)$$

To perform the calculations in these subsections, the values of  $a_j$  and  $b_j$  must be found in (20). We use the prior expectation of  $s(t)$  conditional on  $\beta = \beta_j$ . Thus, from (3) and (20), we get

$$E[s(t) | \beta_j] = \left( 1 + \frac{\log(1 + (t/\beta_j))}{a_j} \right)^{b_j}. \quad (33)$$

## 4. Interval Estimation

This section deals with ACIs, exact CIs, and exact confidence regions for the parameters  $\alpha$  and  $\beta$  of GPD based on Pro-F-F-C.

4.1. *Asymptotic Confidence Intervals.* The asymptotic normality of the MLEs can be used to construct ACIs for parameters  $\alpha$  and  $\beta$  by using Fisher information matrix (FIM). The FIM can be written as  $I = (I_{ij})$  where

$$I_{ij} = E \left[ \frac{-\partial^2 \ell(\Phi)}{\partial \phi_i \partial \phi_j} \right], \quad i, j = 1, 2, \quad (34)$$

where  $\Phi = (\phi_1, \phi_2) = (\alpha, \beta)$ . The asymptotic variance-covariance matrix of the parameters  $\alpha$  and  $\beta$  can be obtained by inverting the observed FIM  $I_{ij}$  as follows:

$$I^{-1}(\hat{\alpha}, \hat{\beta}) = \begin{bmatrix} \frac{\partial^2 \ell}{\partial \alpha^2} & \frac{\partial^2 \ell}{\partial \alpha \partial \beta} \\ \frac{\partial^2 \ell}{\partial \beta \partial \alpha} & \frac{\partial^2 \ell}{\partial \beta^2} \end{bmatrix}_{(\hat{\alpha}, \hat{\beta})}^{-1} = \begin{bmatrix} \text{var}(\hat{\alpha}) & \text{cov}(\hat{\alpha}, \hat{\beta}) \\ \text{cov}(\hat{\beta}, \hat{\alpha}) & \text{var}(\hat{\beta}) \end{bmatrix}, \quad (35)$$

with

$$\begin{aligned} \frac{\partial^2 \ell}{\partial \alpha^2} &= -\frac{m}{\alpha^2}, \\ \frac{\partial^2 \ell}{\partial \alpha \partial \beta} &= \frac{\partial^2 \ell}{\partial \beta \partial \alpha} = \sum_{i=1}^m \frac{k(R_i + 1)}{\beta} - \sum_{i=1}^m \frac{k(R_i + 1)}{(x_i + \beta)}, \\ \frac{\partial^2 \ell}{\partial \beta^2} &= \sum_{i=1}^m \frac{\alpha k(R_i + 1) + 1}{(x_i + \beta)^2} - \sum_{i=1}^m \frac{\alpha k(R_i + 1)}{\beta^2}. \end{aligned} \quad (36)$$

$$\frac{\partial^2 \ell}{\partial \beta^2} = \sum_{i=1}^m \frac{\alpha k(R_i + 1) + 1}{(x_i + \beta)^2} - \sum_{i=1}^m \frac{\alpha k(R_i + 1)}{\beta^2}. \quad (37)$$

Thus,

$$(\hat{\alpha}, \hat{\beta}) \sim N((\alpha, \beta), I_0^{-1}(\hat{\alpha}, \hat{\beta})). \quad (38)$$

The  $(1 - \delta)100\%$  ACIs for  $\alpha$  and  $\beta$  become

$$\begin{aligned} & (\hat{\alpha} - Z_{\delta/2} \sqrt{\text{var}(\hat{\alpha})}, \hat{\alpha} + Z_{\delta/2} \sqrt{\text{var}(\hat{\alpha})}), \\ & \cdot (\hat{\beta} - Z_{\delta/2} \sqrt{\text{var}(\hat{\beta})}, \hat{\beta} + Z_{\delta/2} \sqrt{\text{var}(\hat{\beta})}), \end{aligned} \quad (39)$$

where  $z_\delta$  is 100(1- $\delta$ )th upper percentile of standard normal variate  $N(0, 1)$ .

**4.2. Exact Confidence Intervals.** Let  $x_{1:m:n:k}^R < x_{2:m:n:k}^R < \dots < x_{m:m:n:k}^R$  denote a Pro-F-F-C sample from GPD with parameters  $\alpha$  and  $\beta$ , and let

$$\begin{cases} W_1 = nU_{1:m:n:k}^R \\ W_2 = (n - R_1 - 1)(U_{2:m:n:k}^R - U_{1:m:n:k}^R) \\ W_3 = (n - R_1 - R_2 - 2)(U_{3:m:n:k}^R - U_{2:m:n:k}^R) \\ \vdots \\ W_m = (n - R_1 - \dots - R_{m-1} - m + 1)(U_{m:m:n:k}^R - U_{m-1:m:n:k}^R). \end{cases} \quad (41)$$

According to Thomas and Wilson [41], the generalized spacings  $W_1, W_2, \dots, W_m$  are *iid* as standard ED; hence,

$$\zeta_j = 2 \sum_{i=1}^j W_i, \quad (42)$$

has  $X^2(2j)$ , and

$$\begin{aligned} \xi_j &= \frac{\psi_j / (2(m-j))}{\zeta_j / 2j} = \frac{j}{(m-j)} \cdot \frac{2 \sum_{i=j+1}^m W_i}{2 \sum_{i=1}^j W_i} \\ &= \frac{j}{(m-j)} \cdot \frac{(R_1 + R_2 + \dots + R_j + j - n) + \sum_{i=j+1}^m (R_i + 1) \log(1 + (x_{i:m:n:k}^R / \beta)) / \log(1 + (x_{j:m:n:k}^R / \beta))}{(n - R_1 - R_2 - \dots - R_{j-1} - j + 1) + \sum_{i=1}^{j-1} (R_i + 1) \log(1 + (x_{i:m:n:k}^R / \beta)) / \log(1 + (x_{j:m:n:k}^R / \beta))}, \quad j = 1, 2, \dots, m-1, \end{aligned} \quad (44)$$

$$\begin{aligned} \eta &= (\psi_j + \zeta_j) = 2 \sum_{i=1}^m W_i = 2 \sum_{i=1}^m (R_i + 1) U_{i:m:n:k}^R \\ &= 2k\alpha \sum_{i=1}^m (R_i + 1) \log\left(1 + \frac{x_{i:m:n:k}^R}{\beta}\right). \end{aligned} \quad (45)$$

It can be easily shown that  $\xi_j \sim F(2(m-j), 2j)$  where  $j = 1, 2, \dots, m-1$ ,  $m > 1$ , and  $\eta \sim X^2(2m)$ . Also,  $\xi_j$  and  $\eta$  are independent. To construct an exact confidence interval for  $\beta$  and exact joint confidence region for  $\beta$  and  $\alpha$ , we need to analyze the following two lemmas.

**Lemma 1.** For any positive real numbers  $b > a > 0$ ,  $q(\gamma) = \ln(1 + b^\gamma) / \ln(1 + a^\gamma)$  is a strictly increasing function of  $\gamma$ , where  $\gamma > 0$ .

$$U_{i:m:n:k}^R = k\alpha \log\left(1 + \frac{x_{i:m:n:k}^R}{\beta}\right), \quad i = 1, 2, \dots, m. \quad (40)$$

It is remarked that  $U_{1:m:n:k}^R < U_{2:m:n:k}^R < \dots < U_{m:m:n:k}^R$  is a progressively censored sample of exponential distribution (ED) with mean 1. Let us assume the following:

$$\psi_j = 2 \sum_{i=j+1}^m W_i, \quad (43)$$

has  $X^2(2(m-j))$ . To construct the confidence intervals for  $\alpha$  and  $\beta$ , we consider pivotal quantities:

**Lemma 2.** For a given set of observations  $0 < x_{1:m:n:k}^R < x_{2:m:n:k}^R < \dots < x_{m:m:n:k}^R < \infty$ , the function  $\xi_j$  is a strictly increasing function of  $\beta$  when  $\beta > 0$ . Furthermore,

- (I) For  $x_{m-1:m:n:k}^R \leq 1$ , there is a unique solution for the given equation  $\xi_j = t$ , where  $t > 0$ .
- (II) Let  $x_{0:m:n:k}^R = 0$ . For  $x_{1:m:n:k}^R \leq 1 < x_{l+1:m:n:k}^R$ , there is a unique solution for the given equation  $\xi_j = t$  where

$$0 < t < \frac{j}{(m-j)} \frac{\sum_{i=j+1}^m (R_i + 1) \log(x_{i:m:n:k}^R) - (n - R_1 - R_2 - \dots - R_j - j) \log(x_{j:m:n:k}^R)}{(n - R_1 - R_2 - \dots - R_{j-1} - j + 1) \log(x_{j:m:n:k}^R) + \sum_{i=l+1}^{j-1} (R_i + 1) \log(x_{i:m:n:k}^R)}, \quad (46)$$

for  $l = 0, 1, \dots, j-1$  and  $j = 1, 2, \dots, m-1$ . Using the same arguments and notations in Wu et al. [42], Lemma 1 and Lemma 2 can be proved.

**4.3. Exact Confidence Interval for  $\beta$ .** Suppose that  $x_{i,m,n,k}^R$ ,  $i = 1, 2, \dots, m$ , denote a Pro-F-F-C sample from GPD  $(\alpha, \beta)$ , with censoring scheme  $(R_1, R_2, \dots, R_m)$ . For any  $0 < \delta < 1$ , a  $100(1 - \delta)\%$  confidence interval for  $\beta$  is as follows. We know that  $\xi_j \sim F_{(2(m-j), 2j)}$  by Lemma 1 and Lemma 2  $\xi_j$  strictly increases in  $\beta$  when  $\beta > 0$ , where

- (1) For  $x_{m-1:m:n:k}^R \leq 1$ , there is a unique solution for the given equation  $\xi_j = t$ , where  $t > 0$ .

- (2) Let  $x_{0:m:n:k}^R = 0$ . For  $x_{l:m:n:k}^R \leq 1 < x_{l+1:m:n:k}^R$ , there is a unique solution for the equation  $\xi_j = t$ .

Hence, for  $0 < \delta < 1$ , from (44), we obtain

$$F_{1-\frac{\delta}{2}}(2(m-j), 2j) < \xi_j < F_{\frac{\delta}{2}}(2(m-j), 2j). \quad (47)$$

Thus, a  $100(1 - \delta)\%$  confidence interval for  $\beta$  is

$$\left( \Phi(X^R, F_{1-\delta/2(2(m-j), 2j)}) < \beta < \Phi(X^R, F_{\delta/2(2(m-j), 2j)}) \right), \quad (48)$$

where  $X^R = (X_{1:m:n:k}^R, X_{2:m:n:k}^R, \dots, X_{m:m:n:k}^R)$  and  $\Phi(X^R, t)$  is the solution for  $\beta$  for the equation:

$$\frac{(R_1 + R_2 + \dots + R_j + j - n) + \sum_{i=j+1}^m (R_i + 1) \log(1 + x_{i:m:n:k}^R/\beta) / \log(1 + x_{j:m:n:k}^R/\beta)}{(n - R_1 - R_2 - \dots - R_{j-1} - j + 1) + \sum_{i=1}^{j-1} (R_i + 1) \log(1 + x_{i:m:n:k}^R/\beta) / \log(1 + x_{j:m:n:k}^R/\beta)} = \frac{t(m-j)}{j}. \quad (49)$$

**4.4. Exact Confidence Region for  $\beta$  and  $\alpha$ .** By the same way, from (45), it is clear that

$$\eta = 2k\alpha \sum_{i=1}^m (R_i + 1) \log\left(1 + \frac{x_{i:m:n:k}^R}{\beta}\right), \quad (50)$$

where  $\eta \sim X^2(2m)$ . For  $0 < \delta < 1$ , we have

$$P\left(F_{(1+\sqrt{1-\delta}/2)(2(m-j), 2j)} < \xi_j < F_{1-\sqrt{1-\delta}/2(2(m-j), 2j)}\right) = \sqrt{1-\delta}, \quad (51)$$

$$P\left(\chi_{1+\sqrt{1-\delta}/2(2m)}^2 < \eta < \chi_{1-\sqrt{1-\delta}/2(2m)}^2\right) = \sqrt{1-\delta}. \quad (52)$$

Then, we obtain

$$P\left(F_{1+\sqrt{1-\delta}/2(2(m-j), 2j)} < \xi_j < F_{1-\sqrt{1-\delta}/2(2(m-j), 2j)}\right), \quad (53)$$

$$\chi_{1+\sqrt{1-\delta}/2(2m)}^2 < \eta < \chi_{1-\sqrt{1-\delta}/2(2m)}^2 = 1 - \delta.$$

This is equivalent to

$$P\left(\Phi(X^R, F_{1+\sqrt{1-\delta}/2(2(m-j), 2j)}) < \beta < \Phi(X^R, F_{1-\sqrt{1-\delta}/2(2(m-j), 2j)}), \frac{\chi_{1+\sqrt{1-\delta}/2(2m)}^2}{2k \sum_{i=1}^m (R_i + 1) \log(1 + x_{i:m:n:k}^R/\beta)}\right) < \alpha < \frac{\chi_{1-\sqrt{1-\delta}/2(2m)}^2}{2k \sum_{i=1}^m (R_i + 1) \log(1 + x_{i:m:n:k}^R/\beta)} = 1 - \delta. \quad (54)$$

## 5. Numerical Computations

Consider a Pro-F-F-C sample generated from GPD showing  $\alpha = 0.3$  and  $\beta = 1.5$ . The data consist of 120 observations, grouped into  $n = 30$  sets, with 4 items within each group ( $k = 4$ ). The Pro-F-F-C sample of size 10 out of 30 groups with the corresponding censoring scheme  $R$  is given in Table 1. The MLEs of  $\alpha$  and  $\beta$  using NRM are computed, and then both  $s(t)$  and  $h(t)$  are calculated at  $t = 0.451$ .

To compute the BEs, we first estimate two values of  $s(t)$  using a nonparametric procedure  $s(t_i = x_{i,m,n,k}^R) = m - i + 0.625/m + 0.25$ ,  $i = 1, 2, \dots, m$ . Using the available data, we

obtained  $s(t_1 = 0.1694) = 0.7439$  and  $s(t_2 = 4.8110) = 0.1585$ . These two priors are substituted into (33), where  $a_j$  and  $b_j$  are obtained numerically for each given  $\beta_j$ , and  $\eta_j$ ,  $j = 1, 2, \dots, 10$ , using the NRM. Table 2 displays the values of  $a_j$ ,  $b_j$ , and  $P_j$  for each given  $\beta_j$  and  $\eta_j$ . The results of MLE and BE for  $\alpha$ ,  $\beta$ ,  $s(t)$ , and  $h(t)$  are presented in Table 3. By using (45), the 95% ACIs of  $\alpha$  and  $\beta$  are  $(0, 0.7068)$  and  $(0, 4.4543)$ . For  $j = 2$ , we need the percentiles  $F_{0.025}(18, 2) = 0.2193$  and  $F_{0.975}(18, 2) = 39.4424$  to construct the 95% CI for  $\beta$ . According to (44), the 95% exact confidence interval of  $\beta$  is calculated as  $(0.2193, 7.9943)$ . For the given  $F_{0.0127}(18, 2) = 0.1780$ ,  $F_{0.9873}(18, 2) = 78.1835$ ,  $\chi_{(0.0127)(20)}^2 =$

TABLE 1: Simulated Pro-F-F-C.

$i$	1	2	3	4	5	6	7	8	9	10
$R_i$	10	0	1	1	5	1	1	1	0	0
$x_i^R$	0.0781	0.1582	0.1694	0.2040	0.3066	0.4909	0.8912	1.0705	4.811	14.123

TABLE 2: The hyperparameter values.

$j$	1	2	3	4	5	6	7	8	9	10
$\eta_j$	0.1	0.1	0.1	0.1	0.1	0.1	0.1	0.1	0.1	0.1
$\beta_j$	1.0	1.1	1.2	1.3	1.4	1.5	1.6	1.7	1.8	1.9
$a_j$	0.6995	0.5966	0.5184	0.4571	0.4087	0.3684	0.3349	0.3066	0.2824	0.2615
$b_j$	1.4647	1.3743	1.3054	1.2457	1.1976	1.1574	1.1237	1.0938	1.0664	1.0434
$P_j$	0.1059	0.1058	0.1085	0.1052	0.1041	0.1023	0.0997	0.0961	0.0921	0.0857

TABLE 3: The MLEs and BEs of  $\alpha, \beta, s(t)$ , and  $h(t)$  where  $s(0.450) = 0.9243$  and  $h(0.450) = 0.1538$ .

	$(\cdot)_{ML}$	$(\cdot)_{BS}$	$(\cdot)_{BL}$			$(\cdot)_{BG}$		
			$a$	$q$				
			-1	1	2	-1	1	2
$\alpha$	0.2975	0.3159	0.3213	0.3107	0.3058	0.3159	0.2832	0.2669
$\beta$	1.5521	1.4679	1.5074	1.4279	1.3892	1.4679	1.4108	1.3820
$s(t)$	0.9271	0.9187	0.9189	0.9184	0.9181	0.9187	0.9180	0.9177
$h(t)$	0.1486	0.1653	0.1665	0.1641	0.1629	0.1653	0.1504	0.1428

TABLE 4: The interval lengths for  $\beta$  and 95% confidence area for  $\alpha$  and  $\beta$ .

$j$	Length	Area
1	7.3419	198.238
2	6.1107	74.2141
3	5.7796	61.2357
4	4.3371	66.9821
5	4.7508	64.8714
6	4.2892	59.4761
7	4.2547	55.2478
8	4.0687	62.4790
9	4.3541	67.2178
10	5.1017	55.4785
11	5.1899	61.2587
12	4.6457	56.4512
13	5.2475	42.8979
14	4.5626	39.4872
15	6.9847	41.2789

8.5737, and  $\chi^2_{(0.9873)(20)} = 36.7141$ , the 95% joint confidence region for  $\beta$  and  $\alpha$  is

$$\left\{ \begin{array}{l} 0.2193 < \beta < 709943 \\ \frac{8.5737}{8 \sum_{i=1}^m (R_i + 1) \log(1 + x_{i:m:n:k}^R / \beta)} < \alpha \\ < \frac{36.7141}{8 \sum_{i=1}^m (R_i + 1) \log(1 + x_{i:m:n:k}^R / \beta)} \end{array} \right. \quad (55)$$

After the following integration,

$$\int_{0.2193}^{7.9943} \frac{34.5235}{2k \sum_{i=1}^m (R_i + 1) \log(1 + (x_{i:m:n:k}^R / \beta))} d\beta. \quad (56)$$

We obtain the confidence area at  $j = 2$ , by 74.2141. Similarly, the confidence areas for some values of  $j$  are presented in Table 4. Figure 1 shows the 95% confidence region for  $\beta$  and  $\alpha$ .

## 6. Simulation Study

To compare the proposed BEs with the MLEs, a simulation study is performed using various combinations of  $n$ ,  $m$ , and  $k$  and different censored schemes of  $R$  (different  $R_i$  values). A

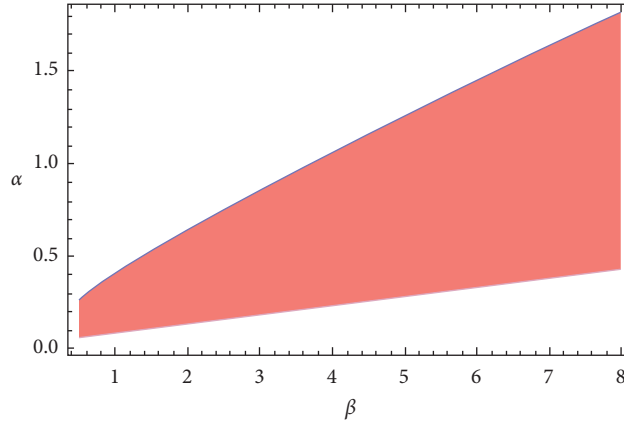


FIGURE 1: Joint confidence region for  $\beta$  and  $\alpha$ .

TABLE 5: MSE of MLEs and BEs with true values.

$k$	$n$	$m$	C.S		$ML$	$BS$	$BL$		$BG$	
							$a$	$q$		
									-1	1
1	30	20	I	$\tilde{\alpha}$	0.1576	0.0920	0.0921	0.0920	0.0920	0.0919
				$\tilde{\beta}$	0.7884	0.5711	0.5744	0.5669	0.5711	0.5655
				$\tilde{s}(t)$	0.0256	0.0223	0.0229	0.0223	0.0223	0.0216
				$\tilde{h}(t)$	0.0056	0.0042	0.0042	0.0041	0.0042	0.0040
			II	$\tilde{\alpha}$	0.1699	0.0922	0.0922	0.0921	0.0922	0.0919
				$\tilde{\beta}$	0.8268	0.5735	0.5770	0.5680	0.5735	0.5584
				$\tilde{s}(t)$	0.0258	0.0236	0.0236	0.0231	0.0236	0.0221
				$\tilde{h}(t)$	0.0058	0.0044	0.0044	0.0042	0.0044	0.0041
			III	$\tilde{\alpha}$	0.1801	0.0956	0.0957	0.0939	0.0956	0.0938
				$\tilde{\beta}$	0.8314	0.5788	0.5789	0.5695	0.5788	0.5595
				$\tilde{s}(t)$	0.0259	0.0237	0.0239	0.0235	0.0237	0.0227
				$\tilde{h}(t)$	0.0061	0.0046	0.0048	0.0045	0.0046	0.0043
5	30	20	I	$\tilde{\alpha}$	0.1588	0.0951	0.0952	0.0948	0.0951	0.0944
				$\tilde{\beta}$	0.6453	0.5717	0.5748	0.5673	0.5717	0.5663
				$\tilde{s}(t)$	0.0160	0.0151	0.0149	0.0147	0.0151	0.0146
				$\tilde{h}(t)$	0.0049	0.0041	0.0042	0.0040	0.0041	0.0039
			II	$\tilde{\alpha}$	0.1597	0.0967	0.0965	0.0963	0.0967	0.0953
				$\tilde{\beta}$	0.6680	0.5724	0.5751	0.5682	0.5724	0.5674
				$\tilde{s}(t)$	0.0168	0.0152	0.0153	0.0149	0.0152	0.0148
				$\tilde{h}(t)$	0.0052	0.0046	0.0049	0.0045	0.0046	0.0043
			III	$\tilde{\alpha}$	0.1602	0.0969	0.0976	0.0968	0.0969	0.0957
				$\tilde{\beta}$	0.6692	0.5755	0.5783	0.5684	0.5755	0.5683
				$\tilde{s}(t)$	0.0175	0.0157	0.0158	0.0155	0.0157	0.0152
				$\tilde{h}(t)$	0.0057	0.0047	0.0051	0.0048	0.0047	0.0045
1	30	25	I	$\tilde{\alpha}$	0.1501	0.0886	0.0889	0.0885	0.0886	0.0881
				$\tilde{\beta}$	0.7861	0.5679	0.5680	0.5593	0.5679	0.5275
				$\tilde{s}(t)$	0.0254	0.0218	0.0222	0.0217	0.0218	0.0215
				$\tilde{h}(t)$	0.0053	0.0040	0.0041	0.0039	0.0040	0.0036
			II	$\tilde{\alpha}$	0.1524	0.0897	0.0898	0.0889	0.0897	0.0886
				$\tilde{\beta}$	0.7952	0.5683	0.5685	0.5596	0.5683	0.5297
				$\tilde{s}(t)$	0.0259	0.0231	0.0239	0.0229	0.0231	0.0227
				$\tilde{h}(t)$	0.0054	0.0041	0.0042	0.0040	0.0041	0.0038
			III	$\tilde{\alpha}$	0.1537	0.0898	0.0899	0.0892	0.0898	0.0889
				$\tilde{\beta}$	0.7959	0.5692	0.5695	0.5608	0.5692	0.5343
				$\tilde{s}(t)$	0.0266	0.0246	0.0248	0.0245	0.0246	0.0239
				$\tilde{h}(t)$	0.0055	0.0045	0.0048	0.0044	0.0045	0.0041



TABLE 5: Continued.

k	n	m	C.S		ML	BS	BL		BG	
							a	q	-1	1
									-1	1
5	30	25	I	$\tilde{\alpha}$	0.1504	0.0894	0.0898	0.0893	0.0894	0.0883
				$\tilde{\beta}$	0.6422	0.5682	0.5687	0.5595	0.5682	0.5361
				$\tilde{s}(t)$	0.0152	0.0143	0.0144	0.0142	0.0143	0.0141
				$\tilde{h}(t)$	0.0041	0.0038	0.0039	0.0037	0.0038	0.0034
			II	$\tilde{\alpha}$	0.1517	0.0926	0.0928	0.0925	0.0926	0.0923
				$\tilde{\beta}$	0.6521	0.5691	0.5695	0.5598	0.5691	0.5369
				$\tilde{s}(t)$	0.0161	0.0146	0.0145	0.0143	0.0146	0.0142
				$\tilde{h}(t)$	0.0047	0.0041	0.0042	0.0039	0.0041	0.0037
			III	$\tilde{\alpha}$	0.1537	0.0954	0.0959	0.0951	0.0954	0.0936
				$\tilde{\beta}$	0.6547	0.5695	0.5707	0.5617	0.5695	0.5487
				$\tilde{s}(t)$	0.0166	0.0149	0.0152	0.0151	0.0149	0.0143
				$\tilde{h}(t)$	0.0052	0.0045	0.0047	0.0042	0.0045	0.0039

TABLE 6: MSE of MLEs and BEs with true values.

k	n	m	C.S		ML	BS	BL		BG	
							a	q	-2	2
									-2	2
1	50	30	I	$\tilde{\alpha}$	0.0914	0.0794	0.0834	0.0756	0.0838	0.0674
				$\tilde{\beta}$	0.6538	0.4130	0.4871	0.3425	0.4389	0.3352
				$\tilde{s}(t)$	0.0242	0.0222	0.0222	0.0222	0.0222	0.0222
				$\tilde{h}(t)$	0.0054	0.0038	0.0037	0.0038	0.0037	0.0036
			II	$\tilde{\alpha}$	0.0942	0.0798	0.0879	0.0788	0.0883	0.0686
				$\tilde{\beta}$	0.6541	0.4140	0.4878	0.3450	0.4397	0.3379
				$\tilde{s}(t)$	0.0255	0.0231	0.0231	0.0231	0.0231	0.0231
				$\tilde{h}(t)$	0.0058	0.0039	0.0040	0.0038	0.0041	0.0037
			III	$\tilde{\alpha}$	0.0945	0.0806	0.0888	0.0796	0.0891	0.0708
				$\tilde{\beta}$	0.6558	0.4304	0.5052	0.3575	0.4566	0.3503
				$\tilde{s}(t)$	0.0279	0.0245	0.0245	0.0245	0.0245	0.0245
				$\tilde{h}(t)$	0.0059	0.0041	0.0042	0.0040	0.0043	0.0039
5	50	30	I	$\tilde{\alpha}$	0.0919	0.0812	0.0843	0.0771	0.0847	0.0698
				$\tilde{\beta}$	0.6483	0.4175	0.4879	0.3633	0.4639	0.3560
				$\tilde{s}(t)$	0.0194	0.0182	0.0182	0.0182	0.0182	0.0182
				$\tilde{h}(t)$	0.0053	0.0034	0.0035	0.0034	0.0035	0.0034
			II	$\tilde{\alpha}$	0.0923	0.0826	0.0861	0.0797	0.0887	0.0727
				$\tilde{\beta}$	0.6499	0.4263	0.4917	0.3721	0.4927	0.3648
				$\tilde{s}(t)$	0.0196	0.0184	0.0184	0.0184	0.0184	0.0184
				$\tilde{h}(t)$	0.0054	0.0037	0.0038	0.0037	0.0038	0.0035
			III	$\tilde{\alpha}$	0.0941	0.0843	0.0877	0.0806	0.0891	0.0756
				$\tilde{\beta}$	0.6512	0.4344	0.5042	0.3852	0.4988	0.3778
				$\tilde{s}(t)$	0.0198	0.0187	0.0187	0.0188	0.0187	0.0188
				$\tilde{h}(t)$	0.0055	0.0038	0.0040	0.0039	0.0040	0.0037

Pro-F-F-C sample from GPD with the parameters  $(\alpha, \beta) = (0.5, 2), (0.3, 1)$  is generated. The true values of  $s(t)$  and  $h(t)$  at time  $t = 0.4$  and  $0.5$  are evaluated to be  $(s(t) = 0.9129, h(t) = 0.2083)$  and  $(s(t) = 0.8855, h(t) = 0.2)$ . The performance of the resulting estimators of  $\alpha, \beta, s(t)$ , and  $h(t)$  has been considered in terms of the mean squared error (MSE), which are computed, for  $l = 1, 2, 3, 4, M = 1000, \phi_1 = \alpha, \phi_2 = \beta, \phi_3 = s(t)$ , and  $\phi_4 = h(t)$  as  $MSE = 1/M \sum_{j=1}^M (\hat{\phi}_l^{(j)} - \phi_l)^2$ . These results were obtained using Mathematica ver. 13. Considering two different group sizes  $k = 1, 5$  and the following censoring schemes,

Scheme I:  $R_1 = n - m$  and  $R_i = 0$  for  $i \neq 1$

Scheme II:  $R_{m+1/2} = n - m$  and  $R_i = 0$  for  $i \neq m + 1/2$  if  $m$  odd, and  $R_{m/2} = n - m$  and  $R_i = 0$  for  $i \neq m/2$  if  $m$  even

Scheme III:  $R_m = n - m$  and  $R_i = 0$  for  $i \neq m$

The results of MSE of estimates are reported in Tables 5 and 6.

### 7. Conclusion

The main aim of this article is to develop different methods to estimate the unknown quantities of the GPD based on a Pro-F-F-C scheme, which was introduced by Wu and Kuş [30]. We applied the classical and the Bayesian inferential procedures for the unknown parameters and reliability measures. The ACIs have been derived based on the asymptotic normality of MLEs. Under the Bayesian approach, we obtained the BEs based on the SE, LINEX, and GE loss functions. Furthermore, we assumed the conjugate gamma prior for the shape parameter and discrete prior for the scale parameter. The exact confidence interval and exact confidence region for the estimators have been constructed based on pivotal quantities. A numerical

example using a simulated data set has been studied to show the practicality of these proposed procedures. The performance of the different estimation methods is realized via a simulation study which is revealed in the following:

- (1) The BEs based on SE, LINEX, and GE loss functions perform better than the MLEs, in terms of MSEs
- (2) The BEs based on LINEX and GE loss functions when  $a = 1$  and  $2$  and  $q = 1$  and  $2$  perform better than BEs based on SE, in terms of MSEs
- (3) The BEs based on the SE loss function perform better than BEs based on LINEX and GE loss functions when  $a = -1$  and  $-2$  and  $q = -1$  and  $-2$ , in terms of MSEs
- (4) From Tables 5 and 6, for a fixed scheme, the MSE values of all estimates, a model's parameters, and the reliability measures decrease as  $m/n$  increases which is consistent with the statistical theory that the larger the sample size, the more accurate the estimate
- (5) It can be seen from Tables 5 and 6 that the three CS methods vary in terms of preference and sometimes CS I is the best while at other times the CS II or III is the best in the sense of having smaller MSEs
- (6) The MSEs for  $\alpha$  and  $\beta$  estimates based on the Pro-F-F-C scheme with  $k = 5$  increase in those for P-type-II-C with  $k = 1$  while the MSEs for  $s(t)$  and  $h(t)$  estimates based on the Pro-F-F-C scheme with  $k = 5$  decrease in those for P-type-II-C with  $k = 1$

## Data Availability

The data used are theoretically generated from the equations in the manuscript.

## Conflicts of Interest

The authors declare that they have no conflicts of interest.

## Acknowledgments

This research was supported by Taif University Researchers Supporting Project (number TURSP-2020/318), Taif University, Taif, Saudi Arabia.

## References

- [1] N. Balakrishnan and R. A. Sandhu, "A simple simulational algorithm for generating progressive type-II censored samples," *The American Statistician*, vol. 49, no. 2, pp. 229-230, 1995.
- [2] N. Balakrishnan and R. A. Sandhu, "Best linear unbiased and maximum likelihood estimation for exponential distributions under general progressive Type-II censored samples," *Sankhya Series B*, vol. 58, no. 1, pp. 1-9, 1996.
- [3] A. C. Cohen, "Progressively censored samples in life testing," *Technometrics*, vol. 5, no. 3, pp. 327-339, 1963.
- [4] N. R. Mann, "Best linear invariant estimation for weibull parameters under progressive censoring," *Technometrics*, vol. 13, no. 3, pp. 521-533, 1971.
- [5] H. K. T. Ng, "Parameter estimation for a modified weibull distribution, for progressively type-II censored samples," *IEEE Transactions on Reliability*, vol. 54, no. 3, pp. 374-380, 2005.
- [6] N. Balakrishnan, N. Kannan, C. T. Lin, and H. K. T. Ng, "Point and interval estimation for Gaussian distribution, based on progressively type-II censored samples," *IEEE Transactions on Reliability*, vol. 52, no. 1, pp. 90-95, 2003.
- [7] D. I. Gibbons and L. C. Vance, "Estimators for the 2-parameter weibull distribution with progressively censored samples," *IEEE Transactions on Reliability*, vol. R-32, no. 1, pp. 95-99, 1983.
- [8] H.-K. Yuen and S.-K. Tse, "Parameters estimation for weibull distributed lifetimes under progressive censoring with random removals," *Journal of Statistical Computation and Simulation*, vol. 55, no. 1-2, pp. 57-71, 1996.
- [9] H. K. T. Ng, P. S. Chan, and N. Balakrishnan, "Estimation of parameters from progressively censored data using EM algorithm," *Computational Statistics & Data Analysis*, vol. 39, no. 4, pp. 371-386, 2002.
- [10] N. Balakrishnan, "Progressive censoring methodology: an appraisal," *Test*, vol. 16, no. 2, pp. 211-259, 2007.
- [11] A. A. Soliman, "Estimation of parameters of life from progressively censored data using Burr-XII model," *IEEE Transactions on Reliability*, vol. 54, no. 1, pp. 34-42, 2005.
- [12] A. A. Soliman, "Estimations for Pareto model using general progressive censored data and asymmetric loss," *Communications in Statistics - Theory and Methods*, vol. 37, no. 9, pp. 1353-1370, 2008.
- [13] M. T. Madi and M. Z. Raqab, "Bayesian inference for the generalized exponential distribution based on progressively censored data," *Communications in Statistics - Theory and Methods*, vol. 38, no. 12, pp. 2016-2029, 2009.
- [14] M. A. W. Mahmoud, M. Moshref, N. M. Yhiew, and N. M. Mohamed, "Progressively censored data from the weibull gamma distribution moments and estimation," *Journal of Statistics Applications & Probability*, vol. 3, no. 1, pp. 45-60, 2014.
- [15] M. A. W. Mahmoud, R. M. El-Sagheer, A. A. Soliman, and A. H. Abd-Allah, "Inferences of the lifetime performance index with Lomax distribution based on progressive type-II censored," *Economic Quality Control*, vol. 29, pp. 39-51, 2014.
- [16] A. A. Soliman, A. H. Abd Allah, N. A. Abou-Elheggag, and R. M. El-Sagheer, "Inferences using type-II progressively censored data with binomial removals," *Arabian Journal of Mathematics*, vol. 4, no. 2, pp. 127-139, 2015.
- [17] R. M. El-Sagheer, "Estimation using progressively Type-II censored data from Rayleigh distribution with binomial removals: Bayesian and non-Bayesian approach," *JP J. Fund. Appl. Stat.* vol. 8, no. 1, pp. 17-39, 2015.
- [18] R. M. El-Sagheer, "Estimation of parameters of Weibull-Gamma distribution based on progressively censored data," *Statistical Papers*, vol. 59, no. 2, pp. 725-757, 2018.
- [19] R. M. El-Sagheer, "Estimating the parameters of Kumaraswamy distribution using progressively censored data," *Journal of Testing and Evaluation*, vol. 47, no. 2, pp. 905-926, 2019.
- [20] M. A. W. Mahmoud, R. M. El-Sagheer, and S. H. M. Abdallah, "Inferences for new Weibull-Pareto distribution based on progressively Type-II censored data," *Journal of Statistics Applications & Probability*, vol. 5, no. 3, pp. 501-514, 2016.
- [21] R. M. El-Sagheer and M. M. Hasaballah, "Inference of process capability Index Cpy for 3-Burr-XII distribution based on progressive Type-II censoring," *International Journal of*

- Mathematics and Mathematical Sciences*, vol. 2020, pp. 1–13, 2020.
- [22] R. M. El-Sagheer, E. M. Shokr, M. A. W. Mahmoud, and B. S. El-Desouky, “Inferences for weibull fréchet distribution using a bayesian and non-bayesian methods on gastric cancer survival times,” *Computational and Mathematical Methods in Medicine*, vol. 2021, pp. 1–12, 2021.
- [23] A. A. Soliman, E. A. Ahmed, A. H. Abd Allah, and A. A. Farghal, “Bayesian estimation from exponentiated Frechet model using MCMC approach based on progressive Type-II censoring data,” *Statistics Applications & Probability*, vol. 4, no. 3, pp. 387–403, 2015.
- [24] Y. Zhang and W. Gui, “Statistical inference for the lifetime performance index of products with Pareto distribution on basis of general progressive type II censored sample,” *Communications in Statistics - Theory and Methods*, vol. 50, no. 16, pp. 3790–3808, 2021.
- [25] R. Viveros and N. Balakrishnan, “Interval estimation of parameters of life from progressively censored data,” *Technometrics*, vol. 36, no. 1, pp. 84–91, 1994.
- [26] J.-W. Wu and H.-Y. Yu, “Statistical inference about the shape parameter of the Burr type XII distribution under the failure-censored sampling plan,” *Applied Mathematics and Computation*, vol. 163, no. 1, pp. 443–482, 2005.
- [27] J.-W. Wu, W.-L. Hung, and C.-H. Tsai, “Estimation of the parameters of the Gompertz distribution under the first failure-censored sampling plan,” *Statistics*, vol. 37, no. 6, pp. 517–525, 2003.
- [28] W.-C. Lee, J.-W. Wu, and H.-Y. Yu, “Statistical inference about the shape parameter of the bathtub-shaped distribution under the failure-censored sampling plan,” *International Journal on Information and Management Sciences*, vol. 18, pp. 157–172, 2007.
- [29] J.-W. Wu, T.-R. Liang-Yuh Ouyang, and L.-Y. Ouyang, “Limited failure-censored life test for the Weibull distribution,” *IEEE Transactions on Reliability*, vol. 50, no. 1, pp. 107–111, 2001.
- [30] S.-J. Wu and C. Kuş, “On estimation based on progressive first-failure-censored sampling,” *Computational Statistics & Data Analysis*, vol. 53, no. 10, pp. 3659–3670, 2009.
- [31] A. A. Soliman, A. H. A. Allah, N. A. Abou-Elheggag, and A. A. Modhesh, “Bayesian inference and prediction of Burr type XII distribution for progressive first failure censored sampling,” *Intelligent Information Management*, vol. 03, no. 05, pp. 175–185, 2011.
- [32] A. A. Soliman, A. H. Abd Allah, N. A. Abou-Elheggag, and A. A. Modhesh, “Estimation of the coefficient of variation for non-normal model using progressive first-failure-censoring data,” *Journal of Applied Statistics*, vol. 39, no. 12, pp. 2741–2758, 2012.
- [33] A. A. Soliman, A. H. Abd-Ellah, N. A. Abou-Elheggag, and G. A. Abd-Elmougod, “Estimation of the parameters of life for Gompertz distribution using progressive first-failure censored data,” *Computational Statistics & Data Analysis*, vol. 56, no. 8, pp. 2471–2485, 2012.
- [34] M. A. W. Mahmoud, A. A. Soliman, A. H. Abd-Ellah, and R. M. El-Sagheer, “Bayesian inference and prediction using progressive first-failure censored from generalized Pareto distribution,” *Journal of Statistics Applications & Probability*, vol. 2, no. 3, pp. 269–279, 2013.
- [35] T. A. Abushal, “Estimation of the unknown parameters for the Compound Rayleigh distribution based on progressive first-failure-censored sampling,” *Open Journal of Statistics*, vol. 01, no. 03, pp. 161–171, 2011.
- [36] E. A. Ahmed, “Estimation and prediction for the generalized inverted exponential distribution based on progressively first-failure-censored data with application,” *Journal of Applied Statistics*, vol. 44, no. 9, pp. 1576–1608, 2017.
- [37] M. M. Mahmoud, M. M. Nassar, and M. A. Aefa, “Bayesian estimation and prediction based on progressively first failure censored scheme from a mixture of Weibull and Lomax distributions,” *Pakistan Journal of Statistics and Operation Research*, vol. 16, no. 2, pp. 357–372, 2020.
- [38] A. A.-E. Soliman, E. A. Ahmed, A. H. Abd Allah, and A. A. Farghal, “Assessing the lifetime performance index using exponentiated Frechet distribution with the progressive first-failure-censoring scheme,” *American Journal of Theoretical and Applied Statistics*, vol. 3, no. 6, pp. 167–176, 2014.
- [39] Y. Cai and W. Gui, “Classical and Bayesian inference for a progressive first-failure censored left-truncated normal distribution,” *Symmetry Plus*, vol. 13, no. 3, p. 490, 2021.
- [40] E. Kremer, “A characterization of the generalized Pareto-distribution with an application to reinsurance,” *Blätter der DGVFM*, vol. 23, no. 1, pp. 17–19, 1997.
- [41] D. R. Thomas and W. M. Wilson, “Linear order statistic estimation for the two-parameter weibull and extreme-value distributions from type II progressively censored samples,” *Technometrics*, vol. 14, no. 3, pp. 679–691, 1972.
- [42] S.-F. Wu, C.-C. Wu, Y.-L. Chen, Y.-R. Yu, and Y. P. Lin, “Interval estimation of a two-parameter Burr-XII distribution under progressive censoring,” *Statistics*, vol. 44, no. 1, pp. 77–88, 2010.

## Research Article

# Maximize Expected Profits by Dynamic After-Sales Service Investment Strategy Based on Word-of-Mouth Marketing in Social Network Shopping

Ying Yu <sup>1,2</sup>, Jiaomin Liu,<sup>1</sup> Jiadong Ren <sup>1,3</sup>, Qian Wang,<sup>1,3</sup> and Cuiyi Xiao<sup>4</sup>

<sup>1</sup>College of Information Science and Engineering, Yanshan University, Qinhuangdao, Hebei, China

<sup>2</sup>Liren College of Yanshan University, Qinhuangdao, Hebei, China

<sup>3</sup>Computer Virtual Technology and System Integration Laboratory of Hebei Province, Qinhuangdao, China

<sup>4</sup>College of Mathematics and Information Technology, Hebei Normal University of Science and Technology, Qinhuangdao, Hebei, China

Correspondence should be addressed to Jiadong Ren; [jdren@ysu.edu.cn](mailto:jdren@ysu.edu.cn)

Received 4 August 2021; Accepted 1 October 2021; Published 11 November 2021

Academic Editor: Sameh S. Askar

Copyright © 2021 Ying Yu et al. This is an open access article distributed under the Creative Commons Attribution License, which permits unrestricted use, distribution, and reproduction in any medium, provided the original work is properly cited.

This paper discusses how word-of-mouth marketing affects the profits of product sales in social network-based shopping under good after-sales service. First, a new word-of-mouth communication model based on silent evaluation, positive evaluation, and negative evaluation is proposed. Second, we use the way of increasing after-sales service to achieve high praise and thereby maximize the expected profits. Thus, the proportion control problem of after-sales service investment is modeled as an optimal control problem. Third, the existence of optimal control is proved, and an optimal control strategy for dynamic proportion of after-sales service investment is proposed. Fourth, through data simulation of different real-world networks, it is verified that the expected profits under the dynamic after-sales service strategy is higher than that under any uniform control strategy. Finally, sensitivity analysis is performed to explore how different parameters affect the expected profits.

## 1. Introduction

With the boom of social networking, more and more consumers are making purchase decisions based on word of mouth (WOM). Nearly three-quarters (73%) of consumers regularly recommend products to their friends, according to an Accenture survey [1]. The rapid advancement of e-commerce and logistics networks has changed the way of shopping in China. Online shopping is characterized by easy access to actual WOM. Compared with traditional advertising strategies, WOM influence strategies cost less and deliver more revenue [2–9].

In recent years, researchers have examined ways to maximize product profits from different perspectives based on WOM marketing. For example, the relationship between users was used to explore the impact of WOM marketing on consumers [10–12]. Users' WOM feedback

data was used to mine information that is conducive to enterprises' innovation or growth [13–15]. A dynamic discount pricing strategy aiming at maximizing product profits based on WOM marketing was proposed [16–18]. Using WOM as an epidemic, a framework was constructed to discuss the impact of WOM on sales based on epidemic models [19–21].

In recent years, social network-based shopping, typified by shopping on WeChat, has emerged in China. The biggest characteristic of this shopping lies in its reliance on social networks for product sales. In particular, since the early 2020, when the COVID-19 outbreak caused a sharp drop in customer visits and product sales in physical stores, more and more sellers have begun to set up shopping groups to sell products on social networks such as WeChat. These shopping groups, which we call community buying groups, tend to have the following characteristics:

Members in such a group are often closely related, i.e., they may be members of the same company, neighbor users, etc. This makes it easy to spread WOM among different nodes within a social network, which directly affects product sales. Since most customers are familiar with each other, reviews are usually truthful and valid. Therefore, positive WOM has a significant impact on product sales.

Community group buying often involves repeat purchases, and positive WOM, in particular, prompts consumers to make repeat purchases. Therefore, WOM affects the initial purchase intention of customers.

After customers buy a product, their evaluation is usually three-fold: silent, positive, and negative. Evidently, positive WOM helps to increase the purchase intention of the remaining customers, and negative WOM reduces their purchase intention.

After-sales service works in two ways for enhancing WOM. On the one hand, it encourages customers who have been remaining silent to post more positive reviews; on the other hand, it helps to reverse customers' negative reviews and finally drive positive WOM publicity.

We note that several studies have been conducted on the positive and negative effects of WOM [22–26]. Based on the cognitive dissonance theory and social support theory, Balaji et al. [27] studied the roles of situational factors, personal factors, and social network factors in determining customers' willingness to use social networking sites for negative WOM communication. Verhagen et al. [28] proposed a sender-oriented model to explore the effects of emotions and negative online WOM on re-sponsorship and switching intention. Dalman et al. [29] investigated how high-equity and low-equity brands attract negative WOM from consumers in the event of market failure. Weitzl et al. [30] suggested that online care (i.e., messages in response to online complaints) can mitigate complainants' adverse attributions of failure (i.e., track, controllability, and stability).

Inspired by the epidemic model, this paper takes WOM as a kind of epidemic and establishes a nodal dynamic WOM propagation model. From the characteristics of community group buying, it can be concluded that WOM has important implications for product sales. However, community group buying is small in scale and the profit it generates is limited. Investing heavy resources to maintain WOM would be costly. In this paper, we focus on how to dynamically invest in after-sales service to maximize profits. The main contributions are as follows:

First, a node-level model based on WOM marketing is established to reveal the influence of WOM on consumers' purchase intention.

Second, on this basis, the dynamic control problem of WOM through after-sales service is modeled as an optimal control problem.

Third, we prove that the model has optimal control and obtain the optimal system for solving the model.

Fourth, by solving the corresponding optimal system, some optimal control strategies are given, which are then compared with uniform control. The comparison demonstrates the superiority of optimal control strategies over uniform control ones.

Finally, the influence of after-sales service on product sales is further discussed through sensitivity analysis of relevant after-sales service parameters.

The remainder of the paper is organized as follows. In Section 2, we establish a node-level Target-Buying-Refusing (TBR) model based on WOM marketing and model the dynamic after-sales service (DAS) problem as an optimal control problem. In Section 3, we perform theoretical analysis on the optimal control problem and give a dynamic strategy for after-sales service investment. Some optimal DAS strategies are given in Section 4. In Section 5, the influence of some after-sales service parameters on expected profits is further revealed. The concluding remarks are drawn in Section 6.

## 2. The Modeling of the DAS Investment Problem

In this section, we consider the WOM marketing problem with DAS investment. In view of the sales activities involved in community group buying, a DAS investment strategy is developed in order to maximize profits for sellers. The highlights of this section are as follows: (1) introducing basic symbols and terms; (2) establishing a TBR model based on WOM marketing; (3) modeling the DAS problem as an optimal control problem.

*2.1. Terms and Notations.* Assuming the number of users for a community group purchase is  $N$ , we let  $G = (V, E)$  denote the topology of this network. Specifically,  $V = (V_1, V_2, \dots, V_N)$  represents the nodes of the network and  $N$  is the number of nodes in the network; furthermore,  $E_{ij} = \{V_i, V_j\} \in E$ , which represents nodes  $V_i$  and  $V_j$  are friends, so  $G$  is an undirected network;  $A = (a_{ij})_{N \times N}$  represents the adjacency matrix of network  $G$ . When  $a_{ij} = 1$ ,  $V_i$  and  $V_j$  can share their reviews on products with each other.

Let the vector  $O(t) = (O_1(t), O_2(t), \dots, O_N(t))$  represent the state of  $N$  nodes in the network at time  $t$ . Assuming that a product is sold in a finite time horizon  $[0, T]$ , individual users may have the following three states in community group buying:  $O_i(t) = 0$ ,  $O_i(t) = 1$ , and  $O_i(t) = 2$ , corresponding to target customers (who have not yet decided whether to buy the product), buying customers (who buy the product), and refusing customers (who refuse to buy the product) at time  $t$ , respectively. Let  $T_i(t)$ ,  $B_i(t)$ , and  $R_i(t)$  denote the expected probabilities of node  $V_i$  being target customers, buying customers, and refusing customers at time  $t$ , respectively:

$$\begin{aligned}
T_i(t) &= \Pr\{O_i(t) = 0\}, \\
B_i(t) &= \Pr\{O_i(t) = 1\}, \\
R_i(t) &= \Pr\{O_i(t) = 2\}.
\end{aligned} \tag{1}$$

Note that  $T_i(t) + B_i(t) + R_i(t) = 1$ . Specifically, buying customers are categorized into three groups in terms of their evaluation: silent, positive, and negative. Let  $S_i(t)$ ,  $P_i(t)$ , and  $N_i(t)$  represent the expected probabilities of buying customers who remain silent and give positive and negative evaluations at time  $t$ , respectively.

To solve the WOM propagation problem with DAS investment, we introduce the following assumptions:

Due to the shopping share of neighbor nodes who buy the products, target customers become buying customers with a probability of  $\rho$  on average

Due to the shopping share of neighbor nodes who refuse to buy the products, target customers become refusing customers with a probability of  $\gamma$  on average

For buying customers,  $\alpha_1$ ,  $\alpha_2$ , and  $\alpha_3$  represent the probabilities of them remaining silent, giving positive evaluation and giving negative evaluation; hence,  $\alpha_1 + \alpha_2 + \alpha_3 = 1$

Due to the positive WOM effect of buyers, target customers become buying customers with a probability of  $\beta_1$  on average

Due to the negative WOM effect of buyers, target customers become refusing customers with a probability of  $\beta_2$  on average

The above assumptions are independent of each other, and the state transition diagram of the node is shown in Figure 1. In practice, parameters  $\rho$ ,  $\gamma$ ,  $\alpha_1$ ,  $\alpha_2$ ,  $\alpha_3$ ,  $\beta_1$ ,  $\beta_2$  can be estimated from the information of the network.

The vector,

$$\mathbf{E}(t) = (T(t), B(t), R(t)), \tag{2}$$

represents the expected state of nodes in the network at time  $t$ , where

$$\begin{cases}
T(t) = (T_1(t), T_2(t), \dots, T_N(t)), \\
B(t) = (B_1(t), B_2(t), \dots, B_N(t)), \\
R(t) = (R_1(t), R_2(t), \dots, R_N(t)).
\end{cases} \tag{3}$$

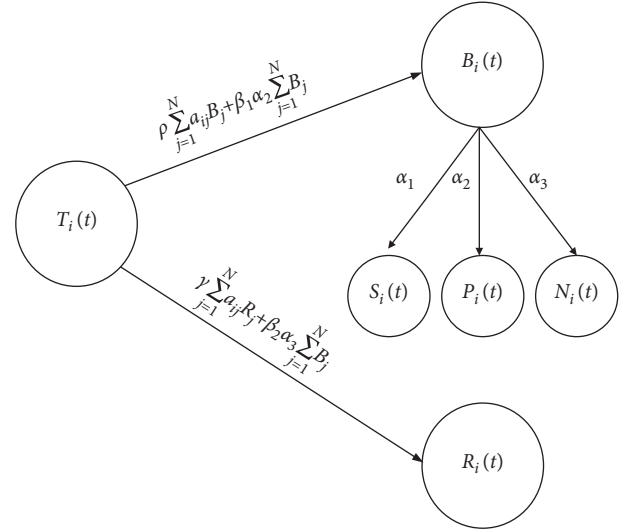


FIGURE 1: State transition diagram of individual  $V_i$  at time  $t$ .

For ease of understanding, a simple example is given. Assume that there is a topological relationship between network nodes, as shown in Figure 2, and the probability that node 1 is a target customer is 1 at time  $t$ , i.e.,  $T_1(t) = \Pr\{O_1(t) = 0\} = 1$ . Suppose the adjacency matrix of nodes in the network is

$$A = \begin{pmatrix} 0 & 1 & 1 & 1 & 0 & 0 \\ 1 & 0 & 1 & 1 & 1 & 0 \\ 1 & 1 & 0 & 0 & 0 & 1 \\ 1 & 1 & 0 & 0 & 0 & 0 \\ 0 & 1 & 0 & 0 & 0 & 0 \\ 0 & 0 & 1 & 0 & 0 & 0 \end{pmatrix}. \tag{4}$$

The probabilities of network nodes being in each state are shown in Table 1.

Parameter values are shown in Table 2.

Then, the probability that node 1 is a buying node at  $t + \Delta t$  is

$$\begin{aligned}
B_1(t + \Delta t) &= \Pr\{O_1(t + \Delta t) = 1\} = \rho \sum_{j=1}^N a_{1j} B_j + \beta_1 \alpha_2 \sum_{j=1}^N B_j \\
&= \rho (a_{12} \cdot B_2 + a_{13} \cdot B_3 + a_{14} \cdot B_4) + \beta_1 \alpha_2 (B_1 + B_2 + B_3 + B_4 + B_5 + B_6) \\
&= 0.1 \cdot (0.7 + 0.7 + 0.2) + 0.02 \cdot (0.7 + 0.7 + 0.2 + 0.6 + 0.2) = 0.208.
\end{aligned} \tag{5}$$

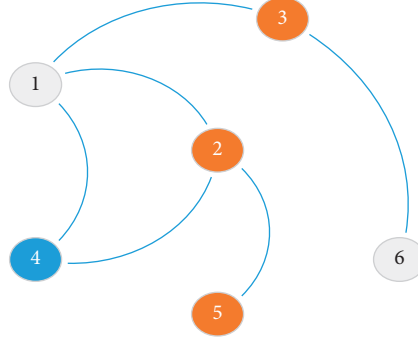


FIGURE 2: A simple network topology.

TABLE 1: Probabilities of nodes being in each state.

Node number	Probability of $T_i$	Probability of $B_i$	Probability of $R_i$
2	0.2	0.7	0.1
3	0.1	0.7	0.2
4	0.2	0.2	0.6
5	0.3	0.6	0.1
6	0.7	0.2	0.1

Then, the probability that node 1 is a refusing node at  $t + \Delta t$  is

$$\begin{aligned}
 R_1(t + \Delta t) &= \Pr(O_1(t + \Delta t) = 2) = \gamma \sum_{j=1}^N a_{ij} R_j + \beta_2 \alpha_3 \sum_{j=1}^N B_j \\
 &= \gamma (a_{12} \cdot R_2 + a_{13} \cdot R_3 + a_{14} \cdot R_4) + \beta_2 \alpha_3 (B_1 + B_2 + B_3 + B_4 + B_5 + B_6) \\
 &= 0.1 \cdot (0.1 + 0.2 + 0.6) + 0.04 \cdot (0.7 + 0.7 + 0.2 + 0.6 + 0.2) = 0.186.
 \end{aligned} \tag{6}$$

Then, the probability that node 1 is a target node at  $t + \Delta t$  is

$$T_1(t + \Delta t) = 1 - 0.208 - 0.186 = 0.606. \tag{7}$$

*2.2. Dynamic TBR Model Based on WOM Marketing.* The TBR model based on WOM marketing to be derived later conforms to the above assumption. The following system gives an equivalent form of the exact TBR model:

$$\begin{cases}
 \frac{dT_i(t)}{dt} = - \left[ \rho \sum_{j=1}^N a_{ij} B_j(t) + \beta_1 \alpha_2 \sum_{j=1}^N B_j(t) + \gamma \sum_{j=1}^N a_{ij} R_j(t) + \beta_2 \alpha_3 \sum_{j=1}^N B_j(t) \right] T_i(t), \\
 \frac{dB_i(t)}{dt} = \left[ \rho \sum_{j=1}^N a_{ij} B_j(t) + \beta_1 \alpha_2 \sum_{j=1}^N B_j(t) \right] T_i(t), \\
 \frac{dR_i(t)}{dt} = \left[ \gamma \sum_{j=1}^N a_{ij} R_j(t) + \beta_2 \alpha_3 \sum_{j=1}^N B_j(t) \right] T_i(t),
 \end{cases} \tag{8}$$

TABLE 2: Values of parameters based on network.

Parameter	$\rho$	$\gamma$	$\alpha_1$	$\alpha_2$	$\alpha_3$	$\beta_1$	$\beta_2$
Value	0.1	0.2	0.4	0.2	0.4	0.1	0.1

under the initial condition  $\mathbf{E}(0) = \mathbf{E}_0$ .

System (8) may be written in system as

$$\begin{cases} \frac{d\mathbf{E}(t)}{dt} = \mathbf{f}_1(\mathbf{E}(t)), & 0 \leq t \leq T, \\ \mathbf{E}(0) = \mathbf{E}_0. \end{cases} \quad (9)$$

**2.3. Optimal Control Modeling of the DAS Problem.** We refer to the function  $\theta = \{\theta_1(t), \theta_2(t)\}$ ,  $0 \leq t \leq T$ , as a DAS strategy.  $\theta_1(t)$  is the proportion of investment in the first type of after-sales service, including the proportion of silent users converted into positive reviews through cash back.  $\theta_2(t)$  is the proportion of investment in the second type of after-sales service, including the proportion of negative reviews converted into positive ones by compensating users for their losses. Therefore, we assume that the DAS strategy is

$$\theta = \{(\theta_1(t), \theta_2(t)) \in L[0, T]^2 \mid 0 \leq \theta_1(t) \leq \bar{\theta}_1, \quad 0 \leq \theta_2(t) \leq \bar{\theta}_2, 0 \leq t \leq T\}, \quad (10)$$

where  $L[0, T]^2$  represents the set of all Lebesgue integrable functions defined on  $[0, T]$  [31].

It is widely known that profits are closely associated with the sales of products. Theoretically, the higher the sales of products is, the more negative reviews there will be. In WOM-oriented community group buying, in particular, negative reviews will directly affect the sales of products, resulting in a decline in profits. The proportion of positive WOM can be increased by investing in after-sales service. However, such investment tends to increase the cost and reduce the profit. In view of this, this paper intends to establish a dynamic proportion of investment in after-sales service to maximize the final profit.

*Remark 1.* Assuming that the profit per unit of a product is  $c_1$ , the total profit from selling the product at time  $[0, T]$  is

$$L_1(\theta) = \int_0^T \sum_{i=1}^N c_1 B_i(t) dt. \quad (11)$$

*Remark 2.* Assuming that the investment proportion of the first type of after-sales service is  $\theta_1(t)$  and its average unit cost is  $c_2$ , the cost of after-sales service at time  $[0, T]$  is

$$L_2(\theta) = \int_0^T \sum_{i=1}^N c_2 \alpha_1 \theta_1(t) B_i(t) dt. \quad (12)$$

*Remark 3.* Assuming that the investment proportion of the second type of after-sales service is  $\theta_2(t)$  and its average unit cost is  $c_3$ , the cost of after-sales service at time  $[0, T]$  is

$$L_3(\theta) = \int_0^T \sum_{i=1}^N c_3 \alpha_3 \theta_2(t) B_i(t) dt. \quad (13)$$

In summary, the expected profit is

$$\begin{aligned} J(\theta) &= L_1(\theta) - L_2(\theta) - L_3(\theta) \\ &= \int_0^T \sum_{i=1}^N (c_1 - c_2 \alpha_1 \theta_1(t) - c_3 \alpha_3 \theta_2(t)) B_i(t) dt \\ &\equiv \int_0^T \mathbf{F}(\mathbf{E}(t), \theta(t)) dt, \end{aligned} \quad (14)$$

where

$$\mathbf{F}(\mathbf{E}(t), \theta(t)) = \sum_{i=1}^N (c_1 - c_2 \alpha_1 \theta_1(t) - c_3 \alpha_3 \theta_2(t)) B_i(t). \quad (15)$$

Based on the above discussions and assumptions, this DAS problem can be modeled as an optimal control problem as follows:



$$\max_{\theta \in \Theta} = \int_0^T \mathbf{F}(\mathbf{E}(t), \theta(t)) dt$$

subject to

$$\left\{ \begin{array}{l} \frac{dT_i(t)}{dt} = \left[ \rho \sum_{j=1}^N a_{ij} B_j(t) + \beta_1 (\alpha_2 + \alpha_1 \theta_1 + \alpha_3 \theta_2) \sum_{j=1}^N B_j(t) \right. \\ \left. + \gamma \sum_{j=1}^N a_{ij} R_j(t) + \beta_2 (\alpha_3 (1 - \theta_2)) \sum_{j=1}^N B_j(t) \right] T_i(t), \\ \frac{dB_i(t)}{dt} = \left[ \rho \sum_{j=1}^N a_{ij} B_j(t) + \beta_1 (\alpha_2 + \alpha_1 \theta_1 + \alpha_3 \theta_2) \sum_{j=1}^N B_j(t) \right] T_i(t), \\ \frac{dR_i(t)}{dt} = \left[ \gamma \sum_{j=1}^N a_{ij} R_j(t) + \beta_2 (\alpha_3 (1 - \theta_2)) \sum_{j=1}^N B_j(t) \right] T_i(t), \\ \mathbf{E}(0) = \mathbf{E}_0. \end{array} \right. \quad (16)$$

The associated TBR model based on WOM can be rewritten as

$$\left\{ \begin{array}{l} \frac{d\mathbf{E}(t)}{dt} = \mathbf{f}_2(\mathbf{E}(t), \theta(t)), \quad 0 \leq t \leq T, \\ \mathbf{E}(0) = \mathbf{E}_0. \end{array} \right. \quad (17)$$

We refer to this optimal control problem as the DAS problem. This model can be described as a 15-tuple problem as follows:

$$\Phi = (G, \rho, \gamma, \alpha_1, \alpha_2, \alpha_3, \beta_1, \beta_2, \bar{\theta}_1, \bar{\theta}_2, c_1, c_2, c_3, \mathbf{E}_0, T). \quad (18)$$

### 3. Theoretical Study of the DAS Control Problem

**3.1. Solvability of the DAS Problem.** First, we prove that the DAS problem is an optimal control problem and is solvable. Hence, we derive Lemma 1 [32].

**Lemma 1.** *The DAS problem is an optimal control problem if all the following five conditions hold.*

- (1)  $\Theta$  is convex and closed
- (2) There exists  $\theta \in \Theta$  such that system (17) is solvable

(3)  $\mathbf{f}_2(\mathbf{E}, \theta)$  is bounded by a linear function in  $\mathbf{E}$

(4)  $\mathbf{F}(\mathbf{E}, \theta)$  is convex on  $\Theta$

(5) There exists  $\delta > 1, d_1 > 0$ , and  $d_2$  such that  $\mathbf{F}(\mathbf{E}, \theta) \geq \|\theta\|_2^\delta + d_2$

Then, we can deduce the following theorem.

**Theorem 1.** *The DAS problem is an optimal control problem.*

*Proof.* First, let  $\theta = (\theta_1(t), \theta_2(t))$  be a limit point of  $\Theta$ . Then, there exists a sequence  $\theta^n(t) = (\theta_1^n(t), \theta_2^n(t))$ ,  $n = 1, 2, \dots$ , of points of  $\Theta$ , which approaches  $\theta(t)$ . Since

$$\begin{aligned} 0 \leq \theta_1(t) &= \lim_{n \rightarrow \infty} \theta_1^n(t) \leq \bar{\theta}_1 \leq 1, \\ 0 \leq \theta_2(t) &= \lim_{n \rightarrow \infty} \theta_2^n(t) \leq \bar{\theta}_2 \leq 1, \quad 0 \leq t \leq T. \end{aligned} \quad (19)$$

$\Theta$  is closed. Let  $\theta^{(1)}, \theta^{(2)} \in \Theta$ ,  $0 < \eta < 1$ ,  $\hat{\theta} = (1 - \eta)\theta^{(1)} + \eta\theta^{(2)}$ . As  $L[0, T]^2$  is a real vector space, we have  $\hat{\theta} \in L[0, T]^2$  and  $0 \leq (1 - \eta)\theta^{(1)}(t) + \eta\theta^{(2)}(t) \leq (1 - \eta)\bar{\theta}_1 + \eta\bar{\theta}_1 = \bar{\theta}_1$ . Hence,  $\Theta$  is convex. Second, let  $\theta^*(t) \in \Theta$ . As  $\mathbf{f}_2(\mathbf{E}, \theta^*)$  is continuously differentiable, it follows by the continuation theorem for differentiable systems [33] that the corresponding state evolution state is solvable.

Third, it follows from (17) that for  $1 \leq i \leq N$ . As  $T_i(t) = 1 - B_i(t) - R_i(t)$  and  $0 \leq \theta(t) \leq 1$ , then we have

$$\begin{aligned}
-\left(\rho \sum_{j=1}^N a_{ij} B_j(t) + \beta_1 \sum_{j=1}^N B_j(t) + \gamma \sum_{j=1}^N a_{ij} R_j(t) + \beta_2 \alpha_3 \sum_{j=1}^N B_j(t)\right) &\leq \frac{dT_i}{dt} \leq \beta_2 \alpha_3 \sum_{j=1}^N B_j, \\
\left(\rho \sum_{j=1}^N a_{ij} B_j(t) + \beta_1 \alpha_2 \sum_{j=1}^N B_j(t)\right) T_i &\leq \frac{dB_i}{dt} \leq \left(\rho \sum_{j=1}^N a_{ij} B_j(t) + \beta_1 \sum_{j=1}^N B_j(t)\right) T_i, \\
\left(\gamma \sum_{j=1}^N a_{ij} R_j(t)\right) T_i &\leq \frac{dR_i}{dt} \leq \left(\gamma \sum_{j=1}^N a_{ij} R_j(t) + \beta_2 \alpha_3 \sum_{j=1}^N B_j(t)\right) T_i.
\end{aligned} \tag{20}$$

Hence,  $f_2(\mathbf{E}, \theta)$  is bounded by a linear function in  $\mathbf{E}$ . The fourth condition follows that  $\mathbf{F}(\mathbf{E}, \theta)$  is linear in  $\Theta$  and is therefore convex.

Finally,  $\mathbf{F}(\mathbf{E}, \theta) \geq 0 \geq (\theta_1^2 + \theta_2^2) - (\bar{\theta}_1^2 + \bar{\theta}_2^2) = \|\theta\|_2^2 - (\bar{\theta}_1^2 + \bar{\theta}_2^2)$ . Then, there exists  $d_1 = 1, \delta = 2, d_2 = -(\bar{\theta}_1^2 + \bar{\theta}_2^2)$  such

that  $\mathbf{F}(\mathbf{E}, \theta) \geq d_1 \|\theta\|_2^\delta + d_2$ . By Lemma 1, Theorem 1 is proved.  $\square$

**3.2. The Optimality System.** According to the optimal control theory, the Hamiltonian function of the DAS problem is

$$\begin{aligned}
H(\mathbf{E}(t), \theta(t), X(t)) &= \sum_{i=1}^N (c_1 - c_2 \alpha_1 \theta_1 - c_3 \alpha_3 \theta_2) B_i(t) \\
&+ \sum_{i=1}^N \lambda_i(t) \left[ -\left(\rho \sum_{j=1}^N a_{ij} B_j(t) + \beta_1 (\alpha_2 + \alpha_1 \theta_1 + \alpha_3 \theta_2) \sum_{j=1}^N B_j(t) \right. \right. \\
&+ \left. \left. \gamma \sum_{j=1}^N a_{ij} R_j(t) + \beta_2 (\alpha_3 (1 - \theta_2)) \sum_{j=1}^N B_j(t)\right) T_i(t) \right] \\
&+ \sum_{i=1}^N \mu_i(t) \left[ \left(\rho \sum_{j=1}^N a_{ij} B_j(t) + \beta_1 (\alpha_2 + \alpha_1 \theta_1 + \alpha_3 \theta_2) \sum_{j=1}^N B_j(t)\right) T_i(t) \right] \\
&+ \sum_{i=1}^N \nu_i(t) \left[ \left(\gamma \sum_{j=1}^N a_{ij} R_j(t) + \beta_2 (\alpha_3 (1 - \theta_2)) \sum_{j=1}^N B_j(t)\right) T_i(t) \right],
\end{aligned} \tag{21}$$

where  $X(t) = (\lambda(t), \mu(t), \nu(t)) = (\lambda_1, \lambda_2, \dots, \lambda_N, \mu_1, \mu_2, \dots, \mu_N, \nu_1, \nu_2, \dots, \nu_N)$  is the adjoint of  $H$ . We give the necessary condition for the optimal control of the DAS problem as follows.

**Theorem 2.** Suppose  $\theta = (\theta_1(t), \theta_2(t))$  is an optimal control of the DAS problem (16) and  $\mathbf{E}$  is the solution to the associated TBR model (17). Then, there exists an adjoint function  $X(t) = (\lambda(t), \mu(t), \nu(t))$  such that the following equations hold:

$$\left\{ \begin{array}{l}
\frac{d\lambda_i(t)}{dt} = (\lambda_i - \mu_i) \sum_{j=1}^N (\rho a_{ij} + \beta_1 (\alpha_2 + \alpha_1 \theta_1 + \alpha_3 \theta_2)) B_j(t) \\
+ (\lambda_i - \nu_i) \sum_{j=1}^N \gamma a_{ij} R_j + (\lambda_i - \nu_i) \sum_{j=1}^N \beta_2 \alpha_3 (1 - \theta_2) B_j, \\
\frac{d\mu_i(t)}{dt} = -c_1 + c_2 \alpha_1 \theta_1 + c_3 \alpha_3 \theta_2 + \sum_{j=1}^N \rho a_{ji} T_j(t) (\lambda_j - \mu_j) \\
+ \beta_1 (\alpha_2 + \alpha_1 \theta_1 + \alpha_3 \theta_2) \sum_{j=1}^N (\lambda_j - \mu_j) T_j(t) + \beta_2 \alpha_3 (1 - \theta_2) \sum_{j=1}^N (\lambda_j - \nu_j) T_j(t) \\
\frac{d\nu_i(t)}{dt} = \gamma \sum_{j=1}^N a_{ji} (\lambda_j - \nu_j) T_j(t), \\
0 \leq t \leq T, i = 1, 2, \dots, N, \\
\lambda(T) = \mu(T) = \nu(T) = 0.
\end{array} \right. \quad (22)$$

Moreover, let

$$\begin{aligned}
g_1(t) &= \beta_1 \alpha_1 \sum_{i=1}^N T_i(t) (\mu_i - \lambda_i) - c_2 \alpha_1, \\
g_2(t) &= \sum_{i=1}^N T_i(t) (\beta_1 \alpha_3 (\mu_i - \lambda_i) + \beta_2 \alpha_3 (\lambda_i - \nu_i)) - c_3 \alpha_3.
\end{aligned} \quad (23)$$

Then, for  $0 \leq t \leq T$ , we have

$$\theta_i(t) = \begin{cases} \bar{\theta}_i, & g_i(t) > 0, \\ 0, & g_i(t) < 0. \end{cases} \quad (24)$$

*Proof.* According to Pontryagin Minimum Principle [32], there exists  $(\lambda, \mu, \nu)$  such that

$$\left\{ \begin{array}{l}
\frac{d\lambda_i}{dt} = -\frac{\partial H(E(t), \theta(t), X(t))}{\partial T_i}, \quad 0 \leq t \leq T, i = 1, 2, \dots, N, \\
\frac{d\mu_i}{dt} = -\frac{\partial H(E(t), \theta(t), X(t))}{\partial B_i}, \quad 0 \leq t \leq T, i = 1, 2, \dots, N, \\
\frac{d\nu_i}{dt} = -\frac{\partial H(E(t), \theta(t), X(t))}{\partial R_i}, \quad 0 \leq t \leq T, i = 1, 2, \dots, N.
\end{array} \right. \quad (25)$$

The first  $3N$  equations in system (22) follow by direct calculations. Since the terminal cost is unspecified and the final state is free, we have  $\lambda(T) = \mu(T) = \nu(T) = 0$ . According to Pontryagin Maximum Principle, we have

$$H(E(t), \theta(t), X(t)) = \arg \max_{\bar{\theta} \in \Theta} H(E(t), \bar{\theta}, X(t)), \quad 0 \leq t \leq T. \quad (26)$$

Equations (23) and (24) follow by the following direct calculations:

$$\begin{aligned}
\frac{\partial H}{\partial \theta_1} &= \sum_{j=1}^N B_j \left( \beta_1 \alpha_1 \sum_{i=1}^N T_i(t) (\mu_i - \lambda_i) - c_2 \alpha_1 \right), \\
\frac{\partial H}{\partial \theta_2} &= \sum_{j=1}^N B_j \left( \sum_{i=1}^N T_i(t) (\beta_1 \alpha_3 (\mu_i - \lambda_i) + \beta_2 \alpha_3 (\lambda_i - \nu_i)) - c_3 \alpha_3 \right).
\end{aligned} \quad (27)$$

□

By the optimal control theory, equations (16) and (22) constitute the optimality system for the TBR model. We refer to the control in each solution to the optimality system as a potential optimal control (POC) of the DAS problem. It is seen from equation (24) that the optimality system may have more than one POC.

#### 4. Examples of the POC

For the notion of POC we introduced earlier for the DAS problem, now we provide some examples of the POC. First, the optimality system (17) and (22) is solved using the Runge–Kutta and backward Runge–Kutta fourth-order iterative procedure [34, 35].

To generate a large number of DAS examples, three real-world networks are selected: Facebook network  $G_{FA}$ , e-mail network  $G_{EM}$ , and Twitter network  $G_{TW}$ . We select the subnet of the network as the total number of nodes of the

three networks with  $N = 100$ . Let  $A_{FA}, A_{EM}$ , and  $A_{TW}$  denote the adjacency matrix of  $G_{FA}, G_{EM}$ , and  $G_{TW}$ , and the network topology is shown in Figure 3. Let the initial value  $E_0 = (T_0, B_0, R_0) = (0.7, \dots, 0.7, 0.2, \dots, 0.2, 0.1, \dots, 0.1)$ .

*Experiment 1.* Stabilities of the three states.

The parameters and their values are shown in Table 3.

As can be seen from Figure 4, in all of three networks, the expected probabilities of the three states are stable at a fixed value. Moreover, when the probability of negative evaluation in the network is larger than that of positive evaluation, nodes tend to refuse to buy the product.

*Experiment 2.* Optimal control strategies in networks.

Consider the TBR model (17) with  $G = G_{FA}, G = G_{EM}, G = G_{TW}$ ,  $\bar{\theta}_1 = 1, \bar{\theta}_2 = 1$ ,  $c_1 = 50, c_2 = 5$ , and  $c_3 = 10$ , and the remaining parameters are shown in Table 3. The optimal control  $\theta_{poc}$  is obtained by solving the optimal system, as shown in Figure 5. Figure 6 exhibits  $\theta_{poc} \cup \theta_{p,q}$ ,  $p = (0, 0.1, 0.2, \dots, 1)$  and  $q = (0, 0.1, 0.2, \dots, 1)$ . It is seen that  $J(\theta_{poc}) > J(\theta_{p,q})$ , for all  $p, q \in [0, 1]$ .  $\theta_{poc}$  is superior to all the uniform controls in the three networks in terms of expected profits. In the above experiment and 100 similar experiments, it is worth emphasizing that  $\theta_{poc}$  outperforms all static controls in terms of expected profits across all the networks, which demonstrates the optimality of  $\theta_{poc}$ .

As can be seen from Figure 6, when there is no after-sales service ( $\theta_{0,0}$ ) in the community group buying network, the expected profit of sales in the whole network is the lowest due to the influence of negative WOM. When  $q = 1$ , although  $p$  is different, the expected profit generated by community group buying is almost the same for the three networks. This phenomenon indicates that reversing negative WOM through after-sales service is more helpful in improving expected profits than operations such as cash back. Moreover, it can be seen from Figures 5 and 6 that the DAS optimal control strategies are concentrated at the initial time, which suggests the importance of timely after-sales service. Delayed or continuous after-sales service has no obvious effect on improving consumers' purchase intention and increasing expected profits.

*Experiment 3.* Effects of optimal control strategies.

As shown in Figure 7, we compare the expected probabilities of buying and refusing states without control and with the optimal control strategy. It can be inferred that, through DAS optimal control strategies, the probability of buying is greatly increased, while that of refusing buying is greatly decreased. This further proves the importance of after-sales service.

## 5. The Influence of Parameters on Expected Profits

In this section, we discuss how different parameters affect the expected profits. On the one hand, taking node 30 as an example, we discuss the effects of different parameters on

purchase intention. On the other hand, given the similar simulation results of the three networks, the e-mail network is taken as an example for illustration, as shown in Figure 8.

*Experiment 4.* Effects of parameters  $\rho, \gamma, \beta_1, \beta_2$  on purchase intention.

Let  $\rho, \gamma, \beta_1, \beta_2 = [0.1, 0.3, 0.5, 0.7, 0.9]$  respectively, and the other parameters are shown in Table 3. The probability of the node's purchase intention increases as  $\rho$  and  $\beta_1$  increase, as shown in Figures 8(a) and 8(c), and decreases as  $\gamma$  and  $\beta_2$  increase, as shown in Figures 8(b) and 8(d). This finding is consistent with the actual representations of the parameters.

*Experiment 5.* Effects of parameters  $\alpha_1, \alpha_2, \alpha_3$  on purchase intention.

Since  $\alpha_1 + \alpha_2 + \alpha_3 = 1$ , let

- (1)  $\alpha_1, \alpha_2 = [0.1, 0.2, 0.3, 0.4, 0.5]$  and  $\alpha_3 = 1 - \alpha_1 - \alpha_2$
- (2)  $\alpha_1, \alpha_3 = [0.1, 0.2, 0.3, 0.4, 0.5]$  and  $\alpha_2 = 1 - \alpha_1 - \alpha_3$
- (3)  $\alpha_2, \alpha_3 = [0.1, 0.2, 0.3, 0.4, 0.5]$  and  $\alpha_1 = 1 - \alpha_2 - \alpha_3$

When  $T = 25$ , take the probability of buying for node 30 as an example. As shown in Figure 9(a), when  $\alpha_2$  is very small, the probability changes little with the increase of  $\alpha_1$ . Specifically, despite the increased probability of silent purchase, the probability of final node purchase does not increase significantly. This is because the probability of positive WOM is fixed at a small value. When  $\alpha_2$  is large, the probability increases significantly as  $\alpha_1$  increases. When the probability of positive WOM is fixed at a large value, the probability of negative WOM decreases as the probability of silent purchase increases, so the probability of final node purchase increases significantly. The situation in Figure 9(b) is similar to that in Figure 9(a). It can be clearly seen from Figure 9(c) that the purchase probability increases with the increase of  $\alpha_2$  and decreases with the increase of  $\alpha_3$ .

Under optimal dynamic after-sales service control, the expected profit exhibits different levels of sensitivity to different parameters. Therefore, we will further discuss how the parameters affect the expected profit of the entire community group buying network later in this section.

*Experiment 6.* Effects of parameters  $\rho, \gamma, \beta_1, \beta_2$  on the expected profit.

Let  $\rho, \gamma, \beta_1, \beta_2 = [0.1, 0.3, 0.5, 0.7, 0.9]$ , respectively, and the other parameters are shown in Table 3. As can be seen from Figure 10, the expected profit of the whole network increases with the increase of  $\rho, \beta_1$  and decreases with the increase of  $\gamma, \beta_2$  after-sales service is available. Based on Figure 8, it can be concluded that when consumers' purchase intention increases, the expected profit also increases in the network.

*Experiment 7.* Effects of parameters  $\alpha_1, \alpha_2, \alpha_3$  on expected profits.

Since  $\alpha_1 + \alpha_2 + \alpha_3 = 1$ , let

- (1)  $\alpha_1, \alpha_2 = [0.1, 0.2, 0.3, 0.4, 0.5]$  and  $\alpha_3 = 1 - \alpha_1 - \alpha_2$
- (2)  $\alpha_1, \alpha_3 = [0.1, 0.2, 0.3, 0.4, 0.5]$  and  $\alpha_2 = 1 - \alpha_1 - \alpha_3$
- (3)  $\alpha_2, \alpha_3 = [0.1, 0.2, 0.3, 0.4, 0.5]$  and  $\alpha_1 = 1 - \alpha_2 - \alpha_3$

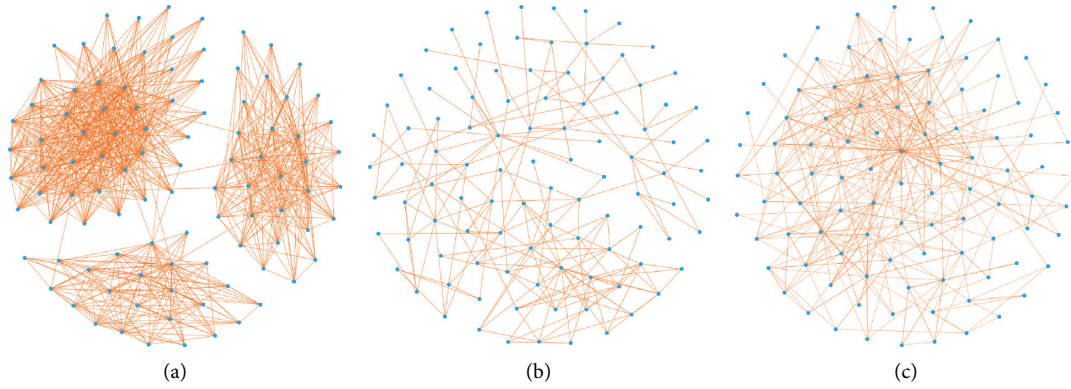


FIGURE 3: (a) Facebook network, (b) e-mail network, and (c) Twitter network.

TABLE 3: Parameters based on the network.

Parameters	$\rho$	$\gamma$	$\alpha_1$	$\alpha_2$	$\alpha_3$	$\beta_1$	$\beta_2$	$T$
Value	0.1	0.2	0.4	0.2	0.4	0.1	0.1	25

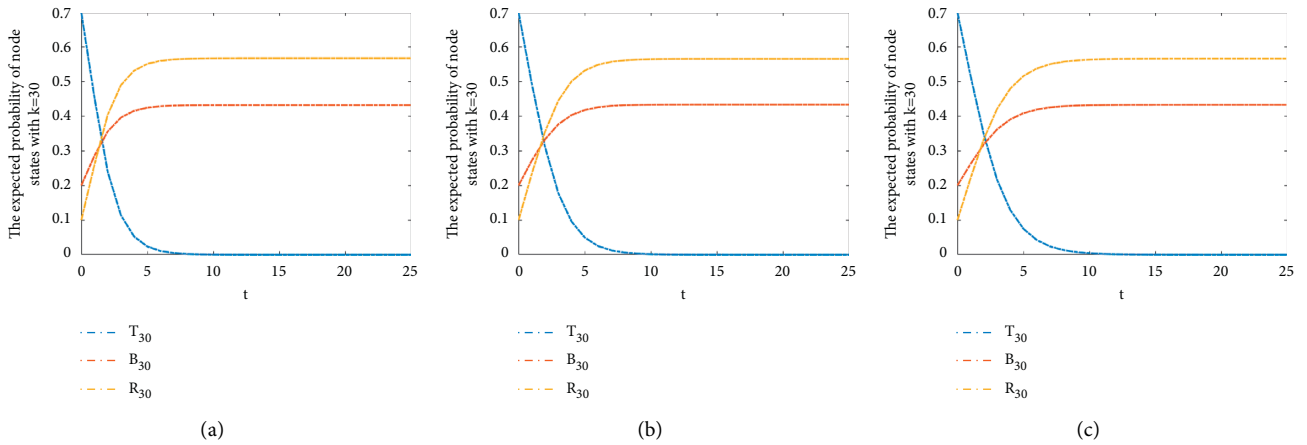


FIGURE 4: (a) Facebook network, (b) e-mail network, and (c) Twitter network.

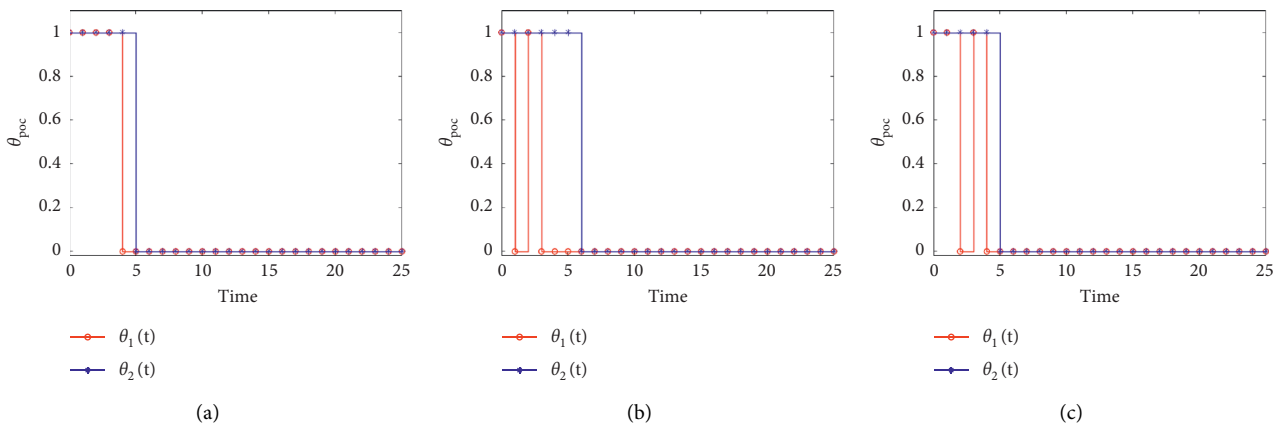


FIGURE 5: Optimal control strategies  $\theta_{poc}$  in networks: (a) Facebook network, (b) e-mail network, and (c) Twitter network.

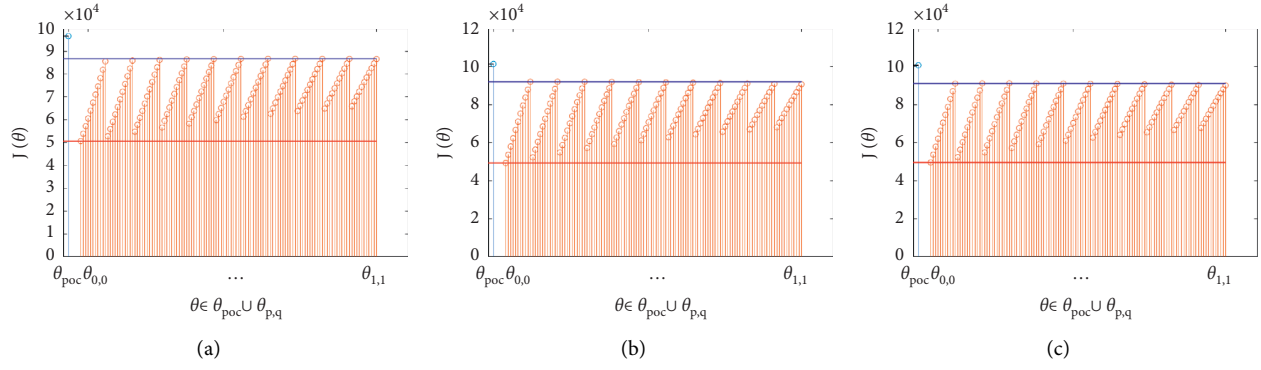


FIGURE 6: Comparison between optimal control strategy  $\theta_{poc}$  and uniform control strategy  $\theta_{p,q}$  in terms of expected profit  $J(\theta)$ : (a) Facebook network, (b) e-mail network, and (c) Twitter network.

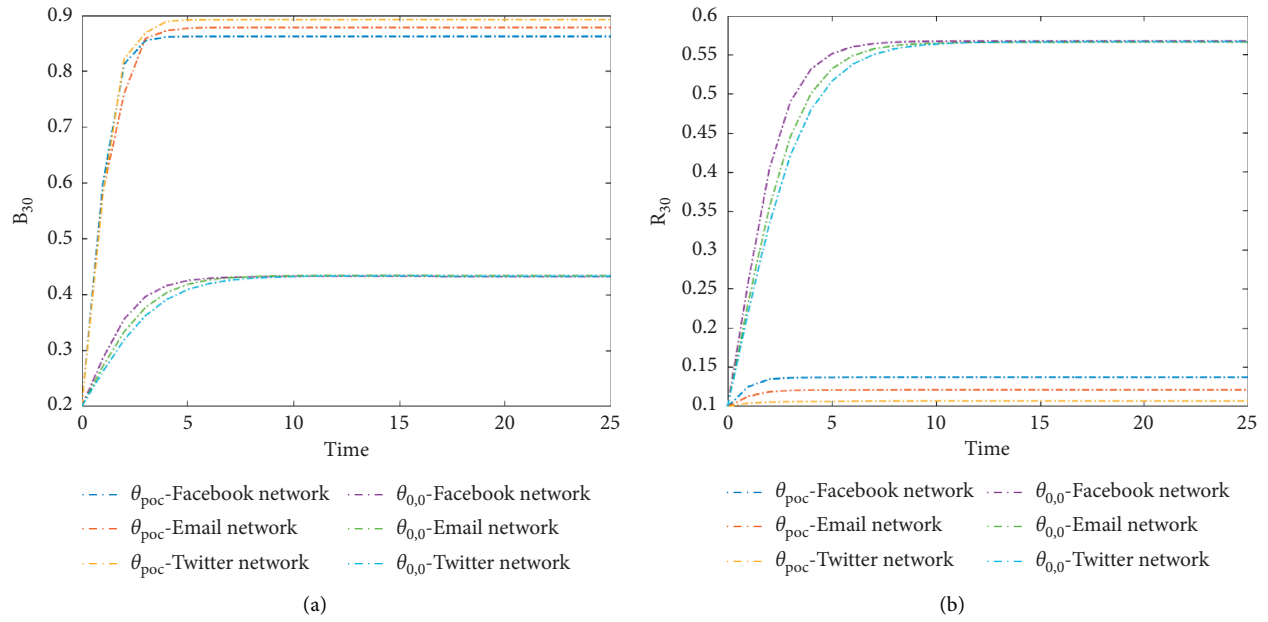


FIGURE 7: (a) Expected probability of buying for node 30 under  $\theta_{poc}$  and without control  $\theta_{0,0}$  and (b) expected probability of refusing for node 30 under  $\theta_{poc}$  and without control  $\theta_{0,0}$ .

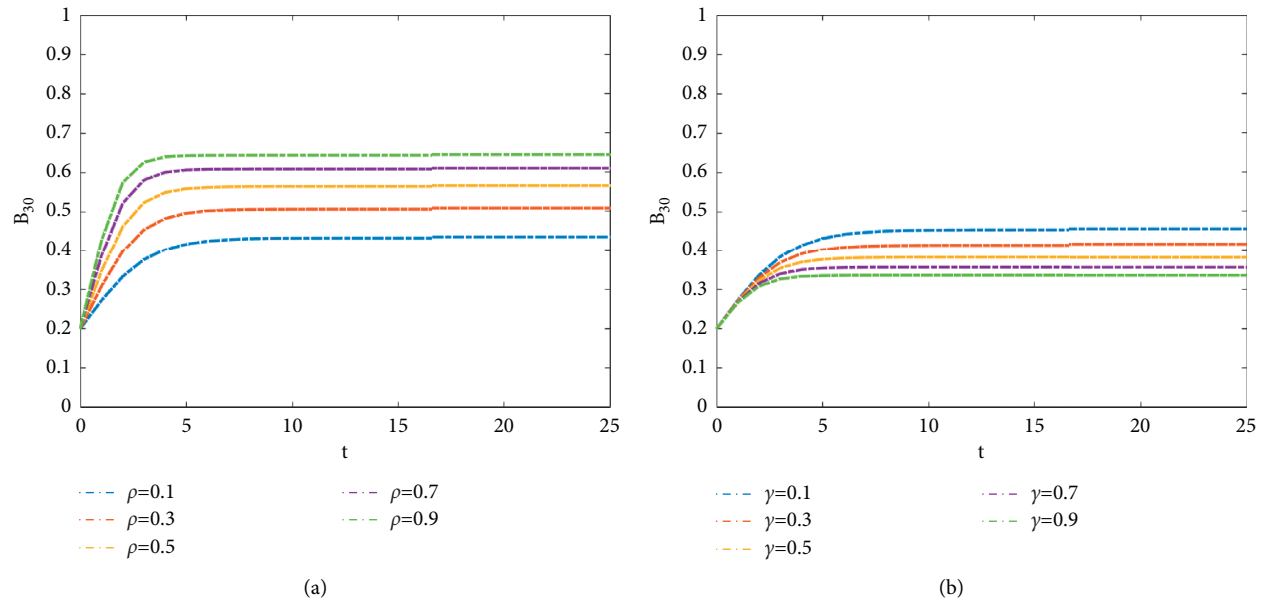


FIGURE 8: Continued.

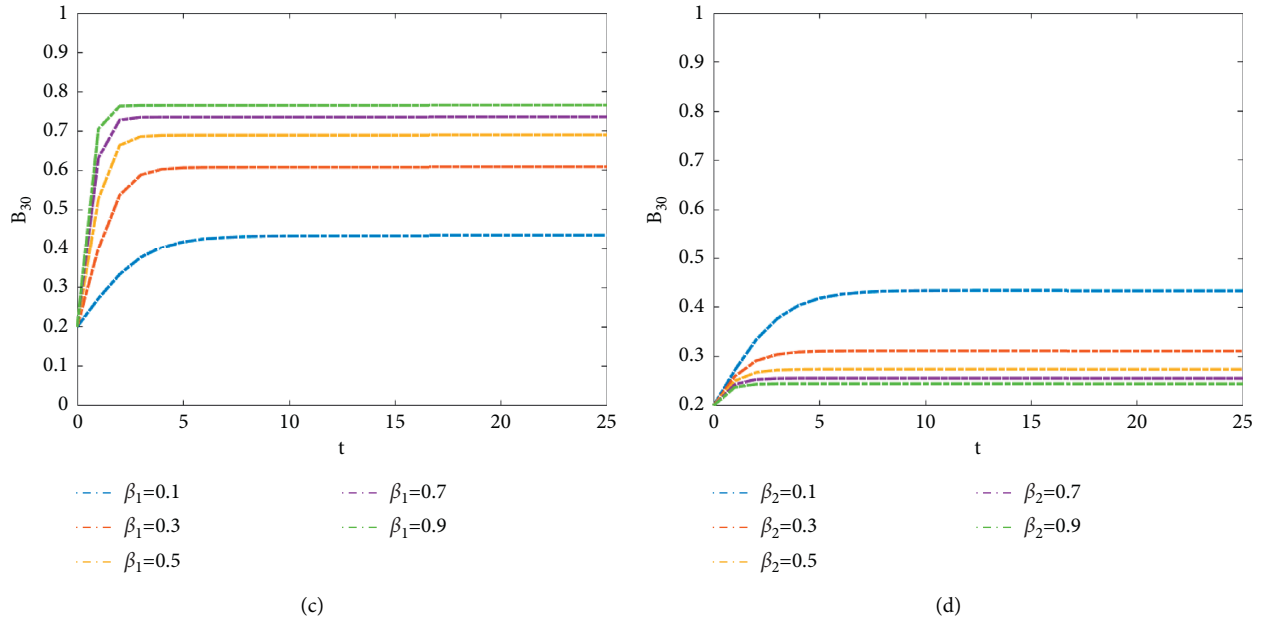


FIGURE 8: Parameters on the expected probability of buying for node 30: (a)  $\rho$ , (b)  $\gamma$ , (c)  $\beta_1$ , and (d)  $\beta_2$ .

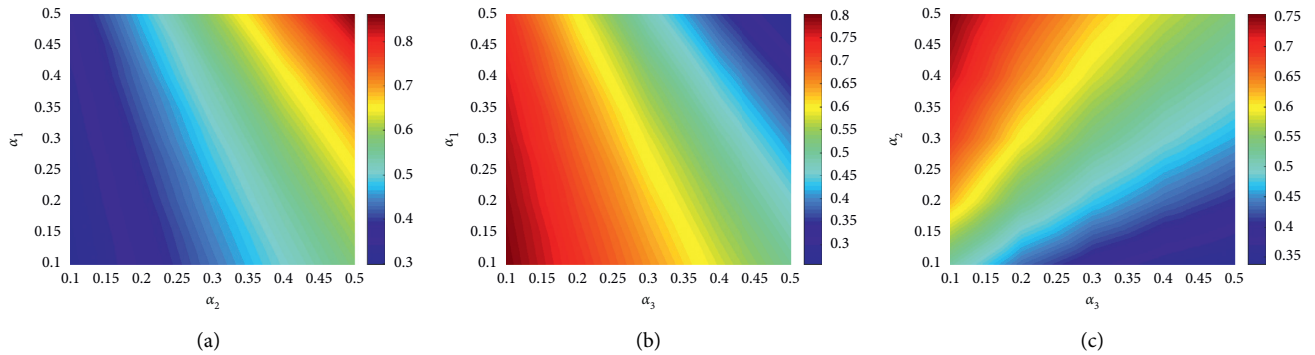


FIGURE 9: Parameters on the expected probability of buying for node 30: (a)  $\alpha_1, \alpha_2$ , (b)  $\alpha_1, \alpha_3$ , and (c)  $\alpha_2, \alpha_3$ .

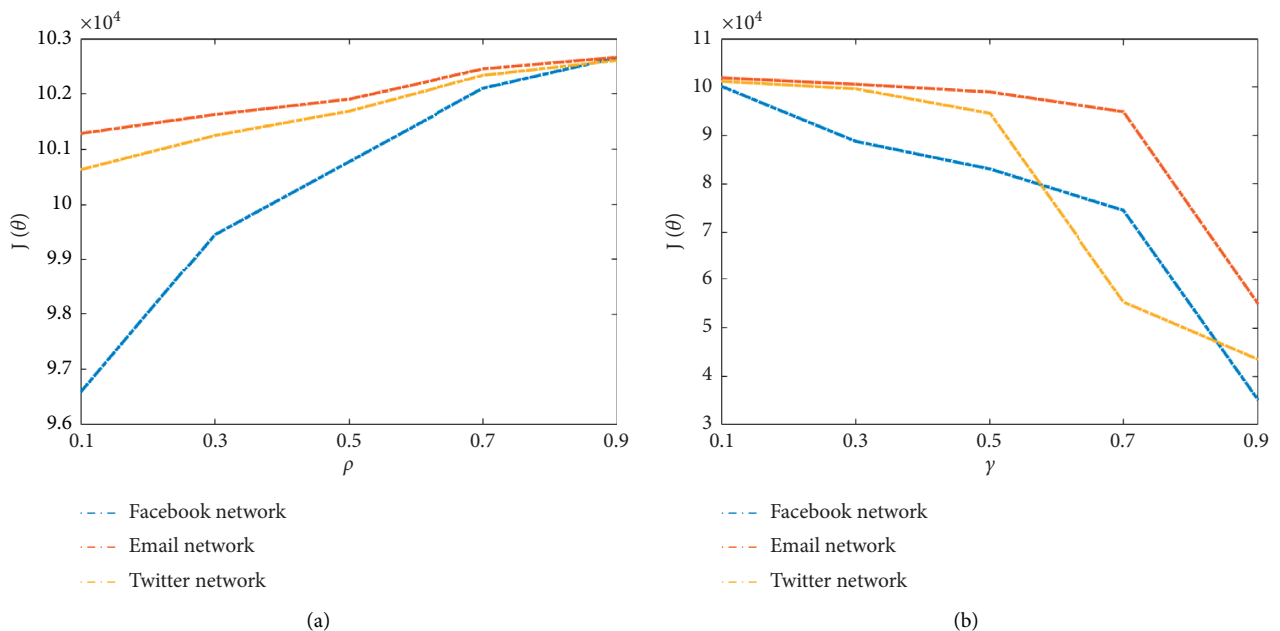


FIGURE 10: Continued.

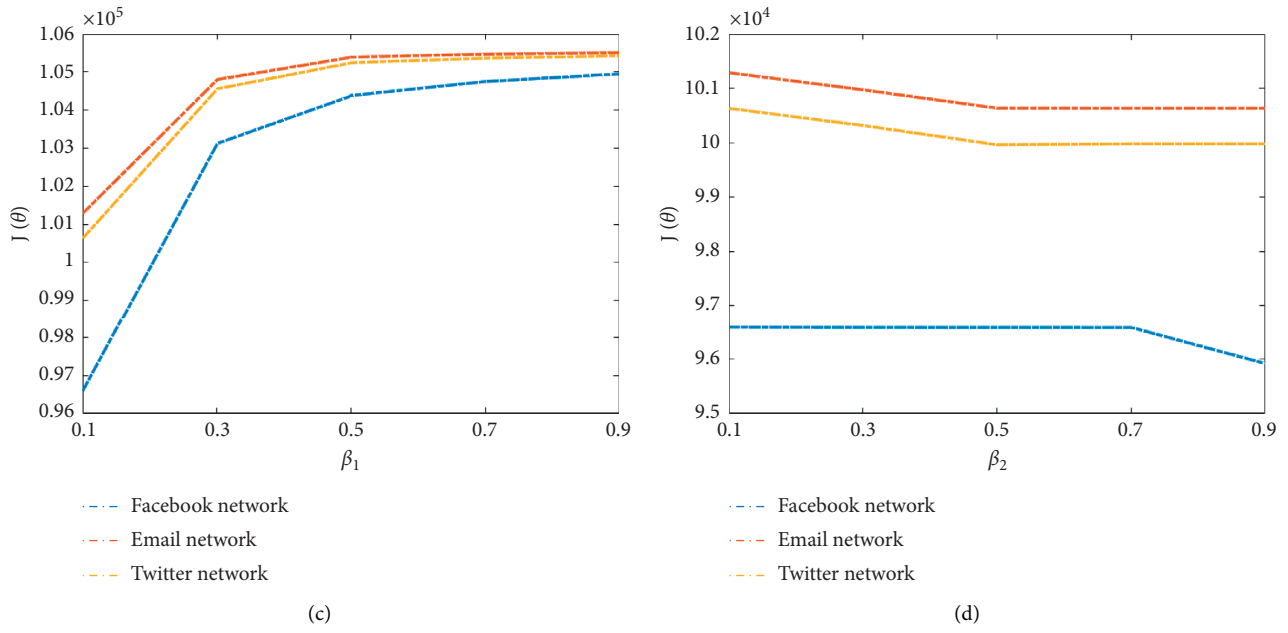


FIGURE 10: Parameters on the expected probability of buying for node 30: (a)  $\rho$ , (b)  $\gamma$ , (c)  $\beta_1$ , and (d)  $\beta_2$ .

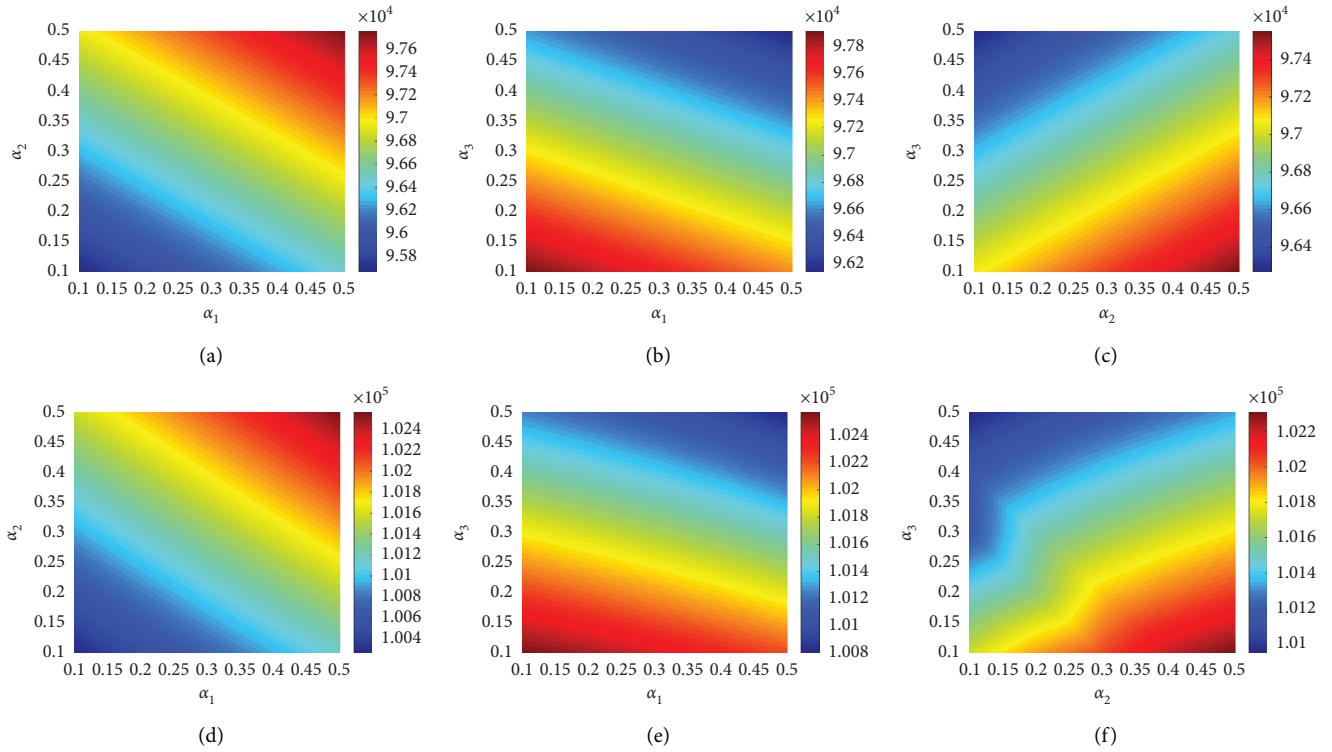


FIGURE 11: Continued.



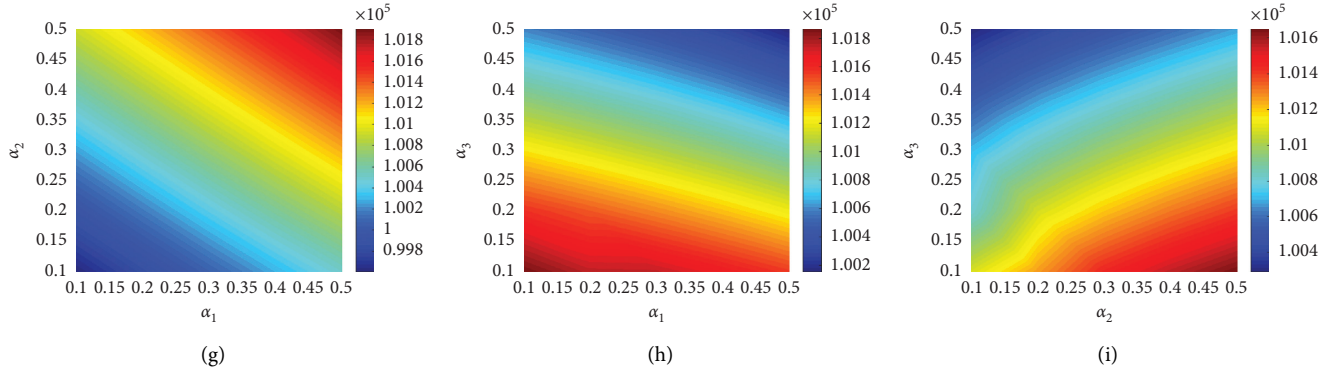


FIGURE 11: Parameters  $\alpha_1, \alpha_2, \alpha_3$  on the expected profit. (a–c)  $\alpha_1, \alpha_2, \alpha_3$  on Facebook network; (d–f)  $\alpha_1, \alpha_2, \alpha_3$  on e-mail network; (g–i)  $\alpha_1, \alpha_2, \alpha_3$  on Twitter network.

TABLE 4: Summary of experimental conclusion.

Number	Conclusion	Supporting experiments
$C_1$	The three states in the network will stabilize to a fixed constant over time	Experiment 1
$C_2$	The DAS optimal control strategy outperforms any uniform control strategy and can greatly improve the expected profit	Experiments 2 and 3
$C_3$	Reversing negative reviews is more helpful in improving expected profits than improve silent evaluation	Experiment 2
$C_4$	The probability $\rho$ of $T_i$ being converted to $B_i$ is positively correlated with expected profits	Experiments 4 and 6
$C_5$	The probability $\gamma$ of $T_i$ being converted to $R_i$ is negatively correlated with expected profits	Experiments 4 and 6
$C_6$	The probability of positive evaluation $\alpha_2$ is positively correlated with expected profits	Experiments 5 and 7
$C_7$	The probability of negative evaluation $\alpha_3$ is positively correlated with expected profits	Experiments 5 and 7
$C_8$	Probability $\beta_1$ influenced by positive WOM is positively correlated with expected profits	Experiments 4 and 6
$C_9$	Probability $\beta_2$ influenced by negative WOM is negatively correlated with expected profits	Experiments 4 and 6
$C_{10}$	When the probability $\alpha_2$ ( $\alpha_3$ ) of positive (negative) WOM is fixed and small, the probability of silent evaluation $\alpha_1$ has a weak positive (negative) correlation with purchase intention	Experiment 5
$C_{11}$	When the probability $\alpha_2$ ( $\alpha_3$ ) of positive (negative) WOM is fixed and large, the probability of silent evaluation $\alpha_1$ has a strong positive (negative) correlation with purchase intention	Experiment 5

As can be seen from Figure 11, the expected profit is not closely related to the proportion of silent customers, but is directly proportional to positive WOM and inversely proportional to negative WOM. This conclusion is consistent with the analysis in Figure 9.

The experimental conclusions are summarized in Table 4.

## 6. Conclusion

This paper aims at maximizing the expected profits of product sales in social network shopping by dynamically controlling the proportion of after-sales service investment based on word-of-mouth marketing. First, the problem is modeled as an optimal control problem. Second, a potential optimal control strategy is proposed and the optimal control problem is identified by solving the optimal system. Finally, some comparative experiments demonstrate that the proposed dynamic control strategy is superior to any uniform control strategy, and the expected profits show different levels of sensitivity to different after-sales service parameters. Therefore, the proposed dynamic after-sales investment strategy can serve as an effective approach to

maximizing the expected profits of product sales in social network shopping. In this regard, there are a number of research topics worthy of further study. The problem of balancing profits and after-sales investment can be modeled as a game theory problem to ensure maximum interests for individuals.

## Data Availability

The data used to support the findings of this study are included within the article.

## Conflicts of Interest

The authors declare no potential conflicts of interest.

## Acknowledgments

This work was supported by the National Natural Science Foundation of China, under Grant nos. 61807028, 61772449, 61572420, and 61802332, and Natural Science Foundation of Hebei Province China, under Grant no. F2019203120.

## References

- [1] “Accenture consulting,” *Report of Chinese Consumer Insight by Accenture*, Dublin, Ireland, 2014.
- [2] Dichter, “How word-of-mouth advertising works,” *Harvard Business Review*, vol. 16, 1966.
- [3] J. Chevalier, *The Effect of Word of Mouth on Sales: Online Book Reviews*, Working Papers – Yale School of Management’s Economics Research Network, Connecticut, CT, USA, 2003.
- [4] L. Leskovec, “Adamic, he dynamics of viral marketing,” *ACM Transactions on the Web*, vol. 1, 2005.
- [5] S. Hill, F. Provost, and C. Volinsky, *Viral Marketing: Identifying Likely Adopters via Consumer Networks*, Social Science Electronic Publishing, New York, NY, USA, 2005.
- [6] S. Hill, F. Provost, and C. Volinsky, “Network-based marketing: identifying likely adopters via consumer networks,” *Statistical Science*, vol. 21, pp. 256–276, 2006.
- [7] A. Vilpponen, S. Winter, and S. Sundqvist, “Network-based marketing: identifying likely adopters via consumer networks,” *Statistical Science*, vol. 21, pp. 256–276, 2006.
- [8] J. Brown, A. J. Broderick, and N. Lee, “Word of mouth communication within online communities: conceptualizing the online social network,” *Journal of Interactive Marketing*, vol. 21, no. 3, pp. 2–20, 2007.
- [9] D. D. Gunawan and K.-H. Huarng, “Viral effects of social network and media on consumers’ purchase intention,” *Journal of Business Research*, vol. 68, no. 11, pp. 2237–2241, 2015.
- [10] D. Godes and D. Mayzlin, “Firm-created word-of-mouth communication: evidence from a field test,” *Marketing Science*, vol. 28, no. 4, pp. 721–739, 2009.
- [11] J. Zhang, Y. Liu, and Y. Chen, *Social Learning in Networks of Friends versus Strangers*, Social Science Electronic Publishing, New York, NY, USA, 2015.
- [12] D. Dubois, A. Bonezzi, and M. De Angelis, “Sharing with friends versus strangers: how interpersonal closeness influences word-of-mouth valence,” *Journal of Marketing Research*, vol. 53, no. 5, pp. 712–727, 2016.
- [13] A. Timoshenko and J. R. Hauser, “Identifying customer needs from user-generated content,” *Marketing Science*, vol. 38, 2019.
- [14] Z. A. Min, B. Bf, Z. C. Ning, and E. Wf, “Mining product innovation ideas from online reviews,” *Information Processing & Management*, vol. 58, 2021.
- [15] R. Y. Du, O. Netzer, D. A. Schweidel, and D. Mitra, “Capturing marketing information to fuel growth,” *Journal of Marketing*, vol. 85, no. 1, pp. 163–183, 2021.
- [16] T. Zhang, P. Li, L.-X. Yang, X. Yang, Y. Y. Tang, and Y. Wu, “A discount strategy in word-of-mouth marketing,” *Communications in Nonlinear Science and Numerical Simulation*, vol. 74, pp. 167–179, 2019.
- [17] J. Chen, L. X. Yang, D. W. Huang, X. Yang, and Y. Y. Tang, “Dynamic discount pricing in competitive marketing,” *IEEE Access*, vol. 7, pp. 14534–145347, 2019.
- [18] H. Peng, K. Huang, L.-X. Yang, X. Yang, and Y. Y. Tang, “Dynamic maintenance strategy for word-of-mouth marketing,” *IEEE Access*, vol. 8, pp. 126496–126503, 2020.
- [19] M. Herrera, G. Armelini, and E. Salvaj, “Understanding social contagion in adoption processes using dynamic social networks,” *PLoS One*, vol. 10, no. 10, Article ID e0140891, 2015.
- [20] M. Wu, L. Wang, L. Ming, and H. Long, “An approach based on the SIR epidemic model and a genetic algorithm for optimizing product feature combinations in feature fatigue analysis,” *Journal of Intelligent Manufacturing*, vol. 26, pp. 1–11, 2015.
- [21] M. Pazoki and H. Samarghandi, “Word-Of-Mouth and estimating demand based on network structure and epidemic models,” *European Journal of Operational Research*, vol. 291, 2021.
- [22] S. Soobin and J. SooCheong, “A negative or positive signal? The impact of food recalls on negative word-of-mouth (N-WOM),” *Journal of Hospitality and Tourism Management*, vol. 47, pp. 150–158, 2021.
- [23] F. Septianto, G. Northey, T. M. Chiew, and L. Ngo, “Hubristic pride & prejudice: the effects of hubristic pride on negative word-of-mouth,” *International Journal of Research in Marketing*, vol. 37, 2020.
- [24] H. H. Chang, Y.-C. Tsai, K. H. Wong, J. W. Wang, and F. J. Cho, “The effects of response strategies and severity of failure on consumer attribution with regard to negative word-of-mouth,” *Decision Support Systems*, vol. 71, pp. 48–61, 2015.
- [25] P. Matthew and A. Laurence, “I should have known better!: when firm-caused failure leads to self-image concerns and reduces negative word-of-mouth,” *Journal of Business Research*, vol. 116, 2020.
- [26] C. Riza and S. Hyunju, “The effects of harm directions and service recovery strategies on customer forgiveness and negative word-of-mouth intentions,” *Journal of Retailing and Consumer Services*, vol. 27, pp. 103–112, 2015.
- [27] M. S. Balaji, K. W. Khong, and A. Chong, “Determinants of negative word-of-mouth communication using social networking,” *Information & Management*, vol. 53, 2016.
- [28] T. Verhagen, A. Nauta, and F. Feldberg, “Negative online word-of-mouth: behavioral indicator or emotional release?” *Serie Research Memoranda*, vol. 29, pp. 1430–1440, 2012.
- [29] M. D. Dalman, S. Chatterjee, and J. Min, “Negative word of mouth for a failed innovation from higher/lower equity brands: moderating roles of opinion leadership and consumer testimonials,” *Journal of Business Research*, vol. 115, pp. 1–13, 2020.
- [30] W. Weitzl, C. Hutzinger, and S. Einwiller, “An empirical study on how webcare mitigates complainants’ failure attributions and negative word-of-mouth,” *Computers in Human Behavior*, vol. 89, pp. 316–327, 2018.
- [31] E. M. Stein and R. Shakarchi, *Real Analysis: Measure Theory, Integration, & Hilbert Spaces*, Princeton University Press, New Jersey, NJ, USA, 2005.
- [32] D. Liberzon, *Calculus of Variations and Optimal Control Theory: A Concise Introduction*, Princeton University Press, New Jersey, NJ, USA, 2012.
- [33] R. C. Robinson, *Calculus of Variations and Optimal Control Theory: A Concise an Introduction to Dynamical Systems: Continuous and Discrete*, American Mathematical Society, Providence, RI, USA, 2004.
- [34] S. Lenhart and J. T. Workman, *Optimal Control Applied to Biological Models*, Champion and Hall/CRC, London, UK, 2007.
- [35] J. T. K. Soovoojeet, “A mathematical study of a prey–predator model in relevance to pest control,” *Nonlinear Dynamics*, vol. 74, no. 3, pp. 667–683, 2013.

## Research Article

# Credit Rating Model of Small Enterprises Based on Optimal Discriminant Ability and Its Empirical Study

Zhanjiang Li  and Lin Guo 

*College of Economics and Management, Inner Mongolia Agricultural University, Hohhot, China*

Correspondence should be addressed to Zhanjiang Li; [lizhanjiang582@163.com](mailto:lizhanjiang582@163.com)

Received 25 September 2021; Accepted 23 October 2021; Published 5 November 2021

Academic Editor: Sameh S. Askar

Copyright © 2021 Zhanjiang Li and Lin Guo. This is an open access article distributed under the Creative Commons Attribution License, which permits unrestricted use, distribution, and reproduction in any medium, provided the original work is properly cited.

As an important part of the national economy, small enterprises are now facing the problem of financing difficulties, so a scientific and reasonable credit rating method for small enterprises is very important. This paper proposes a credit rating model of small enterprises based on optimal discriminant ability; the credit score gap of small enterprises within the same credit rating is the smallest, and the credit score gap of small enterprises between different credit ratings is the largest, which is the dividing principle of credit rating of small enterprises based on the optimal discriminant ability. Based on this principle, a nonlinear optimization model for credit rating division of small enterprises is built, and the approximate solution of the model is solved by a recursive algorithm with strong reproducibility and clear structure. The small enterprise credit rating division not only satisfies the principle that the higher the credit grade, the lower the default loss rate, but also satisfies the principle that the credit group of small enterprises matches the credit grade, with credit data of 3111 small enterprises from a commercial bank for empirical analysis. The innovation of this study is the maximum ratio of the sum of the dispersions of credit scores between different credit ratings and the sum of the dispersions of credit scores within the same credit rating as the objective function, as well as the default loss rate of the next credit grade strictly larger than the default loss rate of the previous credit grade as the inequality constraint; a nonlinear credit rating optimal partition model is constructed. It ensures that the small enterprises with small credit score gap are of the same credit grade, while the small enterprises with large credit score gap are of different credit grades, overcoming the disadvantages of the existing research that only considers the small enterprises with large credit score gap and ignores the small enterprises with small credit score gap. The empirical results show that the credit rating of small enterprises in this study not only matches the reasonable default loss rate but also matches the credit status of small enterprises. The test and comparative analysis with the existing research based on customer number distribution, K-means clustering, and default pyramid division show that the credit rating model in this study is reasonable and the distribution of credit score interval is more stable.

## 1. Introduction

Credit rating plays an extremely important role in the global economy. The unreasonable classification of credit rating may lead to the bankruptcy of enterprises, banks, and other institutions at the least or to financial crisis at the worst. For example, in 2011, Standard & Poor's downgraded the sovereign credit rating of the United States from AAA to AA, causing shocks in the global financial market [1]. With the increasing social development and people's demand, small enterprises are playing an increasingly important role and making great contributions to the development of national

economy. However, due to the characteristics of small enterprises, such as imperfect financial information and nonstandard management, their credit rating is difficult; and, in order to reduce the credit risk, banks and other financial institutions adopt the strategy of reluctance or even not lending to small enterprises, which leads to the difficulty of small enterprises in loan and financing and restricts their development. Therefore, reasonable and scientific credit rating method can enable enterprises to effectively predict their own risk status and timely adjustment of capital structure and reduce the credit risk, and it can provide a basis for banks to make loan pricing and loan decisions,

reduce the potential loss of banks, improve the profitability and core competitiveness of banks, and contribute to the stability of the financial market. This paper proposes a credit rating model of small enterprises based on optimal discriminant ability, which not only matches the reasonable default loss rate but also matches the credit status of small enterprises. This plays a very important role in alleviating the financing difficulties of small enterprises and strengthening the risk control of banks and other financial institutions.

At present, the research on enterprise credit rating is mainly divided into four aspects. The first is a credit rating based on a customer's score. According to the customer's credit score, Bank of China classified the enterprise into ten credit grades, such as AAA, AA, A, BBB, BB, B, and CCC; customers with credit scores of [90,100] were classified as AAA and [80,90) as AA, with each credit rating decreased by 10 points [2]. Agricultural Bank of China divided customers into eight credit grades, namely, AAA+, AAA, AA+, AA, A+, A, B and C; customers with credit scores of [95,100] were classified as AAA+, [90,95) as AAA, and so forth. For every five points that a customer's credit score dropped, it dropped one credit grade [3]. Moon et al. proposed a technology credit rating system based on empirical data of the technology scoring model, called the crossover matrix, which divided customers into ten credit grades according to their credit scores. Customers with credit scores greater than 90 were classified as AAA, those with credit scores between 85 and 89 were classified as AA, and so forth [4]. The second is the credit ratings based on the probability of default. Gupton, based on the credit measurement model of Credit Metrics, divided the loan customers into eight credit grades of AAA, AA, A, BBB, BB, B, CCC, and D according to their different default probabilities [5]. Lyra et al. divided default probability through threshold acceptance method and proposed a new method to calculate the number of defaults of each credit grade to verify the accuracy of the rating system [6]. Zhang used the characteristic function to describe the characteristics of the number of loans during the investigation period and proposed a default probability measurement method based on default intensity, which provided a new idea for banks and other financial institutions to conduct credit rating [7]. Zhu et al. divided enterprises into five credit grades, A, B, C, D, and E, through Lasso logistic regression. Enterprises with default probability less than 0.2 were classified as A, 0.2-0.3 as B, 0.3-0.4 as C, and 0.4-0.5 as D. Enterprises with default probability greater than 0.5 were classified as grade E [8]. The third is the credit rating based on the distribution of the number of customers. Duan and Li improved the PD-implied rating (PDiR) methodology by targeting the historical credit migration matrix rather than simply default rates to classify credit grades [9]. Chi et al. expanded the small sample according to the logarithmic distribution law and finally divided customers into 9 credit grades based on the bell-shaped distribution. The results showed that the rating results of this model are consistent with those of authoritative institutions [10]. According to the bell-shaped distribution of the number of customers, Chi et al. divided peasant households' credit scores into 9 credit grades, such as AAA, AA, and A,

so as to avoid the unreasonable phenomenon of excessive concentration of samples in AAA or C levels and ensure that most samples are concentrated in A and BBB levels [11]. Zhang and Chi established a multiobjective programming model with the minimum absolute value of the difference between the actual customer ratio and the ideal customer ratio based on normal distribution as the first objective function and the minimum difference between the loss rates of adjacent credit grades as the second objective function. The results showed that this method not only ensured the balance between the two criteria but also avoided the phenomenon of excessive concentration of customers on specific credit ratings [12]. The last is a credit rating based on default loss rates. On the basis of considering the default loss rate, Zhao et al. maximized the sum of the difference between the credit score of the last sample of the previous credit grade and the first sample of the next credit grade as the objective function and established the credit rating model with the strict increase of the default loss rate of each grade as the constraint condition, so as to ensure that customers with large credit differences are divided into different credit grades [13]. Shi et al. took the maximum number of loan merchants above the critical point of the bank's target profit and the smallest gap in the default loss rate of adjacent merchants as the objective function and the increasing default loss rate and the realization of the bank's target profit as the constraint conditions. A multiobjective programming model is constructed to classify credit ratings, which can ensure that banks can achieve the target profit [14]. Chi and Yu took the maximum algebraic sum of the maximum absolute values of the difference between the cumulative frequency of nondefaulting customers and the cumulative frequency of defaulting customers as the objective function, with the loss rate of each credit grade strictly increasing as the main constraint condition; a credit rating model was built to ensure that credit grades could significantly distinguish customers with large differences in default possibilities [15]. Shi et al. proposed a credit rating model based on the influence of key macroeconomic variables on credit decisions of commercial banks and loss given default (LGD) and conducted an empirical analysis based on the bank data of 2,044 farmers in China. The results showed that, in some cases, a higher credit rating may lead to a higher LGD [16]. Later, in order to solve the mismatch between credit ratings and default loss rate, Shi et al. proposed a risk rating matching standard to minimize the default loss rate of high credit rating loans and tested the method using three credit datasets from China [17]. Zhou (2021) sorted loan enterprises according to their credit scores from high to low and then found the credit rating results that meet the higher credit rating and lower default loss rate by adjusting the upper and lower limits of credit scores of each grade [18].

Existing credit rating research is divided from the perspectives of customer credit score [2-4], default probability [5-8], and customer number distribution [9-12]; the actual default loss rate of customers is not taken into account, so it may occur that the customer has not only a higher credit grade but also a higher default loss rate. In addition, although there is some research on credit rating from the perspective of default

loss rate [13–18], it is not strictly guaranteed that customers with small credit score gap can be divided into the same credit grade, while customers with large credit score gap can be divided into different credit grades. In view of the above situation, this paper constructs a nonlinear optimal credit rating model, which not only ensures that the credit rating matches the default loss rate but also ensures that the credit rating matches the credit status of small enterprises.

The contribution of this paper is mainly divided into two aspects. First, we propose a credit rating model of small enterprises based on optimal discriminant ability, the maximum ratio of the sum of the dispersions of credit scores between different credit ratings and the sum of the dispersions of credit scores within the same credit rating as the objective function, and the default loss rate of the next credit grade strictly larger than the default loss rate of the previous credit grade as the inequality constraint, as well as through recursive algorithm to solve the model. It ensures that the small enterprises with small credit score gap are of the same credit grade, while the small enterprises with large credit score gap are of different credit grades, which overcomes the disadvantages of the existing research that only considers the small enterprises with large credit score gap and ignores the small enterprises with small credit score gap.

Second, we make empirical analysis of the credit data of 3111 small enterprises from a commercial bank and make comparative analysis with the small business credit rating model based on the distribution of the number of customers, the K-means clustering, and the default pyramid. The results show that the credit rating model constructed in this paper based on the optimal discriminant ability is reasonable and the interval distribution of credit score is more stable.

The article is organized as follows. Section 2 discusses the principle of credit rating model construction; Section 3 describes the methodology of credit rating model construction; Section 4 explains the specific process of credit rating model construction, tests the model, and compares the model to the traditional models; and Section 5 draws conclusions and summarizes the innovative points of the research.

## 2. Principle of Credit Rating Model Based on Optimal Discriminant Ability

*2.1. Principle of Credit Rating Model.* The first principle is that the credit rating matches the default loss rate. A higher credit grade should correspond to a lower default loss rate, and a lower credit grade should correspond to a higher default loss rate. If the credit rating of a small enterprise does not meet this principle, when the credit grade of small enterprise is high, banks and other financial institutions will give the enterprise a lower loan interest rate, but the high default loss rate of the enterprise indicates that the default risk of the enterprise is high, and the banks and other financial institutions may face the risk of not receiving the principal and interest back. When the credit rating of small enterprises is low and the default loss rate is low, the bank and other financial institutions will refuse the loan or loan at a higher interest rate, and the bank will also face the risk of customer loss.

The second principle is that the credit rating matches the credit status of small enterprises. Credit rating should ensure that small enterprises with small credit score gaps are divided into the same credit grade and small enterprise with large credit score gaps are divided into different credit grades. If the credit rating cannot identify the default risk of small enterprises to the maximum extent, it is unreasonable that small enterprises with high default risk and small enterprises with low default risk are in the same credit grade. As a result, the credit rating of small enterprises is chaotic, which is not conducive to the loan pricing and decision-making of banks and other financial institutions.

### 2.2. The Difficulty of the Problem

*Difficulty 1.* The first difficulty of this study is how to avoid ineffective and multiple random classification of credit grade in the case of large sample size.

*Difficulty 2.* The second difficulty of this study is how to ensure that the credit rating can identify the default risk of small enterprises to the greatest extent, so that small enterprises with small credit score gap are in the same credit grade, and small enterprises with large credit score gap are in different credit grades.

### 2.3. The Method to Solve the Difficulty

*The Method to Solve Difficulty 1.* The credit rating should meet the principle of matching the credit rating with the default loss rate. The constraint condition is that the default loss rate of the following credit grade is strictly higher than the default loss rate of the previous credit grade. A nonlinear optimization model is constructed to divide the credit grade and ensure that the divided credit grade matches the default loss rate.

*The Method to Solve Difficulty 2.* The maximum sum of credit score deviations between different credit grades indicates that the credit score gap of small enterprises with different credit grades is large, while the minimum sum of credit score deviations within the same credit grade indicates that the credit score gap of small enterprises with same credit grade is small. Therefore, the maximum ratio of the sum of the deviations of credit scores between different credit grades and the sum of the deviations within the same grade is taken as the objective function, and a nonlinear optimization model is built to divide credit grades to ensure that the divided credit grades match the credit status of small enterprises.

The principle of credit rating model for small enterprises based on optimal discriminant ability is shown in Figure 1.

## 3. Construction of Credit Rating Model Based on Optimal Discriminant Ability

*3.1. Establishment of the Objective Function.* Assume that  $K$  is the number of credit ratings;  $N$  is the total number of small enterprises;  $n_k$  is the number of small enterprises with credit rating  $k$ ;  $\bar{S}^k$  is the average credit score for small enterprises

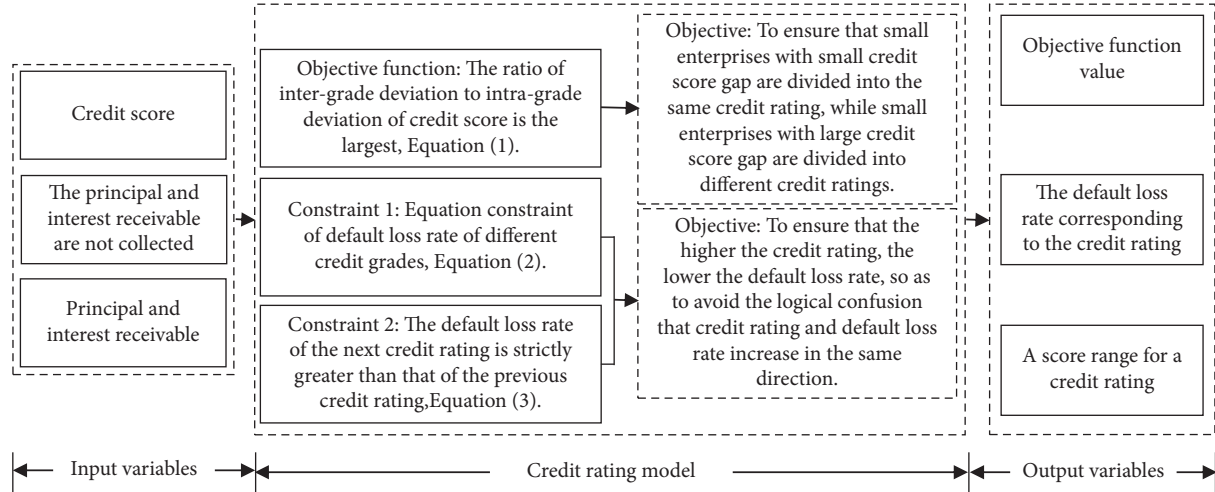


FIGURE 1: The principle of credit rating model for small enterprises based on optimal discriminant ability.

with credit rating  $k$ ;  $\bar{S}$  is the average of all small enterprise credit scores;  $q_k$  is an artificial positive weighting factor;  $q_k$  here takes the prior probability  $n_k/N$ ;  $\sigma_k^2$  is the variance of the credit score of small enterprises with credit rating  $k$ . The objective function is as follows [19]:

$$\text{Obj: } \max f = \frac{\sum_{k=1}^K n_k (\bar{s}^k - \bar{s})^2}{\sum_{k=1}^K q_k \sigma_k^2}. \quad (1)$$

Regarding the economic meaning of equation (1), the molecule of the objective function is the difference between the mean value of the credit scores of small enterprises of each credit grade and the mean value of the credit scores of all small enterprises; the larger the value is, the larger the credit score gap of small enterprises with different credit grades is. The denominator is the credit score deviation of small enterprises within each credit grade; the smaller this value is, the smaller the credit score gap of small enterprises with the same credit grade is. The objective function reflects the principle that credit rating should match the credit status of small enterprises.

For the difference between equation (1) and existing research [13], existing research only considers small enterprises with large credit score gaps and ignores small enterprises with small credit score gaps. This study also considered small enterprise groups with large and small credit score gaps; it avoids the logical confusion that small enterprises with large credit score gaps are divided into the same credit grade, while small enterprises with small credit score gaps are divided into different credit grades.

As regards innovation of equation (1), taking the maximized ratio of the sum of the dispersion of credit scores between different credit grades and the sum of the dispersion of credit scores within the same credit grade as the objective function, a nonlinear optimal division model of credit ratings is established. It ensures that groups of small enterprises with small credit score gaps are divided into the same credit grade and groups of small enterprises with large credit score gaps are divided into different credit grades, and it overcomes the disadvantage that the existing research only

considers the small enterprises with large credit score gap and ignores the small enterprises with small credit score gap.

### 3.2. Establishment of Constraints

**3.2.1. Establishment of the Equation Constraint of Default Loss Rate.** Assume that  $LGD_k$  is the default loss rate of the  $k$ th credit rating;  $L_{ki}$  is the annual receivable and uncollected principal and interest of the  $i$ th small enterprise with the  $k$ th credit rating;  $G_{ki}$  is the annual receivable principal and interest of the  $i$ th small enterprise with the  $k$ th credit rating. The default loss rate of the  $k$ th credit rating is as follows [13]:

$$LGD_k = \frac{\sum_{i=1}^{n_k} L_{ki}}{\sum_{i=1}^{n_k} G_{ki}}. \quad (2)$$

Regarding the economic meaning of equation (2), the default loss rate of each credit grade is the ratio of the sum of the receivable and uncollected principal and interest of all the small enterprises in the grade to the sum of the receivable principal and interest of all the small enterprises in the grade.

For the function of equation (2), the calculation of the default loss rate based on the annual receivable and uncollected principal and interest and annual receivable principal and interest of small enterprises can truly reflect the losses of banks and other financial institutions, avoiding the disadvantages of dividing credit grade only based on default probability and customer number distribution that cannot reflect the real losses of banks.

**3.2.2. Establishment of Inequality Constraint of Default Loss Rate.** In the division of credit grade, the default loss rate of the next credit grade is strictly higher than the default loss rate of the previous credit grade. The inequality constraint of the default loss rate is as follows [13]:

$$\text{s.t.: } 0 < LGD_1 < LGD_2 < \dots < LGD_{k-1} < LGD_k \leq 1. \quad (3)$$

Regarding the economic meaning of equation (3), in practice, only national debt is risk-free; that is, the default

loss rate is 0, so the default loss rate corresponding to the highest credit rating should be greater than 0. When the default loss rate is 1, it means that all the small enterprises corresponding to this grade are in default, which is possible in practice, so the default loss rate corresponding to the lowest credit grade should be less than or equal to 1.

For the function of equation (3), the default loss rate of the next credit grade is strictly higher than the default loss rate of the previous credit grade as the constraint condition for constructing the credit rating model. It ensures that, with the decrease of credit ratings, the corresponding default loss rate rises, which meets the principle that the credit rating should match the default loss rate, and it avoids the unreasonable phenomenon that the credit grade is high but the corresponding default loss rate is also high.

**3.3. Solution of Credit Rating Model.** This research mainly adopts the recursive idea to solve the credit rating model. Here, it directly uses the 9 divided credit grades to illustrate. The specific steps of solving are as follows:

Step 1: Rank small enterprises by credit score from largest to smallest, as shown in columns (2)–(4) of Table 1.

Step 2: Set the credit grade number  $K$  and the threshold value of the objective function.

Step 3: We randomly select a AAA credit grade and then a AA credit grade and calculate the default loss rate for each grade. If the default rate of AA is lower than the default rate of AAA, the AAA grade is reselected at random; if the constraint conditions are satisfied, then we continue to randomly select the credit grade of A and so on, so as to obtain multiple groups of credit rating results satisfying the constraint conditions.

Step 4: We put the credit scores of several groups of small enterprises satisfying the constraint conditions into the objective function and select the credit rating results whose objective function value is greater than the threshold value. At this time, the credit rating results obtained are a set of solutions under the threshold value of the objective function.

Step 5: Select the critical value of the threshold according to the operating efficiency, increase the threshold of the objective function continuously, and continue to repeat Steps 3 and 4. When the objective function value is close to the critical value of the threshold, the dichotomy is used to continuously approach the threshold value to determine the global optimal solution, and the final result of credit rating is obtained. The detailed flowchart is shown in Figure 2.

### 3.4. Test of Credit Rating Model

**3.4.1. Purpose of the Test.** Through the test, it is proved that the nonlinear optimization model of credit rating constructed in this study is reasonable and stable.

**3.4.2. Test Formula.** Use STDEV index value to test the stability of the credit score interval distribution. Assume that  $I_k$  is the length of the credit score interval of the  $k$ th credit grade;  $\bar{I}$  is the mean length of credit score interval of all  $K$  credit grades. The STDEV index value is as follows [20]:

$$\text{STDEV} = \sqrt{\frac{\sum_{i=1}^K (I_k - \bar{I})^2}{K - 1}}. \quad (4)$$

Regarding the economic meaning of equation (4), the smaller the STDEV index value is, the more stable the distribution of credit score interval is.

### 3.4.3. Test Standards

(1) *Reasonableness Standard.* If the final credit rating results meet the standard that the default loss rate increases with the decline of credit rating, it indicates that the credit rating model constructed in this study is reasonable.

(2) *Stability Standard.* By comparison with other models, the smaller the STDEV index value of the credit rating model constructed in this study is, the more stable the distribution of credit score interval in this study is.

## 4. Empirical Study

**4.1. Sample Source.** This study selects the loan data of 3111 small enterprises from a Chinese commercial bank as the empirical sample, including 3040 nondefaulting small enterprises and 71 defaulting small enterprises. The construction process of credit evaluation index system of small enterprises is derived from literature [21], and the results are listed in column 3 of Table 2. The index weights are obtained through logistic regression, and the results are listed in column 4 of Table 2. The standard credit score can be obtained based on the weight of the indicators and standardized data for small enterprises and are listed in column 2 of Table 1 in a descending order. It should be pointed out that the construction of the indicator system of small enterprises, the determination of the weight of the indicator, and the measurement of the credit score are not part of the content of this study, so they will not be repeated here. The specific results are shown in Tables 1 and 2.

**4.2. Determination of Credit Rating Results.** Based on the credit ratings of the international rating agencies Standard & Poor's and Moody's, this study divides small enterprises into 9 credit grades, namely, AAA, AA, A, BBB, BB, B, CCC, CC, and C; that is,  $K$  is 9.

**4.2.1. Credit Rating Satisfying Constraint Conditions and Threshold of Objective Function.** The threshold value of the objective function 35000 and a randomly selected credit rating that meets the constraint conditions are taken as an example to illustrate.

TABLE 1: Small enterprise credit rating data.

(1) No.	(2) Standard credit score	(3) Receivable principal and interest	(4) Receivable and uncollected principal and interest	(5) Default status
1	100.0000	2160388.94	0.00	0
...	...	...	...	...
1408	81.2203	32340576.16	29855947.12	1
1409	81.1925	8443839.30	0.00	0
...	...	...	...	...
3111	0.0000	78904.72	78904.72	1

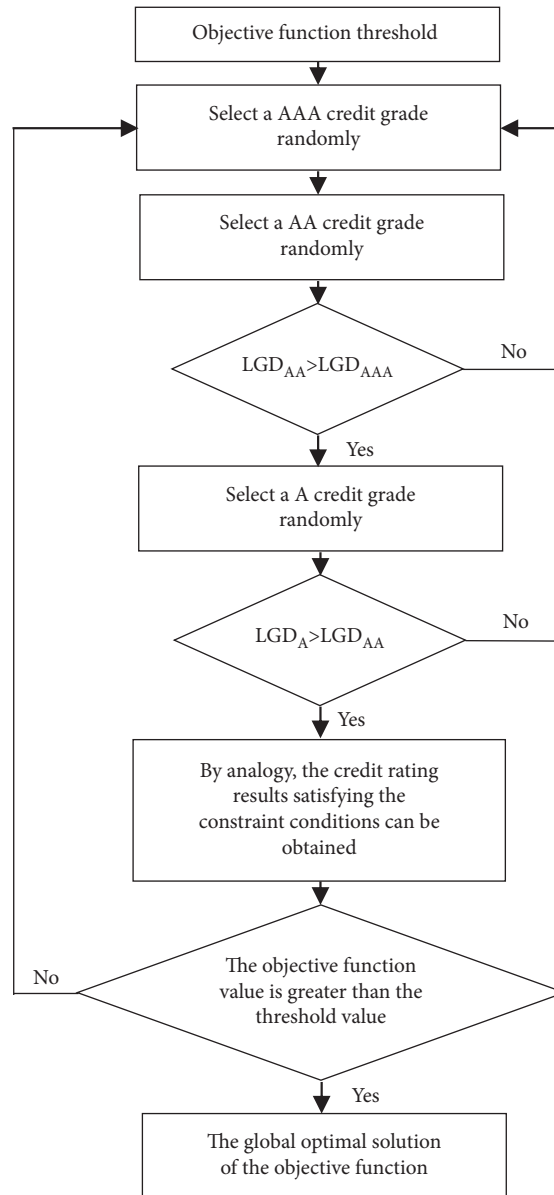


FIGURE 2: Flowchart of solving credit rating model.

(1) *Credit Rating Satisfying Constraint Conditions.* The standard credit score  $S_i$ , receivable principal and interest  $G_i$ , receivable and uncollected principal and interest  $L_i$ , and the default status of small enterprises are listed in the relevant columns in Table 1 according to the credit score from large to small.

Select a AAA credit grade and a AA credit grade at random. Assume that the number of small enterprises with AAA credit grade is 1502 and the number of small enterprises with AA credit grade is 288; that is, the starting and ending numbers of small enterprises with AAA credit grade and AA credit grade are [1–1502] and [1503–1790],



TABLE 2: Small enterprise credit index system and weight.

(1) No.	(2) Criterion layer	(3) Indicator name	(4) Index weight
1		Net profit cash content	0.0124
2		Debt paying ability	Ratio of net cash flow from noncurrent liability operations
3	Internal financial factors	Profitability	Net cash rate of sales
4			Gross profit margin
5	Repayment ability	Operation ability	Speed of turnover of fixed assets
6			Working capital allocation ratio
7	Growth ability		Profit growth rate
8			Growth rate of total assets
9	Internal nonfinancial factors		Working experience in related industry
10			Product sales scope
11			Consumer price index
12	External environment		Per capita disposable income of urban residents
13			Engel coefficient
14	Basic information of legal representative		Legal representative credit card record
15	Repayment willingness		Enterprise credit granting in recent three years
16		Basic credit status	Type of registered capital in place
17	Business reputation		Legal disputes in enterprises
18	Collateral guarantee factor		Collateral score

respectively. Substitute the sum value of the receivable and uncollected principal and interest and the sum value of the receivable principal and interest of the small enterprises in these two grades into equation (2), respectively:

$$\begin{aligned} \text{LGD}_{\text{AAA}} &= \frac{34465964}{5927398089.27} = 0.0058, \\ \text{LGD}_{\text{AA}} &= \frac{3784389.75}{1412429040.39} = 0.0027. \end{aligned} \quad (5)$$

The default loss rate of AAA credit grade is higher than that of AA credit grade, indicating that AAA and AA credit grades do not meet the constraint conditions. Therefore, the numbers of small enterprises with AAA and AA credit grade are randomly selected again.

Assume that the numbers of small enterprises with AAA credit grade and AA credit grade reselected at random are 1783 and 127, respectively; that is, the starting and ending numbers of small enterprises with AAA and AA credit grades are [1–1783] and [1784–1909], respectively. Continue to substitute their sum values of receivable and uncollected principal and interest and their sum values of receivable principal and interest into equation (2), respectively:

$$\begin{aligned} \text{LGD}_{\text{AAA}} &= \frac{38250353.46}{7300129899.68} = 0.0052, \\ \text{LGD}_{\text{AA}} &= \frac{9255986.32}{998518502.37} = 0.0093. \end{aligned} \quad (6)$$

At this point, the default loss rate of AAA credit grade is less than that of AA, indicating that AAA credit grade and

AA credit grade meet the constraint conditions, so A credit grade is selected at random.

Assume that the number of randomly selected small enterprises with A credit grade is 619; that is, the starting and ending number of small enterprises with A credit grade is [1910–2527]. Substitute the sum value of the receivable and uncollected principal and interest and the sum value of the receivable principal and interest of the small enterprise with this credit rating into equation (2):

$$\text{LGD}_A = \frac{485412345.04}{6363741983.55} = 0.0763. \quad (7)$$

At this point, the default loss rate of AA credit grade is less than that of A, indicating that AA credit grade and A credit grade meet the constraint conditions. Therefore, BBB grade is selected at random. If the default loss rate of AA credit grade is greater than that of A, it means that AA and A credit grades do not meet the constraint conditions, and then AAA credit grade shall be reselected.

Assume that the number of small enterprises with BBB credit grade randomly selected is 176; that is, the starting and ending number of small enterprises with BBB credit grade is [2528–2702]. Substitute the sum value of the receivable and uncollected principal and interest and the sum value of the receivable principal and interest of the BBB credit rating small enterprise into equation (2):

$$\text{LGD}_{\text{BBB}} = \frac{197741326.45}{2540497356.76} = 0.0778. \quad (8)$$

At this point, the default loss rate of A credit grade is less than that of BBB, indicating that A and BBB credit grades

meet the constraint conditions, so BB credit grade is selected at random. If the default loss rate of A credit grade is greater than that of BBB at this time, it means that A and BBB credit grades do not meet the constraint conditions, and then the AAA credit grade shall be reselected.

By analogy, a set of credit rating results satisfying the constraint conditions can be obtained. The default loss rates of the nine credit grades are 0.0052, 0.0093, 0.0763, 0.0778, 0.1429, 0.1770, 0.2801, 0.4863, and 0.5000, respectively. The starting and ending numbers of small enterprises with nine credit grades are [1–1783], [1784–1909], [1910–2527], [2528–2702], [2703–3035], [3036–3104], [3105–3107], [3107–3109], and [3110–3111].

Since the number of small enterprises in each credit grade is randomly selected and there is no constraint of objective function threshold, multiple groups of credit rating results satisfying the constraint conditions can be obtained.

(2) *Credit Rating Satisfying the Threshold of Objective Function.* Since the maximum value of the objective function is required to be solved in this study, the threshold value of the objective function needs to be continuously increased to obtain the optimal solution, so the critical value of the threshold value of the objective function is extremely critical.

The threshold value of the objective function in this study is selected according to the actual running efficiency of the program. We first select 5000 and then continue to increase the threshold at intervals of 5000, such as 10000, 15000, and 20000, until the threshold increases to 45000, and the program will run less efficiently. Therefore, 45000 is taken as the threshold critical value of the objective function in this study. Due to the limitation of conditions, the threshold value of the objective function selected in this study is 45000, and the threshold value can be further increased to further increase the objective function value, so as to obtain more superior results of credit rating division.

When the threshold value of the objective function is 35000, according to (1), a set of credit ratings satisfying the constraint conditions will be obtained first, as shown in row 1 of Table 3. Substitute the credit scores of small enterprises corresponding to each credit grade into equation (1):

$$f_1 = \frac{425565.14}{18.18} = 23410.04. \quad (9)$$

Since the objective function value of the first group of credit rating results is less than the threshold value of 35000, AAA and AA credit grades should be randomly selected again until the second group of credit rating results meeting the constraint conditions is obtained, as shown in row 2 of Table 3. Continue to substitute its corresponding credit score into equation (1):

$$f_2 = \frac{403417.05}{25.30} = 15946.58. \quad (10)$$

Since the objective function value of the second group of credit rating results is still less than the threshold value of 35000, it is necessary to continue to randomly select AAA and AA credit grades to obtain the credit rating results of the

third group, the fourth group, and the fifth group that meet the constraint conditions, until the objective function value is greater than the threshold value of 35000.

The credit rating results satisfying the constraint conditions are shown in row 9 of Table 3; that is, the results are listed in process (1) above. Substitute the credit score of the corresponding small enterprise into equation (1):

$$f_9 = \frac{444819.33}{11.99} = 37100.18. \quad (11)$$

At this time, the objective function value corresponding to the credit rating result is greater than the threshold value of 35000, so the credit rating result of this group is a solution of the threshold value of 35000.

What needs to be noted here is that the operation will stop immediately when the credit rating division meeting the constraint conditions appears and the objective function value is greater than 35000. Therefore, the nine groups of division results obtained here are not the results that all meet the constraint conditions when the objective function value is greater than 35000; and, with the number of runs, the results are not exactly the same. The specific results are shown in Table 3.

4.2.2. *Determination of the Global Optimal Solution.* Taking the threshold of objective function 45000 as the boundary, the global optimal solution is approximated by dichotomy. When the threshold value of the objective function is 40000, the credit rating result can still be obtained, and it is close to the critical value. Therefore, 40000 is taken as the starting point here to illustrate the specific process of the dichotomy approach to the global optimal solution.

(1) *The First Approximation to the Global Optimal Solution.* Firstly, the threshold value of the objective function is set as 40000. According to the above process, we can first obtain a solution that satisfies the constraint conditions and the objective function is greater than the threshold value of 40000, that is, a group of credit rating results with the objective function value of 41742.

Continuing on the basis of the above process, we can get another solution that satisfies the constraint conditions and the objective function is greater than the threshold value of 40000, that is, another set of credit rating results with the objective function value of 42650.

Based on the dichotomy, we can calculate and obtain the threshold of the next objective function that approximates the global optimal solution; that is,

$$41742 + \frac{(42650 - 41742)}{2} = 42196. \quad (12)$$

(2) *The Second Approximation to the Global Optimal Solution.* When the objective function threshold is 42196, we can get one solution with the objective function value of 42643 and another solution with the objective function value of

TABLE 3: Credit rating division of 9 groups satisfying constraint conditions.

No.	(1) AAA	(2) AA	(3) A	(4) BBB	(5) BB	(6) B	(7) CCC	(8) CC	(9) C
1	2215	2682	2765	2771	3033	3105	3107	3109	3111
2	2517	2680	2728	2777	3024	3100	3107	3110	3111
3	2366	2688	2735	2754	3028	3106	3107	3110	3111
4	2447	2689	2765	2770	3034	3105	3107	3108	3111
5	1744	2129	2693	2764	3031	3100	3107	3109	3111
6	2657	2688	2738	2753	3026	3105	3107	3108	3111
7	2493	2690	2766	2770	3030	3099	3107	3110	3111
8	1654	1806	2763	2771	3032	3104	3107	3109	3111
9	1783	1909	2527	2702	3035	3104	3107	3109	3111

42657. Therefore, the objective function threshold of the third approximation to the global optimal solution is

$$42643 + \frac{(42657 - 42643)}{2} = 42650. \quad (13)$$

(3) *Obtaining the Global Optimal Solution.* When the objective function threshold is 42650, we can obtain the credit rating result with the objective function value of 44951. At this time, the default loss rate of each credit grade obtained is less different from that obtained in the process of approaching the global optimal solution for several times. Moreover, the objective function value is the maximum value when the threshold critical value is 45000. Therefore, the credit rating result obtained when the objective function value is 44951 is taken as the global optimal solution. The above process is solved by MATLAB programming. The specific results are shown in Table 4. The following LGD is the default loss rate, which is listed in the form of percentages.

4.2.3. *Credit Rating Results Analysis.* When the objective function value is 44951, the sample number and default loss rate corresponding to each credit grade are listed in column 2 and column 6 of Table 5 respectively. The credit score interval is determined by the credit score of the last small enterprise in each credit grade and is listed in column 4 of Table 5. The interval length is the value of the right endpoint of the credit score interval minus the left endpoint. The maximum value of the interval length is 31.3853, and the minimum value of the interval length is 1.6911, which has obvious differentiation and is listed in column 5 of Table 5. The specific results are shown in Table 5.

As can be seen from column 6 of Table 5, the default loss rate of the nine credit grades, such as AAA credit grade and AA credit grade, is strictly increasing, that is,  $0 < 0.52\% < 5.49\% < 7.65\% < 15.42\% < 17.88\% < 20.84\% < 23.01\% < 94.82\% < 100.00\% < 1$ , indicating that the final credit rating result obtained in this study meets the principle that the default loss rate increases with the continuous reduction of credit grade.

The objective function value corresponding to the credit rating result shown in Table 5 is the maximum value that can be obtained when the threshold critical value is 45000, indicating that the credit rating result can ensure that the sum of the dispersions of credit scores between small enterprises with different credit grades is the largest, and the sum of the

dispersions of credit scores for small enterprises within the same credit grade is the smallest. That is, small enterprises with large credit score gap can be divided into different credit grades, while small enterprises with small credit score gap can be divided into the same credit grade, indicating that the credit rating model constructed in this study meets the principle of matching credit rating with the credit status of small enterprises.

By plotting the credit grade in column 3 of Table 5 and the default loss rate in column 6, the relationship between credit grade and default loss rate can be shown more intuitively. The horizontal axis is the length of the default loss rate, and the vertical axis is the corresponding credit grade, as shown in Figure 3. It is important to note that as the number of empirical samples increases, the credit score interval becomes more uniform and Figure 3 becomes smoother.

#### 4.3. Test and Comparative Analysis of Credit Rating Model

##### 4.3.1. Credit Rating Results of Comparative Model

(1) *Credit Rating Based on the Distribution of the Number of Customers.* The sample proportion of each credit grade is determined according to the existing literature [11] on credit rating based on the normal distribution of the number of customers, which is listed in column 2 of Table 6. Then the sample number of small enterprises of each credit grade is calculated to get the starting and ending number of small enterprises of each credit grade, which is listed in column 1 of Table 6. The calculations of credit score interval, interval length, and default loss rate are the same as above, which are, respectively, listed in columns 4–6 of Table 6. The specific results are shown in Table 6.

(2) *Credit Rating Based on K-Means Clustering.* By setting the number of K-means clustering as 9, the division results of 9 credit grades can be obtained directly [22], which are listed in columns 1–3 of Table 7. The calculations of credit score interval, interval length, and default loss rate are the same as above, which are, respectively, listed in columns 4–6 of Table 7. The specific results are shown in Table 7.

4.3.2. *Test of Credit Rating Model.* This study mainly uses two standards to test and compare four credit rating models, which are (1) standard of reasonableness for matching credit

TABLE 4: Default loss rate of different credit ratings.

(1) Objective function threshold	(2) Objective function value	(3) AAA rating LGD	(4) AA rating LGD	(5) A rating LGD	(6) BBB rating LGD	(7) BB rating LGD	(8) B rating LGD	(9) CCC rating LGD	(10) CC rating LGD	(11) C rating LGD
40000	41742	0.52	5.62	8.18	11.10	15.30	22.93	37.89	94.68	100.00
	42650	0.58	5.41	8.20	18.56	19.42	19.52	37.89	94.53	100.00
42196	42643	0.57	5.69	6.74	7.79	18.03	20.48	22.96	94.68	100.00
	42657	0.53	6.08	6.61	8.10	19.40	19.61	22.96	94.53	100.00
42650	44951	0.52	5.49	7.65	15.42	17.44	20.84	23.01	94.82	100.00

TABLE 5: Credit rating results of small enterprises.

(1) No.	(2) Sample size	(3) Credit rating	(4) Credit score interval	(5) Interval length	(6) LGD (%)
1-1458	1458	AAA	[80.8707, 100.0000]	19.1293	0.52
1459-2472	1014	AA	[70.4617, 80.8707)	10.4090	5.49
2473-2690	218	A	[58.3853, 70.4617)	12.0746	7.65
2691-2752	62	BBB	[56.6942, 58.3853)	1.6911	15.42
2753-3033	281	BB	[47.7085, 56.6942)	8.9857	17.44
3034-3099	66	B	[37.1479, 47.7085)	10.5606	20.84
3100-3107	8	CCC	[32.6318, 37.1479)	4.5161	23.01
3108-3110	3	CC	[0, 31.3853)	31.3853	94.82
3111	1	C	0	—	100.00

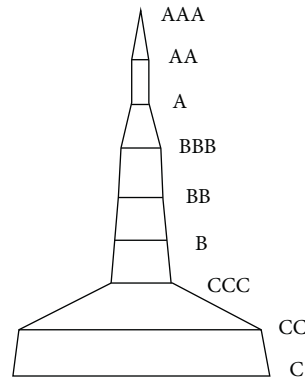


FIGURE 3: Distribution diagram of the relationship between credit rating and default loss rate.

rating with default loss rate and (2) stability standard of credit score interval distribution.

(1) *Standard of Reasonableness for Matching Credit Rating with Default Loss Rate.* According to column 6 of Tables 6 and 7, the default loss rate of AAA credit grade and AA credit grade based on the customer number distribution and K-means clustering credit rating model is 0. This does not satisfy the fact that each credit grade must have a default sample and does not meet the reasonable standard that the default loss rate should rise with the decline of credit grade. The credit rating model constructed in this study strictly meets the inverse relationship between credit grade and default loss rate. The credit rating model based on the distribution of the number of customers is mainly based on the distribution characteristics of “large in the middle and small on both sides” of the number of small enterprises to

divide credit ratings; the credit rating model based on K-means clustering mainly clusters small enterprises with similar credit scores into one category, and neither of which takes into account the internal relationship between credit rating and default loss rate, so these two credit rating models are unreasonable.

(2) *Stability Standard of Credit Score Interval Distribution.* The distribution of credit score interval is stable; that is, the credit score interval should be neither too long nor too short. If the credit score interval is too long, the credit score of small enterprises will change greatly, but the credit grade will remain unchanged. If the credit score interval is too short, the credit grade of small enterprises will change as long as there is a slight change in the credit score. This can mislead banks and other financial institutions in their loan pricing and lending decisions.

TABLE 6: Credit rating results based on customer number distribution.

(1) No.	(2) Sample proportion	(3) Credit rating	(4) Credit score interval	(5) Interval length	(6) LGD (%)
1–249	8	AAA	[88.2830, 100.0000]	11.7170	0.00
250–747	16	AA	[84.7585, 88.2830]	3.5245	0.00
748–1680	30	A	[79.6458, 84.7585]	5.1127	0.89
1681–2178	16	BBB	[75.9311, 79.6458]	3.7147	0.37
2179–2489	10	BB	[69.2688, 75.9311]	6.6623	12.11
2490–2738	8	B	[57.0115, 69.2688]	12.2573	8.64
2739–2925	6	CCC	[50.3302, 57.0115]	6.6813	31.03
2926–3049	4	CC	[44.3122, 50.3302]	6.0810	31.28
3050–3111	2	C	[0, 44.3122]	44.3122	32.04

TABLE 7: Credit rating results based on K-means clustering.

(1) No.	(2) Sample size	(3) Credit rating	(4) Credit score interval	(5) Interval length	(6) LGD (%)
1–80	80	AAA	[91.8873, 100.0000]	8.1127	0.00
81–567	487	AA	[85.9509, 91.8873]	5.9364	0.00
568–1594	1027	A	[80.3318, 85.9509]	5.6191	0.88
1595–2398	804	BBB	[72.3118, 80.3318]	8.0200	6.78
2399–2660	262	BB	[61.2039, 72.3118]	11.1079	5.90
2661–2934	274	B	[50.1150, 61.2039]	11.0889	24.37
2935–3070	136	CCC	[41.5533, 50.1150]	8.5617	21.44
3071–3108	38	CC	[31.3853, 41.5533]	10.1680	2.88
3109–3111	3	C	[0, 31.3853]	31.3853	100.00

TABLE 8: STDEV stability indicators for different models.

(1) Credit rating model	(2) STDEV value	(3) Reasonableness standard	(4) Stability standard
Distribution of the number of customers [11]	12.83	Inconformity	Inconformity
K-means clustering [22]	7.56	Inconformity	Conform
Default pyramid principle [21]	17.93	Conform	Inconformity
This study	9.60	Conform	Conform

The credit rating model based on default pyramid principle [21] is selected for comparative analysis, and the reasons for selecting this literature are as follows: The first reason is that the credit rating model constructed by it and the credit rating model constructed by this study both meet the rationality standard that the corresponding default loss rate keeps rising with the continuous decline of credit grade. The second reason is that the indicator system and empirical data used in this study are the same as those in this literature, and the credit rating results are more comparable.

The stability of credit score interval distribution is tested by STDEV stability index, and the specific results are shown in Table 8.

The STDEV index value of the credit rating model based on K-means clustering is the smallest. However, since this model does not meet the rationality standard of matching credit rating with default loss rate, only the credit rating model based on default pyramid that meets the rationality standard is considered in the comparison model. Because the STDEV value of the credit score interval length of the credit rating model constructed based on the default pyramid principle is larger than that of the interval length of the model constructed in this study, it indicates that the distribution of the credit rating model constructed in this study is more stable.

## 5. Conclusion

### 5.1. Main Conclusions

- (1) Empirical results show that when the threshold value of the objective function is 45000 and the maximum value of the objective function is 44951, the credit score intervals of the nine credit grades from high to low are, respectively, [80.8707, 100.0000], [70.4617, 80.8707], [58.3853, 70.4617], and so forth. The corresponding default loss rates are, respectively, 0.52%, 5.49%, 7.65%, and so forth.
- (2) The comparative analysis shows that the credit rating model constructed in this study is the best, followed by the credit rating model based on default pyramid principle, and the credit rating model based on customer number distribution and K-means clustering is the worst.

### 5.2. Main Features

- (1) The maximum ratio of the sum of the dispersions of credit scores between different credit ratings and the sum of the dispersions of credit scores within the same credit rating is taken as the objective function,

and the default loss rate of the following credit rating strictly larger than the default loss rate of the previous credit rating is taken as the inequality constraint; a nonlinear credit rating optimal partition model is constructed. It ensures that the small enterprises with small credit score gap are of the same credit rating, while the small enterprises with large credit score gap are of different credit ratings, which overcomes the disadvantages of the existing research that only considers the small enterprises with large credit score gap and ignores the small enterprises with small credit score gap.

- (2) The approximate solution of the nonlinear optimization model is solved by a recursive algorithm with strong reproducibility and clear structure, and the credit rating of small enterprises is obtained, which shows that the higher the credit rating, the lower the default loss rate, and the credit group of small enterprises is matched with the credit rating.

## Data Availability

The empirical sample in this paper consists of data on loans for 3111 small enterprises from the database of a Chinese commercial bank.

## Conflicts of Interest

The authors declare that they have no conflicts of interest.

## Acknowledgments

The research was supported by Natural Science Foundation of Inner Mongolia Autonomous Region of China (2020MS07009), the National Natural Science Foundation of China (72161033), Key Projects of National Natural Science Foundation of China (71731003), Science and Technology Project of Inner Mongolia Autonomous Region of China (201605053), and Inner Mongolia Autonomous Region Postgraduate Education Innovation Project of China (SR2020082).

## References

- [1] Q. X. Sun, Y. F. Liu, and Y. Duan, "The impact of the United States sovereign credit rating downgrading," *China Financialist*, vol. 16, pp. 45–46, 2011.
- [2] Bank of China, *Notice on the Sending of Credit Rating Management Measures for Domestic Institutional Clients of Bank of China*, pp. 4–3, Bank of China, Beijing, China, 2003.
- [3] Agricultural Bank of China, *Notice on Printing and Distributing Measures of Customer Credit Rating of Agricultural Bank of China*, pp. 5–6, Agricultural Bank of China, Beijing, China, 2003.
- [4] T. H. Moon, Y. Kim, and S. Y. Sohn, "Technology credit rating system for funding SMEs," *Journal of the Operational Research Society*, vol. 62, no. 4, pp. 608–615, 2011.
- [5] G. Gupton, C. Finger, and M. Bhatia, *CreditMetrics - Technical Document*, pp. 5–22, J. P. Morgan & Co. Incorporated, New York, NY, USA, 1997.
- [6] M. Lyra, J. Paha, S. Paterlini, and P. Winker, "Optimization heuristics for determining internal rating grading scales," *Computational Statistics & Data Analysis*, vol. 54, no. 11, pp. 2693–2706, 2010.
- [7] J. B. Zhang, "A new method for calculating the probability of default of credit rating based on complete information," *The Study of Quantitative and Technical Economics*, vol. 35, no. 6, pp. 149–164, 2018.
- [8] Z. Y. Zhu, W. H. Su, and Q. X. Wang, "Credit risk assessment of small and medium-sized enterprises under the financing environment of the New Third Board," *Statistics and Information Forum*, vol. 33, no. 10, pp. 107–113, 2018.
- [9] J.-C. Duan and S. Li, "Enhanced PD-implied ratings by targeting the credit rating migration matrix," *The Journal of Finance and Data Science*, vol. 7, pp. 115–125, 2021.
- [10] G. T. Chi, M. D. Pan, and F. Qi, "The design and application of a credit risk rating model for banks based on small samples," *The Study of Quantitative and Technical Economics*, vol. 31, no. 6, pp. 02–116, 2014.
- [11] G. T. Chi, M. D. Pan, and Y. Q. Chen, "Rural households' credit evaluation model based on comprehensive discriminant ability," *Management Review*, vol. 27, no. 06, pp. 42–57, 2015.
- [12] Y. Zhang and G. Chi, "A credit rating model based on a customer number bell-shaped distribution," *Management Decision*, vol. 56, no. 5, pp. 987–1007, 2018.
- [13] Z. C. Zhao, G. T. Chi, and M. D. Pan, "An optimization method for credit rating based on the maximum credit difference degree," *Systems Engineering Theory & Practice*, vol. 37, no. 10, pp. 2539–2554, 2017.
- [14] B. F. Shi, J. Wang, and G. T. Chi, "Inclusivity finance, bank credit and merchant microfinance: a perspective of risk level matching," *Chinese Management Science*, vol. 25, no. 9, pp. 28–36, 2017.
- [15] G. T. Chi and S. L. Yu, "The credit rating method based on the maximum default discriminating ability," *Journal of Management Science*, vol. 22, no. 11, pp. 106–126, 2019.
- [16] B. Shi, X. Zhao, B. Wu, and Y. Dong, "Credit rating and microfinance lending decisions based on loss given default (LGD)," *Finance Research Letters*, vol. 30, pp. 124–129, 2019.
- [17] B. Shi, G. Chi, and W. Li, "Exploring the mismatch between credit ratings and loss-given-default: a credit risk approach," *Economic Modelling*, vol. 85, pp. 420–428, 2020.
- [18] Y. Zhou, "Credit rating model of small industrial enterprises based on information gain," *Operations research and management*, vol. 30, no. 1, pp. 209–216, 2021.
- [19] X. S. Ren and X. L. Yu, *Multivariate Statistical Analysis*, China Statistics Press, Beijing, China, 2010.
- [20] F. M. Zhang, W. J. Hua, and R. Y. Li, "Stability analysis of several comprehensive evaluation methods," *System Science and Mathematics*, vol. 39, no. 4, pp. 595–610, 2019.
- [21] B. F. Shi, *Research on Credit Rating Model of Small Enterprise Based on Default Pyramid Principle*, Dalian University of Technology, Dalian, China, 2014.
- [22] F. L. Raquel, "Modelling of insurers' rating determinants. An application of machine learning techniques and statistical models," *European Journal of Operational Research*, vol. 183, no. 3, pp. 1488–1512, 2007.

## Research Article

# Netizens' Perspective towards Electronic Money and Its Essence in the Virtual Economy: An Empirical Analysis with Special Reference to Delhi-NCR, India

Mohammed Arshad Khan 

*Department of Accountancy, College of Administrative and Financial Sciences, Saudi Electronic University, Riyadh 11673, Saudi Arabia*

Correspondence should be addressed to Mohammed Arshad Khan; [m.akhan@seu.edu.sa](mailto:m.akhan@seu.edu.sa)

Received 25 June 2021; Revised 12 October 2021; Accepted 18 October 2021; Published 3 November 2021

Academic Editor: M. M. El-Dessoky

Copyright © 2021 Mohammed Arshad Khan. This is an open access article distributed under the Creative Commons Attribution License, which permits unrestricted use, distribution, and reproduction in any medium, provided the original work is properly cited.

This research attempts to evaluate the ongoing position of the modalities exercised in India concerning digital payments. Largely appraised as a success story in the making, this research examines several instrumental factors in India's digital payment systems. It further extends to identifying the impact of demographic attributes and constructive variables, such as service quality, reliability, satisfaction, and security on digital payment system, Delhi NCR, India. A Google form questionnaire was adopted to collect data through online mode. The researcher collected the primary data from 165 respondents. Purposive sampling method was exercised, along with CFA technique and parameter test used through SPSS (version 25), reliability issue, validity issue, and model fitness achieve through SPSS-AMOS (version 24). The significant peculiarities and analysis are presented further in this research contributing to a precise depiction of findings and then, based on it, the conclusion.

## 1. Introduction

Digital payment, quite simply, is a form of carrying out transactions devoid of any physical exchange of money. However, the said transaction is mandatorily performed via the Internet or applications necessitating its employment. It is the principal branch of digitization, comprising the transition of the natives from the physical exchange of money to digital transactions. The parties involved in the said scenario include a payer and a payee. The individual sending the money is the payer, whereas the recipient or the person to whom the money is transferred is the payee. This contemporary form of exchange of money, mandating the Internet for both parties and eliminating hard currency give-and-take in its entirety, is also known as electronic payment. It is, hence, a rapid and highly convenient method of carrying out transactions [1].

This modern-day method of money exchange comprises several modalities in its application of the Internet. These are

debit card, credit card, net banking, Unified Payments Interface (UPI), digital wallets, etc. Compared with the typical form of carrying out transactions, which is, through currency notes, the employment of the Internet (hence, the word "digital") separates digital payment from the earlier forms of payments, particularly the barter system. The barter system did not have a justifiable give-and-take format along with the previously exercised forms of payments. Coins and currency notes, later on, amended the problems, which is now superseded by, or surging by and large, electronic payments. One of the logical reasons for amelioration is the recurrent issues found in the system, involving cash falsification, cheque bounce, and signature forgery. However, the transition to digital payment is also not infallible. It raises several doubts about frauds happening due to compromised privacy when carrying out transactions digitally on the Internet.

It is also worth mentioning the intensified Internet use in the present time arising from widespread availability, also

accommodating cybercriminals. This decade is witnessing extensive use of smartphones (again, differentiating from regular phones for having Internet applications of all kinds) and enormous access to many products and services via e-commerce applications, which natives greatly enjoy as they happily make payments digitally online [2]. The substantial improvements happening continually in the mobile and broadband industry, leading to cutting-edge technology in rapid succession, and Internet speed, thought of unimaginable some time ago, are also instrumental in the greater use of the Internet and the migration of natives from the currency-based exchange of money to digital payments. The movement from paper to digital, however, was not as smooth [3]. The element of trust was sorely missing initially as people only relied on the cash on delivery method, which they were accustomed to. The lack of proper awareness about the various forms of digital payments largely hindered people from using them [4].

Additionally, various myths acted against the use of digital payment methods. Many believed for the banks to deduct high transaction charges for performing transactions digitally, whether by debit card, credit card, or net banking. Some even criticized the means of payment for the likelihood of overspending, provided the extreme ease of convenience in buying products and services. These myths are still largely present amongst the populace of India, calling for the need for adequate literacy on digital payment systems [5]. It is all more prominent when considered India is undergoing a substantial digital revolution. Appropriate digitization of the payment mechanism will be highly rewarding in the definite possibility of an entirely cashless future economy.

It is also imperative to acknowledge the need for the rightful progression of the Indian digital payment system. It is expectedly the most significant factor that defines how the industry looks in the future [6]. With India shifting to digital means, having an agreeable regulatory environment, the advent of next-generation payment service providers and an improved customer experience are the rudimentary factors contributing to India's overall progression in digital payment systems. That is not to say, various facilitators are encouraging in boosting the means of digital payments, allowing the switch from cash-based to the wholly digital economy [7]. Acting as a bridge to solidifying the Indian digital payment systems, these facilitators comprise the successive advancements done in bolstering Internet connectivity on smartphones, nonbanking financial institutions expediting digital means of carrying out transactions, the emergence of financial technology sectors, and the gradual push by the government through various tax incentives [8]. Hence, all of these factors are helping with an assertive situation for the progression of digital payment systems in India.

The various digital payment systems currently exercised in India comprise banking cards (debit/credit card), digital wallets (Paytm, PhonePe, etc.), National Electronic Fund Transfer (NEFT), Unified Payment Interface (UPI), mobile banking, Real Time Gross Settlement (RTGS), Unstructured Supplementary Service Data (USSD), and Aadhar Enabled Payment System (AEPS) [9].

## 1.1. Types of Digital Payment

*1.1.1. Banking Cards.* The most common types of payment cards are credit cards and debit cards. They are the most easily found and commonly used methods of digital payment. The primary feature of the cards is that they are electronically linked to the holder's bank account and serve as a medium to enable the account holder to purchase commodities without using cash or withdrawing money from an ATM if needed. The cardholder can perform the said actions via a secret code embedded on the backside of the cards, also known as the CVV number (card verification value). The stated number establishes the cardholder's identity and minimises fraud risk [10].

The most influential factors that make banking cards so broadly exercised comprise the ease of convenience and the greater security in making payments. Securitywise, banking cards are quite assuring, most notably, when used in other forms of online payments, such as digital wallets or online transactions [11]. A user may save his or her information on a specific digital app for making digital transactions. The benefit of OTPs (one-time password) ensures, even in the app, either web or mobile-based, at minimal risk. The most recognized banking card payment systems comprise Visa, MasterCard, RuPay, etc. [12]. The usefulness of the cards further extends to making instore purchases via card swiping or a simple tap in POS machines.

*1.1.2. Credit Card.* In today's times, the credit cards are widely used by the customers as they are providing them the facility of making transactions without debiting their account balances. It is the kind of digital banking card that allows the customer to make purchases against a credit amount, which is lent to the customer by the bank, based on various factors, and hence, it needs to be paid off after a month to 45 days [13]. This variable credit amount lent to the customer is generally called the credit limit. If the customer makes purchases from the card, as per his given credit limit and fails to repay the amount, the bank then begins to charge money on the unpaid credit amount, with interest charges and late fees. However, the bank also rewards loyal customers by increasing the credit limit when they are regularly paying the credit amount. Those having a good credit history also benefit with ease in taking bigger loans from a bank.

*1.1.3. Debit Card.* The successor to credit card, and currently, the most found banking card amongst the populace, the debit cards, enjoy simple mechanics. As opposed to spending a credit limit provided by the bank, customers can pay as much money in making a digital purchase as per the amount in their account. It is, otherwise, a very convenient method of utilising the saved amount in a bank, akin to a cheque or cash. For the same reasons, these banking cards are also denoted as "cheque cards" or "bank cards." One differentiating advantage of debit cards over credit cards is the greater cash withdrawal limit. A customer can only withdraw cash of a specific limitation, as provided by the bank, from an ATM with a credit card. However, debit



cards allow customers to draw a much more significant amount (ranging from ₹25,000 to ₹1,00,000) or more, depending on the amount of savings they have in their bank account [14].

*1.1.4. Internet Banking.* While debit and credit cards are convenient and more regularly used, their most significant limitations include spending a substantial amount, or quite precisely, for corporate use. Internet banking, in this case, becomes the most useful, allowing the customers to make online transactions through a web browser, on a bank's official website, with the help of a login ID and a password. Also, denoted as online banking, virtual banking, or more lately, electronic banking (e-banking), this form of digital payment warrants a steady Internet connection to ensure the process of carrying out transaction is not interrupted. While transaction through debit and credit cards is much quicker, Internet banking has a more elaborate approach, more so for security reasons, and hence, it requires a good Internet connection. Necessary details such as the account number of the person or entity to whom the amount is to be sent are needed, along with the IFSC (Indian Financial System Code). For regular transactions, customers can add beneficiaries to simplify the process of adding account number and IFSC daily [15]. In purchasing through e-commerce websites and opting for Internet banking, the portal automatically redirects to the preferred bank's website, and the banking details mentioned above are not required. At present, nearly every bank has an Internet banking service, and all the payment gateways provide the option of virtual banking options. As specified earlier, NEFT, RTGS, and IMPS are the most commonly exercised ways to transact via online banking [16].

*1.1.5. Mobile Banking.* Though introduced two decades ago, the application of mobile banking is still scarce, especially when compared with banking cards and Internet banking. However, their usefulness is equally substantial. Also denoted as M-banking, or SMS banking, this is a kind of digital payment service that incorporates almost all Internet banking features (such as issuing a new cheque book or requesting a new debit/credit card, beyond merely paying money) and is exercised via an official banking software application that needs to be installed via app store of a smartphone or tablet [17]. Nearly every bank has its own application, which, as of late, has been used more than Internet banking, provided similar features but significant ease of accessibility. Many people regard this branch of digital payment services as the future of banking, considering the lot of features, and it provides in a clean user interface [18]. The necessity of a smartphone for using M-banking further bolsters digitization.

*1.1.6. Digital Wallet.* Similar to having a physical wallet, a digital wallet is a virtual case for people to store their money. The application of such wallets is quite identical to modern-day debit and credit cards. However, they come conducive in

carrying out online and instore transactions with a mere tap, saving plenty of time and inconvenience. Also denoted as an E-wallet, or mobile wallet, this digital payment service needs to be connected with an individual's bank account for carrying out transactions. Some service providers (Paytm, PhonePe, MobiKwik, etc.) allow the customers to exercise the services by adding the amount to their digital wallet by debit or credit cards, hence not necessitating linking their bank account. These wallets comprise two vital components: software, which feeds personal data, ensuring its security and encryption [19]. The second component, information, is a database of data rendered by the users, including their name, shipping address, the preferred mode of payments, amount to be paid, and debit/credit card details [20].

## 2. Review of Literature

In their article, Jayakumar and Vincent Sahayaraj [21] have comprehended the factors that make a customer a happy customer. The paper shows that the customers prefer online banking, ATM etc., but some factors like alertness and consistency affect their level of satisfaction. Customer satisfaction increases towards current banking services if the bank provides more consistent services with value as promised and on time. SBI has successfully implemented substantial factors such as modern equipment, infrastructural amenities, and quality of equipment used. They have been flourishing in achieving an amicable relationship with customers. Most of the article respondents felt that the employees of the SBI are very intense to satisfy their customers.

An electronic wallet (E-wallet) is one of the most current digital payment services that provides its users with the comfort of smooth and simplified transactions via allowing them to store amount or otherwise link their bank account or save credit card details faster and easier checkout or instore payments. The benefits associated with E-wallets, mainly saving time and inconvenience, make the mode of payment favourable among the populace [22]. M-wallet, otherwise known as mobile wallet, is distinguished for various advantages over other modes of payments. The most promising benefits comprise customization and instant communication. However, E-wallets have gained a more significant following their usefulness, particularly in the riding industry and food delivery and bill payments. Hence, they are more used than M-wallet and the other forms of digital payment systems [23]. The peculiarities of E-wallets are not merely advantageous to buyers but also for the traders, who have begun to exercise the mode of payment for its ease of convenience and efficacious cash management, ultimately leading to a reduction in the cost of labour. Physical stores, for instance, have witnessed a steep increase in the exercising of E-Wallets, where the customers can make payments swiftly by scanning the QR code, accommodating for a smooth paperless, cashless experience [24]. Near field communications, otherwise known as NFC-supported devices, are placed close by the payment terminals in physical stores to make the transactions convenient. Henceforth, based on the literature mentioned above, it can

be surmised that the usefulness of E-Wallets over the other modes of digital payments, mainly for their high flexibility and adaptability and extremely user-friendly process of carrying out transactions via smartphones or tablets.

Abhijit M. Tadse & Harmeet Singh Nannade [25] tried to analyse the use of Paytm by users of mobile phones and also to find out various issues faced by users of Paytm. The research categorized on the basis of age, purpose of usage, frequency of usage, and average monthly spending on Paytm by the respondents. The study further elaborates that Paytm is quite convenient owing to wide network of partners. This paper concludes that, to improve the transaction efficiency, it needs to work upon the payment gateway as 70% people face issues with it. In order to cater the requirement of maximum customers, the service needs to improvise as indicated by only 5% people respondents to have got help every time they encounter a problem in it.

Revathy and Balaji emphasized the crucial role of the rural populace in the rightful progression of the economy, provided they acquire two-third of the total population. The study highlighted how the IT and Communication sector surge is turning fruitful for the nation, surmising a total of 50% Internet users in India by the end of 2020. The researcher further necessitated the application of digital wallets, underlining the rural populace and the neediness to spread rightful awareness regarding the usage and benefits of using E-wallets amongst them. The study further specified how the Indian Government took the initiative of spreading appropriate awareness amongst the rural populace towards the usefulness of E-wallets, thoroughly covered under their digitization campaign. The timely implementation of advanced and upcoming technology has been unceasingly low in India instead of the other nations. Though the situation has been highly different in this scenario, the country is progressing shoulder to shoulder with other countries to digitize the economy, explicitly exercising E-wallets. Provided two-thirds of the Indian population constitutes the people residing in the rural areas, the timely exercising of digital payment services will ensure the country becomes a cashless economy in mere few years to come. The urban populace is already well-versed with the usefulness of digital payment systems and hence exercising it. By converting, the rural public towards a cashless system of carrying out business will complete the mission of the Indian Government of having a digitized economy. The best step taken forward in this regard is by the National Payments Corporation of India, accommodating for the E-wallets to function on all mobiles, with or without the availability of the Internet [26].

The researcher highlighted how the rapid increase in the number of smartphone, or otherwise, Internet users gave a rise in the total users exercising digital payment services, who found the alternative of cash convenient and more appealing. This research furthermore emphasized the increasing competition in the domain of digital payment services and the willingness to dominate the massive Indian market, specifying those who entered the territory during the phase of demonetization with the prospect of

establishing the company at the right time. Additionally, the study speculated India to become a cashless economy with the appropriate digitization, managing to convert people's behaviour from traditional to the modern-day system of digital payments. The research employed ANOVA to prove no significant variance in consumer perception regarding its demographic factors.

Routray et al. endeavoured to recognize the significant predictors of digital payment services in Middle Eastern Country, Oman. The researcher administered an empirical study for the same and developed a hybrid model through an SEM-neural network model. The study's outcome exhibited that perceived trust, perceived usefulness, and perceived security have a notable impact on the users' intention to exercise digital payment services, specifically M-wallets. In contrast, perceived ease of use does not have a structural effect on the users' intention to exercise M-wallets. Additionally, the study recommended that the service providers maximize social media platforms to produce the rightful awareness among the people for increasing the number of time users spend exercising mobile-based payment services [27].

Tamil Selvi and Balaji [28] strived to recognize whether the demographic profiles of the respondents have any substantial impact on the behavioural intent of the mobile users towards exercising mobile banking services. The researchers, henceforth, carried out an exploratory study for the same in the city of Chennai and Hyderabad. By devising structured questionnaires and distributing them amongst the customers of both public and private banks, the researchers acquired the primary data concerning their viewpoints on the employment of mobile banking. The outcome of the research, thereon, showcased that the performance expectancy, effort expectancy, hedonic motivation, trust, and loyalty are substantially impactful in the behavioural intent of the customers towards exercising mobile banking services.

### 3. Research Gap

The literature review showcased how most of the research is carried out to distinguish the customers' opinion towards the banking payment systems. However, the empirical studies undertaken solely examined the perception of customers towards the digital payment system. This research, however, considered relevant factors such as reliability, service quality, satisfaction, user-friendliness, security, and trustworthy and how they impact the customers.

### 4. Objectives of the Study

The study has the following objectives:

- (1) To examine customer opinion concerning the advantageousness of digital payment system in the perspective of service quality, reliability, satisfaction, trustworthy, user-friendly, and security

- (2) To analyse customers' (on the basis of their demographics) perception towards digital payment system and its importance in the banking sector

## 5. Hypotheses of the Study

The study has formulated the following hypotheses:

H01: the mean score of digital payment system does not differ with gender

H02: the mean score of digital payment system does not differ with age

H03: the mean score of digital payment system does not differ with educational qualification

H04: the mean score of digital payment system does not differ with occupational status

H05: the mean score of digital payment system does not differ with income level

## 6. Research Methodology

This research study is based on descriptive-cum-cross section. Primary data are used to obtain an accurate result. The Google Form of the questionnaire was designed and shared online to acquire users' response in Delhi NCR. The questionnaire was divided into two parts: the first part relevant to the respondent background and the second part based on specific statements pertinent to the digital payment system. All statements are further classified into major 6 sets. These sets (reliability, satisfaction, service-quality, user-friendly, trustworthy, and security) established a relationship with the digital payment system. Apart from this, to check the credibility of the constructs was analysed using Cronbach's alpha, which signifies to which the items in the questionnaire were associated with one another [29]. The online data obtained were collected from February to April 2021. A total of 167 replies were obtained through judgement or purposive sampling technique, out of which 165 respondents were selected, and those 165 responses were utilized further for data analysis. For better result, confirm variables were clearly explaining their interrelated construct. CFA technique was accompanied in the study with the help of AMOS (version 24) software. The investigator employed the relevant statistical tools and methods through SPSS (version 25) software to achieve the study's main objectives.

## 7. Findings and Discussion

The essential purpose of this study was to collect primary data by using a closed-ended questionnaire, which was shared with the help of Google Forms. An adequate number of participants showed interest in this online survey. For this study, the purposive sampling method was used. The questionnaire was designed in English for spread and diversification. It consisted of 29 questions divided into two parts. One part related to the respondent's demographic profile, and the other part divided into six factors: viz., reliability, service quality, satisfaction, user friendly, trustworthy, and security. Summated method of rating scale was

applied to assess the data from participants. It was performed on a five-point scale basis, starting from "strongly disagree (1) to strongly agree (5)." A total of 167 responses were received, but for the study, 165 responses settled to facilitate data analysis. The SPSS (version 25) and SPSS-AMOS software were used to investigate the collected data quantitatively. This segment comprises the results and findings of the research.

*7.1. Background Information of the Respondents.* The details of the respondents who filled the questionnaire are provided in this segment. Table 1 demonstrates the responses of the questions connecting to several demographic variables preferred for the study. The statistics showcased here is accumulated from the primary data.

Table 1 represents the participants' demographic information based on their gender, age group, educational qualification, occupational status, and monthly income. It indicates that most of the sample respondents (70.3%) were males (M), whereas 29.7% were females (F). The above data also indicate that most of the respondents (43%) belong to the age group of 21–30 years, 32.1% were between 31 and 40 years, and 13.3% belonged of age above 40 years, and the last 11.5% fall within the age bracket of up to 20 years.

Educational qualification signifies that 18.8% of respondents belong to undergraduate (U.G), 22.4% represent graduation (G), 26.7% belong to postgraduation (P.G), 13.9% represent doctorate (Dr), and 18.2% represent professional degree holder (PDH). Occupational status represents that 22.4% of respondent belong to government employees, 29.7% represent private employees, 19.4% belong to business or self-employees, and 28.5% represent students.

The monthly income of the respondents illustrates that 23% respondents belong to income of Rs.  $\leq 10000$ , 19.4% respondents belong to income of Rs. 10000–25000, 41.8% respondents belong to income of Rs. 25000–50000, and 15.8% respondents belong to income of Rs.  $< 50000$ .

*7.2. Reliability of the Latent Constructs.* According to [30], "Cronbach's alpha is the standard measure of internal correspondence between items in a scale, facilitating its widespread use with Likert Scale-based questions used in the survey. The fundamental objective of reliability testing was to examine the attributes of the scales of measurement and the items for getting the overall index of internal consistency of the scales."

The result of this test is summarized in the Table 2 provided above. The table represents the reliability analysis of the latent constructs used in the study. The consistency interprets the "high internal reliabilities" as the value of Cronbach's alpha ranges between 0.70 and 0.90. Because of this, it outpaces the threshold limit of 0.70 [31]. Table 2 of reliability result complementary denotes that the coefficient alpha of each latent construct is more than 0.8, revealing that there is strong internal consistency between the variable in a scale elect for the study.

Bartlett's test is used to resolve the requirement for reducing many statements into a smaller number of factors.

TABLE 1: Baseline data of the participants ( $N=165$ ).

Basis	Categories	F	C.F	%
Gender	M	116	116	70.3
	F	49	165	29.7
Age group	Up to 20 years	19	19	11.5
	21–30 years	71	90	43
	31–40 years	53	143	32.1
	41 and above	22	165	13.3
Educational qualification	U.G	31	31	18.8
	G	37	68	22.4
	P.G	44	112	26.7
	Dr	23	135	13.9
	P.D.H	30	165	18.2
Occupational status	Govt. employees	37	37	22.4
	Private. employees	49	86	29.7
	Business and self employees	32	118	19.4
	Students	47	165	28.5
Monthly income	≤Rs. 10000	38	38	23
	Rs. 10000–Rs. 25000	32	70	19.4
	Rs. 25000–Rs. 50000	69	139	41.8
	>Rs. 50000	26	165	15.8
Using the digital payment	Less than 1 year	23	23	13.9
	1–5 years	96	119	58.2
	6–10 years	44	163	26.7
	Above 10 years	2	165	1.2

TABLE 2: Reliability analysis.

Construct	$\alpha$	No. of items
Perception towards digital payment system (PDPS)	0.812	15

KMO describes the ratio of respondents to number of statements. If the KMO value is greater than 0.6, it is accepted for the study. This study revealed 0.813, which was highly accepted [32]. On the other hand, if Bartlett test  $p$  value is less than 5% alpha, it shows that sampling is adequate. The results of the KMO and Bartlett's test are provided in Table 3.

### 7.3. Perception of Customer towards Digital Payment System.

To analyze whether all the manifest variables are clearly explaining their respective latent construct, the CFA technique was applied by the researcher via AMOS (v-24) software in the present study. Conferring to this research study, to scrutinize the perception of customers towards digital payment system, the leading latent construct that is “perceptions towards digital payment system (PDPS)” has been categorized into five subconstructs. Additionally, each is examined by various statements chosen by the analyst to collect responses from the contributors. It is revealed in Figure 1.

The aforesaid CFA measurement model (Figure 1) portrays the “perception of customer towards digital payment system,” the prime latent variable, consistent of six subconstructs: “reliability, service quality, satisfaction, user-

friendly, trustworthy, and security.” Reliability, the first subconstruct, is consistent with three statements (DPS1, DPS2, and DPS3) expressed by rectangles known as observed variables. Service quality, the second subconstruct, is consistent with two items implied as DPS4 and DPS6. Satisfaction, the third subconstructs, is consistent with two items denoted as DPS7 and DPS8. User-friendly, the fourth subconstruct, measured by three statements implied as DPS10, DPS11, and DPS12. Trustworthy, the fifth subconstruct, is analysed through two items implied as DPS14 and DPS16. Security, the last six subconstructs, is examined by three items denoted as DPS19, DPS20, and DPS21. Fifteen statements were selected out of twenty-one, implying six items were deleted. The reason being it creates a model fitness problem.

Table 4 describes the “Chi-square ( $\chi^2$ )” value, i.e., 0.067, which is greater than 5% limit, and the “CMIN/DF” value, i.e., 1.238, which is less than the prescribed limit of 3. These values denote that the deposit sample input is fitting for the model fit. The four indices of goodness, i.e., GFI = 0.927, AGFI = 0.897, CFI = 0.952, and TLI = 0.941, are more than their recommended limits. It shows that the collected sample dataset is suitable for the model fitness. These values surpass their adequate limits, describing that the model is well-fitted. The two “badness-of-fit” indices denoted by RMSEA = 0.038 and SRMR = 0.062 are under the approved limit; it represents that the collected sample input fits the model properly. Hence, it supports that the measurement mentioned above is a well-fitted model.

The term “e” denotes error terms that represent how many parts of variation are unexplained. The standardised regression coefficient represented the arrow leading to the corresponding item, although value over each response item design the squared multiple correlations ( $R^2$ ) of manifest/measured variables. Tables 4 and 5 serve the analysis portion of the earlier model by analysis of moment structure (v-24).

The upstairs examination shows that all the measured variables are significantly connecting to their conforming constructs since their  $p$  values are lower than 5% alpha approved limit. Besides, the standardized regression weight ( $\beta$ ) of each item is above 0.40 which confirm that the “convergent validity” of the earlier discussed that the CFA measurement model is achieved, and it also illustrates that each manifest variable is highly correlated with its respective latent construct [33].

Table 6 shows the responses of customer towards the digital payment system. Draw out the five-point summated scale that stretches from “strongly disagree (1) to strongly agree (5).” Each statement percentage calculated as per the response provided by customers. This table proffers those which statements more positive feedback received from respondent and vice versa. Statements DPS1, DPS2, DPS3, DPS4, DPS6, DPS7, DPS8, DPS10, DPS11, DPS12, DPS14, DPS16, DPS18, DPS19, and DPS21 shows that respondents are more favourable towards digital payment system. On the other hand, DPS5, DPS9, DPS13, DPS15, DPS17, and DPS20 show that respondent least favourable towards digital payment systems.

TABLE 3: Sampling adequacy with the help of KMO and Bartlett’s test.

Construct	KMO	No. of Items	Bartlett’s test of sphericity		p value
			Approx. Chi-square ( $\chi^2$ )	df	
Perception towards digital payment system (PDPS)	0.813	15	509.536	105	$\leq 0.001$

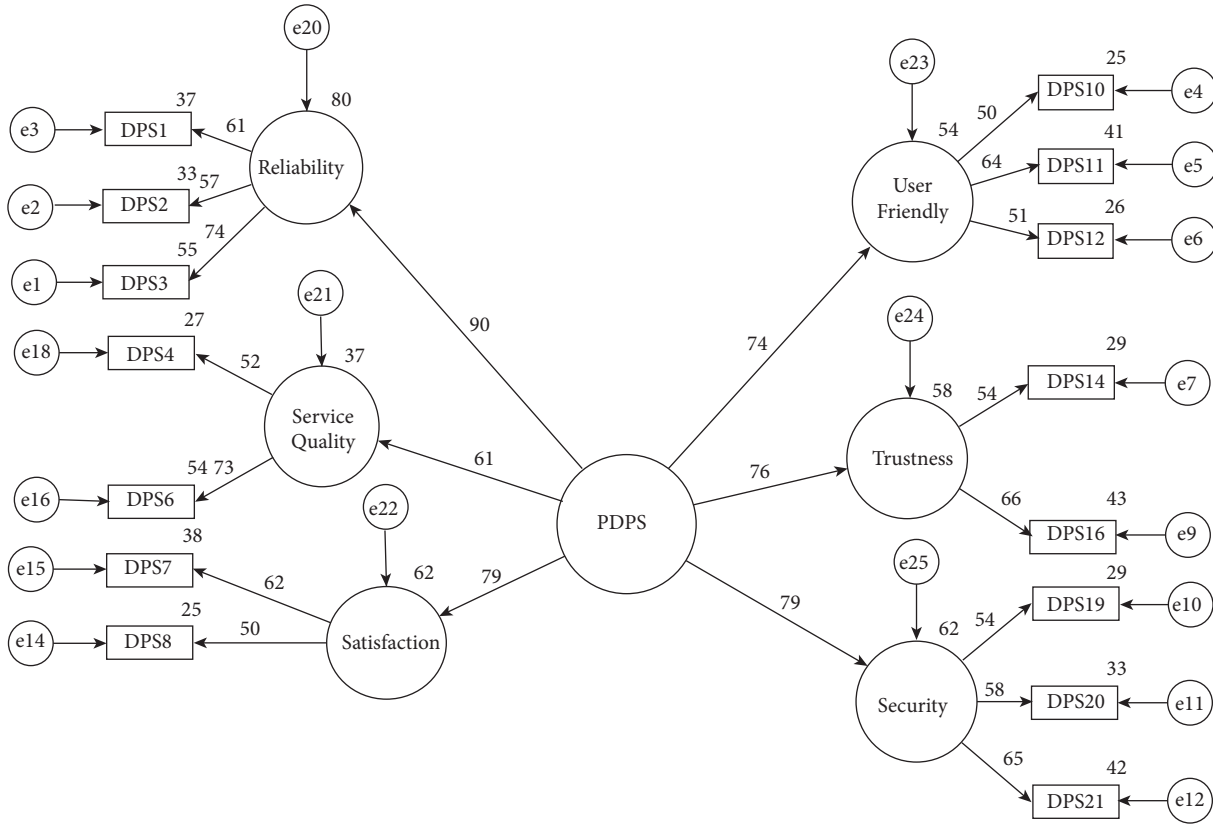


FIGURE 1: CFA measurement model for PDPS.

TABLE 4: Model fit analysis.

Name of category	Required fit indices	Acceptable limits	Values obtained
Absolute fit indices	$\chi^2$	$p$ value $> 0.05$	0.067
	RMSEA	$< 0.05$	0.038
	SRMR	$< 0.09$	0.062
	GFI	$> 0.90$	0.927
Incremental fit indices	AGFI	$> 0.80$	0.897
	CFI	$> 0.90$	0.952
	TLI	$> 0.90$	0.941
Parsimonious fit index	CMIN/DF	$< 3$	1.238

Consistent with the results of the independent sample  $t$ -test (Table 7), H01 is accepted. The value obtains not significant since the  $p$  value (probability value) is more than 0.001. This outcome expresses that gender does not significantly differ from the digital payment system. In some variables such as DPS7, DPS9, DPS12, DPS17, DPS18, and DPS20,  $p$  value is less than 0.005, which means gender significantly differs from the digital payment system.

Consistent with the results of ANOVA (Table 8), H02 is accepted. The value obtains not significant since the  $p$  value

(probability value) is more than 0.001. This outcome expresses that age group does not significantly differ from the digital payment system. In some variables such as DPS6, DPS9, DPS11, and DPS14, the  $p$  value is less than 0.005, which means the age group significantly differs from the digital payment system.

Consistent with the results of ANOVA (Table 9), H03 is accepted. The value obtains not significant since the  $p$  value (probability value) is more than 0.001. This outcome expresses that educational qualification does not significantly

TABLE 5: Analysis summary of scalar estimates.

Path	B	CR	<i>p</i> value
DPS → reliability	0.90	5.691	<0.001
DPS → service quality	0.61	4.051	<0.001
DPS → satisfaction	0.79	4.452	<0.001
DPS → user-friendly	0.72	4.051	<0.001
DPS → trustworthy	0.76	4.301	<0.001
DPS → security	0.79	4.452	<0.001
Reliability → DPS 1	0.61	6.432	<0.001
Reliability → DPS 2	0.57	6.118	<0.001
Reliability → DPS 3	0.74	4.151	<0.001
Service quality → DPS 4	0.52	3.682	<0.001
Service quality → DPS 6	0.73	4.131	<0.001
Satisfaction → DPS 7	0.62	4.716	<0.001
Satisfaction → DPS 8	0.50	3.996	<0.001
User-friendly → DPS 10	0.50	3.996	<0.001
User-friendly → DPS 11	0.64	4.430	<0.001
User-friendly → DPS 12	0.51	4.072	<0.001
Trustworthy → DPS 14	0.54	4.112	<0.001
Trustworthy → DPS 16	0.66	5.229	<0.001
Security → DPS 19	0.54	4.112	<0.001
Security → DPS 20	0.58	4.768	<0.001
Security → DPS 21	0.65	5.001	<0.001

TABLE 6: Responses of customers towards digital payment system.

Code	Variables	S. D (%)	D (%)	N (%)	A (%)	S. A (%)
DPS1	Digital payment system is more user-friendly than previous conventional ones	0.6	0.6	21.8	40	37
DPS2	Digital payment system is better than the traditional payment system	0.6	2.4	13.3	52.1	31.5
DPS3	I am more aware related to digital payment system	15.2	3.6	0.06	46.7	33.9
DPS4	Helpful in saving time, cost, and processing fees	4	12	4.6	39.4	40
DPS5	Update regarding digital payment service available from time to time	26	30	13	21	10
DPS6	I find that it is easier to conduct financial transaction through digital mean	3.9	8	9	49.1	30.3
DPS7	Digital payment system provides good mechanism, so I feel more comfortable while performing digital transaction	5.3	23	8	52.7	11
DPS8	There is well-regulated law relating to digital payment system	5.1	13.4	5.2	52.7	23.6
DPS9	I trust on digital payment system that it will not lead to transaction fraud	30	22	21	12	8
DPS10	It follows simple steps for completing the particular transactions	4.1	13	22	30	30.9
DPS11	An electronic payment system is easy to use	10	21	20	32	17
DPS12	Confidential information is delivered safely to customers	6	21	13	41	19
DPS13	Track and maintain the digital record of every transaction	31	20.1	21	15.6	12.3
DPS14	I trust on the ability of a digital payment system to protect my privacy	21	12	13	33	21
DPS15	Effective complaints and redressal mechanism.	33	24	6	23	14
DPS16	Digital payment system provides good mechanism, so I am not concerned regarding security and data protection issues	15.2	19.8	11	33	21
DPS17	It is providing speedy refund mechanism	41	13	17	18	11
DPS18	Heavily regulated and protected from any risk	13	10	19	31	27
DPS19	Transaction take place in immediate time	14	21	13	41	11
DPS20	The structure and contents of the web site/app are easy to understand	31	21	9	21	18
DPS21	Digital payment offers cash back and reward points to the users	10	19	11	43	21

differ from the digital payment system. In some variables such as DPS9, DPS14, and DPS18, *p* value is less than 0.005, which means educational qualification significantly differ from the digital payment system.

Consistent with the results of ANOVA (Table 10), H04 is accepted. The value obtains not significant since the *p* value (probability value) is more than 0.001. This outcome expresses that occupational status does not significantly differ

with the digital payment system. In some variables such as DPS3, DPS9, DPS14, DPS15, DPS18, and DPS20, *p* value is less than 0.005, which means occupational status significantly differ with the digital payment system.

Consistent with the results of ANOVA (Table 11), H05 is accepted. The value obtains not significant since the *p* value (probability value) is more than 0.001. This outcome expresses that monthly income does not significantly differ

TABLE 7: Gender as independent variable by using independent sample *t*-test.

Variable	Gender	N	Std. error	<i>t</i> -value	d.f	<i>p</i> value
DPS1	M	116	0.073	1.895	163	0.568
	F	49	0.122	1.831	83.896	
DPS2	M	116	0.070	-0.300	163	0.248
	F	49	0.177	-0.290	83.896	
DPS3	M	116	0.072	2.025	163	0.800
	F	49	0.131	1.891	83.896	
DPS4	M	116	0.081	0.115	163	0.944
	F	49	0.118	0.115	83.896	
DPS5	M	116	0.065	1.706	163	0.974
	F	49	0.107	1.662	83.896	
DPS6	M	116	0.072	0.768	163	0.350
	F	49	0.129	0.723	83.896	
DPS7	M	116	0.065	2.041	163	<0.001
	F	49	0.121	1.885	83.896	
DPS8	M	116	0.071	0.421	163	0.293
	F	49	0.116	0.410	83.896	
DPS9	M	116	0.073	1.321	163	<0.001
	F	49	0.129	1.247	83.896	
DPS10	M	116	0.073	0.182	163	0.631
	F	49	0.122	0.176	83.896	
DPS11	M	116	0.065	2.376	163	0.213
	F	49	0.103	2.349	83.896	
DPS12	M	116	0.065	2.361	163	<0.005
	F	49	0.146	2.035	83.896	
DPS13	M	116	0.067	1.177	163	0.761
	F	49	0.113	1.135	83.896	
DPS14	M	116	0.071	1.809	163	0.161
	F	49	0.137	1.653	83.896	
DPS15	M	116	0.082	1.837	163	0.814
	F	49	0.119	1.881	83.896	
DPS16	M	116	0.079	0.664	163	0.079
	F	49	0.137	0.632	83.896	
DPS17	M	116	0.055	0.747	163	<0.001
	F	49	0.109	0.675	83.896	
DPS18	M	116	0.071	2.781	163	<0.001
	F	49	0.129	2.602	83.896	
DPS19	M	116	0.066	1.044	163	0.678
	F	49	0.126	0.958	83.896	
DPS20	M	116	0.069	1.544	163	<0.001
	F	49	0.149	1.352	83.896	
DPS21	M	116	0.069	0.762	163	0.659
	F	49	0.118	0.731	83.896	

with the digital payment system. In some variables such as DPS6, DPS7, DPS9, DPS14, DPS15, and DPS18, *p* value is less than 0.005, which means monthly income significantly differs from the digital payment system.

## 8. Limitations and Future Research

This section points out a few limitations of this research study which should be taken into forethought. First, the sample size in this study is relatively moderate to generalize for India's large population, and in this study, participants of age group response % rate are more or less similar to each other. So, future studies might take a larger sample size and focus on the youth age group of below 30 years as their perception of customers regarding digital payment might be different. Also, the study participants are associated with the urban class of

the population who have more connection to technology. Future research might include the rural class of India in the study as the rural class constitutes a bigger section of the Indian population. If the researcher is unable to reach them through due to technological barriers, then the success of digital system becomes a big question mark. Furthermore, purposive sampling was used to determine the respondents taken in the study. So, in future research, if probability sampling techniques could be used to collect data, and then the generalizability of the findings could be improved.

## 9. Future of Digital Payment in India

The research analysis indicates that the Indian economy will take a substantial time in becoming cashless in its entirety, i.e., with the natives confidently relying on exercising digital

TABLE 8: Age as independent variable by using one-way ANOVA.

Variable	Age group	Sum of square		d. f	F value	p value
		Between groups	Within groups			
DPS1	Up to 20 years	2.367	105.209	3	1.207	0.309
	21–30 years			161		
	31–40 years					
	40 and above					
DPS2	Up to 20 years	3.340	109.109	3	0.161	0.922
	21–30 years			161		
	31–40 years					
	40 and above					
DPS3	Up to 20 years	2.534	116.678	3	1.643	0.182
	21–30 years			161		
	31–40 years					
	40 and above					
DPS4	Up to 20 years	1.199	83.614	3	1.166	0.325
	21–30 years			161		
	31–40 years					
	40 and above					
DPS5	Up to 20 years	7.446	101.063	3	0.769	0.513
	21–30 years			161		
	31–40 years					
	40 and above					
DPS6	Up to 20 years	7.446	101.063	3	3.954	<0.001
	21–30 years			161		
	31–40 years					
	40 and above					
DPS7	Up to 20 years	0.230	92.474	3	0.133	0.940
	21–30 years			161		
	31–40 years					
	40 and above					
DPS8	Up to 20 years	1.633	97.070	3	0.903	0.441
	21–30 years			161		
	31–40 years					
	40 and above					
DPS9	Up to 20 years	11.883	98.929	3	6.446	<0.001
	21–30 years			161		
	31–40 years					
	40 and above					
DPS10	Up to 20 years	1.613	104.362	3	0.830	0.479
	21–30 years			161		
	31–40 years					
	40 and above					
DPS11	Up to 20 years	4.718	79.075	3	3.202	<0.001
	21–30 years			161		
	31–40 years					
	40 and above					
DPS12	Up to 20 years	3.698	106.205	3	1.869	0.137
	21–30 years			161		
	31–40 years					
	40 and above					
DPS13	Up to 20 years	0.076	90.433	3	0.045	0.987
	21–30 years			161		
	31–40 years					
	40 and above					
DPS14	Up to 20 years	5.543	108.239	3	2.748	<0.001
	21–30 years			161		
	31–40 years					
	40 and above					



TABLE 8: Continued.

Variable	Age group	Sum of square		d. f	F value	p value
		Between groups	Within groups			
DPS15	Up to 20 years	5.642	113.782	3	2.547	0.058
	21–30 years			161		
	31–40 years					
	40 and above					
DPS16	Up to 20 years	1.270	125.858	3	0.541	0.655
	21–30 years			161		
	31–40 years					
	40 and above					
DPS17	Up to 20 years	1.673	67.140	3	1.337	0.264
	21–30 years			161		
	31–40 years					
	40 and above					
DPS18	Up to 20 years	4.318	108.130	3	2.143	0.097
	21–30 years			161		
	31–40 years					
	40 and above					
DPS19	Up to 20 years	1.576	94.569	3	0.895	0.445
	21–30 years			161		
	31–40 years					
	40 and above					
DPS20	Up to 20 years	5.447	113.062	3	2.585	0.055
	21–30 years			161		
	31–40 years					
	40 and above					
DPS21	Up to 20 years	0.852	96.785	3	0.472	0.702
	21–30 years			161		
	31–40 years					
	40 and above					

TABLE 9: Educational qualification as independent variable by using one-way ANOVA.

Variable	Educational qualification	Sum of square		d. f	F value	p value
		Between groups	Within groups			
DPS1	U. G	2.144	105.432	3	0.813	0.518
	G			161		
	P. G					
	Dr					
DPS2	P.D.H	3.309	93.503	3	1.415	0.231
	U. G			161		
	G					
	P. G					
DPS3	Dr	3.072	109.377	3	1.123	0.347
	P.D.H			161		
	U. G					
	G					
DPS4	P. G	0.294	118.918	3	0.099	0.983
	G			161		
	P. G					
	Dr					
DPS5	P.D.H	3.854	80.958	3	1.904	0.112
	U. G			161		
	G					
	P. G					

TABLE 9: Continued.

Variable	Educational qualification	Sum of square		d. f	F value	p value
		Between groups	Within groups			
DPS6	U. G	5.966	102.543	3	2.327	0.059
	G					
	P. G					
DPS7	Dr	1.023	91.680	161	0.446	0.775
	P.D.H					
	U. G					
DPS8	G	5.556	93.147	3	2.386	0.053
	P. G					
	Dr					
DPS9	P.D.H	6.466	104.347	161	2.478	<0.001
	U. G					
	G					
DPS10	P. G	3.649	102.327	3	1.426	0.228
	Dr					
	P.D.H					
DPS11	U. G	1.207	82.587	3	0.584	0.674
	G					
	P. G					
DPS12	Dr	1.213	108.691	161	0.446	0.775
	P.D.H					
	U. G					
DPS13	G	0.795	89.715	3	0.354	0.841
	P. G					
	Dr					
DPS14	P.D.H	11.372	102.410	161	4.442	<0.001
	U. G					
	G					
DPS15	P. G	4.685	119.825	3	1.564	0.187
	Dr					
	P.D.H					
DPS16	U. G	5.004	122.123	3	1.639	0.167
	G					
	P. G					
DPS17	Dr	2.151	66.661	161	1.291	0.276
	P.D.H					
	U. G					

TABLE 9: Continued.

Variable	Educational qualification	Sum of square		d. f	F value	p value
		Between groups	Within groups			
DPS18	U. G	7.493	104.955	3	2.856	<0.001
	G					
	P. G					
	Dr					
DPS19	P.D.H	1.333	94.812	161	0.562	0.690
	U. G					
	G					
	P. G					
DPS20	Dr	5.091	113.418	161	1.796	0.132
	P.D.H					
	U. G					
	G					
DPS21	P. G	4.385	93.251	3	1.881	0.116
	G					
	Dr					
	P.D.H					

TABLE 10: Occupational status as independent variable by using one-way ANOVA.

Variable	Occupational status	Sum of square		d. f	F value	p value
		Between groups	Within groups			
DPS 1	Govt. employee	2.115	105.461	3	1.076	0.361
	Private employee					
	Business/self employee					
	Students					
DPS 2	Govt. employee	1.463	95.349	3	0.823	0.483
	Private employee					
	Business/self employee					
	Students					
DPS 3	Govt. employee	5.502	106.946	3	2.761	<0.001
	Private employee					
	Business/self employee					
	Students					
DPS 4	Govt. employee	0.898	118.314	3	0.407	0.748
	Private employee					
	Business/self employee					
	Students					
DPS 5	Govt. employee	1.833	82.979	3	1.186	0.317
	Private employee					
	Business/self employee					
	Students					
DPS 6	Govt. employee	4.418	104.091	3	2.278	0.082
	Private employee					
	Business/self employee					
	Students					
DPS 7	Govt. employee	1.509	91.194	3	0.888	0.449
	Private employee					
	Business/self employee					
	Students					
DPS 8	Govt. employee	2.064	96.639	3	1.146	0.332
	Private employee					
	Business/self employee					
	Students					

TABLE 10: Continued.

Variable	Occupational status	Sum of square		d. f	F value	p value
		Between groups	Within groups			
DPS 9	Govt. employee	8.592	102.220	3	4.511	<0.001
	Private employee			161		
	Business/self employee			161		
	Students			161		
DPS 10	Govt. employee	1.210	104.766	3	0.620	0.603
	Private employee			161		
	Business/self employee			161		
	Students			161		
DPS 11	Govt. employee	0.774	83.020	3	0.500	0.683
	Private employee			161		
	Business/self employee			161		
	Students			161		
DPS 12	Govt. employee	2.203	107.700	3	1.098	0.352
	Private employee			161		
	Business/self employee			161		
	Students			161		
DPS 13	Govt. employee	1.134	89.375	3	0.681	0.565
	Private employee			161		
	Business/self employee			161		
	Students			161		
DPS 14	Govt. employee	11.833	101.949	3	6.229	<0.001
	Private employee			161		
	Business/self employee			161		
	Students			161		
DPS 15	Govt. employee	6.994	117.515	3	3.194	<0.001
	Private employee			161		
	Business/self employee			161		
	Students			161		
DPS 16	Govt. employee	5.134	121.994	3	2.258	0.084
	Private employee			161		
	Business/self employee			161		
	Students			161		
DPS 17	Govt. employee	1.732	67.080	3	1.386	0.249
	Private employee			161		
	Business/self employee			161		
	Students			161		
DPS 18	Govt. employee	6.435	106.014	3	3.257	<0.001
	Private employee			161		
	Business/self employee			161		
	Students			161		
DPS 19	Govt. employee	0.123	96.022	3	0.069	0.976
	Private employee			161		
	Business/self employee			161		
	Students			161		
DPS 20	Govt. employee	5.807	112.702	3	2.765	<0.001
	Private employee			161		
	Business/self employee			161		
	Students			161		
DPS 21	Govt. employee	3.076	94.561	3	1.746	0.160
	Private employee			161		
	Business/self employee			161		
	Students			161		

payment systems and using electronic means of payment. Greater awareness is needed to ensure people in all parts of the country recognize the benefits of carrying out digital transactions through various means. It is imperative to

resolve the scarcity of appropriate digital literacy to advance to make India a digitized economy correctly. Despite the currently provided cashback and relevant promotional offers, a steady, dedicated, and genuinely secure payment

TABLE 11: Monthly income as independent variable by using one-way ANOVA.

Variable	Monthly income	Sum of square		d. f	F value	p value
		Between groups	Within groups			
DPS 1	≤Rs. 10000	1.269	106.307	3	0.641	0.590
	Rs. 10000–Rs. 25000			161		
	Rs. 25000–Rs. 50000			161		
DPS 2	≤Rs.10000	1.475	95.337	3	0.831	0.479
	Rs. 10000–Rs. 25000			161		
	Rs. 25000–Rs. 50000			161		
DPS 3	≤Rs. 10000	2.872	109.576	3	1.407	0.243
	Rs. 10000–Rs. 25000			161		
	Rs. 25000–Rs. 50000			161		
DPS 4	≤Rs. 10000	2.194	117.018	3	1.006	0.392
	Rs. 10000–Rs. 25000			161		
	Rs. 25000–Rs. 50000			161		
DPS 5	≤Rs. 10000	3.552	81.261	3	2.346	0.075
	Rs. 10000–Rs. 25000			161		
	Rs. 25000–Rs. 50000			161		
DPS 6	≤Rs. 10000	9.793	98.716	3	5.324	<0.001
	Rs. 10000–Rs. 25000			161		
	Rs. 25000–Rs. 50000			161		
DPS 7	≤Rs. 10000	4.592	88.111	3	2.797	<0.001
	Rs. 10000–Rs. 25000			161		
	Rs. 25000–Rs. 50000			161		
DPS 8	≤Rs. 10000	1.471	97.232	3	0.812	0.489
	Rs. 10000–Rs. 25000			161		
	Rs. 25000–Rs. 50000			161		
DPS 9	≤Rs. 10000	10.336	100.476	3	5.521	<0.001
	Rs. 10000–Rs. 25000			161		
	Rs. 25000–Rs. 50000			161		
DPS 10	≤Rs. 10000	0.761	105.215	3	0.388	0.762
	Rs. 10000–Rs. 25000			161		
	Rs. 25000–Rs. 50000			161		
DPS 11	≤Rs. 10000	1.219	82.575	3	0.792	0.500
	Rs. 10000–Rs. 25000			161		
	Rs. 25000–Rs. 50000			161		
DPS 12	≤Rs. 10000	3.102	106.801	3	1.559	0.202
	Rs. 10000–Rs. 25000			161		
	Rs. 25000–Rs. 50000			161		
DPS 13	≤Rs. 10000	1.115	89.394	3	0.670	0.572
	Rs. 10000–Rs. 25000			161		
	Rs. 25000–Rs. 50000			161		
DPS 14	≤Rs. 10000	8.521	105.261	3	4.344	<0.001
	Rs. 10000–Rs. 25000			161		
	Rs. 25000–Rs. 50000			161		
DPS 15	≤Rs. 10000	7.666	116.843	3	3.521	<0.001
	Rs. 10000–Rs. 25000			161		
	Rs. 25000–Rs. 50000			161		

TABLE 11: Continued.

Variable	Monthly income	Sum of square		d. f	F value	p value
		Between groups	Within groups			
DPS 16	≤Rs. 10000	2.053	125.075	3	0.881	0.452
	Rs. 10000–Rs. 25000			161		
	Rs. 25000–Rs. 50000					
DPS 17	>Rs. 50000	0.259	68.553	3	0.203	0.894
	≤Rs.10000			161		
	Rs. 10000–Rs. 25000					
DPS 18	Rs. 25000–Rs. 50000	8.334	104.114	3	4.296	<0.001
	>Rs. 50000			161		
	≤Rs. 10000					
DPS 19	Rs. 10000–Rs. 25000	0.761	95.385	3	0.428	0.733
	Rs. 25000–Rs. 50000			161		
	>Rs. 50000					
DPS 20	≤Rs. 10000	3.927	114.582	3	1.839	0.142
	Rs. 10000–Rs. 25000			161		
	Rs. 25000–Rs. 50000					
DPS 21	>Rs. 50000	3.545	94.091	3	2.022	0.113
	≤Rs. 10000			161		
	Rs. 10000–Rs. 25000					
	Rs. 25000–Rs. 50000					
	>Rs. 50000					

network is needed to adequately boost digital transactions in the country, which will enable absolute transparency in transactions, ultimately leading to the identification and eradication of black money.

## 10. Suggestions

- (1) Transaction cost plays a crucial role in encouraging and discouraging at the same time in the adoption of digital payment methods.
- (2) Education-related programs are the best way to provide knowledge to customers about how it is beneficial, less costly, and user-friendly.
- (3) Security and trustiness are complementary. If users feel secure regarding the online platform, it ultimately creates goodwill or trust in service providers.

## 11. Conclusion

This research thoroughly endeavoured towards understanding the viewpoints of the general people towards online means of payment. It is, hence, discovered that a more significant influence is played by the demographic factors in the appropriate adoption of the various digital payment services, which include age, gender, educational qualification, occupational status, and the level of income. On other hand, factors such as reliability, satisfaction, service quality, user-friendly, trustworthy, and security also have positive impact on customer adoption. The study examines that the user provides positive response towards digital payments. Besides, the research outcome emphasises the various

benefits of exercising digital payments, or otherwise, necessitating the neediness to increase e-payments. Digital means of transactions are not merely beneficial concerning the give-and-take of money but also comprise additional benefits. These include timely reminders of unpaid bills, recharges, various cashbacks and rewards scheme, and linking of bank accounts for autopay structure, all leading to greater convenience and efficacy. It is also evident that online means of transactions or digital payment services will become necessary soon. Henceforth, it is imperative for most of the populace, mainly of those belonging to the rural areas, to make the required transition from the traditional means of spending money to modern-day methods that rely on the application of the Internet. It is determined that the online mode of transactions is considerably secure and time-saving, which also accommodates for keeping an easy-to-access record of all the transactions carried out. The continual advancements in the IT and Communications sector have also enhanced the reachability of mobile networks, along with greater availability of electricity and Internet, leading to the increased use of digital services. It can, therefore, be unquestionably stated that the ultimate transaction system would be cashless. There are more significant benefits to be reaped from exercising digital means of payments. Whether it is E-wallets or mobile banking, the modern-day method of transacting allows people to carry out business anywhere, anytime, at their fingertips, with absolute ease of operations. The coming years will bring forward a substantial increase in the use of digital transactions, all ultimately leading to the fulfilment of India's mission of becoming a digitized economy. As more and more advancements are made,

specifically in the digital sphere, our habits have continuously evolved. It is high time for the natives to move forward from sticking to the cash-based commerce format and switch to the digitized payment structure. Its several advantages include a substantial reduction in the cost of currency management and detecting various kinds of fraudulent activities, strengthening the economic position. Besides, the government's continuous efforts in creating adequate awareness, building necessary trust, and providing a concrete cybersecurity framework and infrastructure are likely to fasten the people's receptiveness towards digital payment systems, which is currently, by and large, facilitated by the constant growth in the number of smartphone users and Internet penetration, in both urban as well as rural areas.

### Data Availability

The data used to support the findings of this study are available from the corresponding author upon request.

### Conflicts of Interest

The author declares that there are no conflicts of interest.

### References

- [1] M. Y. Adults, "Factors influencing the use of E-wallet as a payment method among Malaysian young adults," *Journal of International Business and Management*, vol. 3, no. 2, pp. 1–11, 2020.
- [2] A. M. Banu, N. S. Mohamed, and S. Parayitam, "Online banking and customer satisfaction: evidence from India," *Asia-Pacific Journal of Management Research and Innovation*, vol. 15, no. 1-2, pp. 68–80, 2019.
- [3] F. D. Bocell, E. Sanders, R. Abbott, M. Li, D. Mccutchen, and D. Amtmann, "The impact of unmodeled error covariance on measurement models in structural equation modeling," 2015, [https://digital.lib.washington.edu/researchworks/bitstream/handle/1773/33773/Bocell\\_washington\\_0250E\\_14570.pdf?sequence=](https://digital.lib.washington.edu/researchworks/bitstream/handle/1773/33773/Bocell_washington_0250E_14570.pdf?sequence=).
- [4] S. Chakraborty and D. Mitra, "A study on consumers adoption intention for digital wallets in India," *International Journal on Customer Relations*, vol. 6, no. 1, pp. 38–57, 2018.
- [5] M. Chauhan and I. Shingari, "Future of e-wallets: a perspective from under graduates," *International Journal of Advanced Research in Computer Science and Software Engineering*, vol. 7, no. 8, p. 146, 2017.
- [6] G. Ghosh, "Adoption of digital payment system by consumer: a review of literature," vol. 9, no. 2, pp. 412–418, 2021.
- [7] M. Y. Husain, R. Mustapha, and S. A. Malik, "Review of measurement item of engineering students' learning environment: confirmatory factor analysis," *Journal of Technical Education and Training*, vol. 6, no. 1, pp. 42–56, 2014.
- [8] P. Kalyani, "An empirical study about the awareness of paperless E-currency transaction like E-wallet using ICT in the youth of India," *Journal of Management Engineering and Information Technology (JMEIT)*, vol. 3, no. 3, pp. 2394–8124, 2016.
- [9] G Kanimozhi and K. S. Kamatchi, "Security aspects of mobile based E wallet," *International Journal on Recent and Innovation Trends in Computing and Communication*, vol. 5, no. 6, pp. 1223–1228, 2017.
- [10] S. Khatoun, X. Zhengliang, and H. Hussain, "The mediating effect of customer satisfaction on the relationship between electronic banking service quality and customer purchase intention: evidence from the Qatar banking sector," *SAGE Open*, vol. 10, no. 2, 2020.
- [11] A. Krishnan and R. Ramasamy, "Assessing the construct and content validity of uncertainty business using sem approach—an exploratory study of manufacturing firms," *Global Journal of Management and Business Research*, vol. 11, no. 12, pp. 1–9, 2011.
- [12] P. Lai, "Research methodology for novelty technology," *Journal of Information Systems and Technology Management*, vol. 15, 2018.
- [13] F. Li, H. Lu, M. Hou, K. Cui, and M. Darbandi, "Customer satisfaction with bank services: the role of cloud services, security, e-learning and service quality," *Technology in Society*, vol. 64, Article ID 101487, 2021.
- [14] G. M. Ling, Y. S. Fern, L. K. Boon, and T. S. Huat, "Understanding customer satisfaction of Internet banking: a case study in malacca," *Procedia Economics and Finance*, vol. 37, no. 16, pp. 80–85, 2016.
- [15] L. Lu, "Decoding Alipay: mobile payments, a cashless society and regulatory challenges," *Butterworths Journal of International Banking and Financial Law*, vol. 33, no. 1, pp. 40–43, 2018.
- [16] D. A. Malar, V. Arvidsson, and J. Holmstrom, "Digital transformation in banking: exploring value co-creation in online banking services in India," *Journal of Global Information Technology Management*, vol. 22, no. 1, pp. 7–24, 2019.
- [17] L. Malusare, "Digital payments methods in India : a study of problems and prospects," *International Journal of Scientific Research in Engineering and Management (IJSREM)*, vol. 3, no. 8, pp. 1–7, 2019.
- [18] M. Mujjanga, "Online banking service quality: a South African E-S-qual analysis," in *Lecture Notes in Computer Science (including subseries Lecture Notes in Artificial Intelligence and Lecture Notes in Bioinformatics)*, vol. 12066, Berlin, Germany, Springer International Publishing, 2020.
- [19] D. C. Muthurasu and D. M. Suganthi, "An overview on digital library," *Global Journal for Research Analysis*, vol. 8, no. 11, pp. 1–2, 2019.
- [20] T. M. Nisar and G. Prabhakar, "Exploring the key drivers behind the adoption of mobile banking services," *Journal of Marketing Analytics*, vol. 5, no. 3-4, pp. 153–162, 2017.
- [21] P. Jayakumar and M. V. Sahayaraj, "A study on customer satisfaction of modern banking system," *International Journal Advanced Scientific Research and Development*, vol. 50, 2016.
- [22] P. P. Patil, N. P. Rana, and Y. K. Dwivedi, "Digital payments adoption research: a review of factors influencing consumer's attitude, intention and usage," in *Lecture Notes in Computer Science (including subseries Lecture Notes in Artificial Intelligence and Lecture Notes in Bioinformatics)*, vol. 11195, Berlin, Germany, Springer International Publishing, 2018.
- [23] V. K. Research Scholar and M. Sumathy, "Digital payment systems: perception and concerns among urban consumers," vol. 3, no. 6, pp. 1118–1122, 2017.
- [24] I. Researcher and B. Franco Maseke, "Journal of Internet banking and commerce the impact of mobile banking on customer satisfaction: commercial banks of Namibia (keetmanshoop) romario gomachab," *Journal of Internet Banking and Commerce*, vol. 23, no. 2, 2018.
- [25] A. M. Tadse, H. Singh Nannade, A. M. Tadse, and H. S. Nannade, "A study on usage of PAYTM," *Pune Research Scholar*, vol. 3, no. 2, pp. 1–11, 2017.

- [26] C. Revathy and P. Balaji, "Determinants of behavioural intention on E-wallet usage: an empirical examination in amid of COVID-19 lockdown period," *International Journal of Management*, vol. 11, no. 6, pp. 92–104, 2020.
- [27] S. Routray, R. Khurana, R. Payal, and R. Gupta, "A move towards cashless economy: a case of continuous usage of mobile wallets in India," *Theoretical Economics Letters*, vol. 9, no. 4, pp. 1152–1166, 2019.
- [28] R. Tamilselvi and P. Balaji, "The key determinants of behavioural intention towards mobile banking adoption," *International Journal of Innovative Technology and Exploring Engineering*, vol. 8, no. 10, pp. 1124–1130, 2019.
- [29] M. Salah Uddin and A. Yesmin Akhi, "E-wallet system for Bangladesh an electronic payment system," *International Journal of Modeling and Optimization*, vol. 4, no. 3, pp. 216–219, 2014.
- [30] S. Shree, B. Pratap, R. Saroy, and S. Dhal, "Digital payments and consumer experience in India: a survey based empirical study," *Journal of Banking and Financial Technology*, vol. 5, pp. 1–20, Article ID 0123456789, 2021.
- [31] N. Ul Hadia, N. Abdullah, and I. Sentosa, "An easy approach to exploratory factor analysis: marketing perspective," *Journal of Educational and Social Research*, vol. 6, no. 1, 2016.
- [32] A. Upadhayaya, "Electronic commerce and E-wallet," *International Journal of Recent Research and Review*, vol. 1, pp. 37–41, 2012.
- [33] O. Ureche and R. Plamondon, "Digital payment systems for Internet commerce: the state of the art," *World Wide Web*, vol. 3, no. 1, pp. 1–11, 2000.



## Research Article

# The Influence of Industrial Policy on Innovation in Startup Enterprises: An Empirical Study Based on China's GEM Listed Companies

Fang Wang<sup>1</sup> and Deyong Zhu <sup>2</sup>

<sup>1</sup>School of Economics and Management, Wuhan University, Wuhan 430072, China

<sup>2</sup>School of Tourism and Hospitality Management, Wuhan City Polytechnic, Wuhan 430072, China

Correspondence should be addressed to Deyong Zhu; zhudeyong@whcp.edu.cn

Received 4 August 2021; Revised 14 October 2021; Accepted 16 October 2021; Published 29 October 2021

Academic Editor: Sameh S. Askar

Copyright © 2021 Fang Wang and Deyong Zhu. This is an open access article distributed under the Creative Commons Attribution License, which permits unrestricted use, distribution, and reproduction in any medium, provided the original work is properly cited.

This study uses China's Growth Enterprises Market (GEM) listed companies from 2011 to 2017 as samples to examine the impact of industrial policies on innovation in startups from three dimensions, namely, selective industrial policies, government subsidies, and financial support. The results show that selective industrial policies have no effect on the innovation output of startups. Financial support can significantly promote the innovation output of entrepreneurial enterprises; structural differences exist in the impact of government subsidies on the innovation of entrepreneurial enterprises. The influence of industrial policy on the innovation of entrepreneurial enterprises depends on the research and development intensity of enterprises, the level of regional economic development, the leadership structure of enterprises, and other factors. This study's findings have significant practical significance for the implementation of a national innovation-driven development strategy and to guide industrial policies that better promote enterprise innovation.

## 1. Introduction

The term "industrial policy" was put forward by the representative of Japan's Ministry of Trade and Industry at the Organization for Economic Cooperation and Development (OECD) conference in the 1970s. At the time, Japan's economy was advancing rapidly, creating a "post-war miracle." Industrial policy played an important role in this process and has attracted widespread attention ever since. China has gradually developed systematic industrial policies since the late 1980s, and its rapid economic growth since 1978 has benefited from the implementation of various industrial policies [1]. Since the beginning of the 21st century, the Chinese government has strengthened its intervention in the microeconomy and continued to enhance the implementation of industrial policies. Currently, China has many industrial policies and industrial planning documents that cover almost all industries, with their influence reaching all aspects of the national economy. Entering a

period of economic "new normal" (returning to a normal state after a period of abnormality), industrial policies are still required. This is primarily because the technological innovation and industrial upgrade for the promotion of economic development require the efforts of entrepreneurs as well as government assistance to solve difficult externalities and coordinate the corresponding soft and hard infrastructure [2].

Between 2016 and 2020, with the progress of the information age and the deepening of China's economic transformation, the contradiction accumulated by extensive economic growth driven by factor input and investment has become increasingly prominent and has gradually become the bottleneck of sustained economic development [3]. Economic growth is facing a critical stage of transformation from a factor-driven model to an innovation-driven model. The innovation efficiency of microsubjects is high, which is an important carrier of innovation activities [4]. Innovation is an inexhaustible driving force for the progress of

microsubjects. Therefore, the promotion of enterprise innovation has become a focus of society. In the new period, small- and medium-sized enterprises (SMEs) have become an emerging driving force for the transformation and upgradation of China's industrial structure and innovation-driven development. They further influence the guiding effect of industrial policies on enterprise innovation and have become one of the key forces for China's industrial transformation and upgradation as well as the transformation of the mode of economic development.

A section of the literature on the impact of industrial policy on enterprise research and development (R&D) innovation reveals the belief that industrial policy can promote enterprise R&D innovation. Choi et al. [5] believe that certain selective industrial policies directly increase corporate profits that companies can survive a small amount of innovative behavior, and their willingness to innovate will be reduced. Scholars who support industrial policy recognize that such policies promote enterprise R&D innovation, but hold different views on the mechanism of these policies' influence on enterprise R&D innovation [6]. Industrial policies can influence R&D innovation through policy tools such as tax incentives, financial loans, and government subsidies. Many scholars have examined the impact of industrial policy tools such as government subsidies and tax incentives on R&D innovation, but the results are not consistent. Some scholars believe that government subsidies can promote enterprise R&D innovation. Yu [7] believes that, in the short term, government subsidies can promote enterprises' R&D and innovation output. Scott [8] analyzed the data of American companies and found that government R&D subsidies and corporate R&D investment are positively correlated. Liu et al. [9] examined high-tech enterprises in Jiangsu Province and found that government subsidies for R&D play a significant role in promoting R&D expenditures, and private enterprises play a stronger role in promoting R&D than their state-owned counterparts. Jin et al. [10] showed that receiving government subsidies improves private R&D investment and firm performance, that government R&D subsidies can stimulate corporate R&D investment, and that subsidies have no significant impact on innovation performance, while R&D investment has a positive impact. Xu et al. [11] found that government R&D subsidies can stimulate corporate R&D investment, and they have no significant impact on innovation performance, while R&D investment has a positive impact. In addition, environmental policies also affect the innovation efficiency of regions or companies [12, 13]. Some scholars believe that government subsidies have a squeezing effect on enterprises' R&D and innovation. This is because these subsidies can directly increase the profits of enterprises and compensate for the losses of enterprises to a certain extent. Enterprises can obtain profits without innovation, which may lead to them reducing R&D innovation activity. Bound et al. [14] studied large- and medium-sized manufacturing companies in the United States and found that, with an increase in R&D investment, the number of patents obtained by companies declined. Hall [15] believes that government subsidies can increase corporate profits to a certain extent, improve their

survival even with low R&D efforts, and reduce the enthusiasm of corporate R&D, so that it has a crowding-out effect.

This paper details the influence mechanism of entrepreneurial innovation industrial policy and presents corresponding policy recommendations based on the research results to promote China's business enterprise innovation. The marginal contributions of this study are as follows:

- (1) This study introduces the influence of government subsidy policy and financial support (FS) policy on enterprise innovation into the same research framework and further divides the former into science and technology special subsidies and nonscience and technology special subsidies. The research findings support the implementation of different types of industrial policies and improving the efficiency of policy implementation.
- (2) This study provides new evidence based on entrepreneurial enterprises. In previous studies, most research has focused on mature large- and medium-sized enterprises as research samples for the sake of data availability and convenience. This study considers entrepreneurial enterprises as the empirical object and responds to the encouragement to entrepreneurial enterprises through the advocacy of "mass innovation and entrepreneurship" in the 13<sup>th</sup> National Five-Year Plan and other documents.

This study examines the impact of industrial policies on enterprise R&D innovation from three dimensions: selective industrial policy, government subsidies, and FS. It helps to further refine the impact of different industrial policies on enterprise R&D innovation and enrich the impact of industrial policy tools on this process. At the same time, industrial transformation and upgrading are inseparable from enterprise innovation. This study examines industrial policies from the perspective of microenterprises, tests whether industrial policies are based on enterprises, and provides an empirical basis for the formulation and improvement of industrial policies.

## 2. Background and Hypotheses

*2.1. Background.* Generally, industrial policy can be divided into "functional industrial policy" and "selective industrial policy." "Market-friendly" functional industrial policies create an environment for industrial development. More enterprises are allowed to enter the market, and "pre-support" (infrastructure construction, talent cultivation, etc.) influences enterprise behavior as a primary factor. Selective industrial policies provide "after-the-fact support" (subsidies, such as price and operating loss, tax incentives, etc.) to subsidize or protect specific enterprises. In the 21st century, the Chinese government has emphasized the key role of market mechanisms in resource allocation and has gradually paid more attention to the market-friendly "functional industrial policy." However, the history of China's planned economy system results in the continuation of the previous government's intervention regarding industrial policy.

Meanwhile, China is still in the early stage of the transition from a “planned economy” to a “market economy.” The healthy development of the social economy is inseparable from government intervention and guidance. Industrial policy is still dominated by “selective industrial policy,” which remains strong. The characteristics of direct interventions have made the “selective industrial policy” more sophisticated.

Enterprise innovation is “an entrepreneurial combination of production factors or production conditions,” which means “forming a new production function” to realize potential profits. Innovation is a collection of technological innovations in an enterprise. In the era of rapid innovation, innovation is the most important and likely way for a company to achieve sustainable prosperity. Contemporary economist Joseph Schumpeter proposed that a company’s research, together with development and innovation, can not only stabilize its competitive advantage but also break through the inherent system to promote business progress. However, the importance of corporate innovation in social and economic development is unquestionable.

*2.2. Hypotheses.* Most of the existing literature posits that industrial policies have reduced financing constraints to a certain extent and promoted R&D investment [16, 17]. However, some scholars are skeptical, and Li et al. [18] believe that companies with political connections will use support policies for rent seeking and will not increase investment in innovation. For Growth Enterprise Market (GEM) companies, the appropriate implementation of industrial policies will stimulate R&D investment, which will lead to a “seed effect,” an “induced effect,” and even a “self-enhancing effect” on innovation [19]. Financial means and financial policies can effectively change the external economic environment of corporate innovation activities [20–24]; this is conducive to external financing and expansion of investment, which is the basic premise for enterprises carrying out innovation activities. Large enterprises may have the strength to bear the risks brought by the complexity, high investment, and uncertainty of innovation activities, while SMEs lack strength and resources, as well as face serious financing difficulties, high innovation costs, unsustainable scientific and technological innovation, and other practical problems [25].

Based on the above theoretical analysis, this study adopts “industrial policy-driven internal and external factors regulation-enterprise innovation output” as the main line to build the theoretical framework. According to the above analysis, industrial policies can positively stimulate enterprises’ innovation output activities through guidance and support, as shown in Figure 1.

H1: selective industrial policy support can increase the level of innovation output of entrepreneurial enterprises.

*2.2.1. Government Subsidies and Enterprise Innovation Output.* Government subsidies are widely used by governments and research circles as an important method of guiding enterprise innovation. The FS provided by the

government to enterprises tends to focus on the following two projects: the first is technology projects with strategic, high-risk, and frontier characteristics [26–28], such as cutting-edge technologies related to emerging industries, and basic R&D projects, which are characterized by foundation, a long investment period, and high spillover. Such an investment can help solve the problems of promoting the progress of basic technology or breaking through common technical problems. Regardless of the kind of FS, its pertinence is strong, can better guide and support the development of specific industries or regions, and is a direct means of innovation stimulus.

Tax incentives are the government’s care measure for taxed objects. Compared with FS, tax incentives involve the government transferring a portion of fiscal revenue to enterprises, focusing on the use of the market and enterprises’ own power to stimulate the R&D investment of enterprises indirectly, which is more inclusive. However, from the government’s perspective, the effectiveness of the tax incentive policy can only be achieved when the innovation benefit brought by the tax incentive policy is higher than the reduced fiscal revenue [29].

Based on the above analysis, government subsidy policy plays a positive role in promoting enterprise innovation. At the same time, this paper believes that the special subsidy means of science and technology are more targeted at stimulating innovation output. Therefore, the following hypotheses are proposed:

H2: government subsidies can increase the level of innovation output in startups.

H3: special subsidies for science and technology have a greater effect on innovation output in entrepreneurial enterprises than nontechnical special subsidies.

### *2.2.2. Financial Support and Enterprise Innovation Output.*

As an external incentive for enterprise innovation, FS has a positive impact on corporate innovation, mainly by improving the financing environment and playing a signal role. The role of FS is mainly realized by improving the financing environment faced by enterprises or helping them solve the innovation bottleneck of financing difficulty. Generally speaking, FS can be achieved through three aspects: banking, capital markets, and insurance markets [30], through low-interest loans, loan guarantees, and capital market and venture capital market financing measures widely used in China, Japan, Germany, and the United States. FS plays an active role in promoting enterprise innovation. The release of positive signals helps reduce and avoid the information and transaction costs between enterprises and financial institutions and helps enterprises apply for loans [31–33]. FS can not only directly improve the financing environment and solve the capital bottleneck but also indirectly promote enterprise innovation by releasing signals.

In this study, low-interest loans were used as indicators of FS. Since it is difficult to obtain the data of targeted loans provided by state-owned banks or local governments in China, we referred to the treatment method of Aghion et al. [34] in their article “Industrial Policy and Competition” and

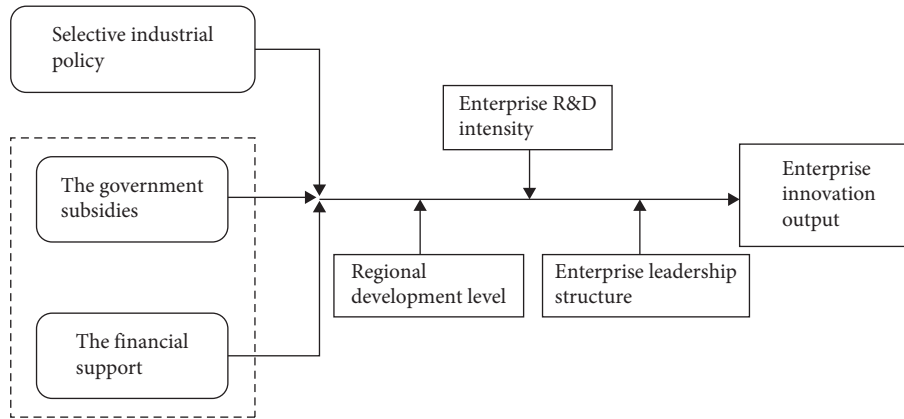


FIGURE 1: The path of industrial policy affecting enterprise innovation.

used the ratio of interest expenditure published by enterprises and current liabilities to form an alternative indicator of low-interest loans. Based on the above analysis, the following hypothesis is proposed:

H4: financial support can improve innovation output level in entrepreneurial enterprises.

*2.2.3. Adjustment of Policy Effects by Internal and External Factors.* Some scholars have researched the role of internal and external factors in regulating the effects of policies. At the enterprise level, most studies are on enterprise scale, property right nature [23, 35], or enterprise type [36, 37]. Since the research object of this paper is a GEM enterprise, the entrepreneurial enterprise is an SME, and the enterprise is small in scale. Next, in order to clarify whether the nature of the enterprise has research value among the GEM enterprises, this study adopts “whether the top ten shareholders have state-owned shares.” The analysis of the two indicators of “the nature of equity” found that the research value was limited. Therefore, this was abandoned in favor of situational factors. The following three aspects are studied under the premise of basic research:

First, analysis of the source of R&D funding in various countries revealed that, among Chinese, Japanese, American, and German societies, the R&D expenditure of enterprises accounted for 74%, 77%, 62%, and 66% of R&D expenditure, respectively, and remained the core support for the R&D expenditures of various countries. Many scholars have confirmed the important role of enterprise R&D intensity in innovation. For example, Benat [38] found that enterprise R&D activities bring innovation growth to enterprises. Research on the influencing factors of enterprise innovation performance [39] also found that innovative resources, including the strength of enterprises’ R&D, help enterprises to introduce advanced R&D equipment, advanced technology, and scientific and technological talents, and have a significant impact on the innovation output of enterprises.

Therefore, this paper refers to the existing research and finds that the R&D intensity of the enterprise itself is included in the scope of examination, and its regulatory effect

on the effect of industrial policy is examined. The following hypothesis is proposed:

H5: the promotion effect of industrial policies on the innovation output of entrepreneurial enterprises is stronger in enterprises with high R&D intensity than those with low R&D intensity.

Second, examining China’s R&D investment revealed that local financial science and technology investment has gradually increased and overtaken that of central government. This result is a normal reaction of the central government’s moderate decentralization, which inevitably increases regional development differences. The influence of factors on the innovation of enterprises in local areas has gradually attracted the attention of scholars. For example, Hao et al. [40] studied the impact mechanism of regional factors on entrepreneurial innovation and found that regional factors significantly affect the innovation performance of enterprises in the region, calling it “the regional gap effect of entrepreneurial innovation performance.” Kong [41] used panel data from seven provinces municipalities, and autonomous regions since 2000 and found that the impact of tax incentives on technological innovation differs in different regions. The author believes that there are more factors that offset the influence of tax incentives on technological innovation in regions with higher or lower degrees of economic development.

This study argues that the level of regional economic development may indeed have an impact on policy outcomes. In economically developed areas, the positive impacts of government subsidies and FS mean they may be better absorbed, the enthusiasm for technological innovation is higher, and the external effects are timelier. Therefore, the following hypothesis is proposed:

H6: the promotion of industrial policies to entrepreneurial innovation is more pronounced in developed regions than in economically backward regions.

Third, regarding the governance structure of entrepreneurial enterprises, Peng’s [42] study of the first batch of listed companies on the GEM as the research object revealed that the family-owned governance model of entrepreneurial enterprises is more important, and that ownership and management rights are unified. The phenomenon of “single

shares,” whereby the Chairman is also the General Manager, exists so that “the two powers are one.” In fact, the influence of the leadership structure of the board of directors on enterprises has long been the focus of scholars, but the research conclusions differ. Zahra et al. [43] found that the separation of the two positions is positively related to the level of enterprise innovation in the study of medium-sized enterprises. Wang [44] and Xu [45] also found that their separation has a positive impact on corporate technological innovation. Some scholars have reached the opposite conclusion. For example, Brickley et al. [46] found that, in most enterprises, the cost of separation of jobs is greater than the benefits.

There is limited research on corporate innovation from the perspective of corporate governance, but the leadership characteristics of the board can indeed affect the innovation activities of enterprises, but it is not the same in different regions and enterprises. This study explores whether the innovation activities of entrepreneurial enterprises are significantly affected by leadership structure is explored in this study. Therefore, in the specific operation, the group’s internal “Chairman and General Manager” is used as a surrogate index to conduct a group study. At the same time, the Herfindahl index of the top ten shareholders of the company is used as a surrogate indicator for the robustness test. Regarding the innovation activities of enterprises, it is assumed that although they can improve the efficiency of decision-making, the correctness of the decision is not guaranteed. When the two are positions are held separately, they can avoid the excessive concentration of power, overcome the rigidity of decision-making and cognitive limitations, and improve the correctness of innovation decisions, which may be more conducive to the innovative growth of the company. The hypothesis is as follows:

H7: when the structure of corporate leadership is dispersed, industrial policies have a more significant effect on the innovation of entrepreneurial enterprises.

### 3. Data and Model

**3.1. Data.** The sample comprised 498 GEM companies listed in the Shenzhen Stock Exchange from 2011 to 2017. Data of GEM companies with stock codes 300001–300498 were adopted to eliminate companies with serious data deficiencies. Finally, the research samples obtained were non-equilibrium panel data, with a total of 2,185 observed values.

In this study, the information on selective industrial policy mainly comes from the Five-Year Plan issued by the Chinese government. As it is difficult to measure, the practices of Yu [23] and Li [18] are referenced to study industrial policies and expressed industrial policies by defining dummy variables at the industry level. In this study, we divided industrial policy into general encouragement policy and key encouragement policy.

The financial data of each company, as well as the basic calculation data of government subsidies and FS, come from the China Stock Market & Accounting Research (CSMAR) database, the China Statistical Yearbook of Science and Technology (2006–2016), and the China Statistical Yearbook

(2006–2016), from which patent data were combined with the CSMAR database and the patent database of the National Intellectual Property Office of China.

The independent variables include selective industrial policy, government subsidy, and FS.

Regarding the specific operation, the analysis is divided into general incentives and key incentives for industrial policies according to the degree of industrial policy encouragement. Industries that are generally encouraged were selected from the documents of the 11<sup>th</sup> and 12<sup>th</sup> Five-Year Plans. If the 11<sup>th</sup> and 12<sup>th</sup> Five-Year Plans mentioned encouragement, support, key development, or vigorous development, they were considered as a general incentive industry, defined as the variable IP\_ind1, and assigned a value of 1, with the others assigned a value of 0. If the 11<sup>th</sup> and 12<sup>th</sup> Five-Year Plans clearly mentioned key development or vigorous development, the industry was considered to be a key incentive industry, defined as the variable IP\_ind2 and assigned the value 1, with the others assigned the value 0, thus generating a new dummy variable.

Industrial policy at this level includes government subsidies and FS:

#### (1) Government subsidy

After studying the breakdown of government subsidies received by GEM companies, this study intended to focus on whether the special subsidies for science and technology play a key role in the innovation output of enterprises and are more targeted. Finally, we compare the government subsidy income obtained by the company with the number of employees and then use the logarithm to define the government subsidy indicators, which were divided into three categories: government total subsidy (Sub), technology special subsidy (Techsub), and non-technology special subsidies. (Ftechsub).

#### (2) Financial support

This study drew on the treatment of “Industry Policy and Competition” by Aghion et al. [34] to compare the ratio of interest expenditure to current liabilities to measure low-interest loan policy as a substitute for FS.

The dependent variable is the startup’s innovative output. Regarding innovation output, there are two main measurement methods in the existing literature. One is the number of patent applications, the number of licenses, or the number of citations [47]; the second is the use of enterprise development or the number of improved new products [48]. This study used the number of patent applications of enterprises to measure enterprises’ innovation output. The patent application year is used as the innovation output year of the enterprise. The patent application data come from the statistics of the CSMAR database and are defined as the variable patent.

With reference to the research of Yu [23]; combined with the actual research needs, when studying the actual impact of selective industrial policies on government subsidies and FS on the number of patent applications, we control important

variables at the enterprise and regional levels. The specific variable definitions are listed in Table 1.

Table 2 presents the descriptive statistics for the main variables. From Table 2, the average number of patent applications (Patent) is 12.66, and the standard deviation is 24.3362. This shows that the number of patents between GEM companies differs greatly, and the level of innovation output is uneven. The average number of patents relative to mature companies is 57.2, and the level of innovation output of entrepreneurial enterprises needs to be improved. The average value of encouraging industrial policies is 0.8492, indicating that 84.92% of the enterprises that participated in the patent application during the research period were in the range of industrial policy incentives in the broadest sense. The average value of the key encouraging industrial policies is 0.3761, indicating that the key support of industrial policies is targeted to some extent, and 37.61% of GEM enterprises are in industries that are mainly encouraged by industrial policies. After comparing the number of employees with government subsidies and taking the natural logarithm, the average value is 8.9514, which is divided into science and technology special projects and nonscience and technology special projects. The average value is 7.4822 and 8.3309, respectively, and the maximum and minimum values of each indicator vary greatly, indicating that, in terms of government subsidies, the types and intensity of subsidies received by each enterprise vary greatly. The standard deviation of FS policies is 2.3106, with a maximum value of 26.3117 and a minimum value of 0, indicating that the FS intensity of each enterprise varies greatly. The average R&D intensity (rde) is 0.069, which means that, on average, the proportion of R&D investment in the sample to operating income is 7%, and the gap between high R&D investment intensity and low R&D investment intensity is obvious. In terms of corporate governance structure, 45.5% of GEM enterprises have the situation in which the Chairman of the Board also serves as the General Manager. The mean value of the regional dummy variable is 0.3807, indicating that approximately 38% of the sample companies are located in developed areas, such as Beijing, Shanghai, Guangzhou, and Shenzhen.

**3.2. Model.** In the empirical study, the patent application data of the dependent variable are discrete variables greater than or equal to 0. According to the research characteristics and variable properties of this study, we refer to Woodridge's "Econometric Analysis of Cross Section and Panel Data." In this book, the counting data model is selected for analysis.

To test the impact of selective industrial policies on the innovation output of start-up enterprises, the following model was constructed:

$$\text{Patent}_{it} = \alpha + \beta_1 \text{IP\_ind1} (\text{IP\_ind2}) + \beta_2 \text{Control}_{it} + \varepsilon_{it}. \quad (1)$$

In the formula, Patent is the number of patent applications of the company, IP\_ind1 and IP\_ind2 are the dummy variables of industrial policy incentives, which are

generally to encourage industrial policies and key industrial policies, and  $\beta$  represents the coefficient of each explanatory variable.

To test the impact of government subsidies on the innovation output (patent application) of entrepreneurial enterprises, it is further divided into technology subsidies (Techsub) and non-technical special subsidies (Ftechsub). The following model was built:

$$\text{Patent}_{it} = \alpha + \beta_1 \text{Insub}_{it} (\text{Intechsub}_{it}, \text{Inftechsub}_{it}) + \beta_2 \text{Control}_{it}. \quad (2)$$

Among them, Insub is the total amount of government subsidies in ten thousand yuan, which is expressed as a logarithm of the number of employees in the company in the current year. Intechsub is a special subsidy for science and technology, and Inftechsub is a special subsidy for non-technical purposes. If H4 is established,  $\beta_1$  is significantly positive when regression is performed with Intechsub as an explanatory variable. To test the impact of FS on entrepreneurs' innovation output, the model is as follows:

$$\text{Patent}_{it} = \alpha + \beta_1 \text{FS}_{it} + \beta_2 \text{Control}_{it} + \varepsilon_{it}, \quad (3)$$

where FS is financial support and is expressed as interest liabilities as a current liability [34], so the positive contribution of FS appears as a negative coefficient. Assuming that the coefficient of  $\beta_1$  is significantly negative, when FS is strengthened, the number of patent applications of startup companies increases.

According to a detailed analysis of the results, the intensity of enterprise R&D is key to the role of industrial policies in innovation output. At the same time, we consider that both the government and enterprises are the two main players supporting China's technological innovation system, and their subjective initiative is the key. The most intuitive manifestation of this initiative is investment in R&D activities. The government relies on policy guidance and support, while the enterprise determines its own investment in R&D, which leads to the intensity of corporate research on government policy, the effect of the regulation of this problem. Therefore, this study used the GEM as a sample to test H5. The models were constructed as follows:

$$\begin{aligned} \text{Patent}_{it} = & \alpha + \beta_1 \text{Insub}_{it} (\text{Intechsub}_{it}, \text{Inftechsub}_{it}) \\ & + \beta_2 \text{Insub}_{it} (\text{Intechsub}_{it}, \text{Inftechsub}_{it}) * \text{RDE} + \beta_3 \text{RDE} \\ & + \beta_4 \text{Control}_{it} + \varepsilon_{it}, \end{aligned} \quad (4)$$

$$\text{Patent}_{it} = \alpha + \beta_1 \text{FS} + \beta_2 \text{FS} * \text{RDE} + \beta_3 \text{RDE} + \beta_4 \text{Control}_{it} + \varepsilon_{it}. \quad (5)$$

According to regional characteristics and corporate leadership structure, specific indicators are used: the former was based on whether the headquarters of the company are located in the developed areas of Beijing, Shanghai, or Shenzhen, indicating the difference in the level of economic development of the region in which the enterprise is located. The latter study in this enterprise, whether the Chairman and the General Manager are concurrently responsible for

TABLE 1: Variable descriptive statistics.

definition	Variables	Description
<i>Dependent variables</i>		
Innovation output	Patent	Number of patent applications
<i>Independent variables</i>		
General incentive policy	IP_ind1	If the “Eleventh Five-Year Plan” and the “Twelfth Five-Year Plan” document mention encouragement, support, key development, or vigorous development, it is considered as a general incentive industry, defined as the variable IP_ind1, assigned the value 1, and the other is 0
Key incentives	IP_ind2	If the “Eleventh Five-Year Plan” and the “Twelfth Five-Year Plan” clearly mention the key development or vigorous development, the industry is considered as the key incentive industry, defined as the variable IP_ind2 and assigned the value 1, the other is 0
Government subsidy policy	Sub	Total subsidy/total number of employees and take the logarithm
Special subsidies for science and technology	Techsub	Total amount of special subsidies for science and technology/total number of employees and take the logarithm
Non-tech special subsidy	Ftechsub	Total non-technical special subsidies/total number of employees and take the logarithm
Financial support	FS	Interest expense/current liabilities
<i>Control variables</i>		
Environment system	IPO	The listing value after listing in 2012 is 1, and the listing value in 2012 and the previous year is 0
Business scale	Size	Logarithm of total assets
Corporate cash flow	Cash	Net cash flow from operating activities/total assets
Asset-liability ratio	LEV	Total liabilities/total assets
Current ratio	CR	Current assets/current liabilities
Return on total assets	ROA	Net profit/average balance of total assets ((end of assets total balance + initial balance of assets)/2)
Business age	Age	The time interval from the date of establishment of the start-up to the statistical year
Adjunct	Dual	The Chairman and general manager have a value of 1, and the others are 0
R&D intensity	RDE	R&D investment amount/operating income
Regional dummy variable	Region	The company’s headquarters is located in Beijing, Shanghai, Guangzhou, Shenzhen, and the value is 1, otherwise 0
Industry dummy variable	Industry	The “2012 Industry Classification Guidelines” issued by the China Securities Regulatory Commission was used to classify and statistic, and two dummy variables of C and I categories were set
Annual dummy variable	Year	There were seven dummies variables from 2011 to 2017

TABLE 2: Descriptive statistics of major variables.

Variable	Symbol	Mean	Max	Min	Standard deviation	Observations
Innovation output	Patent	12.6586	377	0	24.3362	2188
General incentive policy	IP_ind1	0.8492	1	0	0.3580	2188
Key incentives	IP_ind2	0.3761	1	0	0.4845	2188
Government subsidy policy	Sub	8.9514	12.5122	0	1.2452	2179
Special subsidies for science and technology	Techsub	7.4822	12.0637	-2.1107	1.7110	1941
Non-technical special subsidy	Ftechsub	8.3309	12.5122	-0.3381	1.5349	2147
Financial support	FS	1.9197	26.3117	0	2.3106	1965
Environment system	IPO	0.1056	1	0	0.3073	2188
Business scale	Size	20.8941	24.2117	18.6794	0.6970	2188
Corporate cash flow	Cash	0.3480	0.9603	0.0044	0.2117	2188
Asset-liability ratio	LEV	0.2427	0.8864	0.0110	0.1581	2188
Current ratio	CR	6.3588	144	0.38126	8.6600	2188
Return on total assets	ROA	0.7140	0.5589	-0.4620	0.0603	2188
Business age	Age	12.1682	29	2	4.6589	2188
Adjunct	Dual	0.4549	1	0	0.4980	2185
R&D intensity	RDE	0.0690	0.9839	0	0.0721	2188
Regional dummy variable	Region	0.3807	1	0	0.4857	2188

this feature, has an impact on the policy effect. The group study was conducted on the two methods of industrial policy simultaneously for H6 and H7.

#### 4. Results

To explore the impact of selective industrial policies on corporate innovation output, this study conducted a regression test of model 1. From the regression results in Table 3, we observe that the impact of selective industrial policies on the innovation output of entrepreneurial enterprises is not significant, whether the general level of encouragement or the key level of encouragement, so H1 is not supported.

Possible reasons for this result are as follows: first, the lag and timeliness of selective industrial policies (Lin, 2013); the “Five-Year Plan” is a national programmatic document, and specific supporting measures cannot be formulated and implemented in a timely manner, requiring a certain period of time for inspection and implementation. Thus, the current “Five-Year Plan” document’s incentive effect on enterprise innovation cannot be reflected in a timely manner. Second, the innovation promotion effect of key encouragement policies is not significant. One possible reason is that, compared with the generally encouraged industries, the key encouragement industries are largely emerging industries at the stage of cultivation and development, and the demand market and technology level are not mature and perfect. This also indicates that enterprise innovation is in urgent need of government support and guidance.

Next, information agencies such as China’s ratings agencies are still not perfect. Compared with developed countries, there is still a gap between them. This makes the information asymmetry between the government and enterprises more serious. It is difficult for the government to obtain complete information on the growth and technical level of the enterprise, as well as the government. The limitations of professionals in professional knowledge and practice make it difficult to foresee the technological prospects of enterprises and the right antidote [6], which makes industrial policies unable to meet the innovation needs of the most sensitive SMEs in the market, affecting the industry to some extent. This is the support effect of the policy.

Third, the ubiquitous relationship between government and enterprise distorts the government’s allocation of resources such as fiscal subsidies and tax incentives, thus weakening the incentive effect of industrial policies. Enterprises are motivated to establish a good relationship with the government through various methods to obtain additional protection and support, which virtually leads to turning the government’s support for enterprise innovation into a vicious circle. Meanwhile, due to their limited scale, financial resources, and accumulation of social relations, SMEs are far behind large enterprises in terms of social resources and also lack equal competition opportunities. Therefore, the support effect of industrial policies on enterprise innovation in the GEM is not significant.

Fourth, such nondiscriminatory, universal support often brings far more innovation benefits to large enterprises than to small ones. The GEM enterprises are mostly in the early

TABLE 3: The impact of general incentives (key encouragement) on the innovation output of entrepreneurial enterprises.

	Model1	
IP_ind1	0.0252 (0.14)	
IP_ind2		0.133 (1.04)
IPO	0.169 (1.29)	0.164 (1.26)
Size	0.355*** (13.08)	0.355*** (13.10)
Dual	-0.0253 (-0.95)	-0.0257 (-0.97)
Cash	0.0717 (0.89)	0.0722 (0.90)
LEV	-0.0833 (-0.89)	-0.0842 (-0.90)
CR	-0.0167*** (-8.90)	-0.0167*** (-8.91)
ROA	1.316*** (7.08)	1.318*** (7.10)
RDE	2.413*** (11.32)	2.419*** (11.35)
Age	-0.0117 (-0.91)	-0.0121 (-0.95)
Region	-0.0963 (-0.92)	-0.0874 (-0.84)
Industry	Yes	Yes
Year	Yes	Yes
Constant	-6.017*** (-9.31)	-5.956*** (-9.27)
Log likelihood	-10415.8	-10415.3
N	2181	2181

\*, \*\*, and \*\*\*, respectively, indicated that they passed the test at the significance level of 10%, 5%, and 1%.

stage of development or growth stage, with a short time of establishment, immature business model, and relatively small scale. Even if encouraged by national policies, they tend to pursue overall benefits and put more energy and resources into enterprise growth rather than technology R&D and innovation. On the contrary, mature and stable business activities pay more attention to enterprise innovation. Yu Minggui [23], taking the main board listed companies as research samples, concluded that industrial policy can significantly increase the number of invention patents of enterprises in the encouraged industries, and industrial policy in the key industries has a greater impact on enterprise innovation than general encouragement.

We posit that the support effect of selective industrial policy on entrepreneurial innovation is not significant in the short term but will gradually deepen and be reflected over time.

This section examines the role of specific industrial policy instruments on the innovation output of entrepreneurial enterprises and verifies H2, H3, and H4. The Poisson regression results are presented in Table 4.

In model 2, Sub’s coefficient estimate is 0.0002, which is not significant. This indicates that government subsidies have no substantial impact on entrepreneurial innovation output, and H2 is not supported. Possible reasons are as follows.



TABLE 4: Impact of government subsidy policy and financial support policy on entrepreneurial innovation.

	Model2		Model3	
Sub	0.0002 (0.02)			
Techsub		0.0241*** (3.63)		
Ftechsub			-0.0031 (-0.47)	
FS				-0.0177*** (-3.62)
IPO	0.168 (1.3)	0.163 (1.28)	0.162 (1.25)	0.183 (1.37)
Size	0.352*** (12.94)	0.233*** (8.05)	0.350*** (12.87)	0.350*** (12.18)
Dual	-0.0269 (-1.01)	0.0570** (1.95)	-0.0228 (-0.85)	-0.0467* (-1.68)
Cash	0.0755 (0.94)	-0.00709 (-0.08)	0.0907 (1.13)	0.256*** (3.02)
LEV	-0.0819 (-0.87)	-0.378*** (-3.81)	-0.0614 (-0.65)	-0.0203 (-0.21)
CR	-0.0168*** (-8.94)	-0.0160*** (-8.37)	-0.0164*** (-8.78)	-0.0167*** (-7.42)
ROA	1.308*** (6.95)	0.841*** (4.07)	1.324*** (7.08)	1.669*** (8.32)
RDE	2.399*** (11.13)	1.758*** (7.98)	2.252*** (10.31)	3.211*** (13.10)
Age	-0.00994 (-0.79)	-0.0138 (-1.13)	-0.0103 (-0.81)	-0.0147 (-1.14)
Region	-0.103 (-0.98)	-0.0523 (-0.51)	-0.0937 (-0.90)	-0.129 (-1.22)
Industry	Yes	Yes	Yes	Yes
Year	Yes	Yes	Yes	Yes
Constant	-5.922*** (-9.22)	-3.028*** (-4.47)	-5.882*** (-9.15)	-5.895*** (-8.76)
Log likelihood	-10384.3	-9391.85	-10290.1	-9383.2
N	2176	1938	2144	1962

\*, \*\*, and \*\*\*, respectively, indicated that they passed the test at the significance level of 10%, 5%, and 1%.

First, there are many types of government subsidies. Most of them are not specifically targeted at scientific and technological innovation or R&D support, such as the listing of incentives for startup companies. The state's support for certain utilities or socially necessary products only encourages and supports specific industries. These subsidies do not directly affect the R&D of enterprises and technological innovation, and enterprises often have the right to control them. The government's application of this aspect of subsidies and the direction is not supervised and intervened, and startups are likely to choose uses other than R&D innovation.

Second, the government's financial subsidies based on political connections can distort the effective allocation of scarce resources in society [23]. Government subsidies to startup enterprises will objectively motivate these enterprises to establish a good social relationship with the local government so as to obtain additional policy support, that is, "rent seeking." The prevalence of government-enterprise relations makes it inevitable for the government to choose entrepreneurial enterprises with good relations when

selecting funding targets, rather than entrepreneurs with strong technological innovation needs or strong innovation strength.

Third, most startups are in the early stages of development or in the growth stage. Even when government subsidies are used to boost firms' ability to innovate, they are often subject to technological constraints or R&D shortfalls that do not necessarily boost patent output.

The Tech subcoefficient in model 2 is positive ( $\beta_1 = 0.0241$ ,  $p < 0.01$ ), which indicates the positive promotion effect of special subsidies for science and technology on the innovation output of entrepreneurs. The coefficient of Ftechsub is not significant, indicating that nontechnical special subsidies have no obvious effect on corporate patent applications. This result supports H3. We believe that special subsidies for science and technology can better eliminate the negative externalities of enterprise innovation to a certain extent, ease the gap between private income and social benefits of innovation activities, and provide support in resources, funds, or systems to enhance enthusiasm for innovation.

Finally, the impact of the coefficient of FS on innovation output in model 3 is negative ( $\beta_1 = -0.0177$ ,  $p < 0.01$ ). Since FS is measured by the ratio of interest expenses to current liabilities, a negative coefficient indicates positive FS. Therefore, the regression results indicate that the company's patent applications have increased in response to FS, providing evidence for H4.

Accordingly, the FS provided by the government to enterprises can alleviate the financing constraints and capital bottlenecks faced by entrepreneurial innovation, reduce the risk of innovation investment, improve the external environment faced by enterprises, and ultimately promote the innovation output of enterprises.

Table 5 reports the regression results of models 4 and 5, indicating the regulatory role of corporate R&D intensity in the process of policy impacting innovation output.

The coefficient of techsub\*rde ( $\beta_1 = 0.741$ ,  $p < 0.01$ ) in model 4 and the coefficient of fs\*rde in model 5 ( $\beta_1 = 0.0507$ ,  $p < 0.05$ ) are both positive and significant, indicating that in enterprises with high R&D intensity, science and technology special projects, and FS have a higher promoting effect on entrepreneurial enterprises' innovation output. Therefore, when the abovementioned individual research on the impact of industrial policy instruments on innovation output may underestimate the actual effect of the policy, the R&D intensity of the enterprise is indeed the core element of enterprise innovation and has a leading effect on the policy effect. Next, the interaction terms of Ftechsub, Sub, and rde are negative, indicating that R&D intensity does not play a good role in the nontechnical special subsidy form (see Table 2). In summary, the Poisson regression results in Table 5 provide complete support for H5, that is, when the policy means the special subsidy for science and technology and the form of FS, the positive adjustment effect of R&D intensity is obvious.

The adjustment of R&D intensity is obvious in the form of special subsidies for science and technology and FS. The possible reasons are as follows: first, China's GEM enterprises

TABLE 5: Regulation of R&amp;D intensity.

	Model 4		Model 5	
Sub	0.0903*** (7.22)			
Techsub		0.0752*** (8.71)		
Ftechsub			0.0407*** (4.10)	
FS				-0.0260*** (-3.73)
sub*rde	-1.332*** (-12.42)			
Techsub*rde		0.741*** (9.49)		
Ftechsub*rde			-0.618*** (-5.97)	
fs*rde				0.0507** (2.15)
RDE	15.78*** (14.44)	1.786*** (8.20)	7.868*** (8.18)	3.107*** (12.64)
IPO	0.149 (1.14)	0.133 (1.04)	0.169 (1.29)	0.185 (1.39)
Size	0.343*** (12.52)	0.223*** (7.65)	0.351*** (12.86)	0.349*** (12.13)
Dual	-0.0250 (-0.94)	0.0675** (2.31)	-0.0247 (-0.92)	-0.0480* (-1.73)
Cash	0.0511 (0.64)	-0.0208 (-0.24)	0.0661 (0.82)	0.269*** (3.15)
LEV	-0.143 (-1.50)	-0.420*** (-4.21)	-0.0781 (-0.83)	-0.0265 (-0.27)
CR	-0.0177*** (-9.38)	-0.0160*** (-8.43)	-0.0168*** (-8.93)	-0.0165*** (-7.35)
ROA	1.403*** (7.47)	1.016*** (4.90)	1.287*** (6.87)	1.632*** (8.09)
Age	-0.0125 (-0.97)	-0.0146 (-1.19)	-0.0117 (-0.91)	-0.0146 (-1.14)
Region	-0.120 (-1.15)	-0.0616 (-0.59)	-0.0998 (-0.96)	-0.125 (-1.18)
Industry	Yes	Yes	Yes	Yes
Year	Yes	Yes	Yes	Yes
Constant	-6.531*** (-10.03)	-2.726*** (-3.99)	-6.237*** (-9.63)	*** (-8.68)
Log likelihood	-10305.14	-9346.6566	-10272.532	-9377.922
N	2172	1938	2140	1962

\*, \*\*, and \*\*\*, respectively, indicated that they passed the test at the significance level of 10%, 5%, and 1%.

are primarily in the early stages of development or growth, and the proportion of manufacturing and technology industries is large. Therefore, GEM enterprises need a large number of R&D funds for their business development. Effectively increasing the intensity of R&D can promote the development of innovative activities. Second, most GEM enterprises are private enterprises. Compared with state-owned enterprises, their organization structures are flexible and more innovative, which makes them value the government's special support for science and technology, and can improve the allocation efficiency of funds. R&D investment can play a better role in promoting R&D. Third, R&D intensity in research, using the ratio of R&D investment to operating income, represents the

unit revenue spent on R&D projects. A high R&D intensity indicates that the internal decision-making layer of the company attaches great importance to the R&D of products or technologies, and enterprises that attach importance to innovation usually have more abundant innovation output. Fourth, increasing the intensity of R&D investment is conducive to improving the technical level of enterprises and promoting continuous innovation of enterprises. After the implementation of R&D projects, companies often require continuous investment in R&D. Special subsidies for science and technology and FS can help companies avoid capital chain breaks and achieve continuous innovation. R&D intensity plays an indispensable intermediate link in this process and plays a key role in innovation output.

Table 6 reports the impact of government subsidies and FS on innovation output in entrepreneurial conglomerates in different regions. The coefficient of Techsub in model 2 is significantly positive in both the developed and underdeveloped groups, and the Sub and Ftechsub coefficients are still not significant. The coefficients of FS in model 3 are significantly negative in groups in different regions. This implies that special subsidies for science and technology and FS can significantly promote the innovation output of enterprises. The promotion of industrial policies in non-developed regions is slightly stronger than that in developed regions. H6 did not get clear evidence from the empirical research. The possible reasons are as follows: enterprises may face considerable constraints in nondeveloped regions; consequently, the effect of technology subsidies and FS on innovation is prominent. In addition, relevant conclusions can be derived: China's industrial policies cover a wide range, and local governments can respond to China's industrial policies at a basic level; the industrial structure between different regions is similar, and the types of industries tend to be "full"; the enthusiasm for innovation among GEM companies is generally high, and there is almost no geographical difference.

The next step is to examine the impact of different corporate leadership structures in groups (see Table 7). The results of model 2 show that the impact coefficients of Sub and Ftechsub on patent applications are not significant. Tech sub's influence on patent applications is 0.027, which is significant at the 1% level. In the General Manager and concurrently enterprise, the influence coefficient is 0.017, which is significant at the 10% level, that is, it is significantly positive in both the part-time and the suboffice, but the former has a higher level of significance. The results of model 3 found that the influence coefficient of FS on innovation was not significant in the concurrent enterprises; in the "two-job separation" enterprises, the coefficient of FS was significantly negative ( $\beta_1 = -0.022$ ,  $p < 0.01$ ). This shows that, among the enterprises where the Chairman and General Manager are divided, the promotion of science and technology special subsidies and FS to the innovation output of entrepreneurial enterprises is more effective than the two-part enterprises, and H7 is established.

Possible reasons for this result may be: first, the "separation of the two positions" can avoid the excessive concentration of power, ensure effective supervision and

TABLE 6: Grouping study of regional characteristics.

	Model 2				Model 3			
	Developed	Undeveloped	Developed	Undeveloped	Developed	Undeveloped	Developed	Undeveloped
Sub	-0.0104 (-0.63)	0.0180 (1.38)						
Techsub			0.0324*** (3.09)	0.0334*** (3.82)				
Ftechsub					0.0045 (0.38)	-0.0032 (-0.40)		
FS							0.0003 (0.03)	-0.022*** (-3.44)
IPO	0.203 (0.75)	0.146 (1.00)	0.131 (0.51)	0.147 (1.01)	0.172 (0.63)	0.140 (0.95)	0.201 (0.68)	0.146 (0.98)
Size	0.576*** (12.62)	0.221*** (6.34)	0.489*** (10.25)	0.0571 (1.52)	0.572*** (12.50)	0.220*** (6.31)	0.513*** (10.48)	0.238*** (6.45)
Dual	0.0674 (1.58)	-0.107*** (-3.08)	0.0742* (1.68)	0.0613* (1.55)	0.0868** (2.00)	-0.109*** (-3.13)	0.933*** (6.44)	-0.307*** (-2.84)
Cash	0.499*** (3.75)	-0.329*** (-3.20)	0.739*** (5.40)	-0.755*** (-6.61)	0.562*** (4.20)	-0.325*** (-3.15)	-0.175 (-0.98)	-0.192 (-1.54)
LEV	-0.247 (-1.47)	-0.186 (-1.57)	-0.649*** (-3.59)	-0.524*** (-4.22)	-0.182 (-1.08)	-0.178 (-1.50)	-0.015*** (-4.36)	-0.024*** (-7.16)
CR	-0.019*** (-6.83)	-0.02*** (-7.11)	-0.023*** (-7.91)	-0.015*** (-5.55)	-0.018*** (-6.68)	-0.019*** (-7.03)	0.101** (2.27)	-0.155*** (-4.28)
ROA	1.841*** (5.68)	1.098*** (4.57)	1.626*** (5.01)	0.494* (1.77)	1.944*** (6.00)	1.116*** (4.68)	1.972*** (5.81)	1.371*** (5.35)
RDE	3.263*** (11.14)	1.342*** (3.72)	2.440*** (8.14)	0.767** (2.06)	2.987*** (9.96)	1.342*** (3.73)	4.808*** (13.75)	1.141*** (2.97)
Age	-0.0284 (-1.14)	0.00438 (0.29)	-0.0417* (-1.79)	0.00734 (0.50)	-0.0294 (-1.19)	0.00435 (0.29)	-0.0341 (-1.32)	0.00150 (0.10)
Industry	Yes	Yes	Yes	Yes	Yes	Yes	Yes	Yes
Year	Yes	Yes	Yes	Yes	Yes	Yes	Yes	Yes
Constant	-10.59*** (-9.58)	-3.314*** (-4.10)	-8.537*** (-7.50)	0.434 (0.50)	-10.63*** (-9.64)	-3.114*** (-3.84)	-9.418*** (-8.08)	-3.430*** (-4.03)
Log likelihood	-3871.185	-6409.610	-3628.640	-5620.57	-3799.756	-6384.763	-3349.545	-5877.711
N	825	1347	728	1210	803	1337	721	1241

\*, \*\*, and \*\*\*, respectively, indicated that they passed the test at the significance level of 10%, 5%, and 1%.

TABLE 7: Grouping study of corporate governance characteristics.

	Model 2				Model 3			
	Adjunct	Nonparticipating	Adjunct	Nonparticipating	Adjunct	Nonparticipating	Adjunct	Nonparticipating
Sub	0.0307 (1.96)	0.0136 (0.94)						
Techsub			0.017* (1.72)	0.027*** (2.78)	0.0007 (0.06)	0.0047 (0.53)		
Ftechsub								
FS							-0.0016 (-0.19)	-0.022*** (-3.35)
IPO	0.0987 (0.55)	0.133 (0.75)	0.175 (0.96)	0.0928 (0.55)	0.0762 (0.42)	0.130 (0.73)	0.178 (0.94)	0.0324 (0.18)
Size	0.436*** (10.75)	0.235*** (5.92)	0.306*** (7.00)	0.108** (2.52)	0.440*** (10.86)	0.228*** (5.73)	0.525*** (12.25)	0.164*** (3.86)
Cash	-0.215* (-1.79)	0.0659 (0.55)	-0.58*** (-4.50)	0.34*** (2.64)	-0.226* (-1.88)	0.0847 (0.71)	0.122 (0.94)	0.0694 (0.55)
LEV	-0.192 (-1.40)	-0.0808 (-0.55)	-0.88*** (-5.95)	-0.0048 (-0.03)	-0.150 (-1.09)	-0.0865 (-0.58)	-0.151 (-1.04)	-0.000923 (-0.01)
CR	-0.01*** (-3.70)	-0.02*** (-6.16)	-0.01** (-2.27)	-0.02*** (-7.24)	-0.01*** (-3.65)	-0.02*** (-6.17)	-0.01*** (-3.35)	-0.01*** (-4.01)
ROA	2.27*** (7.38)	0.53* (1.95)	1.35*** (4.01)	0.79*** (2.66)	2.38*** (7.79)	0.52* (1.90)	3.11*** (9.49)	1.02*** (3.52)

TABLE 7: Continued.

	Model 2				Model 3			
	Adjunct	Nonparticipating	Adjunct	Nonparticipating	Adjunct	Nonparticipating	Adjunct	Nonparticipating
RDE	2.98*** (9.31)	1.63*** (4.82)	2.33*** (7.13)	0.92*** (2.66)	2.80*** (8.52)	1.59*** (4.69)	3.19*** (9.02)	3.38*** (8.62)
Age	-0.0201 (-1.21)	-0.0171 (-1.03)	-0.028* (-1.74)	-0.0122 (-0.77)	-0.0183 (-1.10)	-0.0173 (-1.04)	-0.0223 (-1.33)	-0.0175 (-1.03)
Region	-0.204* (-1.68)	-0.0611 (-0.38)	-0.0725 (-0.59)	0.0302 (0.20)	-0.167 (-1.36)	-0.0584 (-0.37)	-0.254** (-2.07)	-0.117 (-0.72)
Industry	Yes	Yes	Yes	Yes	Yes	Yes	Yes	Yes
Year	Yes	Yes	Yes	Yes	Yes	Yes	Yes	Yes
Constant	-8.18*** (-8.82)	-3.11*** (-3.31)	-4.68*** (-4.69)	-0.49 (-0.49)	-7.99*** (-8.62)	-2.86*** (-3.06)	-9.88*** (-10.18)	-1.43 (-1.45)
Log likelihood	-4654.952	-5401.916	-4129.150	-4964.780	-4593.495	-5376.288	-4118.095	-4903.139
N	989	1183	870	1068	970	1170	880	1082

\*, \*\*, and \*\*\*, respectively, indicated that they passed the test at the significance level of 10%, 5%, and 1%.

restraint to the management, and establish an effective system of separation of powers, so that enterprises can survive and develop better. On the contrary, a combination of the two will lead to an excessive concentration of power, and the main position of professionals will not be valued, which will reduce the motivation for innovation. Second, the “separation of the two positions” can overcome the limited information sources of individuals and the rigidity of cognitive models, expand the information network, and fully mobilize complementary and innovative information. This will enable companies to search for high-quality innovation projects with greater probability and gain more government support. In addition, if the Chairman serves as the General Manager, it will also limit the information processing capabilities of the board, further hindering the technological innovation of the company. Third, the “separation of the two positions” can overcome the rigidity of decision-making and improve the correctness of innovation decisions, which may be more conducive to the company’s innovative growth. On the contrary, concurrent management gives the management too much power, which can easily cause mistakes in decision-making due to personal mistakes or arbitrary self-seeking behaviors. Fourth, the “separation of the two positions” can be more conducive to the organization of innovative implementation resources, overcome the limited problems of the individual resource circle, make the R&D process of the enterprise more efficient, and ultimately promote the innovation output of the enterprise.

## 5. Conclusions and Recommendations

**5.1. Main Conclusions.** Based on the patent application and financial data of China’s GEM listed companies from 2011 to 2017, as well as the adjustment of the “11th and 12<sup>th</sup> Five-Year Plans” to encourage industry planning, this paper examined the impact of industrial policies on the innovation output of entrepreneurial enterprises. This impact was examined from three perspectives: empirical observation,

theoretical induction and empirical testing, and specific research. The main conclusions are as follows:

- (1) Selective industrial policies have no obvious effect on the innovation output of entrepreneurial enterprises. In contrast to the result in the literature, the effectiveness of selective industrial policies for large- and medium-sized enterprises is minimal in GEM enterprises. This implies that the effects of industrial policies on different enterprises are different.
- (2) There are structural differences in the impact of government subsidies on entrepreneurial innovation: first, government subsidies have no substantial impact on the innovation output of entrepreneurial enterprises. Second, compared with nontechnical special subsidies, special subsidies for science and technology can significantly promote entrepreneurial enterprises. Innovative output levels have superior innovation targeting.
- (3) FS as an important industrial policy implies that its contribution to the innovation output of entrepreneurial enterprises is very significant. As an external incentive for enterprise innovation, FS can help enterprises solve the innovation bottleneck of financing difficulties and play an active “signal” role, effectively improve the financing environment faced by enterprises, promote enterprise R&D investment, and improve innovation output.
- (4) The effect of industrial policy on the innovation output of entrepreneurial enterprises has the characteristics of contingencies. First, the intensity of R&D has a positive adjustment effect on industrial policy support for entrepreneurial enterprise innovation, which indicates the importance of enterprise initiatives in innovation activities. Second, the incentive effects of industrial policies on the innovation output of entrepreneurial enterprises are not significantly different between different regions with different levels of economic development. Finally, in the enterprises that separate the roles of Chairman

and General Manager, the industrial policy plays a stronger role in promoting the innovation output of enterprises on the GEM than in the enterprises with the dual roles.

**5.2. Policy Recommendations.** Based on the above research conclusions, this paper summarizes the following policy recommendations:

First, when implementing the national innovation-driven development strategy, governments at all levels should carefully evaluate the different impacts of selective industrial policies on large enterprises and SMEs and adopt different combinations of policy means based on the actual conditions of enterprises. In this study, we found that the beneficial effects of selective industrial policies are more favorable for large enterprises, but not necessarily applicable to startups.

Second, the impact of government subsidies on SMEs is very important, but this has a wide scope for self-criticism, which is likely to induce more rent-seeking activities and corruption, thus leading to a waste of resources and unhealthy tendencies. Therefore, the government should maintain the market mechanism, reduce direct intervention, and continue to optimize the incentive system of government subsidies to promote SMEs' innovation.

Third, FS is a very important means of industrial policy for SMEs. The government should deepen the reform of finance and other fields, gradually alleviate and eliminate the discrimination and "reluctance to lend" behaviors encountered by start-up enterprises in credit and financing, promote the integration of science and technology, finance, and the transformation of technological achievements, and earnestly build an FS system conducive to the innovation of SMEs.

Fourth, R&D intensity plays an important role in the implementation of industrial policies. Therefore, to ensure that industrial policy can effectively promote the innovation output of enterprises, an effective identification mechanism requires the government to build an effective identification mechanism around the R&D intensity of enterprises. This can not only reduce the risk of enterprise innovation activities but also help solve the problem of information asymmetry, improve the pertinence of industrial policies, and promote enterprise innovation.

Fifth, the leadership structure of entrepreneurial enterprises has an important impact on the effectiveness of industrial policies. The government should actively advocate SMEs to optimize their internal leadership structures and establish a property- rights system that is more conducive to the improvement of enterprise innovation. It is necessary to deepen cooperation among various forces of "official enterprises, universities, and research institutes," actively mobilize various social resources, maintain fair competition in the market, avoid market discrimination against SMEs in terms of opportunities and resources, realize the industrialization and commercialization of the research results of research institutions and universities, and promote resource sharing.

## Data Availability

Data for prefecture level provinces in China used to support the results of this study have been published in the China Statistical Yearbook of Science and Technology (2006–2016) and China Statistical Yearbook (2006–2016) published by the National Bureau of Statistics of China. The data can be downloaded from the National Bureau of Statistics website.

## Conflicts of Interest

The authors declare no conflicts of interest.

## Authors' Contributions

All the authors contributed extensively to the work presented in this paper. F. W. contributed to conceptualization, project administration, methodology, and prepared the original draft. D. Z. provided software and reviewed and edited the manuscript. All authors have read and approved the final manuscript.

## Acknowledgments

This work was supported by the Major Program of the Chinese National Social Science Foundation (Grant no. 21ZDA011).

## References

- [1] W. J. Li and M. N. Zheng, "Substantial innovation or strategic innovation: the impact of macro-industrial policies on micro-enterprise innovation," *Economic Research*, vol. 4, pp. 60–73, 2016.
- [2] Y. F. Lin, "Industrial policy and China's economic development: a perspective of new structural economics," *Journal of Fudan University*, vol. 59, no. 02, pp. 148–153, 2017.
- [3] F. Fan, H. Lian, and S. Wang, "Can regional collaborative innovation improve innovation efficiency? An empirical study of Chinese cities," *Growth and Change*, vol. 51, no. 1, pp. 440–463, 2020.
- [4] F. Fan, S. Dai, K. Zhang, and H. Ke, "Innovation agglomeration and urban hierarchy: evidence from Chinese cities," *Applied Economics*, vol. 53, pp. 1–19, 2021.
- [5] S. B. Choi, S. H. Lee, and C. Williams, "Ownership and firm innovation in a transition economy: evidence from China," *Research Policy*, vol. 40, no. 3, pp. 441–452, 2011.
- [6] S. Zhang, P. Andrews-Speed, and X. Zhao, "Political and institutional analysis of the successes and failures of China's wind power policy," *Energy Policy*, vol. 56, pp. 331–340, 2013.
- [7] F. Yu, "Government R & D subsidies, political relations and technological SMEs innovation transformation," *iBusiness*, vol. 5, no. 3, p. 104, 2013.
- [8] J. T. Scott, *Firm versus Industry Variability in R&D Intensity*, pp. 233–248, University of Chicago Press, Chicago, IL, USA, 2007.
- [9] X. Liu, X. Li, and H. Li, "R&D subsidies and business R&D: evidence from high-tech manufacturing firms in Jiangsu," *China Economic Review*, vol. 41, pp. 1–22, 2016.
- [10] Z. Jin, Y. Shang, and J. Xu, "The impact of government subsidies on private R&D and firm performance: does ownership matter in China's manufacturing industry?" *Sustainability*, vol. 10, no. 7, p. 2205, 2018.

- [11] J. Xu, X. Wang, and F. Liu, "Government subsidies, R&D investment and innovation performance: analysis from pharmaceutical sector in China," *Technology Analysis & Strategic Management*, vol. 33, no. 5, pp. 535–553, 2021.
- [12] F. Fan, H. Lian, and X. Liu, "Can environmental regulation promote urban green innovation efficiency? An empirical study based on Chinese cities," *Journal of Cleaner Production*, vol. 287, Article ID 125060, 2021.
- [13] F. Fan and X. Zhang, "Transformation effect of resource-based cities based on PSM-DID model: an empirical analysis from China," *Environmental Impact Assessment Review*, vol. 91, Article ID 106648, 2021.
- [14] J. Bound, C. Cummins, and Z. Griliches, *Who Does R&D and Who Patents*, University of Chicago Press, Chicago, IL, USA, 2007.
- [15] B. H. Hall, "The financing of research and development," *Oxford Review of Economic Policy*, vol. 18, no. 1, pp. 35–51, 2002.
- [16] L. A. Hall and S. Bagchi-Sen, "A study of R&D, innovation and business performance in the Canadian biotechnology industry," *Technovation*, vol. 22, no. 4, pp. 231–244, 2002.
- [17] J. Wang, "Empirical study on the impact of R&D subsidy on enterprise R&D input and innovation output," *Science of Science Research*, vol. 9, pp. 1368–1374, 2010.
- [18] W. A. Li, H. B. Li, and H. C. Li, "Innovation incentives or tax shields?-research on tax incentives for high-tech enterprises," *Research Management*, vol. 37, no. 11, pp. 61–70, 2016.
- [19] P. Benito, "Choosing among alternative technological strategies: an empirical analysis of formal sources of innovation," *Research Policy*, vol. 32, pp. 693–713, 2003.
- [20] F. Fan and K. K. Zhang, "Decoupling analysis and rebound effect between China's urban innovation capability and resource consumption," *Technology Analysis & Strategic Management*, 2021.
- [21] C. Z. Sun, X. D. Yan, and L. S. Zhao, "Coupling efficiency measurement and spatial correlation characteristic of water-energy-food nexus in China," *Resources, Conservation & Recycling*, vol. 164, pp. 1–11, 2021.
- [22] S. Wang, M. Y. Jia, and Y. H. Zhou, "Impacts of changing urban form on ecological efficiency in China: a comparison between urban agglomerations and administrative areas," *Journal of Environmental Planning and Management*, vol. 63, no. 10, pp. 1834–1856, 2020.
- [23] M. G. Yu, R. Fan, and H. J. Zhong, "China's industrial policy and enterprise technology innovation," *China Industrial Economy*, vol. 12, pp. 5–22, 2016.
- [24] Q. Y. Zhu, C. Z. Sun, and L. S. Zhao, "Effect of the marine system on the pressure of the food-energy-water nexus in the coastal regions of China," *Journal of Cleaner Production*, vol. 319, pp. 1–12, 2021.
- [25] S. Capitalism, *Socialism and Democracy*, The Commercial Press, Beijing, China, 1999.
- [26] H. Q. Ke and S. Z. Dai, "Does innovation efficiency inhibit the ecological footprint? An empirical study of China's provincial regions," *Technology Analysis & Strategic Management*, 2021.
- [27] Z. F. Li and M. S. Zhang, "Research on the impact of government science and technology project input on enterprise innovation performance: data from 95 innovative enterprises in China," *China Soft Science*, vol. 12, pp. 123–132, 2012.
- [28] H. C. Yu, J. Q. Zhang, and M. Q. Zhang, "Cross-national knowledge transfer, absorptive capacity, and total factor productivity: the intermediary effect test of international technology spillover," *Technology Analysis & Strategic Management*, 2021.
- [29] L. Q. Li, "Research on the effectiveness of current R&D tax preferential policies in China," *China Soft Science*, vol. 7, pp. 115–119, 2007.
- [30] J. Qin, "Research on financial support system for independent innovation of SMEs in science and technology," *Research Management*, vol. 32, no. 1, pp. 79–88, 2011.
- [31] N. Liu and F. Fan, "Threshold effect of international technology spillovers on China's regional economic growth," *Technology Analysis & Strategic Management*, vol. 32, no. 8, pp. 923–935, 2020.
- [32] S. Wang and J. Q. Zhang, "The symbiosis of scientific and technological innovation efficiency and economic efficiency in China—an analysis based on data envelopment analysis and logistic model," *Technology Analysis & Strategic Management*, vol. 31, no. 1, pp. 67–80, 2019.
- [33] J. Zhang, D. B. Gao, and Y. L. Xia, "Whether patents can promote China's economic growth: an explanation based on the perspective of Chinese patent subsidy policy," *China Industrial Economy*, vol. 1, pp. 83–98, 2016.
- [34] P. Aghion, J. Cai, and M. Dewatripont, "Industrial policy and competition," *Social Science Electronic Publishing*, vol. 7, no. 4, pp. 1–32, 2015.
- [35] S. Wang and X. L. Wang, "The impact of collaborative innovation on ecological efficiency—empirical research based on China's regions," *Technology Analysis & Strategic Management*, vol. 33, no. 2, pp. 242–256, 2021.
- [36] J. Jiang, "Performance of public policy support for enterprise innovation: a comparative analysis based on direct subsidy and tax preference," *Science Research Management*, vol. 32, no. 4, pp. 1–8, 2011.
- [37] X. L. Wang, L. Wang, and S. Wang, "Marketisation as a channel of international technology diffusion and green total factor productivity: research on the spillover effect from China's first-tier cities," *Technology Analysis & Strategic Management*, vol. 33, no. 5, pp. 491–504, 2021.
- [38] B. O. Benat and R. P. Andres, "From R&D to innovation and economic growth in the EU," *Growth and Change*, vol. 4, pp. 434–455, 2004.
- [39] Y. M. Guo, "An empirical study on the influencing factors of enterprise innovation performance," *Journal of Hebei University of Technology*, vol. 43, no. 1, pp. 101–106, 2014.
- [40] J. X. Hao and Z. Yang, "Analysis of the influence of regional factors on the innovation performance of entrepreneurial enterprises—based on the statistical data of venture enterprises in 52 cities in China," *Jiangsu Social Sciences*, no. 6, pp. 84–89, 2012.
- [41] S. H. Kong, "An empirical analysis of the role of tax preferentials in promoting science and technology innovation: an empirical analysis based on provincial panel data," *Science & Technology Progress and Policy*, vol. 27, no. 24, pp. 32–36, 2010.
- [42] Y. Peng, "Research on agency problem in China's GEM corporate governance," *Accounting News*, vol. 20, pp. 25–26, 2011.
- [43] S. A. Zahra, D. O. Neubaum, and M. Huse, "Entrepreneurship in medium-size companies: exploring the effects of ownership and governance systems," *Journal of Management*, vol. 26, no. 5, pp. 947–976, 2000.
- [44] L. Wang, "Relationship-specific investment and technological innovation performance under the role of VC governance behavior," *Journal of Management*, vol. 12, no. 6, p. 854, 2015.
- [45] J. F. Xu and W. Liu, "Corporate governance structure and technology innovation," *Research Management*, no. 4, pp. 11–15, 2002.

- [46] J. A. Brickley, J. L. Coles, and G. A. Jarrell, "Leadership structure: separating the CEO and chairman of the board," *Journal of Corporate Finance*, vol. 4, pp. 189–220, 1997.
- [47] J. Cornaggia, Y. Mao, X. Tian, and B. Wolfe, "Does banking competition affect innovation," *Journal of Financial Economics*, vol. 115, no. 1, pp. 189–209, 2015.
- [48] C. Lin, P. Lin, and F. M. Song, "Managerial incentives, CEO characteristics and corporate innovation in China's private sector," *Journal of Comparative Economics*, vol. 39, no. 2, pp. 176–190, 2011.

## Research Article

# Truncated Cauchy Power Odd Fréchet-G Family of Distributions: Theory and Applications

M. Shrahili <sup>1</sup> and I. Elbatal<sup>2</sup>

<sup>1</sup>Department of Statistics and Operations Research, College of Science, King Saud University, P. O. Box 2455, Riyadh 11451, Saudi Arabia

<sup>2</sup>Department of Mathematics and Statistics, College of Science, Imam Mohammad Ibn Saud Islamic University (IMSIU), Riyadh, Saudi Arabia

Correspondence should be addressed to M. Shrahili; msharahili@ksu.edu.sa

Received 11 August 2021; Revised 3 October 2021; Accepted 5 October 2021; Published 27 October 2021

Academic Editor: Dan Selişteanu

Copyright © 2021 M. Shrahili and I. Elbatal. This is an open access article distributed under the Creative Commons Attribution License, which permits unrestricted use, distribution, and reproduction in any medium, provided the original work is properly cited.

The truncated Cauchy power odd Fréchet-G family of distributions is presented in this article. This family's unique models are launched. Statistical properties of the new family are proposed, such as density function expansion, moments, incomplete moments, mean deviation, Bonferroni and Lorenz curves, and entropy. We investigate the maximum likelihood method for predicting model parameters of the new family. Two real-world datasets are used to show the importance and flexibility of the new family by using the truncated Cauchy power odd Fréchet exponential model as example of the family and compare it with some known models, and this model proves the importance and the flexibility for the new family.

## 1. Introduction

Many authors have lately made considerable attempts to create new families to expand well-known distributions and give flexible classes to represent data in a wide range of areas, including medical sciences, environmental sciences, engineering, demography, actuarial science, and economics. Many generic families have been developed and are used to explain a wide range of real-world events. Some examples of these families are beta-G [1], gamma-G [2], upper truncated Weibull distribution [3], and truncated Weibull-G more flexible and more reliable than beta-G distribution [4], truncated inverted Kumaraswamy-G by Bantan et al. [5], type II truncated Fréchet-G [6], type II power TL by Bantan et al. [7], odd generalized N-H by Ahmad et al. [8], Topp-Leone (TL) odd Fréchet-G by Al-Marzouki et al. [9], transmuted odd Fréchet-G by Badr et al. [10], and truncated Burr X-G by Bantan et al. [11], among others.

Haq and Elgarhy [12] proposed the odd Fréchet-G (OF, -G) with cumulative function (cdf) as follows, for  $x > 0$ ,

$$H(x; \alpha, \xi) = e^{-(\bar{G}(x, \xi)/G(x, \xi))^\alpha}, \quad \alpha > 0, \quad (1)$$

and probability density function (pdf) is

$$h(x; \alpha, \xi) = \frac{\alpha g(x, \xi) \bar{G}(x, \xi)^{\alpha-1}}{G(x, \xi)^{\alpha+1}} e^{-(\bar{G}(x, \xi)/G(x, \xi))^\alpha}. \quad (2)$$

The Cauchy (C) distribution plays an important role and has applications in different fields such as econometrics, engineering, spectroscopy, biological analysis, reliability, queueing theory, and stochastic modeling of decreasing hazard rate life devices. There are many authors who have been displayed various generalization and extension forms of Cauchy distribution in the statistical literature, for examples, Rider [13] presented generalized C distribution, A truncated C distribution by Nadarajah et al. [14], the existence of the moments of the C distribution by Ohakwe and



Osu [15], Jacob and Jayakumar[16] studied half-C distribution, Kumaraswamy-half-C distribution by Hamedani and Ghosh [17], Alshawarbeh and Famoye [18] presented properties of beta-C distribution, and the power-C negative-binomial distribution by Zubair et al. [19], among others.

Recently, Aldahlan et al. [20] proposed the truncated C power-G (TCP-G) family. The cdf of the TCP-G family is given by

$$F(x; \lambda) = \frac{4}{\pi} \arctan(H(x))^\lambda, \quad x \in R, \quad (3)$$

where  $\lambda > 0$ . The corresponding pdf is

$$f(x; \lambda) = \frac{4\lambda h(x)(H(x))^{\lambda-1}}{\pi[1 + (H(x))^{2\lambda}]}. \quad (4)$$

The aim of this article is to provide a new, broader, and more flexible family of distributions based on the odd Fréchet-G and truncated C power-G (TCP-G) families. The

new proposed family has many wide applications in physics, medicine, engineering, and finance. We construct a new family called TCP odd Fréchet-G (TCPOF – G) family of distributions by inserting equation (1) into equation (3); the cdf and pdf of the TCPOF – G are

$$F(x; \lambda, \alpha, \xi) = \frac{4}{\pi} \arctan e^{-\lambda(\bar{G}(x,\xi)/G(x,\xi))^\alpha}, \quad x > 0, \quad (5)$$

and

$$f(x; \lambda, \alpha, \xi) = \frac{4\lambda\alpha g(x, \xi)\bar{G}(x, \xi)^{\alpha-1}}{\pi G(x, \xi)^{\alpha+1}} e^{-\lambda(\bar{G}(x,\xi)/G(x,\xi))^\alpha} \times \left[ 1 + e^{-2\lambda(\bar{G}(x,\xi)/G(x,\xi))^\alpha} \right]^{-1}. \quad (6)$$

Henceforward, a random variable  $X$  having pdf equation (6) will be defined as  $X \sim \text{TCPOF}(\lambda, \alpha, \xi)$ . The survival and hazard rate functions for the TCPOF – G family are

$$\begin{aligned} \bar{F}(x; \lambda, \alpha, \xi) &= 1 - \frac{4}{\pi} \arctan e^{-\lambda(\bar{G}(x,\xi)/G(x,\xi))^\alpha}, \\ \tau(x; \lambda, \alpha, \xi) &= \frac{4\lambda\alpha g(x, \xi)\bar{G}(x, \xi)^{\alpha-1} e^{-\lambda(\bar{G}(x,\xi)/G(x,\xi))^\alpha}}{\pi G(x, \xi)^{\alpha+1} \left[ 1 + e^{-2\lambda(\bar{G}(x,\xi)/G(x,\xi))^\alpha} \right] \left[ 1 - (4/\pi) \arctan e^{-\lambda(\bar{G}(x,\xi)/G(x,\xi))^\alpha} \right]}. \end{aligned} \quad (7)$$

The quantile function (qf) of TCPOF-G family is given by

$$F^{-1}(u) = Q_G(u) = G^{-1} \left[ \frac{1}{1 + \{-(1/\lambda) \log[\tan(u\pi/4)]\}^{1/\alpha}} \right]. \quad (8)$$

The median is given by

$$M = Q_2 = Q(0.5) = G^{-1} \left[ \frac{1}{1 + \{-(1/\lambda) \log[\tan(0.5\pi/4)]\}^{1/\alpha}} \right]. \quad (9)$$

The structure of this paper is as follows. Section 2 has a useful linear explanation of the TCPOF density as well as several specific models. Section 3 looks at structural

properties of the TCPOF-G. In Section 4, we discuss the suggested family's entropy. The maximum likelihood method is used to estimate the model parameters in Section 5. Section 6 provides applications to real-world datasets to illustrate the proposed family's flexibility.

## 2. Linear Representation of TCPOF

If  $|z| < 1$  and  $b > 0$  is a real noninteger, then the following power series hold:

$$(1+z)^{-b} = \sum_{k=0}^{\infty} \binom{-b}{k} z^k. \quad (10)$$

Applying equation (10) in equation (6), we get

$$f_{\text{TCPOF}_r}(x; \lambda, \alpha, \xi) = \frac{4\lambda\alpha g(x, \xi)\bar{G}(x, \xi)^{\alpha-1}}{\pi G(x, \xi)^{\alpha+1}} \sum_{i=0}^{\infty} (-1)^i e^{-\lambda(2i+1)(\bar{G}(x,\xi)/G(x,\xi))^\alpha}. \quad (11)$$

By using the power series for the exponential function, the last term in equation (11) gives

$$e^{-\lambda(2i+1)(\bar{G}(x,\xi)/G(x,\xi))^\alpha} = \sum_{j=0}^{\infty} \frac{(-1)^j \lambda^j (2i+1)^j \bar{G}(x, \xi)^{\alpha j}}{j! G(x, \xi)^{\alpha j}}. \quad (12)$$

The TCPOF – G density reduces to

$$f_{\text{TCPOF}_r}(x; \lambda, \alpha, \xi) = \frac{4\alpha g(x, \xi)}{\pi} \sum_{i,j=0}^{\infty} \frac{(-1)^{i+j} \lambda^{j+1} (2i+1)^j \overline{G}(x, \xi)^{\alpha(j+1)-1}}{j! G(x, \xi)^{\alpha(j+1)+1}}. \quad (13)$$

Using the general binomial expansion, we can write

$$G(x, \xi)^{-\alpha(j+1)+1} = \sum_{k=0}^{\infty} \frac{\Gamma(\alpha(j+1) + k + 1)}{k! \Gamma(\alpha(j+1) + 1)} (1 - G(x, \xi))^k, \quad (14)$$

and

$$(1 - G(x, \xi))^{\alpha(j+1)+k-1} = \sum_{m=0}^{\infty} (-1)^m \frac{\Gamma(\alpha(j+1) + k)}{m! \Gamma(\alpha(j+1) + k - m)} G(x, \xi)^m. \quad (15)$$

Inserting equations (14) and (15) in equation (13), the TCPOF – G density becomes

$$f_{\text{TCPOF}_r}(x; \lambda, \alpha, \xi) = \sum_{m=0}^{\infty} \psi_m \pi_{(m+1)}(x), \quad (16)$$

where  $h_\nu(x) = \nu g(x; \xi) G(x; \xi)^{\nu-1}$  denotes the pdf of the exponentiated generalized (Exp-G) distribution with power parameter  $\nu$ , and

$$\psi_m = \frac{4\alpha}{\pi} \sum_{i,j,k=0}^{\infty} \frac{(-1)^{i+j+m} \lambda^{j+1} (2i+1)^j \Gamma(\alpha(j+1) + k + 1)}{j! k! m! (m+1) \Gamma(\alpha(j+1) + 1)} \times \frac{\Gamma(\alpha(j+1) + k)}{m! \Gamma(\alpha(j+1) + k - m)}. \quad (17)$$

**2.1. Four Special Models of the TCPOF Family.** In this part, we presented three distinct models of the TCPOF family of distributions. When the cdf  $G(x)$  and pdf  $g(x)$  have simple analytic expressions, the pdf equation (8) will be most tractable. Based on the baseline distributions, we propose four submodels of this family: Weibull, exponential, Rayleigh, and Lomax. The cdf and pdf files for these baseline models are provided in Table 1.

**2.1.1. TCPOF Weibull (TCPOFW) Distribution.** The cdf and pdf of TCPOFW distribution are

$$F(x; \lambda, \alpha, \mu, \beta) = \frac{4}{\pi} \arctan e^{-\lambda (e^{-(\beta x)^\mu} / 1 - e^{-(\beta x)^\mu})^\alpha}, \quad x > 0,$$

$$f(x; \lambda, \alpha, \mu, \beta) = \frac{4\lambda\alpha\mu\beta^\mu x^{\mu-1} e^{-(\beta x)^\mu} (e^{-(\beta x)^\mu})^{\alpha-1}}{\pi(1 - e^{-(\beta x)^\mu})^{\alpha+1}} e^{-\lambda (e^{-(\beta x)^\mu} / 1 - e^{-(\beta x)^\mu})^\alpha},$$

$$\left[ 1 + e^{-2\lambda (e^{-(\beta x)^\mu} / 1 - e^{-(\beta x)^\mu})^\alpha} \right]^{-1}.$$

(18)

**2.1.2. TCPOF Exponential (TCPOFE) Distribution.** The cdf and pdf of the TCPOFE model (for  $x > 0$ ) are

$$F(x; \lambda, \alpha, \beta) = \frac{4}{\pi} \arctan e^{-\lambda (e^{-\beta x} / 1 - e^{-\beta x})^\alpha}, \quad x > 0,$$

$$f(x; \lambda, \alpha, \beta) = \frac{4\lambda\alpha\beta e^{-\beta x} (e^{-\beta x})^{\alpha-1}}{\pi(1 - e^{-\beta x})^{\alpha+1}} e^{-\lambda (e^{-\beta x} / 1 - e^{-\beta x})^\alpha}, \quad (19)$$

$$\left[ 1 + e^{-2\lambda (e^{-\beta x} / 1 - e^{-\beta x})^\alpha} \right]^{-1}.$$

**2.1.3. TCPOF Rayleigh (TCPOFR) Distribution.** The cdf and pdf of the TCPOFR model are

$$F(x; \lambda, \alpha, \beta) = \frac{4}{\pi} \arctan e^{-\lambda (e^{-(\beta x)^2} / 1 - e^{-(\beta x)^2})^\alpha}, \quad x > 0,$$

$$f(x; \lambda, \alpha, \beta) = \frac{4\lambda\alpha\mu\beta^2 x e^{-(\beta x)^2} (e^{-(\beta x)^2})^{\alpha-1}}{\pi(1 - e^{-(\beta x)^2})^{\alpha+1}} e^{-\lambda (e^{-(\beta x)^2} / 1 - e^{-(\beta x)^2})^\alpha}, \quad (20)$$

$$e^{-\lambda (e^{-(\beta x)^2} / 1 - e^{-(\beta x)^2})^\alpha},$$

$$\left[ 1 + e^{-2\lambda (e^{-(\beta x)^2} / 1 - e^{-(\beta x)^2})^\alpha} \right]^{-1}.$$

**2.1.4. TCPOF Lomax (TCPOFL) Distribution.** The cdf and pdf of the TCPOFL model are

TABLE 1: Some new models of the new family.

Model	$G(x; \xi)$	$g(x; \xi)$	$\bar{G}(x; \xi)/G(x; \xi)$
Weibull	$1 - e^{-(\beta x)^\alpha}$	$\mu\beta^\mu x^{\mu-1} e^{-(\beta x)^\mu}$	$e^{-(\beta x)^\mu}/1 - e^{-(\beta x)^\mu}$
$ z  < 1$	$1 - e^{-\beta x}$	$\beta e^{-\beta x}$	$e^{-\beta x}/1 - e^{-\beta x}$
Rayleigh	$1 - e^{-(\beta x)^2}$	$\beta^2 x e^{-(\beta x)^2}$	$e^{-(\beta x)^2}/1 - e^{-(\beta x)^2}$
Lomax	$1 - (1 + (x/b))^{-a}$	$a/b(1 + (x/b))^{-a-1}$	$(1 + (x/b))^{-a}/1 - (1 + (x/b))^{-a}$

$$F(x; \lambda, \alpha, a, b) = \frac{4}{\pi} \arctan e^{-\lambda((1+(x/b))^{-a}/1 - (1+(x/b))^{-a})^\alpha}, \quad x > 0,$$

$$f(x; \lambda, \alpha, a, b) = \frac{4\lambda\alpha(a/b)(1 + (x/b))^{-a-1}((1 + (x/b))^{-a})^{\alpha-1}}{\pi(1 - (1 + (x/b))^{-a})^{\alpha+1}} e^{-\lambda((1+(x/b))^{-a}/1 - (1+(x/b))^{-a})^\alpha} \times \left[ 1 + e^{-2\lambda((1+(x/b))^{-a}/1 - (1+(x/b))^{-a})^\alpha} \right]^{-1}. \quad (21)$$

Plots of the TCPOFW, TCPOFE, TCPOFR, and TCPOFL densities are represented in Figure 1.

### 3. Structural Properties

Our study focused on ordinary moments, incomplete moments (IMs), moment generating functions (MGFs), mean deviations (MD), Lorenz and Bonferroni curves (LBCs), and residual life (RL) functions.

**3.1. Ordinary Moments and Incomplete Moments Functions.** A first formula for the  $r_{\text{th}}$  ordinary moment of  $X$ , say  $\mu'_r$ , is

$$\mu'_r = E(X^r) = \sum_{m=0}^{\infty} \psi_m E(Y_{(m+1)}^r). \quad (22)$$

A second formula depending on the quantile function can be written as  $E(X^r) = (m+1) \int_{-\infty}^{\infty} g(x)G(x)^m dx = (m+1) \int_0^1 Q_G(u; \xi)^r u^d du$ . The  $s_{\text{th}}$  IMs of  $X$  defined by  $\nu_s(t)$  for any real  $s > 0$  can be expressed from equation (16) as

$$\nu_s(t) = \int_{-\infty}^t x^s f(x) dx = \sum_{m=0}^{\infty} \psi_m \int_{-\infty}^t x^s \pi_{(m+1)}(x) dx. \quad (23)$$

Equation (23) denotes the  $s_{\text{th}}$  IMs of  $\pi_{(m+1)}$ . The MDs about the mean  $\mu = E(X)$  and the MDs about the median  $M$  are defined by

$$\begin{aligned} \delta_1(x) &= E|X - \mu'_1| = 2\mu'_1 F(\mu'_1) - 2\nu_1(\mu'_1), \\ \delta_2(x) &= E|X - M| = \mu'_1 - 2\nu_1(M), \end{aligned} \quad (24)$$

respectively, where  $\mu'_1 = E(X)$ ,  $M = \text{median}(X) = Q(1/2)$ ,  $F(\mu'_1)$  is evaluated from equation (5), and  $\nu_1(t)$  is the first IM given by equation (23) with  $s = 1$ , where

$$\begin{aligned} \nu_1(t) &= \int_{-\infty}^t x f(x) dx \\ &= \sum_{m=0}^{\infty} \psi_m \int_{-\infty}^t x \pi_{(m+1)}(x) dx. \end{aligned} \quad (25)$$

We can determine  $\delta_1(x)$  and  $\delta_2(x)$  by two techniques, the first can be obtained from equation (16) as  $\nu_1(t) = \sum_{m=0}^{\infty} \psi_m Y_{(m+1)}(t)$  where  $Y_{(m+1)}(t) = \int_{-\infty}^t x \pi_{(m+1)}(x) dx$  is the first IM of the Exp-G distribution. The second technique is given by  $\nu_1(t) = \sum_{m=0}^{\infty} \psi_m \delta_{(m+1)}(t)$  where

$$\delta_{(m+1)}(t) = (m+1) \int_0^{G(t)} u^{(m+1)} Q_G(u) du. \quad (26)$$

For a positive random variable  $X$ , the LBCs, for a given probability  $p$ , are given by  $L(p) = (1/\mu'_1)\nu_1(q)$  and  $B(p) = (1/p\mu'_1)\nu_1(q)$ , respectively, where  $\mu'_1 = E(X)$ , and  $q = Q(p)$  is the quantile function of  $X$  at  $p$ .

**3.2. Moment Generating Function.** The MGF of  $X$  is

$$M_X(t) = E(e^{tX}) = \sum_{m=0}^{\infty} \psi_m M_{(m+1)}(t), \quad (27)$$

where  $M_{(m+1)}(t)$  denotes the MGF of  $\pi_{(m+1)}$ .

A second alternative formula can be derived from equation (16) as follows:  $M_X(t) = \sum_{m=0}^{\infty} \psi_m \gamma(t, m+1)$ , where  $\gamma(t, m+1) = (m+1) \int_0^1 u^m e^{tQ_G(u)} du$ .

**3.3. Moments of RL and Reversed RL.** The  $r_{\text{th}}$  order moment of the RL is given by

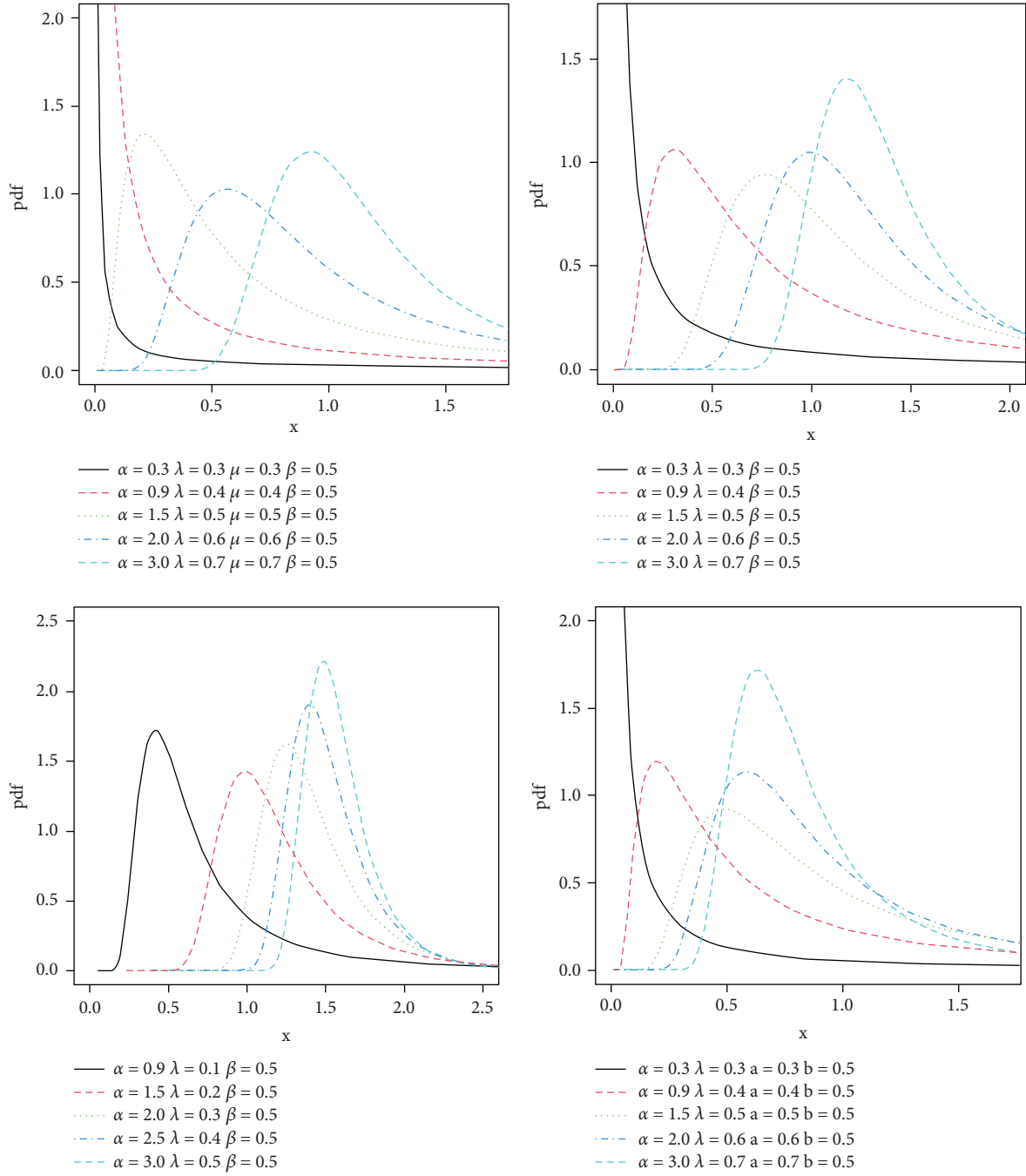


FIGURE 1: TCPOFW, TCPOFE, TCPOFR, and TCPOFL densities for different values of parameters.

$$\begin{aligned} \psi_r(t) &= E((X-t)^r | X > t) = \frac{1}{\bar{F}(t)} \int_t^\infty (x-t)^r f(x) dx, \quad r \geq 1 \\ &= \frac{1}{\bar{F}(t)} \sum_{m=0}^{\infty} \psi_m^* \int_t^\infty x^r \pi_{(m+1)}(x) dx, \end{aligned} \tag{28}$$

where  $\psi_m^* = \sum_{m=0}^{\infty} \sum_{m=0}^r \psi_m \binom{r}{m} (-t)^{r-m}$ . The mean RL (MRL) of TCPOF,  $-G$  family can be obtained by setting  $r = 1$  in equation (28), defined as

$$\psi_1(t) = E(X_t) = E(X | X > t). \tag{29}$$

The  $r^{\text{th}}$  order moment of the reversed RL (or inactivity time) can be obtained by the next equation

$$\begin{aligned}
m_r(t) &= E((t-X)^r | X \leq t) = \frac{1}{F(t)} \int_0^t (t-x)^r f(x) dx, \quad r \geq 1 \\
&= \frac{1}{F(t)} \sum_{m=0}^{\infty} \psi_m^* \int_0^t x^r \pi_{(m+1)}(x) dx.
\end{aligned} \tag{30}$$

#### 4. Entropy

The Rényi entropy is defined by ( $\theta > 0, \theta \neq 1$ )

$$I_R(\theta) = \frac{1}{1-\theta} \log \left[ \int_{-\infty}^{\infty} f^\theta(x) dx \right]. \tag{31}$$

Using the general binomial expansion, applying the same method of the linear representation equation (16) and after some simplifications, we get

$$I_R(\theta) = \frac{1}{1-\theta} \log \left[ \int_{-\infty}^{\infty} f^\theta(x) dx \right], \tag{32}$$

where

$$\begin{aligned}
\Delta_m &= \left( \frac{4\lambda\alpha}{\pi} \right)^\theta \sum_{i,j,k=0}^{\infty} \frac{(-1)^{i+j+m} \lambda^j (2i+\theta)^j}{i!j!k!m!} \\
&\times \frac{\Gamma(\theta+i)\Gamma(\alpha(\theta+j)+k+\theta)\Gamma(\alpha(\theta+j)+k-\theta+1)}{\Gamma(\alpha(\theta+j)+\theta)\Gamma(\alpha(\theta+j)+k-\theta-m+1)}.
\end{aligned} \tag{33}$$

Thus, Rényi entropy of TCPOF,  $-G$  family is given by

$$I_R(\theta) = \frac{1}{1-\theta} \log \left\{ \sum_{m=0}^{\infty} \Delta_m \int_{-\infty}^{\infty} g(x)^\theta G(x)^m dx \right\}. \tag{34}$$

Also,  $\theta$ -entropy can be obtained as

$$\omega_\theta(X) = \frac{1}{1-\theta} \log \left\{ 1 - \sum_{m=0}^{\infty} \Delta_m \int_{-\infty}^{\infty} g(x)^\theta G(x)^m dx \right\}. \tag{35}$$

#### 5. Maximum Likelihood Estimation

Let  $x_1, \dots, x_n$  be a random sample of size  $n$  from the TCPOF  $-G$  given by equation (11). Let  $\Omega = (\lambda, \alpha, \xi)^T$  be  $q \times 1$  vector of parameters. The log-likelihood function is

$$\begin{aligned}
L_n &= n \log \left( \frac{4\lambda}{\pi} \right) + n \log(\alpha) + \sum_{i=1}^n \log g(x_i; \xi) \\
&+ (\alpha-1) \sum_{i=1}^n \log \bar{G}(x_i; \xi) \\
&- (\alpha+1) \sum_{i=1}^n \log(G(x_i; \xi)) - \lambda \sum_{i=1}^n d_i^\alpha \\
&- \sum_{i=1}^n \log \{ 1 + e^{-2\lambda d_i^\alpha} \}.
\end{aligned} \tag{36}$$

$d_i = \bar{G}(x_i; \xi)/G(x_i; \xi)$ . The score vector components, say,  $U(\Omega) = \partial L_n / \partial \Omega = (\partial L_n / \partial \lambda, \partial L_n / \partial \alpha, \partial L_n / \partial \xi)$  are given by

$$\begin{aligned}
U_\lambda &= \frac{\partial L_n}{\partial \lambda} = \frac{n}{\lambda} - \sum_{i=1}^n d_i^\alpha + \sum_{i=1}^n \frac{2d_i^\alpha e^{-2\lambda d_i^\alpha}}{1 + e^{-2\lambda d_i^\alpha}}, \\
U_\alpha &= \frac{\partial L_n}{\partial \alpha} = \frac{n}{\alpha} + \sum_{i=1}^n \log \bar{G}(x_i; \xi) - \sum_{i=1}^n \log(G(x_i; \xi)) \\
&- \lambda \sum_{i=1}^n d_i^\alpha \log d_i + \sum_{i=1}^n \frac{2\lambda d_i^\alpha e^{-2\lambda d_i^\alpha} \log d_i}{1 + e^{-2\lambda d_i^\alpha}}, \\
U_\xi &= \frac{\partial L_n}{\partial \xi_k} = \sum_{i=1}^n \frac{g'(x_i; \xi)}{g(x_i; \xi)} + (\alpha-1) \sum_{i=1}^n \frac{\bar{G}'(x_i; \xi)}{\bar{G}(x_i; \xi)} - (\alpha+1) \sum_{i=1}^n \frac{G'(x_i; \xi)}{G(x_i; \xi)} \\
&- \lambda \alpha \sum_{i=1}^n d_i^{\alpha-1} \left( \frac{\partial d_i}{\partial \xi_k} \right) + \sum_{i=1}^n \frac{2\lambda \alpha d_i^{\alpha-1} e^{-2\lambda d_i^\alpha}}{1 + e^{-2\lambda d_i^\alpha}} \left( \frac{\partial d_i}{\partial \xi_k} \right),
\end{aligned} \tag{37}$$

TABLE 2: Estimates for dataset I.

Distributions	MLEs and SEs
TCPOFE ( $\lambda, \alpha, \beta$ )	0.151, 6.011, 8.084 (0.168), (1.024), (0.6141)
MOE ( $a, b$ )	8.780, 1.380 (3.560), (0.194)
BrXE ( $a, \beta$ )	0.475, 0.2055 (0.060), (0.012)
KE ( $a, b, \beta$ )	3.3041, 1.1002, 1.0371 (1.1061), (0.7642), (0.6141)
GMOE ( $a, b, \beta$ )	0.1789, 47.6350, 4.4652 (0.0702), (44.9011), (1.3270)
BE ( $a, b, \beta$ )	0.8073, 3.4612, 1.3311 (0.6961), (1.0032), (0.8551)
KMOE ( $\alpha, a, b, \beta$ )	0.3731, 3.4782, 3.3063, 0.2990 (0.1358), (0.862), (0.781), (1.113)
MOKE ( $\alpha, a, b, \beta$ )	0.0081, 2.7162, 1.9861, 0.0992 (0.0021), (1.3158), (0.7839), (0.0481)
ME ( $\beta$ )	0.9252 (0.0768)
E ( $\beta$ )	0.540 (0.063)

TABLE 3: Estimates for dataset II.

Distributions	MLEs and SEs
TCPOFE ( $\lambda, \alpha, \beta$ )	1.475, 21.125, 1.295 (5.068), (0.990), (3.816)
MOE ( $a, b$ )	54.470, 2.320 (35.580), (0.370)
BrXE ( $a, \beta$ )	1.1635, 0.3207 (0.330), (0.030)
KE ( $a, b, \beta$ )	83.7558, 0.5679, 3.3329 (42.3612), (0.3261), (1.1880)
GMOE ( $a, b, \beta$ )	0.5192, 89.4623, 3.1691 (0.2561), (66.2782), (0.7721)
BE ( $a, b, \beta$ )	81.6333, 0.5421, 3.5142 (120.4104), (0.3272), (1.4101)
KMOE ( $\alpha, a, b, \beta$ )	8.8679, 34.8258, 0.2989, 4.8988 (9.1459), (22.3119), (0.2387), (3.1757)
MOKE ( $\alpha, a, b, \beta$ )	0.1333, 33.2322, 0.5711, 1.6691 (0.3320), (57.8371), (0.7211), (1.8141)
ME ( $\beta$ )	0.9502 (0.1501)
E ( $\beta$ )	0.526 (0.117)

TABLE 4: Some IC for dataset I.

Distributions	Z1	Z2	Z3	Z4	Z7	Z8
TCPOFE	191.815	191.387	192.168	194.534	0.085	(0.674)
MOE	210.36	214.92	210.53	212.16	0.10	(0.430)
BrXE	235.30	239.90	235.50	237.10	0.22	(0.002)
KE	209.42	216.24	209.77	212.12	0.09	(0.500)
GMOE	210.54	217.38	210.89	213.24	0.09	(0.510)
BE	207.38	214.22	207.73	210.08	0.11	(0.340)
KMOE	207.82	216.94	208.42	211.42	0.09	(0.530)
MOKE	209.44	218.56	210.04	213.04	0.10	(0.440)
ME	210.40	212.68	210.45	211.30	0.14	(0.130)
E	234.63	236.91	234.68	235.54	0.27	(0.060)

TABLE 5: Some IC for dataset II.

Distributions	Z1	Z2	Z3	Z4	Z7	Z8
TCPOFE	37.485	35.388	38.985	38.068	0.108	(0.975)
MOE	43.51	45.51	44.22	43.90	0.18	(0.55)
BrXE	48.10	50.10	48.80	48.50	0.25	(0.17)
KE	41.78	44.75	43.28	42.32	0.14	(0.86)
GMOE	42.75	45.74	44.25	43.34	0.15	(0.78)
BE	43.48	46.45	44.98	44.02	0.16	(0.80)
KMOE	42.80	46.84	45.55	43.60	0.15	(0.86)
MOKE	41.58	45.54	44.25	42.30	0.14	(0.87)
ME	54.32	55.31	54.54	54.50	0.32	(0.07)
E	67.67	68.67	67.89	67.87	0.44	(0.004)

where  $g'(x_i; \xi) = \partial g(x_i; \delta) / \partial \xi_k$ ,  $G'(x_i; \xi) = \partial G(x_i; \xi) / \partial \xi_k$ , and  $\bar{G}'(x_i; \xi) = \partial \bar{G}(x_i; \xi) / \partial \xi_k$ . The maximum likelihood estimation (MLE) of parameters is obtained by setting  $\partial L_n / \partial \lambda = \partial L_n / \partial \alpha = \partial L_n / \partial \xi_k = 0$  and solving these equations simultaneously to get the MLE ( $\hat{\Omega}$ ).

## 6. Applications

In this section, we used two datasets taken from Bjerkedal [21] and Gross and Clark [22]. The TCPOFE model as example of the new family is compared with some other known competitive models to demonstrate its importance in data modeling. The MLE method is used to estimate the parameters of the competitive models. Some information criteria (IC) are as follows: the Akaike IC (Z1), Bayesian IC (Z2), consistent Akaike IC (Z3), Hannan–Quinn IC (Z4), Cramér–Von Mises (Z5), Anderson–Darling (Z6), Kolmogorov–Smirnov (Z7) statistics with its  $p$  value (Z8) model selection criteria, and goodness of fit tests are used to identify the best model.

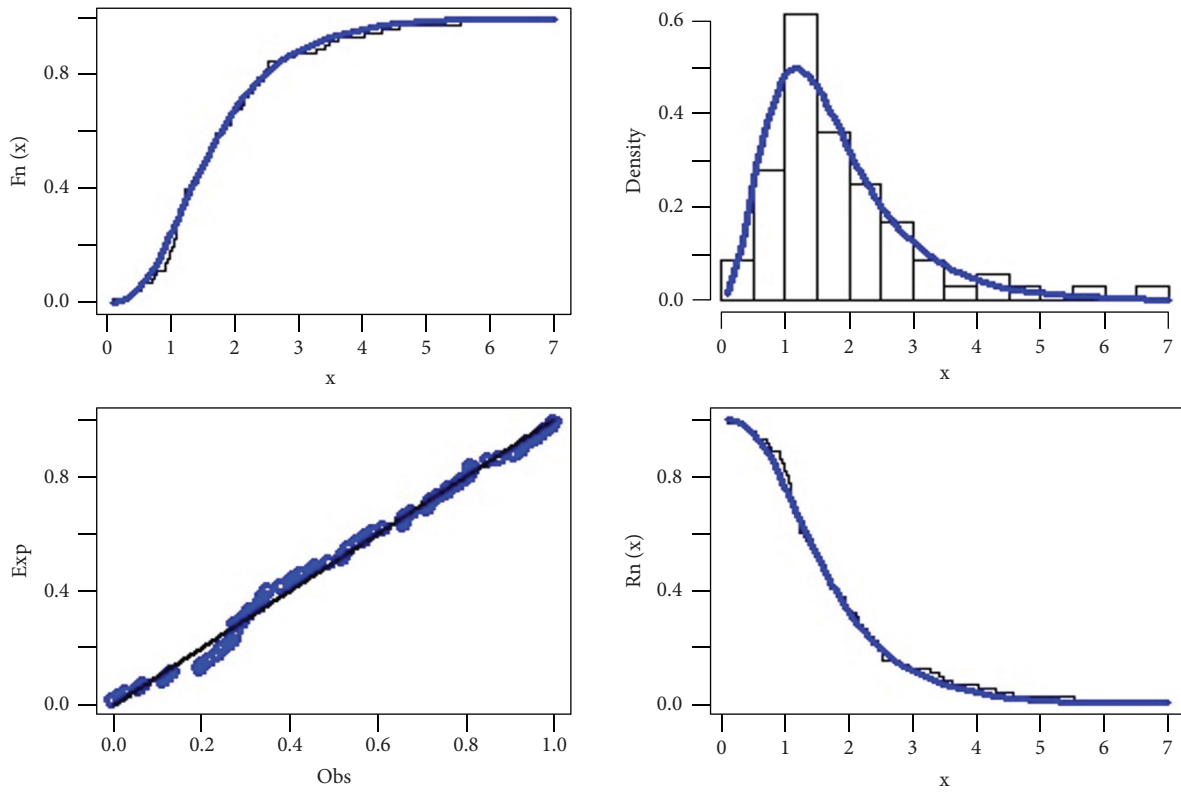


FIGURE 2: Fitted cdf, pdf, and pp plots for dataset I.

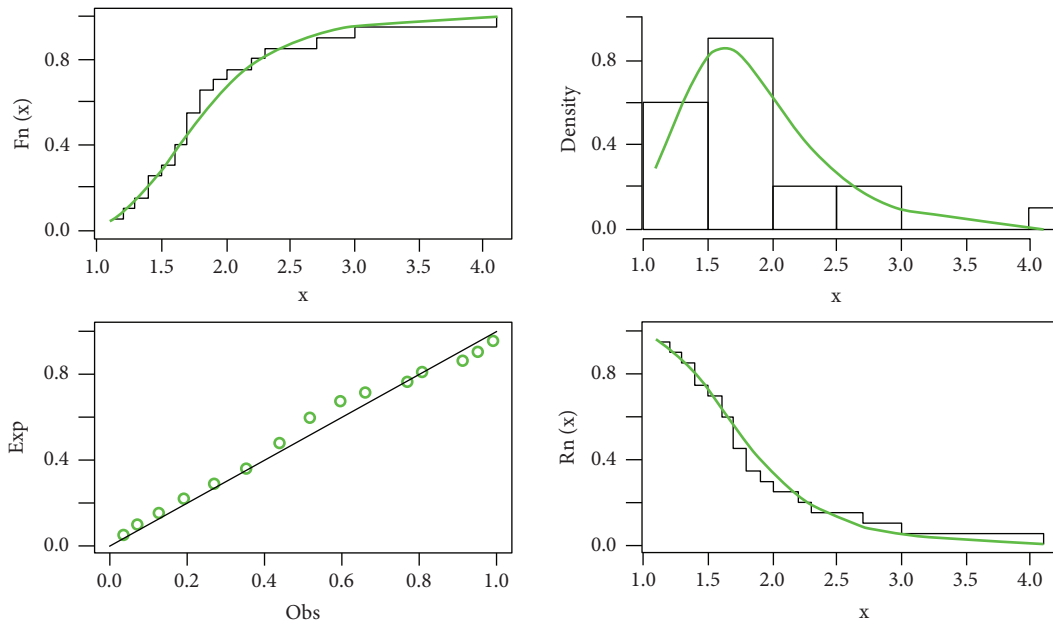


FIGURE 3: Fitted cdf, pdf, and pp plots for dataset II.

The goodness of fits of the TCPOFE model is compared with those of other competitive models, namely, Marshall-Olkin (MO) E (MOE), Burr X-E (BrXE), Kumaraswamy E (KwE), generalized MO exponential (GMOE), beta exponential (BE), Kumaraswamy MO E (KMOE), MO Kumaraswamy E (MOKE), moment exponential (ME), and exponential (E) models.

The MLEs and standard errors (SEs) are calculated for both datasets. The numerical results are listed in Tables 2 and 3. From the numerical values provided in Tables 4 and 5 and the information shown in Figures 2 and 3, the TCPOFE model performs considerably better than the other considered extensions of the E model. Hence, the TCPOFE model is a good alternative over these models for both datasets.

## 7. Conclusion

In this article, we have shown how the use of the “truncated Cauchy power” scheme applied to the odd Fréchet family can lead to new flexible statistical models for the analysis of right-skewed data. Precisely, we have proceeded as follows. First, we have defined the TCPOF-G family of distributions, discussed the motivations behind it, and studied its main properties of interest. Four particular examples of the new family are proposed. Rényi entropy of the TCPOF is calculated. We used the maximum likelihood technique to estimate the parameters. Examples from real-world data demonstrate empirically the significance and promise of the proposed family. In the future, we are planning to use the new family to generate a new model and study its statistical properties and prove the flexibility of it by using more real datasets.

## Data Availability

Please contact the relevant author if you would like to acquire the numerical dataset used to conduct the research described in the paper.

## Conflicts of Interest

The authors declare that they have no conflicts of interest.

## Acknowledgments

The authors extend their appreciation to the deputyship for research and innovation, Ministry of Education in Saudi Arabia, for funding this research work through project no. IFKSURG-1438-086.

## References

- [1] N. Eugene, C. Lee, and F. Famoye, “Beta-normal distribution and its applications,” *Communications in Statistics—Theory and Methods*, vol. 31, no. 4, pp. 497–512, 2002.
- [2] K. Zografos and N. Balakrishnan, “On families of beta and generalized gamma-generated distributions and associated inference,” *Statistical Methodology*, vol. 6, no. 4, pp. 344–362, 2009.
- [3] T. Zhang and M. Xie, “On the upper truncated weibull distribution and its reliability implications,” *Reliability Engineering & System Safety*, vol. 96, no. 1, pp. 194–200, 2011.
- [4] H. Najarzadegan, M. H. Alamatsaz, and S. Hayati, “Truncated weibull-G more flexible and more reliable than beta-G distribution,” *International Journal of Statistics and Probability*, vol. 6, no. 5, pp. 1–17, 2017.
- [5] R. A. R. Bantan, F. Jamal, C. Chesneau, and M. Elgarhy, “Truncated inverted Kumaraswamy generated family of distributions with applications,” *Entropy*, vol. 21, no. 11, p. 1089, 2019.
- [6] M. A. Aldahlan, “Type II truncated Fréchet generated family of distributions,” *International Journal of Machine Intelligence and Applications*, vol. 7, pp. 221–228, 2019.
- [7] R. A. Bantan, F. Jamal, C. Chesneau, and M. Elgarhy, “Type II power topp-leone generated family of distributions with applications,” *Symmetry*, vol. 12, no. 1, pp. 1–22, 2020.
- [8] Z. Ahmad, M. Elgarhy, G. G. Hamedani, and N. S. Butt, “Odd generalized N-H generated family of distributions with application to exponential model,” *Pakistan Journal of Statistics and Operation Research*, vol. 16, no. 1, pp. 53–71, 2020.
- [9] S. Al-Marzouki, F. Jamal, C. Chesneau, and M. Elgarhy, “Topp-leone odd Fréchet generated family of distributions with applications to COVID-19 data sets,” *Computer Modeling in Engineering and Sciences*, vol. 125, no. 1, pp. 437–458, 2020.
- [10] M. M. Badr, I. Elbatal, F. Jamal, C. Chesneau, and M. Elgarhy, “The transmuted odd fréchet-G family of distributions: theory and applications,” *Mathematics*, vol. 8, no. 6, pp. 958–978, 2020.
- [11] R. A. R. Bantan, C. Chesneau, F. Jamal, I. Elbatal, and M. Elgarhy, “The truncated burr X-G family of distributions: properties and applications to actuarial and financial data,” *Entropy*, vol. 23, no. 8, p. 1088, 2021.
- [12] M. A. u. Haq and M. Elgarhy, “The odd fréchet-G family of probability distributions,” *Journal of Statistics Applications & Probability*, vol. 7, no. 1, pp. 189–203, 2018.
- [13] P. Rider, “Generalized cauchy distributions,” *Annals of the Institute of Statistical Mathematics*, vol. 9, no. 1, pp. 215–223, 1957.
- [14] S. Nadarajah and S. Kotz, “A truncated Cauchy distribution,” *International Journal of Mathematical Education in Science & Technology*, vol. 37, no. 5, pp. 605–608, 2006.
- [15] J. Ohakwe and B. Osu, “The existence of the moments of the Cauchy distribution under a simple transformation of dividing with a constant,” *Journal of Theoretical Mathematics and Applications*, vol. 1, pp. 27–35, 2011.
- [16] E. Jacob and K. Jayakumar, “On half-cauchy distribution and process,” *International Journal of Statistika and Matematika*, vol. 3, pp. 77–81, 2012.
- [17] G. Hamedani and I. Ghosh, “Kumaraswamy-half-cauchy distribution: characterizations and related results,” *International Journal of Statistics and Probability*, vol. 4, pp. 94–100, 2015.
- [18] E. Alshawarbeh, F. Famoye, and C. Lee, “Beta-cauchy distribution: some properties and applications,” *Journal of Statistical Theory and Applications*, vol. 12, no. 4, pp. 378–391, 2013.
- [19] M. Zubair, M. H. Tahir, G. M. Cordeiro, A. Alzaatreh, E. M. M. Ortega, and M. Ortega, “The power-cauchy negative-binomial: properties and regression,” *Journal of Statistical Distributions and Applications*, vol. 5, no. 1, pp. 1–17, 2018.
- [20] M. Aldahlan, F. Jamal, C. Chesneau, M. Elgarhy, and I. Elbatal, “The truncated cauchy power family of distributions with inference and applications,” *Entropy*, vol. 22, no. 346, pp. 1–24, 2019.
- [21] T. Bjerkedal, “Acquisition of resistance in guinea pigs infected with different doses of virulent tubercle Bacilli1,” *American Journal of Epidemiology*, vol. 72, no. 1, pp. 130–148, 1960.
- [22] A. J. Gross and V. A. Clark, *Survival Distributions: Reliability Applications in the Biomedical Sciences*, John Wiley & Sons, New York, NY, USA, 1975.



## Research Article

# Regional Bank Consolidation and SMEs' Credit Availability: Evidence from China

Xiaohui Hou <sup>1</sup>, Wei He,<sup>1</sup> and Kong-Lin Ke<sup>2</sup>

<sup>1</sup>School of Economics and Finance, Xi'an Jiaotong University, Xi'an, Shaanxi 710061, China

<sup>2</sup>School of Finance, Zhejiang Gongshang University, Hangzhou, Zhejiang 310018, China

Correspondence should be addressed to Xiaohui Hou; [hxiaoh2006@163.com](mailto:hxiaoh2006@163.com)

Received 5 July 2021; Accepted 15 October 2021; Published 23 October 2021

Academic Editor: Sameh S. Askar

Copyright © 2021 Xiaohui Hou et al. This is an open access article distributed under the Creative Commons Attribution License, which permits unrestricted use, distribution, and reproduction in any medium, provided the original work is properly cited.

We conjecture that locally government-led bank consolidation may negatively affect the SMEs' credit availability in China because the breakdown of privately benefit-based relationships among small business borrowers, loan officers, and senior managers could reduce loan officers' incentives to use their soft information. Empirical results show that this is indeed the case.

## 1. Introduction

Bank consolidation is primarily led by markets in developed countries, whereas the governments are often the driving forces of consolidation in emerging economies. In particular, the effect of regional bank consolidation on credit availability to opaque small businesses is still ambiguous under the current research model of small- and medium-sized enterprise (SME) lending [1].

In this paper, we provide rigorous empirical evidence of the impact of a locally government-led consolidation of regional banks on SMEs' credit availability in China. At the end of 2004, "Outline for the Supervision and Development of City Commercial Banks" was promulgated by China's Banking Regulatory Commission. Since 2005, the reform programs of the consolidation of regional banks were issued successively by each province. Regional city commercial banks and urban credit cooperatives, as the foremost financing source for SMEs, were consolidated and restructured in one province after another.

Berger and Udell [2] show that bank lending can be viewed as the outcome of a hierarchy of contracting problems; the bank's small business borrowers contract with the bank's loan officers who in turn contract with the bank's senior management. Because relationship lending depends on the soft information of the loan officer, the consolidating

banks may reduce credit supply for SMEs when loan officers temporarily leave their jobs. Nevertheless, a government-led consolidation of regional banks may not have a significantly negative impact on SMEs' credit availability because the loan officer is the repository of much of the soft information, and a government-led bank consolidation is very rarely involved in the active job cuts of loan officers for the purpose of maintaining in-system stability.

However, whether consolidated regional banks can access soft information is one thing and whether loan officers have incentives to fully utilize soft information is another. Even when the soft information mainly endures in banks, the breakdown of privately benefit-based relationships among all three parts, namely, small business borrowers, loan officers, and senior management, may negatively affect loan officers' incentives to use their soft information, thus giving rise to a significant decrease in urban manufacturing SMEs' credit availability. In particular, under the circumstances of stringent interest rate control, strong SMEs' credit constraints, and low degree of law enforcement, the implicit value of this privately benefit-based relationship is expected to be revealed by investigating how its breakdown may offset the positive consolidation effects of the advantages of hard-information technologies and stronger credit supply impetus from local governments, thereby reducing regional SMEs' credit availability.

## 2. Related Data

Our SMEs' data are drawn from China's Survey of Manufacturing Firms filed by industrial firms with the National Bureau of Statistics (NBS) from 1998 through 2013. There are no new survey data released by NBS since 2013. Additionally, in the light of hitherto practical interest control, our study can focus on the influence of bank consolidation on credit availability instead of a change of the interest rate. According to the "Classification Standard of Small and Medium-sized Enterprises," formulated by China's Ministry of Industry and Information Technology, a SME is defined as an enterprise whose employees' number is fewer than 1000 and whose operating income is no more than 400 million CNY. The data of the SMEs located in rural areas are eliminated. Our sample totally has 67,611 observations.

To include a set of control variables, we also exploit the information on the regional banking system and socio-economic backgrounds over many years, primarily from the Almanac of China's Finance and Banking, the Almanac of Finance and Banking at Provincial level, the Statistical Yearbook of Commercial Banks, the CEIC Database, Wind Financial Terminal and Economic Database, and the CSMAR Database. The information on the government-led consolidation of regional banks in various provinces employed to construct our treatment variable is manually collected from publicly available provincial official government documents. The impact of price fluctuations on our variables is eliminated. We winsorize the continuous variables within the interval of (1%, 99%).

## 3. Identification Methodology

Following the methodology of [3], we adopt a difference-in-differences (DID) strategy with multiway fixed effects, shown in equation (1), and built on a specification in contributions to credit availability. According to [4], the firm-level individual fixed effects should not be controlled to avoid the estimation problem of too high dimension and the excessive absorption of effects of firm-level variables:

$$Y_{\text{fipt}} = \beta D_{pt} + \theta_{\text{ind}} + \theta_{\text{pro}} + \theta_t + \gamma' X + \varepsilon_{\text{fipt}}, \quad (1)$$

where  $Y_{\text{fipt}}$  is the credit availability variable that are defined as the logarithm of the total amount of credit per firm belonging to an industrial sector in a province and year (Credit1) and the ratio of interest payments to total sales (Credit2) [5], respectively,  $D_{pt}$  is the treatment variable that is equal to 1 if the policy of regional bank consolidation is implemented within a year in a province, and 0 otherwise,  $\varepsilon_{\text{fipt}}$  is an error term, and  $\theta_{\text{ind}}$ ,  $\theta_{\text{pro}}$ , and  $\theta_t$  are industry, province, and time fixed effects, respectively. Following [6],  $X$  is a vector of once-lagged control variables that are pretreated covariates including firm characteristics, regional banking market structures, and socioeconomic backgrounds (see the notes to Table 1). In control variables, firm size is one proxy for whether there is hard information about a firm [7]; soft information is controlled by the provincial-level density of bank branches [8].

Finally, the other determinants of the supply and demand sides of the SMEs for credit are also controlled.

Considering that the industry fixed effects in various provinces may affect both the SMEs' credit availability and the treatment variable, we further implement an even more general research design that accounts for the unobserved confounders that vary at the industry  $\times$  province ( $\delta_{\text{indpro}}$ ) level. A particular version of a triple differenced (DDD) regression model, equation (2), is as follows:

$$Y_{\text{fipt}} = \beta D_{pt} + \theta_{\text{ind}} + \theta_{\text{pro}} + \theta_t + \delta_{\text{indpro}} + \gamma' X + \varepsilon_{\text{fipt}}. \quad (2)$$

Because our treatment, the variable is highly collinear with fixed effects of province  $\times$  year, and it cannot be controlled in our DDD specification; however, the industry  $\times$  year effects reflect a change in the industrial technology over time, which is more difficult to imagine as a confounder affecting both SMEs' credit availability and regional banks.

Finally, we conduct several robustness regressions to address the potential endogeneity problem. First, we employ the fiscal gap (Pfgap) that is defined as a multiple of the fiscal expenditures to fiscal revenues at the provincial level per year as an instrument variable of  $D_{pt}$ . Pfgap is expected to impact the incentives of local governments to carry out the consolidation of regional city commercial banks and urban credit cooperatives to strengthen financial resources while not directly affecting the SMEs' credit availability. Second, to relax the SUTVA, we estimate a model for fitting the average treatment effects of the bank consolidation policy on the SMEs' credit availability in the presence of correlated neighborhood interactions at the provincial level [9]. Third, since a significantly negative treatment effect comes from the attenuated implicit value of privately benefit-based relationships, we should observe that the mechanisms of the negative impact of  $D_{pt}$  on credit availability weakens in the provinces with higher anticorruption efforts (Hnspc), which is a dummy equal to 1 when the logarithm of number of filed duty crimes of officials in a province is greater than its median or have a better market intermediary and legal environment, namely, higher market environment scores (Smlb) [10].

## 4. Results and Discussion

Table 1 reports the coefficient estimates of  $D_{pt}$  for equations (1) and (2). We find that our argument receives empirical support. In the specification of DID equation (1), the implementation of regional bank consolidation reduces SMEs' credit availability by 2.4% and 2.6% without and with our whole control variables, respectively, when the explained variable is Credit1; the consolidation reduces credit availability by 0.058% and 0.086%, respectively, when the explained variable is Credit2. A dynamic DID model, with 2 pretreatment and posttreatment periods, is employed to test for parallel trend. The results show that the parallel trend tests can pass for our equation (1), which alleviates the concern of policy selection bias and justifies our DID settings.

TABLE 1: The impact of bank consolidation on SMEs' credit availability.

	Equation (1)				Equation (2)			
	Credit1		Credit2		Credit1		Credit2	
	(1)	(2)	(1)	(2)	(1)	(2)	(1)	(2)
$D_{pt}$	-0.024*** (0.008)	-0.026** (0.011)	-0.058** (0.025)	-0.086** (0.040)	-0.032*** (0.008)	-0.029*** (0.011)	-0.059** (0.025)	-0.079** (0.040)

Notes: the standard errors, in brackets, are clustered at the firm level. \* is  $p$  val <0.1, \*\* is  $p$  val <0.05, and \*\*\* is  $p$  val <0.01. In columns (1) and (2), we estimate the models without and with control variables, respectively. Control variables consist of the ratio of accounts receivable to total sales, logarithm of annual sales, logarithm of firm age, ROA, ratio of net working capital to total assets, ratio of tangible assets to total assets, firm leverage, state ownership, and internationalization dummy equal to 1 if firms export products, ratio of equity to assets, provincial banking market concentrations calculated in local deposit share of big four state-owned banks and 13 national joint-stock banks, the number of bank branches in a province per million square kilometers, regional GDP per capita, unemployment rate, logarithm of population, GDP growth rate, ratio of output value of the tertiary industry to GDP, and proportion of output value of state-owned firm in the local industry.  $p$  value of F tests are all less than 0.01.

Nevertheless, we still further control for the industry  $\times$  province effects based on equation (2); these negative impacts are 3.2% and 2.9% without and with the control variables, respectively, when the explained variable is Credit1; these negative impacts are 0.059% and 0.079%, respectively, when the explained variable is Credit2. Moreover, Table 2 reports the estimation results using an instrument variable for our treatment variable and fitting the average treatment effects in the presence of correlated neighborhood interactions at the provincial level. Compared with the estimates in Column (2) for Credit1 and Credit2 under equation (1), a reducing effect of bank consolidation seems to be stronger. These findings suggest that our empirical results are truly robust after addressing the main endogeneity concerns.

Finally, some of the reducing effect could be mechanical. We expect to observe that the negative impact of  $D_{pt}$  weakens in the provinces with higher anticorruption efforts or with better market intermediary and legal environments, where the original implicit value of privately benefit-based relationships is lower such that the offsetting effect against bank consolidation advantages would be weaker. It is shown that the moderating effects of  $Hnspc$  and  $Smlb$  are all positive at the 1% significant level, which further supports our argument.

Although to maintain in-system stability, a government-led bank consolidation is very rarely involved in the active job cuts of loan officers, the repository of much of the soft information, and the breakdown of privately benefit-based relationships among all three parts, namely, small business borrowers, loan officers, and senior management, can negatively affect loan officers' incentives to use their soft information, thus giving rise to a significant decrease in urban manufacturing SMEs' credit availability.

The government-led consolidation of regional banks has a significantly negative impact on SMEs' credit availability in the context of an emerging economy such as China even when the soft information still mainly endures in banks. The potential positive consolidation effects of the advantages of hard-information technologies and stronger credit supply impetus from local governments are totally offset by the breakdown of the implicit value derived from the privately benefit-based relationships.

TABLE 2: The impact of bank consolidation on SMEs' credit availability: robustness tests.

	IV estimation for equation (1)		ATE with neighborhood interactions	
	Credit1	Credit2	Credit1	Credit2
$D_{pt}$	-0.642*** (0.250)	-2.270** (0.932)	-0.064* (0.036)	-0.174** (0.072)

Notes: see notes of Table 1. Our estimations pass the tests of under-identification and weak identification. For ATE estimation with neighborhood interactions, only the provincial-level control variables are included, since our focus is provincial average SMEs' credit availability.  $p$  value of F tests are all less than 0.01.

## 5. Conclusions

Our empirical results show that even when soft information mainly endures in banks, hard-information technologies advance, and credit supply impetus from local governments potentially strengthens after consolidation, the breakdown of privately benefit-based relationships among small business borrowers, loan officers, and senior managers may negatively affect loan officers' incentives to use their soft information, giving rise to a significant decrease in SMEs' credit availability. Our primary result has significant implications for the policy practice on the consolidation of regional banks. The regulatory authorities should take account of optimizing the incentive mechanism for the staff of the regional banks suffering from the influences of a government-led consolidation.

## Data Availability

Our SMEs' data are drawn from China's Survey of Manufacturing Firms filed by industrial firms with the National Bureau of Statistics (NBS).

## Conflicts of Interest

The authors declare that there are no conflicts of interest regarding the publication of this paper.

## Acknowledgments

The authors gratefully acknowledge the financial support from a program of “The PATH and Strategy of Micro Finance Development Integrated with the Yangtze River Delta.”

## References

- [1] A. N. Berger, “Small business lending by banks: lending technologies and the effects of banking industry consolidation and technological change,” in *The Oxford Handbook of Banking*, A. N. Berger, P. Molyneux, and J. O. S. Wilson, Eds., pp. 292–311, Oxford University Press, Oxford, UK, 2015.
- [2] A. N. Berger and G. F. Udell, “Small business credit availability and relationship lending: the importance of bank organization structure,” *The Economic Journal*, vol. 112, no. 477, p. 32, 2002.
- [3] S. Correia, “Reghdfe: estimating linear models with multi-way fixed effects,” in *Proceedings of the 2016 Stata Conference 24*, *Stata Users Group*, London, UK, September 2016.
- [4] A. N. Berger, G. Cerqueiro, and M. F. Penas, “Market size structure and small business lending: are crisis times different from normal times?” *Review of Finance*, vol. 19, no. 5, pp. 1965–1995, 2015.
- [5] R. Cull, L. C. Xu, and T. Zhu, “Formal finance and trade credit during China’s transition,” *Journal of Financial Intermediation*, vol. 18, no. 2, pp. 173–192, 2009.
- [6] M. Psillaki and K. Eleftheriou, “Trade credit, bank credit, and flight to quality: evidence from French SMEs,” *Journal of Small Business Management*, vol. 53, no. 4, pp. 1219–1240, 2015.
- [7] A. N. Berger, N. H. Miller, M. A. Petersen, R. G. Rajan, and J. C. Stein, “Does function follow organizational form? Evidence from the lending practices of large and small banks,” *Journal of Financial Economics*, vol. 76, no. 2, pp. 237–269, 2005.
- [8] P. Alessandrini, A. F. Presbitero, and A. Zazzaro, “Banks, distances and firms’ financing constraints,” *Review of Finance*, vol. 13, no. 2, pp. 261–307, 2009.
- [9] G. Cerulli, “Identification and estimation of treatment effects in the presence of (correlated) neighborhood interactions: model and Stata implementation via ntreatreg,” *STATA Journal: Promoting communications on statistics and Stata*, vol. 17, no. 4, pp. 803–833, 2017.
- [10] G. Fan, X. L. Wang, and H. P. Zhu, *NERI INDEX of Marketization of China’s Provinces 2011 Report*, Economic Science Press, Beijing, China, 2011.

## Research Article

# Economic Policy Uncertainty and Chinese Stock Market Volatility: A CARR-MIDAS Approach

Xinyu Wu <sup>1</sup>, Tianyu Liu,<sup>1</sup> and Haibin Xie<sup>2</sup>

<sup>1</sup>School of Finance, Anhui University of Finance and Economics, Bengbu 233030, China

<sup>2</sup>School of Banking and Finance, University of International Business and Economics, Beijing 100029, China

Correspondence should be addressed to Xinyu Wu; xywu@aufe.edu.cn

Received 21 April 2021; Accepted 18 September 2021; Published 30 September 2021

Academic Editor: Zakia Hammouch

Copyright © 2021 Xinyu Wu et al. This is an open access article distributed under the Creative Commons Attribution License, which permits unrestricted use, distribution, and reproduction in any medium, provided the original work is properly cited.

Intraday range (the difference between intraday high and low prices) is often used to measure volatility, which has proven to be a more efficient volatility estimator than the return-based one. Meanwhile, a growing body of studies has found that economic policy uncertainty (EPU) has important impact on stock market volatility. In this paper, building on the range-based volatility model, namely, the conditional autoregressive range (CARR) model, we introduce the CARR-mixed-data sampling (CARR-MIDAS) model framework by considering intraday information to investigate the impact of EPU on the volatility of Chinese stock market and to explore the predictive ability of EPU for Chinese stock market. The empirical results show that both the China EPU (CEPU) and global EPU (GEPU) have a significantly negative effect on the long-run volatility of Chinese stock market. Furthermore, we find that taking into account the CEPU and GEPU leads to substantial improvement in the ability to forecast the volatility of Chinese stock market. We also find that the CEPU provides superior volatility forecasts compared to the GEPU. Our findings are robust to different forecasting windows.

## 1. Introduction

Modelling and forecasting volatility is of great importance for many financial applications such as asset allocation, risk measurement, and option pricing. It is well known that stock market volatility exhibits clustering and high persistence. Although predictable, it is still difficult to forecast accurately. In this paper, we investigate the impact of economic policy uncertainty (EPU) on the volatility of Chinese stock market and explore the predictive ability of EPU for Chinese stock market. By doing so, we shed new light on the role of EPU in Chinese stock market volatility.

Recently, Baker et al. [1] developed an EPU index which is based on newspaper coverage to measure policy-related economic uncertainty, and it has received a great deal of attention in the literature (see Al-Thaqeb and Algharabali [2] for a detailed literature review). As measured by the EPU index of Baker et al. [1], the level of EPU keeps rising since the global financial crisis of 2008. In particular, the current level of EPU is at extremely elevated levels due to a series of

events including the US-China trade war and the coronavirus (COVID-19) pandemic, which have forced governments around the world to make frequent changes to their policies in order to limit the economic impact of these events. Intuitively, this high EPU may affect investors' investment decisions and hence stock markets. Indeed, recent studies have shown that EPU has a significant impact on stock markets. Pástor and Veronesi [3, 4] investigated the impact of EPU and political uncertainty on the volatility of US stock market and observed that policy changes increase volatility, risk premia, and correlations among stocks. Liu and Zhang [5] found that incorporating EPU as an additional predictive variable into the HAR-RV model significantly improves the forecasting ability of the model for the volatility of US stock market. Arouri et al. [6] investigated the impact of EPU on the US stock market returns and found that an increase in EPU significantly decreases stock returns and this effect is stronger and persistent during extreme volatility periods. Liu et al. [7] found that EPU has a significant impact on the volatility of the US stock market.

Moreover, out-of-sample results show that adding EPU as explanatory variable to the volatility model can indeed improve its forecasting performance. Using the VAR model, Tsai [8] analyzed the impact of EPU on the stock returns of 22 stock markets worldwide. Duan et al. [9] investigated the impacts of leverage effect and EPU on future volatility in the framework of regime switching. Mei et al. [10] found that taking into account the US EPU leads to substantial improvement in the ability to forecast the volatility of European stock market. Xiong et al. [11] studied the correlation between China EPU (CEPU) and Chinese stock market returns. Yu and Song [12] found that global EPU (GEPU) has a significant impact on the volatility of US stock market. Balcilar et al. [13] showed that the EPU of major economies is likely to predict stock market volatility in emerging stock markets. Chiang [14] examined EPU and risks on excess stock returns for G7 markets using monthly observations and found that the stock returns are negatively correlated with EPU innovation. However, those studies mainly focus on the US and European stock markets.

To our knowledge, there are few studies investigating the impact of EPU on the volatility of Chinese stock market. Chinese stock market is one of the largest and most important emerging stock markets, which has gained a great deal of attention from investors. It is characterized by large fluctuations, and it is expected that it may be affected by changes in economic policies. Naturally, investigation of the impact of EPU on the volatility of Chinese stock market and exploration of the predictive ability of EPU are important for investors in Chinese stock market, who are eager to understand the dynamics of volatility for the sake of portfolio allocation and risk management.

Previous studies investigated the impact of EPU on the volatility of Chinese stock market relying mainly on the generalized autoregressive conditional heteroskedasticity-mixed-data sampling (GARCH-MIDAS) model by Engle et al. [15]. The choice of MIDAS-based approach is based on the fact that the EPU and stock market data are sampled at different frequencies, i.e., EPU is on a monthly basis, while stock market data are available at a daily frequency. Using the GARCH-MIDAS approach, Yu et al. [16] and Yu and Huang [17] provided evidence that GEPU has a significantly positive effect on the volatility of Chinese stock market and has predictive ability for the volatility of Chinese stock market, while Li et al. [18] explored the effects of directional (up and down) GEPU on Chinese stock market volatility and provided evidence that up and down GEPU have positive impacts on Chinese stock market volatility and the GEPU index predicts Chinese stock market volatility. Furthermore, Wang et al. [19] employed a GARCH-MIDAS model with skew Student's  $t$ -distribution to examine the impact of domestic and foreign EPU on the volatility of China's financial stocks and found that the EPU index has a negative impact on the volatility of China's financial stocks. Recently, Li et al. [20] used a predictive regression approach to investigate the impact of EPU on Chinese stock market volatility and provided evidence that the EPU index has a significantly negative impact on future volatility of Chinese stock market. The predictive regression model adopted by Li

et al. [20] requires the frequency of EPU to match that of predicted (realized) volatility. As a result, Li et al. [20] employed the monthly data to perform the analysis, which may ignore important structural features of stock market data and constrain the choice of forecast horizons (i.e., one month).

The GARCH-MIDAS model offers a convenient framework to combine data that are sampled at different frequencies, avoiding the loss of information. Essentially, the GARCH-MIDAS model is a return-based volatility model that uses daily (squared or absolute) close-to-close returns to estimate volatility, which fails to exploit the intraday information. An alternative approach for estimating volatility is to apply the intraday range, which is based on intraday high and low prices. The main advantage of the range-based volatility estimator over the traditional volatility estimator based on closing prices (or close-to-close returns) is its information content: the range contains information about all intraday price movements. Parkinson [21] showed that the range is a more accurate volatility estimator than the volatility estimator based on the daily returns. Since then, the range-based volatility has received a great deal of attention in the literature (see, e.g., Alizadeh et al. [22], Brandt and Jones [23], Li and Hong [24], Degiannakis and Livada [25], and Chou et al. [26]). In particular, Chou [27] introduced a conditional autoregressive range (CARR) model to model the dynamics of the range, showing that the model yields more accurate volatility estimates than the traditional return-based GARCH model.

Motivated by the above interpretation, in this paper, we aim to introduce the CARR-MIDAS approach to investigate the impact of EPU on the volatility of Chinese stock market and to explore the predictive ability of EPU for Chinese stock market. Importantly, our methodology is founded on the range-based CARR model, which allows us to exploit intraday information. Also, the proposed CARR-MIDAS model builds upon the GARCH-MIDAS model, which features a multiplicative decomposition of volatility into a short-run (high-frequency) component and a long-run (low-frequency) component that allows us to incorporate exogenous explanatory variables such as the EPU. It is claimed that the multiplicative component model is able to capture complex volatility dynamics such as the high persistence of volatility as well as to handle well structural breaks or nonstationarities in volatility (see Wang and Ghysels [28], Conrad and Kleen [29], and Xie [30]).

The contributions of the paper are twofold. First, we introduce a new range-based CARR-MIDAS model framework combining the insights of range-based CARR and return-based GARCH-MIDAS. Compared to the CARR model, the CARR-MIDAS model allows us to incorporate exogenous explanatory variables directly into the long-run component of volatility. Hence, using the CARR-MIDAS model that incorporates EPU, we are able to study the relation between EPU and stock market volatility. Compared to the return-based GARCH-MIDAS model, our proposed range-based CARR-MIDAS model utilizes more (intraday) information for estimating volatility.

Second, using the CARR-MIDAS approach, an empirical analysis based on the Shanghai Stock Exchange Composite Index (SSEC) of China and two EPU indices, namely, the CEPU and GEPU, is conducted. The empirical results show that the CARR-MIDAS models (with the CEPU and GEPU) outperform the CARR model in terms of both in-sample fitting and out-of-sample forecast. Both the CEPU and GEPU have a significantly negative impact on the Chinese stock market volatility. Moreover, both the CEPU and GEPU can greatly improve the forecast accuracy for Chinese stock market volatility for forecast horizons of one-day ahead up to one month. Most importantly, we find that the CEPU provides superior volatility forecasts compared to the GEPU. Our empirical results are robust to different forecasting windows.

The remainder of the paper is organized as follows. In Section 2, we introduce the methodology of our CARR-MIDAS model. Section 3 presents the empirical results, while Section 4 concludes the paper.

## 2. Methodology

**2.1. The Range.** In this paper, we employ the intraday range by considering intraday information to investigate the volatility of Chinese stock market. The intraday range of Parkinson [21] is defined as

$$R_{i,t} = \frac{\log(H_{i,t}) - \log(L_{i,t})}{\sqrt{4 \log(2)}}, \quad (1)$$

where  $H_{i,t}$  and  $L_{i,t}$  are the highest and lowest prices of an asset observed on day  $i$  in month  $t$ , respectively. Parkinson [21] showed that the intraday range given by equation (1) is an unbiased estimator of volatility. Assuming that the log-price of an asset follows a Brownian motion with zero drift, Parkinson [21] proved that the range is 4.9 times more efficient than the daily squared return based on the closing prices. Moreover, Degiannakis and Livada [25] showed that the price range volatility estimator is more accurate compared to the realized volatility estimator constructed from five, or less, intraday returns.

**2.2. The CARR-MIDAS Model.** Inspired by the return-based GARCH-MIDAS model of Engle et al. [15], we propose in the paper the range-based CARR-MIDAS model to describe the dynamics of the range, which can be written as

$$\begin{aligned} R_{i,t} &= \lambda_{i,t} \varepsilon_{i,t}, \quad \varepsilon_{i,t} | \mathcal{F}_{i-1,t} \sim i.i.d. f(\cdot), \\ \lambda_{i,t} &= \tau_t g_{i,t}, \\ g_{i,t} &= (1 - \alpha - \beta) + \alpha \frac{R_{i-1,t}}{\tau_t} + \beta g_{i-1,t}, \end{aligned} \quad (2)$$

$$\log(\tau_t) = m + \theta_1 \sum_{k=1}^K \varphi_k(\gamma_1) \log(RRV_{t-k}),$$

where  $\lambda_{i,t}$  is the conditional mean of the range based on the information set,  $\mathcal{F}_{i-1,t}$ , up to day  $i - 1$  of month  $t$ , the error

term  $\varepsilon_{i,t}$  is assumed to be independent and identically distributed (*i.i.d.*) with unit mean from density  $f(\cdot)$  with positive support, and  $RRV_t = \sum_{i=1}^{N_t} R_{i,t}^2$  is the realized range volatility (RRV) in month  $t$ , where  $N_t$  is the number of trading days in month  $t$ . Note that the conditional range,  $\lambda_{i,t}$ , is multiplicatively decomposed into a short-run (high-frequency) component,  $g_{i,t}$ , and a long-run (low-frequency) component,  $\tau_t$ . The short-run component,  $g_{i,t}$ , is specified as a GARCH(1, 1)-like process. To ensure nonnegativity and stationarity for the short-run component  $g_{i,t}$ , we assume that  $\alpha > 0$ ,  $\beta > 0$ , and  $\alpha + \beta < 1$ . The long-run component,  $\tau_t$ , is modelled in the spirit of the MIDAS regression, which is driven by the smoothing monthly RRV with the weighting scheme  $\varphi_k$ . One-parameter beta polynomial is employed as the weighting scheme due to its parsimony and flexibility:

$$\varphi_k(\gamma) = \frac{(1 - k/K)^{\gamma-1}}{\sum_{j=1}^K (1 - j/K)^{\gamma-1}}, \quad (3)$$

where  $K$  is the number of MIDAS lags with  $\sum_{k=1}^K \varphi_k(\gamma) = 1$ .

The model specification described above is the standard CARR-MIDAS model, which is more flexible than the original CARR model of Chou [27]. It is straightforward to show that

$$\lambda_{i,t} = \omega_t + \alpha R_{i-1,t} + \beta \lambda_{i-1,t}, \quad (4)$$

where  $\omega_t = (1 - \alpha - \beta)\tau_t$  implies the time-varying parameter which allows to capture structural changes in conditional volatility. Lamoureux and Lastrapes [31] showed that structural changes should be taken into account when modelling volatility, otherwise may cause spurious apparent persistence in the volatility process (or long-memory volatility). Assuming constant long-run component, the CARR-MIDAS model reduces to the CARR model:

$$\begin{aligned} R_{i,t} &= \lambda_{i,t} \varepsilon_{i,t}, \quad \varepsilon_{i,t} | \mathcal{F}_{i-1,t} \sim i.i.d. f(\cdot), \\ \lambda_{i,t} &= \omega + \alpha R_{i-1,t} + \beta \lambda_{i-1,t}, \end{aligned} \quad (5)$$

where  $\omega = (1 - \alpha - \beta)\tau$ .

To further explore the explanatory ability of EPU on Chinese stock market volatility, we extend the long-run component in equation (2) by incorporating EPU as

$$\begin{aligned} \log(\tau_t) &= m + \theta_1 \sum_{k=1}^K \varphi_k(\gamma_1) \log(RRV_{t-k}) \\ &\quad + \theta_2 \sum_{k=1}^K \varphi_k(\gamma_2) \log(\text{EPU}_{t-k}), \end{aligned} \quad (6)$$

where  $\text{EPU}_t$  is the EPU index in month  $t$ . In regard to the EPU index, we consider in this paper the CEPU and GEPU.

**2.3. Maximum Likelihood Estimation.** The CARR-MIDAS model is easy to estimate. We use the quasimaximum likelihood method to estimate the parameters of the CARR-MIDAS model. The log-likelihood function of the CARR-MIDAS model can be written as

$$\ell(\Theta) = - \sum_{t=1}^T \sum_{i=1}^{N_t} \left[ \log(\lambda_{i,t}) - \log\left(f\left(\frac{R_{i,t}}{\lambda_{i,t}}\right)\right) \right], \quad (7)$$

where  $\Theta$  is the vector of all model parameters.

To implement the CARR-MIDAS model, we need to specify the density  $f(\cdot)$  (or the distribution of the error term  $\varepsilon_{i,t}$ ). We choose the Gamma density function, which can be written as

$$f(\varepsilon_t) = \frac{\nu}{\Gamma(\nu)} (\nu \varepsilon_{i,t})^{\nu-1} \exp(-\nu \varepsilon_{i,t}), \quad \varepsilon_{i,t} \geq 0, \quad (8)$$

$$\ell(\Theta) = - \sum_{t=1}^T \sum_{i=1}^{N_t} \left[ \log(\lambda_{i,t}) + \log(\Gamma(\nu)) - \nu \log(\nu) - (\nu - 1) \log\left(\frac{R_{i,t}}{\lambda_{i,t}}\right) + \nu \frac{R_{i,t}}{\lambda_{i,t}} \right]. \quad (9)$$

Hence, the maximum likelihood estimators,  $\hat{\Theta}$ , can be obtained by maximizing the log-likelihood function in equation (9):

$$\hat{\Theta} = \arg \max_{\Theta} \ell(\Theta). \quad (10)$$

### 3. Empirical Results

**3.1. Data.** We use the CARR-MIDAS approach to investigate the impact of EPU on the volatility of Chinese stock market and to explore the predictive ability of EPU for Chinese stock market. The data used in the paper consist of daily open, high, low, and close prices for the Shanghai Stock Exchange Composite Index (SSEC) of China from January 4, 2005, to December 31, 2020, resulting in a total of 3889 daily observations. The data are obtained from Wind Database of China. The intraday range is computed using equation (1). As EPU, we consider the monthly CEPU index and GEPU (current) index constructed by Baker et al. [1], which are obtained from <https://www.policy.uncertainty.com/>. The daily range of SSEC and monthly EPU (CEPU and GEPU) are presented in Figure 1, which shows that the well-known behaviors of volatility clustering in the Chinese stock market are apparent, and Chinese stock market experienced particularly strong fluctuations during the periods of global financial crisis of 2007-2008 and Chinese stock market turbulence of 2015-2016. In addition, we find that the EPU indices seem to increase over the sample period particularly in the recent years. Moreover, it is interesting to note that the CEPU is generally larger and significantly more volatile than the GEPU, suggesting that Chinese government makes more frequent adjustments of economic policy.

Table 1 presents summary statistics. Panel A reports summary statistics of the daily range for the SSEC. The results show that the SSEC range is positively skewed and highly leptokurtic. From the Jarque–Bera statistics, we observe that the SSEC range fails the normality assumption. The Ljung–Box Q statistics for autocorrelation up to 10 lags provide evidence of high persistence (or long-memory property) for the SSEC range, suggesting that our proposed

where  $\nu$  ( $\nu > 0$ ) is the shape parameter. It is important to note that the Gamma distribution is flexible and includes the exponential distribution as a special case when  $\nu$  takes the value of 1. Moreover, Xie and Wu [32] showed that the Gamma distribution can reduce both the inlier and outlier problems.

Then, the log-likelihood function can be written as

CARR-MIDAS framework that assumes a multiplicative component structure might be appropriate for modelling the conditional range. Panel B reports summary statistics of the monthly CEPU and GEPU. It is worth noting that the CEPU is significantly larger and more volatile than the GEPU, which is consistent with the findings in Figure 1, indicating that economic policy changes more often in China.

**3.2. Estimation Results.** Table 2 reports the estimation results for the standard CARR-MIDAS model and its specification with the EPU (CARR-MIDAS-CEPU and CARR-MIDAS-GEPU) discussed in Section 2.2. In addition, estimates for the CARR model are presented for the purpose of comparison. For the CARR-MIDAS specifications, we employ three MIDAS lag years, i.e., we choose  $K = 36$  for the monthly RRV and EPU. Conrad and Kleen [29] showed that the data will identify the optimal weighting scheme as long as  $K$  is chosen reasonably large.

As can be seen from the table, the estimate of the persistence coefficient  $\alpha + \beta$  in the CARR model is close to one, showing high persistence in the conditional range process. Note also that, in the CARR-MIDAS estimation results, the estimates of the persistence coefficient of the short-run component,  $\alpha + \beta$ , are less than one, with its magnitude smaller than that of the CARR, indicating that accounting for long-run component reduces persistence in the short-run component. Additionally, the estimates of the parameter  $\theta_1$  are significant positive, which suggests that the monthly RRV is positively related to long-run volatility of Chinese stock market. It is interesting to note that the estimates of the parameter  $\theta_2$  in the CARR-MIDAS-CEPU and CARR-MIDAS-GEPU models are all negative and statistically significant, implying that both CEPU and GEPU have significantly negative effect on long-run volatility of Chinese stock market. That is, an increase in CEPU or GEPU predicts lower levels of long-run volatility of Chinese stock market. This result is consistent with the findings of Li et al. [20] and Wang et al. [19].

Figure 2 plots the conditional range ( $\lambda_{i,t}$ ) along with the long-run component ( $\tau_t$ ) from the CARR-MIDAS



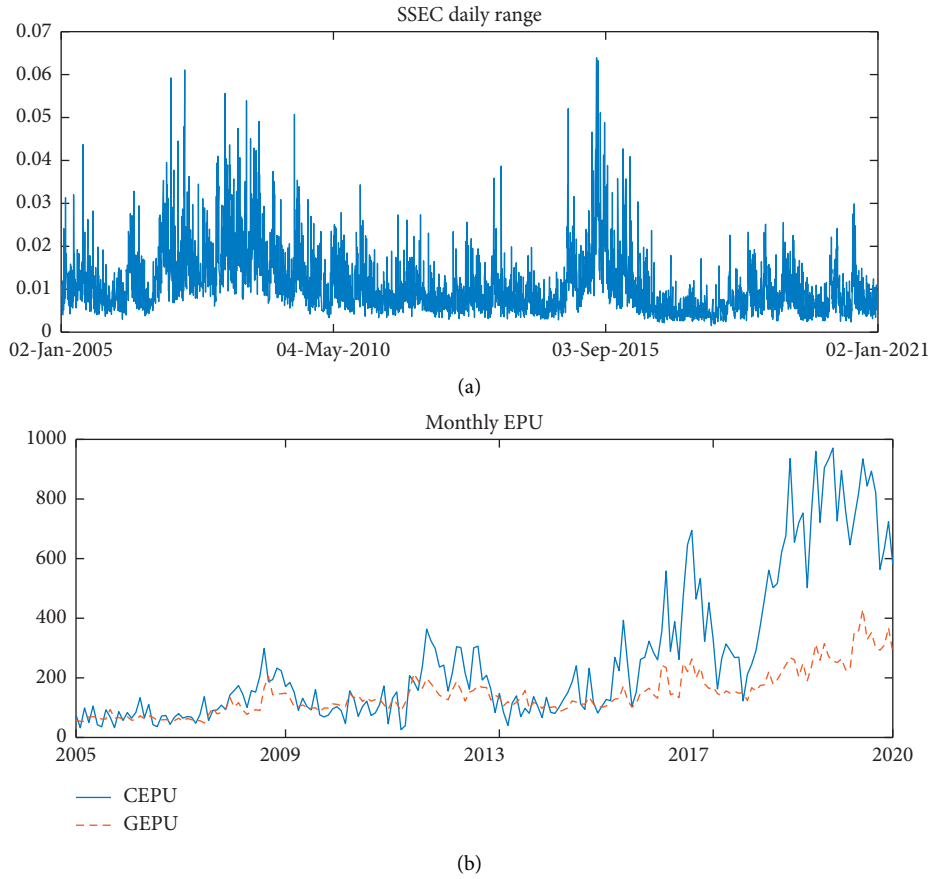


FIGURE 1: Daily range of SSEC and monthly EPU (CEPU and GEPU).

TABLE 1: Summary statistics.

	Mean	Min.	Max.	Std. dev.	Skewness	Kurtosis	Jarque-Bera	Q(10)
<i>Panel A: daily range</i>								
SSEC	0.0110	0.0015	0.0639	0.0075	2.1969	9.9680	10995.7980	9176.8674
<i>Panel B: monthly EPU</i>								
CEPU	261.6636	26.1441	970.8299	242.6354	1.4383	4.0095	74.3495	1240.5849
GEPU	145.2330	48.8196	429.5147	72.9342	1.2406	4.4544	66.1778	1015.1523

Q(10) is the Ljung-Box statistic for autocorrelation up to 10 lags.

TABLE 2: Estimation results.

	CARR	CARR-MIDAS	CARR-MIDAS-CEPU	CARR-MIDAS-GEPU
$\alpha$	0.1532 (0.0075)	0.1739 (0.0024)	0.1731 (0.0024)	0.1726 (0.0024)
$\beta$	0.8340 (0.0080)	0.7705 (0.0027)	0.7677 (0.0028)	0.7679 (0.0028)
$m(\omega)$	0.0001 (0.0000)	-2.1709 (0.0060)	-1.8975 (0.0053)	-1.5643 (0.0045)
$\theta_1$		0.3976 (0.0020)	0.3456 (0.0024)	0.3506 (0.0023)
$\gamma_1$		11.1079 (0.0544)	12.3186 (0.0061)	11.7892 (0.0721)
$\theta_2$			-0.1172 (0.0027)	-0.1854 (0.0027)
$\gamma_2$			1.9172 (0.0122)	7.3200 (0.0405)
$\nu$	5.6010 (0.1266)	5.6324 (0.0092)	5.6420 (0.0096)	5.6443 (0.0087)
Log-lik	15970.0035	15981.5230	15985.0211	15985.8600
AIC	-31932.0070	-31951.0460	-31954.0421	-31955.7200

Log-lik is the log-likelihood, and AIC is the Akaike information criterion. Numbers in parentheses are standard errors for the model parameters.

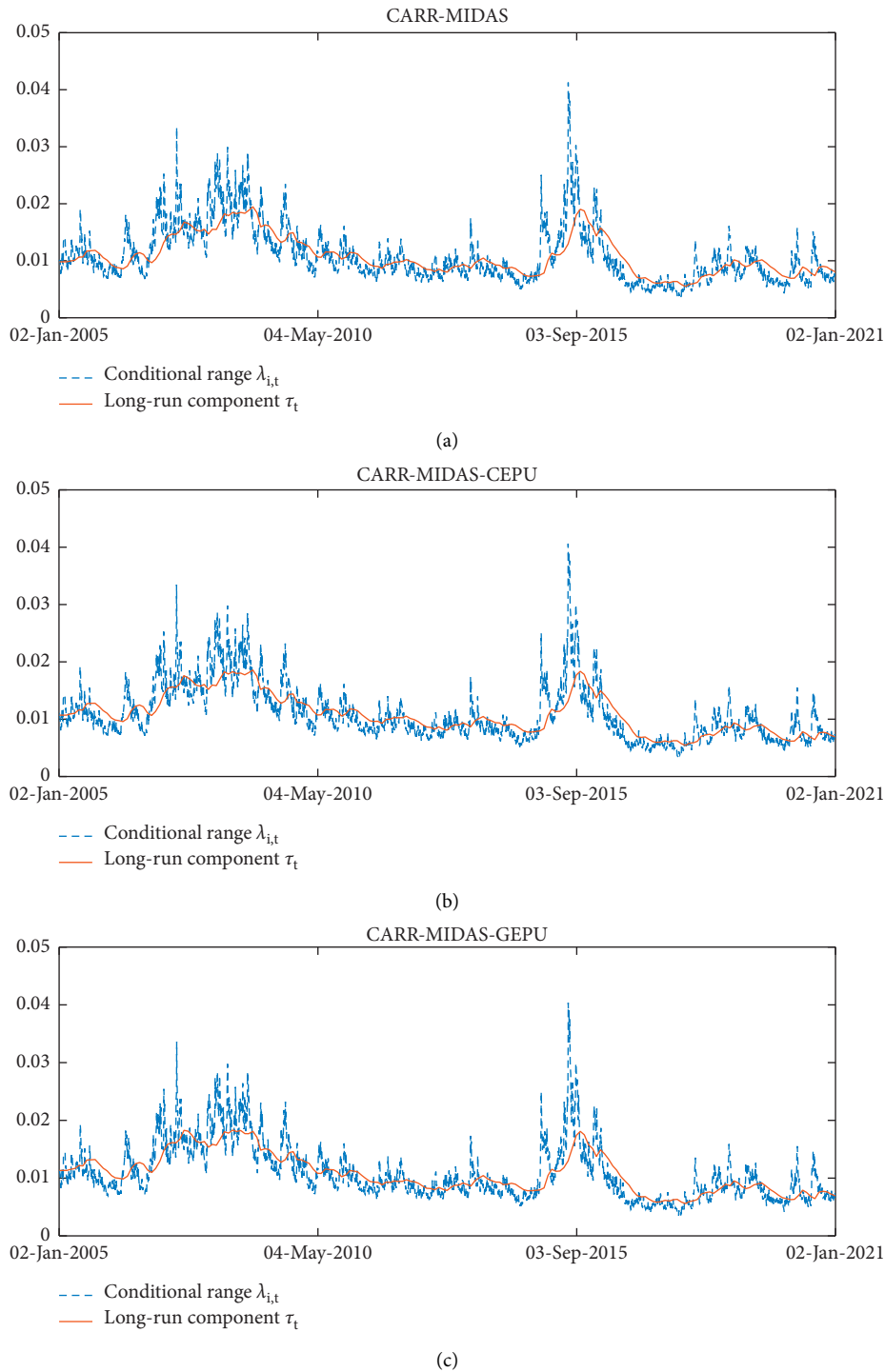


FIGURE 2: Conditional range ( $\lambda_{i,t}$ ) and the long-run component ( $\tau_t$ ) from the CARR-MIDAS framework.

framework. It is obvious that the long-run component of volatility appears smooth and tracks secular volatility trends over the sample period. All of the CARR-MIDAS models (the standard CARR-MIDAS, the CARR-MIDAS-CEPU, and the CARR-MIDAS-GEPU) do a good job in capturing the long-run trend of Chinese stock market volatility.

Turning to the shape parameter of the Gamma distribution,  $\nu$ 's in the models are estimated to be significantly larger than

one, ranging from 5.60 to 5.65. The estimates of  $\nu$  indicate a significant deviation from the exponential distribution.

Finally, we find that the standard CARR-MIDAS model significantly improves the CARR model, in terms of the log-likelihood and the Akaike information criterion (AIC). The result demonstrates that the multiplicative component structure for the conditional range is important to improve the model fit. Moreover, the extended CARR-MIDAS

TABLE 3: Out-of-sample forecast evaluation results.

Horizon	CARR	CARR-MIDAS	CARR-MIDAS-CEPU	CARR-MIDAS-GEPU
<i>Panel A: MSE loss function</i>				
1	6.4698e-06	5.6615e-06	<b>4.0326e-06</b>	4.7452e-06
5	8.7122e-06	7.4566e-06	<b>4.9309e-06</b>	5.9348e-06
10	1.0675e-05	8.7959e-06	<b>5.4236e-06</b>	6.6263e-06
22	1.3883e-05	9.8059e-06	<b>5.5660e-06</b>	6.7895e-06
<i>Panel B: QLIKE loss function</i>				
1	5.3383e-02	4.8970e-02	<b>3.6363e-02</b>	4.2160e-02
5	6.9746e-02	6.4000e-02	<b>4.5982e-02</b>	5.3552e-02
10	8.3782e-02	7.4541e-02	<b>5.1807e-02</b>	6.0427e-02
22	1.0811e-01	8.5781e-02	<b>5.8370e-02</b>	6.6381e-02

MSE is the mean squared error, and QLIKE is the quaslikelihood. Bold entries indicate the model with the lowest loss value per horizon (in each row). Shaded entries indicate the model is included in the MCS at a 10% significance level.

models (CARR-MIDAS-CEPU and CARR-MIDAS-GEPU) outperform the standard CARR-MIDAS model, which highlights the value of incorporating EPU into range (volatility) modelling. Note also that the CARR-MIDAS-GEPU model provides a slightly better performance in empirical fit than the CARR-MIDAS-CEPU model.

**3.3. Out-of-Sample Results.** In this section, we investigate whether EPU has predictive ability on Chinese stock market volatility using the CARR-MIDAS approach. The out-of-sample exercise is performed based on a rolling window (parameter estimates) scheme with a fixed window size of 3000 trading days. For each new forecast, we roll the window forward daily. The forecast horizon is set to one day, one week, two weeks, and one month, i.e., 1-day, 5-days, 10-days, and 22-days ahead forecasts.

As volatility cannot be observed directly, we require a proxy of the true volatility for forecast evaluation. In this paper, we use the daily realized range volatility (RRV) based on 5-min high-frequency data as the proxy of the true volatility, which is defined as

$$\text{RRV}_{i,t} = \sum_{j=1}^J R_{j,i,t}^2, \quad (11)$$

where  $R_{j,i,t}$  is the  $j$ th intraday range at day  $i$  in month  $t$ . It has been documented in the literature that RRV is five times more efficient than the realized volatility measure (see, e.g., Christensen and Podolskij [33]).

To assess the forecast performance of the CARR-MIDAS approach, we use two robust loss functions, the mean squared error (MSE) and the quaslikelihood (QLIKE), which are given by

$$\begin{aligned} \text{MSE: } \text{loss}_{i,t} &= (\text{MV}_{i,t} - \text{FV}_{i,t})^2, \\ \text{QLIKE: } \text{loss}_{i,t} &= \frac{\text{MV}_{i,t}}{\text{FV}_{i,t}} - \log \frac{\text{MV}_{i,t}}{\text{FV}_{i,t}} - 1, \end{aligned} \quad (12)$$

where  $\text{MV}_{i,t} = \sqrt{\text{RRV}_{i,t}}$  is the measured volatility (Since RRV measures the variance (squared volatility), we take the square root transformation for RRV as the measured (true)

volatility.) and  $\text{FV}_{i,t}$  is the forecasted volatility. Patton [34] showed that the MSE and QLIKE loss functions are robust to imperfect volatility proxies and provide consistent ranking of forecasts.

Moreover, we evaluate the predictive ability of the CARR-MIDAS approach by employing the model confidence set (MCS) test of Hansen et al. [35]. The MCS procedure examines a given set of competing models and identifies the set of the best performing models with some confidence level, namely, the MCS. This procedure is performed based on an equivalence test and an elimination rule. To be specific, let  $\mathcal{M}^0$  be an initial set of all competing models. The null hypothesis for the equivalence test is given by

$$H_{0,\mathcal{M}}: E(d_{uv,i,t}) = 0, \quad \forall u, v \in \mathcal{M}, \mathcal{M} \subset \mathcal{M}^0, \quad (13)$$

where  $d_{uv,i,t} \equiv \text{loss}_{i,t}(u) - \text{loss}_{i,t}(v)$  denotes the difference in the MSE or QLIKE loss of models  $u$  and  $v$ . Following Hansen et al. [35], the test statistic for the null hypothesis  $H_{0,\mathcal{M}}$  is given by

$$\begin{aligned} T_{\mathcal{M}} &= \max_{u,v \in \mathcal{M}} |t_{uv}|, \\ t_{uv} &= \frac{\bar{d}_{uv}}{\sqrt{\widehat{\text{var}}(\bar{d}_{uv})}}, \end{aligned} \quad (14)$$

where  $\bar{d}_{uv}$  is the average loss difference and  $\widehat{\text{var}}(\bar{d}_{uv})$  denotes a bootstrapped estimate of  $\text{var}(\bar{d}_{uv})$ . If the null hypothesis  $H_{0,\mathcal{M}}$  is rejected, the set  $\mathcal{M}$  is reduced using the elimination rule,  $e_{\mathcal{M}} = \text{argmax}_{u \in \mathcal{M}} \sup_{v \in \mathcal{M}} t_{uv}$ . The test is performed iteratively, until no further model can be eliminated. The final set of surviving models are denoted by  $\mathcal{M}_{\text{MCS}}$ . Following Hansen et al. [35], we implement the MCS procedure using a block bootstrap of  $10^5$  replications and a significance level of 10%.

Table 3 presents the out-of-sample forecast evaluation results. It can be seen from the table that the standard CARR-MIDAS model improves upon the forecasting performance of the CARR model for all forecast horizons in terms of the two loss functions. This indicates the usefulness of modelling a long-run component (or multiplicative component structure). More importantly, by incorporating

TABLE 4: Out-of-sample forecast evaluation results for forecast window of 500.

Horizon	CARR	CARR-MIDAS	CARR-MIDAS-CEPU	CARR-MIDAS-GEPU
<i>Panel A: MSE loss function</i>				
1	5.8635e-06	5.3300e-06	<b>3.9646e-06</b>	4.2818e-06
5	8.0498e-06	7.2398e-06	<b>5.0020e-06</b>	5.4611e-06
10	9.9444e-06	8.7142e-06	<b>5.6484e-06</b>	6.2006e-06
22	1.3656e-05	1.0430e-05	<b>6.3693e-06</b>	6.9867e-06
<i>Panel B: QLIKE loss function</i>				
1	4.6432e-02	4.5667e-02	<b>3.4571e-02</b>	3.7338e-02
5	6.1724e-02	6.1738e-02	<b>4.4787e-02</b>	4.8592e-02
10	7.4483e-02	7.3153e-02	<b>5.1065e-02</b>	5.5565e-02
22	1.0084e-01	8.8528e-02	<b>6.1062e-02</b>	6.5505e-02

MSE is the mean squared error, and QLIKE is the quaslikelihood. Bold entries indicate the model with the lowest loss value per horizon (in each row). Shaded entries indicate the model is included in the MCS at a 10% significance level.

TABLE 5: Out-of-sample forecast evaluation results for forecast window of 1000.

Horizon	CARR	CARR-MIDAS	CARR-MIDAS-CEPU	CARR-MIDAS-GEPU
<i>Panel A: MSE loss function</i>				
1	6.3291e-06	5.4761e-06	<b>3.8849e-06</b>	4.5401e-06
5	8.6110e-06	7.2356e-06	<b>4.7254e-06</b>	5.6592e-06
10	1.0671e-05	8.5469e-06	<b>5.1621e-06</b>	6.2875e-06
22	1.4443e-05	9.6989e-06	<b>5.2976e-06</b>	6.4651e-06
<i>Panel B: QLIKE loss function</i>				
1	5.6089e-02	5.0384e-02	<b>3.7588e-02</b>	4.2935e-02
5	7.3891e-02	6.5760e-02	<b>4.6985e-02</b>	5.4085e-02
10	8.9510e-02	7.6431e-02	<b>5.2300e-02</b>	6.0477e-02
22	1.1905e-01	8.9079e-02	<b>5.8530e-02</b>	6.6474e-02

MSE is the mean squared error, and QLIKE is the quaslikelihood. Bold entries indicate the model with the lowest loss value per horizon (in each row). Shaded entries indicate the model is included in the MCS at a 10% significance level.

C(G)EPU, the extended CARR-MIDAS model, the CARR-MIDAS-C(G)EPU model, provides better performance than the standard CARR-MIDAS model, suggesting that volatility forecasting can be improved when the C(G)EPU is taken into consideration. It is interesting to note the CARR-MIDAS-CEPU model outperforms the CARR-MIDAS-GEPU model in all cases. The results demonstrate that the CEPU is more important than the GEPU for forecasting volatility of Chinese stock market. Overall, the CARR-MIDAS-CEPU model consistently gives the lowest loss values and is clearly the preferred and best forecasting model, followed by the CARR-MIDAS-GEPU model.

The shaded entries in Table 3 identify the model included in the MCS at the significance level of 10%. The results show that the CARR-MIDAS-CEPU model is the only model that includes in the MCS for all forecast horizons, suggesting that the CARR-MIDAS-CEPU model significantly outperforms all other models.

*3.4. Robustness Check.* For the robustness check, out-of-sample forecast is also performed on the SSEC over different forecast windows (out-of-sample periods). We choose two different forecast windows, 500 and 1000. The out-of-sample forecast evaluation results are reported in Tables 4 and 5 for the two forecast windows, respectively. As is consistent with the results in Table 3, the CARR-MIDAS-CEPU model performs significantly better than the others.

## 4. Conclusions

Motivated by the return-based GARCH-MIDAS model, we introduce in this paper the range-based CARR-MIDAS model that exploits intraday information from the high and low prices. The proposed CARR-MIDAS model allows for exogenous explanatory variable such as EPU to model the time-varying long-run volatility. We employ the CARR-MIDAS approach to investigate the impact of EPU on the volatility of Chinese stock market and to explore the predictive ability of EPU for Chinese stock market. We perform an analysis on the SSEC of China and use two EPU indices including CEPU and GEPU. We find that both the CEPU and GEPU have a significantly negative effect on the long-run volatility of Chinese stock market. The multiplicative component MIDAS structure for the conditional range is important to improve the model fit. The CARR-MIDAS models significantly improve upon the empirical fit of the original CARR model. Moreover, the extended CARR-MIDAS models (CARR-MIDAS-CEPU and CARR-MIDAS-GEPU) outperform the standard CARR-MIDAS model, which highlights the value of incorporating EPU into range (volatility) modelling. Furthermore, out-of-sample results demonstrate that taking into account the CEPU and GEPU substantially improves our ability to forecast 1-day, 5-days (one week), 10-days (two weeks), and 22-days (one month) ahead volatility of Chinese stock market. In particular, we find that the CEPU provides superior volatility forecasts

compared to the GEPU. According to the robustness check, our empirical results are robust to different forecasting windows. Overall, the findings highlight the role of EPU particularly the CEPU as predictor of Chinese stock market volatility.

Finally, future research could be extended to consider application of our approach to risk management, or to option pricing relying on EPU. Moreover, our proposed model could be extended to incorporate regime switching in the short-run component of volatility in the spirit of the regime switching GARCH-MIDAS model of Pan et al. [36]. The regime switching model has the capacity to accommodate structural breaks, which is a well-known stylized feature of financial volatility.

### Data Availability

The data on the SSEC index of China are obtained from Wind Database of China, and the data on the monthly CEPU and GEPU indices are obtained from <https://www.policy.uncertainty.com/>. All the data are available from the corresponding author upon request.

### Conflicts of Interest

The authors declare that there are no conflicts of interest regarding the publication of this paper.

### Acknowledgments

This research was supported by the National Natural Science Foundation of China (No. 71971001), the University Natural Science Research Project of Anhui Province (No. KJ2019A0659), and the Innovative Research Project for Graduates of Anhui University of Finance and Economics (No. ACYC2020186).

### References

- [1] S. R. Baker, N. Bloom, and S. J. Davis, "Measuring economic policy uncertainty," *Quarterly Journal of Economics*, vol. 131, no. 4, pp. 1593–1636, 2016.
- [2] S. A. Al-Thaqeb and B. G. Algharabali, "Economic policy uncertainty: a literature review," *The Journal of Economic Asymmetries*, vol. 20, Article ID e00133, 2019.
- [3] L. Pástor and P. Veronesi, "Uncertainty about government policy and stock prices," *The Journal of Finance*, vol. 67, no. 4, pp. 1219–1264, 2012.
- [4] L. Pástor and P. Veronesi, "Political uncertainty and risk premia," *Journal of Financial Economics*, vol. 110, no. 3, pp. 520–545, 2013.
- [5] L. Liu and T. Zhang, "Economic policy uncertainty and stock market volatility," *Finance Research Letters*, vol. 15, pp. 99–105, 2015.
- [6] M. Arouri, C. Estay, C. Rault, and D. Roubaud, "Economic policy uncertainty and stock markets: long-run evidence from the US," *Finance Research Letters*, vol. 18, pp. 136–141, 2016.
- [7] Z. Liu, Y. Ye, F. Ma, and J. Liu, "Can economic policy uncertainty help to forecast the volatility: a multifractal perspective," *Physica A: Statistical Mechanics and Its Applications*, vol. 482, pp. 181–188, 2017.
- [8] I.-C. Tsai, "The source of global stock market risk: a viewpoint of economic policy uncertainty," *Economic Modelling*, vol. 60, pp. 122–131, 2017.
- [9] Y. Duan, W. Chen, Q. Zeng, and Z. Liu, "Leverage effect, economic policy uncertainty and realized volatility with regime switching," *Physica A: Statistical Mechanics and Its Applications*, vol. 493, pp. 148–154, 2018.
- [10] D. Mei, Q. Zeng, Y. Zhang, and W. Hou, "Does US economic policy uncertainty matter for European stock markets volatility?" *Physica A: Statistical Mechanics and Its Applications*, vol. 512, pp. 215–221, 2018.
- [11] X. Xiong, Y. Bian, and D. Shen, "The time-varying correlation between policy uncertainty and stock returns: evidence from China," *Physica A: Statistical Mechanics and Its Applications*, vol. 499, pp. 413–419, 2018.
- [12] M. Yu and J. Song, "Volatility forecasting: global economic policy uncertainty and regime switching," *Physica A: Statistical Mechanics and Its Applications*, vol. 511, pp. 316–323, 2018.
- [13] M. Balciar, R. Gupta, W. J. Kim, and C. Kyei, "The role of economic policy uncertainties in predicting stock returns and their volatility for Hong Kong, Malaysia and South Korea," *International Review of Economics & Finance*, vol. 59, pp. 150–163, 2019.
- [14] T. C. Chiang, "Economic policy uncertainty, risk and stock returns: evidence from G7 stock markets," *Finance Research Letters*, vol. 29, pp. 41–49, 2019.
- [15] R. F. Engle, E. Ghysels, and B. Sohn, "Stock market volatility and macroeconomic fundamentals," *The Review of Economics and Statistics*, vol. 95, no. 3, pp. 776–797, 2013.
- [16] H. Yu, L. Fang, and W. Sun, "Forecasting performance of global economic policy uncertainty for volatility of Chinese stock market," *Physica A: Statistical Mechanics and Its Applications*, vol. 505, pp. 931–940, 2018.
- [17] X. Yu and Y. Huang, "The impact of economic policy uncertainty on stock volatility: evidence from GARCH-MIDAS approach," *Physica A*, vol. 570, Article ID 125794, 2021.
- [18] T. Li, F. Ma, X. Zhang, and Y. Zhang, "Economic policy uncertainty and the Chinese stock market volatility: novel evidence," *Economic Modelling*, vol. 87, pp. 24–33, 2020.
- [19] X. Wang, Y. Luo, Z. Wang, Y. Xu, and C. Wu, "The impact of economic policy uncertainty on volatility of China's financial stocks: An empirical analysis," *Finance Research Letters*, Forthcoming.
- [20] Y. Li, F. Ma, Y. Zhang, and Z. Xiao, "Economic policy uncertainty and the Chinese stock market volatility: new evidence," *Applied Economics*, vol. 51, no. 49, pp. 5398–5410, 2019.
- [21] M. Parkinson, "The extreme value method for estimating the variance of the rate of return," *Journal of Business*, vol. 53, no. 1, pp. 61–65, 1980.
- [22] S. Alizadeh, M. W. Brandt, and F. X. Diebold, "Range-based estimation of stochastic volatility models," *The Journal of Finance*, vol. 57, no. 3, pp. 1047–1091, 2002.
- [23] M. W. Brandt and C. S. Jones, "Volatility forecasting with range-based EGARCH models," *Journal of Business & Economic Statistics*, vol. 24, no. 4, pp. 470–486, 2006.
- [24] H. Li and Y. Hong, "Financial volatility forecasting with range-based autoregressive volatility model," *Finance Research Letters*, vol. 8, no. 2, pp. 69–76, 2011.
- [25] S. Degiannakis and A. Livada, "Realized volatility or price range: evidence from a discrete simulation of the continuous time diffusion process," *Economic Modelling*, vol. 30, pp. 212–216, 2013.

- [26] R. Y. Chou, H. Chou, and N. Liu, "Range volatility: a review of models and empirical studies," in *Handbook of Financial Econometrics and Statistics*, C.-F. Lee and J. Lee, Eds., Springer, New York, NY, USA, pp. 2029–2050, 2015.
- [27] R. Y. Chou, "Forecasting financial volatilities with extreme values: the conditional autoregressive range (CARR) model," *Journal of Money, Credit, and Banking*, vol. 37, no. 3, pp. 561–582, 2005.
- [28] F. Wang and E. Ghysels, "Econometric analysis of volatility component models," *Econometric Theory*, vol. 31, no. 2, pp. 362–393, 2015.
- [29] C. Conrad and O. Kleen, "Two are better than one: volatility forecasting using multiplicative component GARCH-MIDAS models," *Journal of Applied Econometrics*, vol. 35, no. 1, pp. 19–45, 2020.
- [30] H. B. Xie, "Range-based volatility forecasting: a multiplicative component conditional autoregressive range model," *Journal of Risk*, vol. 22, no. 5, pp. 1–23, 2020.
- [31] C. G. Lamoureux and W. D. Lastrapes, "Persistence in variance, structural change, and the GARCH model," *Journal of Business & Economic Statistics*, vol. 8, no. 2, pp. 225–234, 1990.
- [32] H. Xie and X. Wu, "A conditional autoregressive range model with gamma distribution for financial volatility modelling," *Economic Modelling*, vol. 64, pp. 349–356, 2017.
- [33] K. Christensen and M. Podolskij, "Realized range-based estimation of integrated variance," *Journal of Econometrics*, vol. 141, no. 2, pp. 323–349, 2007.
- [34] A. J. Patton, "Volatility forecast comparison using imperfect volatility proxies," *Journal of Econometrics*, vol. 160, no. 1, pp. 246–256, 2011.
- [35] P. R. Hansen, A. Lunde, and J. M. Nason, "The model confidence set," *Econometrica*, vol. 79, no. 2, pp. 453–497, 2011.
- [36] Z. Pan, Y. Wang, C. Wu, and L. Yin, "Oil price volatility and macroeconomic fundamentals: a regime switching GARCH-MIDAS model," *Journal of Empirical Finance*, vol. 43, pp. 130–142, 2017.

## Research Article

# Asymmetric Risk Spillover Networks and Risk Contagion Driver in Chinese Financial Markets: The Perspective of Economic Policy Uncertainty

Zongxin Zhang,<sup>1</sup> Ying Chen ,<sup>2</sup> and Weijie Hou<sup>3</sup>

<sup>1</sup>*Institute of Finance, Fudan University, Shanghai 200433, China*

<sup>2</sup>*School of Economics, Fudan University, Shanghai 200433, China*

<sup>3</sup>*Antai College of Economics and Management, Shanghai Jiao Tong University, Shanghai 200030, China*

Correspondence should be addressed to Ying Chen; [chenying18@fudan.edu.cn](mailto:chenying18@fudan.edu.cn)

Received 9 May 2021; Accepted 3 September 2021; Published 14 September 2021

Academic Editor: Ning Cai

Copyright © 2021 Zongxin Zhang et al. This is an open access article distributed under the Creative Commons Attribution License, which permits unrestricted use, distribution, and reproduction in any medium, provided the original work is properly cited.

The global financial market shocks have intensified due to the COVID-19 epidemic and other impacts, and the impacts of economic policy uncertainty on the financial system cannot be ignored. In this paper, we construct asymmetric risk spillover networks of Chinese financial markets based on five sectors: bank, securities, insurance, diversified finance, and real estate. We investigate the complexity of the risk spillover effect of Chinese financial markets and the impact of economic policy uncertainty on the level of network contagion of financial risk. The study yields three findings. First, the cross-sectoral risk spillover effects of Chinese financial markets are asymmetric in intensity. The bank sector is systemically important in the risk spillover network. Second, the level of risk stress in the real estate sector has increased in recent years, and it plays an important role in the path of financial risk contagion. Third, Economic policy uncertainty has a significant positive impact on the level of network contagion of financial risk of Chinese financial markets.

## 1. Introduction

Corresponding to the three main elements of systemic financial risk: shocks, contagion mechanisms, and the consequences of macroeconomic losses. The generation mechanism of systemic financial risk consists of three main processes: the emergence of systemic financial risk triggers, cross-sectoral risk contagion, and the generation of systemic financial risk. In particular, the cross-sectoral risk contagion is the core process of the outbreak of the financial crisis. At present, the global economic and political situation is volatile. The COVID-19 epidemic and the Sino-US trade war have intensified economic policy uncertainty, financial market shocks, and cross-market risk spillover have subsequently increased. It is of great academic value and practical significance to quantify the level of financial market risk spillover, clarify the role of different submarkets in the

financial risk spillover network, and explore the driving impact of economic policy uncertainty on financial risk contagion and financial stability.

The paths of systemic financial risk generation and contagion are increasingly complex, with dynamic evolution, nonlinear and networked characteristics. Complex network technology can incorporate financial market complexity into spatial network models and provide a parsing framework for systemic financial risk networked generation mechanisms through network topology analysis, which is an important tool for risk derivation and contagion analysis in financial markets (Caccioli et al. [1]). Traditional risk network models tend to construct risk spillover networks among banks based on asset-liability linkages. While these models are able to capture risk linkages among banks, they neglect cross-sectoral risk spillover arising from indirect linkages and information channel linkages. For

example, financial risk contagion triggered by the monsoon effect (risk contagion triggered by shocks in macro-fundamentals) and pure infection effect (extreme risk contagion) is still in the risk controlling gap. Furthermore, the frequency of balance sheet data is low, and the risk spillover networks constructed from them are often measured after the risk spillover effects have occurred. In addition, Anand et al. [2] point out that stock price is a market representation of a firm's operating conditions and it is more scientific to build a risk spillover network based on the return series of stock price.

Based on the above analysis, this paper constructs asymmetric risk spillover networks of the Chinese financial market using stock market return series of five sectors: banking, securities, insurance, diversified finance, and real estate, and explores the driving impact of economic policy uncertainty on the level of network contagion of financial risk. The main content of this paper consists of three parts as follows. First, constructing cross-sectoral risk spillover networks of Chinese financial markets and second, analyzing the risk spillover characteristics of the Chinese financial market and quantifying the level of network contagion of financial risk, finally, exploring the driving role of economic policy uncertainty on the level of financial risk network contagion through empirical analysis.

The main innovations and contributions of this paper are threefold. First, we construct an asymmetric cross-sectoral risk spillover network to analyze the risk linkage and contagion effects among various sectors within the Chinese financial markets. Second, the existing studies on risk contagion mostly focus on the risk association between two pairs. This paper implements an effective measurement of the overall risk contagion level of Chinese financial markets. Third, this paper explores the driving role of economic policy uncertainty on the overall risk contagion level of financial markets, further enriching the researches about economic policy uncertainty and financial stability, which provide references for financial risk prevention and control.

The rest of this paper is organized as follows. Part 2 is the literature review and Part 3 is the model construction. Part 4 reports and discusses the main empirical results in terms of the risk spillover networks and the driving impact of economic policy uncertainty on the level of network contagion of financial risk. Part 5 concludes the study and puts forward the policy implications.

## 2. Literature Review

*2.1. Network Contagion of Financial Risk.* The network contagion of financial risk refers to the characteristics of the association in the process of systemic financial risk generation due to the cross-contagion of risks within the financial system, i.e., between financial markets and financial institutions (Acemoglu et al. [3]). Complex network modeling is one of the important methods for studying the contagion effects of financial risk networks. The construction of risk networks in financial markets has led to a deeper study of risk contagion. Silva et al. [4] found that the network

structure can attenuate or amplify shocks from the real sector by simulating shocks to the real sector and plays an important role in the risk contagion process.

The core of financial risk spillover network construction is the identification of risk spillover intensity and risk spillover direction. Hong et al. [5] study the risk Granger causality to the network system, and Billio et al. [6] extend their study by proposing a systemic financial risk measure based on principal component analysis and Granger causality network. Billio et al. [6] solve the network causal direction identification, then Diebold and Yilmaz [7] propose weighted directed networks based on the variance decomposition method for studying systemic risk spillover. Paltalidis et al. [8] use the maximum entropy method to construct dynamic financial networks, through which they study systemic financial risk and the contagion of crises within the euro area banking system. They confirm the vulnerability of the European banking system by simulating the shocks of systemic financial risk sources through counterfactuals. Regarding the formation of complex risk networks of financial markets, Berndsen et al. [9] propose an interdependent network that couples multiple layers of transmission paths of financial institutions to facilitate a more accurate understanding of the true connectivity architecture of the financial system. Anderson et al. [10] show that transactional behaviors among financial institutions lead financial markets to form a complex network, and the degree of network centrality has an inconsistent effect on the stability of financial markets. They suggest that small and medium-sized financial institutions with a more centralized network structure have better risk diversification, while central banks are exposed to larger shocks that increase network vulnerability.

The network contagion of financial risks is an important link of the outbreak of the financial crisis, Elliott et al. [11] investigate the failure cascade in interdependent financial organization networks, i.e., how discontinuous changes in asset values trigger further failures and their relationship with the structure of financial organization networks. Acemoglu et al. [3] further suggest that the degree of financial contagion manifests itself as a phase transition, where the propagation mechanism of mutual shocks in financial networks leads to a more vulnerable financial system. How to construct cross-sectoral risk spillover networks of financial markets, analyzing the characteristics of risk contagion within financial markets, and quantify the level of the network contagion of financial risk are important to improve the efficiency of financial risk monitoring and control.

*2.2. Economic Policy Uncertainty and Financial Risk Contagion.* As a significant factor influencing macro-fundamental trends, the role of economic policy uncertainty in the cross-market contagion of risk cannot be ignored (Baker et al. [12]). The impact of economic policy uncertainty on the degree of risk contagion of financial markets is often accompanied by unusual volatility in financial markets, which can affect the stock price by influencing inflation,



interest rates, and expected risk premiums (Pástor and Veronesi [13, 14]). Dakhlaoui and Aloui [15] find that there is strong evidence of a time-varying correlation between US economic uncertainty and BRIC stock market volatility, and the correlation is highly volatile during periods of global economic instability. Hoque and Zaidi [16] suggest that global economic policy uncertainty can be a systemic risk factor and predictor of stock market returns.

In addition, increased economic policy uncertainty can also exacerbate financial market risk contagion. Dicks and Fulghieri [17] propose that uncertainty is a driver of new systemic risk contagion. Increasing uncertainty makes the financial system more fragile and more prone to crises. Yang et al. [18] use a nonlinear correlation network to study cross-country systemic financial risk and find that the stock market is the main risk exporter, and the foreign exchange market is the main risk inputter. Their study proves that the economic policy uncertainty plays an important mediating role in both cross-country and cross-market contagion of systemic financial risk. Sharif et al. [19] find that COVID-19 is expected to have a long-term negative effect on the geopolitical risk levels and economic uncertainty. And Li et al. [20] propose that the interaction between EPU in the US and stock returns in China and India is weak in the short term but gradually becomes stronger in the long term, especially when significant financial events occur. The impact of economic policy uncertainty on the level of systemic financial risk contagion has further increased due to the COVID-19 epidemic and the Sino-US trade friction. Li et al. [21] suggest that the correlations between the EPU and financial networks increased significantly during the COVID-19 period.

The study of risk contagion should not be limited to the level of risk of individual systemically important financial institutions. Systemic risk contagion is also crucial (Minoiu et al. [22]). However, existing researches are mostly focused on the impact of economic policy uncertainty on abnormal financial market volatility. There are still research gaps with respect to the role of economic policy uncertainty in driving the level of contagion in financial risk networks, which is important for maintaining financial stability and is an important task for global risk management.

### 3. Research Design and Methods

*3.1. Sample Selection and Data Acquisition.* Data from financial markets are characterized by high frequency, timeliness, and availability (Diebold and Yilmaz [7]; Benoit et al. [23]; Li et al. [21]; Yang et al. [18]). The study of comovements and risk spillover effects within Chinese financial markets based on data from financial markets can provide a global measure of financial risk contagion. Moreover, the construction of the proxy variables for each sector of Chinese financial markets according to the industry classification criteria has become a common approach to study cross-sector risk spillover (Yang et al. [18]; Li et al. [21]; Gong and Xiong [24]).

In this paper, the stock market sector indices of banking, securities, insurance, and diversified finance are selected as

proxy variables for each sector of the Chinese financial markets according to the industry classification criteria of Shenyn Wanguo. In addition, considering the increasing risk contagion effect between the real estate sector and the traditional financial sector in the Chinese financial market (Yang et al. [18]; Bai et al. [25]), we add the real estate sector to the financial risk spillover network to study cross-sectoral risk contagion effects. Since the sector indices are nonstationary time series, thus we calculate the daily log returns of each sector index first. The sample period covers from March 2, 2007, to March 5, 2021, and the descriptive statistics of the daily log returns of each index are shown in Table 1.

According to Table 1, the static correlation coefficients among banking, securities, insurance, real estate, and diversified finance are high. The correlation coefficient between the bank sector and the insurance sector is the highest at approximately 0.81, the correlation coefficients between the securities sector and the other four sectors are greater than 0.7, and the correlation coefficient between the diversified finance and insurance sector is the lowest at approximately 0.642.

*3.2. Model Construction.* This paper uses generalized variance decomposition to construct asymmetric risk spillover networks including five sectors: bank, securities, insurance, diversified finance, and real estate (Diebold and Yilmaz [7]; Diebold and Yilmaz [26]), to measure network contagion of financial risk due to direct linkages, indirect linkages, and information channel linkages. As for the stationary multivariate time series  $X_t$ , the VAR(p) model is constructed with an autoregressive process as equation (1), the autoregressive process is transformed into the form of the lag operator as equation (2), and then it is transformed into a moving average process as equation (3).

$$X_t = \sum_{i=1}^p \varphi_i X_{t-i} + \varepsilon_t, \quad (1)$$

$$X_t = \Theta(L)\varepsilon_t, \quad (2)$$

$$X_t = \sum_{i=0}^{\infty} A_i \varepsilon_{t-i}, \quad (3)$$

where  $\varepsilon \sim N(0, \Sigma)$ ,  $A_i$  is a coefficient matrix of order  $N \times N$ , obeying the recursive process shown in equation (4), where  $A_0$  is a unitary array of order  $N$ ,  $i \geq 0$ .

$$A_i = \varphi_1 A_{i-1} + \varphi_2 A_{i-2} + \dots + \varphi_p A_{i-p}. \quad (4)$$

The key to constructing a risk spillover network based on the generalized variance decomposition is the calculation of the variance contribution, i.e., the proportion of the  $H$ -step forecast error of  $x_i$  that is explained by  $x_j$  when the variable  $x_i$  is subject to an external shock:  $d_{ij}(H)$ , it is also known as the forecast error variance ratio. The essence of the variance contribution variance ratio  $d_{ij}(H)$  is the extent to which the variable  $x_i$  is affected by itself and other variables in the system when faced with a market shock, i.e., the distribution

TABLE 1: Descriptive statistics of variables.

	Bank	Securities	Insurance	Estate	Diversified finance
Mean	0.0098	0.0048	-0.0003	0.0089	0.0105
Median	-0.0172	-0.0188	0.0183	0.0228	-0.0090
Maximum	4.1478	4.1394	4.1469	4.0845	4.1455
Minimum	-4.5626	-4.5761	-4.5764	-4.2359	-4.5758
Std. dev.	0.7969	1.1528	1.0248	0.9198	0.9884
Skewness	0.0194	-0.0378	-0.5070	-0.4888	-0.0063
Kurtosis	7.8855	5.6911	6.1296	5.7515	5.8542
Static correlation matrix					
Bank	1.0000	0.7160	0.8101	0.6845	0.6420
Securities	0.7160	1.0000	0.7530	0.7503	0.7997
Insurance	0.8101	0.7530	1.0000	0.6699	0.6454
Estate	0.6845	0.7503	0.6699	1.0000	0.7555
Diversified finance	0.6420	0.7997	0.6454	0.7555	1.0000

of incremental risk across sectors of the financial system between its own risk derivation and cross-sectoral risk contagion effects.  $d_{ij}(H)$  is calculated as shown in the following equation:

$$d_{ij}(H) = \frac{\sigma_{jj}^{-1} \sum_{h=0}^{H-1} (e_i' A_i \Sigma e_j)^2}{\sum_{h=0}^{H-1} (e_i' A_i \Sigma A_i' e_i)^2}, i, j = 1, 2, \dots, N, i \neq j, \quad (5)$$

where  $\Sigma$  is the variance covariance matrix of  $\varepsilon_t$  and  $\sigma_{jj}$  is the standard deviation of  $\varepsilon_t$ . The  $i$ -th element of  $e_i$  is 1 and the remaining elements are 0.  $H$  denotes the prediction period and  $h$  is the lag order of the perturbation term  $\varepsilon_t$ . Equation (6) is a variance decomposition matrix of order  $N \times N$ , consisting of the prediction error variance ratio  $d_{ij}(H)$ .

$$D_{ij}(H) = \begin{pmatrix} d_{11} & d_{12} & \dots & d_{1N} \\ d_{21} & d_{22} & \dots & d_{2N} \\ \vdots & \vdots & \ddots & \vdots \\ d_{N1} & d_{N2} & \dots & d_{NN} \end{pmatrix}. \quad (6)$$

The standardized risk spillover matrix  $S_{ij}(H)$  can be obtained using the elements of each row of  $D_{ij}(H)$  divided by the sum of the elements of the row in which they are located, respectively. Assume the corresponding element of  $S_{ij}$  is  $zd_{ij}$ , as shown in the following equation:

$$S_{ij}(H) = \begin{pmatrix} zd_{11} & zd_{12} & \dots & zd_{1N} \\ zd_{21} & zd_{22} & \dots & zd_{2N} \\ \vdots & \vdots & \ddots & \vdots \\ zd_{N1} & zd_{N2} & \dots & zd_{NN} \end{pmatrix}. \quad (7)$$

In this paper, we use five sectors: bank, securities, insurance, diversified finance, and real estate as the nodes of the risk spillover network, and the standardized risk spillover matrix  $S_{ij}(H)$  between different dimensions as the network weights to construct directed and weighted cross-sector risk spillover networks.

The overall connectivity indicator of risk spillover network can denote the level of network contagion of financial risk. In this paper, we use the total risk network connectivity index to measure the level of network contagion of financial risk (Cindex), which is calculated as shown in the following equation:

$$\text{Cindex} = \frac{1}{N} \sum_{\substack{i,j=1 \\ i \neq j}}^N d_{ij}^H. \quad (8)$$

This paper constructs an empirical model using the total risk network connectivity index as the explanatory variable and the Chinese economic policy uncertainty index (CEPU) as the core explanatory variable while controlling for the relevant macroeconomic variables: inflation rate (CPI), CSI 300 index turnover rate (HSTR), CSI 300 index price-to-earnings ratio (HSPE), industrial value added (IAV), and Treasury term spread (BSPREAD), for investigating the driving impact of economic policy uncertainty on the network contagion level of risk. The regression model is constructed as shown in equation (9), where  $X_t$  is a vector consisting of control variables and  $\beta_1$  is the corresponding vector of coefficients to be estimated.

$$\text{Cindex}_t = \alpha_0 + \alpha_1 * \text{CEPU}_t + \beta_1 * X_t. \quad (9)$$

## 4. Empirical Analysis

**4.1. Risk Spillover Networks Based on Different Financial Sectors.** The VAR model is constructed based on five sectors: bank, securities, insurance, diversified finance, and real estate. From Table 1, we can see that the daily log returns of these five sectors are stationary time series, and Table 2 shows the lagged order test of the VAR model.

Combining the lag order test and the parameter significance test of the VAR model with lag order 2, we choose to construct the VAR model with lag order 2, as in

TABLE 2: Test of lagged order of VAR model.

Lag	LogL	LR	FPE	AIC	SC	HQ
0	-17614.6	NA	0.021	10.349	10.358*	10.352
1	-17529.9	169.264	0.021	10.314	10.368	10.333*
2	-17496.7	66.096	0.021*	10.309*	10.408	10.345
3	-17474.5	44.282	0.021	10.311	10.455	10.362
4	-17452.7	43.214	0.021	10.313	10.502	10.380

Joint significance test of VAR (2) parameters						
	Bank	Securities	Insurance	Estate	Diversified finance	General
Lag 1	30.216 [0.000]	13.304 [0.021]	23.982 [0.000]	18.077 [0.003]	22.359 [0.000]	166.458 [0.000]
Lag 2	3.421 [0.635]	12.296 [0.031]	2.909 [0.714]	4.840 [0.436]	16.368 [0.006]	68.247 [0.000]

\* $p < 0.1$ , \*\* $p < 0.05$ , \*\*\* $p < 0.01$ .

equation (10), and then construct the prediction error variance ratio  $d_{ij}(H)$ .

$$\begin{pmatrix} \text{bank}_t \\ \text{security}_t \\ \text{insurance}_t \\ \text{estate}_t \\ \text{mvfinance}_t \end{pmatrix} = A_1 \begin{pmatrix} \text{bank}_{t-1} \\ \text{security}_{t-1} \\ \text{insurance}_{t-1} \\ \text{estate}_{t-1} \\ \text{mvfinance}_{t-1} \end{pmatrix} + A_2 \begin{pmatrix} \text{bank}_{t-2} \\ \text{security}_{t-2} \\ \text{insurance}_{t-2} \\ \text{estate}_{t-2} \\ \text{mvfinance}_{t-2} \end{pmatrix} + \begin{pmatrix} \varepsilon_{1t} \\ \varepsilon_{2t} \\ \varepsilon_{3t} \\ \varepsilon_{4t} \\ \varepsilon_{5t} \end{pmatrix}. \quad (10)$$

Table 3 shows the estimation results of VAR (2) model, where the first- and second-order lagged returns of the bank and real estate sectors have an overall positive impact on themselves versus each of the other sectors. The insurance sector with first-order lag has an overall positive impact on other sectors, and the insurance sector with second-order lag has an overall negative impact on other sectors. The overall impact of the diversified financial sector on other sectors is negative with a first-order lag, and the overall impact of the diversified financial sector on other sectors is positive with a second-order lag. The impact of the securities sector on the bank sector and the insurance sector with a first-order lag is negative, and the impact of the securities sector returns on the insurance sector with a second-order lag is negative, and the impact of the returns on the other sectors is positive.

We define  $H$  as 10 when calculating the proportion of forecast error variance  $d_{ij}(H)$ , and Table 4 shows the matrix of risk spillover effects. The element in row  $i$  and column  $j$  of the matrix corresponds to  $d_{ij}(H)$ , the proportion of the  $H$ -step forecast error of  $x_i$  that is explained by  $x_j$ , and  $d_{ii}(H)$  denotes the proportion of the forward  $H$ -step forecast error of the variable  $x_i$  that is explained by the variable  $x_i$  itself. In this paper, we define  $d_{ij}(H)$  as the proportion of the risk spilled from sector  $j$  to sector  $i$  to the total risk of sector  $i$ . The larger the value of  $d_{ij}(H)$ , the greater the impact of sector  $i$  on sector  $j$ , and the larger the  $d_{ii}(H)$ , the greater the risk derived by sector  $i$  itself than the risk of contagion from other sectors when facing market shocks.

According to Table 4, there is a distinct asymmetry in the intensity of risk spillover effects between different sectors,

i.e.,  $d_{ij}(H) \neq d_{ji}(H)$ . In the face of market shocks, the risk of the bank sector is mainly derived from the bank system, with its internal derivative risk accounting for about 64.994% of the total risk. However, the percentage of risk spillover from the securities, insurance, real estate, and diversified financial sectors to the bank sector is relatively low, at 15.835%, 21.012%, 15.862%, and 12.235% of the total bank sector risk, respectively. The ratio of derivative risk within the securities sector to total risk is about 33.348%, which is smaller than the total cross-sectoral risk spillover effect of the other four sectors (66.652%). Meanwhile, the ratio of risk spillover from the bank sector, insurance sector, real estate sector, and diversified financial sector to the securities sector was 15.058%, 16.343%, 16.426%, and 18.825%, respectively. The ratio of derivative risk within the insurance sector to total risk is about 34.988%, which is smaller than the sum of cross-sectoral risk spillover effects from the other four sectors. In particular, the ratio of risk spillover from the bank sector to the insurance sector is the largest, with a value of 20.959%. The risk of the real estate sector is mainly generated within itself, accounting for about 34.657% of the total risk, while the risk spillover from the bank, securities, insurance, and diversified finance sectors to the real estate sector accounts for 15.651%, 17.189%, 14.193%, and 18.311%, respectively. The share of internal derivative risk of the diversified financial sector is 35.736%, and the risk spillovers to it from the bank, securities, insurance, and real estate sectors are 12.364%, 20.310%, 12.669%, and 18.921%, respectively. In particular, the securities sector has the largest share of contagion risk to the diversified financial sector at 20.31%.

TABLE 3: Estimation results of VAR (2).

Coefficient matrix A1					
L1.bank	0.0291	0.0288	0.0307	-0.0164	0.0528
L1.estate	-0.0369	0.0100	-0.0602	0.0251	-0.0648
L1.insurance	0.0509	-0.0007	0.0610	0.0228	0.0311
L1.mvfinance	-0.0645	-0.0183	-0.0629	0.0306	-0.0430
L1.securities	-0.0134	0.0490	-0.0065	0.0247	0.0526
Coefficient matrix A2					
L2.bank	-0.0030	0.0135	0.0514	0.0837	0.1149
L2.estate	0.0289	-0.0455	-0.0347	-0.0373	0.0033
L2.insurance	-0.0293	-0.0297	-0.0206	-0.0685	-0.0836
L2.mvfinance	-0.0196	0.0254	0.0079	0.0440	0.0209
L2.securities	0.0168	0.0231	-0.0039	0.0360	0.0087

TABLE 4: Cross-sectoral risk contagion effect matrix (%).

	Bank	Securities	Insurance	Estate	Diversified finance	Risk absorption
Bank	35.056	15.835	21.012	15.862	12.235	64.944
Securities	15.058	33.348	16.343	16.426	18.825	66.652
Insurance	20.959	17.183	34.988	14.383	12.486	65.012
Estate	15.651	17.189	14.193	34.657	18.311	65.343
Diversified finance	12.364	20.310	12.669	18.921	35.736	64.264
Risk spillover	64.032	70.516	64.217	65.592	61.858	326.215
Sum	99.088	103.864	99.205	100.249	97.594	65.243

Figure 1 shows the cross-sectoral risk spillover networks constructed based on the risk contagion effect matrix. In order to identify the asymmetry of risk spillover networks, this paper constructs the upper triangular network of risk contagion matrix and the lower triangular network of risk contagion matrix, respectively. In Figure 1, (a) shows the upper triangular network of risk spillover, and (b) shows the lower triangular network of risk spillover. The risk absorption effect portrays the risk transfer taken by each sector from other sectors, and the risk sending effect portrays the risk spillover from each sector to other sectors. According to Figure 1, the risk sending and risk absorbing effects of each sector are asymmetric. According to Figure 1, the risk sending and risk absorbing effects of each sector are asymmetric; i.e., the risk network is asymmetric in intensity. And we find that the securities and bank sectors are most vulnerable to risk fluctuations from other sectors (with the largest risk absorption effect), and the risk absorption effect is stronger in the securities sector than in the bank sector. In addition, the securities sector has the largest risk sending effect.

**4.2. Dynamic Movements of Network Contagion of Financial Risk.** Risk linkages and risk contagion within financial markets have a dynamic change pattern. This paper employs the moving window approach to construct a cross-sectoral risk spillover network of financial markets and further investigates the dynamic changes of the level of the network contagion of financial risk. Figure 2 shows the movement of the risk contagion index (Cindex).

In 2008, due to the global financial crisis caused by the “subprime mortgage crisis,” the risk contagion effect of Chinese financial markets intensified, and the risk contagion

index rose from around 53% to around 70%. During 2008–2010, the risk contagion effect weakened, and the risk contagion index fell to around 63%. In early 2011, the cross-sectoral risk contagion effect increased for a short period of time due to the shocks from the bond market, the risk contagion index exceeded 70%, but it decreased in the first quarter of 2012. During the “stock market crash” in 2015, the risk contagion effect of Chinese financial markets reached a new peak, with the risk contagion index at about 72%. But it dropped to its lowest level (around 32%) from March 2, 2007, to March 5, 2021, due to risk management measures taken by the regulatory authorities. Along with the Sino-US trade war, the risk contagion effect of Chinese financial markets started to increase in the first quarter of 2018, at approximately 70%. Adding the impact of COVID-19, the risk contagion index further enlarged and persists at a high level of 70% for about two years. With the effective prevention and gradual mitigation of the epidemic in China, the risk contagion effect diminishes in the second half of 2020, with the risk contagion index at about 65%.

Overall, the risk contagion index is an important proxy variable for the level of overall risk contagion in the financial market. It portrays the movement of risk contagion accurately and identifies the rising trend of risk contagion effect during the crisis period.

**4.3. Driving Impact of Economic Policy Uncertainty on the Level of Risk Contagion.** In this paper, we use risk network connectivity index as the explanatory variable, economic policy uncertainty index as the core explanatory variable, and these variables that reflect domestic macroeconomic and financial fundamentals: inflation, CSI 300 index turnover rate, industrial value added, CSI 300 index PE ratio, and 5-

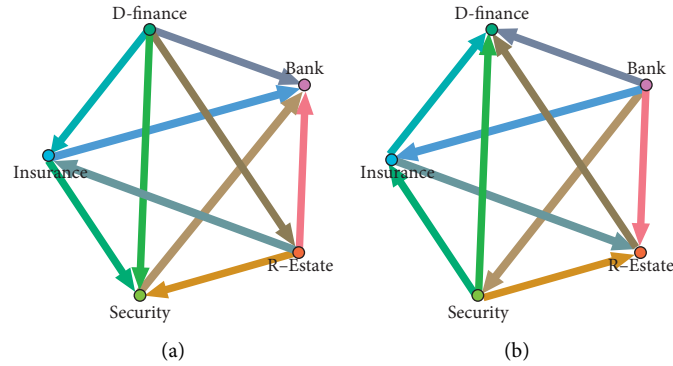


FIGURE 1: Cross-sectoral risk spillover networks. In the risk spillover networks constructed in this paper, the risk absorption effect mainly refers to how many arrows point to the node, the more arrows pointing to the node, the more cross-sectoral risk contagion sources of the node, the thicker the pointing arrows, the stronger the risk spillover effect. The risk sending effect mainly refers to how many arrows point to other nodes at the node, and the more arrows point from the node, the more sectors are affected by the risk spillover from the node, and the thicker the pointing arrow, the stronger the risk spillover effect. (a) The upper triangular network of risk spillover, (b) The lower triangular network of risk spillover.

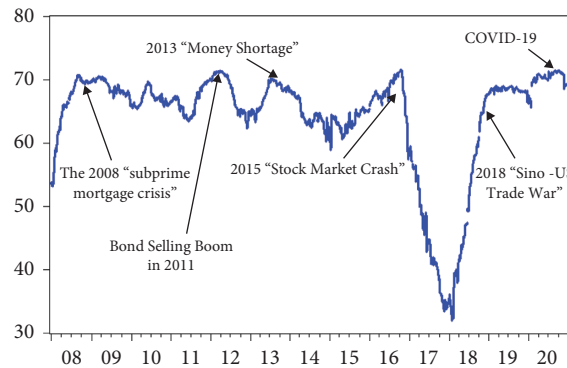


FIGURE 2: Risk contagion index of Chinese financial markets (%).

year and 6-month treasury term spread as control variables to empirically test the driving impact of economic policy uncertainty on risk contagion in Chinese financial markets. To avoid the pseudoregression that arises from the common trend of variables, we use the HP filtering method to separate the trend terms of all explanatory variables, leaving the periodic terms for model estimation. The periodic terms of the variables separated by HP filtering are all stationary time series, and Table 5 shows the model estimation results.

In Table 5, models (1), (2), and (3) all use risk contagion index as the explanatory variables, the explanatory variable in model (1) is the Chinese economic policy uncertainty index, the explanatory variables in model (2) are control variables such as inflation rate, and model (3) adds control variables based on model (1). From Table 5, we can know that the economic policy uncertainty index has a significant positive effect on the risk contagion index of Chinese financial markets. That is, the higher the economic policy uncertainty, the higher the level of risk contagion. After adding macroeconomic and financial variables, the effect of economic policy uncertainty on the level of risk contagion is still significantly positive.

**4.4. Robustness Test.** This paper selects 19 financial institutions belonging to the banking, securities, and insurance sectors and 5 firms belonging to the real estate sector to construct interinstitutional asymmetric risk spillover networks and risk contagion index for testing the robustness of the driving impact of economic policy uncertainty on the level of risk contagion. Considering the availability of data, the 19 financial institutions include 7 banks, 3 insurance companies, and 9 securities companies. Since the number of listed companies of the real estate sector is large and the time span is long, we select five real estate companies with the largest market capitalization. The names of selected institutions in each sector are shown in Table 6, and each financial institution is used as the central node to construct an interinstitutional asymmetric risk spillover network.

Figure 3 shows the risk spillover networks diagram constructed based on the risk spillover matrix between 19 financial institutions and 5 real estate companies. In Figure 3, (a) shows the network of upper triangular, (b) shows the network of lower triangular. According to Figure 3, we can see that the risk spillover effect of bank sector firms to firms belong to securities, real estate, and insurance sectors is

TABLE 5: Estimation results of regression.

	(1)	(2)	(3)
CEPU			0.0058**
CPI		0.2370	0.3378
CSI 300 turnover rate	0.0058**	-1.2281	-0.8497
Industrial value added		-0.1038	-0.1130
CSI 300 PE ratio		-0.6000***	-0.5929***
Treasury term spread		5.5265**	5.6745**
C	$3.36E - 12$	$2.94E - 12$	$2.8E - 12$
R-squared	0.0250	0.1869	0.2112
Adjusted $R^2$	0.0188	0.1601	0.1799

\* $p < 0.1$ , \*\* $p < 0.05$ , \*\*\* $p < 0.01$ .

TABLE 6: Selection of the nodes of institutional risk spillover network.

Department	Name of institution	Node number
Bank	Ping An Bank, Shanghai Pudong Development Bank, Huaxia bank, China Minsheng Bank, China Merchant's Bank, Industrial and Commercial Bank of China	node1–node7
Estate	Vanke, Shenzhen Zhenye, Shenzhen Property, Shahe industry, Grandjoy	node8–node12
Insurance	Hubei Biocause Pharmaceutical, Ping An Insurance of China, China Life Insurance	node13–node15
Securities	Northeast Securities, Guangdong Golden Dragon Development, Guangzhou Yuexiu Financial Holdings Group, CITIC Securities, SDIC Capital, Xiangcai, China Fortune Securities Investment Company, Haitong Securities, Harbin Hatou Investment	node16–node24

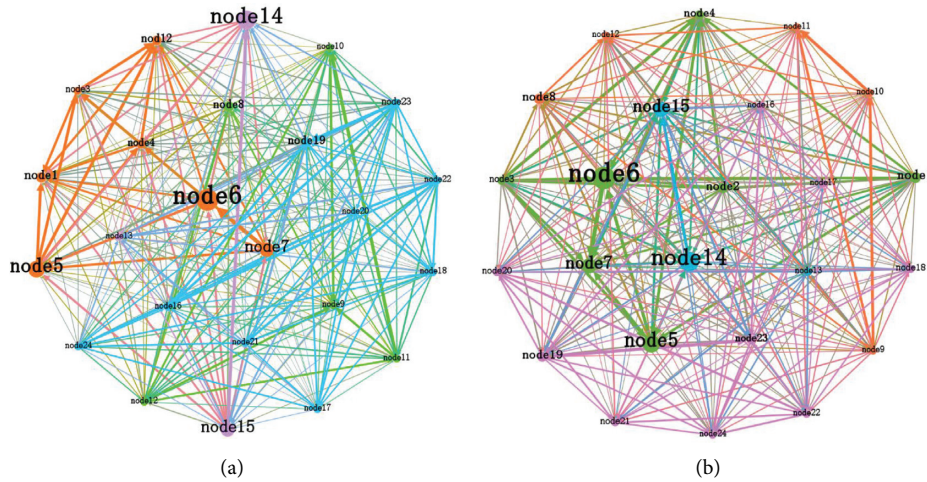


FIGURE 3: Interinstitutional risk spillover networks (average). Consistent with the risk spillover networks constructed for each sector of Chinese financial markets, the return series of 19 financial institutions, and 5 real estate companies are all stationary time series. Based on the lag order test, we construct a second-order VAR model and calculate the proportion of variation in forecast error  $d_{ij}$  (10) for the forward 10-step forecast. In a single risk spillover network, network nodes and connected edges are identified using the same color for institutions belonging to the same sector. The node size of the interinstitutional risk spillover network corresponds to the market capitalization of the institution. The larger the market capitalization, the larger the network node, and the thickness of the contiguous edges of the network nodes indicates the strength of the risk contagion level. The thicker the contiguous edges of the network, the stronger the risk spillover effect. (a) The upper triangular network of risk spillover. (b) The lower triangular network of risk spillover.

large, while companies in the securities, real estate, and insurance sectors have relatively small risk spillover effects on companies in the banking sector. Risk spillover networks are typically asymmetric.

Table 7 presents the estimation results of the robustness test of the risk contagion index constructed based on the interinstitutional asymmetric risk spillover networks. According to Table 7, the conclusion that the economic

policy uncertainty index has a significant positive driving impact on the risk contagion index still holds.

In addition, this paper tests the robustness of the impact of economic policy uncertainty on the level of risk contagion by using the Global Economic Policy Uncertainty (GEPY) Index instead of the Chinese Economic Policy Uncertainty Index. The model estimation results are shown in Table 8. According to Table 8, this conclusion still holds.

TABLE 7: Robustness tests based on risk contagion index of 24 firms.

	(1)	(2)	(3)
CEPU			0.0038*
CPI		-0.2678	-0.2011
CSI 300 turnover rate	0.0040**	-0.9505	-0.7003
Industrial value added		-0.0940	-0.1001
CSI 300 PE ratio		-0.3782***	-0.3735***
Treasury term spread		5.1000***	5.1979***
C	-8.87E-12	-9.49E-12	-9.59E-12
R-squared	0.0216	0.2067	0.2251
Adjusted R <sup>2</sup>	0.0153	0.1807	0.1943

\* $p < 0.1$ , \*\* $p < 0.05$ , \*\*\* $p < 0.01$ .

TABLE 8: Robustness test based on the global economic policy uncertainty index.

	(1)	(2)	(3)
GEPU			0.0475***
CPI		0.2370	0.2517
CSI 300 turnover rate	0.0604***	-0.1038	-0.0550
Industrial value added		-1.2281	-0.9464
CSI 300 PE ratio		-0.6000***	-0.4755***
Treasury term spread		5.5265***	5.8121***
C	4.55E-12	2.94E-12	3.93E-12
R-squared	0.1380	0.1869	0.2624
Adjusted R <sup>2</sup>	0.1325	0.1601	0.2331

\* $p < 0.1$ , \*\* $p < 0.05$ , \*\*\* $p < 0.01$ .

## 5. Conclusion

This paper constructs asymmetric risk spillover networks and risk contagion index for Chinese financial markets based on the bank, securities, insurance, diversified finance, and real estate sectors. The driving impact of economic policy uncertainty on the level of risk contagion in financial markets is investigated. This paper draws the following conclusions. First, the risk contagion effect within Chinese financial markets has dynamic change characteristics, and the risk spillover effects among different sectors are asymmetric in intensity. Second, the risk spillover effect of the real estate sector does not diminish with the mitigation of the COVID-19 epidemic, and the current potential risk in the Chinese real estate market is larger. Third, economic policy uncertainty has a significant positive impact on the level of overall risk contagion in Chinese financial markets.

Based on a comprehensive analysis of the level of risk contagion in Chinese financial markets, this paper proposes the following implications. First, economic policy uncertainty is tightly related to risk contagion and shocks of financial markets. Therefore, regulatory authorities should be cautious in dealing with the adverse effects of economic policy uncertainty on financial markets to avoid the spread of negative public emotion due to economic policy uncertainty, which could lead to financial crises. Second, the contagion of financial risks is an asymmetric network that intersects with each other, and the regulatory authorities should distinguish the role of different sectors in risk contagion. Third, the trend of financialization of real estate is

increasingly obvious, and regulatory authorities should focus on potential sources of systemic financial risk induced by the real estate sector by actively studying the risk transmission mechanism between the real estate market and the financial markets.

## Data Availability

The data used in this study are available from the corresponding author upon request.

## Conflicts of Interest

The authors declare that there are no conflicts of interest regarding the publication of this paper.

## Acknowledgments

This work was supported by the National Natural Science Foundation of China (7207030651).

## References

- [1] F. Caccioli, P. Barucca, and T. Kobayashi, "Network models of financial systemic risk: a review," *Journal of Computational Social Science*, vol. 1, no. 1, pp. 81–114, 2018.
- [2] K. Anand, B. Craig, and G. Von Peter, "Filling in the blanks: network structure and interbank contagion," *Quantitative Finance*, vol. 15, no. 4, pp. 625–636, 2015.
- [3] D. Acemoglu, A. Ozdaglar, and A. Tahbaz-Salehi, "Systemic risk and stability in financial networks," *The American Economic Review*, vol. 105, no. 2, pp. 564–608, 2015.
- [4] T. C. Silva, M. A. Da Silva, and B. M. Tabak, "Bank lending and systemic risk: a financial-real sector network approach with feedback," *Journal of Financial Stability*, vol. 38, pp. 98–118, 2017.
- [5] Y. Hong, Y. Liu, and S. Wang, "Granger causality in risk and detection of extreme risk spillover between financial markets," *Journal of Econometrics*, vol. 150, no. 2, pp. 271–287, 2009.
- [6] M. Billio, M. Getmansky, A. W. Lo, and L. Pelizzon, "Econometric measures of connectedness and systemic risk in the finance and insurance sectors," *Journal of Financial Economics*, vol. 104, no. 3, pp. 535–559, 2012.
- [7] F. X. Diebold and K. YiLmaz, "Measuring financial asset return and volatility spillovers, with application to global equity markets," *The Economic Journal*, vol. 119, no. 534, pp. 158–171, 2009.
- [8] N. Paltalidis, D. Gounopoulos, R. Kizys, and Y. Koutelidakis, "Transmission channels of systemic risk and contagion in the European financial network," *Journal of Banking & Finance*, vol. 61, pp. 36–52, 2015.
- [9] R. J. Berndsen, C. León, and L. Renneboog, "Financial stability in networks of financial institutions and market infrastructures," *Journal of Financial Stability*, vol. 35, pp. 120–135, 2016.
- [10] H. Anderson, M. Paddrik, and J. J. Wang, "Bank networks and systemic risk: evidence from the national banking acts," *The American Economic Review*, vol. 109, no. 9, pp. 3125–3161, 2019.
- [11] M. Elliott, B. Golub, and M. O. Jackson, "Financial networks and contagion," *The American Economic Review*, vol. 104, no. 10, pp. 3115–3153, 2014.

- [12] S. R. Baker, N. Bloom, and S. J. Davis, "Measuring economic policy uncertainty\*," *Quarterly Journal of Economics*, vol. 131, no. 4, pp. 1593–1636, 2016.
- [13] L. Pástor and P. Veronesi, "Uncertainty about government policy and stock prices," *The Journal of Finance*, vol. 67, no. 4, pp. 1219–1264, 2012.
- [14] L. Pástor and P. Veronesi, "Political uncertainty and risk premia," *Journal of Financial Economics*, vol. 110, no. 3, pp. 520–545, 2013.
- [15] I. Dakhlaoui and C. Aloui, "The interactive relationship between the US economic policy uncertainty and BRIC stock markets," *International Economics*, vol. 146, pp. 141–157, 2016.
- [16] M. E. Hoque and M. A. S. Zaidi, "The impacts of global economic policy uncertainty on stock market returns in regime switching environment: evidence from sectoral perspectives," *International Journal of Finance & Economics*, vol. 24, no. 2, pp. 991–1016, 2019.
- [17] D. L. Dicks and P. Fulghieri, "Uncertainty aversion and systemic risk," *Journal of Political Economy*, vol. 127, no. 3, pp. 1118–1155, 2019.
- [18] Z. H. Yang, R. X. Chen, and Y. T. Chen, "Economic policy uncertainty and cross-market contagion of systemic financial risk: a study based on nonlinear network correlation," *Economic Research*, vol. 55, no. 1, pp. 65–81, 2020.
- [19] A. Sharif, C. Aloui, and L. Yarovaya, "COVID-19 pandemic, oil prices, stock market, geopolitical risk and policy uncertainty nexus in the US economy: fresh evidence from the wavelet-based approach," *International Review of Financial Analysis*, vol. 70, Article ID 101496, 2020.
- [20] R. Li, S. Li, D. Yuan, and K. Yu, "Does economic policy uncertainty in the U.S. influence stock markets in China and India? time-frequency evidence," *Applied Economics*, vol. 52, no. 39, pp. 4300–4316, 2020.
- [21] Y. Li, J. Luo, and Y. Jiang, "Policy uncertainty spillovers and financial risk contagion in the Asia-Pacific network," *Pacific-Basin Finance Journal*, vol. 67, Article ID 101554, 2021.
- [22] C. Minoui, C. Kang, V. S. Subrahmanian, and A. Berea, "Does financial connectedness predict crises?" *Quantitative Finance*, vol. 15, no. 4, pp. 607–624, 2015.
- [23] S. Benoit, J.-E. Colliard, C. Hurlin, and C. Pérignon, "Where the risks lie: a survey on systemic risk\*," *Review of Finance*, vol. 21, no. 1, pp. 109–152, 2017.
- [24] X. L. Gong, X. Xiong, and W. Zhang, "Research on systemic risk measures and spillover effects of financial institutions in China," *Management World*, vol. 36, no. 8, pp. 65–83, 2020.
- [25] H. X. Bai, S. F. Liu, X. W. Luo, L. L. Liu, and W. Y. Hao, "Research on the measurement and early warning of systemic financial risk in China based on real estate market," *Financial Research*, vol. 8, pp. 54–73, 2020.
- [26] F. X. Diebold and K. Yilmaz, "On the network topology of variance decompositions: measuring the connectedness of financial firms," *Journal of Econometrics*, vol. 182, no. 1, pp. 119–134, 2014.